ISSN 1007-9327 (print)
ISSN 2219-2840 (online)

World Journal of *Gastroenterology*

World J Gastroenterol 2015 January 21; 21(3): 711-1048

Published by Baishideng Publishing Group Inc

World Journal of Gastroenterology

A peer-reviewed, online, open-access journal of gastroenterology and hepatology

Editorial Board

2014-2017

The *World Journal of Gastroenterology* Editorial Board consists of 1379 members, representing a team of worldwide experts in gastroenterology and hepatology. They are from 68 countries, including Algeria (2), Argentina (7), Australia (31), Austria (9), Belgium (11), Brazil (20), Brunei Darussalam (1), Bulgaria (2), Cambodia (1), Canada (26), Chile (4), China (163), Croatia (2), Cuba (1), Czech (6), Denmark (2), Egypt (9), Estonia (2), Finland (6), France (20), Germany (58), Greece (31), Guatemala (1), Hungary (15), Iceland (1), India (33), Indonesia (2), Iran (10), Ireland (9), Israel (18), Italy (195), Japan (151), Jordan (1), Kuwait (1), Lebanon (7), Lithuania (1), Malaysia (1), Mexico (11), Morocco (1), Netherlands (5), New Zealand (4), Nigeria (3), Norway (6), Pakistan (6), Poland (12), Portugal (8), Puerto Rico (1), Qatar (1), Romania (10), Russia (3), Saudi Arabia (2), Singapore (7), Slovenia (2), South Africa (1), South Korea (70), Spain (51), Sri Lanka (1), Sudan (1), Sweden (12), Switzerland (5), Thailand (7), Trinidad and Tobago (1), Tunisia (2), Turkey (56), United Kingdom (49), United States (179), Venezuela (1), and Vietnam (1).

Daniel A Lemberg, *Sydney*
Rupert W Leong, *Sydney*
Finlay A Macrae, *Victoria*
Vance Matthews, *Melbourne*
David L Morris, *Sydney*
Reme Mountifield, *Bedford Park*
Hans J Netter, *Melbourne*
Nam Q Nguyen, *Adelaide*
Liang Qiao, *Westmead*
Rajvinder Singh, *Adelaide*
Ross Cyril Smith, *StLeonards*
Kevin J Spring, *Sydney*
Debbie Trinder, *Fremantle*
Daniel R van Langenberg, *Box Hill*
David Ian Watson, *Adelaide*
Desmond Yip, *Garran*
Li Zhang, *Sydney*

Austria

Felix Aigner, *Innsbruck*
Gabriela A Berlakovich, *Vienna*
Herwig R Cerwenka, *Graz*
Peter Ferenci, *Wien*
Alfred Gangl, *Vienna*
Kurt Lenz, *Linz*
Markus Peck-Radosavljevic, *Vienna*
Markus Raderer, *Vienna*
Stefan Riss, *Vienna*

Belgium

Michael George Adler, *Brussels*
Benedicte Y De Winter, *Antwerp*
Mark De Ridder, *Jette*
Olivier Detry, *Liege*
Denis Dufrane Dufrane, *Brussels*
Sven M Francque, *Edegem*
Nikos Kotzampassakis, *Liège*
Geert KMM Robaeys, *Genk*
Xavier Sagaert, *Leuven*
Peter Starkel, *Brussels*
Eddie Wisse, *Keerbergen*

Brazil

SMP Balzan, *Santa Cruz do Sul*
JLF Caboclo, *Sao jose do rio preto*
Fábio Guilherme Campos, *Sao Paulo*
Claudia RL Cardoso, *Rio de Janeiro*
Roberto J Carvalho-Filho, *Sao Paulo*
Carla Daltro, *Salvador*
José Sebastiao dos Santos, *Ribeirao Preto*
Eduardo LR Mello, *Rio de Janeiro*
Sthela Maria Murad-Regadas, *Fortaleza*
Claudia PMS Oliveira, *Sao Paulo*
Júlio C Pereira-Lima, *Porto Alegre*
Marcos V Perini, *Sao Paulo*
Vietla Satyanarayana Rao, *Fortaleza*
Raquel Rocha, *Salvador*
AC Simoes e Silva, *Belo Horizonte*
Mauricio F Silva, *Porto Alefre*
Aytan Miranda Sipahi, *Sao Paulo*
Rosa Leonôra Salerno Soares, *Niterói*
Cristiane Valle Tovo, *Porto Alegre*
Eduardo Garcia Vilela, *Belo Horizonte*

Brunei Darussalam

Vui Heng Chong, *Bandar Seri Begawan*

Bulgaria

Tanya Kirilova Kadiyska, *Sofia*
Mihaela Petrova, *Sofia*

Cambodia

Francois Rouet, *Phnom Penh*

Canada

Brian Bressler, *Vancouver*
Frank J Burczynski, *Winnipeg*
Wangxue Chen, *Ottawa*
Francesco Crea, *Vancouver*
Mirko Diksic, *Montreal*
Jane A Foster, *Hamilton*
Hugh J Freeman, *Vancouver*
Shahrokh M Ghobadloo, *Ottawa*
Yuewen Gong, *Winnipeg*
Philip H Gordon, *Quebec*
Rakesh Kumar, *Edmonton*
Wolfgang A Kunze, *Hamilton*
Patrick Labonte, *Laval*
Zhikang Peng, *Winnipeg*
Jayadev Raju, *Ottawa*
Maitreyi Raman, *Calgary*
Giada Sebastiani, *Montreal*
Maida J Sewitch, *Montreal*
Eldon A Shaffer, *Alberta*
Christopher W Teshima, *Edmonton*
Jean Sévigny, *Québec*
Pingchang Yang, *Hamilton*
Pingchang Yang, *Hamilton*
Eric M Yoshida, *Vancouver*
Bin Zheng, *Edmonton*

Chile

Marcelo A Beltran, *La Serena*
Flavio Nervi, *Santiago*
Adolfo Parra-Blanco, *Santiago*
Alejandro Soza, *Santiago*

China

Zhao-Xiang Bian, *Hong Kong*
San-Jun Cai, *Shanghai*
Guang-Wen Cao, *Shanghai*
Long Chen, *Nanjing*
Ru-Fu Chen, *Guangzhou*
George G Chen, *Hong Kong*
Li-Bo Chen, *Wuhan*
Jia-Xu Chen, *Beijing*
Hong-Song Chen, *Beijing*
Lin Chen, *Beijing*
Yang-Chao Chen, *Hong Kong*
Zhen Chen, *Shanghai*
Ying-Sheng Cheng, *Shanghai*
Kent-Man Chu, *Hong Kong*
Zhi-Jun Dai, *Xi'an*
Jing-Yu Deng, *Tianjin*
Yi-Qi Du, *Shanghai*
Zhi Du, *Tianjin*
Hani El-Nezami, *Hong Kong*
Bao-Ying Fei, *Hangzhou*
Chang-Ming Gao, *Nanjing*
Jian-Ping Gong, *Chongqing*
Zuo-Jiong Gong, *Wuhan*
Jing-Shan Gong, *Shenzhen*
Guo-Li Gu, *Beijing*
Yong-Song Guan, *Chengdu*
Mao-Lin Guo, *Luoyang*
Jun-Ming Guo, *Ningbo*
Yan-Mei Guo, *Shanghai*
Xiao-Zhong Guo, *Shenyang*
Guo-Hong Han, *Xi'an*
Ming-Liang He, *Hong Kong*
Peng Hou, *Xi'an*
Zhao-Hui Huang, *Wuxi*
Feng Ji, *Hangzhou*
Simon Law, *Hong Kong*
Yu-Yuan Li, *Guangzhou*
Meng-Sen Li, *Haikou*
Shu-De Li, *Shanghai*
Zong-Fang Li, *Xi'an*
Qing-Quan Li, *Shanghai*
Kang Li, *Lasa*
Han Liang, *Tianjin*
Xing'e Liu, *Hangzhou*
Zheng-Wen Liu, *Xi'an*
Xiao-Fang Liu, *Yantai*
Bin Liu, *Tianjin*
Quan-Da Liu, *Beijing*
Hai-Feng Liu, *Beijing*
Fei Liu, *Shanghai*
Ai-Guo Lu, *Shanghai*
He-Sheng Luo, *Wuhan*
Xiao-Peng Ma, *Shanghai*
Yong Meng, *Shantou*
Ke-Jun Nan, *Xi'an*
Siew Chien Ng, *Hong Kong*
Simon SM Ng, *Hong Kong*
Zhao-Shan Niu, *Qingdao*
Bo-Rong Pan, *Xi'an*
Di Qu, *Shanghai*
Rui-Hua Shi, *Nanjing*
Bao-Min Shi, *Shanghai*
Xiao-Dong Sun, *Hangzhou*
Si-Yu Sun, *Shenyang*
Guang-Hong Tan, *Haikou*
Wen-Fu Tang, *Chengdu*
Anthony YB Teoh, *Hong Kong*
Wei-Dong Tong, *Chongqing*
Eric Tse, *Hong Kong*
Hong Tu, *Shanghai*
Rong Tu, *Haikou*
Jian-She Wang, *Shanghai*
Kai Wang, *Jinan*
Xiao-Ping Wang, *Xianyang*
Dao-Rong Wang, *Yangzhou*
De-Sheng Wang, *Xi'an*
Chun-You Wang, *Wuhan*
Ge Wang, *Chongqing*
Xi-Shan Wang, *Harbin*
Wei-hong Wang, *Beijing*
Zhen-Ning Wang, *Shenyang*

Wai Man Raymond Wong, *Hong Kong*
Chun-Ming Wong, *Hong Kong*
Jian Wu, *Shanghai*
Sheng-Li Wu, *Xi'an*
Wu-Jun Wu, *Xi'an*
Qing Xia, *Chengdu*
Yan Xin, *Shenyang*
Dong-Ping Xu, *Beijing*
Jian-Min Xu, *Shanghai*
Wei Xu, *Changchun*
Ming Yan, *Jinan*
Xin-Min Yan, *Kunming*
Yi-Qun Yan, *Shanghai*
Feng Yang, *Shanghai*
Yong-Ping Yang, *Beijing*
He-Rui Yao, *Guangzhou*
Thomas Yau, *Hong Kong*
Winnie Yeo, *Hong Kong*
Jing You, *Kunming*
Jian-Qing Yu, *Wuhan*
Ying-Yan Yu, *Shanghai*
Wei-Zheng Zeng, *Chengdu*
Zong-Ming Zhang, *Beijing*
Dian-Liang Zhang, *Qingdao*
Ya-Ping Zhang, *Shijiazhuang*
You-Cheng Zhang, *Lanzhou*
Jian-Zhong Zhang, *Beijing*
Ji-Yuan Zhang, *Beijing*
Hai-Tao Zhao, *Beijing*
Jian Zhao, *Shanghai*
Jian-Hong Zhong, *Nanning*
Ying-Qiang Zhong, *Guangzhou*
Ping-Hong Zhou, *Shanghai*
Yan-Ming Zhou, *Xiamen*
Tong Zhou, *Nanchong*
Li-Ming Zhou, *Chengdu*
Guo-Xiong Zhou, *Nantong*
Feng-Shang Zhu, *Shanghai*
Jiang-Fan Zhu, *Shanghai*
Zhao-Hui Zhu, *Beijing*

Croatia

Tajana Filipec Kanizaj, *Zagreb*
Mario Tadic, *Zagreb*

Cuba

Damian Casadesus, *Havana*

Czech

Jan Bures, *Hradec Kralove*
Marcela Kopacova, *Hradec Kralove*
Otto Kucera, *Hradec Kralove*
Marek Minarik, *Prague*
Pavel Soucek, *Prague*
Miroslav Zavoral, *Prague*

Denmark

Vibeke Andersen, *Odense*
E Michael Danielsen, *Copenhagen*

Egypt

Mohamed MM Abdel-Latif, *Assiut*
Hussein Atta, *Cairo*
Ashraf Elbahrawy, *Cairo*
Mortada Hassan El-Shabrawi, *Cairo*
Mona El Said El-Raziky, *Cairo*
Elrashdy M Redwan, *New Borg Alrab*
Zeinab Nabil Ahmed Said, *Cairo*
Ragaa HM Salama, *Assiut*
Maha Maher Shehata, *Mansoura*

Estonia

Margus Lember, *Tartu*
Tamara Vorobjova, *Tartu*

Finland

Marko Kalliomäki, *Turku*
Thomas Kietzmann, *Oulu*
Kaija-Leena Kolho, *Helsinki*
Eija Korkeila, *Turku*
Heikki Makisalo, *Helsinki*
Tanja Pessi, *Tampere*

France

Armando Abergel Clermont, *Ferrand*
Elie K Chouillard, *Polssy*
Pierre Cordelier, *Toulouse*
Pascal P Crenn, *Garches*
Catherine Daniel, *Lille*
Fanny Daniel, *Paris*
Cedric Dray, *Toulouse*
Benoit Foligne, *Lille*
Jean-Noel Freund, *Strasbourg*
Hervé Guillou, *Toulouse*
Nathalie Janel, *Paris*
Majid Khatib, *Bordeaux*
Jacques Marescaux, *Strasbourg*
Jean-Claude Marie, *Paris*
Driffa Moussata, *Pierre Benite*
Hang Nguyen, *Clermont-Ferrand*
Hugo Perazzo, *Paris*
Alain L Servin, *Chatenay-Malabry*
Chang Xian Zhang, *Lyon*

Germany

Stavros A Antoniou, *Monchengladbach*
Erwin Biecker, *Siegburg*
Hubert E Blum, *Freiburg*
Thomas Bock, *Berlin*
Katja Breitkopf-Heinlein, *Mannheim*
Elke Cario, *Essen*
Güralp Onur Ceyhan, *Munich*
Angel Cid-Arregui, *Heidelberg*
Michael Clemens Roggendorf, *München*
Christoph F Dietrich, *Bad Mergentheim*
Valentin Fuhrmann, *Hamburg*
Nikolaus Gassler, *Aachen*
Andreas Geier, *Wuerzburg*
Markus Gerhard, *Munich*
Anton Gillessen, *Muenster*
Thorsten Oliver Goetze, *Offenbach*
Daniel Nils Gotthardt, *Heidelberg*
Robert Grützmann, *Dresden*
Thilo Hackert, *Heidelberg*
Joerg Haier, *Muenster*
Claus Hellerbrand, *Regensburg*
Harald Peter Hoensch, *Darmstadt*
Jens Hoeppner, *Freiburg*
Richard Hummel, *Muenster*
Jakob Robert Izbicki, *Hamburg*
Gernot Maximilian Kaiser, *Essen*
Matthias Kapischke, *Hamburg*
Michael Keese, *Frankfurt*
Andrej Khandoga, *Munich*
Jorg Kleeff, *Munich*
Alfred Koenigsrainer, *Tuebingen*
Peter Christopher Konturek, *Saalfeld*
Michael Linnebacher, *Rostock*
Stefan Maier, *Kaufbeuren*
Oliver Mann, *Hamburg*
Marc E Martignoni, *Munic*
Thomas Minor, *Bonn*
Oliver Moeschler, *Osnabrueck*
Jonas Mudter, *Eutin*
Sebastian Mueller, *Heidelberg*
Matthias Ocker, *Berlin*
Andreas Ommer, *Essen*
Albrecht Piiper, *Frankfurt*
Esther Raskopf, *Bonn*
Christoph Reichel, *Bad Brückenau*
Elke Roeb, *Giessen*
Udo Rolle, *Frankfurt*
Karl-Herbert Schafer, *Zweibrücken*
Peter Schemmer, *Heidelberg*
Andreas G Schreyer, *Regensburg*
Manuel A Silva, *Penzberg*
Georgios C Sotiropoulos, *Essen*
Ulrike S Stein, *Berlin*
Dirk Uhlmann, *Leipzig*
Michael Weiss, *Halle*
Hong-Lei Weng, *Mannheim*
Karsten Wursthorn, *Hamburg*

Greece

Alexandra Alexopoulou, *Athens*
Nikolaos Antonakopoulos, *Athens*
Stelios F Assimakopoulos, *Patras*
Grigoris Chatzimavroudis, *Thessaloniki*
Evangelos Cholongitas, *Thessaloniki*
Gregory Christodoulidis, *Larisa*
George N Dalekos, *Larissa*
Maria Gazouli, *Athens*
Urania Georgopoulou, *Athens*
Eleni Gigi, *Thessaloniki*
Stavros Gourgiotis, *Athens*
Leontios J Hadjileontiadis, *Thessaloniki*
Thomas Hyphantis, *Ioannina*
Ioannis Kanellos, *Thessaloniki*
Stylianos Karatapanis, *Rhodes*
Michael Koutsilieris, *Athens*
Spiros D Ladas, *Athens*
Theodoros K Liakakos, *Athens*
Emanuel K Manesis, *Athens*
Spilios Manolakopoulos, *Athens*
Gerassimos John Mantzaris, *Athens*
Athanasios D Marinis, *Piraeus*
Nikolaos Ioannis Nikiteas, *Athens*
Konstantinos X Papamichael, *Athens*
George Sgourakis, *Athens*
Konstantinos C Thomopoulos, *Patras*
Konstantinos Triantafyllou, *Athens*
Christos Triantos, *Patras*
Georgios Zacharakis, *Athens*
Petros Zezos, *Alexandroupolis*

Demosthenes E Ziogas, *Ioannina*

Guatemala

Carlos Maria Parellada, *Guatemala*

Hungary

Mihaly Boros, *Szeged*
Tamás Decsi, *Pécs*
Gyula Farkas, *Szeged*
Andrea Furka, *Debrecen*
Y vette Mandi, *Szeged*
Peter L Lakatos, *Budapest*
Pal Miheller, *Budapest*
Tamás Molnar, *Szeged*
Attila Olah, *Gyor*
Maria Papp, *Debrecen*
Zoltan Rakonczay, *Szeged*
Ferenc Sipos, *Budapest*
Miklós Tanyi, *Debrecen*
Tibor Wittmann, *Szeged*

Iceland

Tryggvi Bjorn Stefánsson, *Reykjavík*

India

Brij B Agarwal, *New Delhi*
Deepak N Amarapurkar, *Mumbai*
Shams ul Bari, *Srinagar*
Sriparna Basu, *Varanasi*
Runu Chakravarty, *Kolkata*
Devendra C Desai, *Mumbai*
Nutan D Desai, *Mumbai*
Suneela Sunil Dhaneshwar, *Pune*
Radha K Dhiman, *Chandigarh*
Pankaj Garg, *Mohali*
Uday C Ghoshal, *Lucknow*
Kalpesh Jani, *Vadodara*
Premashis Kar, *New Delhi*
Jyotdeep Kaur, *Chandigarh*
Rakesh Kochhar, *Chandigarh*
Pradyumna K Mishra, *Mumbai*
Asish K Mukhopadhyay, *Kolkata*
Imtiyaz Murtaza, *Srinagar*
P Nagarajan, *New Delhi*
Samiran Nundy, *Delhi*
Gopal Pande, *Hyderabad*
Benjamin Perakath, *Vellore*
Arun Prasad, *New Delhi*
D Nageshwar Reddy, *Hyderabad*
Lekha Saha, *Chandigarh*
Sundeep Singh Saluja, *New Delhi*
Mahesh Prakash Sharma, *New Delhi*
Sadiq Saleem Sikora, *Bangalore*
Sarman Singh, *New Delhi*
Rajeev Sinha, *Jhansi*
Rupjyoti Talukdar, *Hyderabad*
Rakesh Kumar Tandon, *New Delhi*
Narayanan Thirumoorthy, *Coimbatore*

Indonesia

David Handojo Muljono, *Jakarta*
Andi Utama, *Jakarta*

Iran

Arezoo Aghakhani, *Tehran*
Seyed Mohsen Dehghani, *Shiraz*
Ahad Eshraghian, *Shiraz*
Hossein Khedmat, *Tehran*
Sadegh Massarrat, *Tehran*
Marjan Mohammadi, *Tehran*
Roja Rahimi, *Tehran*
Farzaneh Sabahi, *Tehran*
Majid Sadeghizadeh, *Tehran*
Farideh Siavoshi, *Tehran*

Ireland

Gary Alan Bass, *Dublin*
David J Brayden, *Dublin*
Ronan A Cahill, *Dublin*
Glen A Doherty, *Dublin*
Liam J Fanning, *Cork*
Barry Philip McMahon, *Dublin*
RossMcManus, *Dublin*
Dervla O'Malley, *Cork*
Sinead M Smith, *Dublin*

Israel

Dan Carter, *Ramat Gan*
Jorge-Shmuel Delgado, *Metar*
Eli Magen, *Ashdod*
Nitsan Maharshak, *Tel Aviv*
Shaul Mordechai, *Beer Sheva*
Menachem Moshkowitz, *Tel Aviv*
William Bahij Nseir, *Nazareth*
Shimon Reif, *Jerusalem*
Ram Reifen, *Rehovot*
Ariella Bar-Gil Shitrit, *Jerusalem*
Noam Shussman, *Jerusalem*
Igor Sukhotnik, *Haifa*
Nir Wasserberg, *Petach Tiqwa*
Jacob Yahav, *Rehovot*
Doron Levi Zamir, *Gedera*
Shira Zelber-Sagi, *Haifa*
Romy Zemel, *Petach-Tikva*

Italy

Ludovico Abenavoli, *Catanzaro*
Luigi Elio Adinolfi, *Naples*
Carlo Virginio Agostoni, *Milan*
Anna Alisi, *Rome*
Piero Luigi Almasio, *Palermo*
Donato Francesco Altomare, *Bari*
Amedeo Amedei, *Florence*
Pietro Andreone, *Bologna*
Imerio Angriman, *Padova*
Vito Annese, *Florence*
Paolo Aurello, *Rome*
Salavtore Auricchio, *Naples*
Gian Luca Baiocchi, *Brescia*
Gianpaolo Balzano, *Milan*
Antonio Basoli, *Rome*
Gabrio Bassotti, *San Sisto*
Mauro Bernardi, *Bologna*
Alberto Biondi, *Rome*
Ennio Biscaldi, *Genova*
Massimo Bolognesi, *Padua*
Luigi Bonavina, *Milano*
Aldo Bove, *Chieti*
Raffaele Bruno, *Pavia*
Luigi Brusciano, *Napoli*
Giuseppe Cabibbo, *Palermo*
Carlo Calabrese, *Bologna*
Daniele Calistri, *Meldola*
Vincenza Calvaruso, *Palermo*
Lorenzo Camellini, *Reggio Emilia*
Marco Candela, *Bologna*
Raffaele Capasso, *Naples*
Lucia Carulli, *Modena*
Renato David Caviglia, *Rome*
Luigina Cellini, *Chieti*
Giuseppe Chiarioni, *Verona*
Claudio Chiesa, *Rome*
Michele Cicala, *Roma*
Rachele Ciccocioppo, *Pavia*
Sandro Contini, *Parma*
Gaetano Corso, *Foggia*
Renato Costi, *Parma*
Alessandro Cucchetti, *Bologna*
Rosario Cuomo, *Napoli*
Giuseppe Currò, *Messina*
Paola De Nardi, *Milano*
Giovanni D De Palma, *Naples*
Raffaele De Palma, *Napoli*
Giuseppina De Petro, *Brescia*
Valli De Re, *Aviano*
Paolo De Simone, *Pisa*
Giuliana Decorti, *Trieste*
Emanuele Miraglia del Giudice, *Napoli*
Isidoro Di Carlo, *Catania*
Matteo Nicola Dario Di Minno, *Naples*
Massimo Donadelli, *Verona*
Mirko D'Onofrio, *Verona*
Maria Pina Dore, *Sassari*
Luca Elli, *Milano*
Massimiliano Fabozzi, *Aosta*
Massimo Falconi, *Ancona*
Ezio Falletto, *Turin*
Silvia Fargion, *Milan*
Matteo Fassan, *Verona*
Gianfranco Delle Fave, *Roma*
Alessandro Federico, *Naples*
Francesco Feo, *Sassari*
Davide Festi, *Bologna*
Natale Figura, *Siena*
Vincenzo Formica, *Rome*
Mirella Fraquelli, *Milan*
Marzio Frazzoni, *Modena*
Walter Fries, *Messina*
Gennaro Galizia, *Naples*
Andrea Galli, *Florence*
Matteo Garcovich, *Rome*
Eugenio Gaudio, *Rome*
Paola Ghiorzo, *Genoa*
Edoardo G Giannini, *Genova*
Luca Gianotti, *Monza*
Maria Cecilia Giron, *Padova*
Alberto Grassi, *Rimini*
Gabriele Grassi, *Trieste*
Francesco Greco, *Bergamo*
Luigi Greco, *Naples*
Antonio Grieco, *Rome*
Fabio Grizzi, *Rozzano*

Laurino Grossi, *Pescara*
Simone Guglielmetti, *Milan*
Tiberiu Hershcovici, *Jerusalem*
Calogero Iacono, *Verona*
Enzo Ierardi, *Bari*
Amedeo Indriolo, *Bergamo*
Raffaele Iorio, *Naples*
Paola Iovino, *Salerno*
Angelo A Izzo, *Naples*
Loreta Kondili, *Rome*
Filippo La Torre, *Rome*
Giuseppe La Torre, *Rome*
Giovanni Latella, *L'Aquila*
Salvatore Leonardi, *Catania*
Massimo Libra, *Catania*
Anna Licata, *Palermo*
C armela Loguercio, *Naples*
Amedeo Lonardo, *Modena*
Carmelo Luigiano, *Catania*
Francesco Luzza, *Catanzaro*
Giovanni Maconi, *Milano*
Antonio Macrì, *Messina*
Mariano Malaguarnera, *Catania*
Francesco Manguso, *Napoli*
Tommaso Maria Manzia, *Rome*
Daniele Marrelli, *Siena*
Gabriele Masselli, *Rome*
Sara Massironi, *Milan*
Giuseppe Mazzarella, *Avellino*
Michele Milella, *Rome*
Giovanni Milito, *Rome*
Antonella d'Arminio Monforte, *Milan*
Fabrizio Montecucco, *Genoa*
Giovanni Monteleone, *Rome*
Mario Morino, *Torino*
Vincenzo La Mura, *Milan*
Gerardo Nardone, *Naples*
Riccardo Nascimbeni, *Brescia*
Gabriella Nesi, *Florence*
Giuseppe Nigri, *Rome*
Erica Novo, *Turin*
Veronica Ojetti, *Rome*
Michele Orditura, *Naples*
Fabio Pace, *Seriate*
Lucia Pacifico, *Rome*
Omero Alessandro Paoluzi, *Rome*
Valerio Pazienza, *San Giovanni Rotondo*
Rinaldo Pellicano, *Turin*
Adriano M Pellicelli, *Rome*
Nadia Peparini, *Ciampino*
Mario Pescatori, *Rome*
Antonio Picardi, *Rome*
Alberto Pilotto, *Padova*
Alberto Piperno, *Monza*
Anna Chiara Piscaglia, *Rome*
Maurizio Pompili, *Rome*
Francesca Romana Ponziani, *Rome*
Cosimo Prantera, *Rome*
Girolamo Ranieri, *Bari*
Carlo Ratto, *Tome*
Barbara Renga, *Perugia*
Alessandro Repici, *Rozzano*
Maria Elena Riccioni, *Rome*
Lucia Ricci-Vitiani, *Rome*
Luciana Rigoli, *Messina*
Mario Rizzetto, *Torino*
Ballarin Roberto, *Modena*
Roberto G Romanelli, *Florence*
Claudio Romano, *Messina*
Luca Roncucci, *Modena*
Cesare Ruffolo, *Treviso*
L ucia Sacchetti, *Napoli*
Rodolfo Sacco, *Pisa*
Lapo Sali, *Florence*
Romina Salpini, *Rome*
Giulio Aniello, *Santoro Treviso*
Armando Santoro, *Rozzano*
Edoardo Savarino, *Padua*
Marco Senzolo, *Padua*
Annalucia Serafino, *Rome*
Giuseppe S Sica, *Rome*
Pierpaolo Sileri, *Rome*
Cosimo Sperti, *Padua*
Vincenzo Stanghellini, *Bologna*
Cristina Stasi, *Florence*
Gabriele Stocco, *Trieste*
Roberto Tarquini, *Florence*
Mario Testini, *Bari*
Guido Torzilli, *Milan*
Guido Alberto Massimo, *Tiberio Brescia*
Giuseppe Toffoli, *Aviano*
Alberto Tommasini, *Trieste*
Francesco Tonelli, *Florence*
Cesare Tosetti Porretta, *Terme*
Lucio Trevisani, *Cona*
Guglielmo M Trovato, *Catania*
Mariapia Vairetti, *Pavia*
Luca Vittorio Valenti, *Milano*
Mariateresa T Ventura, *Bari*
Giuseppe Verlato, *Verona*
Alessandro Vitale, *Padova*
Marco Vivarelli, *Ancona*
Giovanni Li Volti, *Catania*
Giuseppe Zanotti, *Padua*
Vincenzo Zara, *Lecce*
Gianguglielmo Zehender, *Milan*
Anna Linda Zignego, *Florence*
Rocco Antonio Zoccali, *Messina*
Angelo Zullo, *Rome*

Japan

Yasushi Adachi, *Sapporo*
Takafumi Ando, *Nagoya*
Masahiro Arai, *Tokyo*
Makoto Arai, *Chiba*
Takaaki Arigami, *Kagoshima*
Itaru Endo,*Yokohama*
Munechika Enjoji, *Fukuoka*
Shunji Fujimori, *Tokyo*
Yasuhiro Fujino, *Akashi*
Toshiyoshi Fujiwara, *Okayama*
Yosuke Fukunaga, *Tokyo*
Toshio Fukusato, *Tokyo*
Takahisa Furuta, *Hamamatsu*
Osamu Handa, *Kyoto*
Naoki Hashimoto, *Osaka*
Yoichi Hiasa, *Toon*
Masatsugu Hiraki, *Saga*
Satoshi Hirano, *Sapporo*
Keiji Hirata, *Fukuoka*
Toru Hiyama, *Higashihiroshima*
Akira Hokama, *Nishihara*
Shu Hoteya, *Tokyo*
Masao Ichinose, *Wakayama*
Tatsuya Ide, *Kurume*
Masahiro Iizuka, *Akita*
Toshiro Iizuka, *Tokyo*
Kenichi Ikejima, *Tokyo*
Tetsuya Ikemoto, *Tokushima*
Hiroyuki Imaeda, *Saitama*
Atsushi Imagawa, *Kan-onji*
Hiroo Imazu, *Tokyo*
Shuji Isaji, *Tsu*
Toru Ishikawa, *Niigata*
Toshiyuki Ishiwata, *Tokyo*
Soichi Itaba, *Kitakyushu*
Yoshiaki Iwasaki, *Okayama*
Tatehiro Kagawa, *Isehara*
Satoru Kakizaki, *Maebashi*
Naomi Kakushima, *Shizuoka*
Terumi Kamisawa, *Tokyo*
Akihide Kamiya, *Isehara*
Osamu Kanauchi, *Tokyo*
Tatsuo Kanda, *Chiba*
Shin Kariya, *Okayama*
Shigeyuki Kawa, *Matsumoto*
Takumi Kawaguchi, *Kurume*
Takashi Kawai, *Tokyo*
Soo Ryang Kim, *Kobe*
Shinsuke Kiriyama, *Gunma*
Tsuneo Kitamura, *Urayasu*
Masayuki Kitano, *Osakasayama*
Hirotoshi Kobayashi, *Tokyo*
Hironori Koga, *Kurume*
Takashi Kojima, *Sapporo*
Satoshi Kokura, *Kyoto*
Shuhei Komatsu, *Kyoto*
Tadashi Kondo, *Tokyo*
Yasuteru Kondo, *Sendai*
Yasuhiro Kuramitsu, *Yamaguchi*
Yukinori Kurokawa, *Osaka*
Shin Maeda, *Yokohama*
Koutarou Maeda, *Toyoake*
Hitoshi Maruyama, *Chiba*
Atsushi Masamune, *Sendai*
Hiroyuki Matsubayashi, *Suntogun*
Akihisa Matsuda, *Inzai*
Hirofumi Matsui, *Tsukuba*
Akira Matsumori, *Kyoto*
Yoichi Matsuo, *Nagoya*
Y Matsuzaki, *Ami*
Toshihiro Mitaka, *Sapporo*
Kouichi Miura, *Akita*
Shinichi Miyagawa, *Matumoto*
Eiji Miyoshi, *Suita*
Toru Mizuguchi, *Sapporo*
Nobumasa Mizuno, *Nagoya*
Zenichi Morise, *Nagoya*
Tomohiko Moriyama, *Fukuoka*
Kunihiko Murase, *Tusima*
Michihiro Mutoh, *Tsukiji*
Akihito Nagahara, *Tokyo*
Hikaru Nagahara, *Tokyo*
Hidenari Nagai, *Tokyo*
Koichi Nagata, *Shimotsuke-shi*
Masaki Nagaya, *Kawasaki*
Hisato Nakajima, *Nishi-Shinbashi*
Toshifusa Nakajima, *Tokyo*
Hiroshi Nakano, *Kawasaki*
Hiroshi Nakase, *Kyoto*
Toshiyuki Nakayama, *Nagasaki*
Takahiro Nakazawa, *Nagoya*
Shoji Natsugoe, *Kagoshima City*

Tsutomu Nishida, *Suita*
Shuji Nomoto, *Naogya*
Sachiyo Nomura, *Tokyo*
Takeshi Ogura, *Takatsukishi*
Nobuhiro Ohkohchi, *Tsukuba*
Toshifumi Ohkusa, *Kashiwa*
Hirohide Ohnishi, *Akita*
Teruo Okano, *Tokyo*
Satoshi Osawa, *Hamamatsu*
Motoyuki Otsuka, *Tokyo*
Michitaka Ozaki, *Sapporo*
Satoru Saito, *Yokohama*
Chouhei Sakakura, *Kyoto*
Naoaki Sakata, *Sendai*
Ken Sato, *Maebashi*
Toshiro Sato, *Tokyo*
Tomoyuki Shibata, *Toyoake*
H Shimada, *Tokyo*
Tomohiko Shimatani, *Kure*
Yukihiro Shimizu, *Nanto*
Tadashi Shimoyama, *Hirosaki*
Masayuki Sho, *Nara*
Ikuo Shoji, *Kobe*
Atsushi Sofuni, *Tokyo*
Takeshi Suda, *Niigata*
M Sugimoto, *Hamamatsu*
Ken Sugimoto, *Hamamatsu*
Haruhiko Sugimura, *Hamamatsu*
Shoichiro Sumi, *Kyoto*
Hidekazu Suzuki, *Tokyo*
Masahiro Tajika, *Nagoya*
Hitoshi Takagi, *Takasaki*
Toru Takahashi, *Niigata*
Yoshihisa Takahashi, *Tokyo*
Shinsuke Takeno, *Fukuoka*
Akihiro Tamori, *Osaka*
Kyosuke Tanaka, *Tsu*
Shinji Tanaka, *Hiroshima*
Atsushi Tanaka, *Tokyo*
Yasuhito Tanaka, *Nagoya*
Shinji Tanaka, *Tokyo*
Minoru Tomizawa, *Yotsukaido City*
Kyoko Tsukiyama-Kohara, *Kagoshima*
Takuya Watanabe, *Niigata*
Kazuhiro Watanabe, *Sendai*
Satoshi Yamagiwa, *Niigata*
Takayuki Yamamoto, *Yokkaichi*
Hiroshi Yamamoto, *Otsu*
Kosho Yamanouchi, *Nagasaki*
Ichiro Yasuda, *Gifu*
Yutaka Yata, *Maebashi-city*
Shin-ichi Yokota, *Sapporo*
Norimasa Yoshida, *Kyoto*
Hiroshi Yoshida, *Tama-City*
Hitoshi Yoshiji, *Kashihara*
Kazuhiko Yoshimatsu, *Tokyo*
Kentaro Yoshioka, *Toyoake*
Nobuhiro Zaima, *Nara*

Jordan

Khaled Ali Jadallah, *Irbid*

Kuwait

Islam Khan, *Kuwait*

Lebanon

Bassam N Abboud, *Beirut*
Kassem A Barada, *Beirut*
Marwan Ghosn, *Beirut*
Iyad A Issa, *Beirut*
Fadi H Mourad, *Beirut*
AIa Sharara, *Beirut*
Rita Slim, *Beirut*

Lithuania

Antanas Mickevicius, *Kaunas*

Malaysia

Huck Joo Tan, *Petaling Jaya*

Mexico

Richard A Awad, *Mexico City*
Carlos R Camara-Lemarroy, *Monterrey*
Norberto C Chavez-Tapia, *Mexico City*
Wolfgang Gaertner, *Mexico City*
Diego Garcia-Compean, *Monterrey*
Arturo Panduro, *Guadalajara*
OT Teramoto-Matsubara, *Mexico City*
Felix Tellez-Avila, *Mexico City*
Omar Vergara-Fernandez, *Mexico City*
Saúl Villa-Trevino, *Cuidad de México*

Morocco

Samir Ahboucha, *Khouribga*

Netherlands

Robert J de Knegt, *Rotterdam*
Tom Johannes Gerardus Gevers, *Nijmegen*
Menno Hoekstra, *Leiden*
BW Marcel Spanier, *Arnhem*
Karel van Erpecum, *Utrecht*

New Zealand

Leo K Cheng, *Auckland*
Andrew Stewart Day, *Christchurch*
Jonathan Barnes Koea, *Auckland*
Max Petrov, *Auckland*

Nigeria

Olufunmilayo Adenike Lesi, *Lagos*
Jesse Abiodun Otegbayo, *Ibadan*
Stella Ifeanyi Smith, *Lagos*

Norway

Trond Berg, *Oslo*
Trond Arnulf Buanes, *Krokkleiva*
Thomas de Lange, *Rud*
Magdy El-Salhy, *Stord*
Rasmus Goll, *Tromso*
Dag Arne Lihaug Hoff, *Aalesund*

Pakistan

Zaigham Abbas, *Karachi*
Usman A Ashfaq, *Faisalabad*
Muhammad Adnan Bawany, *Hyderabad*
Muhammad Idrees, *Lahore*
Saeed Sadiq Hamid, *Karachi*
Yasir Waheed, *Islamabad*

Poland

Thomas Brzozowski, *Cracow*
Magdalena Chmiela, *Lodz*
Krzysztof Jonderko, *Sosnowiec*
Anna Kasicka-Jonderko, *Sosnowiec*
Michal Kukla, *Katowice*
Tomasz Hubert Mach, *Krakow*
Agata Mulak, *Wroclaw*
Danuta Owczarek, *Kraków*
Piotr Socha, *Warsaw*
Piotr Stalke, *Gdansk*
Julian Teodor Swierczynski, *Gdansk*
Anna M Zawilak-Pawlik, *Wroclaw*

Portugal

Marie Isabelle Cremers, *Setubal*
Ceu Figueiredo, *Porto*
Ana Isabel Lopes, *LIsbon*
M Paula Macedo, *Lisboa*
Ricardo Marcos, *Porto*
Rui T Marinho, *Lisboa*
Guida Portela-Gomes, *Estoril*
Filipa F Vale, *Lisbon*

Puerto Rico

Caroline B Appleyard, *Ponce*

Qatar

Abdulbari Bener, *Doha*

Romania

Mihai Ciocirlan, *Bucharest*
Dan LucianDumitrascu, *Cluj-Napoca*
Carmen Fierbinteanu-Braticevici, *Bucharest*
Romeo G Mihaila, *Sibiu*
Lucian Negreanu, *Bucharest*
Adrian Saftoiu, *Craiova*
Andrada Seicean, *Cluj-Napoca*
Ioan Sporea, *Timisoara*
Letiția Adela Maria Streba, *Craiova*
Anca Trifan, *Iasi*

Russia

Victor Pasechnikov, *Stavropol*
Vasiliy Ivanovich Reshetnyak, *Moscow*
Vitaly Skoropad, *Obninsk*

Saudi Arabia

Abdul-Wahed N Meshikhes, *Dammam*

M Ezzedien Rabie, *Khamis Mushait*

Singapore

Brian KP Goh, *Singapore*
Richie Soong, *Singapore*
Ker-Kan Tan, *Singapore*
Kok-Yang Tan, *Singapore*
Yee-Joo Tan, *Singapore*
Mark Wong, *Singapore*
Hong Ping Xia, *Singapore*

Slovenia

Matjaz Homan, *Ljubljana*
Martina Perse, *Ljubljana*

South Korea

Sang Hoon Ahn, *Seoul*
Seung Hyuk Baik, *Seoul*
Soon Koo Baik, *Wonju*
Soo-Cheon Chae, *Iksan*
Byung-Ho Choe, *Daegu*
Suck Chei Choi, *Iksan*
Hoon Jai Chun, *Seoul*
Yeun-Jun Chung, *Seoul*
Young-Hwa Chung, *Seoul*
Ki-Baik Hahm, *Seongnam*
Sang Young Han, *Busan*
Seok Joo Han, *Seoul*
Seung-Heon Hong, *Iksan*
Jin-Hyeok Hwang, *Seoungnam*
Jeong Won Jang, *Seoul*
Jin-Young Jang, *Seoul*
Dae-Won Jun, *Seoul*
Young Do Jung, *Kwangju*
Gyeong Hoon Kang, *Seoul*
Sung-Bum Kang, *Seoul*
Koo Jeong Kang, *Daegu*
Ki Mun Kang, *Jinju*
Chang Moo Kang, *Seodaemun-gu*
Gwang Ha Kim, *Busan*
Sang Soo Kim, *Goyang-si*
Jin Cheon Kim, *Seoul*
Tae Il Kim, *Seoul*
Jin Hong Kim, *Suwon*
Kyung Mo Kim, *Seoul*
Kyongmin Kim, *Suwon*
Hyung-Ho Kim, *Seongnam*
Seoung Hoon Kim, *Goyang*
Sang Il Kim, *Seoul*
Hyun-Soo Kim, *Wonju*
Jung Mogg Kim, *Seoul*
Dong Yi Kim, *Gwangju*
Kyun-Hwan Kim, *Seoul*
Jong-Han Kim, *Ansan*
Sang Wun Kim, *Seoul*
Ja-Lok Ku, *Seoul*
Kyu Taek Lee, *Seoul*
Hae-Wan Lee, *Chuncheon*
Inchul Lee, *Seoul*
Jung Eun Lee, *Seoul*
Sang Chul Lee, *Daejeon*
Song Woo Lee, *Ansan-si*
Hyuk-Joon Lee, *Seoul*
Seong-Wook Lee, *Yongin*
Kil Yeon Lee, *Seoul*
Jong-Inn Lee, *Seoul*
Kyung A Lee, *Seoul*
Jong-Baeck Lim, *Seoul*
Eun-Yi Moon, *Seoul*
SH Noh, *Seoul*
Seung Woon Paik, *Seoul*
Won Sang Park, *Seoul*
Sung-Joo Park, *Iksan*
Kyung Sik Park, *Daegu*
Se Hoon Park, *Seoul*
Yoonkyung Park, *Gwangju*
Seung-Wan Ryu, *Daegu*
Dong Wan Seo, *Seoul*
Il Han Song, *Cheonan*
Myeong Jun Song, *Daejeon*
Yun Kyoung Yim, *Daejeon*
Dae-Yeul Yu *Daejeon*

Spain

Mariam Aguas, *Valencia*
Raul J Andrade, *Málaga*
Antonio Arroyo, *Elche*
Josep M Bordas, *Barcelona*
Lisardo Boscá, *Madrid*
Ricardo Robles Campos, *Murcia*
Jordi Camps, *Reus*
Carlos Cervera *Barcelona*
Alfonso Clemente, *Granada*
Pilar Codoner-Franch, *Valencia*
Fernando J Corrales, *Pamplona*
Fermin Sánchez de Medina, *Granada*
Alberto Herreros de Tejada, *Majadahonda*
Enrique de-Madaria, *Alicante*
JE Dominguez-Munoz, *Santiago de Compostela*
Vicente Felipo, *Valencia*
CM Fernandez-Rodriguez, *Madrid*
Carmen Frontela-Saseta, *Murcia*
Julio Galvez, *Granada*
Maria Teresa García, *Vigo*
MI Garcia-Fernandez, *Málaga*
Emilio Gonzalez-Reimers, *La Laguna*
Marcel Jimenez, *Bellaterra*
Angel Lanas, *Zaragoza*
Juan Ramón Larrubia, *Guadalajara*
Antonio Lopez-Sanroman, *Madrid*
Vicente Lorenzo-Zuniga, *Badalona*
Alfredo J Lucendo, *Tomelloso*
Vicenta Soledad Martinez-Zorzano, *Vigo*
José Manuel Martin-Villa, *Madrid*
Julio Mayol, *Madrid*
Manuel Morales-Ruiz, *Barcelona*
Alfredo Moreno-Egea, *Murcia*
Albert Pares, *Barcelona*
Maria Pellise, *Barcelona*
José Perea, *Madrid*
Miguel Angel Plaza, *Zaragoza*
María J Pozo, *Cáceres*
Enrique Quintero, *La Laguna*
Jose M Ramia, *Madrid*
Francisco Rodriguez-Frias, *Barcelona*
Silvia Ruiz-Gaspa, *Barcelona*
Xavier Serra-Aracil, *Barcelona*
Vincent Soriano, *Madrid*
Javier Suarez, *Pamplona*
Carlos Taxonera, *Madrid*
M Isabel Torres, *Jaén*
Manuel Vazquez-Carrera, *Barcelona*
Benito Velayos, *Valladolid*
Silvia Vidal, *Barcelona*

Sri Lanka

Arjuna Priyadarsin De Silva, *Colombo*

Sudan

Ishag Adam, *Khartoum*

Sweden

Roland G Andersson, *Lund*
Bergthor Björnsson, *Linkoping*
Johan Christopher Bohr, *Örebro*
Mauro D'Amato, *Stockholm*
Thomas Franzen, *Norrkoping*
Evangelos Kalaitzakis, *Lund*
Riadh Sadik, *Gothenburg*
Per Anders Sandstrom, *Linkoping*
Ervin Toth, *Malmö*
Konstantinos Tsimogiannis, *Vasteras*
Apostolos V Tsolakis, *Uppsala*

Switzerland

Gieri Cathomas, *Liestal*
Jean Louis Frossard, *Geneve*
Christian Toso, *Geneva*
Stephan Robert Vavricka, *Zurich*
Dominique Velin, *Lausanne*

Thailand

Thawatchai Akaraviputh, *Bangkok*
P Yoysungnoen Chintana, *Pathumthani*
Veerapol Kukongviriyapan, *Muang*
Vijittra Leardkamolkarn, *Bangkok*
Varut Lohsiriwat, *Bangkok*
Somchai Pinlaor, *Khaon Kaen*
D Wattanasirichaigoon, *Bangkok*

Trinidad and Tobago

B Shivananda Nayak, *Mount Hope*

Tunisia

Ibtissem Ghedira, *Sousse*
Lilia Zouiten-Mekki, *Tunis*

Turkey

Sami Akbulut, *Diyarbakir*
Inci Alican, *Istanbul*
Mustafa Altindis, *Sakarya*
Mutay Aslan, *Antalya*
Oktar Asoglu, *Istanbul*
Yasemin Hatice Balaban, *Istanbul*
Metin Basaranoglu, *Ankara*
Yusuf Bayraktar, *Ankara*
Süleyman Bayram, *Adiyaman*
Ahmet Bilici, *Istanbul*

Ahmet Sedat Boyacioglu, *Ankara*
Züleyha Akkan Cetinkaya, *Kocaeli*
Cavit Col, *Bolu*
Yasar Colak, *Istanbul*
Cagatay Erden Daphan, *Kirikkale*
Mehmet Demir, *Hatay*
Ahmet Merih Dobrucali, *Istanbul*
Gülsüm Ozlem Elpek, *Antalya*
Ayse Basak Engin, *Ankara*
Eren Ersoy, *Ankara*
Osman Ersoy, *Ankara*
Yusuf Ziya Erzin, *Istanbul*
Mukaddes Esrefoglu, *Istanbul*
Levent Filik, *Ankara*
Ozgur Harmanci, *Ankara*
Koray Hekimoglu, *Ankara*
Abdurrahman Kadayifci, *Gaziantep*
Cem Kalayci, *Istanbul*
Selin Kapan, *Istanbul*
Huseyin Kayadibi, *Adana*
Sabahattin Kaymakoglu, *Istanbul*
Metin Kement, *Istanbul*
Mevlut Kurt, *Bolu*
Resat Ozaras, *Istanbul*
Elvan Ozbek, *Adapazari*
Cengiz Ozcan, *Mersin*
Hasan Ozen, *Ankara*
Halil Ozguc, *Bursa*
Mehmet Ozturk, *Izmir*
Orhan V Ozkan, *Sakarya*
Semra Paydas, *Adana*
Ozlem Durmaz Suoglu, *Istanbul*
Ilker Tasci, *Ankara*
Müge Tecder-ünal, *Ankara*
Mesut Tez, *Ankara*
Serdar Topaloglu, *Trabzon*
Murat Toruner, *Ankara*
Gokhan Tumgor, *Adana*
Oguz Uskudar, *Adana*
Mehmet Yalniz, *Elazig*
Mehmet Yaman, *Elazig*
Veli Yazisiz, *Antalya*
Yusuf Yilmaz, *Istanbul*
Ozlem Yilmaz, *Izmir*
Oya Yucel, *Istanbul*
Ilhami Yuksel, *Ankara*

United Kingdom

Nadeem Ahmad Afzal, *Southampton*
Navneet K Ahluwalia, *Stockport*
Yeng S Ang, *Lancashire*
Ramesh P Arasaradnam, *Coventry*
Ian Leonard Phillip Beales, *Norwich*
John Beynon, *Swansea*
Barbara Braden, *Oxford*
Simon Bramhall, *Birmingham*
Geoffrey Burnstock, *London*
Ian Chau, *Sutton*
Thean Soon Chew, *London*
Helen G Coleman, *Belfast*
Anil Dhawan, *London*
Sunil Dolwani, *Cardiff*
Piers Gatenby, *London*
Anil T George, *London*
Pasquale Giordano, *London*
Paul Henderson, *Edinburgh*
Georgina Louise Hold, *Aberdeen*
Stefan Hubscher, *Birmingham*
Robin D Hughes, *London*
Nusrat Husain, *Manchester*
Matt W Johnson, *Luton*
Konrad Koss, *Macclesfield*
Anastasios Koulaouzidis, *Edinburgh*
Simon Lal, *Salford*
John S Leeds, *Aberdeen*
JK K Limdi, *Manchester*
Hongxiang Liu, *Cambridge*
Michael Joseph McGarvey, *London*
Michael Anthony Mendall, *London*
Alexander H Mirnezami, *Southampton*
J Bernadette Moore, *Guildford*
Claudio Nicoletti, *Norwich*
Savvas Papagrigoriadis, *London*
Sylvia LF Pender, *Southampton*
David Mark Pritchard, *Liverpool*
James A Ross, *Edinburgh*
Kamran Rostami, *Worcester*
Xiong Z Ruan, *London*
Dina Tiniakos, *Newcastle upon Tyne*
Frank I Tovey, *London*
Dhiraj Tripathi, *Birmingham*
Vamsi R Velchuru, *Great Yarmouth*
Nicholas T Ventham, *Edinburgh*
Diego Vergani, *London*
Jack Westwood Winter, *Glasgow*
Terence Wong, *London*
Ling Yang, *Oxford*

United States

Daniel E Abbott, *Cincinnati*
Ghassan K Abou-Alfa, *New York*
Julian Abrams, *New York*
David William Adelson, *Los Angeles*
Jonathan Steven Alexander, *Shreveport*
Tauseef Ali, *Oklahoma City*
Mohamed R Ali, *Sacramento*
Rajagopal N Aravalli, *Minneapolis*
Hassan Ashktorab, *Washington*
Shashi Bala, *Worcester*
Charles F Barish, *Raleigh*
P Patrick Basu, *New York*
Robert L Bell, *Berkeley Heights*
David Bentrem, *Chicago*
Henry J Binder, *New Haven*
Joshua Bleier, *Philadelphia*
Wojciech Blonski, *Johnson City*
Kenneth Boorom, *Corvallis*
Brian Boulay, *Chicago*
Carla W Brady, *Durham*
Kyle E Brown, *Iowa City*
Adeel A Butt, *Pittsburgh*
Weibiao Cao, *Providence*
Andrea Castillo, *Cheney*
Fernando J Castro, *Weston*
Adam S Cheifetz, *Boston*
Xiaoxin Luke Chen, *Durham*
Ramsey Cheung, *Palo Alto*
Parimal Chowdhury, *Little Rock*
Edward John Ciaccio, *New York*
Dahn L Clemens, *Omaha*
Yingzi Cong, *Galveston*
Laura Iris Cosen-Binker, *Boston*
Joseph John Cullen, *Lowa*
Mark J Czaja, *Bronx*
Mariana D Dabeva, *Bronx*
Christopher James Damman, *Seattle*
Isabelle G De Plaen, *Chicago*
Punita Dhawan, *Nashville*
Hui Dong, *La Jolla*
Wael El-Rifai, *Nashville*
Sukru H Emre, *New Haven*
Paul Feuerstadt, *Hamden*
Josef E Fischer, *Boston*
Laurie N Fishman, *Boston*
Joseph Che Forbi, *Atlanta*
Temitope Foster, *Atlanta*
Amy E Foxx-Orenstein, *Scottsdale*
Daniel E Freedberg, *New York*
Shai Friedland, *Palo Alto*
Virgilio George, *Indianapolis*
Ajay Goel, *Dallas*
Oliver Grundmann, *Gainesville*
Stefano Guandalini, *Chicago*
Chakshu Gupta, *St. Joseph*
Grigoriy E Gurvits, *New York*
Xiaonan Han, *Cincinnati*
Mohamed Hassan, *Jackson*
Martin Hauer-Jensen, *Little Rock*
Koichi Hayano, *Boston*
Yingli Hee, *Atlanta*
Samuel B Ho, *San Diego*
Jason Ken Hou, *Houston*
Lifang Hou, *Chicago*
K-Qin Hu, *Orange*
Jamal A Ibdah, *Columbia*
Robert Thomas Jensen, *Bethesda*
Huanguang "Charlie" Jia, *Gainesville*
Rome Jutabha, *Los Angeles*
Andreas M Kaiser, *Los Angeles*
Avinash Kambadakone, *Boston*
David Edward Kaplan, *Philadelphia*
Randeep Kashyap, *Rochester*
Rashmi Kaul, *Tulsa*
Ali Keshavarzian, *Chicago*
Amir Maqbul Khan, *Marshall*
Nabeel Hasan Khan, *New Orleans*
Sahil Khanna, *Rochester*
Kusum K Kharbanda, *Omaha*
Hyun Sik Kim, *Pittsburgh*
Joseph Kim, *Duarte*
Jae S Kim, *Gainesville*
Miran Kim, *Providence*
Timothy R Koch, *Washington*
Burton I Korelitz, *New York*
Betsy Kren, *Minneapolis*
Shiu-Ming Kuo, *Buffalo*
Michelle Lai, *Boston*
Andreas Larentzakis, *Boston*
Edward Wolfgang Lee, *Los Angeles*
Daniel A Leffler, *Boston*
Michael Leitman, *New York*
Suthat Liangpunsakul, *Indianapolis*
Joseph K Lim, *New Haven*
Elaine Y Lin, *Bronx*
Henry C Lin, *Albuquerque*
Rohit Loomba, *La Jolla*
James David Luketich, *Pittsburgh*
Mohammad F Madhoun, *Oklahoma City*
Thomas C Mahl, *Buffalo*

World Journal of Gastroenterology

Contents

Weekly Volume 21 Number 3 January 21, 2015

World Journal of Gastroenterology
Volume 21 Number 3 January 21, 2015

Contents

EDITORS FOR THIS ISSUE

Responsible Assistant Editor: *Xiang Li*
Responsible Electronic Editor: *Xiao-Mei Liu*
Proofing Editor-in-Chief: *Lian-Sheng Ma*
Responsible Science Editor: *Ya-Juan Ma*
Proofing Editorial Office Director: *Jin-Lei Wang*

NAME OF JOURNAL
World Journal of Gastroenterology

ISSN
ISSN 1007-9327 (print)
ISSN 2219-2840 (online)

LAUNCH DATE
October 1, 1995

FREQUENCY
Weekly

EDITORIAL OFFICE
Jin-Lei Wang, Director
Xiu-Xia Song, Vice Director
World Journal of Gastroenterology
Room 903, Building D, Ocean International Center,
No. 62 Dongsihuan Zhonglu, Chaoyang District,
Beijing 100025, China
Telephone: +86-10-59080039
Fax: +86-10-85381893
E-mail: editorialoffice@wjgnet.com
Help Desk: http://www.wjgnet.com/esps/helpdesk.aspx
http://www.wjgnet.com

PUBLISHER
Baishideng Publishing Group Inc
8226 Regency Drive,
Pleasanton, CA 94588, USA
Telephone: +1-925-223-8242
Fax: +1-925-223-8243
E-mail: bpgoffice@wjgnet.com
Help Desk: http://www.wjgnet.com/esps/helpdesk.aspx
http://www.wjgnet.com

PUBLICATION DATE
January 21, 2015

INSTRUCTIONS TO AUTHORS
Full instructions are available online at http://www.wjgnet.com/1007-9327/g_info_20100315215714.htm

ONLINE SUBMISSION
http://www.wjgnet.com/esps/

World Journal of Gastroenterology

Submit a Manuscript: http://www.wjgnet.com/esps/
Help Desk: http://www.wjgnet.com/esps/helpdesk.aspx
DOI: 10.3748/wjg.v21.i3.711

World J Gastroenterol 2015 January 21; 21(3): 711-725
ISSN 1007-9327 (print) ISSN 2219-2840 (online)

EDITORIAL

Liver enzymes, metabolomics and genome-wide association studies: From systems biology to the personalized medicine

Silvia Sookoian, Carlos J Pirola

Silvia Sookoian, Department of Clinical and Molecular Hepatology, Institute of Medical Research A Lanari-IDIM, University of Buenos Aires - National Scientific and Technical Research Council Ciudad Autónoma de Buenos Aires, Buenos Aires 1427, Argentina
Carlos J Pirola, Department of Molecular Genetics and Biology of Complex Diseases, Institute of Medical Research A Lanari-IDIM, University of Buenos Aires - National Scientific and Technical Research Council, Ciudad Autónoma de Buenos Aires, Buenos Aires 1427, Argentina
Author contributions: Pirola CJ and Sookoian S contributed to study concept and design; acquisition of data; analysis and interpretation of data; statistical analysis; drafting of the manuscript; obtained funding and study supervision.
Supported by (in part) Grants PICT 2010-0441 and PICT 2012-0159 (Agencia Nacional de Promoción Científica y Tecnológica) and UBACYT CM04 (Universidad de Buenos Aires).
Conflict-of-interest: The authors have no conflict of interest to declare.

Correspondence to: Silvia Sookoian, MD, PhD, Department of Clinical and Molecular Hepatology, Institute of Medical Research A Lanari-IDIM, University of Buenos Aires - National Scientific and Technical Research Council, Ciudad Autónoma de Buenos Aires, Combatiente de Malvinas 3150, Buenos Aires 1427, Argentina. sookoian.silvia@lanari.fmed.uba.ar
Telephone: +54-11-45148701
Fax: +54-11-45238947
Received: September 4, 2014
Peer-review started: September 4, 2014
First decision: October 14, 2014
Revised: October 18, 2014
Accepted: December 14, 2014
Article in press: December 16, 2014
Published online: January 21, 2015

Abstract

For several decades, serum levels of alanine (ALT) and aspartate (AST) aminotransferases have been regarded as markers of liver injury, including a wide range of etiologies from viral hepatitis to fatty liver. The increasing worldwide prevalence of metabolic syndrome and cardiovascular disease revealed that transaminases are strong predictors of type 2 diabetes, coronary heart disease, atherothrombotic risk profile, and overall risk of metabolic disease. Therefore, it is plausible to suggest that aminotransferases are surrogate biomarkers of "liver metabolic functioning" beyond the classical concept of liver cellular damage, as their enzymatic activity might actually reflect key aspects of the physiology and pathophysiology of the liver function. In this study, we summarize the background information and recent findings on the biological role of ALT and AST, and review the knowledge gained from the application of genome-wide approaches and "omics" technologies that uncovered new concepts on the role of aminotransferases in human diseases and systemic regulation of metabolic functions. Prediction of biomolecular interactions between the candidate genes recently discovered to be associated with plasma concentrations of liver enzymes showed interesting interconnectivity nodes, which suggest that regulation of aminotransferase activity is a complex and highly regulated trait. Finally, links between aminotransferase genes and metabolites are explored to understand the genetic contributions to the metabolic diversity.

Key words: Transaminases; Aminotransferases; Alanine-aminotransferase; Aspartate-aminotransferase; Glutamate-oxalacetate transaminase; Glutamate-pyruvate tran-saminase; Glutamic acid; Metabolism; Nonalcoholic fatty liver; Nonalcoholic fatty liver disease; Nonalcoholic steatohepatitis; Gene variants; Single nucleotide polymorphisms; *PNPLA3*; Genetics; Metabolomics; Metabolic

syndrome; Systems biology

Core tip: Genomic, transcriptomic, proteomic, and metabolomic information has changed the classical conception of the meaning that serum concentrations of alanine- (ALT) and aspartate (AST) aminotransferase are merely indicators of hepatocyte membrane disruption. It has given way to a more complex and interconnected view of the importance of liver transaminases in the regulation of systemic metabolic function.

Sookoian S, Pirola CJ. Liver enzymes, metabolomics and genome-wide association studies: From systems biology to the personalized medicine. *World J Gastroenterol* 2015; 21(3): 711-725 Available from: URL: http://www.wjgnet.com/1007-9327/full/v21/i3/711.htm DOI: http://dx.doi.org/10.3748/wjg.v21.i3.711

INTRODUCTION

For several decades, serum levels of alanine (ALT) and aspartate (AST) aminotransferases have been regarded as markers of liver injury, including a wide range of etiologies from viral hepatitis to fatty liver[1]. The first report of the role of liver transaminases in the prediction of liver cellular damage was published in 1955 by Molander and colleagues, after noticing that the levels of glutamic oxalacetic transaminase (GOT or AST) were elevated after acute myocardial infarction[2]. It is noteworthy to mention that high serum GOT activity observed in patients with myocardial infarction and acute heart failure is mostly attributed to the accompanying acute central necrosis of the liver associated with circulatory changes, as elegantly demonstrated by Killip *et al*[3].

Although the chemical reaction mediated by a transaminase was initially described in 1950[4], measurement of ALT and AST enzymatic activity in circulation is still the most commonly used biochemistry test in clinical practice, when the aim is to evaluate putative liver injury[5]. Notably, while the correlation between the degree of hepatocyte injury and amininotransferase levels is poor[1], it is accepted that blood levels of ALT and AST are a consequence of the liver cell membrane damage, with the subsequent leakage of intracellular enzymes into the circulation, especially the cytosolic ones[6,7].

The increasing worldwide prevalence of metabolic syndrome (Met Synd) and cardiovascular disease (CVD) has revealed that transaminases are reliable predictors of the individual components of this very complex trait, including type 2 diabetes[8] and decreased hepatic insulin sensitivity[9], coronary heart disease[10], atherothrombotic risk profile[11], and overall risk of cardiovascular[12] and metabolic disease[13].

Therefore, routine testing of aminotransferases ALT and AST, initially regarded as markers of liver injury, is increasingly being considered as an indicator of the "liver metabolic function"[14]. Based upon this evidence, it is reasonable to speculate that the ALT and AST enzymatic activity measured in circulation actually reflects relevant aspects of the physiology and pathophysiology of the liver function beyond hepatocyte membrane disruption.

In this study, we summarize the background information and recent findings on the biological function of ALT and AST, and review the knowledge gained from the application of genome-wide approaches and "omics" technologies that uncovered new concepts of the role of aminotransferases in human diseases and systemic regulation of metabolic functions.

BRIEF OVERVIEW OF ALT AND AST GENE AND PROTEIN FUNCTION: A PIVOTAL ROLE IN GLUCOSE METABOLISM

Aminotransferases are enzymes that catalyze the transfer of an alpha-amino group from an amino acid to an alpha-keto acid. They share certain mechanistic features with other pyridoxal-phosphate-dependent enzymes. With respect to the domain features, aminotransferases are grouped into different classes, including class Ⅰ, Ⅱ, Ⅲ, Ⅳ and Ⅴ. ALT and AST belong to the class- Ⅰ pyridoxal-phosphate-dependent aminotransferase, which comprises 11 proteins in the human proteome, as shown in Table 1. In this review, we will refer to aminotransferase genes as to *GPT* and *GOT,* including their related isoforms.

While there are two isoforms of human ALT, namely ALT1 and ALT2, when referring to the protein, we will use the ALT name. The gene that encodes for the cytosolic alanine aminotransaminase 1 protein (ALT1), also known as glutamate-pyruvate transaminase 1 (*GPT1* or formally *GPT*), is located in chromosome 8 (8q24.3) and has 11 exons.

This enzyme catalyzes the reversible transamination between alanine and 2-oxoglutarate to generate pyruvate and glutamate, playing a key role in the intermediary metabolism of glucose and amino acids. *ALT1* is expressed in liver, kidney, heart, and skeletal muscle, and at moderate levels in the adipose tissue[15].

ALT2 is encoded by a different gene (*GPT2*), located in chromosome 16 (16q12.1). The *GPT2* mRNA is expressed at high levels in muscle, fat, kidney, and brain, and at lower levels in liver and breast[16]. As, in some studies, neither liver nor kidney showed ALT2 expression[17], this issue clearly requires further investigation.

According to available evidence, ALT1 and ALT2 seem to have not only different tissue source, but cellular localization as well, suggesting a dissimilar biological meaning in the context of acute or chronic liver disease pathogenesis. Figure 1 depicts a schematic representation of ALT1 and ALT2 protein localization at the cellular level. For example, in the liver, ALT1 localizes only in the cytosol and endoplasmic reticulum, with no presence in

Table 1 List of enzymes of the Class- I pyridoxal-phosphate-dependent aminotransferase family: Evidence from the human proteome

Protein name	Gene name	Chromosome	Number of isoforms
1-aminocyclopropane-1-carboxylate synthase-like protein 1	*ACCS*	11p11.2	1
Alanine aminotransferase 1	*GPT1*	8q24.3	1
Alanine aminotransferase 2	*GPT2*	16q11.2	2
Aspartate aminotransferase, cytoplasmic	*GOT1*	10q24.2	1
Aspartate aminotransferase, mitochondrial	*GOT2*	16q21	2
Kynurenine/alpha-aminoadipate aminotransferase, mitochondrial	*AADAT*	4q33	2
Kynurenine--oxoglutarate transaminase 1	*CCBL1*	9q34.11	3
Kynurenine--oxoglutarate transaminase 3	*CCBL2*	1p22.2	3
Probable inactive 1-aminocyclopropane-1-carboxylate synthase-like protein 2	*ACCSL*	11p11.2	1
Putative aspartate aminotransferase, cytoplasmic 2	*GOT1L1*	8p11.23	1
Tyrosine aminotransferase	*TAT*	16q22.2	1

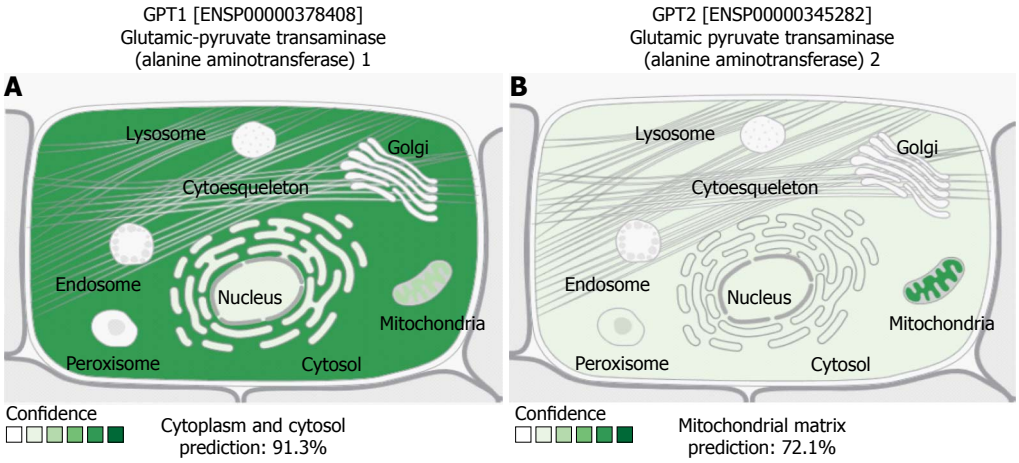

Figure 1 Schematic representation of different localizations of ALT1 (GPT1) and ALT2 (GPT2) proteins at the cellular level. Prediction was performed by the open access web resource "COMPARTMENTS" available at http://compartments.jensenlab.org, which predicts protein localization according to information extracted from different databases, including UniProtKB, as well as cellular component ontologies visualized by the Gene Ontology Consortium. The program generates unified confidence scores of the localization evidence; confidence scale is color coded, ranging from light green (1) indicating low confidence, to dark green (5), corresponding to high confidence, with absence of localization evidence depicted in white (0). The evidence score is expressed in %.

mitochondria[18]. Conversely, ALT2 is preferably localized in the mitochondrial matrix (Figure 1). Thus, while current evidence from human studies is scarce, it is plausible to suggest that ALT1 and ALT2 might reflect hepatocyte membrane disruption and mitochondrial dysfunction, respectively. Unfortunately, current biochemical tests aimed at measuring ALT in circulation are incapable of identifying the cellular source. Nevertheless, while routine assessment of ALT activity does not discriminate between ALT isoforms, a recent study demonstrated that most of the activity in circulation is given by ALT1[19].

In addition, supporting the notion that elevation of ALT levels does not necessarily denote hepatocellular damage, Kechagias *et al*[20] showed that fast-food-based hyper-alimentation in combination with a sedentary lifestyle, when followed for four weeks, was associated with pathological serum ALT levels. Notably, the authors showed that the significant elevation of aminotransferases (up to 447 U/L) associated with the hyper-alimentation regimen were not related to the development of liver steatosis[20]. This clinical finding reinforces the hypothesis that an increase in the ALT enzymatic activity is an adaptive response to the liver metabolic demands[14]. Table 2 summarizes the main features of ALT1 and ALT2, including novel aspects on their biological function and gene regulation, such as modulation of *GPT1* by miR-122 to enhance ALT enzymatic activity, as recently reported by our group[21].

Glutamate-oxalacetate transaminase (GOT) is a pyridoxal phosphate-dependent enzyme that exists in cytoplasmic and mitochondrial forms, GOT1 and GOT2, respectively. As previously noted, the two enzymes belong to the class-I pyridoxal-phosphate-dependent aminotransferase family, and are homodimeric, showing close homology.

The gene that encodes for the soluble GOT1 (*GOT1*) is located in chromosome 10 (10q24.2), while the one that encodes for the mitochondrial GOT2 (*GOT2*) is located in chromosome 16 (16q21). GOT1 is an important regulator of glutamate levels, as it is involved in the biosynthesis of L-glutamate from L-aspartate or L-cysteine. The catalytic unit of GOT1 is responsible for the following reactions: L-aspartate + 2-oxoglutarate = oxaloacetate + L-glutamate and L-cysteine + 2-oxoglutarate = mercaptopyruvate + L-glutamate. GOT1 aliases are cysteine aminotransferase and transaminase A. In addition, the aspartate aminotransferase activity is involved in hepatic glucose synthesis during

Table 2 Comparison of biological and protein function of ALT1 and ALT2: Background information and recent findings

Features and function	Glutamic-pyruvate transaminase 1 (alanine aminotransferase 1) GPT1	Glutamic pyruvate transaminase 2 (alanine aminotransferase) 2 GPT2
Gene and protein Id in data-bases	Entrez Gene: 2875 Ensembl gene: ENSG00000167701 UniProtKB: P24298	Entrez gene: 84706 Ensemble: ENSG00000166123 UniProtKB: Q8TD30
Genomic location	Entrez Gene cytogenetic band: 8q24.3	Entrez gene cytogenetic band: 16q12.1
Number of gene transcripts	7 transcripts (splice variants), 28 exons on the forward strand	5 transcripts (splice variants), 26 exons on the forward strand
Variation	*GPT1* has 210 SNPs	*GPT2* has 819 SNPs
Orthologues	*GPT1* has 69 orthologues in Ensembl	*GPT2* has 63 orthologues in Ensembl
Regulation	There are 2 regulatory elements located in the region of *GPT1* gene miR-122 may interact with *GPT1* at multiple sites of the coding region to enhance translation[21] Microsomal triglyceride transfer protein inhibition augments plasma ALT/AST levels in response to endoplasmic reticulum stress[66] *GPT1*, but not *GPT2* promoter is induced by PPAR agonists[67] ALT1 catalytic activity is inhibited by the effect of glycation[68]	There are 13 regulatory elements located in the region of *GPT2* *GPT2* promoter has a putative ATF4 (Activating transcription factor 4 binding site[69] *GPT2* is regulated by androgens in non-hepatic tissues[70]
Protein features	Size: 496 amino acids; 54637 Da Cofactor: Pyridoxal phosphate Subunit: Homodimer	Size: 523 amino acids; 57904 Da Cofactor: Pyridoxal phosphate Subunit: Homodimer (By similarity)
Cellular localization in human cells[1]	Cytosol of hepatocytes[18]	ER and mitochondrial fraction[18]
Measurement in plasma (catalytic activity)	Represents 90% of total ALT in circulation[17,18]	Represents 10% of total ALT in circulation[17,18]
Tissue expression in humans	Evidence: WB: Liver and kidney[18] Evidence: NB: GPT mRNA is moderately expressed in kidney, liver, heart, and fat[15]	Evidence: WB and IHQ (protein): Pancreas (islets of Langerhans), brain, adrenal gland, skeletal muscle, heart (cardiomyocytes)[18] Evidence: NB: mRNA is expressed at high levels in muscle, fat, kidney, and brain, and at lower levels in liver and breast[15]
Tissue expression in rodents	Evidence: NB (mRNA): Highly expressed in liver and moderately expressed in white adipose tissue (WAT), intestine, and colon[71]	Evidence: NB (mRNA): muscle, liver, and white adipose tissue (WAT), at moderate levels in brain and kidney, and at a low level in heart[71] Gene expression analysis suggests a sex-dependent difference in *GPT2*-mRNA in the liver and muscle[15] Hepatic and muscle ALT2 protein activity was higher in males than in females; while no sex-dependent difference was noted in the liver for ALT1, it appears 20% higher in muscle in females[15]
Biological meaning and metabolic function	ALT1 contributes to "basal" serum ALT activity, most likely associated with normal cell turnover in liver and other tissues that would release ALT1 into the circulation[15,17-19]	Generation of pyruvate for gluconeogenesis under stressful living conditions, such as starvation[18] ALT2 is involved in the metabolic adaptation of the cell to stress[69] ALT2 is associated with a liver progluconeogenic metabolic adaptive response without hepatocellular necrosis after exposure to dexamethasone[72] ALT2 may participate in the generation of pyruvate and glyceroneogenesis, contributing to the homeostasis of fatty acid metabolism and storage[16]
Biological meaning in human disease	NAFLD: ALT1 represented 94% of total ALT levels in circulation[19] HCV: High levels in circulation of ALT1 (about 5-fold increase as compared to the controls)[19] Ultra-endurance exercise: no significant changes after exercise[19]	NAFLD: ALT2 represented 6% of total ALT levels in circulation[19] HCV: Moderate levels in circulation of ALT1 (about 2.5 fold increase as compared to the controls)[19] Ultra-endurance exercise: High levels in circulation of ALT2 (about 2-fold increase as compared to the baseline conditions)[19]
Biological meaning in experimental models of disease	NAFLD (*ob/ob*): Compared to the normal liver of lean mice, the expression of *GPT1* mRNA remained unchanged[71] Both ALT1 and ALT2 increased in the liver of mice induced liver steatosis by a deficient methionine-choline diet[73]	NAFLD (*ob/ob*): Compared to the normal liver of lean mice, the expression of *GPT2* mRNA was elevated by about 2-fold, suggesting ALT2 induction during fatty liver[71]

[1]Cellular localization differs among species. ER: Endoplasmic reticulum; WB: Western blotting; IHQ: Immunohistochemistry; NB: Northern blot analysis; HCV: Hepatitis C virus; NAFLD: Non-alcoholic fatty liver disease.

Table 3 Evidence from genome-wide association studies on the heritability of circulating levels of alanine-aminotransferase and aspartate-aminotransferase

Ref.	Number of participants/ study design	GWAS strategy (genotyping)	Number of variants	Phenotype	Identified locus
Chambers *et al*[36]	*n* = 61089 Population-based Adults	Affymetrix, Illumina and perlegen sciences arrays	About 2.6 million directly genotyped or imputed autosomal SNPs	Plasma levels of ALT	*HSD17B13, MAPK10, TRIB1, CPN1, PNPLA3, SAMM50*
Yuan *et al*[74]	Initial study *n* = 7715 Replication *n* = 704 Population-based Adults	Affymetrix	-	Plasma levels of ALT	*CHUK, PNPLA3, SAMM50, CPN1*
Park *et al*[75]	*n* = 532	Illumina HumanOmni1-Quad BeadChip	747076 SNPs	Plasma levels of ALT	*ST6GALNAC3, MMADHC, CCDC102B, RGS5, BRD7, GALNT13, SIRPA, CD93, SLC39A11, ADAMTS9, CELF2*
	Population-based Children			Plasma levels of AST	*CYB5APS, CELF2, GOT1, ST6GALNAC3, ADAMTS9, THSD7B, EIF4A1P1, ROBO1, THSD7B*
Shen *et al*[76]	*n* = 866 Population-based adults	Affymetrix GeneChip Human Mapping 500 K Array set	500568 SNPs	Plasma levels of AST	*GOT1*

GWAS: Genome-wide association studies; SNPs: Single nucleotide polymorphisms; ALT: Alanine-aminotransferase; AST: Aspartate-aminotransferase.

development and in adipocyte glyceroneogenesis.

GOT2 catalyzes the irreversible transamination of the L-tryptophan metabolite L-kynurenine to form kynurenic acid (L-kynurenine + 2-oxoglutarate = 4-(2-aminophenyl)-2,4-dioxobutanoate + L-glutamate) and the reversible transamination of L-aspartate + 2-oxoglutarate = oxaloacetate + L-glutamate. GOT2 plays a key role in amino acid metabolism and the metabolite exchange between mitochondria and cytosol. It also facilitates cellular uptake of long-chain free fatty acids. Of note, GOT2 is also known by the following aliases: fatty acid-binding protein, kynurenine aminotransferase 4, plasma membrane-associated fatty acid-binding protein and kynurenine-oxoglutarate transaminase Ⅳ.

GENETIC HERITABILITY ON THE SERUM LEVELS OF LIVER AMINOTRANSFERASES: EVIDENCE FROM GENOME-WIDE ASSOCIATION STUDIES

The serum level of transaminases is highly variable and is affected by a myriad of factors, including demographic ones, such as sex, age and ethnicity; anthropometric features, such as waist circumference and body mass index; and environmental factors, such as alcohol consumption[22]. Serum level of transaminases is also subject to diurnal variation[23,24].

In addition, it is known that ALT and AST concentrations in circulation are heritable[25]. In fact, studies have shown that ALT and AST levels are highly heritable, with additive genetic effects accounting for 48% and 32% of the variation, respectively[26]. Furthermore, results from a population-based study in twins showed that the heritability for ALT and AST is not gender specific[27].

To examine the genetic influence on plasma/serum levels of aminotransferases, four genome-wide association studies (GWAS) exploring a large number of SNPs were conducted in different populations around the world, as summarized in Table 3. Findings of these studies have shed light on new interesting candidate genes associated with liver enzymes, including the largely replicated *PNPLA3* (patatin-like phospholipase domain containing 3) gene that is not only associated with nonalcoholic fatty liver disease (NAFLD)[28] and nonalcoholic steatohepatitis (NASH)[29,30], but also a wide spectrum of chronic liver diseases, as recently highlighted[31], including alcoholic liver disease[32], viral hepatitis C[33] and B[34] and hepatocellular carcinoma[35]. Interestingly, the rs738409 located in *PNPLA3* reached the most significant p value for association with liver enzyme levels (1.2×10^{-45}) in the larger GWAS performed in Caucasians[36]. As expected, most of the associated variants with liver enzyme levels are either intergenic or intronic single nucleotide polymorphisms (SNPs), and the loci or nearest gene in which they are located has either an unknown function or a biological role not known to be associated with liver enzymes. Moreover, with the exception of the rs738409[37-39], there is presently no evidence supporting a putative pathogenic, damaging or deleterious effect of the discovered variants, either on the protein function or in the regulation of the related gene.

A detailed overview of the associated variants with aminotransaminase levels, their main features, and the biological role of the gene where are they located is shown in Table 4.

Table 4 Summary of the variants associated with alanine-aminotransferase and aspartate-aminotransferase levels in population-based genome-wide association studies: Biological function and variants characteristics

Variant ID	Variant features	Significant *P* value for GWAS association	Gene or nearest gene	Reported biological function of the associated locus
ALT				
rs6834314	Intergenic	3.1×10^{-9}	*HSD17B13/ MAPK10*	Oxidoreductase involved in the metabolism of steroid hormones, prostaglandins, retinoids, lipids and xenobiotics A member of the MAP kinase family
rs2954021	Intron variant	5.3×10^{-9}	*TRIB1*	Involved in protein amino acid phosphorylation and controlling mitogen-activated protein kinase cascades. Potent negative regulator of MAPK pathways influencing apoptosis. Regulates hepatic lipogenesis and very low density lipoprotein production
rs10883437	Intergenic	4.0×10^{-9}	*CPN1*	A plasma metallo-protease that cleaves basic amino acids from the C terminal of peptides and proteins
rs11597390	intergenic	2.9×10^{-8}		
rs738409	Missense p.Ile148Met	1.2×10^{-45}	*PNPLA3*	Acylglycerol O-acyltransferase and triacylglycerol lipase that mediates triacylglycerol hydrolysis
rs2281135	Intron variant	8.2×10^{-12}		
rs3761472	Missense p.Asp110Gly	3.7×10^{-29}	*SAMM50*	Component of the sorting and assembly machinery (SAM) of the mitochondrial outer membrane
rs2143571	Intron variant	9.4×10^{-7}		
rs11597086	Non coding exon variant	3.6×10^{-7}	*CHUK*	Member of the serine/threonine protein kinase family; a component of a cytokine-activated protein complex that is an inhibitor of the essential transcription factor NF-kappa-B complex
rs11591741	Intron variant	4.5×10^{-7}		
rs4949718	Intron variant	1.87×10^{-7}	*ST6GALNAC3*	Transfer sialic acids from CMP-sialic acid to terminal positions of carbohydrate groups in glycoproteins and glycolipids
rs17801127	Intergenic	2.37×10^{-7}	*MMADHC*	Mitochondrial protein that is involved in an early step of vitamin B12 metabolism
rs1539893	Intron variant	3.40×10^{-6}	*CCDC102B*	Unknown
rs12035879	Intron variant	3.97×10^{-6}	*RGS5*	Member of the regulators of G protein signaling (RGS) family
rs9941219	Intergenic	4.06×10^{-6}	*BRD7*	Member of the bromodomain-containing protein family
rs731660	Intergenic			
rs12621256	Intron variant	4.36×10^{-6}	*GALNT13*	Member of the glycosyltransferase 2 family; catalyzes the initial reaction in oligosaccharide biosynthesis; neurons cell biogenesis
rs6035126	Intergenic	4.94×10^{-6}	*SIRPA*	Receptor-type transmembrane glycoproteins involved in the negative regulation of receptor tyrosine kinase-coupled signaling processes
rs13433286	Intergenic			
rs844917	Intergenic	5.64×10^{-6}	*CD93*	Cell-surface glycoprotein and type I membrane protein
rs844914	Intergenic	5.98×10^{-6}		
rs903107	Intron variant	6.11×10^{-6}	*SLC39A11*	Mediates zinc uptake
rs80311637	Missense p.Val653Met	7.18×10^{-6}	*ADAMTS9*	Disintegrin and metalloproteinase with thrombospondin motifs
rs596406	Intron variant	9.18×10^{-6}	*CELF2*	RNA-binding protein implicated in the regulation of several post-transcriptional events
AST				
rs11597390	Intergenic	0.0009	*CHUK*	Explained previously
rs2281135	Intron variant	5.7×10^{-6}	*PNPLA3*	Explained previously
rs862946	Intergenic	2.41×10^{-7}	*CYB5AP5*	Pseudogene
rs596406	Intron variant	3.69×10^{-7}	*CELF2*	Explained previously
rs76850691	Missense p.Gln349Glu	8.55×10^{-7}	*GOT1*	Biosynthesis of L-glutamate from L-aspartate or L-cysteine
rs17109512	Intergenic	2.80×10^{-14}		
rs4949718	Intron variant	1.49×10^{-6}	*ST6GALNAC3*	Explained previously
rs80311637	Missense p.Val1597Met	1.85×10^{-6}	*ADAMTS9*	Explained previously
rs892877	Intron variant	3.75×10^{-6}	*THSD7B*	Unknown
rs984295	Intron variant	5.86×10^{-6}		
rs457603	Intergenic	4.57×10^{-6}	*EIF4A1P1*	Pseudogene
rs452621	Intergenic			
rs7617400	Intron variant	6.16×10^{-6}	*ROBO1*	Neuronal development
rs11924965	Intron variant			
rs7644918	Intron variant			

HSD17B13: Hydroxysteroid (17-beta) dehydrogenase 13; *MAPK10*: Mitogen-activated protein kinase 10; *TRIB1*: Tribbles pseudokinase 1; *CPN1*: Carboxypeptidase N, polypeptide 1; PNPLA3: Patatin-like phospholipase domain containing 3; *SAMM50*: Sorting and assembly machinery component; CHUK: Conserved helix-loop-helix ubiquitous kinase; ST6GALNAC3: ST6 (alpha-N-acetyl-neuraminyl-2,3-beta-galactosyl-1,3)-N-acetylgalactosaminide alpha-2,6-sialyltransferase 3; MMADHC: Methylmalonic aciduria (cobalamin deficiency) cblD type, with homocystinuria; CCDC102B: Coiled-Coil Domain Containing 102B; RGS5: Regulator of G-protein signaling 5; *BRD7*: Bromodomain containing 7; *GALNT13*: Polypeptide N-acetylgalactosaminyltransferase 13; *SIRPA*: Signal-regulatory protein alpha; *CD93*: *CD93* molecule; *SLC39A11*: Solute carrier family 39, member 11; *ADAMTS9*: ADAM metallopeptidase with thrombospondin type 1 motif, 9; *CYB5AP5*: Cytochrome b5 type A (microsomal) pseudogene 5; *CELF2*: CUGBP, Elav-like family member 2; *GOT1*: Glutamic-oxaloacetic transaminase 1, soluble; *THSD7B*: thrombospondin, type I, domain containing 7B; *EIF4A1P1*: Eukaryotic translation initiation factor 4A1 pseudogene 1; *ROBO1*: Roundabout, axon guidance receptor, homolog 1. Biological function was extracted from Gene Atlas (http://genatlas.medecine.univ-paris5.fr).

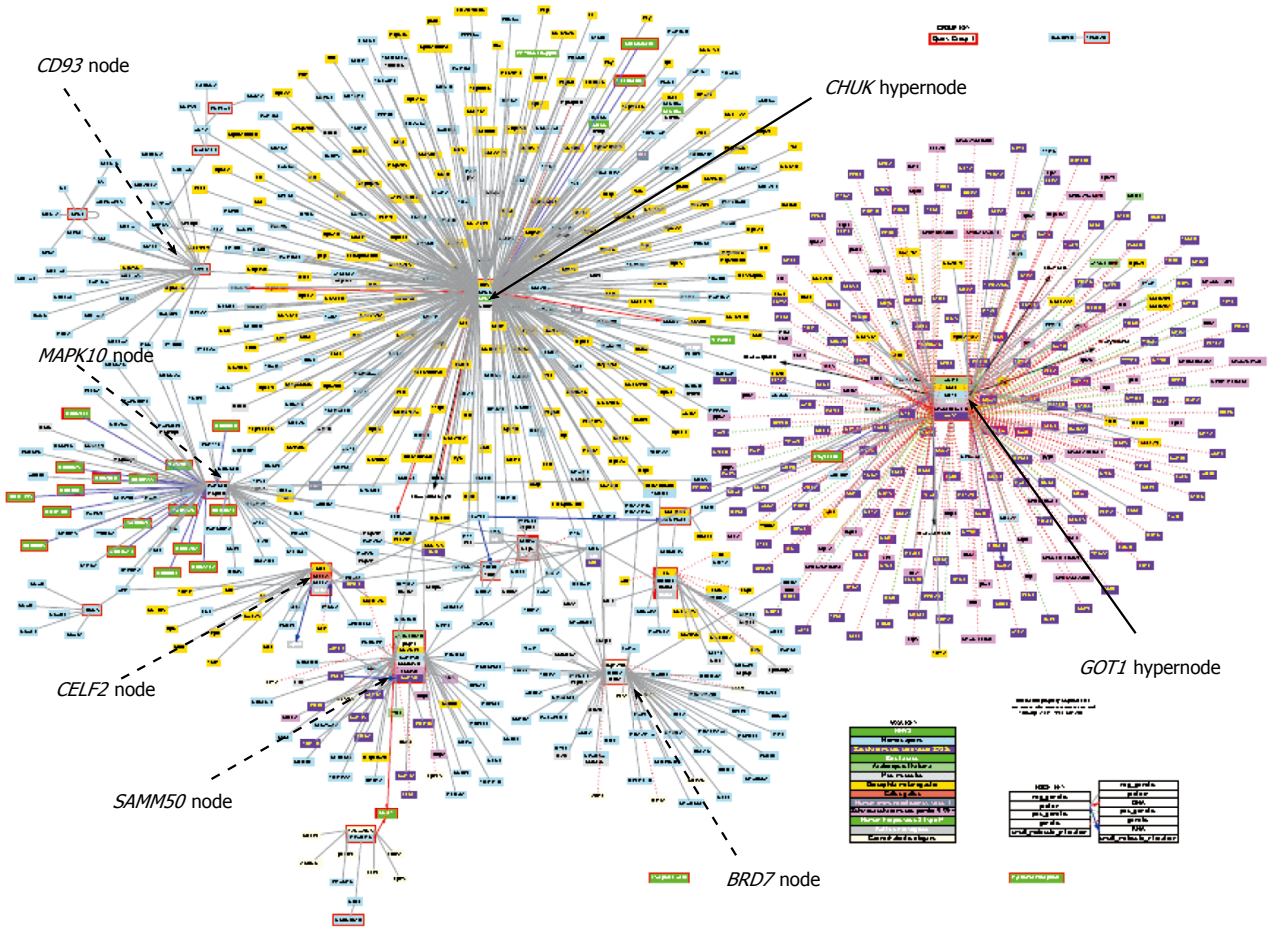

Figure 2 Visualization of biomolecular interactions among associated loci with serum levels of alanine-aminotransferase and aspartate-aminotransferase in published genome-wide association studies. Prediction was based on the Cognoscente program, freely available at the web-based submission portal: http://vanburenlab.tamhsc.edu/cognoscente.html. The interaction network image shows 828 nodes with different levels of complexity; black arrows indicate the major nodes. Additional interconnectivity nodes of importance (highlighted in black dashed arrows) are *SAMM50*, *CD93* (highly connected with *CHUK*), *MAPK10*, *CELF2* and *BRD7*. Prediction by Cognoscente supports multiple organisms in the same query, as well as gene-gene, gene-protein, protein-RNA and protein-DNA interactions, and multi-molecule queries[77]. The input list was based on the gene list presented in Table 4, while the graph depicts known interactions the query list members.

SYSTEMS BIOLOGY APPROACHES TO EXPLORING A PUTATIVE CONNECTION BETWEEN THE SIGNIFICANTLY ASSOCIATED LOCUS WITH LIVER TRANSAMINASES

To understand a putative biological connection between the significantly associated locus with levels of liver transaminases, we used a strategy for exploring biomolecular interactions, based on the Cognoscente program, freely available at http://vanburenlab.tamhsc.edu/cognoscente.html. The interaction network image is shown in Figure 2, and comprises 828 nodes with different levels of complexity. Hypernodes, such as the ones centered on *CHUK* and *GOT1*, and nodes-such as the ones centered on *SAMM50*, *MAPK10*, *CD93*, *CELF2* and *BRD7*-are highlighted in Figure 2. The results of the prediction of biomolecular interactions revealed some attractive findings that deserve further exploration in future experimental or functional studies. For example, *GOT1* was predicted to have a significant number of gene-gene interactions, including *IDH1* (isocitrate dehydrogenase 1 (NADP+), soluble) that catalyzes the oxidative decarboxylation of isocitrate to 2-oxoglutarate, *SCD1* (stearoyl-CoA desaturase) involved in fatty acid biosynthesis, which we and others found deregulated in fatty liver[40,41], *GDH2* (glutamate dehydrogenase 2) that catalyzes the reversible oxidative deamination of glutamate to 2-ketoglutarate, and *CHD1* (chromodomain helicase DNA binding protein 1), an ATP-dependent chromatin-remodeling factor that functions as substrate recognition component of the transcription regulatory histone acetylation (HAT) complex SAGA, (Figure 3A, arrow).

Likewise, remarkable gene-gene interactions were noted for *CHUK* and *PPARGC1β* (peroxisome proliferator-activated receptor gamma, coactivator 1 beta), whereby the last one is involved in fat oxidation, non-oxidative glucose metabolism, and the regulation of energy expenditure (Figure 3B, arrow). Gene-protein interactions between *CHUK* and CCND1 (cyclin D1), a highly conserved

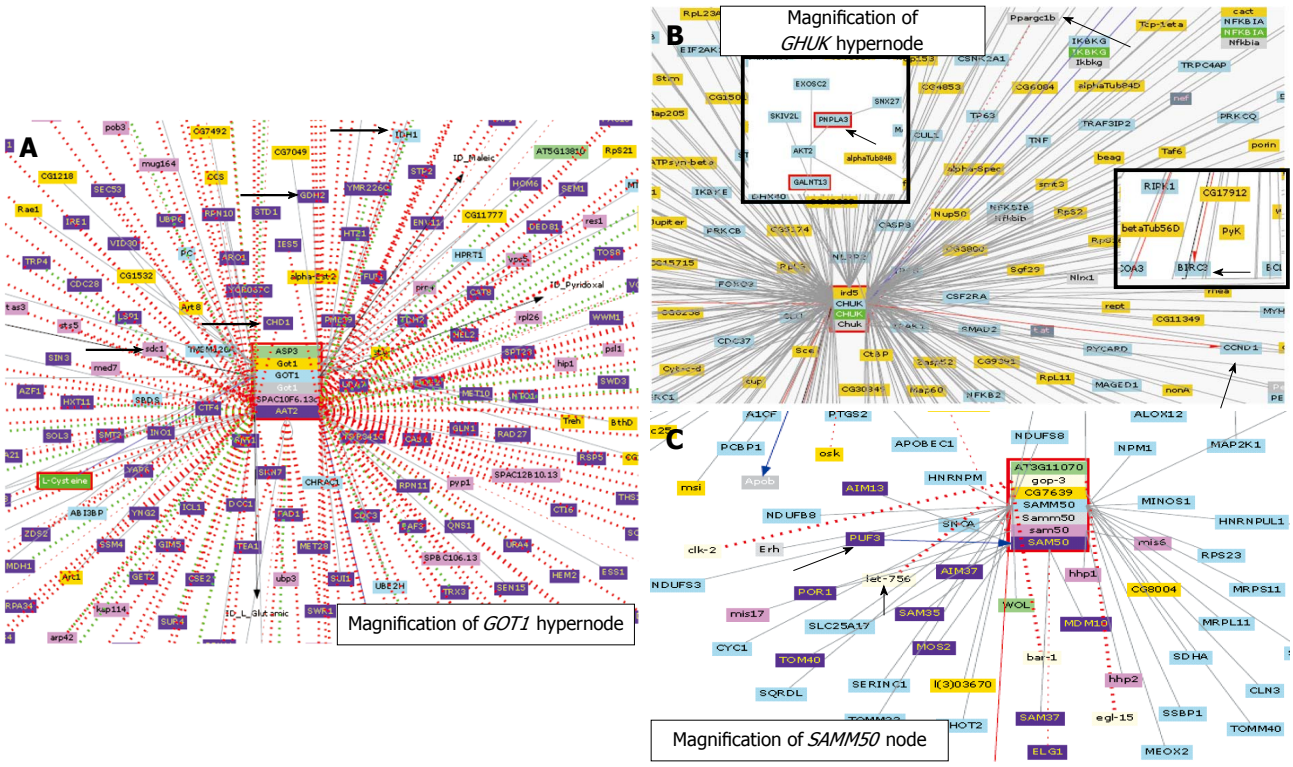

Figure 3 Biomolecular interactions focused on hypernodes (*GOT1* and *CHUK*) and nodes (*SAMM50*) predicted by the visualization tool for systems biology Cognoscente. Cognoscente currently contains over 413000 documented interactions, with coverage across multiple species, including Homo sapiens, Saccharomyces cerevisiae, Drosophila melanogaster, Schizosaccharomyces pombe, Arabidopsis thaliana, Mus musculus, and Caenorhabditis elegans, among others[74]. Colors under the hypernode/node gene name denote different species; for example, light blue corresponds to homo sapiens, blue to saccharomyces cerevisiae S288c and violet to schizosaccharomyces pombe; light green is arabidopsis thaliana, orange is Drosophila melanogaster, red is Gallus gallus, gray is rattus norvegicus and pale gray is caenorhabditis elegans. Arrows highlight biomolecular interactions discussed in the body of the manuscript.

member of the cyclin family (Figure 3B, arrow), and BIRC3 (baculoviral IAP repeat containing 3) (Figure 3B, inset), a gene activated by hypoxia we previously found associated with NAFLD in a human study[42], were predicted. PNPLA3 showed a connection with the CHUK hypernode (Figure 3B, inset) by a putative protein-protein interaction with AKT2 (v-akt murine thymoma viral oncogene homolog 2), which regulates many processes, including metabolism, proliferation, cell survival, growth and angiogenesis.

Systems Biology modeling also predicted presence of gene-gene biomolecular interaction between *SAMM50* and let-756 (Figure 3C, arrow), whereby the latter is involved in fibroblast growth factor receptor signaling pathway in Caenorhabditis elegans. In addition, a protein-RNA prediction between SAMM50 and PUF3 was found (Figure 3C, arrow); PUF proteins bind to related sequence motifs in the 3' untranslated region of specific target mRNAs and repress their translation[43].

GWAS COUPLED WITH METABOLOMICS ANALYSIS: UNDERSTANDING THE GENETIC CONTRIBUTIONS TO METABOLIC DIVERSITY

The use of GWAS studies, coupled with large scale metabolomics analysis, is a powerful strategy that can assist in better understanding genetic contributions to metabolic diversity and its importance in the biological context. For instance, Geiger and colleagues performed a GWAS with metabolomics based on the quantitative measurement of 363 metabolites in serum, and found that common variants might explain up to 12% of the observed variance in metabolite concentration[44]. Examples of GWAS relevance are the discovery of SNPs in *GLS2* (glutamine synthase 2) associated with glutamine levels, such as the rs2638315[45]. Furthermore, a recently reported large GWAS coupled with high-throughput metabolomics demonstrated the role of genetic loci in influencing human metabolism, including liver enzymes[46]. Shin *et al*[46] explored genome-wide associations at 145 metabolic loci and their biochemical connectivity with more than 400 metabolites in human blood and found that a variant in *GOT2,* the rs12709013, was associated with the phenyllactate/phenylalanine ratio. In addition, the *GOT2*-rs4784054 was associated with phenyllactate levels[46]. Interestingly, the rs12709013 and the rs4784054, located in chromosome 16, at positions 58795886 and 58742410, respectively (both in the forward strand), are intronic variants that reside in a genomic region encoding a noncoding RNA (ncRNA) transcript (Gene: RNU6-1155P ENSG00000200424). Genetic regulation of these metabolites may indicate that *GOT2* would be not only involved in the maintenance of the equilibrium of amino

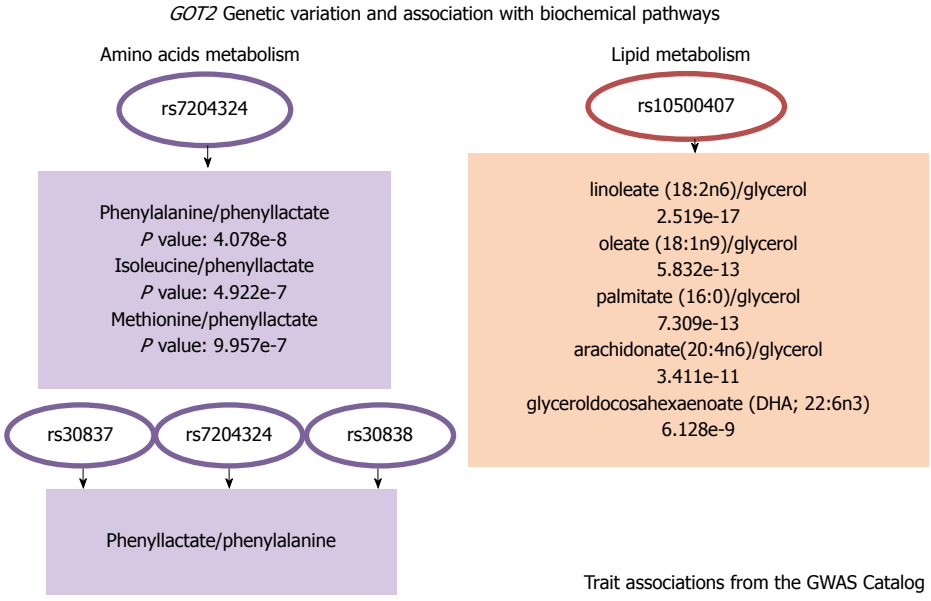

Figure 4 *GOT2*: Trait associations from the genome-wide association studies Catalog. Significant associations were extracted from the Metabolomics genome-wide association studies Server, freely available at http://metabolomics.helmholtz-muenchen.de/gwas/index.php. This site contains the association results of two genome-wide association studies on the human metabolome[46,78]. GWAS: Genome-wide association studies.

acid levels in circulation, including the regulation of the glucose-alanine cycle, but also in the control of energy balance. Figure 4 depicts additional variants in *GOT2* with genome-wide significant associations with metabolites of the amino acid and lipid metabolism. Surprisingly, these findings indicate that the metabolites associated with *GOT2* locus surpass the current knowledge of classical GOT2 protein function. They thus offer novel biochemical and functional insights into poorly explored roles of GOT2, such as fatty acid and glycerolipid metabolism. For instance, a significant association between the intronic *GOT2*-rs10500407 and arachidonate (20:4n6)/glycerol ratio was recently reported[46] (Figure 4), suggesting that GOT2 participates in the arachidonate and docosahexaenoic acid (DHA)-related metabolic pathways. Likewise, variants located in *GOT1* (rs11867, *P* value < 0.0008 and rs10748775, *P* value < 0.001) were associated with N-(2-h) glycine and glycerol 2-phosphate, respectively.

Overall, these observations are in line with the functional data from comparative genomics, indicating that the domain and molecular function of aminotransferases, including GOT2, are highly conserved among species, thus suggesting an important role in metabolic functioning. For instance, the orthologue of *GOT2* in drosophila melanogaster, known as Dmel/Got2, is involved in glutamate[47] and aspartate metabolic process[48]. Moreover, tissue localization yielded evidence, indicating that Dmel\Got2 is expressed in embryonic larval fat body and midgut[49], and in adult heart[50]. Furthermore, subcellular localization showed evidence of Dmel\Got2 localized to lipid particles[51] and mitochondria[52]. Notably, drosophila lipid droplets are ubiquitous organelles, which play a central role in cholesterol homeostasis and lipid metabolism. Taken together, these observations suggest that metabolism regulation is the "ancestral" GOT2 protein function. A representative figure of *GOT2* gene phylogenetic tree is depicted in Figure 5, where, supporting the aforementioned concept, the high conservation of the aminotransferase I and II domains among species, including fruit fly, is clearly visible.

On the other hand, variants located in *GPT1* were associated with epiandrosterone sulfate and androsterone sulfate (rs1063739, *P* value < 0.0002 and 0.0007, respectively), and variants located in *GPT2* were associated with 3-phenylpropionate (hydrocinnamate) (rs734309, *P* value < 0.00001) and the ratio between biliverdin and glycoursodeoxycholate (rs754043, *P* value < 1×10^{-7}).

Finally, metabolite associations with *PNPLA3*-rs738409 are summarized in Table 5. Notably, while no significant associations were found for the rs738409 and human metabolites, some other SNPs in disequilibrium with this variant reached GWAS significance with metabolite ratios of interest, for example cholesterol/gamma-glutamyltyrosine, docosapentaenoate (n3 DPA; 22:5n3)/eicosapentaenoate (EPA; 20:5n3), and aspartylphenylalanine/docosapentaenoate (n3 DPA; 22:5n3) (Table 5). Remarkably, eicosapentaenoic acid (EPA) is an important polyunsaturated fatty acid that serves as a precursor for the prostaglandin-3 and thromboxane-3 families. In our previous works, putative disease-related mechanisms associated with PNPLA3 severity in NASH and its relationship with prostaglandins were postulated[53,54]. Furthermore, aspartylphenylalanine results from an incomplete breakdown of protein digestion products, or protein catabolism, and might have a physiological involvement in cell-signaling. Recently, we described a novel role of PNPLA3, beyond its classical participation in triacylglycerol remodeling that involves amino acid metabolism[55]. Furthermore, the importance of amino acid metabolism in the pathogenesis of

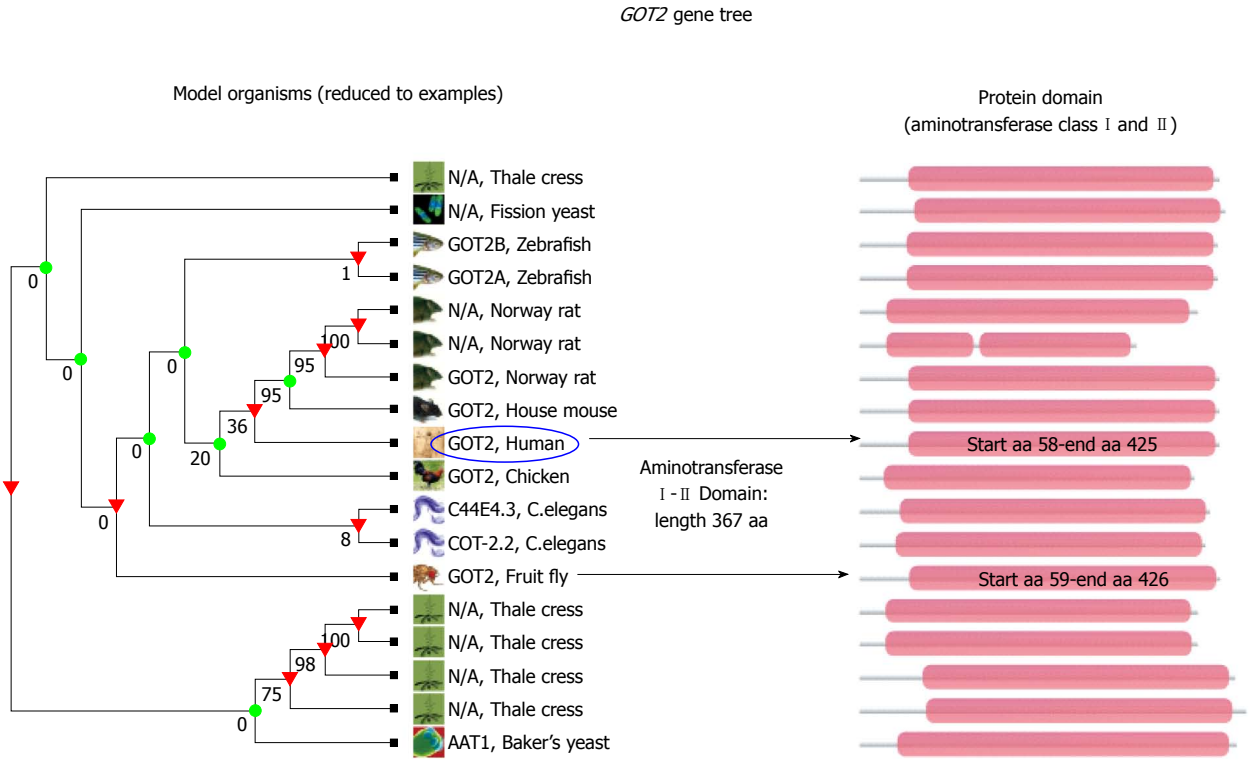

Figure 5 Conservation analysis of *GOT2* between species. Cladogram shows the relationships between *GOT2* genes in different species; for simplicity reasons species were restricted to few models. An alignment of all homologous sequences (protein domain) in the TreeFam family is represented in pink, displayed on the left side of the graph. Numbers below branches are bootstrap values, whereby 100% indicates strong support for these nodes, whereas other nodes receive much weaker support (*e.g.*, 0%). Arrows highlight aminotransferase class Ⅰ and Ⅱ domain in human and fruit fly (aa: amino acid). TreeFam gene was created by using the resource TreeFam, freely available at http://www.treefam.org/family.

NAFLD was recently highlighted[56,57]. Finally, a significant association was found between the intronic *PNPLA3*-rs2281135 and the glycocholate (glycocholic acid) to levulinate (4-oxovalerate) ratio. The secondary bile glycocholic acid is a bile acid-glycine conjugate produced by the action of enzymes existing in the microbial flora of the colonic environment. Metabolomic data on *PNPLA3* also indicated that this gene plays an important role in bile acid metabolism[55].

A comprehensive summary of SNPs and their role in the regulation of metabolites can be found at the freely available web resource "Metabolomics GWAS server" (http://metabolomics.helmholtz-muenchen.de/)[46].

CONCLUSION

The reaction of transamination from glutamine to alpha-keto acids was first described in 1950[4]. Since then, clinicians have been using serum measurement of ALT and AST for the evaluation of liver injury. Nearly 50 years later, the rise in the worldwide prevalence of obesity, type 2 diabetes and CVD brought into the clinical scenario a new concept, associating increased levels of liver enzymes with long-term development of multiple metabolic and CV disorders. In addition, GWAS coupled with metabolomics uncovered key roles of transaminases in the global metabolism. In particular, "omics" studies have led to interesting insights into the biology of liver metabolic function and its relationship with liver transaminases.

Of note, background knowledge on liver enzymes functioning indicates that liver concentrations of ALT and AST are not significantly higher relative to the pool of major liver enzymes[58]. In contrast, liver concentrations of LDH (lactate dehydrogenase) and MD (malate dehydrogenase), for instance, rank first and second, respectively. At 50% of their concentrations, AST and ALT respectively take the third and fourth place (Figure 6)[58].

Wieme *et al*[58] made an interesting observation about the relationship between liver and plasma concentration of enzymes, reporting that the localization of the enzymes at the cellular level very much conditions the concentration in the circulation. The authors further showed that mild cell damage tends to release the enzymes in the soluble fraction only, while severe necrotic lesions, which also affect the mitochondria, release enzymes from both fractions[58]. Hence, it is plausible to suggest that enzymes that are present in high concentrations in the liver tissue, such as LDH, might better and more accurately reflect liver injury. Nevertheless, LDH levels are not commonly used in clinical practice for the diagnosis or monitoring of acute or chronic liver damage. Indeed, serum LDH was reported to be markedly elevated in ischemic, but not viral hepatitis[59,60], indicating that severe cell necrosis is needed for the leaking of the liver-LDH content into the blood to occur.

Table 5 *PNPLA3*-rs738409 metabolite trait associations from the genome-wide association studies catalog

Variant ID	LD with rs738409	Metabolite ratio	*P* value for association
rs12483959	0.657	Cholesterol/gamma-glutamyltyrosine	7.76×10^{-6}
rs2076211	0.657	Cholesterol/gamma-glutamyltyrosine	1.19×10^{-5}
rs2076211	0.657	Aspartylphenylalanine/docosapentaenoate (n3 DPA; 22:5n3)	5.26×10^{-6}
rs2294922	0.657	Docosapentaenoate (n3 DPA; 22:5n3)/eicosapentaenoate (EPA; 20:5n3)	4.64×10^{-7}
rs2073081	0.568	3-methoxytyrosine/gamma-glutamylthreonine	2.14×10^{-5}
rs2281135	0.609	Glycocholate/levulinate (4-oxovalerate)	3.26×10^{-5}
rs1010023	0.609	Docosapentaenoate (n3 DPA; 22:5n3)/phenylacetylglutamine	1.43×10^{-5}
rs926633	0.609	Docosapentaenoate (n3 DPA; 22:5n3)/myristate (14:0)	1.08×10^{-5}
rs2896019	0.607	Aspartylphenylalanine/docosapentaenoate (n3 DPA; 22:5n3)	1.31×10^{-5}

Information was retrieved from the GWAS server at the freely accessible URL: http://metabolomics.helmholtz-muenchen.de. This server combines data on large GWAS and non-targeted and metabolome-wide panel of small molecules, using blood samples and phenotype data from 2824 individuals of two major population-based European cohorts: the German KORA study and the British TWINs UK study. LD: Linkage disequilibrium that refers to a non-random association in the occurrence of alleles at two loci was assessed by R^2 (the square of the correlation coefficient between the presence or absence of a particular allele at the first locus and the other representing the presence or absence of a particular allele at the second locus). GWAS: Genome-wide association studies.

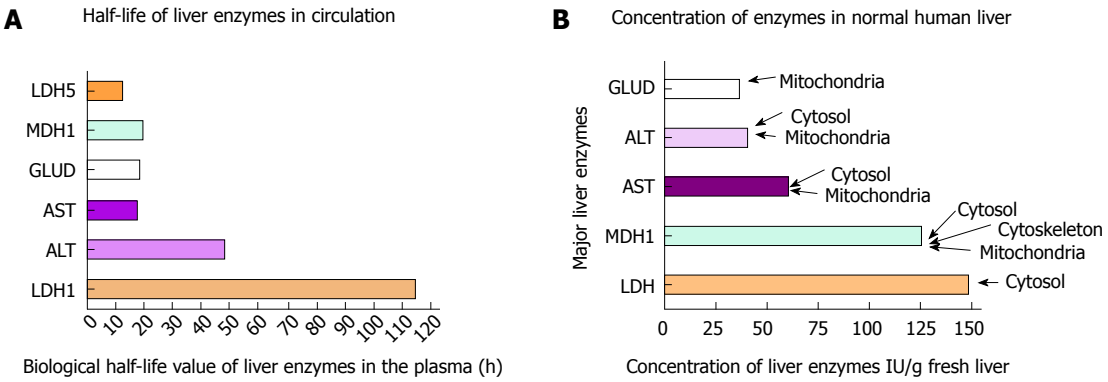

Figure 6 Liver enzyme concentrations in normal human liver. Information of the liver concentration of major liver enzymes was extracted from the report published by Wieme *et al*[58]. Evidence of subcellular locations from the Compartments database (http://compartments.jensenlab.org) is highlighted. LDH5: Human isoform-5 of lactate dehydrogenase, which is normally present in the liver; GLUD: Glutamate dehydrogenase; ALT: Alanine aminotransferase; AST: Aspartate aminotransferase; MDH1: Malate dehydrogenase; LDH: Lactate dehydrogenase.

A second factor in determining the rise of liver enzymes in the circulation seems to be its biological half-life as, according to the observation of Wieme *et al*[58], the longer the half-life the greater the accumulation of the enzymes in the serum (Figure 6 depicts the half-life of liver enzymes in serum). Based on the above, the findings reported by Wieme *et al*[58] may explain why ALT, which seems to have a half-life of 50 h, is more likely to be found elevated in serum than the LDH isoform 5, which is normally present in the liver and has a very short half-life of 10 h.

Taken together, the observations made in the GWAS studies, coupled with metabolomics, in conjunction with past knowledge on the traditional biochemistry explorations (presently referred to as "quantitative biology"), are of particular significance in providing a plausible biological explanation to the meaning of elevated ALT and AST levels in the clinical setting. Indeed, these findings suggest that restricting the biological role of elevated aminotransferase levels to liver injury has not only been a misinterpretation but an underestimation of the biological role of these enzymes. Interestingly, *in vitro* studies showed that even ethanol might increase transaminases, mitochondrial AST in particular, by up-regulating gene expression, rather than by inducing its release owing to cell injury[61].

Data from the Third National Health and Nutrition Examination Survey, the largest epidemiological study in the United States, showed that the prevalence of aminotransferase elevation in the general population is about 9%[22]. Notably, unexplained enzyme elevations were associated with adiposity and other features of the metabolic syndrome[22,62]. On the other hand, presence of a considerable inter-individual variation in the level of transaminases is widely acknowledged, and this variability is explained in part by genetic variation. Links between aminotransferase genes and metabolites demonstrated important contributions to the metabolic diversity. In fact, evidence from high-throughput studies of genetic influences on human metabolites demonstrated that aminotransferases ALT and AST are not solely involved in gluconeogenesis and amino acid synthesis, but also regulate other functions of the liver metabolism, such as fatty acid, glycerolipid and bile acids metabolism. In addition, an interesting study highlighted a putative relationship between iron stores, ALT activity

and the risk of metabolic disturbances in adolescents that deserves further follow-up[63].

Finally, the role of the newly described TM6SF2 rs58542926 nonsynonymous variant in genetic susceptibility to NAFLD and disease severity[64] deserves follow-up as this variant was associated in population-based studies but not in NAFLD patients with levels of transaminases in circulation[65].

In conclusion, genomic, transcriptomic, proteomic, and metabolomic information has changed the classical conception of the meaning that serum concentrations of ALT and ALT are merely indicators of hepatocyte membrane disruption. It has given way to a more complex and interconnected view of the importance of liver transaminases in the regulation of systemic metabolic function.

REFERENCES

1 **Pratt DS**, Kaplan MM. Evaluation of abnormal liver-enzyme results in asymptomatic patients. *N Engl J Med* 2000; **342**: 1266-1271 [PMID: 10781624 DOI: 10.1056/NEJM200004273421707]

2 **Molander DW**, Wroblewski F, Ladue JS. Serum glutamic oxalacetic transaminase as an index of hepatocellular integrity. *J Lab Clin Med* 1955; **46**: 831-839 [PMID: 13271882]

3 **Killip T**, Payne MA. High serum transaminase activity in heart disease. Circulatory failure and hepatic necrosis. *Circulation* 1960; **21**: 646-660 [PMID: 14409072]

4 **Meister A**, Tice SV. Transamination from glutamine to alpha-keto acids. *J Biol Chem* 1950; **187**: 173-187 [PMID: 14794702]

5 **Sherman KE**. Alanine aminotransferase in clinical practice. A review. *Arch Intern Med* 1991; **151**: 260-265 [PMID: 1992953]

6 **Kamiike W**, Fujikawa M, Koseki M, Sumimura J, Miyata M, Kawashima Y, Wada H, Tagawa K. Different patterns of leakage of cytosolic and mitochondrial enzymes. *Clin Chim Acta* 1989; **185**: 265-270 [PMID: 2620458]

7 **Reichling JJ**, Kaplan MM. Clinical use of serum enzymes in liver disease. *Dig Dis Sci* 1988; **33**: 1601-1614 [PMID: 2904353]

8 **Sattar N**, Scherbakova O, Ford I, O'Reilly DS, Stanley A, Forrest E, Macfarlane PW, Packard CJ, Cobbe SM, Shepherd J. Elevated alanine aminotransferase predicts new-onset type 2 diabetes independently of classical risk factors, metabolic syndrome, and C-reactive protein in the west of Scotland coronary prevention study. *Diabetes* 2004; **53**: 2855-2860 [PMID: 15504965]

9 **Vozarova B**, Stefan N, Lindsay RS, Saremi A, Pratley RE, Bogardus C, Tataranni PA. High alanine aminotransferase is associated with decreased hepatic insulin sensitivity and predicts the development of type 2 diabetes. *Diabetes* 2002; **51**: 1889-1895 [PMID: 12031978]

10 **Ioannou GN**, Weiss NS, Boyko EJ, Mozaffarian D, Lee SP. Elevated serum alanine aminotransferase activity and calculated risk of coronary heart disease in the United States. *Hepatology* 2006; **43**: 1145-1151 [PMID: 16628637 DOI: 10.1002/hep.21171]

11 **Kain K**, Carter AM, Grant PJ, Scott EM. Alanine aminotransferase is associated with atherothrombotic risk factors in a British South Asian population. *J Thromb Haemost* 2008; **6**: 737-741 [PMID: 18315552 DOI: 10.1111/j.1538-7836.2008.02935.x]

12 **Song HR**, Yun KE, Park HS. Relation between alanine aminotransferase concentrations and visceral fat accumulation among nondiabetic overweight Korean women. *Am J Clin Nutr* 2008; **88**: 16-21 [PMID: 18614719]

13 **Goessling W**, Massaro JM, Vasan RS, D'Agostino RB, Ellison RC, Fox CS. Aminotransferase levels and 20-year risk of metabolic syndrome, diabetes, and cardiovascular disease. *Gastroenterology* 2008; **135**: 1935-1944, 1944.e1 [PMID: 19010326 DOI: 10.1053/j.gastro.2008.09.018]

14 **Sookoian S**, Pirola CJ. Alanine and aspartate aminotransferase and glutamine-cycling pathway: their roles in pathogenesis of metabolic syndrome. *World J Gastroenterol* 2012; **18**: 3775-3781 [PMID: 22876026 DOI: 10.3748/wjg.v18.i29.3775]

15 **Yang RZ**, Blaileanu G, Hansen BC, Shuldiner AR, Gong DW. cDNA cloning, genomic structure, chromosomal mapping, and functional expression of a novel human alanine aminotransferase. *Genomics* 2002; **79**: 445-450 [PMID: 11863375 DOI: 10.1006/geno.2002.6722]

16 **Uhlen M**, Oksvold P, Fagerberg L, Lundberg E, Jonasson K, Forsberg M, Zwahlen M, Kampf C, Wester K, Hober S, Wernerus H, Björling L, Ponten F. Towards a knowledge-based Human Protein Atlas. *Nat Biotechnol* 2010; **28**: 1248-1250 [PMID: 21139605 DOI: 10.1038/nbt1210-1248]

17 **Lindblom P**, Rafter I, Copley C, Andersson U, Hedberg JJ, Berg AL, Samuelsson A, Hellmold H, Cotgreave I, Glinghammar B. Isoforms of alanine aminotransferases in human tissues and serum--differential tissue expression using novel antibodies. *Arch Biochem Biophys* 2007; **466**: 66-77 [PMID: 17826732 DOI: 10.1016/j.abb.2007.07.023]

18 **Glinghammar B**, Rafter I, Lindström AK, Hedberg JJ, Andersson HB, Lindblom P, Berg AL, Cotgreave I. Detection of the mitochondrial and catalytically active alanine aminotransferase in human tissues and plasma. *Int J Mol Med* 2009; **23**: 621-631 [PMID: 19360321]

19 **Rafter I**, Gråberg T, Kotronen A, Strömmer L, Mattson CM, Kim RW, Ehrenborg E, Andersson HB, Yki-Järvinen H, Schuppe-Koistinen I, Ekblom B, Cotgreave I, Glinghammar B. Isoform-specific alanine aminotransferase measurement can distinguish hepatic from extrahepatic injury in humans. *Int J Mol Med* 2012; **30**: 1241-1249 [PMID: 22922605 DOI: 10.3892/ijmm.2012.1106]

20 **Kechagias S**, Ernersson A, Dahlqvist O, Lundberg P, Lindström T, Nystrom FH. Fast-food-based hyper-alimentation can induce rapid and profound elevation of serum alanine aminotransferase in healthy subjects. *Gut* 2008; **57**: 649-654 [PMID: 18276725 DOI: 10.1136/gut.2007.131797]

21 **Pirola CJ**, Fernández Gianotti T, Castaño GO, Mallardi P, San Martino J, Mora Gonzalez Lopez Ledesma M, Flichman D, Mirshahi F, Sanyal AJ, Sookoian S. Circulating microRNA signature in non-alcoholic fatty liver disease: from serum non-coding RNAs to liver histology and disease pathogenesis. *Gut* 2014: Epub ahead of print [PMID: 24973316 DOI: 10.1136/gutjnl-2014-306996]

22 **Ioannou GN**, Boyko EJ, Lee SP. The prevalence and predictors of elevated serum aminotransferase activity in the United States in 1999-2002. *Am J Gastroenterol* 2006; **101**: 76-82 [PMID: 16405537 DOI: 10.1111/j.1572-0241.2005.00341.x]

23 **Statland BE**, Winkel P, Bokelund H. Factors contributing to intra-individual variation of serum constituents. 2. Effects of exercise and diet on variation of serum constituents in healthy subjects. *Clin Chem* 1973; **19**: 1380-1383 [PMID: 4757367]

24 **Statland BE**, Winkel P, Bokelund H. Factors contributing to intra-individual variation of serum constituents. 1. Within-day variation of serum constituents in healthy subjects. *Clin Chem* 1973; **19**: 1374-1379 [PMID: 4757366]

25 **Rahmioglu N**, Andrew T, Cherkas L, Surdulescu G, Swaminathan R, Spector T, Ahmadi KR. Epidemiology and genetic epidemiology of the liver function test proteins. *PLoS One* 2009; **4**: e4435 [PMID: 19209234 DOI: 10.1371/journal.pone.0004435]

26 **Whitfield JB**, Zhu G, Nestler JE, Heath AC, Martin NG. Genetic covariation between serum gamma-glutamyltransferase activity and cardiovascular risk factors. *Clin Chem* 2002; **48**: 1426-1431 [PMID: 12194918]

27 **Bathum L**, Petersen HC, Rosholm JU, Hyltoft Petersen P, Vaupel J, Christensen K. Evidence for a substantial genetic influence on biochemical liver function tests: results from a population-based Danish twin study. *Clin Chem* 2001; **47**: 81-87 [PMID: 11148181]

28 **Romeo S**, Kozlitina J, Xing C, Pertsemlidis A, Cox D, Pennacchio LA, Boerwinkle E, Cohen JC, Hobbs HH. Genetic variation in PNPLA3 confers susceptibility to nonalcoholic fatty liver disease. *Nat Genet* 2008; **40**: 1461-1465 [PMID: 18820647 DOI: 10.1038/ng.257]

29 **Sookoian S**, Castaño GO, Burgueño AL, Gianotti TF, Rosselli MS, Pirola CJ. A nonsynonymous gene variant in the adiponutrin gene is associated with nonalcoholic fatty liver disease severity. *J Lipid Res* 2009; **50**: 2111-2116 [PMID: 19738004 DOI: 10.1194/jlr.P900013-JLR200]

30 **Sookoian S**, Pirola CJ. Meta-analysis of the influence of I148M variant of patatin-like phospholipase domain containing 3 gene (PNPLA3) on the susceptibility and histological severity of nonalcoholic fatty liver disease. *Hepatology* 2011; **53**: 1883-1894 [PMID: 21381068 DOI: 10.1002/hep.24283]

31 **Sookoian S**, Pirola CJ. PNPLA3, the history of an orphan gene of the potato tuber protein family that found an organ: the liver. *Hepatology* 2014; **59**: 2068-2071 [PMID: 24122882 DOI: 10.1002/hep.26895]

32 **Chamorro AJ**, Torres JL, Mirón-Canelo JA, González-Sarmiento R, Laso FJ, Marcos M. Systematic review with meta-analysis: the I148M variant of patatin-like phospholipase domain-containing 3 gene (PNPLA3) is significantly associated with alcoholic liver cirrhosis. *Aliment Pharmacol Ther* 2014; **40**: 571-581 [PMID: 25060292 DOI: 10.1111/apt.12890]

33 **Valenti L**, Rumi M, Galmozzi E, Aghemo A, Del Menico B, De Nicola S, Dongiovanni P, Maggioni M, Fracanzani AL, Rametta R, Colombo M, Fargion S. Patatin-like phospholipase domain-containing 3 I148M polymorphism, steatosis, and liver damage in chronic hepatitis C. *Hepatology* 2011; **53**: 791-799 [PMID: 21319195 DOI: 10.1002/hep.24123]

34 **Viganò M**, Valenti L, Lampertico P, Facchetti F, Motta BM, D'Ambrosio R, Romagnoli S, Dongiovanni P, Donati B, Fargion S, Colombo M. Patatin-like phospholipase domain-containing 3 I148M affects liver steatosis in patients with chronic hepatitis B. *Hepatology* 2013; **58**: 1245-1252 [PMID: 23564580 DOI: 10.1002/hep.26445]

35 **Trépo E**, Nahon P, Bontempi G, Valenti L, Falleti E, Nischalke HD, Hamza S, Corradini SG, Burza MA, Guyot E, Donati B, Spengler U, Hillon P, Toniutto P, Henrion J, Franchimont D, Devière J, Mathurin P, Moreno C, Romeo S, Deltenre P. Association between the PNPLA3 (rs738409 C& gt; G) variant and hepatocellular carcinoma: Evidence from a meta-analysis of individual participant data. *Hepatology* 2014; **59**: 2170-2177 [PMID: 24114809 DOI: 10.1002/hep.26767]

36 **Chambers JC**, Zhang W, Sehmi J, Li X, Wass MN, Van der Harst P, Holm H, Sanna S, Kavousi M, Baumeister SE, Coin LJ, Deng G, Gieger C, Heard-Costa NL, Hottenga JJ, Kühnel B, Kumar V, Lagou V, Liang L, Luan J, Vidal PM, Mateo Leach I, O'Reilly PF, Peden JF, Rahmioglu N, Soininen P, Speliotes EK, Yuan X, Thorleifsson G, Alizadeh BZ, Atwood LD, Borecki IB, Brown MJ, Charoen P, Cucca F, Das D, de Geus EJ, Dixon AL, Döring A, Ehret G, Eyjolfsson GI, Farrall M, Forouhi NG, Friedrich N, Goessling W, Gudbjartsson DF, Harris TB, Hartikainen AL, Heath S, Hirschfield GM, Hofman A, Homuth G, Hyppönen E, Janssen HL, Johnson T, Kangas AJ, Kema IP, Kühn JP, Lai S, Lathrop M, Lerch MM, Li Y, Liang TJ, Lin JP, Loos RJ, Martin NG, Moffatt MF, Montgomery GW, Munroe PB, Musunuru K, Nakamura Y, O'Donnell CJ, Olafsson I, Penninx BW, Pouta A, Prins BP, Prokopenko I, Puls R, Ruokonen A, Savolainen MJ, Schlessinger D, Schouten JN, Seedorf U, Sen-Chowdhry S, Siminovitch KA, Smit JH, Spector TD, Tan W, Teslovich TM, Tukiainen T, Uitterlinden AG, Van der Klauw MM, Vasan RS, Wallace C, Wallaschofski H, Wichmann HE, Willemsen G, Würtz P, Xu C, Yerges-Armstrong LM, Abecasis GR, Ahmadi KR, Boomsma DI, Caulfield M, Cookson WO, van Duijn CM, Froguel P, Matsuda K, McCarthy MI, Meisinger C, Mooser V, Pietiläinen KH, Schumann G, Snieder H, Sternberg MJ, Stolk RP, Thomas HC, Thorsteinsdottir U, Uda M, Waeber G, Wareham NJ, Waterworth DM, Watkins H, Whitfield JB, Witteman JC, Wolffenbuttel BH, Fox CS, Ala-Korpela M, Stefansson K, Vollenweider P, Völzke H, Schadt EE, Scott J, Järvelin MR, Elliott P, Kooner JS. Genome-wide association study identifies loci influencing concentrations of liver enzymes in plasma. *Nat Genet* 2011; **43**: 1131-1138 [PMID: 22001757 DOI: 10.1038/ng.970]

37 **Smagris E**, BasuRay S, Li J, Huang Y, Lai KM, Gromada J, Cohen JC, Hobbs HH. Pnpla3I148M knockin mice accumulate PNPLA3 on lipid droplets and develop hepatic steatosis. *Hepatology* 2015; **61**: 108-118 [PMID: 24917523 DOI: 10.1002/hep.27242]

38 **Huang Y**, Cohen JC, Hobbs HH. Expression and characterization of a PNPLA3 protein isoform (I148M) associated with nonalcoholic fatty liver disease. *J Biol Chem* 2011; **286**: 37085-37093 [PMID: 21878620 DOI: 10.1074/jbc.M111.290114]

39 **He S**, McPhaul C, Li JZ, Garuti R, Kinch L, Grishin NV, Cohen JC, Hobbs HH. A sequence variation (I148M) in PNPLA3 associated with nonalcoholic fatty liver disease disrupts triglyceride hydrolysis. *J Biol Chem* 2010; **285**: 6706-6715 [PMID: 20034933 DOI: 10.1074/jbc.M109.064501]

40 **Fernández Gianotti T**, Burgueño A, Gonzales Mansilla N, Pirola CJ, Sookoian S. Fatty liver is associated with transcriptional downregulation of stearoyl-CoA desaturase and impaired protein dimerization. *PLoS One* 2013; **8**: e76912 [PMID: 24098813 DOI: 10.1371/journal.pone.0076912]

41 **Silbernagel G**, Kovarova M, Cegan A, Machann J, Schick F, Lehmann R, Häring HU, Stefan N, Schleicher E, Fritsche A, Peter A. High hepatic SCD1 activity is associated with low liver fat content in healthy subjects under a lipogenic diet. *J Clin Endocrinol Metab* 2012; **97**: E2288-E2292 [PMID: 23015656 DOI: 10.1210/jc.2012-2152]

42 **Sookoian S**, Gianotti TF, Rosselli MS, Burgueño AL, Castaño GO, Pirola CJ. Liver transcriptional profile of atherosclerosis-related genes in human nonalcoholic fatty liver disease. *Atherosclerosis* 2011; **218**: 378-385 [PMID: 21664615 DOI: 10.1016/j.atherosclerosis.2011.05.014]

43 **Spassov DS**, Jurecic R. The PUF family of RNA-binding proteins: does evolutionarily conserved structure equal conserved function? *IUBMB Life* 2003; **55**: 359-366 [PMID: 14584586 DOI: 10.1080/15216540310001603093]

44 **Gieger C**, Geistlinger L, Altmaier E, Hrabé de Angelis M, Kronenberg F, Meitinger T, Mewes HW, Wichmann HE, Weinberger KM, Adamski J, Illig T, Suhre K. Genetics meets metabolomics: a genome-wide association study of metabolite profiles in human serum. *PLoS Genet* 2008; **4**: e1000282 [PMID: 19043545 DOI: 10.1371/journal.pgen.1000282]

45 **Kettunen J**, Tukiainen T, Sarin AP, Ortega-Alonso A, Tikkanen E, Lyytikäinen LP, Kangas AJ, Soininen P, Würtz P, Silander K, Dick DM, Rose RJ, Savolainen MJ, Viikari J, Kähönen M, Lehtimäki T, Pietiläinen KH, Inouye M, McCarthy MI, Jula A, Eriksson J, Raitakari OT, Salomaa V, Kaprio J, Järvelin MR, Peltonen L, Perola M, Freimer NB, Ala-Korpela M, Palotie A, Ripatti S. Genome-wide association study identifies multiple loci influencing human serum metabolite levels. *Nat Genet* 2012; **44**: 269-276 [PMID: 22286219 DOI: 10.1038/ng.1073]

46 **Shin SY**, Fauman EB, Petersen AK, Krumsiek J, Santos R, Huang J, Arnold M, Erte I, Forgetta V, Yang TP, Walter K, Menni C, Chen L, Vasquez L, Valdes AM, Hyde CL, Wang V, Ziemek D, Roberts P, Xi L, Grundberg E, Waldenberger M, Richards JB, Mohney RP, Milburn MV, John SL, Trimmer J, Theis FJ, Overington JP, Suhre K, Brosnan MJ, Gieger C, Kastenmüller G, Spector TD, Soranzo N. An atlas of genetic influences on human blood metabolites. *Nat Genet* 2014; **46**:

543-550 [PMID: 24816252 DOI: 10.1038/ng.2982]
47 **Chase BA**, Kankel DR. A genetic analysis of glutamatergic function in Drosophila. *J Neurobiol* 1987; **18**: 15-41 [PMID: 3106567 DOI: 10.1002/neu.480180104]
48 **Sardiello M**, Licciulli F, Catalano D, Attimonelli M, Caggese C. MitoDrome: a database of Drosophila melanogaster nuclear genes encoding proteins targeted to the mitochondrion. *Nucleic Acids Res* 2003; **31**: 322-324 [PMID: 12520013]
49 **Tomancak P**, Beaton A, Weiszmann R, Kwan E, Shu S, Lewis SE, Richards S, Ashburner M, Hartenstein V, Celniker SE, Rubin GM. Systematic determination of patterns of gene expression during Drosophila embryogenesis. *Genome Biol* 2002; **3**: RESEARCH0088 [PMID: 12537577]
50 **Cammarato A**, Ahrens CH, Alayari NN, Qeli E, Rucker J, Reedy MC, Zmasek CM, Gucek M, Cole RN, Van Eyk JE, Bodmer R, O'Rourke B, Bernstein SI, Foster DB. A mighty small heart: the cardiac proteome of adult Drosophila melanogaster. *PLoS One* 2011; **6**: e18497 [PMID: 21541028 DOI: 10.1371/journal.pone.001849]
51 **Cermelli S**, Guo Y, Gross SP, Welte MA. The lipid-droplet proteome reveals that droplets are a protein-storage depot. *Curr Biol* 2006; **16**: 1783-1795 [PMID: 16979555 DOI: 10.1016/j.cub.2006.07.062]
52 **Alonso J**, Rodriguez JM, Baena-López LA, Santarén JF. Characterization of the Drosophila melanogaster mitochondrial proteome. *J Proteome Res* 2005; **4**: 1636-1645 [PMID: 16212416 DOI: 10.1021/pr050130c]
53 **Sookoian S**, Pirola CJ. The genetic epidemiology of nonalcoholic fatty liver disease: toward a personalized medicine. *Clin Liver Dis* 2012; **16**: 467-485 [PMID: 22824476 DOI: 10.1016/j.cld.2012.05.011]
54 **Sookoian S**, Pirola CJ. PNPLA3, the triacylglycerol synthesis/hydrolysis/storage dilemma, and nonalcoholic fatty liver disease. *World J Gastroenterol* 2012; **18**: 6018-6026 [PMID: 23155331 DOI: 10.3748/wjg.v18.i42.6018]
55 **Min HK**, Sookoian S, Pirola CJ, Cheng J, Mirshahi F, Sanyal AJ. Metabolic profiling reveals that PNPLA3 induces widespread effects on metabolism beyond triacylglycerol remodeling in Huh-7 hepatoma cells. *Am J Physiol Gastrointest Liver Physiol* 2014; **307**: G66-G76 [PMID: 24763554 DOI: 10.1152/ajpgi.00335.2013]
56 **Sookoian S**, Pirola CJ. NAFLD. Metabolic make-up of NASH: from fat and sugar to amino acids. *Nat Rev Gastroenterol Hepatol* 2014; **11**: 205-207 [PMID: 24566880 DOI: 10.1038/nrgastro.2014.25]
57 **Mardinoglu A**, Agren R, Kampf C, Asplund A, Uhlen M, Nielsen J. Genome-scale metabolic modelling of hepatocytes reveals serine deficiency in patients with non-alcoholic fatty liver disease. *Nat Commun* 2014; **5**: 3083 [PMID: 24419221 DOI: 10.1038/ncomms4083]
58 **Wieme RJ**, Demeulenaere L. Enzyme assays in liver disease. *J Clin Pathol Suppl* (Assoc Clin Pathol) 1970; **4**: 51-59 [PMID: 4143914]
59 **Cassidy WM**, Reynolds TB. Serum lactic dehydrogenase in the differential diagnosis of acute hepatocellular injury. *J Clin Gastroenterol* 1994; **19**: 118-121 [PMID: 7963356]
60 **Rotenberg Z**, Weinberger I, Davidson E, Fuchs J, Harell D, Agmon J. Alterations in total lactate dehydrogenase and its isoenzyme-5 in hepatic disorders. *Ann Clin Lab Sci* 1990; **20**: 268-273 [PMID: 2403242]
61 **Zhou SL**, Gordon RE, Bradbury M, Stump D, Kiang CL, Berk PD. Ethanol up-regulates fatty acid uptake and plasma membrane expression and export of mitochondrial aspartate aminotransferase in HepG2 cells. *Hepatology* 1998; **27**: 1064-1074 [PMID: 9537447 DOI: 10.1002/hep.510270423]
62 **Clark JM**, Brancati FL, Diehl AM. The prevalence and etiology of elevated aminotransferase levels in the United States. *Am J Gastroenterol* 2003; **98**: 960-967 [PMID: 12809815 DOI: 10.1111/j.1572-0241.2003.07486.x]
63 **Aigner E**, Hinz C, Steiner K, Rossmann B, Pfleger J, Hohla F, Steger B, Stadlmayr A, Patsch W, Datz C. Iron stores, liver transaminase levels and metabolic risk in healthy teenagers. *Eur J Clin Invest* 2010; **40**: 155-163 [PMID: 20050877 DOI: 10.1111/j.1365-2362.2009.02238.x]
64 **Sookoian S**, Castaño GO, Scian R, Mallardi P, Fernández Gianotti T, Burgueño AL, San Martino J, Pirola CJ. Genetic variation in transmembrane 6 superfamily member 2 and the risk of nonalcoholic fatty liver disease and histological disease severity. *Hepatology* 2014; Epub ahead of print [PMID: 25302781 DOI: 10.1002/hep.27556]
65 **Holmen OL**, Zhang H, Fan Y, Hovelson DH, Schmidt EM, Zhou W, Guo Y, Zhang J, Langhammer A, Løchen ML, Ganesh SK, Vatten L, Skorpen F, Dalen H, Zhang J, Pennathur S, Chen J, Platou C, Mathiesen EB, Wilsgaard T, Njølstad I, Boehnke M, Chen YE, Abecasis GR, Hveem K, Willer CJ. Systematic evaluation of coding variation identifies a candidate causal variant in TM6SF2 influencing total cholesterol and myocardial infarction risk. *Nat Genet* 2014; **46**: 345-351 [PMID: 24633158 DOI: 10.1038/ng.2926]
66 **Josekutty J**, Iqbal J, Iwawaki T, Kohno K, Hussain MM. Microsomal triglyceride transfer protein inhibition induces endoplasmic reticulum stress and increases gene transcription via Ire1α/cJun to enhance plasma ALT/AST. *J Biol Chem* 2013; **288**: 14372-14383 [PMID: 23532846 DOI: 10.1074/jbc.M113.459602]
67 **Thulin P**, Rafter I, Stockling K, Tomkiewicz C, Norjavaara E, Aggerbeck M, Hellmold H, Ehrenborg E, Andersson U, Cotgreave I, Glinghammar B. PPARalpha regulates the hepatotoxic biomarker alanine aminotransferase (ALT1) gene expression in human hepatocytes. *Toxicol Appl Pharmacol* 2008; **231**: 1-9 [PMID: 18455211 DOI: 10.1016/j.taap.2008.03.007]
68 **Beránek M**, Drsata J, Palicka V. Inhibitory effect of glycation on catalytic activity of alanine aminotransferase. *Mol Cell Biochem* 2001; **218**: 35-39 [PMID: 11330835]
69 **Salgado MC**, Metón I, Anemaet IG, Baanante IV. Activating transcription factor 4 mediates up-regulation of alanine aminotransferase 2 gene expression under metabolic stress. *Biochim Biophys Acta* 2014; **1839**: 288-296 [PMID: 24418603 DOI: 10.1016/j.bbagrm.2014.01.005]
70 **Coss CC**, Bauler M, Narayanan R, Miller DD, Dalton JT. Alanine aminotransferase regulation by androgens in non-hepatic tissues. *Pharm Res* 2012; **29**: 1046-1056 [PMID: 22167351 DOI: 10.1007/s11095-011-0649-5]
71 **Jadhao SB**, Yang RZ, Lin Q, Hu H, Anania FA, Shuldiner AR, Gong DW. Murine alanine aminotransferase: cDNA cloning, functional expression, and differential gene regulation in mouse fatty liver. *Hepatology* 2004; **39**: 1297-1302 [PMID: 15122758]
72 **Reagan WJ**, Yang RZ, Park S, Goldstein R, Brees D, Gong DW. Metabolic adaptive ALT isoenzyme response in livers of C57/BL6 mice treated with dexamethasone. *Toxicol Pathol* 2012; **40**: 1117-1127 [PMID: 22609950 DOI: 10.1177/0192623312447550]
73 **Liu R**, Pan X, Whitington PF. Increased hepatic expression is a major determinant of serum alanine aminotransferase elevation in mice with nonalcoholic steatohepatitis. *Liver Int* 2009; **29**: 337-343 [PMID: 18710424 DOI: 10.1111/j.1478-3231.2008.01862.x]
74 **Yuan X**, Waterworth D, Perry JR, Lim N, Song K, Chambers JC, Zhang W, Vollenweider P, Stirnadel H, Johnson T, Bergmann S, Beckmann ND, Li Y, Ferrucci L, Melzer D, Hernandez D, Singleton A, Scott J, Elliott P, Waeber G, Cardon L, Frayling TM, Kooner JS, Mooser V. Population-based genome-wide association studies reveal six loci influencing plasma levels of liver enzymes. *Am J Hum Genet* 2008; **83**: 520-528 [PMID: 18940312 DOI: 10.1016/j.ajhg.2008.09.012]
75 **Park TJ**, Hwang JY, Go MJ, Lee HJ, Jang HB, Choi Y, Kang JH, Park KH, Choi MG, Song J, Kim BJ, Lee JY. Genome-wide association study of liver enzymes in korean children. *Genomics Inform* 2013; **11**: 149-154 [PMID: 24124411 DOI: 10.5808/GI.2013.11.3.149]

76 **Shen H**, Damcott C, Shuldiner SR, Chai S, Yang R, Hu H, Gibson Q, Ryan KA, Mitchell BD, Gong DW. Genome-wide association study identifies genetic variants in GOT1 determining serum aspartate aminotransferase levels. *J Hum Genet* 2011; **56**: 801-805 [PMID: 21900944 DOI: 10.1038/jhg.2011.105]

77 **Vanburen V**, Chen H. Managing biological complexity across orthologs with a visual knowledgebase of documented biomolecular interactions. *Sci Rep* 2012; **2**: 1011 [PMID: 23264875 DOI: 10.1038/srep01011]

78 **Suhre K**, Shin SY, Petersen AK, Mohney RP, Meredith D, Wägele B, Altmaier E, Deloukas P, Erdmann J, Grundberg E, Hammond CJ, de Angelis MH, Kastenmüller G, Köttgen A, Kronenberg F, Mangino M, Meisinger C, Meitinger T, Mewes HW, Milburn MV, Prehn C, Raffler J, Ried JS, Römisch-Margl W, Samani NJ, Small KS, Wichmann HE, Zhai G, Illig T, Spector TD, Adamski J, Soranzo N, Gieger C. Human metabolic individuality in biomedical and pharmaceutical research. *Nature* 2011; **477**: 54-60 [PMID: 21886157 DOI: 10.1038/nature10354]

P- Reviewer: del Giudice EM, Duryee MJ, Mascitelli L, Tarquini R
S- Editor: Ma YJ **L- Editor**: A **E- Editor**: Liu XM

World Journal of Gastroenterology

Submit a Manuscript: http://www.wjgnet.com/esps/
Help Desk: http://www.wjgnet.com/esps/helpdesk.aspx
DOI: 10.3748/wjg.v21.i3.726

World J Gastroenterol 2015 January 21; 21(3): 726-741
ISSN 1007-9327 (print) ISSN 2219-2840 (online)

REVIEW

Endoscopic ultrasonography guided drainage: Summary of consortium meeting, May 21, 2012, San Diego, California

Michel Kahaleh, Everson LA Artifon, Manuel Perez-Miranda, Monica Gaidhane, Carlos Rondon, Takao Itoi, Marc Giovannini

Michel Kahaleh, Monica Gaidhane, Carlos Rondon, Division of Gastroenterology and Hepatology, Department of Medicine, Weill Cornell Medical Center, New York, NY 10021, United States
Everson LA Artifon, Department of Surgery, University of Sao Paulo Medical School, Sao Paulo 05403-000, Brazil
Manuel Perez-Miranda, Endoscopy Unit, Hospital Universitario Rio Hortega, 47012 Valladolid, Spain
Takao Itoi, Department of Gastroenterology and Hematology, Tokyo Medical University, Tokyo 160-0023, Japan
Marc Giovannini, Department of Gastroenterology, Paoli-Calmettes Institute, 13273 Marseille, France
Author contributions: Kahaleh M, Artifon ELA, Perez-Miranda M and Giovannini M designed and organized the meeting and provided summary results; Kahaleh M, Gaidhane M and Rondon C summarized the data and wrote the paper; Itoi T helped write the manuscript.

Correspondence to: Michel Kahaleh, MD, AGAF, FACG, FASGE, Chief of Endoscopy, Professor of Clinical Medicine, Division of Gastroenterology and Hepatology, Department of Medicine, Weill Cornell Medical College, 1305 York Avenue, 4th Floor, New York, NY 10021, United States. mkahaleh@gmail.com
Telephone: +1-646-9624000
Fax: +1-646-9620110
Received: February 18, 2014
Peer-review started: February 21, 2014
First decision: March 13, 2014
Revised: April 29, 2014
Accepted: June 21, 2014
Article in press: June 23, 2014
Published online: January 21, 2015

Abstract

Endoscopic retrograde cholangiopancreatography (ERCP) is the preferred procedure for biliary and pancreatic drainage. While ERCP is successful in about 95% of cases, a small subset of cases are unsuccessful due to altered anatomy, peri-ampullary pathology, or malignant obstruction. Endoscopic ultrasound-guided drainage is a promising technique for biliary, pancreatic and recently gallbladder decompression, which provides multiple advantages over percutaneous or surgical biliary drainage. Multiple retrospective and some prospective studies have shown endoscopic ultrasound-guided drainage to be safe and effective. Based on the currently reported literature, regardless of the approach, the cumulative success rate is 84%-93% with an overall complication rate of 16%-35%. endoscopic ultrasound-guided drainage seems a viable therapeutic modality for failed conventional drainage when performed by highly skilled advanced endoscopists at tertiary centers with expertise in both echo-endoscopy and therapeutic endoscopy

Key words: Endoscopic ultrasound; Endoscopic ultrasound-guided biliary drainage; Consortium; Biliary drainage; Pancreatic drainage; Endoscopic ultrasound-guided

Core tip: This summary of the endoscopic ultrasound (EUS)-guided biliary drainage consortium held in 2012 focuses on technical improvements in both EUS-Guided biliary and pancreatic drainage techniques. This summary also provides a detailed overview of EUS-guided choledochoduodenostomy compared to percutaneous transhepatic cholangiography and surgical drainage. Other EUS Guided techniques such as endoscopic ultrasound-guided pancreatico-gastrostomy and endoscopic ultrasonography-guided cholecystoduodenostomy and cholecystogastrostomy have been discussed. Lastly, an extensive review of therapeutic endoscopic interventions in surgically

altered anatomy has been provided as well.

Kahaleh M, Artifon ELA, Perez-Miranda M, Gaidhane M, Rondon C, Itoi T, Giovannini M. Endoscopic ultrasonography guided drainage: Summary of consortium meeting, May 21, 2012, San Diego, California. *World J Gastroenterol* 2015; 21(3): 726-741 Available from: URL: http://www.wjgnet.com/1007-9327/full/v21/i3/726.htm DOI: http://dx.doi.org/10.3748/wjg.v21.i3.726

INTRODUCTION

Endoscopic ultrasound (EUS) has evolved from a simple diagnostic procedure in the last two decades. This is in part due to the landmark study published by Wiersema[1], whom first used the EUS to guide a cholangiography to define the anatomy of the biliary tree. This shifting paradigm paper paved the ground for the subsequent evolution of the EUS as a powerful therapeutic tool. Giovannini *et al*[2] was the first article describing the use of EUS guiding biliary drainage, follow by Kahaleh *et al*[3] characterizing the "rendezvous" techniques.

Endoscopic transpapillary biliary drainage is the procedure of choice for biliary decompression in patients with unresectable pancreatic cancer associated to obstructive jaundice[3-6]. However, endoscopic retrograde cholangio-pancreatography (ERCP) failure can occur in 3%-10% of cases[3-5]. This failure can be due to operator inexperience, anatomic variation, tumor extension, prior surgery or incomplete drainage[3-9].

The indications for EUS-Guided biliary drainage include (1) failed conventional ERCP; (2) altered anatomy; (3) tumor preventing access into the biliary tree; and (4) contraindication to percutaneous access (*i.e.*, ascites, *etc.*). The Consensus guidelines for the management of biliary obstruction using EUS guided biliary drainage were reviewed and updated to reflect practice patterns, techniques and new indications among the field.

TECHNIQUES APPROACHES IN EUS-GUIDED BILIARY DRAINAGE

Access

Biliary drainage guided by EUS can be performed at two locations, depending on the level of access to the biliary system.

Intrahepatic: The intrahepatic biliary system can be reached either transesophageal, transgastric or transjejunal (in altered anatomy), being the biliary segment Ⅲ of the left hepatic lobe the most frequent and best visualized duct, especially when the EUS probe is placed at the stomach cardia and lesser curvature[9-11].

Extrahepatic: This technique can be performed having the needle accessing the common bile duct (CBD) directly, either using the transmural access from the antral part of the stomach or duodenum. In one hand, this approach provide not only a better visualization of the CBD, that some endoscopist considered advantageous at the time to select the route of access to the biliary system, but also due to the anatomical position of the CBD (located in the retroperitoneal space) might be safer in patients with ascites[10]. On the other hand, the major limitation for this technique is the difficulty inherent in the anterograde placement of the stent because of the angle of the needle entering the biliary duct.

Drainage

Rendezvous: Modality that allows advancing a guided wire through the papilla in antegrade fashion in which the bile duct is located and cannulated using the EUS rather than by retrograde cannulation with a duodenoscope. Technique especially used in those cases where biliary drainage is needed, ERCP failed and the duodenal anatomy allows the placement of the scope at the ampulla and the wire is identified traversing the papilla. Therefore, duodenal anatomy will determine the feasibility of the procedure, and that represent the main limitation[9].

Antegrade: In those cases where the luminal obstruction can not be overcome and the papilla is not visualized; but, the transpapillary wire access was obtained with EUS-guidance, then the alternative for biliary drainage is the antegrade placement of a biliary stent across the obstruction.

Transmural: Biliary drainage is obtained by creating a fistula in those cases where the wire cannot be positioned across the papilla due to either anomaly in the anatomy (biliary obstruction by a tumor) or technical complication (difficult position)[9].

ENDOSCOPIC ULTRASOUND-GUIDED BILIARY DRAINAGE

There is no consensus among the experts in the field of advance endoscopy regarding when to use EUS-BD, however, most of them can agree that failure in the use of conventional ERCP might be used as main explanation to justify the procedure, however, the indications for EUS-BD are not being established yet[12]. Therefore, EUS-BD has been rapidly being accepted as an alternative and reasonable option in those cases where bile duct cannulation cannot be achieved[11]. Either surgically altered anatomy (bariatric surgery or intestinal diversion for pancreatic cancer or other diseases) or obstruction of the gastrointestinal (GI) tract or bile duct (must often due to malignant causes) can be considered the principal causes for unsuccessful ERCP[13,14].

Most recent data reports that the accumulative success rate for extrahepatic EUS-BD (Table 1) is approximately

Table 1 Studies on extrahepatic endoscopic ultrasound-guided biliary drainage

Ref.	No./total sample	Method	Disease	Approach	Initial stent	Percent success rate	Complications
Giovannini *et al*[27] (2001)	1/1	Direct (1)	Malignant (1)	Duodenum	PS (1)	100	None
Burmester *et al*[6] (2003)	3/4	Direct (4)	Malignant (4)	Duodenum (2), stomach (1), jejunum (1)	PS (3)	75	Bile leak (1)
Mallery *et al*[28] (2004)	2/2	Rendez-vous (2)	Malignant (2)	Duodenum (2)	MS (2)	100	None
Lai and Freeman[29] (2005)	1/1	Rendez-vous (1)	Malignant (1)	Duodenum (1)	MS (1)	100	None
Püspök *et al*[13] (2005)	5/5	Direct (5)	Malignant (4), benign (1)	Duodenum (5)	PS (5)	80	Subacute phlegmonous cholecystitis (1)
Kahaleh *et al*[3] (2006)	10/23	Direct (2), rendez-vous (7)	Malignant (8), benign (2)	Duodenum (5), jejunum (5)	PS (4), MS (5)	90	Bile leak (1), pneumoperitoneum (2)
Yamao *et al*[20] (2006)	2/2	Direct (2)	Malignant (2)	Duodenum (2)	PS (2)	100	None
Ang *et al*[4] (2007)	2/2	Direct (2)	Malignant (2)	Duodenum (2)	PS (2)	100	None
Fujita *et al*[30] (2007)	1/1	Direct (1)	Malignant (1)	Duodenum (1)	PS (1)	100	None
Will *et al*[31] (2007)	8/8	Direct (8)	Malignant (7), benign (1)	Stomach (4), jejunum (3), esophagus (1)	PS (2), MS (5)	88	Slight pain (2), cholangitis (1)
Yamao *et al*[21] (2008)	3/3	Direct (3)	Malignant (3)	Duodenum (3)	PS (3)	100	Pneumoperitoneum (1)
Tarantino *et al*[19] (2008)	8/8	Direct (4), Rendez-vous (4)	Malignant (7), benign (1)	Duodenum (8)	PS (8)	100	None
Itoi *et al*[32] (2008)	4/4	direct (4)	Malignant (4)	Duodenum (4)	PS (3), NBD (1)	100	Focal peritonitis (1), bleeding (1)
Brauer *et al*[33] (2009)	12/12	Direct (4), Rendez-vous (7)	Malignant (8), benign (4)	NA	PS (5), SEMS (5)	92	Pneumoperitoneum (1), respiratory failure (1)
Horaguchi *et al*[14] (2009)	9/16	NA	Malignant (9)	Duodenum (8), stomach (1)	PS (14), plastic PT (1), NBT (1)	100	Peritonitis (1)
Hanada *et al*[17] (2009)	4/4	Direct (4)	Malignant (4)	Duodenum (4)	PS (4)	100	None
Maranki *et al*[34] (2009)	14/49	Direct (6), Rendez-vous (8)	Malignant (9), benign (5)	NA	NA	86	Biliary peritonitis (1), abdominal pain (1), pneumoperitoneum (1)
Kim *et al*[35] (2010)	15/15	Rendez-vous (15)	Malignant (10), benign (5)	Duodenum (15)	PS (4), MS (8)	80	Pancreatitis (1)
Nguyen-Tang *et al*[36] (2010)	1/5	Rendez-vous (1)	Malignant (1)	NA	MS (1)	100	None
Iwamuro *et al*[37] (2010)	7/7	Direct (7)	Malignant (7)	Duodenum (5), stomach (2)	PS (7)	100	Bile peritonitis (2)
Artifon *et al*[38] (2010)	3/3	Direct (3)	Malignant (3)	Duodenum (3)	MS (3)	100	None
Belletrutti *et al*[39] (2010)	1/1	Direct (1)	Malignant (1)	Duodenum (1)	MS (1)	100	None
Park do *et al*[40] (2011)	31/57	Direct (31)	Malignant (51), benign (6)	Duodenum (31)	PS (6), MS (25)	87	Pneumoperitoneum (6), mild bleeding (2)
Fabbri *et al*[41] (2011)	16/16	Direct (13), Rendez-vous (3)	Malignant (16)	Duodenum (15), stomach (1)	PS (4), MS (8)	80	Pancreatitis (1)
Hara *et al*[42] (2011)	18/18	Direct (18)	Malignant (18	NA	PS (17)	94	Peritonitis (2), bleeding (1)
Ramírez-Luna *et al*[43] (2011)	9/11	Direct (9)	Malignant (9)	Duodenum (9)	plastic DPT (9)	89	Biloma (1)
Siddiqui *et al*[44] (2011)	8/8	Direct (8)	Malignant (8)	Duodenum (80	MS (8)	100	Stent migration (1), duodenal perforation (1)
Komaki *et al*[45] (2011)	15/15	Direct (14), Rendez-vous (1)	Malignant (15)	Duodenum (15)	PS (15)	100	None
Prachayakul *et al*[46] (2011)	1/1	Direct (1)	Malignant (1)	Duodenum (1)	PS (1)	100	None
Artifon *et al*[22] (2012)	13/13	Direct (13)	Malignant (13)	Duodenum (13)	MS (13)	100	Bile leak (1), bleeding (1)
Attasaranya *et al*[47] (2012)	10/31	Direct (9), Antegrade (1)	Malignant (23), benign (8)	Duodenum	NA	60	4/10 (40%)
Katanuma *et al*[48] (2012)	1/1	Direct (1)	Benign (1)	Duodenum (1)	PS (1)	100	None
Kawakubo *et al*[49] (2012)	2/2	Direct (2)	Malignant (2)	Duodenum (2)	PS (2)	100	None
Khashab *et al*[50] (2012)	7/9	Direct (2), antegrade (2), Rendez-vous (3)	Malignant (7)	Duodenum (6), gastric (1)	MS (7)	100	Pancreatitis (1), cholecystitis (1), abdominal pain (1)
Kim *et al*[51] (2012)	9/13	Direct (9)	Malignant (9)	Duodenum (9)	MS (9)	100	Pneumoperitoneum (2), migration (2), peritonitis (1)
Song *et al*[52] (2012)	15/15	Direct (15)	Malignant (15)	Duodenum (15)	MS (15)	100	Pneumoperitoneum (2), cholangitis (1)
Dhir *et al*[53] (2012)	58/58	Rendez-vous (58)	Malignant (43), benign (15)	Duodenum (58)	NA	98	Bile leak (2)

Hara *et al*[54] (2013)	18/18	Direct (18)	Malignant (18)	Duodenum (18)	MS (18)	94	Bile peritonitis (2)
Park do *et al*[55] (2013)	16/45	Direct (2), Rendez-Vous (14)	Malignant (39), benign (6)	Duodenum (16)	MS (16)	88	Pancreatitis (1), bile peritonitis (1)
Itoi *et al*[56] (2013)	1/1	Direct (1)	Malignant (1)	Stomach (1)	MS (1)	100	None
Total	365					338/365 (93%)	58/365 (16%)

Table 2 Studies on intrahepatic endoscopic ultrasound-guided biliary drainage

Ref.	No./total sample	Method	Disease	Approach	Initial stent	Percent success rate	Complications
Burmester *et al*[6] (2003)	1/4	Direct (1)	Malignant (1)	Stomach (1)	PS (1)	100	Bile leak (1)
Püspök *et al*[13] (2005)	1/1	Direct (1)	Malignant (1)	jejunum (1)	PS (1), MS (1)	100	None
Kahaleh *et al*[3] (2006)	13/23	Direct (1), Rendez-vous (12)	Malignant (9), benign (4)	Stomach (13)	PS (6), MS (6)	92	Minor bleeding (1)
Bories *et al*[16] (2007)	11/11	Direct (9), Antegrade (2)	Malignant (3), benign (8)	Stomach (3), Duodenum (3), stenosis (5)	PS (7), MS (3)	91	Transient ileus (1), biloma (1), cholangitis (1)
Horaguchi *et al*[14] (2009)	7/16	NA	Malignant (7)	Stomach (5), esophagus (2)	PS (2), MS (5)	100	None
Maranki *et al*[34] (2009)	35/49	Direct (9), Antegrade (24)	Malignant (26), benign (9)	NA	NA	83	Bleeding (1), pneumoperitoneum (3), aspiration pneumonia (1)
Nguyen-Tang *et al*[36] (2010)	4/5	Rendez-vous (4)	Malignant (3), benign (1)	Duodenum (1), Stomach (3)	MS (5)	100	None
Park do *et al*[40] (2011)	31/57	Direct (31)	Malignant (51), benign (6)	Duodenum (31)	PS (6) MS (25)	87	Pneumoperitoneum (1), bile peritonitis (2)
Ramírez-Luna *et al*[43] (2011)	2/11	Direct (2)	Malignant (2)	Stomach (2)	PS (2)	100	Stent migration (1)
Attasaranya *et al*[47] (2012)	16/31	Direct (16)	Malignant (23), benign (8)	NA	NA	81	6/16 (38%)
Khashab *et al*[50] (2012)	2/9	Antegrade (1), rendez-vous (1)	Malignant (2)	Stomach	MS (2)	100	Nausea (1)
Kim *et al*[51] (2012)	4/13	Direct (4)	Malignant (4)	Stomach (4)	MS (3)	75	Peritonitis (1), stent migration (1)
Park do *et al*[55] (2013)	29/45	Direct (9), antegrade (14), rendez-vous (5)	Malignant (39), benign (6)	Stomach (29)	NA	66	Biloma (1)
Iwashita *et al*[57] (2013)	6/6	Direct (1)	Malignant (1), benign (5)	NA	MS (1)	100	Pancreatitis (1), abdominal pain (1)
Total	162					136/162 (84%)	26/162 (16%)

93% over the last 12 years[3,4,6,13-56], and in case of intrahepatic EUS-BD (Table 2) the cumulative success rate published is 84%[3,6,13,14,34,36,40,43,47,50-52,57]. However, data from two large multicenter retrospective trials failed to report advantages of any of these techniques[58,59].

EUS-guided rendezvous

This procedure is performed inserting a needle under EUS and doppler guidance into either left intrahepatic duct or common bile duct. Here, the FNA needle will permit also the advance of guidewire distally into the duodenum. Upon insertion of the needle into the duct, suspected by EUS imaging, the aspiration of the bile will confirm the intraductal placement of the needle, which is follow by injection of contrast drawing the biliary tree (cholangiogram). Next, the insertion of the guidewire through the FNA needle toward the duodenum and perform the conversion to a conventional ERCP in a retrograde fashion. If by any reason the transpapillary passage is not successfully accomplish, then the FNA needle need to be replaced by the sphincterotome or dilating bougie, allowing the manipulation of the wire freely and safely to facilitate the passage through the ampulla. At this point, the EUS scope is removed leaving the wire in the duodenum and the duodenoscope is advanced to the ampulla where the guidewire can be grasped using a snare or forceps and pulled it back through the working channel of the duodenoscope and permit the subsequent over-the-wire cannulation or alternately use the duodenoscope to cannulate the common bile duct next to the prior placed guidewire. Now the procedure can be completed by conventional endoscopic retrograde cholangiography with stent placement in retrograde manner[11].

EUS-guided choledochoduodenostomy vs other techniques (percutaneous transhepatic cholangiography and surgical drainage)

Burmester *et al*[6] described a one-step method using a new device consisted of a 19 gauge fistulotome with a 0.25-inch

guidewire, a pusher tube and an 8.5F plastic stent fixed with a 3.0 nylon-suture. This method of direct puncture of the extrahepatic or an intrahepatic duct could reduce the risk of guidewire dislocation during the instrument change, what must be made with the two-step method[17]. However, more studies with this device are needed.

EUS-guided biliary drainage has many advantages over PTBD[3,4,16,17]. The proximity of the transducer to the bile duct during EUS is the major advantage[3,19]. Even in patients who have undergone total gastrectomy or partial gastrectomy with a Billroth Ⅱ reconstruction, EUS can reveal the etiology of extrahepatic cholestasis, situations in that ERCP may not be possible[1,3,4,15,16]. Other advantages include puncture of the biliary tree with color-Doppler information to avoid vascular injury, the lack of ascites in the interventional field and the lack of an external tube, improving the quality of life of the patients[4,20].

Choledochoduodenostomy can prevent clogging and tumor ingrowth and/or overgrowth, because it creates a fistula far from the obstructing tumor[20,21]. Many studies described this procedure with high success rates (more than 90%) and low rate of procedure-related complications (around 19%)[18]. The main risk of EUS-guided biliary drainage is bile leakage, especially if stent insertion is unsuccessful[4]. Burmester *et al*[6] reported the failure of stent placement in 1 of their 4 patients, causing bile peritonitis[17]. They also reported that only local peritonitis developed, which did not contribute to the death of the patient. Some investigators recommend the transhepatic approach to decrease the risk of biliary peritonitis in case of stent failure[17]. Other complications include pneumoperitoneum and minor bleeding[4,5,1].

EUS-guided choledochoduodenostomy for malignant biliary obstruction has been shown to be an effective alternative to PTBD or surgery when ERCP fails. Artifon *et al*[22] compared EUSCD and PTC in 25 patients with distal biliary malignant obstruction. The 2 groups were similar before intervention in terms of quality of life [EUS-CD (58.3) *vs* PTBD (57.8), $P = 0.78$], total bilirubin (16.4 *vs* 17.2, $P = 0.7$), alkaline phosphatase (539 *vs* 518, $P = 0.7$), and gamma-glutamyl transferase (554.3 *vs* 743.5, $P = 0.56$). All procedures were technically and clinically successful in both groups. The study concluded that EUS-CD can be an effective and safe alternative to PTBD with similar success, complication rate, cost, and quality of life.

Another Study conducted by Artifon *et al*[23] showed results on comparative trial between EUS CD and surgery to patients with biliary distal cancer. There was no significant difference in the technical and clinical outcomes in the two groups. Cost analysis demonstrated a significantly increased cost per patient in the surgical group ($P = 0.039$). Complications were significantly higher in the surgical group ($P = 0.041$). There was one case of self-limited bleeding on group EUSCD and one case each of wound abscess, abdominal abscess, internal fistula and pneumonia on group Surgery. All patients in surgical group were managed conservatively.

ENDOSCOPIC ULTRASOUND-GUIDED PANCREATICO-GASTROSTOMY

Main indications are stenosis of pancreatico-jejunal or pancreatico-gastric anstomosis after Whipple resection, which induce recurrent acute pancreatitis, main pancreatic duct stenosis due to chronic pancreatitis, post-acute pancreatitis or post pancreatic trauma after failure of ERCP. EUS guided pancreatico-gastro or bulbostomy offers an alternative to surgery (Figure 1).

By using a linear interventional echoendoscope, the dilated main pancreatic duct (MPD) was well visualized. Endoscopic pancreatico-gastrostomy (EPG) was then performed under combined fluoroscopic and ultrasound guidance, with the tip of the echoendoscope positioned such that the inflated balloon was in the duodenal bulb while the accessory channel remained in the antrum. A needle was inserted transgastrically into the proximal pancreatic duct and contrast medium was injected. Opacification demonstrated a pancreaticogram the needle was exchanged over a guidewire, which was then used to enlarge the channel between the stomach and MPD. The sheath was introduced by using cutting current. After exchange over a guidewire (rigid 0.035 inch diameter), a 7F, 8-cm-long pancreaticogastric stent was positioned. This stent will be exchanged for two 7F or one 8.5F stents one month after the first procedure.

The results of the fours series[3,24-26] of patients published are much too preliminary in nature to recommend wider use of EPG, which in any case should be restricted to tertiary centers specializing in biliopancreatic therapy with a pain relief in 70% of cases. But the complication rate is still high around 15% including bleeding, pancreatic collection and perforation. The largest series was published by Tessier *et al*[24] on 36 patients. Indications were chronic pancreatitis, with complete obstruction (secondary to a tight stenosis, a stone, or MPD rupture); inaccessible papilla or impossible cannulation ($n = 20$); anastomotic stenosis after a Whipple procedure ($n = 12$); complete MPD rupture after acute pancreatitis (AP); or trauma ($n = 4$). EPG or EPB was unsuccessful in 3 patients; 1 was lost to follow-up. Major complications occurred in 2 patients and included 1 hematoma and 1 severe AP. The median follow-up was 14.5 mo (range: 4-55 mo). Pain relief was complete or partial in 25 patients (69%, intention to treat). Eight patients treated had no improvement of their symptoms (4 were subsequently diagnosed with cancer). Stent dysfunction occurred in 20 patients (55%) and required a total of 29 repeat endoscopies. The last study published by Ergun *et al*[26] reported the long-term follow-up (37 mo) of 18 patients who underwent a EUS guided pancreatico-gastrostomy. Stent occlusion occurred in 50%, pain relief was always present in 70% and the mean pain score decreased

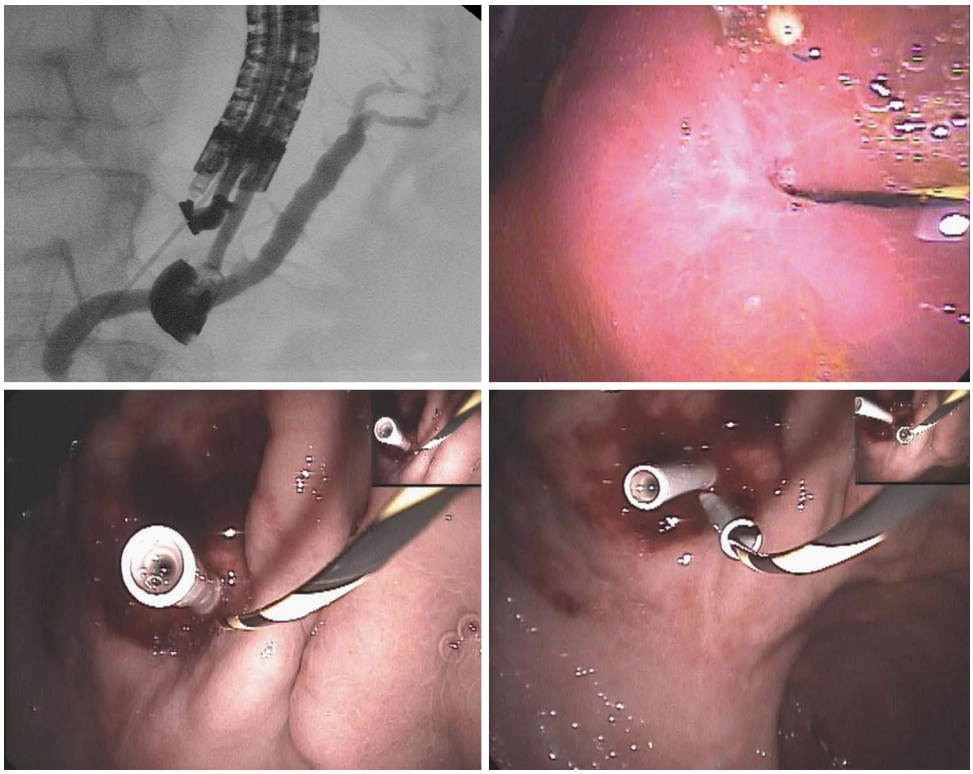

Figure 1 Pancreatico-gastrostomy/stenosis of a wirsung-gastro anastomosis after whipple resection for benign cystic lesion of the head of the pancreas.

dramatically from 7.5 to 1.6.

It's very difficult to find today the place of EGD in our experience the best indication is anastomotic stenosis after Whipple procedure for benign pancreatic lesions (cystadenoma, IPMN, NET). EGD offers an alternative to surgery and the best results in the 3 series published (Table 3) were showed in this indication. In another hand, surgery should be considered as the elective treatment of CP after failure of the endoscopic route.

ENDOSCOPIC ULTRASONOGRAPHY-GUIDED CHOLECYSTODUODENOSTOMY AND CHOLECYSTOGASTROSTOMY

Revised Tokyo Guideline (TG13) proposes that early or emergency cholecystectomy should be conducted as the gold standard of treatment for acute cholecystitis[60-63]. In general, cholecystectomy is relatively safe. However, the mortality rate of cholecystectomy in patients at high risk due to comorbid conditions is not lower than in non-critical ill patients[64,65]. Therefore, several literatures advocates that high-risk patients should be tentatively treated by decompress the gallbladder, *e.g.*, percutaneous transhepatic gallbladder drainage (PTGBD), percutaneous transhepatic gallbladder aspiration, endoscopic transpapillary gallbladder drainage[66-69]. Recently, as a novel translumenal access, endoscopic ultrasonography-guided gallbladder drainage (EUS-GBD) has been performed.

Technique of EUS-guided gallbladder drainage

The gallbladder is visualized from the duodenal bulb or the antrum of the stomach using a curved linear array echoendoscope in a long scope position (pushing scope position)[69].

After depiction of neck and body of the gallbladder, a 19-gauge needle is inserted transduodenally or transgastrically into the gallbladder under EUS visualization. After the stylet is removed, bile is aspirated approximately 3 cc and same 3 cc contrast medium is then injected to confirm the tip of a needle is in the gallbladder. Then, a 0.025-inch or 0.035-inch guidewire was inserted through the 19-gauge needle and looped in the gallbladder. A biliary catheter for dilation up to 8-Fr or 4-mm to 6-mm papillary balloon dilator if necessary, are used for dilation of the cholecystoentero fistula. Finally, a 5-8.5-Fr pigtail type naso-gallbladder drainage catheter, double pigtail type plastic stent, or fully-covered self-expandable metal stent are inserted through the gastric or duodenal fistula into the gallbladder.

Ten reports describe the outcome of EUS-guided gallbladder drainage (Table 4)[70-81]. In total, the technical success and clinical success rate were 98.7% (74/74) and 100% (74/74), respectively. As a first puncture, a 19-gauge needle was mainly used. A 5- to 8.5-F plastic stents or naso-gallbladder catheters were used for drainage. In 2 institutions, dedicated fully-covered metal stents, which had double flanges were used.

As an adverse events, 6 of self-limited pneumoperitoneum, 2 of bile leakage, and 1 distal stent migration without bile

Table 3 Studies on endoscopic ultrasound-guided pancreatico-gastrostomy

Ref.	NB PTS	Success	Complication	Follow-up
Tessier *et al*[24] (2007)	36	70%	11%	16.5 mo
Kahaleh *et al*[3] (2006)	13	92%	16%	14 mo
Barkay *et al*[25] (2010)	21	48%	2%	13 mo
Ergun *et al*[26] (2011)	20	90%	10%	37 mo

leakage 3 wk after stent insertion. Interestingly, Jang *et al*[79] conducted randomized control study, PTGBD *vs* EUS-guided naso-gallbladder drainage (EUS-NGBD). EUS-NGBD and PTGBD showed similar technical [97% (29/30) *vs* 97% (28/29); 95%] and clinical [100% (29/29) *vs* 96% (27/28)] success rates, and similar rates of complications [7% (2/30) *vs* 3% (1/29)]. The median post-procedure pain score was significantly lower after EUS- NGBD than after PTGBD (1 *vs* 5, $P < 0.001$). On the basis of the results, they suggested that EUS-NGBD is comparable with PTGBD in terms of the technical feasibility and efficacy; there were no statistical differences in the safety. EUS-GBD is a good alternative for high-risk patients with acute cholecystitis who cannot undergo an emergency cholecystectomy.

EUS-guided gallbladder drainage has been developed as an alternative drainage method for acute cholecystitis. However, there are several limitations of this procedure. One of the big issues is that basically there is no adhesion and relatively distance between the GI tract including gastric and duodenal wall and the gallbladder wall. In addition, tubular biliary plastic and metal stents for biliary decompression have significant shortcomings when used for transenteric drainage. Plastic stents have the disadvantage of a small lumen diameter, which can limit drainage and may necessitate reintervention. Currently available SEMSs have a larger lumen diameter but may show inward and outward migration. Furthermore, abutment of the end of a tubular SEMS against the lumen wall may cause tissue injury and bleeding. Although serious adverse events have never been reported, we should consider the possibility of such unexpected events.

Recently, Itoi *et al*[78] de la Serna-Higuera *et al*[80] and Jang *et al*[79] reported a newly designed fully-covered metallic stent with anchor for EUS-guided gallbladder drainage. These dedicated devices may suggest that this procedure is becoming safer and more reliable. That causes reducing the risk of serious complications like bile leakage and stent migration.

SURGICALLY ALTERED ANATOMY

Surgery of the upper gastrointestinal (GI) tract involving change in the configuration of the antro-duodenal C-loop is commonly referred to as postoperative or surgically altered anatomy (SAA). Obesity surgery, peptic ulcer disease, iatrogenic bile-duct injury and chronic pancreatitis are common benign causes of SAA. Gastric, biliary and pancreatic malignancies also lead to radical resections with curative intent or to palliative bypass procedures resulting in SAA. Interventions performed for both benign and malignant disease include Billroth Ⅱ, variations on the Whipple operation, and Roux-en-Y reconstructions, either with intact papillae[82] or with bilio-enteric anastomoses[83]. Most of these interventions result in long afferent limbs of small bowel (jejunum) impairing endoscopic access to the papilla.

Indications for biliary drainage in SAA patients

More insidious biliary obstructive symptoms caused by recurrent malignancy are seen in afferent limb syndrome, a condition difficult to diagnose and challenging to treat[84]. Obesity and weight loss are associated with common bile duct stones. Gallstones are almost always present in patients undergoing cholecystectomy, which is the major cause of bile-duct injury. Chronic reflux of GI contents across widely patent bilio-enteric anastomoses causes sump syndrome and stone formation. Leakage or anastomotic strictures may develop acutely after bilio-digestive bypass surgery. Anastomotic strictures more commonly cause chronic cholestasis and/or recurrent cholangitis over the long-term, with a reported incidence up to 30% after a mean follow-up of six years[85].

Dominant ERCP strategies in SAA

Access to the papilla and ease of en-face view are nearly normal in some cases with past SAA for benign conditions, such as Billroth I for peptic ulcer or choledochoduodenostomy for common bile duct stones. Nowadays, experienced operators report similarly high success rates for duodenoscope-based ERCP in patients with Billroth Ⅱ. Whipple and Roux-en-Y reconstructions, particularly Roux-en-Y gastric by-pass (RYGB) for obesity, have ultra-long afferent limbs. Special endoscopes are usually required to access the proximal afferent limb for ERCP in these patients. Balloon or spiral enteroscopes are currently used at expert centers[86]. Enteroscopy-based ERCP is nonetheless a labor-intensive procedure with limited overall success rates of 60%. Seventy-five percent of failures occur because the papilla or bilio-enteric anastomosis cannot be identified, cannulated or drained, even despite successful limb intubation[86,87]. These figures underscore the limitations to ERCP using long, narrow channel, forward viewing enteroscopes.

An alternative approach to enteroscopy-based ERCP in long limb SAA patients is percutaneous transenteric access under open[6] or laparoscopic[88] surgical assistance. Typically, laparoscopic surgeons access the distal gastric remnant of RYGB, allowing intraoperative transgastric insertion of a duodenoscope and antegrade ERCP[87-89]. Bariatric procedures involving distal gastrectomy are less readily amenable to laparoscopically-assisted ERCP, often requiring open surgery for duodenoscope passage[87]. The complex logistics of intraoperative ERCP help understand its limited dissemination. It should be noted nonetheless that higher success rates have been reported with laparoscopy-assisted transgastric ERCP compared

Table 4 Summary of published data on endoscopic ultrasound-guided gallbladder drainage

Ref.	No. of cases	Device for puncture	Approach route	Technical success	Clinical success	Stent	Complication (No. of cases)
Baron *et al*[70] (2007)	1	19 G FN	TD	100%	100%	7F PS	None
Kwan *et al*[71] (2007)	3	19 G FN/FT/CT	TD	100%	100%	8.5F NBD	Bile leakage (1)
Lee *et al*[72] (2007)	9	19 G FN	TD	100%	100%	5F NBD	Pneumoperitoneum (1)[1]
Kamata *et al*[74] (2009)	1	19 G FN	TG	100%	100%	7F PS	None
Takasawa *et al*[73] (2009)	1	NK	TG	100%	100%	7F PS	None
Song *et al*[75] (2010)	8	19 G FN +/- NK	1TG/7TD	100%	100%	7F PS	Bile Leakage (1), pneumoperitoneum (1), stent migration (1)
Súbtil *et al*[81] (2010)	4	CT/NK	TG	100%	100%	8.5F PS	None
Jang *et al*[77] (2011)	15	19 G FN/NK	10TG/5TD	100%	100%	New SEMS	Pneumoperitoneum (2)
Jang *et al*[79] (2012)	30	19 G FN/NK	TG/TD	97%	100%	5F NBD	Pneumoperitoneum (2)
Itoi *et al*[78] (2012)	5	19 G FN/1 CT	1TG/4TD	100%	100%	New SEMS	Mild bleeding (1)
de la Serna-Higuera *et al*[80] (2013)	13	CT	12TG/1TD	84.6%	100%	New SEMS	Hematochezia (1/11), pain (1/11)

[1]Minor bile leakage without serious bile peritonitis. G: Gauge; NK: Needle knife; FT: Fistulotome; CT: Cystotome; PS: Plastic stent; NBD: Naso-Gallbladder Drain; TD: TransDuodenal; Approach TG: TransGastric approach; Partially covered SEMS: Partially cover self expandable metallic stent.

to enteroscopy ERCP in RYGB patients, especially when Roux limbs are longer than 150 cm from the ligament of Treitz to the jejuno-jejunal anastomosis[90].

Non-standard approaches to ERCP in SAA

Prior indwelling transenteric feeding tubes may allow percutaneous ERCP through mature tracks in the occasional SAA patient. A standard duodenoscope was passed percutaneously into the jejunum after jejunostomy track dilation and ERCP with sphincterotomy was performed uneventfully in a patient with Roux-en-Y gastrectomy[91]. However, a two-step approach is usually required in RYGB. Gastrostomy to the distal gastric remnant is first performed for the purpose of providing a conduit for duodenoscope passage, so that elective ERCP can be carried out through the mature gastrostomy track 2-4 wk later. In this two-step approach, percutaneous gastrostomy to the remnant stomach can be performed by surgery[92-94], interventional radiology[95] or endoscopy[96]. In keeping with data from the intraoperative transgastric approach, ERCP success rates using this two-step percutaneous transgastric approach are significantly higher than success rates for enteroscopy-based ERCP[94]. Complications related to the gastrostomy are however not negligible[93,94]. Successful therapeutic ERCP through gastrostomy to the remnant stomach placed by interventional radiology has been reported in a single RYGB case[95]. However, radiographically guided percutaneous access to the non-distended remnant stomach entails risk and difficulty. EUS-guided puncture and distension of the remnant stomach from the proximal gastric pouch by injecting contrast and air appears to facilitate percutaneous radiographic gastrostomy[97]. Double-balloon enteroscopy retrograde access to the remnant stomach for PEG placement prior to transgastric antegrade ERCP appears a reasonable option, given the high failure rate of enteroscopy-based ERCP even after successful limb intubation. Retrograde enteroscopy PEG placement has been reported as the initially chosen approach for ERCP in RYGB[96], and it might become a convenient same-session salvage procedure in cases of failed enteroscopy ERCP despite successful limb intubation.

Antegrade endoscopic access to the gastric remnant through spontaneous gastro-gastric communications across the staple line has successfully used for ERCP in two RYGB patients. The defect was large enough to allow passage of a duodenoscope for sphincterotomy and stone removal in one case[98]. Another patient, however, required balloon dilation. A covered self-expandable esophageal stent was placed across the staple line to provide a conduit for iterative ERCP. Once final resolution of a benign biliary stricture was achieved, the transgastric covered stent was removed[99]. The concept of temporary covered metal stents serving as conduits for endoscope passage and therapeutic ERCP has also been applied to the percutaneous[96,100,101] or transluminal EUS-guided routes[102].

Afferent loop syndrome resulting in chronic biliary obstruction caused by recurrent malignancy is an increasingly frequent clinical problem. Palliation often involves permanent percutaneous drains, which adversely impact quality of life[84]. A novel EUS-based approach was used at two different institutions in three patients. The distended afferent loop was punctured from the distal antrum or duodenum, and a double plastic pigtail placed transmurally. Cholangitis or cholestasis resolved in all three case[103,104].

EUS-guided access and drainage routes in SAA

EUS-guided biliary drainage (EUSBD) is carried out by any of three possible routes, transmural, transpapillary antegrade or transpapillary retrograde (rendezvous) encompassed under a procedure hybrid between EUS and ERCP known as endosonography-guided cholangiopancreatography (ESCP)[105]. Patients with SAA represent around a fourth of cases in both current[55,58,106] and early[2,6,13] ESCP series inclusive of both intrahepatic and extrahepatic EUS-guided access (Table 5). Patients with SAA are not present however in ESCP series reporting predominantly on choledocho-duodenostomy

Table 5 Outcomes of biliary drainage in endosonographic cholangiopancreatography series including surgically altered anatomy patients *n* (%)

Ref.	*n*	Patients with SAA	Overall technical success	Type of ESCP drainage				Complications
				Transpapillary		Transmural		
				RV	AG	HG	CD	
Will *et al*[31] (2007)	8	7 (87)	7 (87)	1	-	6	-	2 (25)
Bories *et al*[16] (2007)	11	4 (36)	10 (91)	-	-	10	-	4 (36)
Horaguchi *et al*[14] (2009)	16	4 (25)	16 (100)	-	-	8	8	2 (12)
Maranki *et al*[34] (2009)	49	7 (14)	41 (84)	20[1]	14[1]	3	4	8 (16)
Shah *et al*[106] (2012)	68	19 (28)	58 (85)	39[2]	10[2]	8	1	6 (9)
Iwashita *et al*[118] (2012)	40	9 (40)	29 (73)	29	-	-	-	5 (13)
Park *et al*[55] (2013)	45	14 (31)	41 (95)	16	9	14	2	5 (11)
Total	237	64 (27)	202 (85)	105	33	49	15	32 (13)
				138 (68)		64 (32)		

[1]Not specified in the original report, data provided by the author; [2]Not specified in the original report. Data estimated from prior detailed series[48]. SAA: Surgically altered anatomy; ESCP: Endosonographic cholangiopancreatography; RV: Rendezvous; AG: Antegrade; HG: Hepatico-gastrostomy; CD: Choledochoduodenostomy.

or extrahepatic rendezvous, which represent two thirds of the total ESCP cases reported[105]. Direct drainage routes (transmural and antegrade transpapillary) are typically chosen for EUSBD in patients with SAA instead of rendezvous. The ability to endoscopically reach the papilla is a requisite for rendezvous, and in most patients with SAA the reason for ERCP failure dictating the need for ESCP is precisely failed access to the papilla. EUS rendezvous has nonetheless been attempted in patients with past Billroth Ⅱ from an extrahepatic[107] or an intrahepatic[108] approach to extract CBD stones or to relieve malignant obstruction.

The dominant EUS-guided access route in SAA patients is intrahepatic into the left hepatic duct branches from the cardia region: either transgastric from the proximal stomach, transesophageal from the abdominal esophagus, or transjejunal in patients with esophago-jejunostomy[31]. Even if left intrahepatic duct branches are less obvious target for EUS-guided puncture than the CBD, the rationale for it in SAA patients is strong. SAA frequently involves distal gastrectomy, as in Roux-en-Y gastrectomy for gastric cancer, or an excluded distal stomach, as in RYGB for obesity. As the CBD is typically imaged under EUS from the distal antrum or the duodenal bulb, extrahepatic EUS-guided access is usually not possible in SAA. An exception to this rule would be the occasional patient with distal biliary obstruction in whom the common hepatic duct can be imaged and accessed under EUS from the mid stomach. This frequently overlooked transgastric access site into the proximal extrahepatic bile duct may be useful in those SAA patients without dilated intrahepatics. Kahaleh *et al*[107] reported this option in 2 out of their first 5 cases. Another potentially useful secondary EUS-guided access route in highly selected SAA patients with intact stomach and proximal biliary obstruction but no left intrahepatic dilation, would be transduodenal from the bulb into the right hepatic duct or its branches. This recently reported access site was chosen in 6 cases with selective right intrahepatic dilation not amenable to standard left intrahepatic or extrahepatic access. Three of these 6 patients had Roux-en-Y hepaticojejunostomy. Hepaticoduodenostomy and antegrade transanastomotic intervention (stenting and balloon dilation) were used to carry out drainage[109]. EUSBD in patients with SAA usually involves transmural or antegrade transpapillary (or transanastomotic) stenting after left intrahepatic duct puncture. Exceptions to these general rules may nonetheless allow salvage of specific patient subsets, such as secondary access sites for those without left intrahepatic dilation[109] or retrograde rendezvous drainage for those requiring cross-over after failed antegrade or transmural ESCP approaches[55,106]. EUSBD has been reported to date in around a hundred patients with SAA. Only two small series focus specifically on EUSBD in SAA[57,110], patient specifics can be traced to procedural approach and outcomes in just 47 cases, 22 malignant (Table 6) and 25 benign (Table 7).

ESCP interventions for malignant biliary obstruction in SAA

Recurrent gastric, pancreatic and biliary malignancy after surgical resection usually present as obstructive jaundice. Roux-en-Y gastrectomy or hepatico-jejunostomy, pancreatico-duodenectomy and palliative bypass gastro-jejunostomy are the most commonly SAA encountered. PTBD has been classically used in this setting, as it is much simpler and more readily available than the combinations of surgical, percutaneous or enteroscopy-based ERCP described earlier. Two important limitations of PTBD in these patients are failure to provide internal biliary drainage occasionally[16] and the management of relapsing stent dysfunction[2].

As in other settings, EUSBD may overcome those limitations, improving management in patients with SAA and malignant biliary obstruction over that afforded by PTBD. Internal biliary drainage has been provided by hepaticogastrostomy (n = 10) or any of its variants (n = 7), with either plastic or metal stents placed in about half of the cases each (Table 6). Transmural metal stent

Table 6 Patients with malignant biliary obstruction and surgically altered anatomy drained by endosonographic cholangiopancreatography

Ref.	No. of patients[1]	Type of SAA				Etiology			Type of ESCP drainage[2]				Success/complex[4]	
									Transpapillary		*Transmural*			
		RYG	RYHJ	PD	Other	Gast	Panc	Other	RV	AG	HG	Other[3]	Sn	Cn
Burmester *et al*[6] (2003)	2/4	1	-	-	1	1	1	-	-	-	1 (0)	1 (0)	2/2	0
Giovannini *et al*[2] (2003)	1/1	1	-	-	-	1	-	-	-	-	1 (1)[5]	-	1/1	0
Püspök *et al*[13] (2005)	1/6	1	-	-	-	1	-	-	-	1 (1)	-	1 (0)[6]	1/1	0
Kahaleh *et al*[3] (2006)	2/23	-	-	-	2	-	1	1	2 (1)	-	-	-	2/2	0
Will *et al*[31] (2007)	6/8	4	1	1	-	4	-	2	-	-	3 (3)	3 (1)	5/6	2
Bories *et al*[16] (2007)	1/11	-	-	1	-	-	1	-	-	-	1 (0)	-	1/1	0
Horaguchi *et al*[14] (2009)	4/16	-	2	-	2	1	1	2	-	-	2 (2)[5]	2 (1)[5]	4/4	1
Chopin-Laly *et al*[115] (2009)	1/1	-	-	-	1	-	1	-	-	-	1 (1)	-	1/1	0
Nguyen-Tang *et al*[36] (2010)	1/5	-	1	-	-	-	-	1	-	1 (1)	-	-	1/1	0
Ma *et al*[117] (2011)	1/1	-	-	1	-	-	-	1	-	-	1 (0)	-	1/1	0
Henry *et al*[116] (2011)	1/1	-	-	-	1	-	-	1	-	-	-	1 (0)[7]	1/1	1
Iwashita *et al*[118] (2012)	1/7	1	-	-	-	1	-	-	-	1 (1)	-	-	1/1	1
Total	22	8	4	3	7		5	8	2 (1)	3 (3)	10 (7)	7 (1)		
		22				9 (40%)	13 (60%)		5 (23%)		17 (77%)		21 (95%)	5 (23%)

[1]Number of surgically altered anatomy (SAA) patients with malignant biliary obstruction per total number of patients in the series; [2]Number of patients with attempted stent placement (ITT), followed by number of metal stents in parentheses; [3]Transmural variants of HG (hepatico-esophagostomy/jejunostomy) following intrahepatic access, except when stated otherwise; [4]Number of successful cases or complications per number of SAA patients with malignant biliary obstruction; [5]Initial plastic stent replaced at follow-up. Only final stent tallied in the total count; [6]Additional hepato-esophageal plastic stent combined with AG metal stent in recurrent gastric cancer after RYG. Not tallied in the total count; [7]Choledochoduodenostomy after palliative gastrojejunostomy. SAA: Surgically altered anatomy; ESCP: Endosonographic cholangiopancreatography; RYG: Roux-en-Y gastrectomy; RYHJ: Roux-en-Y hepatico-jejunostomy; PD: Pancreatico-duodenectomy; Gast: Gastric; Panc: Pancreatic; RV: Rendezvous; AG: Antegrade; HG: Hepatico-gastrostomy; ITT: Intention-to-treat; Sn: Successful cases; Cn: Complications.

Table 7 Patients with benign biliary obstruction and surgically altered anatomy drained by endosonographic cholangiopancreatography

Ref.	No. of patients[1]	Type of SAA				Etiology		Type of ESCP drainage					Success/complex[5]	
								Transpapillary[2]			*Transmural*[3]			
		RYG	RYGB	RYHJ	Other	Stone	Strx	RV	AGS	AGB	HG	Other[4]	Sn	Cn
Püspök *et al*[13] (2005)	1/6	-	-	-	1	1	-	-	-	-	-	1 (0)[6]	1/1	0
Kahaleh *et al*[3] (2006)	2/23	-	-	1	1	1	1	2	-	-	-	-	1/2	1
Will *et al*[31] (2007)	1/8	-	-	1	-	-	1	1[7]	-	-	-	1 (0)	1/1	0
Bories *et al*[16] (2007)	3/11	-	-	-	3	-	3	1[7]	-	-	3 (1)	-	2/3	1
Weilert *et al*[110] (2011)	6/6	-	6	-	-	6	-	2	-	4	-	-	6/6	1
Artifon *et al*[112] (2011)	1/1	-	-	1	-	-	1	-	1	1[9]	-	-	1/1	0
Park *et al*[113] (2012)	1/1	-	-	1	-	-	1	-	-	1	-	-	1/1	0
Bapaye *et al*[114] (2012)	1/1	-	-	1	-	-	1	-	-	1	-	-	1/1	0
Iwashita *et al*[57] (2013)	6/7	4	-	-	2	5	1	-	-	5[9]	-	-	6/6	1
Park *et al*[109] (2013)	3/6	-	-	3	-	-	3	-	1	3[8]	-	-	2/3	0
Total	25	4	6	8	7			6	2	13	3 (1)	2 (0)		
		25				13 (52%)	12 (48%)		21 (84%)		5 (20%)		22 (88%)	4 (16%)

[1]Number of surgically altered anatomy (SAA) patients with benign biliary obstruction per total number of patients in the series; [2]Number of patients with attempted drainage by stent insertion and/or balloon dilation with/without stone removal (ITT); [3]Number of patients with attempted stent placement (ITT), followed by number of metal stents in parentheses; [4]Transmural variants of HG (hepatico-esophagostomy/jejunostomy) following intrahepatic access, except when stated otherwise; [5]Number of successful cases or complications per number of SAA patients with benign biliary obstruction; [6]Choledochoduodenostomy with plastic stents used for transmural stone extraction in Billroth I; [7]Transpapillary AG metal stent placed at follow-up of prior transmural intrahepatic stenting in anastomotic Strx. Tallied in the total count; [8]AGB prior to AGS in a single case. AGS tallied as main intervention and AGB not tallied in the total count; [9]AGB with stone removal plus temporary NBD placement in four patients. AGB of anastomotic Strx and normal cholangiogram in one each. SAA: Surgically altered anatomy; ESCP: Endosonographic cholangiopancreatography; RYG: Roux-en-Y gastrectomy; RYGB: Roux-en-Y gastric bypass; RYHJ: Roux-en-Y hepatico-jejunostomy; RV: Rendezvous; AGS: Antegrade stent insertion; AGB: Antegrade balloon dilation; HG: Hepatico-gastrostomy; ITT: Intention-to-treat; Sn: Successful cases; Cn: Complications.

placement carries the risk of severe bile leakage into the peritoneum caused by stent foreshortening[16]. This risk can be minimized by initial placement of transmural plastic stents followed by elective stent exchange after track maturation[2,14,16]. The recommended technique for plastic stent replacement after transmural EUSBD is over-the-wire snare removal after guide-wire cannulation of the stent[14,111]. The snare over-the-wire technique prevents track disruption and avoids the need for a repeat transhepatic (PTBD or EUSBD) puncture should stent occlusion lead to dysfunction.

As an alternative to transmural stenting, transductal

(transpapillary or transanastomotic) stent placement has been reported in just five patients with SAA and malignant biliary obstruction, by means of rendezvous ERCP after antegrade guide-wire passage in 2 cases, and by direct antegrade stent insertion in a further 3 (Table 6). The final position of the stent in antegrade or rendezvous approaches is the same as in internal drainage by PTBD. Püspök *et al*[13] associated 7F plastic stent hepatico-jejunostomy in a patient with recurrent gastric cancer and prior Roux-en-Y total gastrectomy to antegrade transpapillary metal stent placement. Although their goal in placing this second transmural stent was to minimize the risk of acute leakage, this dual approach might well serve the purpose of avoiding a repeat transhepatic puncture in case of stent dysfunction, the transmural stent serving as an entry point to the bile-duct. A similar strategy to manage stent dysfunction was reported by Bories *et al*[16]. After initial transmural stenting, they converted drainage electively to antegrade stent placement at follow-up in two cases and to rendezvous in a further case. These authors highlight the ease of endoscopic re-intervention through a transmural metal stent in case of stent dysfunction.

ESCP interventions for benign biliary obstruction in SAA

Stones and anastomotic strictures are the most common benign causes requiring intervention after SAA, about half each in the 25 patients reported so far in the literature (Table 7). In contrast to SAA patients with malignant biliary obstruction in whom EUSBD is predominantly transmural, transductal intervention is the dominant approach to benign disease, chosen in 84% of SAA cases (Table 7). Antegrade balloon dilation with or without stone removal is the major ESCP intervention performed in this setting[57,110], with rendezvous[3,16,31,110] and antegrade stenting[109,112] having a secondary role.

Only two small series have specifically reported these EUSBD interventions in the setting of SAA. Weilert *et al*[110] succeeded at antegrade CBD stone removal in four RYGB patients and managed to salvage a further two with rendezvous enteroscopy-ERCP. These authors found rendezvous enteroscopy-ERCP with retrograde balloon dilation and stone removal helpful as a cross-over strategy following failed antegrade puncture track dilation. Iwashita *et al*[57] replicated their approach in patients with CBD stones following Roux-en-Y gastrectomy. To prevent leakage and to allow serial cholangiography, these authors left a nasobiliary drainage tube in place during 2-4 wk. Serial cholangiograms led to repeat intervention in one out of four patients with CBD stones.

Antegrade ESCP balloon dilation of anastomotic strictures without additional stenting has been reported as an effective measure to relieve biliary obstruction by several authors[34,109,113,114]. As effective remodeling of benign biliary strictures usually requires serial endotherapy[85,99], the long-term outcomes of single session balloon dilation remain unproven. A seemingly more effective two-step stricture remodeling strategy was used by Artifon *et al*[112], who *via* ESCP placed a temporary covered metal stent in an antegrade fashion across an anastomotic stricture. The stent was removed at follow-up using balloon enteroscopy. Authors limiting intervention to antegrade balloon dilation base the potential compromise in efficacy on concerns about transmural stenting when only minimal intrahepatic dilation is present[109], or about stent removability secondary to impaired access caused by SAA[114].

REFERENCES

1 **Wiersema MJ**, Sandusky D, Carr R, Wiersema LM, Erdel WC, Frederick PK. Endosonography-guided cholangiopancreatography. *Gastrointest Endosc* 1996; **43**: 102-106 [PMID: 8635700 DOI: 10.1016/s0016-5107(06)80108-2]

2 **Giovannini M**, Dotti M, Bories E, Moutardier V, Pesenti C, Danisi C, Delpero JR. Hepaticogastrostomy by echo-endoscopy as a palliative treatment in a patient with metastatic biliary obstruction. *Endoscopy* 2003; **35**: 1076-1078 [PMID: 14648424 DOI: 10.1055/s-2003-44596]

3 **Kahaleh M**, Hernandez AJ, Tokar J, Adams RB, Shami VM, Yeaton P. Interventional EUS-guided cholangiography: evaluation of a technique in evolution. *Gastrointest Endosc* 2006; **64**: 52-59 [PMID: 16813803 DOI: 10.1016/j.gie.2006.01.063]

4 **Ang TL**, Teo EK, Fock KM. EUS-guided transduodenal biliary drainage in unresectable pancreatic cancer with obstructive jaundice. *JOP* 2007; **8**: 438-443 [PMID: 17625296]

5 **Marinone MG**, Rizzoni D, Ferremi P, Rossi G, Izzi T, Brusotti C. Late taste disorders in bone marrow transplantation: clinical evaluation with taste solutions in autologous and allogeneic bone marrow recipients. *Haematologica* 1991; **76**: 519-522 [PMID: 1820992]

6 **Burmester E**, Niehaus J, Leineweber T, Huetteroth T. EUS-cholangio-drainage of the bile duct: report of 4 cases. *Gastrointest Endosc* 2003; **57**: 246-251 [PMID: 12556796 DOI: 10.1067/mge.2003.85]

7 **Giovannini M**, Pesenti Ch, Bories E, Caillol F. Interventional EUS: difficult pancreaticobiliary access. *Endoscopy* 2006; **38** Suppl 1: S93-S95 [PMID: 16802236 DOI: 10.1055/s-2006-946665]

8 **Irisawa A**, Hikichi T, Shibukawa G, Takagi T, Wakatsuki T, Takahashi Y, Imamura H, Sato A, Sato M, Ikeda T, Suzuki R, Obara K, Ohira H. Pancreatobiliary drainage using the EUS-FNA technique: EUS-BD and EUS-PD. *J Hepatobiliary Pancreat Surg* 2009; **16**: 598-604 [PMID: 19649561 DOI: 10.1007/s00534-009-0131-5]

9 **Kedia P**, Gaidhane M, Kahaleh M. Endoscopic guided biliary drainage: how can we achieve efficient biliary drainage? *Clin Endosc* 2013; **46**: 543-551 [PMID: 24143319 DOI: 10.5946/ce.2013.46.5.543]

10 **Kahaleh M**, Artifon EL, Perez-Miranda M, Gupta K, Itoi T, Binmoeller KF, Giovannini M. Endoscopic ultrasonography guided biliary drainage: summary of consortium meeting, May 7th, 2011, Chicago. *World J Gastroenterol* 2013; **19**: 1372-1379 [PMID: 23538784 DOI: 10.3748/wjg.v19.i9.1372]

11 **Sarkaria S**, Lee HS, Gaidhane M, Kahaleh M. Advances in endoscopic ultrasound-guided biliary drainage: a comprehensive review. *Gut Liver* 2013; **7**: 129-136 [PMID: 23560147 DOI: 10.5009/gnl.2013.7.2.129]

12 **Ito K**, Fujita N, Horaguchi J, Noda Y, Kobayashi G. Current issues regarding endosonography-guided biliary drainage for biliary obstruction. *Dig Endosc* 2010; **22** Suppl 1: S132-S136 [PMID: 20590762]

13 **Püspök A**, Lomoschitz F, Dejaco C, Hejna M, Sautner T, Gangl A. Endoscopic ultrasound guided therapy of benign and malignant biliary obstruction: a case series. *Am J Gastroenterol* 2005; **100**: 1743-1747 [PMID: 16086710 DOI: 10.1016/s0016-5107(05)01508-7]

14 **Horaguchi J**, Fujita N, Noda Y, Kobayashi G, Ito K, Obana T, Takasawa O, Koshita S, Kanno Y. Endosonography-guided biliary drainage in cases with difficult transpapillary endoscopic biliary drainage. *Dig Endosc* 2009; **21**: 239-244 [PMID: 19961522 DOI: 10.1111/j.1443-1661.2009.00899.x]

15 **Ashida R**, Chang KJ. Interventional EUS for the treatment of pancreatic cancer. *J Hepatobiliary Pancreat Surg* 2009; **16**: 592-597 [PMID: 19547908 DOI: 10.1007/s00534-009-0129-z]

16 **Bories E**, Pesenti C, Caillol F, Lopes C, Giovannini M. Transgastric endoscopic ultrasonography-guided biliary drainage: results of a pilot study. *Endoscopy* 2007; **39**: 287-291 [PMID: 17357952 DOI: 10.1055/s-2007-966212]

17 **Hanada K**, Iiboshi T, Ishii Y. Endoscopic ultrasound-guided choledochoduodenostomy for palliative biliary drainage in cases with inoperable pancreas head carcinoma. *Dig Endosc* 2009; **21** Suppl 1: S75-S78 [PMID: 19691742 DOI: 10.1111/j.1443-1661.2009.00855.x]

18 **Itoi T**, Yamao K. EUS 2008 Working Group document: evaluation of EUS-guided choledochoduodenostomy (with video). *Gastrointest Endosc* 2009; **69**: S8-12 [PMID: 19179177 DOI: 10.1016/j.gie.2008.11.003]

19 **Tarantino I**, Barresi L, Repici A, Traina M. EUS-guided biliary drainage: a case series. *Endoscopy* 2008; **40**: 336-339 [PMID: 18264890 DOI: 10.1055/s-2007-995455]

20 **Yamao K**, Sawaki A, Takahashi K, Imaoka H, Ashida R, Mizuno N. EUS-guided choledochoduodenostomy for palliative biliary drainage in case of papillary obstruction: report of 2 cases. *Gastrointest Endosc* 2006; **64**: 663-667 [PMID: 16996372 DOI: 10.1016/j.gie.2006.07.003]

21 **Yamao K**, Bhatia V, Mizuno N, Sawaki A, Ishikawa H, Tajika M, Hoki N, Shimizu Y, Ashida R, Fukami N. EUS-guided choledochoduodenostomy for palliative biliary drainage in patients with malignant biliary obstruction: results of long-term follow-up. *Endoscopy* 2008; **40**: 340-342 [PMID: 18389451 DOI: 10.1055/s-2007-995485]

22 **Artifon EL**, Aparicio D, Paione JB, Lo SK, Bordini A, Rabello C, Otoch JP, Gupta K. Biliary drainage in patients with unresectable, malignant obstruction where ERCP fails: endoscopic ultrasonography-guided choledochoduodenostomy versus percutaneous drainage. *J Clin Gastroenterol* 2012; **46**: 768-774 [PMID: 22810111 DOI: 10.1097/mcg.0b013e31825f264c]

23 **Artifon EL**, Silva R, Gupta K, Ferreira FC, De Moura EG, Sakai P, Rassian S. Guided Choledochoduodenostomy Versus Surgical Drainage in Patients With Unresectable Distal Malignant Biliary Obstruction: A Randomized Prospective Trial. *Gastrointest Endosc* 2012; **75**: AB162-AB163 [DOI: 10.1016/j.gie.2012.04.122]

24 **Tessier G**, Bories E, Arvanitakis M, Hittelet A, Pesenti C, Le Moine O, Giovannini M, Devière J. EUS-guided pancreatogastrostomy and pancreatobulbostomy for the treatment of pain in patients with pancreatic ductal dilatation inaccessible for transpapillary endoscopic therapy. *Gastrointest Endosc* 2007; **65**: 233-241 [PMID: 17258981 DOI: 10.1016/j.gie.2006.06.029]

25 **Barkay O**, Sherman S, McHenry L, Yoo BM, Fogel EL, Watkins JL, DeWitt J, Al-Haddad MA, Lehman GA. Therapeutic EUS-assisted endoscopic retrograde pancreatography after failed pancreatic duct cannulation at ERCP. *Gastrointest Endosc* 2010; **71**: 1166-1173 [PMID: 20303489 DOI: 10.1016/j.gie.2009.10.048]

26 **Ergun M**, Aouattah T, Gillain C, Gigot JF, Hubert C, Deprez PH. Endoscopic ultrasound-guided transluminal drainage of pancreatic duct obstruction: long-term outcome. *Endoscopy* 2011; **43**: 518-525 [PMID: 21437853 DOI: 10.1016/j.gie.2010.03.447]

27 **Giovannini M**, Moutardier V, Pesenti C, Bories E, Lelong B, Delpero JR. Endoscopic ultrasound-guided bilioduodenal anastomosis: a new technique for biliary drainage. *Endoscopy* 2001; **33**: 898-900 [PMID: 11571690 DOI: 10.1055/s-2001-17324]

28 **Mallery S**, Matlock J, Freeman ML. EUS-guided rendezvous drainage of obstructed biliary and pancreatic ducts: Report of 6 cases. *Gastrointest Endosc* 2004; **59**: 100-107 [PMID: 14722561 DOI: 10.1016/s0016-5107(03)02300-9]

29 **Lai R**, Freeman ML. Endoscopic ultrasound-guided bile duct access for rendezvous ERCP drainage in the setting of intradiverticular papilla. *Endoscopy* 2005; **37**: 487-489 [PMID: 15844030 DOI: 10.1055/s-2005-861250]

30 **Fujita N**, Noda Y, Kobayashi G, Ito K, Obana T, Horaguchi J, Takasawa O, Nakahara K. Histological changes at an endosonography-guided biliary drainage site: a case report. *World J Gastroenterol* 2007; **13**: 5512-5515 [PMID: 17907298 DOI: 10.1111/j.1443-1661.2010.01027.x]

31 **Will U**, Thieme A, Fueldner F, Gerlach R, Wanzar I, Meyer F. Treatment of biliary obstruction in selected patients by endoscopic ultrasonography (EUS)-guided transluminal biliary drainage. *Endoscopy* 2007; **39**: 292-295 [PMID: 17357950 DOI: 10.1055/s-2007-966215]

32 **Itoi T**, Itokawa F, Sofuni A, Kurihara T, Tsuchiya T, Ishii K, Tsuji S, Ikeuchi N, Moriyasu F. Endoscopic ultrasound-guided choledochoduodenostomy in patients with failed endoscopic retrograde cholangiopancreatography. *World J Gastroenterol* 2008; **14**: 6078-6082 [PMID: 18932289 DOI: 10.3748/wjg.14.6078]

33 **Brauer BC**, Chen YK, Fukami N, Shah RJ. Single-operator EUS-guided cholangiopancreatography for difficult pancreaticobiliary access (with video). *Gastrointest Endosc* 2009; **70**: 471-479 [PMID: 19560768 DOI: 10.1016/j.gie.2008.12.233]

34 **Maranki J**, Hernandez AJ, Arslan B, Jaffan AA, Angle JF, Shami VM, Kahaleh M. Interventional endoscopic ultrasound-guided cholangiography: long-term experience of an emerging alternative to percutaneous transhepatic cholangiography. *Endoscopy* 2009; **41**: 532-538 [PMID: 19533558 DOI: 10.1055/s-0029-1214712]

35 **Kim YS**, Gupta K, Mallery S, Li R, Kinney T, Freeman ML. Endoscopic ultrasound rendezvous for bile duct access using a transduodenal approach: cumulative experience at a single center. A case series. *Endoscopy* 2010; **42**: 496-502 [PMID: 20419625 DOI: 10.1055/s-0029-1244082]

36 **Nguyen-Tang T**, Binmoeller KF, Sanchez-Yague A, Shah JN. Endoscopic ultrasound (EUS)-guided transhepatic anterograde self-expandable metal stent (SEMS) placement across malignant biliary obstruction. *Endoscopy* 2010; **42**: 232-236 [PMID: 20119894 DOI: 10.1055/s-0029-1243858]

37 **Iwamuro M**, Kawamoto H, Harada R, Kato H, Hirao K, Mizuno O, Ishida E, Ogawa T, Okada H, Yamamoto K. Combined duodenal stent placement and endoscopic ultrasonography-guided biliary drainage for malignant duodenal obstruction with biliary stricture. *Dig Endosc* 2010; **22**: 236-240 [PMID: 20642617 DOI: 10.1111/j.1443-1661.2010.00997.x]

38 **Artifon EL**, Takada J, Okawa L, Moura EG, Sakai P. EUS-guided choledochoduodenostomy for biliary drainage in unresectable pancreatic cancer: a case series. *JOP* 2010; **11**: 597-600 [PMID: 21068493 DOI: 10.1016/j.gie.2010.10.041]

39 **Belletrutti PJ**, Gerdes H, Schattner MA. Successful endoscopic ultrasound-guided transduodenal biliary drainage through a pre-existing duodenal stent. *JOP* 2010; **11**: 234-236 [PMID: 20442518]

40 **Park do H**, Jang JW, Lee SS, Seo DW, Lee SK, Kim MH. EUS-guided biliary drainage with transluminal stenting after failed ERCP: predictors of adverse events and long-term results. *Gastrointest Endosc* 2011; **74**: 1276-1284 [PMID: 21963067 DOI: 10.1016/j.gie.2011.07.054]

41 **Fabbri C**, Luigiano C, Fuccio L, Polifemo AM, Ferrara F, Ghersi S, Bassi M, Billi P, Maimone A, Cennamo V, Masetti M, Jovine E, D'Imperio N. EUS-guided biliary drainage with placement of a new partially covered biliary stent for palliation of malignant biliary obstruction: a case series. *Endoscopy* 2011; **43**: 438-441 [PMID: 21271507 DOI: 10.1055/s-0030-1256097]

42 **Hara K**, Yamao K, Niwa Y, Sawaki A, Mizuno N, Hijioka S, Tajika M, Kawai H, Kondo S, Kobayashi Y, Matumoto K, Bhatia V, Shimizu Y, Ito A, Hirooka Y, Goto H. Prospective clinical study of EUS-guided choledochoduodenostomy for malignant lower biliary tract obstruction. *Am J Gastroenterol* 2011; **106**: 1239-1245 [PMID: 21448148 DOI: 10.1055/s-0031-1292133]

43 **Ramírez-Luna MA**, Téllez-Ávila FI, Giovannini M, Valdovinos-Andraca F, Guerrero-Hernández I, Herrera-Esquivel J. Endoscopic ultrasound-guided biliodigestive drainage is a good alternative in patients with unresectable cancer. *Endoscopy* 2011; **43**: 826-830 [PMID: 21833899 DOI: 10.1055/s-0030-1256406]

44 **Siddiqui AA**, Sreenarasimhaiah J, Lara LF, Harford W, Lee C, Eloubeidi MA. Endoscopic ultrasound-guided transduodenal placement of a fully covered metal stent for palliative biliary drainage in patients with malignant biliary obstruction. *Surg Endosc* 2011; **25**: 549-555 [PMID: 20632191 DOI: 10.1007/s00464-010-1216-6]

45 **Komaki T**, Kitano M, Sakamoto H, Kudo M. Endoscopic ultrasonography-guided biliary drainage: evaluation of a choledochoduodenostomy technique. *Pancreatology* 2011; **11** Suppl 2: 47-51 [PMID: 21464587 DOI: 10.1159/000323508]

46 **Prachayakul V**, Aswakul P, Kachintorn U. EUS-guided choledochoduodenostomy for biliary drainage using tapered-tip plastic stent with multiple fangs. *Endoscopy* 2011; **43** Suppl 2 UCTN: E109-E110 [PMID: 21424999 DOI: 10.1055/s-0030-1256140]

47 **Attasaranya S**, Netinasunton N, Jongboonyanuparp T, Sottisuporn J, Witeerungrot T, Pirathvisuth T, Ovartlarnporn B. The Spectrum of Endoscopic Ultrasound Intervention in Biliary Diseases: A Single Center's Experience in 31 Cases. *Gastroenterol Res Pract* 2012; **2012**: 680753 [PMID: 22654900 DOI: 10.1155/2012/680753]

48 **Katanuma A**, Maguchi H, Osanai M, Takahashi K. Endoscopic ultrasound-guided biliary drainage performed for refractory bile duct stenosis due to chronic pancreatitis: a case report. *Dig Endosc* 2012; **24** Suppl 1: 34-37 [PMID: 22533749 DOI: 10.1111/j.1443-1661.2012.01256.x]

49 **Kawakubo K**, Isayama H, Nakai Y, Sasahira N, Kogure H, Sasaki T, Hirano K, Tada M, Koike K. Simultaneous Duodenal Metal Stent Placement and EUS-Guided Choledochoduodenostomy for Unresectable Pancreatic Cancer. *Gut Liver* 2012; **6**: 399-402 [PMID: 22844572 DOI: 10.1055/s-0031-1292132]

50 **Khashab MA**, Fujii LL, Baron TH, Canto MI, Gostout CJ, Petersen BT, Okolo PI, Topazian MD, Levy MJ. EUS-guided biliary drainage for patients with malignant biliary obstruction with an indwelling duodenal stent (with videos). *Gastrointest Endosc* 2012; **76**: 209-213 [PMID: 22726485 DOI: 10.1016/j.gie.2012.03.170]

51 **Kim TH**, Kim SH, Oh HJ, Sohn YW, Lee SO. Endoscopic ultrasound-guided biliary drainage with placement of a fully covered metal stent for malignant biliary obstruction. *World J Gastroenterol* 2012; **18**: 2526-2532 [PMID: 22654450 DOI: 10.3748/wjg.v18.i20.2526]

52 **Song TJ**, Hyun YS, Lee SS, Park do H, Seo DW, Lee SK, Kim MH. Endoscopic ultrasound-guided choledochoduodenostomies with fully covered self-expandable metallic stents. *World J Gastroenterol* 2012; **18**: 4435-4440 [PMID: 22969210 DOI: 10.3748/wjg.v18.i32.4435]

53 **Dhir V**, Bhandari S, Bapat M, Maydeo A. Comparison of EUS-guided rendezvous and precut papillotomy techniques for biliary access (with videos). *Gastrointest Endosc* 2012; **75**: 354-359 [PMID: 22248603 DOI: 10.1016/j.gie.2011.07.075]

54 **Hara K**, Yamao K, Hijioka S, Mizuno N, Imaoka H, Tajika M, Kondo S, Tanaka T, Haba S, Takeshi O, Nagashio Y, Obayashi T, Shinagawa A, Bhatia V, Shimizu Y, Goto H, Niwa Y. Prospective clinical study of endoscopic ultrasound-guided choledochoduodenostomy with direct metallic stent placement using a forward-viewing echoendoscope. *Endoscopy* 2013; **45**: 392-396 [PMID: 23338620 DOI: 10.1055/s-0032-1326076]

55 **Park do H**, Jeong SU, Lee BU, Lee SS, Seo DW, Lee SK, Kim MH. Prospective evaluation of a treatment algorithm with enhanced guidewire manipulation protocol for EUS-guided biliary drainage after failed ERCP (with video). *Gastrointest Endosc* 2013; **78**: 91-101 [PMID: 23523301 DOI: 10.1016/j.gie.2013.01.042]

56 **Itoi T**, Itokawa F, Tsuchiya T, Tsuji S, Tonozuka R. Endoscopic ultrasound-guided choledochoantrostomy as an alternative extrahepatic bile duct drainage method in pancreatic cancer with duodenal invasion. *Dig Endosc* 2013; **25** Suppl 2: 142-145 [PMID: 23617666 DOI: 10.1111/den.12065]

57 **Iwashita T**, Yasuda I, Doi S, Uemura S, Mabuchi M, Okuno M, Mukai T, Itoi T, Moriwaki H. Endoscopic ultrasound-guided antegrade treatments for biliary disorders in patients with surgically altered anatomy. *Dig Dis Sci* 2013; **58**: 2417-2422 [PMID: 23535877 DOI: 10.1016/j.gie.2013.03.1219]

58 **Gupta K**, Perez-Miranda M, Kahaleh M, Artifon EL, Itoi T, Freeman ML, de-Serna C, Sauer B, Giovannini M. Endoscopic ultrasound-assisted bile duct access and drainage: multicenter, long-term analysis of approach, outcomes, and complications of a technique in evolution. *J Clin Gastroenterol* 2014; **48**: 80-87 [PMID: 23632351 DOI: 10.1097/mcg.0b013e31828c6822]

59 **Kahaleh M**, Perez-Miranda M, Artifon EL, Gupta K, Park DH, Moon JH, Choi HJ, De La Serna C, De La Mora-Levy JG, Alonso-Larraga JO, Ramirez M, Shah RJ, Brauer BC, Fukami N, Gaidhane M, Bories E, Giovannini M. 140 Endoscopic ultrasound (EUS) guided biliary drainage: what have we learned? *Gastrointest Endosc* 2013; **77** (5 Suppl): AB127-AB128 [DOI: 10.1016/j.gie.2013.04.021]

60 **Miura F**, Takada T, Strasberg SM, Solomkin JS, Pitt HA, Gouma DJ, Garden OJ, Büchler MW, Yoshida M, Mayumi T, Okamoto K, Gomi H, Kusachi S, Kiriyama S, Yokoe M, Kimura Y, Higuchi R, Yamashita Y, Windsor JA, Tsuyuguchi T, Gabata T, Itoi T, Hata J, Liau KH. TG13 flowchart for the management of acute cholangitis and cholecystitis. *J Hepatobiliary Pancreat Sci* 2013; **20**: 47-54 [PMID: 23307003 DOI: 10.1007/s00534-012-0563-1]

61 **Takada T**, Strasberg SM, Solomkin JS, Pitt HA, Gomi H, Yoshida M, Mayumi T, Miura F, Gouma DJ, Garden OJ, Büchler MW, Kiriyama S, Yokoe M, Kimura Y, Tsuyuguchi T, Itoi T, Gabata T, Higuchi R, Okamoto K, Hata J, Murata A, Kusachi S, Windsor JA, Supe AN, Lee S, Chen XP, Yamashita Y, Hirata K, Inui K, Sumiyama Y. TG13: Updated Tokyo Guidelines for the management of acute cholangitis and cholecystitis. *J Hepatobiliary Pancreat Sci* 2013; **20**: 1-7 [PMID: 23307006 DOI: 10.1007/s00534-006-1150-0]

62 **Tsuyuguchi T**, Itoi T, Takada T, Strasberg SM, Pitt HA, Kim MH, Supe AN, Mayumi T, Yoshida M, Miura F, Gomi H, Kimura Y, Higuchi R, Okamoto K, Yamashita Y, Gabata T, Hata J, Kusachi S. TG13 indications and techniques for gallbladder drainage in acute cholecystitis (with videos). *J Hepatobiliary Pancreat Sci* 2013; **20**: 81-88 [PMID: 23307009 DOI: 10.1007/s00534-012-0570-2]

63 **Yokoe M**, Takada T, Strasberg SM, Solomkin JS, Mayumi T, Gomi H, Pitt HA, Gouma DJ, Garden OJ, Büchler MW, Kiriyama S, Kimura Y, Tsuyuguchi T, Itoi T, Yoshida M, Miura F, Yamashita Y, Okamoto K, Gabata T, Hata J,

Higuchi R, Windsor JA, Bornman PC, Fan ST, Singh H, de Santibanes E, Kusachi S, Murata A, Chen XP, Jagannath P, Lee S, Padbury R, Chen MF. New diagnostic criteria and severity assessment of acute cholecystitis in revised Tokyo Guidelines. *J Hepatobiliary Pancreat Sci* 2012; **19**: 578-585 [PMID: 22872303 DOI: 10.1007/s00534-012-0548-0]

64 **Houghton PW**, Jenkinson LR, Donaldson LA. Cholecystectomy in the elderly: a prospective study. *Br J Surg* 1985; **72**: 220-222 [PMID: 3978383]

65 **Frazee RC**, Nagorney DM, Mucha P. Acute acalculous cholecystitis. *Mayo Clin Proc* 1989; **64**: 163-167 [PMID: 2921875]

66 **Hirota M**, Takada T, Kawarada Y, Nimura Y, Miura F, Hirata K, Mayumi T, Yoshida M, Strasberg S, Pitt H, Gadacz TR, de Santibanes E, Gouma DJ, Solomkin JS, Belghiti J, Neuhaus H, Büchler MW, Fan ST, Ker CG, Padbury RT, Liau KH, Hilvano SC, Belli G, Windsor JA, Dervenis C. Diagnostic criteria and severity assessment of acute cholecystitis: Tokyo Guidelines. *J Hepatobiliary Pancreat Surg* 2007; **14**: 78-82 [PMID: 17252300 DOI: 10.1007/s00534-006-1159-4]

67 **Itoi T**, Sofuni A, Itokawa F, Tsuchiya T, Kurihara T, Ishii K, Tsuji S, Ikeuchi N, Tsukamoto S, Takeuchi M, Kawai T, Moriyasu F. Endoscopic transpapillary gallbladder drainage in patients with acute cholecystitis in whom percutaneous transhepatic approach is contraindicated or anatomically impossible (with video). *Gastrointest Endosc* 2008; **68**: 455-460 [PMID: 18561927 DOI: 10.1016/j.gie.2008.02.052]

68 **Itoi T**, Coelho-Prabhu N, Baron TH. Endoscopic gallbladder drainage for management of acute cholecystitis. *Gastrointest Endosc* 2010; **71**: 1038-1045 [PMID: 20438890 DOI: 10.1016/j.gie.2010.01.026]

69 **Nahrwold DL**. Acute cholecystitis. In: Sabiston D Jr, editor. Textbook of surgery. 15th ed. Philadelphia: Saunders, 1997: 1126-1131

70 **Baron TH**, Topazian MD. Endoscopic transduodenal drainage of the gallbladder: implications for endoluminal treatment of gallbladder disease. *Gastrointest Endosc* 2007; **65**: 735-737 [PMID: 17141230 DOI: 10.1016/j.gie.2006.07.041]

71 **Kwan V**, Eisendrath P, Antaki F, Le Moine O, Devière J. EUS-guided cholecystenterostomy: a new technique (with videos). *Gastrointest Endosc* 2007; **66**: 582-586 [PMID: 17725950 DOI: 10.1016/j.gie.2007.02.065]

72 **Lee SS**, Park do H, Hwang CY, Ahn CS, Lee TY, Seo DW, Lee SK, Kim MW. EUS-guided transmural cholecystostomy as rescue management for acute cholecystitis in elderly or high-risk patients: a prospective feasibility study. *Gastrointest Endosc* 2007; **66**: 1008-1012 [PMID: 17767933 DOI: 10.1016/j.gie.2007.03.1080]

73 **Takasawa O**, Fujita N, Noda Y, Kobayashi G, Ito K, Horaguchi J, Obana T. Endosonography-guided gallbladder drainage for acute cholecystitis following covered metal stent deployment. *Dig Endosc* 2009; **21**: 43-47 [PMID: 19691802 DOI: 10.1111/j.1443-1661.2008.00822.x]

74 **Kamata K**, Kitano M, Komaki T, Sakamoto H, Kudo M. Transgastric endoscopic ultrasound (EUS)-guided gallbladder drainage for acute cholecystitis. *Endoscopy* 2009; **41** Suppl 2: E315-E316 [PMID: 19921608 DOI: 10.1055/s-0029-1215258]

75 **Song TJ**, Park do H, Eum JB, Moon SH, Lee SS, Seo DW, Lee SK, Kim MH. EUS-guided cholecystoenterostomy with single-step placement of a 7F double-pigtail plastic stent in patients who are unsuitable for cholecystectomy: a pilot study (with video). *Gastrointest Endosc* 2010; **71**: 634-640 [PMID: 20189528 DOI: 10.1016/j.gie.2009.11.024]

76 **Itoi T**, Itokawa F, Kurihara T. Endoscopic ultrasonography-guided gallbladder drainage: actual technical presentations and review of the literature (with videos). *J Hepatobiliary Pancreat Sci* 2011; **18**: 282-286 [PMID: 20652716 DOI: 10.1007/s00534-010-0310-4]

77 **Jang JW**, Lee SS, Park do H, Seo DW, Lee SK, Kim MH. Feasibility and safety of EUS-guided transgastric/transduodenal gallbladder drainage with single-step placement of a modified covered self-expandable metal stent in patients unsuitable for cholecystectomy. *Gastrointest Endosc* 2011; **74**: 176-181 [PMID: 21704816 DOI: 10.1016/j.gie.2011.03.1120]

78 **Itoi T**, Binmoeller KF, Shah J, Sofuni A, Itokawa F, Kurihara T, Tsuchiya T, Ishii K, Tsuji S, Ikeuchi N, Moriyasu F. Clinical evaluation of a novel lumen-apposing metal stent for endosonography-guided pancreatic pseudocyst and gallbladder drainage (with videos). *Gastrointest Endosc* 2012; **75**: 870-876 [PMID: 22301347 DOI: 10.1016/j.gie.2011.10.020]

79 **Jang JW**, Lee SS, Song TJ, Hyun YS, Park do H, Seo DW, Lee SK, Kim MH, Yun SC. Endoscopic ultrasound-guided transmural and percutaneous transhepatic gallbladder drainage are comparable for acute cholecystitis. *Gastroenterology* 2012; **142**: 805-811 [PMID: 22245666 DOI: 10.1053/j.gastro.2011.12.051]

80 **de la Serna-Higuera C**, Pérez-Miranda M, Gil-Simón P, Ruiz-Zorrilla R, Diez-Redondo P, Alcaide N, Sancho-del Val L, Nuñez-Rodriguez H. EUS-guided transenteric gallbladder drainage with a new fistula-forming, lumen-apposing metal stent. *Gastrointest Endosc* 2013; **77**: 303-308 [PMID: 23206813 DOI: 10.1016/j.gie.2012.09.021]

81 **Súbtil JC**, Betes M, Muñoz-Navas M. Gallbladder drainage guided by endoscopic ultrasound. *World J Gastrointest Endosc* 2010; **2**: 203-209 [PMID: 21160934 DOI: 10.4253/wjge.v2.i6.203]

82 **Feitoza AB**, Baron TH. Endoscopy and ERCP in the setting of previous upper GI tract surgery. Part I: reconstruction without alteration of pancreaticobiliary anatomy. *Gastrointest Endosc* 2001; **54**: 743-749 [PMID: 11726851 DOI: 10.1067/mge.2001.120169]

83 **Feitoza AB**, Baron TH. Endoscopy and ERCP in the setting of previous upper GI tract surgery. Part II: postsurgical anatomy with alteration of the pancreaticobiliary tree. *Gastrointest Endosc* 2002; **55**: 75-79 [PMID: 11756919 DOI: 10.1067/mge.2002.120385]

84 **Pannala R**, Brandabur JJ, Gan SI, Gluck M, Irani S, Patterson DJ, Ross AS, Dorer R, Traverso LW, Picozzi VJ, Kozarek RA. Afferent limb syndrome and delayed GI problems after pancreaticoduodenectomy for pancreatic cancer: single-center, 14-year experience. *Gastrointest Endosc* 2011; **74**: 295-302 [PMID: 21689816 DOI: 10.1016/j.gie.2011.04.029]

85 **Costamagna G**, Tringali A, Mutignani M, Perri V, Spada C, Pandolfi M, Galasso D. Endotherapy of postoperative biliary strictures with multiple stents: results after more than 10 years of follow-up. *Gastrointest Endosc* 2010; **72**: 551-557 [PMID: 20630514 DOI: 10.1016/j.gie.2010.04.052]

86 **Shah RJ**, Smolkin M, Yen R, Ross A, Kozarek RA, Howell DA, Bakis G, Jonnalagadda SS, Al-Lehibi AA, Hardy A, Morgan DR, Sethi A, Stevens PD, Akerman PA, Thakkar SJ, Brauer BC. A multicenter, U.S. experience of single-balloon, double-balloon, and rotational overtube-assisted enteroscopy ERCP in patients with surgically altered pancreaticobiliary anatomy (with video). *Gastrointest Endosc* 2013; **77**: 593-600 [PMID: 23290720 DOI: 10.1016/j.gie.2012.10.015]

87 **Mergener K**, Kozarek RA, Traverso LW. Intraoperative transjejunal ERCP: case reports. *Gastrointest Endosc* 2003; **58**: 461-463 [PMID: 14528232 DOI: 10.1067/s0016-5107(03)00032-4]

88 **Pimentel RR**, Mehran A, Szomstein S, Rosenthal R. Laparoscopy-assisted transgastrostomy ERCP after bariatric surgery: case report of a novel approach. *Gastrointest Endosc* 2004; **59**: 325-328 [PMID: 14745421 DOI: 10.1016/s0016-5107(03)02549-5]

89 **Bertin PM**, Singh K, Arregui ME. Laparoscopic transgastric endoscopic retrograde cholangiopancreatography (ERCP) after gastric bypass: case series and a description of technique. *Surg Endosc* 2011; **25**: 2592-2596 [PMID: 21416184 DOI: 10.1007/s00464-011-1593-5]

90 **Schreiner MA**, Chang L, Gluck M, Irani S, Gan SI, Brandabur JJ, Thirlby R, Moonka R, Kozarek RA, Ross AS. Laparoscopy-assisted versus balloon enteroscopy-assisted ERCP in bariatric post-Roux-en-Y gastric bypass patients. *Gastrointest Endosc* 2012; **75**: 748-756 [PMID: 22301340 DOI: 10.1016/j.gie.2011.11.019]

91 **Baron TH**, Chahal P, Ferreira LE. ERCP *via* mature feeding jejunostomy tube tract in a patient with Roux-en-Y anatomy (with video). *Gastrointest Endosc* 2008; **68**: 189-191 [PMID: 18308307 DOI: 10.1016/j.gie.2007.11.016]

92 **Baron TH**, Vickers SM. Surgical gastrostomy placement as access for diagnostic and therapeutic ERCP. *Gastrointest Endosc* 1998; **48**: 640-641 [PMID: 9852460 DOI: 10.1016/s0016-5107(98)70052-5]

93 **Tekola B**, Wang AY, Ramanath M, Burnette B, Ellen K, Schirmer BD, Hallowell PT, Sauer BG, Kahaleh M. Percutaneous gastrostomy tube placement to perform transgastrostomy endoscopic retrograde cholangiopancreaticography in patients with Roux-en-Y anatomy. *Dig Dis Sci* 2011; **56**: 3364-3369 [PMID: 21625965 DOI: 10.1007/s10620-011-1743-6]

94 **Choi EK**, Chiorean MV, Coté GA, El Hajj II, Ballard D, Fogel EL, Watkins JL, McHenry L, Sherman S, Lehman GA. ERCP *via* gastrostomy vs. double balloon enteroscopy in patients with prior bariatric Roux-en-Y gastric bypass surgery. *Surg Endosc* 2013; **27**: 2894-2899 [PMID: 23793801 DOI: 10.1007/s00464-013-3129-7]

95 **Martinez J**, Guerrero L, Byers P, Lopez P, Scagnelli T, Azuaje R, Dunkin B. Endoscopic retrograde cholangiopancreatography and gastroduodenoscopy after Roux-en-Y gastric bypass. *Surg Endosc* 2006; **20**: 1548-1550 [PMID: 16897292 DOI: 10.1007/s00464-005-0267-6]

96 **Baron TH**, Song LM, Ferreira LE, Smyrk TC. Novel approach to therapeutic ERCP after long-limb Roux-en-Y gastric bypass surgery using transgastric self-expandable metal stents: experimental outcomes and first human case study (with videos). *Gastrointest Endosc* 2012; **75**: 1258-1263 [PMID: 22624815 DOI: 10.1016/j.gie.2012.02.026]

97 **Attam R**, Leslie D, Freeman M, Ikramuddin S, Andrade R. EUS-assisted, fluoroscopically guided gastrostomy tube placement in patients with Roux-en-Y gastric bypass: a novel technique for access to the gastric remnant. *Gastrointest Endosc* 2011; **74**: 677-682 [PMID: 21872717 DOI: 10.1016/j.gie.2011.05.018]

98 **Madan A**, Urayama S. Successful ERCP in a Roux-en-Y gastric bypass patient, performed *via* a small remnant of gastrogastric communication. *Endoscopy* 2011; **43** Suppl 2 UCTN: E73-E74 [PMID: 21341190 DOI: 10.1055/s-0030-1256038]

99 **Shear W**, Gaidhane M, Kahaleh M. ERCP in Roux-en-Y gastric bypass: creation of an antegrade gastrogastric conduit using a fully covered metal esophageal stent. *Endoscopy* 2012; **44** Suppl 2 UCTN: E58-E59 [PMID: 22396279 DOI: 10.1055/s-0031-1291562]

100 **Perez-Miranda M**, Mata L, Saracibar E, Sanchez-Antolin G, Barrio J, Caro-Paton A. Temporary access fistulas (TAFs) using covered self-expandable metal stents (cSEMS): a feasible tool for interventional pancreaticobiliary endoscopy [abstract]. *Gastrointest Endosc* 2007; **65**: AB123 [DOI: 10.1016/j.gie.2007.03.122]

101 **Baron TH**, Song LM. Percutaneous assisted transprosthetic endoscopic therapy (PATENT): expanding gut access to infinity and beyond! (with video). *Gastrointest Endosc* 2012; **76**: 641-644 [PMID: 22898421 DOI: 10.1016/j.gie.2012.05.027]

102 **Perez-Miranda M**, Sancho-Del VL, Lorenzo Pelayo S, Ruiz-Zorrilla R, Alcaide N, Herranz MT, de-Serna C, Caro-Paton A. Transmural Access and therapy of bile-duct disease in patients with complex anatomy using temporary covered self-expandable metal stents (CSEMS) [abstract]. *Gastrointest Endosc* 2011; **73**: AB126 [DOI: 10.1016/j.gie.2011.03.050]

103 **Jürgensen C**, Wentrup R, Zeitz M. Endoscopic ultrasound (EUS)-guided transduodenal drainage of an obstructed jejunal loop after hepaticojejunostomy as treatment for recurrent biliary sepsis. *Endoscopy* 2013; **45** Suppl 2 UCTN: E40-E41 [PMID: 23526508 DOI: 10.1055/s-0032-1325891]

104 **Matsumoto K**, Kato H, Tomoda T, Sakakihara I, Yamamoto N, Noma Y, Sonoyama T, Tsutsumi K, Okada H, Yamamoto K, Kawamoto H. A case of acute afferent loop syndrome treated by transgastric drainage with EUS. *Gastrointest Endosc* 2013; **77**: 132-133 [PMID: 23261104 DOI: 10.1016/j.gie.2012.09.016]

105 **Perez-Miranda M**, Barclay RL, Kahaleh M. Endoscopic ultrasonography-guided endoscopic retrograde cholangiopancreatography: endosonographic cholangiopancreatography. *Gastrointest Endosc Clin N Am* 2012; **22**: 491-509 [PMID: 22748245 DOI: 10.1016/j.giec.2012.05.004]

106 **Shah JN**, Marson F, Weilert F, Bhat YM, Nguyen-Tang T, Shaw RE, Binmoeller KF. Single-operator, single-session EUS-guided anterograde cholangiopancreatography in failed ERCP or inaccessible papilla. *Gastrointest Endosc* 2012; **75**: 56-64 [PMID: 22018554 DOI: 10.1016/j.gie.2011.08.032]

107 **Kahaleh M**, Yoshida C, Kane L, Yeaton P. Interventional EUS cholangiography: A report of five cases. *Gastrointest Endosc* 2004; **60**: 138-142 [PMID: 15229448 DOI: 10.1016/s0016-5107(04)01528-7]

108 **Kahaleh M**, Wang P, Shami VM, Tokar J, Yeaton P. EUS-guided transhepatic cholangiography: report of 6 cases. *Gastrointest Endosc* 2005; **61**: 307-313 [PMID: 15729253 DOI: 10.1016/s0016-5107(04)02585-4]

109 **Park SJ**, Choi JH, Park do H, Choi JH, Lee SS, Seo DW, Lee SK, Kim MH. Expanding indication: EUS-guided hepaticoduodenostomy for isolated right intrahepatic duct obstruction (with video). *Gastrointest Endosc* 2013; **78**: 374-380 [PMID: 23711555 DOI: 10.1016/j.gie.2013.03.1302]

110 **Weilert F**, Binmoeller KF, Marson F, Bhat Y, Shah JN. Endoscopic ultrasound-guided anterograde treatment of biliary stones following gastric bypass. *Endoscopy* 2011; **43**: 1105-1108 [PMID: 22057823 DOI: 10.1055/s-0030-1256961]

111 **Fujita N**, Sugawara T, Noda Y, Kobayashi G, Ito K, Obana T, Horaguchi J, Takasawa O. Snare-over-the-wire technique for safe exchange of a stent following endosonography-guided biliary drainage. *Dig Endosc* 2009; **21**: 48-52 [PMID: 19691803 DOI: 10.1111/j.1443-1661.2008.00821.x]

112 **Artifon EL**, Safatle-Ribeiro AV, Ferreira FC, Poli-de-Figueiredo L, Rasslan S, Carnevale F, Otoch JP, Sakai P, Kahaleh M. EUS-guided antegrade transhepatic placement of a self-expandable metal stent in hepatico-jejunal anastomosis. *JOP* 2011; **12**: 610-613 [PMID: 22072253 DOI: 10.1016/j.gie.2011.03.1186]

113 **Park do H**, Jang JW, Lee SS, Seo DW, Lee SK, Kim MH. EUS-guided transhepatic antegrade balloon dilation for benign bilioenteric anastomotic strictures in a patient with hepaticojejunostomy. *Gastrointest Endosc* 2012; **75**: 692-693 [PMID: 21679943 DOI: 10.1016/j.gie.2011.04.013]

114 **Bapaye A**, Dubale N. Endoscopic ultrasound-guided antegrade dilation of a stenosed hepaticojejunostomy. *Endoscopy* 2012; **44** Suppl 2 UCTN: E435-E436 [PMID: 23299469 DOI: 10.1055/s-0032-1325894]

115 **Chopin-Laly X**, Ponchon T, Guibal A, Adham M. Endoscopic biliogastric stenting: a salvage procedure. *Surgery* 2009; **145**: 123 [PMID: 19081487 DOI: 10.1016/j.surg.2008.07.019]

116 **Henry WA**, Singh VK, Kalloo AN, Khashab MA. Simultaneous EUS-guided transbulbar pancreaticobiliary drainage (with video). *Gastrointest Endosc* 2012; **76**: 1065-1067, 1067.e1-e2 [PMID: 22197478 DOI: 10.1016/j.gie.2011.09.046]

117 **Ma J**, Liu Y, Li Z, Jin Z. Endoscopic ultrasound-guided transgastric biliary drainage after partial gastrectomy. *Endoscopy* 2011; **43** Suppl 2 UCTN: E102 [PMID: 21424995 DOI: 10.1055/s-0030-1256104]

118 **Iwashita T**, Lee JG, Shinoura S, Nakai Y, Park DH,

Muthusamy VR, Chang KJ. Endoscopic ultrasound-guided rendezvous for biliary access after failed cannulation. *Endoscopy* 2012; **44**: 60-65 [PMID: 22127960 DOI: 10.1055/s-0030-1256871]

P- Reviewer: Aytac E, Leitman IM, Li XL, Tsai HH, Yan SL
S- Editor: Qi Y **L- Editor**: A **E- Editor**: Zhang DN

World Journal of Gastroenterology

Submit a Manuscript: http://www.wjgnet.com/esps/
Help Desk: http://www.wjgnet.com/esps/helpdesk.aspx
DOI: 10.3748/wjg.v21.i3.742

World J Gastroenterol 2015 January 21; 21(3): 742-758
ISSN 1007-9327 (print) ISSN 2219-2840 (online)

REVIEW

Use of mesenchymal stem cells to treat liver fibrosis: Current situation and future prospects

Silvia Berardis, Prenali Dwisthi Sattwika, Mustapha Najimi, Etienne Marc Sokal

Silvia Berardis, Prenali Dwisthi Sattwika, Mustapha Najimi, Etienne Marc Sokal, Laboratory of Pediatric Hepatology and Cell Therapy, Institut de Recherche Expérimentale et Clinique, Cliniques Universitaires St Luc, Université Catholique de Louvain, 1200 Brussels, Belgium
Author contributions: Berardis S, Dwisthi Sattwika P, Najimi M and Sokal EM wrote the paper.

Correspondence to: Silvia Berardis, MD, Laboratory of Pediatric Hepatology and Cell Therapy, Institut de Recherche Expérimentale et Clinique, Cliniques Universitaires St Luc, Université Catholique de Louvain, Avenue Hippocrate 10, 1200 Brussels, Belgium. silvia.berardis@uclouvain.be
Telephone: +32-2-7645285
Fax: +32-2-7648909
Received: July 29, 2014
Peer-review started: July 31, 2014
First decision: August 15, 2014
Revised: September 5, 2014
Accepted: November 18, 2014
Article in press: November 19, 2014
Published online: January 21, 2015

Abstract

Progressive liver fibrosis is a major health issue for which no effective treatment is available, leading to cirrhosis and orthotopic liver transplantation. However, organ shortage is a reality. Hence, there is an urgent need to find alternative therapeutic strategies. Cell-based therapy using mesenchymal stem cells (MSCs) may represent an attractive therapeutic option, based on their immunomodulatory properties, their potential to differentiate into hepatocytes, allowing the replacement of damaged hepatocytes, their potential to promote residual hepatocytes regeneration and their capacity to inhibit hepatic stellate cell activation or induce their apoptosis, particularly *via* paracrine mechanisms. The current review will highlight recent findings regarding the input of MSC-based therapy for the treatment of liver fibrosis, from *in vitro* studies to pre-clinical and clinical trials. Several studies have shown the ability of MSCs to reduce liver fibrosis and improve liver function. However, despite these promising results, some limitations need to be considered. Future prospects will also be discussed in this review.

Key words: Liver fibrosis; Cirrhosis; Mesenchymal stem cells; Cell therapy; Hepatic stellate cells

Core tip: Liver fibrosis is a major public health issue for which no treatment is available. Cell therapy and, in particular, mesenchymal stem cells (MSCs), represent a promising strategy, based mainly on their immunomodulatory properties and differentiation capa-city. In the current review, we discuss the rationale to propose cell therapy and, in particular, MSCs to treat liver fibrosis, overview of the current knowledge in this field and highlight future prospects.

Berardis S, Dwisthi Sattwika P, Najimi M, Sokal EM. Use of mesenchymal stem cells to treat liver fibrosis: Current situation and future prospects. *World J Gastroenterol* 2015; 21(3): 742-758 Available from: URL: http://www.wjgnet.com/1007-9327/full/v21/i3/742.htm DOI: http://dx.doi.org/10.3748/wjg.v21.i3.742

LIVER FIBROSIS: A MAJOR HEALTH ISSUE

Liver fibrosis refers to the excessive accumulation of extracellular matrix into the liver parenchyma in response to chronic injury. Injuries may result from viral, autoimmune, cholestatic, toxic or metabolic disease, including nonalcoholic steatohepatitis. Chronic fibrosis progresses from fibrosis to cirrhosis characterised by septa formation and rings of scar tissue surrounding nodules of surviving hepatocytes[1]. Epidemiological data suggest that cirrhosis affects hundreds of millions people worldwide[1]. It represents the 14th most common cause of death in adults worldwide (resulting in 1.03 million death per year) but the fourth in central Europe[2]. In the European population, less than 1% (approximately 0.1%) of the population is affected by cirrhosis, corresponding to 14-26 new cases per 100000 inhabitants per year or an estimated 170000 deaths per year[3].

CLINICAL ASPECTS

Although mild fibrosis remains largely asymptomatic, its progression towards cirrhosis is a major cause of morbidity and mortality. Fibrosis and distorted vasculature lead to portal hypertension and related complications, namely upper gastrointestinal bleeding from ruptured gastro-oesophageal varices, portal hypertensive gastropathy, ascites, renal dysfunction, and hypersplenism leading to thrombocytopenia and hepatopulmonary syndrome[4]. Furthermore, cirrhosis is associated with hepatocellular insufficiency, impaired metabolic capacity and dysfunction of other organs such as the gastrointestinal tract[5] and kidneys[6], as well as the cardiovascular[7], respiratory[8] and skeletal systems[9]. Cirrhosis can lead to hepatocellular carcinoma[10].

HISTOLOGY OF LIVER FIBROSIS

Following acute injury, liver parenchymal cells regenerate and replace the necrotic damaged cells. During this process, an inflammatory response is observed accompanied by limited deposition of extracellular matrix in the liver parenchyma. In the case of persistence of the injury, the regenerative capacity of parenchymal cells is impaired and dead hepatocytes are replaced by an abundant accumulation of the extracellular matrix, mainly secreted by activated hepatic stellate cells[11]. The pattern of fibrosis is related to the pathogenic mechanism of the underlying disease. In chronic viral hepatitis, autoimmune hepatitis and chronic cholestatic disorders, the fibrotic tissue will initially be located in the periportal areas. However, in alcohol-induced liver disease, the pericentral and perisinusoidal areas represent the initial localisation of extracellular matrix deposition[12], most likely because alcohol is mainly metabolised in these regions.

Following disease progression, the collagen fibres will progressively evolve to bridging fibrosis, leading finally to cirrhosis. Cirrhosis is defined histologically as a diffuse process characterised by fibrosis and the conversion of normal liver architecture into structurally abnormal nodules[13].

In the advanced stages of fibrosis, the liver contains approximately 6 times more extracellular matrix deposition levels than a normal liver, including collagens (types Ⅰ, Ⅲ and Ⅳ), fibronectin, undulin, elastin, laminin, hyaluronan and proteoglycans[11]. The accumulation of extracellular matrix in the liver parenchyma results from both increased synthesis and decreased degradation by matrix metalloproteinases.

PHYSIOPATHOLOGY OF LIVER FIBROSIS

Cellular effectors: Extracellular matrix producing cells

Extracellular matrix is mainly produced by hepatic stellate cells (HSCs), located in the space of Disse between the hepatocytes and sinusoids. Following liver injury, HSCs are "activated" and evolve to myofibroblast-like cells following paracrine and autocrine signalling. This activation is characterised by an increase in cell proliferation and extracellular matrix protein deposition, loss of vitamin A droplets and acquisition of contractile features. HSC activation has been well identified as a key event in the fibrotic response to liver injury. Proliferating activated HSCs are typically located in the regions of greatest injury. This phenomenon is preceded by an influx of inflammatory cells and is associated with extracellular matrix accumulation[14].

Initiation represents the first activation phase and refers to early changes in gene expression and phenotype. HSCs are stimulated by paracrine signals, including exposure to lipid peroxides and products released from damaged hepatocytes as well as biochemical signals from Kupffer and endothelial cells. In the perpetuation phase, the activated phenotype is maintained, and fibrosis is generated. Autocrine as well as paracrine loops are implicated. Resolution refers either to the reversion to a quiescent phenotype or to clearance through apoptosis[14]. At the structural level, activated HSCs lose their large vitamin A-containing lipid droplets and up-regulate the expression of cell adhesion molecules such as intercellular adhesion molecule-1 (ICAM-1) and vascular cell adhesion molecule-1 (VCAM-1), promoting the recruitment of inflammatory cells to the injured liver. The up-regulation of adhesion molecules expression has been studied *in vitro* and *in vivo*[15]. The expression of α-smooth muscle actin is also up-regulated and the secretion of pro-inflammatory cytokines is increased[14,16]. During fibrosis, the enhanced expression of the cytoskeletal protein alpha-smooth muscle actin (α-SMA) confers a contractile potential to HSCs, that is a determinant of increased portal resistance[14]. High expression level of α-SMA correlates with an extent of disease progression. Some particularities have been documented as in kidney. Indeed, renal fibrosis progression (in experimental glomerulonephritis model) was enhanced in mice lacking

this protein in myofibroblasts, while tissue fibrosis was ameliorated by forced expression of α-SMA in renal interstitial myofibroblasts[17]. These data suggest that α-SMA expression could play a role in moderating chronic organ fibrosis.

In addition to HSCs, other cellular sources contributing to extracellular matrix accumulation have been identified. These cells include portal fibroblasts (mainly implicated in biliary fibrosis)[18], circulating fibrocytes, and bone-marrow derived cells[19], as well as fibroblasts derived from epithelial-mesenchymal transition (EMT) of hepatocytes and bile duct epithelial cells[20]. EMT is characterised by the loss of cell adhesion, repression of E-cadherin expression and increased cell mobility. Transforming growth factor beta (TGFβ) induces the acquisition of a fibroblastoid phenotype by hepatocytes and their expression of proteins characteristic for EMT and fibrogenesis. After EMT, hepatocytes will contribute to the population of myofibroblasts and consequently, participate to fibrogenesis[21]. This phenomenon represents an attractive target for liver fibrosis treatment.

Other cellular sources involved in fibrogenesis

Biliary progenitor cells: In biliary fibrosis, the proliferating biliary progenitor cells secrete several factors that attract and activate HSCs into proliferative and extracellular matrix-producing cells. This phenomenon is amplified by several molecules secreted by the surrounding myofibroblasts and by inflammatory cells, such as interleukin (IL)-6 and fibroblast growth factor[22].

Liver sinusoidal endothelial cells: In perisinusoidal fibrosis, liver sinusoidal endothelial cells (LSECs) are activated and proliferate. LSECs contribute to extracellular matrix production and secrete cytokines and growth factors [such as TGFβ and platelet-derived growth factor (PDGF)] that activate HSCs as well as factors contributing to intrahepatic vasoconstriction. Myofibroblasts activate LSECs *via* the secretion of angiogenic factors such as vascular endothelial growth factor (VEGF) and angiopoietin-1[23].

Inflammatory cells: $CD4^+$T cells with Th2 polarization also promote fibrogenesis. These cells secrete IL-4 and IL-13, which can stimulate the differentiation of fibrogenic myeloid cells and macrophages[24]. Th17 cells, induced by TGF-β1 and IL-6, secrete IL-17A, which activates myofibroblasts directly and indirectly by stimulating TGF-β1 release by inflammatory cells[25]. Regulatory T cells can either favour or inhibit fibrogenesis by secreting TGF-β1 (profibrotic) or IL-10 (anti-fibrotic)[22]. $CD4^+$ Th1 cells have an anti-fibrotic effect[22].

NK cells can reduce fibrosis by killing activated HSCs and by producing interferon γ[26]. Monocytes play a key role in inflammation and fibrosis. They are precursors of fibrocytes, macrophages and dendritic cells[27]. Macrophages are fibrogenic during fibrosis progression and fibrolytic during its reversal[22].

Key factors

Factors involved in HSC proliferation: PDGF-β signaling is one of the best characterised pathways involved in the HSC activation process. After PDGF-β binding to its receptor, several intracellular pathways are activated (including the Ras-MAPK, PI3K-AKT/PKB and PKC pathways) supporting cellular proliferation. In early HSC activation, a rapid induction of PDGF-β receptor is observed[28,29].

Even if PDGF is the most potent mitogen towards HSC, other growth factors such as TGFα, epidermal growth factor and VEGF can also stimulate HSC proliferation[30].

Fibrogenic molecules: TGFβ1 is derived from both autocrine and paracrine sources and represents the most potent fibrogenic cytokine in the liver. TGFβ1 recruits Smad2/3, leading to its phosphorylation and stimulation of fibrogenic gene expression[31]. Leptin also has a pro-fibrotic action through suppression of peroxisome proliferator-activated receptor-γ (PPARγ)[32]. Connective tissue growth factor, secreted by HSCs, is also fibrogenic.

Chemokines: The migration of HSCs to the site of injury is promoted by several chemokines (such as CCL5) secreted by HSCs which express the respective receptors[30].

Neurotransmitters: Following chronic liver injury, the local neuroendocrine system is up-regulated, and HSCs express different receptors, including those regulating cannabinoid signalling, and secrete endogenous cannabinoid. The activation of CB1 receptor is pro-fibrogenic, but the CB2 receptor is anti-fibrotic. Opioid and serotonin pathways, as well as thyroid hormones, have a pro-fibrotic effect[30].

Inflammatory pathways: Finally, inflammatory pathways are also involved in the HSC activation process. HSCs secrete inflammatory chemokines and interact directly with immune cells through the expression of adhesion molecules, including ICAM-1 and VCAM-1[33]. Moreover, apoptotic hepatocyte DNA can interact with Toll-like receptor 9 expressed on HSCs, repressing HSC migration and increasing collagen production[34].

CURRENT THERAPEUTIC APPROACHES

Anti-fibrotic drugs

Liver fibrosis is a dynamic process that may undergo reversal[35]. The best aim of anti-fibrotic therapy is to eliminate the underlying disease process. For chronic viral hepatitis, anti-viral treatment efficacy has been recently documented to improve liver fibrosis. In the context of chronic hepatitis B, prevention of developing cirrhosis and fibrosis regression has been demonstrated

for entecavir and tenofovir, two third-generation nucleotide analogues. Chang *et al*[36] firstly documented histological improvements and reversal of fibrosis/cirrhosis in patients with chronic hepatitis B treated with entecavir for a period of at least 3 years. More recently, Marcellin and colleagues reported regression of fibrosis and cirrhosis among patients with chronic hepatitis B infection treated for 5 years with tenofovir disoproxil fumarate. Seventy-four percent of the patients with cirrhosis were no longer cirrhotic at year 5[37]. With respect to chronic hepatitis C, significant regression of fibrosis has been shown among patients presenting mild-to-moderate fibrosis after treatment with Peginterferon alpha-2a or alpha-2b plus ribavirin during 24 or 48 wk, depending on genotype[38]. However, beyond the strict enrolment criteria of the studies, the long term efficacy and safety of these anti-viral treatments have to be confirmed with older patients presenting several comorbidities and treated with other medications.

In the case of impossibility to treat the underlying process, anti-fibrotic therapy would be ideal. Currently, there is no anti-fibrotic drugs available in a clinical setting[1,39,40]. Although specific agents are under investigation, none has been approved as anti-fibrotic therapy.

The use of anti-fibrotic drugs has been reported in preclinical and clinical studies. This approach targets several aims[41-43], such as: (1) downregulation of HSC activation[44-51]; (2) neutralisation of the proliferative, fibrogenic, and contractile responses of HSCs[52-58]; (3) promotion of HSC apoptosis[59,60]; (4) promotion of matrix degradation[61,62]; (5) reduction of inflammation[63-68]; and (6) inhibition of collagen I cross-linking[69], as shown in Table 1. Overall, anti-fibrotic agents have been shown to be highly effective in animal models and represent potential anti-fibrotic drugs. Several anti-fibrotic agents that have been transitioned to clinical studies are PPAR-γ agonist[45,46], interferon γ (IFN-γ)[48,49], angiotensin Ⅱ antagonist[55], colchicine[57], interleukin 10 (IL-10)[64], anti-tumour necrosis factor alpha (TNF-α)[66], ursodeoxycolic acid[68], and antioxidants[51].

Given the supportive preclinical data, however, the data in human are mixed. Moreover, most of these studies were performed in small numbers of patients over a short period of time, but fibrosis is a long lasting, slowly progressive event. Human studies have examined the effect of PPAR-γ agonist[45] and IFN-γ[48] in patients with liver fibrosis. In addition to the promising results in small-scale studies[45,48], longer and larger studies have failed to demonstrate any beneficial effect[46,49].

Compared with preclinical studies, clinical studies of several anti-fibrotic agents have been shown to yield dramatically different results[51,57,64] that may be due to several reasons. In animal models, anti-fibrotic drugs were investigated against the development of fibrosis. On the other hand, in real clinical settings, and in most clinical trials, patients had advanced fibrosis. The potential of collagen degradation also differs between the rodent model and humans because of difference in the cross-linking of ECM. Compared with human fibrosis, which requires years to develop, fibrosis in rodents occurs over weeks or months and contains less chemical cross linking. In addition, differences in the pharmacokinetics of anti-fibrotic drugs between animal models and humans contribute to the different results[42].

Furthermore, a crucial issue that remains to be investigated is how to translate the preclinical evidence of other potential anti-fibrotic agents into a benefit for patients. In general, the development of anti-fibrotic drugs in humans meets several obstacles[41]. First, liver fibrosis is a slowly progressive event, most likely requiring several years of follow up to establish efficacy. Second, the gold-standard tool to evaluate fibrosis remains to be histology. Patients and physicians may be reluctant to perform repeated biopsies due to possible adverse events[70]. Moreover, sampling error in liver biopsy and inter-observer variability may interfere with the results[71]. For all of these reasons, noninvasive diagnostic tools would be highly desirable, ranging from physical examination, laboratory investigation, radiographic testing, to specific serum markers[42]. Transient elastography has also been developed to measure liver stiffness using ultrasound principles[72].

Orthotopic liver transplantation

Currently, orthotopic liver transplantation (OLT) remains the most effective treatment for this condition. Over time, the survival rate after OLT has progressively increased, reaching currently 83% after 1 year. Liver cirrhosis remains the main indication for OLT in Europe (59%) (EASL 2013). In children, a survival rate above 80% has been reported 10 years after OLT[73]. However, over the last 10 years, the annual number of OLTs has stopped growing because organ donation has not kept up with demand, leading to increased mortality and morbidity[74]. Moreover, some limitations such as operative risk, post-transplant rejection, recurrence of the pre-existing liver disease and high costs must be considered[75]. Moreover, fibrosis often develops in the liver grafts as early as one year after transplantation. One year after paediatric OLT, portal fibrosis is present in 31% of liver grafts[76].

The prevalence of fibrosis increases to 65% five years after OLT and to 71% at 10 years, with 29% of severe fibrosis[77].

Cell-based therapy

Cell-based therapy has been proposed as a less invasive potential alternative to OLT. The rationale is mainly based on the ability of several cells to: (1) improve the hepatic inflammatory microenvironment; (2) inhibit the activation or induce apoptosis of HSCs; (3) replace damaged hepatocytes; and (4) promote the regeneration of residual hepatocytes.

Isolated hepatocytes: Hepatocyte transplantation has

Table 1 Preclinical and clinical studies representing the development of anti-fibrotic strategies

Antifibrotic drug	Preclinical/clinical results	Disease model	Ref.
Downregulation of hepatic stellate cell (HSC) activation			
Peroxisomal proliferator-activated receptor gamma agonist (pioglitazone)	Inhibition of HSC activation and amelioration of hepatocyte necroinflammation in rats after 8 wk	Carbon tetrachloride (CCl_4)-induced liver fibrosis	[44]
	Reduction of steatosis, but not fibrosis compared to placebo, in patients with NASH after 6 mo (26 pioglitazone; 21 placebo)	Nonalcoholic steatohepatitis (NASH)	[45]
	No benefit of pioglitazone over placebo in term of steatosis and fibrosis in patients with NASH after 96 wk (80 pioglitazone; 83 placebo)	NASH	[46]
Interferon gamma (IFN-γ)	Inhibition of the activation of HSC and extracellular matrix production	CCl_4-induced liver fibrosis	[47]
	Improvement of fibrosis scores in patients with chronic hepatitis B virus (HBV) infection after 9 mo (54 IFN-γ; 29 control)	Chronic HBV infection	[48]
Antioxidant (vitamin E)	No reversion of fibrosis in patients with advanced liver disease after 1 yr (IFN-γ1b 100 μg 169; IFN-γ1b 200 μg 157; placebo 162)	Chronic hepatitis C virus (HCV) infection	[49]
	Protective effects against liver damage and cirrhosis in rats	CCl_4-induced liver fibrosis	[50]
	No benefit on liver function tests in patients with mild to moderate alcoholic hepatitis after 1 yr (25 vitamin E, 26 placebo)	Alcoholic hepatitis	[51]
Neutralization of proliferative, fibrogenic and contractile responses of HSC			
Anti-transforming growth factor beta (TGF-β)	Supression of fibrosis in rats after 3 wk	Dimethylnitrosamine-induced liver fibrosis	[52]
Short interference RNA	Inhibition of the expression of TGF-β1 and attenuation of liver fibrosis in rats	High-fat diet and CCl_4-induced model of liver fibrosis	[58]
Endothelin antagonist	Nonpeptide endothelin-A receptor antagonist, LU 135252, reduced collagen accumulation in rats after 6 wk	Secondary biliary fibrosis	[53]
Angiotensin system inhibitor	Olmesartan, an angiotensin Ⅱ type 1 receptor blocker, decreased expression of collagen genes and attenuated liver fibrosis in rats after 15 wk	Methionine-choline-deficient rat model of NASH	[54]
	Angiotensin-converting enzyme inhibitors (ACEi) and angiotensin receptor-1 blocker (ARB) did not retard the progression of liver fibrosis in patients with advanced liver fibrosis after 3.5 yr (66 ACEi/ARB, 126 non-ACEi/ARB, 343 no antihypertensive medication)	Chronic hepatitis C	[55]
Colchicine	Colchicine and colchiceine (metabolite of colchicine) prevented the increase in collagen synthesis and increased the intracellular degradation of collagen rats	CCl_4-induced liver fibrosis	[56]
	Colchicine improved fibrosis marker expression, but not histological finding, in patients with hepatic fibrosis after 12 mo (21 colchicine; 17 control)	Liver fibrosis of various etiologies	[57]
Promotion of HSC apoptosis			
Gliotoxin	Morphologic alterations typical of HSC apoptosis *in vitro* (activated rat and human HSCs) and reduction of the number of activated HSCs in rats	CCl_4-induced liver fibrosis	[59]
Sulfasalazine	Induction of activated HSC apoptosis, by inhibiting nuclear factor kappa B-dependent gene transcription, both *in vitro* (activated rat and human HSC) and *in vivo*	CCl_4-induced liver fibrosis	[60]
Promotion of matrix degradation			
Matrix metalloproteinase (MMP) inducer	Urokinase-type plasminogen activator, an initiator of the matrix proteolysis cascade, induced collagenase expression and reversal of fibrosis rats	CCl_4-induced liver fibrosis	[61]
Tissue inhibitor of matrix metalloproteinase (TIMP) inhibitor	Polaprezinc, a zinc-carnosine chelate compound, attenuated fibrosis by inhibiting TIMP expression during a later phase, thus promoting fibrinolysis, in mice after 10 wk	Dietary methionine and choline deficient (MCD)-induced NASH	[62]
Reduce inflammation			
Interleukin 10	Inhibition of HSC activation and decrease of the expression of TGF-β1, MMP-2, and TIMP-1 in rats	CCl_4-induced liver fibrosis	[63]
	Anti-inflammatory effect, but increased HCV viral burden *via* alterations in immunologic viral surveillance, in patients (30 subjects for 3-dose trial)	Chronic hepatitis C	[64]
Anti-tumour necrosis factor-α	Infliximab decreased necrosis, inflammation, and fibrosis in rats	Dietary MCD-induced NASH	[65]
	Infliximab improved Maddrey's score in patients after 28 d (20 subjects)	Alcoholic hepatitis	[66]
Ursodeoxycholic acid (UDCA)	Reversion of liver damage in rats	CCl_4-induced liver fibrosis	[67]
	Reduction of periportal necroinflammation and, if initiated at the earlier stages Ⅰ-Ⅱ of the disease, delay of the progression of histologic stage in patients after 2 yr (200 UDCA, 167 placebo)	Primary biliary cirrhosis	[68]

Inhibition of collagen I cross-linking			
Anti-Lysyl oxidase-like-2	Reduction of liver fibrosis, decrease in the number of myofibroblasts and lower p-Smad3 signal	CCl_4-induced liver fibrosis	[69]

provided the proof-of-concept that cell therapy could be used to treat some liver diseases such as metabolic disorders and acute liver failure[78-80]. A decrease in liver fibrosis and restoration of phospholipid secretion were also observed in a mouse model of progressive familial intrahepatic cholestasis type Ⅲ after hepatocyte transplantation[81]. The feasibility and safety of this technique are supported by the numerous clinical trials performed with hepatocytes.

However, the efficacy of hepatocyte transplantation seems to have a limited durability, with a progressive decrease in the observed effects[82]. Moreover, hepatocytes are poorly resistant to cryopreservation, which can be limitative as fresh hepatocytes are not always available[83]. Moreover, hepatocytes are rare materials and cannot be expanded *in vitro*. Therefore, finding a new and readily available cell source was primordial.

Stem/progenitor cells: Stem/progenitor cells have progressively emerged as an attractive alternative to hepatocytes in the context of cell-based therapy. Stem/progenitor cells are can proliferate in culture, are resistant to cryopreservation and have three interesting characteristics: plasticity, migration and engraftment.

Embryonic stem cells and induced pluripotent stem cells

Pluripotent embryonic stem cells (ESCs) are derived from the inner cell mass of blastocyst embryos. Several *in vivo* studies have revealed the potency of ESCs to differentiate into hepatocyte-like cells and reduce induced liver fibrosis. Mouse ESC-derived green fluorescent protein$^+$ cells injected into CCl_4-injured mice[84], undifferentiated mouse ESCs injected into CCl_4-treated mice[85,86], and human differentiated ESCs transplanted into CCl_4-injured SCID mice[87] showed hepatic differentiation, integrated into the liver parenchyma, and reduced liver fibrosis without evidence of tumourigenicity. The result of these studies should be further confirmed, however, because teratoma formation was observed in other studies. Splenic teratomas were formed in mice with induced hepatocellular injury 35 d after the administration of undifferentiated mouse ESCs and 60 d after the transplantation of mouse ESC-derived alpha-fetoprotein-producing cells[88]. Injection of undifferentiated mouse ESCs into the spleen of immunosuppressed nude mice also gave rise to splenic teratomas[89]. Although ESCs have the ability to differentiate into hepatocytes, their malignant potential and ethical issues remain the major obstacles to develop ESC treatment in clinical settings. Moreover, there may be genetic/epigenetic changes and immune rejection problems when ESCs are transplanted, due to their allogeneic nature[90].

To avoid these issues, new technologies have enabled tissue cells to become induced pluripotent stem cells (iPSCs). Along with the development in the field of stem cell reprogramming, iPSCs represent promising stem cells in cell-based liver therapy. Song and colleagues provided evidence of hepatocyte differentiation of human iPSCs for the first time[91]. At various differentiation stages, human iPSC-derived hepatic cells from different organs repopulated the liver of mice with induced liver cirrhosis. The engraftment potential of differentiated iPSCs was comparable to that of human hepatocytes and was higher than that of undifferentiated human ESCs or iPSCs[92]. iPSCs provide an unlimited source for regenerative medicine since patient-specific cells produce no ethical issue and problem of cell rejection. Despite the promise of iPSCs, the potential risk of genetic manipulation and mutagenesis should be considered before any clinical application. Other issues that remain to be addressed in recruiting iPSCs are (1) the source of iPSCs, whether patient-specific iPSCs should be derived from the diseased tissue portion; (2) the directed hepatic differentiation protocol; and (3) extensive characterisation of hepatic differentiation[93].

Mesenchymal stem cells

Mesenchymal stem cells (MSCs) have extensively been investigated as potential therapeutic options for the treatment of various degenerative diseases and immune disorders, mainly because of their differentiation potential and immunoregulatory properties[94]. The MSC secretion profile also represents an attractive property, as MSCs are known to secrete several anti-fibrotic molecules such as hepatocyte growth factor (HGF)[95]. Compared with embryonic stem cells, MSCs do not cause ethical problems and have a safer profile in terms of oncogenicity[96].

The different properties of MSCs make them an attractive therapeutic tool in the context of liver fibrosis, a topic that will be discussed in the following paragraphs.

PROPERTIES OF MSCs AND THEIR POTENTIAL USE IN REGENERATIVE MEDICINE

General features

In 2006, the International Society for Cellular Therapy proposed minimal criteria to define human MSCs[97]. First, MSCs must be plastic-adherent when maintained under standard culture conditions. Second, $\geqslant$ 95% of the MSC population must express CD105, CD73 and CD90, and lack the expression ($\leqslant$ 2% positive) of CD45, CD34, CD14 or CD11b, CD79α or CD19 and HLA class Ⅱ

surface molecules. Third, MSCs must differentiate into osteoblasts, adipocytes and chondroblasts under standard *in vitro* differentiating conditions[97].

MSCs are spindle-shaped fibroblast-like cells and have the ability of self-renewal. They can be isolated and expanded with high efficiency[98].

Differentiation potential

The high degree of plasticity of MSCs has widely been described during the last decade[99-102].

MSCs have been shown to differentiate into various mesodermal cell lineages (including adipocytes, osteoblasts, chondroblasts, myocytes and cardiomyocytes) and into non-mesodermal cells (such as hepatocytes and neurons), depending on their microenvironment[103].

In particular, *in vitro* models have provided evidence of the differentiation potential of MSCs into hepatocyte-like cells with functional properties such as albumin and urea production, glycogen storage, LDL uptake and phenobarbital-induced cytochrome p450 expression[104,105].

Moreover, the *in vivo* hepatic differentiation of MSCs has been demonstrated in rats[106,107], mice[108], sheep[109] and humans[110].

In comparison with extra-hepatic MSCs, adult-derived human liver stem/progenitor cell, a subtype of MSCs derived from the adult human liver, has a preferential hepatocyte differentiation pattern[111,112].

This hepatic differentiation potential is essential for MSC-based therapies in the context of chronic liver diseases in which the injured hepatocytes cannot regenerate[74].

Immunomodulatory properties

The ability of MSCs to modulate the immune response has attracted great interest, in the context of cell-based therapy and allogeneic transplantation.

It is well known that MSCs suppress the activity of cells from both adaptive and innate immunity. Indeed, MSCs can inhibit the proliferation of $CD8^+$ cytotoxic lymphocytes and increase the relative proportion of $CD4^+$ T helper-2 lymphocytes and $CD4^+$ regulatory T lymphocytes[113,114]. This effect on T lymphocytes indirectly suppresses the function of B lymphocytes because their activation is mainly T cell dependent. Moreover, MSCs can modulate B cell functions by inhibiting their proliferation, differentiation into antibody-secreting cells and chemotaxis. Soluble factors such as transforming growth factor β1, hepatocyte growth factor, prostaglandin E2 and indoleamine 2,3-dioxygenase seem to be implicated in this immunosuppressive activity[115].

MSCs also exert inhibitory effects on monocytes, dendritic cells, macrophages and NK cells, which belong to the innate immune system. MSCs inhibit the maturation of monocytes into dendritic cells, which play a role in antigen presentation to naïve T-cells. MSCs also inhibit the secretion of TNF-α, INF-γ and interleukin-12 by dendritic cells and increase their secretion of IL-10, reducing their proinflammatory potential[116,117]. This inhibitory effect exerted by MSCs seems to be mediated by soluble factors, including prostaglandin E2 (PGE2)[118]. MSCs can also suppress NK cell's proliferation, cytolytic activity and secretion of cytokines. The role of PGE2 and indoleamine 2,3- dioxygenase has been established[119].

Because of all these characteristics, MSCs have generated a great interest for their potential use in regenerative medicine.

In summary, although having less potential to differentiate into endodermal cells compared with ESCs and iPSCs, MSCs can be readily obtained and expanded into large quantities. Moreover, MSCs are resistant to cryopreservation and maintain a stable phenotype following passages in culture[120]. Furthermore, the use of MSCs sidesteps many obstacles for conducting human trials, such as ethical concerns, the risk of rejection, and teratoma formation. Considering the unrelieved concerns regarding safety and efficacy, there has not been a clinical trial using human ESCs and iPSC-derived hepatocytes for liver regeneration.

Homing and engraftment

MSCs have the potential to migrate to the injured site and thereafter to engraft into the concerned organ. This involves their ability to migrate across the endothelial cells and to integrate the organ.

It is well known that injured tissues express several receptors and ligands (such as CXCR4 and SDF-1) that facilitate the migration of MSCs to the damaged sites. Furthermore, chemokines are released following injury, creating a gradient followed by MSCs[121]. This represents a key mediator of the trafficking of MSCs to the site of injury. Finally, MSCs also express some integrins, selectins and chemokine receptors involved in the adhesion and migration of leucocytes[122,123].

The advantage of this property is that MSCs can participate in liver regeneration and ensure continued delivery of trophic signal molecules. However, follow-up studies are necessary to assess the long-term engraftment rate of MSCs.

Therapeutic significance of the MSC secretome

Soluble factors secreted by MSCs have been described to play an important role in liver regeneration and to protect hepatocytes from cell death. It has been demonstrated that bone marrow MSC conditioned medium has anti-apoptotic and pro-mitotic effects on cultured hepatocytes. Moreover, systemic infusion of MSC conditioned medium could inhibit hepatocyte cell death and enhance liver regeneration *in vivo*, in a *D*-galactosamine-induced rat model of acute liver injury[124]. Zhang and colleagues demonstrated that human umbilical cord matrix stem cells provide a significant survival benefit in mice with CCl_4-induced acute liver failure, through paracrine effects, by stimulating endogenous liver regeneration[125].

In addition to liver regeneration, the MSC secretome has also been described to have anti-fibrotic properties. Li *et al*[126] demonstrated that transplantation of exosomes

derived from human umbilical cord MSCs could alleviate CCl_4-induced liver fibrosis by inhibiting EMT and by protecting hepatocytes.

MSC-BASED THERAPY FOR LIVER FIBROSIS TREATMENT: FROM *IN VITRO* STUDIES TO CLINICAL TRIALS

Over the past few years, an increasing number of studies have evaluated the anti-fibrotic potential of MSCs. *In vivo* studies have highlighted the ability of MSCs to reduce liver fibrosis in animal models. *In vitro* studies have been aimed to elucidate the underlying mechanisms by which MSC could modulate HSC activation. Finally, clinical trials have evaluated the efficiency of MSC transplantation for the treatment of liver fibrosis in humans.

Preclinical studies

Several *in vivo* studies were performed to evaluate the therapeutic potential of mesenchymal stem cells in the context of liver fibrosis (Table 2)[127-135].

In most of the studies, liver fibrosis was induced by intraperitoneal or subcutaneous injection of CCl_4. This model has the advantage of being the best characterized model with respect to histological, biochemical, cellular and molecular changes associated with the development of liver fibrosis. Moreover, it can reproduce the pattern of most of the diseases observed in human fibrosis. However, this model has some limitations. First, it is not a suitable model to study all types of liver fibrosis, such as biliary fibrosis. Second, it cannot provide a perfect simulation of a human disease because there are large species differences in immune reactions, gene expression/regulation, and metabolic, pharmacological and tissue responses[136].

The most studied MSCs are those from the bone marrow. These cells have been reported to be beneficial in the prevention of pulmonary fibrotic lesions[137]. However, aspiration of the bone marrow remains an invasive procedure. The bleeding tendency of cirrhotic patients and their general condition may represent an obstacle for autologous cell transplantation.

Alternative sources of MSCs such as adipose tissue and umbilical blood cord have subsequently been proposed but the number of studies in the context of liver fibrosis treatment remains limited, such as studies using human MSCs in animal models. Most of the cell sources used in the *in vivo* studies are murine MSCs. To our knowledge, tissue based MSCs and bone marrow-derived MSCs have not been compared in terms of efficacy for liver fibrosis treatment until now. The beneficial effects were observed regardless of the origin of MSCs, even if the superiority in terms of immunomodulation has been demonstrated *in vitro* for adipose tissue-derived MSCs in comparison with bone marrow-derived MSCs[138].

The results of the *in vivo* studies are promising because they report a decrease in the liver fibrosis with frequent improvement of hepatic functions. Most of the time, these results are observed 4 wk after cell infusion. Long-term studies would be of great interest to evaluate whether the observed anti-fibrotic effect persists over time. However, the CCl_4 injections need to be continued after MSC injection to avoid a regression of liver fibrosis. This represents an obstacle to long-term studies, because animals can hardly support CCl_4 injections over a long period of time. In addition to an improvement in liver fibrosis and liver function, one study reported an improvement in liver microcirculation after MSC injection[128]. In two other studies, the decrease in the collagen deposition was correlated to a decrease in α-SMA expression, a classical marker of activated stellate cells[133,135].

In vivo studies highlight the controversy that remains concerning the exact mechanisms by which MSCs exert their beneficial effect. Indeed, some studies have mentioned the differentiation of MSCs into hepatocyte-like cells[127,131] and/or the expression of metalloproteinases by MSCs[131,132,135]. The promotion of hepatocyte proliferation and modulation of inflammation have also been proposed[130].

The question of the ideal route of MSC administration remains one of the main unsolved issues regarding efficient injection of MSCs. Even if the tail vein seems to be the most often used administration route in animals, the portal vein[128,131] and intrahepatic injections[129] also seem to be efficient. The optimal doses of cells also need to be evaluated because there are significant variations among studies in terms of the number of cells injected per animal.

In vitro studies

As mentioned above, following liver injury, hepatic stellate cells (HSCs) are activated into proliferative, α-smooth muscle actin positive, myofibroblast-like and extracellular matrix-producing cells[14]. Hence, activated HSCs represent an attractive target for antifibrotic therapy.

Several *in vitro* studies have demonstrated the ability of MSCs to modulate HSC activation indirectly *via* paracrine mechanisms and directly through cell-cell contacts. The use of *in vitro* models is supported by the ability of HSC activation to be mimicked *in vitro*, when HSCs are in contact with the plastic culture dishes[14].

Paracrine mechanisms: Using indirect co-culture systems, Parekkadan *et al*[139] showed that human bone marrow-derived MSCs could inhibit collagen synthesis in activated HSCs from rats and, to a lesser extent, in immortalized human HSCs, as demonstrated by a significant reduction in the procollagen type I C-peptide secretion level. Moreover, MSCs could inhibit HSC's proliferation and induce their apoptosis, even if HSCs did nott revert to a quiescent state. The underlying

Table 2 ***In vivo*** **studies using mesenchymal stem cells to treat liver fibrosis**

Species	Fibrosis induction	Administration route	MSC source	Number of cells injected/ animal	Results	Anti-fibrotic mechanisms proposed	Ref.
Rats	CCl_4 IP	Tail vein	Human umbilical cord blood	1×10^6	Liver fibrosis alleviated 4 wk post-infusion Improvement of liver function	Differentiation into hepatocyte-like cells	[127]
Rats	CCl_4 IP	Portal vein	Rat adipose tissue	2×10^6	Improvement of liver functional tests, histological findings and microcirculation 6 wk post-infusion	Not mentioned	[128]
Mice	CCl_4 IP	Intrahepatic	Murine bone marrow	1×10^6	Reduced fibrosis and apoptosis 30 d post-infusion Improvement of liver function	Not mentioned	[129]
Mice	CCl_4 IP	Tail vein	Murine bone marrow	1×10^6	Thinner fibrotic areas and decreased collagen depositions 4 wk post-infusion Improvement of liver function	Promotion of hepatocyte proliferation and modulation of inflammation	[130]
Rats	CCl_4 SC	Portal vein	Human bone marrow	1×10^6	Reduced fibrosis 4 wk post-infusion Improvement of liver function	Differentiation into hepatocyte-like cells expression of MMPs by MSCs	[131]
Mice	CCl_4 IP	Tail vein	Murine bone marrow	1×10^6	Decrease in liver fibrosis 4 wk after transplantation	Increased expression of MMPs	[132]
Rats	CCl_4 SC/DMN IP	Intraveinous	Rat bone marrow	3×10^6	Decrease in collagen deposition and of α-SMA expression Improvement of liver function	Not mentioned	[133]
Rats	CCl_4 SC	Tail vein	Rat bone marrow	3×10^6	Decrease in collagen deposition Elevation of serum albumin	Not mentioned	[134]
Mice	CCl_4 IP	Tail vein	Human bone marrow	5×10^5	Reduction in fibrosis 4 wk after cell infusion	Enhanced expression of MMP-9 and decreased expression of α-SMA, TNFα and TGFβ	[135]

MSC: Mesenchymal stem cell; DMN: Dimethylnitrosamine; MMP: Matrix metalloproteinase; α-SMA: Alpha-smooth muscle actin; TNFα: Tumour necrosis factor-α; TGFβ: Transforming growth factor beta.

mechanisms in the modulation of HSC activity by MSCs were attributed to IL-10, TNFα and HGF. IL-10 and TNFα secretion by MSCs seemed to inhibit synergistically the collagen secretion and the proliferation of HSCs but MSC-derived HGF induced apoptosis in activated HSCs, as demonstrated by antibody-neutralisation studies.

Adipose tissue derived human MSCs could also indirectly inhibit murine HSC proliferation. This growth inhibition is partially mediated by TGF-β3 and HGF, which are secreted by MSCs. Neutralisation of both cytokines synergistically decreased the percentage of cells in the G0/G1 cell cycle phase. A decrease in the phosphorylation of extracellular signal-regulated kinase ½ by MSCs seemed to be partially involved in the suppressive effect of MSCs on HSCs. Gene expression of collagen type Ⅰ and Ⅲ was also inhibited by MSCs[140].

NGF released from human bone marrow-derived MSCs may also represent an important paracrine loop by which human HSC activation can be modulated. Using indirect co-culture systems, Lin and colleagues demonstrated that NGF could inhibit HSC proliferation and promote their apoptosis. The same effect was reproduced using recombinant NGF. NF-κB and its target gene, Bcl-xl, seem to participate in the regulation of this process[141].

Cell-cell contacts: Other studies have evaluated the effects of direct interplay and juxtacrine signaling between MSCs and HSCs.

Rat bone marrow-derived MSCs were shown to significantly inhibit rat HSC proliferation and reduce their α-SMA expression level, through a cell-cell contact mode. The Notch pathway, known to induce cell cycle arrest, is activated following MSC-HSC contact. This signalling pathway may participate in the inhibition of HSC proliferation. In addition, the PI3k/Akt pathway seems to be involved in the growth inhibition of HSCs by the Notch pathway[142].

Human bone marrow-derived MSCs were also shown to inhibit the proliferation and activation of HSCs (LX-2 cell line) through cell-cell contact and through the secretion of HGF. This HSC modulation is mediated by an inhibition of the TLR4/NF-κB signaling pathway[143].

Taken together, these studies shed light on new insights regarding the mechanisms responsible for the anti-fibrotic effects of MSCs.

Clinical trials

Over the past few years, nine clinical trials using human MSCs to treat patients presenting liver fibrosis have been published (Table 3)[144-152].

The endpoints of the studies were to evaluate the safety and efficacy of bone marrow and umbilical cord MSCs transplantation. The cells were mostly infused

Table 3 Clinical trials using mesenchymal stem cell to treat liver fibrosis

Cell source	Administration route	Number of cells infused	Patient population	Number of patients	Follow up period	Endpoints	Efficacy	Ref.
Umbilical cord	Intravenous	5×10^5/kg, 3 times	Chronic hepatitis B	30 treatment 15 control	1 yr	Safety/efficacy	Improvement of liver function and MELD score Reduced acites	[144]
Umbilical cord	Intravenous	5×10^5/kg, 3 times	Chronic hepatitis B	24 treatment 19 control	48 or 72 wk	Safety/efficacy	Improvement of liver function and MELD score Increased survival rates	[145]
Umbilical cord	Intravenous	5×10^5/kg, 3 times	Primary biliary cirrhosis	7	48 wk	Safety/efficacy	Decrease in serum alkaline phosphatase and γ-glutamyltransferase levels Alleviation of fatigue and pruritus Decrease of ascites	[146]
Bone marrow (autologous)	Intravenous	30×10^6/patient	3 cryptogenic 1 autoimmune hepatitis	4	1 yr	Safety/efficacy	Improvement of MELD score	[147]
Bone marrow (autologous)	Intravenous (peripheral vein or portal vein)	30×10^6-50×10^6/patient	4 chronic hepatitis B 1 chronic hepatitis C 1 alcoholic cirrhosis 2 cryptogenic	8	24 wk	Safety/efficacy	Improvement of liver function and MELD score	[148]
Bone marrow (autologous)	Hepatic artery	$3,4 \times 10^8$/patient	Chronic hepatitis B	53 treatment 105 control	192 wk	Safety/efficacy	Improvement of Alb, TBIL, PT and MELD score	[149]
Bone marrow (autologous)	Intravenous	1×10^6/kg	Chronic hepatitis C	15 treatment 10 control	6 mo	Efficacy	Improvement of liver function and MELD score	[150]
Bone marrow (autologous)	Intrasplenic	10×10^6/patient	Chronic hepatitis C	20	6 mo	Safety/efficacy	Decrease od TBIL, AST, ALT, PT and INR Increase of the albumin levels	[151]
Bone marrow (autologous)	Hepatic artery	5×10^7/patient, twice	Alcoholic cirrhosis	12	12 wk	Efficacy	Histological improvements Improvement of Child-Pugh score Decrease of TGF-β1, collagen type 1 and α-SMA	[152]

MELD: Model for end-stage liver disease; Alb: Albumin; TBIL: Total bilirubin; PT: Prothrombin time; TGF-β: Transforming growth factor beta; α-SMA: Alpha-smooth muscle actin; AST: Aspartate aminotransferase; ALT: Alanine aminotransferase; INR: International normalised ratio.

intravenously even if two studies reported infusions *via* the hepatic artery[149,152]. Additionally, in one study, the cells were even injected into the spleen[151]. There is a great variation in the number of cells infused per patient and in the frequency of injection in the different trials. The results of the studies seemed promising in terms of improvement of liver function and model for end-stage liver disease score. This score is based on objective variables (INR, serum albumin and serum bilirubin) and has been validated as a predictor of survival among patients with advanced liver disease[153].

However, there is a lack of data regarding the evaluation of liver histology after cell transplantation, except in one study reporting histological improvements[152].

Globally, the size of the samples is small in most studies and there is a lack of controls in five studies. The follow up period is quite short, except in one study with a 192-wk follow up. We believe that it is crucial to evaluate the long term efficacy, prognosis and safety before proposing this therapy routinely in the clinical practice. Using other types of MSCs and other patient populations could also be of great interest to evaluate the best therapeutic option for each pathology.

The use of MSCs in clinical practice is currently hindered by the incapacity to monitor the transplanted cells in the patients and by the lack of standardised transplantation protocols. Standardised protocols providing information concerning the timing of cell injection following the stage of liver fibrosis, number of cells and administration route would be useful.

Only randomised controlled clinical trials can assess the potential clinical benefit of MSCs for patients affected by liver fibrosis. According to the clinical trials Website of the United States sponsored by the National Institutes of Health (http://clinicaltrials.gov), approximately 24 clinical trials are currently ongoing.

FUTURE PROSPECTS

MSCs may represent a clinically relevant solution for the treatment of liver fibrosis, given their interesting properties and the promising results of preclinical and clinical studies.

However, several issues need to be clarified before MSCs can be routinely proposed as a therapeutic option to treat liver fibrosis.

Over the past few years, concerns have been raised about the long-term effectiveness of MSC-based the-

rapy and the potential tumorigenic risk. Several lines of evidence have suggested that MSCs might promote tumour growth *in vivo*[154-156]. On the other hand, because of their immunomodulatory properties, MSCs may have an antitumour effect, in relation with the modulation of the inflammatory environment that characterizes many tumors[157-159]. MSCs can also interact with cancer cells and inhibit signalling pathways associated with tumour growth and cell division[160,161].

Moreover, there is a lack of standardised protocols for MSC transplantation. The optimal MSC doses, timing and frequency of injection and administration route differ considerably among the different studies.

For all of these reasons, we believe that further studies, particularly randomised controlled trials, are needed to evaluate the long-term safety and efficacy of MSC-based treatment. Moreover, potency tests performed on MSCs before injection in patients could be useful.

CONCLUSION

Although considerable advances have been made in the past decade to better understand the cellular and molecular mechanisms underlying liver fibrogenesis, no efficient therapy is available so far to treat this serious condition.

Further investigations and efforts are currently being conducted to efficiently reverse liver fibrosis. MSC-based therapy has been shown to have a significant potential to decrease mortality and improve the quality of life of patients with liver fibrosis. However, a standardisation is needed before proposing this strategy routinely in clinical practice.

REFERENCES

1 **Friedman SL**. Liver fibrosis -- from bench to bedside. *J Hepatol* 2003; **38** Suppl 1: S38-S53 [PMID: 12591185 DOI: 10.1016/S0168-8278(02)00429-4]

2 **Lozano R**, Naghavi M, Foreman K, Lim S, Shibuya K, Aboyans V, Abraham J, Adair T, Aggarwal R, Ahn SY, Alvarado M, Anderson HR, Anderson LM, Andrews KG, Atkinson C, Baddour LM, Barker-Collo S, Bartels DH, Bell ML, Benjamin EJ, Bennett D, Bhalla K, Bikbov B, Bin Abdulhak A, Birbeck G, Blyth F, Bolliger I, Boufous S, Bucello C, Burch M, Burney P, Carapetis J, Chen H, Chou D, Chugh SS, Coffeng LE, Colan SD, Colquhoun S, Colson KE, Condon J, Connor MD, Cooper LT, Corriere M, Cortinovis M, de Vaccaro KC, Couser W, Cowie BC, Criqui MH, Cross M, Dabhadkar KC, Dahodwala N, De Leo D, Degenhardt L, Delossantos A, Denenberg J, Des Jarlais DC, Dharmaratne SD, Dorsey ER, Driscoll T, Duber H, Ebel B, Erwin PJ, Espindola P, Ezzati M, Feigin V, Flaxman AD, Forouzanfar MH, Fowkes FG, Franklin R, Fransen M, Freeman MK, Gabriel SE, Gakidou E, Gaspari F, Gillum RF, Gonzalez-Medina D, Halasa YA, Haring D, Harrison JE, Havmoeller R, Hay RJ, Hoen B, Hotez PJ, Hoy D, Jacobsen KH, James SL, Jasrasaria R, Jayaraman S, Johns N, Karthikeyan G, Kassebaum N, Keren A, Khoo JP, Knowlton LM, Kobusingye O, Koranteng A, Krishnamurthi R, Lipnick M, Lipshultz SE, Ohno SL, Mabweijano J, MacIntyre MF, Mallinger L, March L, Marks GB, Marks R, Matsumori A, Matzopoulos R, Mayosi BM, McAnulty JH, McDermott MM, McGrath J, Mensah GA, Merriman TR, Michaud C, Miller M, Miller TR, Mock C, Mocumbi AO, Mokdad AA, Moran A, Mulholland K, Nair MN, Naldi L, Narayan KM, Nasseri K, Norman P, O'Donnell M, Omer SB, Ortblad K, Osborne R, Ozgediz D, Pahari B, Pandian JD, Rivero AP, Padilla RP, Perez-Ruiz F, Perico N, Phillips D, Pierce K, Pope CA, Porrini E, Pourmalek F, Raju M, Ranganathan D, Rehm JT, Rein DB, Remuzzi G, Rivara FP, Roberts T, De León FR, Rosenfeld LC, Rushton L, Sacco RL, Salomon JA, Sampson U, Sanman E, Schwebel DC, Segui-Gomez M, Shepard DS, Singh D, Singleton J, Sliwa K, Smith E, Steer A, Taylor JA, Thomas B, Tleyjeh IM, Towbin JA, Truelsen T, Undurraga EA, Venketasubramanian N, Vijayakumar L, Vos T, Wagner GR, Wang M, Wang W, Watt K, Weinstock MA, Weintraub R, Wilkinson JD, Woolf AD, Wulf S, Yeh PH, Yip P, Zabetian A, Zheng ZJ, Lopez AD, Murray CJ, AlMazroa MA, Memish ZA. Global and regional mortality from 235 causes of death for 20 age groups in 1990 and 2010: a systematic analysis for the Global Burden of Disease Study 2010. *Lancet* 2012; **380**: 2095-2128 [PMID: 23245604 DOI: 10.1016/S0140-6736(12)61728-0]

3 **Zatoński WA**, Sulkowska U, Mańczuk M, Rehm J, Boffetta P, Lowenfels AB, La Vecchia C. Liver cirrhosis mortality in Europe, with special attention to Central and Eastern Europe. *Eur Addict Res* 2010; **16**: 193-201 [PMID: 20606444 DOI: 10.1159/000317248]

4 **Bosch J**, García-Pagán JC. Complications of cirrhosis. I. Portal hypertension. *J Hepatol* 2000; **32**: 141-156 [PMID: 10728801 DOI: 10.1016/S0168-8278(00)80422-5]

5 **Quigley EM**. Gastrointestinal dysfunction in liver disease and portal hypertension. Gut-liver interactions revisited. *Dig Dis Sci* 1996; **41**: 557-561 [PMID: 8617136 DOI: 10.1007/BF02282341]

6 **Cárdenas A**. Hepatorenal syndrome: a dreaded complication of end-stage liver disease. *Am J Gastroenterol* 2005; **100**: 460-467 [PMID: 15667508 DOI: 10.1111/j.1572-0241.2005.40952.x]

7 **Wong F**, Girgrah N, Graba J, Allidina Y, Liu P, Blendis L. The cardiac response to exercise in cirrhosis. *Gut* 2001; **49**: 268-275 [PMID: 11454805 DOI: 10.1136/gut.49.2.268]

8 **Huffmyer JL**, Nemergut EC. Respiratory dysfunction and pulmonary disease in cirrhosis and other hepatic disorders. *Respir Care* 2007; **52**: 1030-1036 [PMID: 17650360]

9 **Collier J**. Bone disorders in chronic liver disease. *Hepatology* 2007; **46**: 1271-1278 [PMID: 17886334 DOI: 10.1002/hep.21852]

10 **de Franchis R**, Dell'Era A. Non-invasive diagnosis of cirrhosis and the natural history of its complications. *Best Pract Res Clin Gastroenterol* 2007; **21**: 3-18 [PMID: 17223493 DOI: 10.1016/j.bpg.2006.07.001]

11 **Bataller R**, Brenner DA. Liver fibrosis. *J Clin Invest* 2005; **115**: 209-218 [PMID: 15690074 DOI: 10.1172/JCI24282]

12 **Pinzani M**. Liver fibrosis. *Springer Semin Immunopathol* 1999; **21**: 475-490 [PMID: 10945037 DOI: 10.1007/BF00870306]

13 **Anthony PP**, Ishak KG, Nayak NC, Poulsen HE, Scheuer PJ, Sobin LH. The morphology of cirrhosis. Recommendations on definition, nomenclature, and classification by a working group sponsored by the World Health Organization. *J Clin Pathol* 1978; **31**: 395-414 [PMID: 649765 DOI: 10.1136/jcp.31.5.395]

14 **Friedman SL**. Hepatic stellate cells: protean, multifunctional, and enigmatic cells of the liver. *Physiol Rev* 2008; **88**: 125-172 [PMID: 18195085 DOI: 10.1152/physrev.00013.2007]

15 **Knittel T**, Dinter C, Kobold D, Neubauer K, Mehde M, Eichhorst S, Ramadori G. Expression and regulation of cell adhesion molecules by hepatic stellate cells (HSC) of rat liver: involvement of HSC in recruitment of inflammatory cells during hepatic tissue repair. *Am J Pathol* 1999; **154**: 153-167 [PMID: 9916930 DOI: 10.1016/S0002-9440(10)65262-5]

16 **Sancho-Bru P**, Bataller R, Gasull X, Colmenero J, Khurdayan V, Gual A, Nicolás JM, Arroyo V, Ginès P. Genomic and functional characterization of stellate cells isolated from

human cirrhotic livers. *J Hepatol* 2005; **43**: 272-282 [PMID: 15964095 DOI: 10.1016/j.jhep.2005.02.035]
17 **Takeji M**, Moriyama T, Oseto S, Kawada N, Hori M, Imai E, Miwa T. Smooth muscle alpha-actin deficiency in myofibroblasts leads to enhanced renal tissue fibrosis. *J Biol Chem* 2006; **281**: 40193-40200 [PMID: 17090535 DOI: 10.1074/jbc.M602182200]
18 **Wells RG**, Kruglov E, Dranoff JA. Autocrine release of TGF-beta by portal fibroblasts regulates cell growth. *FEBS Lett* 2004; **559**: 107-110 [PMID: 14960316 DOI: 10.1016/S0014-5793(04)00037-7]
19 **Forbes SJ**, Russo FP, Rey V, Burra P, Rugge M, Wright NA, Alison MR. A significant proportion of myofibroblasts are of bone marrow origin in human liver fibrosis. *Gastroenterology* 2004; **126**: 955-963 [PMID: 15057733 DOI: 10.1053/j.gastro.2004.02.025]
20 **Kalluri R**, Neilson EG. Epithelial-mesenchymal transition and its implications for fibrosis. *J Clin Invest* 2003; **112**: 1776-1784 [PMID: 14679171 DOI: 10.1172/JCI200320530]
21 **Meindl-Beinker NM**, Dooley S. Transforming growth factor-beta and hepatocyte transdifferentiation in liver fibrogenesis. *J Gastroenterol Hepatol* 2008; **23** Suppl 1: S122-S127 [PMID: 18336655 DOI: 10.1111/j.1440-1746.2007.05297.x]
22 **Schuppan D**, Kim YO. Evolving therapies for liver fibrosis. *J Clin Invest* 2013; **123**: 1887-1901 [PMID: 23635787 DOI: 10.1172/JCI66028]
23 **Thabut D**, Shah V. Intrahepatic angiogenesis and sinusoidal remodeling in chronic liver disease: new targets for the treatment of portal hypertension? *J Hepatol* 2010; **53**: 976-980 [PMID: 20800926 DOI: 10.1016/j.jhep.2010.07.004]
24 **Lee CG**, Homer RJ, Zhu Z, Lanone S, Wang X, Koteliansky V, Shipley JM, Gotwals P, Noble P, Chen Q, Senior RM, Elias JA. Interleukin-13 induces tissue fibrosis by selectively stimulating and activating transforming growth factor beta(1). *J Exp Med* 2001; **194**: 809-821 [PMID: 11560996 DOI: 10.1084/jem.194.6.809]
25 **Meng F**, Wang K, Aoyama T, Grivennikov SI, Paik Y, Scholten D, Cong M, Iwaisako K, Liu X, Zhang M, Osterreicher CH, Stickel F, Ley K, Brenner DA, Kisseleva T. Interleukin-17 signaling in inflammatory, Kupffer cells, and hepatic stellate cells exacerbates liver fibrosis in mice. *Gastroenterology* 2012; **143**: 765-776.e1-e3 [PMID: 22687286 DOI: 10.1053/j.gastro.2012.05.049]
26 **Gao B**, Radaeva S. Natural killer and natural killer T cells in liver fibrosis. *Biochim Biophys Acta* 2013; **1832**: 1061-1069 [PMID: 23022478 DOI: 10.1016/j.bbadis.2012.09.008]
27 **Marra F**, Aleffi S, Galastri S, Provenzano A. Mononuclear cells in liver fibrosis. *Semin Immunopathol* 2009; **31**: 345-358 [PMID: 19533130 DOI: 10.1007/s00281-009-0169-0]
28 **Kelly JD**, Haldeman BA, Grant FJ, Murray MJ, Seifert RA, Bowen-Pope DF, Cooper JA, Kazlauskas A. Platelet-derived growth factor (PDGF) stimulates PDGF receptor subunit dimerization and intersubunit trans-phosphorylation. *J Biol Chem* 1991; **266**: 8987-8992 [PMID: 1709159]
29 **Wong L**, Yamasaki G, Johnson RJ, Friedman SL. Induction of beta-platelet-derived growth factor receptor in rat hepatic lipocytes during cellular activation in vivo and in culture. *J Clin Invest* 1994; **94**: 1563-1569 [PMID: 7929832 DOI: 10.1172/JCI117497]
30 **Lee UE**, Friedman SL. Mechanisms of hepatic fibrogenesis. *Best Pract Res Clin Gastroenterol* 2011; **25**: 195-206 [PMID: 21497738 DOI: 10.1016/j.bpg.2011.02.005]
31 **Inagaki Y**, Okazaki I. Emerging insights into Transforming growth factor beta Smad signal in hepatic fibrogenesis. *Gut* 2007; **56**: 284-292 [PMID: 17303605 DOI: 10.1136/gut.2005.088690]
32 **Zhou Y**, Jia X, Wang G, Wang X, Liu J. PI-3 K/AKT and ERK signaling pathways mediate leptin-induced inhibition of PPARgamma gene expression in primary rat hepatic stellate cells. *Mol Cell Biochem* 2009; **325**: 131-139 [PMID: 19191008 DOI: 10.1007/s11010-009-0027-3]
33 **Hellerbrand SC**, Tsukamoto H, Brenner DA, Rippe RA. Expression of intracellular adhesion molecule 1 by activated hepatic stellate cells. *Hepatology* 1996; **24**: 670-676 [PMID: 8781341 DOI: 10.1002/hep.510240333]
34 **Watanabe A**, Hashmi A, Gomes DA, Town T, Badou A, Flavell RA, Mehal WZ. Apoptotic hepatocyte DNA inhibits hepatic stellate cell chemotaxis via toll-like receptor 9. *Hepatology* 2007; **46**: 1509-1518 [PMID: 17705260 DOI: 10.1002/hep.21867]
35 **Cohen-Naftaly M**, Friedman SL. Current status of novel antifibrotic therapies in patients with chronic liver disease. *Therap Adv Gastroenterol* 2011; **4**: 391-417 [PMID: 22043231 DOI: 10.1177/1756283X11413002]
36 **Chang TT**, Liaw YF, Wu SS, Schiff E, Han KH, Lai CL, Safadi R, Lee SS, Halota W, Goodman Z, Chi YC, Zhang H, Hindes R, Iloeje U, Beebe S, Kreter B. Long-term entecavir therapy results in the reversal of fibrosis/cirrhosis and continued histological improvement in patients with chronic hepatitis B. *Hepatology* 2010; **52**: 886-893 [PMID: 20683932 DOI: 10.1002/hep.23785]
37 **Marcellin P**, Gane E, Buti M, Afdhal N, Sievert W, Jacobson IM, Washington MK, Germanidis G, Flaherty JF, Schall RA, Bornstein JD, Kitrinos KM, Subramanian GM, McHutchison JG, Heathcote EJ. Regression of cirrhosis during treatment with tenofovir disoproxil fumarate for chronic hepatitis B: a 5-year open-label follow-up study. *Lancet* 2013; **381**: 468-475 [PMID: 23234725 DOI: 10.1016/S0140-6736(12)61425-1]
38 **Vukobrat-Bijedic Z**, Husic-Selimovic A, Mehinovic L, Mehmedovic A, Junuzovic D, Bjelogrlic I, Sofic A, Djurovic A. Analysis of effect of antiviral therapy on regression of liver fibrosis in patient with HCV infection. *Mater Sociomed* 2014; **26**: 172-176 [PMID: 25126010 DOI: 10.5455/msm.2014.26.172-176]
39 **Mormone E**, George J, Nieto N. Molecular pathogenesis of hepatic fibrosis and current therapeutic approaches. *Chem Biol Interact* 2011; **193**: 225-231 [PMID: 21803030 DOI: 10.1016/j.cbi.2011.07.001]
40 **Li JT**, Liao ZX, Ping J, Xu D, Wang H. Molecular mechanism of hepatic stellate cell activation and antifibrotic therapeutic strategies. *J Gastroenterol* 2008; **43**: 419-428 [PMID: 18600385 DOI: 10.1007/s00535-008-2180-y]
41 **Albanis E**, Friedman SL. Antifibrotic agents for liver disease. *Am J Transplant* 2006; **6**: 12-19 [PMID: 16433751 DOI: 10.1111/j.1600-6143.2005.01143.x]
42 **Rockey DC**. Current and future anti-fibrotic therapies for chronic liver disease. *Clin Liver Dis* 2008; **12**: 939-962, xi [PMID: 18984475 DOI: 10.1016/j.cld.2008.07.011]
43 **Ismail MH**, Pinzani M. Reversal of hepatic fibrosis: pathophysiological basis of antifibrotic therapies. *Hepat Med* 2011; **3**: 69-80 [PMID: 24367223 DOI: 10.2147/HMER.S9051]
44 **Yuan GJ**, Zhang ML, Gong ZJ. Effects of PPARg agonist pioglitazone on rat hepatic fibrosis. *World J Gastroenterol* 2004; **10**: 1047-1051 [PMID: 15052691]
45 **Belfort R**, Harrison SA, Brown K, Darland C, Finch J, Hardies J, Balas B, Gastaldelli A, Tio F, Pulcini J, Berria R, Ma JZ, Dwivedi S, Havranek R, Fincke C, DeFronzo R, Bannayan GA, Schenker S, Cusi K. A placebo-controlled trial of pioglitazone in subjects with nonalcoholic steatohepatitis. *N Engl J Med* 2006; **355**: 2297-2307 [PMID: 17135584 DOI: 10.1056/NEJMoa060326]
46 **Sanyal AJ**, Chalasani N, Kowdley KV, McCullough A, Diehl AM, Bass NM, Neuschwander-Tetri BA, Lavine JE, Tonascia J, Unalp A, Van Natta M, Clark J, Brunt EM, Kleiner DE, Hoofnagle JH, Robuck PR. Pioglitazone, vitamin E, or placebo for nonalcoholic steatohepatitis. *N Engl J Med* 2010; **362**: 1675-1685 [PMID: 20427778 DOI: 10.1056/NEJMoa0907929]
47 **Rockey DC**, Chung JJ. Interferon gamma inhibits lipocyte activation and extracellular matrix mRNA expression during experimental liver injury: implications for treatment of hepatic fibrosis. *J Investig Med* 1994; **42**: 660-670 [PMID:

8521029]
48 **Weng HL**, Wang BE, Jia JD, Wu WF, Xian JZ, Mertens PR, Cai WM, Dooley S. Effect of interferon-gamma on hepatic fibrosis in chronic hepatitis B virus infection: a randomized controlled study. *Clin Gastroenterol Hepatol* 2005; **3**: 819-828 [PMID: 16234012 DOI: 10.1016/S1542-3565(05)00404-0]
49 **Pockros PJ**, Jeffers L, Afdhal N, Goodman ZD, Nelson D, Gish RG, Reddy KR, Reindollar R, Rodriguez-Torres M, Sullivan S, Blatt LM, Faris-Young S. Final results of a double-blind, placebo-controlled trial of the antifibrotic efficacy of interferon-gamma1b in chronic hepatitis C patients with advanced fibrosis or cirrhosis. *Hepatology* 2007; **45**: 569-578 [PMID: 17326152 DOI: 10.1002/hep.21561]
50 **Naziroğlu M**, Cay M, Ustündağ B, Aksakal M, Yekeler H. Protective effects of vitamin E on carbon tetrachloride-induced liver damage in rats. *Cell Biochem Funct* 1999; **17**: 253-259 [PMID: 10587612]
51 **Mezey E**, Potter JJ, Rennie-Tankersley L, Caballeria J, Pares A. A randomized placebo controlled trial of vitamin E for alcoholic hepatitis. *J Hepatol* 2004; **40**: 40-46 [PMID: 14672612 DOI: 10.1016/S0168-8278(03)00476-8]
52 **Nakamura T**, Sakata R, Ueno T, Sata M, Ueno H. Inhibition of transforming growth factor beta prevents progression of liver fibrosis and enhances hepatocyte regeneration in dimethylnitrosamine-treated rats. *Hepatology* 2000; **32**: 247-255 [PMID: 10915731 DOI: 10.1053/jhep.2000.9109]
53 **Cho JJ**, Hocher B, Herbst H, Jia JD, Ruehl M, Hahn EG, Riecken EO, Schuppan D. An oral endothelin-A receptor antagonist blocks collagen synthesis and deposition in advanced rat liver fibrosis. *Gastroenterology* 2000; **118**: 1169-1178 [PMID: 10833492 DOI: 10.1016/S0016-5085(00)70370-2]
54 **Hirose A**, Ono M, Saibara T, Nozaki Y, Masuda K, Yoshioka A, Takahashi M, Akisawa N, Iwasaki S, Oben JA, Onishi S. Angiotensin II type 1 receptor blocker inhibits fibrosis in rat nonalcoholic steatohepatitis. *Hepatology* 2007; **45**: 1375-1381 [PMID: 17518368 DOI: 10.1002/hep.21638]
55 **Abu Dayyeh BK**, Yang M, Dienstag JL, Chung RT. The effects of angiotensin blocking agents on the progression of liver fibrosis in the HALT-C Trial cohort. *Dig Dis Sci* 2011; **56**: 564-568 [PMID: 21136163 DOI: 10.1007/s10620-010-1507-8]
56 **Rodríguez L**, Cerbón-Ambriz J, Muñoz ML. Effects of colchicine and colchiceine in a biochemical model of liver injury and fibrosis. *Arch Med Res* 1998; **29**: 109-116 [PMID: 9650324]
57 **Nikolaidis N**, Kountouras J, Giouleme O, Tzarou V, Chatzizisi O, Patsiaoura K, Papageorgiou A, Leontsini M, Eugenidis N, Zamboulis C. Colchicine treatment of liver fibrosis. *Hepatogastroenterology* 2006; **53**: 281-285 [PMID: 16608040]
58 **Lang Q**, Liu Q, Xu N, Qian KL, Qi JH, Sun YC, Xiao L, Shi XF. The antifibrotic effects of TGF-β1 siRNA on hepatic fibrosis in rats. *Biochem Biophys Res Commun* 2011; **409**: 448-453 [PMID: 21600192 DOI: 10.1016/j.bbrc.2011.05.023]
59 **Wright MC**, Issa R, Smart DE, Trim N, Murray GI, Primrose JN, Arthur MJ, Iredale JP, Mann DA. Gliotoxin stimulates the apoptosis of human and rat hepatic stellate cells and enhances the resolution of liver fibrosis in rats. *Gastroenterology* 2001; **121**: 685-698 [PMID: 11522753 DOI: 10.1053/gast.2001.27188]
60 **Oakley F**, Meso M, Iredale JP, Green K, Marek CJ, Zhou X, May MJ, Millward-Sadler H, Wright MC, Mann DA. Inhibition of inhibitor of kappaB kinases stimulates hepatic stellate cell apoptosis and accelerated recovery from rat liver fibrosis. *Gastroenterology* 2005; **128**: 108-120 [PMID: 15633128 DOI: 10.1053/j.gastro.2004.10.003]
61 **Salgado S**, Garcia J, Vera J, Siller F, Bueno M, Miranda A, Segura A, Grijalva G, Segura J, Orozco H, Hernandez-Pando R, Fafutis M, Aguilar LK, Aguilar-Cordova E, Armendariz-Borunda J. Liver cirrhosis is reverted by urokinase-type plasminogen activator gene therapy. *Mol Ther* 2000; **2**: 545-551 [PMID: 11124055 DOI: 10.1006/mthe.2000.0210]
62 **Sugino H**, Kumagai N, Watanabe S, Toda K, Takeuchi O, Tsunematsu S, Morinaga S, Tsuchimoto K. Polaprezinc attenuates liver fibrosis in a mouse model of non-alcoholic steatohepatitis. *J Gastroenterol Hepatol* 2008; **23**: 1909-1916 [PMID: 18422963 DOI: 10.1111/j.1440-1746.2008.05393.x]
63 **Zhang LJ**, Zheng WD, Chen YX, Huang YH, Chen ZX, Zhang SJ, Shi MN, Wang XZ. Antifibrotic effects of interleukin-10 on experimental hepatic fibrosis. *Hepatogastroenterology* 2007; **54**: 2092-2098 [PMID: 18251166]
64 **Nelson DR**, Tu Z, Soldevila-Pico C, Abdelmalek M, Zhu H, Xu YL, Cabrera R, Liu C, Davis GL. Long-term interleukin 10 therapy in chronic hepatitis C patients has a proviral and anti-inflammatory effect. *Hepatology* 2003; **38**: 859-868 [PMID: 14512873 DOI: 10.1053/jhep.2003.50427]
65 **Koca SS**, Bahcecioglu IH, Poyrazoglu OK, Ozercan IH, Sahin K, Ustundag B. The treatment with antibody of TNF-alpha reduces the inflammation, necrosis and fibrosis in the non-alcoholic steatohepatitis induced by methionine- and choline-deficient diet. *Inflammation* 2008; **31**: 91-98 [PMID: 18066656 DOI: 10.1007/s10753-007-9053-z]
66 **Spahr L**, Rubbia-Brandt L, Frossard JL, Giostra E, Rougemont AL, Pugin J, Fischer M, Egger H, Hadengue A. Combination of steroids with infliximab or placebo in severe alcoholic hepatitis: a randomized controlled pilot study. *J Hepatol* 2002; **37**: 448-455 [PMID: 12217597 DOI: 10.1016/S0168-8278(02)00230-1]
67 **Nava-Ocampo AA**, Suster S, Muriel P. Effect of colchiceine and ursodeoxycholic acid on hepatocyte and erythrocyte membranes and liver histology in experimentally induced carbon tetrachloride cirrhosis in rats. *Eur J Clin Invest* 1997; **27**: 77-84 [PMID: 9041381 DOI: 10.1046/j.1365-2362.1997.910615.x]
68 **Poupon RE**, Lindor KD, Parés A, Chazouillères O, Poupon R, Heathcote EJ. Combined analysis of the effect of treatment with ursodeoxycholic acid on histologic progression in primary biliary cirrhosis. *J Hepatol* 2003; **39**: 12-16 [PMID: 12821038 DOI: 10.1016/S0168-8278(03)00192-2]
69 **Barry-Hamilton V**, Spangler R, Marshall D, McCauley S, Rodriguez HM, Oyasu M, Mikels A, Vaysberg M, Ghermazien H, Wai C, Garcia CA, Velayo AC, Jorgensen B, Biermann D, Tsai D, Green J, Zaffryar-Eilot S, Holzer A, Ogg S, Thai D, Neufeld G, Van Vlasselaer P, Smith V. Allosteric inhibition of lysyl oxidase-like-2 impedes the development of a pathologic microenvironment. *Nat Med* 2010; **16**: 1009-1017 [PMID: 20818376 DOI: 10.1038/nm.2208]
70 **Cadranel JF**, Rufat P, Degos F. Practices of liver biopsy in France: results of a prospective nationwide survey. For the Group of Epidemiology of the French Association for the Study of the Liver (AFEF). *Hepatology* 2000; **32**: 477-481 [PMID: 10960438 DOI: 10.1053/jhep.2000.16602]
71 **Regev A**, Berho M, Jeffers LJ, Milikowski C, Molina EG, Pyrsopoulos NT, Feng ZZ, Reddy KR, Schiff ER. Sampling error and intraobserver variation in liver biopsy in patients with chronic HCV infection. *Am J Gastroenterol* 2002; **97**: 2614-2618 [PMID: 12385448 DOI: 10.1111/j.1572-0241.2002.06038.x]
72 **Sandrin L**, Fourquet B, Hasquenoph JM, Yon S, Fournier C, Mal F, Christidis C, Ziol M, Poulet B, Kazemi F, Beaugrand M, Palau R. Transient elastography: a new noninvasive method for assessment of hepatic fibrosis. *Ultrasound Med Biol* 2003; **29**: 1705-1713 [PMID: 14698338 DOI: 10.1016/j.ultrasmedbio.2003.07.001]
73 **Kelly DA**. Current issues in pediatric transplantation. *Pediatr Transplant* 2006; **10**: 712-720 [PMID: 16911496 DOI: 10.1111/j.1399-3046.2006.00567.x]
74 **Forbes SJ**. Stem cell therapy for chronic liver disease--choosing the right tools for the job. *Gut* 2008; **57**: 153-155 [PMID: 18192451 DOI: 10.1136/gut.2007.134247]
75 **Francoz C**, Belghiti J, Durand F. Indications of liver transplantation in patients with complications of cirrhosis. *Best Pract Res Clin Gastroenterol* 2007; **21**: 175-190 [PMID: 17223504 DOI: 10.1016/j.bpg.2006.07.007]

76 **Peeters PM**, Sieders E, vd Heuvel M, Bijleveld CM, de Jong KP, TenVergert EM, Slooff MJ, Gouw AS. Predictive factors for portal fibrosis in pediatric liver transplant recipients. *Transplantation* 2000; **70**: 1581-1587 [PMID: 11152219 DOI: 10.1097/00007890-200012150-00008]

77 **Scheenstra R**, Peeters PM, Verkade HJ, Gouw AS. Graft fibrosis after pediatric liver transplantation: ten years of follow-up. *Hepatology* 2009; **49**: 880-886 [PMID: 19101912 DOI: 10.1002/hep.22686]

78 **Sokal EM**, Smets F, Bourgois A, Van Maldergem L, Buts JP, Reding R, Bernard Otte J, Evrard V, Latinne D, Vincent MF, Moser A, Soriano HE. Hepatocyte transplantation in a 4-year-old girl with peroxisomal biogenesis disease: technique, safety, and metabolic follow-up. *Transplantation* 2003; **76**: 735-738 [PMID: 12973120 DOI: 10.1097/01.TP.0000077420.81365.53]

79 **Stéphenne X**, Najimi M, Sibille C, Nassogne MC, Smets F, Sokal EM. Sustained engraftment and tissue enzyme activity after liver cell transplantation for argininosuccinate lyase deficiency. *Gastroenterology* 2006; **130**: 1317-1323 [PMID: 16618422 DOI: 10.1053/j.gastro.2006.01.008]

80 **Stéphenne X**, Najimi M, Smets F, Reding R, de Ville de Goyet J, Sokal EM. Cryopreserved liver cell transplantation controls ornithine transcarbamylase deficient patient while awaiting liver transplantation. *Am J Transplant* 2005; **5**: 2058-2061 [PMID: 15996260 DOI: 10.1111/j.1600-6143.2005.00935.x]

81 **De Vree JM**, Ottenhoff R, Bosma PJ, Smith AJ, Aten J, Oude Elferink RP. Correction of liver disease by hepatocyte transplantation in a mouse model of progressive familial intrahepatic cholestasis. *Gastroenterology* 2000; **119**: 1720-1730 [PMID: 11113093 DOI: 10.1053/gast.2000.20222]

82 **Smets F**, Najimi M, Sokal EM. Cell transplantation in the treatment of liver diseases. *Pediatr Transplant* 2008; **12**: 6-13 [PMID: 18186884 DOI: 10.1111/j.1399-3046.2007.00788.x]

83 **Stéphenne X**, Najimi M, Ngoc DK, Smets F, Hue L, Guigas B, Sokal EM. Cryopreservation of human hepatocytes alters the mitochondrial respiratory chain complex 1. *Cell Transplant* 2007; **16**: 409-419 [PMID: 17658131 DOI: 10.3727/000000007783464821]

84 **Yamamoto H**, Quinn G, Asari A, Yamanokuchi H, Teratani T, Terada M, Ochiya T. Differentiation of embryonic stem cells into hepatocytes: biological functions and therapeutic application. *Hepatology* 2003; **37**: 983-993 [PMID: 12717379 DOI: 10.1053/jhep.2003.50202]

85 **Moriya K**, Yoshikawa M, Saito K, Ouji Y, Nishiofuku M, Hayashi N, Ishizaka S, Fukui H. Embryonic stem cells develop into hepatocytes after intrasplenic transplantation in CCl4-treated mice. *World J Gastroenterol* 2007; **13**: 866-873 [PMID: 17352015 DOI: 10.3748/wjg.v13.i6.866]

86 **Moriya K**, Yoshikawa M, Ouji Y, Saito K, Nishiofuku M, Matsuda R, Ishizaka S, Fukui H. Embryonic stem cells reduce liver fibrosis in CCl4-treated mice. *Int J Exp Pathol* 2008; **89**: 401-409 [PMID: 19134049 DOI: 10.1111/j.1365-2613.2008.00607.x]

87 **Cai J**, Zhao Y, Liu Y, Ye F, Song Z, Qin H, Meng S, Chen Y, Zhou R, Song X, Guo Y, Ding M, Deng H. Directed differentiation of human embryonic stem cells into functional hepatic cells. *Hepatology* 2007; **45**: 1229-1239 [PMID: 17464996 DOI: 10.1002/hep.21582]

88 **Ishii T**, Yasuchika K, Machimoto T, Kamo N, Komori J, Konishi S, Suemori H, Nakatsuji N, Saito M, Kohno K, Uemoto S, Ikai I. Transplantation of embryonic stem cell-derived endodermal cells into mice with induced lethal liver damage. *Stem Cells* 2007; **25**: 3252-3260 [PMID: 17885077 DOI: 10.1634/stemcells.2007-0199]

89 **Choi D**, Oh HJ, Chang UJ, Koo SK, Jiang JX, Hwang SY, Lee JD, Yeoh GC, Shin HS, Lee JS, Oh B. In vivo differentiation of mouse embryonic stem cells into hepatocytes. *Cell Transplant* 2002; **11**: 359-368 [PMID: 12162376]

90 **Gilchrist ES**, Plevris JN. Bone marrow-derived stem cells in liver repair: 10 years down the line. *Liver Transpl* 2010; **16**: 118-129 [PMID: 20104479 DOI: 10.1002/lt.21965]

91 **Song Z**, Cai J, Liu Y, Zhao D, Yong J, Duo S, Song X, Guo Y, Zhao Y, Qin H, Yin X, Wu C, Che J, Lu S, Ding M, Deng H. Efficient generation of hepatocyte-like cells from human induced pluripotent stem cells. *Cell Res* 2009; **19**: 1233-1242 [PMID: 19736565 DOI: 10.1038/cr.2009.107]

92 **Liu H**, Kim Y, Sharkis S, Marchionni L, Jang YY. In vivo liver regeneration potential of human induced pluripotent stem cells from diverse origins. *Sci Transl Med* 2011; **3**: 82ra39 [PMID: 21562231 DOI: 10.1126/scitranslmed.3002376]

93 **Chun YS**, Chaudhari P, Jang YY. Applications of patient-specific induced pluripotent stem cells; focused on disease modeling, drug screening and therapeutic potentials for liver disease. *Int J Biol Sci* 2010; **6**: 796-805 [PMID: 21179587 DOI: 10.7150/ijbs.6.796]

94 **Ren G**, Chen X, Dong F, Li W, Ren X, Zhang Y, Shi Y. Concise review: mesenchymal stem cells and translational medicine: emerging issues. *Stem Cells Transl Med* 2012; **1**: 51-58 [PMID: 23197640 DOI: 10.5966/sctm.2011-0019]

95 **Berardis S**, Lombard C, Evraerts J, El Taghdouini A, Rosseels V, Sancho-Bru P, Lozano JJ, van Grunsven L, Sokal E, Najimi M. Gene expression profiling and secretome analysis differentiate adult-derived human liver stem/progenitor cells and human hepatic stellate cells. *PLoS One* 2014; **9**: e86137 [PMID: 24516514 DOI: 10.1371/journal.pone.0086137]

96 **Prockop DJ**, Brenner M, Fibbe WE, Horwitz E, Le Blanc K, Phinney DG, Simmons PJ, Sensebe L, Keating A. Defining the risks of mesenchymal stromal cell therapy. *Cytotherapy* 2010; **12**: 576-578 [PMID: 20735162 DOI: 10.3109/14653249.2010.507330]

97 **Dominici M**, Le Blanc K, Mueller I, Slaper-Cortenbach I, Marini F, Krause D, Deans R, Keating A, Prockop Dj, Horwitz E. Minimal criteria for defining multipotent mesenchymal stromal cells. The International Society for Cellular Therapy position statement. *Cytotherapy* 2006; **8**: 315-317 [PMID: 16923606 DOI: 10.1080/14653240600855905]

98 **Barry FP**, Murphy JM. Mesenchymal stem cells: clinical applications and biological characterization. *Int J Biochem Cell Biol* 2004; **36**: 568-584 [PMID: 15010324 DOI: 10.1016/j.biocel.2003.11.001]

99 **Barry F**, Boynton RE, Liu B, Murphy JM. Chondrogenic differentiation of mesenchymal stem cells from bone marrow: differentiation-dependent gene expression of matrix components. *Exp Cell Res* 2001; **268**: 189-200 [PMID: 11478845 DOI: 10.1006/excr.2001.5278]

100 **Johnstone B**, Hering TM, Caplan AI, Goldberg VM, Yoo JU. In vitro chondrogenesis of bone marrow-derived mesenchymal progenitor cells. *Exp Cell Res* 1998; **238**: 265-272 [PMID: 9457080 DOI: 10.1006/excr.1997.3858]

101 **Pittenger MF**, Mackay AM, Beck SC, Jaiswal RK, Douglas R, Mosca JD, Moorman MA, Simonetti DW, Craig S, Marshak DR. Multilineage potential of adult human mesenchymal stem cells. *Science* 1999; **284**: 143-147 [PMID: 10102814 DOI: 10.1126/science.284.5411.143]

102 **Sanchez-Ramos J**, Song S, Cardozo-Pelaez F, Hazzi C, Stedeford T, Willing A, Freeman TB, Saporta S, Janssen W, Patel N, Cooper DR, Sanberg PR. Adult bone marrow stromal cells differentiate into neural cells in vitro. *Exp Neurol* 2000; **164**: 247-256 [PMID: 10915564 DOI: 10.1006/exnr.2000.7389]

103 **Jiang Y**, Jahagirdar BN, Reinhardt RL, Schwartz RE, Keene CD, Ortiz-Gonzalez XR, Reyes M, Lenvik T, Lund T, Blackstad M, Du J, Aldrich S, Lisberg A, Low WC, Largaespada DA, Verfaillie CM. Pluripotency of mesenchymal stem cells derived from adult marrow. *Nature* 2002; **418**: 41-49 [PMID: 12077603 DOI: 10.1038/nature00870]

104 **Schwartz RE**, Reyes M, Koodie L, Jiang Y, Blackstad M, Lund

T, Lenvik T, Johnson S, Hu WS, Verfaillie CM. Multipotent adult progenitor cells from bone marrow differentiate into functional hepatocyte-like cells. *J Clin Invest* 2002; **109**: 1291-1302 [PMID: 12021244 DOI: 10.1172/JCI0215182]

105 **Taléns-Visconti R**, Bonora A, Jover R, Mirabet V, Carbonell F, Castell JV, Gómez-Lechón MJ. Hepatogenic differentiation of human mesenchymal stem cells from adipose tissue in comparison with bone marrow mesenchymal stem cells. *World J Gastroenterol* 2006; **12**: 5834-5845 [PMID: 17007050]

106 **Sato Y**, Araki H, Kato J, Nakamura K, Kawano Y, Kobune M, Sato T, Miyanishi K, Takayama T, Takahashi M, Takimoto R, Iyama S, Matsunaga T, Ohtani S, Matsuura A, Hamada H, Niitsu Y. Human mesenchymal stem cells xenografted directly to rat liver are differentiated into human hepatocytes without fusion. *Blood* 2005; **106**: 756-763 [PMID: 15817682 DOI: 10.1182/blood-2005-02-0572]

107 **Shu SN**, Wei L, Wang JH, Zhan YT, Chen HS, Wang Y. Hepatic differentiation capability of rat bone marrow-derived mesenchymal stem cells and hematopoietic stem cells. *World J Gastroenterol* 2004; **10**: 2818-2822 [PMID: 15334677]

108 **Theise ND**, Badve S, Saxena R, Henegariu O, Sell S, Crawford JM, Krause DS. Derivation of hepatocytes from bone marrow cells in mice after radiation-induced myeloablation. *Hepatology* 2000; **31**: 235-240 [PMID: 10613752 DOI: 10.1002/hep.510310135]

109 **Chamberlain J**, Yamagami T, Colletti E, Theise ND, Desai J, Frias A, Pixley J, Zanjani ED, Porada CD, Almeida-Porada G. Efficient generation of human hepatocytes by the intrahepatic delivery of clonal human mesenchymal stem cells in fetal sheep. *Hepatology* 2007; **46**: 1935-1945 [PMID: 17705296 DOI: 10.1002/hep.21899]

110 **Alison MR**, Poulsom R, Jeffery R, Dhillon AP, Quaglia A, Jacob J, Novelli M, Prentice G, Williamson J, Wright NA. Hepatocytes from non-hepatic adult stem cells. *Nature* 2000; **406**: 257 [PMID: 10917519 DOI: 10.1038/35018642]

111 **Najimi M**, Khuu DN, Lysy PA, Jazouli N, Abarca J, Sempoux C, Sokal EM. Adult-derived human liver mesenchymal-like cells as a potential progenitor reservoir of hepatocytes? *Cell Transplant* 2007; **16**: 717-728 [PMID: 18019361 DOI: 10.3727/000000007783465154]

112 **Khuu DN**, Scheers I, Ehnert S, Jazouli N, Nyabi O, Buc-Calderon P, Meulemans A, Nussler A, Sokal E, Najimi M. In vitro differentiated adult human liver progenitor cells display mature hepatic metabolic functions: a potential tool for in vitro pharmacotoxicological testing. *Cell Transplant* 2011; **20**: 287-302 [PMID: 20719066 DOI: 10.3727/096368910X516655]

113 **Aggarwal S**, Pittenger MF. Human mesenchymal stem cells modulate allogeneic immune cell responses. *Blood* 2005; **105**: 1815-1822 [PMID: 15494428 DOI: 10.1182/blood-2004-04-1559]

114 **Puglisi MA**, Tesori V, Lattanzi W, Piscaglia AC, Gasbarrini GB, D'Ugo DM, Gasbarrini A. Therapeutic implications of mesenchymal stem cells in liver injury. *J Biomed Biotechnol* 2011; **2011**: 860578 [PMID: 22228987 DOI: 10.1155/2011/860578]

115 **Corcione A**, Benvenuto F, Ferretti E, Giunti D, Cappiello V, Cazzanti F, Risso M, Gualandi F, Mancardi GL, Pistoia V, Uccelli A. Human mesenchymal stem cells modulate B-cell functions. *Blood* 2006; **107**: 367-372 [PMID: 16141348 DOI: 10.1182/blood-2005-07-2657]

116 **Jiang XX**, Zhang Y, Liu B, Zhang SX, Wu Y, Yu XD, Mao N. Human mesenchymal stem cells inhibit differentiation and function of monocyte-derived dendritic cells. *Blood* 2005; **105**: 4120-4126 [PMID: 15692068 DOI: 10.1182/blood-2004-02-0586]

117 **Zhang W**, Ge W, Li C, You S, Liao L, Han Q, Deng W, Zhao RC. Effects of mesenchymal stem cells on differentiation, maturation, and function of human monocyte-derived dendritic cells. *Stem Cells Dev* 2004; **13**: 263-271 [PMID: 15186722 DOI: 10.1089/154732804323099190]

118 **Spaggiari GM**, Abdelrazik H, Becchetti F, Moretta L. MSCs inhibit monocyte-derived DC maturation and function by selectively interfering with the generation of immature DCs: central role of MSC-derived prostaglandin E2. *Blood* 2009; **113**: 6576-6583 [PMID: 19398717 DOI: 10.1182/blood-2009-02-203943]

119 **Spaggiari GM**, Capobianco A, Abdelrazik H, Becchetti F, Mingari MC, Moretta L. Mesenchymal stem cells inhibit natural killer-cell proliferation, cytotoxicity, and cytokine production: role of indoleamine 2,3-dioxygenase and prostaglandin E2. *Blood* 2008; **111**: 1327-1333 [PMID: 17951526 DOI: 10.1182/blood-2007-02-074997]

120 **Basciano L**, Nemos C, Foliguet B, de Isla N, de Carvalho M, Tran N, Dalloul A. Long term culture of mesenchymal stem cells in hypoxia promotes a genetic program maintaining their undifferentiated and multipotent status. *BMC Cell Biol* 2011; **12**: 12 [PMID: 21450070 DOI: 10.1186/1471-2121-12-12]

121 **Salem HK**, Thiemermann C. Mesenchymal stromal cells: current understanding and clinical status. *Stem Cells* 2010; **28**: 585-596 [PMID: 19967788 DOI: 10.1002/stem.269]

122 **Kansas GS**. Selectins and their ligands: current concepts and controversies. *Blood* 1996; **88**: 3259-3287 [PMID: 8896391]

123 **Rüster B**, Göttig S, Ludwig RJ, Bistrian R, Müller S, Seifried E, Gille J, Henschler R. Mesenchymal stem cells display coordinated rolling and adhesion behavior on endothelial cells. *Blood* 2006; **108**: 3938-3944 [PMID: 16896152 DOI: 10.1182/blood-2006-05-025098]

124 **van Poll D**, Parekkadan B, Cho CH, Berthiaume F, Nahmias Y, Tilles AW, Yarmush ML. Mesenchymal stem cell-derived molecules directly modulate hepatocellular death and regeneration in vitro and in vivo. *Hepatology* 2008; **47**: 1634-1643 [PMID: 18395843 DOI: 10.1002/hep.22236]

125 **Zhang S**, Chen L, Liu T, Zhang B, Xiang D, Wang Z, Wang Y. Human umbilical cord matrix stem cells efficiently rescue acute liver failure through paracrine effects rather than hepatic differentiation. *Tissue Eng Part A* 2012; **18**: 1352-1364 [PMID: 22519429 DOI: 10.1089/ten.tea.2011.0516]

126 **Li T**, Yan Y, Wang B, Qian H, Zhang X, Shen L, Wang M, Zhou Y, Zhu W, Li W, Xu W. Exosomes derived from human umbilical cord mesenchymal stem cells alleviate liver fibrosis. *Stem Cells Dev* 2013; **22**: 845-854 [PMID: 23002959 DOI: 10.1089/scd.2012.0395]

127 **Jung KH**, Shin HP, Lee S, Lim YJ, Hwang SH, Han H, Park HK, Chung JH, Yim SV. Effect of human umbilical cord blood-derived mesenchymal stem cells in a cirrhotic rat model. *Liver Int* 2009; **29**: 898-909 [PMID: 19422480 DOI: 10.1111/j.1478-3231.2009.02031.x]

128 **Wang Y**, Lian F, Li J, Fan W, Xu H, Yang X, Liang L, Chen W, Yang J. Adipose derived mesenchymal stem cells transplantation via portal vein improves microcirculation and ameliorates liver fibrosis induced by CCl4 in rats. *J Transl Med* 2012; **10**: 133 [PMID: 22735033 DOI: 10.1186/1479-5876-10-133]

129 **Nasir GA**, Mohsin S, Khan M, Shams S, Ali G, Khan SN, Riazuddin S. Mesenchymal stem cells and Interleukin-6 attenuate liver fibrosis in mice. *J Transl Med* 2013; **11**: 78 [PMID: 23531302 DOI: 10.1186/1479-5876-11-78]

130 **Li Q**, Zhou X, Shi Y, Li J, Zheng L, Cui L, Zhang J, Wang L, Han Z, Han Y, Fan D. In vivo tracking and comparison of the therapeutic effects of MSCs and HSCs for liver injury. *PLoS One* 2013; **8**: e62363 [PMID: 23638052 DOI: 10.1371/journal.pone.0062363]

131 **Chang YJ**, Liu JW, Lin PC, Sun LY, Peng CW, Luo GH, Chen TM, Lee RP, Lin SZ, Harn HJ, Chiou TW. Mesenchymal stem cells facilitate recovery from chemically induced liver damage and decrease liver fibrosis. *Life Sci* 2009; **85**: 517-525 [PMID: 19686763 DOI: 10.1016/j.lfs.2009.08.003]

132 **Rabani V**, Shahsavani M, Gharavi M, Piryaei A, Azhdari Z, Baharvand H. Mesenchymal stem cell infusion therapy in a carbon tetrachloride-induced liver fibrosis model affects matrix metalloproteinase expression. *Cell Biol Int* 2010; **34**:

601-605 [PMID: 20178458 DOI: 10.1042/CBI20090386]
133 **Zhao DC**, Lei JX, Chen R, Yu WH, Zhang XM, Li SN, Xiang P. Bone marrow-derived mesenchymal stem cells protect against experimental liver fibrosis in rats. *World J Gastroenterol* 2005; **11**: 3431-3440 [PMID: 15948250]
134 **Abdel Aziz MT**, Atta HM, Mahfouz S, Fouad HH, Roshdy NK, Ahmed HH, Rashed LA, Sabry D, Hassouna AA, Hasan NM. Therapeutic potential of bone marrow-derived mesenchymal stem cells on experimental liver fibrosis. *Clin Biochem* 2007; **40**: 893-899 [PMID: 17543295 DOI: 10.1016/j.clinbiochem.2007.04.017]
135 **Tanimoto H**, Terai S, Taro T, Murata Y, Fujisawa K, Yamamoto N, Sakaida I. Improvement of liver fibrosis by infusion of cultured cells derived from human bone marrow. *Cell Tissue Res* 2013; **354**: 717-728 [PMID: 24104560 DOI: 10.1007/s00441-013-1727-2]
136 **Starkel P**, Leclercq IA. Animal models for the study of hepatic fibrosis. *Best Pract Res Clin Gastroenterol* 2011; **25**: 319-333 [PMID: 21497748 DOI: 10.1016/j.bpg.2011.02.004]
137 **Ortiz LA**, Gambelli F, McBride C, Gaupp D, Baddoo M, Kaminski N, Phinney DG. Mesenchymal stem cell engraftment in lung is enhanced in response to bleomycin exposure and ameliorates its fibrotic effects. *Proc Natl Acad Sci USA* 2003; **100**: 8407-8411 [PMID: 12815096 DOI: 10.1073/pnas.1432929100]
138 **Schubert T**, Xhema D, Vériter S, Schubert M, Behets C, Delloye C, Gianello P, Dufrane D. The enhanced performance of bone allografts using osteogenic-differentiated adipose-derived mesenchymal stem cells. *Biomaterials* 2011; **32**: 8880-8891 [PMID: 21872925 DOI: 10.1016/j.biomaterials.2011.08.009]
139 **Parekkadan B**, van Poll D, Megeed Z, Kobayashi N, Tilles AW, Berthiaume F, Yarmush ML. Immunomodulation of activated hepatic stellate cells by mesenchymal stem cells. *Biochem Biophys Res Commun* 2007; **363**: 247-252 [PMID: 17869217 DOI: 10.1016/j.bbrc.2007.05.150]
140 **Wang J**, Bian C, Liao L, Zhu Y, Li J, Zeng L, Zhao RC. Inhibition of hepatic stellate cells proliferation by mesenchymal stem cells and the possible mechanisms. *Hepatol Res* 2009; **39**: 1219-1228 [PMID: 19788697 DOI: 10.1111/j.1872-034X.2009.00564.x]
141 **Lin N**, Hu K, Chen S, Xie S, Tang Z, Lin J, Xu R. Nerve growth factor-mediated paracrine regulation of hepatic stellate cells by multipotent mesenchymal stromal cells. *Life Sci* 2009; **85**: 291-295 [PMID: 19559033 DOI: 10.1016/j.lfs.2009.06.007]
142 **Chen S**, Xu L, Lin N, Pan W, Hu K, Xu R. Activation of Notch1 signaling by marrow-derived mesenchymal stem cells through cell-cell contact inhibits proliferation of hepatic stellate cells. *Life Sci* 2011; **89**: 975-981 [PMID: 22056375 DOI: 10.1016/j.lfs.2011.10.012]
143 **Wang PP**, Xie DY, Liang XJ, Peng L, Zhang GL, Ye YN, Xie C, Gao ZL. HGF and direct mesenchymal stem cells contact synergize to inhibit hepatic stellate cells activation through TLR4/NF-kB pathway. *PLoS One* 2012; **7**: e43408 [PMID: 22927965 DOI: 10.1371/journal.pone.0043408]
144 **Zhang Z**, Lin H, Shi M, Xu R, Fu J, Lv J, Chen L, Lv S, Li Y, Yu S, Geng H, Jin L, Lau GK, Wang FS. Human umbilical cord mesenchymal stem cells improve liver function and ascites in decompensated liver cirrhosis patients. *J Gastroenterol Hepatol* 2012; **27** Suppl 2: 112-120 [PMID: 22320928 DOI: 10.1111/j.1440-1746.2011.07024.x]
145 **Shi M**, Zhang Z, Xu R, Lin H, Fu J, Zou Z, Zhang A, Shi J, Chen L, Lv S, He W, Geng H, Jin L, Liu Z, Wang FS. Human mesenchymal stem cell transfusion is safe and improves liver function in acute-on-chronic liver failure patients. *Stem Cells Transl Med* 2012; **1**: 725-731 [PMID: 23197664 DOI: 10.5966/sctm.2012-0034]
146 **Wang L**, Li J, Liu H, Li Y, Fu J, Sun Y, Xu R, Lin H, Wang S, Lv S, Chen L, Zou Z, Li B, Shi M, Zhang Z, Wang FS. Pilot study of umbilical cord-derived mesenchymal stem cell transfusion in patients with primary biliary cirrhosis. *J Gastroenterol Hepatol* 2013; **28** Suppl 1: 85-92 [PMID: 23855301 DOI: 10.1111/jgh.12029]
147 **Mohamadnejad M**, Alimoghaddam K, Mohyeddin-Bonab M, Bagheri M, Bashtar M, Ghanaati H, Baharvand H, Ghavamzadeh A, Malekzadeh R. Phase 1 trial of autologous bone marrow mesenchymal stem cell transplantation in patients with decompensated liver cirrhosis. *Arch Iran Med* 2007; **10**: 459-466 [PMID: 17903050]
148 **Kharaziha P**, Hellström PM, Noorinayer B, Farzaneh F, Aghajani K, Jafari F, Telkabadi M, Atashi A, Honardoost M, Zali MR, Soleimani M. Improvement of liver function in liver cirrhosis patients after autologous mesenchymal stem cell injection: a phase I-II clinical trial. *Eur J Gastroenterol Hepatol* 2009; **21**: 1199-1205 [PMID: 19455046 DOI: 10.1097/MEG.0b013e32832a1f6c]
149 **Peng L**, Xie DY, Lin BL, Liu J, Zhu HP, Xie C, Zheng YB, Gao ZL. Autologous bone marrow mesenchymal stem cell transplantation in liver failure patients caused by hepatitis B: short-term and long-term outcomes. *Hepatology* 2011; **54**: 820-828 [PMID: 21608000 DOI: 10.1002/hep.24434]
150 **El-Ansary M**, Abdel-Aziz I, Mogawer S, Abdel-Hamid S, Hammam O, Teaema S, Wahdan M. Phase II trial: undifferentiated versus differentiated autologous mesenchymal stem cells transplantation in Egyptian patients with HCV induced liver cirrhosis. *Stem Cell Rev* 2012; **8**: 972-981 [PMID: 21989829 DOI: 10.1007/s12015-011-9322-y]
151 **Amin MA**, Sabry D, Rashed LA, Aref WM, el-Ghobary MA, Farhan MS, Fouad HA, Youssef YA. Short-term evaluation of autologous transplantation of bone marrow-derived mesenchymal stem cells in patients with cirrhosis: Egyptian study. *Clin Transplant* 2013; **27**: 607-612 [PMID: 23923970 DOI: 10.1111/ctr.12179]
152 **Jang YO**, Kim YJ, Baik SK, Kim MY, Eom YW, Cho MY, Park HJ, Park SY, Kim BR, Kim JW, Soo Kim H, Kwon SO, Choi EH, Kim YM. Histological improvement following administration of autologous bone marrow-derived mesenchymal stem cells for alcoholic cirrhosis: a pilot study. *Liver Int* 2014; **34**: 33-41 [PMID: 23782511]
153 **Kamath PS**, Kim WR. The model for end-stage liver disease (MELD). *Hepatology* 2007; **45**: 797-805 [PMID: 17326206 DOI: 10.1002/hep.21563]
154 **Zhu W**, Xu W, Jiang R, Qian H, Chen M, Hu J, Cao W, Han C, Chen Y. Mesenchymal stem cells derived from bone marrow favor tumor cell growth in vivo. *Exp Mol Pathol* 2006; **80**: 267-274 [PMID: 16214129 DOI: 10.1016/j.yexmp.2005.07.004]
155 **Djouad F**, Plence P, Bony C, Tropel P, Apparailly F, Sany J, Noël D, Jorgensen C. Immunosuppressive effect of mesenchymal stem cells favors tumor growth in allogeneic animals. *Blood* 2003; **102**: 3837-3844 [PMID: 12881305 DOI: 10.1182/blood-2003-04-1193]
156 **Yu JM**, Jun ES, Bae YC, Jung JS. Mesenchymal stem cells derived from human adipose tissues favor tumor cell growth in vivo. *Stem Cells Dev* 2008; **17**: 463-473 [PMID: 18522494 DOI: 10.1089/scd.2007.0181]
157 **Khakoo AY**, Pati S, Anderson SA, Reid W, Elshal MF, Rovira II, Nguyen AT, Malide D, Combs CA, Hall G, Zhang J, Raffeld M, Rogers TB, Stetler-Stevenson W, Frank JA, Reitz M, Finkel T. Human mesenchymal stem cells exert potent antitumorigenic effects in a model of Kaposi's sarcoma. *J Exp Med* 2006; **203**: 1235-1247 [PMID: 16636132 DOI: 10.1084/jem.20051921]
158 **Qiao L**, Xu Z, Zhao T, Zhao Z, Shi M, Zhao RC, Ye L, Zhang X. Suppression of tumorigenesis by human mesenchymal stem cells in a hepatoma model. *Cell Res* 2008; **18**: 500-507 [PMID: 18364678 DOI: 10.1038/cr.2008.40]
159 **Lu YR**, Yuan Y, Wang XJ, Wei LL, Chen YN, Cong C, Li SF, Long D, Tan WD, Mao YQ, Zhang J, Li YP, Cheng JQ.

The growth inhibitory effect of mesenchymal stem cells on tumor cells in vitro and in vivo. *Cancer Biol Ther* 2008; **7**: 245-251 [PMID: 18059192]

160 **Gao P**, Ding Q, Wu Z, Jiang H, Fang Z. Therapeutic potential of human mesenchymal stem cells producing IL-12 in a mouse xenograft model of renal cell carcinoma. *Cancer Lett* 2010; **290**: 157-166 [PMID: 19786319 DOI: 10.1016/j.canlet.2009.08.031]

161 **Abdel aziz MT**, El Asmar MF, Atta HM, Mahfouz S, Fouad HH, Roshdy NK, Rashed LA, Sabry D, Hassouna AA, Taha FM. Efficacy of mesenchymal stem cells in suppression of hepatocarcinorigenesis in rats: possible role of Wnt signaling. *J Exp Clin Cancer Res* 2011; **30**: 49 [PMID: 21545718]

P- Reviewer: Enomoto H, Huang L, Nevzorova YA, Pixley J
S- Editor: Gou SX **L- Editor**: A **E- Editor**: Liu XM

World Journal of Gastroenterology

Submit a Manuscript: http://www.wjgnet.com/esps/
Help Desk: http://www.wjgnet.com/esps/helpdesk.aspx
DOI: 10.3748/wjg.v21.i3.759

World J Gastroenterol 2015 January 21; 21(3): 759-785
ISSN 1007-9327 (print) ISSN 2219-2840 (online)

REVIEW

Technical skills and training of upper gastrointestinal endoscopy for new beginners

Seung-Hwa Lee, Young-Kyu Park, Sung-Min Cho, Joon-Koo Kang, Duck-Joo Lee

Seung-Hwa Lee, Duck-Joo Lee, Health Promotion Center, Ajou University School of Medicine, Suwon 443-380, South Korea
Young-Kyu Park, Sung-Min Cho, Health Promotion Center, Bundang Jaesang Hospital, Kwandong University School of Medicine, Seongnam 463-774, South Korea
Joon-Koo Kang, Department of Gastroenterology, Ajou University School of Medicine, Suwon 443-380, South Korea
Author contributions: Lee SH, Park YK and Cho SM contributed equally to this paper; Lee SH, Park YK and Cho SM contributed in the study concept and design, acquisition of data, and drafting of the manuscript; Lee SH and Kang JK were involved in the acquisition, ascertainment of data and revision of manuscript; Lee DJ contributed to a critical revision of the manuscript regarding its intellectual content, and supervised the study overall; all the authors read and approved the final draft of this manuscript.

Correspondence to: Duck-Joo Lee, President and Professor, Health Promotion Center, Ajou University School of Medicine, Gyeonggi-do, Suwon 443-380, South Korea. fmdr@medimail.co.kr
Telephone: +82-10-87710911
Fax: +82-31-2195561
Received: August 5, 2014
Peer-review started: August 6, 2014
First decision: September 15, 2014
Revised: October 17, 2014
Accepted: December 1, 2014
Article in press: December 1, 2014
Published online: January 21, 2015

Abstract

The incidence of gastric cancer remains high in South Korea. Upper gastrointestinal (GI) endoscopy, *i.e.*, esophagogastroduodenoscopy (EGD), has a higher diagnostic specificity and sensitivity than the upper GI series. Additionally, EGD has the ability to biopsy, through taking a tissue of the pathologic lesion. Successful training of EGD procedural skills require a few important things to be learned and remembered, including the posture of an examinee (*e.g.*, left lateral decubitus and supine) and examiner (*e.g.*, one-man standing method *vs* one-man sitting method), basic skills (*e.g.*, tip deflection, push forward and pull back, and air suction and infusion), advanced skills (*e.g.*, paradoxical movement, J-turn, and U-turn), and intubation techniques along the upper GI tract (*e.g.*, oral cavity, pharynx, larynx including vocal cord, upper and middle and lower esophagus, gastroesophageal junction, gastric fundus, body, and antrum, duodenal bulb, and descending part of duodenum). In the current review, despite several limitations, we explained the intubation method of EGD for beginners. We hope this will be helpful to beginners who wish to learn the procedure.

Key words: Upper gastrointestinal endoscopy; Esophagogastroduodenoscopy; Beginner; Procedure; Technical skill

Core tip: The demand for esophagogastroduodenoscopy (EGD) has been increasing annually, especially in Asian countries. However, it is challenging to learn the procedure, due to its long learning curve. Therefore, care must be taken in teaching, learning, and practicing the procedure. We believe that if beginners learn how to perform EGD properly through an adequate training program and then perform the procedure effectively on patients, the safety and satisfaction of patients undergoing EGD will be improving.

Lee SH, Park YK, Cho SM, Kang JK, Lee DJ. Technical

skills and training of upper gastrointestinal endoscopy for new beginners. *World J Gastroenterol* 2015; 21(3): 759-785 Available from: URL: http://www.wjgnet.com/1007-9327/full/v21/i3/759.htm DOI: http://dx.doi.org/10.3748/wjg.v21.i3.759

INTRODUCTION

South Korea has a high prevalence of gastric cancer[1], hence upper gastrointestinal (GI) endoscopy, *i.e.*, esophagogastroduodenoscopy (EGD), potentially has great significance in terms of gastric cancer screening[2]. EGD is a useful procedure for the diagnosis of various abnormalities of the upper GI tract[3-6]. The sensitivity and specificity of EGD exceeds those of radiographs such as an upper GI barium series, for the diagnosis of upper GI tract inflammations, ulcers, and neoplasms. EGD is one of the most common procedures in South Korean clinical practice[7], hence acquisition of the skills and expertise for this technique is highly desired among beginners, including primary care physicians[8-11]. It is important for new practitioners of EGD to have a theoretical knowledge of pathological GI lesions in order to correctly interpret findings during endoscopic procedures and to arrive at the right clinical decision[9,12]. However, even those armed with an in-depth theoretical knowledge of pathological legions may end up doing an incomplete examination, if they are unable correctly to insert the scope into the oral cavity of the examinee or advance it properly along each portion of the upper GI tract. Additionally, it is necessary to thoroughly observe throughout the procedure, considering the possibility of blind spots, so as not to miss any pathological legions. Consequently, it is nearly impossible to perform a successful EGD without procedural skills. Therefore, an early session of endoscopy-training programs must focus on procedural skills of upper GI endoscopy[12,13].

Like all other procedures, upper GI endoscopy is difficult to explain verbally and in writing because the standards of endoscopy procedural skill assessment are very subjective. Furthermore, an EGD is a relatively invasive procedure carried out on a real human body (examinee), which can make practice and teaching difficult for residents, fellows, and even instructors. Endoscopy without proper preparation is inadvisable. It is helpful and has been repeatedly proven effective to acquire endoscopy procedural skills from text and photos[14-16]. Therefore, we explain the operation in depth, including insertion and advancement techniques of the scope in addition to providing the background knowledge that will help beginners, including residents and fellows, who are undergoing training to learn the procedure.

EXTENT OF EXAMINATION AND PROPER POSTURE IN UPPER GI ENDOSCOPY

Examination range

Typically EGD is performed to observe the oral cavity and larynx including the vocal cord, in addition the esophagus, stomach, duodenal bulb, and second portion (descending part) of duodenum. It is desirable to observe and take images of even the ampulla of Vater (AOV) while the endoscope is advanced into the second portion of the duodenum, however, it is not always possible to take such images, because the endoscope used is not a side-viewing endoscope, but is a kind of forward-viewing endoscope[17]. An examiner may need to abandon AOV imaging after, several attempts, as continued attempts would aggravate the examinee's discomfort.

Proper postures for upper GI endoscopy

Examinee (patient): The basic posture that examinees often take during EGD is the left lateral decubitus position, or if they experience difficulty lying in that manner, they can be examined in the supine position (Figure 1)[18]. However, except for cases in which the left lateral decubitus position is contra-indicated, such as hemiplegia, quadriplegia or tracheotomy, it is extremely rare that the EGD is performed in a supine posture.

The abdomen is dilated by injecting air into the lumen, allowing for accurate observation. As a result, an examinee should wear comfortable patient clothing, or if casually attired, the patient should loosen tops, bottoms, and belts. As the stomach can be dilated by increasing intra-abdominal pressure, an examinee lying in the left lateral decubitus posture is required to bend the legs by flexing the knee and hip joints, or straighten the left leg while bending only the right leg during the examination.

Examiner (endoscopist): While a colonoscopy can be done by either by the one-man or the two-man method[19], EGD is performed by the one-man method. While it can be done with the one-man standing method or the one-man sitting method depending on the examiner preference, EGD is usually performed using the one-man standing method because it is faster; however, if an examiner is required to do a large number of examinations in a short time or if the standing posture exerts too much strain on the examiner, such as in cases of pregnancy, the sitting posture may be recommended (Figure 2)[20,21].

ENDOSCOPY EQUIPMENT AND BASIC TECHNIQUE OF UPPER GI ENDOSCOPY

Just as understanding the basics of a vehicle is helpful in

Figure 1 Examinee. A, B: Example of left lateral decubitus position. To avoid an increased intra-abdominal pressure while lying in a left lateral decubitus position, it is recommended to bend the legs; C: Example of supine position; D, E: The examinee is undergoing an upper gastrointestinal endoscopy while lying in a supine posture due to hemiplegia and tracheotomy (arrow mark).

Figure 2 Standing and sitting method. A: As the upper gastrointestinal endoscopy takes a relatively short time, most examiners conduct the procedure in the standing posture; B: If the standing method puts too much strain on the body of an examiner such as in case of pregnancy, she can use the sitting method to perform the procedure.

learning to drive, understanding the upper GI endoscopy equipment can be helpful in developing procedural skills. Endoscopic equipment consists of two sections; the main body including the central processing unit and the endoscope. The endoscope is the main tool of EGD.

Components of the endoscope

The endoscope consists of a control section, an instrument channel (forcep, snare, injector, and clip device), a shaft (the endoscope portion actually inserted into the patient), the tip (the distal end of the shaft; controlled by the control section), the connection section, and a line (Figure 3).

Basic technique

Tip deflection: Vertical (up/down) and lateral (left/right) tip deflection is a basic technique for EGD, performed using a control knob. There are two control knobs in the control section of endoscope. The larger, outer control knob is used for the vertical (up or down) movement of the tip and the smaller, inner knob is used for the lateral (left or right) movement of the tip.

Push forward and pull back: Push forward (PF) is the action of pushing the endoscope tip forward through the anus, whereas pull back (PB) is the action of pulling it backward. PF is essential for advancing the endoscope. However, PB is also important in some cases, such as when there is a red-out sign. If the endoscopist uses force despite a red-out sign, complications such as mucosal damage and perforation may occur.

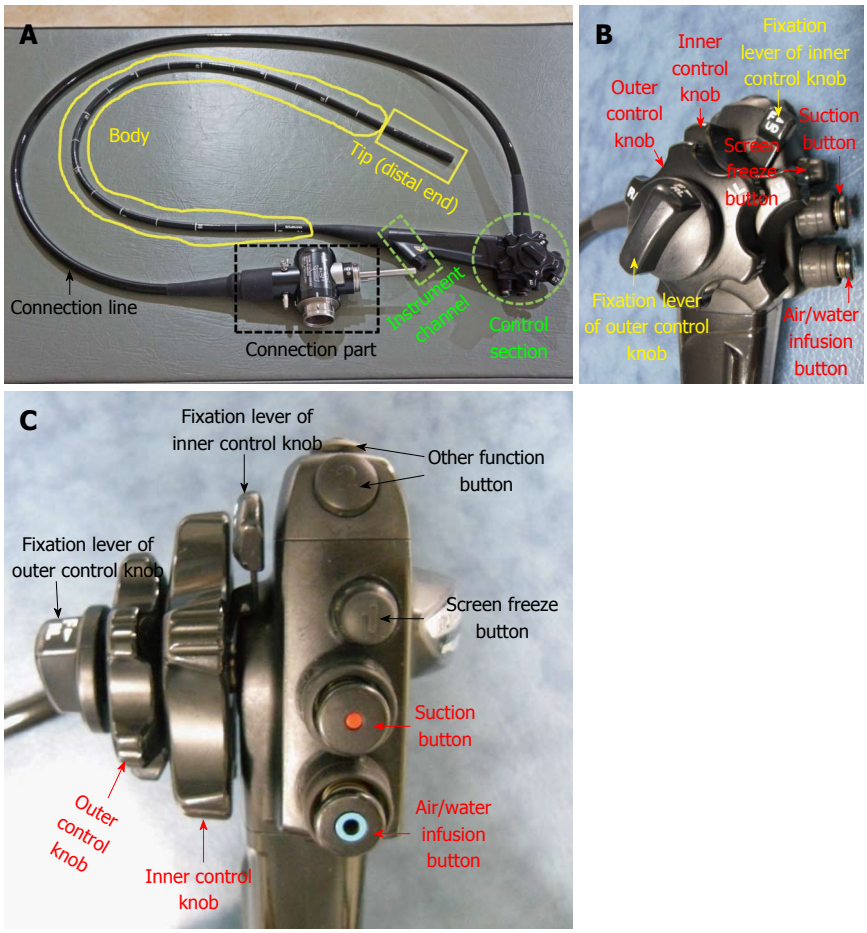

Figure 3 Components of the endoscope. A: Typical upper gastrointestinal endoscope (Olympus GIF-H260). Although there might be slight differences in the structure of the endoscope between manufacturing companies, the overall structure will be nearly identical; B, C: Magnified view of control section; lateral and forward views.

Right and left turn: Right or left turns are accomplished by twisting the body of the endoscope to the right (clockwise) or left (counter-clockwise) direction using the right hand. The body of the endoscope is grasped by the right hand, angling the tip using the inner control knob by left hand. Similarly, applying a twisting (right or left) motion when the tip is deflected upward has the effect of turning the endoscope to the right or left without using the left/right control knob. Alternatively, the outer control knob (left/right) can be used. However, during EGD, the former method is far more preferable.

Air insufflation and suction: Air infusion and suction are performed by using the air/water infusion valve button and the suction valve button, respectively. In EGD, optimal visualization required so that pathologic lesions are not missed. Adequate visualization of the upper GI tract, especially the stomach, may be achieved by distending the stomach with air. Thus, in clinical practice, the air infusion level is set to a high level and endoscopists are required to infuse sufficient air into stomach in order to fully observe the organ and remove any blind spots (Figure 4).

INTUBATION TECHNIQUE OF ENDOSCOPE ALONG EACH SECTION OF THE UPPER GI TRACT

The methods of inserting the endoscope and advancing it along each section of the upper GI tract may vary depending on the endoscopists; there is no single definite way of intubation. However, if one beginner carefully observes how a skilled endoscopist performs the procedure, he or she will find slight but consistent differences in the way of inserting and advancing the scope. Herein, we delineated a universal insertion method for each anatomical part of the upper GI tract and offer related knowledge helpful to the beginner.

Endoscope gripping method

Although gripping methods are based on examiner preference, the left hand usually grabs the control section and the right hand pinches the distal end of the scope. After resting the control section in the left palm, the left hand grips the scope with the fourth and fifth fingers. With the first finger on the large

Figure 4 Basic technique. A: Up deflection; B: Down deflection; C: Left deflection; D: Right deflection; E: Push forward (red arrow) and pull back (blue arrow); F: Air inflation. Simple closure of hole in the Air/Water infusion button activates it, one is not required to push the button. If an endoscopist wishes to infuse air into lumen, he or she should close the hole of this button, and should not push the button; G: An example of air inflation; H: Air suction. If an endoscopist wants to suction air or fluid, he needs to push the suction button; I: An example of water suction.

angle knob, the second finger on the suction button and the third finger on the air/water supply button, an examiner can freely manipulate the scope with the tip of each finger. The right hand holds the distal end of the scope at the correct distance from the tip. If held it too far from the tip, the scope will bend, and force is not transmitted to the tip. If held too close to the tip, an examiner will have less flexibility in advancing the

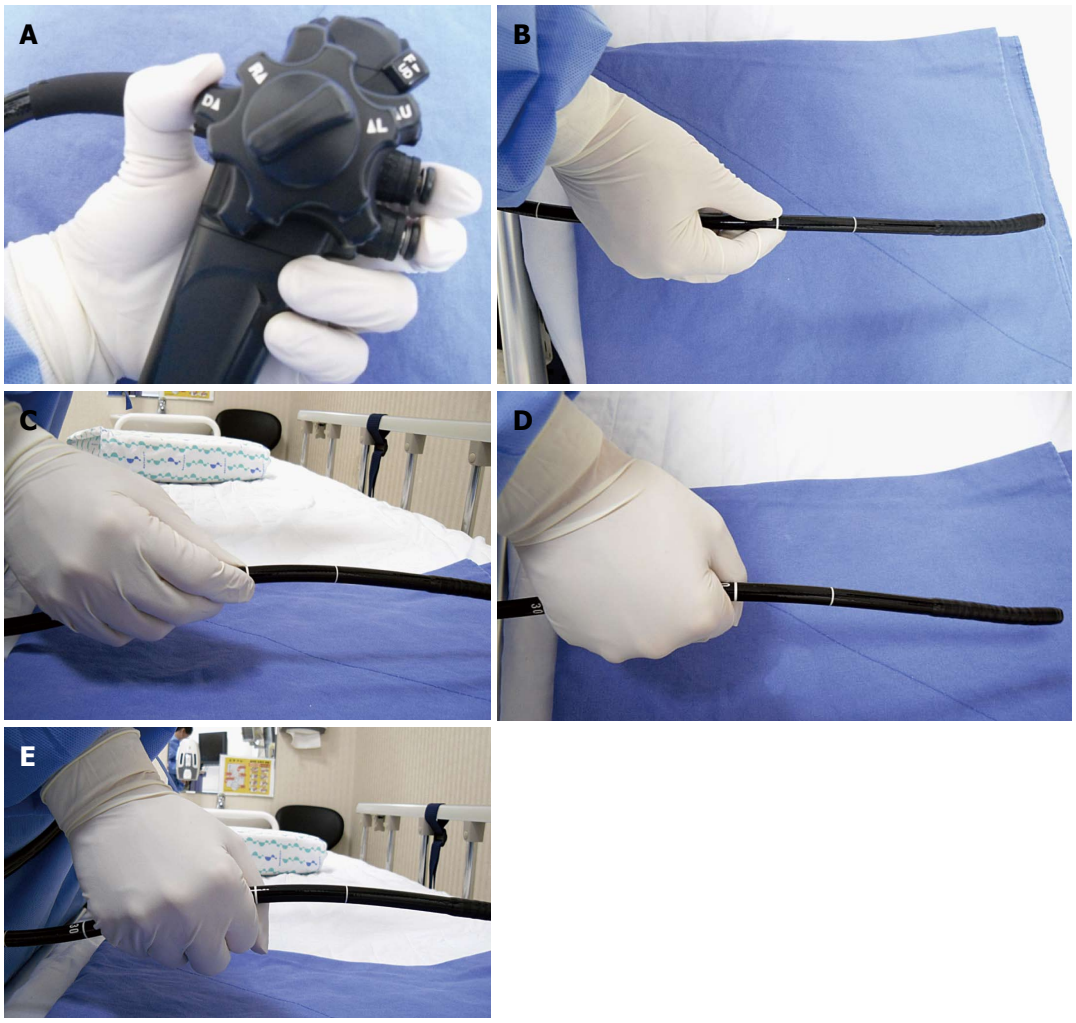

Figure 5 Endoscope gripping method. A: Holding the control part of the endoscope with the left hand; B, C: Grabbing the distal end of the endoscope with the right hand. It is recommended than one gently hold the shaft approximately 15-20 cm away from the tip as if to shake hands; D, E: Wrong gripping methods. If the shaft is held with a firmly clenched fist, the endoscopist will have difficulty handling the scope. Therefore, the shaft should not be held too tightly.

scope. In ordinary situations, the endoscopist holds the scope approximately 15-20 cm from the tip. However, as a stronger force is required to advance the scope from the pyloric ring into the duodenal bulb, an examiner may hold it closer to the tip than usual. When holding the distal end of the scope, an examiner can grip it with either the shake hand method or the pen holder method. Regardless, the physician should avoid holding the tip of the scope with a clenched fist, as that will result in a loss of flexibility (Figure 5).

Pre-intubation preparation

Overview: (1) Before EGD is performed on a patient, an endoscopist is required to quickly check all the necessary conditions, including the function of the endoscope, his or her own physical condition, and the examinee's posture and preference of sedation[22]; and (2) as a beginner, it is not so important to identify how an examiner manipulates an endoscope during insertion to influence the movement and location of the scope within the body. It is more important is to keep in mind that the movement of the endoscope should coincide with the location and movement displayed on the screen. Although a well-skilled endoscopist may be well aware of the 3-dimensional movements and deflections of the scope within the patients' body, a beginner is required to concentrate on the scope's upward and downward movements displayed on the screen (Figure 6).

Important points for beginners: (1) It is important to check whether the scope is well connected to the mainframe before examination. An examiner will encounter problems during examination due to poor air-insufflation if the connection is sub-optimal; (2) it is especially important during EGD to rapidly dilate and contract the stomach to enable advancement of the scope at a high level of air insufflation; and (3) as mentioned above, the examinee should lie in the left lateral decubitus posture during the upper GI endoscopy. If the arm of an examinee protrudes out of the bed during this time, it can interfere with the examination. The right arm of an examinee should be placed on his or her hip, while the left

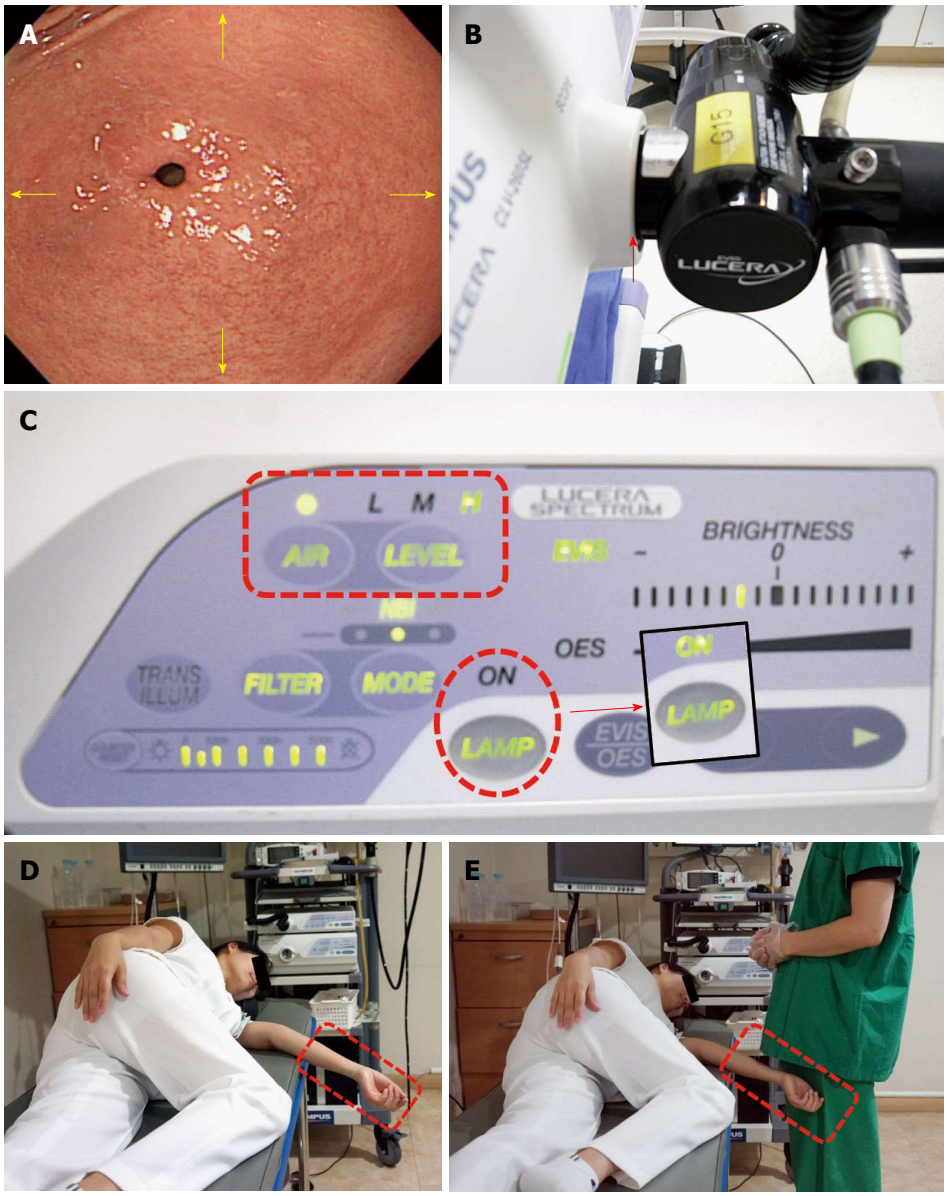

Figure 6 Pre-intubation preparation. A: The endoscopic image displayed on the monitor. A beginner endoscopist must remember that the direction (arrow marks) on the screen coincides with that of the movement of the endoscope. Therefore, for example, if one wants to see a lesion on the upper side, one can angle the tip of the endoscope upward; if one wants to see a lesion on the lower side, one can angle it downward; if one wants to see a lesion on the left or right side, you can angle it to the left or right, respectively; B: Connection part where the endoscope is plugged into the mainframe. If there is any defect in the arrow-marked part, an endoscopist will encounter difficulty advancing the scope due to insufficient air insufflation; C: Mainframe. There are many buttons to control a variety of functions. Among them, the control button for air insufflation (dotted rectangle) is set to a low level for the colonoscopy, while the esophagogastroduodenoscopy is performed at a high level of air insufflation. Apart from them, there is the light source button (dotted circle). If the light source button turns off, an image on the screen becomes invisible, which makes it impossible to proceed with an endoscopy. Therefore, endoscopies must be always performed after checking whether the light source functions properly; D, E: Wrong position of arm. If an arm of an examinee is protruding out of the bed, it can touch the body of the endoscopist and interfere with the examination.

arm should be on the chest. Alternatively, an examinee can fold their arms across the chest.

Intubation of scope from oral cavity into pharynx

Overview: (1) It is important to check whether the mouthpiece is properly placed in the mouth of an examinee; if the tongue blocks the opening, an examiner should instruct an examinee to place his or her tongue in the lower part of the mouth. If an examinee does not follow the instruction well or in case of a sedated endoscopy, an examiner should insert his or her index finger into the examinee's mouth to place the tongue in the lower part of the mouth. A mouthpiece with a tongue restrainer can be of great help; (2) after securing the space above the tongue (in the lower side on the screen), an examiner should insert the scope through the mouthpiece. Before inserting the scope, it is important to check the location of the tongue on the screen of the monitor and ensure that it is placed between the 9 o' clock (the upper left on the screen and 12 o'clock (the upper side on the screen) positions; and (3) once the tongue is properly placed, an examiner should insert the

scope along the middle line of the soft palate. When advanced approximately 5-7 cm, the scope will reach the tongue base (tongue root), where the uvular can be observed. The anatomical location of the uvula is curved in a downward direction but will appear bent at an upward direction, on the screen. If the section is only slightly curved in an upward direction with the scope in in a neutral position, the endoscopist can advance the scope further without manipulating the scope. However, if the upward curve angle is sharp, an examiner can use the up/down angulation control knob to deflect the distal end of the scope more acutely upwards. At this point, it is important to deflect the scope slightly to the left (left turn) toward the space on the left side of the uvula. When the uvula is irritated during the insertion of the scope, an examinee may feel uncomfortable or nauseous. After passing this section, the scope will enter the hypopharynx or laryngeal pharynx, which is the distal end of the pharynx where the vocal cord, both pyriform sinuses, and various cartilages are observed.

Important points for beginners: (1) The section from oval cavity to the pharynx is one of the most difficult parts of upper GI endoscopy. It is important for a beginner to carefully observe an advanced endoscopist performing EGD; when given a chance the beginner should attempt a careful insertion of the scope into an examine. We recommend practicing with a model of a human body which can also be helpful in learning the procedure[23]; (2) just as in the oral cavity to pharynx section, an examiner must not insufflate air through the section comprising the pharynx to the esophagus, which will be explained later in this review. Air insufflation in this section can irritate the vocal cord, which in turn causes a coughing reflex. According to the operating principle of an endoscope, air is infused when the air/water control button is in the neutral position (located right below the suction button), whereas a few droplets of water can emerge from the distal end when the air/water button is depressed. Since air and water are supplied through the same channel, a few droplets of water can emerge together with air and enter the esophagus even when the vent is blocked for air insufflation, which can also trigger the coughing and vomiting reflexes. Therefore, a beginner should bear in mind that an examiner should not block the vent on the air/water button (*i.e.*, insufflate air) after inserting the scope into the oral cavity, until the distal tip is advanced into the upper esophagus; (3) saliva can physiologically drain into the examinee mouth, if opened. There are two important factors regarding this point: if an examinee swallows saliva, it can cause coughing and vomiting reflexes; and saliva can compromise the visibility of the scope and interfere with its advancement[24]. Therefore, it is very important for an examiner to instruct an examinee prior examination not to swallow saliva but let it fall from the mouth into the collecting container; it can be helpful to push the suction button to remove saliva from the mouth during the insertion; and (4) even though adults usually do not have enlarged tonsils, some patients can have swollen tonsil either due to inflammation, such as tonsillitis and pharyngolaryngitis, or due to anatomical traits. In this case, even though the uvula and the tonsil appear to block the opening, it is still possible to perform the procedure. Advancement of the scope between the uvula and the tonsil should be attempted, as it will cause the soft tissues of the tonsil to be pushed back and allow for the smooth passage of the scope (Figure 7, Figure 8, Figure 9, Figure 10, Figure 11, Figure 12).

Intubation from hypopharynx to upper esophagus

Overview: (1) The vocal cord is clearly observed below the epiglottis when the distal tip reaches the lower end of pharynx. The scope should by no means be inserted into the vocal cord. If the scope is mistakenly inserted into the vocal cord, the cricoid cartilage can be observed, and this causes a severe cough reflex and dyspnea. If this occurs, the scope must be pulled back immediately; (2) the larynx is mainly involved in sound production and is located above the air way, situated the trachea below and the hypopharynx posteriorly. The larynx is strongly pulled back by the cricopharyngeal muscles, while the hypopharynx is divided at the esophageal entrance into the right and left sides. Therefore, the center of the hypopharynx connected to the esophagus appears blocked, while the left and right sides appear slightly recessed. Usually, the hypopharynx appears to be closed ended, as it is contracted by the upper sphincter. The hypopharynx is connected to a upper esophagus through a section termed the pyriform fossa, or pyriform recess, or pyriform sinus, whose unique shape has earned it nickname descriptors such as gourd-shaped conclave and pear-shaped conclave; (3) we have provided several tips for advancing the scope through this section. First of all, as an examinee lies in the left lateral decubitus posture in most cases, the scope should be advanced into the left side of the pyriform sinus in keeping with gravity. While advancing along the left side of the pyriform sinus, the examiner should begin to insufflate air by placing a finger on the vent of the air/water button. In the pharynx, air infusion is contra-indicated. At the same time, the examiner is required to push the scope carefully with just a little force. It can be helpful for the examiner to raise his or her left hand holding the control shaft, above the head of an examine, or to slightly twist his or her right hand, which is holding the scope in a clockwise direction; and (4) as the passage of the scope through the larynx occurs continuously, an examiner can momentarily lose sight of it. However, if an examiner attentively employs the above mentioned operating skills, he or she will ultimately be able to advance the scope into the upper esophagus.

Important points for beginners: Unlike the colonoscopy,

Figure 7 Intubation of scope from oral cavity into pharynx. A: The examiner is inserting a mouthpiece into the mouth of the examinee (dotted circle). The pillow (arrow mark) helps keep the neck and head straight with the trunk; B: To ensure a smooth insertion of the endoscope, the examiner needs to raise the chin of the examinee and have the head protrude a little bit forward. If this happens, the tongue base separates from the hypopharynx so that the insertion of the endoscope is easier; C: A small container is placed close to the mouth of a patient to collect saliva during and after the esophagogastroduodenoscopy; D: The examinee with a mouthpiece placed in the mouth is fully ready for the examination.

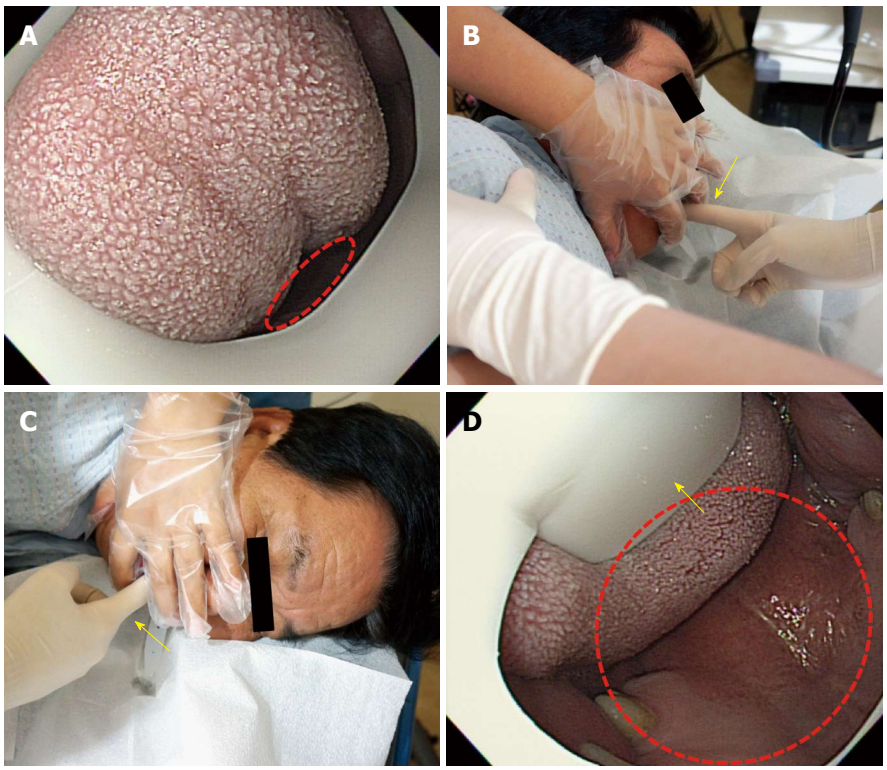

Figure 8 Intubation of scope from oral cavity into pharynx. A: Tongue blocking the oral cavity. As the oral cavity has a very narrow space (dotted circle) in this case, it is difficult to insert the scope (B, C). The examiner pushes aside the examinee's tongue with his or her index finger (arrow mark) to secure more space; D: Tongue placed under the tongue restrainer (arrow mark). After securing more space, the insertion of the scope is easier.

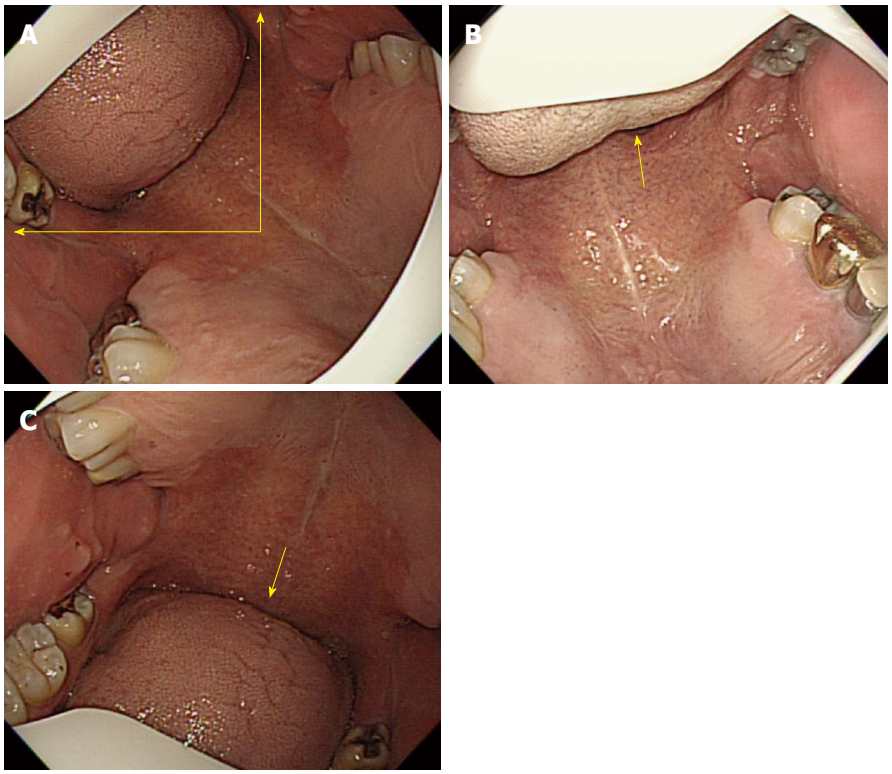

Figure 9 Intubation of scope from oral cavity into pharynx. A: The right position of the tongue. Before inserting the endoscope into the oral cavity, it is recommended the the tongue be positioned between the 9 o'clock and 12 o'clock directions on the screen. An advanced endoscopist usually inserts the endoscope into the oral cavity after placing the tongue to the upper left side (11 o'clock direction) on the screen; B: Another example of a properly positioned tongue. In this case, the tongue is placed nearly to the 12 o'clock direction on the screen; C: Inadequately positioned tongue. As the tongue is placed in a wrong position (about 6 o'clock direction in this examinee's case) on the screen, it becomes difficult to advance the scope further because the intended manipulation of the scope does not coincide with the subsequent movement of the scope displayed on the screen.

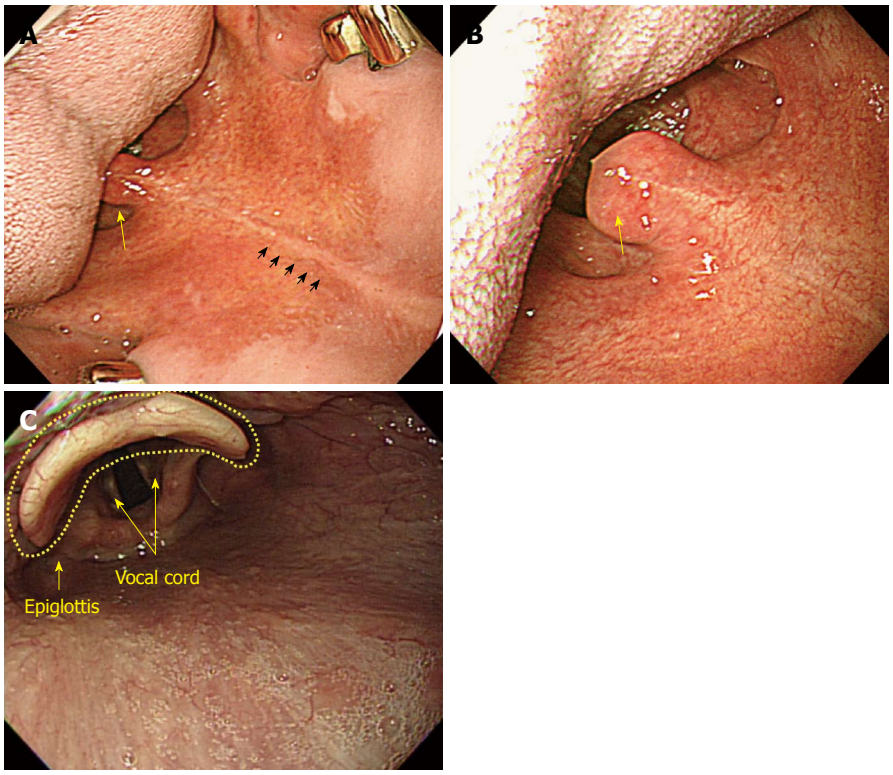

Figure 10 Intubation of scope from oral cavity into pharynx. A: After placing the tongue in a right position on the screen, an examiner has to advance the scope along the middle line (small arrow marks) of the soft palate. The uvula is observed in the upper side of the tongue (lower side); B: The uvula is observed more clearly at the end of the tongue (tongue base). After that, rotate the scope a little bit to the left and advance it further; C: If the scope is advanced further, it will enter the hypopharynx where the epiglottis is observed together with the vocal cord.

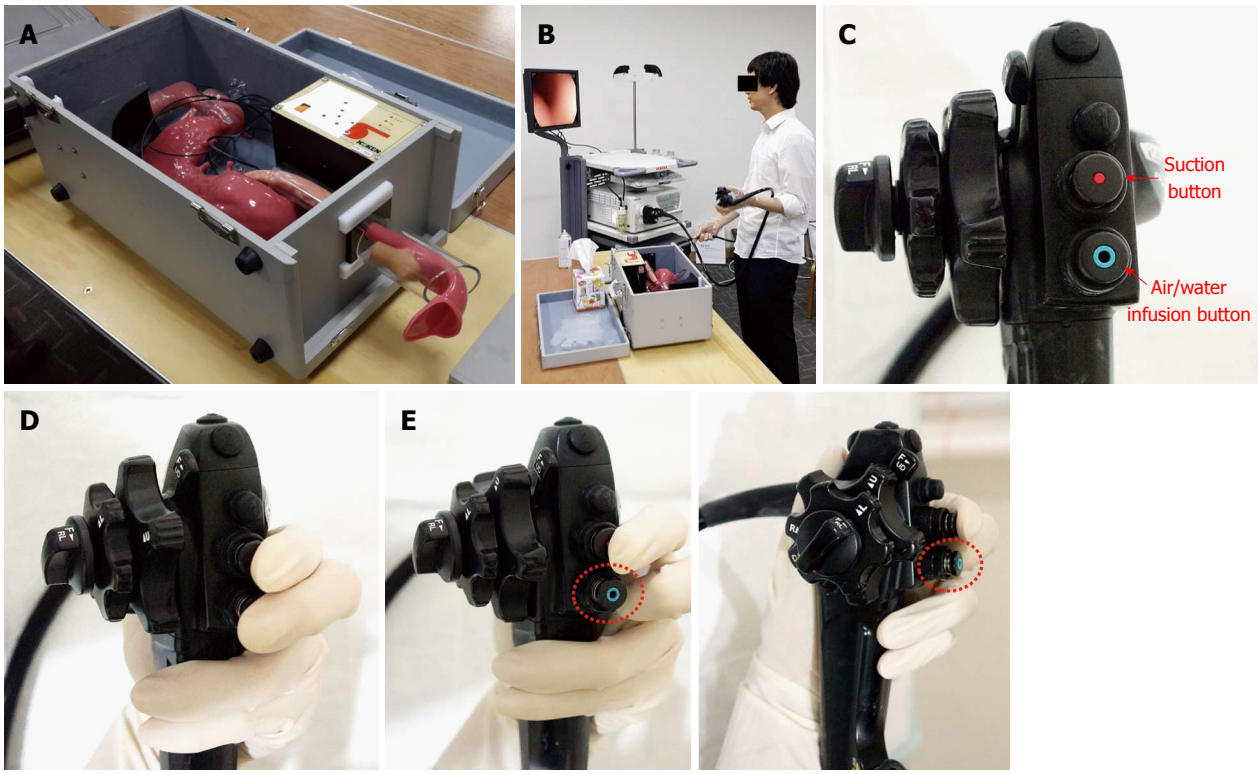

Figure 11 Intubation of scope from oral cavity into pharynx. A: The human body model for esophagogastroduodenoscopy (EGD) training; B: Practicing the endoscopic procedure using a model of a human body. This human body model is specially designed for EGD training, and if beginners practice EGD using a human body model, it will be helpful for them to acquire and improve their capacity to perform the procedure; C: The control part of the endoscope has several buttons to manipulate various functions. Among them, there are two buttons that play a critical role in relation to the procedure; the "suction button" and the "air/water infusion button"; D: When one is advancing the scope, it is recommended to place the second and third fingers on the suction button and the air/water infusion button, respectively, after inserting the distal tip into the upper esophagus. The reason for placing the fingers on the buttons is to continuously insufflate air into the lumen during the upper GI endoscopy; of course, an excessive air infusion is absolutely taboo, and in that case, an endoscopist should stop air insufflation and begin to suction the air. Another reason is it makes it easier to immediately suction liquid or air whenever it is judged to be necessary by the examiner; E: The recommended position of the third finger until advancement into the upper esophagus (the cervical part of esophagus). As mentioned above, if a finger is placed on the air/water infusion button (that is to say, if the vent is blocked by a finger), this itself can irritate the airway (trachea) and trigger coughing and vomiting reflexes. As the air insufflation and water infusion use the same channel, a few droplets of water can be released when an examiner starts to do an air infusion, which can also cause coughing or vomiting reflexes. Therefore, it is recommended that an examiner not block the vent on the top of the air/water infusion button with the third finger of the left hand, until the distal tip reaches the entrance of the upper esophagus, as shown in the picture.

EGD has almost no risks of perforation. The only section with a potential risk of perforation is the pyriform fossa, which is the entrance into the upper esophagus from the hypopharynx[25]. Actually, several EGD research reports have emphasized that an examiner should not exert too much pressure when passing the scope through this section. However, it has been my experience that beginners are often overly and unduly obsessed with it and consequently experience difficulty advancing the scope through this section. As a result, the typical beginner does not exert enough force, and ultimately failure to enter the esophagus. However, it should be emphasized that when the scope is advanced through the pyriform fossa, too much strain must be avoided due to the potential risk of perforation. Conversely, if an examiner does not place enough force to the shaft, he or she may fail to penetrate the upper esophagus even in normal situations, due to resistance from the upper esophagus sphincter. Therefore, an adequate amount of force is recommended to penetrate the shaft into the upper esophagus. An "adequate amount of force" is very subjective, hence an examiner will benefit from prior experience. Broadly stated despite its subjectivity, endoscopists are required to exert force as if gently making a fist with the right hand.

Propofol used for a sedated endoscopy, is effective in preventing vomiting and relaxing the upper esophageal sphincter (UES). Combinations with or a single administration of propofol can help the beginner to successfully penetrate the distal tip of the scope into the esophagus[26]. Additionally, when performing an endoscopy without sedation, it can be of great help if an examiner verbally instructs an examinee to "try to swallow the scope" or pushes the scope in synchronization with the examinee's swallowing movement.

Although advancing the scope in the left side of pyriform sinus is recommend based on the examinee's posture as mentioned above, it is not applicable to every case. There are some cases in which advancing the scope through the left side of the pyriform sinus is quite difficult. In such cases, it is better to redirect the scope toward the right side of the pyriform fossa rather than attempt to

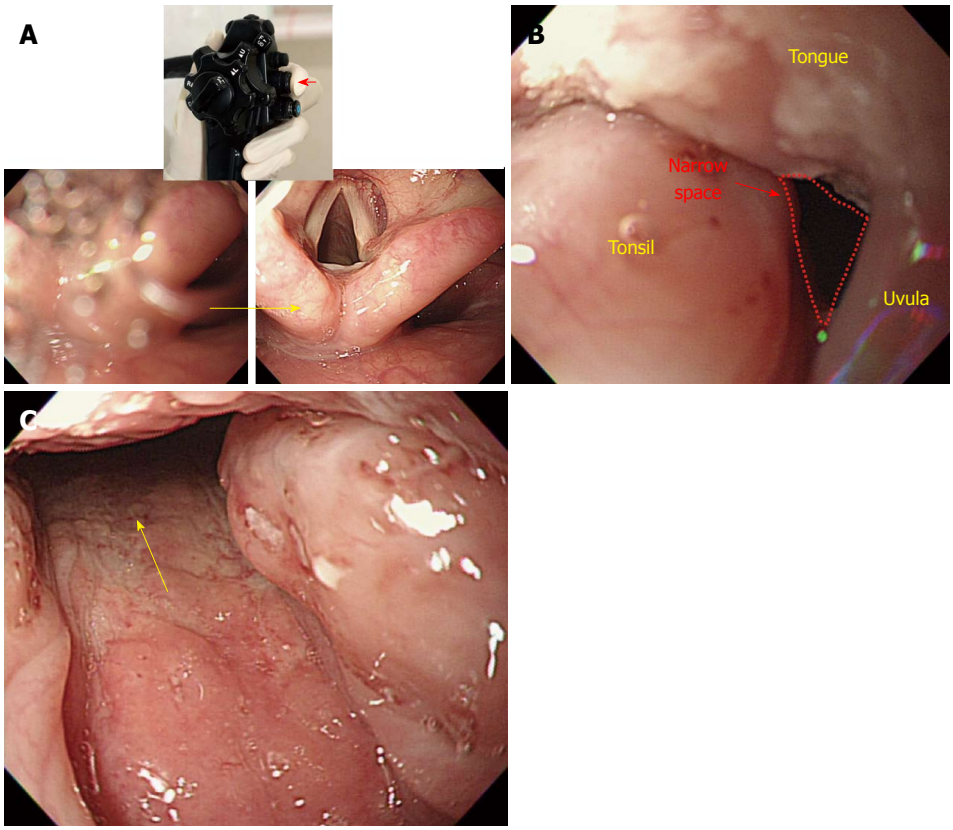

Figure 12 Intubation of scope from oral cavity into pharynx. A: If the visibility is compromised by saliva in the process of advancement after inserting the scope into the oral cavity (left), one can secure clear visualization of the entrance route (right) by suctioning the saliva with a push on the suction button (small arrow mark). If one advances the scope into the esophagus without suctioning the saliva, an examinee may inhale saliva, which can cause a severe coughing reflex. Therefore, it is recommended to suction saliva during the advancement process; B: Swollen tonsil. As the pathway where the tongue, uvula and tonsil are located together is narrow due to a swollen tonsil, it can be difficult to advance the scope, and a beginner may feel frustrated. However, as the endoscope is ductile, the scope can pass into the oropharynx if it is twisted carefully (to the right, in this case); C: Passage through the swollen tonsil.

proceed along the left side.

The primary focus of EGD is the examination of the esophagus, stomach, and proximal duodenum (usually up to the second portion). Incidental upper airway lesions can be identified in the pharynx and larynx, including those of the epiglottis and vocal cords, during the insertion and withdrawal of the endoscope to and from the esophagus. Therefore, this area should be examined thoroughly during the insertion as well as the withdrawal of the endoscope (Figure 13 and Figure 14).

Insertion from esophagus to stomach

Overview: (1) The advancement of the scope into esophagus is not difficult, and may be one of the easiest parts of EGD intubation. The esophagus refers to the anatomical region which ranges from the UES to the gastroesophageal junction (GEJ), which is subdivided into three portions: upper, middle, and lower. Despite possible differences between examinees, the UES is usually located about 15 cm away from the incisor, while the GEJ lies 45 cm away from it; (2) Overall, it can be said that the scope is advanced in a straight linear direction in the esophagus, though there are times when slight twisting and deflection of the scope are required. When the scope advances into a section that is 10 cm away from the UES (the starting point of the upper esophagus), tracheoesophageal compression by the aortic arch can be visualized, which is commonly called the upper esophagus. By dividing the remaining portion from this point (tracheoesophageal compression by aortic arch; physiologically the second constriction) to the GEJ, the upper half is termed the middle esophagus, while the remaining half is the lower esophagus; and (3) Similar to the advancement of the scope into the esophagus, it is also difficult to insert the scope from the GEJ (the end part of the esophagus) into the lumen of the stomach. However, it is more important to observe the GEJ; if an examinee follows the instructions of an endoscopist well in a non-sedated or even a sedated endoscopy, an endoscopist should ask the examinee to breathe in to inflate the GEJ so that he or she can clearly observe it.

Important points for beginners: Intubation into the esophagus is not difficult. Hence a detailed explanation is not required. Instead, we would like to provide beginners with some helpful tips to advance the scope into the esophagus as follows: (1) continuous air insufflation throughout the entire esophagus is helpful in advancing the endoscope. The lumen of the esophagus is 15-20

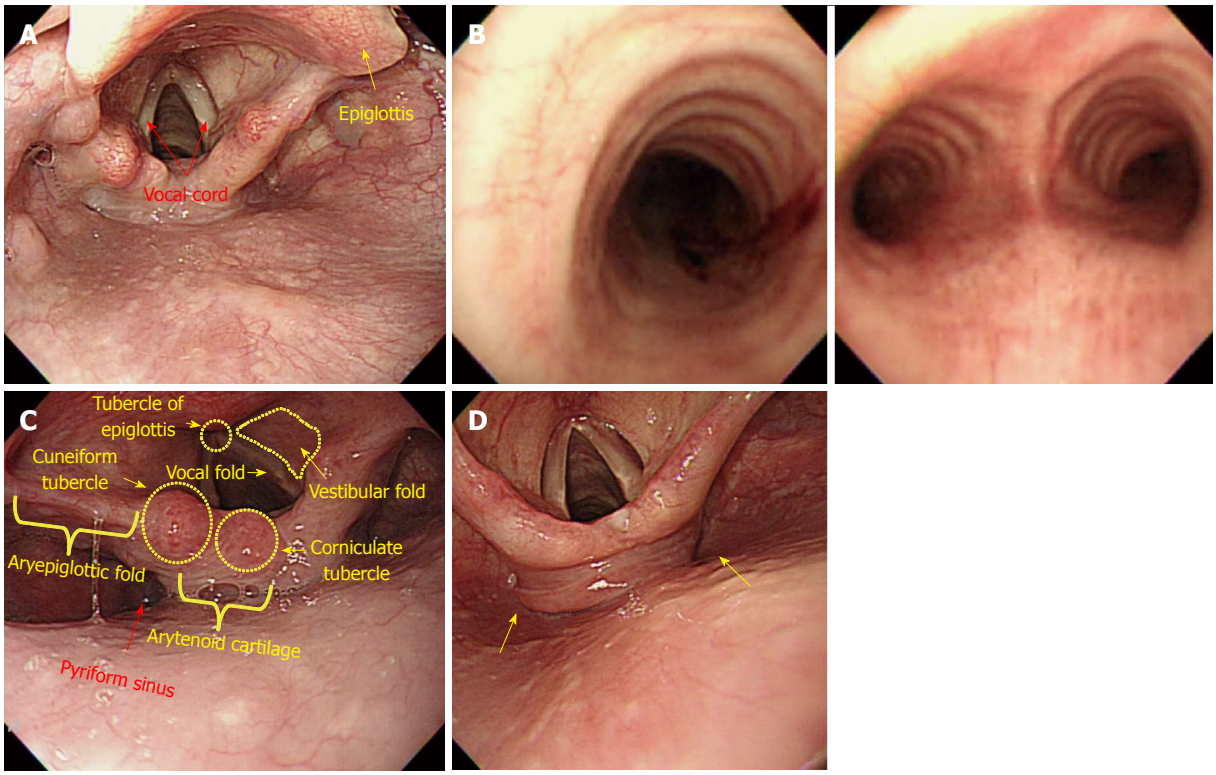

Figure 13 Intubation from hypopharynx to upper esophagus. A: Hypopharynx. The hypopharynx refers to a part of the pharynx located in the posterior of the larynx (usually from the epiglottis to the vocal cord); B: Bronchus. If the scope is mistakenly inserted into the vocal cord, the circular cricoid cartilage, which belongs to the main bronchus (left), is observed. If the scope is passed further without noticing that it has been placed in a wrong position, the scope will enter the area (right) where it bifurcates into the left and right sides. When an examinee suffers a coughing reflex together with severe dyspnea, the scope must be immediately withdrawn; C: Anatomical structures of hypopharynx and larynx; D: Left- and right-sided pyriform fossa. As an examinee lies in a left lateral decubitus position, it is usually recommended to insert the scope into the left sided pyriform fossa. However, after several attempts to insert the scope have failed and ended with damaged tissues, advancement into the right-sided pyriform fossa should be attempted.

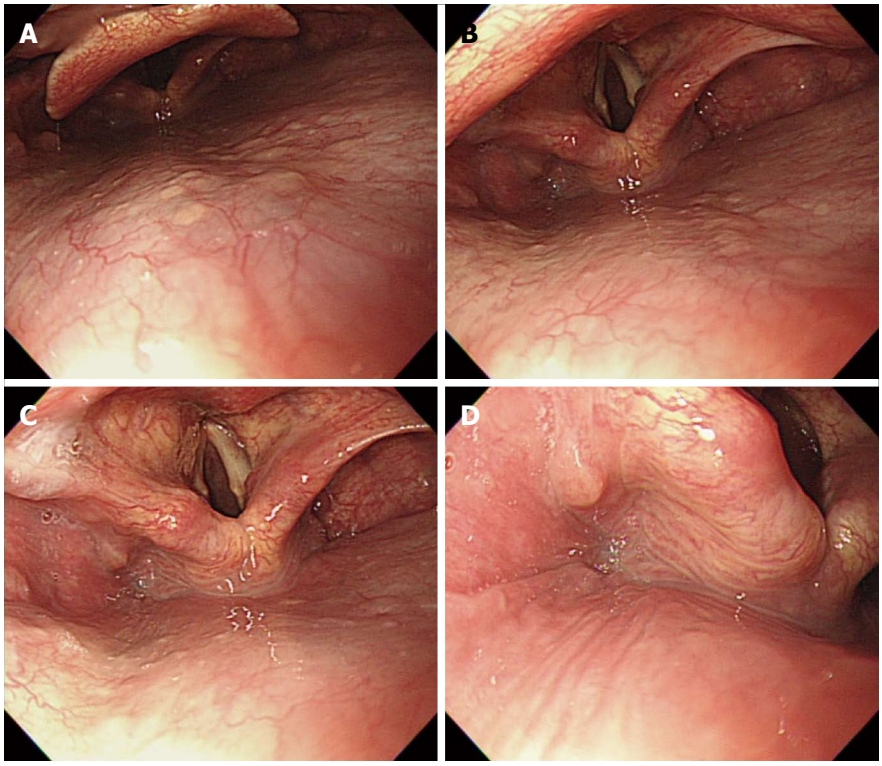

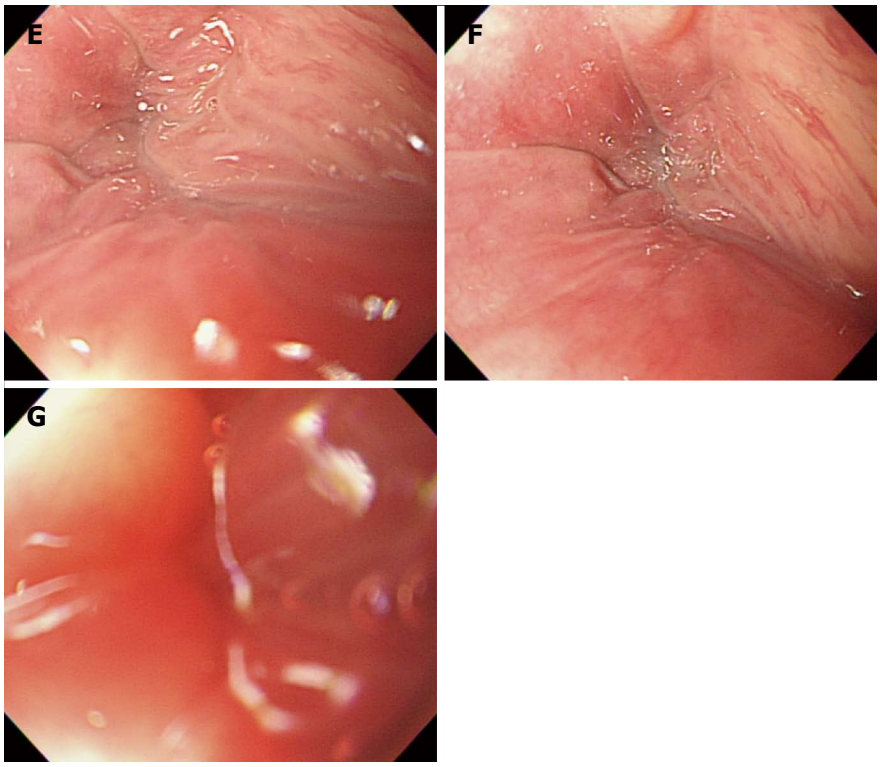

Figure 14 Intubation from hypopharynx to upper esophagus. A-E: Images were continuously taken during the advancement of the scope through the left-sided pyriform fossa into the upper esophagus. Although it appears to have a blind ending shape, upon further examination, a tiny furrow will be observed. With air insufflation and by a little bit of force, the scope can be moved into the upper esophagus, despite resistance from its sphincter; F, G: In this process, a red-out sign can occur. Continue to insert the scope gradually and carefully while observing the surface in the process of the advancement into the lumen.

cm wide, which is not spacious enough to comfortably advance the scope. Therefore, air insufflation is required to guide the endoscope into the esophagus as well as for observation. The next portion into which the endoscope is advanced after the esophagus, is the stomach. While a well-skilled endoscopist can advance the scope into the stomach without even inflating the stomach, it is difficult for a beginner to advance the scope without air insufflation. Continuous air insufflation into the lumen of the esophagus, while the scope is being advanced from the esophagus, can help the examiner to insert the scope into the stomach through the GEJ without triggering the vomiting reflex. Therefore, the EGD has an advantage, in that intubation from the esophagus into the stomach can be done without much difficulty; (2) In principle, the intubation from the esophagus into the stomach is done in a straight linear direction as mentioned above. However, a beginner should remember that the distal tip of the endoscope needs be slightly deflected in some parts of the esophagus unlike the straight line intubation displayed in the schematic diagram. There are some cases in which an esophageal web is observed especially in the GEJ section. In that case, an examiner should avoid using too much power when pushing the scope. Instead, it is recommended to advance the scope using a slight rotation in order to position the center of the esophageal lumen in the middle of the screen; (3) although extremely rare, great attention and care is required when a diverticulum is observed in the esophagus. A diverticulum is made up of very thin walled pouches or sacs formed by herniated protrusion of mucous membranes, without a muscle layer. Therefore, the scope must be pulled back immediately, if it is mistakenly inserted in a wrong direction. If a diverticulum is mistaken as the lumen and the scope is advanced in that direction, there is a risk of perforation; and (4) an endoscopist should use extra attention and care when advancing the scope in case an esophageal varix is observed in an examinee. The surface of an esophageal varix is extremely thin, hence great care is required to ensure that the scope does not touch it. If an examinee has a vomiting reflex, the examination should be quickly done to ensure that the examinee becomes stabilized. In this instance, where the examinee has a known severe vomiting reflex, an EGD in a deep sedation state can be paradoxically safer than a non-sedated procedure. An endoscopist must make an informed decision, taking all these factors into consideration (Figure 15).

Intubation from stomach to duodenal bulb

Overview: (1) on the basis of anatomical landmarks of high reproducibility such as the cardia, gastric angle and pyloric ring, the stomach is subdivided into the fundus (fornix), body and antrum. The gastric body is further subdivided into the upper body (UB), middle body and lower body, while the antrum is subdivided into the prepyloric antrum, distal antrum and proximal

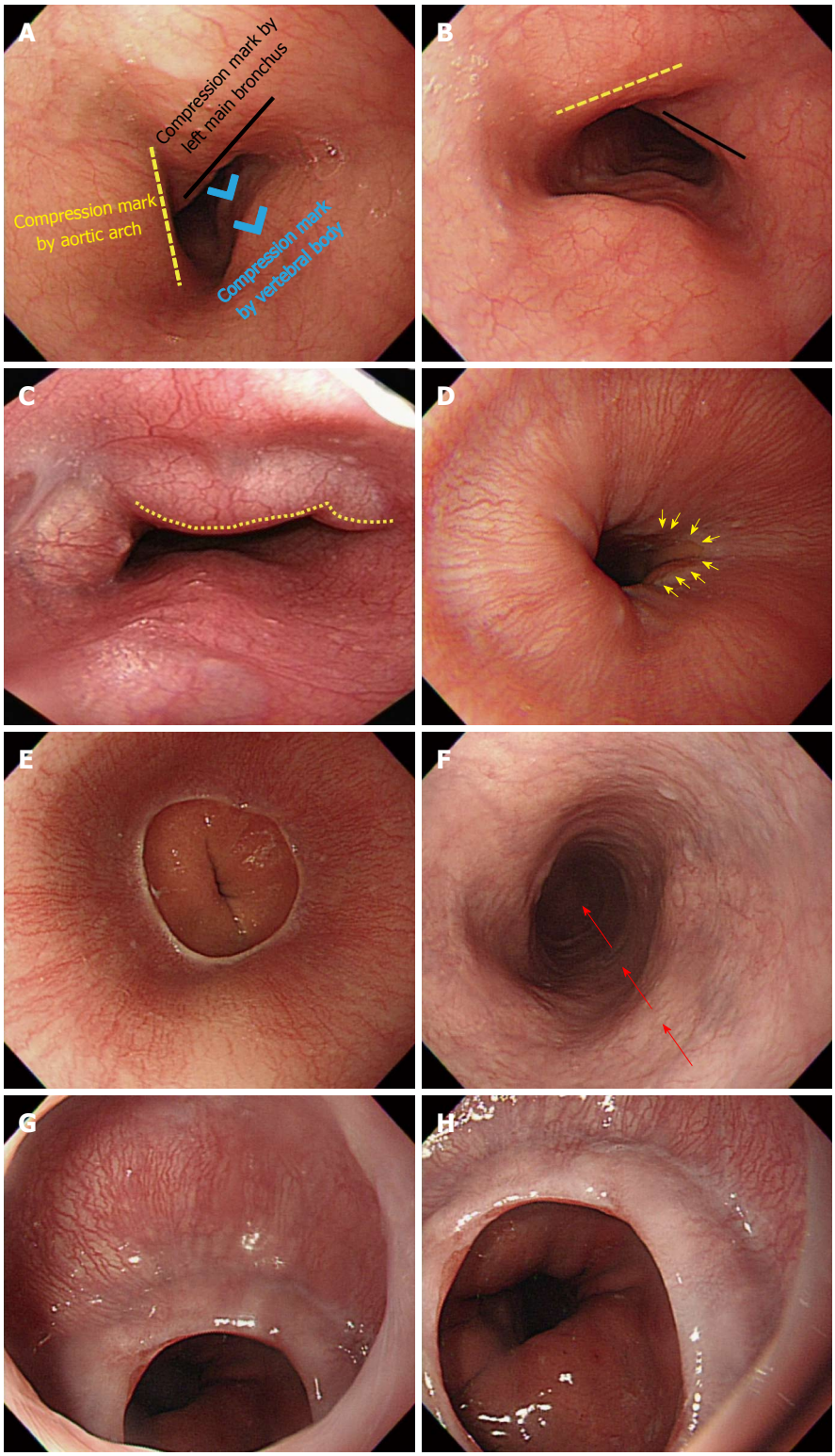
A
Compression mark by left main bronchus
Compression mark by aortic arch
Compression mark by vertebral body
B
C
D
E
F
G
H

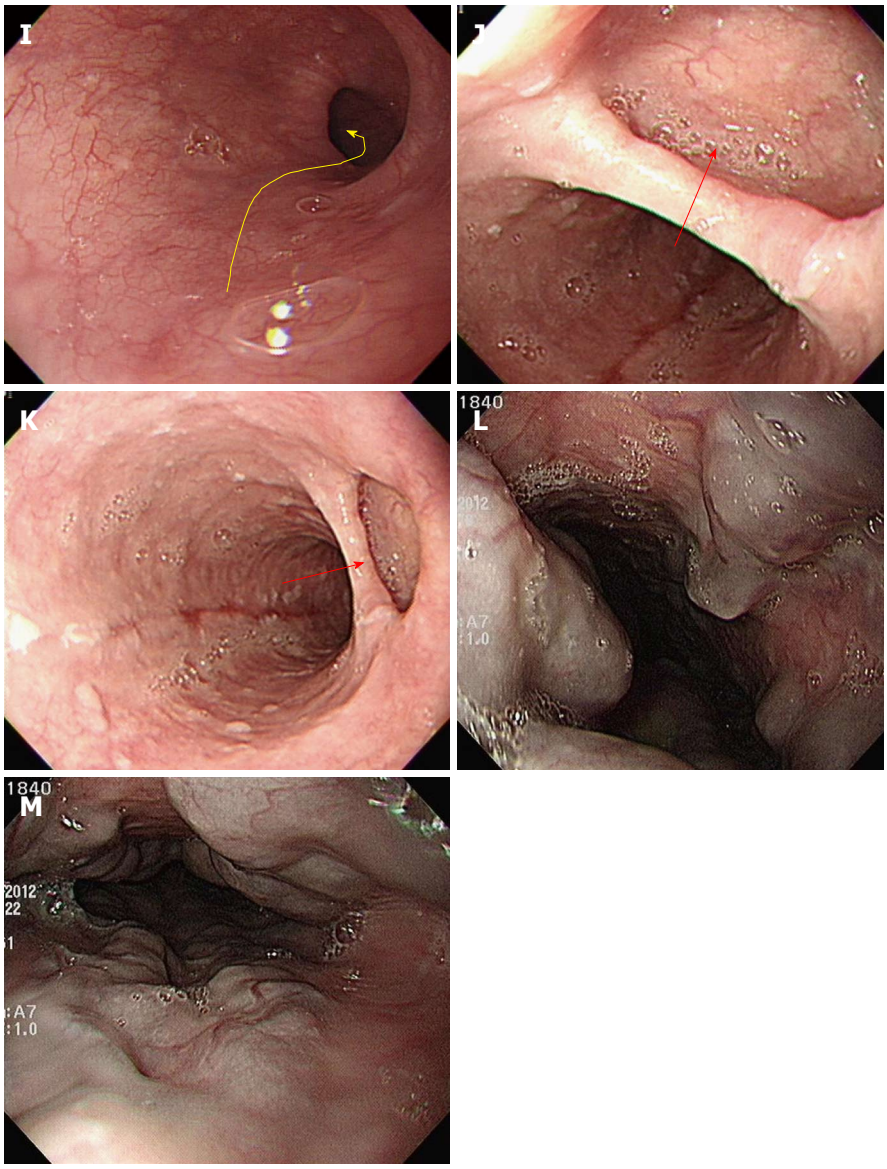

Figure 15 Insertion from esophagus to stomach. A: Esophageal physiology, the second stenosis. If the scope is advanced 10 cm further after passing it through the sphincter of the upper esophagus, a high pressure zone caused by aortic arch (dotted line) on the left side, and another high pressure zone by the left main bronchus on the right side of the distal antrum can be seen. Depending on the examinees's posture, or condition, state of air insufflation, there are some cases where such pressure marks are clearly visible; B: Pressure marks by the aortic arch and the left main bronchus, with a pressure zone caused by a vertebral body positioned in the 6 o'clock direction on the screen with a slightly rotation of the scope (knuckle line). The advancement direction inside the esophagus is usually described based on the condition that a high pressure zone by the vertebral body is positioned toward the 6 o'clock direction on the screen. However, if those pressure marks by the vertebral body are not clearly visible, the lumen of the esophagus is not wide enough. In that case, it is acceptable to describe their vertical locations (usually the insertion length from the incisor) unlike the description of directions inside the stomach; C: Pressure by a calcified aortic arc. A severe case of calcification can look like a submucosal tumor, due to the conspicuous appearance of pressure marks; D: Gastroesophageal junction (GEJ) before suctioning air. The boundaries of the GEJ (arrow mark) are not clearly visible; E: GEJ after suctioning air. As the GEJ unfolds, the boundaries of the GEJ become clear; F: The direction of the scope in the esophagus. The scope is inserted using a straight line progression (arrow mark) in the esophagus; G-I: An esophageal web around the GEJ. If the mucous membrane of the esophagus has a rather curved progression (arrow mark in I), it is recommended to insert the scope by slightly rotating the shaft rather than pushing it straight ahead forcefully; I: Esophageal diverticulum: it appears as though the progression of the esophagus has two different directions. If being pushed in a hurry, a scope can enter the esophageal diverticulum, which can cause a perforation; J: Esophageal diverticulum after pulling back the scope. After filming the entire entrance of the esophageal diverticulum by pulling back the scope, advance it into the lumen of the esophagus; K, L: Endoscopic image of a severe case of esophageal diverticulum. In the case of a patient with a severe esophageal varix, extra caution needs to be taken during the insertion and advancement of the scope into the esophagus. A massive hemorrhage here can lead to the death of an examinee.

antrum; (2) the lower esophagus passes through the diaphragm near the GEJ and has a curved progression toward the left posterior side. Therefore, when the scope passes through the GEJ into the stomach for the first time, the scope needs to be rotated anticlockwise (left turn); in some cases, the distal tip of the shaft needs to be deflected in the upward direction. If the scope is pushed in a linear fashion without such manipulations, the scope will penetrate the GEJ to reach the posterior wall of the UB. This will lead to a "red-out" sign, which

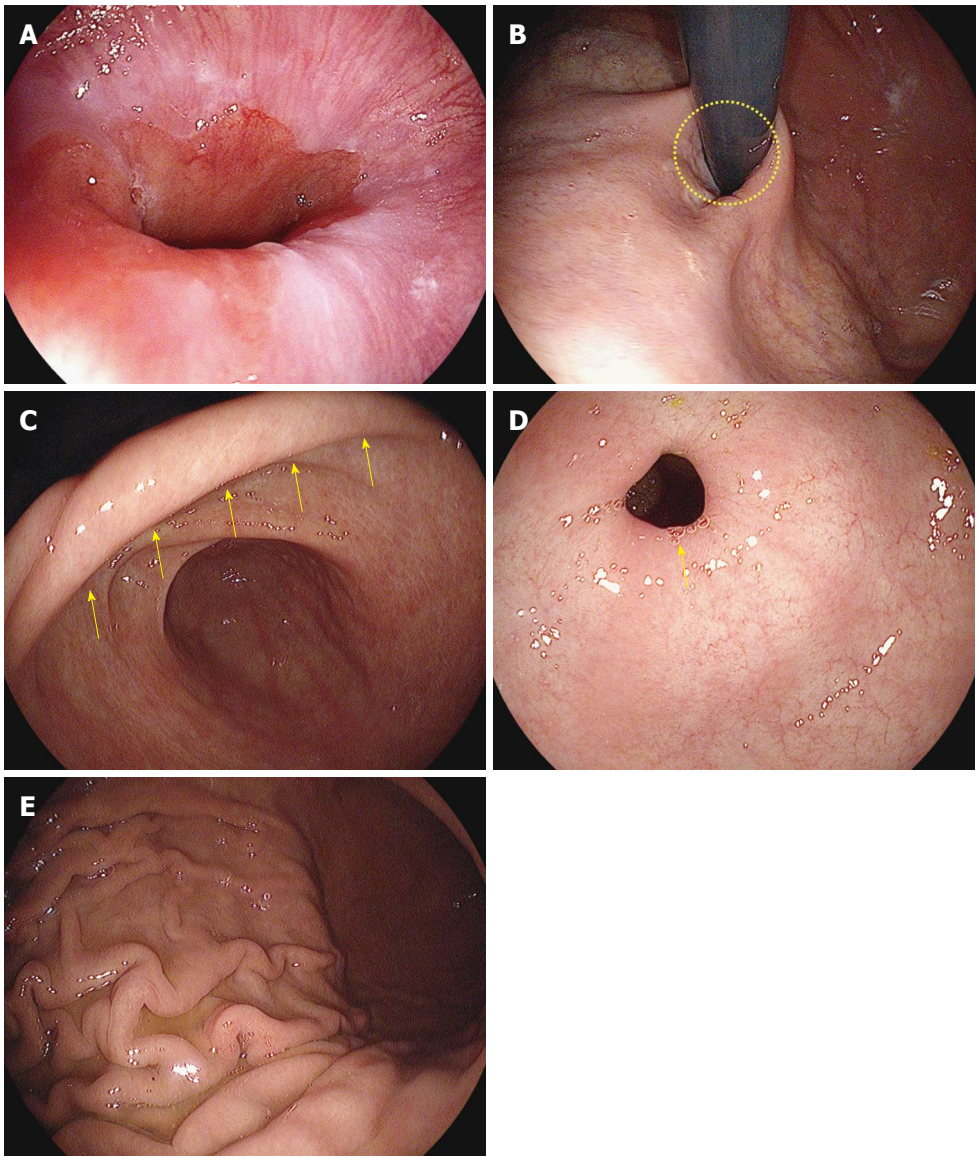

Figure 16 Intubation from stomach to duodenal bulb. A: Gastroesophageal junction (GEJ). In absence of hiatal hernia, the GEJ lies next to the cardia; B: Gastric cardia observed in retroflexion of the scope. Likewise, in the absence of hiatal hernia, the gastric cardia is located next to the gastroesophageal junction; C: Gastric angle. If the distal tip of the scope is deflected upward in the distal antrum, the gastric angle (arrow marks) in an arched shape will be observed; D: Pyloric ring. The pyloric ring is usually observed to have a circular shape (arrow mark); E: Gastric fold. For a patient who does not have a severe case of atrophic gastritis, the gastric fold serves as a landmark to distinguish the body of stomach from the antrum of stomach.

will compromise visibility; (3) a "red-out" sign is not inherently problematic. The scope must be pulled back just a little. At this point, it is recommended that the endoscopist secures better visibility using air inflation. If clear visibility is not achieved after pulling the scope slightly backward, it may be withdrawn as far as the lower esophagus through the GEJ. Then, it is recommended that the scope be inserted from the lower esophagus into the stomach again, while continuing to insufflate air into the lumen of the stomach from the GEJ; (4) if the scope is properly inserted into the stomach, a gastric fold, the greater curvature of the body of the stomach will be typically observed. There are many cases wherein gastric juice retention is detected. The watershed, which is an elevated area, along which the gastric fundus and body are divided, can be observed depending on the individual examinees or the air insufflation; (5) unless the stomach is reversed to the right side (situs inversus), the direction of insertion is mostly oriented to the right side (right middle, right upper or right lower). Therefore, if an examinee pushes the scope by rotating it to the right, which is the same direction as the fold, the scope can enter the antrum of stomach without much difficulty; (6) there are some cases where beginners feel embarrassed to see that the intubation is oriented to the left side on the screen. However, as a right-sided stomach is extremely rare, it is reasonable to first suspect that a beginner might have made a mistake operating the scope rather than of a case of situs inversus. This is caused mainly by a manipulation mistake of rotating the scope to the left too sharply when inserting the scope into the cardia from the GEJ. In that case, the

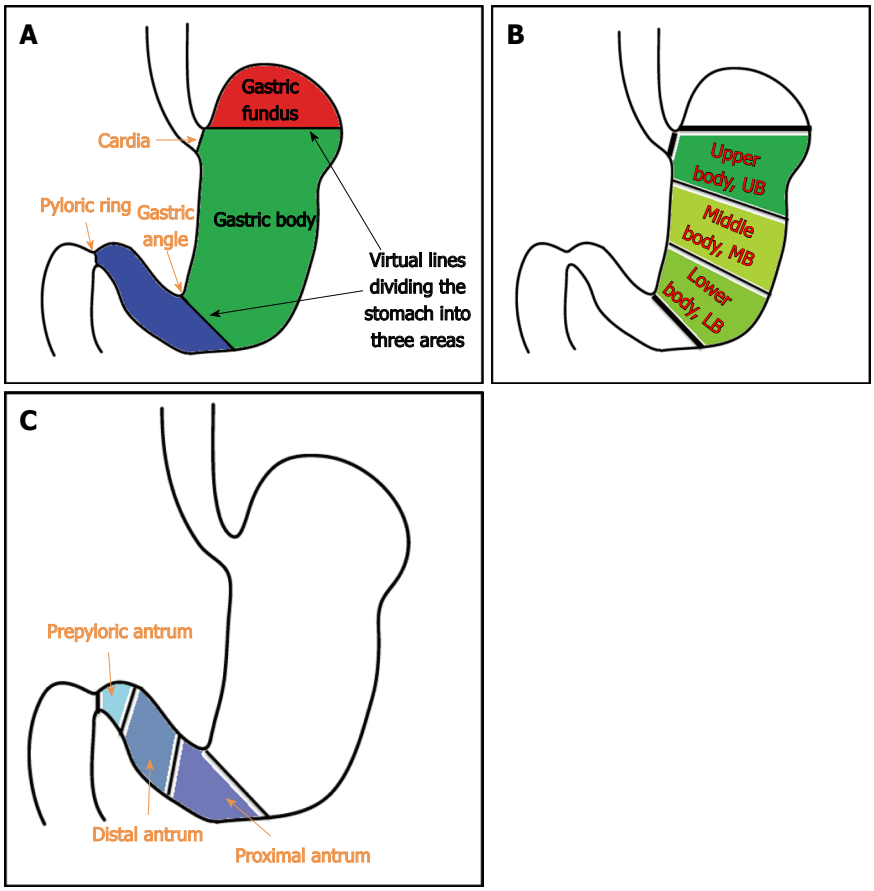

Figure 17 Intubation from stomach to duodenal bulb. A: Schematic diagram of the anatomy of the stomach. Based on the landmarks, the stomach is divided into three parts: the gastric fundus, gastric body and gastric antrum; B: A schematic diagram of gastric body subdivided into three areas. The gastric body is the largest among the three parts. Therefore, the gastric body can be subdivided into three areas: upper body, middle body and lower body; C: Schematic diagram of three subdivided areas of the gastric antrum.

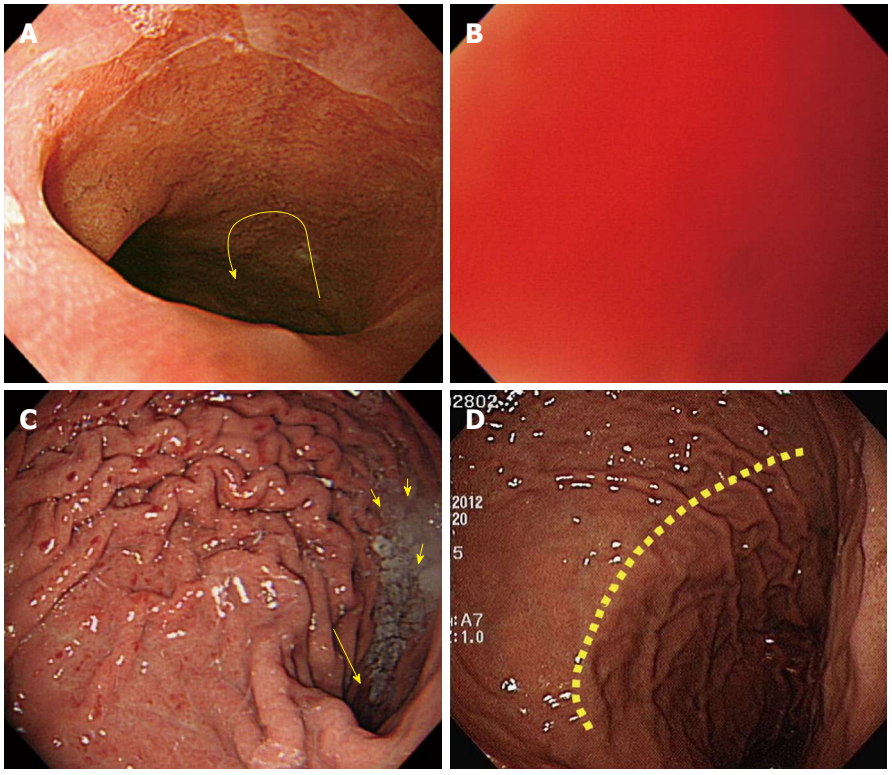

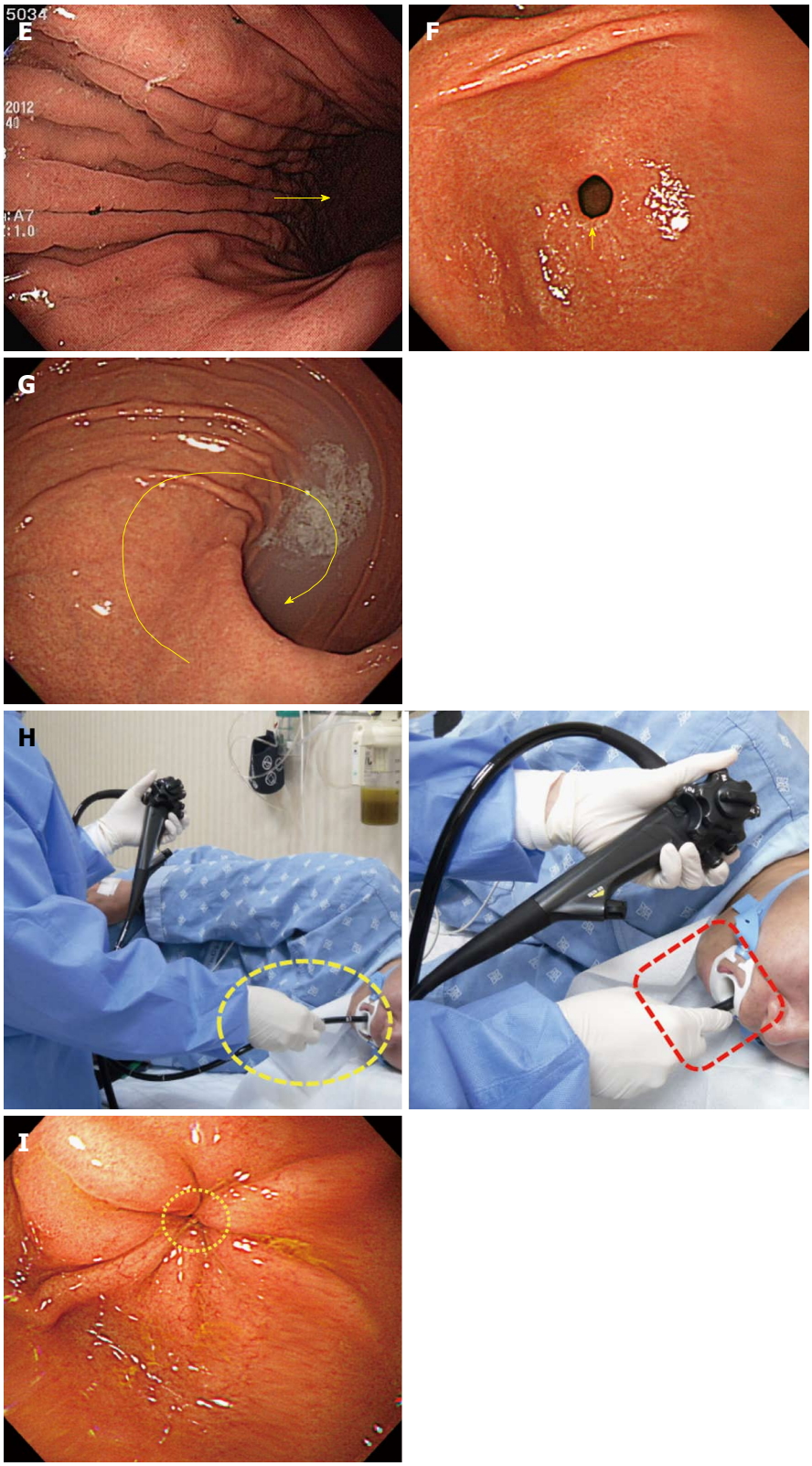
E
F
G
H
I

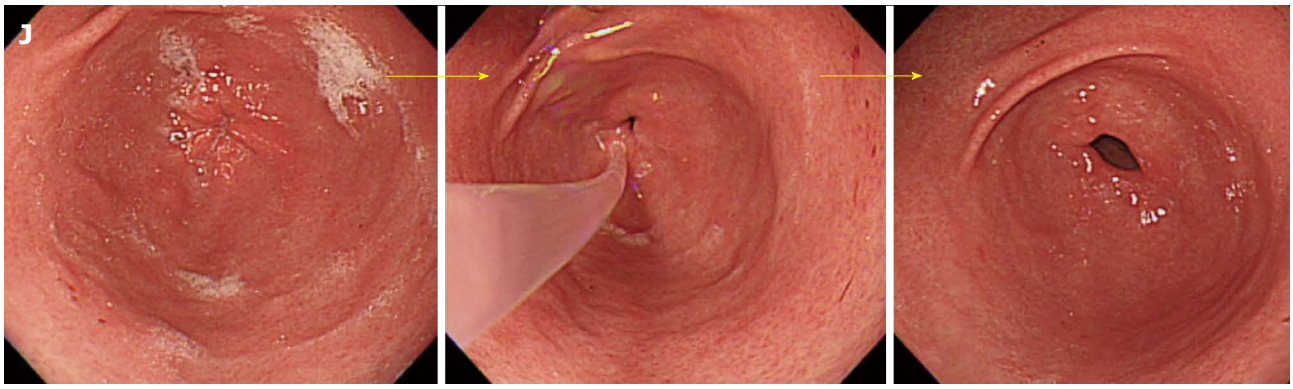

Figure 18 Intubation from stomach to duodenal bulb. A: Gastroesophageal junction (GEJ). As the lower esophagus penetrates through the diaphragm and then starts to progress in the left posterior direction at a point where it is connected to the stomach, it is recommendable to insert the scope by twisting the shaft to the left side (arrow mark) during intubation into the stomach; B: Red-out sign. If the scope is only pushed in a straight line, it can subsequently touch the posterior wall of the gastric body, in which a red-out sign appears. If this happens, just pull back the scope a little. If air is insufflated, clear visibility will result; C: Gastric fold. When the scope is first inserted from the GEJ into the lumen of the stomach, a gastric fold is observed. Gastric fluid (small arrow marks) is usually retained in the gastric fold (greater curvature). The progression direction into the antrum of stomach is usually to the right side. The examinee in this image has a right sided progression of the surface into the antrum of stomach (5 o'clock direction, big arrow mark); D: Watershed. The watershed is also often called the saddle area, which serves as a landmark to divide the stomach into the gastric fold, fundus, and gastric body. It may not be clearly visible depending on the examinees or the condition of air insufflation; E: Advancement into the antrum of stomach; F: Distal antrum. The pyloric ring in a circle-shape is observed (arrow mark); G: Endoscopic image of cascade stomach. As the deflection angle of the cascade stomach is extremely sharp, a beginner may encounter difficulty advancing the scope into it; H: Tips for the insertion of the scope into the pyloric ring. When the endoscopy is performed in the stomach, it is a common practice to hold a shaft by keeping some distance from the mouth of the examinee (approximately 10 cm). However, especially when inserting the distal tip into the pyloric ring, it is advisable to hold it short (dotted rectangle) because it can transfer force to the tip more efficiently, to help advance it into the pyloric ring; I: Closed pyloric ring, a challenging configuration for beginners; J: Injection of warm water into the pyloric ring. The injection of warm water is helpful in inserting the scope into the pyloric ring.

scope must be withdrawn to be reinserted, or it must be redirected toward the right side by readjusting the left rotation angle. It is recommended that the endoscopist manipulates the scope as described above, when such a problem is encountered; (7) when the scope is inserted along the fold of the greater curvature of the body of stomach, the endoscopist will observe the antrum of stomach where there is no fold. Advancing the scope further into the distal antrum will allow the examiner to observe the pyloric ring, which leads to the duodenal bulb; and (8) unless the pyloric ring is deformed due to ulcer scars in the duodenum, it is usually observed to have a circular shape. At this point, it is important for an endoscopist to place the pyloric ring in the middle of the screen before trying to insert the scope into the duodenal bulb. After positioning the pyloric ring at the center of the screen with a combination of up/bottom and left/right deflections and twists, the endoscopist will be able to pass the scope through the pyloric ring to enter the duodenal bulb without much difficulty, if he or she gently pushes the tip of the scope into the pyloric ring.

Important points for beginners: (1) a limited low level of air insufflation during the advancement of the scope into the stomach can help reduce the insertion route and time by shortening the stomach's longitudinal axis. Therefore in principle, it is recommended to use the smallest amount of air insufflation necessary during the EGD; an experienced endoscopist is able to pass the scope through the anatomical section without any air insufflation of the stomach. However, a beginner cannot identify the direction of scope's advancement without inflating the stomach somewhat. Accordingly, it is recommended that beginners infuse air into the stomach, even though it will extend the insertion route. In particular, when the scope is inserted into the stomach through the GEJ, the examiner should provide enough air into the lumen of the stomach so he or she can determine the direction of scope advancement; (2) retention of gastric juice occurs in the greater curvature of the body of stomach in normal conditions, even if an examinee went on a fast prior to the examination. It appears opaque when mixed with a premedication (*e.g.*, simethicone solution) for the EGD or mucus materials. In principle, an examiner should suction the gastric liquid when it is observed, while withdrawing the scope. But if an excessive amount of gastric liquid interferes with the advancement of the scope, it may be helpful to suction while inserting the scope into the stomach; (3) the most challenging stomach shape for beginners is the so-called "cascade stomach"[27]. When the scope is advanced into the stomach through the GEJ, the watershed between the gastric body and fundus can be observed, and the greater curvature of stomach can be seen on the right side of the watershed. The cascade stomach refers to the one that appears like a waterfall due to an acute bi-directional angle and curve. In the cascade stomach, the fundus descends into the "body" of the stomach and makes a sudden turn or curve, to move upward toward the examinee's back. Therefore, if the scope is pushed while rotating to the right side as usual, the scope will bend in the fundus, which makes it impossible to advance further. For the smooth

advancement of the scope into the cascade stomach, it is recommended that the endoscopist push the shaft hard while twisting it at a sharp angle with the right hand, after flattening an acute curve angle from the fundus to the gastric body by relieving the inflation pressure in the lumen of the stomach with air suction; (4) the insertion through the pyloric ring to the fundus can be more difficult, especially for a beginner, than any other parts of the stomach. The location of the pyloric ring is constantly changing due to peristalsis and the examinee' s respiration. In order to safely navigate this area, it is important for the examiner to hold the shaft rather short or closer to the mouth of the examinee. Furthermore, it can be helpful to hold the shaft in this manner while advancing it into the pyloric ring, because it can transfer force more effectively to the distal tip of the scope. In such conditions, the examiner should push the shaft with minimal force (as when getting close to the examinee). The scope will then advance through the pyloric ring into the duodenal bulb. An examiner must relax his or her grip immediately after entering the pyloric ring, as a precautionary measure, so that the distal tip does not hit into the wall of the duodenal bulb; and (5) the opening and closing degree and the diameter of the pyloric ring may vary depending on each examinee. Advancing the scope through an open pyloric sphincter with a wide diameter is straightforward, even for beginners. However, if a pyloric ring has a narrow diameter or is closed, a beginner may have difficulty advancing the scope (Figure 18I). To avoid such a situation in the case of a non-sedated endoscopy, an examiner can ask an examinee to make the sound "Ah" which will open the pyloric ring by relieving the abdominal pressure and reducing peristalsis. If an examinee undergoes a sedated endoscopy, the endoscopist can instead insufflate air or inject warm water toward the pyloric ring after positioning the tip of the scope close to it (Figures 16-18).

Insertion from duodenal bulb into the descending portion of duodenum

Overview: (1) Typically, villi of the mucosa of the small intestine can be observed at this point since the duodenal bulb is part of the small intestine. These villi are more clearly visible with the water-filling method or with narrow-band imaging[28,29]; (2) It is important to observe the superior duodenal angle (SDA) in the duodenal bulb. The SDA plays an important role as a landmark in identifying the location of the scope in the duodenal bulb; as the scope progresses through the second portion of the duodenum on the right side of the SDA, the angle can be used to help identify the direction an examiner should take to insert the scope into the second part of the duodenum; (3) The duodenum is subdivided into the first, second, third and the fourth portion, also referred to as the bulb, descending portion, horizontal portion and ascending portion, respectively. EGD usually progresses only through the first and second portions of the duodenum. In addition, an examiner should try to observe the AOV, while examining the second portion of the duodenum. However, it can occasionally be impossible to observe the AOV with a straight-view endoscope due to its limited visibility, and it is not always necessary to take images of the AOV; (4) to insert the scope from the duodenal bulb into the descending portion; the examiner should first position the SDA on the right side on the screen and move the scope close to the SDA. When the scope reaches the SDA, the examiner needs to advance the scope while rotating the shaft to the right. To rotate the scope to the right, an examiner can twist the shaft with his or her right hand to the right, and then the endoscopist can raise his or her left hand, which holds the control shaft toward the examiner's chest, which is a more convenient way to penetrate the duodenal bulb. If an endoscopist fails to insert the scope into the second portion of the duodenum with right rotation alone, an endoscopist can also manipulate the up/down control knob on the inner side of the control unit to deflect the distal tip of the scope upward. After a series of such manipulations consecutively without any hinderance, the typical circular fold (Kerckring) of the descending portion of the duodenum can be observed, signifying that the tip of the scope has been inserted into the descending portion of duodenum; and (5) To take images of the AOV displayed on the screen or make a more thorough observation of the descending portion of the duodenum, a paradoxical maneuver of the scope is required. The "paradoxical movement" of the scope refers to a phenomenon where the tip of the shaft is paradoxically advanced when an endoscopist attempts to withdraw the scope from the descending portion of the duodenum.

Important points for beginners: (1) Beginners often experience difficulty performing the paradoxical movement in the descending portion of the duodenum, in which the distal tip of the scope advances as the shaft is withdrawn. It is important to know that, as the shaft is withdrawn, it is not just simply pulled back. If it were pulled back in a straight linear direction, in most cases, the distal end of the scope will end up falling into the duodenal bulb. The scope is reversed at this point because it pulled back in order to be advanced; accordingly, the scope must be reversed while being rotated to the right. This concept is similar to a torque maneuver in colonoscopies. In addition, when an endoscopist starts to withdraw the scope, it will be reversed at first. This is not a cause for concern. If it is pulled back further, the distal end of the scope continue to advance after being reversed; and (2) in principle, the upper GI endoscope will take images in reverse order after inserting the distal dip into the second portion of the duodenum. However, the authors recommend that the endoscopist take images of the pyloric ring and the duodenal bulb first before inserting the scope into the second portion of the duodenum, even if these endoscopic images

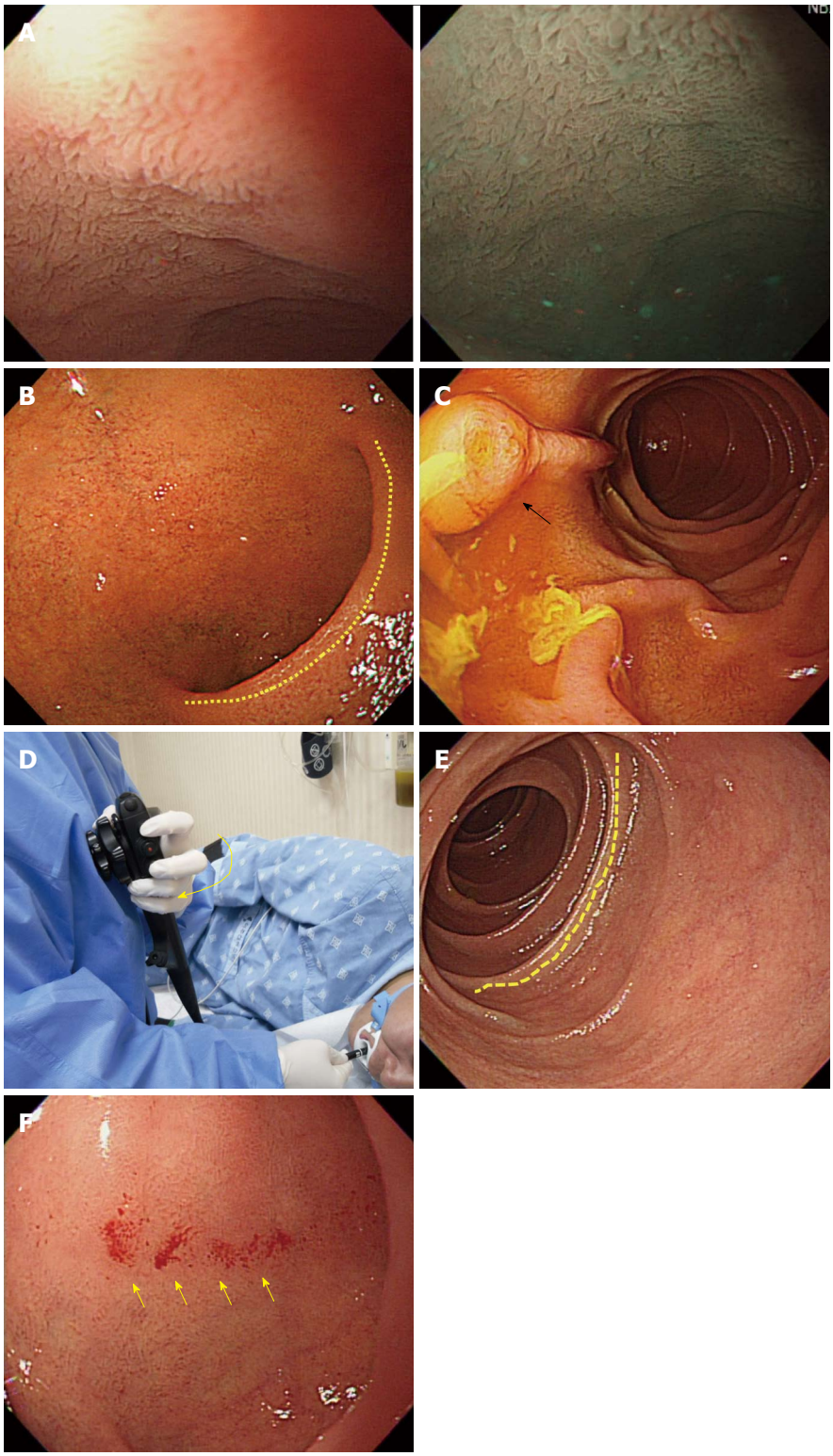

Figure 19 Insertion from duodenal bulb into the descending portion of duodenum. A: Villi in the duodenal bulb. Water-filling method (left) and narrow-banding image (right); B: Typical image of a normal duodenal bulb. The superior duodenal angle in a crescent shape is observed on the right side. This direction coincides with the progression direction into the second portion of duodenum (descending part); C: Descending part of duodenum. The AOV is observed; D: Image of the left hand when inserting the scope into the descending part of duodenum from the duodenal bulb. It is advisable to pull the left hand holding the control part close to the chest (arrow mark), as it will help insert the scope into the descending part of duodenum. If one fails to advance the scope into the descending part of duodenum by rotating the shaft to the right in the SDA, it is recommendable to try to angle the scope more sharply to the right side or to do it in combination with an upward deflection of the distal tip of the endoscope; E: Circular fold (Kerckring) observed in the descending part of duodenum; F: Bleeding marks on the mucous membrane due to a collision with the endoscope during the advancement from the ampulla into the descending part of duodenum. A smooth insertion of the scope is needed in order to avoid leaving bleeding marks during the advancement into the entrance to the descending part of duodenum. However, if the body of an examinee moves during the endoscopy, even a skilled endoscopist can leave bleeding marks while trying to insert the scope into the descending part of duodenum. Therefore, it is recommended to film the images of the duodenal bulb before inserting the scope into the descending part from the duodenal bulb.

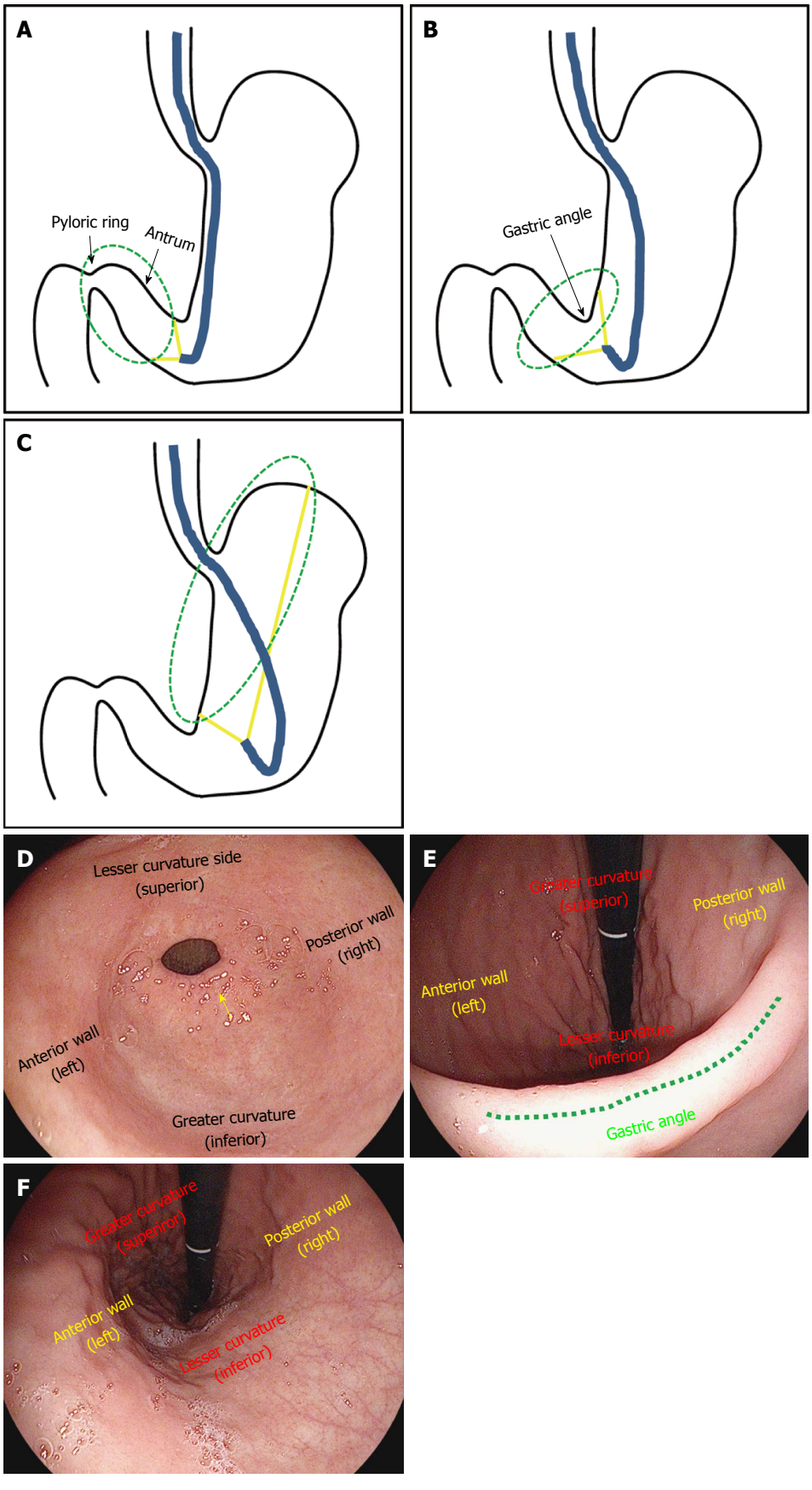
A
Pyloric ring
Antrum
B
Gastric angle
C
D
Lesser curvature side
(superior)
Posterior wall
(right)
Anterior wall
(left)
Greater curvature
(inferior)
E
Greater curvature
(superior)
Posterior wall
(right)
Anterior wall
(left)
Lesser curvature
(inferior)
Gastric angle
F
Greater curvature
(superior)
Posterior wall
(right)
Anterior wall
(left)
Lesser curvature
(inferior)

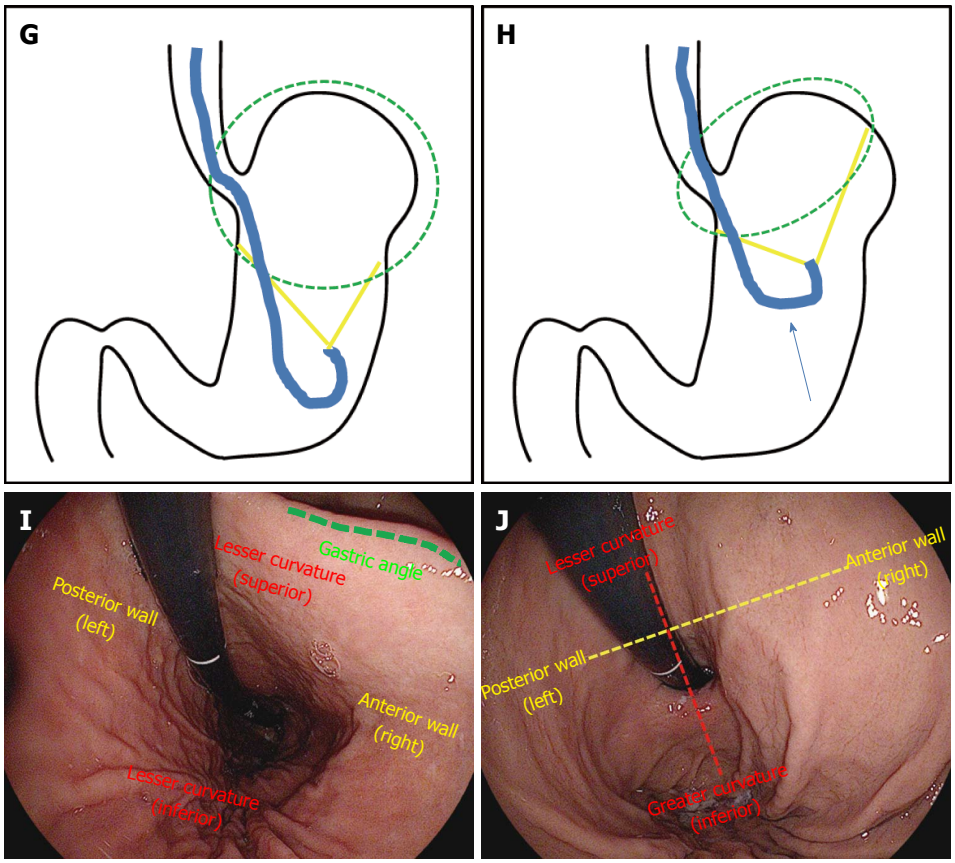

Figure 20 Withdrawal of scope and observation, J-turn and U-turn. A: Schematic diagram of the J-turn. Deflect the distal tip of the scope upward in the antrum of the stomach; B: The shaft of the scope is bent in a J-shape, as the gastric angle in an arched shape is observed; C: If the scope tip is deflected upward more sharply, the lesser curvature of the gastric body can be observed; D: Endoscopic image of the antrum of stomach before maneuvering a J-turn. The pyloric ring (arrow mark) is observed in the front; E: Endoscopic image of the antrum of stomach after maneuvering a J-turn. If the distal tip of the endoscope is deflected upward, the gastric angle (dotted line) in an arched shape is observed. At this point, the upper side is the greater curvature; the lower side is the lesser curvature; the left side is the anterior wall; the right side is the posterior wall. The left and right directions on an endoscopic image taken during a J-turn maneuver are not reversed; F: Endoscopic image taken in the J-turn. In this case, the distal tip of the endoscope is deflected upward too sharply and the gastric angle cannot be observed. Likewise, the left and right directions on an image taken in J-turn do not change, but only the up and down directions are reversed in this case; G: Schematic diagram of the U-turn. The U-turn can be maneuvered by rotating the scope in a J-turn by 180 degree; H: In the U-turn, the observation is usually done while pulling the scope up toward the gastric cardia; I: Endoscopic image taken in the U-turn. A U-turn changes the directions of the left and right sides; the upper side is the lesser curvature; the lower side is the greater curvature; the left side is the posterior wall; the right side is the anterior wall; J: Endoscopic image after pulling up the scope in a U-turn toward the gastric cardia. The directions of the left and right sides still remain reversed.

overlap with the ones that are to be taken while the scope is being reversed. The reason is that even a skilled practitioner can leave scars (iatrogenic legions) owing to contact with the scope. Therefore, it is helpful to take images of the condition of the mucous membrane before trying to insert the distal tip of the scope, which can be helpful when analyzing results or explaining the results to an examinee (Figure 19).

Others: Withdrawal of scope and observation, J-turn and U-turn

Withdrawal of scope and observation: (1) even though observation can be accomplished before the distal tip being inserted, upper GI endoscopy usually inspects the mucosa in greater detail during the withdrawal phase. The endoscopic images are usually taken in reverse starting from the second portion of the duodenum, but it is highly recommended that images of some portions such as the GEJ, pyloric ring and duodenal bulb be taken in advance; (2) in the earlier Polaroid digital photo printing system, 4 or 8 images were usually taken and more were filmed in case of pathological legions. Recently, most medical institutions have introduced picture archiving communication systems (PACS), which allow for unlimited photo-taking. Therefore, a large number of images can be taken on a certain anatomical part depending on the judgment of an endoscopist, in addition to photos of the mandatory sections. Images that are required to be recorded include the upper esophagus, middle esophagus, lower esophagus, GEJ, front and reverse images of the fundus, front and reverse images of the gastric body (upper, middle, lower), antrum of stomach (proximal, distal, pylorus), gastric angle, pyloric ring, duodenal bulb and the lower portion of duodenum; and (3) according to the principle of withdrawal, an observation should be thoroughly conducted without missing blind spots. The possible blind spots include the cardia, lesser

curvature and posterior wall of the body of stomach and all other spots which are hidden by the scope. An examiner should take extra care and attention to observe these areas in detail. It is highly recommended that the stomach be observed by adjusting the inflation with an adequate use of air insufflation and air suction.

J-turn and U-turn: (1) The gastric fundus and body can be observed in anteversion during the withdrawal of the scope, but need to be inspected in retroversion in order to examine blind spots thoroughly[30]. If the scope gets deflected upward when the distal antrum is observed along with the pyloric ring, the scope will be deflected in a J-shape, which is termed as a "J-turn maneuver", where the gastric angle is observed and the gastric body can be seen if the scope is angled up even further; (2) when maneuvering a J-turn, the location of the anterior wall is not simply replaced with the posterior wall. When observed on gastric endoscopy, the left side is the anterior wall, while the right side is the posterior wall. In contrast, the location of the greater curvature of the body of stomach is replaced with the lesser curvature; the lower side is the lesser curvature, whereas the upper side is the greater curvature. However, it is not difficult to distinguish the greater curvature from the lesser curvature, thanks to the unique appearance of their respective folds, and it is important to remember that during J-turn, the direction of the scope usually coincides with those of the anterior and posterior walls observed on the screen; and (3) a U-turn maneuver is a 180° rotation of the endoscope in a J-turn. The U-turn allows for a good visualization of the greater curvature of the gastric body, cardia and fundus. In a U-turn, a detailed observation is possible when the scope is angled upward. As a precaution, note that the orientation is different: the anterior and posterior abdominal walls are visible in the opposite direction; the right side is the posterior abdominal wall of abdomen, whereas the left side is the anterior wall (Figure 20).

CONCLUSION

The overall incidence rates for gastric cancer have steadily declined over the past 50 years[31,32]. However, gastric cancer is one of the most common causes of cancer deaths worldwide, particularly in Asian countries such as China, South Korea, and Japan[33,34]. Although it is relatively invasive procedure compared to the other examination tools such as an upper GI barium series, computed tomography (CT), magnetic resonance imaging (MRI), and capsule endoscope[35], EGD is the only method that allows for the biopsy and/or removal of pathologic lesions during the procedure, if indicated[36,37]. Furthermore, in the case a lesion suspected to be a malignant tumor or an ulcerous disease observed during the upper GI series, EGD is used to perform a biopsy and confirm the diagnosis, which makes the gastric cancer screening method quite inconvenient. Additionally, upper GI endoscopy offers color visualization of the upper GI tract with real time assessment and interpretation of the findings, through which an examiner can easily identity pathological lesions. Therefore, EGD is actively performed in South Korea as a primary screening tool for patients with upper GI diseases including gastric cancer currently[38].

EGD requires practical skills obtained by extensive training[39]. Endoscopic education is based predominantly on practicing on patients under the supervision of teaching staff (experienced endoscopists) and upper GI endoscopy dexterity is acquired over several hundred procedures. However, trainees may differ considerably in the rate at which they acquire the necessary psychomotor skills, although evidence suggests that most will arrive at the common end point, *i.e.*, procedural competence, in time. Active performance of the technical skills cannot be substituted with didactic demonstrations; the skills require hands-on teaching. Thus, it is hard to convey verbally or in writing precisely how an EGD should be performed because the assessment of procedural skills is very subjective. However, it is not desirable to attempt an endoscopy without proper preparation. This manuscript can be helpful in acquiring endoscopy procedural skills from a theoretical perspective, through text and photos. In conclusion, we hope our elaborate manuscript helps to improve the performance of EGD by beginners. Additionally, we believe that, if beginners learn how to perform EGD properly through an adequate training program, and then offer the service on patients, it can promote public health.

REFERENCES

1 **Oh MG**, Han MA, Park J, Ryu SY, Park CY, Choi SW. Health behaviors of cancer survivors: the Fourth Korea National Health and Nutrition Examination Survey (KNHANES IV, 2007-09). *Jpn J Clin Oncol* 2013; **43**: 981-987 [PMID: 23975890 DOI: 10.1093/jjco/hyt118]

2 **Park CH**, Kim EH, Chung H, Lee H, Park JC, Shin SK, Lee YC, An JY, Kim HI, Cheong JH, Hyung WJ, Noh SH, Kim CB, Lee SK. The optimal endoscopic screening interval for detecting early gastric neoplasms. *Gastrointest Endosc* 2014; **80**: 253-259 [PMID: 24613579 DOI: 10.1016/j.gie.2014.01.030]

3 **Early DS**, Ben-Menachem T, Decker GA, Evans JA, Fanelli RD, Fisher DA, Fukami N, Hwang JH, Jain R, Jue TL, Khan KM, Malpas PM, Maple JT, Sharaf RS, Dominitz JA, Cash BD. Appropriate use of GI endoscopy. *Gastrointest Endosc* 2012; **75**: 1127-1131 [PMID: 22624807 DOI: 10.1016/j.gie.2012.01.011]

4 **Evans JA**, Early DS, Fukami N, Ben-Menachem T, Chandrasekhara V, Chathadi KV, Decker GA, Fanelli RD, Fisher DA, Foley KQ, Hwang JH, Jain R, Jue TL, Khan KM, Lightdale J, Malpas PM, Maple JT, Pasha SF, Saltzman JR, Sharaf RN, Shergill A, Dominitz JA, Cash BD. The role of endoscopy in Barrett's esophagus and other premalignant conditions of the esophagus. *Gastrointest Endosc* 2012; **76**: 1087-1094 [PMID: 23164510 DOI: 10.1016/j.gie.2012.08.004]

5 **Evans JA**, Early DS, Chandraskhara V, Chathadi KV, Fanelli RD, Fisher DA, Foley KQ, Hwang JH, Jue TL, Pasha SF, Sharaf R, Shergill AK, Dominitz JA, Cash BD. The role of

endoscopy in the assessment and treatment of esophageal cancer. *Gastrointest Endosc* 2013; **77**: 328-334 [PMID: 23410694 DOI: 10.1016/j.gie.2012.10.001]
6 **Hirota WK**, Zuckerman MJ, Adler DG, Davila RE, Egan J, Leighton JA, Qureshi WA, Rajan E, Fanelli R, Wheeler-Harbaugh J, Baron TH, Faigel DO. ASGE guideline: the role of endoscopy in the surveillance of premalignant conditions of the upper GI tract. *Gastrointest Endosc* 2006; **63**: 570-580 [PMID: 16564854 DOI: 10.1016/j.gie.2006.02.004]
7 **Kim HS**, Baik SJ, Kim KH, Oh CR, Lee JH, Jo WJ, Kim HK, Kim EY, Kim MJ. Prevalence of and risk factors for gastrointestinal diseases in korean americans and native koreans undergoing screening endoscopy. *Gut Liver* 2013; **7**: 539-545 [PMID: 24073311 DOI: 10.5009/gnl.2013.7.5.539]
8 **Joo NS**. Esophagastroduodenoscopic Training in the Family Physician Residency Program. *Korean J Fam Med* 2010; **31**: 585-586 [DOI: 10.4082/kjfm.2010.31.8.585]
9 **Lee KM**, Choi SR, Jang BI, Kim SH, Kang CD, Kim YD, Park JY, Chung IK. Education and Training Guidelines for the Board of the Korean Society of Gastrointestinal Endoscopy. *Korean J Gastrointest Endosc* 2011; **42**: 207-214
10 **Chun JH**, Yoon YS, Oh SW, Lee ES, Kim MG, Kim YS, Kim YH, Yang J. Current State and Demand of Esophagogastroduodenoscopy Training in Family Practice Residency Programs. *J Korean Acad Fam Med* 2003; **24**: 1092-1098
11 **Coleman WH**. Gastroscopy: a primary diagnostic procedure. *Prim Care* 1988; **15**: 1-11 [PMID: 3043490]
12 **Park KH**, Sung NJ, Lee DW, Jeong HS. Technical Competency of the Esophgogastroduodenoscopy (EGD) during the First 50 EGDs: The Training Result of Family Medicine Residents in a University Hospital. *Korean J Fam Med* 2010; **31**: 595-599 [DOI: 10.4082/kjfm.2010.31.8.595]
13 **Catalano MF**. Training in upper gastrointestinal endoscopy. *Gastrointest Endosc Clin N Am* 1994; **4**: 623-638 [PMID: 8069479]
14 **Xiong X**, Barkun AN, Waschke K, Martel M. Current status of core and advanced adult gastrointestinal endoscopy training in Canada: Survey of existing accredited programs. *Can J Gastroenterol* 2013; **27**: 267-272 [PMID: 23712301]
15 ASGE guidelines for clinical application. Statement on role of short courses in endoscopic training. American Society for Gastrointestinal Endoscopy. *Gastrointest Endosc* 1999; **50**: 913-914 [PMID: 10644190]
16 **Dumonceau JM**, Riphaus A, Beilenhoff U, Vilmann P, Hornslet P, Aparicio JR, Dinis-Ribeiro M, Giostra E, Ortmann M, Knape JT, Ladas S, Paspatis G, Ponsioen CY, Racz I, Wehrmann T, Walder B. European curriculum for sedation training in gastrointestinal endoscopy: position statement of the European Society of Gastrointestinal Endoscopy (ESGE) and European Society of Gastroenterology and Endoscopy Nurses and Associates (ESGENA). *Endoscopy* 2013; **45**: 496-504 [PMID: 23702777 DOI: 10.1055/s-0033-1344142]
17 **Chini P**, Draganov PV. Diagnosis and management of ampullary adenoma: The expanding role of endoscopy. *World J Gastrointest Endosc* 2011; **3**: 241-247 [PMID: 22195233 DOI: 10.4253/wjge.v3.i12.241]
18 **Taylor H**. Position of Patient in Gastroscopy. *Br Med J* 1938; **1**: 892-894 [PMID: 20781408]
19 **Lee IL**, Wu CS. Less patient discomfort by one-man colonoscopy examination. *Int J Clin Pract* 2006; **60**: 635-638 [PMID: 16805744 DOI: 10.1111/j.1368-5031.2006.00891.x]
20 **Byun YH**, Lee JH, Park MK, Song JH, Min BH, Chang DK, Kim YH, Son HJ, Rhee PL, Kim JJ, Rhee JC, Hwang JH, Park DI, Shim SG, Sung IK. Procedure-related musculoskeletal symptoms in gastrointestinal endoscopists in Korea. *World J Gastroenterol* 2008; **14**: 4359-4364 [PMID: 18666326]
21 **Kuwabara T**, Urabe Y, Hiyama T, Tanaka S, Shimomura T, Oko S, Yoshihara M, Chayama K. Prevalence and impact of musculoskeletal pain in Japanese gastrointestinal endoscopists: a controlled study. *World J Gastroenterol* 2011; **17**: 1488-1493 [PMID: 21472109 DOI: 10.3748/wjg.v17.i11.1488]
22 **Kang SH**, Hyun JJ. Preparation and patient evaluation for safe gastrointestinal endoscopy. *Clin Endosc* 2013; **46**: 212-218 [PMID: 23767028 DOI: 10.5946/ce.2013.46.3.212]
23 **Ende A**, Zopf Y, Konturek P, Naegel A, Hahn EG, Matthes K, Maiss J. Strategies for training in diagnostic upper endoscopy: a prospective, randomized trial. *Gastrointest Endosc* 2012; **75**: 254-260 [PMID: 22153875 DOI: 10.1016/j.gie.2011.07.063]
24 **Maekita T**, Kato J, Nakatani Y, Enomoto S, Takano E, Tsuji M, Nakaya T, Moribata K, Muraki Y, Shingaki N, Niwa T, Deguchi H, Ueda K, Inoue I, Iguchi M, Tamai H, Ichinose M. Usefulness of continuous suction mouthpiece during esophagogastroduodenoscopy: A single-center, prospective, randomized study. *World J Gastrointest Endosc* 2013; **5**: 508-513 [PMID: 24147195 DOI: 10.4253/wjge.v5.i10.508]
25 **Safránek J**, Geiger J, Klecka J, Skalický T, Spidlen V, Veselý V, Vodicka J. [Mediastinitis after esophageal perforation]. *Rozhl Chir* 2013; **92**: 195-200 [PMID: 23965005]
26 **Koo JS,** Choi JH. Conscious Sedation During Gastrointestinal Endoscopy: Midazolam vs Propofol. *Korean J Gastrointest Endosc* 2011; **42**: 67-73
27 **Kusano M**, Hosaka H, Moki H, Shimoyama Y, Kawamura O, Kuribayashi S, Mori M, Akuzawa M. Cascade stomach is associated with upper gastrointestinal symptoms: a population-based study. *Neurogastroenterol Motil* 2012; **24**: 451-455, e214 [PMID: 22288935 DOI: 10.1111/j.1365-2982.2012.01876.x]
28 **Cammarota G**, Cesaro P, Cazzato A, Cianci R, Fedeli P, Ojetti V, Certo M, Sparano L, Giovannini S, Larocca LM, Vecchio FM, Gasbarrini G. The water immersion technique is easy to learn for routine use during EGD for duodenal villous evaluation: a single-center 2-year experience. *J Clin Gastroenterol* 2009; **43**: 244-248 [PMID: 18813029 DOI: 10.1097/MCG.0b013e318159c654]
29 **Cammarota G**, Pirozzi GA, Martino A, Zuccalà G, Cianci R, Cuoco L, Ojetti V, Landriscina M, Montalto M, Vecchio FM, Gasbarrini G, Gasbarrini A. Reliability of the "immersion technique" during routine upper endoscopy for detection of abnormalities of duodenal villi in patients with dyspepsia. *Gastrointest Endosc* 2004; **60**: 223-228 [PMID: 15278049]
30 **Singer HC**, Reichbach EJ, Fagin RR, Kobayashi S. Retroversion as a routine gastroscopic maneuver. *Gastrointest Endosc* 1971; **17**: 112-114 passim [PMID: 5546137]
31 **Parkin DM**, Bray F, Ferlay J, Pisani P. Global cancer statistics, 2002. *CA Cancer J Clin* 2005; **55**: 74-108 [PMID: 15761078]
32 **Ellis L**, Woods LM, Estève J, Eloranta S, Coleman MP, Rachet B. Cancer incidence, survival and mortality: explaining the concepts. *Int J Cancer* 2014; **135**: 1774-1782 [PMID: 24945976 DOI: 10.1002/ijc.28990]
33 **Shin A**, Kim J, Park S. Gastric cancer epidemiology in Korea. *J Gastric Cancer* 2011; **11**: 135-140 [PMID: 22076217 DOI: 10.5230/jgc.2011.11.3.135]
34 **Fock KM**. Review article: the epidemiology and prevention of gastric cancer. *Aliment Pharmacol Ther* 2014; **40**: 250-260 [PMID: 24912650 DOI: 10.1111/apt.12814]
35 **Lapalus MG**, Dumortier J, Fumex F, Roman S, Lot M, Prost B, Mion F, Ponchon T. Esophageal capsule endoscopy versus esophagogastroduodenoscopy for evaluating portal hypertension: a prospective comparative study of performance and tolerance. *Endoscopy* 2006; **38**: 36-41 [PMID: 16429353 DOI: 10.1055/s-2006-924975]
36 **Choi KS**, Jun JK, Park EC, Park S, Jung KW, Han MA, Choi IJ, Lee HY. Performance of different gastric cancer screening methods in Korea: a population-based study. *PLoS One* 2012; **7**: e50041 [PMID: 23209638 DOI: 10.1371/journal.pone.0050041]
37 **Cho E**, Kang MH, Choi KS, Suh M, Jun JK, Park EC. Cost-effectiveness outcomes of the national gastric cancer screening program in South Korea. *Asian Pac J Cancer Prev* 2013; **14**: 2533-2540 [PMID: 23725170]
38 **Kim N**. Screening and Diagnosis of Early Gastric Cancer.

J Korean Med Assoc 2010; **53**: 290-298 [DOI: 10.5124/jkma.2010.53.4.290]
39 **Ponich T**, Enns R, Romagnuolo J, Springer J, Armstrong D, Barkun AN. Canadian credentialing guidelines for esophagogastroduodenoscopy. *Can J Gastroenterol* 2008; **22**: 349-354 [PMID: 18414707]

P- Reviewer: Homan M, Tan HJ
S- Editor: Ma YJ **L- Editor**: A **E- Editor**: Liu XM

World Journal of Gastroenterology

Submit a Manuscript: http://www.wjgnet.com/esps/
Help Desk: http://www.wjgnet.com/esps/helpdesk.aspx
DOI: 10.3748/wjg.v21.i3.786

World J Gastroenterol 2015 January 21; 21(3): 786-793
ISSN 1007-9327 (print) ISSN 2219-2840 (online)

REVIEW

Role of E3 ubiquitin ligases in gastric cancer

Ya-Chao Hou, Jing-Yu Deng

Ya-Chao Hou, Jing-Yu Deng, Department of Gastroenterology, Cancer Hospital of Tianjin Medical University, City Key Laboratory of Tianjin Cancer Center, and National Clinical Research Center of Cancer, Tianjin 300060, China
Author contributions: Hou YC and Deng JY contributed equally to this work; Hou YC wrote the paper; and Deng JY designed the research.

Correspondence to: Jing-Yu Deng, MD, PhD, Department of Gastroenterology, Cancer Hospital of Tianjin Medical University, City Key Laboratory of Tianjin Cancer Center, and National Clinical Research Center of Cancer, Huanhuxi Road, Hexi District, Tianjin 300060, China. dengery@126.com
Telephone: +86-22-23340123
Fax: +86-22-23359904
Received: September 1, 2014
Peer-review started: September 7, 2014
First decision: October 14, 2014
Revised: November 1, 2014
Accepted: December 1, 2014
Article in press: December 1, 2014
Published online: January 21, 2015

Abstract

E3 ubiquitin ligases have an important role in carcinogenesis and include a large family of proteins that catalyze the ubiquitination of many protein substrates for targeted degradation by the 26S proteasome. So far, E3 ubiquitin ligases have been reported to have a role in a variety of biological processes including cell cycle regulation, cell proliferation, and apoptosis. Recently, several kinds of E3 ubiquitin ligases were demonstrated to be generally highly expressed in gastric cancer (GC) tissues and to contribute to carcinogenesis. In this review, we summarize the current knowledge and information about the clinical significance of E3 ubiquitin ligases in GC. Bortezomib, a proteasome inhibitor, encouraged the evaluation of other components of the ubiquitin proteasome system for pharmaceutical intervention. The clinical value of novel treatment strategies targeting aberrant E3 ubiquitin ligases for GC are discussed in the review.

Key words: E3 ubiquitin ligases; Gastric cancer; Oncogene; Tumor suppressor gene; Target therapy

Core tip: E3 biquitin ligases are a large family of proteins that catalyze the ubiquitination of many protein substrates for targeted degradation by the 26S proteasome. They play an essential role in a variety of biological processes, including cell cycle regulation, proliferation and apoptosis. They are often found overexpressed in gastric cancer (GC) and their deregulation has been shown to contribute to GC development. The mechanisms of E3 ubiquitin ligases in the regulation of biological functions and their exact roles in carcinogenesis can help to develop specific E3 ubiquitin ligase inhibitors to improve the treatment strategies for GC patients.

Hou YC, Deng JY. Role of E3 ubiquitin ligases in gastric cancer. *World J Gastroenterol* 2015; 21(3): 786-793 Available from: URL: http://www.wjgnet.com/1007-9327/full/v21/i3/786.htm DOI: http://dx.doi.org/10.3748/wjg.v21.i3.786

INTRODUCTION

Gastric cancer (GC) is one of the most common malignancies worldwide, as well as one of the leading causes of cancer-related death[1]. More than half of these cases occur in Eastern Asia. It is well known that GC is highly invasive and metastatic, which is the main

factor contributing to the high mortality rate of GC patients[2-4]. Although there are many studies of novel diagnostic and therapeutic interventions, the prognosis of patients with advanced GC remains poor[5]. It is well known that GC is a multifactorial and multistep disease which involves activation of oncogenes and inactivation of tumor suppressor genes during GC progression[6]. Genetic and epigenetic alterations, occurring in genes and molecules, occur in proliferation, invasion and metastasis of GC and influence its prognosis[7-10]. An understanding of these alterations may be critical for improvements in the diagnosis, treatment or prediction of prognosis of GC.

The ubiquitin-proteasome system (UPS) plays a key role in the regulation of many cellular pathways by controlling the abundance, activity and localization of an enormous variety of cellular proteins[11-14]. The UPS targets a variety of proteins, including those that are misfolded, mutated, or otherwise damaged - the cellular version of quality control[15]. The attachment of ubiquitin to target proteins is mediated by three enzymes: E1, E2, E3. E1 involved in the ubiquitination process. E1 is the ubiquitin-activating enzyme recruiting ubiquitin. E2 is the ubiquitin-conjugating enzyme that transfers the ubiquitin to the targeted protein. E3 is the ubiquitin ligase acting as a scaffold protein that interacts with the E2 enzyme and transfers ubiquitin to the target protein[16,17]. This process is reversible through the action of deubiquitinases (DUBs) that remove ubiquitin chains linked to the target protein[18]. DUBs are also involved in ubiquitin processing and recycling[19]. In this process, E3 ubiquitin ligases perform a critical role through the selective binding of protein substrates. This review will focus on the role of E3 ubiquitin ligases in GC and their potential as a novel anticancer target.

E3 UBIQUITIN LIGASES

More than 600 E3 ubiquitin ligases are expressed in the human genome, allowing for the specificity of the ubiquitination system[20]. E3 enzymes are divided into subclasses based on their biochemical and structural features: HECT (homologous to E6-AP carboxy terminus), *RING* (a very interesting new gene) fingers, and U-box domains[21]. There are about 30 proteins containing the HECT domain. The *RING* fingers and U-box quitin ligases contain the new gene (*RING*) finger domain[22]. There are over 700 proteins containing the *RING* finger domain, but only a small part functions as an E3 ubiquitin ligase. Unlike RING proteins, most HECT proteins, if not all, are believed to function as E3 ubiquitin ligases. RING and HECT E3 ubiquitin ligases use different catalytic mechanisms to promote the transfer of ubiquitin to targeted substrates. RING E3 ubiquitin ligases can promote the direct transfer of ubiquitin from E2 to the targeted substrate, whereas HECT E3 ubiquitin ligases interact with the cognate E2, followed by the formation of a thiolester linkage with ubiquitin and subsequent transfer of ubiquitin to the targeted substrate[23]. Many E3 ubiquitin ligases could be oncogenes or tumor suppressor genes because frequent deregulation of E3 ubiquitin ligases has been shown in gastric carcinogenesis. The function of E3 ubiquitin ligases in GC are discussed in detail below.

E3 UBIQUITIN LIGASES AS ONCOGENES IN GASTRIC CANCER

Some E3 ubiquitin ligases, such as MDM2 and MKRN1, have established roles in the cell cycle and apoptosis. Other E3 ubiquitin ligases, such as Cbl/Cbl-b/c-Cbl, Cullin1, and Hakai, may be similarly important in gastric carcinogenesis. These E3 ubiquitin ligases are overexpressed in GC, and their inhibition leads to cells growth arrest or apoptosis. The oncogenic E3 ubiquitin ligases in GC are discussed in detail below.

Murine double minute 2

The murine double minute 2 (*MDM2*) gene encodes an important negative regulating protein which promotes ubiquitin-dependent proteasomal degradation of P53 by functioning as an E3 ubiquitin ligase[24,25]. SNP309, a T to G change at the 309th nucleotide in the first intron of the *MDM2* gene, has been characterized and shown to increase the affinity of the transcriptional activator Sp1, resulting in higher levels of MDM2 RNA and protein and subsequent attenuation of the p53 pathway. Numerous studies have shown that MDM2 SNP309 is associated with increased risk and poor prognosis of GC[26-31]. Although MDM2 was characterized as a RING finger E3 for the tumor suppressor p53[32], its interaction with Nbs1 inhibited DNA break repair, leading to chromosome instability and subsequent transformation that was independent of p53[25,33]. MDM2 is expressed at higher levels in GC tissues than in non-cancerous gastric mucosa. In addition, MDM2 expression is associated with clinicopathologic features in patients treated only with surgery[34]. Moreover, MDM2 is a potential predictive factor for benefit from adjuvant chemotherapy with fluorouracil-leucovorin-oxaliplatin in patients with resectable GC[34].

Cullin1

Cullin1 is a scaffold protein of the ubiquitin E3 ligase Skp1/Cullin1/Rbx1/F-box protein complex, which ubiquitinates a broad range of proteins involved in cell-cycle progression, signal transduction, and transcription. Cullin1 is involved in the progression of several cancers[35-37], including GC. The high expression of Cullin1 was significantly correlated with poorer overall survival and lymph node metastasis of GC[7]. On the other hand, Korzeniewski demonstrated that Cullin1 may act as a tumor suppressor by regulating PLK4 protein levels[38].

Cbl/Cbl-b/c-Cbl

The Casitas B-lineage lymphoma (Cbl) family of

ubiquitin ligases were identified as negative regulators of non-receptor tyrosine kinases or activated signaling pathways[39]. Some studies showed Cbl in conjunction with epidermal growth factor receptor (EGFR) system might be associated with gastric carcinogenesis, invasion and metastasis[40,41]. Other authors showed that cCbl, Cblb, and EGFR are highly expressed in GC tissue and their expression levels are related to the invasion and development of GC. Both cCb l and Cblb were positively correlated with EGFR, suggesting that they may interact in the proliferation, infiltration, and metastasis of GC[42]. So Cbl, cCbl, Cblb might be deemed novel molecular markers for aggressive GC. However, another study found that the Cbl-b repressed insulin-like growth factor-1(IGF-1)-induced epithelial to mesenchymal transition, likely through targeting the IGF-1 receptor, resulting in degradation and further inhibition of the Akt/ERK-miR-200c-ZEB2 axis in GC cells and a decrease in the risk of developing lymph node metastasis in patients with GC[43]. Some studies demonstrated an important role of Cbl-b in reversing Pgp-mediated GC multi-drug resistance through suppression of the PI3K/Akt signaling pathway and down-regulation of P-gp expression[44].

Hakai

Hakai was originally identified as an E3 ubiquitin-ligase for the E-cadherin complex[45]. Hakai contains Src homology (SH)2, RING-finger, and proline-rich domains, and it is structurally and functionally related to c-Cbl, a RING-finger type E3 ubiquitin ligase for receptor tyrosine kinases[46,47]. High expression of Hakai induced weakness of cell-cell adhesions and enhanced cell proliferation[48]. Overexpression of Hakai in GC and colon adenocarcinomas was reported to occur in the early stages of carcinogenesis and up-regulated cell proliferation[48,49]. Therefore, Hakai may be a valuable new biomarker or drug target for GC treatment.

Makorin ring finger protein 1

Makorin ring finger protein 1 (MKRN1) was reported to be a transcriptional co-regulator and an E3 ligase for hTERT[50]. MKRN1 simultaneously induced p53 and p21 ubiquitination and proteasome-dependent degradation. This suggested that the presence of MKRN1 in cancer cells may affect p53- and p21-dependent apoptosis and cell growth. MKRN1 remains unique in its ability to negatively regulate the major tumor suppressors including p14ARF and p53[51]. MKRN1 may induce gastric carcinogenesis by regulating the p14ARF-associated pathways, and thus potentially represent an important therapeutic target in GC[52].

E3 UBIQUITIN LIGASES AS TUMOR SUPPRESSOR GENES INS GASTRIC CANCER

Numerous E3 ubiquitin ligases, including FBXW7 and CHIP, have been shown to be tumor suppressors in GC. Frequent inactivating mutations or downregulated expression of these E3 ubiquitin ligases have been detected in GC. Several discovered E3 ubiquitin ligases, such as CHFR, ZNRF3, and RNF180, may play an important role in regulating gastric carcinogenesis. Besides mutation and gene copy loss, epigenetic alteration (*i.e.*, promoter methylation) also contributed to inactivation of these tumor suppressors. E3 ubiquitin ligases with tumor suppressor activity in GC are discussed in detail below.

FBXW7/CDC4

The *FBXW7/CDC4* gene, which maps to 4q32, encodes a ubiquitin ligase and has been implicated as a tumor suppressor gene in many tumor types, including GC. *FBXW7/CDC4* targets several oncoproteins, including cyclin-E, c-myc, c-jun, Notch 1 and Notch 4, for degradation. and its tumor suppressor function was thought to be exerted through these substrates[53]. Loss of *FBXW7/CDC4* was seen in both early-onset GC and advanced GC[54]. *FBXW7* inactivation contributed to poor prognosis *via* genome instability and cell cycle progression. Recent studies suggested that GC patients with inactivation of *FBXW7* had aggressive cancer and a poor prognosis[55,56]. Loss of *FBXW7* expression could lead to MYC overexpression, and was associated with poor prognosis in GC patients[56]. In the future, *FBXW7/CDC4* may be a potential diagnostic biomarker and therapeutic target for GC.

Ring finger protein 180

Ring finger protein 180 (RNF180), a novel member of the RING finger protein family and function as an E3 ubiquitin ligase, is well conserved among vertebrates[57]. High expression of RNF180 suppressed cell growth and induced apoptosis, which were mediated by upregulating the antiproliferation regulators MTSS1 and CDKN2A and the proapoptotic mediator TIMP3[58]. Promoter methylation of RNF180 was detected in 76% of primary GC and 55% of intestinal metaplasia, but was not detected in any of the normal gastric tissues, suggesting methylation of this gene was a common and early event in gastric carcinogenesis. Promoter methylation of RNF180 DNA was more frequently detected in the GC tissue samples, which led to low or loss of RNF180 expression in GC patients with poor overall survival[58]. Our study showed that methylation of CpG sites(-116, -80, +97, and +102) in the RNF180 DNA promoter predicted poor prognosis of GC[10].

CHIP

CHIP (carboxy terminus of Hsc70 interacting protein) was reported to be an E3 ubiquitin ligase that could induce ubiquitination and degradation of several tumor-related proteins, and acted as a suppressor of tumor metastasis. CHIP inactivation was significantly correlated with GC progression, lymph node metastasis, TNM

stage, and tumor differentiation. Therefore, CHIP inactivation was an independent prognostic marker of poor survival in GC patients as well as added significant prognostic value to the well known clinical prognostic factors[8,59]. Moreover, CHIP suppresses GC angiogenesis by inhibiting nuclear factor (NF)-κB activity through ubiquitin-proteasome-dependent degradation of the NF-κBep65 and downregulation of the proangiogenic cytokine interleukin-8[8]. Therefore, CHIP may be as a potential diagnostic biomarker and therapeutic target for GC.

CHFR

The *CHFR* gene encodes a RING finger domain containing E3, as a tumor suppressor gene, which was shown to play an important role in mitosis through targeting key mitotic proteins Aurora A and Plk for ubiquitin-mediated proteolysis[60,61]. Loss of *CHFR* mRNA expression was a consequence of promoter methylation, suggesting that it played a tumor suppressor role in gastric carcinogenesis[62,63]. *CHFR* promoter methylation status may be of value in predicting malignant behavior or as a molecular diagnostic marker for GC[64-66]. Moreover, *CHFR* promoter methylation was a sensitive marker for the effect of docetaxel in GC patients[67].

COP1

COP1 (constitutive photomorphogenic 1, also known as RFWD2) is a p53-targeting E3 ubiquitin ligase, containing RING-finger, WD40-repeat domains, and coiled-coil[68-70]. Whether the *COP1* gene is an oncogene or a tumor suppressor gene remains controversial. Some studies showed that *COP1* acted as a tumor suppressor[71-73]. However, other studies indicated that *COP1* acted as an oncogene[74]. One study showed that loss of *COP1* expression determined poor prognosis in patients with GC[9]. However, another study showed that *COP1* overexpression was associated with poor prognosis in primary GC[75]. Therefore, *COP1* may be worth further investigation to determine the fundamental biology of GC.

ZNRF3

ZNRF3, a unique transmembrane E3 ubiquitin ligase, suppresses the β-catenin signaling initiated by endogenous Wnt proteins[76]. ZNRF3 was reported as a negative regulator of the Wnt pathway that inhibited cancer cell growth and promoted cell apoptosis. ZNRF3 inhibited GC cell growth and promoted the cell apoptosis by limiting the Wnt/beta-catenin/TCF signaling pathway[77]. In the future, a novel therapeutic strategy based on ZNRF3 may be of value in patients with GC.

TARGETING E3 UBIQUITIN LIGASES FOR GC THERAPY

The success of bortezomib, a selective proteasome inhibitor, for treating refractory myeloma and mantle cell lymphoma, showed that modulation of UPS may represent a novel strategy for GC. However, in a nonrandomized Phase Ⅱ clinical trial conducted in 16 patients with advanced GC, bortezomib, at a dose of 1.3 mg/m^2 *i.v.* twice weekly for 2 wk (days 1, 4, 8 and 11) every 21 d, did not show any clinical activity (no patient responded and only one patient achieved stable disease as the best response)[78]. In addition, 14 out of 16 patients experienced grade 2 or greater toxicity. Similar outcomes were obtained in another clinical trial[79]. These studies showed that proteasome inhibition in GC should include combination therapy with targeted agents focusing on nonoverlapping oncogenic pathways.

By selectively inhibiting an E3 ubiquitin ligase, the proteins that are regulated by this E3 ubiquitin ligase can be stabilized, thereby avoiding any unwanted effects on other cellular proteins. Targeting of the E3 ubiquitin ligase has gained increasing attention, and has led to the development of high-throughput screening assays to identify inhibitors of multiple E3 ubiquitin ligases[80]. Nutlin-3 has potent antitumor activity against human GC cells with wt p53 and has shown promise as a single agent and in combination with conventional anticancer drugs[81]. Small molecule compounds, such as Nutlin-3a, RITA, and MI-219, have been identified as potent MDM2 inhibitors[82-85]. These small molecule compounds disrupted MDM2-mediated p53 degradation and thus led to tumor regression by inducing p53-mediated cell cycle arrest and cell death[82-85]. Therefore, using analogs of MDM2, or using agonists of Mdm2 with other therapeutic modalities may be of use as neoadjuvant therapy for GC within a few years.

Recognition of molecules that could promote the activity of FBXW7 and subsequently enhance the degradation of its oncogenic substrates could also be a very good anticancer treatment strategy. It has been shown that a natural dietary agent genistein inhibited miR-223 expression and subsequently up-regulated FBXW7, leading to cell growth inhibition and apoptosis in pancreatic cancer cells[86]. Another study indicated that rapamycin suppressed FBXW7 loss-induced epithelial-mesenchymal transition and cancer stem cell-like characteristics in colorectal cancer cells[87]. However, there are no inhibitors targeting FBXW7 that is currently being tested in preclinical and clinical trials in GC. In the future, targeting FBXW7 may be useful in patients with GC.

SCF ligases, also known as CRL (Cullin-RING ubiquitin Ligases), are the largest family of ubiquitin ligases, and promote the degradation of about 20% of UPS-regulated proteins[88,89], including cell cycle regulatory proteins, transcription factors, oncoproteins and tumor suppressors among others[90,91]. Post-translational neddylation of CUL, a process triggered by the NEDD8-activating enzyme E1 subunit 1 (NAE1), is required for CRL/SCF activation. Recently, MLN4924 was discovered *via* a high-throughput screen as a specific NAE1 inhibitor and first-in-class anticancer drug[92,93]. The efficacy and

mechanism of action of MLN4924 has been tested *in vitro* and in mouse models and has shown promising anticancer activity in a wide-range of malignancies[94-99], though these did not include GC. MLN4924 is currently in multiple phase I clinical trials for both solid tumors and hematological malignancies[88]. We believe that MLN4924 may be used in patients with GC in the near future.

CONCLUSION

The E3 ubiquitin ligases play an essential role in a variety of biological processes including cell cycle regulation, cell proliferation, and apoptosis. Although further research is necessary to better understand the biological functions of E3 ubiquitin ligases, it has become clear that some E3 ubiquitin ligases, such as those described in this review, are promising targets for GC therapy. Perhaps the greatest challenge for scientists trying to manipulate the E3 ubiquitin ligases in GC cells will be to delineate the role of targeted proteins as tumor suppressors or oncogenes. The effect of such proteins can be influenced by many factors, some of which are still unknown. There remain other obstacles to overcome before targeting E3 ubiquitin ligases as a viable treatment option. The main obstacle is selectivity, and any new therapies must target only cancer cells and not healthy ones. While targeting of E3 ubiquitin ligases in GC therapy is still at an early stage, continued research on the E3 ubiquitin ligases should lead to the discovery of new therapeutic targets that may boost the development of more specific, less toxic, and more efficacious anti-cancer therapeutics.

REFERENCES

1 **Jemal A**, Bray F, Center MM, Ferlay J, Ward E, Forman D. Global cancer statistics. *CA Cancer J Clin* 2011; **61**: 69-90 [PMID: 21296855 DOI: 10.3322/caac.20107]

2 **Steeg PS**. Tumor metastasis: mechanistic insights and clinical challenges. *Nat Med* 2006; **12**: 895-904 [PMID: 16892035 DOI: 10.1038/nm1469]

3 **Huo ZB**, Chen SP, Li H, Wu DC. Defining a subgroup treatable for laparoscopic surgery in poorly differentiated early gastric cancer: the role of lymph node metastasis. *Cancer Biol Med* 2012; **9**: 54-56 [PMID: 23691456 DOI: 10.3969/j.issn.2095-3941]

4 **López-Basave HN**, Morales-Vásquez F, Ruiz-Molina JM, Namendys-Silva SA, Vela-Sarmiento I, Ruan JM, Rosciano AE, Calderillo-Ruiz G, Díaz-Romero C, Herrera-Gómez A, Meneses-García AA. Gastric cancer in young people under 30 years of age: worse prognosis, or delay in diagnosis? *Cancer Manag Res* 2013; **5**: 31-36 [PMID: 23580357 DOI: 10.2147/CMAR.S40377]

5 **Zheng L**, Wang L, Ajani J, Xie K. Molecular basis of gastric cancer development and progression. *Gastric Cancer* 2004; **7**: 61-77 [PMID: 15224192 DOI: 10.1007/s10120-004-0277-4]

6 **Chen CN**, Lin JJ, Chen JJ, Lee PH, Yang CY, Kuo ML, Chang KJ, Hsieh FJ. Gene expression profile predicts patient survival of gastric cancer after surgical resection. *J Clin Oncol* 2005; **23**: 7286-7295 [PMID: 16145069 DOI: 10.1200/JCO.2004.00.2253]

7 **Bai J**, Zhou Y, Chen G, Zeng J, Ding J, Tan Y, Zhou J, Li G. Overexpression of Cullin1 is associated with poor prognosis of patients with gastric cancer. *Hum Pathol* 2011; **42**: 375-383 [PMID: 21190721 DOI: 10.1016/j.humpath.2010.09.003]

8 **Wang S**, Wu X, Zhang J, Chen Y, Xu J, Xia X, He S, Qiang F, Li A, Shu Y, Røe OD, Li G, Zhou JW. CHIP functions as a novel suppressor of tumour angiogenesis with prognostic significance in human gastric cancer. *Gut* 2013; **62**: 496-508 [PMID: 22535373 DOI: 10.1136/gutjnl-2011-301522]

9 **Sawada G**, Ueo H, Matsumura T, Uchi R, Ishibashi M, Mima K, Kurashige J, Takahashi Y, Akiyoshi S, Sudo T, Sugimachi K, Doki Y, Mori M, Mimori K. Loss of COP1 expression determines poor prognosisin patients with gastric cancer. *Oncol Rep* 2013; **30**: 1971-1975 [PMID: 23933908 DOI: 10.3892/or.2013.2664]

10 **Deng J**, Liang H, Ying G, Zhang R, Wang B, Yu J, Fan D, Hao X. Methylation of CpG sites in RNF180 DNA promoter prediction poor survival of gastric cancer. *Oncotarget* 2014; **5**: 3173-3183 [PMID: 24833402]

11 **Reinstein E**, Ciechanover A. Narrative review: protein degradation and human diseases: the ubiquitin connection. *Ann Intern Med* 2006; **145**: 676-684 [PMID: 17088581 DOI: 10.7326/0003-4819-145-9-200611070-00010]

12 **Varshavsky A**. The ubiquitin system, an immense realm. *Annu Rev Biochem* 2012; **81**: 167-176 [PMID: 22663079 DOI: 10.1146/annurev-biochem-051910-094049]

13 **Eldridge AG**, O'Brien T. Therapeutic strategies within the ubiquitin proteasome system. *Cell Death Differ* 2010; **17**: 4-13 [PMID: 19557013 DOI: 10.1038/cdd.2009.82]

14 **Hoeller D**, Dikic I. Targeting the ubiquitin system in cancer therapy. *Nature* 2009; **458**: 438-444 [PMID: 19325623 DOI: 10.1038/nature07960]

15 **Hershko A**. The ubiquitin system for protein degradation and some of its roles in the control of the cell division cycle. *Cell Death Differ* 2005; **12**: 1191-1197 [PMID: 16094395 DOI: 10.1038/sj.cdd.4401702]

16 **Komander D**. The emerging complexity of protein ubiquitination. *Biochem Soc Trans* 2009; **37**: 937-953 [PMID: 19754430 DOI: 10.1042/BST0370937]

17 **Dikic I**, Wakatsuki S, Walters KJ. Ubiquitin-binding domains - from structures to functions. *Nat Rev Mol Cell Biol* 2009; **10**: 659-671 [PMID: 19773779 DOI: 10.1038/nrm2767]

18 **Komander D**, Clague MJ, Urbé S. Breaking the chains: structure and function of the deubiquitinases. *Nat Rev Mol Cell Biol* 2009; **10**: 550-563 [PMID: 19626045 DOI: 10.1038/nrm2731]

19 **Nijman SM**, Luna-Vargas MP, Velds A, Brummelkamp TR, Dirac AM, Sixma TK, Bernards R. A genomic and functional inventory of deubiquitinating enzymes. *Cell* 2005; **123**: 773-786 [PMID: 16325574 DOI: 10.1016/j.cell.2005.11.007]

20 **Li W**, Bengtson MH, Ulbrich A, Matsuda A, Reddy VA, Orth A, Chanda SK, Batalov S, Joazeiro CA. Genome-wide and functional annotation of human E3 ubiquitin ligases identifies MULAN, a mitochondrial E3 that regulates the organelle's dynamics and signaling. *PLoS One* 2008; **3**: e1487 [PMID: 18213395 DOI: 10.1371/journal.pone.0001487]

21 **Ardley HC**, Robinson PA. E3 ubiquitin ligases. *Essays Biochem* 2005; **41**: 15-30 [PMID: 16250895 DOI: 10.1042/EB0410015]

22 **Hershko A**, Ciechanover A. The ubiquitin system. *Annu Rev Biochem* 1998; **67**: 425-479 [PMID: 9759494 DOI: 10.1146/annurev.biochem.67.1.425]

23 **Berndsen CE**, Wolberger C. New insights into ubiquitin E3 ligase mechanism. *Nat Struct Mol Biol* 2014; **21**: 301-307 [PMID: 24699078 DOI: 10.1038/nsmb.2780]

24 **Oren M**, Damalas A, Gottlieb T, Michael D, Taplick J, Leal JF, Maya R, Moas M, Seger R, Taya Y, Ben-Ze'Ev A. Regulation of p53: intricate loops and delicate balances. *Ann N Y Acad Sci* 2002; **973**: 374-383 [PMID: 12485897 DOI: 10.1016/S0006-2952(02)01149-8]

25 **Bouska A**, Lushnikova T, Plaza S, Eischen CM. Mdm2 promotes genetic instability and transformation independent

of p53. *Mol Cell Biol* 2008; **28**: 4862-4874 [PMID: 18541670 DOI: 10.1128/MCB.01584-07]
26 **Yang M**, Guo Y, Zhang X, Miao X, Tan W, Sun T, Zhao D, Yu D, Liu J, Lin D. Interaction of P53 Arg72Pro and MDM2 T309G polymorphisms and their associations with risk of gastric cardia cancer. *Carcinogenesis* 2007; **28**: 1996-2001 [PMID: 17638920 DOI: 10.1093/carcin/bgm168]
27 **Wang X**, Yang J, Ho B, Yang Y, Huang Z, Zhang Z, Zhang G. Interaction of Helicobacter pylori with genetic variants in the MDM2 promoter, is associated with gastric cancer susceptibility in Chinese patients. *Helicobacter* 2009; **14**: 114-119 [PMID: 19751436 DOI: 10.1111/j.1523-5378]
28 **Pan X**, Li Y, Feng J, Wang X, Hao B, Shi R, Zhang G. A functional polymorphism T309G in MDM2 gene promoter, intensified by Helicobacter pylori lipopolysaccharide, is associated with both an increased susceptibility and poor prognosis of gastric carcinoma in Chinese patients. *BMC Cancer* 2013; **13**: 126 [PMID: 23506213 DOI: 10.1186/1471-2407-13-126]
29 **Tian X**, Tian Y, Ma P, Sui CG, Meng FD, Li Y, Fu LY, Jiang T, Wang Y, Ji FJ, Fang XD, Jiang YH. Association between MDM2 SNP309 T& gt; G and risk of gastric cancer: a meta-analysis. *Asian Pac J Cancer Prev* 2013; **14**: 1925-1929 [PMID: 23679294 DOI: 10.7314/APJCP.2013.14.3.1925]
30 **Chen B**, Cao L, Hu KW, Zhang JW, Meng XL, Xiong MM. MDM2 SNP309 is an ethnicity-dependent risk factor for digestive tract cancers. *Tumour Biol* 2014; **35**: 3431-3438 [PMID: 24338709 DOI: 10.1007/s13277-013-1453-0]
31 **Chen W**, Wu Q, Ren H. Meta-analysis of associations between MDM2 SNP309 polymorphism and gastric cancer risk. *Biomed Rep* 2014; **2**: 105-111 [PMID: 24649079 DOI: 10.3892/br.2013.181]
32 **Haupt Y**, Maya R, Kazaz A, Oren M. Mdm2 promotes the rapid degradation of p53. *Nature* 1997; **387**: 296-299 [PMID: 9153395 DOI: 10.1038/387296a0]
33 **Piette J**, Neel H, Maréchal V. Mdm2: keeping p53 under control. *Oncogene* 1997; **15**: 1001-1010 [PMID: 9285554 DOI: 10.1038/sj.onc.1201432]
34 **Ye Y**, Li X, Yang J, Miao S, Wang S, Chen Y, Xia X, Wu X, Zhang J, Zhou Y, He S, Tan Y, Qiang F, Li G, Røe OD, Zhou J. MDM2 is a useful prognostic biomarker for resectable gastric cancer. *Cancer Sci* 2013; **104**: 590-598 [PMID: 23347235 DOI: 10.1111/cas.12111]
35 **Bai J**, Yong HM, Chen FF, Mei PJ, Liu H, Li C, Pan ZQ, Wu YP, Zheng JN. Cullin1 is a novel marker of poor prognosis and a potential therapeutic target in human breast cancer. *Ann Oncol* 2013; **24**: 2016-2022 [PMID: 23592700 DOI: 10.1093/annonc/mdt147]
36 **Xu M**, Yang X, Zhao J, Zhang J, Zhang S, Huang H, Liu Y, Liu J. High expression of Cullin1 indicates poor prognosis for NSCLC patients. *Pathol Res Pract* 2014; **210**: 397-401 [PMID: 24767980 DOI: 10.1016/j.prp.2014.01.015]
37 **Chen G**, Li G. Increased Cul1 expression promotes melanoma cell proliferation through regulating p27 expression. *Int J Oncol* 2010; **37**: 1339-1344 [PMID: 20878082]
38 **Korzeniewski N**, Zheng L, Cuevas R, Parry J, Chatterjee P, Anderton B, Duensing A, Münger K, Duensing S. Cullin 1 functions as a centrosomal suppressor of centriole multiplication by regulating polo-like kinase 4 protein levels. *Cancer Res* 2009; **69**: 6668-6675 [PMID: 19679553 DOI: 10.1158/0008-5472]
39 **Mohapatra B**, Ahmad G, Nadeau S, Zutshi N, An W, Scheffe S, Dong L, Feng D, Goetz B, Arya P, Bailey TA, Palermo N, Borgstahl GE, Natarajan A, Raja SM, Naramura M, Band V, Band H. Protein tyrosine kinase regulation by ubiquitination: critical roles of Cbl-family ubiquitin ligases. *Biochim Biophys Acta* 2013; **1833**: 122-139 [PMID: 23085373 DOI: 10.1016/j.bbamcr]
40 **Ito R**, Nakayama H, Yoshida K, Matsumura S, Oda N, Yasui W. Expression of Cbl linking with the epidermal growth factor receptor system is associated with tumor progression and poor prognosis of human gastric carcinoma. *Virchows Arch* 2004; **444**: 324-331 [PMID: 14991403 DOI: 10.1007/s00428-004-0982-8]
41 **Lai AZ**, Durrant M, Zuo D, Ratcliffe CD, Park M. Met kinase-dependent loss of the E3 ligase Cbl in gastric cancer. *J Biol Chem* 2012; **287**: 8048-8059 [PMID: 22262855 DOI: 10.1074/jbc.M112.339820]
42 **Dong Q**, Liu YP, Qu XJ, Hou KZ, Li LL. [Expression of c-Cbl, Cbl-b, and epidermal growth factor receptor in gastric carcinoma and their clinical significance]. *Chin J Cancer* 2010; **29**: 59-64 [PMID: 20038312 DOI: 10.5732/cjc.009.10342]
43 **Li H**, Xu L, Li C, Zhao L, Ma Y, Zheng H, Li Z, Zhang Y, Wang R, Liu Y, Qu X. Ubiquitin ligase Cbl-b represses IGF-I-induced epithelial mesenchymal transition via ZEB2 and microRNA-200c regulation in gastric cancer cells. *Mol Cancer* 2014; **13**: 136 [PMID: 24885194 DOI: 10.1186/1476-4598-13-136]
44 **Zhang Y**, Qu X, Hu X, Yang X, Hou K, Teng Y, Zhang J, Sada K, Liu Y. Reversal of P-glycoprotein-mediated multidrug resistance by the E3 ubiquitin ligase Cbl-b in human gastric adenocarcinoma cells. *J Pathol* 2009; **218**: 248-255 [PMID: 19274672 DOI: 10.1002/path.2533]
45 **Mukherjee M**, Chow SY, Yusoff P, Seetharaman J, Ng C, Sinniah S, Koh XW, Asgar NF, Li D, Yim D, Jackson RA, Yew J, Qian J, Iyu A, Lim YP, Zhou X, Sze SK, Guy GR, Sivaraman J. Structure of a novel phosphotyrosine-binding domain in Hakai that targets E-cadherin. *EMBO J* 2012; **31**: 1308-1319 [PMID: 22252131 DOI: 10.1038/emboj.2011.496]
46 **Joazeiro CA**, Wing SS, Huang H, Leverson JD, Hunter T, Liu YC. The tyrosine kinase negative regulator c-Cbl as a RING-type, E2-dependent ubiquitin-protein ligase. *Science* 1999; **286**: 309-312 [PMID: 10514377 DOI: 10.1126/science.286.5438.309]
47 **Levkowitz G**, Waterman H, Ettenberg SA, Katz M, Tsygankov AY, Alroy I, Lavi S, Iwai K, Reiss Y, Ciechanover A, Lipkowitz S, Yarden Y. Ubiquitin ligase activity and tyrosine phosphorylation underlie suppression of growth factor signaling by c-Cbl/Sli-1. *Mol Cell* 1999; **4**: 1029-1040 [PMID: 10635327 DOI: 10.1016/S1097-2765(00)80231-2]
48 **Figueroa A**, Kotani H, Toda Y, Mazan-Mamczarz K, Mueller EC, Otto A, Disch L, Norman M, Ramdasi RM, Keshtgar M, Gorospe M, Fujita Y. Novel roles of hakai in cell proliferation and oncogenesis. *Mol Biol Cell* 2009; **20**: 3533-3542 [PMID: 19535458 DOI: 10.1091/mbc.E08-08-0845]
49 **Abella V**, Valladares M, Rodriguez T, Haz M, Blanco M, Tarrío N, Iglesias P, Aparicio LA, Figueroa A. miR-203 regulates cell proliferation through its influence on Hakai expression. *PLoS One* 2012; **7**: e52568 [PMID: 23285092 DOI: 10.1371/journal.pone.0052568]
50 **Kim JH**, Park SM, Kang MR, Oh SY, Lee TH, Muller MT, Chung IK. Ubiquitin ligase MKRN1 modulates telomere length homeostasis through a proteolysis of hTERT. *Genes Dev* 2005; **19**: 776-781 [PMID: 15805468 DOI: 10.1101/gad.1289405]
51 **Lee EW**, Lee MS, Camus S, Ghim J, Yang MR, Oh W, Ha NC, Lane DP, Song J. Differential regulation of p53 and p21 by MKRN1 E3 ligase controls cell cycle arrest and apoptosis. *EMBO J* 2009; **28**: 2100-2113 [PMID: 19536131 DOI: 10.1038/emboj.2009.164]
52 **Ko A**, Shin JY, Seo J, Lee KD, Lee EW, Lee MS, Lee HW, Choi IJ, Jeong JS, Chun KH, Song J. Acceleration of gastric tumorigenesis through MKRN1-mediated posttranslational regulation of p14ARF. *J Natl Cancer Inst* 2012; **104**: 1660-1672 [PMID: 23104211 DOI: 10.1093/jnci/djs424]
53 **Wang L**, Ye X, Liu Y, Wei W, Wang Z. Aberrant regulation of FBW7 in cancer. *Oncotarget* 2014; **5**: 2000-2015 [PMID: 24899581]
54 **Milne AN**, Leguit R, Corver WE, Morsink FH, Polak M, de Leng WW, Carvalho R, Offerhaus GJ. Loss of CDC4/

FBXW7 in gastric carcinoma. *Cell Oncol* 2010; **32**: 347-359 [PMID: 20448329 DOI: 10.3233/CLO-2010-523]
55 **Yokobori T**, Mimori K, Iwatsuki M, Ishii H, Onoyama I, Fukagawa T, Kuwano H, Nakayama KI, Mori M. p53-Altered FBXW7 expression determines poor prognosis in gastric cancer cases. *Cancer Res* 2009; **69**: 3788-3794 [PMID: 19366810 DOI: 10.1158/0008-5472.CAN-08-2846]
56 **Calcagno DQ**, Freitas VM, Leal MF, de Souza CR, Demachki S, Montenegro R, Assumpção PP, Khayat AS, Smith Mde A, dos Santos AK, Burbano RR. MYC, FBXW7 and TP53 copy number variation and expression in gastric cancer. *BMC Gastroenterol* 2013; **13**: 141 [PMID: 24053468 DOI: 10.1186/1471-230X-13-141]
57 **Ogawa M**, Mizugishi K, Ishiguro A, Koyabu Y, Imai Y, Takahashi R, Mikoshiba K, Aruga J. Rines/RNF180, a novel RING finger gene-encoded product, is a membrane-bound ubiquitin ligase. *Genes Cells* 2008; **13**: 397-409 [PMID: 18363970 DOI: 10.1111/j.1365-2443.2008.01169.x]
58 **Cheung KF**, Lam CN, Wu K, Ng EK, Chong WW, Cheng AS, To KF, Fan D, Sung JJ, Yu J. Characterization of the gene structure, functional significance, and clinical application of RNF180, a novel gene in gastric cancer. *Cancer* 2012; **118**: 947-959 [PMID: 21717426 DOI: 10.1002/cncr.26189]
59 **Gan L**, Liu DB, Lu HF, Long GX, Mei Q, Hu GY, Qiu H, Hu GQ. Decreased expression of the carboxyl terminus of heat shock cognate 70 interacting protein in human gastric cancer and its clinical significance. *Oncol Rep* 2012; **28**: 1392-1398 [PMID: 22895543 DOI: 10.3892/or.2012.1957]
60 **Kang D**, Chen J, Wong J, Fang G. The checkpoint protein Chfr is a ligase that ubiquitinates Plk1 and inhibits Cdc2 at the G2 to M transition. *J Cell Biol* 2002; **156**: 249-259 [PMID: 11807090 DOI: 10.1083/jcb.200108016]
61 **Yu X**, Minter-Dykhouse K, Malureanu L, Zhao WM, Zhang D, Merkle CJ, Ward IM, Saya H, Fang G, van Deursen J, Chen J. Chfr is required for tumor suppression and Aurora A regulation. *Nat Genet* 2005; **37**: 401-406 [PMID: 15793587 DOI: 10.1038/ng1538]
62 **Gao YJ**, Xin Y, Zhang JJ, Zhou J. Mechanism and pathobiologic implications of CHFR promoter methylation in gastric carcinoma. *World J Gastroenterol* 2008; **14**: 5000-5007 [PMID: 18763281 DOI: 10.3748/wjg.14.5000]
63 **Hu SL**, Kong XY, Cheng ZD, Sun YB, Shen G, Xu WP, Wu L, Xu XC, Jiang XD, Huang DB. Promoter methylation of p16, Runx3, DAPK and CHFR genes is frequent in gastric carcinoma. *Tumori* 2010; **96**: 726-733 [PMID: 21302620]
64 **Hu SL**, Huang DB, Sun YB, Wu L, Xu WP, Yin S, Chen J, Jiang XD, Shen G. Pathobiologic implications of methylation and expression status of Runx3 and CHFR genes in gastric cancer. *Med Oncol* 2011; **28**: 447-454 [PMID: 20300977 DOI: 10.1007/s12032-010-9467-6]
65 **Honda T**, Tamura G, Waki T, Kawata S, Nishizuka S, Motoyama T. Promoter hypermethylation of the Chfr gene in neoplastic and non-neoplastic gastric epithelia. *Br J Cancer* 2004; **90**: 2013-2016 [PMID: 15138487 DOI: 10.1038/sj.bjc.6601849]
66 **Morioka Y**, Hibi K, Sakai M, Koike M, Fujiwara M, Kodera Y, Ito K, Nakao A. Aberrant methylation of the CHFR gene in digestive tract cancer. *Anticancer Res* 2006; **26**: 1791-1795 [PMID: 16827108]
67 **Li Y**, Yang Y, Lu Y, Herman JG, Brock MV, Zhao P, Guo M. Predictive value of CHFR and MLH1 methylation in human gastric cancer. *Gastric Cancer* 2014; Epub ahead of print [PMID: 24748501 DOI: 10.1007/s10120-014-0370-2]
68 **Bianchi E**, Denti S, Catena R, Rossetti G, Polo S, Gasparian S, Putignano S, Rogge L, Pardi R. Characterization of human constitutive photomorphogenesis protein 1, a RING finger ubiquitin ligase that interacts with Jun transcription factors and modulates their transcriptional activity. *J Biol Chem* 2003; **278**: 19682-19690 [PMID: 12615916 DOI: 10.1074/jbc.M212681200]
69 **Kato S**, Ding J, Pisck E, Jhala US, Du K. COP1 functions as a FoxO1 ubiquitin E3 ligase to regulate FoxO1-mediated gene expression. *J Biol Chem* 2008; **283**: 35464-35473 [PMID: 18815134 DOI: 10.1074/jbc.M801011200]
70 **Wang L**, He G, Zhang P, Wang X, Jiang M, Yu L. Interplay between MDM2, MDMX, Pirh2 and COP1: the negative regulators of p53. *Mol Biol Rep* 2011; **38**: 229-236 [PMID: 20333547 DOI: 10.1007/s11033-010-0099-x]
71 **Migliorini D**, Bogaerts S, Defever D, Vyas R, Denecker G, Radaelli E, Zwolinska A, Depaepe V, Hochepied T, Skarnes WC, Marine JC. Cop1 constitutively regulates c-Jun protein stability and functions as a tumor suppressor in mice. *J Clin Invest* 2011; **121**: 1329-1343 [PMID: 21403399 DOI: 10.1172/JCI45784]
72 **Vitari AC**, Leong KG, Newton K, Yee C, O'Rourke K, Liu J, Phu L, Vij R, Ferrando R, Couto SS, Mohan S, Pandita A, Hongo JA, Arnott D, Wertz IE, Gao WQ, French DM, Dixit VM. COP1 is a tumour suppressor that causes degradation of ETS transcription factors. *Nature* 2011; **474**: 403-406 [PMID: 21572435 DOI: 10.1038/nature10005]
73 **Shao J**, Teng Y, Padia R, Hong S, Noh H, Xie X, Mumm JS, Dong Z, Ding HF, Cowell J, Kim J, Han J, Huang S. COP1 and GSK3β cooperate to promote c-Jun degradation and inhibit breast cancer cell tumorigenesis. *Neoplasia* 2013; **15**: 1075-1085 [PMID: 24027432]
74 **Dornan D**, Bheddah S, Newton K, Ince W, Frantz GD, Dowd P, Koeppen H, Dixit VM, French DM. COP1, the negative regulator of p53, is overexpressed in breast and ovarian adenocarcinomas. *Cancer Res* 2004; **64**: 7226-7230 [PMID: 15492238 DOI: 10.1158/0008-5472.CAN-04-2601]
75 **Li YF**, Wang DD, Zhao BW, Wang W, Huang CY, Chen YM, Zheng Y, Keshari RP, Xia JC, Zhou ZW. High level of COP1 expression is associated with poor prognosis in primary gastric cancer. *Int J Biol Sci* 2012; **8**: 1168-1177 [PMID: 23091414 DOI: 10.7150/ijbs.4778]
76 **Hao HX**, Xie Y, Zhang Y, Charlat O, Oster E, Avello M, Lei H, Mickanin C, Liu D, Ruffner H, Mao X, Ma Q, Zamponi R, Bouwmeester T, Finan PM, Kirschner MW, Porter JA, Serluca FC, Cong F. ZNRF3 promotes Wnt receptor turnover in an R-spondin-sensitive manner. *Nature* 2012; **485**: 195-200 [PMID: 22575959 DOI: 10.1038/nature11019]
77 **Zhou Y**, Lan J, Wang W, Shi Q, Lan Y, Cheng Z, Guan H. ZNRF3 acts as a tumour suppressor by the Wnt signalling pathway in human gastric adenocarcinoma. *J Mol Histol* 2013; **44**: 555-563 [PMID: 23504200 DOI: 10.1007/s10735-013-9504-9]
78 **Shah MA**, Power DG, Kindler HL, Holen KD, Kemeny MM, Ilson DH, Tang L, Capanu M, Wright JJ, Kelsen DP. A multicenter, phase II study of bortezomib (PS-341) in patients with unresectable or metastatic gastric and gastroesophageal junction adenocarcinoma. *Invest New Drugs* 2011; **29**: 1475-1481 [PMID: 20574790 DOI: 10.1007/s10637-010-9474-7]
79 **Jatoi A**, Dakhil SR, Foster NR, Ma C, Rowland KM, Moore DF, Jaslowski AJ, Thomas SP, Hauge MD, Flynn PJ, Stella PJ, Alberts SR. Bortezomib, paclitaxel, and carboplatin as a first-line regimen for patients with metastatic esophageal, gastric, and gastroesophageal cancer: phase II results from the North Central Cancer Treatment Group (N044B). *J Thorac Oncol* 2008; **3**: 516-520 [PMID: 18449005 DOI: 10.1097/JTO.0b013e31816de276]
80 **Goldenberg SJ**, Marblestone JG, Mattern MR, Nicholson B. Strategies for the identification of ubiquitin ligase inhibitors. *Biochem Soc Trans* 2010; **38**: 132-136 [PMID: 20074047 DOI: 10.1042/BST0380132]
81 **Endo S**, Yamato K, Hirai S, Moriwaki T, Fukuda K, Suzuki H, Abei M, Nakagawa I, Hyodo I. Potent in vitro and in vivo antitumor effects of MDM2 inhibitor nutlin-3 in gastric cancer cells. *Cancer Sci* 2011; **102**: 605-613 [PMID: 21205074 DOI: 10.1111/j.1349-7006.2010.01821.x]
82 **Haaland I**, Opsahl JA, Berven FS, Reikvam H, Fredly HK,

Haugse R, Thiede B, McCormack E, Lain S, Bruserud O, Gjertsen BT. Molecular mechanisms of nutlin-3 involve acetylation of p53, histones and heat shock proteins in acute myeloid leukemia. *Mol Cancer* 2014; **13**: 116 [PMID: 24885082 DOI: 10.1186/1476-4598-13-116]

83 **Wang H**, Chen G, Wang H, Liu C. RITA inhibits growth of human hepatocellular carcinoma through induction of apoptosis. *Oncol Res* 2013; **20**: 437-445 [PMID: 24308154 DOI: 10.3727/096504013X13685487925059]

84 **Tsao CC**, Corn PG. MDM-2 antagonists induce p53-dependent cell cycle arrest but not cell death in renal cancer cell lines. *Cancer Biol Ther* 2010; **10**: 1315-1325 [PMID: 20953142 DOI: 10.4161/cbt.10.12.13612]

85 **Tovar C**, Rosinski J, Filipovic Z, Higgins B, Kolinsky K, Hilton H, Zhao X, Vu BT, Qing W, Packman K, Myklebost O, Heimbrook DC, Vassilev LT. Small-molecule MDM2 antagonists reveal aberrant p53 signaling in cancer: implications for therapy. *Proc Natl Acad Sci USA* 2006; **103**: 1888-1893 [PMID: 16443686 DOI: 10.1073/pnas.0507493103]

86 **Ma J**, Cheng L, Liu H, Zhang J, Shi Y, Zeng F, Miele L, Sarkar FH, Xia J, Wang Z. Genistein down-regulates miR-223 expression in pancreatic cancer cells. *Curr Drug Targets* 2013; **14**: 1150-1156 [PMID: 23834147 DOI: 10.2174/13894501113149990187]

87 **Wang Y**, Liu Y, Lu J, Zhang P, Wang Y, Xu Y, Wang Z, Mao JH, Wei G. Rapamycin inhibits FBXW7 loss-induced epithelial-mesenchymal transition and cancer stem cell-like characteristics in colorectal cancer cells. *Biochem Biophys Res Commun* 2013; **434**: 352-356 [PMID: 23558291 DOI: 10.1016/j.bbrc.2013.03.077]

88 **Soucy TA**, Smith PG, Milhollen MA, Berger AJ, Gavin JM, Adhikari S, Brownell JE, Burke KE, Cardin DP, Critchley S, Cullis CA, Doucette A, Garnsey JJ, Gaulin JL, Gershman RE, Lublinsky AR, McDonald A, Mizutani H, Narayanan U, Olhava EJ, Peluso S, Rezaei M, Sintchak MD, Talreja T, Thomas MP, Traore T, Vyskocil S, Weatherhead GS, Yu J, Zhang J, Dick LR, Claiborne CF, Rolfe M, Bolen JB, Langston SP. An inhibitor of NEDD8-activating enzyme as a new approach to treat cancer. *Nature* 2009; **458**: 732-736 [PMID: 19360080 DOI: 10.1038/nature07884]

89 **Deshaies RJ**. SCF and Cullin/Ring H2-based ubiquitin ligases. *Annu Rev Cell Dev Biol* 1999; **15**: 435-467 [PMID: 10611969]

90 **Petroski MD**, Deshaies RJ. Function and regulation of cullin-RING ubiquitin ligases. *Nat Rev Mol Cell Biol* 2005; **6**: 9-20 [PMID: 15688063]

91 **Deshaies RJ**, Joazeiro CA. RING domain E3 ubiquitin ligases. *Annu Rev Biochem* 2009; **78**: 399-434 [PMID: 19489725 DOI: 10.1146/annurev.biochem.78.101807.093809]

92 **Blank JL**, Liu XJ, Cosmopoulos K, Bouck DC, Garcia K, Bernard H, Tayber O, Hather G, Liu R, Narayanan U, Milhollen MA, Lightcap ES. Novel DNA damage checkpoints mediating cell death induced by the NEDD8-activating enzyme inhibitor MLN4924. *Cancer Res* 2013; **73**: 225-234 [PMID: 23100467 DOI: 10.1158/0008-5472.CAN-12-1729]

93 **Nawrocki ST**, Griffin P, Kelly KR, Carew JS. MLN4924: a novel first-in-class inhibitor of NEDD8-activating enzyme for cancer therapy. *Expert Opin Investig Drugs* 2012; **21**: 1563-1573 [PMID: 22799561 DOI: 10.1517/13543784.2012.707192]

94 **McMillin DW**, Jacobs HM, Delmore JE, Buon L, Hunter ZR, Monrose V, Yu J, Smith PG, Richardson PG, Anderson KC, Treon SP, Kung AL, Mitsiades CS. Molecular and cellular effects of NEDD8-activating enzyme inhibition in myeloma. *Mol Cancer Ther* 2012; **11**: 942-951 [PMID: 22246439 DOI: 10.1158/1535-7163.MCT-11-0563]

95 **Milhollen MA**, Traore T, Adams-Duffy J, Thomas MP, Berger AJ, Dang L, Dick LR, Garnsey JJ, Koenig E, Langston SP, Manfredi M, Narayanan U, Rolfe M, Staudt LM, Soucy TA, Yu J, Zhang J, Bolen JB, Smith PG. MLN4924, a NEDD8-activating enzyme inhibitor, is active in diffuse large B-cell lymphoma models: rationale for treatment of NF-{kappa}B-dependent lymphoma. *Blood* 2010; **116**: 1515-1523 [PMID: 20525923 DOI: 10.1182/blood-2010-03-272567]

96 **Li L**, Wang M, Yu G, Chen P, Li H, Wei D, Zhu J, Xie L, Jia H, Shi J, Li C, Yao W, Wang Y, Gao Q, Jeong LS, Lee HW, Yu J, Hu F, Mei J, Wang P, Chu Y, Qi H, Yang M, Dong Z, Sun Y, Hoffman RM, Jia L. Overactivated neddylation pathway as a therapeutic target in lung cancer. *J Natl Cancer Inst* 2014; **106**: dju083 [PMID: 24853380 DOI: 10.1093/jnci/dju083]

97 **Wang X**, Li L, Liang Y, Li C, Zhao H, Ye D, Sun M, Jeong LS, Feng Y, Fu S, Jia L, Guo X. Targeting the neddylation pathway to suppress the growth of prostate cancer cells: therapeutic implication for the men's cancer. *Biomed Res Int* 2014; **2014**: 974309 [PMID: 25093192 DOI: 10.1155/2014/974309]

98 **Gao Q**, Yu GY, Shi JY, Li LH, Zhang WJ, Wang ZC, Yang LX, Duan M, Zhao H, Wang XY, Zhou J, Qiu SJ, Jeong LS, Jia LJ, Fan J. Neddylation pathway is up-regulated in human intrahepatic cholangiocarcinoma and serves as a potential therapeutic target. *Oncotarget* 2014; **5**: 7820-7832 [PMID: 25229838]

99 **Yang D**, Tan M, Wang G, Sun Y. The p21-dependent radiosensitization of human breast cancer cells by MLN4924, an investigational inhibitor of NEDD8 activating enzyme. *PLoS One* 2012; **7**: e34079 [PMID: 22457814 DOI: 10.1371/journal.pone.0034079]

P- Reviewer: Marrelli D, Wang WH **S- Editor**: Ma YJ
L- Editor: Cant MR **E- Editor**: Ma S

World Journal of Gastroenterology

Submit a Manuscript: http://www.wjgnet.com/esps/
Help Desk: http://www.wjgnet.com/esps/helpdesk.aspx
DOI: 10.3748/wjg.v21.i3.794

World J Gastroenterol 2015 January 21; 21(3): 794-802
ISSN 1007-9327 (print) ISSN 2219-2840 (online)

REVIEW

PNPLA3 I148M variant in nonalcoholic fatty liver disease: Demographic and ethnic characteristics and the role of the variant in nonalcoholic fatty liver fibrosis

Li-Zhen Chen, Yong-Ning Xin, Ning Geng, Man Jiang, Ding-Ding Zhang, Shi-Ying Xuan

Li-Zhen Chen, Yong-Ning Xin, Ning Geng, Man Jiang, Ding-Ding Zhang, Shi-Ying Xuan, Department of Gastroenterology, Qingdao Municipal Hospital, Qingdao 266071, Shandong Province, China
Li-Zhen Chen, Ning Geng, Medical College of Qingdao University, Qingdao 266021, Shandong Province, China
Author contributions: Chen LZ drafted and wrote the manuscript; Xin YN, Geng N, Jiang M and Zhang DD revised the manuscript; and Xuan SY approved the final version.
Supported by National Natural Science Foundation of China No. 81170337/H0304.

Correspondence to: Shi-Ying Xuan, PhD, Professor, Department of Gastroenterology, Qingdao Municipal Hospital, 1 Jiaozhou Road, Qingdao 266071, Shandong Province, China. dxyxyn@163.com
Telephone: +86-532-88905508
Fax: +86-532-88905293
Received: August 12, 2014
Peer-review started: August 13, 2014
First decision: September 15, 2014
Revised: September 25, 2014
Accepted: October 20, 2014
Article in press: October 21, 2014
Published online: January 21, 2015

Abstract

Patatin-like phospholipase domain-containing 3 (PNPLA3 or adiponutrin) displays anabolic and catabolic activities in lipid metabolism, and has been reported to be significantly associated with liver fat content. Various studies have established a strong link between the 148 isoleucine to methionine protein variant (I148M) of PNPLA3 and liver diseases, including nonalcoholic fatty liver disease (NAFLD). However, detailed demographic and ethnic characteristics of the I148M variant and its role in the development of nonalcoholic fatty liver fibrosis have not been fully elucidated. The present review summarizes the current knowledge on the association between the *PNPLA3* I148M variant and NAFLD, and especially its role in the development of nonalcoholic fatty liver fibrosis. First, we analyze the impact of demographic and ethnic characteristics of the *PNPLA3* I148M variant and the presence of metabolic syndrome on the association between *PNPLA3* I148M and NAFLD. Then, we explore the role of the *PNPLA3* I148M in the development of nonalcoholic fatty liver fibrosis, and hypothesize the underlying mechanisms by speculating a pro-fibrogenic network. Finally, we briefly highlight future research that may elucidate the specific mechanisms of the *PNPLA3* I148M variant in fibrogenesis, which, in turn, provides a theoretical foundation and valuable experimental data for the clinical management of nonalcoholic fatty liver fibrosis.

Key words: *PNPLA3* I148M variant; Polymorphism; Nonalcoholic fatty liver disease; Nonalcoholic fatty liver fibrosis

Core tip: In this review, we summarize the association between the *PNPLA3* I148M variant and nonalcoholic fatty liver disease (NAFLD), and especially its role in nonalcoholic fatty liver fibrosis. The variant is associated with NAFLD, but is predominant in women, not in men. The association may vary among different ethnic populations, but is not affected by the presence of metabolic syndrome. We speculate there is a pro-

fibrogenic network that the *PNPLA3* I148M variant may promote the development of fibrogenesis by activating the hedgehog signaling pathway, which, in turn, leads to the activation and proliferation of hepatic stellate cells, and excessive generation and deposition of extracellular matrix.

Chen LZ, Xin YN, Geng N, Jiang M, Zhang DD, Xuan SY. *PNPLA3* I148M variant in nonalcoholic fatty liver disease: Demographic and ethnic characteristics and the role of the variant in nonalcoholic fatty liver fibrosis. *World J Gastroenterol* 2015; 21(3): 794-802 Available from: URL: http://www.wjgnet.com/1007-9327/full/v21/i3/794.htm DOI: http://dx.doi.org/10.3748/wjg.v21.i3.794

INTRODUCTION

Nonalcoholic fatty liver disease (NAFLD) is defined histologically or by proton magnetic resonance spectroscopy as hepatic fat accumulation (steatosis) exceeding 5% in the absence of excessive ethanol consumption, drugs, toxins, infectious diseases or any other specific etiologic factors of liver disease[1]. NAFLD embraces a morphological spectrum of hepatic diseases, ranging from nonalcoholic fatty liver (NAFL) to nonalcoholic steatohepatitis (NASH). NASH is the late stage of NAFLD, in which hepatic inflammation and fibrosis co-exist. In a proportion of patients, NASH can progress towards cirrhosis and even hepatocellular carcinoma (HCC)[2]. With a general prevalence of 25%-30%, NAFLD currently represents the most common cause of liver dysfunction, and is now the most prevalent liver disorder in Western countries[3].

It is well known that metabolic risk factors such as obesity, insulin resistance, type 2 diabetes mellitus and dyslipidemia are deeply associated with the pathophysiology of NAFLD[2,4]. Moreover, genetic mutations also play a significant role in predisposition to the development and progression of NAFLD[5].

In 2008, a single nucleotide polymorphism (SNP) in the patatin-like phospholipase domain-containing 3 (*PNPLA3*, also known as adiponutrin) gene, or rs738409 polymorphism, which represents a substitution from cytosine to guanine that results in a switch from isoleucine to methionine at residue 148 (I148M), was reported to be significantly associated with liver fat content[6].

Since then, extensive investigations of the association between the *PNPLA3* I148M variant (or rs738409 polymorphism) and NAFLD have been carried out, and various studies have established a strong link between the *PNPLA3* I148M variant and the development and progression of NAFLD, including nonalcoholic fatty liver fibrosis[7-12]. These results indicate that this variant may be a potential modifier of NAFLD, especially nonalcoholic fatty liver fibrosis. However, detailed demographic and ethnic characteristics of the I148M variant and its role in the development of nonalcoholic fatty liver fibrosis, along with the specific molecular mechanisms, have not been fully elucidated. Therefore, the present review summarizes the current knowledge on the association between the *PNPLA3* I148M variant and NAFLD, and the variant's role in the development of nonalcoholic fatty liver fibrosis.

EXPRESSION AND FUNCTION OF THE *PNPLA3* GENE AND *PNPLA3* I148M VARIANT

The *PNPLA3* gene is located in the long branch of human chromosome 22, and encodes a transmembrane polypeptides chain containing 481 amino acids[13]. PNPLA3 protein is highly expressed on the endoplasmic reticulum and lipid membranes of hepatocytes as well as adipose tissue[14], and changes in the expression are closely associated with the nutrient status[15]. Rae-Whitcombe and colleagues reported that the promoter region of the *PNPLA3* gene is regulated by glucose and insulin[16]. Consistently, *PNPLA3* mRNA levels have been demonstrated to decrease after fasting and increased by refeeding in mice[17]. The nutritional regulation of *PNPLA3* has further been confirmed, as the gene is shown to be regulated by sterol regulatory element binding protein 1c (SREBP-1c) in mouse liver and human hepatocytes[17-19], which responds in turn to insulin and glucose.

With the conserved patatin domain at its N-terminal, the PNPLA3 protein demonstrates a predominant triglyceride hydrolase activity with mild lysophosphatidic acid acyltransferase activity[13]. It has been shown that substitution of methionine for isoleucine at residue 148 does not alter the orientation of the catalytic dyad, but the longer side chain of methionine restricts access of substrate to the catalytic serine at residue 47[20]. The size of the substrate-access entry site is significantly reduced in mutants, which limits the access of palmitic acid to the catalytic dyad[21]. Recently, Kumari and colleagues determined that the *PNPLA3* I148M variant induced an increase in lipogenic activity, leading to increased hepatic triglyceride synthesis[22]. Similarly, Li *et al*[23] generated transgenic mice over-expressing PNPLA3 in the liver and observed that the *PNPLA3* I148M variant exerted three effects on hepatic triglyceride metabolism: increased synthesis of fatty acids and triglyceride; impaired hydrolysis of triglyceride; and depletion of triglyceride long-chain polyunsaturated fatty acids. These findings suggest that the increase in hepatic triglyceride levels associated with the *PNPLA3* I148M variant is induced by multiple changes in triglyceride metabolism. These previous studies showed that acid modification within the catalytic patatin domain of the *PNPLA3* protein acts as a kind of "gain of function" mutation enhancing the accumulation of lipids in the hepatocytes.

PNPLA3 I148M VARIANT AND NAFLD

In 2008, Romeo and colleagues first reported a genome-wide association study to explore the genes associated with susceptibility to NAFLD[6]. They demonstrated that the *PNPLA3* 148M allele was robustly associated with increased liver fat content, and the association remained highly significant after adjusting for body mass index (BMI), diabetes status, ethanol use, as well as global and local ancestry. In addition, the *PNPLA3* I148M variant was also found to be associated with elevated serum aminotransferase levels[6,24] and increased computed tomography-measured hepatic steatosis and histological NAFLD[25]. A series of subsequent candidate gene studies[26,29,36,37] have verified the association between the *PNPLA3* I148M variant and NAFLD.

*PNPLA3*I148M variant is associated with NAFLD in adults

The *PNPLA3* I148M variant is reported to be dose-dependently associated with increased levels of serum triglyceride, alanine aminotransferase (ALT) and aspartate aminotransferase (AST)[26]. In addition, numerous studies have demonstrated that the *PNPLA3* I148M variant is associated with liver fat content[27-29]. These findings confirm that the *PNPLA3* I148M variant is associated not only with fat accumulation in the liver, but also with liver injury since aminotransferases are the most sensitive liver function parameters. Liver injury is believed to be triggered by lipotoxicity, which results from hepatic fat accumulation. It has been previously reported that liver necrosis induced by intracellular lipotoxicity parallels liver fat accumulation[30], and the degree of steatosis correlates with the severity of liver injury in NAFLD[31].

Currently, liver biopsy is used as the gold standard for diagnosis of NAFLD. Although it is expensive and not ethically feasible, especially in uninvestigated patients, there are still some studies on NAFLD based on histological diagnosis. The *PNPLA3* I148M variant has been confirmed to be strongly associated with an increased risk of histological NAFLD[32]. In a case-control study, patients who were homozygotes of the 148M allele had higher steatosis scores (33.3% ± 4.0%) compared with heterozygotes of the 148IM allele (26.3% ± 3.5%) and 148I allele (14.9% ± 3.9%), indicating that the variant was significantly associated with the degree of liver steatosis[27].

PNPLA3 I148M variant is associated with pediatric NAFLD

NAFLD is not only a disease affecting the adult population, but also a leading liver disease in children worldwide[8,33]. A study of Hispanic children and adolescents in the Unites States showed that the 148M allele was associated with higher liver fat content and lower HDL cholesterol levels[34]. This is consistent with the observation that Hispanic children who were homozygotes of the 148MM allele were susceptible to increased hepatic fat when dietary carbohydrate intake was high[35]. In addition, a study of obese Taiwanese children also showed that the *PNPLA3* I148M variant was associated with an increase in ALT levels and an increased risk of NAFLD[36,37].

In a more extensive study of pediatric patients with biopsy-proven NAFLD, the *PNPLA3* I148M variant was associated with the severity of steatosis, hepatocellular ballooning and lobular inflammation, and the presence of NASH and fibrosis, but not with BMI, adiposity, lipid levels, insulin resistance and ALT levels[8]. In another large study[7] to determine the association between SNPs and the histological severity of NAFLD, 223 children with histologically confirmed NAFLD were investigated. It was observed that the 148M allele was associated with an earlier presentation of the disease, but not with histological severity. However, the association was marginal in the multivariate analysis ($P = 0.045$).

Therefore, although the currently available findings suggest that the *PNPLA3* I148M variant confers genetic susceptibility to liver injury in children at a young age, most subjects studied were obese children or pediatric NAFLD patients, and the samples were relatively small in most of the studies. Thus, well-designed large studies that include pediatric NAFLD patients and matched healthy children are required to confirm the association. At the very least, a meta-analysis would offer valuable information.

ASSOCIATION BETWEEN *PNPLA3* I148M VARIANT AND NAFLD IS AFFECTED BY GENDER AND PROBABLY BY ETHNICITY, BUT NOT BY METABOLIC SYNDROME

The *PNPLA3* I148M variant shows a potential sexual dimorphism on NAFLD susceptibility[9,32]. In a gender-specific analysis of a NASH cohort, Speliotes *et al*[32] observed that the effect of the *PNPLA3*I148M variant on histological NAFLD was higher in women than in men. Indeed, a meta-regression analysis showed a negative correlation between male gender and the effect of the *PNPLA3* I148M variant on liver fat content[9].

The above findings suggest a predominant association between the *PNPLA3* I148M variant with NAFLD in women, but not in men. It is known that estrogen levels are different in men and women, and estrogen is a critical hormone involved in lipid metabolism. Therefore, the gender differences may mainly result from the variations in the hormone, the variation in the gene, or the interaction of the two. However, it is necessary to test whether there is a true and reproducible interaction between estrogen and *PNPLA3* I148M in well-defined population-based cohorts.

The prevalence of NAFLD differs among different populations. Hispanics have been demonstrated to have a higher prevalence of hepatic steatosis compared with European-Americans, whereas African-Americans have a lower prevalence[38]. In addition, Asian-Indian men have

more liver fat and are more insulin-resistant than BMI- and age-matched white individuals[39].

Romeo and colleagues found that the frequencies of the 148M allele matched the prevalence of NAFLD in the Dallas Heart Study, and Hispanics had a higher frequency of the 148M allele (49%) compared with European Americans (23%) and African Americans (17%)[6]. Another study by Wagenknecht *et al*[40] suggested that the *PNPLA3* I148M variant contributed to the variation in NAFLD across multiple ethnicities. These findings indicate that the *PNPLA3* I148M variant may explain ethnic differences in the prevalence of NAFLD, and that some of the ethnic variations in NAFLD are genetic.

On the other hand, in a study of 144 biopsy-proven NAFLD patients and 198 controls in Malaysia, the *PNPLA3* I148M variant was associated with susceptibility to NAFLD (OR = 2.34; 95%CI: 1.69-3.24)[12]. However, the association remained similar in three ethnic groups, namely Chinese (OR = 1.94; 95%CI: 1.12-3.37), Indian (OR = 3.51; 95%CI: 1.69-7.26) and Malay (OR = 2.05; 95%CI: 1.25-3.35), which indicates no effect of ethnicity on the association between the *PNPLA3* I148M variant and NAFLD. Nevertheless, these three ethnic groups all belong to Asian populations, which may be different from Hispanics, Europeans and Africans in terms of association between the *PNPLA3* I148M variant and NAFLD.

NAFLD is now considered the hepatic manifestation of metabolic syndrome[41]. Insulin resistance in adipose tissue induces an excess of free fatty acid supply to the liver, which may lead to lipotoxicity, oxidative stress, and apoptosis[42]. Whether the association between the *PNPLA3* I148M variant and NAFLD is confounded by the presence of metabolic syndrome has been investigated. Although a few studies have suggested an association between the *PNPLA3* I148M variant and metabolic syndrome, such as insulin resistance[26,43], other studies have failed to reveal the association[9,32,44,45]. For example, in a study of 592 cases with European ancestry, there were no associations of the *PNPLA3* I148M variant with BMI, triglyceride levels, high- and low-density lipoprotein levels, or diabetes[32]. Moreover, a study of 330 German subjects showed that the *PNPLA3* I148M variant was strongly associated with fatty liver, but not with insulin resistance or estimates of liver injury[44]. In addition, in a study of 218 French type 2 diabetic patients, the *PNPLA3* I148M variant was not correlated with visceral obesity and was inversely associated with carotid intima media thickness, suggesting that fatty liver associated with the *PNPLA3* I148M variant may not be linked to metabolic disorders[45]. Indeed, in a recent meta-analysis, all included studies showed a lack of a significant difference among genotypes for BMI, glucose and insulin levels, and homeostasis model assessment of insulin resistance[9].

Furthermore, there appears to be no association between the *PNPLA3* I148M variant and metabolic syndrome in children. In a study of obese children and adolescents, the *PNPLA3* I148M variant was associated with increased levels of ALT and AST, but not with glucose tolerance and insulin sensitivity[46]. The *PNPLA3*I148M variant also conferred susceptibility to hepatic steatosis in obese youths, but without increasing insulin resistance[47].

In summary, the *PNPLA3* I148M variant is associated with NAFLD both in adults and children, and the association is affected by gender and ethnicity, but not by the presence of metabolic syndrome (Table 1).

ROLE OF THE *PNPLA3* I148M VARIANT IN NONALCOHOLIC FATTY LIVER FIBROSIS

Nonalcoholic fatty liver fibrosis represents a necessary pathological pathway that patients with NAFLD undergo and then progress to cirrhosis, HCC and end-stage liver disease, and poses a noteworthy economic burden worldwide. Liver fibrosis is a reversible wound-healing response to continuous chronic liver injuries[48], and the most characteristic hallmark is the excessive production and accumulation of intrahepatic extracellular matrix (ECM), including fibronectin, type I collagen, proteoglycan, *etc*., which eventually lead to hepatic structural change and dysfunction. Therefore, whether or not to control or reverse liver fibrosis affects the prognosis of patients to a great extent. However, challenges remain, as the underlying specific pathogenesis of liver fibrosis is still unclear.

Various studies have established that the *PNPLA3* I148M variant is significantly associated with the development of fibrogenesis and the severity of nonalcoholic fatty liver fibrosis[7,8,10,11,32,49]. In 2010, Valenti and colleagues demonstrated that the *PNPLA3* I148M variant influenced both the presence of NASH (OR = 1.5; 95%CI: 1.12-2.04) and the severity of liver fibrosis (OR = 1.5; 95%CI: 1.09-2.12) in a large series of 591 biopsied patients with NAFLD independently of the degree of obesity, diabetes and steatosis[11]. In addition, Rotman *et al*[7] carried out a study in a large cohort of 894 adults and 223 children with histopathological markers of NAFLD, and confirmed that the *PNPLA3* I148M variant was associated with portal ($P < 0.001$) and lobular inflammation ($P = 0.005$), Mallory-Denk bodies ($P = 0.020$), and fibrosis ($P < 0.001$). Furthermore, in an observational cross-sectional study of 899 European patients with chronic liver diseases, there was a prominent association between the *PNPLA3* I148M variant and enhanced liver stiffness by using a non-invasive transient elastography[10]. This association between the *PNPLA3* I148M variant and the severity of fibrosis in patients with histologically confirmed NAFLD was replicated in a case-control analysis (OR = 3.37; 95%CI: 2.85-3.97; $P < 0.001$)[32]. More importantly, consistent with previous findings in adults, a prospective study of 149 consecutive Caucasian children and adolescents with biopsy-proven

Table 1 Studies evaluating the association between the *PNPLA3* I148M variant and nonalcoholic fatty liver disease

Ref.	Population/Ethnicity country	*n*	Age	Diagnosis criteria	Key findings
Wang *et al*[26]	Asian Tai Wan	879	Adult	US	Increase in TG, ALT and AST
Sookoian *et al*[27]	Caucasian Argentina	266	Adult	US Liver biopsy	Increased liver fat and liver Injury
Kollerits *et al*[28]	Italy/Austria/United States	4290	Adult	NA	Increase in ALT and AST
Xu *et al*[29]	Chinese China	651	Adult	US	Increased ALT, GGT and related to development and progression of NAFLD
Speliotes *et al*[32]	Caucasian United States	1597	Adult	Liver biopsy	Increased risk of histological NAFLD, but not associated with metabolic syndrome
Rotman *et al*[7]	Caucasian United States	1117	Adult Pediatric	Liver biopsy	Earlier presentation of NAFLD in pediatric patients
Valenti *et al*[8]	Caucasian Italian	149	Pediatric	Liver biopsy	Associated with steatosis, NASH and fibrosis
Goran *et al*[34]	Hispanic United States	327	Pediatric	MRS	Higher liver fat and lower HDL-C
Davis *et al*[35]	Hispanic United States	153	Pediatric	MRI	Increased liver fat when dietary carbohydrate intake
Lin *et al*[36]	Asian Tai Wan	520	Pediatric	US	Increased ALT and risk of NAFLD
Viitasalo *et al*[37]	Caucasian Finland	481	Pediatric	NA	Increase in ALT
Sookoian *et al*[9]	Meta-analysis				A negative correlation between male sex and the variant on liver fat, and a lack of significant difference among genotypes for metabolic syndrome
Romeo *et al*[6]	Hispanic/ European American/ African American United States	9229	Adult	H-MRS	Hispanics have a higher frequency of the 148M allele than European Americans and African Americans
Zain *et al*[12]	Chinese, Indian and Malay Malaysia	342	Adult	Liver biopsy	No effect of ethnicity on the association between the variant and NAFLD
Browning *et al*[38]	White/Black/Hispanic United States	2287	Adult	H-MRS	Frequency of hepatic steatosis varied with ethnicity and gender
Petersen *et al*[39]	Caucasian/ Eastern Asian/ Asian-Indian/Black/ Hispanic United States	482	Pediatric Adult	Proton MRS	Asian-Indians have increased liver fat and prevalence of insulin resistance compared with all other ethnic groups
Wagenknecht *et al*[40]	Hispanic American/ African American United States	1214	Adult	Abdominal CT scanning	Hispanic Americans have a higher frequency of the 148M allele than African Americans
Kantartzis *et al*[44]	Caucasian Germany	330	Adult	H-MRS MRT	Higher liver fat but not insulin sensitivity, lipids, or liver enzymes
Petit *et al*[45]	Caucasian France	218	Adult	H-MRS	Not associated with BMI or visceral fat area
Romeo *et al*[46]	Caucasian Italy	475	Pediatric	US	Increased ALT and AST, but not glucose tolerance and insulin sensitivity
Santoro *et al*[47]	Caucasian/ Hispanic/ African American United States	85	Pediatric	MRI	Increase susceptibility to hepatic steatosis, but without increasing insulin resistance

PNPLA3: Patatin-like phospholipase domain-containing 3; NAFLD: Nonalcoholic fatty liver disease; NASH: Nonalcoholic steatohepatitis; US: Ultrasonography; H-MRS: Hydrogen magnetic resonance spectroscopy; MRI: Magnetic resonance imaging; MRT: Magnetic resonance tomography; CT: Computed tomography; TG: Triglyceride; ALT: Alanine aminotransferase; AST: Aspartate aminotransferase; GGT: Gamma-glutamyl transferase; HDL-C: High-density lipoprotein cholesterol; LDL-C: Low-density lipoprotein cholesterol; BMI: Body mass index; NA: Not available.

NAFLD showed stronger evidence that the *PNPLA3* I148M variant significantly influenced the occurrence of fibrosis ($P = 0.01$) irrespective of confounding factors[8].

Recently, a meta-analysis established a significant association between the *PNPLA3* I148M variant and advanced nonalcoholic fatty liver fibrosis[49]. In a dominant model, patients with PNPLA3 148MM or 148IM exhibited a significantly increased risk of developing advanced fibrosis compared with 148Ⅱ carriers (OR = 1.29; 95%CI: 1.21-1.38). In line with the dominant model, a recessive model yielded a similar strength of the association (OR = 1.32; 95%CI: 1.20-1.45)[49]. Therefore, there is little doubt that there exists an association between the *PNPLA3* I148M variant and nonalcoholic fatty liver

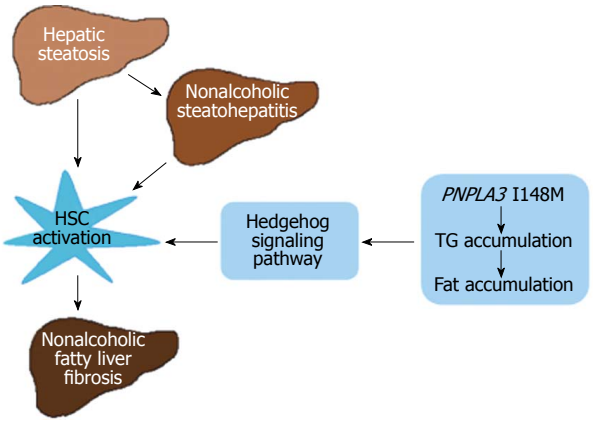

Figure 1 Simplified schematic model showing the hypothetical molecular mechanism by which the *PNPLA3* I148M variant participates in the development and progression of nonalcoholic fatty liver fibrosis. The hedgehog signaling pathway links *PNPLA3* with the activation of hepatic stellate cells, which is considered as the central part of fibrogenesis. PNPLA3 protein exhibits activities of lysophosphatidic acid acyltransferase and acylglycerol hydrolase to maintain the Triglyceride (TG) balance in the liver. The "gain function" of the *PNPLA3* I148M variant causes TG accumulation in the liver, which accelerates the progression of nonalcoholic fatty liver disease. HSC: Hepatic stellate cell.

fibrosis. Continuous research on the strategies for potential prevention or even curative intervention of nonalcoholic fatty liver fibrosis is warranted.

However, the specific mechanism of the *PNPLA3* I148M variant in the development and progression of nonalcoholic fatty liver fibrosis is still not clear. Up to now, abnormal activation of hepatic stellate cells (HSCs) characterized by retinoid loss was considered as the key contributor to fibrogenesis irrespective of the underlying disease[50]. The hedgehog (Hh) signaling pathway, consisting of Hh ligands, transmembrane protein receptors patched and smoothened, and Gli family transcription factors, is one of the most classic signaling pathways participating in the process of cell differentiation and proliferation during embryonic development[51,52].

Recent studies have shown a strong association between the Hh signaling pathway and the development and progression of nonalcoholic fatty liver fibrosis[53-55]. Guy *et al*[53] demonstrated that the activation of the Hh pathway paralleled histological severity of injury and liver fibrosis in a cross-sectional immunohistochemical study of a large cohort of biopsy-proven adult NAFLD patients. Moreover, a study of 56 children with NAFLD at the University of California, San Diego, United States, also showed significant associations between sonic Hh grade, the numbers of Hh-ligand-producing cells, Hh-responsive cells, and fibrosis stage[55]. In addition, it has been reported that the Hh signaling pathway regulates the HSC-to-myofibroblast transition[56,57], the expansion of hepatic progenitor cells[53,54], and the expression of cholangiocyte chemokines[58,59]. Meanwhile, cholangiocytes and hepatic progenitor cells can activate the Hh signaling pathway by generating Hh ligands[59] and increasing the expression of Gli2[54] (a Hh-regulated target gene), which, in turn, activates HSCs. Based on the available evidence, it is speculated that cross-talk between the Hh signaling pathway and activated HSCs, as well as progenitor cells and cholangiocytes, forms a pro-fibrogenic network together and leads to excessive generation and deposition of ECM and eventually fibrogenesis. Accordingly, we hypothesize that the *PNPLA3* I148M variant promotes the development of fibrogenesis by activating the Hh signaling pathway, which, in turn, leads to the activation and proliferation of HSCs, and excessive generation and deposition of ECM (Figure 1). To test this hypothesis, future studies are needed to established *PNPLA3* I148M transgenic mouse models, which can be used to establish transgenic mouse models of nonalcoholic fatty liver fibrosis. With such models, the role of the *PNPLA3* I148M variant in nonalcoholic fatty liver fibrosis and the underlying mechanisms can be further explored. Consequently, the association between the *PNPLA3* I148M variant and the Hh signaling pathway, and the precise mechanisms at molecular, cellular and genetic levels by which the *PNPLA3* I148M variant participates in the development of fibrogenesis are expected to be elucidated, which will lay a theoretical foundation and provide valuable experimental data for the clinical management of nonalcoholic fatty liver fibrosis.

CONCLUSION

The *PNPLA3* I148M variant is associated with NAFLD, but is predominant in women, not in men. The association may vary among different ethnic populations, but is not affected by the presence of metabolic syndrome. The *PNPLA3* I148M variant may promote the development of fibrogenesis by activating the Hh signaling pathway, which, in turn, leads to the activation and proliferation of HSCs, and excessive generation and deposition of ECM. Further studies are needed to understand the underlying mechanisms.

REFERENCES

1 **Gao X**, Fan JG. Diagnosis and management of non-alcoholic fatty liver disease and related metabolic disorders: consensus statement from the Study Group of Liver and Metabolism, Chinese Society of Endocrinology. *J Diabetes* 2013; **5**: 406-415 [PMID: 23560695 DOI: 10.1111/1753-0407.12056]

2 **Chalasani N**, Younossi Z, Lavine JE, Diehl AM, Brunt EM, Cusi K, Charlton M, Sanyal AJ. The diagnosis and management of non-alcoholic fatty liver disease: practice guideline by the American Gastroenterological Association, American Association for the Study of Liver Diseases, and American College of Gastroenterology. *Gastroenterology* 2012; **142**: 1592-1609 [PMID: 22656328 DOI: 10.1053/j.gastro.2012.04.001]

3 **Bhala N**, Jouness RI, Bugianesi E. Epidemiology and natural history of patients with NAFLD. *Curr Pharm Des* 2013; **19**: 5169-5176 [PMID: 23394091]

4 **Anstee QM**, Targher G, Day CP. Progression of NAFLD to diabetes mellitus, cardiovascular disease or cirrhosis. *Nat Rev Gastroenterol Hepatol* 2013; **10**: 330-344 [PMID: 23507799 DOI: 10.1038/nrgastro.2013.41]

5 **Erickson SK**. Nonalcoholic fatty liver disease. *J Lipid Res* 2009; **50** Suppl: S412-S416 [PMID: 19074370 DOI: 10.1194/jlr.R800089-JLR200]

6 **Romeo S**, Kozlitina J, Xing C, Pertsemlidis A, Cox D, Pennacchio LA, Boerwinkle E, Cohen JC, Hobbs HH. Genetic variation in PNPLA3 confers susceptibility to nonalcoholic fatty liver disease. *Nat Genet* 2008; **40**: 1461-1465 [PMID: 18820647 DOI: 10.1038/ng.257]

7 **Rotman Y**, Koh C, Zmuda JM, Kleiner DE, Liang TJ. The association of genetic variability in patatin-like phospholipase domain-containing protein 3 (PNPLA3) with histological severity of nonalcoholic fatty liver disease. *Hepatology* 2010; **52**: 894-903 [PMID: 20684021 DOI: 10.1002/hep.23759]

8 **Valenti L**, Alisi A, Galmozzi E, Bartuli A, Del Menico B, Alterio A, Dongiovanni P, Fargion S, Nobili V. I148M patatin-like phospholipase domain-containing 3 gene variant and severity of pediatric nonalcoholic fatty liver disease. *Hepatology* 2010; **52**: 1274-1280 [PMID: 20648474 DOI: 10.1002/hep.23823]

9 **Sookoian S**, Pirola CJ. Meta-analysis of the influence of I148M variant of patatin-like phospholipase domain containing 3 gene (PNPLA3) on the susceptibility and histological severity of nonalcoholic fatty liver disease. *Hepatology* 2011; **53**: 1883-1894 [PMID: 21381068 DOI: 10.1002/hep.24283]

10 **Krawczyk M**, Grünhage F, Zimmer V, Lammert F. Variant adiponutrin (PNPLA3) represents a common fibrosis risk gene: non-invasive elastography-based study in chronic liver disease. *J Hepatol* 2011; **55**: 299-306 [PMID: 21168459 DOI: 10.1016/j.jhep.2010.10.042]

11 **Valenti L**, Al-Serri A, Daly AK, Galmozzi E, Rametta R, Dongiovanni P, Nobili V, Mozzi E, Roviaro G, Vanni E, Bugianesi E, Maggioni M, Fracanzani AL, Fargion S, Day CP. Homozygosity for the patatin-like phospholipase-3/adiponutrin I148M polymorphism influences liver fibrosis in patients with nonalcoholic fatty liver disease. *Hepatology* 2010; **51**: 1209-1217 [PMID: 20373368 DOI: 10.1002/hep.23622]

12 **Zain SM**, Mohamed R, Mahadeva S, Cheah PL, Rampal S, Basu RC, Mohamed Z. A multi-ethnic study of a PNPLA3 gene variant and its association with disease severity in non-alcoholic fatty liver disease. *Hum Genet* 2012; **131**: 1145-1152 [PMID: 22258181 DOI: 10.1007/s00439-012-1141-y]

13 **Pingitore P**, Pirazzi C, Mancina RM, Motta BM, Indiveri C, Pujia A, Montalcini T, Hedfalk K, Romeo S. Recombinant PNPLA3 protein shows triglyceride hydrolase activity and its I148M mutation results in loss of function. *Biochim Biophys Acta* 2014; **1841**: 574-580 [PMID: 24369119 DOI: 10.1016/j.bbalip.2013.12.006]

14 **He S**, McPhaul C, Li JZ, Garuti R, Kinch L, Grishin NV, Cohen JC, Hobbs HH. A sequence variation (I148M) in PNPLA3 associated with nonalcoholic fatty liver disease disrupts triglyceride hydrolysis. *J Biol Chem* 2010; **285**: 6706-6715 [PMID: 20034933 DOI: 10.1074/jbc.M109.064501]

15 **Baulande S**, Lasnier F, Lucas M, Pairault J. Adiponutrin, a transmembrane protein corresponding to a novel dietary- and obesity-linked mRNA specifically expressed in the adipose lineage. *J Biol Chem* 2001; **276**: 33336-33344 [PMID: 11431482]

16 **Rae-Whitcombe SM**, Kennedy D, Voyles M, Thompson MP. Regulation of the promoter region of the human adiponutrin/PNPLA3 gene by glucose and insulin. *Biochem Biophys Res Commun* 2010; **402**: 767-772 [PMID: 21036152 DOI: 10.1016/j.bbrc.2010.10.106]

17 **Liu YM**, Moldes M, Bastard JP, Bruckert E, Viguerie N, Hainque B, Basdevant A, Langin D, Pairault J, Clément K. Adiponutrin: A new gene regulated by energy balance in human adipose tissue. *J Clin Endocrinol Metab* 2004; **89**: 2684-2689 [PMID: 15181042]

18 **Huang Y**, He S, Li JZ, Seo YK, Osborne TF, Cohen JC, Hobbs HH. A feed-forward loop amplifies nutritional regulation of PNPLA3. *Proc Natl Acad Sci USA* 2010; **107**: 7892-7897 [PMID: 20385813 DOI: 10.1073/pnas.1003585107]

19 **Dubuquoy C**, Robichon C, Lasnier F, Langlois C, Dugail I, Foufelle F, Girard J, Burnol AF, Postic C, Moldes M. Distinct regulation of adiponutrin/PNPLA3 gene expression by the transcription factors ChREBP and SREBP1c in mouse and human hepatocytes. *J Hepatol* 2011; **55**: 145-153 [PMID: 21145868 DOI: 10.1016/j.jhep.2010.10.024]

20 **Wilson PA**, Gardner SD, Lambie NM, Commans SA, Crowther DJ. Characterization of the human patatin-like phospholipase family. *J Lipid Res* 2006; **47**: 1940-1949 [PMID: 16799181]

21 **Xin YN**, Zhao Y, Lin ZH, Jiang X, Xuan SY, Huang J. Molecular dynamics simulation of PNPLA3 I148M polymorphism reveals reduced substrate access to the catalytic cavity. *Proteins* 2013; **81**: 406-414 [PMID: 23042597 DOI: 10.1002/prot.24199]

22 **Kumari M**, Schoiswohl G, Chitraju C, Paar M, Cornaciu I, Rangrez AY, Wongsiriroj N, Nagy HM, Ivanova PT, Scott SA, Knittelfelder O, Rechberger GN, Birner-Gruenberger R, Eder S, Brown HA, Haemmerle G, Oberer M, Lass A, Kershaw EE, Zimmermann R, Zechner R. Adiponutrin functions as a nutritionally regulated lysophosphatidic acid acyltransferase. *Cell Metab* 2012; **15**: 691-702 [PMID: 22560221 DOI: 10.1016/j.cmet.2012.04.008]

23 **Li JZ**, Huang Y, Karaman R, Ivanova PT, Brown HA, Roddy T, Castro-Perez J, Cohen JC, Hobbs HH. Chronic overexpression of PNPLA3I148M in mouse liver causes hepatic steatosis. *J Clin Invest* 2012; **122**: 4130-4144 [PMID: 23023705]

24 **Yuan X**, Waterworth D, Perry JR, Lim N, Song K, Chambers JC, Zhang W, Vollenweider P, Stirnadel H, Johnson T, Bergmann S, Beckmann ND, Li Y, Ferrucci L, Melzer D, Hernandez D, Singleton A, Scott J, Elliott P, Waeber G, Cardon L, Frayling TM, Kooner JS, Mooser V. Population-based genome-wide association studies reveal six loci influencing plasma levels of liver enzymes. *Am J Hum Genet* 2008; **83**: 520-528 [PMID: 18940312 DOI: 10.1016/j.ajhg.2008.09.012]

25 **Speliotes EK**, Yerges-Armstrong LM, Wu J, Hernaez R, Kim LJ, Palmer CD, Gudnason V, Eiriksdottir G, Garcia ME, Launer LJ, Nalls MA, Clark JM, Mitchell BD, Shuldiner AR, Butler JL, Tomas M, Hoffmann U, Hwang SJ, Massaro JM, O'Donnell CJ, Sahani DV, Salomaa V, Schadt EE, Schwartz SM, Siscovick DS, Voight BF, Carr JJ, Feitosa MF, Harris TB, Fox CS, Smith AV, Kao WH, Hirschhorn JN, Borecki IB. Genome-wide association analysis identifies variants associated with nonalcoholic fatty liver disease that have distinct effects on metabolic traits. *PLoS Genet* 2011; **7**: e1001324 [PMID: 21423719 DOI: 10.1371/journal.pgen.1001324]

26 **Wang CW**, Lin HY, Shin SJ, Yu ML, Lin ZY, Dai CY, Huang JF, Chen SC, Li SS, Chuang WL. The PNPLA3 I148M polymorphism is associated with insulin resistance and nonalcoholic fatty liver disease in a normoglycaemic population. *Liver Int* 2011; **31**: 1326-1331 [PMID: 21745282 DOI: 10.1111/j.1478-3231]

27 **Sookoian S**, Castaño GO, Burgueño AL, Gianotti TF, Rosselli MS, Pirola CJ. A nonsynonymous gene variant in the adiponutrin gene is associated with nonalcoholic fatty liver disease severity. *J Lipid Res* 2009; **50**: 2111-2116 [PMID: 19738004 DOI: 10.1194/jlr.P900013-JLR200]

28 **Kollerits B**, Coassin S, Kiechl S, Hunt SC, Paulweber B, Willeit J, Brandstätter A, Lamina C, Adams TD, Kronenberg F. A common variant in the adiponutrin gene influences liver enzyme values. *J Med Genet* 2010; **47**: 116-119 [PMID: 19542081 DOI: 10.1136/jmg.2009.066597]

29 **Xu J**, Xin YN, Lü WH, Lin ZH, Zhang DD, Zhang M, Dong QJ, Jiang XJ, Xuan SY. [Polymorphism rs738409 in PNPLA3 is associated with inherited susceptibility to non-alcoholic fatty liver disease]. *Zhonghua Ganzangbing Zazhi* 2013; **21**: 619-623 [PMID: 24119744 DOI: 10.3760/cma.j.issn.1007-3418]

30 **Wanless IR**, Shiota K. The pathogenesis of nonalcoholic steatohepatitis and other fatty liver diseases: a four-step model including the role of lipid release and hepatic venular obstruction in the progression to cirrhosis. *Semin Liver Dis*

2004; **24**: 99-106 [PMID: 15085490]
31 **Chalasani N**, Wilson L, Kleiner DE, Cummings OW, Brunt EM, Unalp A. Relationship of steatosis grade and zonal location to histological features of steatohepatitis in adult patients with non-alcoholic fatty liver disease. *J Hepatol* 2008; **48**: 829-834 [PMID: 18321606 DOI: 10.1016/j.jhep.2008.01.016]
32 **Speliotes EK**, Butler JL, Palmer CD, Voight BF, Hirschhorn JN. PNPLA3 variants specifically confer increased risk for histologic nonalcoholic fatty liver disease but not metabolic disease. *Hepatology* 2010; **52**: 904-912 [PMID: 20648472 DOI: 10.1002/hep.23768]
33 **Pacifico L**, Nobili V, Anania C, Verdecchia P, Chiesa C. Pediatric nonalcoholic fatty liver disease, metabolic syndrome and cardiovascular risk. *World J Gastroenterol* 2011; **17**: 3082-3091 [PMID: 21912450 DOI: 10.3748/wjg.v17.i26.3082]
34 **Goran MI**, Walker R, Le KA, Mahurkar S, Vikman S, Davis JN, Spruijt-Metz D, Weigensberg MJ, Allayee H. Effects of PNPLA3 on liver fat and metabolic profile in Hispanic children and adolescents. *Diabetes* 2010; **59**: 3127-3130 [PMID: 20852027 DOI: 10.2337/db10-0554]
35 **Davis JN**, Lê KA, Walker RW, Vikman S, Spruijt-Metz D, Weigensberg MJ, Allayee H, Goran MI. Increased hepatic fat in overweight Hispanic youth influenced by interaction between genetic variation in PNPLA3 and high dietary carbohydrate and sugar consumption. *Am J Clin Nutr* 2010; **92**: 1522-1527 [PMID: 20962157 DOI: 10.3945/ajcn.2010.30185]
36 **Lin YC**, Chang PF, Hu FC, Yang WS, Chang MH, Ni YH. A common variant in the PNPLA3 gene is a risk factor for non-alcoholic fatty liver disease in obese Taiwanese children. *J Pediatr* 2011; **158**: 740-744 [PMID: 21168155 DOI: 10.1016/j.jpeds.2010.11.016]
37 **Viitasalo A**, Pihlajamaki J, Lindi V, Atalay M, Kaminska D, Joro R, Lakka TA. Associations of I148M variant in PNPLA3 gene with plasma ALT levels during 2-year follow-up in normal weight and overweight children: the PANIC Study. *Pediatr Obes* 2014; Epub ahead of print [PMID: 24916969 DOI: 10.1111/ijpo.234]
38 **Browning JD**, Szczepaniak LS, Dobbins R, Nuremberg P, Horton JD, Cohen JC, Grundy SM, Hobbs HH. Prevalence of hepatic steatosis in an urban population in the United States: impact of ethnicity. *Hepatology* 2004; **40**: 1387-1395 [PMID: 15565570]
39 **Petersen KF**, Dufour S, Feng J, Befroy D, Dziura J, Dalla Man C, Cobelli C, Shulman GI. Increased prevalence of insulin resistance and nonalcoholic fatty liver disease in Asian-Indian men. *Proc Natl Acad Sci USA* 2006; **103**: 18273-18277 [PMID: 17114290]
40 **Wagenknecht LE**, Palmer ND, Bowden DW, Rotter JI, Norris JM, Ziegler J, Chen YD, Haffner S, Scherzinger A, Langefeld CD. Association of PNPLA3 with non-alcoholic fatty liver disease in a minority cohort: the Insulin Resistance Atherosclerosis Family Study. *Liver Int* 2011; **31**: 412-416 [PMID: 21281435 DOI: 10.1111/j.1478-3231.2010.02444.x]
41 **Marchesini G**, Brizi M, Bianchi G, Tomassetti S, Bugianesi E, Lenzi M, McCullough AJ, Natale S, Forlani G, Melchionda N. Nonalcoholic fatty liver disease: a feature of the metabolic syndrome. *Diabetes* 2001; **50**: 1844-1850 [PMID: 11473047]
42 **Day CP**. From fat to inflammation. *Gastroenterology* 2006; **130**: 207-210 [PMID: 16401483]
43 **Sevastianova K**, Kotronen A, Gastaldelli A, Perttilä J, Hakkarainen A, Lundbom J, Suojanen L, Orho-Melander M, Lundbom N, Ferrannini E, Rissanen A, Olkkonen VM, Yki-Järvinen H. Genetic variation in PNPLA3 (adiponutrin) confers sensitivity to weight loss-induced decrease in liver fat in humans. *Am J Clin Nutr* 2011; **94**: 104-111 [PMID: 21525193 DOI: 10.3945/ajcn.111.012369]
44 **Kantartzis K**, Peter A, Machicao F, Machann J, Wagner S, Königsrainer I, Königsrainer A, Schick F, Fritsche A, Häring HU, Stefan N. Dissociation between fatty liver and insulin resistance in humans carrying a variant of the patatin-like phospholipase 3 gene. *Diabetes* 2009; **58**: 2616-2623 [PMID: 19651814 DOI: 10.2337/db09-0279]
45 **Petit JM**, Guiu B, Masson D, Duvillard L, Jooste V, Buffier P, Terriat B, Bouillet B, Brindisi MC, Loffroy R, Robin I, Hillon P, Cercueil JP, Verges B. Specifically PNPLA3-mediated accumulation of liver fat in obese patients with type 2 diabetes. *J Clin Endocrinol Metab* 2010; **95**: E430-E436 [PMID: 20826584 DOI: 10.1210/jc.2010-0814]
46 **Romeo S**, Sentinelli F, Cambuli VM, Incani M, Congiu T, Matta V, Pilia S, Huang-Doran I, Cossu E, Loche S, Baroni MG. The 148M allele of the PNPLA3 gene is associated with indices of liver damage early in life. *J Hepatol* 2010; **53**: 335-338 [PMID: 20546964 DOI: 10.1016/j.jhep.2010.02.034]
47 **Santoro N**, Kursawe R, D'Adamo E, Dykas DJ, Zhang CK, Bale AE, Calí AM, Narayan D, Shaw MM, Pierpont B, Savoye M, Lartaud D, Eldrich S, Cushman SW, Zhao H, Shulman GI, Caprio S. A common variant in the patatin-like phospholipase 3 gene (PNPLA3) is associated with fatty liver disease in obese children and adolescents. *Hepatology* 2010; **52**: 1281-1290 [PMID: 20803499 DOI: 10.1002/hep.23832]
48 **Chiang DJ**, Roychowdhury S, Bush K, McMullen MR, Pisano S, Niese K, Olman MA, Pritchard MT, Nagy LE. Adenosine 2A receptor antagonist prevented and reversed liver fibrosis in a mouse model of ethanol-exacerbated liver fibrosis. *PLoS One* 2013; **8**: e69114 [PMID: 23874883 DOI: 10.1371/journal.pone.0069114]
49 **Singal AG**, Manjunath H, Yopp AC, Beg MS, Marrero JA, Gopal P, Waljee AK. The effect of PNPLA3 on fibrosis progression and development of hepatocellular carcinoma: a meta-analysis. *Am J Gastroenterol* 2014; **109**: 325-334 [PMID: 24445574 DOI: 10.1038/ajg.2013.476]
50 **Ray K**. Liver: hepatic stellate cells hold the key to liver fibrosis. *Nat Rev Gastroenterol Hepatol* 2014; **11**: 74 [PMID: 24322897 DOI: 10.1038/nrgastro.2013.244]
51 **Scales SJ**, de Sauvage FJ. Mechanisms of Hedgehog pathway activation in cancer and implications for therapy. *Trends Pharmacol Sci* 2009; **30**: 303-312 [PMID: 19443052 DOI: 10.1016/j.tips.2009.03.007]
52 **Omenetti A**, Choi S, Michelotti G, Diehl AM. Hedgehog signaling in the liver. *J Hepatol* 2011; **54**: 366-373 [PMID: 21093090 DOI: 10.1016/j.jhep.2010.10.003]
53 **Guy CD**, Suzuki A, Zdanowicz M, Abdelmalek MF, Burchette J, Unalp A, Diehl AM. Hedgehog pathway activation parallels histologic severity of injury and fibrosis in human nonalcoholic fatty liver disease. *Hepatology* 2012; **55**: 1711-1721 [PMID: 22213086 DOI: 10.1002/hep.25559]
54 **Friedman SL**. Liver fibrosis in 2012: Convergent pathways that cause hepatic fibrosis in NASH. *Nat Rev Gastroenterol Hepatol* 2013; **10**: 71-72 [PMID: 23296246 DOI: 10.1038/nrgastro.2012.256]
55 **Swiderska-Syn M**, Suzuki A, Guy CD, Schwimmer JB, Abdelmalek MF, Lavine JE, Diehl AM. Hedgehog pathway and pediatric nonalcoholic fatty liver disease. *Hepatology* 2013; **57**: 1814-1825 [PMID: 23300059 DOI: 10.1002/hep.26230]
56 **Choi SS**, Omenetti A, Witek RP, Moylan CA, Syn WK, Jung Y, Yang L, Sudan DL, Sicklick JK, Michelotti GA, Rojkind M, Diehl AM. Hedgehog pathway activation and epithelial-to-mesenchymal transitions during myofibroblastic transformation of rat hepatic cells in culture and cirrhosis. *Am J Physiol Gastrointest Liver Physiol* 2009; **297**: G1093-G1106 [PMID: 19815628 DOI: 10.1152/ajpgi.00292.2009]
57 **Swiderska-Syn M**, Syn WK, Xie G, Krüger L, Machado MV, Karaca G, Michelotti GA, Choi SS, Premont RT, Diehl AM. Myofibroblastic cells function as progenitors to regenerate murine livers after partial hepatectomy. *Gut* 2014; **63**: 1333-1344 [PMID: 24173292 DOI: 10.1136/gutjnl-2013-305962]

58 **Omenetti A**, Syn WK, Jung Y, Francis H, Porrello A, Witek RP, Choi SS, Yang L, Mayo MJ, Gershwin ME, Alpini G, Diehl AM. Repair-related activation of hedgehog signaling promotes cholangiocyte chemokine production. *Hepatology* 2009; **50**: 518-527 [PMID: 19575365 DOI: 10.1002/hep.23019]
59 **Omenetti A**, Diehl AM. Hedgehog signaling in cholangiocytes. *Curr Opin Gastroenterol* 2011; **27**: 268-275 [PMID: 21423008 DOI: 10.1097/MOG.0b013e32834550b4]

P- Reviewer: Fan JG, Fouad YM, Morales-Gonzalez JA, Mikolasevic I
S- Editor: Qi Y **L- Editor**: Cant MR **E- Editor**: Liu XM

World Journal of Gastroenterology

Submit a Manuscript: http://www.wjgnet.com/esps/
Help Desk: http://www.wjgnet.com/esps/helpdesk.aspx
DOI: 10.3748/wjg.v21.i3.803

World J Gastroenterol 2015 January 21; 21(3): 803-814
ISSN 1007-9327 (print) ISSN 2219-2840 (online)

REVIEW

Application of metagenomics in the human gut microbiome

Wei-Lin Wang, Shao-Yan Xu, Zhi-Gang Ren, Liang Tao, Jian-Wen Jiang, Shu-Sen Zheng

Wei-Lin Wang, Shao-Yan Xu, Zhi-Gang Ren, Liang Tao, Jian-Wen Jiang, Shu-Sen Zheng, Department of Hepatobiliary and Pancreatic Surgery, First Affiliated Hospital, Zhejiang University School of Medicine, Hangzhou 310003, Zhejiang Province, China

Author contributions: Wang WL and Xu SY contributed equally to the writing of the paper; Ren ZG, Tao L and Jiang JW revised the paper and prepared the figures; and Zheng SS is the supervisor of the study.

Supported by National Basic Research Program (973 Program) of China, No. 2013CB531403.

Correspondence to: Shu-Sen Zheng, PhD, MD, Department of Hepatobiliary and Pancreatic Surgery, First Affiliated Hospital, Zhejiang University School of Medicine, 79 Qingchun Road, Hangzhou 310003, Zhejiang Province, China. shusenzheng@zju.edu.cn
Telephone: +86-571-87236466
Fax: +86-571-87236466

Received: July 15, 2014
Peer-review started: July 16, 2014
First decision: September 15, 2014
Revised: September 30, 2014
Accepted: November 7, 2014
Article in press: November 11, 2014
Published online: January 21, 2015

Abstract

There are more than 1000 microbial species living in the complex human intestine. The gut microbial community plays an important role in protecting the host against pathogenic microbes, modulating immunity, regulating metabolic processes, and is even regarded as an endocrine organ. However, traditional culture methods are very limited for identifying microbes. With the application of molecular biologic technology in the field of the intestinal microbiome, especially metagenomic sequencing of the next-generation sequencing technology, progress has been made in the study of the human intestinal microbiome. Metagenomics can be used to study intestinal microbiome diversity and dysbiosis, as well as its relationship to health and disease. Moreover, functional metagenomics can identify novel functional genes, microbial pathways, antibiotic resistance genes, functional dysbiosis of the intestinal microbiome, and determine interactions and co-evolution between microbiota and host, though there are still some limitations. Metatranscriptomics, metaproteomics and metabolomics represent enormous complements to the understanding of the human gut microbiome. This review aims to demonstrate that metagenomics can be a powerful tool in studying the human gut microbiome with encouraging prospects. The limitations of metagenomics to be overcome are also discussed. Metatranscriptomics, metaproteomics and metabolomics in relation to the study of the human gut microbiome are also briefly discussed.

Key words: Human gut microbiome; Metabolomics; Metagenomics; Metaproteomics; Metatranscriptomics

Core tip: Metagenomics plays a role in understanding the human gut microbiome, including the diversity of the gut microbiome, identifying novel genes, and determining the etiology of functional dysbiosis. A combination of metagenomics, metatranscriptomics, metaproteomics and metabolomics can also promote an understanding of the functional activity of the human gut microbiome and possibly provide a new strategy for disease diagnosis and treatment.

Wang WL, Xu SY, Ren ZG, Tao L, Jiang JW, Zheng SS. Application of metagenomics in the human gut microbiome. *World J Gastroenterol* 2015; 21(3): 803-814 Available from:

URL: http://www.wjgnet.com/1007-9327/full/v21/i3/803.htm
DOI: http://dx.doi.org/10.3748/wjg.v21.i3.803

INTRODUCTION

The human gastrointestinal tract harbors an extremely complex and dynamic microbial community, including archaea, bacteria, viruses and eukaryota[1]. Most of the microorganisms residing in the gastrointestinal tract are bacteria, with a density of approximately 10^{13}-10^{14} cells/g fecal matter, in which 70% of the total microbes colonize the colon[2]. The gut microbial community plays an important role in protecting the host against pathogenic microbes[3-5], modulating immunity[6,7], regulating metabolic processes[8,9], and is regarded as a neglected endocrine organ[10]. Recently, the role of the human gut microbiome has been well reviewed[11-13].

Classical studies of the gut microbiome have been largely dependent on cultivation techniques. However, traditional culture methods only cultivate 10%-30% of gut microbiota[14-16]. With the rapid development of advanced molecular technologies such as PCR-denaturing gradient gel electrophoresis, it has been shown that the gut microbial ecosystem is far more complex than previously thought[17]. In recent years, several next-generation sequencing technologies have been developed[18,19], which further facilitate the analysis of a large number of microorganisms in different environments[20-22] and human body sites[23], including the human gut[24-26]. 16S rDNA sequence analysis and metagenomics are two effective DNA sequencing approaches, and both have been used to study uncultivated gut microbial communities. The former focuses on the sequencing of the conserved 16S rDNA gene present in all microbes[27,28], and has established a series of novel connections between intestinal microbiota composition and disease[29-31]. The research based on 16S rDNA sequence attempts to reveal "who's there?" in a given microbial community, while shotgun metagenomic sequencing can be used to answer the complementary question of "what can they do?"[32,33].

Metagenomics was first described in 1998 by Handelsman and Rodon[34,35], and became another DNA sequencing approach to study the complex gut microbial community. It aims to catalog all the genes from a community by the random sequencing of all DNA extracted from the sample[36-38]. Firstly, the total DNA of all microorganisms is extracted from fecal samples. Before being sequenced, total DNA samples are randomly sheared by a "shotgun" approach. The comprehensive sequences are then analyzed to obtain either species profiles based on phylogenetic markers (16S rDNA)[39] or genomic profiles based on whole genomes[22]. The shotgun sequence reads are filtered to obtain the high-quality sequences for the whole genomic profile by metagenomics. Based on sequence overlaps, the filtered sequences are then assembled to form longer genomic sequence contigs. Computational methods are needed to code sequences in the contigs. Data mining and database searches applying different powerful algorithms are then used to annotate genes[40]. The information obtained from the sequence-based and functional metagenomics enables a more comprehensive understanding of the structure and function of microbial communities than ever before.

METAGENOMICS IN STUDYING THE HUMAN GUT MICROBIOME

Metagenomics: Revealing the diversity of the human gut microbiome

The European project, MetaHIT[37], and the American Human Microbiome Project[25,41] have contributed to the availability of the reference gene catalog. These projects have facilitated the study of the human intestinal microbiome using metagenomics. By applying metagenomics to investigate fecal samples from 124 European individuals, the MetaHIT consortium found 3.3 million non-redundant genes in the human gut microbiome for the first time. Surprisingly, the gene set was 150 times larger than the human gene complement. Moreover, over 99% of the genes in the human gut microbial communities were bacterial, which indicated that the entire cohort harbored more than 1000 bacterial species[37]. However, the number of genes in the human gut microbiome was expanded more than threefold by subsequent analyses[42,43]. These observations further completed the catalog of reference genes in the human gut microbiome.

A core human gut microbiome has also been explored[44]. The average human intestinal microbiome is now better defined and comprises approximately 160 bacterial species in each individual[37]. Moreover, on average, individual microbiota could have long-term stability[45,46]. By applying low-error 16S ribosomal RNA amplicon sequencing and whole-genome sequencing methods to characterize bacterial strain composition in the fecal microbiota of 37 patients in the United States, Jeremiah and colleagues[45] found that on average, their individual microbiota was remarkably stable and 60% of strains remained over the course of five years. From the in-depth profiling of metagenomic datasets derived from fecal metagenomes of healthy individuals, the human gut has been postulated to consist of three enterotypes, typified by the relative dominance of particular groups of organisms: *Prevotella*, *Ruminococcus* and *Bactericides* spp[47].

In addition, studies using different methods including metagenomics have found a series of factors that can influence the composition and diversity of the gut microbiome, such as diet[48-50], age[51,52], geography[51,53], drugs[54,55], and environmental substances[56]. For example, a study found that due to the difference in long-term dietary habits, human gut microbiome abundance and proportions varied between United States individuals. Furthermore, species composition, but not enterotype, in these subjects was affected by short-term changes in diet[57]. In the MARS-500 study, Mardanov *et al*[58] found dynamic changes in the gut microbiome in participants

using metagenomic analysis.

Functional metagenomics: Discovering novel genes and microbial pathways

In recent years, due to the rapidly developing computational methods critical for the analysis of metagenomic data and earlier surveys performed on marine and other environmental microbiome, more and more studies have focused on functional metagenomics of the human gut microbiome[37,38,51,59]. *Escherichia coli* (*E. coli*) is the most commonly used host for functional metagenomics, and genes from a large diversity of bacteria can be expressed within *E. coli*[33]. Furthermore, other species such as *Streptomyces*, *Bacillus subtilis* and *Lactococcus lactis* can also be used to promote the heterologous expression of Gram-positive bacterial DNA[60].

Hehemann and colleagues[61] found genes encoding the enzymes porphyranase and agarase from the gut microbiome in Japanese individuals, but not in North Americans. Interestingly, the marine Bacteroidetes are widely found in seaweed, and many Japanese eat seaweed regularly[61], thus it is likely that these functions were acquired from these organisms by lateral gene transfer.

The catabolism of dietary fibers is important for human health[32]. Carbohydrate active enzymes (CAZymes), produced by human intestinal microorganisms, can degrade components of dietary fiber into metabolizable monosaccharides and disaccharides. However, before metagenomics were used to study the human gut microbiome, the study of CAZymes was restricted to cultivated bacterial species. Several metagenomics studies focusing on the gut microbiome determined the diversity of CAZymes, revealing the human gut microbiome to be a surprisingly rich source of carbohydrate active enzymes[36,38,62,63]. In addition, Tasse *et al*[64] detected novel CAZymes using functional metagenomics on human gut microbial genes. The function-based screening of intestinal metagenome libraries also identified a large genetic repertoire of genes encoding bile-salt hydrolase enzymes[65]. These functions were selectively enriched in intestinal microorganisms. Furthermore, novel β-glucuronidase activity, dominant in healthy adults and children, from Firmicutes was revealed by the functional screening of large insert metagenomic libraries of *E. coli* clones independent of culturability[66].

Recently Vital and colleagues[67] performed an extensive analysis of butyrate-producing pathways and individual genes by screening thousands of sequenced bacterial genomes from the Integrated Microbial Genome database. They found that the genomes of 225 bacteria had the potential to produce butyrate, including many previously unknown candidates. Most candidates belonged to distinct families within Firmicutes[67]. These authors also used the established gene catalog to screen for butyrate synthesis pathways in 15 metagenomes obtained from the fecal samples of healthy individuals. The results revealed that a high percentage of total genomes exhibited a butyrate-producing pathway, and the most prevalent was the acetyl-coenzyme A pathway, followed by the lysine pathway[67].

Functional metagenomics: Investigating antibiotic-resistance genes

Many bacterial infections are becoming more and more difficult to treat, partly due to the increasing antibiotic resistance of human pathogens[68-70]. Recent studies have revealed that some human commensal microbiota harbor numerous antibiotic-resistance genes (ARGs), which have led to the human gut-associated resistome[71,72]. Thus, it is important to understand the contribution of the whole microbiota of particular systems to antibiotic resistance[73].

The first population-level analysis of resistance gene prevalence in the human gut was performed by Seville *et al*[74]. Interestingly, they found that several of the tested genes were common in human microbiomes using microarray probes to identify 14 tetracycline and macrolide-resistance genes in the fecal and saliva samples of 20 healthy volunteers from England, Finland, France, Italy, Norway, and Scotland. However, the fecal samples from France and Italy showed significantly higher levels of some tetracycline and erythromycin genes than those of the samples from Scandinavia or the United Kingdom.

Compared with previous methods, the metagenomic approach is a powerful tool that can help us to gain a more comprehensive understanding of the ARGs in human gut microbes. By analyzing the genomic content of a microorganism, it is possible to predict the resistance phenotype and adapt a specific treatment. Functional metagenomics can be used to isolate completely novel ARGs from the non-cultivable fraction of the microbiota and reveal the complex background context in which antibiotic resistance evolves in both microbial and host communities.

By employing fecal metagenomic data from different countries, studies have confirmed that resistance gene prevalence exists in the human gut microbiome and the distribution of ARGs are different between countries[75,76]. Moreover, Forslund *et al*[75] found associations between transposable elements in the tested genes, which is consistent with the finding that ARGs can be exchanged among gastrointestinal microbes[77], particularly during host stress[78].

Sommer *et al*[72] screened the gene inserts that caused resistance in *E. coli* to 13 different antibiotics by performing functional metagenomics screening of fecal and oral samples from two human donors. They then compared these genes with previous homologs in pathogens and found a considerable diversity of ARGs in the microbes. Cheng *et al*[79] first applied the strategy of screening a relatively large-insert fosmid library generated from the gut microbiota of four healthy candidates. The library was used to screen for ARGs against seven antibiotics. The authors identified a variety of previously unknown resistance determinants and found that only the N-terminus conferred kanamycin resistance following a functional

study on the new kanamycin resistance gene.

Recently, Moore *et al*[80] used functional metagenomics in fecal microbiota from 22 healthy infants and children to identify ARGs. They not only identified three novel resistance genes, but also reported their results on resistance to folate-synthesis inhibitors conferred by a predicted Nudix hydrolase, which was an important part of the folate-synthesis pathway. In addition, their functional metagenomic investigations demonstrated that fecal resistomes of healthy children had a higher diversity than previously suspected.

Metagenomics: Finding functional dysbiosis

As reported, dysbiosis of the intestinal microbial community is associated with some diseases, including inflammatory bowel disease[81-83], obesity[38,84-86], diabetes[87-89], allergy[90,91], irritable bowel syndrome (IBS)[92], colorectal cancer[93-96], liver cirrhosis[97-99], nonalcoholic steatohepatitis[100,101], neurodevelopmental disorders[102,103], cardiovascular disorders[104], cholesterol gallstones[105], diarrhea[106], malnutrition[107], kidney disease[108], and colon polyps[109]. Recently, in a metagenomic analysis of the stool microbiome in patients receiving allogeneic stem cell transplantation, Holler *et al*[110] found a relative shift from a predominance of commensal bacteria toward *Enterococci*, which was particularly marked in patients who subsequently developed or suffered from active gastrointestinal graft-*vs*-host disease.

In addition to identifying dysbiosis of the human gut microbiome in some diseases, metagenomics can determine novel changes in microbial functions. A study using the metagenomic approach in patients with type 2 diabetes performed by Qin *et al*[87] found a moderate variation in the microbial composition of the gut between cases and controls. Microbial functions conferring sulfate reduction and oxidative stress resistance were also more abundant in patients with type 2 diabetes than in healthy controls. Similarly, Wei *et al*[98] analyzed the fecal microbiota of 20 hepatitis B liver cirrhosis patients and 20 healthy controls using metagenomic methods, and found an obvious change in fecal microbiota between the two groups. Importantly, compared with the controls, functional diversity was significantly reduced in the fecal microbiota in the patients. In addition, the fecal microbiota in the patients showed abundant metabolism of glutathione, gluconeogenesis, branched-chain amino acids, nitrogen and lipids, but a decrease in the level of aromatic amino acids, bile acid and cell cycle related metabolism.

Metagenomics can also be used to determine the interactions between intestinal bacteria and the host. Intestinal bacteria play an integral role in human health. However, the possible mechanisms related to the interactions between intestinal bacteria and the host are not understood. Lakhdari *et al*[111] used high-throughput screening technology to investigate intestinal microbial pathways, and found that *E. coli* metagenomic clones could modulate intestinal mucosal proliferation by activating the nuclear factor-κB pathway in epithelial cells[112-114]. Recently, by applying functional metagenomics, Dobrijevic *et al*[115] found that secreted and surface-exposed proteins from Gram-positive bacteria in the human gut microbiota played a role in immune modulation.

Metagenomics is also helpful in screening plasmid-encoding elements, especially with the improvement of methods for purifying high-quality and high-yield plasmid DNA[116]. The plasmid harbors numerous mobile genetic elements. A profound understanding of the mobile genetic elements associated with the human gut microbiota is meaningful as they can reflect the co-evolution of host and microbe in the human gut[32].

Jones and Marchesi[117] isolated novel plasmids from the human gut microbiota and revealed that some crucial genes were enriched in the human gut compared with other systems using the culture independent transposon-aided capture system. Recently, based on metagenomic analysis, several studies indicated that the horizontal gene could transfer between phylogenetically distant bacterial groups[64,65,118]. However, the triggers that promote this gene exchange are not known. Smillie *et al*[119] showed that ecology could be the main driver of gene exchange.

LIMITATIONS IN APPLYING METAGENOMICS

From the above findings (Figure 1), metagenomics have been shown to be an incredibly powerful technology in studying the human gut microbiome. However, there are still some limitations in the use of metagenomics, as shown in Figure 2. Firstly, it is not possible to identify microbial expression. Secondly, as metagenomics require much higher sequence coverage than 16S rDNA sequence analysis[120], the costs and time involved in DNA sequencing projects for gut metagenomics are far greater than those of 16S rDNA sequence analysis. Thirdly, to obtain high coverage required for metagenomics, a sufficient quantity and high quality of DNA samples are essential. Although precautionary steps are performed, human contaminants are found in 50%-90% of sequences[24]. Different DNA extraction kits and laboratories also have an impact on the assessment of human gut microbiota[121]. Comparing data across studies that use different bacterial DNA extraction methods is difficult[122]. Fourthly, to perform a metagenomic study successfully, the quality of the underlying functional annotations of metagenomic sequence fragments is very important. However, a significant proportion of data cannot be assigned a function due to a lack of close matches in reference databases[37]. For viral data, this situation is particularly severe, as 80% or more of sequence reads lack known matches[123].

Millions of sequences in each sample are required for functional gene analysis of a complex microbial community. It is difficult to identify and improve the accuracy of information derived from the relatively short gene fragments generated by next-generation sequencing,

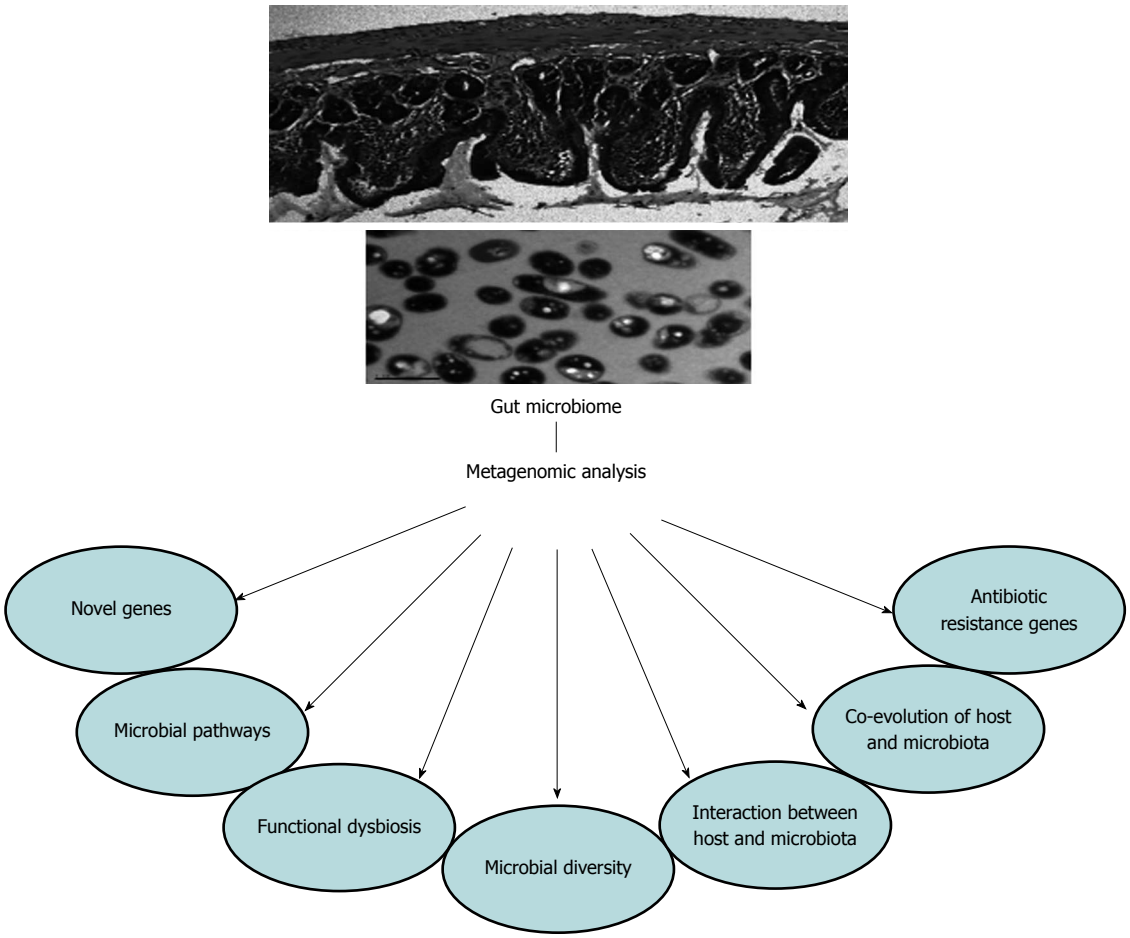

Figure 1 Application of metagenomics in the human gut microbiome. In studying the human gut microbiome, metagenomic analysis has the potential to provide sufficient information in the following research areas: The detection of microbial composition and diversity, novel genes, microbial pathways, functional dysbiosis, antibiotic resistance genes, and the determination of interactions and co-evolution between microbiota and host.

due to the many bioinformatics challenges proposed by the huge metagenomic shotgun sequencing. It is also difficult to assign function unambiguously based on sequence similarity alone, which may cause misannotation[124]. Moreover, when there are less abundant members of the microbiome or a community containing many closely related species, it may be difficult to assemble genomes[125]. This can lead to a situation where, even if a function can be ascertained, it may be a challenge to assign it to specific species within the microbial community. In addition, DNA is the material used in metagenomic sequencing, and the expression of each functional gene in a sample in a given environment is very difficult to determine.

METATRANSCRIPTOMICS, METAPROTEOMICS AND METABOLOMICS

Metagenomics is an extremely powerful tool that can be used to describe the genetic potential of the microorganisms present in a given environment. However, it has a very limited function in revealing their activity or gene expression. With the rapid development of metatranscriptomics[126], metaproteomics[127] and metabolomics[128], the functional activity of a microbial community can be identified.

Metatranscriptomic sequencing can be used to determine the activity of genes in a defined environment. Gosalbes *et al*[129] used metatranscriptomic analysis of fecal microbiomes from ten healthy humans, and found that carbohydrate metabolism, energy production and synthesis of cellular components were the main functional roles of the gut microbiota. In contrast, amino acid and lipid metabolism were reduced in the metatranscriptome.

Metatranscriptomics also has some limitations. Firstly, it is very difficult to obtain high-quality and sufficient amounts of RNA from environmental samples. Secondly, it is a challenge to separate the mRNA of interest from the more abundant types of RNA such as rRNA. Thirdly, the short half-life of mRNA leads to difficulty in the detection of rapid and short-term responses to environmental changes[130]. Fourthly, the reference databases are insufficient.

An analysis of proteins is also important to understand microbial functions. Recently, a study demonstrated that the fecal metaproteome in healthy adults was subject-specific and relatively stable over a one-year period[131]. In addition, some core functions, including carbohydrate metabolism

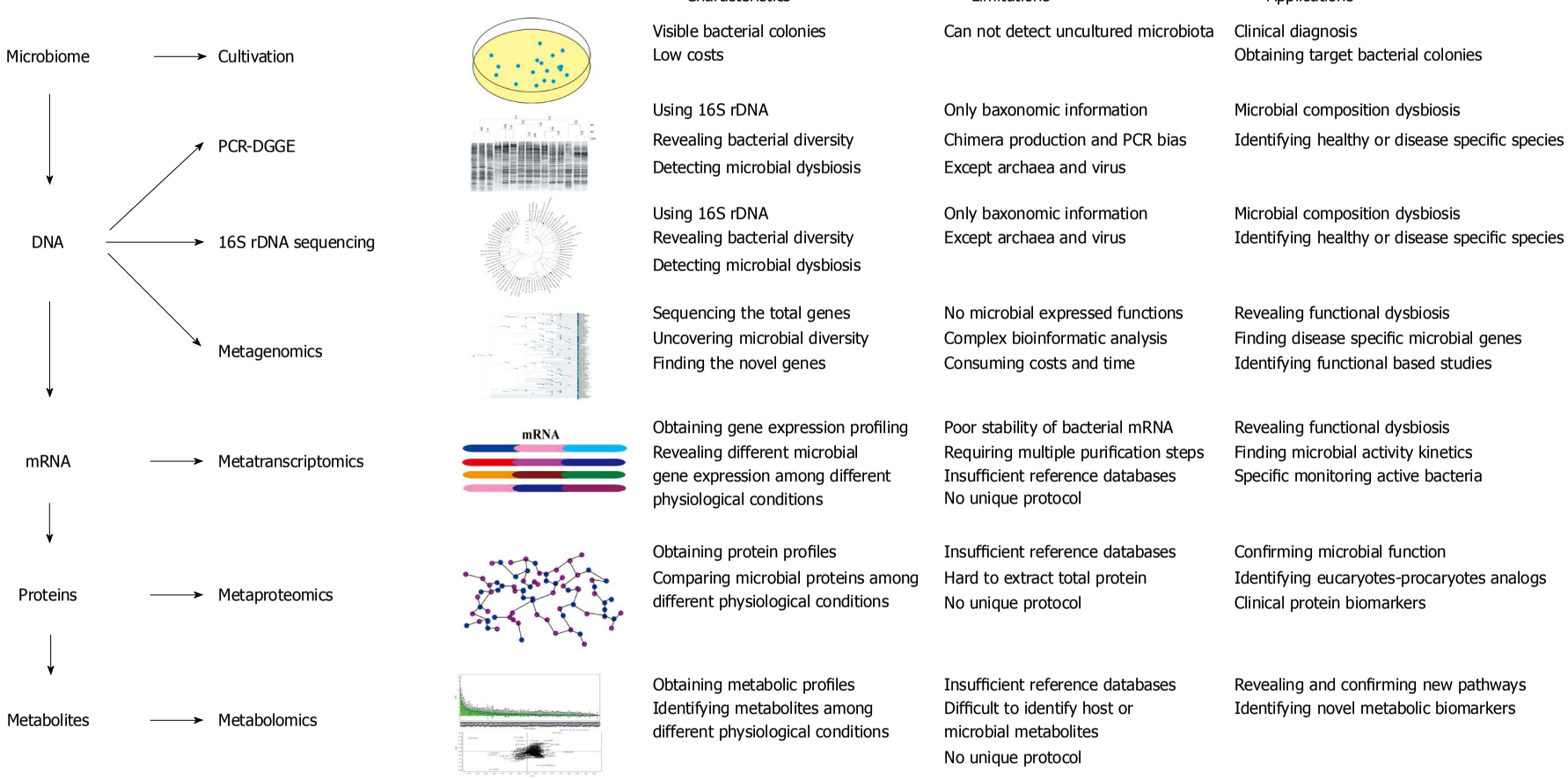

Figure 2 Comparison of different gut microbiome study approaches. The characteristics, limitations, and applications of different gut microbiome approaches from cultivation to metabolomics are presented. DGGE: Denaturing gradient gel electrophoresis.

and transport, were also determined. However, similar to metatranscriptomics, the ability to assign functional classifications is limited due to insufficient reference databases. It is a significant challenge to disentangle the complex array of proteins produced by the intestinal microbiota.

Currently, metabolomics is increasingly used to study the gut microbiome[132]. Some human intestinal disorders, such as colorectal cancer, inflammatory bowel disease and IBS, have been studied using metabolomics[133-136]. For instance, a study on patients with ulcerative colitis and IBS revealed that, compared with controls, the patients with ulcerative colitis had increased quantities of taurine and cadaverine. Importantly, a higher bile acid concentration and lower levels of branched-chain fatty acids were found in IBS patients[136]. Moreover, no significant changes were found in short-chain fatty acid and amino acid concentrations. However, some limitations restrict the development and clinical application of metabolomics. On the one hand, the metabolomics databases are incomplete and insufficient, and there are many metabolites that are not included

in the databases. On the other hand, the obtained metabolites are mixed, thus it is very difficult to identify the information from the host and the microbial metabolites.

As shown in Figure 2, though there are some limitations with these approaches, they have significant potential clinical applications. The combination of the meta-omics may be sufficiently powerful to elucidate the ecologic roles of the human gut microbiome[137].

CONCLUSION

In conclusion, metagenomics can not only identify the diversity of the human gut microbiome, but can also reveal new genes and microbial pathways, and uncover functional dysbiosis. The application of metagenomics has huge potential in revealing the mechanisms and correlations between the human intestinal microbiome and diseases. However, metagenomics also has limitations and requires improvement[138].

With the rapid development and application of metagenomics, as well as metatranscriptomics, metaproteomics and metabolomics, it is possible to identify new microbial diagnostic markers that will provide early diagnosis and novel treatments. Maximizing the contribution of microorganisms and identifying more probiotics are also very promising. Based on an increased understanding of the role of the human microbiome in diseases and their interactions, as well as inter-individual differences and physiologic parameters, the exploration of personalized medicine will progress immensely. In addition, it is possible to explore new antibiotics that target antibiotic resistance microbiomes based on a profound understanding of ARGs in the gut microbiome.

Current metagenomic studies of the human gut microbiome have been performed in limited cohorts, thus, it is necessary to enhance our understanding of the human gut microbiome by investigating human populations from different countries, for longer periods, and include multiple age groups[32], and various disease stages. A study of the characteristics of the human gut microbiome in different disease stages would help us understand the relationship between the gut microbiome and disease development, and thus would help to establish the optimal strategies for preventing, improving and even reversing diseases.

As metagenomics still has some limitations, it is necessary to combine other microbiome approaches, including cultivation methods, with a study of metagenomics in the intestinal microbiome. This will ensure that the results are more accurate and convincing. Recently, several studies have successfully used this combination and obtained meaningful findings[56,139-141]. To overcome the limitations of metagenomics, it is also important to create a unified microbial DNA extraction method, improve computational algorithms, and complete the reference databases.

The application of metagenomic technology in the human gut microbiome is in its infancy. However, it has been used in other environments, including soil and the sea, for some time. Thus, the success of applying metagenomic technology in studying these environments can be followed by further study in the human gut microbiome. In addition, the human gut harbors not only bacteria, but also eukaryota and viruses. To date, few studies on eukaryota and viruses using the metagenomics approach have been carried out, thus, the future study of the human gut microbiome using the metagenomics approach is promising and more efforts are urgently needed.

REFERENCES

1 **Weinstock GM**. Genomic approaches to studying the human microbiota. *Nature* 2012; **489**: 250-256 [PMID: 22972298 DOI: 10.1038/nature11553]

2 **Ley RE**, Turnbaugh PJ, Klein S, Gordon JI. Microbial ecology: human gut microbes associated with obesity. *Nature* 2006; **444**: 1022-1023 [PMID: 17183309 DOI: 10.1038/4441022a]

3 **Endt K**, Stecher B, Chaffron S, Slack E, Tchitchek N, Benecke A, Van Maele L, Sirard JC, Mueller AJ, Heikenwalder M, Macpherson AJ, Strugnell R, von Mering C, Hardt WD. The microbiota mediates pathogen clearance from the gut lumen after non-typhoidal Salmonella diarrhea. *PLoS Pathog* 2010; **6**: e1001097 [PMID: 20844578 DOI: 10.1371/journal.ppat.1001097]

4 **Fukuda S**, Toh H, Taylor TD, Ohno H, Hattori M. Acetate-producing bifidobacteria protect the host from enteropathogenic infection via carbohydrate transporters. *Gut Microbes* 2012; **3**: 449-454 [PMID: 22825494 DOI: 10.4161/gmic.21214]

5 **Fukuda S**, Toh H, Hase K, Oshima K, Nakanishi Y, Yoshimura K, Tobe T, Clarke JM, Topping DL, Suzuki T, Taylor TD, Itoh K, Kikuchi J, Morita H, Hattori M, Ohno H. Bifidobacteria can protect from enteropathogenic infection through production of acetate. *Nature* 2011; **469**: 543-547 [PMID: 21270894 DOI: 10.1038/nature09646]

6 **Maynard CL**, Elson CO, Hatton RD, Weaver CT. Reciprocal interactions of the intestinal microbiota and immune system. *Nature* 2012; **489**: 231-241 [PMID: 22972296 DOI: 10.1038/nature11551]

7 **Viaud S**, Saccheri F, Mignot G, Yamazaki T, Daillère R, Hannani D, Enot DP, Pfirschke C, Engblom C, Pittet MJ, Schlitzer A, Ginhoux F, Apetoh L, Chachaty E, Woerther PL, Eberl G, Bérard M, Ecobichon C, Clermont D, Bizet C, Gaboriau-Routhiau V, Cerf-Bensussan N, Opolon P, Yessaad N, Vivier E, Ryffel B, Elson CO, Doré J, Kroemer G, Lepage P, Boneca IG, Ghiringhelli F, Zitvogel L. The intestinal microbiota modulates the anticancer immune effects of cyclophosphamide. *Science* 2013; **342**: 971-976 [PMID: 24264990 DOI: 10.1126/science.1240537]

8 **Tremaroli V**, Bäckhed F. Functional interactions between the gut microbiota and host metabolism. *Nature* 2012; **489**: 242-249 [PMID: 22972297 DOI: 10.1038/nature11552]

9 **Cani PD**. Metabolism in 2013: The gut microbiota manages host metabolism. *Nat Rev Endocrinol* 2014; **10**: 74-76 [PMID: 24322652 DOI: 10.1038/nrendo.2013.240]

10 **Clarke G**, Stilling RM, Kennedy PJ, Stanton C, Cryan JF, Dinan TG. Minireview: Gut microbiota: the neglected endocrine organ. *Mol Endocrinol* 2014; **28**: 1221-1238 [PMID: 24892638 DOI: 10.1210/me.2014-1108]

11 **Sommer F**, Bäckhed F. The gut microbiota--masters of host development and physiology. *Nat Rev Microbiol* 2013; **11**: 227-238 [PMID: 23435359 DOI: 10.1038/nrmicro2974]

12 **Clemente JC**, Ursell LK, Parfrey LW, Knight R. The impact

of the gut microbiota on human health: an integrative view. *Cell* 2012; **148**: 1258-1270 [PMID: 22424233 DOI: 10.1016/j.cell.2012.01.035]
13 **Owyang C**, Wu GD. The gut microbiome in health and disease. *Gastroenterology* 2014; **146**: 1433-1436 [PMID: 24675436 DOI: 10.1053/j.gastro.2014.03.032]
14 **Suau A**, Bonnet R, Sutren M, Godon JJ, Gibson GR, Collins MD, Doré J. Direct analysis of genes encoding 16S rRNA from complex communities reveals many novel molecular species within the human gut. *Appl Environ Microbiol* 1999; **65**: 4799-4807 [PMID: 10543789]
15 **Sokol H**, Seksik P. The intestinal microbiota in inflammatory bowel diseases: time to connect with the host. *Curr Opin Gastroenterol* 2010; **26**: 327-331 [PMID: 20445446 DOI: 10.1097/MOG.0b013e328339536b]
16 **Tannock GW**. Molecular assessment of intestinal microflora. *Am J Clin Nutr* 2001; **73**: 410S-414S [PMID: 11157350]
17 **Eckburg PB**, Bik EM, Bernstein CN, Purdom E, Dethlefsen L, Sargent M, Gill SR, Nelson KE, Relman DA. Diversity of the human intestinal microbial flora. *Science* 2005; **308**: 1635-1638 [PMID: 15831718 DOI: 10.1126/science.1110591]
18 **Shendure J**, Ji H. Next-generation DNA sequencing. *Nat Biotechnol* 2008; **26**: 1135-1145 [PMID: 18846087 DOI: 10.1038/nbt1486]
19 **Fuller CW**, Middendorf LR, Benner SA, Church GM, Harris T, Huang X, Jovanovich SB, Nelson JR, Schloss JA, Schwartz DC, Vezenov DV. The challenges of sequencing by synthesis. *Nat Biotechnol* 2009; **27**: 1013-1023 [PMID: 19898456 DOI: 10.1038/nbt.1585]
20 **Venter JC**, Remington K, Heidelberg JF, Halpern AL, Rusch D, Eisen JA, Wu D, Paulsen I, Nelson KE, Nelson W, Fouts DE, Levy S, Knap AH, Lomas MW, Nealson K, White O, Peterson J, Hoffman J, Parsons R, Baden-Tillson H, Pfannkoch C, Rogers YH, Smith HO. Environmental genome shotgun sequencing of the Sargasso Sea. *Science* 2004; **304**: 66-74 [PMID: 15001713 DOI: 10.1126/science.1093857]
21 **Tyson GW**, Chapman J, Hugenholtz P, Allen EE, Ram RJ, Richardson PM, Solovyev VV, Rubin EM, Rokhsar DS, Banfield JF. Community structure and metabolism through reconstruction of microbial genomes from the environment. *Nature* 2004; **428**: 37-43 [PMID: 14961025 DOI: 10.1038/nature02340]
22 **Tringe SG**, von Mering C, Kobayashi A, Salamov AA, Chen K, Chang HW, Podar M, Short JM, Mathur EJ, Detter JC, Bork P, Hugenholtz P, Rubin EM. Comparative metagenomics of microbial communities. *Science* 2005; **308**: 554-557 [PMID: 15845853 DOI: 10.1126/science.1107851]
23 **Ding T**, Schloss PD. Dynamics and associations of microbial community types across the human body. *Nature* 2014; **509**: 357-360 [PMID: 24739969 DOI: 10.1038/nature13178]
24 **Human Microbiome Project Consortium**. A framework for human microbiome research. *Nature* 2012; **486**: 215-221 [PMID: 22699610 DOI: 10.1038/nature11209]
25 **Human Microbiome Project Consortium**. Structure, function and diversity of the healthy human microbiome. *Nature* 2012; **486**: 207-214 [PMID: 22699609 DOI: 10.1038/nature11234]
26 **Tyakht AV**, Kostryukova ES, Popenko AS, Belenikin MS, Pavlenko AV, Larin AK, Karpova IY, Selezneva OV, Semashko TA, Ospanova EA, Babenko VV, Maev IV, Cheremushkin SV, Kucheryavyy YA, Shcherbakov PL, Grinevich VB, Efimov OI, Sas EI, Abdulkhakov RA, Abdulkhakov SR, Lyalyukova EA, Livzan MA, Vlassov VV, Sagdeev RZ, Tsukanov VV, Osipenko MF, Kozlova IV, Tkachev AV, Sergienko VI, Alexeev DG, Govorun VM. Human gut microbiota community structures in urban and rural populations in Russia. *Nat Commun* 2013; **4**: 2469 [PMID: 24036685 DOI: 10.1038/ncomms3469]
27 **Cole JR**, Chai B, Farris RJ, Wang Q, Kulam-Syed-Mohideen AS, McGarrell DM, Bandela AM, Cardenas E, Garrity GM, Tiedje JM. The ribosomal database project (RDP-II): introducing myRDP space and quality controlled public data. *Nucleic Acids Res* 2007; **35**: D169-D172 [PMID: 17090583 DOI: 10.1093/nar/gkl889]
28 **Woese CR**, Fox GE. Phylogenetic structure of the prokaryotic domain: the primary kingdoms. *Proc Natl Acad Sci USA* 1977; **74**: 5088-5090 [PMID: 270744]
29 **Blaser M**, Bork P, Fraser C, Knight R, Wang J. The microbiome explored: recent insights and future challenges. *Nat Rev Microbiol* 2013; **11**: 213-217 [PMID: 23377500 DOI: 10.1038/nrmicro2973]
30 **Cho I**, Blaser MJ. The human microbiome: at the interface of health and disease. *Nat Rev Genet* 2012; **13**: 260-270 [PMID: 22411464 DOI: 10.1038/nrg3182]
31 **Ren Z**, Cui G, Lu H, Chen X, Jiang J, Liu H, He Y, Ding S, Hu Z, Wang W, Zheng S. Liver ischemic preconditioning (IPC) improves intestinal microbiota following liver transplantation in rats through 16s rDNA-based analysis of microbial structure shift. *PLoS One* 2013; **8**: e75950 [PMID: 24098410 DOI: 10.1371/journal.pone.0075950]
32 **Lepage P**, Leclerc MC, Joossens M, Mondot S, Blottière HM, Raes J, Ehrlich D, Doré J. A metagenomic insight into our gut's microbiome. *Gut* 2013; **62**: 146-158 [PMID: 22525886 DOI: 10.1136/gutjnl-2011-301805]
33 **Handelsman J**. Metagenomics: application of genomics to uncultured microorganisms. *Microbiol Mol Biol Rev* 2004; **68**: 669-685 [PMID: 15590779 DOI: 10.1128/MMBR.68.4.669-685.2004]
34 **Handelsman J**, Rondon MR, Brady SF, Clardy J, Goodman RM. Molecular biological access to the chemistry of unknown soil microbes: a new frontier for natural products. *Chem Biol* 1998; **5**: R245-R249 [PMID: 9818143]
35 **Rondon MR**, Raffel SJ, Goodman RM, Handelsman J. Toward functional genomics in bacteria: analysis of gene expression in Escherichia coli from a bacterial artificial chromosome library of Bacillus cereus. *Proc Natl Acad Sci USA* 1999; **96**: 6451-6455 [PMID: 10339608]
36 **Gill SR**, Pop M, Deboy RT, Eckburg PB, Turnbaugh PJ, Samuel BS, Gordon JI, Relman DA, Fraser-Liggett CM, Nelson KE. Metagenomic analysis of the human distal gut microbiome. *Science* 2006; **312**: 1355-1359 [PMID: 16741115 DOI: 10.1126/science.1124234]
37 **Qin J**, Li R, Raes J, Arumugam M, Burgdorf KS, Manichanh C, Nielsen T, Pons N, Levenez F, Yamada T, Mende DR, Li J, Xu J, Li S, Li D, Cao J, Wang B, Liang H, Zheng H, Xie Y, Tap J, Lepage P, Bertalan M, Batto JM, Hansen T, Le Paslier D, Linneberg A, Nielsen HB, Pelletier E, Renault P, Sicheritz-Ponten T, Turner K, Zhu H, Yu C, Li S, Jian M, Zhou Y, Li Y, Zhang X, Li S, Qin N, Yang H, Wang J, Brunak S, Doré J, Guarner F, Kristiansen K, Pedersen O, Parkhill J, Weissenbach J, Bork P, Ehrlich SD, Wang J. A human gut microbial gene catalogue established by metagenomic sequencing. *Nature* 2010; **464**: 59-65 [PMID: 20203603 DOI: 10.1038/nature08821]
38 **Turnbaugh PJ**, Hamady M, Yatsunenko T, Cantarel BL, Duncan A, Ley RE, Sogin ML, Jones WJ, Roe BA, Affourtit JP, Egholm M, Henrissat B, Heath AC, Knight R, Gordon JI. A core gut microbiome in obese and lean twins. *Nature* 2009; **457**: 480-484 [PMID: 19043404 DOI: 10.1038/nature07540]
39 **Sunagawa S**, Mende DR, Zeller G, Izquierdo-Carrasco F, Berger SA, Kultima JR, Coelho LP, Arumugam M, Tap J, Nielsen HB, Rasmussen S, Brunak S, Pedersen O, Guarner F, de Vos WM, Wang J, Li J, Doré J, Ehrlich SD, Stamatakis A, Bork P. Metagenomic species profiling using universal phylogenetic marker genes. *Nat Methods* 2013; **10**: 1196-1199 [PMID: 24141494 DOI: 10.1038/nmeth.2693]
40 **Thomas T**, Gilbert J, Meyer F. Metagenomics - a guide from sampling to data analysis. *Microb Inform Exp* 2012; **2**: 3 [PMID: 22587947 DOI: 10.1186/2042-5783-2-3]
41 **Blottière HM**, de Vos WM, Ehrlich SD, Doré J. Human intestinal metagenomics: state of the art and future. *Curr Opin Microbiol* 2013; **16**: 232-239 [PMID: 23870802 DOI: 10.1016/j.mib.2013.06.006]

42 **Gevers D**, Knight R, Petrosino JF, Huang K, McGuire AL, Birren BW, Nelson KE, White O, Methé BA, Huttenhower C. The Human Microbiome Project: a community resource for the healthy human microbiome. *PLoS Biol* 2012; **10**: e1001377 [PMID: 22904687 DOI: 10.1371/journal.pbio.1001377]

43 **Li J**, Jia H, Cai X, Zhong H, Feng Q, Sunagawa S, Arumugam M, Kultima JR, Prifti E, Nielsen T, Juncker AS, Manichanh C, Chen B, Zhang W, Levenez F, Wang J, Xu X, Xiao L, Liang S, Zhang D, Zhang Z, Chen W, Zhao H, Al-Aama JY, Edris S, Yang H, Wang J, Hansen T, Nielsen HB, Brunak S, Kristiansen K, Guarner F, Pedersen O, Doré J, Ehrlich SD, Bork P, Wang J. An integrated catalog of reference genes in the human gut microbiome. *Nat Biotechnol* 2014; **32**: 834-841 [PMID: 24997786 DOI: 10.1038/nbt.2942]

44 **Turnbaugh PJ**, Gordon JI. The core gut microbiome, energy balance and obesity. *J Physiol* 2009; **587**: 4153-4158 [PMID: 19491241 DOI: 10.1113/jphysiol.2009.174136]

45 **Faith JJ**, Guruge JL, Charbonneau M, Subramanian S, Seedorf H, Goodman AL, Clemente JC, Knight R, Heath AC, Leibel RL, Rosenbaum M, Gordon JI. The long-term stability of the human gut microbiota. *Science* 2013; **341**: 1237439 [PMID: 23828941 DOI: 10.1126/science.1237439]

46 **Lee SM**, Donaldson GP, Mikulski Z, Boyajian S, Ley K, Mazmanian SK. Bacterial colonization factors control specificity and stability of the gut microbiota. *Nature* 2013; **501**: 426-429 [PMID: 23955152 DOI: 10.1038/nature12447]

47 **Arumugam M**, Raes J, Pelletier E, Le Paslier D, Yamada T, Mende DR, Fernandes GR, Tap J, Bruls T, Batto JM, Bertalan M, Borruel N, Casellas F, Fernandez L, Gautier L, Hansen T, Hattori M, Hayashi T, Kleerebezem M, Kurokawa K, Leclerc M, Levenez F, Manichanh C, Nielsen HB, Nielsen T, Pons N, Poulain J, Qin J, Sicheritz-Ponten T, Tims S, Torrents D, Ugarte E, Zoetendal EG, Wang J, Guarner F, Pedersen O, de Vos WM, Brunak S, Doré J, Antolín M, Artiguenave F, Blottiere HM, Almeida M, Brechot C, Cara C, Chervaux C, Cultrone A, Delorme C, Denariaz G, Dervyn R, Foerstner KU, Friss C, van de Guchte M, Guedon E, Haimet F, Huber W, van Hylckama-Vlieg J, Jamet A, Juste C, Kaci G, Knol J, Lakhdari O, Layec S, Le Roux K, Maguin E, Mérieux A, Melo Minardi R, M'rini C, Muller J, Oozeer R, Parkhill J, Renault P, Rescigno M, Sanchez N, Sunagawa S, Torrejon A, Turner K, Vandemeulebrouck G, Varela E, Winogradsky Y, Zeller G, Weissenbach J, Ehrlich SD, Bork P. Enterotypes of the human gut microbiome. *Nature* 2011; **473**: 174-180 [PMID: 21508958 DOI: 10.1038/nature09944]

48 **Claesson MJ**, Jeffery IB, Conde S, Power SE, O'Connor EM, Cusack S, Harris HM, Coakley M, Lakshminarayanan B, O'Sullivan O, Fitzgerald GF, Deane J, O'Connor M, Harnedy N, O'Connor K, O'Mahony D, van Sinderen D, Wallace M, Brennan L, Stanton C, Marchesi JR, Fitzgerald AP, Shanahan F, Hill C, Ross RP, O'Toole PW. Gut microbiota composition correlates with diet and health in the elderly. *Nature* 2012; **488**: 178-184 [PMID: 22797518 DOI: 10.1038/nature11319]

49 **Chewapreecha C**. Your gut microbiota are what you eat. *Nat Rev Microbiol* 2014; **12**: 8 [PMID: 24336181 DOI: 10.1038/nrmicro3186]

50 **David LA**, Maurice CF, Carmody RN, Gootenberg DB, Button JE, Wolfe BE, Ling AV, Devlin AS, Varma Y, Fischbach MA, Biddinger SB, Dutton RJ, Turnbaugh PJ. Diet rapidly and reproducibly alters the human gut microbiome. *Nature* 2014; **505**: 559-563 [PMID: 24336217 DOI: 10.1038/nature12820]

51 **Yatsunenko T**, Rey FE, Manary MJ, Trehan I, Dominguez-Bello MG, Contreras M, Magris M, Hidalgo G, Baldassano RN, Anokhin AP, Heath AC, Warner B, Reeder J, Kuczynski J, Caporaso JG, Lozupone CA, Lauber C, Clemente JC, Knights D, Knight R, Gordon JI. Human gut microbiome viewed across age and geography. *Nature* 2012; **486**: 222-227 [PMID: 22699611 DOI: 10.1038/nature11053]

52 **Biagi E**, Candela M, Turroni S, Garagnani P, Franceschi C, Brigidi P. Ageing and gut microbes: perspectives for health maintenance and longevity. *Pharmacol Res* 2013; **69**: 11-20 [PMID: 23079287 DOI: 10.1016/j.phrs.2012.10.005]

53 **Suzuki TA**, Worobey M. Geographical variation of human gut microbial composition. *Biol Lett* 2014; **10**: 20131037 [PMID: 24522631 DOI: 10.1098/rsbl.2013.1037]

54 **Xu D**, Gao J, Gillilland M, Wu X, Song I, Kao JY, Owyang C. Rifaximin alters intestinal bacteria and prevents stress-induced gut inflammation and visceral hyperalgesia in rats. *Gastroenterology* 2014; **146**: 484-496.e4 [PMID: 24161699 DOI: 10.1053/j.gastro.2013.10.026]

55 **Vrieze A**, Out C, Fuentes S, Jonker L, Reuling I, Kootte RS, van Nood E, Holleman F, Knaapen M, Romijn JA, Soeters MR, Blaak EE, Dallinga-Thie GM, Reijnders D, Ackermans MT, Serlie MJ, Knop FK, Holst JJ, van der Ley C, Kema IP, Zoetendal EG, de Vos WM, Hoekstra JB, Stroes ES, Groen AK, Nieuwdorp M. Impact of oral vancomycin on gut microbiota, bile acid metabolism, and insulin sensitivity. *J Hepatol* 2014; **60**: 824-831 [PMID: 24316517 DOI: 10.1016/j.jhep.2013.11.034]

56 **Guo M**, Huang K, Chen S, Qi X, He X, Cheng WH, Luo Y, Xia K, Xu W. Combination of metagenomics and culture-based methods to study the interaction between ochratoxin a and gut microbiota. *Toxicol Sci* 2014; **141**: 314-323 [PMID: 24973096 DOI: 10.1093/toxsci/kfu128]

57 **Wu GD**, Chen J, Hoffmann C, Bittinger K, Chen YY, Keilbaugh SA, Bewtra M, Knights D, Walters WA, Knight R, Sinha R, Gilroy E, Gupta K, Baldassano R, Nessel L, Li H, Bushman FD, Lewis JD. Linking long-term dietary patterns with gut microbial enterotypes. *Science* 2011; **334**: 105-108 [PMID: 21885731 DOI: 10.1126/science.1208344]

58 **Mardanov AV**, Babykin MM, Beletsky AV, Grigoriev AI, Zinchenko VV, Kadnikov VV, Kirpichnikov MP, Mazur AM, Nedoluzhko AV, Novikova ND, Prokhortchouk EB, Ravin NV, Skryabin KG, Shestakov SV. Metagenomic Analysis of the Dynamic Changes in the Gut Microbiome of the Participants of the MARS-500 Experiment, Simulating Long Term Space Flight. *Acta Naturae* 2013; **5**: 116-125 [PMID: 24303207]

59 **Koenig JE**, Spor A, Scalfone N, Fricker AD, Stombaugh J, Knight R, Angenent LT, Ley RE. Succession of microbial consortia in the developing infant gut microbiome. *Proc Natl Acad Sci USA* 2011; **108** Suppl 1: 4578-4585 [PMID: 20668239 DOI: 10.1073/pnas.1000081107]

60 **Gabor EM**, Alkema WB, Janssen DB. Quantifying the accessibility of the metagenome by random expression cloning techniques. *Environ Microbiol* 2004; **6**: 879-886 [PMID: 15305913 DOI: 10.1111/j.1462-2920.2004.00640.x]

61 **Hehemann JH**, Correc G, Barbeyron T, Helbert W, Czjzek M, Michel G. Transfer of carbohydrate-active enzymes from marine bacteria to Japanese gut microbiota. *Nature* 2010; **464**: 908-912 [PMID: 20376150 DOI: 10.1038/nature08937]

62 **Turnbaugh PJ**, Henrissat B, Gordon JI. Viewing the human microbiome through three-dimensional glasses: integrating structural and functional studies to better define the properties of myriad carbohydrate-active enzymes. *Acta Crystallogr Sect F Struct Biol Cryst Commun* 2010; **66**: 1261-1264 [PMID: 20944220 DOI: 10.1107/S1744309110029088]

63 **Li LL**, McCorkle SR, Monchy S, Taghavi S, van der Lelie D. Bioprospecting metagenomes: glycosyl hydrolases for converting biomass. *Biotechnol Biofuels* 2009; **2**: 10 [PMID: 19450243 DOI: 10.1186/1754-6834-2-10]

64 **Tasse L**, Bercovici J, Pizzut-Serin S, Robe P, Tap J, Klopp C, Cantarel BL, Coutinho PM, Henrissat B, Leclerc M, Doré J, Monsan P, Remaud-Simeon M, Potocki-Veronese G. Functional metagenomics to mine the human gut microbiome for dietary fiber catabolic enzymes. *Genome Res* 2010; **20**: 1605-1612 [PMID: 20841432 DOI: 10.1101/gr.108332.110]

65 **Jones BV**, Begley M, Hill C, Gahan CG, Marchesi JR.

Functional and comparative metagenomic analysis of bile salt hydrolase activity in the human gut microbiome. *Proc Natl Acad Sci USA* 2008; **105**: 13580-13585 [PMID: 18757757 DOI: 10.1073/pnas.0804437105]
66 **Gloux K**, Berteau O, El Oumami H, Béguet F, Leclerc M, Doré J. A metagenomic β-glucuronidase uncovers a core adaptive function of the human intestinal microbiome. *Proc Natl Acad Sci USA* 2011; **108** Suppl 1: 4539-4546 [PMID: 20615998 DOI: 10.1073/pnas.1000066107]
67 **Vital M**, Howe AC, Tiedje JM. Revealing the bacterial butyrate synthesis pathways by analyzing (meta)genomic data. *MBio* 2014; **5**: e00889 [PMID: 24757212 DOI: 10.1128/mBio.00889-14]
68 **Fischbach MA**, Walsh CT. Antibiotics for emerging pathogens. *Science* 2009; **325**: 1089-1093 [PMID: 19713519 DOI: 10.1126/science.1176667]
69 **Alekshun MN**, Levy SB. Molecular mechanisms of antibacterial multidrug resistance. *Cell* 2007; **128**: 1037-1050 [PMID: 17382878 DOI: 10.1016/j.cell.2007.03.004]
70 **Robicsek A**, Jacoby GA, Hooper DC. The worldwide emergence of plasmid-mediated quinolone resistance. *Lancet Infect Dis* 2006; **6**: 629-640 [PMID: 17008172 DOI: 10.1016/S1473-3099(06)70599-0]
71 **Salyers AA**, Gupta A, Wang Y. Human intestinal bacteria as reservoirs for antibiotic resistance genes. *Trends Microbiol* 2004; **12**: 412-416 [PMID: 15337162 DOI: 10.1016/j.tim.2004.07.004]
72 **Sommer MO**, Dantas G, Church GM. Functional characterization of the antibiotic resistance reservoir in the human microflora. *Science* 2009; **325**: 1128-1131 [PMID: 19713526 DOI: 10.1126/science.1176950]
73 **D'Costa VM**, McGrann KM, Hughes DW, Wright GD. Sampling the antibiotic resistome. *Science* 2006; **311**: 374-377 [PMID: 16424339 DOI: 10.1126/science.1120800]
74 **Seville LA**, Patterson AJ, Scott KP, Mullany P, Quail MA, Parkhill J, Ready D, Wilson M, Spratt D, Roberts AP. Distribution of tetracycline and erythromycin resistance genes among human oral and fecal metagenomic DNA. *Microb Drug Resist* 2009; **15**: 159-166 [PMID: 19728772 DOI: 10.1089/mdr.2009.0916]
75 **Forslund K**, Sunagawa S, Kultima JR, Mende DR, Arumugam M, Typas A, Bork P. Country-specific antibiotic use practices impact the human gut resistome. *Genome Res* 2013; **23**: 1163-1169 [PMID: 23568836 DOI: 10.1101/gr.155465.113]
76 **Hu Y**, Yang X, Qin J, Lu N, Cheng G, Wu N, Pan Y, Li J, Zhu L, Wang X, Meng Z, Zhao F, Liu D, Ma J, Qin N, Xiang C, Xiao Y, Li L, Yang H, Wang J, Yang R, Gao GF, Wang J, Zhu B. Metagenome-wide analysis of antibiotic resistance genes in a large cohort of human gut microbiota. *Nat Commun* 2013; **4**: 2151 [PMID: 23877117 DOI: 10.1038/ncomms3151]
77 **Karami N**, Martner A, Enne VI, Swerkersson S, Adlerberth I, Wold AE. Transfer of an ampicillin resistance gene between two Escherichia coli strains in the bowel microbiota of an infant treated with antibiotics. *J Antimicrob Chemother* 2007; **60**: 1142-1145 [PMID: 17768176 DOI: 10.1093/jac/dkm327]
78 **Stecher B**, Denzler R, Maier L, Bernet F, Sanders MJ, Pickard DJ, Barthel M, Westendorf AM, Krogfelt KA, Walker AW, Ackermann M, Dobrindt U, Thomson NR, Hardt WD. Gut inflammation can boost horizontal gene transfer between pathogenic and commensal Enterobacteriaceae. *Proc Natl Acad Sci USA* 2012; **109**: 1269-1274 [PMID: 22232693 DOI: 10.1073/pnas.1113246109]
79 **Cheng G**, Hu Y, Yin Y, Yang X, Xiang C, Wang B, Chen Y, Yang F, Lei F, Wu N, Lu N, Li J, Chen Q, Li L, Zhu B. Functional screening of antibiotic resistance genes from human gut microbiota reveals a novel gene fusion. *FEMS Microbiol Lett* 2012; **336**: 11-16 [PMID: 22845886 DOI: 10.1111/j.1574-6968.2012.02647.x]
80 **Moore AM**, Patel S, Forsberg KJ, Wang B, Bentley G, Razia Y, Qin X, Tarr PI, Dantas G. Pediatric fecal microbiota harbor diverse and novel antibiotic resistance genes. *PLoS One* 2013; **8**: e78822 [PMID: 24236055 DOI: 10.1371/journal.pone.0078822]
81 **Manichanh C**, Rigottier-Gois L, Bonnaud E, Gloux K, Pelletier E, Frangeul L, Nalin R, Jarrin C, Chardon P, Marteau P, Roca J, Dore J. Reduced diversity of faecal microbiota in Crohn's disease revealed by a metagenomic approach. *Gut* 2006; **55**: 205-211 [PMID: 16188921 DOI: 10.1136/gut.2005.073817]
82 **Ray K**. IBD. Understanding gut microbiota in new-onset Crohn's disease. *Nat Rev Gastroenterol Hepatol* 2014; **11**: 268 [PMID: 24662277 DOI: 10.1038/nrgastro.2014.45]
83 **Bye W**, Ishaq N, Bolin TD, Duncombe VM, Riordan SM. Overgrowth of the indigenous gut microbiome and irritable bowel syndrome. *World J Gastroenterol* 2014; **20**: 2449-2455 [PMID: 24627582 DOI: 10.3748/wjg.v20.i10.2449]
84 **Le Chatelier E**, Nielsen T, Qin J, Prifti E, Hildebrand F, Falony G, Almeida M, Arumugam M, Batto JM, Kennedy S, Leonard P, Li J, Burgdorf K, Grarup N, Jørgensen T, Brandslund I, Nielsen HB, Juncker AS, Bertalan M, Levenez F, Pons N, Rasmussen S, Sunagawa S, Tap J, Tims S, Zoetendal EG, Brunak S, Clément K, Doré J, Kleerebezem M, Kristiansen K, Renault P, Sicheritz-Ponten T, de Vos WM, Zucker JD, Raes J, Hansen T, Bork P, Wang J, Ehrlich SD, Pedersen O. Richness of human gut microbiome correlates with metabolic markers. *Nature* 2013; **500**: 541-546 [PMID: 23985870 DOI: 10.1038/nature12506]
85 **Tarantino G**. Gut microbiome, obesity-related comorbidities, and low-grade chronic inflammation. *J Clin Endocrinol Metab* 2014; **99**: 2343-2346 [PMID: 25003243 DOI: 10.1210/jc.2014-2074]
86 **Ohtani N**, Yoshimoto S, Hara E. Obesity and cancer: a gut microbial connection. *Cancer Res* 2014; **74**: 1885-1889 [PMID: 24638983 DOI: 10.1158/0008-5472.CAN-13-3501]
87 **Qin J**, Li Y, Cai Z, Li S, Zhu J, Zhang F, Liang S, Zhang W, Guan Y, Shen D, Peng Y, Zhang D, Jie Z, Wu W, Qin Y, Xue W, Li J, Han L, Lu D, Wu P, Dai Y, Sun X, Li Z, Tang A, Zhong S, Li X, Chen W, Xu R, Wang M, Feng Q, Gong M, Yu J, Zhang Y, Zhang M, Hansen T, Sanchez G, Raes J, Falony G, Okuda S, Almeida M, LeChatelier E, Renault P, Pons N, Batto JM, Zhang Z, Chen H, Yang R, Zheng W, Li S, Yang H, Wang J, Ehrlich SD, Nielsen R, Pedersen O, Kristiansen K, Wang J. A metagenome-wide association study of gut microbiota in type 2 diabetes. *Nature* 2012; **490**: 55-60 [PMID: 23023125 DOI: 10.1038/nature11450]
88 **de Goffau MC**, Fuentes S, van den Bogert B, Honkanen H, de Vos WM, Welling GW, Hyöty H, Harmsen HJ. Aberrant gut microbiota composition at the onset of type 1 diabetes in young children. *Diabetologia* 2014; **57**: 1569-1577 [PMID: 24930037 DOI: 10.1007/s00125-014-3274-0]
89 **Tilg H**, Moschen AR. Microbiota and diabetes: an evolving relationship. *Gut* 2014; **63**: 1513-1521 [PMID: 24833634 DOI: 10.1136/gutjnl-2014-306928]
90 **Abrahamsson TR**, Jakobsson HE, Andersson AF, Björkstén B, Engstrand L, Jenmalm MC. Low diversity of the gut microbiota in infants with atopic eczema. *J Allergy Clin Immunol* 2012; **129**: 434-440, 440.e1-e2 [PMID: 22153774 DOI: 10.1016/j.jaci.2011.10.025]
91 **Abrahamsson TR**, Jakobsson HE, Andersson AF, Björkstén B, Engstrand L, Jenmalm MC. Low gut microbiota diversity in early infancy precedes asthma at school age. *Clin Exp Allergy* 2014; **44**: 842-850 [PMID: 24330256 DOI: 10.1111/cea.12253]
92 **Carroll IM**, Ringel-Kulka T, Siddle JP, Ringel Y. Alterations in composition and diversity of the intestinal microbiota in patients with diarrhea-predominant irritable bowel syndrome. *Neurogastroenterol Motil* 2012; **24**: 521-530, e248 [PMID: 22339879 DOI: 10.1111/j.1365-2982.2012.01891.x]
93 **Ahn J**, Sinha R, Pei Z, Dominianni C, Wu J, Shi J, Goedert JJ, Hayes RB, Yang L. Human gut microbiome and risk for colorectal cancer. *J Natl Cancer Inst* 2013; **105**: 1907-1911

[PMID: 24316595 DOI: 10.1093/jnci/djt300]
94 **Ou J**, Carbonero F, Zoetendal EG, DeLany JP, Wang M, Newton K, Gaskins HR, O'Keefe SJ. Diet, microbiota, and microbial metabolites in colon cancer risk in rural Africans and African Americans. *Am J Clin Nutr* 2013; **98**: 111-120 [PMID: 23719549 DOI: 10.3945/ajcn.112.056689]
95 **Candela M**, Turroni S, Biagi E, Carbonero F, Rampelli S, Fiorentini C, Brigidi P. Inflammation and colorectal cancer, when microbiota-host mutualism breaks. *World J Gastroenterol* 2014; **20**: 908-922 [PMID: 24574765 DOI: 10.3748/wjg.v20.i4.908]
96 **Yang T**, Owen JL, Lightfoot YL, Kladde MP, Mohamadzadeh M. Microbiota impact on the epigenetic regulation of colorectal cancer. *Trends Mol Med* 2013; **19**: 714-725 [PMID: 24051204 DOI: 10.1016/j.molmed.2013.08.005]
97 **Chen Y**, Yang F, Lu H, Wang B, Chen Y, Lei D, Wang Y, Zhu B, Li L. Characterization of fecal microbial communities in patients with liver cirrhosis. *Hepatology* 2011; **54**: 562-572 [PMID: 21574172 DOI: 10.1002/hep.24423]
98 **Wei X**, Yan X, Zou D, Yang Z, Wang X, Liu W, Wang S, Li X, Han J, Huang L, Yuan J. Abnormal fecal microbiota community and functions in patients with hepatitis B liver cirrhosis as revealed by a metagenomic approach. *BMC Gastroenterol* 2013; **13**: 175 [PMID: 24369878 DOI: 10.1186/1471-230X-13-175]
99 **Qin N**, Yang F, Li A, Prifti E, Chen Y, Shao L, Guo J, Le Chatelier E, Yao J, Wu L, Zhou J, Ni S, Liu L, Pons N, Batto JM, Kennedy SP, Leonard P, Yuan C, Ding W, Chen Y, Hu X, Zheng B, Qian G, Xu W, Ehrlich SD, Zheng S, Li L. Alterations of the human gut microbiome in liver cirrhosis. *Nature* 2014; **513**: 59-64 [PMID: 25079328 DOI: 10.1038/nature13568]
100 **Zhu L**, Baker SS, Gill C, Liu W, Alkhouri R, Baker RD, Gill SR. Characterization of gut microbiomes in nonalcoholic steatohepatitis (NASH) patients: a connection between endogenous alcohol and NASH. *Hepatology* 2013; **57**: 601-609 [PMID: 23055155 DOI: 10.1002/hep.26093]
101 **Miura K**, Ohnishi H. Role of gut microbiota and Toll-like receptors in nonalcoholic fatty liver disease. *World J Gastroenterol* 2014; **20**: 7381-7391 [PMID: 24966608 DOI: 10.3748/wjg.v20.i23.7381]
102 **Hsiao EY**, McBride SW, Hsien S, Sharon G, Hyde ER, McCue T, Codelli JA, Chow J, Reisman SE, Petrosino JF, Patterson PH, Mazmanian SK. Microbiota modulate behavioral and physiological abnormalities associated with neurodevelopmental disorders. *Cell* 2013; **155**: 1451-1463 [PMID: 24315484 DOI: 10.1016/j.cell.2013.11.024]
103 **Flight MH**. Neurodevelopmental disorders: the gut-microbiome-brain connection. *Nat Rev Neurosci* 2014; **15**: 65 [PMID: 24370876 DOI: 10.1038/nrn3669]
104 **Karlsson FH**, Fåk F, Nookaew I, Tremaroli V, Fagerberg B, Petranovic D, Bäckhed F, Nielsen J. Symptomatic atherosclerosis is associated with an altered gut metagenome. *Nat Commun* 2012; **3**: 1245 [PMID: 23212374 DOI: 10.1038/ncomms2266]
105 **Wu T**, Zhang Z, Liu B, Hou D, Liang Y, Zhang J, Shi P. Gut microbiota dysbiosis and bacterial community assembly associated with cholesterol gallstones in large-scale study. *BMC Genomics* 2013; **14**: 669 [PMID: 24083370 DOI: 10.1186/1471-2164-14-669]
106 **Pop M**, Walker AW, Paulson J, Lindsay B, Antonio M, Hossain MA, Oundo J, Tamboura B, Mai V, Astrovskaya I, Corrada Bravo H, Rance R, Stares M, Levine MM, Panchalingam S, Kotloff K, Ikumapayi UN, Ebruke C, Adeyemi M, Ahmed D, Ahmed F, Alam MT, Amin R, Siddiqui S, Ochieng JB, Ouma E, Juma J, Mailu E, Omore R, Morris JG, Breiman RF, Saha D, Parkhill J, Nataro JP, Stine OC. Diarrhea in young children from low-income countries leads to large-scale alterations in intestinal microbiota composition. *Genome Biol* 2014; **15**: R76 [PMID: 24995464 DOI: 10.1186/gb-2014-15-6-r76]
107 **Subramanian S**, Huq S, Yatsunenko T, Haque R, Mahfuz M, Alam MA, Benezra A, DeStefano J, Meier MF, Muegge BD, Barratt MJ, VanArendonk LG, Zhang Q, Province MA, Petri WA, Ahmed T, Gordon JI. Persistent gut microbiota immaturity in malnourished Bangladeshi children. *Nature* 2014; **510**: 417-421 [PMID: 24896187 DOI: 10.1038/nature13421]
108 **Ramezani A**, Raj DS. The gut microbiome, kidney disease, and targeted interventions. *J Am Soc Nephrol* 2014; **25**: 657-670 [PMID: 24231662 DOI: 10.1681/ASN.2013080905]
109 **Brim H**, Yooseph S, Zoetendal EG, Lee E, Torralbo M, Laiyemo AO, Shokrani B, Nelson K, Ashktorab H. Microbiome analysis of stool samples from African Americans with colon polyps. *PLoS One* 2013; **8**: e81352 [PMID: 24376500 DOI: 10.1371/journal.pone.0081352]
110 **Holler E**, Butzhammer P, Schmid K, Hundsrucker C, Koestler J, Peter K, Zhu W, Sporrer D, Hehlgans T, Kreutz M, Holler B, Wolff D, Edinger M, Andreesen R, Levine JE, Ferrara JL, Gessner A, Spang R, Oefner PJ. Metagenomic analysis of the stool microbiome in patients receiving allogeneic stem cell transplantation: loss of diversity is associated with use of systemic antibiotics and more pronounced in gastrointestinal graft-versus-host disease. *Biol Blood Marrow Transplant* 2014; **20**: 640-645 [PMID: 24492144 DOI: 10.1016/j.bbmt.2014.01.030]
111 **Lakhdari O**, Cultrone A, Tap J, Gloux K, Bernard F, Ehrlich SD, Lefèvre F, Doré J, Blottière HM. Functional metagenomics: a high throughput screening method to decipher microbiota-driven NF-κB modulation in the human gut. *PLoS One* 2010; **5**: e13092 [PMID: 20927194 DOI: 10.1371/journal.pone.0013092]
112 **Karlsson FH**, Tremaroli V, Nookaew I, Bergström G, Behre CJ, Fagerberg B, Nielsen J, Bäckhed F. Gut metagenome in European women with normal, impaired and diabetic glucose control. *Nature* 2013; **498**: 99-103 [PMID: 23719380 DOI: 10.1038/nature12198]
113 **Lakhdari O**, Tap J, Béguet-Crespel F, Le Roux K, de Wouters T, Cultrone A, Nepelska M, Lefèvre F, Doré J, Blottière HM. Identification of NF-κB modulation capabilities within human intestinal commensal bacteria. *J Biomed Biotechnol* 2011; **2011**: 282356 [PMID: 21765633 DOI: 10.1155/2011/282356]
114 **Gloux K**, Leclerc M, Iliozer H, L'Haridon R, Manichanh C, Corthier G, Nalin R, Blottière HM, Doré J. Development of high-throughput phenotyping of metagenomic clones from the human gut microbiome for modulation of eukaryotic cell growth. *Appl Environ Microbiol* 2007; **73**: 3734-3737 [PMID: 17400773 DOI: 10.1128/AEM.02204-06]
115 **Dobrijevic D**, Di Liberto G, Tanaka K, de Wouters T, Dervyn R, Boudebbouze S, Binesse J, Blottière HM, Jamet A, Maguin E, van de Guchte M. High-throughput system for the presentation of secreted and surface-exposed proteins from Gram-positive bacteria in functional metagenomics studies. *PLoS One* 2013; **8**: e65956 [PMID: 23799065 DOI: 10.1371/journal.pone.0065956]
116 **Brown Kav A**, Benhar I, Mizrahi I. A method for purifying high quality and high yield plasmid DNA for metagenomic and deep sequencing approaches. *J Microbiol Methods* 2013; **95**: 272-279 [PMID: 24055388 DOI: 10.1016/j.mimet.2013.09.008]
117 **Jones BV**, Marchesi JR. Transposon-aided capture (TRACA) of plasmids resident in the human gut mobile metagenome. *Nat Methods* 2007; **4**: 55-61 [PMID: 17128268 DOI: 10.1038/nmeth964]
118 **Kurokawa K**, Itoh T, Kuwahara T, Oshima K, Toh H, Toyoda A, Takami H, Morita H, Sharma VK, Srivastava TP, Taylor TD, Noguchi H, Mori H, Ogura Y, Ehrlich DS, Itoh K, Takagi T, Sakaki Y, Hayashi T, Hattori M. Comparative metagenomics revealed commonly enriched gene sets in human gut microbiomes. *DNA Res* 2007; **14**: 169-181 [PMID: 17916580 DOI: 10.1093/dnares/dsm018]
119 **Smillie CS**, Smith MB, Friedman J, Cordero OX, David LA, Alm EJ. Ecology drives a global network of gene exchange connecting the human microbiome. *Nature* 2011; **480**: 241-244 [PMID: 22037308 DOI: 10.1038/nature10571]

120 **Raes J**, Korbel JO, Lercher MJ, von Mering C, Bork P. Prediction of effective genome size in metagenomic samples. *Genome Biol* 2007; **8**: R10 [PMID: 17224063 DOI: 10.1186/gb-2007-8-1-r10]

121 **Kennedy NA**, Walker AW, Berry SH, Duncan SH, Farquarson FM, Louis P, Thomson JM, Satsangi J, Flint HJ, Parkhill J, Lees CW, Hold GL. The impact of different DNA extraction kits and laboratories upon the assessment of human gut microbiota composition by 16S rRNA gene sequencing. *PLoS One* 2014; **9**: e88982 [PMID: 24586470 DOI: 10.1371/journal.pone.0088982]

122 **Wesolowska-Andersen A**, Bahl MI, Carvalho V, Kristiansen K, Sicheritz-Pontén T, Gupta R, Licht TR. Choice of bacterial DNA extraction method from fecal material influences community structure as evaluated by metagenomic analysis. *Microbiome* 2014; **2**: 19 [PMID: 24949196 DOI: 10.1186/2049-2618-2-19]

123 **Reyes A**, Haynes M, Hanson N, Angly FE, Heath AC, Rohwer F, Gordon JI. Viruses in the faecal microbiota of monozygotic twins and their mothers. *Nature* 2010; **466**: 334-338 [PMID: 20631792 DOI: 10.1038/nature09199]

124 **Schnoes AM**, Brown SD, Dodevski I, Babbitt PC. Annotation error in public databases: misannotation of molecular function in enzyme superfamilies. *PLoS Comput Biol* 2009; **5**: e1000605 [PMID: 20011109 DOI: 10.1371/journal.pcbi.1000605]

125 **Albertsen M**, Hugenholtz P, Skarshewski A, Nielsen KL, Tyson GW, Nielsen PH. Genome sequences of rare, uncultured bacteria obtained by differential coverage binning of multiple metagenomes. *Nat Biotechnol* 2013; **31**: 533-538 [PMID: 23707974 DOI: 10.1038/nbt.2579]

126 **Poretsky RS**, Hewson I, Sun S, Allen AE, Zehr JP, Moran MA. Comparative day/night metatranscriptomic analysis of microbial communities in the North Pacific subtropical gyre. *Environ Microbiol* 2009; **11**: 1358-1375 [PMID: 19207571 DOI: 10.1111/j.1462-2920.2008.01863.x]

127 **Verberkmoes NC**, Russell AL, Shah M, Godzik A, Rosenquist M, Halfvarson J, Lefsrud MG, Apajalahti J, Tysk C, Hettich RL, Jansson JK. Shotgun metaproteomics of the human distal gut microbiota. *ISME J* 2009; **3**: 179-189 [PMID: 18971961 DOI: 10.1038/ismej.2008.108]

128 **Nicholson JK**, Holmes E, Wilson ID. Gut microorganisms, mammalian metabolism and personalized health care. *Nat Rev Microbiol* 2005; **3**: 431-438 [PMID: 15821725 DOI: 10.1038/nrmicro1152]

129 **Gosalbes MJ**, Durbán A, Pignatelli M, Abellan JJ, Jiménez-Hernández N, Pérez-Cobas AE, Latorre A, Moya A. Metatranscriptomic approach to analyze the functional human gut microbiota. *PLoS One* 2011; **6**: e17447 [PMID: 21408168 DOI: 10.1371/journal.pone.0017447]

130 **Simon C**, Daniel R. Metagenomic analyses: past and future trends. *Appl Environ Microbiol* 2011; **77**: 1153-1161 [PMID: 21169428 DOI: 10.1128/AEM.02345-10]

131 **Kolmeder CA**, de Been M, Nikkilä J, Ritamo I, Mättö J, Valmu L, Salojärvi J, Palva A, Salonen A, de Vos WM. Comparative metaproteomics and diversity analysis of human intestinal microbiota testifies for its temporal stability and expression of core functions. *PLoS One* 2012; **7**: e29913 [PMID: 22279554 DOI: 10.1371/journal.pone.0029913]

132 **Heinken A**, Khan MT, Paglia G, Rodionov DA, Harmsen HJ, Thiele I. Functional metabolic map of Faecalibacterium prausnitzii, a beneficial human gut microbe. *J Bacteriol* 2014; **196**: 3289-3302 [PMID: 25002542 DOI: 10.1128/JB.01780-14]

133 **Phua LC**, Chue XP, Koh PK, Cheah PY, Ho HK, Chan EC. Non-invasive fecal metabonomic detection of colorectal cancer. *Cancer Biol Ther* 2014; **15**: 389-397 [PMID: 24424155 DOI: 10.4161/cbt.27625]

134 **Marchesi JR**, Holmes E, Khan F, Kochhar S, Scanlan P, Shanahan F, Wilson ID, Wang Y. Rapid and noninvasive metabonomic characterization of inflammatory bowel disease. *J Proteome Res* 2007; **6**: 546-551 [PMID: 17269711 DOI: 10.1021/pr060470d]

135 **Jansson J**, Willing B, Lucio M, Fekete A, Dicksved J, Halfvarson J, Tysk C, Schmitt-Kopplin P. Metabolomics reveals metabolic biomarkers of Crohn's disease. *PLoS One* 2009; **4**: e6386 [PMID: 19636438 DOI: 10.1371/journal.pone.0006386]

136 **Le Gall G**, Noor SO, Ridgway K, Scovell L, Jamieson C, Johnson IT, Colquhoun IJ, Kemsley EK, Narbad A. Metabolomics of fecal extracts detects altered metabolic activity of gut microbiota in ulcerative colitis and irritable bowel syndrome. *J Proteome Res* 2011; **10**: 4208-4218 [PMID: 21761941 DOI: 10.1021/pr2003598]

137 **Franzosa EA**, Morgan XC, Segata N, Waldron L, Reyes J, Earl AM, Giannoukos G, Boylan MR, Ciulla D, Gevers D, Izard J, Garrett WS, Chan AT, Huttenhower C. Relating the metatranscriptome and metagenome of the human gut. *Proc Natl Acad Sci USA* 2014; **111**: E2329-E2338 [PMID: 24843156 DOI: 10.1073/pnas.1319284111]

138 **Nielsen HB**, Almeida M, Juncker AS, Rasmussen S, Li J, Sunagawa S, Plichta DR, Gautier L, Pedersen AG, Le Chatelier E, Pelletier E, Bonde I, Nielsen T, Manichanh C, Arumugam M, Batto JM, Quintanilha Dos Santos MB, Blom N, Borruel N, Burgdorf KS, Boumezbeur F, Casellas F, Doré J, Dworzynski P, Guarner F, Hansen T, Hildebrand F, Kaas RS, Kennedy S, Kristiansen K, Kultima JR, Léonard P, Levenez F, Lund O, Moumen B, Le Paslier D, Pons N, Pedersen O, Prifti E, Qin J, Raes J, Sørensen S, Tap J, Tims S, Ussery DW, Yamada T, Renault P, Sicheritz-Ponten T, Bork P, Wang J, Brunak S, Ehrlich SD. Identification and assembly of genomes and genetic elements in complex metagenomic samples without using reference genomes. *Nat Biotechnol* 2014; **32**: 822-828 [PMID: 24997787 DOI: 10.1038/nbt.2939]

139 **Mitra S**, Förster-Fromme K, Damms-Machado A, Scheurenbrand T, Biskup S, Huson DH, Bischoff SC. Analysis of the intestinal microbiota using SOLiD 16S rRNA gene sequencing and SOLiD shotgun sequencing. *BMC Genomics* 2013; **14** Suppl 5: S16 [PMID: 24564472 DOI: 10.1186/1471-2164-14-S5-S16]

140 **Culligan EP**, Marchesi JR, Hill C, Sleator RD. Combined metagenomic and phenomic approaches identify a novel salt tolerance gene from the human gut microbiome. *Front Microbiol* 2014; **5**: 189 [PMID: 24808895 DOI: 10.3389/fmicb.2014.00189]

141 **Lee S**, Cantarel B, Henrissat B, Gevers D, Birren BW, Huttenhower C, Ko G. Gene-targeted metagenomic analysis of glucan-branching enzyme gene profiles among human and animal fecal microbiota. *ISME J* 2014; **8**: 493-503 [PMID: 24108330 DOI: 10.1038/ismej.2013.167]

P- Reviewer: Chen CY, Chen YC, Streba LAM
S- Editor: Qi Y **L- Editor**: AmEditor **E- Editor**: Liu XM

World Journal of Gastroenterology

Submit a Manuscript: http://www.wjgnet.com/esps/
Help Desk: http://www.wjgnet.com/esps/helpdesk.aspx
DOI: 10.3748/wjg.v21.i3.815

World J Gastroenterol 2015 January 21; 21(3): 815-819
ISSN 1007-9327 (print) ISSN 2219-2840 (online)

Gastroesophageal reflux disease and non-esophageal cancer

Fernando AM Herbella, Sebastião Pannocchia Neto, Ilka Lopes Santoro, Licia Caldas Figueiredo

Fernando AM Herbella, Sebastião Pannocchia Neto, Department of Surgery, Federal University of Sao Paulo, Sao Paulo 04037-003, Brazil
Ilka Lopes Santoro, Licia Caldas Figueiredo, Pneumology Division, Department of Medicine, Federal University of Sao Paulo, Sao Paulo 04037-003, Brazil
Author contributions: Both Herbella FAM and Neto SP designed research and wrote the paper; and all authors performed research and analyzed data.

Correspondence to: Fernando AM Herbella, MD, Department of Surgery, Federal University of Sao Paulo, Rua Diogo de Faria 1087 cj 301, Sao Paulo 04037-003, Brazil. herbella.dcir@epm.br
Telephone: +55-11-99922824
Fax: +55-11-99922824
Received: July 28, 2014
Peer-review started: July 29, 2014
First decision: August 15, 2014
Revised: August 29, 2014
Accepted: October 15, 2014
Article in press: October 15, 2014
Published online: January 21, 2015

Abstract

The association of gastroesophageal reflux disease (GERD) and esophageal cancer is well known. The carcinogenic properties of the gastroduodenal contents may also lead to cancer in target organs for GERD especially considering that they do not have intrinsic protective mechanisms as found in the esophagus. This review focuses on the putative relation between GERD and non-esophageal cancer. Most of the papers reviewed are far from ideal to prove the relationship of extra-esophageal cancer and GERD since a small number of patients is presented, most do not control cases based on tobacco usage and obesity, and the diagnosis of GERD is variable, not always from an objective measurement such as pH monitoring but relying on symptoms in most reports. Nevertheless, head and neck and lung cancer have a growing incidence parallel to GERD and a shift towards non-smoking, female gender and adenocarcinoma (compared to squamous cell carcinoma) is arising, similar to the example of esophageal cancer with the exception of the female gender.

Key words: Gastroesophageal reflux; Cancer; Pharynx; Larynx; Trachea; Lung

Core tip: Gastroesophageal reflux disease (GERD) is a very prevalent disease with a rising incidence. The disease is certainly linked to the pathogenesis of esophageal adenocarcinoma originated in the Barrett's esophagus. The carcinogenic properties of the gastroduodenal contents may also lead to cancer in target organs for GERD, especially considering that they do not have intrinsic protective mechanisms as found in the esophagus. Although strong conclusions cannot be drawn due to lack of good quality published studies, GERD may also be linked to the pathogenesis of head and neck and lung cancers.

Herbella FAM, Neto SP, Santoro IL, Figueiredo LC. Gastroesophageal reflux disease and non-esophageal cancer. *World J Gastroenterol* 2015; 21(3): 815-819 Available from: URL: http://www.wjgnet.com/1007-9327/full/v21/i3/815.htm DOI: http://dx.doi.org/10.3748/wjg.v21.i3.815

INTRODUCTION

Gastroesophageal reflux disease (GERD) is a very prevalent disease, affecting 18%-27% of the population

in North America, 9%-25% in Europe, 2%-8% in East Asia, 9%-33% in the Middle East, 11% in Australia and 23% in South America[1]. Moreover, the incidence of GERD seems to be increasing with time[2]. It accounts for almost 9000000 outpatient visits, 65000 hospitalizations and costs of over US $9000000000 per year only in the United States[3,4]. The association of GERD and esophageal cancer is well known, with a metaplasia-dysplasia-carcinoma sequence leading ultimately to esophageal adenocarcinoma[5]. Esophageal adenocarcinoma also showed a significant increase in incidence in the last decades[6].

Virtually all adjacent organs to the esophagus may be affected by the gastric refluxate and new discoveries are made on a regular basis showing that even distant organs may be affected by GERD. It seems logical that the carcinogenic properties of the gastroduodenal contents may also lead to cancer in target organs for GERD especially considering that they do not have intrinsic protective mechanisms as found in the esophagus.

This review focuses on the putative relation between GERD and non-esophageal cancer.

MECHANISM OF GERD-INDUCED CARCINOGENESIS

Esophageal adenocarcinoma originated in a Barrett's esophagus is the most studied cancer linked to GERD; however, its cellular origins and molecular mechanisms are still not fully understood[7]. GERD induces esophageal inflammation and consequent oxidative stress leading to DNA damage. Both acid and bile are active on oncogenic pathways. Acid induces DNA damage, decreases proliferation, and increases apoptosis. Bile salts induce DNA damage, affect proliferation in a pH-dependent manner, and cause resistance to apoptosis[7,8]. More detailed molecular mechanisms are available in recent reviews[7-9].

Apart from the direct effect of gastric refluxate, other variables link GERD and cancer. Obesity is a risk factor for different cancers, including esophageal adenocarcinoma[10]. Fat tissue increases the release of proinflammatory molecules and induces insulin resistance, all of them linked to carcinogenesis[7,11]. GERD is strongly associated to obesity as well[12]. It has been shown that for each 5-point increase in body mass index, the DeMeester GERD score increases by 3 units[13]. Parallel to GERD, the prevalence of obesity more than doubled between 1980 and 2009 in the United States, as indicated by Centers for Disease Control and Prevention Surveys.

Smoking is also linked to esophageal[14], head and neck[15] and lung cancer[16] and, again, is a risk factor for GERD[17].

ORAL/LARYNX/PHARYNX CANCER

Gastric contents reach the larynx/pharynx in healthy volunteers and in patients with GERD[18]. This has been proven by different methods, such as dual probe pH monitoring[18], multichannel intraluminal impedance[19], and aerosolized reflux detection[20]. In fact, refluxate may reach up to the mouth and GERD is thought to cause tooth wearing[21].

GERD has long been considered a risk factor for laryngeal/pharyngeal cancer[22]. Few studies did not show GERD as an independent risk factor for cancer in multivariate analysis when tobacco and alcohol consumption are considered[23]; however, other studies, including a meta-analysis, do show GERD as an independent risk factor especially in non-smokers[24-27]. Also, the incidence of these tumors is increasing parallel to GERD.

Another piece of evidence that links GERD and laryngeal/pharyngeal cancer is the putative higher risk in patients with heterotopic acid-producing gastric mucosa in the proximal esophagus (inlet patch)[28].

The literature on oral cancer and GERD is scarce even though they also may be associated[29].

LUNG

Similar to the proximal respiratory organs, duodenogastric contents may also reflux to the lungs. Pepsin and biliary salts can be recovered from the lungs in patients with end-stage pulmonary diseases[30]. GERD is associated with different lung diseases[31]; however, the association of GERD and lung cancer is unknown. A single preliminary report showed significant GERD in lung cancer patients irrespective of histology[32].

The link between GERD and lung cancer seems plausible based on the following facts: (1) Lung adenocarcinoma has a growing incidence with a trend to surpass squamous cell carcinoma[33,34], similar to esophageal cancer; (2) Lung adenocarcinoma is the most frequent histologic type in non-smokers and a clear risk factor has not been attributed to it[35]; (3) Connective tissue diseases are common risk factors for lung adenocarcinoma[36] and GERD[37]; and (4) Centrally located lung adenocarcinoma (area of the lung closer to the esophagus and more prone to aspirate gastrodudodenal refluxate) is likely to arise from the glandular epithelium (superficial layer more susceptible to contact with refluxate). In contrast, peripheral adenocarcinoma is likely to originate in type II pneumocytes and Clara cells[38].

CONCLUSION

GERD is a common and costly disease; however, despite great achievements in the understanding of the pathophysiology and treatment of the disease, medicine is not winning the battle against GERD. The incidence of GERD is escalating (Figure 1)[39-59] and, even though old complications attributed to this illness, such as esophageal stenosis and ulceration, have almost disappeared, a new spectrum of the disease is surging with extra-esophageal manifestations and cancer. Thus, esophageal cancer

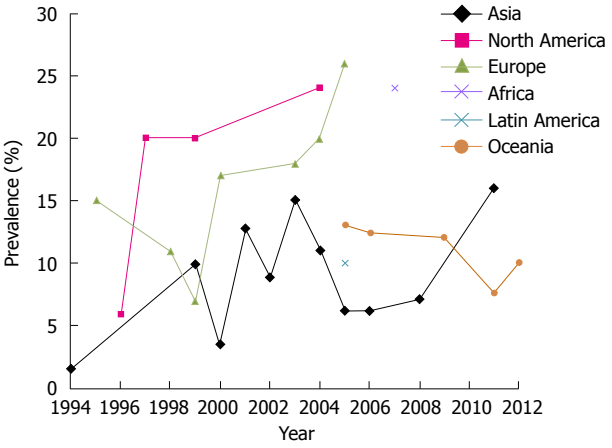

Figure 1 Worldwide prevalence of gastroesophageal reflux disease[39-59]. Gastroesophageal reflux disease defined by symptoms with a weekly frequency or according to the author's definition.

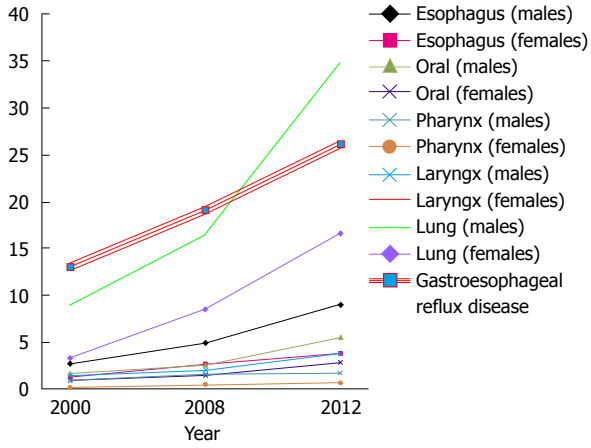

Figure 2 Worldwide incidence of cancers putatively associated to gastroesophageal reflux disease[62-64].

should also be added to the burden of GERD and probably head and neck and lung cancers as well.

Head and neck and lung cancer both have smoking as the main etiologic factor. Even though the prevalence of smokers is decreasing[60], the incidence of the aforementioned tumors is not (Figure 2). Obviously, a proportional increase in the incidences of two separate diseases does not necessarily indicate an etiological relationship but more than that, a shift towards non-smoking, female gender and adenocarcinoma (compared to squamous cell carcinoma) is arising[61], similar to the example of the esophageal cancer with the exception of the female gender[62-64].

It must be said that most of the papers reviewed are far from ideal to prove the relationship of extra-esophageal cancer and GERD. A single study addressed the association of lung cancer and GERD. Not all studies showed a relationship between GERD and head and neck cancer, and even in studies showing positive association this is not too strong. Some present with a small number of patients, most do not control cases based on tobacco usage and obesity. Moreover, the diagnosis of GERD is variable, not always from an objective measurement such as pH monitoring but relying on symptoms that has been shown not to be a trustworthy method for correct GERD diagnosis. Different previous publications showed that symptoms are unreliable for the diagnosis of GERD[65,66] although the labeling of patients as refluxers based on symptom questionnaires is still a common practice, in spite of the fact that most of these questionnaires were not validated in comparison to esophageal ambulatory pH monitoring[67].

In conclusion, laryngeal and pharyngeal tumors are highly associated to GERD. Oral and lung cancers probably are also connected to GERD.

REFERENCES

1 **El-Serag HB**, Sweet S, Winchester CC, Dent J. Update on the epidemiology of gastro-oesophageal reflux disease: a systematic review. *Gut* 2014; **63**: 871-880 [PMID: 23853213 DOI: 10.1136/gutjnl2012-304269]

2 **Rubenstein JH**, Chen JW. Epidemiology of gastroesophageal reflux disease. *Gastroenterol Clin North Am* 2014; **43**: 1-14 [PMID: 24503355 DOI: 10.1016/j.gtc.2013.11.006]

3 **Sandler RS**, Everhart JE, Donowitz M, Adams E, Cronin K, Goodman C, Gemmen E, Shah S, Avdic A, Rubin R. The burden of selected digestive diseases in the United States. *Gastroenterology* 2002; **122**: 1500-1511 [PMID: 11984534 DOI: 10.1053/gast.2002.32978]

4 **Peery AF**, Dellon ES, Lund J, Crockett SD, McGowan CE, Bulsiewicz WJ, Gangarosa LM, Thiny MT, Stizenberg K, Morgan DR, Ringel Y, Kim HP, Dibonaventura MD, Carroll CF, Allen JK, Cook SF, Sandler RS, Kappelman MD, Shaheen NJ. Burden of gastrointestinal disease in the United States: 2012 update. *Gastroenterology* 2012; **143**: 1179-1187.e1-e3 [PMID: 22885331 DOI: 10.1053/j.gastro.2012.08.002]

5 **Oh DS**, Demeester SR. Pathophysiology and treatment of Barrett's esophagus. *World J Gastroenterol* 2010; **16**: 3762-3772 [PMID: 20698038 DOI: 10.3748/wjg.v16.i30.3762]

6 **Hur C**, Miller M, Kong CY, Dowling EC, Nattinger KJ, Dunn M, Feuer EJ. Trends in esophageal adenocarcinoma incidence and mortality. *Cancer* 2013; **119**: 1149-1158 [PMID: 23303625 DOI: 10.1002/cncr.27834]

7 **Fang Y**, Chen X, Bajpai M, Verma A, Das KM, Souza RF, Garman KS, Donohoe CL, O'Farrell NJ, Reynolds JV, Dvorak K. Cellular origins and molecular mechanisms of Barrett's esophagus and esophageal adenocarcinoma. *Ann N Y Acad Sci* 2013; **1300**: 187-199 [PMID: 24117642 DOI: 10.1111/nyas.12249]

8 **Denlinger CE**, Thompson RK. Molecular basis of esophageal cancer development and progression. *Surg Clin North Am* 2012; **92**: 1089-1103 [PMID: 23026271 DOI: 10.1016/j.suc.2012.07.002]

9 **Wang DH**, Souza RF. Biology of Barrett's esophagus and esophageal adenocarcinoma. *Gastrointest Endosc Clin N Am* 2011; **21**: 25-38 [PMID: 21112495 DOI: 10.1016/j.giec.2010.09.011]

10 **Donohoe CL**, Pidgeon GP, Lysaght J, Reynolds JV. Obesity and gastrointestinal cancer. *Br J Surg* 2010; **97**: 628-642 [PMID: 20306531 DOI: 10.1002/bjs.7079]

11 **Alemán JO**, Eusebi LH, Ricciardiello L, Patidar K, Sanyal AJ, Holt PR. Mechanisms of obesity-induced gastrointestinal neoplasia. *Gastroenterology* 2014; **146**: 357-373 [PMID: 24315827 DOI: 10.1053/j.gastro.2013.11.051]

12 **Fisichella PM**, Patti MG. Gastroesophageal reflux disease and morbid obesity: is there a relation? *World J Surg* 2009; **33**: 2034-2038 [PMID: 19404705 DOI: 10.1007/s00268-009-0045-z]

13 **Herbella FA**, Sweet MP, Tedesco P, Nipomnick I, Patti MG. Gastroesophageal reflux disease and obesity. Pathophysiology and implications for treatment. *J Gastrointest Surg* 2007; **11**:

286-290 [PMID: 17458599 DOI: 10.1007/s1605-007-0097-z]
14 **Navarro Silvera SA**, Mayne ST, Gammon MD, Vaughan TL, Chow WH, Dubin JA, Dubrow R, Stanford JL, West AB, Rotterdam H, Blot WJ, Risch HA. Diet and lifestyle factors and risk of subtypes of esophageal and gastric cancers: classification tree analysis. *Ann Epidemiol* 2014; **24**: 50-57 [PMID: 24239095 DOI: 10.1016/j.annepidem.2013.10.009]
15 **Maasland DH**, van den Brandt PA, Kremer B, Goldbohm RA, Schouten LJ. Alcohol consumption, cigarette smoking and the risk of subtypes of head-neck cancer: results from the Netherlands Cohort Study. *BMC Cancer* 2014; **14**: 187 [PMID: 24629046 DOI: 10.1186/1471-2407-14-187]
16 **Samet JM**. Tobacco smoking: the leading cause of preventable disease worldwide. *Thorac Surg Clin* 2013; **23**: 103-112 [PMID: 23566962 DOI: 10.1016/j.thorsurg.2013.01.009]
17 **Pandolfino JE**, Kahrilas PJ. Smoking and gastro-oesophageal reflux disease. *Eur J Gastroenterol Hepatol* 2000; **12**: 837-842 [PMID: 10958210]
18 **Neto SC**, Herbella FA, Silva LC, Patti MG. Ratio between proximal/distal gastroesophageal reflux does not discriminate abnormal proximal reflux. *World J Surg* 2014; **38**: 890-896 [PMID: 24305918 DOI: 10.1007/s00268-013-2341-x]
19 **Oelschlager BK**, Quiroga E, Isch JA, Cuenca-Abente F. Gastroesophageal and pharyngeal reflux detection using impedance and 24-hour pH monitoring in asymptomatic subjects: defining the normal environment. *J Gastrointest Surg* 2006; **10**: 54-62 [PMID: 16368491 DOI: 10.1016/j.gassur.2005.09.005]
20 **Sun G**, Muddana S, Slaughter JC, Casey S, Hill E, Farrokhi F, Garrett CG, Vaezi MF. A new pH catheter for laryngopharyngeal reflux: Normal values. *Laryngoscope* 2009; **119**: 1639-1643 [PMID: 19504553 DOI: 10.1002/lary.20282]
21 **Holbrook WP**, Furuholm J, Gudmundsson K, Theodórs A, Meurman JH. Gastric reflux is a significant causative factor of tooth erosion. *J Dent Res* 2009; **88**: 422-426 [PMID: 19493884 DOI: 10.1177/0022034509336530]
22 **Ward PH**, Hanson DG. Reflux as an etiological factor of carcinoma of the laryngopharynx. *Laryngoscope* 1988; **98**: 1195-1199 [PMID: 3185074 DOI: 10.1288/00005537-198811000-00009]
23 **Francis DO**, Maynard C, Weymuller EA, Reiber G, Merati AL, Yueh B. Reevaluation of gastroesophageal reflux disease as a risk factor for laryngeal cancer. *Laryngoscope* 2011; **121**: 102-105 [PMID: 21046549 DOI: 10.1002/lary.21165]
24 **Langevin SM**, Michaud DS, Marsit CJ, Nelson HH, Birnbaum AE, Eliot M, Christensen BC, McClean MD, Kelsey KT. Gastric reflux is an independent risk factor for laryngopharyngeal carcinoma. *Cancer Epidemiol Biomarkers Prev* 2013; **22**: 1061-1068 [PMID: 23703970 DOI: 10.1158/1055-9965.EPI-13-0183]
25 **Qadeer MA**, Colabianchi N, Vaezi MF. Is GERD a risk factor for laryngeal cancer? *Laryngoscope* 2005; **115**: 486-491 [PMID: 15744163 DOI: 10.1097/01.mlg.0000157851.24272.41]
26 **Vaezi MF**, Qadeer MA, Lopez R, Colabianchi N. Laryngeal cancer and gastroesophageal reflux disease: a case-control study. *Am J Med* 2006; **119**: 768-776 [PMID: 16945612 DOI: 10.1016/j.amjmed.2006.01.019]
27 **Bacciu A**, Mercante G, Ingegnoli A, Ferri T, Muzzetto P, Leandro G, Di Mario F, Bacciu S. Effects of gastroesophageal reflux disease in laryngeal carcinoma. *Clin Otolaryngol Allied Sci* 2004; **29**: 545-548 [PMID: 15373871 DOI: 10.1111/j.1365-2273.2004.00851-x]
28 **Chong VH**. Clinical significance of heterotopic gastric mucosal patch of the proximal esophagus. *World J Gastroenterol* 2013; **19**: 331-338 [PMID: 23372354 DOI: 10.3748/wjg.v19.i3.331]
29 **Mercante G**, Bacciu A, Ferri T, Bacciu S. Gastroesophageal reflux as a possible co-promoting factor in the development of the squamous-cell carcinoma of the oral cavity, of the larynx and of the pharynx. *Acta Otorhinolaryngol Belg* 2003; **57**: 113-117 [PMID: 12836467]
30 **Reder NP**, Davis CS, Kovacs EJ, Fisichella PM. The diagnostic value of gastroesophageal reflux disease (GERD) symptoms and detection of pepsin and bile acids in bronchoalveolar lavage fluid and exhaled breath condensate for identifying lung transplantation patients with GERD-induced aspiration. *Surg Endosc* 2014; **28**: 1794-1800 [PMID: 24414458 DOI: 10.1007/s00464-013-3388-3]
31 **Sweet MP**, Patti MG, Hoopes C, Hays SR, Golden JA. Gastro-oesophageal reflux and aspiration in patients with advanced lung disease. *Thorax* 2009; **64**: 167-173 [PMID: 19176842 DOI: 10.1136/thx.2007.082719]
32 **Vereczkei A**, Horvath OP, Varga G, Molnar TF. Gastroesophageal reflux disease and non-small cell lung cancer. Results of a pilot study. *Dis Esophagus* 2008; **21**: 457-460 [PMID: 19125801 DOI: 10.1111/j.1442-2050.2007.00796.x]
33 **Etzel CJ**, Lu M, Merriman K, Liu M, Vaporciyan A, Spitz MR. An epidemiologic study of early onset lung cancer. *Lung Cancer* 2006; **52**: 129-134 [PMID: 16564601 DOI: 10.1016/j.lungcan.2005.11.018]
34 **Liam CK**, Pang YK, Leow CH, Poosparajah S, Menon A. Changes in the distribution of lung cancer cell types and patient demography in a developing multiracial Asian country: experience of a university teaching hospital. *Lung Cancer* 2006; **53**: 23-30 [PMID: 16690159 DOI: 10.1016/j.lungcan.2006.03.009]
35 **Couraud S**, Zalcman G, Milleron B, Morin F, Souquet PJ. Lung cancer in never smokers--a review. *Eur J Cancer* 2012; **48**: 1299-1311 [PMID: 22464348 DOI: 10.1016/j.ejca.2012.03.007]
36 **Yang Y**, Fujita J, Tokuda M, Bandoh S, Ishida T. Lung cancer associated with several connective tissue diseases: with a review of literature. *Rheumatol Int* 2001; **21**: 106-111 [PMID: 11765223 DOI: 10.1007/s00296-001-0141-3]
37 **Patti MG**, Gasper WJ, Fisichella PM, Nipomnick I, Palazzo F. Gastroesophageal reflux disease and connective tissue disorders: pathophysiology and implications for treatment. *J Gastrointest Surg* 2008; **12**: 1900-1906 [PMID: 18766408 DOI: 10.1007/s11605-008-0674-9]
38 **Fukui T**, Shaykhiev R, Agosto-Perez F, Mezey JG, Downey RJ, Travis WD, Crystal RG. Lung adenocarcinoma subtypes based on expression of human airway basal cell genes. *Eur Respir J* 2013; **42**: 1332-1344 [PMID: 23645403 DOI: 10.1183/09031936.00144012]
39 **Goh KL**. Gastroesophageal reflux disease in Asia: A historical perspective and present challenges. *J Gastroenterol Hepatol* 2011; **26** Suppl 1: 2-10 [PMID: 21199509 DOI: 10.1111/j.1440-1746.2010.06534.x]
40 **Bhatia SJ**, Reddy DN, Ghoshal UC, Jayanthi V, Abraham P, Choudhuri G, Broor SL, Ahuja V, Augustine P, Balakrishnan V, Bhasin DK, Bhat N, Chacko A, Dadhich S, Dhali GK, Dhawan PS, Dwivedi M, Goenka MK, Koshy A, Kumar A, Misra SP, Mukewar S, Raju EP, Shenoy KT, Singh SP, Sood A, Srinivasan R. Epidemiology and symptom profile of gastroesophageal reflux in the Indian population: report of the Indian Society of Gastroenterology Task Force. *Indian J Gastroenterol* 2011; **30**: 118-127 [PMID: 21792655 DOI: 10.1007/s12664-011-0112-x]
41 **Hung LJ**, Hsu PI, Yang CY, Wang EM, Lai KH. Prevalence of gastroesophageal reflux disease in a general population in Taiwan. *J Gastroenterol Hepatol* 2011; **26**: 1164-1168 [PMID: 21517967 DOI: 10.1111/j.1440-1746.2011.06750.x]
42 **El-Serag HB**, Petersen NJ, Carter J, Graham DY, Richardson P, Genta RM, Rabeneck L. Gastroesophageal reflux among different racial groups in the United States. *Gastroenterology* 2004; **126**: 1692-1699 [PMID: 15188164 DOI: 10.1053/j.gastro.2004.03.077]
43 **Locke GR**, Talley NJ, Fett SL, Zinsmeister AR, Melton LJ. Risk factors associated with symptoms of gastroesophageal reflux. *Am J Med* 1999; **106**: 642-649 [PMID: 10378622 DOI: 10.1016/S0002-9343(99)00121-7]
44 **Frank L**, Kleinman L, Ganoczy D, McQuaid K, Sloan S, Eggleston A, Tougas G, Farup C. Upper gastrointestinal symptoms in North America: prevalence and relationship to

healthcare utilization and quality of life. *Dig Dis Sci* 2000; **45**: 809-818 [PMID: 10759254]
45 **Diaz-Rubio M**, Moreno-Elola-Olaso C, Rey E, Locke GR, Rodriguez-Artalejo F. Symptoms of gastro-oesophageal reflux: prevalence, severity, duration and associated factors in a Spanish population. *Aliment Pharmacol Ther* 2004; **19**: 95-105 [PMID: 14687171 DOI: 10.1046/j.1365-2036.2003.01769-x]
46 **Louis E**, DeLooze D, Deprez P, Hiele M, Urbain D, Pelckmans P, Devière J, Deltenre M. Heartburn in Belgium: prevalence, impact on daily life, and utilization of medical resources. *Eur J Gastroenterol Hepatol* 2002; **14**: 279-284 [PMID: 11953693]
47 **Agréus L**, Svärdsudd K, Talley NJ, Jones MP, Tibblin G. Natural history of gastroesophageal reflux disease and functional abdominal disorders: a population-based study. *Am J Gastroenterol* 2001; **96**: 2905-2914 [PMID: 11693325 DOI: 10.1111/j.1572-0241.2001.04680.x]
48 **Isolauri J**, Laippala P. Prevalence of symptoms suggestive of gastro-oesophageal reflux disease in an adult population. *Ann Med* 1995; **27**: 67-70 [PMID: 7742002 DOI: 10.3109/07853899509031939]
49 **Ronkainen J**, Aro P, Storskrubb T, Johansson SE, Lind T, Bolling-Sternevald E, Graffner H, Vieth M, Stolte M, Engstrand L, Talley NJ, Agréus L. High prevalence of gastroesophageal reflux symptoms and esophagitis with or without symptoms in the general adult Swedish population: a Kalixanda study report. *Scand J Gastroenterol* 2005; **40**: 275-285 [PMID: 15932168 DOI: 10.1080/00365520510011579]
50 **Valle C**, Broglia F, Pistorio A, Tinelli C, Perego M. Prevalence and impact of symptoms suggestive of gastroesophageal reflux disease. *Dig Dis Sci* 1999; **44**: 1848-1852 [PMID: 10505724 DOI: 10.1023/A:1018846807296]
51 **Terry P**, Lagergren J, Wolk A, Nyrén O. Reflux-inducing dietary factors and risk of adenocarcinoma of the esophagus and gastric cardia. *Nutr Cancer* 2000; **38**: 186-191 [PMID: 11525596 DOI: 10.1207/S15327914NC382_7]
52 **Mohammed I**, Cherkas LF, Riley SA, Spector TD, Trudgill NJ. Genetic influences in gastro-oesophageal reflux disease: a twin study. *Gut* 2003; **52**: 1085-1089 [PMID: 12865263 DOI: 10.1136/gut.52.8.1085]
53 **Eslick GD**, Talley NJ. Gastroesophageal reflux disease (GERD): risk factors, and impact on quality of life-a population-based study. *J Clin Gastroenterol* 2009; **43**: 111-117 [PMID: 18838922 DOI: 10.1097/MCG.0b013e31815ea27b]
54 **Pandeya N**, Green AC, Whiteman DC; Australian Cancer Study. Prevalence and determinants of frequent gastroesophageal reflux symptoms in the Australian community. *Dis Esophagus* 2012; **25**: 573-583 [PMID: 22128757 DOI: 10.1111/j.1442-2050.2011.01287.x]
55 **Ben Chaabane N**, El Jeridi N, Ben Salem K, Hellara O, Loghmari H, Melki W, Bdioui F, Safer L, Soltani M, Saffar H. Prevalence of gastroesophageal reflux in a Tunisian primary care population determined by patient interview. *Dis Esophagus* 2012; **25**: 4-9 [PMID: 21595777 DOI: 10.1111/j.1442-2050.2011.01205.x]
56 **Chen Z**, Thompson SK, Jamieson GG, Devitt PG, Watson DI. Effect of sex on symptoms associated with gastroesophageal reflux. *Arch Surg* 2011; **146**: 1164-1169 [PMID: 22006875 DOI: 10.1001/archsurg.2011.248]
57 **Watson DI**, Lally CJ. Prevalence of symptoms and use of medication for gastroesophageal reflux in an Australian community. *World J Surg* 2009; **33**: 88-94 [PMID: 18949510 DOI: 10.1007/s00268-008-9780-9]
58 **Knox SA**, Harrison CM, Britt HC, Henderson JV. Estimating prevalence of common chronic morbidities in Australia. *Med J Aust* 2008; **189**: 66-70 [PMID: 18637769]
59 **Chiocca JC**, Olmos JA, Salis GB, Soifer LO, Higa R, Marcolongo M; Argentinean Gastro-oesophageal Reflux Study Group. Prevalence, clinical spectrum and atypical symptoms of gastro-oesophageal reflux in Argentina: a nationwide population-based study. *Aliment Pharmacol Ther* 2005; **22**: 331-342 [PMID: 16098000 DOI: 10.1111/j.1365-2036.2005.02565.x]
60 **Center for Diseases Control**. Trends in Current Cigarette Smoking Among High School Students and Adults, United States, 1965-2011. Available from: URL: http://www.cdc.gov/tobacco/data_statistics/tables/trends/cig_smoking/ accessed 07-26-2014
61 **Lortet-Tieulent J**, Renteria E, Sharp L, Weiderpass E, Comber H, Baas P, Bray F, Coebergh JW, Soerjomataram I. Convergence of decreasing male and increasing female incidence rates in major tobacco-related cancers in Europe in 1988-2010. *Eur J Cancer* 2013; Epub ahead of print [PMID: 24269041 DOI: 10.1016/j.ejca.2013.10.014]
62 **Ferlay J**, Shin HR, Bray F, Forman D, Mathers C, Parkin DM. Estimates of worldwide burden of cancer in 2008: GLOBOCAN 2008. *Int J Cancer* 2010; **127**: 2893-2917 [PMID: 21351269 DOI: 10.1002/ijc.25516]
63 **Parkin DM**, Bray F, Ferlay J, Pisani P. Estimating the world cancer burden: Globocan 2000. *Int J Cancer* 2001; **94**: 153-156 [PMID: 11668491 DOI: 10.1002/ijc.1440]
64 **Ferlay J**, Soerjomataram I, Ervik M, Dikshit R, Eser S, Mathers C, Rebelo M, Parkin DM, Forman D, Bray F. GLOBOCAN 2012 v1.0, Cancer Incidence and Mortality Worldwide: IARC CancerBase No. 11[Internet]. Lyon, France: International Agency for Research on Cancer, 2013. Available from: URL: http://globocan.iarc.fr
65 **Bello B**, Zoccali M, Gullo R, Allaix ME, Herbella FA, Gasparaitis A, Patti MG. Gastroesophageal reflux disease and antireflux surgery-what is the proper preoperative work-up? *J Gastrointest Surg* 2013; **17**: 14-20; discussion p. 20 [PMID: 23090280 DOI: 10.1007/s11605-012-2057-5]
66 **Chan K**, Liu G, Miller L, Ma C, Xu W, Schlachta CM, Darling G. Lack of correlation between a self-administered subjective GERD questionnaire and pathologic GERD diagnosed by 24-h esophageal pH monitoring. *J Gastrointest Surg* 2010; **14**: 427-436 [PMID: 20066567 DOI: 10.1007/s11605-009-1137-7]
67 **Vakil NB**, Halling K, Becher A, Rydén A. Systematic review of patient-reported outcome instruments for gastroesophageal reflux disease symptoms. *Eur J Gastroenterol Hepatol* 2013; **25**: 2-14 [PMID: 23202695 DOI: 10.1097/MEG.0b013e328358bf74]

P- Reviewer: Ding GQ, Mickevicius A, Thomopoulos KC
S- Editor: Gou SX **L- Editor**: O'Neill M **E- Editor**: Wang CH

World Journal of Gastroenterology

Submit a Manuscript: http://www.wjgnet.com/esps/
Help Desk: http://www.wjgnet.com/esps/helpdesk.aspx
DOI: 10.3748/wjg.v21.i3.820

World J Gastroenterol 2015 January 21; 21(3): 820-828
ISSN 1007-9327 (print) ISSN 2219-2840 (online)

MINIREVIEWS

Technical tips of endoscopic ultrasound-guided choledochoduodenostomy

Takeshi Ogura, Kazuhide Higuchi

Takeshi Ogura, Kazuhide Higuchi, Second Department of Internal Medicine, Osaka Medical College, Osaka 569-8686, Japan
Author contributions: Ogura T and Higuchi K equally contributed to this paper.

Correspondence to: Takeshi Ogura, MD, PhD, Second Department of Internal Medicine, Osaka Medical College, 2-7 Daigaku-machi, Takatsuki, Osaka 569-8686, Japan. oguratakeshi0411@yahoo.co.jp
Telephone: +81-7-26831221
Fax: +81-7-26846532
Received: August 2, 2014
Peer-review started: August 2, 2014
First decision: August 27, 2014
Revised: September 12, 2014
Accepted: November 18, 2014
Article in press: November 19, 2014
Published online: January 21, 2015

Abstract

Endoscopic ultrasound (EUS) is clinically useful not only as a diagnostic tool during EUS-guided fine needle aspiration, but also during interventional EUS. EUS-guided biliary drainage has been developed and performed by experienced endoscopists. EUS-guided choledocoduodenostomy (EUS-CDS) is relatively well established as an alternative biliary drainage method for biliary decompression in patients with biliary obstruction. The reported technical success rate of EUS-CDS ranges from 50% to 100%, and the clinical success rate ranges from 92% to 100%. Further, the over-all technical success rate was 93%, and clinical success rate was 98%. Based on the currently available literature, the overall adverse event rate for EUS-CDS is 16%. The data on the cumulative technical and clinical success rate for EUS-CDS is promising. However, EUS-CDS can still lead to several problems, so techniques or devices that are more feasible and safe need to be established. EUS-CDS has the potential to become a first-line biliary drainage procedure, although standardizing the technique in multicenter clinical trials and comparisons with endoscopic biliary drainage by randomized clinical trials are still needed.

Key words: Endoscopic ultrasound; Endoscopic ultrasound-guided choledochoduodenostomy; Endoscopic ultrasound-guided biliary drainage; Percutaneous transhepatic biliary drainage

Core tip: Endoscopic ultrasound-guided choledocoduod enostomy (EUS-CDS) is relatively well established as an alternative biliary drainage method. The reported technical success rate of EUS-CDS ranges from 50% to 100%, and the clinical success rate ranges from 92% to 100%. Further, the over-all technical success rate was 93%, and clinical success rate was 98%. Based on the currently available literature, the overall adverse event rate for EUS-CDS is 16%. EUS-CDS may become the first choice of the biliary tract drainage procedure in the local cases such as poor prognosis, the contraindication of percutaneous transhepatic biliary drainage.

Ogura T, Higuchi K. Technical tips of endoscopic ultrasound-guided choledochoduodenostomy. *World J Gastroenterol* 2015; 21(3): 820-828 Available from: URL: http://www.wjgnet.com/1007-9327/full/v21/i3/820.htm DOI: http://dx.doi.org/10.3748/wjg.v21.i3.820

INTRODUCTION

Obstructive jaundice is a major adverse effect of pancreatic or biliary carcinoma. This adverse event requires treatment, especially in patients who cannot be treated surgically due to concurrent chemotherapy. Endoscopic biliary stenting (EBS) is a gold standard method of treatment for obstructive jaundice[1,2]. However, this method is associated with several problems, such as post-endoscopic retrograde cholangiopancreatography (ERCP) pancreatitis. In addition, EBS cannot be performed in patients with selective cannulation failure of the major papilla or an inaccessible papilla due to duodenal invasion. The alternative method under these conditions is percutaneous transhepatic biliary drainage (PTBD)[3,4]. However, PTBD can lead to several adverse events, such as cholangitis, bile leakage and pneumothorax. Moreover, the frequency of major complications, such as prolonged hospital stay and permanent adverse sequelae, is 4.6%-25%, and that of procedure-related deaths is 0%-5.6%[5,6]. Cosmetic issues due to external drainage also compromise the patient's quality of life.

Endoscopic ultrasound (EUS) is clinically useful not only as a diagnostic tool during EUS-guided fine needle aspiration (FNA), but also during interventional EUS. Among the different types of interventional EUS, endoscopic ultrasound-guided biliary drainage (EUS-BD) has been developed and performed by experienced endoscopists. The technique of EUS-BD depends on the approach route. For transgastric EUS-BD, EUS-guided hepaticogastrostomy (EUS-HGS) is performed, in which the intrahepatic bile duct (usually segment 3; B3) is punctured *via* the stomach, and stent placement is performed from the intrahepatic bile duct to the stomach[7]. For transduodenal EUS-BD, EUS-guided choledochoduodenostomy (EUS-CDS) is performed, in which the common bile duct (CBD) is punctured, and stent placement is performed from the CBD to the duodenum. For transgastric or transduodenal EUS-BD, EUS-guided gallbladder drainage (EUS-GBD) is performed, in which the gallbladder is punctured and a stent is placed from the gallbladder to the stomach or duodenum[8]. In addition, the EUS-guided rendezvous technique (EUS-RV) is also included as EUS-BD[9].

While EUS-HGS and EUS-GBD have clinical benefits in certain patients, their use is associated with several adverse events, including stent migration. If stent migration does occur, it is sometimes fatal. Therefore, novel methods or new devices are required to prevent the complications associated with these procedures. EUS-RV is only indicated for patients in whom the ampulla of Vater is accessible by duodenoscopy. This procedure is sometimes difficult and requires a long procedure time[9].

On the other hand, EUS-CDS is relatively well established as an alternative biliary drainage method with a relatively low rate of adverse events, for biliary decompression in patients with biliary obstruction. However, EUS-CDS can still lead to several problems, so techniques or devices that are more feasible and safe need to be established.

Table 1 shows an overview of previous reports of EUS-CDS[10-45]. Herein, we present technical tips on the performance of EUS-CDS and review of the literature on EUS-CDS, especially its techniques and adverse events.

INDICATIONS

EUS-CDS is mainly performed for patients with failed EBS excluded prospective clinical trial, as was previously described by Hara *et al*[26] and Itoi *et al*[42]. This procedure can be performed for obstructions in the middle and lower bile duct.

The primary diseases in patients who underwent EUS-CDS were pancreatic carcinoma (n = 98), ampullary carcinoma (n = 14), and cholangiocarcinoma (n = 13). This indicates that pancreato-biliary carcinoma is the main indication for EUS-CDS. On the other hand, EUS-CDS for benign biliary stricture was only performed in 2 patients, as previously reported.

EUS-CDS is contraindicated in patients with surgically altered anatomy, such as a Roux-en-Y anastomosis or duodenal obstruction caused by tumor invasion, through which an endoscope cannot be passed. In such cases, EUS-guided hepaticogastrostomy may be indicated. However, if the duodenal bulb is not involved, EUS-CDS can be performed in combination with duodenal stenting (Figure 1).

The indications for EUS-CDS *vs* ERCP for benign disease are still not completely known. Therefore, prospective randomized controlled trials comparing EUS-CDS with ERCP are needed to assess the clinical efficacy of the procedure.

Hence, the following are the indications for EUS-CDS: (1) failed EBS; (2) inaccessibility of the ampulla of Vater, such as due to duodenal invasion by the tumor; (3) contraindications for percutaneous transhepatic biliary drainage (PTBD); and (4) middle or lower bile duct obstruction.

DEVICE SELECTION AND TECHNICAL TIPS

Puncture of the common bile duct

To visualize the CBD on EUS, the EUS scope is advanced into the duodenum, turned slightly to the left and angled downwards. The CBD is punctured using a 19-G needle under Doppler visualization, to avoid any intervening vessels. Bile juice is aspirated and a small amount of contrast medium is injected. During this step, it is important to avoid puncturing the duodenal mucosa and cystic duct. As shown in Figure 2, when a double duodenal mucosal line is visualized on EUS, the CBD should not be punctured to avoid puncture and stenting through double duodenal mucosa.

According to previous reports, a 19G or 22G FNA needle or needle knife is used to puncture the CBD. As of now, there are no randomized controlled trials

Table 1 Overview of reports on endoscopic ultrasound-guided choledocoduodenostomy *n* (%)

Ref.	*n*	Disease (*n*)	Indications	Technical success	Clinical success	Puncture devise (*n*)	Dilation devise	Stents	Adverse events (*n*)
Giovannini *et al*[10]	1	Pancreatic carcinoma	Faild EBD	1 (100)	1 (100)	5 Fr needle knife	6.5 Fr dilataor	10 Fr PS	None
Burmester *et al*[11]	2	Pancreatic carcinoma (2)	Faild EBD	1 (50)	1 (100)	19 G fistulome	None	8.5 Fr PS	Bile peritonitis (1)
Püspök *et al*[12]	5	N/D	Faild EBD	4 (80)	4 (100)	Needle knife, 19 G FNA needle	8 mm balloon	7-10 Fr PS	None
Kahaleh *et al*[13]	1	Pancreatic carcinoma	Faild EBD	1 (100)	1 (100)	19 G FNA needle	N/D	10 mm MS	Pneumoperitoneum (1)
Yamao *et al*[14]	5	Pancreatic carcinoma (3), ampulla carcinoma (2)	Faild EBD	2 (100)	2 (100)	Needle knife	7 Fr, 9 Fr dilator	7-8.5 Fr PS	Pneumoperitoneum (1)
Ang *et al*[16]	2	Pancreatic carcinoma (2)	Faild EBD	2 (100)	2 (100)	19 G FNA needle	7 Fr dilator	7 Fr PS	Pneumoperitoneum (1)
Fujita *et al*[17]	1	Ampulla carcinoma	Faild EBD	1 (100)	1 (100)	19 G FNA needle	Dilator	7 Fr PS	None
Tarantino *et al*[18]	4	Pancreatic carcinoma (2), cholangiocarcinoma (1), malignant lymphoma (1)	Faild EBD	4 (100)	4 (100)	19 G, 22 G FNA needle, needle knife	4 mm balloon	PS	None
Itoi *et al*[19]	4	Pancreatic carcinoma (2), ampulla carcinoma (2)	Faild EBD	4 (100)	4 (100)	Needle knife, 19 G FNA needle	7 Fr, 9 Fr dilator, balloon	7 Fr PS (3), NBD (1)	Bleeding (1), peritonitis (1)
Brauer *et al*[20]	3	Pancreatic carcinoma (1), gastric carcinoma (1), choledocholithiasis (1)	Faild EBD	3 (100)	3 (100)	19 G FNA needle, needle knife	N/D	5 Fr, 10 Fr PS	Cardicac and respiratory failure (1), pneumoperitoneum (1)
Horaguchi *et al*[21]	8	Pancreatic carcinoma (5), ampulla carcinoma (1), choledocholithiasis (1), Lymph note metastasis (1)	Faild EBD	8 (100)	8 (100)	19 G FNA needle	5 Fr dilator, 4 mm balloon	7 Fr PS (7), NBD (1)	Peritonitis (1)
Hanada *et al*[22]	4	Pancreatic carcinoma (4)	Faild EBD	4 (100)	4 (100)	19 G FNA needle	6 Fr, 7 Fr dilator	6 Fr, 7 Fr PS	None
Iwamuro *et al*[23]	5	Pancreatic carcinoma (4), ampulla carcinoma (1)	Duodenal obstruction	5 (100)	5 (100)	Needle knife	7 Fr dilator	7 Fr PS	Abdominal pain, fever (1)
Artifon *et al*[24]	3	Pancreatic carcinoma (3), ampulla carcinoma (2)	Faild EBD (2), duodenal invasion (1)	3 (100)	3 (100)	19 G FNA needle	Needle knife	10 mm MS	None
Belletrutii *et al*[25]	1	Pancreatic carcinoma	Faild EBD	1 (100)	1 (100)	19 G FNA needle	6 mm balloon	10 mm MS	None
Hara *et al*[26]	18	Pancreatic carcinoma (15), uterus carcinoma (1), gastric carcinoma (1), gallbladder carcinoma (1)	Lower biliary obstruction	17 (94)	17 (100)	22G FNA needle, needle knife	6, 7, 9 Fr dilator	7, 8.5 Fr PS	Bile peritonitis (2), hemobilia (1)
Siddiqu *et al*[27]	8	Pancreatic carcinoma (6), cholangiocarcinoma (2)	Faild EBD	8 (100)	8 (100)	19 G FNA needle	Needle knife	10 mm MS	Stent migration/ duodenal perforation (1), abdominal pain (1)
Fabbri *et al*[28]	12	Pancreatic carcinoma (7), cholangiocarcinoma (4), ampulla carcinoma (1), gallbladder carcinoma (1)	Faild EBD	9 (75)	9 (100)	19 G FNA needle, needle knife	4 mm balloon	MS	Pneumoperitoneum (1)
Komaki *et al*[29]	15	Unresectable malignant biliary obstruction	Faild EBD	14 (93)	14 (100)	19 G FNA needle	Dilator	7 Fr PS	None
Prachayakul *et al*[30]	1	Pancreatic carcinoma	Duodenal obstruction	1 (100)	1 (100)	N/D	Dilator	PS	None
Ramírez-Luna *et al*[31]	9	Pancreatic carcinoma (4), cholangiocarcinoma (2), metastases (1), ampulla carcinoma (1), neuroendocrine (1)	Faild EBD	8 (89)	8 (100)	19 G FNA needle	Needle knife, 6, 7, 10 Fr dilator	7, 8, 10 Fr PS	Biloma (1)
Park do *et al*[32]	26	N/D	Faild EBD	24 (92)	22 (92.9)	19 G FNA needle	4 Fr ERCP cannula, 6, 7 Fr dilator, needle knife	PS, MS	Bile peritonitis (2), unknown (3)

Artifon *et al*[33]	13	Unresectable malignant biliary obstruction	Faild EBD	13 (100)	13 (100)	19 G FNA needle	Needle knife	10 mm MS	Biloma (1), bleeding (1)
Attasaranya *et al*[34]	9	N/D	Faild EBD	5 (56)	N/D	19 G FNA needle	ERCP catheter, 6, 7 Fr dilator, 8 mm balloon, needle knife	N/D	Unknown (4)
Katanuma *et al*[35]	1	Chronic pancreatitis	Relapsing cholangitis, duodena stenosis	1 (100)	1 (100)	19 G FNA needle	Needle knife, dilator	7 Fr PS	None
kawakubo *et al*[36]	2	Pancreatic carcinoma (2)	Duodenal obstruction	2 (100)	2 (100)	19 G FNA needle	7 Fr dilator, 4 mm balloon	7 Fr PS	None
Khashab *et al*[37]	2	Pancreatic carcinoma (2)	Duodenal obstruction	2 (100)	2 (100)	19 G FNA needle	Needle knife, 7 Fr dilator	10 mm MS	None
Kim *et al*[38]	9	Pancreatic carcinoma (5), cholangiocarcinoma (4)	Faild EBD	9 (100)	9 (100)	19 G FNA needle	ERCP catheter, cystostome, needle knife, dilator	10 mm MS	Bile peritonitis (1)
Song *et al*[39]	15	Pancreatic carcinoma (9), ampulla carcinoma (2), renal cell carcinoma (1), lymphoma (1), gastric carcinoma (1), duodenal carcinoma (1)	Faild EBD	13 (87)	13 (100)	19 G FNA needle	6, 7 Fr dilator, needle knife	8, 10 mm MS	Pneumoperitoneum (2), cholngitis (1)
Vila *et al*[40]	26	Malignant (22), benign (4)	NA	19 (86)	NA	NA	NA	NA	Biloma (1), bleeding (1), pancreatitis (1), cholangitis (1)
Maluf-Filho *et al*[41]	5	Pancreatic carcinoma (3), colonic carcinoma (1), cervix carcinoma (1)	Duodenal obstruction	3 (60)	5 (100)	19 G FNA needle	Diathermic sheath	10 mm MS	Biliary fistula (1), cardiogenic shock (1)
Itoi *et al*[42]	1	Pancreatic carcinoma (1)	Duodenal obstruction	1 (100)	1 (100)	19 G FNA needle	ERCP catheter, 4 mm balloon	10 mm MS	None
Tonozuka *et al*[43]	4	Pancreatic carcinoma (4)	Duodenal obstruction	4 (100)	4 (100)	19 G FNA needle	Dilator, balloon, diathermic sheath	MS	None
Hara *et al*[44]	18	Pancreatic carcinoma (17), ampulla carcinoma (1)	Lower biliary obstruction	17 (94)	17 (100)	22G FNA needle, needle knife	6, 7, 9 Fr dilator	10 mm MS, 8.5 Fr PS	Peritonitis (2)
Khashab *et al*[45]	20	Malignant (15)	NA	20 (100)	19 (95)	19 G FNA needle	Dilator, balloon	PS, MS	NA
Kawakubo *et al*[46]	44	Pancreatic carcinoma (31), ampullary carcinoma (8), cholangiocarcinoma (2), metastatic lymph nodes (3)	Periampullary tumor invasion, failed EBS	42 (95)	NA	19 G FNA needle, needle knife	Dilator, balloon	PS, MS	Bile leak (3), stent misplacement (1), bleeding (1), pneumoperitoneum (1), perforation (1)

EBD: Endoscopic biliary drainage; FNA: Fine needle aspiration; EBS: Endoscopic biliary stenting; ERCP: Endoscopic retrograde cholangiopancreatography; NBD: Negative binomial distribution; NA: Not applicable; PS: Plastic stent; MS: Metal stent; N/D: Not determined.

comparing the outcomes of various FNA needles in EUS-CDS. Recently, a novel FNA needle (Sono Tip Pro Control 19G needle, Medi-Globe GmbH, Rosenheim, Germany) (Figure 3) has become available. The cut surface of this FNA needle is 5 mm long, and is believed to be extremely sharp. Therefore, we think this needle is appropriate for use in interventional EUS.

Guidewire insertion into the bile duct

After the contrast is injected into the CBD, the guidewire is placed deep in the intrahepatic bile duct. On EUS imaging, when the CBD is aligned parallel to the FNA needle, the guidewire can be easily advanced toward the hepatic hilum.

To enable passage of a 0.035 inch stiff guidewire into the needle, a 19-gauge needle should be selected. A 0.025 inch guidewire with a highly flexible tip, sufficient stiffness, and easily seeking ability (VisiGlide; Olympus Medical Systems, Tokyo, Japan) is preferable. To avoid wire sharing, a novel guidewire which top formation is coil (Cyst-wire, Medi-Globe) (Figure 4) is also useful.

When the guidewire is inserted along with other

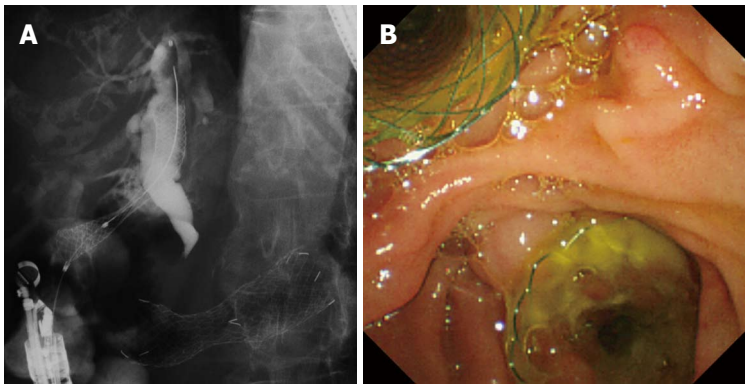

Figure 1 Endoscopic ultrasound-guided choledocoduodenostomy combined with duodenal stent. A: Endoscopic ultrasound-guided choledocoduodenostomy (EUS-CDS) was performed from duodenal bulb after duodenal stenting; B: Endoscopic view of EUS-CDS combined with duodenal stent.

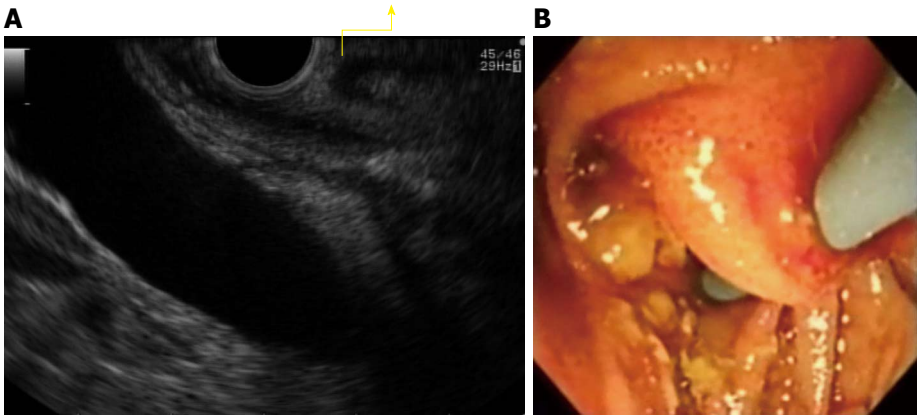

Figure 2 Double puncture of duodenal mucosa. A: Double mucosa of duodenum on endoscopic ultrasound view (arrow); B: Endoscopic view of double puncture of duodenal mucosa.

Figure 3 Novel endoscopic ultrasound-guided fine needle aspiration needle (Sono Tip Pro Control 19 G needle, Medi-Globe GmbH, Rosenheim, Germany). The cut surface of this fine needle aspiration needle is 5 mm, and this needle has sharpness.

Figure 4 Cyst-wire (Medi-Globe GmbH, Rosenheim, Germany). To avoid wire sharing, top formation of this guidewire is coil.

devices, it is important to be able to view the devices under both EUS and fluoroscopic guidance, to ensure that they fit the axis.

Devices used to dilate the fistula

Various devices have been previously described for dilatation of the fistula after puncturing the CBD. The most common devices for transmural tract dilation are the dilator (6 to 10 Fr; Soehendra biliary dilation catheters, Cook Medical), balloon catheter (4-8 mm; MaxForce or Hurricane RX; Boston Scientific), or needle knife (Microtome, Boston Scientific). Park reported that the overall adverse event rate of EUS-BD, including EUS-CDS and EUS-HGS, was 27% (15/55)[32]. They also described the use of a needle

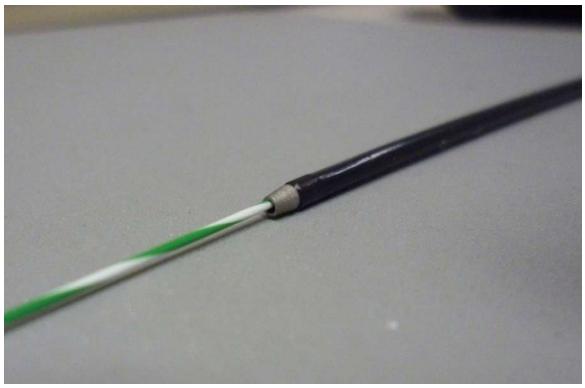

Figure 5 Cysto-Gastro-Set (Endoflex, GmbH, Voerde, Germany). This devise is always coaxial with the guidewire.

knife for fistula dilation as the single risk factor for adverse procedural events after EUS-BD (P = 0.01, HR = 12.4, 95%CI: 1.83-83.5). Due to the acute angulation of the EUS scope, following deployment of the catheter at the duodenal bulb, the needle knife, when deployed, points tangentially, which can lead to accidental incision with a chance of pneumoperitoneum or bleeding. Therefore, they concluded that fistula dilation should be avoided if possible.

However, it is true that fistula dilation is easier if a needle knife is used. Recently, a diathermic dilator (Cysto Gastro Set; Endoflex, GmbH, Voerde, Germany) has become available. This device is always coaxial with the guidewire (Figure 5). Hence, its use for fistula dilation may reduce the incidence of EUS-BD-related adverse events compared with those using a needle knife. Studies comparing these devices are, therefore, warranted.

Stent selection

Both plastic and metallic stents have been used during EUS-CDS. Previously, plastic stents with diameters ranging from 5 to 10 Fr were used. Generally, because the diameter of the working channel of the EUS is 3.7 mm, a 7 or 8.5 Fr plastic stent is used. However, as shown in Figure 6, bile leak can occur with plastic stent placement. This patient had abdominal pain and fever for up to 3 d after EUS-CDS, and computed tomography and duodenoscopy showed bile leakage. If a large fistula is created during stent placement, bile leakage from the gap between the stent and the fistula is likely to occur because of the fine gauge of the plastic stent.

On the other hand, although no comparative studies exist, metallic stents are expected to offer several clinical benefits. First, because of their large diameter, metallic stents have a longer patency than plastic stents. Second, due to the close proximity between the metallic stent and the duodenal wall and bile duct, bile leak is less likely to occur. Use of an uncovered metallic stent, however, can easily cause bile leakage, which is sometimes fatal[43]. Therefore, partially or fully covered self-expandable metal stents (SEMS) should be selected. However, although these SEMS have the advantage of preventing bile leakage, they also have the disadvantage of causing occlusion of the side branch of the bile duct. This suggests that if the distance between the site of the puncture and the hepatic hilar portion is short, a partially covered SEMS should be selected to prevent occlusion of the intrahepatic bile duct. Unfortunately, when a partially covered SEMS is used, bile leak can occur from the uncovered part, particularly between the bile duct and the gastrointestinal tract.

Stent migration is also usually a challenging complication of EUS-BD. With the use of the standard metallic stent, some authors described that a double pigtail plastic stent can be placed inside the metal stent, with the pigtail functioning as an anchor[47]. Among standard metallic stents, metallic stents with a wide flange should be selected, and stent shortening to a length of 60 mm may be preferable in order to avoid stent migration.

Recently, a novel SEMS has been developed. The NAGI-Stent (Taewoong-Medical Co., Seoul, South Korea) is delivered through a 10.5 Fr catheter, and consists of a fully covered 20 mm long and 16 mm diameter stent with bilateral anchor flanges. The AXIOS stent (Xlumena Inc., Mountain View, CA, United States) is a fully covered, 10 mm diameter, 10 mm long, braided stent with bilateral 20 mm diameter anchor flanges. These novel SEMSs are used for EUS-guided pseudocystic drainage and EUS-guided cholecystogastrostomy[48-50]. This SEMS seems to be useful for EUS-CDS as well, although clinical trials are needed to confirm its utility.

According to previous reports, the mean stent patency in EUS-CDS was similar to PTBD (198 d *vs* 184 d, P = 0.86)[51]. Although there were no reports of comparison between EUS-CDS and EBS, stent patency of EBS (covered metallic stent; 585 d, uncovered metallic stent; 314 d) may be longer than EUS-CDS according to previously described report[52]. Randomized clinical trials are needed with standardizing kinds of biliary stents.

SUCCESS RATE

The reported technical success rate of EUS-CDS ranges from 50% to 100%, and the clinical success rate ranges from 92% to 100%. Further, the over-all technical success rate was 93% (199/213), and clinical success rate was 98% (183/187). This is a relatively high success rate compared with ERCP. Therefore, if EUS-CDS is associated with a low rate of adverse events and long stent patency, it has the potential to be the bile drainage method of choice instead of EBS. A prospective randomized clinical trial is needed to compare endoscopic biliary drainage and EUS-CDS.

ADVERSE EVENTS

Based on the currently available literature, the overall adverse event rate for EUS-CDS is 16% (34/213). EUS-CDS has the potential to cause several adverse

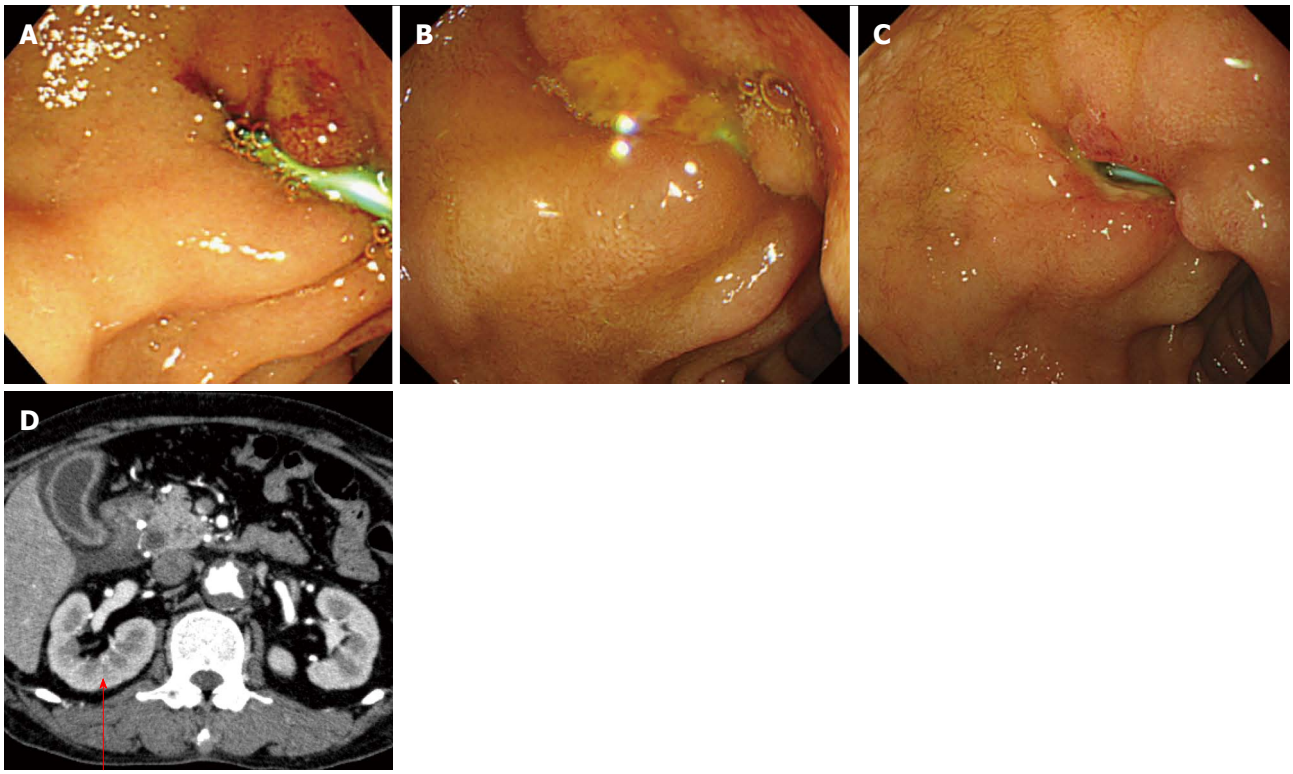

Figure 6 Bile leak due to plastic stent of endoscopic ultrasound-guided choledocoduodenostomy. A: Endoscopic view of day 1; B: Day 2; C: Day 3; D: Computed tomography showed bile leak (arrow).

events, including: (1) infection (peritonitis, cholangitis, cholecystitis); (2) pneumoperitoneum; (3) bile leakage, biloma; (4) bleeding; (5) abdominal pain; (6) perforation; and (7) stent migration.

Based on previous reports, the most frequent adverse events were pneumoperitoneum (28%, 9/34). In most EUS-CDS cases, if adverse events do occur, they can be treated conservatively. However, two deaths related to EUS-CDS, due to cardiogenic shock and bile leakage, were also reported by Maluf-Filho *et al*[41]. In both these patients, the bile leak occurred because of use of an uncovered SEMS. However, even if a fully covered SEMS is selected, the risk of bile peritonitis still remains. This adverse event may occur because of bile or air leak during dilation of the fistula while inserting the stent delivery system. Therefore, to avoid these adverse events, more developed devices that would enable one-step stent placement (without dilation of the fistula) are strongly needed. To avoid bleeding, use of color Doppler ultrasound to detect vascular structures can decrease the risk of bleeding.

CONCLUSION

SEM stents should be selected during EUS-CDS to avoid several adverse events, although the possibility of stent migration still remains. The data on the cumulative technical and clinical success rate for EUS-CDS is promising. EUS-CDS may become the first choice of the biliary tract drainage procedure in the local cases such as poor prognosis, the contraindication of PTBD.

REFERENCES

1 **Fogel EL**, Sherman S, Devereaux BM, Lehman GA. Therapeutic biliary endoscopy. *Endoscopy* 2001; **33**: 31-38 [PMID: 11204985 DOI: 10.1055/s-2001-11186]
2 **Williams EJ**, Taylor S, Fairclough P, Hamlyn A, Logan RF, Martin D, Riley SA, Veitch P, Wilkinson M, Williamson PJ, Lombard M. Are we meeting the standards set for endoscopy? Results of a large-scale prospective survey of endoscopic retrograde cholangio-pancreatograph practice. *Gut* 2007; **56**: 821-829 [PMID: 17145737 DOI: 10.1136/gut.2006.097543]
3 **Oh HC**, Lee SK, Lee TY, Kwon S, Lee SS, Seo DW, Kim MH. Analysis of percutaneous transhepatic cholangioscopy-related complications and the risk factors for those complications. *Endoscopy* 2007; **39**: 731-736 [PMID: 17661249 DOI: 10.1055/s-2007-966577]
4 **Winick AB**, Waybill PN, Venbrux AC. Complications of percutaneous transhepatic biliary interventions. *Tech Vasc Interv Radiol* 2001; **4**: 200-206 [PMID: 11748558]
5 **Carrasco CH**, Zornoza J, Bechtel WJ. Malignant biliary obstruction: complications of percutaneous biliary drainage. *Radiology* 1984; **152**: 343-346 [PMID: 6739796 DOI: 10.1148/radiology.152.2.6739796]
6 **Günther RW**, Schild H, Thelen M. Percutaneous transhepatic biliary drainage: experience with 311 procedures. *Cardiovasc Intervent Radiol* 1988; **11**: 65-71 [PMID: 2455599]
7 **Giovannini M**, Dotti M, Bories E, Moutardier V, Pesenti C, Danisi C, Delpero JR. Hepaticogastrostomy by echo-endoscopy as a palliative treatment in a patient with metastatic biliary obstruction. *Endoscopy* 2003; **35**: 1076-1078 [PMID: 14648424 DOI: 10.1055/s-2003-44596]
8 **Itoi T**, Itokawa F, Kurihara T. Endoscopic ultrasonography-guided gallbladder drainage: actual technical presentations

and review of the literature (with videos). *J Hepatobiliary Pancreat Sci* 2011; **18**: 282-286 [PMID: 20652716 DOI: 10.1007/s00534-010-0310-4]

9 **Kim YS**, Gupta K, Mallery S, Li R, Kinney T, Freeman ML. Endoscopic ultrasound rendezvous for bile duct access using a transduodenal approach: cumulative experience at a single center. A case series. *Endoscopy* 2010; **42**: 496-502 [PMID: 20419625 DOI: 10.1007/s-0029-1244082]

10 **Giovannini M**, Moutardier V, Pesenti C, Bories E, Lelong B, Delpero JR. Endoscopic ultrasound-guided bilioduodenal anastomosis: a new technique for biliary drainage. *Endoscopy* 2001; **33**: 898-900 [PMID: 11571690 DOI: 10.1055/s-2001-17324]

11 **Burmester E**, Niehaus J, Leineweber T, Huetteroth T. EUS-cholangio-drainage of the bile duct: report of 4 cases. *Gastrointest Endosc* 2003; **57**: 246-251 [PMID: 12556796]

12 **Püspök A**, Lomoschitz F, Dejaco C, Hejna M, Sautner T, Gangl A. Endoscopic ultrasound guided therapy of benign and malignant biliary obstruction: a case series. *Am J Gastroenterol* 2005; **100**: 1743-1747 [PMID: 16086710 DOI: 10.11111/j.1572-0241.2005.41806]

13 **Kahaleh M**, Hernandez AJ, Tokar J, Adams RB, Shami VM, Yeaton P. Interventional EUS-guided cholangiography: evaluation of a technique in evolution. *Gastrointest Endosc* 2006; **64**: 52-59 [PMID: 16813803]

14 **Yamao K**, Sawaki A, Takahashi K, Imaoka H, Ashida R, Mizuno N. EUS-guided choledochoduodenostomy for palliative biliary drainage in case of papillary obstruction: report of 2 cases. *Gastrointest Endosc* 2006; **64**: 663-667 [PMID: 16996372]

15 **Yamao K**, Bhatia V, Mizuno N, Sawaki A, Ishikawa H, Tajika M, Hoki N, Shimizu Y, Ashida R, Fukami N. EUS-guided choledochoduodenostomy for palliative biliary drainage in patients with malignant biliary obstruction: results of long-term follow-up. *Endoscopy* 2008; **40**: 340-342 [PMID: 18389451 DOI: 10.1055/s-2007-995485]

16 **Ang TL**, Teo EK, Fock KM. EUS-guided transduodenal biliary drainage in unresectable pancreatic cancer with obstructive jaundice. *JOP* 2007; **8**: 438-443 [PMID: 17625296]

17 **Fujita N**, Noda Y, Kobayashi G, Ito K, Obana T, Horaguchi J, Takasawa O, Nakahara K. Histological changes at an endosonography-guided biliary drainage site: a case report. *World J Gastroenterol* 2007; **13**: 5512-5515 [PMID: 17907298 DOI: 10.3748/wjg.v13.i41.5512]

18 **Tarantino I**, Barresi L, Repici A, Traina M. EUS-guided biliary drainage: a case series. *Endoscopy* 2008; **40**: 336-339 [PMID: 18264890 DOI: 10.1055/s-2007-995455]

19 **Itoi T**, Itokawa F, Sofuni A, Kurihara T, Tsuchiya T, Ishii K, Tsuji S, Ikeuchi N, Moriyasu F. Endoscopic ultrasound-guided choledochoduodenostomy in patients with failed endoscopic retrograde cholangiopancreatography. *World J Gastroenterol* 2008; **14**: 6078-6082 [PMID: 18932289 DOI: 10.3748/wjg.14.6078]

20 **Brauer BC**, Chen YK, Fukami N, Shah RJ. Single-operator EUS-guided cholangiopancreatography for difficult pancreaticobiliary access (with video). *Gastrointest Endosc* 2009; **70**: 471-479 [PMID: 19560768 DOI: 10.1016/j.gie.2008.12.233]

21 **Horaguchi J**, Fujita N, Noda Y, Kobayashi G, Ito K, Obana T, Takasawa O, Koshita S, Kanno Y. Endosonography-guided biliary drainage in cases with difficult transpapillary endoscopic biliary drainage. *Dig Endosc* 2009; **21**: 239-244 [PMID: 19961522 DOI: 10.1111/j.1443-1661.2009.00899.x]

22 **Hanada K**, Iiboshi T, Ishii Y. Endoscopic ultrasound-guided choledochoduodenostomy for palliative biliary drainage in cases with inoperable pancreas head carcinoma. *Dig Endosc* 2009; **21** Suppl 1: S75-S78 [PMID: 19691742 DOI: 10.1111/j.1443-1661.2009.00855.x]

23 **Iwamuro M**, Kawamoto H, Harada R, Kato H, Hirao K, Mizuno O, Ishida E, Ogawa T, Okada H, Yamamoto K. Combined duodenal stent placement and endoscopic ultrasonography-guided biliary drainage for malignant duodenal obstruction with biliary stricture. *Dig Endosc* 2010; **22**: 236-240 [PMID: 20642617 DOI: 10.1111/j.1443-1661.2010.00997.x]

24 **Artifon EL**, Takada J, Okawa L, Moura EG, Sakai P. EUS-guided choledochoduodenostomy for biliary drainage in unresectable pancreatic cancer: a case series. *JOP* 2010; **11**: 597-600 [PMID: 21068493]

25 **Belletrutti PJ**, Gerdes H, Schattner MA. Successful endoscopic ultrasound-guided transduodenal biliary drainage through a pre-existing duodenal stent. *JOP* 2010; **11**: 234-236 [PMID: 20442518]

26 **Hara K**, Yamao K, Niwa Y, Sawaki A, Mizuno N, Hijioka S, Tajika M, Kawai H, Kondo S, Kobayashi Y, Matumoto K, Bhatia V, Shimizu Y, Ito A, Hirooka Y, Goto H. Prospective clinical study of EUS-guided choledochoduodenostomy for malignant lower biliary tract obstruction. *Am J Gastroenterol* 2011; **106**: 1239-1245 [PMID: 21448148 DOI: 10.1038/ajg.2011.84]

27 **Siddiqui AA**, Sreenarasimhaiah J, Lara LF, Harford W, Lee C, Eloubeidi MA. Endoscopic ultrasound-guided transduodenal placement of a fully covered metal stent for palliative biliary drainage in patients with malignant biliary obstruction. *Surg Endosc* 2011; **25**: 549-555 [PMID: 20632191 DOI: 10.1007/s00464-010-1216-6]

28 **Fabbri C**, Luigiano C, Fuccio L, Polifemo AM, Ferrara F, Ghersi S, Bassi M, Billi P, Maimone A, Cennamo V, Masetti M, Jovine E, D'Imperio N. EUS-guided biliary drainage with placement of a new partially covered biliary stent for palliation of malignant biliary obstruction: a case series. *Endoscopy* 2011; **43**: 438-441 [PMID: 21271507 DOI: 10.1055/s-0030-1256097]

29 **Komaki T**, Kitano M, Sakamoto H, Kudo M. Endoscopic ultrasonography-guided biliary drainage: evaluation of a choledochoduodenostomy technique. *Pancreatology* 2011; **11** Suppl 2: 47-51 [PMID: 21464587 DOI: 10.1159/000323508]

30 **Prachayakul V**, Aswakul P, Kachintorn U. EUS-guided choledochoduodenostomy for biliary drainage using tapered-tip plastic stent with multiple fangs. *Endoscopy* 2011; **43** Suppl 2 UCTN: E109-E110 [PMID: 21424999 DOI: 10.1055/s-0030-1256140]

31 **Ramírez-Luna MA**, Téllez-Ávila FI, Giovannini M, Valdovinos-Andraca F, Guerrero-Hernández I, Herrera-Esquivel J. Endoscopic ultrasound-guided biliodigestive drainage is a good alternative in patients with unresectable cancer. *Endoscopy* 2011; **43**: 826-830 [PMID: 21833899 DOI: 10.1055/s-0030-1256406]

32 **Park do H**, Jang JW, Lee SS, Seo DW, Lee SK, Kim MH. EUS-guided biliary drainage with transluminal stenting after failed ERCP: predictors of adverse events and long-term results. *Gastrointest Endosc* 2011; **74**: 1276-1284 [PMID: 21963067 DOI: 10.1016/j.gie.2011.07.054]

33 **Artifon EL**, Aparicio D, Paione JB, Lo SK, Bordini A, Rabello C, Otoch JP, Gupta K. Biliary drainage in patients with unresectable, malignant obstruction where ERCP fails: endoscopic ultrasonography-guided choledochoduodenostomy versus percutaneous drainage. *J Clin Gastroenterol* 2012; **46**: 768-774 [PMID: 22810111 DOI: 10.1097/MCG.0b013e31825f264c]

34 **Attasaranya S**, Netinasunton N, Jongboonyanuparp T, Sottisuporn J, Witeerungrot T, Pirathvisuth T, Ovartlarnporn B. The Spectrum of Endoscopic Ultrasound Intervention in Biliary Diseases: A Single Center's Experience in 31 Cases. *Gastroenterol Res Pract* 2012; **2012**: 680753 [PMID: 22654900 DOI: 10.1155/2012/680753]

35 **Katanuma A**, Maguchi H, Osanai M, Takahashi K. Endoscopic ultrasound-guided biliary drainage performed for refractory bile duct stenosis due to chronic pancreatitis: a case report. *Dig Endosc* 2012; **24** Suppl 1: 34-37 [PMID: 22533749 DOI: 10.1111/j.1443-1661]

36 **Kawakubo K**, Isayama H, Nakai Y, Sasahira N, Kogure H, Sasaki T, Hirano K, Tada M, Koike K. Simultaneous Duodenal Metal Stent Placement and EUS-Guided Choledochoduodenostomy for Unresectable Pancreatic Cancer. *Gut Liver* 2012; **6**: 399-402 [PMID: 22844572 DOI: 10.5009/gnl.2012.6.3.399]

37 **Khashab MA**, Fujii LL, Baron TH, Canto MI, Gostout CJ, Petersen BT, Okolo PI, Topazian MD, Levy MJ. EUS-guided biliary drainage for patients with malignant biliary obstruction with an indwelling duodenal stent (with videos). *Gastrointest Endosc* 2012; **76**: 209-213 [PMID: 22726485 DOI: 10.1016/j.gie.2012.03.170]

38 **Kim TH**, Kim SH, Oh HJ, Sohn YW, Lee SO. Endoscopic ultrasound-guided biliary drainage with placement of a fully covered metal stent for malignant biliary obstruction. *World J Gastroenterol* 2012; **18**: 2526-2532 [PMID: 22654450 DOI: 10.3748/wjg.v18.i20.2526]

39 **Song TJ**, Hyun YS, Lee SS, Park do H, Seo DW, Lee SK, Kim MH. Endoscopic ultrasound-guided choledochoduodenostomies with fully covered self-expandable metallic stents. *World J Gastroenterol* 2012; **18**: 4435-4440 [PMID: 22969210 DOI: 10.3748/wjg.v18.i32.4435]

40 **Vila JJ**, Pérez-Miranda M, Vazquez-Sequeiros E, Abadia MA, Pérez-Millán A, González-Huix F, Gornals J, Iglesias-Garcia J, De la Serna C, Aparicio JR, Subtil JC, Alvarez A, de la Morena F, García-Cano J, Casi MA, Lancho A, Barturen A, Rodríguez-Gómez SJ, Repiso A, Juzgado D, Igea F, Fernandez-Urien I, González-Martin JA, Armengol-Miró JR. Initial experience with EUS-guided cholangiopancreatography for biliary and pancreatic duct drainage: a Spanish national survey. *Gastrointest Endosc* 2012; **76**: 1133-1141 [PMID: 23021167 DOI: 10.1016/j.gie.2012.08.001]

41 **Maluf-Filho F**, Retes FA, Neves CZ, Sato CF, Kawaguti FS, Jureidini R, Ribeiro U, Bacchella T. Transduodenal endosonography-guided biliary drainage and duodenal stenting for palliation of malignant obstructive jaundice and duodenal obstruction. *JOP* 2012; **13**: 210-214 [PMID: 22406603]

42 **Itoi T**, Itokawa F, Tsuchiya T, Tsuji S, Tonozuka R. Endoscopic ultrasound-guided choledochoantrostomy as an alternative extrahepatic bile duct drainage method in pancreatic cancer with duodenal invasion. *Dig Endosc* 2013; **25** Suppl 2: 142-145 [PMID: 23617666 DOI: 10.1111/den.12063]

43 **Tonozuka R**, Itoi T, Sofuni A, Itokawa F, Moriyasu F. Endoscopic double stenting for the treatment of malignant biliary and duodenal obstruction due to pancreatic cancer. *Dig Endosc* 2013; **25** Suppl 2: 100-108 [PMID: 23617659 DOI: 10.1111/den.12065]

44 **Hara K**, Yamao K, Hijioka S, Mizuno N, Imaoka H, Tajika M, Kondo S, Tanaka T, Haba S, Takeshi O, Nagashio Y, Obayashi T, Shinagawa A, Bhatia V, Shimizu Y, Goto H, Niwa Y. Prospective clinical study of endoscopic ultrasound-guided choledochoduodenostomy with direct metallic stent placement using a forward-viewing echoendoscope. *Endoscopy* 2013; **45**: 392-396 [PMID: 23338620 DOI: 10.1055/s-0032-1326076]

45 **Khashab MA**, Valeshabad AK, Modayil R, Widmer J, Saxena P, Idrees M, Iqbal S, Kalloo AN, Stavropoulos SN. EUS-guided biliary drainage by using a standardized approach for malignant biliary obstruction: rendezvous versus direct transluminal techniques (with videos). *Gastrointest Endosc* 2013; **78**: 734-741 [PMID: 23886353 DOI: 10.1016/j.gie.2013.05.013]

46 **Kawakubo K**, Isayama H, Kato H, Itoi T, Kawakami H, Hanada K, Ishiwatari H, Yasuda I, Kawamoto H, Itokawa F, Kuwatani M, Iiboshi T, Hayashi T, Doi S, Nakai Y. Multicenter retrospective study of endoscopic ultrasound-guided biliary drainage for malignant biliary obstruction in Japan. *J Hepatobiliary Pancreat Sci* 2014; **21**: 328-334 [PMID: 24026963 DOI: 10.1002/jhbp.27]

47 **Sarkaria S**, Lee HS, Gaidhane M, Kahaleh M. Advances in endoscopic ultrasound-guided biliary drainage: a comprehensive review. *Gut Liver* 2013; **7**: 129-136 [PMID: 23560147 DOI: 10.5009/gnl.2013.7.2.129]

48 **Itoi T**, Binmoeller KF, Shah J, Sofuni A, Itokawa F, Kurihara T, Tsuchiya T, Ishii K, Tsuji S, Ikeuchi N, Moriyasu F. Clinical evaluation of a novel lumen-apposing metal stent for endosonography-guided pancreatic pseudocyst and gallbladder drainage (with videos). *Gastrointest Endosc* 2012; **75**: 870-876 [PMID: 22301347 DOI: 10.1016/j.gie.2011.10.020]

49 **Itoi T**, Nageshwar Reddy D, Yasuda I. New fully-covered self-expandable metal stent for endoscopic ultrasonography-guided intervention in infectious walled-off pancreatic necrosis (with video). *J Hepatobiliary Pancreat Sci* 2013; **20**: 403-406 [PMID: 22926337 DOI: 10.1007/s00534-012-0551-5]

50 **Binmoeller KF**, Shah J. A novel lumen-apposing stent for transluminal drainage of nonadherent extraintestinal fluid collections. *Endoscopy* 2011; **43**: 337-342 [PMID: 21264800 DOI: 10.1055/s-0030-1256127]

51 **Khashab MA**, Valeshabad AK, Afghani E, Singh VK, Kumbhari V, Messallam A, Saxena P, El Zein M, Lennon AM, Canto MI, Kalloo AN. A Comparative Evaluation of EUS-Guided Biliary Drainage and Percutaneous Drainage in Patients with Distal Malignant Biliary Obstruction and Failed ERCP. *Dig Dis Sci* 2014; Epub ahead of print [PMID: 25081224]

52 **Kitano M**, Yamashita Y, Tanaka K, Konishi H, Yazumi S, Nakai Y, Nishiyama O, Uehara H, Mitoro A, Sanuki T, Takaoka M, Koshitani T, Arisaka Y, Shiba M, Hoki N, Sato H, Sasaki Y, Sato M, Hasegawa K, Kawabata H, Okabe Y, Mukai H. Covered self-expandable metal stents with an anti-migration system improve patency duration without increased complications compared with uncovered stents for distal biliary obstruction caused by pancreatic carcinoma: a randomized multicenter trial. *Am J Gastroenterol* 2013; **108**: 1713-1722 [PMID: 24042190 DOI: 10.1038/ajg.2013.305]

P- Reviewer: Matsumoto K, Mentes O, Tsai HH
S- Editor: Gou SX **L- Editor**: A **E- Editor**: Liu XM

World Journal of Gastroenterology

Submit a Manuscript: http://www.wjgnet.com/esps/
Help Desk: http://www.wjgnet.com/esps/helpdesk.aspx
DOI: 10.3748/wjg.v21.i3.829

World J Gastroenterol 2015 January 21; 21(3): 829-835
ISSN 1007-9327 (print) ISSN 2219-2840 (online)

Recent advances in prevention of hepatitis B recurrence after liver transplantation

Zhi-Feng Xi, Qiang Xia

Zhi-Feng Xi, Qiang Xia, Department of Liver Surgery, Ren Ji Hospital, School of Medicine, Shanghai Jiaotong University, Shanghai 200127, China
Author contributions: Xi ZF designed the research and wrote the paper; and Xia Q coordinated the research and approved the final manuscript for publication.
Supported by Shanghai Jiaotong University School of Medicine Science and Technology Fund, No. 11XJ21016; and Training Program for Super Academic Leaders in the Shanghai Health System, No. XBR2011029.

Correspondence to: Qiang Xia, Professor, Department of Liver Surgery, Ren Ji Hospital, School of Medicine, Shanghai Jiaotong University, No. 160 Pujian Road, Shanghai 200127, China. xiaqiang@medmail.com.cn
Telephone: +86-21-68383775
Fax: +86-21-58737232
Received: June 29, 2014
Peer-review started: June 29, 2014
First decision: August 6, 2014
Revised: August 31, 2014
Accepted: December 5, 2014
Article in press: December 8, 2014
Published online: January 21, 2015

Abstract

Liver transplantation is the only effective treatment for hepatitis B virus (HBV)-related end-stage liver disease. However, without antiviral prophylaxis, the recurrence rate of hepatitis B is as high as 80%-100%, which leads to a 50% mortality rate in the first 2 years after liver transplantation. Combination therapy of hepatitis B immunoglobulin (HBIG) and lamivudine demonstrated a higher efficacy of prophylaxis and further reduced the rate of recurrence to < 10%. The strategy of HBIG combined with lamivudine has been the standard treatment in many centers. However, the high rate of lamivudine resistance and the many disadvantages of HBIG have compelled surgeons to reconsider the long-term efficacy of this strategy for the prevention of HBV reinfection. Recently, new nucleos(t)ide analogues, such as entecavir and tenofovir, have been approved as first-line monotherapies for the treatment of chronic hepatitis B infection. These antiviral medicines have replaced lamivudine as the first choice in the prevention of HBV recurrence after liver transplantation. Various therapies that are composed of entecavir, tenofovir, and lamivudine plus adefovir, with or without HBIG have been adopted in several liver transplant centers. This article reviews the recent advances in prophylaxis for the recurrence of hepatitis B after liver transplantation.

Key words: Liver transplantation; Hepatitis B recurrence; Hepatitis B immunoglobulin; Lamivudine; Entecavir; Tenofovir

Core tip: The strategy of hepatitis B immunoglobulin (HBIG) combined with lamivudine has been the standard treatment for the prophylaxis of hepatitis B virus recurrence after liver transplantation. However, the high rate of lamivudine resistance and the many disadvantages of HBIG have compelled surgeons to reconsider the long-term efficacy of this strategy for the prevention of hepatitis B virus reinfection. This review discusses new strategies for prophylaxis of the recurrence of hepatitis B after liver transplantation.

Xi ZF, Xia Q. Recent advances in prevention of hepatitis B recurrence after liver transplantation. *World J Gastroenterol* 2015; 21(3): 829-835 Available from: URL: http://www.

wjgnet.com/1007-9327/full/v21/i3/829.htm DOI: http://dx.doi.org/10.3748/wjg.v21.i3.829

INTRODUCTION

Hepatitis B infection is a major global health problem. More than 240 million people have been chronically infected, and more than 780000 people die every year due to the acute or chronic effects of hepatitis B[1]. Liver transplantation is the only effective treatment for hepatitis B virus (HBV)-related end-stage liver disease[2]. However, without antiviral prophylaxis, the recurrence rate of hepatitis B is as high as 80%-100%, which leads to a 50% mortality rate within the first 2 years after liver transplantation[3-5]. The introduction of hepatitis B immunoglobulin (HBIG) in the early 1990s has dramatically reduced the incidence of hepatitis B recurrence and has raised the survival rate after transplantation[6-8]. Subsequently, oral nucleos(t)ide analogues, such as lamivudine (LAM), were used in perioperative transplant patients. The combination of HBIG and LAM demonstrated a higher efficacy of prophylaxis and further reduced the recurrence rate to < 10%[9-12]. Until recently, the strategy of LAM combined with HBIG has been the standard of care of prophylaxis for the recurrence of HBV after orthotropic liver transplantation (OLT) in many liver transplant centers. However, the long-term use of HBIG has many disadvantages, including high cost, the need for lifelong monthly parenteral injections, headache, flushing, and chest pain[13,14] . In addition, the long-term use of both LAM and HBIG induces viral resistance, which leads to a high rate of recurrence after liver transplantation[15]. On the contrary, more potent nucleos(t)ide analogues with a higher genetic barrier, such as entecavir and tenofovir, have been used in liver transplant patients. Therefore, developing more effective therapies of prophylaxis for the recurrence of hepatitis B after liver transplantation is urgently needed.

NEW NUCLEOS(T)IDE ANALOGUES COMBINED WITH LONG-TERM HBIG TREATMENT

Entecavir

Entecavir, a guanosine nucleoside analogue with activity against HBV polymerase, is effective in both hepatitis B e antigen (HBeAg)-positive and -negative hepatitis B infected-patients[16]. In two phase Ⅲ trials, nucleoside-naïve HBeAg-positive or -negative patients with chronic hepatitis B (CHB) who received 0.5 mg of entecavir per day for 48 wk achieved a superior virological, histologic, and biochemical efficacy than the patients who received 100 mg per day of LAM[17,18]. Entecavir is an antiviral medicine with a high genetic barrier. The resistance is associated with the LAM-resistance substitutions M204 V/ I and L180 M in combination with an additional substitution at residue T184, S202 or M250 in the reverse-transcriptase region of the HBV polymerase[19-21]. In nucleoside-naïve patients, the probability of the development of resistance to entecavir remains consistently low (< 1.2%) even after 96 wk of treatment[20]. A recent article reported that the strategy that included entecavir yielded the most quality-adjusted life years (QALYs) for both HBeAg-positive and -negative patients compared with the strategies that encompassed "no treatment," or treatment with LAM, adefovir, or telbivudine[22]. Therefore, entecavir is not only effective but also cost-effective as an antiviral treatment. Recently, entecavir and tenofovir have been approved as first-line monotherapies for the treatment of CHB according to the practice guidelines of the EASL (European Association for the Study of the Liver) for the management of chronic hepatitis B[23]. The guidelines also proposed that a potent nucleos(t)ide analogue with a high barrier to resistance is recommended for all HBsAg-positive patients undergoing liver transplantation for HBV-related end-stage liver disease or HCC, to achieve the lowest possible level of HBV DNA before transplantation. With regards to the use of entecavir in the prevention of HBV reinfection after liver transplantation, one abstract in 2008 showed that entecavir, in addition to HBIG, was effective and tolerable in patients with HBV-related post-transplantation hepatic decompensation. However, only 9 patients were included in this study[24]. A study by Xi *et al*[25] compared the efficiency of entecavir with LAM in patients who received a liver transplant. Thirty patients with end-stage hepatitis B-related liver disease received entecavir, and 90 patients received LAM after liver transplantation. HBV reinfection was not detected in any patient at the time of the latest follow-up in the entecavir group. However, 10 patients were diagnosed with HBV reinfection in the LAM group (0% *vs* 11%, $P = 0.049$). It was concluded that entecavir was superior to LAM in the prevention of hepatitis B recurrence after liver transplantation. In recent years, many other articles that concern the efficacy of entecavir have been published. Different rates of recurrence of hepatitis B were reported in those articles. Kim *et al*[26] retrospectively assessed the clinical outcomes in 154 patients who received entecavir and HBIG after liver transplantation. A total of 5 patients (3.2%) were diagnosed with HBV reinfection without entecavir resistance. In 4 of those 5 patients, recurrence of HCC was detected prior to the recurrence of HBV. Recurrent HCC was an independent risk factor for the recurrence of HBV ($P = 0.06$). In a trial by Cai *et al*[27], no recurrence of HBV occurred in patients who received entecavir after liver transplantation during the median 41.2-mo follow-up period. However, 18 patients in the LAM group developed HBV reinfection during the median 38.5-mo follow-up period (0/63 *vs* 18/189, $P < 0.01$). Similar results were shown in a study by a Japanese group. Ueda *et al*[28] evaluated the efficacy and safety of prophylaxis with entecavir and HBIG in the prevention of hepatitis B recurrence after living-donor liver transplantation.

Twenty-six patients who received entecavir plus HBIG after liver transplantation were compared with 63 patients who received LAM and HBIG. No HBV recurrence was detected during the median follow-up period of 25.1 mo in the entecavir group, whereas the HBV recurrence rate was 4% at 3 years and 6% at 5 years in the LAM group. Hu *et al*[29] showed a lower hepatitis B recurrence rate in patients who received entecavir rather than LAM. A total of 145 patients were administered entecavir plus low-dose on-demand HBIG, and 171 patients in the control group received LAM plus HBIG. Two of the 145 patients in the entecavir group developed HBV reinfection with no evidence of viral resistance in the median 36-mo follow-up period. A total of 11 of 171 patients in the LAM group developed HBV reinfection, 3 of whom demonstrated HBV resistance in the median 77-mo follow-up period. Further analysis showed that HCC at the time of liver transplantation and low anti-HBs titer post-liver transplantation were independent risk factors for the recurrence of HBV infection. Perrillo *et al*[30] assessed the efficacy of entcavir together with various HBIG regimens after liver transplantation. Sixty-one patients with HBV-related liver disease took 1.0 mg of entecavir combined with various HBIG regimens. In the median 72-wk follow-up time, only 2 patients demonstrated positivity for HBsAg while HBV DNA remained undetected. Na *et al*[31] reported that 4 of 262 recipients who received entecavir combined with HBIG experienced a recurrence of HBV infection after liver transplantation during the median 49-mo follow-up period. Among the 4 patients with recurrence, three had received LAM followed by entecavir. They also showed that the incidence of pre-transplant HCC was significantly associated with the recurrence of hepatitis B. Currently, most liver transplant centers have converted to the combination of entecavir and low-dose HBIG as the standard treatment for the prevention of hepatitis B recurrence after liver transplantation.

Tenofovir

Tenofovir disoproxil fumarate, a nucleotide analogue, inhibits viral polymerases by directly binding to the DNA or by the termination of the DNA chain due to the absence of a requisite 3' hydroxyl on the tenofovir molecule[32,33]. It has been found to be efficient in the treatment of HBV infection in patients who have not received a liver transplant[34-37]. It was further shown that resistance to tenofovir did not emerge in patients in six years of follow-up time after transplant[38]. Together with entecavir, tenofovir has been recommended as the first-line therapy for patients with hepatitis B infection[23]. Studies regarding the efficacy of tenofovir in the prevention of hepatitis B recurrence after liver transplantation are limited. A small trial[39] reported that four patients received tenofovir plus HBIG with or without entecavir for the prevention of hepatitis B recurrence. After 12 mo, no hepatitis B recurrence was observed in these four patients. In a study by Teperman *et al*[40], 19 patients were administered emtricitabine/tenofovir combined with HBIG post-liver transplantation. No patient experienced a recurrence of HBV infection at 96 wk, and no tenofovir-related renal failure was observed in the study.

DISCONTINUATION OF HBIG FOLLOWED BY NUCLEOS(T)IDE ANALOGUE

HBIG plus a nucleos(t)ide analogue was the standard treatment for the prevention of hepatitis B recurrence. However, the long-term use of HBIG has many disadvantages, including high cost, the need for lifelong monthly parenteral injections, headache, flushing, and chest pain. Recently, more potent antiviral agents, such as tenofovir and entecavir, have been introduced which challenge the necessity of the long-term use of HBIG in combination therapy[41]. Many centers have adopted the strategy of treatment with HBIG for a finite period of time but in conjunction with one or two nucleos(t)ide analogues.

LAM alone

Although several studies have been performed to determine the efficacy of the withdrawal of HBIG with concurrent LAM treatment[42-45], the long-term effects of LAM treatment after HBIG withdrawal should be established due to the increasing resistance rate associated with the long-term use of this drug[15]. In a retrospective study by Tanaka *et al*[46], 132 patients who presented with positive HBsAg at the time of post-liver transplantation and received a nucleos(t)ide analogue with one year of HBIG post-transplant were included. A total of 97 patients received LAM + HBIG (LAM group) while 35 received a non-LAM nucleos(i)de analogue + HBIG. Recurrent hepatitis B was observed only in the LAM group during the follow-up period of 1752 d. In another randomized study by Buti *et al*[45], 29 patients with undetectable HBV DNA at the time of post-liver transplantation were randomized to receive HBIG with LAM for 1 mo followed by LAM (n = 14) or both drugs (n = 15) for 17 mo. After 18 mo of follow-up, all patients survived without recurrence of HBV. However, in the subsequent follow-up trial[46], 15% of these patients developed a recurrence of HBV infection after a mean follow-up period of 91 mo. Therefore, additional studies regarding HBIG withdrawal followed by treatment with a new nucleos(t)ide analogue other than LAM were conducted.

LAM and adefovir

In a trial conducted by Neff *et al*[47], the treatment strategy of HBIG and LAM was replaced with adefovir and LAM at 6 mo post-transplantation in 10 patients. After 31 mo of follow-up, no patients experienced a recurrence of hepatitis B. The cost of adefovir and LAM vastly outweighed that of HBIG and LAM ($7235 *vs* $110700 per year for adefovir/LAM and HBIG/LAM, respectively). An abstract published in 2007[48] showed that no recurrence of hepatitis B was observed during an 11.7-mo follow-

up period after the conversion from HBIG with LAM to adefovir with LAM one week after liver transplantation. The subsequent outcome of the study was reported in 2013. Gane *et al*[49] showed that all patients who received LAM and adefovir remained alive and healthy with no recurrence of HBV infection (defined as both detectable HBsAg and HBV DNA in the serum) after a median follow-up of 22 mo after transplantation. One patient who experienced a recurrence of HCC developed HBsAg positivity 41 mo after transplantation. Serological tests for HBV DNA in this patient remained negative throughout the follow-up period. Serum levels of HBsAg became undetectable again 1 mo after the excision of this metastasis. In another randomized study by Angus *et al*[50], 34 patients who received LAM together with low-dose HBIG who did not experience a recurrence of hepatitis B at least one year post-transplantation were enrolled. Patients were randomized to receive both adefovir and LAM (n = 16) or to receive the current standard of HBIG and LAM (n = 18). One patient in the adefovir/LAM group presented with a detectable level of HBsAg (titer 0.05 IU/mL) at 5 mo; however, HBV DNA was undetectable until the last follow-up time point. The total cost per year for the treatment of patients in the adefovir/LAM group was less than that for patients in the HBIG/LAM group ($8290 *vs* $13718). Cholongitas *et al*[51] evaluated the risk of recurrence of HBV infection after the withdrawal of HBIG in patients who had received HBIG and nucleos(t)ide analogues after liver transplantation. A total of 47 patients who had received a combination of HBIG and LAM for at least one year after liver transplantation discontinued treatment with HBIG and received treatment with new nucleos(t)ide analogues *(i.e.*, adefovir, entecavir or tenofovir). The median follow-up time after HBIG withdrawal was 24 mo. In all, 28 patients continued treatment with LAM in combination with adefovir (n = 23) or tenofovir (n = 5); 10 and 9 of the 47 patients continued on tenofovir and entecavir monoprophylaxis, respectively. Three patients developed transiently detectable levels of HBsAg. Nath *et al*[52] reported that high-dose HBIG (10000 IU) was administered only 7 d after liver transplantation, which was followed by treatment with adefovir combined with LAM. With a mean duration of follow-up of 14.1 mo, one patient remained HBsAg-positive but had normal lab values.

Entecavir or tenofovir

Entecavir and tenofovir are potent antiviral agents with a high genetic barrier that are both recommended as the first-line nucleos(t)ide analogues for the treatment of patients with CHB. In a study in 2014 by Cholongitas *et al*[53], 28 patients who received entecavir (n = 11) or tenofovir (n = 17) combined with HBIG discontinued use of HBIG but continued treatment with nucleostide analogue monotherapy 6 mo after liver transplantation. No hepatitis B recurrence occurred during the follow-up period of 21 mo. Three patients who received tenofovir (17%) and 2 (18%) who received entecavir required a reduction in dosage frequency (alternate day) at some points during the follow-up period because the estimated glomerular filtration rate of these patients was less than 50 mL/min. Yi *et al*[54] reported the efficacy of entecavir monotherapy following HBIG withdrawal one year after liver transplantation. In that study, 29 patients with undetectable levels of HBV DNA who were negative for HBeAg at the time of transplantation were enrolled. After the first 12 mo of primary combination therapy of HBIG and entecavir, HBIG was discontinued. During the follow-up period of 31 mo, only one patient experienced a recurrence of HBV infection after the recurrence of HCC. Tanaka *et al*[55] showed that none of the 29 patients who received tenofovir in combination with one year of low-dose HBIG developed a recurrence of hepatitis B. In a randomized trial by Teperman *et al*[40], patients who were administered emtricitabine/tenofovir and HBIG for at least 24 wk were randomized to receive emtricitabine/tenofovir plus HBIG (n = 19) or emtricitabine/tenofovir alone (n = 18) for an additional 72 wk. No patient experienced a recurrence of HBV infection throughout the 72 wk. Both the combination of emtricitabine/tenofovir and HBIG and the treatment with emtricitabine/tenofovir alone were effective in the prevention of HBV reinfection. Another study in 2013 by Wesdorp *et al*[56] reported the safety and efficacy of tenofovir and emtricitabine after the cessation of HBIG after OLT in patients with chronic HBV infection. A total of 17 consecutive patients who were administered HBIG for at least 6 mo before the discontinuation of HBIG converted from their current HBV prophylaxis regimen (LAM + adefovir) to tenofovir/emtricitabine. HBsAg positivity without detectable levels of HBV DNA was demonstrated in one patient during the 26-mo follow-up period. Renal function remained stable during follow-up for most patients. The authors also showed that the use of tenofovir/emtricitabine saved €16262/year over the standard of care (HBIG + LAM). Stravitz *et al*[57] assigned 21 patients without recurrence of HBV infection who were treated with HBIG ± a nucleos(t)ide analogue for at least 6 mo to receive treatment with tenofovir/emtricitabine for the prophylaxis against HBV reinfection. HBIG was discontinued when they began to receive the tenofovir/emtricitabine therapy. Three patients tested positive for HBsAg after 31 mo. Three patients developed acute renal failure during the study, one of whom demonstrated a tenofovir-related acute tubular necrosis. Tenofovir/emtricitabine treatment was discontinued in two patients due to a suspicion of drug toxicity. All 3 recovered normal renal function and were withdrawn from hemodialysis during the treatment. Although only one patient in this study demonstrated convincing evidence of tenofovir-related nephrotoxicity, renal function should be closely monitored when tenofovir/emtricitabine is given.

NUCLEOS(T)IDE ANALOGUE MONOTHERAPY

In recent years, new nucleos(t)ide analogues have been approved for the treatment of hepatitis B. Higher efficacy and lower rates of resistance have transformed these new oral medicines such as entecavir and tenofovir into first-line treatments for chronic hepatitis B patients. Entecavir was also recommended as the first choice treatment for the prevention of HBV reinfection after liver transplantation. A strategy with new nucleos(t)ide analogue monotherapies for the prevention of HBV reinfection may avoid the disadvantages associated with HBIG and may achieve effective outcomes. However, studies that have focused on an HBIG-free prophylactic approach are limited. Fung *et al*[58] reported that 80 patients received entecavir without HBIG as a primary prophylaxis for the prevention of HBV recurrence. Throughout the median follow-up period of 26 mo, 10 patients tested positive for HBsAg, and 8 patients remained HBsAg-positive without seroclearance after liver transplantation. No entecavir-related viral resistance was detected in these 18 patients. In a prospective trial by Wadhawan *et al*[59], 75 patients tested negative for HBV DNA or who had levels < 2000 IU/mL at the time of transplantation were not given HBIG. Nineteen patients received a combination of LAM and adefovir, 42 received entecavir, 12 received tenofovir, and 2 received a combination of entecavir and tenofovir. At the last follow-up (median 21 mo, range: 1-83 mo), all patients were HBV DNA-negative. HBV DNA reappeared in 6 patients during the median 21-mo follow-up. Five of the 6 patients had stopped treatment with oral antiviral medication on their own. All of these patients with recurrence were HBV DNA-negative at the last follow-up after they changed their antiviral therapy. Nine patients never experienced HBsAg clearance but were negative for HBV DNA at the last follow-up. Additional studies that focus on the long-term efficacy and safety of nucleos(t)ide analogue monotherapy for the prevention of hepatitis B infection should be performed.

CONCLUSION

Patients with high levels of HBV DNA in serum at the time of liver transplantation were considered to be at a higher risk for the recurrence of HBV infection after transplantation[60,61]. The choice of an antiviral medicine with a high genetic barrier in order to achieve the lowest level of HBV DNA in serum before transplantation was crucial for the prevention of hepatitis B recurrence after liver transplantation. From our experience in the prevention of hepatitis B recurrence post-transplantation, entecavir seems to be more cost-effective than tenofovir because of the high cost of tenofovir in China.

A recent trend in liver transplantation is the increased use of new strategies for prophylaxis of hepatitis B recurrence after transplantation. Highly potent antiviral medicines with minimal or risk-free viral resistance have replaced LAM as the first-line therapy in patients who undergo a liver transplant. As a high rate of resistance occurred with LAM treatment, the discontinuation of HBIG was not recommended for patients who were treated with LAM and HBIG[62]. HBIG withdrawal followed by treatment with new nucleos(t)ide analogues, such as entecavir and tenofovir, is a promising alternative strategy for the prevention of hepatitis B recurrence. The timing of HBIG withdrawal is still controversial; however, one year post-transplantation seems to be safe and feasible[50,51]. New oral antiviral monotherapies without HBIG may be effective in patients at low risk of HBV recurrence at the time of transplantation. However, the long-term efficacy and safety of these therapies need to be determined with more adequately powered studies in the future.

REFERENCES

1 **WHO**. Hepatitis B fact sheet [cited 2014 Jun]. Available from: URL: http://www.who.int/mediacentre/factsheets/fs204/en/

2 **Pfitzmann R**, Nüssler NC, Hippler-Benscheidt M, Neuhaus R, Neuhaus P. Long-term results after liver transplantation. *Transpl Int* 2008; **21**: 234-246 [PMID: 18031464 DOI: 10.1111/j.1432-2277.2007.00596.x]

3 **O'Grady JG**, Smith HM, Davies SE, Daniels HM, Donaldson PT, Tan KC, Portmann B, Alexander GJ, Williams R. Hepatitis B virus reinfection after orthotopic liver transplantation. Serological and clinical implications. *J Hepatol* 1992; **14**: 104-111 [PMID: 1737910 DOI: 10.1016/0168-8278(92)90138-F]

4 **Todo S**, Demetris AJ, Van Thiel D, Teperman L, Fung JJ, Starzl TE. Orthotopic liver transplantation for patients with hepatitis B virus-related liver disease. *Hepatology* 1991; **13**: 619-626 [PMID: 2010156 DOI: 10.1016/0270-9139(91)92554-L]

5 **Lake JR**, Wright TL. Liver transplantation for patients with hepatitis B: what have we learned from our results? *Hepatology* 1991; **13**: 796-799 [PMID: 2010175]

6 **Samuel D**, Muller R, Alexander G, Fassati L, Ducot B, Benhamou JP, Bismuth H. Liver transplantation in European patients with the hepatitis B surface antigen. *N Engl J Med* 1993; **329**: 1842-1847 [PMID: 8247035 DOI: 10.1056/NEJM199312163292503]

7 **Markowitz JS**, Martin P, Conrad AJ, Markmann JF, Seu P, Yersiz H, Goss JA, Schmidt P, Pakrasi A, Artinian L, Murray NG, Imagawa DK, Holt C, Goldstein LI, Stribling R, Busuttil RW. Prophylaxis against hepatitis B recurrence following liver transplantation using combination lamivudine and hepatitis B immune globulin. *Hepatology* 1998; **28**: 585-589 [PMID: 9696028 DOI: 10.1002/hep.510280241]

8 **Terrault NA**, Wright TL. Hepatitis B virus infection and liver transplantation. *Gut* 1997; **40**: 568-571 [PMID: 9203930 DOI: 10.1136/gut.40.5.568]

9 **Fan XL**, Zhang JS, Zhang XQ, Yue W, Ma L. Differential regulation of beta-arrestin 1 and beta-arrestin 2 gene expression in rat brain by morphine. *Neuroscience* 2003; **117**: 383-389 [PMID: 12614678 DOI: 10.1034/j.1600-6143.2003.00063.x]

10 **Katz LH**, Paul M, Guy DG, Tur-Kaspa R. Prevention of recurrent hepatitis B virus infection after liver transplantation: hepatitis B immunoglobulin, antiviral drugs, or both? Systematic review and meta-analysis. *Transpl Infect Dis* 2010; **12**: 292-308 [PMID: 20002355 DOI: 10.1111/j.1399-3062.2009.00470.x]

11 **Riediger C**, Berberat PO, Sauer P, Gotthardt D, Weiss KH, Mehrabi A, Merle U, Stremmel W, Encke J. Prophylaxis and treatment of recurrent viral hepatitis after liver transplantation.

Nephrol Dial Transplant 2007; **22** Suppl 8: viii37-viii46 [PMID: 17890261 DOI: 10.1093/ndt/gfm655]
12 **Angus PW**, McCaughan GW, Gane EJ, Crawford DH, Harley H. Combination low-dose hepatitis B immune globulin and lamivudine therapy provides effective prophylaxis against posttransplantation hepatitis B. *Liver Transpl* 2000; **6**: 429-433 [PMID: 10915163]
13 **Terrault NA**, Vyas G. Hepatitis B immune globulin preparations and use in liver transplantation. *Clin Liver Dis* 2003; **7**: 537-550 [PMID: 14509525 DOI: 10.1016/S1089-3261(03)00045-X]
14 **Terrault NA**, Zhou S, Combs C, Hahn JA, Lake JR, Roberts JP, Ascher NL, Wright TL. Prophylaxis in liver transplant recipients using a fixed dosing schedule of hepatitis B immunoglobulin. *Hepatology* 1996; **24**: 1327-1333 [PMID: 8938155]
15 **Lok AS**, Lai CL, Leung N, Yao GB, Cui ZY, Schiff ER, Dienstag JL, Heathcote EJ, Little NR, Griffiths DA, Gardner SD, Castiglia M. Long-term safety of lamivudine treatment in patients with chronic hepatitis B. *Gastroenterology* 2003; **125**: 1714-1722 [PMID: 14724824 DOI: 10.1053/j.gastro.2003.09.033]
16 **Cheng PN**, Chang TT. Entecavir: a potent antiviral with minimal long-term resistance in nucleoside-naive chronic hepatitis B patients. *Expert Rev Anti Infect Ther* 2008; **6**: 569-579 [PMID: 18847396 DOI: 10.1586/14787210.6.5.569]
17 **Chang TT**, Gish RG, de Man R, Gadano A, Sollano J, Chao YC, Lok AS, Han KH, Goodman Z, Zhu J, Cross A, DeHertogh D, Wilber R, Colonno R, Apelian D. A comparison of entecavir and lamivudine for HBeAg-positive chronic hepatitis B. *N Engl J Med* 2006; **354**: 1001-1010 [PMID: 16525137 DOI: 10.1056/NEJMoa051285]
18 **Lai CL**, Shouval D, Lok AS, Chang TT, Cheinquer H, Goodman Z, DeHertogh D, Wilber R, Zink RC, Cross A, Colonno R, Fernandes L. Entecavir versus lamivudine for patients with HBeAg-negative chronic hepatitis B. *N Engl J Med* 2006; **354**: 1011-1020 [PMID: 16525138 DOI: 10.1056/NEJMoa051287]
19 **Baldick CJ**, Tenney DJ, Mazzucco CE, Eggers BJ, Rose RE, Pokornowski KA, Yu CF, Colonno RJ. Comprehensive evaluation of hepatitis B virus reverse transcriptase substitutions associated with entecavir resistance. *Hepatology* 2008; **47**: 1473-1482 [PMID: 18435459 DOI: 10.1002/hep.22211]
20 **Colonno RJ**, Rose R, Baldick CJ, Levine S, Pokornowski K, Yu CF, Walsh A, Fang J, Hsu M, Mazzucco C, Eggers B, Zhang S, Plym M, Klesczewski K, Tenney DJ. Entecavir resistance is rare in nucleoside naïve patients with hepatitis B. *Hepatology* 2006; **44**: 1656-1665 [PMID: 17133475 DOI: 10.1002/hep.21422]
21 **Tenney DJ**, Rose RE, Baldick CJ, Pokornowski KA, Eggers BJ, Fang J, Wichroski MJ, Xu D, Yang J, Wilber RB, Colonno RJ. Long-term monitoring shows hepatitis B virus resistance to entecavir in nucleoside-naïve patients is rare through 5 years of therapy. *Hepatology* 2009; **49**: 1503-1514 [PMID: 19280622 DOI: 10.1002/hep.22841]
22 **Wu B**, Li T, Chen H, Shen J. Cost-effectiveness of nucleoside analog therapy for hepatitis B in China: a Markov analysis. *Value Health* 2010; **13**: 592-600 [PMID: 20561341 DOI: 10.1111/j.1524-4733.2010.00733.x]
23 **European Association For The Study Of The Liver**. EASL clinical practice guidelines: Management of chronic hepatitis B virus infection. *J Hepatol* 2012; **57**: 167-185 [PMID: 22436845 DOI: 10.1016/j.jhep.2012.02.010]
24 **Samuelson A**, Morgan M, Reynolds J, Morgan M, Reynolds J, Lee M, Kamal A, Ahmed A. The Use of Entecavir Following Liver Transplantation: Pilot Safety and Tolerability Data. *Amer J Gastroenterol* 2008; **103** Suppl 1: S160.415 Abstract
25 **Xi ZF**, Xia Q, Zhang JJ, Chen XS, Han LZ, Wang X, Shen CH, Luo Y, Xin TY, Wang SY, Qiu de K. The role of entecavir in preventing hepatitis B recurrence after liver transplantation. *J Dig Dis* 2009; **10**: 321-327 [PMID: 19906113 DOI: 10.1111/j.1751-2980.2009.00403.x]
26 **Kim YK**, Kim SH, Lee SD, Park SJ. Clinical outcomes and risk factors of hepatitis B virus recurrence in patients who received prophylaxis with entecavir and hepatitis B immunoglobulin following liver transplantation. *Transplant Proc* 2013; **45**: 3052-3056 [PMID: 24157034 DOI: 10.1016/j.transproceed.2013.08.065]
27 **Cai CJ**, Lu MQ, Chen YH, Zhao H, Li MR, Chen GH. Clinical study on prevention of HBV re-infection by entecavir after liver transplantation. *Clin Transplant* 2012; **26**: 208-215 [PMID: 21981656 DOI: 10.1111/j.1399-0012.2011.01448.x]
28 **Ueda Y**, Marusawa H, Kaido T, Ogura Y, Ogawa K, Yoshizawa A, Hata K, Fujimoto Y, Nishijima N, Chiba T, Uemoto S. Efficacy and safety of prophylaxis with entecavir and hepatitis B immunoglobulin in preventing hepatitis B recurrence after living-donor liver transplantation. *Hepatol Res* 2013; **43**: 67-71 [PMID: 22548744 DOI: 10.1111/j.1872-034X.2012.01020.x]
29 **Hu TH**, Chen CL, Lin CC, Wang CC, Chiu KW, Yong CC, Liu YW, Eng HL. Section 14. Combination of entecavir plus low-dose on-demand hepatitis B immunoglobulin is effective with very low hepatitis B recurrence after liver transplantation. *Transplantation* 2014; **97** Suppl 8: S53-S59 [PMID: 24849836 DOI: 10.1097/01.tp.0000446278.43804.f9]
30 **Perrillo R**, Buti M, Durand F, Charlton M, Gadano A, Cantisani G, Loong CC, Brown K, Hu W, Lopez-Talavera JC, Llamoso C. Entecavir and hepatitis B immune globulin in patients undergoing liver transplantation for chronic hepatitis B. *Liver Transpl* 2013; **19**: 887-895 [PMID: 23788462 DOI: 10.1002/lt.23690]
31 **Na GH**, Kim DG, Han JH, Kim EY, Lee SH, Hong TH, You YK, Choi JY. Prevention and risk factors of hepatitis B recurrence after living donor liver transplantation. *J Gastroenterol Hepatol* 2014; **29**: 151-156 [PMID: 24117684 DOI: 10.1111/jgh.12403]
32 **De Clercq E**. Clinical potential of the acyclic nucleoside phosphonates cidofovir, adefovir, and tenofovir in treatment of DNA virus and retrovirus infections. *Clin Microbiol Rev* 2003; **16**: 569-596 [PMID: 14557287 DOI: 10.1128/CMR.16.4.569-596.2003]
33 **Gallant JE**, Deresinski S. Tenofovir disoproxil fumarate. *Clin Infect Dis* 2003; **37**: 944-950 [PMID: 13130407 DOI: 10.1086/378068]
34 **Jones J**, Colquitt J, Shepherd J, Harris P, Cooper K. Tenofovir disoproxil fumarate for the treatment of chronic hepatitis B infection. *Health Technol Assess* 2010; **14** Suppl 1: 23-29 [PMID: 20507800 DOI: 10.3310/hta14Suppl1/04]
35 **Lee CI**, Kwon SY, Kim JH, Choe WH, Lee CH, Yoon EL, Yeon JE, Byun KS, Kim YS, Kim JH. Efficacy and safety of tenofovir-based rescue therapy for chronic hepatitis B patients with previous nucleo(s/t)ide treatment failure. *Gut Liver* 2014; **8**: 64-69 [PMID: 24516703 DOI: 10.5009/gnl.2014.8.1.64]
36 **Snow-Lampart A**, Chappell B, Curtis M, Zhu Y, Myrick F, Schawalder J, Kitrinos K, Svarovskaia ES, Miller MD, Sorbel J, Heathcote J, Marcellin P, Borroto-Esoda K. No resistance to tenofovir disoproxil fumarate detected after up to 144 weeks of therapy in patients monoinfected with chronic hepatitis B virus. *Hepatology* 2011; **53**: 763-773 [PMID: 21374657 DOI: 10.1002/hep.24078]
37 **Gordon SC**, Krastev Z, Horban A, Petersen J, Sperl J, Dinh P, Martins EB, Yee LJ, Flaherty JF, Kitrinos KM, Rustgi VK, Marcellin P. Efficacy of tenofovir disoproxil fumarate at 240 weeks in patients with chronic hepatitis B with high baseline viral load. *Hepatology* 2013; **58**: 505-513 [PMID: 23364953 DOI: 10.1002/hep.26277]
38 **Heathcote EJ**, Marcellin P, Buti M, Gane E, De Man RA, Krastev Z, Germanidis G, Lee SS, Flisiak R, Kaita K, Manns M, Kotzev I, Tchernev K, Buggisch P, Weilert F, Kurdas OO, Shiffman ML, Trinh H, Gurel S, Snow-Lampart A, Borroto-Esoda K, Mondou E, Anderson J, Sorbel J, Rousseau F. Three-year efficacy and safety of tenofovir disoproxil fumarate treatment for chronic hepatitis B. *Gastroenterology* 2011; **140**: 132-143 [PMID: 20955704 DOI: 10.1053/j.gastro.2010.10.011]
39 **Jiménez-Pérez M**, Sáez-Gómez AB, Mongil Poce L, Lozano-

Rey JM, de la Cruz-Lombardo J, Rodrigo-López JM. Efficacy and safety of entecavir and/or tenofovir for prophylaxis and treatment of hepatitis B recurrence post-liver transplant. *Transplant Proc* 2010; **42**: 3167-3168 [PMID: 20970638 DOI: 10.1016/j.transproceed.2010.05.127]

40 **Teperman LW**, Poordad F, Bzowej N, Martin P, Pungpapong S, Schiano T, Flaherty J, Dinh P, Rossi S, Subramanian GM, Spivey J. Randomized trial of emtricitabine/tenofovir disoproxil fumarate after hepatitis B immunoglobulin withdrawal after liver transplantation. *Liver Transpl* 2013; **19**: 594-601 [PMID: 23447407 DOI: 10.1002/lt.23628]

41 **Fox AN**, Terrault NA. The option of HBIG-free prophylaxis against recurrent HBV. *J Hepatol* 2012; **56**: 1189-1197 [PMID: 22274310 DOI: 10.1016/j.jhep.2011.08.026]

42 **Naoumov NV**, Lopes AR, Burra P, Caccamo L, Iemmolo RM, de Man RA, Bassendine M, O'Grady JG, Portmann BC, Anschuetz G, Barrett CA, Williams R, Atkins M. Randomized trial of lamivudine versus hepatitis B immunoglobulin for long-term prophylaxis of hepatitis B recurrence after liver transplantation. *J Hepatol* 2001; **34**: 888-894 [PMID: 11451173 DOI: 10.1016/S0168-8278(01)00039-3]

43 **Buti M**, Mas A, Prieto M, Casafont F, González A, Miras M, Herrero JI, Jardí R, Cruz de Castro E, García-Rey C. A randomized study comparing lamivudine monotherapy after a short course of hepatitis B immune globulin (HBIg) and lamivudine with long-term lamivudine plus HBIg in the prevention of hepatitis B virus recurrence after liver transplantation. *J Hepatol* 2003; **38**: 811-817 [PMID: 12763375 DOI: 10.1016/S0168-8278(03)00087-4]

44 **Park SJ**, Paik SW, Choi MS, Lee JH, Koh KC, Kim SJ, Joh JW, Lee SK. Is lamivudine with 1-week HBlg as effective as long-term high-dose HBlg in HBV prophylaxis after liver transplantation? *Transplant Proc* 2002; **34**: 1252-1254 [PMID: 12072331 DOI: 10.1016/S0041-1345(02)02637-4]

45 **Buti M**, Mas A, Prieto M, Casafont F, González A, Miras M, Herrero JI, Jardi R, Esteban R. Adherence to Lamivudine after an early withdrawal of hepatitis B immune globulin plays an important role in the long-term prevention of hepatitis B virus recurrence. *Transplantation* 2007; **84**: 650-654 [PMID: 17876280 DOI: 10.1097/01.tp.0000277289.23677.0a]

46 **Tanaka T**, Benmousa A, Marquez M, Therapondos G, Renner EL, Lilly LB. The long-term efficacy of nucleos(t)ide analog plus a year of low-dose HBIG to prevent HBV recurrence post-liver transplantation. *Clin Transplant* 2012; **26**: E561-E569 [PMID: 23061767 DOI: 10.1111/ctr.12022]

47 **Neff GW**, Kemmer N, Kaiser TE, Zacharias VC, Alonzo M, Thomas M, Buell J. Combination therapy in liver transplant recipients with hepatitis B virus without hepatitis B immune globulin. *Dig Dis Sci* 2007; **52**: 2497-2500 [PMID: 17404847 DOI: 10.1007/s10620-006-9658-3]

48 **Gane EJ**, Strasser S, Patterson S, McCaughan GW, Angus PW. A prospective study on the safety and efficacy of lamivudine and adefovir dipivoxil prophylaxis in HBsAg positive liver transplantation candidates. *Hepatology* 2007; **46** suppl 1: abstracts. 479A

49 **Gane EJ**, Patterson S, Strasser SI, McCaughan GW, Angus PW. Combination of lamivudine and adefovir without hepatitis B immune globulin is safe and effective prophylaxis against hepatitis B virus recurrence in hepatitis B surface antigen-positive liver transplant candidates. *Liver Transpl* 2013; **19**: 268-274 [PMID: 23447403 DOI: 10.1002/lt.23600]

50 **Angus PW**, Patterson SJ, Strasser SI, McCaughan GW, Gane E. A randomized study of adefovir dipivoxil in place of HBIG in combination with lamivudine as post-liver transplantation hepatitis B prophylaxis. *Hepatology* 2008; **48**: 1460-1466 [PMID: 18925641 DOI: 10.1002/hep.22524]

51 **Cholongitas E**, Vasiliadis T, Antoniadis N, Goulis I, Papanikolaou V, Akriviadis E. Hepatitis B prophylaxis post liver transplantation with newer nucleos(t)ide analogues after hepatitis B immunoglobulin discontinuation. *Transpl Infect Dis* 2012; **14**: 479-487 [PMID: 22624695 DOI: 10.1111/j.1399-3062.2012.00741.x]

52 **Nath DS**, Kalis A, Nelson S, Payne WD, Lake JR, Humar A. Hepatitis B prophylaxis post-liver transplant without maintenance hepatitis B immunoglobulin therapy. *Clin Transplant* 2006; **20**: 206-210 [PMID: 16640528]

53 **Cholongitas E**, Goulis I, Antoniadis N, Fouzas I, Imvrios G, Papanikolaou V, Akriviadis E. New nucleos(t)ide analogue monoprophylaxis after cessation of hepatitis B immunoglobulin is effective against hepatitis B recurrence. *Transpl Int* 2014; **27**: 1022-1028 [PMID: 24909714 DOI: 10.1111/tri.12370]

54 **Yi NJ**, Choi JY, Suh KS, Cho JY, Baik M, Hong G, Lee KW, Kim W, Kim YJ, Yoon JH, Lee HS, Kim DG. Post-transplantation sequential entecavir monotherapy following 1-year combination therapy with hepatitis B immunoglobulin. *J Gastroenterol* 2013; **48**: 1401-1410 [PMID: 23463400 DOI: 10.1007/s00535-013-0761-x]

55 **Tanaka T**, Renner EL, Selzner N, Therapondos G, Lilly LB. One year of hepatitis B immunoglobulin plus tenofovir therapy is safe and effective in preventing recurrent hepatitis B post-liver transplantation. *Can J Gastroenterol Hepatol* 2014; **28**: 41-44 [PMID: 24212911]

56 **Wesdorp DJ**, Knoester M, Braat AE, Coenraad MJ, Vossen AC, Claas EC, van Hoek B. Nucleoside plus nucleotide analogs and cessation of hepatitis B immunoglobulin after liver transplantation in chronic hepatitis B is safe and effective. *J Clin Virol* 2013; **58**: 67-73 [PMID: 23880162]

57 **Stravitz RT**, Shiffman ML, Kimmel M, Puri P, Luketic VA, Sterling RK, Sanyal AJ, Cotterell AH, Posner MP, Fisher RA. Substitution of tenofovir/emtricitabine for Hepatitis B immune globulin prevents recurrence of Hepatitis B after liver transplantation. *Liver Int* 2012; **32**: 1138-1145 [PMID: 22348467 DOI: 10.1111/j.1478-3231.2012.02770.x]

58 **Fung J**, Cheung C, Chan SC, Yuen MF, Chok KS, Sharr W, Dai WC, Chan AC, Cheung TT, Tsang S, Lam B, Lai CL, Lo CM. Entecavir monotherapy is effective in suppressing hepatitis B virus after liver transplantation. *Gastroenterology* 2011; **141**: 1212-1219 [PMID: 21762659 DOI: 10.1053/j.gastro.2011.06.083]

59 **Wadhawan M**, Gupta S, Goyal N, Taneja S, Kumar A. Living related liver transplantation for hepatitis B-related liver disease without hepatitis B immune globulin prophylaxis. *Liver Transpl* 2013; **19**: 1030-1035 [PMID: 23788470 DOI: 10.1002/lt.23692]

60 **Marzano A**, Gaia S, Ghisetti V, Carenzi S, Premoli A, Debernardi-Venon W, Alessandria C, Franchello A, Salizzoni M, Rizzetto M. Viral load at the time of liver transplantation and risk of hepatitis B virus recurrence. *Liver Transpl* 2005; **11**: 402-409 [PMID: 15776431 DOI: 10.1002/lt.20402]

61 **Wu LM**, Xu X, Zheng SS. Hepatitis B virus reinfection after liver transplantation: related risk factors and perspective. *Hepatobiliary Pancreat Dis Int* 2005; **4**: 502-508 [PMID: 16286252]

62 **Kasraianfard A**, Watt KD, Lindberg L, Alexopoulos S, Rezaei N. HBIG Remains Significant in the Era of New Potent Nucleoside Analogues for Prophylaxis Against Hepatitis B Recurrence After Liver Transplantation. *Int Rev Immunol* 2014; Epub ahead of print [PMID: 24911598 DOI: 10.3109/08830185.2014.921160]

P- Reviewer: Chiu KW, Quintero J
S- Editor: Yu J **L- Editor**: Wang TQ **E- Editor**: Liu XM

World Journal of Gastroenterology

Submit a Manuscript: http://www.wjgnet.com/esps/
Help Desk: http://www.wjgnet.com/esps/helpdesk.aspx
DOI: 10.3748/wjg.v21.i3.836

World J Gastroenterol 2015 January 21; 21(3): 836-853
ISSN 1007-9327 (print) ISSN 2219-2840 (online)

ORIGINAL ARTICLE

Basic Study

Pharmacological attenuation of chronic alcoholic pancreatitis induced hypersensitivity in rats

Sabrina L McIlwrath, Karin N Westlund

Sabrina L McIlwrath, Karin N Westlund, Department of Physiology, University of Kentucky, Lexington, KY 40536-0298, United States
Author contributions: Westlund KN designed the research and edited the paper; McIlwrath SL performed the research, analyzed the data, and wrote the paper.
Supported by National Institutes of Health, No. NINDS R01 NS39041.

Correspondence to: Karin N Westlund, PhD, Professor, Department of Physiology, University of Kentucky, MS-508 Medical Center, 800 Rose St., Lexington, KY 40536-0298, United States. kwhigh2@uky.edu
Telephone: +1-859-3233668
Fax: +1-859-3231070
Received: June 20, 2014
Peer-review started: June 20, 2014
First decision: August 6, 2014
Revised: August 16, 2014
Accepted: September 29, 2014
Article in press: September 30, 2014
Published online: January 21, 2015

Abstract

AIM: To characterize an alcohol and high fat diet induced chronic pancreatitis rat model that mimics poor human dietary choices.

METHODS: Experimental rats were fed a modified Lieber-DeCarli alcohol (6%) and high-fat (65%) diet (AHF) for 10 wk while control animals received a regular rodent chow diet. Weekly behavioral tests determined mechanical and heat sensitivity. In week 10 a fasting glucose tolerance test was performed, measuring blood glucose levels before and after a 2 g/kg bodyweight intraperitoneal (i.p.) injection of glucose. Post mortem histological analysis was performed by staining pancreas and liver tissue sections with hematoxylin and eosin. Pancreas sections were also stained with Sirius red and fast green to quantify collagen content. Insulin-expressing cells were identified immunohistochemically in separate sections. Tissue staining density was quantified using Image J software. After mechanical and heat sensitivity became stable (weeks 6-10) in the AHF-fed animals, three different drugs were tested for their efficacy in attenuating pancreatitis associated hypersensitivity: a Group Ⅱ metabotropic glutamate receptor specific agonist (2R,4R)-4-Aminopyrrolidine-2,4-dicarboxylate (APDC, 3 mg/kg, ip; Tocris, Bristol, United Kingdom), nociceptin (20, 60, 200 nmol/kg, ip; Tocris), and morphine sulfate (3 mg/kg, μ-opioid receptor agonist; Baxter Healthcare, Deerfield, IL, United States).

RESULTS: Histological analysis of pancreas and liver determined that unlike control rats, AHF fed animals had pancreatic fibrosis, acinar and beta cell atrophy, with steatosis in both organs. Fat vacuolization was significantly increased in AHF fed rats (6.4% ± 1.1% in controls *vs* 23.8% ± 4.2%, $P < 0.05$). Rats fed the AHF diet had reduced fasting glucose tolerance in week 10 when peak blood glucose levels reached significantly higher concentrations than controls (127.4 ± 9.2 mg/dL in controls *vs* 161.0 ± 8.6 mg/dL, $P < 0.05$). This concurred with a 3.5 fold higher incidence of single and small 2-10 cell insulin-positive cell clusters ($P < 0.05$). Insulin expressing islet of Langerhans cells appeared hypertrophied while islet number and area measurements were not different from controls. Weekly behavioral tests determined that mechanical and heat sensitivities were significantly increased by 4 wk on AHF diet compared to controls. Hypersensitivity

was attenuated with efficacy similar to morphine with single dose treatment of either metabotropic glutamate receptor 2/3 agonist APDC, or nociceptin, the endogenous ligand for opioid-receptor-like 1 receptor.

CONCLUSION: The AHF diet induces a chronic alcoholic pancreatitis in rats with measurable features resembling clinical patients with chronic pancreatitis and type 3c diabetes mellitus.

Key words: Lieber-DeCarli diet; Orphanin FQ receptor; Metabotropic glutamate receptor; Liver steatosis; Pain; Behavior; Glucose tolerance; Type 3c diabetes mellitus

Core tip: Chronic pancreatitis is a progressive and potentially fatal disease caused by persistent unresolved inflammation and pancreatic fibrosis. It can be accompanied by intractable abdominal pain and progress to type 3c diabetes mellitus (T3cDM) and pancreatic cancer. Animal models of acute pancreatitis are typically chemically induced, invasive, of short duration, and have a high mortality rate. This study characterizes a diet-induced chronic rat model closely mimicking poor human dietary choices to investigate therapies for alcoholic chronic pancreatitis with developing T3cDM. The efficacy of acute opioid and non-opioid pharmacological interventions are compared to morphine in pain-related behavior tests.

McIlwrath SL, Westlund KN. Pharmacological attenuation of chronic alcoholic pancreatitis induced hypersensitivity in rats. *World J Gastroenterol* 2015; 21(3): 836-853 Available from: URL: http://www.wjgnet.com/1007-9327/full/v21/i3/836.htm DOI: http://dx.doi.org/10.3748/wjg.v21.i3.836

INTRODUCTION

Chronic pancreatitis is a progressive and potentially fatal disease caused by persistent unresolved inflammation and pancreatic fibrosis typically accompanied by intractable abdominal pain, particularly during the early phase[1,2]. Other symptoms include weight loss due to insufficiency of the exocrine pancreas, type 3c diabetes mellitus (T3cDM), and an increased risk of developing pancreatic cancer[3-13]. Factors that increase susceptibility to the diverse etiology of chronic pancreatitis include lifestyle choices such as regular alcohol consumption, particularly binge drinking, hyperlipidemia/hypertriglyceridemia caused by a diet high in saturated fat, and smoking, as well as heritable factors[1,12,14-21]. Although 50%-70% of patients with chronic pancreatitis regularly consume alcohol, only around 10% of patients with alcohol use disorders develop this disease, indicating other contributing factors[1,22-25]. Worldwide the incidence of chronic pancreatitis is higher in the male population, partially explained by the recently identified X chromosome linked genetic polymorphism in the claudin-2 gene[19]. Chief clinical complaint of afflicted patients is intractable pain and currently recommended pain management therapies range from non-narcotic analgesics increasing to strong opiates depending on the patient's complaints[25-27]. Concurrent analysis of amino acids in plasma and serum of patients with chronic pancreatitis identified a doubling of the glutamate concentration, the main excitatory neurotransmitter of the nervous system and a known facilitator of pain, while other amino acid levels are unaffected or decreased[28,29]. Knowledge of the underlying pathophysiology of chronic pancreatitis resulting in this severe abdominal pain is still limited and is needed for the development of better pharmacological treatments. Presently employed animal models poorly reproduce the clinical etiology of chronic pancreatitis as they are highly invasive, requiring laparotomy surgery and/or utilize repetitive dosing with caustic chemicals. The abdominal hypersensitivity induced with these experimental procedures is better suited for modeling acute pancreatitis[30,31].

Chronic pancreatitis is a multifactorial disease. Clinical observations indicate that diets high in fat facilitate the progression of alcoholic chronic pancreatitis[12,18,21,25]. Animal studies modeling chronic pancreatitis have reported limited or no success when ethanol is used alone[32-36]. The combination of fatty acids and ethanol is required to induce noticeable cell damage to cultured pancreatic cells while the application of individual compounds alone is unable to injure these cells[37-39]. Recently, we established a rat model of chronic pancreatitis using a modified Lieber-DeCarli diet with increased dietary saturated fat content (28%)[40,41]. In the present study, the alcoholic chronic pancreatitis rat model was modified by further increasing the dietary saturated fat content to 65%. Unique to the current model is developing T3cDM, recognized by the American Diabetes Association and the National Institutes of Health, is an underdiagnosed secondary disease associated with exocrine pancreatic damage[6,8,12,13]. Clinically, between 5%-10% of patients with diabetes are diagnosed with T3cDM[6,13]. This is the first animal model of chronic pancreatitis that develops T3cDM. The model is utilized here to quantify chronic pancreatitis induced pain related behaviors that persist at least 10 wk for analgesic testing.

Using the alcohol and high fat diet (AHF) induced rat chronic pancreatitis model, the efficacy of acute pharmacological activation of three inhibitory metabotropic G_i protein-coupled receptors (GPCR) was tested. The agonists activate either Group II metabotropic glutamate receptor 2 and receptor 3 (mGluR2/3), μ-opioid receptor (MOR), or the opioid receptor like-1 receptor (ORL-1). Signaling through mGluR2/3 receptors was initiated by glutamate binding[42,43], while the opioid receptors ORL-1 and μ-opioid receptor MOR are activated by the endogenous neuropeptides nociceptin (also called orphanin FQ[44,45]), enkephalins and beta-

endorphins, respectively[46,47]. Their activation results in downstream signaling events that activate voltage-gated potassium channels to inhibit voltage-gated calcium channels. Thus, activating these metabotropic receptors on peripheral nociceptors activated by noxious stimuli inhibits the release of neuropeptide modulators and glutamate, the main excitatory neurotransmitter in the nervous system[48-50].

Agonists for mGluR2/3 have been shown to be analgesic in animal models of somatic inflammatory and neuropathic pain[51-55]. Information about ORL-1 activation indicates that intrathecal and peripheral applications of nociceptin attenuate hypersensitivity in inflammatory and neuropathic rodent pain models[56-59], while intracerebroventricular injections produce hyperalgesia[60]. The efficacy of their activation in reducing hypersensitivity in the chronic alcoholic pancreatitis model in the present study is compared to morphine, the customary opiate utilized for experimental comparisons. Using the AHF rat chronic pancreatitis model with developing T3cDM, we provide the first evidence that peripheral activation of inhibitory GPCR-mediated signaling cascades through mGluR2/3 or ORL-1 are similarly efficacious to morphine in reversing hypersensitivity induced in this chronic visceral pain model.

MATERIALS AND METHODS

Ethics statement

All animal procedures were conducted according to the guidelines for the ethical treatment of experimental animals published by the Internal Association for the Study of Pain and approved by the University of Kentucky Institutional Animal Care and Use Committee (IACUC#2007-0113).

Induction of alcohol pancreatitis

Experiments were performed using a total of 16 male Fischer rats weighing 230-250 g (Harlan Laboratories, Indianapolis, IN). Animals were housed individually on a 12/12 h reverse light cycle so that behavioral assays were conducted during their active night phase. Food and water were given *ad libitum* and animals were divided into two groups: (1) controls (n = 7) received regular low soy rodent chow (Teklab #8626, Harlan, Indianapolis, IN) and (2) alcohol and high fat (AHF) diet fed animals (n = 9) received a modified Lieber-DeCarli diet. Along with the 6% ethanol liquid diet, a daily portion of 8 g lard was provided. The liquid diet (1000 g) contained 14% LD101A (TestDiet, Richmond, IN), 9% maltodextrin, 10% apple juice, 6% ethanol, and 3.3% corn oil. The AHF liquid diet was initially introduced without ethanol and corn oil. On a weekly basis the ethanol content of the food was increased from 4%-6% and finally corn oil was also added, resulting in a liquid maintenance diet containing 6% ethanol and 30% corn oil in AHF fed animals. Throughout this time AHF fed animals also received the 8 g lard supplement daily. Consumed liquid diet and lard were measured daily and averaged throughout the experimental time period to calculate the percentage of consumed dietary fat. Average daily liquid diet consumption was 20 g, of which 27.6% was nutritional value and 72.6% was water. Of this 5.48 g with nutritional value, 28% was fat (1.5 g). Animals consumed an average of 6 g of lard daily, resulting in 7.5 g total fat consumption per day out of the total 11.5 g of nutritional diet. Thus, total daily dietary fat consumption was about 65%.

Behavioral testing

Weekly behavioral assays to determine mechanical and heat sensitivity were performed on all animals. The abdomen was shaved at least 24 h prior to testing. Alcohol was removed 4 h prior to behavioral testing and drug application to minimize potential interference of alcohol on motor control and interactions with the compound of interest. Previous studies had shown that alcohol withdrawal in this experimental setting did not interfere with outcomes of these behavioral assays[41].

Animals were placed in individual Plexiglas boxes on an elevated metal screen mesh (3 mm^2 holes). Mechanical sensitivity of the abdomen and hindpaws was tested by probing the animal through the mesh from below using two different experimental methods. Abdominal referred sensitivity was characterized as previously reported by Vera-Portocarrero *et al*[61] (2003). Briefly, the upper right abdominal quadrant overlaying the pancreas was probed 10 times each in ascending order with 2 different von Frey filaments eliciting 1.0 or 6.0 g bending force equivalent to 9.8 or 58.8 mN. This assessed behavior in response to both sub- and supra-threshold mechanical stimuli, *i.e.*, touch and poke, to identify the time course for development of chronic mechanical hypersensitivity. Stimuli were applied at 10 s intervals and the number of abdominal withdrawals counted. A single trial to determine the number of responses to application of 10 stimuli with a single von Frey filament was performed per animal per time point. Mechanical hypersensitivity thresholds of the hindpaw footpads were subsequently determined while the animals were still on the elevated mesh screen table. For this measure, the up-down method was used incorporating a series of 8 von Frey filaments exerting calibrated bending forces (0.4, 0.6, 1.0, 2.0, 4.0, 6.0, 8.0, 15.0 g or 3.9, 5.9, 9.8, 19.6, 39.2, 58.8, 98.0 mN[62]).

Heat sensitivity was determined using a hot plate analgesiometer apparatus set at 50 ℃ (Columbus Instruments, Columbus, OH). Animals were placed individually on the hotplate (254 mm × 254 mm heated surface) surrounded by a 30 cm high Plexiglas barrier and the latency until a nocifensive response occurred, such as shaking or licking the paw, jumping, or running was recorded. Animals were immediately removed after the initial response and a cut-off time of 25 s prevented burn injury. The heat test was performed 3 times at 20 min

intervals and the latencies averaged.

Drug treatments

After mechanical and heat sensitivity developed in the AHF-fed animals, the efficacy of three different drugs in attenuation of pancreatitis associated hypersensitivity was determined to identify contributing signaling pathways: a Group II metabotropic glutamate receptor specific agonist, (2*R*,4*R*)-4-Aminopyrrolidine-2,4-dicarboxylate (APDC, 3 mg/kg, ip; Tocris, Bristol, United Kingdom), nociceptin (20, 60, 200 nmol/kg, ip; Tocris), and morphine sulfate (3 mg/kg, subcutaneous (s.c.); Baxter Healthcare, Deerfield, IL, United States). All drugs were diluted in sterile saline and tested after hypersensitivity became stable (weeks 6-10). Mechanical and heat sensitivity were determined 24 h before treatment and 1, 4, and 24 h after intraperitoneal (ip) injection of a single dose of drug or vehicle (saline) was administered. Efficacy of drug treatments was tested once a week in the same animals since no long-lasting changes for acute use of these drugs is reported nor noted in the present study.

Glucose tolerance test

Prior to euthanasia, a glucose tolerance test was performed with all animals[63]. Rats were fasted for 6 h and then given glucose (2 g/kg body weight, ip) in distilled sterile water (25% w/v solution). Glucose levels in tail vein blood samples were measured prior to and at several timepoints after giving glucose (15, 30, 60, 120, 180 min) using a blood glucose meter and appropriate test strips (FreeStyle, Abbott Diabetes Care, Alameda, CA).

Histology

Liver and pancreas samples were collected prior to perfusion of the animal and immerse fixed overnight in 4% paraformaldehyde in phosphate buffered saline, transferred into 70% ethanol, and paraffin embedded. Sections were cut (5 μm), rehydrated, stained for collagen fibers with Sirius red (Electron Microscopy Sciences, #26357-02), and counterstained with fast green. Other sections were stained with Sirius red and hematoxylin and eosin (HE) using routine histological protocols. Liver and pancreas samples were analyzed after acquiring five random images per slide using ACT software and a Nikon microscope for analysis using Image J. A red color threshold macro was used to measure the image areas with fibrous collagen stained red by Sirius red in 5 random fast green stained sections per group. The area quantified is presented as a ratio of the total tissue area. Islets of Langerhans were identified optically in HE and Sirius red stained sections. Images were taken of all Islets, their sizes measured, and their ratio normalized to total tissue area. Quantification of white space among the lobules of condensed pancreas tissue was performed taking 5 random images in HE and Sirius red stained tissue sections, quantifying the ratio of unstained to stained tissue area. A threshold macro determining white areas was used to assess the fat content leached out in paraffin processing in HE and Sirius red stained tissue, and the ratio of unstained white area to total tissue area per image was determined.

Immunofluorescent tissue staining

Deparaffinized and rehydrated pancreas tissue on slides was incubated overnight in a primary rabbit antibody against insulin (H-86, sc-9168; Santa Cruz Biotechnology, Santa Cruz, CA) 1:400 at room temperature. Tissue was washed, incubated in a goat anti-rabbit secondary antibody conjugated to Alexa Fluor 488 (Life Technologies, Grand Island, NY) 1:1000 for 2 h at room temperature, washed and coverslipped in VectaShield hard set mounting medium with DAPI (Vectorlabs, Burlingame, CA). Fluorescent staining of all proliferating insulin-positive cells in images of whole pancreas sectioned head to tail was analyzed using a Nikon microscope with Metamorph software. Post-processing and quantitative analyses were conducted using Photoshop and Image J. Colocalization of DAPI and insulin was used to count the number of cells in small clusters of under 10 cells and the counts normalized to total tissue area in each pancreatic section. Graph Pad Prism and Excel Microsoft software were used for statistical analysis and graphing of the data.

Statistical analysis

Data are expressed as mean ± SE. Statistical significance of behavioral and immunohistochemical data was determined using analysis of variance tests and Student *t* test with the significance level set at $P < 0.05$. *Post hoc* comparison included Student *t* tests to test statistical differences between control and experimental groups before and after drug treatments.

RESULTS

Chronic consumption of AHF diet induces histopathological changes in pancreas and liver indicative of alcoholic pancreatitis

Adult male Fischer rats were fed the alcohol and high fat diet (AHF) *ad libitum* for 10 wk. The liquid diet contains 6% (wt/vol) ethanol and 3.3% (wt/vol) corn oil supplemented with a daily dose of 6 g saturated fat resulting in the daily consumed diet to contain 65% fat, modified from Lieber-DeCarli and others[35,41,64,65]. Control animals received standard rat chow pellets (Harlan Teklad 8626). Post mortem histopathological analysis of the pancreas using Sirius red, hematoxylin, and eosin staining revealed acinar atrophy, fibrosis, and necrosis in all of the tissue samples from AHF diet fed rats (Figure 1A and B). Pancreata of AHF fed rats developed enlarged interlobular spaces, and cellular atrophy. Pancreatic interlobular spaces, measured as the percent white area to stained tissue, were significantly increased in AHF fed rats (Figure 1C; control = 8.9% ± 1.0%, $n = 4$; AHF =

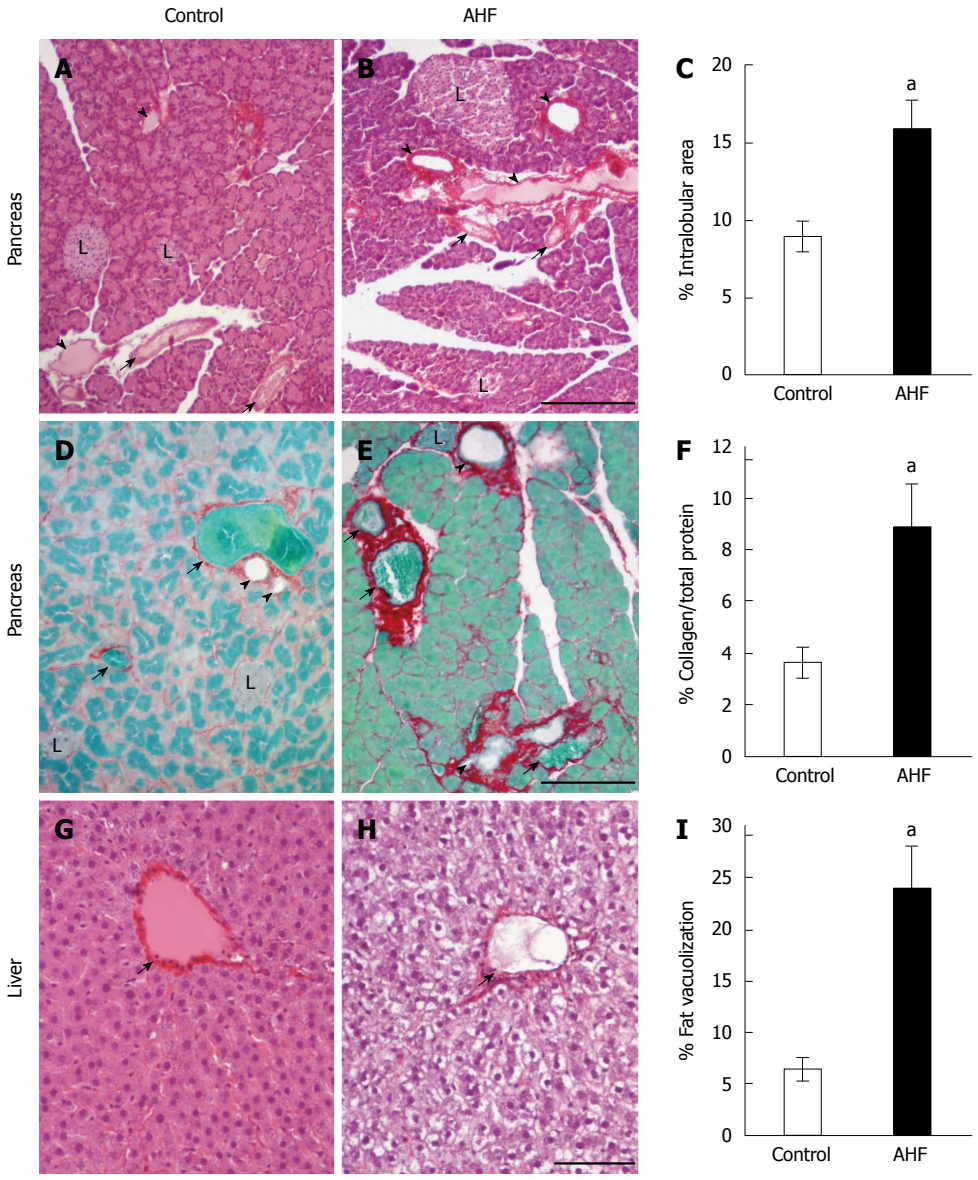

Figure 1 Histopathological analysis of the effects of alcohol and high fat diet fat diet on pancreas and liver. A: Micrograph of pancreas from a control regular chow fed rat stained with hematoxylin and eosin (HE); B: Micrograph of pancreas from an alcohol and high fat diet (AHF) fed rat stained with HE; C: Quantification of intralobular spaces (area percentage) determined there was a significant increase in pancreata from AHF fed rats; D: Micrograph of pancreas from a control rat fed regular chow with Sirius red stained collagen fibrosis and fast green counterstain; E: Micrograph of pancreas from an AHF fed rat with Sirius red stained collagen fibrosis and fast green counterstain; F: Quantification of extracellular collagen deposits (stained red) as a percent of total tissue area. A significant increase in collagen staining was detected in pancreata of AHF fed rats; G: Micrograph of liver from a control rat fed regular chow stained with HE; H: Micrograph of liver from an AHF fed rat stained with HE; I: Quantification of intracellular fat vacuolization (area percentage). Unstained areas are fat vacuoles that were significantly increased in liver samples from AHF fed rats. [a]$P < 0.05$, AHF *vs* control. L: Islet of Langerhans; Solid arrow head: Pancreatic duct; Small arrow: Blood vessel. A, B: Scalebar 50 μm; D, E: Scalebar 100 μm; G, H: Scalebar 100 μm.

15.7% ± 2.0%, $n = 6$; $P < 0.05$) indicating cell shrinkage and/or necrosis. Parenchymal fibrosis was determined histologically as the ratio of the area of pancreatic tissue collagen proteins stained with Sirius red to staining of non-collagenous proteins with fast green[66-68]. Small amounts of interstitial collagen were detected in control tissue samples while the ratio of collagenous and non-collagenous protein staining was significantly increased in AHF fed animals (Figure 1D, F; control = 3.6% ± 0.6%; AHF = 8.8% ± 1.7%; $P < 0.05$). Collagen bundles were increased in particular and clearly visible surrounding pancreatic ducts, lobes, and blood vessels in tissue samples from the AHF experimental group, while only diffuse staining localized within and among the acinar cells was observed in control animals. In the liver, chronic AHF diet consumption produced clearly visible steatosis when tissue was stained with Sirius red, hematoxylin, and eosin. Alcoholic fatty liver was quantified by measuring the unstained intracellular area in liver tissue samples remaining of the severe fat vacuolization after graded alcohol removal of the paraffin. Fat vacuolization was significantly increased in AHF fed animals compared to controls (Figure 1G-I; control = 6.4% ± 1.1%; AHF = 23.8% ± 4.2%; $P < 0.05$).

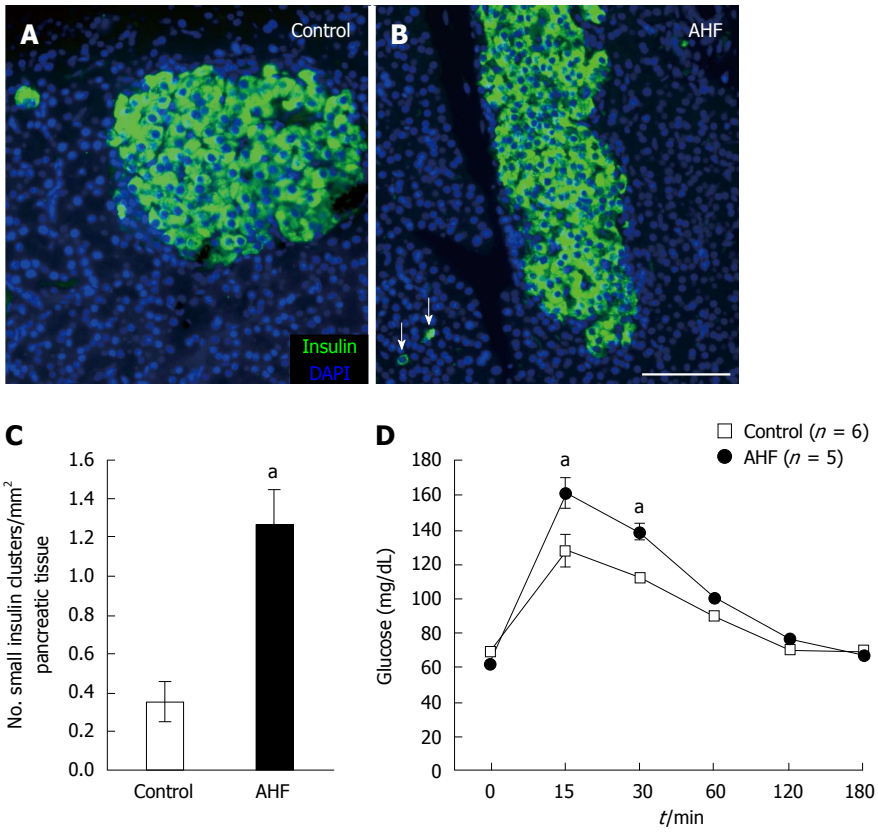

Figure 2 Chronic alcohol and high fat diet induced insulin cell proliferation and decreased glucose tolerance. A: Micrograph of insulin immunoreactivity in pancreas from a control rat fed regular chow; B: Micrograph of insulin immunoreactivity in pancreas from a rat fed alcohol and high fat (AHF). In tissue samples from AHF fed rats insulin producing cells in the islets are atrophied and an increase of spurious proliferating insulin expressing cells (arrows) is detected in the pancreas; C: Quantification of the number of single cells or small insulin cell clusters per mm^2 pancreas tissue detected a significant increase in AHF fed rats; D: Intraperitoneal glucose tolerance test at 10 wk determined that glucose tolerance was reduced in fasted AHF fed animals. Blood glucose levels of AHF fed animals peaked to significantly higher levels 15 and 30 min post injection. [a]$P < 0.05$, AHF *vs* control. A-B: Scalebar 100 μm.

Immunohistochemical analysis of insulin expression in pancreas tissue stained from animals fed (A) regular chow or (B) AHF diet determined there was prominent proliferation of insulin immunoreactive cells evident in AHF fed animals (Figure 2A-C). After chronic AHF diet for 10 wk the pancreas had atrophy of insulin producing cells in the islets and an increase of spurious proliferating insulin expressing cells. The number of single to small cell clusters of 10 or less was 3.5 fold higher in AHF fed animals (1.29 ± 0.19 per mm^2) compared to controls (0.33 ± 0.09 per mm^2, $P < 0.05$) (Figure 2C).

Chronic AHF diet consumption decreases glucose tolerance

Weekly monitoring of blood glucose levels in naïve control and AHF fed rats did not detect significant differences throughout the experiment. Unfasted blood glucose concentrations remained constant at 85.1 ± 3.1 mg/dL in controls and 83.4 ± 4.6 mg/dL in AHF fed rats. Glucose tolerance testing following ip injection of 2 g glucose per kg bodyweight was performed in week 10 after fasting animals for 6 h to measure metabolic efficiency of glucose clearance from the blood stream (Figure 2D). Animals fed AHF had significantly higher peak blood glucose levels 15 and 30 min after glucose injection (control 15 min: 127.4 ± 9.2 mg/dL, 30 min: 112.0 ± 3.9 mg/dL; AHF 15 min: 161.0 ± 8.6 mg/dL, 30 min: 138.4 ± 4.4 mg/dL, $P < 0.05$), indicating reduced glucose tolerance.

Chronic AHF diet consumption causes mechanical and heat hypersensitivity

A chief complaint of clinical patients with chronic pancreatitis is intractable pain. The pain is commonly focused in the upper abdomen but can radiate to the back with some patients reporting overall sensitivity. In the animal model, mechanical and heat sensitivity were monitored weekly (Figure 3). Abdominal sensitivity was assayed by testing the reflexive responses to low intensity (1 g = 9.8 mN force; Figure 3A) and higher intensity (6 g = 58.8 mN force; Figure 3B) mechanical stimuli applied with von Frey filaments[61]. The Y-axis indicates the average number of abdominal withdrawals in response to the bending force stimulations (10 ×). Low intensity (1 g) mechanical stimulation applied on the abdomen elicited an average of 3 of 10 responses from control rats fed a standard chow diet (Figure 3A, open squares). Baseline responses to low intensity and

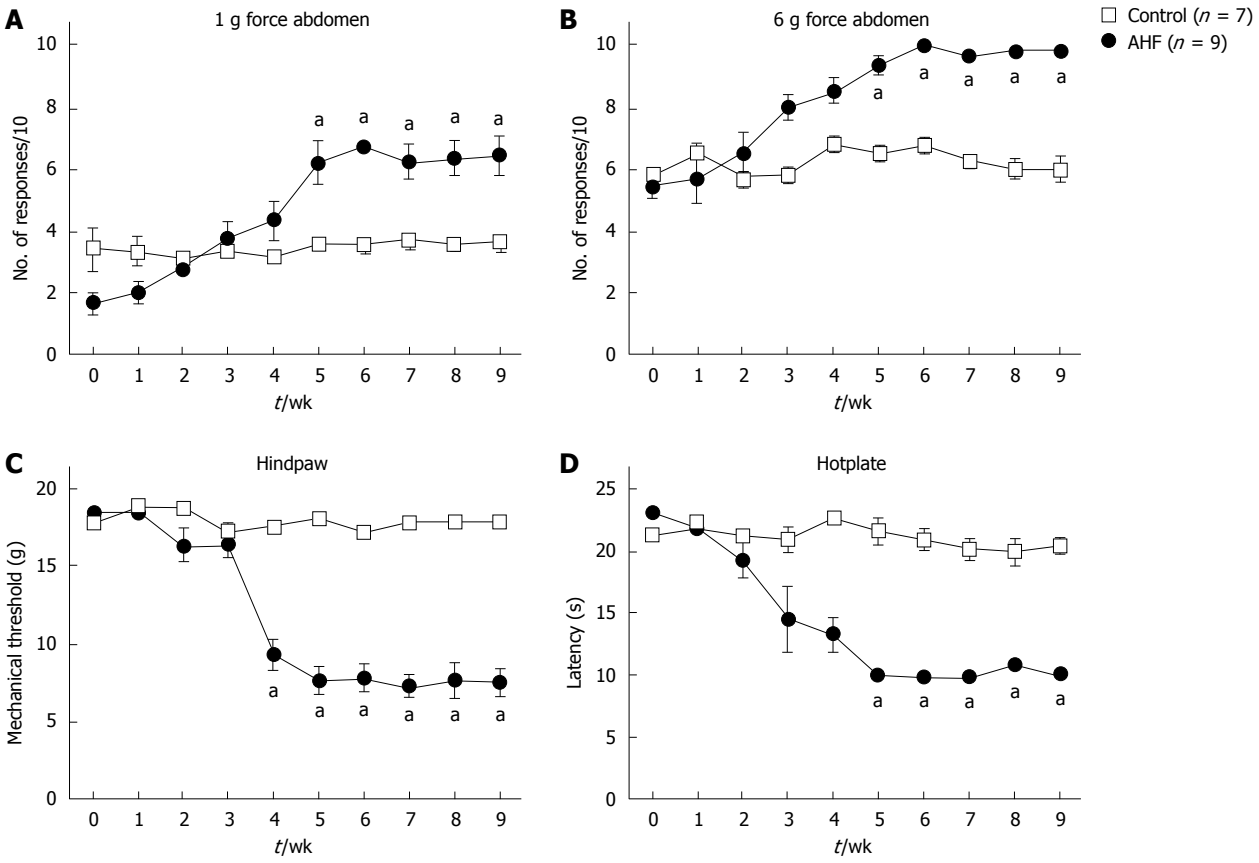

Figure 3 Time course of nociceptive behaviors in rats with chronic pancreatitis evoked by mechanical and heat stimuli. A, B: Abdominal sensitivity is determined by the number of abdominal withdrawals in response to von Frey filament bending force stimulations (× 10). Responses to (A) low intensity (1 g) and (B) high intensity (6 g) mechanical stimulation elicited significantly more responses in alcohol and high fat (AHF) fed rats starting in week 5; C: Mechanical thresholds of the hindpaws were determined with von Frey filaments using the up-down method. In week 4 mechanical sensitivity thresholds of AHF fed rats were significantly reduced and did not recover while on the AHF diet; D: Heat sensitivity was determined by measuring the response latency (s) in the hotplate test (50 ℃). In week 4, AHF fed rats demonstrated reduced response latencies in the hotplate test which did not recover during the 10 wk experimental time course. Open squares: control animals. Solid circles: AHF fed animals. [a]$P < 0.05$, AHF *vs* control.

higher intensity stimulation on the abdomen skin were not different between groups [1 g: control = 2.3 ± 0.5; AHF = (1.8 ± 0.5 responses)/10; N.S.; 6 g: control = 5.8 ± 0.5; AHF = (5.5 ± 0.5 responses)/10; N.S]. Responses increased significantly during the experiment's duration in the AHF group (1 g: $P < 0.01$; 6 g: $P < 0.0001$). In week 5, AHF fed rats responded with almost twice as many abdominal withdrawals to low intensity mechanical stimulation than controls [control = 3.6 ± 0.2; AHF = (6.2 ± 0.7 responses)/10; $P < 0.05$; Figure 3A]. Similarly, the responses to 6 g mechanical stimulation of the abdomen was significantly increased in AHF animals in week 5 [control = 6.6 ± 0.4; AHF = (9.2 ± 0.3 responses)/10; $P < 0.05$]. Higher intensity (6 g) mechanical stimulation of the abdomen consistently elicited an average of 6 of 10 responses from control rats while AHF fed animals responded every time after week 5. Mechanical and heat sensitivity of control animals did not change during the study.

Similarly, mechanical thresholds for eliciting hindpaw withdrawal in AHF fed rats decreased significantly in week 4 from 18.72 g force to 9.3 ± 1.0 g force ($P < 0.05$; Figure 3C). This referred hypersensitivity of the hindpaw plantar surface was characterized by determining the mechanical withdrawal threshold using the up-down method[62]. The mechanical thresholds of the hindpaws of control animals did not change throughout the experiment (17.8 ± 0.6 g force). Hindpaw mechanical thresholds for AHF fed rats remained decreased at 7.6 ± 0.9 g force ($P < 0.01$) through the experiment end at week 10.

Heat sensitivity was determined indirectly by measuring the latency (s) to an escape response in the hotplate test (50 ℃) (Figure 3D). Response latencies on the hotplate, *i.e.*, the time until animals displayed signs of nociception such as shaking the paw, licking, agitation, were not different between groups at baseline (control = 21.2 ± 0.1 s; AHF = 22.9 ± 0.5 s; N.S). In week 4 hotplate sensitivity was significantly decreased in the AHF fed group (control = 22.6 ± 0.2 s; AHF = 13.3 ± 1.4 s; $P < 0.05$; Figure 3D). The reduced latencies did not recover during the 10 wk experimental time course. At the end of the experiment (10 wk), control animals spend 18.3 ± 0.4 s on the hotplate before showing signs of distress while AHF animals reacted within 10.0 ± 0.3 s ($P < 0.05$).

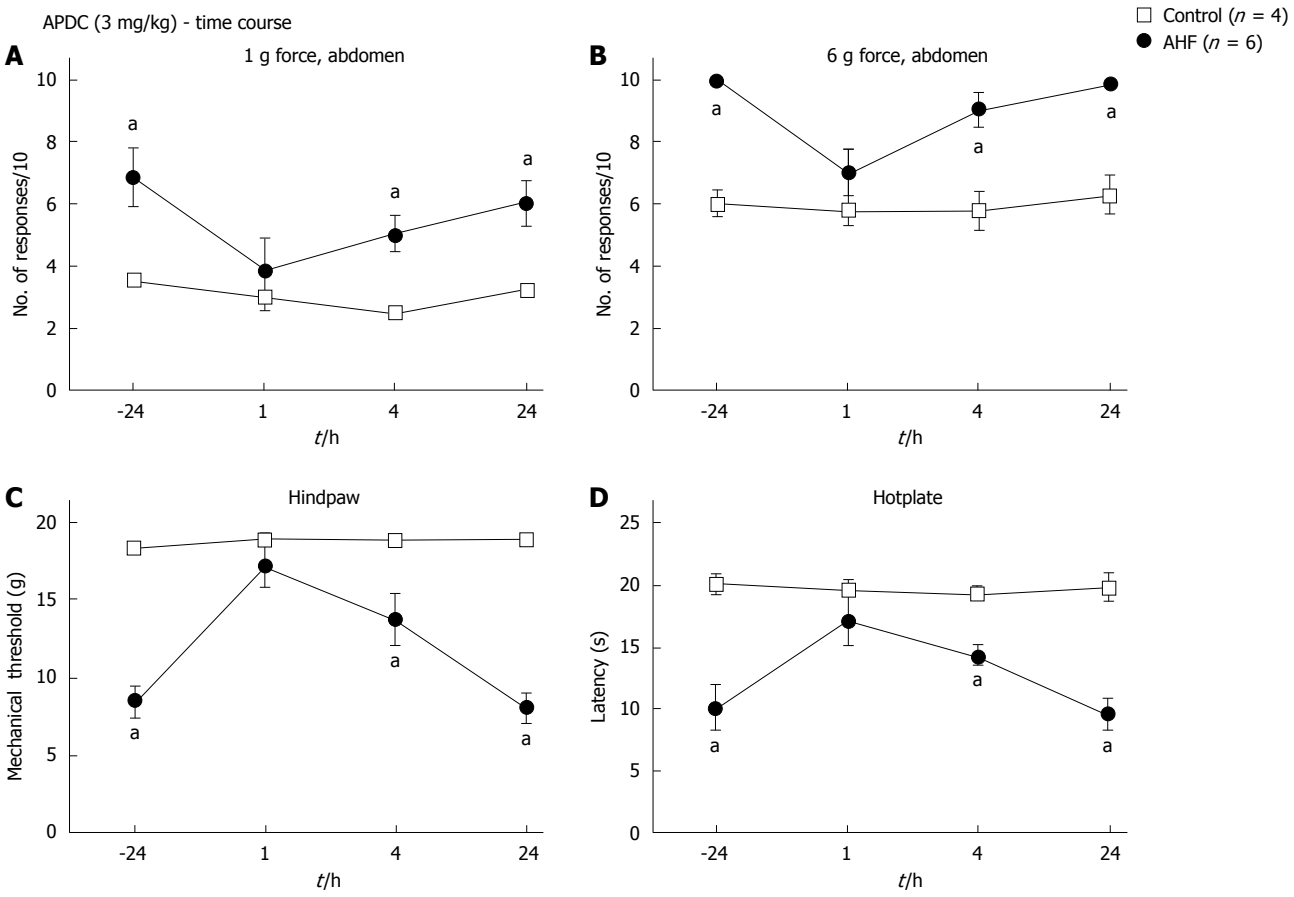

Figure 4 Time course of nociceptive responses to mechanical and heat stimuli after a single systemic treatment with (2R,4R)-4-Aminopyrrolidine-2,4-dicarboxylate. A, B: Animals were treated with a single ip dose of (2R,4R)-4-Aminopyrrolidine-2,4-dicarboxylate (APDC) (3 mg/kg). APDC reversed the increase in nociception responses 1 h post treatment evoked by (A) low intensity (1 g) abdominal stimulation and (B) high intensity (6 g) abdominal stimulation; C: Alcohol and high fat (AHF) fed rats had increased hindpaw mechanical withdrawal thresholds; D: Response latencies of AHF fed rats increased 1 h after APDC treatment in the hotplate test, but sensitivity of the controls was not altered. [a]$P < 0.05$, AHF *vs* control.

Analgesic effects of APDC on AHF diet induced hypersensitivity

Glutamate is a widely expressed neuropeptide within the nervous system. When binding to group Ⅱ metabotropic glutamate receptors, mGluR2 and mGluR3, G_i-protein coupled receptors, their activation inhibits adenylyl cyclase. This initiates inhibitory signaling cascades that result in reduced neuronal activity and decrease the release of further glutamate[49,50]. The mGluR2/3 agonist APDC has been shown to reduce inflammation induced mechanical and heat hypersensitivity in mouse models of somatic pain[51,52]. Here we used a single dose of 3 mg/kg APDC (ip) to decrease mechanical and heat hypersensitivity induced by chronic pancreatitis, a concentration previously shown to optimally reduce hypersensitivity in acute somatic inflammatory animal models. Within 1 h of APDC treatment, reversal was noted of the increased nociceptive response evoked by low intensity abdominal stimulation in AHF fed rats (Figure 4A). Responses to low intensity mechanical stimulation of the abdomen were 3.8 ± 1.0, instead of 6.8 ± 0.9 responses to 10 stimuli observed at baseline. Responses of the controls 1 h after APDC treatment (1 h: 3.5 ± 0.3 responses) remained the same (-24 h: 3.0 ± 0.4 responses; Figure 4A). Responses of AHF fed rats to higher intensity mechanical stimulation of the abdomen were similarly reduced at the 1 h timepoint [-24 h: (10 ± 0 responses)/10; 1 h: (7.0 ± 0.7 responses)/10; $P < 0.05$; Figure 4B].

Mechanical thresholds of the hindpaws (-24 h: 8.4 ± 1.0 g force; 1h: 17.0 ± 1.3 g force; AHF $n = 6$, $P < 0.05$; Figure 4C) and latencies on the hotplate (-24 h: 10.2 ± 0.5 s; 1 h: 17.3 ± 1.0 s; AHF $n = 6$, $P < 0.05$) improved significantly to values indistinguishable from control animals (Figure 4D). The effect of APDC was abolished 24 h after treatment.

Nociceptin treatment reverses AHF diet induced hypersensitivity

Nociceptin, an endogenous opioid-related neuropeptide, binds to the opioid receptor like-1 receptor (ORL-1) whose peripheral activation and activation in the spinal cord has been shown to be anti-nociceptive[57,58,69]. Both control and AHF fed animals received single ip injections of vehicle only, 20, 60, or 200 nmol/kg nociceptin. Nociceptive responses to mechanical and heat stimulation 1 h after treatment with a single ip dose of nociceptin in animals with AHF induced pancreatitis were compared

to controls.

Dose-dependent improvement was observed after the single dose of nociceptin for responses to low intensity mechanical stimulation of the abdomen (Figure 5A), responses to higher intensity mechanical stimulation of the abdomen (Figure 5B), and mechanical thresholds on the hindpaws (Figure 5C). In AHF fed animals 20 nmol/kg nociceptin decreased abdominal hypersensitivity to low intensity (1 g) mechanical stimulation [vehicle: control = 2.8 ± 0.5; AHF = (6.3 ± 0.7 responses)/10; $P < 0.05$; 20 nmol nociceptin: control = 3.5 ± 0.3; AHF = (4.7 ± 0.4 responses)/10; n.s.; Figure 5A]. Abdominal withdrawal of AHF animals to higher intensity (6 g) mechanical stimulation decreased from 9.8 ± 0.3 to 6.5 ± 0.4 responses after treatment with the highest dose of nociceptin. This was not different from vehicle treated control animals [(6.5 ± 0.5 responses)/10; Figure 5B]. Treatment of AHF fed animals with 20 nmol/kg nociceptin increased mechanical thresholds on the hindpaws so that they were no longer different from controls while not altering the sensitivity in control animals (vehicle: control = 18.2 ± 0.5; AHF = 6.3 ± 0.7 g force; $P < 0.05$; 20 nmol: control = 18.7 ± 0.0; AHF = 15.7 ± 1.6 g force; $P < 0.05$; Figure 5C).

Thus, a dose of 200 nmol nociceptin per kg body weight was determined to be the most effective in reducing sensitized nociceptive responses in all four behavioral assays in AHF fed rats (Figure 5E-H). With this dose, abdominal withdrawals of AHF fed rats in response to low intensity mechanical stimulation decreased to control levels at the 1 and 4 h timepoints. Responses of AHF fed animals to mechanical stimulation of the abdomen at 1 h were significantly decreased [1 g: -24 h = 6.0 ± 0.5; 1 h = (3.2 ± 1.1 responses)/10; $P < 0.05$; 6 g: -24 h = 9.8 ± 0.2; 1 h = (6.5 ± 0.4 responses)/10; $P < 0.05$; Figure 5E, F] and returned to pre-treatment levels 24 h after the injection [1 g: 24 h = (6.2 ± 0.9 responses)/10; 6 g: 24 h = (9.5 ± 0.3 responses)/10]. Nociceptive responses of AHF fed rats to higher intensity abdominal mechanical stimulation were decreased to control values only at the 1 h time point after nociceptin treatment (Figure 5F). Mechanical withdrawal thresholds of the hindpaws of AHF fed animals also increased significantly from 8.4 ± 1.0 g force prior to treatment to 17.0 ± 1.3 g force 1 h after treatment (Figure 5G). Four hours after nociceptin treatment, the mechanical thresholds of AHF fed animals with chronic pancreatitis decreased again, returning to their previous hypersensitive level within 24 h (4 h = 13.3 ± 2.2; 24 h = 7.5 ± 1.0 g force; Figure 5G). Nociceptin treatments had no effect on mechanical sensitivity in control animals. In control animals the 200 nmol/kg dose increased hypersensitivity but was not significant [(7.5 ± 0.3 responses)/10]. Vehicle treatments did not alter nociceptive responses of naïve or AHF fed animals.

Hotplate response latencies of AHF animals were increased dose dependently from 10.4 ± 0.2 s (vehicle) to 15.1 ± 0.4 s (200 nmol/kg nociceptin), but the improvement was significant only at the highest dose of nociceptin (Figure 5D). After systemic injection of 200 nmol/kg nociceptin, for AFH animals, the hotplate response latency increased from 10.1 ± 0.7 s prior to treatment to 15.1 ± 0.4 s 1 h afterwards ($P < 0.05$; Figure 5H). This improvement remained significantly lower than in untreated control (20.0 ± 0.9 s; $P < 0.05$). Heat responses of control animals slightly decreased 1 h after injection of 200 nmol/kg nociceptin (vehicle: 19.2 ± 0.3 s; 200 nmol: 16.7 ± 1.0 s; Figure 5H). The ability of nociceptin to reverse hypersensitivity of AHF fed animals was optimal at 1 h after which it decreased and was completely absent 24 h after injection.

Comparison to effects of morphine on AHF diet induced hypersensitivity

Many studies have demonstrated the efficacy of morphine in reversal of acute and chronic pancreatitis associated hypersensitivity in animal models as well as its use for pain management of chronic pancreatitis patients with pain. Single dose s.c. treatment with 3 mg/kg morphine sulfate solution resulted in significant reduction of mechanical and heat hypersensitivity in AHF fed rats (Figure 6). Responses of AHF fed rats to low intensity mechanical stimulation of the abdomen [-24 h: (5.5 ± 0.3 responses)/10; 1 h: 1.8 ± 0.5 responses /10; 4 h: (2.0 ± 0.8 responses)/10; AHF $n = 4$; $P < 0.05$; Figure 6A] was significantly reduced for up to 4 h compared to responses before treatment. Similarly, responses of AHF fed rats to higher intensity mechanical stimulation of the abdomen [-24 h: (9.0 ± 0.6 responses)/10; 1 h: (2.3 ± 0.8 responses)/10; 4 h: (6.0 ± 0.4 responses)/10; AHF $n = 4$; $P < 0.05$; Figure 6B] was significantly reduced for up to 4 h compared to responses before treatment. Naïve animals responded to higher intensity mechanical stimulation of the abdomen with 6.5 ± 0.6 responses/10 which was significantly reduced 1 h after morphine treatment to 3.3 ± 0.5 responses/10 ($P < 0.05$; Figure 6B). Mechanical thresholds of the hindpaws in the AHF diet group improved after morphine treatment for up to 4 h (-24 h: 7.6 ± 1.0 g force; 1h: 18.7 ± 0 g force; 4h: 18.2 ± 0.4 g force; AHF $n = 4$, $P < 0.05$; Figure 6C). No changes in naïve animals were measured after morphine treatment for either on the hindpaw nociceptive withdrawal thresholds for low intensity mechanical stimulation or the responses to low threshold (1 g) abdominal stimulation. Morphine treatment reversed heat sensitivity of AHF fed animals back to response levels recorded in naïve animals for up to 4 h (-24 h: 10.7 ± 0.1 s; 1h: 20.4 ± 0.7 s; 4h: 18.2 ± 0.7 s; AHF $n = 4$, $P < 0.05$; Figure 6D). Responses of naïve rats on the hotplate were not affected by the 3 mg/kg morphine. Animals were tested during their active period and did not appear somnolent for any of the testing. After 24 h no effects of morphine were detected in any of the tests.

DISCUSSION

Here we present a non-invasive dietary animal model of alcoholic chronic pancreatitis induced in 3 wk but

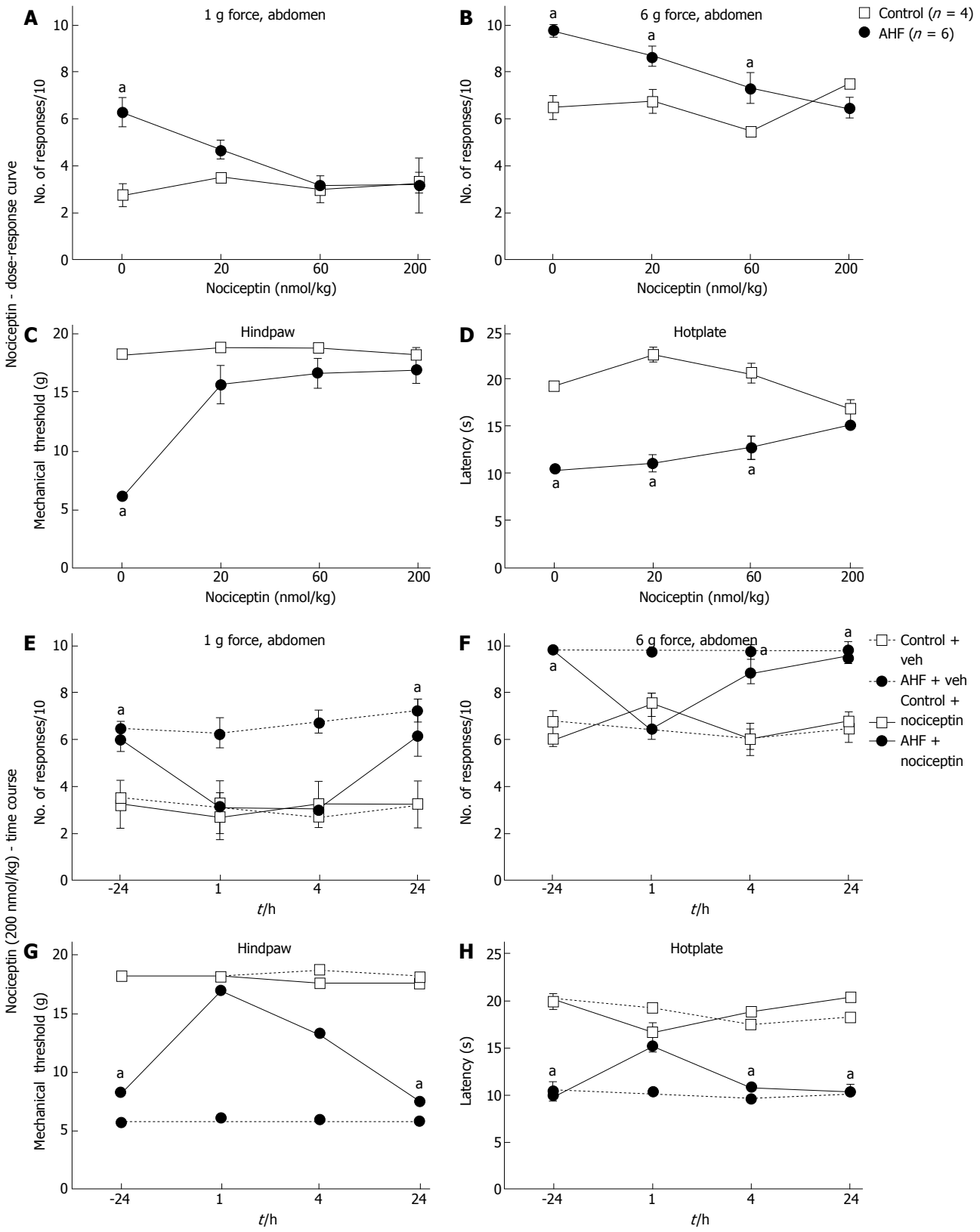

Figure 5 Dose-response curves and time course of nociceptive responses to mechanical and heat stimuli after a single systemic treatment with nociceptin. A, B: Comparisons of the number of responses to mechanical stimulation on the abdomen skin 1 h after treatment with nociceptin (ip) for control and alcohol and high fat (AHF) fed rats. Dose-dependent responses were reduced to (A) low intensity (1 g) and (B) high intensity (6 g) mechanical stimulation of the abdomen; C: Nociceptin increased hindpaw mechanical withdrawal threshold in AHF fed rats; D: Hotplate response latencies of AHF fed animals improved with the highest dose of nociception. In control animals nociceptin did not alter mechanical and heat sensitivity. Vehicle treatments had no effect on mechanical or heat sensitivity of animals from either group; E-H: Mechanical and heat responses in animals treated with either a single systemic injection of nociceptin (200 nmol/kg in saline) or with the saline vehicle; E: Abdominal withdrawals in response to low intensity (1 g) mechanical stimulation decreased to control levels at the 1 and 4 h post injection timepoints of AHF fed rats. Mechanical hypersensivity of vehicle treated AHF diet fed rats did not improve; F: Responses of AHF fed rats to high intensity (6 g) abdominal mechanical stimulation were decreased to control values only 1 h after injection of nociception; G: Hindpaws mechanical withdrawal thresholds of AHF fed rats recovered to control values for up to 4 h post injection; H: Hotplate response latencies of AHF fed rats improved only at the 1 h time point after nociceptin treatment. [a]$P < 0.05$, AHF *vs* control.

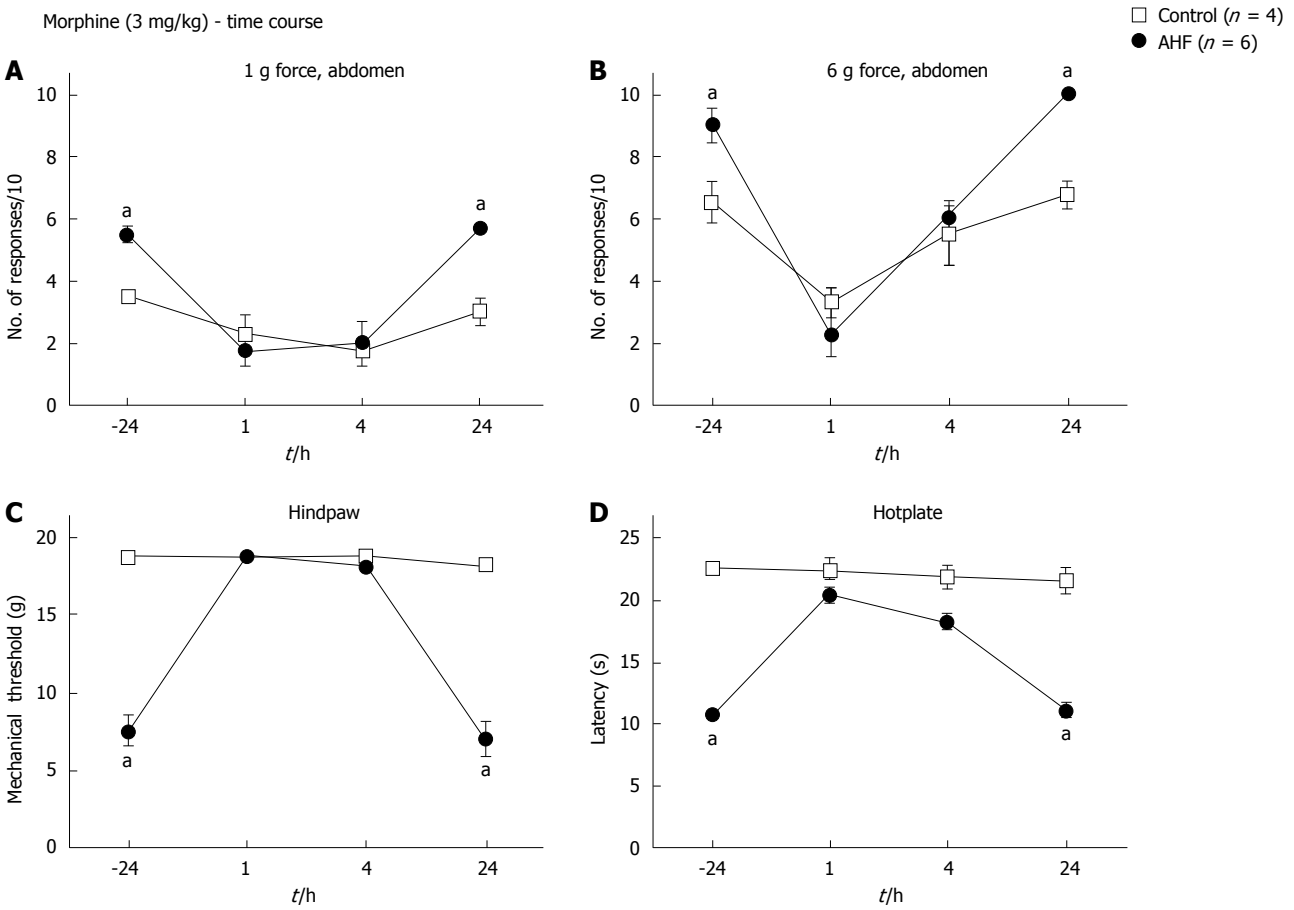

Figure 6 Time course of nociceptive responses to mechanical and heat stimuli after a single systemic treatment with morphine. Animals were injected with morphine (3 mg/kg, subcutaneous) and responses to mechanical and heat stimuli measured. Morphine treatment of alcohol and high fat (AHF) fed rats decreased the number of responses to (A) low (1 g) and (B) high intensity (6 g) mechanical stimulation of the abdominal skin for up to 4 h. Abdominal withdrawal responses of controls evoked by high intensity (6 g) mechanical stimulation were reduced 1 h after treatment compared to before morphine. Hindpaw (C) mechanical withdrawal thresholds and (D) response latencies on the hot plate test of AHF fed rats were improved at 1 and 4 h after morphine treatment. Controls were unaffected by the low dose morphine. $^{a}P < 0.05$, AHF *vs* control.

persisting for at least 10 wk. The model replicates poor dietary choices of clinical patients diagnosed with alcoholic chronic pancreatitis. Recent estimates reported that 51%-67% of Americans consume 3-5 alcoholic beverages per day which concurs with a decrease in diet quality and an increase of dietary fat intake[70-72]. Concurrently, the Food and Agriculture Organization (FAO) of the United Nations reported a steady increase of the average daily dietary fat consumption per capita in the United States from 140 g in 1990/92 to 161 g in 2005/7 while it averaged 131 g fat in the developed world[73]. Comparison of nutritional profiles identified that patients with chronic alcoholic pancreatitis consumed significantly more saturated fat and animal protein compared to patients suffering from alcohol consumption induced cirrhosis of the liver[21,74,75]. Other studies have shown that drinkers consume significantly more dietary fat and calories on drinking days[71,72,76]. Exactly this combination is described as inducing chronic alcoholic pancreatitis, with alcohol being the leading and diet the secondary cause[77,78]. Animal models of alcoholic chronic pancreatitis and fatty liver disease have shown that increased dietary fat consumption results in higher hepatic triglycerides and associated fat vacuolization[64,65,79]. Hence, the AHF rat model of chronic pancreatitis described here closely mimics high-risk human dietary choices that are part of the etiology of chronic alcoholic pancreatitis with liver steatosis.

Presently favored rodent models of pancreatitis are highly invasive and poorly reproduce disease progression seen in clinical patients. They often require laparotomy surgery to obstruct the pancreatic duct, or direct instill chemical irritants such as the aromatic nitro compound trinitrobenzene sulfonic acid or ethanol into the pancreatic duct. Other models utilize the repeated supraphysiological ip injections of caerulein, an analog of the gastrointestinal peptide hormone cholecystokinin, in combination with an ip lipopolysaccharide injection or a single dose of the highly toxic organotin dibutyltin chloride into the tail vein[30,31,80]. All of these models induce a rapid immune response that is focused primarily on the pancreas. By chemically modifying cell surface proteins an inflammatory cell reaction is induced which ultimately results in acinar cell death with or without prior dysregulated digestive enzyme release. Thus, other current models of pancreatitis are better suited for study of acute

pancreatitis[31,81,82]. Animals can recover in these acute models within 48-72 h as in most cases of acute pancreatitis. However, in the AHF model the pathological and functional symptomatology of chronic alcoholic pancreatitis persists. Regeneration of the damaged tissue is impaired by the continued alcohol consumption, facilitating the establishment of chronic pancreatitis[83].

Chronic pancreatitis is a multifactorial disease caused by a combination of regular alcohol consumption, a low quality diet high with high fat content producing hyperlipidemia, smoking, and hereditary factors[12,19,21,23,75,84]. The AHF model of chronic pancreatitis focuses on the combined effects of alcohol and a diet high in fat on the pancreatitis and associated comorbidities. Chronic consumption of alcohol results in its metabolism not only in the liver, but also in the pancreas. Alcohol is typically metabolized *via* acetaldehyde into acetyl which is used for energy production. In the results presented here, liver steatosis induced by alcohol consumption[40,85] was visible not only in the centrilobular region of the liver where lipids are predominantly stored in fatty vacuoles[86], but was detected throughout the large area of sampled tissue in the AHF fed animals indicating severity of disease progression. Metabolism of dietary alcohol and fat converges on the same enzymes, so that when high amounts of alcohol and fatty acids are consumed, cellular signaling molecules anandamide and arachidonic acid, and cytotoxic acetaldehydes accumulate within liver and pancreas that are able to directly activate ion channels such as Transient Receptor Potential Cation Channel, Subfamily A, Member 1 (TRPA1); Transient Receptor Potential Cation Channel, Subfamily V, Member 1 (TRPV1); and Transient Receptor Potential Cation Channel, Subfamily V, Member 4 (TRPV4) localized in the cell membranes of nociceptive sensory neurons innervating the pancreas as well as on local cells to induce cellular damage[84,87-90]. In the pancreas acetaldehydes and fatty acid ethyl esters can further induce fragility of pancreatic zymogen granules and cause cellular damage to pancreatic cells[7,84,90,91]. Resulting cellular atrophy and necrosis induce separation of pancreatic lobules as well as peri- and intralobular fibrosis, indicators of severe damage to parenchymal tissue, were visible throughout the examined pancreatic tissue of AHF fed animals. Cell damage and necrosis directly and indirectly activate the pancreatic local immune stellate cells, and activate nociceptors innervating the pancreas, amplifying pain sensation and pancreatic tissue damage through neurogenic inflammation[89,92,93].

Alcoholic chronic pancreatitis not only results in damage to the exocrine pancreas but can also impair and dysregulate insulin metabolism in the endocrine pancreas which in patients results in the development of diabetes mellitus type 3c[10,13]. In the present study, 10 wk of AHF diet resulted in decreased glucose tolerance in rats. While no changes in islet of Langerhans number and size distribution were detected (data not shown), fasting glucose tolerance was impaired, cellular atrophy of insulin cells was evident histologically, and a 3.5 fold increase of small clusters of insulin producing cells were detected in AHF fed rats. This suggested a compensatory reaction to beta cell atrophy and decreased effectiveness. In a Korean study increased alcohol consumption coincided with increased dietary fat which concurred with decreased pancreatic beta cell function[75]. Low-density lipoproteins, metabolic products of saturated fats, have been shown to reduce beta-cell function, decreasing glucose-stimulated insulin secretion and causing beta-cell proliferation in primary cell culture experiments[94].

Exposure of cultured beta cells to combined fatty acids and ethanol has been shown to decrease their mitochondrial activity and adenosine triphosphate (ATP) production and increase released reactive oxygen species, indicators of their decreased function[38]. Platelet-derived growth factor as well as interleukin-1β, two pro-inflammatory cytokines and signaling molecules that are increased in pancreatitis, have been reported to induce beta-cell proliferation[95]. The proliferation of small beta-cell groups observed in AHF fed pancreas tissue suggest a regenerative mechanism is active in the rats to compensate for ethanol and fatty acid induced cell damage.

As in our previous study using a similar protocol to induce chronic pancreatitis, animals fed AHF diet developed mechanical hypersensitivity of the abdomen and hindpaws as well as increased heat sensitivity. Alcohol metabolism in chronic alcoholism is not confined to visceral organs but occurs in every tissue. As a result of cellular damage produced by chronic alcoholism, resulting oxidative stress can also be measured in skeletal muscle[96]. Cellular damage releases molecules such as ATP and incompletely metabolized alcohol products activate and sensitize nociceptors throughout the body, resulting in hypersensitivity that is not confined to the abdominal region. Activity induced central sensitization further exacerbates hypersensitivity to noxious and normally innocuous stimuli. Clinically, 85% of chronic pancreatitis patients require treatment for pain at some point during disease progression and are treated depending on severity of the pain with non-narcotic analgesics and as pain increases, ever increasing doses of opiates as well as pancreatic enzyme therapy. In extreme cases, nerve blocks and eventually surgical intervention may be required[26,27]. While opioids are efficacious in patients as well as in animal models of chronic pancreatitis, even acute doses have severe side effects and may lead to overdose. Long term use of morphine can cause addiction and constipation, its efficacy to reduce pain decreases with duration of use, while ongoing pancreatic inflammation is not improved. Yet, despite the side effects, prescription rates for opioids have increased almost exponentially in the last decade and non-addictive alternatives are very much needed[97,98]. We therefore investigated the hypothesis that activation of other G_i-coupled GPCRs would decrease nociceptive signaling.

Initial focus was on the inhibitory mGluR2/3 signaling pathway. Glutamate is the main excitatory

neurotransmitter that depolarizes neurons by binding to its ionotropic and metabotropic receptors. However, glutamate initiates inhibitory signaling cascades when bound to the group Ⅱ metabotropic glutamate receptors, mGluR2 and mGluR3 to dampen cellular excitability[99,100]. Activation of these G_i-coupled GPCRs negatively modulate adenylate cyclase, alter synaptic connectivity, and decrease release of glutamate[101]. Group Ⅱ mGluRs are expressed throughout the nervous system, in primary sensory neurons, predominantly presumed nociceptors, in the dorsal horn of the spinal cord, as well as in visceral organs such as beta-cells of the pancreas[102-105]. After acute single dose treatment with the mGluR2/3 agonist APDC in the present study, the hypersensitized responses to mechanical and heat stimuli of AHF animals were no longer significantly different from those of controls. This attenuation was of short duration (1 h) suggesting that systemic administration of APDC may have activated mGluR2/3 receptors on peripheral nociceptive sensory neurons, thus reducing nociception. Previous studies have reported efficacious use of group Ⅱ agonists as analgesics without any apparent side effects in animal models of neuropathic and acute inflammatory pain without altering nociceptive responses of control animals[51,52,54,106-108]. Systemic use of mGluR2/3 agonists is able to activate receptors on peripheral sensory neurons to decrease their activity and central release of glutamate, thus interrupting neurogenic inflammation and facilitating tissue regeneration. Due to their expression within the limbic system, mGluR2/3 receptors have been studied in connection with schizophrenia, alcohol and drug addiction, and anxiety[109-111]. The potential ability of a single drug to be used not only for pain management in alcoholic chronic pancreatitis, but also to support patients' alcohol cessation and dietary management would be of immense benefit, simplifying dosing and regular use of pharmacological therapy. Prolonged use of a different mGluR2/3 agonist, LY379268, for pain management in somatic pain models showed that repeated daily systemic dosing quickly resulted in desensitization and lost ability to reverse hypersensitivity[53,55]. Long-term experiments utilizing lower doses or novel mGluR2/3 agonists for repeated treatments are needed to investigate its efficacy in reversing alcoholic chronic pancreatitis associated hypersensitivity.

Nociceptin, also called orphanin FQ, is an endogenous opioid-like peptide that does not bind to the classical opioid receptors but to ORL-1. Like mGluR2/3, activation of this G_i-coupled GPCR also inhibits adenylate cyclase and voltage-gated Ca^{2+}-channels while activating voltage-gated K^+-channels which results in decreased neuronal activity and decreased glutamate release[44,45,112]. In the AHF diet induced chronic pancreatitis animal group, acute systemic treatments with nociceptin successfully reversed the induced mechanical and heat hypersensitivity in AHF fed animals. Unlike morphine, these treatments did not alter nociceptive responses of control animals. Morphine decreases mechanical and heat sensitivity concentration-dependently in control animals. In the present experiments morphine decreased mechanical sensitivity in control rats while response latencies in the hotplate test were not affected. The Fischer F344 rat strain is known for having higher anxiety compared to other rat strains[113]. Animals were acclimated to the experimental set-up for mechanical sensitivity assays whereas the hotplate test posed a novel environment which may have altered the effects of morphine in control Fischer F344 rats.

Nociceptin and downstream signaling pathways initiated by binding to the ORL-1 receptor have been enigmatic. Initial reports described that intracerebroventricular injections induced hyperalgesia and high doses inhibited locomotion[44,45]. Subsequent studies using intrathecal injections demonstrated analgesic properties of ORL-1 activation by reducing acute inflammatory and nerve injury induced neuropathic hypersensitivity[56,57,69,114]. Intrathecal nociceptin reduced peripheral release of vasodilatory neuropeptides co-expressed with ORL-1, thus decreasing edema after acute inflammatory insult by decreasing dorsal root potentials and glutamatergic transmission[115-117]. Due to the absence of reliable antibodies for ORL-1, its localization still relies on *in situ* hybridization studies. Its mRNA has been localized throughout nociceptive signaling pathways, including small diameter, presumably nociceptive sensory neurons, within the superficial dorsal horn as well as around the central canal, and in multiple regions throughout the brain[116,118]. Reduction of hypersensitivity in AHF animals after systemic treatment with nociceptin was most likely achieved by ORL-1 activation within the peripheral nervous system and resulting decrease in neuronal activity and glutamate release. While activation of ORL-1 within the spinal cord is predicted to also be able to attenuate chronic pancreatitis induced hypersensitivity, repeated use of systemic nociceptin may result in increased crossing of the blood brain barrier which can be compromised in cases of severe peripheral inflammation thus promoting pro-nociceptive effects similar to intracerebroventricular injections[119,120]. Combined treatment using morphine and nociceptin provided synergistic analgesia thus diminishing the amount of morphine needed to attenuate pain sensation and reducing the risk of sensitization to morphine in a previous study[2]. This opens the possible therapeutic option of employing the nociceptin-NOP system for more efficient pain management of chronic pancreatitis-associated pain while reducing side effects.

In summary, the G_i-coupled GPCR signaling pathways downstream from mGluR2/3 and ORL-1 receptors investigated here, presented good alternatives to presently employed opioid pain therapies for the treatment of chronic pancreatitis induced pain. Likewise, these studies suggest these agents have potential as adjuvant therapy to reduce the dosage of morphine derivatives and related side effects.

COMMENTS

Background

Chronic pancreatitis is a progressive and potentially fatal disease caused by persistent unresolved inflammation and pancreatic fibrosis. Pancreatitis can be accompanied by severe intractable abdominal pain. Currently recommended pain management therapies range from non-narcotic analgesics to strong opiates with their accompanying side-effects, but are not effective as long term treatments. Presently employed animal models poorly reproduce the clinical etiology of chronic pancreatitis as they are highly invasive, requiring laparotomy surgery and/or utilize repetitive dosing with caustic chemicals. The abdominal hypersensitivity induced with these experimental procedures is better suited for modeling acute pancreatitis.

Research frontiers

To date no satisfactory pain therapy is available for treatment of chronic pancreatitis nor is there a suitable experimental model for the study of chronic pancreatitis resembling the clinical syndrome with which to test potential therapeutics. Knowledge of the underlying pathophysiology of chronic pancreatitis resulting in this severe abdominal pain is needed for the development of better pharmacological interventions.

Innovations and breakthroughs

The animal model of chronic pancreatitis is induced with a 6% alcohol and high fat diet similar to poor human dietary choices. It produces hypersensitivity to touch with fine filaments on the abdomen and has characteristics of type 3c diabetes mellitus (T3cDM), *i.e.*, abnormal insulin histology and intolerance to glucose. Reduction of hypersensitivity induced by the model was demonstrated with the pharmacological activation of three inhibitory metabotropic G_i protein-coupled receptors. Analgesia was demonstrated with single doses of drugs activating inhibitory glutamate and opiate-like receptors, mGluR2/3 and ORL-1, respectively, in comparisons to morphine.

Applications

These therapies for the treatment of chronic pancreatitis associated pain are suggested as good alternatives to presently employed opioid pain therapies. Used as adjuvant therapy with morphine derivatives for more effective relief of chronic pancreatitis pain, these agents would have potential to reduce the opiate dosage and related side effects.

Terminology

Intractable pancreatic pain cannot be alleviated with current therapies. Using the 6% alcohol and high fat diet (AHF) induced rat chronic pancreatitis model, two therapies were tested, including nociceptin, an endogenous ligand for the opioid-receptor-like 1 receptor, and (2R,4R)-4-Aminopyrrolidine-2,4-dicarboxylate, an activator of inhibitory mGluR2/3 glutamate receptors. These therapies reduced the hypersensitivity that develops on the abdominal skin of the rats with chronic pancreatitis as effectively as morphine.

Peer review

This study demonstrated that the AHF diet replicating high risk human dietary choices induced a chronic alcoholic pancreatitis in rats with histological features and developing glucose intolerance resembling clinical patients with chronic pancreatitis and T3cDM. So, this paper has novelty and innovation.

REFERENCES

1 **Coté GA**, Yadav D, Slivka A, Hawes RH, Anderson MA, Burton FR, Brand RE, Banks PA, Lewis MD, Disario JA, Gardner TB, Gelrud A, Amann ST, Baillie J, Money ME, O'Connell M, Whitcomb DC, Sherman S. Alcohol and smoking as risk factors in an epidemiology study of patients with chronic pancreatitis. *Clin Gastroenterol Hepatol* 2011; **9**: 266-273; quiz e27 [PMID: 21029787 DOI: 10.1016/j.cgh.2010.10.015]

2 **Nøjgaard C**, Becker U, Matzen P, Andersen JR, Holst C, Bendtsen F. Progression from acute to chronic pancreatitis: prognostic factors, mortality, and natural course. *Pancreas* 2011; **40**: 1195-1200 [PMID: 21926938 DOI: 10.1097/MPA.0b013e318221f569]

3 **Malka D**, Hammel P, Maire F, Rufat P, Madeira I, Pessione F, Lévy P, Ruszniewski P. Risk of pancreatic adenocarcinoma in chronic pancreatitis. *Gut* 2002; **51**: 849-852 [PMID: 12427788]

4 **Malka D**, Hammel P, Sauvanet A, Rufat P, O'Toole D, Bardet P, Belghiti J, Bernades P, Ruszniewski P, Lévy P. Risk factors for diabetes mellitus in chronic pancreatitis. *Gastroenterology* 2000; **119**: 1324-1332 [PMID: 11054391]

5 **Howes N**, Neoptolemos JP. Risk of pancreatic ductal adenocarcinoma in chronic pancreatitis. *Gut* 2002; **51**: 765-766 [PMID: 12427771]

6 **Hardt PD**, Brendel MD, Kloer HU, Bretzel RG. Is pancreatic diabetes (type 3c diabetes) underdiagnosed and misdiagnosed? *Diabetes Care* 2008; **31** Suppl 2: S165-S169 [PMID: 18227480 DOI: 10.2337/dc08-s244]

7 **Apte MV**, Pirola RC, Wilson JS. Pancreas: alcoholic pancreatitis--it's the alcohol, stupid. *Nat Rev Gastroenterol Hepatol* 2009; **6**: 321-322 [PMID: 19494819 DOI: 10.1038/nrgastro.2009.84]

8 **American Diabetes Association**. Diagnosis and classification of diabetes mellitus. *Diabetes Care* 2010; **33** Suppl 1: S62-S69 [PMID: 20042775 DOI: 10.2337/dc10-S062]

9 **Raimondi S**, Lowenfels AB, Morselli-Labate AM, Maisonneuve P, Pezzilli R. Pancreatic cancer in chronic pancreatitis; aetiology, incidence, and early detection. *Best Pract Res Clin Gastroenterol* 2010; **24**: 349-358 [PMID: 20510834 DOI: 10.1016/j.bpg.2010.02.007]

10 **Cui Y**, Andersen DK. Pancreatogenic diabetes: special considerations for management. *Pancreatology* 2011; **11**: 279-294 [PMID: 21757968 DOI: 10.1159/000329188]

11 **Cui Y**, Andersen DK. Diabetes and pancreatic cancer. *Endocr Relat Cancer* 2012; **19**: F9-F26 [PMID: 22843556 DOI: 10.1530/ERC-12-0105]

12 **Andersen DK**, Andren-Sandberg Å, Duell EJ, Goggins M, Korc M, Petersen GM, Smith JP, Whitcomb DC. Pancreatitis-diabetes-pancreatic cancer: summary of an NIDDK-NCI workshop. *Pancreas* 2013; **42**: 1227-1237 [PMID: 24152948 DOI: 10.1097/MPA.0b013e3182a9ad9d]

13 **Ewald N**, Bretzel RG. Diabetes mellitus secondary to pancreatic diseases (Type 3c)--are we neglecting an important disease? *Eur J Intern Med* 2013; **24**: 203-206 [PMID: 23375619 DOI: 10.1016/j.ejim.2012.12.017]

14 **Dufour MC**, Adamson MD. The epidemiology of alcohol-induced pancreatitis. *Pancreas* 2003; **27**: 286-290 [PMID: 14576488]

15 **Rosendahl J**, Bödeker H, Mössner J, Teich N. Hereditary chronic pancreatitis. *Orphanet J Rare Dis* 2007; **2**: 1 [PMID: 17204147]

16 **Lieb JG**, Forsmark CE. Review article: pain and chronic pancreatitis. *Aliment Pharmacol Ther* 2009; **29**: 706-719 [PMID: 19284407 DOI: 10.1111/j.1365-2036.2009.03931.x]

17 **Affronti J**. Chronic pancreatitis and exocrine insufficiency. *Prim Care* 2011; **38**: 515-537; ix [PMID: 21872095 DOI: 10.1016/j.pop.2011.05.007]

18 **Nitsche C**, Simon P, Weiss FU, Fluhr G, Weber E, Gärtner S, Behn CO, Kraft M, Ringel J, Aghdassi A, Mayerle J, Lerch MM. Environmental risk factors for chronic pancreatitis and pancreatic cancer. *Dig Dis* 2011; **29**: 235-242 [PMID: 21734390 DOI: 10.1159/000323933]

19 **Whitcomb DC**. Genetic risk factors for pancreatic disorders. *Gastroenterology* 2013; **144**: 1292-1302 [PMID: 23622139 DOI: 10.1053/j.gastro.2013.01.069]

20 **National Institute of Health. Pancreatitis**. NIH Publication 2008; No. 08-1596. Available from: URL: http://digestive.niddk.nih.gov/ddiseases/pubs/pancreatitis/index.aspx

21 **Rajesh G**, Girish BN, Vaidyanathan K, Balakrishnan V. Diet, nutrient deficiency and chronic pancreatitis. *Trop Gastroenterol* 2013; **34**: 68-73 [PMID: 24377152]

22 **Ammann RW**, Buehler H, Bruehlmann W, Kehl O, Muench R, Stamm B. Acute (nonprogressive) alcoholic pancreatitis: prospective longitudinal study of 144 patients with recurrent alcoholic pancreatitis. *Pancreas* 1986; **1**: 195-203 [PMID:

3575305]
23 **Apte MV**, Wilson JS, Korsten MA. Alcohol-related pancreatic damage: mechanisms and treatment. *Alcohol Health Res World* 1997; **21**: 13-20 [PMID: 15706759]
24 **Thrower EC**, Gorelick FS, Husain SZ. Molecular and cellular mechanisms of pancreatic injury. *Curr Opin Gastroenterol* 2010; **26**: 484-489 [PMID: 20651589 DOI: 10.1097/MOG.0b013e32833d119e]
25 **Goulden MR**. The pain of chronic pancreatitis: a persistent clinical challenge. *Br J Pain* 2013; **7**: 8-22 [DOI: 10.1177/2049463713479230]
26 **Gachago C**, Draganov PV. Pain management in chronic pancreatitis. *World J Gastroenterol* 2008; **14**: 3137-3148 [PMID: 18506917]
27 **Burton F**, Alkaade S, Collins D, Muddana V, Slivka A, Brand RE, Gelrud A, Banks PA, Sherman S, Anderson MA, Romagnuolo J, Lawrence C, Baillie J, Gardner TB, Lewis MD, Amann ST, Lieb JG, O'Connell M, Kennard ED, Yadav D, Whitcomb DC, Forsmark CE. Use and perceived effectiveness of non-analgesic medical therapies for chronic pancreatitis in the United States. *Aliment Pharmacol Ther* 2011; **33**: 149-159 [PMID: 21083584 DOI: 10.1111/j.1365-2036.2010.04491.x]
28 **Adrych K**, Smoczynski M, Stojek M, Sledzinski T, Slominska E, Goyke E, Smolenski RT, Swierczynski J. Decreased serum essential and aromatic amino acids in patients with chronic pancreatitis. *World J Gastroenterol* 2010; **16**: 4422-4427 [PMID: 20845509]
29 **Girish BN**, Rajesh G, Vaidyanathan K, Balakrishnan V. Zinc status in chronic pancreatitis and its relationship with exocrine and endocrine insufficiency. *JOP* 2009; **10**: 651-656 [PMID: 19890187]
30 **Aghdassi AA**, Mayerle J, Christochowitz S, Weiss FU, Sendler M, Lerch MM. Animal models for investigating chronic pancreatitis. *Fibrogenesis Tissue Repair* 2011; **4**: 26 [PMID: 22133269 DOI: 10.1186/1755-1536-4-26]
31 **Lerch MM**, Gorelick FS. Models of acute and chronic pancreatitis. *Gastroenterology* 2013; **144**: 1180-1193 [PMID: 23622127 DOI: 10.1053/j.gastro.2012.12.043]
32 **Singh M**, LaSure MM, Bockman DE. Pancreatic acinar cell function and morphology in rats chronically fed an ethanol diet. *Gastroenterology* 1982; **82**: 425-434 [PMID: 6172313]
33 **Letko G**, Nosofsky T, Lessel W, Siech M. Transition of rat pancreatic juice edema into acute pancreatitis by single ethanol administration. *Pathol Res Pract* 1991; **187**: 247-250 [PMID: 2068007]
34 **Siech M**, Heinrich P, Letko G. Development of acute pancreatitis in rats after single ethanol administration and induction of a pancreatic juice edema. *Int J Pancreatol* 1991; **8**: 169-175 [PMID: 2033327]
35 **Kono H**, Nakagami M, Rusyn I, Connor HD, Stefanovic B, Brenner DA, Mason RP, Arteel GE, Thurman RG. Development of an animal model of chronic alcohol-induced pancreatitis in the rat. *Am J Physiol Gastrointest Liver Physiol* 2001; **280**: G1178-G1186 [PMID: 11352811]
36 **Li J**, Guo M, Hu B, Liu R, Wang R, Tang C. Does chronic ethanol intake cause chronic pancreatitis?: evidence and mechanism. *Pancreas* 2008; **37**: 189-195 [PMID: 18665082 DOI: 10.1097/MPA.0b013e31816459b7]
37 **Norton ID**, Apte MV, Lux O, Haber PS, Pirola RC, Wilson JS. Chronic ethanol administration causes oxidative stress in the rat pancreas. *J Lab Clin Med* 1998; **131**: 442-446 [PMID: 9605109]
38 **Dembele K**, Nguyen KH, Hernandez TA, Nyomba BL. Effects of ethanol on pancreatic beta-cell death: interaction with glucose and fatty acids. *Cell Biol Toxicol* 2009; **25**: 141-152 [PMID: 18330713 DOI: 10.1007/s10565-008-9067-9]
39 **Siech M**, Zhou Z, Zhou S, Bair B, Alt A, Hamm S, Gross H, Mayer J, Beger HG, Tian X, Kornmann M, Bachem MG. Stimulation of stellate cells by injured acinar cells: a model of acute pancreatitis induced by alcohol and fat (VLDL). *Am J Physiol Gastrointest Liver Physiol* 2009; **297**: G1163-G1171 [PMID: 19779015 DOI: 10.1152/ajpgi.90468.2008]
40 **DeCarli LM**, Lieber CS. Fatty liver in the rat after prolonged intake of ethanol with a nutritionally adequate new liquid diet. *J Nutr* 1967; **91**: 331-336 [PMID: 6021815]
41 **Yang H**, McNearney TA, Chu R, Lu Y, Ren Y, Yeomans DC, Wilson SP, Westlund KN. Enkephalin-encoding herpes simplex virus-1 decreases inflammation and hotplate sensitivity in a chronic pancreatitis model. *Mol Pain* 2008; **4**: 8 [PMID: 18307791 DOI: 10.1186/1744-8069-4-8]
42 **Bischofberger J**, Schild D. Glutamate and N-acetylaspartylglutamate block HVA calcium currents in frog olfactory bulb interneurons via an mGluR2/3-like receptor. *J Neurophysiol* 1996; **76**: 2089-2092 [PMID: 8890318]
43 **Petralia RS**, Wang YX, Niedzielski AS, Wenthold RJ. The metabotropic glutamate receptors, mGluR2 and mGluR3, show unique postsynaptic, presynaptic and glial localizations. *Neuroscience* 1996; **71**: 949-976 [PMID: 8684625 DOI: 10.1016/0306-4522(95)00533-1]
44 **Meunier JC**, Mollereau C, Toll L, Suaudeau C, Moisand C, Alvinerie P, Butour JL, Guillemot JC, Ferrara P, Monsarrat B. Isolation and structure of the endogenous agonist of opioid receptor-like ORL1 receptor. *Nature* 1995; **377**: 532-535 [PMID: 7566152 DOI: 10.1038/377532a0]
45 **Reinscheid RK**, Nothacker HP, Bourson A, Ardati A, Henningsen RA, Bunzow JR, Grandy DK, Langen H, Monsma FJ, Civelli O. Orphanin FQ: a neuropeptide that activates an opioidlike G protein-coupled receptor. *Science* 1995; **270**: 792-794 [PMID: 7481766 DOI: 10.1126/science.270.5237.792]
46 **Waterfield AA**, Leslie FM, Lord JA, Ling N, Kosterlitz HW. Opioid activities of fragments of beta-endorphin and of its leucine65-analogue. Comparison of the binding properties of methionine- and leucine-enkephalin. *Eur J Pharmacol* 1979; **58**: 11-18 [PMID: 499333 DOI: 10.1016/0014-2999(79)90334-0]
47 **Kosterlitz HW**. Opioid peptides and their receptors. *Prog Biochem Pharmacol* 1980; **16**: 3-10 [PMID: 6255487]
48 **Malmberg AB**, Yaksh TL. The effect of morphine on formalin-evoked behaviour and spinal release of excitatory amino acids and prostaglandin E2 using microdialysis in conscious rats. *Br J Pharmacol* 1995; **114**: 1069-1075 [PMID: 7780642 DOI: 10.1111/j.1476-5381.1995.tb13315.x]
49 **Tang FR**, Bradford HF, Ling EA. Metabotropic glutamate receptors in the control of neuronal activity and as targets for development of anti-epileptogenic drugs. *Curr Med Chem* 2009; **16**: 2189-2204 [PMID: 19519386 DOI: 10.2174/092986709788612710]
50 **Niswender CM**, Conn PJ. Metabotropic glutamate receptors: physiology, pharmacology, and disease. *Annu Rev Pharmacol Toxicol* 2010; **50**: 295-322 [PMID: 20055706 DOI: 10.1146/annurev.pharmtox.011008.145533]
51 **Yang D**, Gereau RW. Peripheral group II metabotropic glutamate receptors (mGluR2/3) regulate prostaglandin E2-mediated sensitization of capsaicin responses and thermal nociception. *J Neurosci* 2002; **22**: 6388-6393 [PMID: 12151517]
52 **Yang D**, Gereau RW. Peripheral group II metabotropic glutamate receptors mediate endogenous anti-allodynia in inflammation. *Pain* 2003; **106**: 411-417 [PMID: 14659524 DOI: 10.1016/j.pain.2003.08.011]
53 **Jones CK**, Eberle EL, Peters SC, Monn JA, Shannon HE. Analgesic effects of the selective group II (mGlu2/3) metabotropic glutamate receptor agonists LY379268 and LY389795 in persistent and inflammatory pain models after acute and repeated dosing. *Neuropharmacology* 2005; **49** Suppl 1: 206-218 [PMID: 15998527 DOI: 10.1016/j.neuropharm.2005.05.008]
54 **Du J**, Zhou S, Carlton SM. Group II metabotropic glutamate receptor activation attenuates peripheral sensitization in

inflammatory states. *Neuroscience* 2008; **154**: 754-766 [PMID: 18487022 DOI: 10.1016/j.neuroscience.2008.03.084]
55 **Zammataro M**, Chiechio S, Montana MC, Traficante A, Copani A, Nicoletti F, Gereau RW. mGlu2 metabotropic glutamate receptors restrain inflammatory pain and mediate the analgesic activity of dual mGlu2/mGlu3 receptor agonists. *Mol Pain* 2011; **7**: 6 [PMID: 21235748 DOI: 10.1186/1744-8069-7-6]
56 **Hao JX**, Xu IS, Wiesenfeld-Hallin Z, Xu XJ. Anti-hyperalgesic and anti-allodynic effects of intrathecal nociceptin/orphanin FQ in rats after spinal cord injury, peripheral nerve injury and inflammation. *Pain* 1998; **76**: 385-393 [PMID: 9718257 DOI: 10.1016/S0304-3959(98)00071-2]
57 **Kolesnikov YA**, Pasternak GW. Peripheral orphanin FQ/nociceptin analgesia in the mouse. *Life Sci* 1999; **64**: 2021-2028 [PMID: 10374927 DOI: 10.1016/S0024-3205(99)00149-6]
58 **Fu X**, Zhu ZH, Wang YQ, Wu GC. Regulation of proinflammatory cytokines gene expression by nociceptin/orphanin FQ in the spinal cord and the cultured astrocytes. *Neuroscience* 2007; **144**: 275-285 [PMID: 17069983 DOI: 10.1016/j.neuroscience.2006.09.016]
59 **Agostini S**, Eutamene H, Broccardo M, Improta G, Petrella C, Theodorou V, Bueno L. Peripheral anti-nociceptive effect of nociceptin/orphanin FQ in inflammation and stress-induced colonic hyperalgesia in rats. *Pain* 2009; **141**: 292-299 [PMID: 19147291 DOI: 10.1016/j.pain.2008.12.007]
60 **Suaudeau C**, Florin S, Meunier JC, Costentin J. Nociceptin-induced apparent hyperalgesia in mice as a result of the prevention of opioid autoanalgesic mechanisms triggered by the stress of an intracerebroventricular injection. *Fundam Clin Pharmacol* 1998; **12**: 420-425 [PMID: 9711464 DOI: 10.1111/j.1472-8206.1998.tb00966.x]
61 **Vera-Portocarrero LP**, Lu Y, Westlund KN. Nociception in persistent pancreatitis in rats: effects of morphine and neuropeptide alterations. *Anesthesiology* 2003; **98**: 474-484 [PMID: 12552208 DOI: 10.1097/00000542-200302000-00029]
62 **Chaplan SR**, Bach FW, Pogrel JW, Chung JM, Yaksh TL. Quantitative assessment of tactile allodynia in the rat paw. *J Neurosci Methods* 1994; **53**: 55-63 [PMID: 7990513 DOI: 10.1016/0165-0270(94)90144-9]
63 **Williams DB**, Wan Z, Frier BC, Bell RC, Field CJ, Wright DC. Dietary supplementation with vitamin E and C attenuates dexamethasone-induced glucose intolerance in rats. *Am J Physiol Regul Integr Comp Physiol* 2012; **302**: R49-R58 [PMID: 22031784 DOI: 10.1152/ajpregu.00304.2011]
64 **Lieber CS**, DeCarli LM. Quantitative relationship between amount of dietary fat and severity of alcoholic fatty liver. *Am J Clin Nutr* 1970; **23**: 474-478 [PMID: 5462407]
65 **Tsukamoto H**, Towner SJ, Yu GS, French SW. Potentiation of ethanol-induced pancreatic injury by dietary fat. Induction of chronic pancreatitis by alcohol in rats. *Am J Pathol* 1988; **131**: 246-257 [PMID: 3358454]
66 **Reber PU**, Patel AG, Toyama MT, Ashley SW, Reber HA. Feline model of chronic obstructive pancreatitis: effects of acute pancreatic duct decompression on blood flow and interstitial pH. *Scand J Gastroenterol* 1999; **34**: 439-444 [PMID: 10365907 DOI: 10.1080/00365529750026489]
67 **Demols A**, Van Laethem JL, Quertinmont E, Degraef C, Delhaye M, Geerts A, Deviere J. Endogenous interleukin-10 modulates fibrosis and regeneration in experimental chronic pancreatitis. *Am J Physiol Gastrointest Liver Physiol* 2002; **282**: G1105-G1112 [PMID: 12016137]
68 **van Westerloo DJ**, Florquin S, de Boer AM, Daalhuisen J, de Vos AF, Bruno MJ, van der Poll T. Therapeutic effects of troglitazone in experimental chronic pancreatitis in mice. *Am J Pathol* 2005; **166**: 721-728 [PMID: 15743784 DOI: 10.1016/S0002-9440(10)62293-6]
69 **Kamei J**, Ohsawa M, Kashiwazaki T, Nagase H. Antinociceptive effects of the ORL1 receptor agonist nociceptin/orphanin FQ in diabetic mice. *Eur J Pharmacol* 1999; **370**: 109-116 [PMID: 10323258 DOI: 10.1016/S0014-2999(99)00112-0]
70 **Breslow RA**, Smothers BA. Drinking patterns and body mass index in never smokers: National Health Interview Survey, 1997-2001. *Am J Epidemiol* 2005; **161**: 368-376 [PMID: 15692081 DOI: 10.1093/aje/kwi061]
71 **Breslow RA**, Guenther PM, Juan W, Graubard BI. Alcoholic beverage consumption, nutrient intakes, and diet quality in the US adult population, 1999-2006. *J Am Diet Assoc* 2010; **110**: 551-562 [PMID: 20338281 DOI: 10.1016/j.jada.2009.12.026]
72 **Food and Agriculture Organization of the United Nations**. FAO Statistics Division 2010. Available from: URL: http://faostat.fao.org/
73 **Noel-Jorand MC**, Bras J. A comparison of nutritional profiles of patients with alcohol-related pancreatitis and cirrhosis. *Alcohol Alcohol* 1994; **29**: 65-74 [PMID: 8003119]
74 **Chung HK**, Cho Y, Shin MJ. Alcohol use behaviors, fat intake and the function of pancreatic β-cells in non-obese, healthy Korean males: findings from 2010 Korea National Health and Nutrition Examination Survey. *Ann Nutr Metab* 2013; **62**: 129-136 [PMID: 23392227 DOI: 10.1159/000345587]
75 **Manari AP**, Preedy VR, Peters TJ. Nutritional intake of hazardous drinkers and dependent alcoholics in the UK. *Addict Biol* 2003; **8**: 201-210 [PMID: 12850779 DOI: 10.1080/13556210310001174437]
76 **Sarles H**. An international survey on nutrition and pancreatitis. *Digestion* 1973; **9**: 389-403 [PMID: 4206286 DOI: 10.1159/000197468]
77 **Durbec JP**, Sarles H. Multicenter survey of the etiology of pancreatic diseases. Relationship between the relative risk of developing chronic pancreaitis and alcohol, protein and lipid consumption. *Digestion* 1978; **18**: 337-350 [PMID: 750261 DOI: 10.1159/000198221]
78 **Sarles H**, Lebreuil G, Tasso F, Figarella C, Clemente F, Devaux MA, Fagonde B, Payan H. A comparison of alcoholic pancreatitis in rat and man. *Gut* 1971; **12**: 377-388 [PMID: 4329553 DOI: 10.1136/gut.12.5.377]
79 **Schwartz ES**, La JH, Scheff NN, Davis BM, Albers KM, Gebhart GF. TRPV1 and TRPA1 antagonists prevent the transition of acute to chronic inflammation and pain in chronic pancreatitis. *J Neurosci* 2013; **33**: 5603-5611 [PMID: 23536075 DOI: 10.1523/JNEUROSCI.1806-12.2013]
80 **Zaninovic V**, Gukovskaya AS, Gukovsky I, Mouria M, Pandol SJ. Cerulein upregulates ICAM-1 in pancreatic acinar cells, which mediates neutrophil adhesion to these cells. *Am J Physiol Gastrointest Liver Physiol* 2000; **279**: G666-G676 [PMID: 11005752]
81 **Gumy C**, Chandsawangbhuwana C, Dzyakanchuk AA, Kratschmar DV, Baker ME, Odermatt A. Dibutyltin disrupts glucocorticoid receptor function and impairs glucocorticoid-induced suppression of cytokine production. *PLoS One* 2008; **3**: e3545 [PMID: 18958157 DOI: 10.1371/journal.pone.0003545]
82 **Schneider KJ**, Scheer M, Suhr M, Clemens DL. Ethanol administration impairs pancreatic repair after injury. *Pancreas* 2012; **41**: 1272-1279 [PMID: 22617711 DOI: 10.1097/MPA.0b013e31824bde37]
83 **Apte M**, Pirola R, Wilson J. New insights into alcoholic pancreatitis and pancreatic cancer. *J Gastroenterol Hepatol* 2009; **24** Suppl 3: S51-S56 [PMID: 19799699 DOI: 10.1111/j.1440-1746.2009.06071.x]
84 **Lieber CS**, DeCarli LM, Feinman L, Hasumura Y, Korsten M, Matsuzaki S, Teschke R. Effect of chronic alcohol consumption on ethanol and acetaldehyde metabolism. *Adv Exp Med Biol* 1975; **59**: 185-227 [PMID: 241214]
85 **Petersen P**. Ultrastructure of periportal and centrilobular hepatocytes in human fatty liver of various aetiology. *Acta Pathol Microbiol Scand A* 1977; **85**: 421-427 [PMID: 878877]
86 **Bang S**, Kim KY, Yoo S, Kim YG, Hwang SW. Transient receptor potential A1 mediates acetaldehyde-evoked

pain sensation. *Eur J Neurosci* 2007; **26**: 2516-2523 [PMID: 17970723]
87 **Schwartz ES**, Christianson JA, Chen X, La JH, Davis BM, Albers KM, Gebhart GF. Synergistic role of TRPV1 and TRPA1 in pancreatic pain and inflammation. *Gastroenterology* 2011; **140**: 1283-1291.e1-e2 [PMID: 21185837 DOI: 10.1053/j.gastro.2010.12.033]
88 **Zhang LP**, Ma F, Abshire SM, Westlund KN. Prolonged high fat/alcohol exposure increases TRPV4 and its functional responses in pancreatic stellate cells. *Am J Physiol Regul Integr Comp Physiol* 2013; **304**: R702-R711 [PMID: 23447134 DOI: 10.1152/ajpregu.00296.2012]
89 **Haber PS**, Apte MV, Moran C, Applegate TL, Pirola RC, Korsten MA, McCaughan GW, Wilson JS. Non-oxidative metabolism of ethanol by rat pancreatic acini. *Pancreatology* 2004; **4**: 82-89 [PMID: 15056978]
90 **Haber PS**, Apte MV, Applegate TL, Norton ID, Korsten MA, Pirola RC, Wilson JS. Metabolism of ethanol by rat pancreatic acinar cells. *J Lab Clin Med* 1998; **132**: 294-302 [PMID: 9794700]
91 **McCarroll JA**, Phillips PA, Park S, Doherty E, Pirola RC, Wilson JS, Apte MV. Pancreatic stellate cell activation by ethanol and acetaldehyde: is it mediated by the mitogen-activated protein kinase signaling pathway? *Pancreas* 2003; **27**: 150-160 [PMID: 12883264 DOI: 10.1097/00006676-200308000-00008]
92 **Vera-Portocarrero L**, Westlund KN. Role of neurogenic inflammation in pancreatitis and pancreatic pain. *Neurosignals* 2005; **14**: 158-165 [PMID: 16215298 DOI: 10.1159/000087654]
93 **Rütti S**, Ehses JA, Sibler RA, Prazak R, Rohrer L, Georgopoulos S, Meier DT, Niclauss N, Berney T, Donath MY, von Eckardstein A. Low- and high-density lipoproteins modulate function, apoptosis, and proliferation of primary human and murine pancreatic beta-cells. *Endocrinology* 2009; **150**: 4521-4530 [PMID: 19628574 DOI: 10.1210/en.2009-0252]
94 **Sjöholm A**. Intracellular signal transduction pathways that control pancreatic beta-cell proliferation. *FEBS Lett* 1992; **311**: 85-90 [PMID: 1327880 DOI: 10.1016/0014-5793(92)81373-T]
95 **Fernández-Solà J**, García G, Elena M, Tobías E, Sacanella E, Estruch R, Nicolás JM. Muscle antioxidant status in chronic alcoholism. *Alcohol Clin Exp Res* 2002; **26**: 1858-1862 [PMID: 12500110 DOI: 10.1111/j.1530-0277.2002.tb02493.x]
96 **Pade PA**, Cardon KE, Hoffman RM, Geppert CM. Prescription opioid abuse, chronic pain, and primary care: a Co-occurring Disorders Clinic in the chronic disease model. *J Subst Abuse Treat* 2012; **43**: 446-450 [PMID: 22980449 DOI: 10.1016/j.jsat.2012.08.010]
97 **Mehendale AW**, Goldman MP, Mehendale RP. Opioid overuse pain syndrome (OOPS): the story of opioids, prometheus unbound. *J Opioid Manag* 2013; **9**: 421-438 [PMID: 24481931 DOI: 10.5055/jom.2013.0185]
98 **Pin JP**, Duvoisin R. The metabotropic glutamate receptors: structure and functions. *Neuropharmacology* 1995; **34**: 1-26 [PMID: 7623957 DOI: 10.1016/0028-3908(94)00129-G]
99 **Blackshaw LA**, Page AJ, Young RL. Metabotropic glutamate receptors as novel therapeutic targets on visceral sensory pathways. *Front Neurosci* 2011; **5**: 40 [PMID: 21472028 DOI: 10.3389/fnins.2011.00040]
100 **Moldrich RX**, Beart PM. Emerging signalling and protein interactions mediated via metabotropic glutamate receptors. *Curr Drug Targets CNS Neurol Disord* 2003; **2**: 109-122 [PMID: 12769803 DOI: 10.2174/1568007033482922]
101 **Carlton SM**, Hargett GL, Coggeshall RE. Localization of metabotropic glutamate receptors 2/3 on primary afferent axons in the rat. *Neuroscience* 2001; **105**: 957-969 [PMID: 11530234 DOI: 10.1016/S0306-4522(01)00238-X]
102 **Carlton SM**, Hargett GL. Colocalization of metabotropic glutamate receptors in rat dorsal root ganglion cells. *J Comp Neurol* 2007; **501**: 780-789 [PMID: 17299761 DOI: 10.1002/cne.21285]
103 **Brice NL**, Varadi A, Ashcroft SJ, Molnar E. Metabotropic glutamate and GABA(B) receptors contribute to the modulation of glucose-stimulated insulin secretion in pancreatic beta cells. *Diabetologia* 2002; **45**: 242-252 [PMID: 11935156 DOI: 10.1007/s00125-001-0750-0]
104 **Volpi C**, Fazio F, Fallarino F. Targeting metabotropic glutamate receptors in neuroimmune communication. *Neuropharmacology* 2012; **63**: 501-506 [PMID: 22640632 DOI: 10.1016/j.neuropharm.2012.05.024]
105 **Valli MJ**, Schoepp DD, Wright RA, Johnson BG, Kingston AE, Tomlinson R, Monn JA. Synthesis and metabotropic glutamate receptor antagonist activity of N1-substituted analogs of 2R,4R-4-aminopyrrolidine-2,4-dicarboxylic acid. *Bioorg Med Chem Lett* 1998; **8**: 1985-1990 [PMID: 9873471 DOI: 10.1016/S0960-894X(98)00352-7]
106 **Chiechio S**, Nicoletti F. Metabotropic glutamate receptors and the control of chronic pain. *Curr Opin Pharmacol* 2012; **12**: 28-34 [PMID: 22040745 DOI: 10.1016/j.coph.2011.10.010]
107 **Osikowicz M**, Mika J, Przewlocka B. The glutamatergic system as a target for neuropathic pain relief. *Exp Physiol* 2013; **98**: 372-384 [PMID: 23002244 DOI: 10.1113/expphysiol.2012.069922]
108 **Vinson PN**, Conn PJ. Metabotropic glutamate receptors as therapeutic targets for schizophrenia. *Neuropharmacology* 2012; **62**: 1461-1472 [PMID: 21620876 DOI: 10.1016/j.neuropharm.2011.05.005]
109 **Spooren W**, Lesage A, Lavreysen H, Gasparini F, Steckler T. Metabotropic glutamate receptors: their therapeutic potential in anxiety. *Curr Top Behav Neurosci* 2010; **2**: 391-413 [PMID: 21309118 DOI: 10.1007/7854_2010_36]
110 **Moussawi K**, Kalivas PW. Group II metabotropic glutamate receptors (mGlu2/3) in drug addiction. *Eur J Pharmacol* 2010; **639**: 115-122 [PMID: 20371233 DOI: 10.1016/j.ejphar.2010.01.030]
111 **Bruchas MR**, Chavkin C. Kinase cascades and ligand-directed signaling at the kappa opioid receptor. *Psychopharmacology* (Berl) 2010; **210**: 137-147 [PMID: 20401607 DOI: 10.1007/s00213-010-1806-y]
112 **Langen B**, Fink H. Anxiety as a predictor of alcohol preference in rats? *Prog Neuropsychopharmacol Biol Psychiatry* 2004; **28**: 961-968 [PMID: 15380856 DOI: 10.1016/j.pnpbp.2004.05.002]
113 **Chen Y**, Sommer C. Activation of the nociceptin opioid system in rat sensory neurons produces antinociceptive effects in inflammatory pain: involvement of inflammatory mediators. *J Neurosci Res* 2007; **85**: 1478-1488 [PMID: 17387690 DOI: 10.1002/jnr.21272]
114 **Dong XW**, Williams PA, Jia YP, Priestley T. Activation of spinal ORL-1 receptors prevents acute cutaneous neurogenic inflammation: role of nociceptin-induced suppression of primary afferent depolarization. *Pain* 2002; **96**: 309-318 [PMID: 11973003 DOI: 10.1016/S0304-3959(01)00460-2]
115 **Pettersson LM**, Sundler F, Danielsen N. Expression of orphanin FQ/nociceptin and its receptor in rat peripheral ganglia and spinal cord. *Brain Res* 2002; **945**: 266-275 [PMID: 12126889 DOI: 10.1016/S0006-8993(02)02817-2]
116 **Mika J**, Li Y, Weihe E, Schafer MK. Relationship of pronociceptin/orphanin FQ and the nociceptin receptor ORL1 with substance P and calcitonin gene-related peptide expression in dorsal root ganglion of the rat. *Neurosci Lett* 2003; **348**: 190-194 [PMID: 12932825 DOI: 10.1016/S0304-3940(03)00786-9]
117 **Houtani T**, Nishi M, Takeshima H, Sato K, Sakuma S, Kakimoto S, Ueyama T, Noda T, Sugimoto T. Distribution of nociceptin/orphanin FQ precursor protein and receptor in brain and spinal cord: a study using in situ hybridization and X-gal histochemistry in receptor-deficient mice. *J Comp Neurol* 2000; **424**: 489-508 [PMID: 10906715]
118 **Brooks TA**, Hawkins BT, Huber JD, Egleton RD, Davis TP. Chronic inflammatory pain leads to increased blood-brain barrier permeability and tight junction protein alterations. *Am J Physiol Heart Circ Physiol* 2005; **289**: H738-H743 [PMID:

15792985 DOI: 10.1152/ajpheart.01288.2004]

119 **Ronaldson PT**, Davis TP. Targeting blood-brain barrier changes during inflammatory pain: an opportunity for optimizing CNS drug delivery. *Ther Deliv* 2011; **2**: 1015-1041 [PMID: 22468221 DOI: 10.4155/tde.11.67]

120 **Tian JH**, Xu W, Fang Y, Mogil JS, Grisel JE, Grandy DK, Han JS. Bidirectional modulatory effect of orphanin FQ on morphine-induced analgesia: antagonism in brain and potentiation in spinal cord of the rat. *Br J Pharmacol* 1997; **120**: 676-680 [PMID: 9051307 DOI: 10.1038/sj.bjp.0700942]

P- Reviewer: Zhang ZM **S- Editor**: Ma YJ **L- Editor**: A
E- Editor: Wang CH

World Journal of Gastroenterology

Submit a Manuscript: http://www.wjgnet.com/esps/
Help Desk: http://www.wjgnet.com/esps/helpdesk.aspx
DOI: 10.3748/wjg.v21.i3.854

World J Gastroenterol 2015 January 21; 21(3): 854-861
ISSN 1007-9327 (print) ISSN 2219-2840 (online)

ORIGINAL ARTICLE

Basic Study

Antiproliferative effects of cinobufacini on human hepatocellular carcinoma HepG2 cells detected by atomic force microscopy

Qing Wu, Wei-Dong Lin, Guan-Qun Liao, Li-Guo Zhang, Shun-Qian Wen, Jia-Ying Lin

Qing Wu, Wei-Dong Lin, Guan-Qun Liao, Li-Guo Zhang, Shun-Qian Wen, Jia-Ying Lin, Department of General Surgery, the Affiliated Foshan Hospital of Southern Medical University, Foshan 528000, Guangdong Province, China

Author contributions: Wu Q and Lin WD designed the research and wrote the paper; Wu Q and Liao GQ performed the research; Zhang LG, Wen SQ and Lin JY analyzed the data.

Correspondence to: Wei-Dong Lin, Chief, Professor, Department of General Surgery, the Affiliated Foshan Hospital of Southern Medical University, No. 78 Weiguo Road, Foshan 528000, Guangdong Province, China. 13433123361@163.com
Telephone: +86-757-88032005
Fax: +86-757-88032005

Received: May 13, 2014
Peer-review started: May 13, 2014
First decision: July 9, 2014
Revised: July 30, 2014
Accepted: September 18, 2014
Article in press: September 19, 2014
Published online: January 21, 2015

Abstract

AIM: To investigate the antiproliferative activity of cinobufacini on human hepatocellular carcinoma HepG2 cells and the possible mechanism of its action.

METHODS: HepG2 cells were treated with different concentrations of cinobufacini. Cell viability was measured by methylthiazolyl tetrazolium (MTT) assay. Cell cycle distribution was analyzed by flow cytometry (FCM). Cytoskeletal and nuclear alterations were observed by fluorescein isothiocyanate-phalloidin and DAPI staining under a laser scanning confocal microscope. Changes in morphology and ultrastructure of cells were detected by atomic force microscopy (AFM) at the nanoscale level.

RESULTS: MTT assay indicated that cinobufacini significantly inhibited the viability of HepG2 cells in a dose-dependent manner. With the concentration of cinobufacini increasing from 0 to 0.10 mg/mL, the cell viability decreased from 74.9% ± 2.7% to 49.41% ± 2.2% and 39.24% ± 2.1% ($P < 0.05$). FCM analysis demonstrated cell cycle arrest at S phase induced by cinobufacini. The immunofluorescence studies of cytoskeletal and nuclear morphology showed that after cinobufacini treatment, the regular reorganization of actin filaments in HepG2 cells become chaotic, while the nuclei were not damaged seriously. Additionally, high-resolution AFM imaging revealed that cell morphology and ultrastructure changed a lot after treatment with cinobufacini. It appeared as significant shrinkage and deep pores in the cell membrane, with larger particles and a rougher cell surface.

CONCLUSION: Cinobufacini inhibits the viability of HepG2 cells *via* cytoskeletal destruction and cell membrane toxicity.

Key words: Cinobufacini; Cell viability; Atomic force microscopy; HepG2 cells; Hepatocarcinoma

Core tip: Cinobufacini is effective against hepatocarcinoma. However, its mechanism of action has not been determined. The present study investigated the effect of cinobufacini

on HepG2 cells and the alterations in cell morphology and membrane ultrastructure. We used atomic force microscopy (AFM) to study the changes in cell membrane ultrastructure induced by cinobufacini. We demonstrated that AFM is a useful tool in verifying cell response to cinobufacini treatment. We observed nuclear morphology and actin filaments in the cytoskeleton by laser scanning confocal microscopy. The cellular changes allowed us to understand better the biophysical functions of HepG2 cells induced by cinobufacini.

Wu Q, Lin WD, Liao GQ, Zhang LG, Wen SQ, Lin JY. Antiproliferative effects of cinobufacini on human hepatocellular carcinoma HepG2 cells detected by atomic force microscopy. *World J Gastroenterol* 2015; 21(3): 854-861 Available from: URL: http://www.wjgnet.com/1007-9327/full/v21/i3/854.htm DOI: http://dx.doi.org/10.3748/wjg.v21.i3.854

INTRODUCTION

Cinobufacini is a water-soluble Chinese medicine that is extracted from the skin of *Bufo bufo gargarizans* Cantor[1]. It has been proven to be effective against a variety of malignant tumor cells, such as breast cancer[2], lung cancer[3] and hepatocellular carcinoma[1,4] cells. In recent years, it has also shown satisfactory therapeutic effects against cancer in clinical studies[5-7]. Although cinobufacini is widely used clinically, little is known about its anti-tumor mechanisms. In particular, there are no detailed data on the changes it induces in cell membrane morphology. The present study sought to investigate the effect of cinobufacini on human hepatoma cell line HepG2 and the alterations in cell morphology and cell membrane ultrastructure.

Atomic force microscopy (AFM) is a powerful tool for nanoscale imaging of cells[8-10], and an important diagnostic instrument[11]. In this study, AFM was used to visualize cell morphology and membrane ultrastructure, which can provide information about the surface topography of the cell at the nanometric level. We used AFM to image the changes in HepG2 cell membrane ultrastructure induced by cinobufacini. We also demonstrated that AFM is a useful tool in discerning and verifying cell response to cinobufacini. In addition, we also analyzed the cell cycle by flow cytometry (FCM), and observed the nuclear morphology and actin filaments in the cytoskeleton by laser scanning confocal microscopy (LSCM). The changes observed in the cells allow us to understand better the biophysical functions of HepG2 cells treated by cinobufacini.

MATERIALS AND METHODS

Materials

All reagents used in the experiments were of analytical grade. Fetal bovine serum (FBS), 2.5% trypsin, RPMI-1640 medium, methylthiazolyl tetrazolium (MTT) and DMSO were purchased from Gibco (Carlsbad, CA, United States). Glutamine, penicillin and streptomycin were purchased from Hyclone (Logan, UT, United States). Triton X-100 and 4% paraformaldehyde were purchased from Sigma (St Louis, MO, United States). Fluorescein isothiocyanate (FITC)-phalloidin and DAPI were purchased from Biyuntian Biological (Shanghai, China). Cell cycle phase determination kit was bought from Keygen Biotechnology (Nanjing, China). Cinobufacini was provided by Jinchan Biochemistry Company Ltd. (Anhui, China). Human hepatoma cell line HepG2 was donated by the First Affiliated Hospital of Jinan University.

Cell culture and treatment with cinobufacini

HepG2 cells were cultured in RPMI-1640 medium supplemented with 10% FBS at 37 ℃ in a humidified atmosphere containing 5% CO_2, and the medium was refreshed every 2-3 d. The cinobufacini was diluted to appropriate concentrations with free medium. Cells were harvested with 0.25% trypsin when needed.

MTT assay

The effect of cinobufacini on cell viability was detected by MTT assay. HepG2 cells were plated at a density of 5000 cells/well in 96-well plates. After 24 h of culture, the cells were treated with cinobufacini at a final concentrations of 0, 0.01, 0.05 or 0.1 mg/mL. After incubation for 48 h, 20 μL MTT dye solution (5 mg/mL) was added to each well and incubated at 37 ℃ for 4 h. The medium was removed and formazan was dissolved in 150 μL DMSO. A_{570} of each group was then measured with a spectrophotometer (Tecan, Switzerland). Cell viability was expressed by the following formula: Viability (%) = $(A_{treated}/A_{control}) \times 100\%$. Experiments were repeated three times.

Cell cycle analysis

The effect of cinobufacini on the cell cycle of HepG2 cells was analyzed by FCM (Becton Dickinson, CA, United States). HepG2 cells were seeded at a density of 1×10^6 cells/mL in six-well plates, and treated with different concentrations of cinobufacini (0, 0.05 or 0.1 mg/mL) for 48 h. Cells were harvested and fixed in 70% ethanol and stored at 4 ℃ overnight. The fixed cells were centrifuged at 1000 *g* for 5 min and washed with cold PBS three times. At last, cells were incubated with 50 μg/mL propidium iodide (PI) containing 8 μg/mL RNase in the dark at 37 ℃ for 30 min. The DNA content of cells was quantified by FCM.

Immunofluorescence staining

HepG2 cells grown on coverslips were treated with 0.1 mg/mL cinobufacini or free medium for 48 h. The actin filaments in HepG2 cells were visualized by staining with FITC-phalloidin. Cells in each group were fixed with 4% paraformaldehyde for 15 min, rinsed three times with PBS, then treated with 0.2% Triton X-100 for 20 min at room temperature, and rinsed with PBS three times

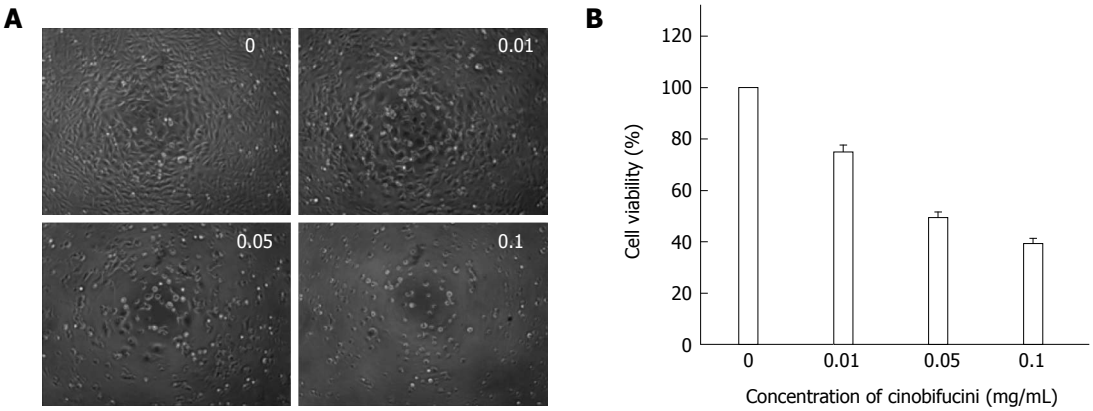

Figure 1 Growth inhibitory effect of cinobufacini on HepG2 cells. Cells were treated with different concentrations (0-0.1 mg/mL) of cinobufacini for 48 h. A: Changes in morphology observed under a phase microscope; B: Viability of HepG2 cells measured by methylthiazolyl tetrazolium (MTT) assay. The results reveal that the cytotoxic effect of cinobufacini on HepG2 cells was dose dependent. All studies are representative of at least three independent experiments.

again. The cells were incubated with 1 mmol/L FITC-phalloidin for 1 h in the dark at room temperature. Subsequently, we added 50 mmol/L DAPI to label the nuclei, for 15 min in the dark at room temperature. The cells were washed in PBS to remove the unbound FITC-phalloidin and DAPI. Finally, the cytoskeletal and nuclear morphology was imaged by LSCM (LSCM510 Meta Duo Scan; Carl Zeiss, Jena, Germany).

Single cell AFM measurement

HepG2 cells were seeded on the slide and treated with different concentrations of cinobufacini (0, 0.05 or 0.1 mg/mL) for 48 h at 37 ℃ in 5% CO_2. The cells were fixed with 4% paraformaldehyde for 15 min, washed three times with PBS, and air dried at room temperature. An atomic force microscope (Autoprobe CP Research, Veeco, CA, United States) was used in the contact mode to obtain topographic images. The silicon nitride tips (UL20B; Park Scientific Instruments) used in all AFM measurements were irradiated with UV in air for 15 min, to remove any organic contaminants prior to use. The curvature radius of the tips was < 10 nm, with a force constant set at 2.8 N/m and oscillation frequency set at 255 kHz. The prepared samples were placed on the XY scanning station of AFM, and > 5 cells were measured. The acquired images were only processed with the instrument-equipped software (Image Processing Software Version 2.1, IP 2.1) to eliminate low-frequency background noise in the scanning direction.

Statistical analysis

All data are presented as mean ± SD from at least three independent experiments. Statistical analyses were performed with SPSS version 13.0 software. Comparisons between groups were performed using two independent samples *t*-test; comparisons between multiple groups were tested by one-way analysis of variance; and comparison between any group using the Student-Newman-Keuls test. A *P*-value < 0.05 was considered statistically significant.

RESULTS

Effect of cinobufacini on HepG2 cell viability

HepG2 cells were treated with different concentration of cinobufacini for 48 h. Under the inverted microscope (Figure 1A), the cells in the control group were closely arranged and well adherent in large numbers. After treatment with different concentrations of cinobufacini (0, 0.01, 0.05 or 0.10 mg/mL), the cells became round and had poor adherence, and were fewer in number, especially at a high concentration of cinobufacini.

As shown in Figure 1B, MTT assay showed that proliferation of HepG2 cells was significantly inhibited. With the concentration of cinobufacini increasing, the cell viability decreased from 74.9% ± 2.7% to 49.41% ± 2.2% and 39.24% ± 2.1%, which suggested that the inhibitory effect of cinobufacini on HepG2 cell viability was dose-dependent ($P < 0.05$).

Effect of cinobufacini on cell cycle distribution of HepG2 cells

After treatment with cinobufacini at different concentrations for 48 h, cell cycle distribution of HepG2 cells was analyzed by FCM through PI staining. Figure 2 shows that the percentage of HepG2 cells in S phase increased when the concentration of cinobufacini increased. After treatment with cinobufacini at a concentration of 0.10 mg/mL, the percentage of cells in S phase increased to 61.60%, which was significantly higher than that in the control group (23.92%). These results suggested that cinobufacini caused cell cycle arrest in S phase.

Alterations in cytoskeleton and nuclei

The cytoskeleton plays an important role in cell morphology, movement, and even apoptosis[2]. Actin microfilaments are important constituents of the cytoskeleton. To observe the organization of the cytoskeleton, actin was stained by FITC-phalloidin and imaged by LSCM. The cells in the control group were rich in actin with regular, parallel organization (Figure 3A). After treatment with

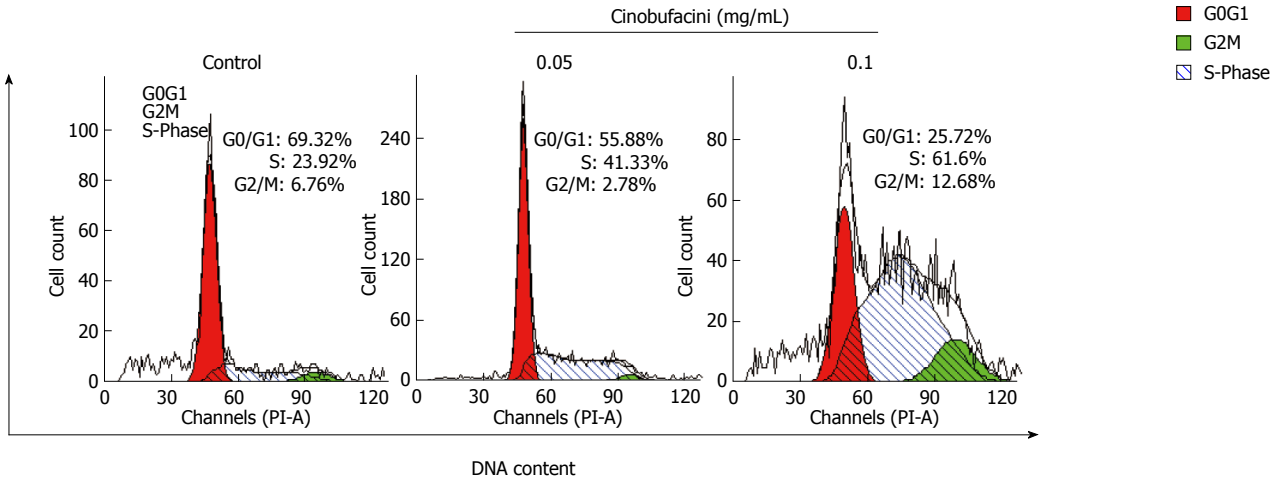

Figure 2 Cell cycle distribution of HepG2 cells analyzed by flow cytometry. Cells were incubated with cinobufacini (0, 0.05 or 0.1 mg/mL) for 48 h. Cell cycle was arrested at S phase.

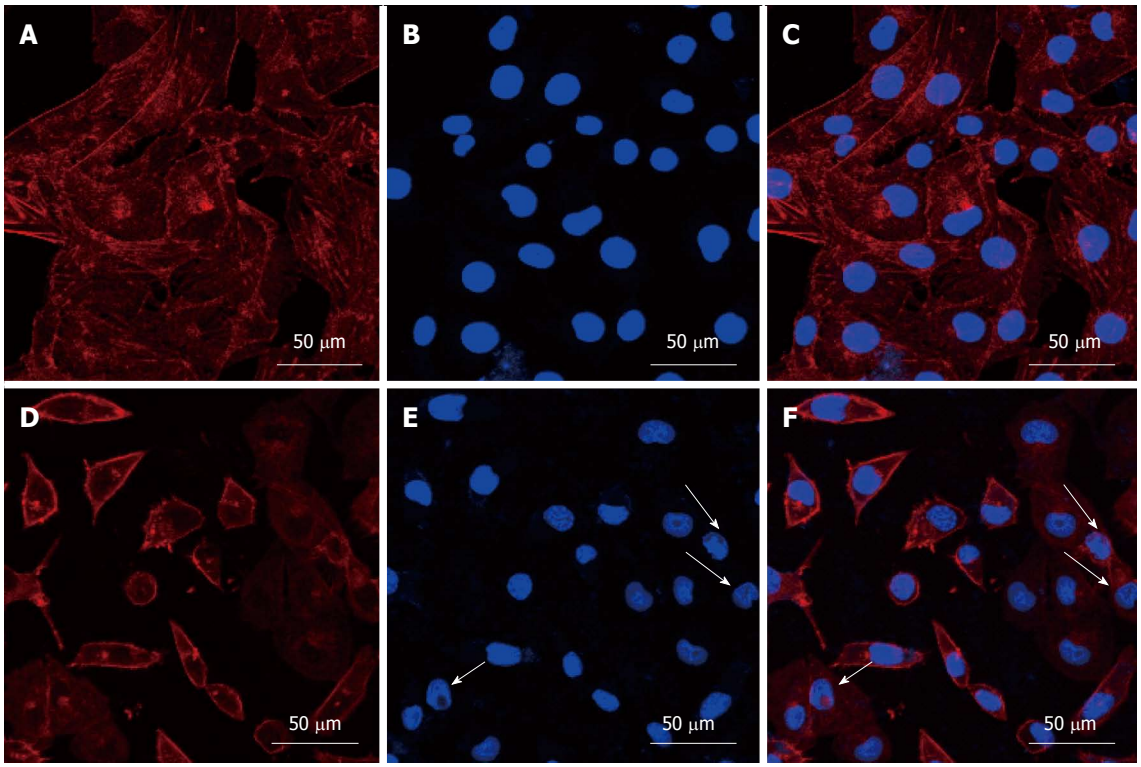

Figure 3 Morphology of the cytoskeleton and nuclei in HepG2 cells before (A-C) and after (D-F) treatment with cinobufacini. The cytoskeleton and nuclei were stained with rhodamine-phalloidin and DAPI. (C) and (F) were merged images of (A, B) and (D, E). White arrow: Fragmented nuclei.

cinobufacini, actin assembly changed dramatically. It became disordered with fewer filaments in the cells (Figure 3D). We used DAPI to stain the cell nuclei. The nuclear morphology of control HepG2 cells was intact and plump (Figure 3B). After treatment with cinobufacini for 48 h, most of the nuclei shrank, and some of the nuclei were condensed, but few were fragmented (Figure 3E, white arrows). Figure 3C and Figure 3F were merged images of (Figure 3A, B) and (Figure 3D, E).

Changes in cell morphology

AFM was used for cell imaging and observing various changes in surface morphology and ultrastructure of HepG2 cells after treatment with different concentrations of cinobufacini. HepG2 cells in the control group were fusiform in shape (Figure 4A). The ultrastructure of the cell surface was homogeneous and displayed granular morphology, with uniform particles, and the cell membrane was relatively smooth with intact and

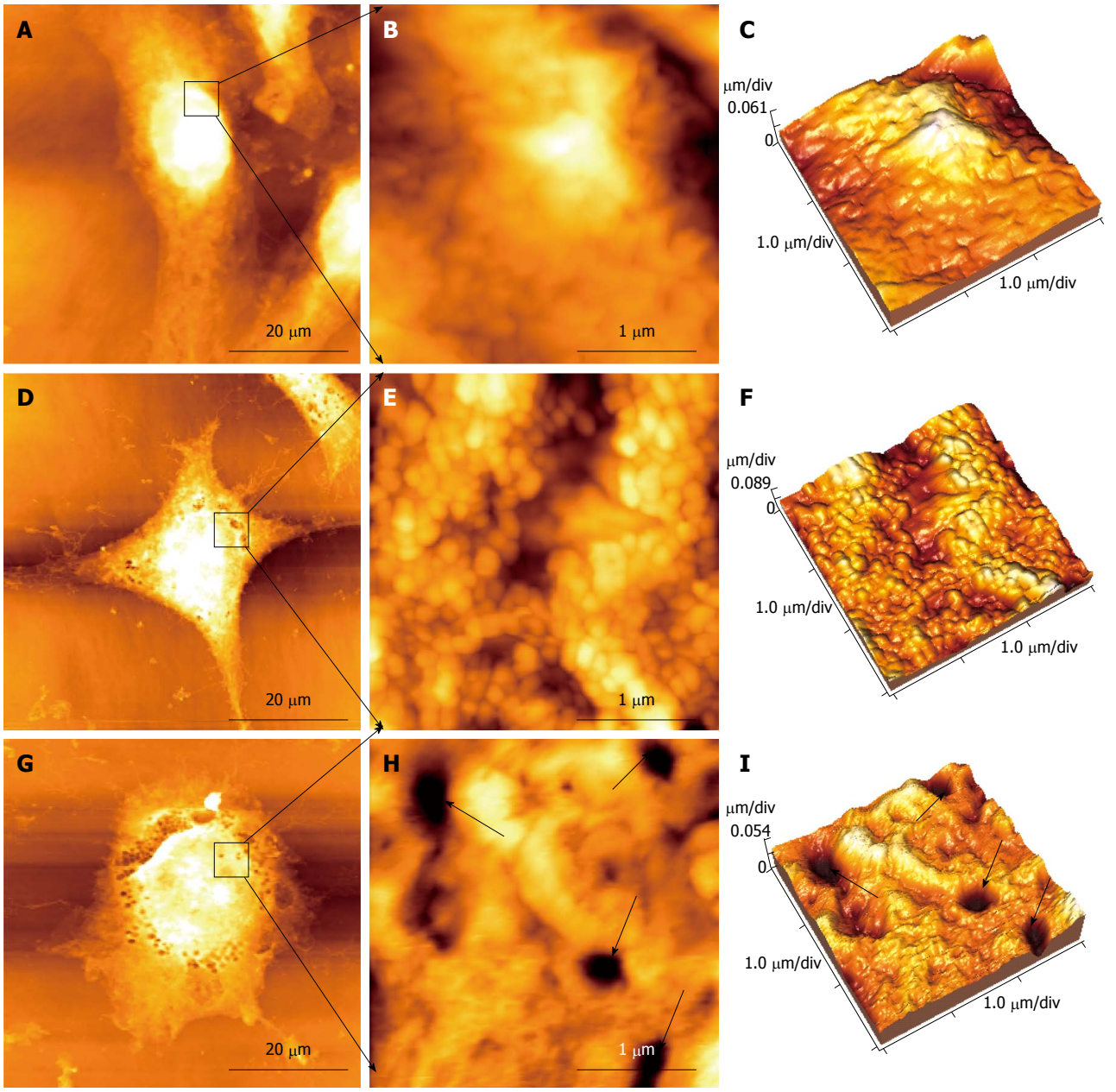

Figure 4 Changes in morphology and ultrastructure of HepG2 cells detected by atomic force microscopy. A-C: Control HepG2 cells; D-F: HepG2 cells treated with 0.05 mg/mL cinobufacini for 48 h; G-I: HepG2 cells treated with 0.1 mg/mL cinobufacini for 48 h; A, D and G: Morphology of HepG2 cells (60 μm × 60 μm); B, E and H: Ultrastructure images (3 μm × 3 μm) on corresponding cell region indicated by black frame; C, F and I: Corresponding 3D images of ultrastructure in B, E and H. Black arrows: Some pores in the cell membrane.

plump cells (Figure 4B, C). After treatment with 0.05 mg/mL cinobufacini for 48 h, cell morphology changed to polygonal (Figure 4D), and the cell surface also became rougher with particles of different size (Figure 4E, F). As the concentration increased to 0.1 mg/mL, further changes in cell morphology were seen, and they appeared to be irregular and even became rounded (Figure 4G), with some pores in the cell membrane (Figure 4H, I, black arrows). These results could help us to acquire more detailed information about the toxic effect of cinobufacini on the cell membrane.

Analysis of cell membrane roughness

By measuring and comparing different areas of cellular ultrastructure, we observed that the average size of surface particles on control HepG2 cells was about 71.5 nm, which increased to 97.0 nm and 142.0 nm for cells treated with 0.05 mg/mL and 0.1 mg/mL cinobufacini, respectively (Figure 5A). We detected that peak to valley roughness (Rp-v), root-mean-square roughness (Rq), average roughness (Ra) and mean height (mean Ht) of the cell membrane surface increased with cinobufacini concentration. As shown in Figure 5B, Rp-v was 55.70 ± 14.74, 92.03 ± 12.03 and 174.53 ± 16.56 nm (F = 56.580, P = 0.000); Rq was 7.32 ± 1.69, 11.66 ± 2.79 and 23.35 ± 6.04 nm (F = 14.136, P = 0.000); Ra was 5.72 ± 1.07, 9.02 ± 2.15 and 17.82 ± 4.66 nm (F = 13.683, P = 0.000). Mean Ht was 30.46 ± 4.82, 54.29 ± 9.99 and

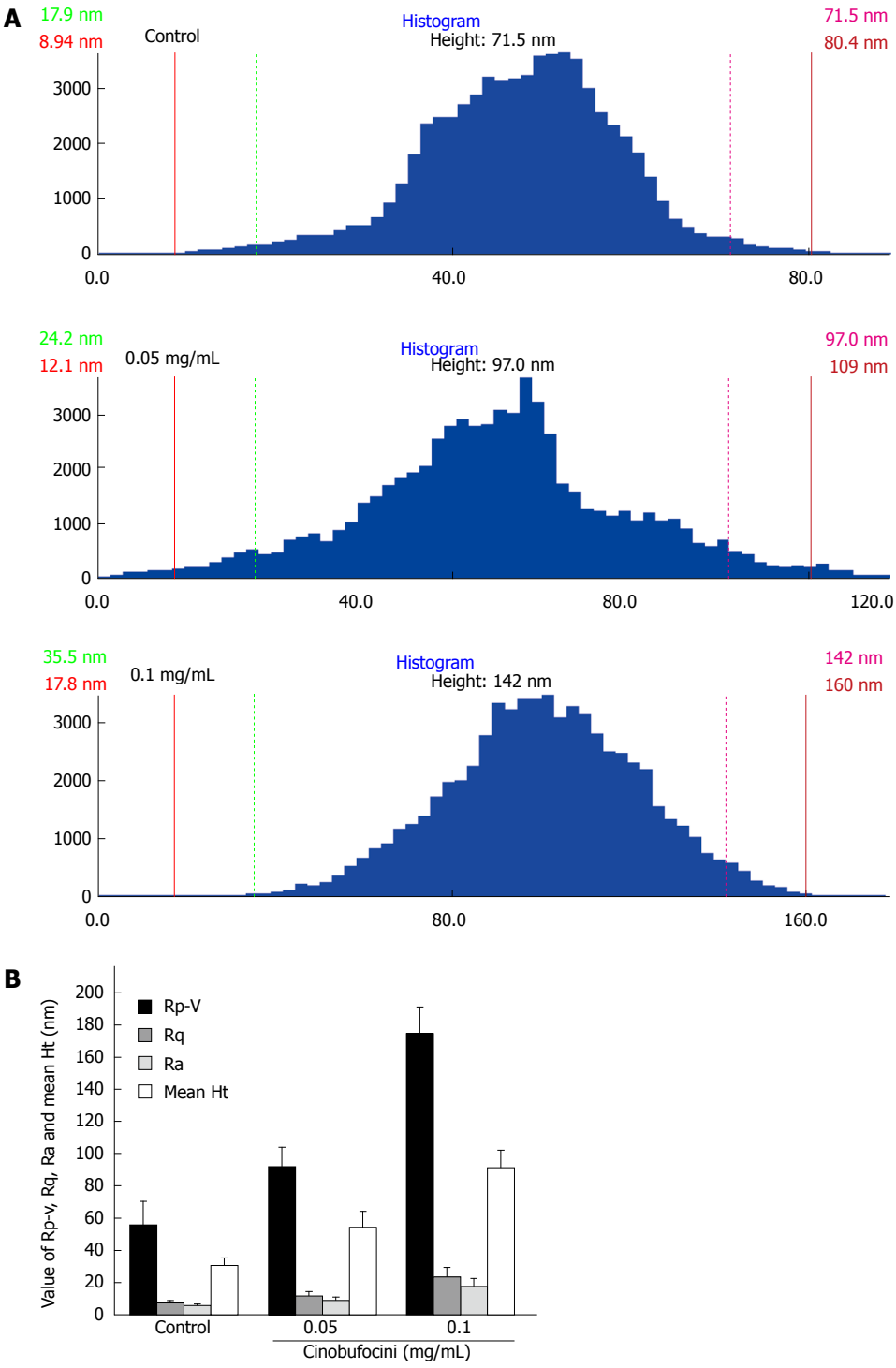

Figure 5 Average size of surface particles on control HepG2 cells. A: Histograms of cell membrane particle size distributions of ultrastructure in Figure 4; B: Statistical analysis of the membrane Rp-v, Rq, Ra and mean Ht of HepG2 cell surface; these values increased as cinobufacini concentration increased (P = 0.000). The data showed that cinobufacini treatment induced rougher cell membranes.

91.35 ± 11.05 nm (F = 23.895, P = 0.000). All these data showed that cinobufacini treatment induced much rougher cell membranes.

DISCUSSION

As a traditional Chinese antineoplastic drug, cinobufacini has been proved to be effective against hepatocarcinoma, and is extensively used clinically[4,7]. Clinical data indicate that total effective rate of cinobufacini against hepatocarcinoma is 44.4%, and cinobufacini can also improve quality of life[12]. However, the mechanism of cinobufacini against hepatocarcinoma has not yet been identified, and especially little is known about its effect on membrane morphology and the mechanism involved. In the present investigation, human HepG2 cells were

treated with different concentrations of cinobufacini for 48 h. AFM was used to visualize cell morphology and membrane ultrastructure, which can show the surface topography of the cell at the nanometer scale. Moreover, MTT assay and FCM were used to analyze cell viability and cell cycle distribution, and LSCM was used to observe the alterations in the cytoskeleton and cell nuclei. Our results demonstrated that cinobufacini could induce cytotoxicity, growth inhibition and S phase arrest in HepG2 cells, which were associated with prominent alterations in cell membrane ultrastructure and cytoskeleton.

MTT assay showed that cinobufacini significantly inhibited the viability of HepG2 cells in a dose-dependent manner. Interruption of the tumor cell cycle so as to inhibit cell growth is the main mechanism of current antineoplastic drugs[13]. Cells are damaged by anti-cancer drugs at different phases of the cell cycle: G1 (growth and preparation of the chromosomes), S (synthesis of DNA), G2 (preparation to divide), and M (cell division). Our study showed that cinobufacini could induce cell cycle arrest at S phase. This observation is consistent with previous studies that showed cinobufacini-induced arrest of several types of human cancer cells in S phase[2,13]. S phase arrest implies that the effects of cinobufacini involve disruption of DNA synthesis and replication, which lead to in inhibition of cell proliferation.

For further investigation of the inhibitory effect of cinobufacini, we observed the alterations in cytoskeleton by staining with FITC-phalloidin and LSCM, and detected the changes in cell membrane ultrastructure by AFM. Immunofluorescence images showed the regular organization of actin filaments in HepG2 cells became chaotic and significantly reduced after treatment with cinobufacini, suggesting that cinobufacini disrupts polymerization of the actin filaments network. It is well known that the cytoskeleton contains three major constitutes: actin microfilaments, intermediate filaments, and microtubules. The cytoskeleton can be remodeled during the cellular processes, including motility, migration, adhesion, and proliferation[14]. Besides, the cytoskeletal network plays vital roles in cell morphology maintenance[2]. It was found that the course of the cell cycle depends on correct cytoskeletal arrangement[15]. As a result, cinobufacini can induce cytoskeletal rearrangement. Moreover, to detect the morphology of cell nuclei, DAPI was used to stain the cells by binding to double-stranded DNA in the nuclei. After treatment with cinobufacini for 48 h, cell nuclei showed shrinkage and chromatin condensation, but not fragmentation, which implied that the nuclear damage was less serious than cytoskeletal damage induced by cinobufacini. Taken together, these data suggest that cinobufacini inhibits the proliferation of HepG2 cells *via* disorganization of the cytoskeleton.

As a nondestructive surface imaging tool, AFM can obtain images of the cell surface at the nanoscale, which can provide us with qualitative and quantitative information on the architecture of cell membranes[10,16]. AFM was widely used in cell imaging, especially in cancer detection[17,18]. It can probe modifications of cell morphology induced by drugs in the imaging mode[19]. The tapping mode of AFM was used to detect the variety of changes in surface morphology and ultrastructure of HepG2 cells treated with different concentrations of cinobufacini. AFM images revealed that cinobufacini could damage the cell membrane in a dose-dependent manner. It appeared to be significant shrinkage and deep pores in the cell membrane, which were similar to the signs of apoptosis[20], especially after treatment with 0.1 mg/mL cinobufacini. With AFM at the subcellular level, we visualized that after treatment with cinobufacini, particles on the cell membrane were bigger than in the control group. It has been reported that the visible protruding particles are clusters of membrane proteins[21], which means that some biological events have occurred, such as opening/closing of ion channels, structural disruption, or changes in the chemical composition of the outer membrane proteins[22]. Changes in cell morphology and ultrastructure are closely related to cell function[23-25]. AFM images provided evidence for the toxic effects of cinobufacini on HepG2 cell membranes, which help us to achieve a better understanding of the mechanism of action of cinobufacini.

In conclusion, the present study demonstrated that cinobufacini inhibited the viability of HepG2 cells and arrested the cell cycle at S phase, which were due to the cytoskeletal destruction and membrane toxicity induced by cinobufacini. These would be the therapeutic targets of cinobufacini.

COMMENTS

Background

Cinobufacini is a traditional Chinese antineoplastic medicine and widely used in clinical cancer therapy in China. As an anti-tumor drug, it has been used in clinical cancer research in recent years. Atomic force microscopy (AFM) is a nondestructive surface imaging tool, which can provide the qualitative and quantitative information on cancer research.

Research frontiers

Cinobufacini has been proven to be effective against a variety of malignant tumor cells, such as breast cancer, lung cancer and hepatocellular carcinoma cells. It has also achieved satisfactory therapeutic results in cancer. Little is known about its anti-tumor mechanisms in the cancer cells. In particular, there are no detailed data on changes in cell membrane morphology and the mechanism involved.

Innovations and breakthroughs

This is believed to be the first study to use AFM to image the changes in cell membrane ultrastructure in HepG2 cells induced by cinobufacini. These AFM images provide evidence for the toxic effects of cinobufacini on the HepG2 cell membrane, which help us to achieve a better understanding of the mechanism of action of cinobufacini.

Applications

This study demonstrated that AFM is a useful tool in discerning and verifying cell response to cinobufacini treatment.

Peer review

This is an original molecular research investigating the possible anti-cancer effect of cinobufacini on a hepatocellular cancer cell line. Previous studies of this traditional Chinese medicine have shown the possible involvement of apoptotic pathways in its anti-cancer effect. Here, the authors' study revealed the morphological changes in cancer cells by AFM after treatment with different

concentrations of cinobufacini. These findings also suggest apoptotic cell death.

REFERENCES

1 **Qi FH**, Li AY, Lv H, Zhao L, Li JJ, Gao B, Tang W. Apoptosis-inducing effect of cinobufacini, Bufo bufo gargarizans Cantor skin extract, on human hepatoma cell line BEL-7402. *Drug Discov Ther* 2008; **2**: 339-343 [PMID: 22504743]

2 **Ma L**, Song B, Jin H, Pi J, Liu L, Jiang J, Cai J. Cinobufacini induced MDA-MB-231 cell apoptosis-associated cell cycle arrest and cytoskeleton function. *Bioorg Med Chem Lett* 2012; **22**: 1459-1463 [PMID: 22225634 DOI: 10.1016/j.bmcl.2011.11.095]

3 **Wang JY**, Chen L, Zheng Z, Wang Q, Guo J, Xu L. Cinobufocini inhibits NF-κB and COX-2 activation induced by TNF-α in lung adenocarcinoma cells. *Oncol Rep* 2012; **27**: 1619-1624 [PMID: 22267101 DOI: 10.3892/or.2012.1647]

4 **Xie RF**, Li ZC, Gao B, Shi ZN, Zhou X. Bufothionine, a possible effective component in cinobufocini injection for hepatocellular carcinoma. *J Ethnopharmacol* 2012; **141**: 692-700 [PMID: 22210051 DOI: 10.1016/j.jep.2011.12.018]

5 **Qin TJ**, Zhao XH, Yun J, Zhang LX, Ruan ZP, Pan BR. Efficacy and safety of gemcitabine-oxaliplatin combined with huachansu in patients with advanced gallbladder carcinoma. *World J Gastroenterol* 2008; **14**: 5210-5216 [PMID: 18777599]

6 **Qi F**, Li A, Zhao L, Xu H, Inagaki Y, Wang D, Cui X, Gao B, Kokudo N, Nakata M, Tang W. Cinobufacini, an aqueous extract from Bufo bufo gargarizans Cantor, induces apoptosis through a mitochondria-mediated pathway in human hepatocellular carcinoma cells. *J Ethnopharmacol* 2010; **128**: 654-661 [PMID: 20193751 DOI: 10.1016/j.jep.2010.02.022]

7 **Meng Z**, Yang P, Shen Y, Bei W, Zhang Y, Ge Y, Newman RA, Cohen L, Liu L, Thornton B, Chang DZ, Liao Z, Kurzrock R. Pilot study of huachansu in patients with hepatocellular carcinoma, nonsmall-cell lung cancer, or pancreatic cancer. *Cancer* 2009; **115**: 5309-5318 [PMID: 19701908 DOI: 10.1002/cncr.24602]

8 **Müller DJ**, Dufrêne YF. Atomic force microscopy: a nanoscopic window on the cell surface. *Trends Cell Biol* 2011; **21**: 461-469 [PMID: 21664134 DOI: 10.1016/j.tcb.2011.04.008]

9 **Kim KS**, Cho CH, Park EK, Jung MH, Yoon KS, Park HK. AFM-detected apoptotic changes in morphology and biophysical property caused by paclitaxel in Ishikawa and HeLa cells. *PLoS One* 2012; **7**: e30066 [PMID: 22272274 DOI: 10.1371/journal.pone.0030066]

10 **Pi J**, Jin H, Liu R, Song B, Wu Q, Liu L, Jiang J, Yang F, Cai H, Cai J. Pathway of cytotoxicity induced by folic acid modified selenium nanoparticles in MCF-7 cells. *Appl Microbiol Biotechnol* 2013; **97**: 1051-1062 [PMID: 22945264 DOI: 10.1007/s00253-012-4359-7]

11 **Ji XL**, Ma YM, Yin T, Shen MS, Xu X, Guan W. Application of atomic force microscopy in blood research. *World J Gastroenterol* 2005; **11**: 1709-1711 [PMID: 15786556]

12 **Sun Y**, Lu XX, Liang XM, Cui XN. The impact of Cinobufacini injection on proliferation and apoptosis of human hepatoma HepG-2 cells. *Zhongde Linchuang Zhongliu Zazhi* 2011; **10**: 27-30

13 **Sun Y**, Lu XX, Liang XM, Cui XN. Impact of Cinobufacini injection on proliferation and cell cycle of human hepatoma HepG-2 cells. *Zhongde Linchuang Zhongliu Zazhi* 2011; **10**: 321-324

14 **Jin H**, Pi J, Huang X, Huang F, Shao W, Li S, Chen Y, Cai J. BMP2 promotes migration and invasion of breast cancer cells via cytoskeletal reorganization and adhesion decrease: an AFM investigation. *Appl Microbiol Biotechnol* 2012; **93**: 1715-1723 [PMID: 22270235 DOI: 10.1007/s00253-011-3865-3]

15 **Jiang J**, Jin H, Liu L, Pi J, Yang F, Cai J. Curcumin disturbed cell-cycle distribution of HepG2 cells via cytoskeletal arrangement. *Scanning* 2013; **35**: 253-260 [PMID: 23070725 DOI: 10.1002/sca.21058]

16 **Shao W**, Jin H, Huang J, Qiu B, Xia R, Deng Z, Cai J, Chen Y. AFM investigation on Ox-LDL-induced changes in cell spreading and cell-surface adhesion property of endothelial cells. *Scanning* 2013; **35**: 119-126 [PMID: 22833475 DOI: 10.1002/sca.21040]

17 **Wang J**, Wan Z, Liu W, Li L, Ren L, Wang X, Sun P, Ren L, Zhao H, Tu Q, Zhang Z, Song N, Zhang L. Atomic force microscope study of tumor cell membranes following treatment with anti-cancer drugs. *Biosens Bioelectron* 2009; **25**: 721-727 [PMID: 19734031 DOI: 10.1016/j.bios.2009.08.011]

18 **Lekka M**, Laidler P. Applicability of AFM in cancer detection. *Nat Nanotechnol* 2009; **4**: 72; author reply 72-73 [PMID: 19197298 DOI: 10.1038/nnano.2009.004]

19 **Pillet F**, Chopinet L, Formosa C, Dague E. Atomic Force Microscopy and pharmacology: from microbiology to cancerology. *Biochim Biophys Acta* 2014; **1840**: 1028-1050 [PMID: 24291690 DOI: 10.1016/j.bbagen.2013.11.019]

20 **Jin H**, Zhong X, Wang Z, Huang X, Ye H, Ma S, Chen Y, Cai J. Sonodynamic effects of hematoporphyrin monomethyl ether on CNE-2 cells detected by atomic force microscopy. *J Cell Biochem* 2011; **112**: 169-178 [PMID: 21053362 DOI: 10.1002/jcb.22912]

21 **Le Grimellec C**, Lesniewska E, Giocondi MC, Finot E, Vié V, Goudonnet JP. Imaging of the surface of living cells by low-force contact-mode atomic force microscopy. *Biophys J* 1998; **75**: 695-703 [PMID: 9675171]

22 **Wang M**, Ruan Y, Chen Q, Li S, Wang Q, Cai J. Curcumin induced HepG2 cell apoptosis-associated mitochondrial membrane potential and intracellular free Ca(2+) concentration. *Eur J Pharmacol* 2011; **650**: 41-47 [PMID: 20883687 DOI: 10.1016/j.ejphar.2010.09.049]

23 **Ke C**, Jin H, Cai J. AFM studied the effect of celastrol on β1 integrin-mediated HUVEC adhesion and migration. *Scanning* 2013; **35**: 316-326 [PMID: 23239560 DOI: 10.1002/sca.21070]

24 **Pan Y**, Wu Q, Liu R, Shao M, Pi J, Zhao X, Qin L. Inhibition effects of gold nanoparticles on proliferation and migration in hepatic carcinoma-conditioned HUVECs. *Bioorg Med Chem Lett* 2014; **24**: 679-684 [PMID: 24365157 DOI: 10.1016/j.bmcl.2013.11.045]

25 **Pan Y**, Wu Q, Qin L, Cai J, Du B. Gold nanoparticles inhibit VEGF165-induced migration and tube formation of endothelial cells via the Akt pathway. *Biomed Res Int* 2014; **2014**: 418624 [PMID: 24987682 DOI: 10.1155/2014/418624]

P- Reviewer: Doganay L, Li ZF **S- Editor**: Qi Y
L- Editor: Wang TQ **E- Editor**: Liu XM

World Journal of Gastroenterology

Submit a Manuscript: http://www.wjgnet.com/esps/
Help Desk: http://www.wjgnet.com/esps/helpdesk.aspx
DOI: 10.3748/wjg.v21.i3.862

World J Gastroenterol 2015 January 21; 21(3): 862-867
ISSN 1007-9327 (print) ISSN 2219-2840 (online)

ORIGINAL ARTICLE

Basic Study

Experimental infection of Z:ZCLA Mongolian gerbils with human hepatitis E virus

Yan Hong, Zhuo-Jing He, Wei Tao, Ting Fu, Yan-Kun Wang, Yong Chen

Yan Hong, Zhuo-Jing He, Wei Tao, Ting Fu, Yan-Kun Wang, Yong Chen, Institute of Bioengineering, Zhejiang Academy of Medical Science, Hangzhou 310013, Zhejiang Province, China

Author contributions: Hong Y, He ZJ, Tao W, Fu T and Chen Y designed the study; Hong Y, He ZJ, Tao W, Fu T and Wang YK performed the experiments; Tao W, Fu T and Wang YK analyzed the data; Hong Y, He ZJ and Chen Y wrote the paper.

Supported by Science Technology Department of Zhejiang Province No. 2011F20015; and Health and Family Planning Commission of Zhejiang Province, No. XKQ-010001.

Correspondence to: Yan Hong, Professor, Institute of Bioengineering, Zhejiang Academy of Medical Science, 182 Tianmushan Road, Xihu District, Hangzhou 310013, Zhejiang Province, China. hongy1008@163.com
Telephone: +86-571-88215588
Fax: +86-571-88215588

Received: May 27, 2014
Peer-review started: May 27, 2014
First decision: June 27, 2014
Revised: July 22, 2014
Accepted: September 5, 2014
Article in press: September 5, 2014
Published online: January 21, 2015

Abstract

AIM: To investigate whether Z:ZCLA Mongolian gerbils are readily susceptible to infection by human hepatitis E virus (HEV).

METHODS: Z:ZCLA Mongolian gerbils were infected with a clinical HEV strain isolated from an acute hepatitis E patient, and virus pathogenesis was assessed in this host. Non-infected gerbils served as the control group. Feces samples from gerbils were collected weekly for reverse transcription-nested polymerase chain reaction. Serum anti-HEV IgG and alanine aminotransferase (ALT) were detected by enzyme linked immunosorbent assay. At sacrifice, each animal's liver, spleen and kidney were collected for histopathologic examination.

RESULTS: HEV-infected gerbils showed fatigue, with histopathological changes observed in the liver, spleen and kidney. HEV RNA was detected in fecal samples taken at day 7 after inoculation and the detectable levels lasted out to day 42 after inoculation. Interestingly, ALT levels were only moderately increased in the HEV-infected animals compared with the non-infected control group.

CONCLUSION: Z:ZCLA Mongolian gerbils are susceptible to human HEV.

Key words: Hepatitis E virus; Mongolian gerbils; Infection; Interspecies transmission; Zoonosis

Core tip: Z:ZCLA Mongolian gerbils were infected with human hepatitis E virus (HEV). Feces samples from gerbils were collected weekly for reverse transcription-nested polymerase chain reaction. Serum anti-HEV IgG and alanine aminotransferase (ALT) detection was carried out by enzyme linked immunosorbent assay. At sacrifice, liver, spleen and kidney were collected from infected animals and non-infected controls for histopathologic examination. Detectable HEV RNA in fecal samples appeared at post-inoculation day 7 and persisted through day 42. Interestingly, ALT levels were only moderately increased in infected animals compared with control animals. These findings indicate

that Z:ZCLA Mongolian gerbils are susceptible to human HEV.

Hong Y, He ZJ, Tao W, Fu T, Wang YK, Chen Y. Experimental infection of Z:ZCLA Mongolian gerbils with human hepatitis E virus. *World J Gastroenterol* 2015; 21(3): 862-867 Available from: URL: http://www.wjgnet.com/1007-9327/full/v21/i3/862.htm DOI: http://dx.doi.org/10.3748/wjg.v21.i3.862

INTRODUCTION

Hepatitis E virus (HEV) infection is a significant public health problem in many developing countries, causing large outbreaks of acute hepatitis. It is known that HEV transmission occurs primarily by the fecal-oral route, mainly through contaminated drinking water in areas with poor sanitation. However, hepatitis E has recently been diagnosed with increasing frequency in industrialized countries[1], and seroreactivity is observed in 5% to 21% of asymptomatic individuals[2].

Interestingly, antibodies to HEV have been detected in a wide range of domestic and feral mammals, and HEV RNA has been isolated from pig[3-5], deer[6], wild boar[7], rodents[8-10] and chickens[11]. The prevalence of HEV-specific antibodies in wild rodents is well documented[12-15], and HEV was recently isolated from rats trapped in several cities of industrialized countries[8]. Thus, it is important to assess whether rodents constitute a potential source of human HEV infection. Wild gerbils, commonly known as midday jird [*Meriones meridianus* (*M. meridianus*)], have been experimentally infected with human HEV, and lesions similar to those found in human hepatitis E patients were observed[16]. However, *M. meridianus* is not a breeding species and the animal's biological characteristics are unknown. Other studies have reported the transmission of HEV from swine feces in southern China to the Mongolian gerbil *M. unguiculatus*, which serves as an animal model for a wide range of diseases[17].

The Z:ZCLA Mongolian gerbil (*M. unguiculatus*) is a relatively new laboratory stock, domesticated by Zhejiang Experimental Animal Center, a branch of our institution. The animals originated from Inner Mongolia of China and have been artificially propagated for more than 30 years. So far, the gerbils have been bred for 46 generations and systematically characterized for basic biological attributes. The aim of the present study was to assess whether the Z:ZCLA Mongolian gerbils are readily susceptible to infection by human HEV.

MATERIALS AND METHODS

Virus

A clinical strain of HEV was isolated from a fecal sample of an acute hepatitis E patient (Hangzhou, China). A 221-nt product was amplified from the fecal sample by reverse transcription-nested polymerase chain reaction (RT-nPCR) and directly sequenced to yield the consensus sequence. The virus sequence showed 99% homology with the Xinjiang strain D11092 (genotype 1). For virus preparation, 5 g of the patient's feces were resuspended in phosphate-buffered saline (PBS, pH 7.4) containing 0.01% diethyl pyrocarbonate (DEPC), at a proportion of 10% (w/v). After centrifugation of the suspension at 12000 × g for 20 min, the resulting supernatant was filtered sequentially through 0.45 and 0.22 μm filters before inoculation. The viruses were inoculated into each gerbil at a minimum viral count of 5.5×10^2/mL of feces supernatant, as calculated by viral genomic titer determined by real-time reverse quantitative PCR.

Animals and infection

Twenty-one specific pathogen-free male Z:ZCLA Mongolian gerbils with an average body mass of 40 ± 5 g (approximately 5 wk of age) were provided by the Experimental Animal Center at the Zhejiang Academy of Medical Sciences (China) and maintained in a pathogen-free animal facility. Adequate measures were taken to minimize animal discomfort. All procedures involving animals in this study were approved by the local committee of Animal Use and Protection.

Gerbils were divided into two groups, with 14 in the virus infection group and 7 in the control group. The day before infection, each gerbil was injected with 6×10^4-8×10^4 units of penicillin intraperitoneally. The infection group was inoculated intraperitoneally with 100 μL of the virus suspension described above. Gerbils in the control group were inoculated with 100 μL PBS. All animals were provided with food and water *ad libitum* during the 7-wk study course. Fecal samples were collected each week post-inoculation and stored at -20 ℃ until use. Two gerbils from the infection group and 1 from the control group were humanely euthanized each week post-inoculation. Serum was obtained from blood samples collected weekly and stored at -20 ℃. Liver, spleen and kidney were fixed in 10% neutral buffered formalin immediately upon sampling for subsequent histopathologic examination.

Serologic tests

Serum specimens were assessed for IgG antibodies to HEV by using a commercial enzyme-linked immunosorbent assay (ELISA) kit (Wantai Biological Pharmacy Co., Beijing, China), according to the manufacturer's instructions. The absorbance was determined at 450 nm (Multiscan MCC microplate reader; Titertek Instruments, Huntsville, AL, United States).

ALT levels were detected in serum samples with an automated biochemistry analyzer (AU2700 chemistry immune-analyzer; Olympus, Tokyo, Japan).

Histopathological studies

For histological studies, fixed tissues (liver, spleen, and kidney) were dehydrated with increasing concentrations

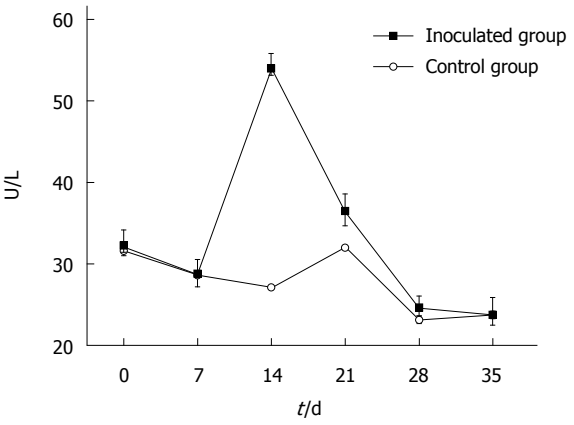

Figure 1 Changes in alanine aminotransferase levels after hepatitis E virus infection. Z:ZCLA Mongolian gerbils showed alanine aminotransferase (ALT) level changes upon hepatitis E virus infection. The ALT levels were moderately increased in the inoculated group compared with the control group at days 14 and 21 post-inoculation. No changes were observed in the control group.

Table 1 Hepatitis E virus RNA-positive rate in experimental and control Mongolian gerbils

	Post-inoculation day							
Group	0	7	14	21	28	35	42	49
HEV-inoculated	0/14	5/14	10/12	10/10	8/8	6/6	1/4	0/2
Control	0/7	0/7	0/6	0/5	0/4	0/3	0/2	0/1

The viral shedding in feces was detected by reverse transcription-nested polymerase chain reaction. HEV: Hepatitis E virus.

of ethanol and embedded in paraffin according to standard laboratory procedures. Tissues were cut into 7 μm sections and stained with hematoxylin and eosin for histological evaluation. Observation was carried out on an Olympus CX41 microscope.

RNA extraction and RT-nPCR

Total RNA was extracted from the 10% fecal supernatants. After centrifugation of the suspensions at 12000 × g for 15 min, the resulting supernatant was mixed with 10% PEG 6000 (w/v) and 2.3% NaCl (w/v), and stored at 4 ℃ overnight. The solution was centrifuged at 12000 × g for 20 min the following day. Total RNA was extracted from the sediment by the TRIzol reagent (Invitrogen, Carlsbad, CA, United States), according to the manufacturer's instructions, and dissolved in 20 μL ribonuclease (RNase)-free water. Reverse transcription was performed using a commercially available Primescript first-strand cDNA synthesis kit (TaKaRa, Dalian, China) following the manufacturer's instructions. The resulting cDNA was amplified by nested PCR using primers based on sequences of the open reading frame 2 (5123-7105 nt) of the Chinese HEV isolate (sites based on L08816.1)[18]. The external forward primer (6272-6294 nt, PCR1) was 5'-CCGACAGAATTGATTTCGTCGGC-3' and the reverse primer (6579-6557 nt, PCR4) was 5'-CCGTAAGTGGACTGGTCATACTC-3'; the internal forward primer (6323-6345 nt, PCR2) was 5'-GTCGTCTCAGCCAATGGCGAGCC-3', and the reverse primer (6521-6543 nt, PCR3) was 5'-GAAAGCCAAAGCACATCATTAGC-3'. The RT-nPCR product was expected to be 221 base pairs. The first round PCR was set up at 94 ℃ for 5 min, followed by 33 cycles of 94 ℃ for 30 s, 55 ℃ for 30 s and 72 ℃ for 10 min. The second round PCR protocol was the same as the first one except that the melting temperature of 57 ℃ was used. The PCR products were assessed by electrophoresis on 1% agarose gel. A negative control (water only) was included, and the PCR products were identified by sequencing to exclude the possibility of contamination and failure of amplification.

RESULTS

Clinical evaluation

The HEV-infected gerbils showed fatigue and loose hair. As expected, no evidence of clinical disease was observed in the control gerbils.

Serological analysis

Serum specimens were examined using an automatic biochemical analyzer to determine serum ALT levels. As shown in Figure 1, ALT levels were moderately increased in gerbils infected with HEV, compared with control animals, at days 14 and 21 post-inoculation. Assays were performed in triplicate and data expressed as mean ± SD. In addition, serum anti-HEV antibodies were assessed in HEV-inoculated and non-inoculated groups by ELISA, and no anti-HEV IgG was detected in either group.

Detection of HEV RNA by RT-nPCR

Viral shedding in feces was detected intermittently by RT-nPCR, beginning at day 7 post-inoculation for all infected gerbils. Indeed, correct sized PCR products were detected by electrophoresis on a 1% agarose gel, which showed a 221 bp DNA fragment (Figure 2). The fecal excretion of HEV lasted for 42 d post-inoculation. All data obtained for the 7-wk experimental period are summarized in Table 1.

Histopathologic examination

To determine whether gerbils responded to the HEV-containing inoculum with histopathologic signs of injury, tissues (liver, spleen and kidney) from inoculated and control gerbils were sectioned, stained, and examined by light microscopy. We observed changes attributable to inoculation in the liver, spleen and kidney. Hepatic inflammation and focal hepatocellular necrosis were observed in inoculated gerbils. In addition, mixed infiltration of lymphocytes and eosinophils in the portal tracts was observed (Figure 3A). Enlarged splenocytes and multiple vacuolar degeneration were observed in the spleens of inoculated gerbils (Figure 3B). Moreover,

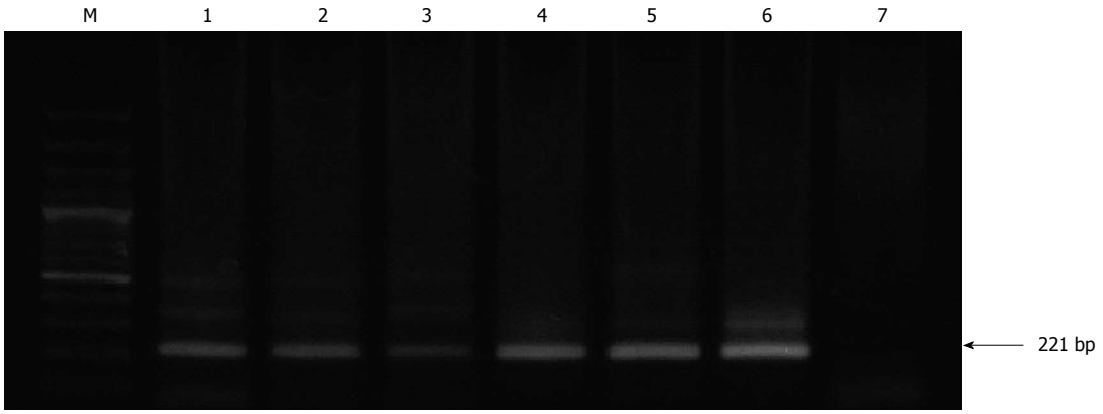

Figure 2 Reverse transcription-nested polymerase chain reaction detection of viral shedding in feces. Hepatitis E virus RNA was detected by reverse transcription-nested polymerase chain reaction (RT-nPCR) in feces from all inoculated gerbils. Lane M: DNA marker; Lanes 1-6 represent experimental time points (in weeks): the second round PCR products of gerbil feces samples on intermittent days; Lane 7: a negative control containing water.

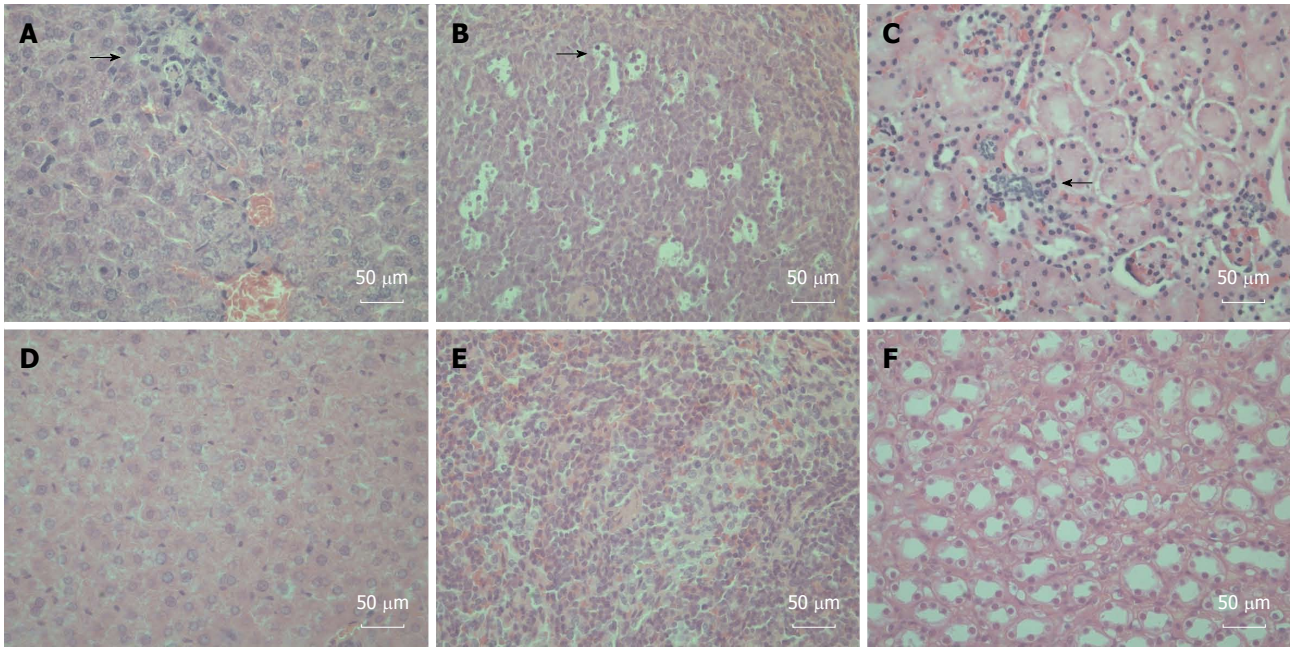

Figure 3 Histopathologic changes in the hepatitis E virus-inoculated Mongolian gerbils. A: A representative liver sample showing slight histiocytic hepatitis and focal accumulation of inflammatory cells surrounding hepatocytes [21 d post-inoculation (DPI)]; B: A representative spleen sample showing ruptured and enlarged splenocytes with multiple vacuolar degeneration (21 DPI); C: A representative kidney showing disarranged kidney cells with increased infiltrating lymphocytes and macrophages (35 DPI); D: A representative negative control liver; E: A representative negative control spleen; F: A representative Negative control kidney. All tissues were stained with hematoxylin and eosin. Original magnifications × 400.

increased lymphocyte and macrophage infiltration was observed in renal tissues after HEV infection (Figure 3C). Of note, no damage was observed in any tissue from control animals (Figure 3D-F).

DISCUSSION

Hepatitis E genotype 1 is an infectious agent, which causes a disease considered to be endemic in developing countries, due to poor sanitary conditions. However, recent reports have drawn attention to hepatitis E appearance in developed countries; the most recent survey showed that 21% of United States' residents are seropositive for anti-HEV IgG[19]. Although some research assays could yield "false-positive" results, with controversy surrounding current enzyme immunoassays used for HEV detection[2], more thorough HEV studies are urgently needed.

HEV infection is described as a disease transmitted primarily *via* the fecal-oral route through contaminated drinking water[20]. In addition, wild or domestic swine consumption probably plays an important role in the occurrence of hepatitis E genotype 3 or 4[21,22]. However, as evidences began to accumulate, recent investigations suggested the possibility of other modes of transmission. It was reported that HEV can be transmitted from person to person[23], despite the fact that HEV presence in stool

is acknowledged as a major source of transmission by contact exposure to other animals[24]. Because rodents and humans often share the environment, especially in inner cities, there is a possibility for rodents to come in contact with human feces. Therefore, rodents are particularly interesting as a potential source of human HEV infections.

Currently, the Mongolian gerbil is a used widely model animal for scientific studies. However, the Z:ZCLA Mongolian gerbil is a relatively new closed colony, of which ancestors were obtained in Inner Mongolia of China by the Zhejiang Experimental Animal Center in 1978. This population has stable biological characteristics, and lives longer than other Mongolian gerbil populations in China. Moreover, these animals have been used in investigations in multiple fields: parasitology, cerebral hemorrhage, virology, bacteriology, lipometabolism, and carbohydrate metabolism. The results presented here suggest that Z:ZCLA Mongolian gerbils are susceptible to human HEV, as evidenced by clinical signs of HEV infection, changes in serum ALT levels, fecal viral shedding, and lesions of organs, including liver, spleen and kidney. As shown above, fecal virus shedding was detected at day 7 post-inoculation and lasted for 5 wk. Similar findings were previously described by Li *et al*[25], who detected HEV RNA in fecal excretions obtained from gerbils inoculated with swine HEV at 3-4 wk post-inoculation. With the large number of rodents in large cities, HEV can be spread easily and for a long time through rat feces; therefore, the effects of HEV *via* the fecal-oral route are difficult to predict.

During the experimental infection course of the current study, no anti-HEV antibodies were detected in the inoculated gerbils. Similar to a previous study, in which Wistar rats were infected with human HEV, seroconversion could not be detected out to the experiment-end day 35 of post-inoculation[26]. In another study, gerbils infected with swine HEV produced anti-HEV antibodies at 49 d after inoculation, with noticeably lower optical density values than the positive control[25]. Therefore, the magnitude of rat viremia might be reduced in comparison to that of other inoculated mammals.

The results presented here indicate that Z:ZCLA Mongolian gerbils could be experimentally infected by human HEV; therefore, this rodent should be considered a helpful animal model for HEV studies. Specifically, it might be used to further describe the mechanism of HEV interspecies transmission. In addition, rodent control in inner cities may help prevent HEV transmission.

COMMENTS

Background

Hepatitis E virus (HEV) infection is a significant public health problem in many developing countries, causing large outbreaks of acute hepatitis. However, in industrialized countries, hepatitis E has recently been diagnosed with increasing frequency as a cause of sporadic hepatitis, and seroreactivity has been recorded frequently in asymptomatic persons. Because antibodies to HEV have been detected in a wide range of domestic and feral mammals, and HEV RNA has been recently isolated from rats trapped in several cities in industrialized countries, it is important to understand whether rodents are a potential source of human HEV infection.

Research frontiers

HEV infection is known as a disease transmitted primarily *via* the fecal-oral route through contaminated drinking water. However, recent investigations have suggested the possibility of other modes of transmission. It was reported that HEV can be transmitted from person to person despite the fact that HEV presence in stool is a major source of transmission by contact exposure to other animals. Because rodents and humans often share the environment, especially in inner cities, rodents could come in contact with human feces easily. Therefore, rodents are particularly interesting as a potential source of human HEV infections.

Innovations and breakthroughs

It has been shown that wild gerbils, commonly known as midday jird [*Meriones meridianus* (*M. meridianus*)], can be experimentally infected by human HEV and present with lesions similar to those found in human hepatitis E patients. However, *M. meridianus* is not a breeding species and their biological characteristics are unknown. Other studies have reported the transmission of HEV from swine feces to the Mongolian gerbil (*Meriones unguiculatus*), which serves as an animal model for a wide range of diseases. The Z:ZCLA Mongolian gerbil (*M. unguiculatus*) is a relatively new laboratory stock, domesticated by the Zhejiang Experimental Animal Center, a branch of our institution. The animals originated from Inner Mongolia of China, and have been artificially propagated for more than 30 years. So far, the gerbils have been bred for 46 generations and their basic biological characteristics have been systematically described. The aim of the present study was to investigate whether Z:ZCLA Mongolian gerbils are readily susceptible to infection with human HEV.

Applications

The study results suggest that Z:ZCLA Mongolian gerbils could be experimentally infected by human HEV; therefore, *M. unguiculatus* should be considered a helpful animal model for HEV studies. Specifically, it can be used to further describe the mechanism of HEV interspecies transmission.

Terminology

HEV is an emerging pathogen and the most common cause of acute viral hepatitis worldwide.

Peer review

This manuscript comprises the experimental infection of a novel laboratory stock of Mongolian gerbils with a clinical strain of human HEV. Apart from the introduction of an animal model for HEV (interspecies) infection, the authors raise the question about the influence of rodents on HEV transmission to humans.

REFERENCES

1 **Purcell RH**, Emerson SU. Hepatitis E virus. In: Knipe, DM, Howley PM, eds. Fields virology. 4th ed. Philadelphia: Lippincott Williams & Wilkins, 2001: 3051-3061

2 **Teshale EH**, Hu DJ, Holmberg SD. The two faces of hepatitis E virus. *Clin Infect Dis* 2010; **51**: 328-334 [PMID: 20572761 DOI: 10.1086/653943]

3 **van der Poel WH**, Verschoor F, van der Heide R, Herrera MI, Vivo A, Kooreman M, de Roda Husman AM. Hepatitis E virus sequences in swine related to sequences in humans, The Netherlands. *Emerg Infect Dis* 2001; **7**: 970-976 [PMID: 11747723 DOI: 10.3201/eid0706.010608]

4 **Huang FF**, Haqshenas G, Guenette DK, Halbur PG, Schommer SK, Pierson FW, Toth TE, Meng XJ. Detection by reverse transcription-PCR and genetic characterization of field isolates of swine hepatitis E virus from pigs in different geographic regions of the United States. *J Clin Microbiol* 2002; **40**: 1326-1332 [PMID: 11923352 DOI: 10.1128/JCM.40.4.1326-1332.2002]

5 **Pei Y**, Yoo D. Genetic characterization and sequence heterogeneity of a canadian isolate of Swine hepatitis E virus. *J Clin Microbiol* 2002; **40**: 4021-4029 [PMID: 12409369 DOI: 10.1128/JCM.40.11.4021-4029.2002]

6 **Tei S**, Kitajima N, Takahashi K, Mishiro S. Zoonotic transmission of hepatitis E virus from deer to human beings. *Lancet* 2003; **362**: 371-373 [PMID: 12907011 DOI: 10.1016/

S0140-6736(03)14025-1]
7 **Takahashi K**, Kitajima N, Abe N, Mishiro S. Complete or near-complete nucleotide sequences of hepatitis E virus genome recovered from a wild boar, a deer, and four patients who ate the deer. *Virology* 2004; **330**: 501-505 [PMID: 15567444 DOI: 10.1016/j.virol.2004.10.006]
8 **Purcell RH**, Engle RE, Rood MP, Kabrane-Lazizi Y, Nguyen HT, Govindarajan S, St Claire M, Emerson SU. Hepatitis E virus in rats, Los Angeles, California, USA. *Emerg Infect Dis* 2011; **17**: 2216-2222 [PMID: 22172320 DOI: 10.3201/eid1712.110482]
9 **Johne R**, Plenge-Bönig A, Hess M, Ulrich RG, Reetz J, Schielke A. Detection of a novel hepatitis E-like virus in faeces of wild rats using a nested broad-spectrum RT-PCR. *J Gen Virol* 2010; **91**: 750-758 [PMID: 19889929 DOI: 10.1099/vir.0.016584-0]
10 **Kanai Y**, Miyasaka S, Uyama S, Kawami S, Kato-Mori Y, Tsujikawa M, Yunoki M, Nishiyama S, Ikuta K, Hagiwara K. Hepatitis E virus in Norway rats (Rattus norvegicus) captured around a pig farm. *BMC Res Notes* 2012; **5**: 4 [PMID: 22217009 DOI: 10.1186/1756-0500-5-4]
11 **Huang FF**, Sun ZF, Emerson SU, Purcell RH, Shivaprasad HL, Pierson FW, Toth TE, Meng XJ. Determination and analysis of the complete genomic sequence of avian hepatitis E virus (avian HEV) and attempts to infect rhesus monkeys with avian HEV. *J Gen Virol* 2004; **85**: 1609-1618 [PMID: 15166445 DOI: 10.1099/vir.0.79841-0]
12 **Arankalle VA**, Joshi MV, Kulkarni AM, Gandhe SS, Chobe LP, Rautmare SS, Mishra AC, Padbidri VS. Prevalence of anti-hepatitis E virus antibodies in different Indian animal species. *J Viral Hepat* 2001; **8**: 223-227 [PMID: 11380801 DOI: 10.1046/j.1365-2893.2001.00290.x]
13 **Hirano M**, Ding X, Li TC, Takeda N, Kawabata H, Koizumi N, Kadosaka T, Goto I, Masuzawa T, Nakamura M, Taira K, Kuroki T, Tanikawa T, Watanabe H, Abe K. Evidence for widespread infection of hepatitis E virus among wild rats in Japan. *Hepatol Res* 2003; **27**: 1-5 [PMID: 12957199 DOI: 10.1016/S1386-6346(03)00192-X]
14 **Favorov MO**, Kosoy MY, Tsarev SA, Childs JE, Margolis HS. Prevalence of antibody to hepatitis E virus among rodents in the United States. *J Infect Dis* 2000; **181**: 449-455 [PMID: 10669325 DOI: 10.1086/315273]
15 **Vitral CL**, Pinto MA, Lewis-Ximenez LL, Khudyakov YE, dos Santos DR, Gaspar AM. Serological evidence of hepatitis E virus infection in different animal species from the Southeast of Brazil. *Mem Inst Oswaldo Cruz* 2005; **100**: 117-122 [PMID: 16021297 DOI: 10.1590/S0074-02762005000200003]
16 **Zhao SY**, Liao LF, Zou LY, Yu ZY. Study of experiment on HEV infection in Gerbil (Merionesmeridianus) from generation to generation. *Zhongguo Meijie Shengwuxue and Kongzhi Zazhi* 2001; **12**: 215-218
17 **Gaucher D**, Chadee K. Molecular cloning and expression of gerbil granulocyte/macrophage colony-stimulating factor. *Gene* 2002; **294**: 233-238 [PMID: 12234685 DOI: 10.1016/S0378-1119(02)00795-3]
18 **Bi SL**, Purdy MA, McCaustland KA, Margolis HS, Bradley DW. The sequence of hepatitis E virus isolated directly from a single source during an outbreak in China. *Virus Res* 1993; **28**: 233-247 [PMID: 8346669 DOI: 10.1016/0168-1702(93)90024-H]
19 **Kuniholm MH**, Purcell RH, McQuillan GM, Engle RE, Wasley A, Nelson KE. Epidemiology of hepatitis E virus in the United States: results from the Third National Health and Nutrition Examination Survey, 1988-1994. *J Infect Dis* 2009; **200**: 48-56 [PMID: 19473098 DOI: 10.1086/599319]
20 **Balayan MS**, Andjaparidze AG, Savinskaya SS, Ketiladze ES, Braginsky DM, Savinov AP, Poleschuk VF. Evidence for a virus in non-A, non-B hepatitis transmitted via the fecal-oral route. *Intervirology* 1983; **20**: 23-31 [PMID: 6409836 DOI: 10.1159/000149370]
21 **Li TC**, Chijiwa K, Sera N, Ishibashi T, Etoh Y, Shinohara Y, Kurata Y, Ishida M, Sakamoto S, Takeda N, Miyamura T. Hepatitis E virus transmission from wild boar meat. *Emerg Infect Dis* 2005; **11**: 1958-1960 [PMID: 16485490 DOI: 10.3201/eid1112.051041]
22 **Mizuo H**, Yazaki Y, Sugawara K, Tsuda F, Takahashi M, Nishizawa T, Okamoto H. Possible risk factors for the transmission of hepatitis E virus and for the severe form of hepatitis E acquired locally in Hokkaido, Japan. *J Med Virol* 2005; **76**: 341-349 [PMID: 15902701 DOI: 10.1002/jmv.20364]
23 **Teshale EH**, Grytdal SP, Howard C, Barry V, Kamili S, Drobeniuc J, Hill VR, Okware S, Hu DJ, Holmberg SD. Evidence of person-to-person transmission of hepatitis E virus during a large outbreak in Northern Uganda. *Clin Infect Dis* 2010; **50**: 1006-1010 [PMID: 20178415 DOI: 10.1086/651077]
24 **Huang F**, Zhang W, Gong G, Yuan C, Yan Y, Yang S, Cui L, Zhu J, Yang Z, Hua X. Experimental infection of Balb/c nude mice with Hepatitis E virus. *BMC Infect Dis* 2009; **9**: 93 [PMID: 19523236 DOI: 10.1186/1471-2334-9-93]
25 **Li W**, Sun Q, She R, Wang D, Duan X, Yin J, Ding Y. Experimental infection of Mongolian gerbils by a genotype 4 strain of swine hepatitis E virus. *J Med Virol* 2009; **81**: 1591-1596 [PMID: 19623666 DOI: 10.1002/jmv.21573]
26 **Maneerat Y**, Clayson ET, Myint KS, Young GD, Innis BL. Experimental infection of the laboratory rat with the hepatitis E virus. *J Med Virol* 1996; **48**: 121-128 [PMID: 8835343]

P- Reviewer: Kim SR **S- Editor**: Ma YJ
L- Editor: AmEditor **E- Editor**: Liu XM

World Journal of Gastroenterology

Submit a Manuscript: http://www.wjgnet.com/esps/
Help Desk: http://www.wjgnet.com/esps/helpdesk.aspx
DOI: 10.3748/wjg.v21.i3.868

World J Gastroenterol 2015 January 21; 21(3): 868-877
ISSN 1007-9327 (print) ISSN 2219-2840 (online)

ORIGINAL ARTICLE

Basic Study

NOB1 is essential for the survival of RKO colorectal cancer cells

Xiao-Wen He, Tao Feng, Qiao-Ling Yin, Yuan-Wei Jian, Ting Liu

Xiao-Wen He, Tao Feng, Qiao-Ling Yin, Department of General Surgery, Shaoxing People's Hospital, Shaoxing Hospital of Zheijiang University, Shaoxing 312000, Zhejiang Province, China
Yuan-Wei Jian, Ting Liu, Department of Gastroenterology, Xiangya Hospital of Central South University, Changsha 410008, Hunan Province, China
Author contributions: He XW and Feng T developed the concept and design of the research; Jian YW and Liu T analyzed the data; and Yin QL wrote the manuscript.
Supported by National Natural Science Foundation of China, No. 81272735; Class A Medical and Health Technology Program Project from Zhejiang Province, No. 2010KY178; and the Science and Technology Department of Hunan Province, No. 2010Ck3013.

Correspondence to: Ting Liu, PhD, Department of Gastroenterology, Xiangya Hospital of Central South University, 87 Xiangya Road, Changsha 410008, Hunan Province, China. liuting818@126.com
Telephone: +86-731-89753023
Fax: +86-731-89753723
Received: March 1, 2014
Peer-review started: March 5, 2014
First decision: March 27, 2014
Revised: June 13, 2014
Accepted: July 22, 2014
Article in press: July 22, 2014
Published online: January 21, 2015

Abstract

AIM: To determine the role of NOB1, a regulator of cell survival in yeast, in human colorectal cancer cells.

METHODS: Lentivirus-mediated small interfering RNA (siRNA) was used to inhibit NOB1 expression in RKO human colorectal cancer cells *in vitro* and *in vivo* in a mouse xenograft model. The *in vitro* and *in vivo* knockdown efficacy was determined using both Western blot and quantitative reverse transcription polymerase chain reaction (qRT-PCR). qRT-PCR was also used to analyze the downstream signals following NOB1 knockdown. Cell growth and colony formation assays were used to determine the effect of NOB1 inhibition on RKO proliferation and their ability to form colonies. Endonuclease activity, as evaluated by terminal deoxytransferase-mediated dUTP nick end labeling (TUNEL), and annexin V staining were used to determine the presence of apoptotic cell death prior to and following NOB1 inhibition. Cell cycle analysis was used to determine the effect of NOB1 inhibition on RKO cell cycle. A cDNA microarray was used to determine global differential gene expression following NOB1 knockdown.

RESULTS: Virus-mediated siRNA inhibition of NOB1 resulted in (1) the down-regulation of NOB1 expression in RKO cells for both the mRNA and protein; (2) inhibition of NOB1 expression both *in vitro* and *in vivo* experimental systems; (3) cell growth inhibition *via* significant induction of cell apoptosis, without alteration of the cell cycle distribution; and (4) a significant decrease in the average weight and volume of xenograft tumors in the NOB1-siRNA group compared to the control scr-siRNA group ($P = 0.001$, $P < 0.05$). Significantly more apoptosis was detected within tumors in the NOB1-siRNA group than in the control group. Microarray analysis detected 2336 genes potentially regulated by NOB1. Most of these genes are associated with the WNT, cell proliferation, apoptosis, fibroblast growth factor, and angiogenesis signaling pathways, of which BAX and WNT were validated by qRT-PCR. Among them, 1451 probes, representing 963 unique genes, were upregulated; however, 2308 probes,

representing 1373 unique genes, were downregulated.

CONCLUSION: *NOB1* gene silencing by lentivirus-mediated RNA interference can inhibit tumor growth by inducing apoptosis of cancerous human colorectal cells.

Key words: NOB1; Small RNA interference; Apoptosis; Colorectal cancer; BAX; WNT

Core tip: NOB1, a critically important regulator in yeast, is also required for regulation of cell growth and survival in RKO human colorectal cancer cells. NOB1 knockdown promotes cell apoptosis in both *in vitro* and *in vivo* model systems. The gene expression profile suggests the importance of the WNT pathway, cell proliferation, apoptosis, the fibroblast growth factor, and angiogenesis signaling pathways in the function of NOB1.

He XW, Feng T, Yin QL, Jian YW, Liu T. NOB1 is essential for the survival of RKO colorectal cancer cells. *World J Gastroenterol* 2015; 21(3): 868-877 Available from: URL: http://www.wjgnet.com/1007-9327/full/v21/i3/868.htm DOI: http://dx.doi.org/10.3748/wjg.v21.i3.868

INTRODUCTION

Colorectal cancer (CRC), one of the most common malignancies worldwide, and is the result of a multi-step and multi-mechanistic process. Abnormalities in apoptotic function have been shown to contribute to both CRC pathogenesis as well as its resistance to chemotherapeutic drugs and radiotherapy[1-3]. Understanding the molecular and cellular mechanisms which contribute to the carcinogenesis and CRC development could facilitate diagnosis and treatment of the disease.

The proteasome, a highly selective proteinase complex, is considered a promising therapeutic target for CRC treatment[4,5]. The proteasome is required for the degradation of many endogenous proteins, including transcriptional factors, cyclins, and tumor suppressors[6-9]. The proteasome 19S regulatory particle (RP) recognizes and degrades ubiquitin-marked proteins[10]. The ubiquitin-proteasome system, one of the most important intracellular degradative pathways, plays a critical role in the regulation of various cellular processes, such as cell cycle progression, differentiation, apoptosis, and angiogenesis[11].

Ribosome biogenesis, a high-energy and essential process, plays a crucial role in cell growth, proliferation, and differentiation[12,13]. The rate of ribosomal processing is highly in tune with extracellular growth signals[14], and is, therefore, tightly coordinated with cell growth and proliferation. An emerging line of evidence suggests that altered ribosome biogenesis may be associated with tumorigenesis[15-17].

The human *NOB1* gene encodes a putative protein with a PIN (PilT amino terminus) domain and a zinc ribbon domain[18]. The yeast Nob1p (Nin one binding protein) is required for 26S proteasome function and ribosome biogenesis. Nob1p has an endonuclease-containing PIN domain responsible for cleavage of the 20S pre-rRNA at site D generating the mature 18S-rRNA[19-22]. Granneman *et al*[22] was able to show the importance of RNA restructuring and protein remodeling in the 3' region of the 18S rRNA in the Nob1p-dependent cleavage at site D. In addition, using a two-hybrid screen, Nob1p was identified as a protein interacting with Nin1p/Rpn12p (a subunit of the 19S RP of the yeast 26S proteasome)[23,24]. The interaction between Nob1p and 19S RP subunit appears to be crucial for the maturation of the 20S RP[24]. Thus, the human NOB1 might also be involved in ribosome biogenesis and 26S proteasome function in the nucleus[20], and play an important role in cell growth and proliferation.

A recent study indicated that NOB1 RNA interference inhibits human ovarian cancer cell growth through G_0/G_1 arrest[25]. However, the NOB1 potential role in colorectal cancer has not been demonstrated. A recent study, using immunohistochemistry to determine the expression of NOB1, found that NOB1 was up-regulated in 60 colorectal cancer tissues[26]. RKO, a well-established poorly differentiated human colon carcinoma cell line with wild-type *p53*, is used as the model for studying *NOB1* gene due to the relatively short doubling time and established genetic profile of the cell line. Lentiviral-mediated small interfering RNA (siRNA) was used to inhibit NOB1 expression and investigate the effects of NOB1 knockdown on cell proliferation, cell cycle progression, and apoptosis in RKO. Microarray and qPCR were used to detect and validate NOB1-targeted genes and pathways in colorectal cancer. Herein, a specific downregulation of NOB1 inhibited RKO cell proliferation by inducing cell apoptosis, but not cell cycle arrest. Therefore, NOB1 may serve as a therapeutic target for CRC.

MATERIALS AND METHODS

Reagents and antibodies

RPMI 1640, fetal bovine serum (FBS), Trizol Reagent, and Lipofectamine 2000 were purchased from Invitrogen (Carlsbad, CA, United States). Propidium iodide (PI) was obtained from Sigma-Aldrich (St. Louis, MO, United States). RNase A was from MBI Fermentas (St. Leon-Rot, Germany). The Annexin V-APC Apoptosis Detection Kit was acquired from eBioscience (San Diego, CA, United States). The bicinchoninic acid (BCA) protein assay was purchased from HyClone-Pierce (South Logan, UT, United States). M-MLV Reverse Transcriptase was bought from Promega (Madison, WI, United States).

Oligo-dT was procured from Sangon Biotech (Shanghai, China). SYBR Green Master Mixture was purchased from Takara (Otsu, Japan). pGCSIL-green fluorescent protein (GFP), vector and virion-packaging elements (pHelper 1.0 and pHelper 2.0) were obtained from Genechem (Shanghai, China). Rabbit anti-NOB1 polyclonal antibody was bought from either Abcam (Cambridge, MA, United States) or ProteinTech Group (Chicago, IL, United States). Mouse anti-glyceraldehyde-3-phosphate dehydrogenase (GAPDH), goat anti-rabbit IgG, and goat anti-mouse IgG were from Santa Cruz Biotechnology (Santa Cruz, CA, United States). All other chemicals were of analytical grade.

siRNA construction and lentivirus production

Previously described methods, with minimal modifications, were used to construct siRNA and to produce lentivirus[27]. A 19-nucleotide (CCTGGAGCCAATCTTCAAGAA) siRNA was designed against the human NOB1 mRNA (GenBank accession number NM_014062). In the experiment, siRNA with a scrambled sequence (scr-siRNA; TTCTCCGAACGTGTCACGT) was used as a negative control. siRNAs were synthesized and inserted between the *Age*I and *Eco*RI restriction sites of the pGCSIL-GFP plasmid. The correct siRNA insertion was confirmed by restriction mapping and direct DNA sequencing.

Using Lipofectamine 2000, a recombinant lentiviral vector, pGCSIL-GFP, with pHelper 1.0 [encoding human immunodeficiency virus (HIV) gag, pol, and rev] and pHelper 2.0 (encoding for the VSV-G envelope) was used to co-transfect 293T cells, according to the manufacturer's instructions. Infectious lentivirus was harvested at 48 h post-transfection, centrifuged to remove cell debris, and then filtered through a 0.45 μm cellulose acetate filter.

Cell culture and infection

The RKO (human colorectal cancer) cell line, purchased from the American Type Culture Collection (ATCC, Manassas, VA, United States), was maintained in RPMI 1640 medium supplemented with 10% FBS, 100 U/mL penicillin, and 100 μg/mL streptomycin, at 37 ℃ in a 5% CO_2 humidified incubator. RKO cells were subcultured in 6-well tissue culture plates at a density of 5×10^4 cells/well. Lentivirus infection was conducted at 30% cell confluency. Lentivirus was added at different MOIs in serum-free medium at 37 ℃ in 5% humidified CO_2. After 24 h, complete medium was added to the cells. More than 90% of the cells were infected at 4 d post-infection as indicated by the expression of GFP.

Quantitative reverse transcription polymerase chain reaction analysis

The total RNA from scr-siRNA and NOB1-siRNA infected cells was extracted with Trizol reagent according to the manufacturer's protocol. The RNA quantity and purity were determined by UV absorbance spectroscopy. cDNA was generated by reverse transcription with oligo-dT primer using M-MLV. The quantitative reverse transcription polymerase chain reaction (qRT-PCR) was performed using SYBR Green Master Mixture and analyzed on the TAKARA TP800-Thermal Cycler Dice™ Real-Time System. The qRT-PCR primers of each gene are listed in Table 1. The thermal cycling conditions were 15 s at 95 ℃, 45 cycles of 5 s at 95 ℃, and 30 s at 60 ℃. Data were analyzed with TAKARA Thermal Dice Real Time System software Ver3.0. Each reaction was performed with triplicate samples in each group and analyzed individually relative to GAPDH (a normalization control), and differential gene expression was calculated using the $2^{-\Delta\Delta Ct}$ method[28]. Thereafter, data for mRNA expression levels were expressed as a fold difference relative to that of negative control cells.

Table 1 Primers used in this study

Genes	Sequence	Length (bp)
GAPDH-F	TGACTTCAACAGCGACACCCA	121
GAPDH-R	CACCCTGTTGCTGTAGCCAAA	
NOB1-F	ATCTGCCCTACAAGCCTAAAC	184
NOB1-R	TCCTCCTCCTCCTCCTCAC	
BAX-F	TGCTTCAGGGTTTCATCCA	296
BAX-R	GGCCTTGAGCACCAGTTT	
WNT7B-F	TCCACTGGTGCTGCTTCG	300
WNT7B-R	GTCACGGGTGCTGTTCTGC	

GAPDH: Glyceraldehyde-3-phosphate dehydrogenase.

Western blot analysis

The infected cells were washed twice with PBS, suspended in a lysis buffer (2% mercaptoethanol, 20% glycerol, 4% SDS in 100 mmol/L Tris-HCl buffer, pH 6.8), and placed on ice for 15 min. The suspension was collected after centrifugation at 12000 *g* for 15 min at 4 ℃. Protein concentration was determined by the BCA Protein assay. From each sample, 30 μg of protein was subjected to electrophoresis on 10% SDS-polyacrylamide gel and transferred to a PVDF membrane. TBST (Tris-buffered saline, 0.1% Tween-20) buffer containing 5% non-fat dry milk was used to block non-specific binding for 1 h at room temperature. Membranes were then incubated with the indicated antibodies overnight at 4 ℃, and washed three times with TBST. Membranes were incubated with secondary antibodies conjugated to horseradish peroxidase for 2 h at room temperature, and washed three times with TBST. The detected protein signals were visualized by the ECL Plus Western Blotting Detection System (Amersham). GAPDH protein levels were used as a control to verify equal protein loading.

Cell growth

Cell growth was assessed using the Cellomics ArrayScan High Content Screening (HCS) system (Thermo Fisher Scientific, Pittsburgh, PA, United States). Briefly, RKO cells infected with lentivirus-mediated NOB1-siRNA or scr-siRNA were seeded in 96-well plates at a density of 2×10^3 cells/well and cultured at 37 ℃ in a 5% CO_2

humidified incubator. The infected GFP-expressing cells were imaged and counted on the Cellomics ArrayScan HCS Reader once a day for 5 d. The experiment was performed at least three times, independently. The growth curves of the infected cells were constructed.

Colony formation assay

To analyze cell growth, the colony formation analysis was performed using the Cellomics ArrayScan HCS system. Briefly, RKO cells infected with lentivirus-mediated NOB1-siRNA or scr-siRNA were seeded in 96-well plates at a density of 500 cells/well. Cells were cultured for 14 d at 37 ℃ in a 5% CO_2 humidified incubator. Culture medium was changed every 3 d. Cell colonies were imaged and counted using the Cellomics HCS Reader. The experiment was performed in triplicate.

Cell cycle distribution analysis

The cell cycle distribution was determined by DNA staining with propidium iodide (PI) and flow cytometric analysis[29]. In summary, RKO cells seeded in 6 cm culture dishes were infected with lentivirus-mediated NOB1-siRNA or scr-siRNA for 6 d. After infection, the cells were trypsinized, washed with PBS, and fixed in 70% ethanol for at least 1 h at 4 ℃. After two washing steps in cold PBS, the cells were resuspended in 1 mL of PBS containing 100 μg/mL RNase A and 50 μg/mL PI, and incubated for 30 min in the dark at room temperature. The percentages of cells in different phases of cell cycle were measured with the Becton Dickinson FACSCalibur flow cytometer using dedicated software. The experiment was repeated three times.

Annexin V apoptosis assay

Annexin V-APC (apoptosis detection kit) was used to detect apoptosis as described by the manufacturer. Briefly, RKO cells seeded in 6-well culture plates were infected with lentivirus-mediated NOB1-siRNA or scr-siRNA for 7 d. After infection, attached cells were trypsinized, washed with PBS, and centrifuged. The cells were washed with 1 × binding buffer, centrifuged, and resuspended in 1 mL 1 × staining buffer. To 100 μL of cell suspension, prepared as described above, 5 μL Annexin V-APC was added, followed by a gentle vortex, and 10 min incubation at room temperature in the dark. Data acquisition and analysis were performed by the Becton Dickinson FACSCalibur flow cytometer using dedicated software. The experiment was repeated three times.

In vivo xenograft tumor model

This animal experiment was approved by the Shanghai Laboratory Animal Ethics Committee. Four to five week old female nude mice were purchased from the Shanghai Laboratory Animal Center of the Chinese Academy of Science and were treated according to the ethics guidelines for animal research. To produce tumors, using a 24-gauge needle, 1×10^6 RKO cells in 0.1 mL of serum-free RPMI 1640 were injected subcutaneously into the right flank of each nude mouse. The mice were randomized into three groups ($n = 5$ each group). After 2 wk, the first group of nude mice was injected intratumorally with PBS, the second group with lentivirus-mediated scr-siRNA, and the third group with lentivirus-NOB1-siRNA. All of the mice were injected weekly until the completion of experiments. Tumor growth was monitored weekly and measured in two dimensions. Tumor volume was calculated using the $V = W2 \times L/2$ formula, where W and L are the shortest and longest diameters, respectively. After 5 wk, mice were killed and the tumors were immediately fixed in formalin for terminal deoxynucleotidyl transferase mediated dUTP nick end labeling (TUNEL) analysis.

Terminal deoxytransferase-mediated dUTP nick end labeling procedure

Apoptosis was detected using the TUNEL *in situ* apoptosis detection kit (Roche, Basel, Switzerland) according to the manufacturer's instructions. After deparaffinization, dehydration, and inactivation of intrinsic peroxidase activity, 20 paraffin sections of each tumor specimen were incubated with 2 μg/mL proteinase K at 37 ℃ for 15 min. Afterward, the sections were treated with terminal deoxynucleotidyl transferase and biotinylated dUTP. The reaction was stopped with TB buffer (30 mmol/L sodium chloride, 30 mmol/L sodium citrate), followed by microscopic observation of the samples. The controls for the TUNEL procedure were treated in the same manner as the test samples except dH_2O was used instead of using TdT enzyme in both kits. No labeling was found in the controls.

Microarray analysis

The scr-siRNA and NOB1-siRNA infected RKO cell gene expression profiles were obtained and compared using the Agilent Human Gene Expression 4 × 44K v2 Microarray kit (Agilent Technologies, Santa Clara, CA, United States). The microarrays were performed following the manufacturer's protocol. Briefly, the total RNA was extracted using Trizol and further purified with the Qiagen RNeasy kit (Valencia, CA, United States). RNA quantity, quality, and size distribution were checked by the Nanodrop 2000C (A_{260}/A_{280}) and Agilent 2100 Bioanalyzer system (Agilent Technologies, Santa Clara, CA, United States). cDNA was generated by reverse transcription using 0.2 μg of the total RNA. Cy3-CTP-labeled cRNA was synthesized by *in vitro* transcription (IVT), which was purified by Qiagen RNeasy kit and hybridized to the Agilent Whole Human Genome Oligo Microarrays 4 × 44K. After hybridization, the array was washed and processed using an Agilent DNA microarray scanner (Agilent Technologies). Agilent Feature Extraction Software (FES) was used to read and process the microarray image files. Genespring was employed to determine feature intensities and ratios (including background subtraction and normalization). Genes

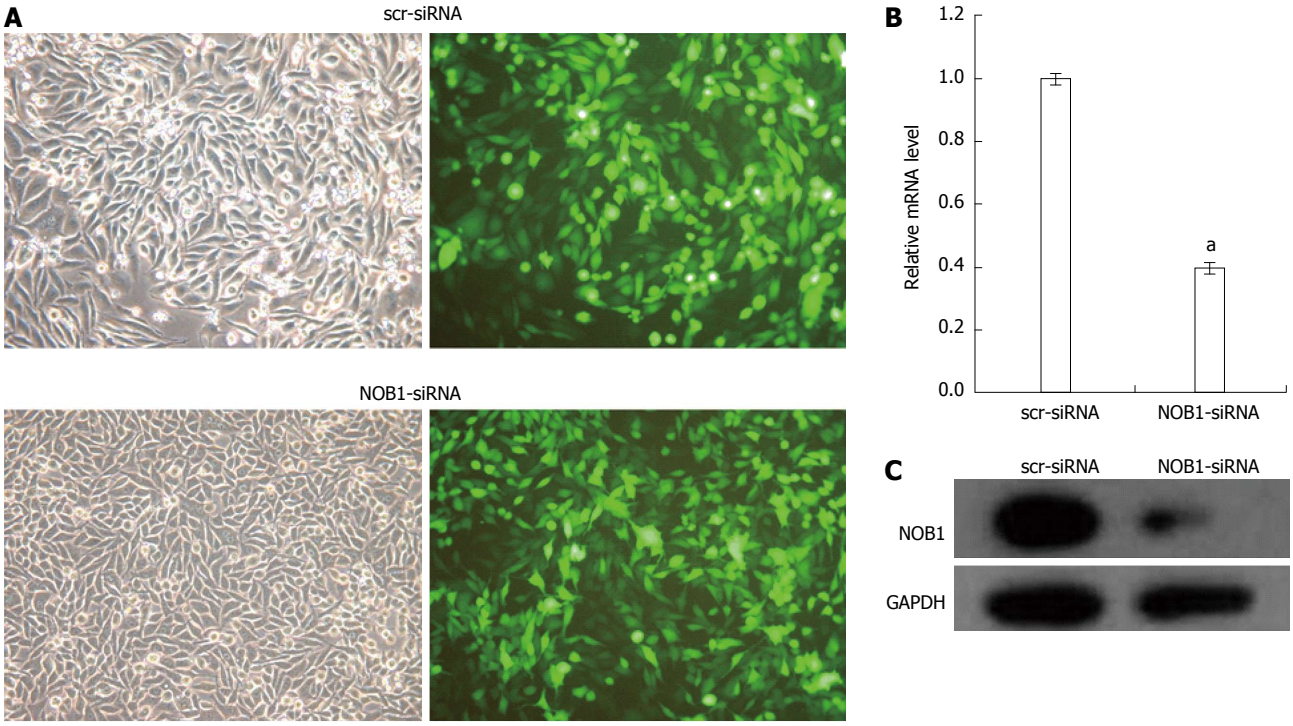

Figure 1 Lentivirus-mediated siRNA decreased *NOB1* expression in RKO cells. A: Infection efficiency was estimated 4 d after infection at MOI of 10. Green fluorescent protein (GFP) expression in infected cells was observed under light and fluorescence microscopy, respectively. Light micrograph (left); Fluorescent micrograph (right) (× 200); B: Total RNA was extracted 5 d after infection, and relative NOB1 mRNA expression was determined by qRT-PCR. GAPDH expression was used as a loading control. Data are presented as mean ± SD of three independent experiments. $^{a}P < 0.05$ *vs* scr-siRNA; C: Total cellular protein was extracted 7 d after infection and determined by western blot analysis using antibodies against NOB1. GAPDH was used as an internal control. MOI: Multiplicity of infection; GFP: Green fluorescent protein; GAPDH: Glyceraldehyde-3-phosphate dehydrogenase.

with ratios > 2 or < 0.5 were considered differentially expressed. The KEGG pathway and Gene Ontology (GO) enrichment analyses, for differentially expressed genes, were performed using the *NIH* gene annotation software, DAVID[30]. Heat maps were presented using Cluster 3.0 and the Tree View software[31].

Statistical analysis

Statistical analysis was performed using SPSS software version 10.0 (SPSS Inc, Chicago, IL, United States). Data were expressed as the mean of at least three different experiments ± SD. The statistical difference was evaluated using the χ^2 test and Student's *t* test. Statistically significant differences were defined as $P < 0.05$.

RESULTS

Downregulation of NOB1 expression by lentivirus-mediated NOB1-siRNA in RKO cells

The efficiency of lentiviral infection of RKO cells was determined through microscopic examination of GFP expression at an MOI of 10 on day 4 after infection (Figure 1A). More than 90% of RKO cells were infected.

qRT-PCR and Western blot examination of the effect of lentivirus-mediated NOB1-siRNA infection on the silencing of NOB1 expression showed a 60.9% reduction in NOB1 mRNA expression after 5 d of infection compared to scr-siRNA infection ($P < 0.05$, Figure 1B). Western blot analysis, performed 7 d after infection, showed a significant decrease in NOB1 protein expression in NOB1-siRNA infected RKO cells, as compared to the scr-siRNA infected cells (Figure 1C).

Effects of NOB1 knockdown on cell growth in RKO cells

The effects of NOB1 knockdown on cell function, cell growth, and colony formation were assessed using the Cellomics ArrayScan™ HCS system. As shown in Figure 2A, the GFP-expressing infected cells were counted once a day for 5 d. NOB1-siRNA inhibited cell proliferation in a time-dependent manner. After 5 d of infection, the number of NOB1-siRNA-infected RKO cells was reduced by 92.8% as compared with scr-siRNA infected cells ($P < 0.05$). Furthermore, NOB1-siRNA infected cells exhibited significant attenuation in the ability to form colonies. After 14 d of infection, the number of cell colonies in NOB1-siRNA infected RKO cells was reduced by 89.7%, as compared with scr-siRNA infected cells ($P < 0.05$, Figure 2B).

Effects of NOB1 knockdown on cell cycle progression and apoptosis in RKO cells

The effects of NOB1 knockdown on cell cycle progression and apoptosis in RKO cells were examined in an effort to further explore the reason for cell growth reduction. As shown in Figure 3A, there were no significant differences in cell cycle progression, including G_0/G_1, S, and G_2/M

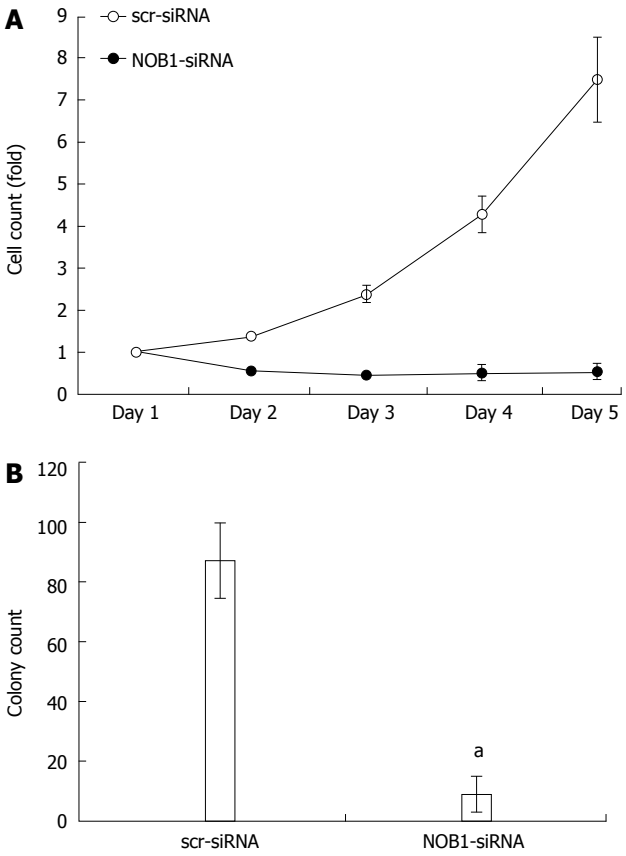

Figure 2 Effect of NOB1 knockdown on cell growth in RKO cells. A: The infected cells expressing GFP were imaged and counted using the Cellomics ArrayScan™ High Content Screening (HCS) Reader once a day for 5 d. Cell growth curves in scr-siRNA and NOB1-siRNA infected RKO cells are shown; B: Cell growth was detected by the colony formation assay in RKO cells 14 d after infection of scr-siRNA and NOB1-siRNA cells. RKO cells were seeded at 500 cells/well and allowed to form colonies. Cell colonies were imaged and counted using the Cellomics ArrayScan™ HCS Reader. Data are presented as mean ± SD of three independent experiments. $^{a}P < 0.05$ *vs* scr-siRNA. scr-siRNA: Cells infected with lentivirus-mediated scramble small interfering RNA; NOB1-siRNA: Cells infected with lentivirus-mediated NOB1-siRNA; GFP: Green fluorescent protein; qRT-PCR: Quantitative reverse transcription polymerase chain reaction.

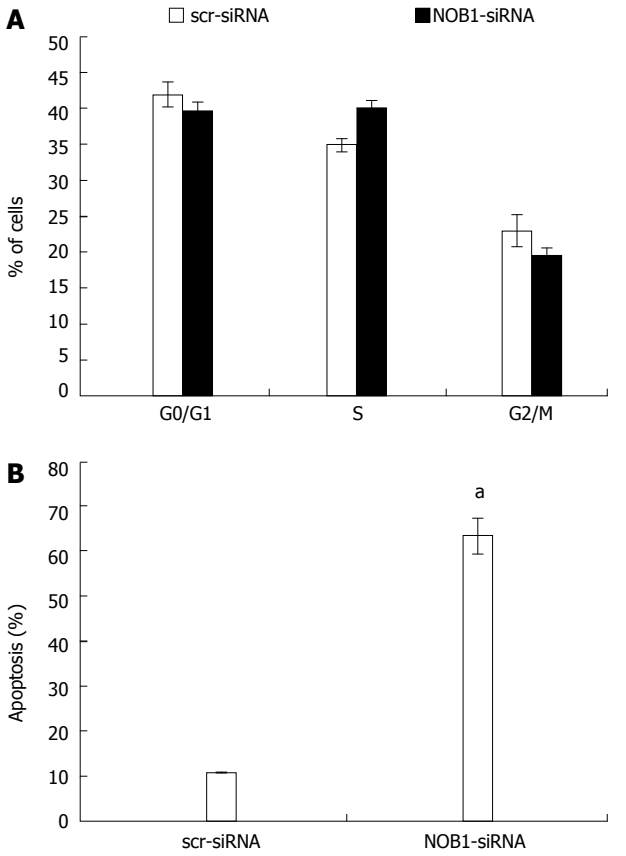

Figure 3 Effects of NOB1 downregulation on cell cycle progression and apoptosis in RKO cells. A: Cell cycle distribution was determined by flow cytometric analysis at day 6 of infection; B: Flow cytometric analysis of cell apoptosis was performed on day 7 of infection. Data are presented as mean ± SD of three independent experiments. $^{a}P < 0.05$ *vs* scr-siRNA. scr-siRNA: Cells infected with lentivirus-mediated scramble small interfering RNA; NOB1-siRNA: Cells infected with lentivirus-mediated NOB1-siRNA.

phases, between the cells infected with NOB1-siRNA or scr-siRNA.

NOB1 knockdown resulted in a marked increase in cell apoptosis (Figure 3B). The percentage of apoptotic cells was 63.2% ± 4.2% in NOB1-siRNA infected RKO cells, and 10.9% ± 0.2% in scr-siRNA infected RKO cells ($P < 0.05$). To validate the current finding in another colon cancer cell line, HCT116 cells were also infected with NOB1-siRNA and resulted in efficient NOB1 knockdown (Figure 1A). Flow cytometry analysis of cell death revealed that NOB1 knockdown induced significant apoptosis in HCT116 cells (Figure 1B).

Effects of NOB1 knockdown on tumor growth and cell survival in the xenograft mouse model

The effect of lentivirus-mediated Nob1-siRNA on tumor growth in the xenograft mouse model was examined. Western blot showed a reduction in NOB1 expression in xenograft tissue (Figure 4A). Furthermore, NOB1-siRNA also induced extensive cell death as detected by TUNEL assay (Figure 4B, C). After 2 wk the xenograft tumor began to grow; and at week 5 after injection, the xenograft tumor size was as follows (means ± SE): 910 ± 180 mm^3 in the PBS control group, 870 ± 1650 mm^3 in the scr-siRNA group, and 405 ± 102 mm^3 in the NOB1-siRNA group (Figures 4D, E, and F). ANOVA analysis revealed that the inhibitory effect of NOB1-siRNA infection was significant compared with scr-siRNA or PBS injections ($P < 0.05$). Compared with the starting volume, there was a significant retardation of tumor growth in xenograft mice treated with NOB1-siRNA.

Microarray analysis identified genes and pathways potentially targeted by NOB1

To determine the NOB1-targeted genes and -pathways in colorectal cancer, the total RNA was extracted from scr-siRNA and NOB1-siRNA infected RKO cells, and was hybridized on the Human Gene Expression 4 × 44K v2 Microarray chip containing 41093 probes, representing 27958 Entrez genes. Among them, 2336 genes with ratio > 2 or < 0.5 were defined as differentially expressed genes and potential NOB1 targets. In an indirect way,

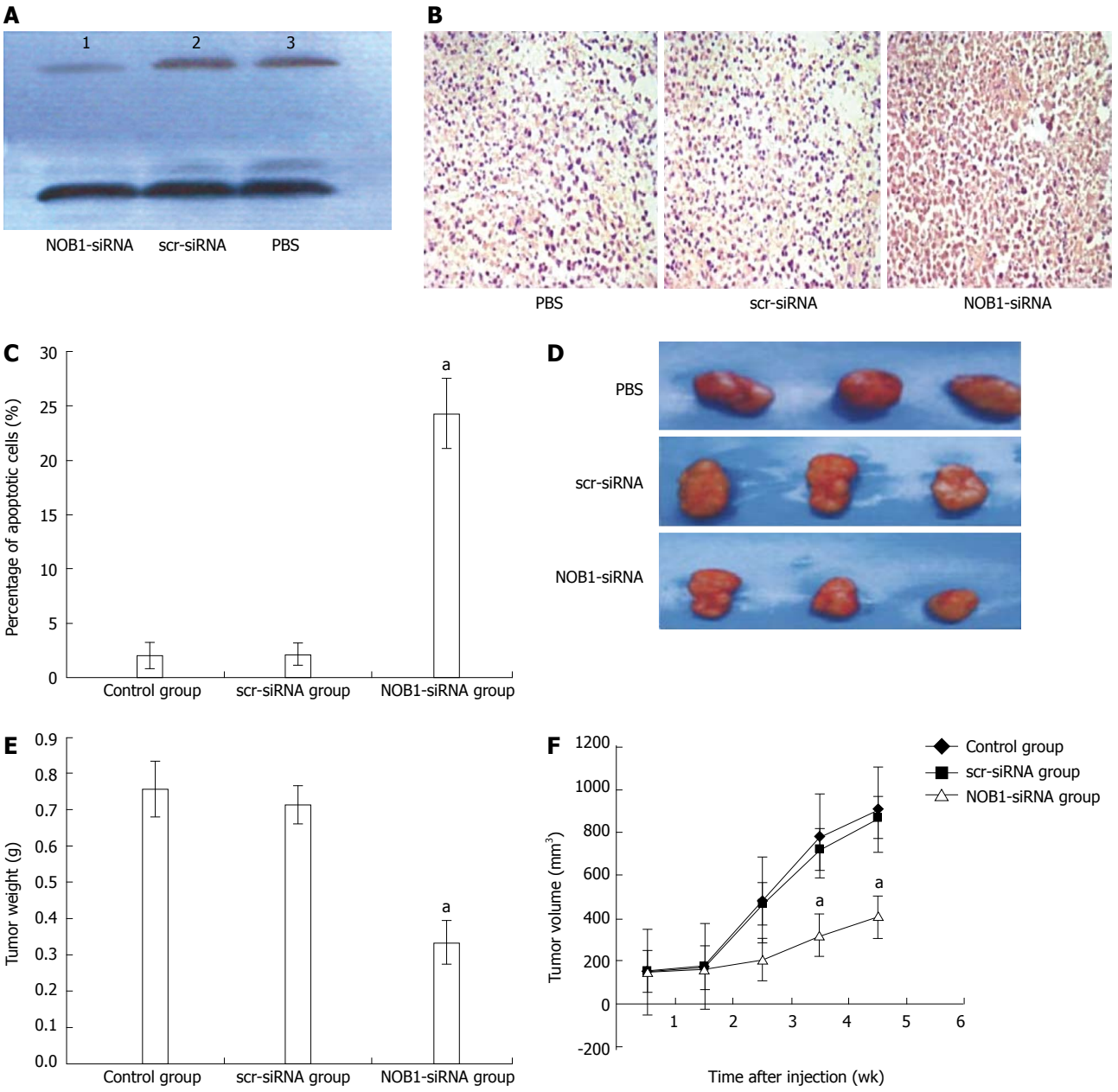

Figure 4 Suppression of tumor growth by lentivirus-mediated NOB1-siRNA in RKO cell xenograft mouse model. A: RKO cell xenograft mice were injected intratumorally with lentivirus-mediated NOB1-siRNA, scr-siRNA, or PBS. The size of the primary tumors was measured every week. Mice were sacrificed after 5 wk. NOB1-siRNA reduced NOB-1 expression in xenografted tumor tissue as determined by Western blot; B: NOB1-siRNA induced significant apoptosis in xenografted tumor tissue detected by TUNEL staining as shown in representative images; C: Plotted percentages of apoptotic cells; D: Typical pictures from RKO cell xenografted tumors infected by PBS, src-RNA and NOB1-siRNA; E: Plotted tumor weight; F: Tumor volume in RKO cell xenograft mouse model after NOB1-siRNA infection. $^{a}P < 0.05$ *vs* scr-siRNA. scr-siRNA: Cells infected with lentivirus-mediated scramble small interfering RNA; NOB1-siRNA: Cells infected with lentivirus-mediated NOB1-siRNA; PBS: Phosphate buffered saline.

NOB1 potentially upregulated 1451 probes representing 963 unique genes. There were also 2308 downregulated probes, representing 1373 unique genes, which may possibly be regulated by NOB1 directly.

NIH DAVID enrichment analysis of 2336 differentially expressed genes demonstrated NOB1 targeting KEGG pathways in cancer [$P = 0.001$, false discovery rate (FDR) = 1.23%]. With a total of 328 genes in cancer pathways, 56 genes are potentially targeted by NOB1 (Figure 5). Gene Ontology analysis indicated that these 56 genes are found in the WNT, cell proliferation, apoptosis, fibroblast growth factor (FGF), and angiogenesis signaling pathways (Table 2). The expressions of WNT7B and BAX were validated by qRT-PCR (Figure 6), which was consistent with microarray data.

DISCUSSION

There has been little research conducted in order to understand the role of human *NOB1* gene in colorectal cancer development and treatment. In an effort to expand our understanding, we employed lentiviral-

Figure 5 Heat map showing 56 genes differentially expressed in NOB1-siRNA infected RKO cells and enriched in the cancer pathway.

Table 2 Gene Ontology enrichment analysis showing NOB1-targeted pathways and genes involved in cancer development

Gene ontology	Genes	*P* value	Fold enrichment	FDR
WNT pathway	*WNT4, WNT7B, WNT5B, MITF, LEF1, WNT9A, TCF7L1, WNT8B, APC*	4.32×10^{-8}	16.9523	7.00×10^{-5}
Proliferation	*PRKCA, CEBPA, FGFR3, IL-8, FGF9, MITF, TGFBR2, EGLN3, NFKBIA, CDKN1A, CASP3, BAX, VEGFA, FGF1, EGF, APC*	2.03×10^{-7}	5.0931	3.28×10^{-4}
Apoptosis	*PRKCA, TRAF1, MITF, MLH1, NFKBIA, FADD, BIRC3, DAPK3, CDKN1A, CASP3, NTRK1, BAX, VEGFA, FAS, TRAF4, APC*	2.67×10^{-7}	4.9854	4.33×10^{-4}
FGF pathway	*FGF5, FGFR3, FGF9, FGF16, FGF1*	4.64×10^{-6}	43.1928	0.007516
Angiogenesis	*IL-8, EPAS1, FGF9, VEGFA, TGFBR2, EGF, FGF1*	2.33×10^{-5}	11.8488	0.037727

FDR: False discovery rate; APC: Adenomatous polyposis coli; IL: Interleukin; VEGFA: Vascular endothelial growth factor A; FGF: Fibroblast growth factor; TGF: Transforming growth factor.

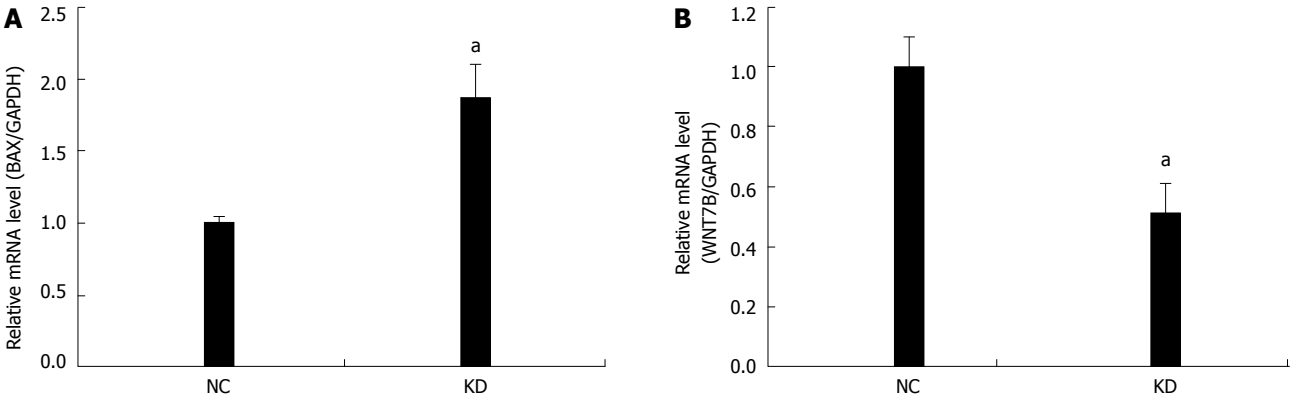

Figure 6 Quantitative reverse transcription polymerase chain reaction demonstrated NOB1-siRNA up-regulating BAX and down-regulating WNT7B mRNA in RKO cells. GAPDH expression was used as a loading control. Data are presented by the mean ± SD of three independent experiments. $^{a}P < 0.05$ *vs* scr-siRNA; scr-siRNA: Cells infected with lentivirus-mediated scramble small interfering RNA; NOB1-siRNA: Cells infected with lentivirus-mediated NOB1-siRNA.

mediated siRNA to inhibit NOB1 expression in RKO human colorectal cancer cells. The efficiency of lentiviral infection in RKO cells was more than 90% at an MOI of 10 on day 4 after infection. The NOB1-siRNA infection effectively reduced the expression of NOB1 in RKO cells, which was confirmed by qRT-PCR and Western blot analysis.

Carcinogenesis upsets the normal balance between cell proliferation and cell death[32]. Our results showed a significant inhibition of RKO cell growth as a result of NOB1 knockdown (Figure 2). The inhibition seemed to be due to induction of cell apoptosis, but not cell cycle arrest, in RKO cells (Figure 3). Furthermore, this phenomenon was validated in HCT116 cells, a p53 null cell line, suggesting that NOB1 is required for the survival of various colon cancer cells and its function is independent of p53. Given that RKO is a p53-positive cell line, our results suggest that apoptosis induced by NOB1-knockdown is p53 independent. The greatest apoptosis-inducing effect occurred 7 d after NOB1-siRNA infection. At 4 d after infection, the cell morphology looked largely normal, which could be explained by the relatively long half-life of NOB1 protein. Although, the most efficient NOB1 knockdown occurred on day 7, mRNA was markedly reduced on day 5 after infection. To explore the underlying mechanisms, microarray analysis was used to identify 2336 genes potentially targeted by NOB1. Further bioinformatic analysis suggested that NOB1 inhibited colorectal cancer through the oncogenic pathways, such as the WNT, cell proliferation, apoptosis, FGF, and angiogenesis signaling pathways. qRT-PCR confirmed that the expression of WNT7B and BAX were altered when NOB1 was knocked down.

Nob1p is required for 26S proteasome function, ribosome biogenesis, and cell viability in yeast[19-24]. Depletion of Nob1p leads to a defect in the processing of 40S ribosome subunits or small subunits[19]. Specifically, it results in the accumulation of 20S rRNA, the precursor of 18S rRNA, which is the primary rRNA component of the small subunit in yeast. Because Nob1p contains a PIN domain, it is believed to be the endonuclease responsible for the site D cleavage producing the mature 18S rRNA[20].

In addition to the PIN domain, Nob1p also contains a zinc ribbon domain, a well-known RNA binding domain. Thus, Nob1p-like proteins may potentially be required for ribosome biogenesis in other eukaryotes. A report showed that Nob1p assists in joining of the 20S core particle with the 19S RP in the nucleus as well as facilitating the 20S core particle maturation. Furthermore, 26S proteasome biogenesis is completed upon Nob1p internalization and degradation by the 26S proteasome[24]. Thus, Nob1p may also be required for ribosome biogenesis and 26S proteasome function in other eukaryotes.

The ubiquitin-proteasome pathway is responsible for most of the intracellular protein degradation[33]. The ribosome is a large protein-RNA complex essential for protein synthesis, a characteristic of cell viability[34]. Because protein synthesis malfunction and protein degradation cause cell apoptosis in tumor cells[35-37], the ubiquitin-proteasome pathway and ribosome biogenesis have become attractive targets in anticancer drug development. Due to the potentially important role of the human NOB1 in 26S proteasome function and ribosome biogenesis, we presumed that NOB1 knockdown might induce cell apoptosis. Considering that genes involved with WNT, apoptosis, FGF and angiogenesis signaling were altered in microarray profiling, further investigations should be focused on deciphering the connection between the role of NOB1 in the ubiquitin-proteasome pathway and ribosome biogenesis with these signaling/ pathways.

In conclusion, NOB1 expression can be downregulated specifically and effectively by lentivirus-mediated siRNA. NOB1 knockdown significantly inhibited RKO cell growth by inducing cell apoptosis, but not cell cycle arrest. Furthermore, NOB1 knockdown led to the altered expression of genes involved in multiple pathways or cellular functions, such as the WNT, cell proliferation, apoptosis, FGF, and angiogenesis signaling cascades. Thus, NOB1 should be considered a potential therapeutic target for the treatment of CRC.

COMMENTS

Background

Human *NOB1* encodes a protein with a PIN (PilT amino terminus) domain and a zinc ribbon domain. The yeast homolog Nob1p is required for 26S proteasome function and ribosome biogenesis; hence, Nob1p is essential for cell growth. However, the role of NOB1 in human cells remains largely unknown.

Research frontiers

Colorectal cancer (CRC) is one of the most common malignancies worldwide. The molecular events that trigger CRC development remain largely unexplored. Identification of novel therapeutic targets is urgently needed to improve the outcomes of patients suffering from CRC.

Innovations and breakthroughs

The role of NOB1 in CRC is unknown. The results of this study show that NOB1 is required for the survival of CRC cells. siRNA knockdown of NOB1 induced significant cell apoptosis in both *in vitro* and *in vivo* model systems. Microarray analysis showed that the WNT, cell proliferation, apoptosis, fibroblast growth factor, and angiogenesis signaling cascades contribute to NOB1 function.

Applications

Given the critical role of NOB1 in CRC, NOB1 may be a novel therapeutic target in the treatment of CRC patients.

Peer review

The role of human *NOB1* gene is largely unknown. The authors provide solid evidence to show the importance of NOB1 in the survival of colorectal cancer cells. Inhibition of the NOB1 function by siRNA greatly induces cell apoptosis both *in vitro* and *in vivo*. NOB1 seems to be an important and poorly investigated molecular target in colorectal cancer.

REFERENCES

1 **Watson AJ**. An overview of apoptosis and the prevention of colorectal cancer. *Crit Rev Oncol Hematol* 2006; **57**: 107-121 [PMID: 16326109 DOI: 10.1016/j.critrevonc.2005.06.005]

2 **Grady WM**, Markowitz SD. Genetic and epigenetic alterations in colon cancer. *Annu Rev Genomics Hum Genet* 2002; **3**: 101-128 [PMID: 12142355 DOI: 10.1146/annurev.genom.3.022502.103043]

3 **Yang SY**, Sales KM, Fuller B, Seifalian AM, Winslet MC. Apoptosis and colorectal cancer: implications for therapy. *Trends Mol Med* 2009; **15**: 225-233 [PMID: 19362056 DOI: 10.1016/j.molmed.2009.03.003]

4 **Adams J**. Potential for proteasome inhibition in the treatment of cancer. *Drug Discov Today* 2003; **8**: 307-315 [PMID: 12654543 DOI: 10.1016/S1359-6446(03)02647-3]

5 **Voorhees PM**, Dees EC, O'Neil B, Orlowski RZ. The proteasome as a target for cancer therapy. *Clin Cancer Res* 2003; **9**: 6316-6325 [PMID: 14695130]

6 **Baumeister W**, Walz J, Zühl F, Seemüller E. The proteasome: paradigm of a self-compartmentalizing protease. *Cell* 1998; **92**: 367-380 [PMID: 9476896 DOI: 10.1016/S0092-8674(00)80929-0]

7 **Glotzer M**, Murray AW, Kirschner MW. Cyclin is degraded by the ubiquitin pathway. *Nature* 1991; **349**: 132-138 [PMID: 1846030 DOI: 10.1038/349132a0]

8 **Pagano M**, Tam SW, Theodoras AM, Beer-Romero P, Del Sal G, Chau V, Yew PR, Draetta GF, Rolfe M. Role of the ubiquitin-proteasome pathway in regulating abundance of the cyclin-dependent kinase inhibitor p27. *Science* 1995; **269**: 682-685 [PMID: 7624798 DOI: 10.1126/science.7624798]

9 **Chen ZJ**, Parent L, Maniatis T. Site-specific phosphorylation of IkappaBalpha by a novel ubiquitination-dependent protein kinase activity. *Cell* 1996; **84**: 853-862 [PMID: 8601309 DOI: 10.1016/S0092-8674(00)81064-8]

10 **Nandi D**, Tahiliani P, Kumar A, Chandu D. The ubiquitin-proteasome system. *J Biosci* 2006; **31**: 137-155 [PMID: 16595883 DOI: 10.1158/0008-5472]

11 **Orlowski RZ**, Dees EC. The role of the ubiquitination-proteasome pathway in breast cancer: applying drugs that affect the ubiquitin-proteasome pathway to the therapy of breast cancer. *Breast Cancer Res* 2003; **5**: 1-7 [PMID: 12559038 DOI: 10.1186/bcr460]

12 **Hernandez-Verdun D**, Roussel P. Regulators of nucleolar functions. *Prog Cell Cycle Res* 2003; **5**: 301-308 [PMID: 14593725]

13 **Thomas G**. An encore for ribosome biogenesis in the control of cell proliferation. *Nat Cell Biol* 2000; **2**: E71-E72 [PMID: 10806485 DOI: 10.1038/35010581]

14 **Schmidt EV**. The role of c-myc in cellular growth control. *Oncogene* 1999; **18**: 2988-2996 [PMID: 10378694 DOI: 10.1038/sj.onc.1202751]

15 **Belin S**, Beghin A, Solano-Gonzàlez E, Bezin L, Brunet-Manquat S, Textoris J, Prats AC, Mertani HC, Dumontet C, Diaz JJ. Dysregulation of ribosome biogenesis and translational capacity is associated with tumor progression of human breast cancer cells. *PLoS One* 2009; **4**: e7147 [PMID: 19779612 DOI: 10.1371/journal.pone.0007147]

16 **Drygin D**, Siddiqui-Jain A, O'Brien S, Schwaebe M, Lin A, Bliesath J, Ho CB, Proffitt C, Trent K, Whitten JP, Lim JK, Von Hoff D, Anderes K, Rice WG. Anticancer activity of CX-3543: a direct inhibitor of rRNA biogenesis. *Cancer Res* 2009; **69**: 7653-7661 [PMID: 19738048]

17 **Montanaro L**, Treré D, Derenzini M. Nucleolus, ribosomes, and cancer. *Am J Pathol* 2008; **173**: 301-310 [PMID: 18583314

DOI: 10.2353/ajpath.2008.070752]
18 **Zhang Y**, Ni J, Zhou G, Yuan J, Ren W, Shan Y, Tang W, Yu L, Zhao S. Cloning, expression and characterization of the human NOB1 gene. *Mol Biol Rep* 2005; **32**: 185-189 [PMID: 16172919 DOI: 10.1007/s11033-005-3141-7]
19 **Fatica A**, Oeffinger M, Dlakić M, Tollervey D. Nob1p is required for cleavage of the 3' end of 18S rRNA. *Mol Cell Biol* 2003; **23**: 1798-1807 [PMID: 12588997 DOI: 10.1128/MCB.23.5.1798-1807.2003]
20 **Fatica A**, Tollervey D, Dlakić M. PIN domain of Nob1p is required for D-site cleavage in 20S pre-rRNA. *RNA* 2004; **10**: 1698-1701 [PMID: 15388878 DOI: 10.1261/rna.7123504]
21 **Lamanna AC**, Karbstein K. Nob1 binds the single-stranded cleavage site D at the 3′-end of 18S rRNA with its PIN domain. *Proc Natl Acad Sci USA* 2009; **106**: 14259-14264 [PMID: 19706509 DOI: 10.1073/pnas.0905403106]
22 **Granneman S**, Petfalski E, Swiatkowska A, Tollervey D. Cracking pre-40S ribosomal subunit structure by systematic analyses of RNA-protein cross-linking. *EMBO J* 2010; **29**: 2026-2036 [PMID: 20453830 DOI: 10.1038/emboj.2010.86]
23 **Tone Y**, Tanahashi N, Tanaka K, Fujimuro M, Yokosawa H, Toh-e A. Nob1p, a new essential protein, associates with the 26S proteasome of growing saccharomyces cerevisiae cells. *Gene* 2000; **243**: 37-45 [PMID: 10675611 DOI: 10.1016/S0378-1119(99)00566-1]
24 **Tone Y**, Toh-E A. Nob1p is required for biogenesis of the 26S proteasome and degraded upon its maturation in Saccharomyces cerevisiae. *Genes Dev* 2002; **16**: 3142-3157 [PMID: 12502737 DOI: 10.1101/gad.1025602]
25 **Lin Y**, Peng S, Yu H, Teng H, Cui M. RNAi-mediated downregulation of NOB1 suppresses the growth and colony-formation ability of human ovarian cancer cells. *Med Oncol* 2012; **29**: 311-317 [PMID: 21287298 DOI: 10.1007/s12032-010-9808-5]
26 **Wu DP**, He XW. [Expression of NOB1 and its significance in colorectal cancer]. *Nanfang Yike Daxue Xuebao* 2012; **32**: 420-422 [PMID: 22445998]
27 **Rubinson DA**, Dillon CP, Kwiatkowski AV, Sievers C, Yang L, Kopinja J, Rooney DL, Zhang M, Ihrig MM, McManus MT, Gertler FB, Scott ML, Van Parijs L. A lentivirus-based system to functionally silence genes in primary mammalian cells, stem cells and transgenic mice by RNA interference. *Nat Genet* 2003; **33**: 401-406 [PMID: 12590264 DOI: 10.1038/ng1117]
28 **Livak KJ**, Schmittgen TD. Analysis of relative gene expression data using real-time quantitative PCR and the 2(-Delta Delta C(T)) Method. *Methods* 2001; **25**: 402-408 [PMID: 11846609 DOI: 10.1006/meth.2001.1262]
29 **Nunez R**. DNA measurement and cell cycle analysis by flow cytometry. *Curr Issues Mol Biol* 2001; **3**: 67-70 [PMID: 11488413]
30 **Dennis G**, Sherman BT, Hosack DA, Yang J, Gao W, Lane HC, Lempicki RA. DAVID: Database for Annotation, Visualization, and Integrated Discovery. *Genome Biol* 2003; **4**: P3 [PMID: 12734009 DOI: 10.1186/gb-2003-4-5-p3]
31 **Eisen MB**, Spellman PT, Brown PO, Botstein D. Cluster analysis and display of genome-wide expression patterns. *Proc Natl Acad Sci USA* 1998; **95**: 14863-14868 [PMID: 9843981]
32 **Green DR**, Evan GI. A matter of life and death. *Cancer Cell* 2002; **1**: 19-30 [PMID: 12086884 DOI: 10.1016/S1535-6108(02)00024-7]
33 **Goldberg AL**, Stein R, Adams J. New insights into proteasome function: from archaebacteria to drug development. *Chem Biol* 1995; **2**: 503-508 [PMID: 9383453 DOI: 10.1016/1074-5521(95)90182-5]
34 **Wilson KS**, Noller HF. Molecular movement inside the translational engine. *Cell* 1998; **92**: 337-349 [PMID: 9476894 DOI: 10.1016/S0092-8674(00)80927-7]
35 **Wertz IE**, Hanley MR. Diverse molecular provocation of programmed cell death. *Trends Biochem Sci* 1996; **21**: 359-364 [PMID: 8918187 DOI: 10.1016/S0968-0004(96)40002-0]
36 **Nadano D**, Sato TA. Caspase-3-dependent and -independent degradation of 28 S ribosomal RNA may be involved in the inhibition of protein synthesis during apoptosis initiated by death receptor engagement. *J Biol Chem* 2000; **275**: 13967-13973 [PMID: 10788523 DOI: 10.1074/jbc.275.18.13967]
37 **Almond JB**, Cohen GM. The proteasome: a novel target for cancer chemotherapy. *Leukemia* 2002; **16**: 433-443 [PMID: 11960320 DOI: 10.1038/sj.leu.2402417]

P- Reviewer: Chae SC **S- Editor**: Ding Y **L- Editor**: Webster JR
E- Editor: Zhang DN

World Journal of Gastroenterology

Submit a Manuscript: http://www.wjgnet.com/esps/
Help Desk: http://www.wjgnet.com/esps/helpdesk.aspx
DOI: 10.3748/wjg.v21.i3.878

World J Gastroenterol 2015 January 21; 21(3): 878-887
ISSN 1007-9327 (print) ISSN 2219-2840 (online)

ORIGINAL ARTICLE

Basic Study

Hes1, an important gene for activation of hepatic stellate cells, is regulated by Notch1 and TGF-β/BMP signaling

Kai Zhang, Yan-Qiong Zhang, Wen-Bing Ai, Qing-Ting Hu, Qiao-Juan Zhang, Lin-Yan Wan, Xiao-Lian Wang, Chang-Bai Liu, Jiang-Feng Wu

Kai Zhang, Yan-Qiong Zhang, Qing-Ting Hu, Qiao-Juan Zhang, Lin-Yan Wan, Xiao-Lian Wang, Chang-Bai Liu, Jiang-Feng Wu, Medical College, China Three Gorges University, Yichang 443002, Hubei Province, China

Wen-Bing Ai, the Second College of Clinical Medical Science, China Three Gorges University, Yichang 443000, Hubei Province, China

Chang-Bai Liu, Jiang-Feng Wu, Institute of Molecular Biology, Medical College, China Three Gorges University, Yichang 443002, Hubei Province, China

Author contributions: Zhang K, Zhang YQ and Ai WB contributed equally to this work and wrote the manuscript; Hu QT, Zhang QJ, Wan LY and Wang XL give some help for this work; Wu JF and Liu CB guide the research; Wu JF and Liu CB revised and approved the article to be published.

Supported by National Natural Science Foundation of China, No. 81170412, No. 81070348 and No. 81200307; Health Department of Hubei Province of China, No. JX6C-26.

Correspondence to: Jiang-Feng Wu, Professor, Institute of Molecular Biology, Medical College, China Three Gorges University, 8 Daxue Road, Xiling District, Yichang 443002, Hubei Province, China. 313229177@qq.com
Telephone: +86-717-6397328
Fax: +86-717-6397328

Received: April 23, 2014
Peer-review started: April 24, 2014
First decision: May 29, 2014
Revised: June 18, 2014
Accepted: July 15, 2014
Article in press: July 16, 2014
Published online: January 21, 2015

Abstract

AIM: To determine the role of Notch1 and Hes1 in regulating the activation of hepatic stellate cells (HSCs) and whether Hes1 is regulated by transforming growth factor (TGF)/bone morphogenetic protein (BMP) signaling.

METHODS: Immunofluorescence staining was used to detect the expression of desmin, glial fibrillary acidic protein and the myofibroblastic marker α-smooth muscle actin (α-SMA) after freshly isolated, normal rat HSCs had been activated in culture for different numbers of days (0, 1, 3, 7 and 10 d). The expression of α-SMA, collagen1α2 (COL1α2), Notch receptors (Notch1-4), and the Notch target genes Hes1 and Hey1 were analyzed by reverse transcriptase-polymerase chain reaction. Luciferase reporter assays and Western blot were used to study the regulation of α-SMA, COL1α1, COL1α2 and Hes1 by NICD1, Hes1, CA-ALK3, and CA-ALK5 in HSC-T6 cells. Moreover, the effects of inhibiting Hes1 function in HSC-T6 cells using a Hes1 decoy were also investigated.

RESULTS: The expression of Notch1 and Hes1 mRNAs was significantly down-regulated during the culture of freshly isolated HSCs. In HSC-T6 cells, Notch1 inhibited the promoter activities of α-SMA, COL1α1 and COL1α2. On the other hand, Hes1 enhanced the promoter activities of α-SMA and COL1α2, and this effect could be blocked by inhibiting Hes1 function with a Hes1 decoy. Furthermore, co-transfection of pcDNA3-CA-ALK3 (BMP signaling activin receptor-like kinase 3) and pcDNA3.1-NICD1 further increased the expression of Hes1 compared with transfection of either vector alone in HSC-T6 cells, while pcDNA3-CA-ALK5 (TGF-β signaling activin receptor-like kinase 5) reduced the effect of NICD1 on Hes1 expression.

CONCLUSION: Selective interruption of Hes1 or maintenance of Hes1 at a reasonable level decreases the promoter activities of α-SMA and COL1α2, and these conditions may provide an anti-fibrotic strategy against hepatic fibrosis.

Key words: Hes1; Notch1; TGF-β/BMP; Hepatic stellate cells; Hepatic fibrosis

Core tip: In our paper, we found that Notch signaling appears to crosstalk with TGF-β/BMP signaling and co-regulates the expression of Hes1 in hepatic stellate cells. Notch1 may keep Hes1 protein in a reasonable range due to Hes1 auto-negative feedback, allowing Notch1 to repress the expression of α-SMA and collagen1α2 (COL1α2). Over-expression of Hes1 *via* transfection, thus lacking the negative feedback, enhances the promoter activities of α-smooth muscle actin (α-SMA) and COL1α2, consistent with the finding when Hes1 is captured by a Hes1-decoy oligodeoxynucleotide. This may provide an anti-fibrotic strategy against hepatic fibrosis. Further investigations in the future on the molecular mechanism by which Hes1 regulates the expression of α-SMA and COL1α2 should provide additional support for such an approach.

Zhang K, Zhang YQ, Ai WB, Hu QT, Zhang QJ, Wan LY, Wang XL, Liu CB, Wu JF. *Hes1*, an important gene for activation of hepatic stellate cells, is regulated by Notch1 and TGF-β/BMP signaling. *World J Gastroenterol* 2015; 21(3): 878-887 Available from: URL: http://www.wjgnet.com/1007-9327/full/v21/i3/878.htm DOI: http://dx.doi.org/10.3748/wjg.v21.i3.878

INTRODUCTION

The activation of hepatic stellate cells (HSCs), a key step in liver fibrosis, can lead to the development of myofibroblast-like cells and contribute to liver fibrosis[1]. The main characteristics of the formation of myofibroblast-like cells are the expression of α-smooth muscle actin (α-SMA) and extracellular matrix (ECM) proteins, particularly collagen I[2]. Because of the importance of myofibroblasts in liver fibrosis, the majority of antifibrotic therapies are designed to inhibit the formation of myofibroblastic cells[3].

Previous studies have revealed that the transforming growth factor-β (TGF-β)/bone morphogenetic protein (BMP) signaling pathway is a pivotal player in the activation of HSCs[4,5]. TGF-β is a key mediator in the activation of HSCs[6]. BMPs are also members of the TGF-β superfamily and are antagonistic against TGF-β[7].

Notch signaling is an evolutionarily conserved pathway controlling diverse aspects of development and disease[8]. In mammals, the Notch family contains five Notch ligands (Jagged1, Jagged2, Delta-like1, Delta-like3, and Delta-like4) and four Notch receptors (Notch1-4). Among the Notch target genes are the basic helix-loop-helix (bHLH) transcription factors of the Hes (Hairy-Enhancer of Split) and HERP (Hes-related repressor protein) families, which function as transcriptional repressors[9,10].

During hematopoiesis and immune development, Notch is critical for T/B lineage specification and for the generation of splenic marginal zone B cells[11,12]. Earlier research has mainly focused on the interconnections between Notch and hematopoiesis or immune system-related molecules, aiming to find a preferable method to modulate hematopoiesis or treat immune disorders.

Recently, several studies have implicated Notch signaling in some human fibrosis diseases, such as renal, pulmonary and even liver fibrosis[13,14]. Evidence suggests that TGF-β/BMP signaling, as a key mediator in the process of HSC activation, has a synergistic effect with Notch in many cell types, enhancing the expression of target genes[15,16]. While the Jagged/Notch pathway may selectively mediate the fibrogenic properties of TGF-β1, which are essential to promote the production and deposition of the ECM[17,18], whether Notch signaling regulates TGF-β/BMP in HSCs remains largely unclear.

We hypothesized that Notch signaling can interact with TGF-β/BMP signaling and play a role in HSC activation. To test this hypothesis, we investigated the relationship between the activation of HSCs and Notch signaling pathways. Our findings demonstrate a pivotal role for Notch signaling in this process.

MATERIALS AND METHODS

HSC preparation and HSC-T6 cell line

The use of animals for this study was approved by the laboratory animal center of China, Three Gorges University. Primary rat HSCs were isolated using a previously described method with minor modifications[19]. Freshly isolated, normal rat HSCs were cultured on 6- or 24-well plates in low glucose DMEM (Invitrogen) supplemented with 10% FBS and antibiotics for 0, 1, 3, 7, or 10 d to examine the quiescent, activating, or fully activated cells. HSC-T6 cells, an immortalized rat HSC line provided by the institute of liver disease at Shanghai University of Traditional Chinese Medicine, were cultured in low glucose DMEM supplemented with 10% FBS.

Western blot analysis

Cells were lysed in lysis buffer (25 mmol/L Tris-HCl pH 7.5, 2.5 mmol/L EDTA, 137 mmol/L NaCl, 2.7 mmol/L KCl, 1% sodium deoxycholic acid, 0.1% SDS, 1% TritonX-100, and 2 mmol/L PMSF) and protease inhibitor cocktail for 30 min at 4 ℃. The cell lysates were clarified by centrifugation at 12000 rpm for 20 min at 4 ℃, and the supernatants were collected. The protein concentrations were measured using a BCA Protein Assay kit (Thermo). An equal amount of protein from

Table 1 Primers for reverse transcriptase-polymerase chain reaction

Gene	Forward primer	Reverse primer	Bp	Accession No.
Notch1	AGAGCTTTTCCTGTGTCTGTCC	CGGTACAGTCAGGTGTGTTGTT	414	NM_001105721
Notch2	GACTGCCAATACTCGACCTC	TTCAGAAGTGAAGTCTCCAG	438	NM_024358.1
Notch3	CCTCTTTCACCTGTACCTGTCC	ACACAGTAGTGGGAGTGGTCCT	496	NM_020087
Notch4	CAACTCTGCGAGAACGGTGG	TGGAAGGAGCCCAAGGTGTT	443	NM_001002827.1
hes1	GCCAGCTGATATAATGGA	TAGGTCATGGCGTTGATC	462	NM_024360.3
hey1	CTACAGCTCCTCTGATAGTG	GAGGCATCGAGTCCTTCAAT	420	NM_001191845
TGF-β1	GGTGAAACGGAAGCGCATCG	CTTGAATCTCTGCAGGCGCA	364	NM_021578.2
E-cadherin	CTCGTGGCTTTGTCAGCA	GACCCAGTCTCGTTTCTG	432	NM_031334.1
α-SMA	GTGTGAAGAGGAAGACAG	TTGGCCTTAGGGTTCAGC	348	NM_031004.2
β-catenin	CTGACAGAGTTGCTCCACTC	CAGCCCATCAACTGGATAGT	342	NM_053357.2
Bmp7	CAGAGCATCAACCCCAAGTT	GATGAAGTGAACCAGTGTCT	396	NM_001191856.1
COL1α2	ACCTCAGGGTGTTCAAGGTG	CGGATTCCAATAGGACCAGA	222	NM_053356
GAPDH	ACCACAGTCCATGCCATCAC	TCCACCACCCTGTTGCTGTA	480	NM_017008.4

each sample was separated by sodium dodecyl sulfate-polyacrylamide gel electrophoresis (SDS-PAGE) and transferred to a polyvinylidene difluoride membrane. The membrane was incubated with a mouse monoclonal anti-α-SMA antibody (1:1000 dilution) (Sigma), a goat polyclonal anti-Hes1 antibody (1:1000 dilution) (SANTA CRUZ), a rabbit polyclonal anti-TGF-β(R) antibody (1:1000 dilution) (SANTA CRUZ), a mouse monoclonal anti-HA antibody (1:3000 dilution) (Abmart), a mouse monoclonal anti-c-myc antibody (1:3000 dilution) (Abmart) or a mouse monoclonal anti-β-actin antibody (1:3000 dilution) (Sigma) for 24 h at 4 ℃. This primary antibody incubation was followed by incubation with HRP-conjugated anti-mouse (1:3000 dilution), anti-rabbit (1:3000 dilution) or anti-goat (1:12000 dilution) antibody as the secondary antibody for 1 h at RT. These membranes were developed using Immobilon Western Detection Reagents (Millipore) according to the manufacturer's instructions. The chemiluminescence on the membrane was detected using the VersaDoc system (Bio-Rad). Densitometric analyses of the band intensities were performed using ImageJ software (version 1.38 ×; National Institutes of Health).

RNA extraction and reverse transcriptase-polymerase chain reaction

Total RNA from freshly isolated HSCs or HSC-T6 cells was extracted using TRIzol reagent (Axygen). The RNA (2 mg) was reverse transcribed using a Transcriptor First Strand cDNA Synthesis Kit according to the manufacturer's instructions (Fermentas). The primers used in the polymerase chain reaction (PCR) reactions to detect the mRNA levels were synthesized by Sangon Biotech (Shanghai, China) and are described in Table 1.

Immunofluorescence analysis

Freshly isolated, normal rat HSCs cultured for varying lengths of time (1, 3, 7, 10 d) were fixed in phosphate buffered saline containing 4% paraformaldehyde at room temperature for 30 min and were then treated with blocking solution containing 0.1% Triton X-100. The fixed and blocked cells were incubated for 1 h with either a mouse monoclonal anti-α-SMA (1:100) (Sigma), a mouse monoclonal anti-GFAP (1:250) (Sigma) or a mouse monoclonal anti-desmin (1:600) (Sigma) antibody in 3% NCBS. The cells were then incubated with a Cy3-conjugated anti-mouse secondary antibody (1:1000) (NovoGene) for 1 h at 37 ℃. After incubation, the cells were stained with the nuclear stain 4',6-diamidino-2-phenyl-indole (DAPI). The cells were then examined under a fluorescence microscope (Nikon, Japan).

Constructs, transfection and luciferase reporter assay

The pcDNA3-CA-ALK3 (BMP signaling activin receptor-like kinase 3)[20] and pcDNA3-CA-ALK5 (TGF-β signaling activin receptor-like kinase 5)[21] plasmids were gifts from Professor Miyazono at Tokyo University. The rat Notch1 intracellular domain (*NICD1*) and Hes1 cDNA (Hes1) were cloned into the pcDNA3.1(+) vector. The promoters of α-SMA (*pSMA*), COL1α1 (*P-COL1α1*), COL1α2 (*P-COL1α2*) and Hes1 (P-Hes1) were cloned into the pGLuc-Basic vector (N8082S, NEB, United States) for luciferase assays. The HSC-T6 cells were seeded in a 24- or 6-well plate at 60% confluence. After 24 h, the cells were transfected with different plasmids using the FuGENE HD Transfection Reagent (Roche) according to the manufacturer's instructions. The cells were lysed after 36 h in culture for Western blot analyses. For luciferase assays, the supernatants were collected 24 h after transfection, and the assays were performed using the Gaussia Luciferase Assay Kit (BioLux) according to the manufacturer's instructions. The reactions were examined using a Fluorescence Detector (Brethold).

Synthesis of oligodeoxynucleotides and selection of sequence targets

The Hes1 oligodeoxynucleotide (ODN) decoy (5'-TTT CAC GAG TTT TCA CGA GTT T-3', 5'-AAA CTC GTG AAA ACT CGT GAA A-3') and scrambled (Scr) ODN decoy (5'-TTT ACA GAG TTT TAC AGA GTT T-3', 5'- AAA CTC TGT AAA ACT CTG TAA A-3') were synthesized by Sangon Biotech (Shanghai, China). These ODN decoys were annealed overnight while the temperature decreased from 80 ℃ to 25 ℃. After GLuc

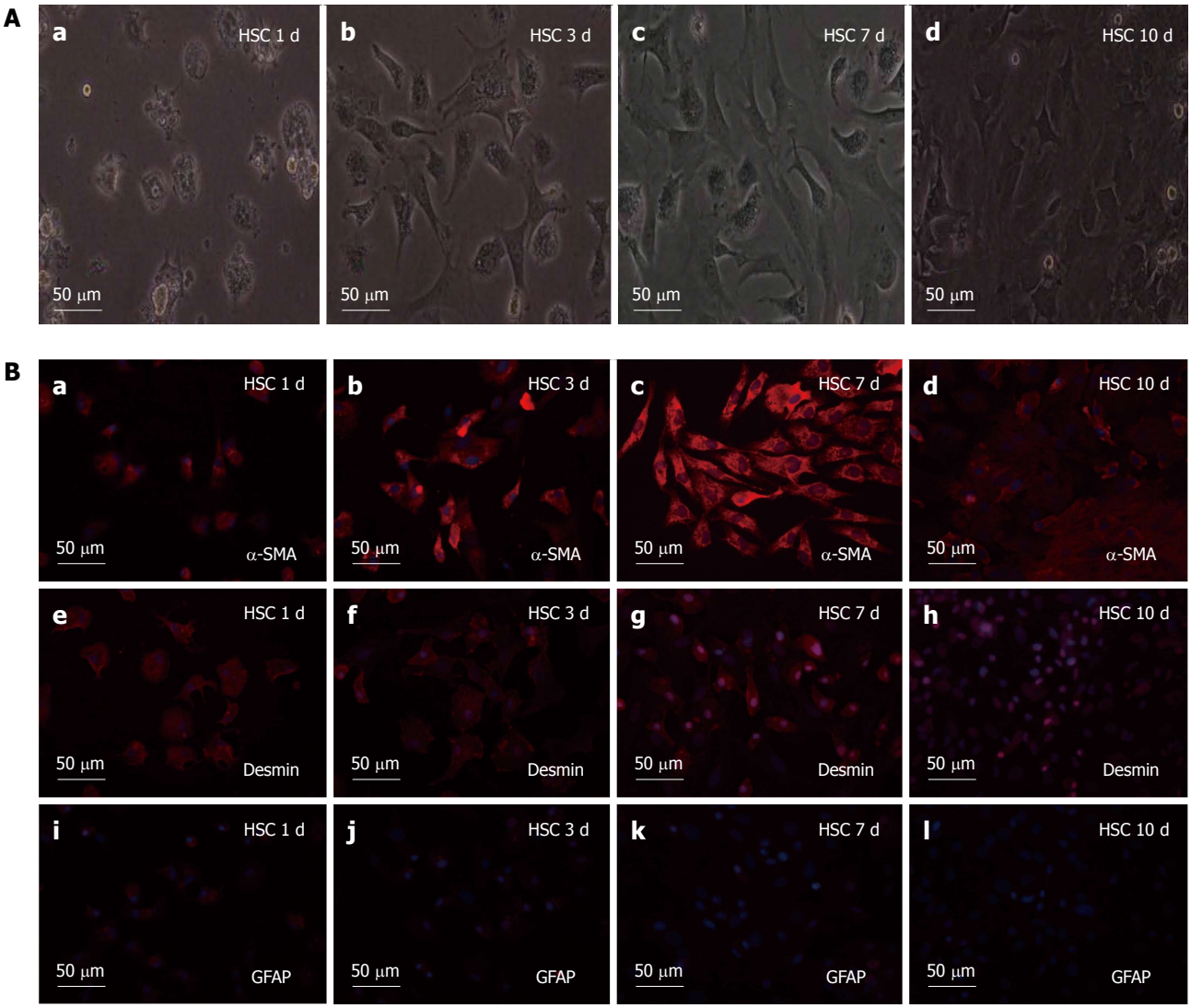
A
a HSC 1 d
b HSC 3 d
c HSC 7 d
d HSC 10 d
50 μm
B
a HSC 1 d
b HSC 3 d
c HSC 7 d
d HSC 10 d
50 μm α-SMA
e HSC 1 d
f HSC 3 d
g HSC 7 d
h HSC 10 d
50 μm Desmin
i HSC 1 d
j HSC 3 d
k HSC 7 d
l HSC 10 d
50 μm GFAP

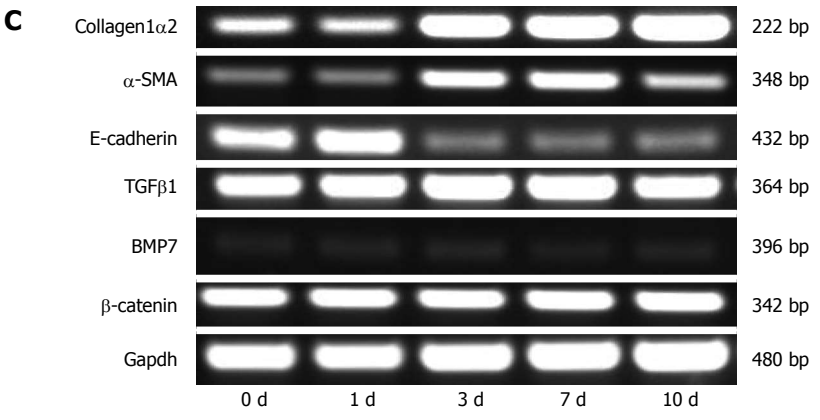
C
Collagen1α2 222 bp
α-SMA 348 bp
E-cadherin 432 bp
TGFβ1 364 bp
BMP7 396 bp
β-catenin 342 bp
Gapdh 480 bp
0 d 1 d 3 d 7 d 10 d

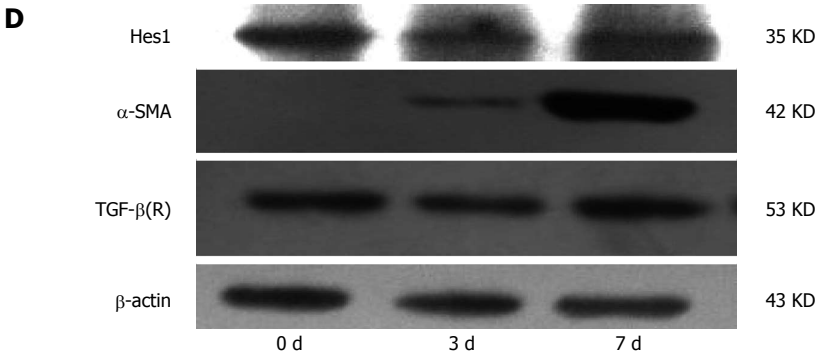
D
Hes1 35 KD
α-SMA 42 KD
TGF-β(R) 53 KD
β-actin 43 KD
0 d 3 d 7 d

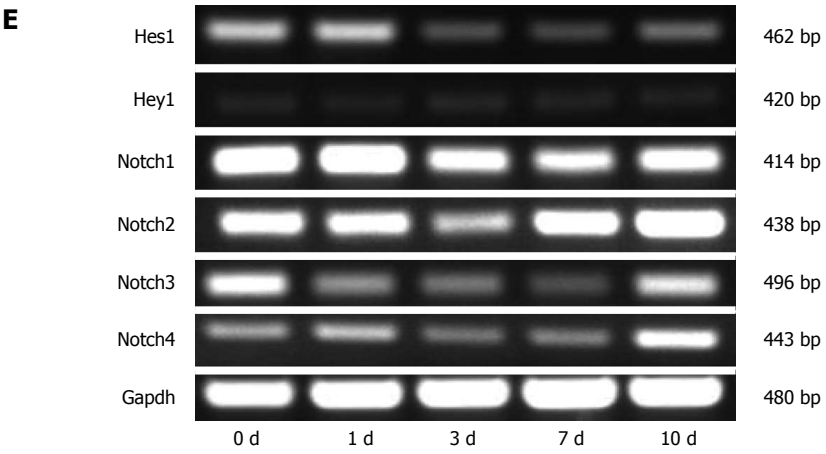

Figure 1 Characteristics of quiescent and activated hepatic stellate cells. A: Microscopic pictures of freshly isolated hepatic stellate cells (HSCs) after 1, 3, 7 and 10 d of culture; B: The expression of α-smooth muscle actin (α-SMA), desmin and GFAP detected by immunofluorescence staining. Red fluorescence represents α-SMA in pictures a, b, c, and d; desmin in pictures e, f, g, and h; and GFAP in pictures i, j, k, and l. The cell nuclei were visualized by DAPI (4, 6-diamidino-2-phenylindole) staining (blue). C: Expression analysis of collagen1α2, α-SMA, E-cadherin, transforming growth factor-β1 (TGFβ1), bone morphogenetic protein-7 (BMP7), and β-catenin in the cells in (A) measured by RT-PCR. RT-PCR of Gapdh served as a control; D: Analysis of α-SMA, Hes1 and TGF-β (R) by Western blotting of the cells in (A). The β-actin protein served as a control; E: RT-PCR analysis of Notch receptors (Notch1-4) and the Notch target genes Hes1 and Hey1. Notably, the data for Hes1 in D and E do not agree with each other.

reporter plasmids were transfected into HSC-T6 cells for 12 h, the Hes1 ODN decoy was delivered by Mirus (Mirus Bio Corporation). The supernatant was collected for luciferase reporter analysis after 24 h of culture.

Statistical analysis

Data are presented as mean ± SE of several experiments. The statistical significance was assessed using a two-tailed Student's *t*-test. $P < 0.05$ was considered statistically significant.

RESULTS

Expression of Notch1 and Hes1 is reduced in activated HSCs

The activation of HSCs can be modeled *in vitro* by culturing freshly isolated (quiescent) rodent or human HSCs on plastic in serum-containing media. Freshly isolated HSCs from normal rats were cultured for various lengths of time (1, 3, 7 and 10 d), and the results showed that the HSCs lost their typical lipid droplets and developed into myofibroblast-like cells during culture (Figure 1A). When various HSC markers were analyzed by immunofluorescence, the expression of the HSC marker GFAP had decreased, desmin synthesis had increased, and the myofibroblast marker α-SMA had also increased (Figure 1B). To further characterize the quiescent and activated HSCs, we analyzed the expression of α-SMA, COL1α2, E-cadherin, TGF-β1, BMP7, and β-catenin on different days during the culture period (0, 1, 3, 7, and 10 d) by RT-PCR. The results showed that the mRNA levels of TGF-β1, BMP7 and β-catenin did not change during the activation of HSCs; the mRNA levels of E-cadherin, a marker of epithelial-mesenchymal transition (EMT), decreased, while the mRNA levels of the hepatic fibrosis-related genes α-SMA and COL1α2 increased (Figure 1C). We also used RT-PCR to analyze the expression of the Notch receptors (Notch1-4) and their target genes *Hes1* and *Hey1* on different days during the culture period. The mRNA levels of the Notch1 receptor decreased during culture, while the mRNA levels of the other Notch receptors (Notch2-4) changed inconsistently (Figure 1E). The mRNA levels of the Notch target gene Hes1 decreased, but the protein did not significantly change (Figure 1D).

Over-expression of Notch1 decreases the expression of myofibroblastic markers in HSC-T6 cells

To investigate the role of Notch1 on the activation of HSCs, we examined the effect of over-expression of Notch1 in the HSC-T6 cell line. After the pcDNA3.1-NICD1 was co-transfected with reporter plasmids of GLuc-pSMA, GLuc-P-COL1α1 or GLuc-P-COL1α2, respectively, into HSC-T6 for 24 h, the supernatant was collected for a luciferase reporter assay. The results revealed that the promoter activities of α-SMA, COL1α1 and COL1α2 were reduced (Figure 2).

Over-expression of Hes1 increases the expression of myofibroblastic markers in HSC-T6

To determine whether the Notch1 target gene Hes1 is involved in the activation of HSCs, the pcDNA-Hes1 plasmid was co-transfected with the reporter plasmids GLuc-pSMA, GLuc-P-COL1α1 or GLuc-P-COL1α2 into HSC-T6 cells for 24 h. The supernatant was collected for luciferase assays. The activities of GLuc-pSMA and GLuc-P-COL1α2 were higher in the pcDNA-Hes1 transfected cells than in the empty vector control cells (Figure 3A, C), while over-expression of Hes1 did not alter the activity of the COL1α1 promoter (Figure 3B). Over-expression of Hes1 also increased the expression of endogenous α-SMA, as revealed by Western blot analysis (Figure 3D). Thus, Hes1, a Notch signaling target gene,

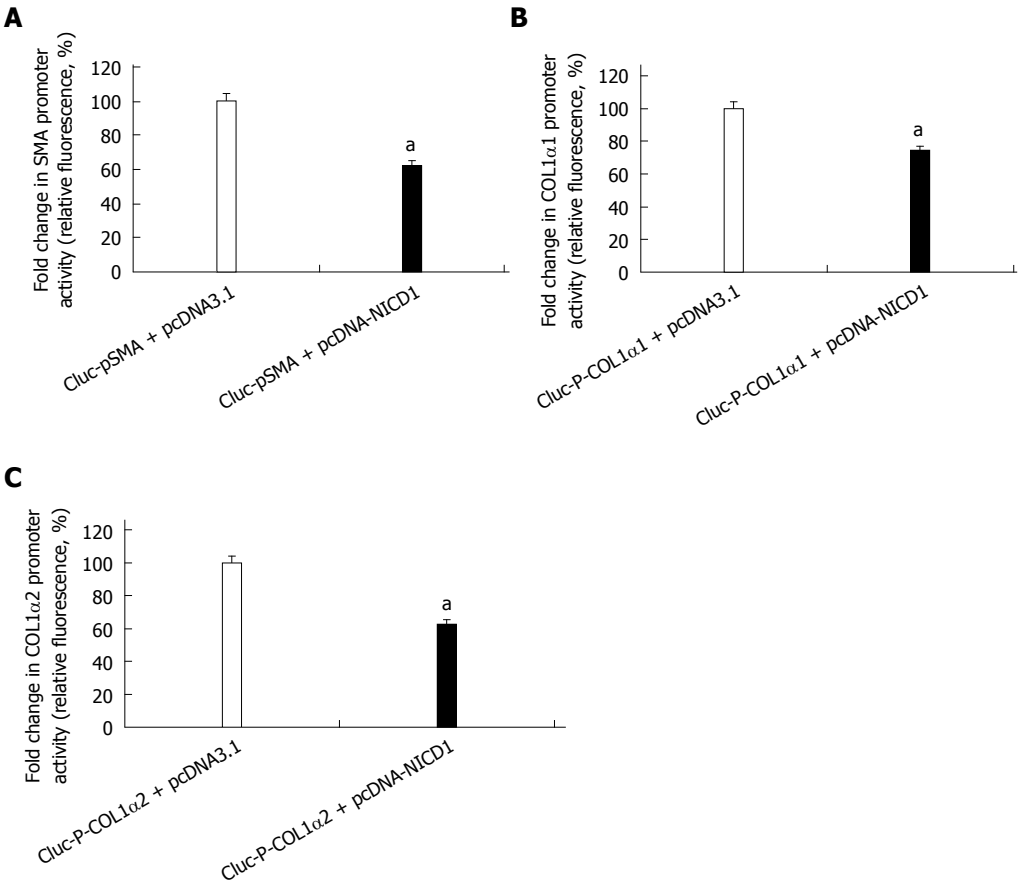

Figure 2 NICD1 suppresses the expression of myofibroblastic markers in hepatic stellate cell-T6 cells. A-C: Luciferase reporter assays for the promoter activities of α-SMA, COL1α1, COL1α2 in cells transfected with empty plasmid-pcDNA3.1(+) as a control or with pcDNA3.1-NICD1 ($^{a}P < 0.05$ *vs* the control group, $n = 8$). α-SMA: α-smooth muscle actin; COL1α1: Collagen1α1.

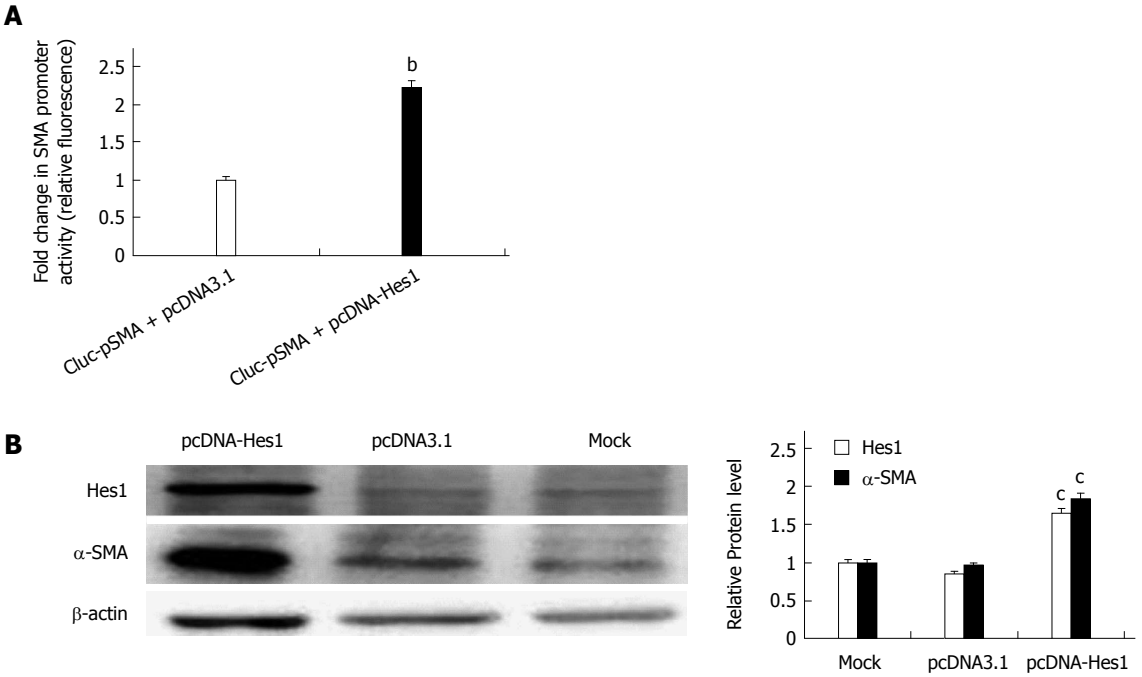

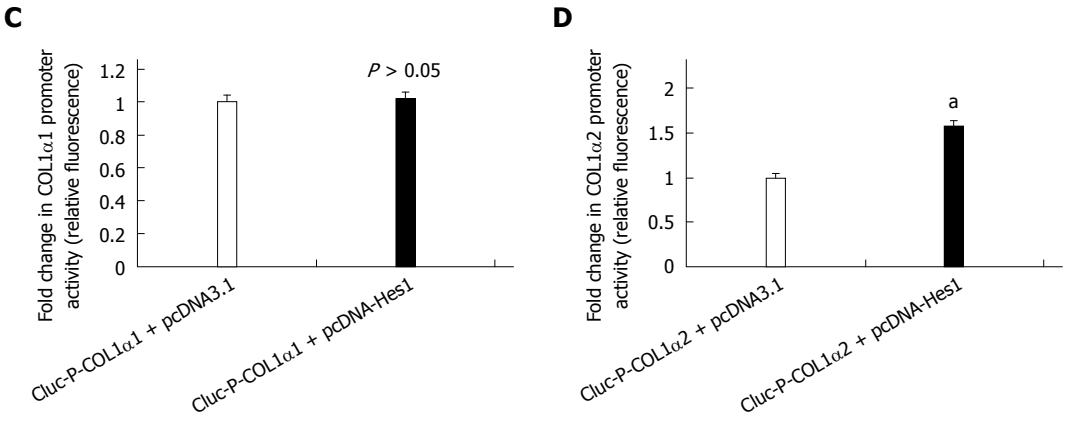

Figure 3 Over-expression of the Notch target gene *Hes1* increases the expression of α-smooth muscle actin and Collagen1α2 in hepatic stellate cell-T6 cells but has no effect on the expression of Collagen1α1. A, C, D: Luciferase reporter assays for the promoter activities of α-SMA, COL1α1 and COL1α2 in cells transfected with pcDNA-Hes1 or empty plasmid-pcDNA3.1(+) as a control ($^aP < 0.05$, $^bP < 0.01$ *vs* the control group, $n = 8$); B: Analysis of α-SMA and Hes1 by Western blot analysis of transfected cells. The β-actin protein served as a control ($^cP < 0.05$ *vs* all the control groups). α-SMA: α-smooth muscle actin; COL1α1: Collagen1α1.

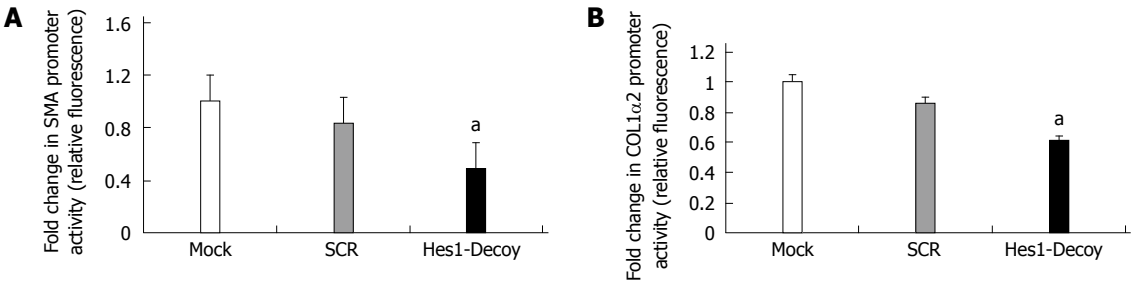

Figure 4 Inhibition of Hes1 transcription factor function by a Hes1 decoy down-regulates the promoter activities of α-smooth muscle actin and Collagen1α2 in hepatic stellate cell-T6 cells. The promoter activities of α-SMA and col1α2 decreased in cells treated with a Hes1 ODN decoy compared with the control (SCR) (A, B). ($^aP < 0.05$ *vs* the control and SCR groups, $n = 8$). α-SMA: α-smooth muscle actin; ODN: Oligodeoxynucleotide.

has an opposite effect on the activation of HSCs to that of the Notch1 receptor.

Inhibiting the function of the Hes1 transcription factor with a Hes1 ODN decoy down-regulates the expression of α-SMA and collagen1 in HSC-T6 cells

To inhibit Hes1, an ODN decoy was transfected into the HSCs. The Hes1 ODN decoy is a double-stranded DNA containing a Hes1 binding site. After the Hes1 ODN decoy was delivered into the HSC-T6 cells, the luciferase reporter activities for the pSMA and P-COL1α2 reporter constructs decreased compared with those in the control group (Scr) (Figure 4A, B). Thus, inhibiting the function of the Hes1 transcription factor in HSC-T6 cells could down-regulate the expression of α-SMA and COL1α2.

Notch1 target gene Hes1 is regulated by TGF/BMP signaling in HSC-T6 cells

It is well known that Notch1 can induce the expression of Hes1 directly in many mammalian cell types. To determine whether Notch1 up-regulates the expression of Hes1 in HSC-T6 cells, the GLuc-P-Hes1 and pcDNA3.1-NICD1 plasmids were co-transfected into HSC-T6 cells, and GLuc reporter analysis showed that the promoter activity of Hes1 was enhanced approximately 5.5-fold compared with the activity in cells transfected with the empty plasmid pcDNA3.1 (Figure 5B). At the protein level, pcDNA3.1-NICD1 also increased the expression of Hes1 based on Western blot analysis (Figure 5A). Next, we studied the relationship between the TGF-β/BMP signaling pathway and Hes1. To investigate whether the Notch pathway interacts with the TGF-β/BMP signaling pathway in HSC-T6 cells, a pcDNA3-CA-ALK3 (BMP signaling activin receptor-like kinase 3) expression vector was transfected into HSC-T6 cells, and the Notch target gene Hes1 and the TGF-β receptor were analyzed by Western blot. We found that over-expression of CA-ALK3 increased the expression of Hes1 approximately 2.5-fold (Figure 5C), while the expression of the TGF-β receptor was not altered (Figure 5C). We also obtained the same results using a luciferase reporter assay. When pcDNA3-CA-ALK3 and GLuc-P-Hes1 were co-transfected into HSC-T6 cells, the reporter activity increased approximately 2-fold compared with the control (empty vector pcDNA3.1). In addition, co-transfection with pcDNA3-CA-ALK3 and pcDNA3.1-NICD1 cooperatively enhanced the expression of Hes1 compared to transfection with pcDNA3-CA-ALK3 or pcDNA3.1-NICD1 alone in HSC-T6 cells (Figure

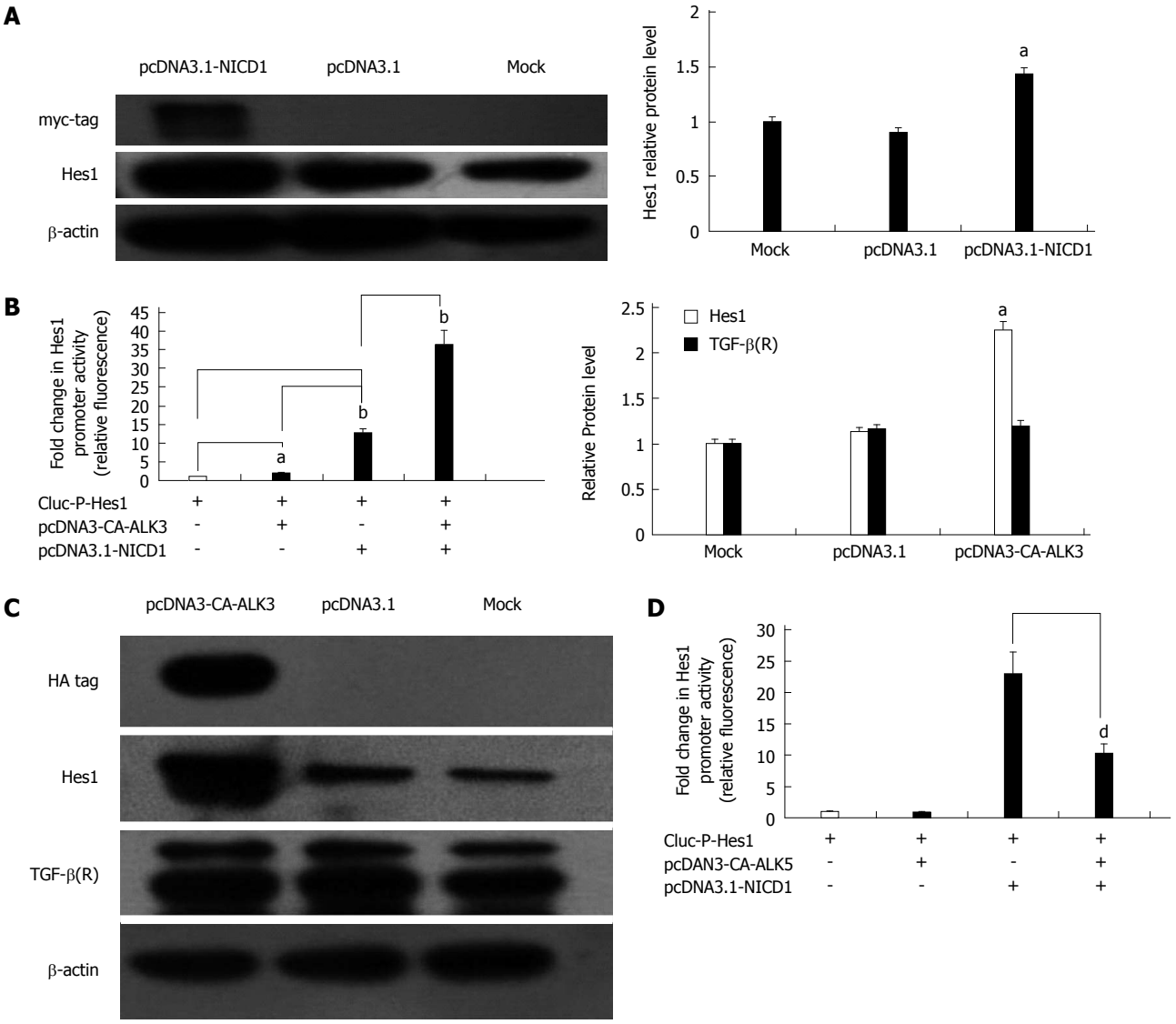

Figure 5 Notch target gene *Hes1* is regulated by the transforming growth factor-β/bone morphogenetic protein signaling pathway in hepatic stellate cell-T6 cells. A: Western blot analysis of Hes1 expression in cells transfected with pcDNA3.1-NICD1. The β-actin protein served as a control; B: Luciferase reporter assays for the Hes1 promoter in cells transfected with pcDNA3-NICD1 and/or pcDNA3-CA-ALK3 ($^aP < 0.05$, $^bP < 0.01$ *vs* all the control groups, $n = 8$); C: Analysis of Hes1 and TGF-β(R) by Western blot analysis of cells transfected with pcDNA3-CA-ALK3 with the β-actin protein as a control; D: Luciferase reporter assays for the Hes1 promoter in cells transfected with pcDNA3.1-NICD1 and/or pcDNA3-CA-ALK5 together ($^dP < 0.01$ *vs* the control group, $n = 8$). TGF: Transforming growth factor.

5B). Thus, CA-ALK3 enhances NICD1-mediated up-regulation of Hes1 in HSC-T6 cells. We also analyzed the effect of CA-ALK5, an antagonist of CA-ALK3, and found that it could not affect Hes1 expression by itself in HSC-T6 cells but reduced the effects of NICD1 on Hes1 expression (Figure 5D).

DISCUSSION

It is well accepted that HSCs play a major role in the progression of liver fibrosis because the cells can develop into myofibroblast cells that synthesize extracellular matrix proteins[22]. Thus, a better understanding of the molecular mechanisms underlying HSC activation is an important prerequisite for developing new therapeutic modalities for liver fibrosis. TGF-β signaling has been shown to be the key event in promoting fibrogenesis *in vivo* and *in vitro*; however, the development of anti-fibrotic strategies targeting the TGF-β axis is uncertain because of the pleiotropic nature of TGF-β action[23].

Notch signaling is critical for the regulation of cell differentiation, and its aberrant activation has been implicated in human fibrosis diseases. It has ben confirmed that Notch3 may regulate the activation of HSCs, but it is unknown whether other members of the Notch family, such as Notch1, Notch2 and Notch4, play a part in activating HSCs and if so, what the underlying mechanism may be[24]. In studies of the HSC niche in the rat liver, it has been found that Notch1 is involved in the regulation of β-catenin-dependent Wnt signaling and may be a marker for activated somatic stem/progenitor cells[25,26]. Some studies have also shown that, in response to inflammatory zone 1, Notch1 signaling may play a significant role in myofibroblast differentiation during lung fibrosis[14].

Thus, we hypothesized that Notch1 signaling may play an important role in liver fibrosis.

Our present study suggests that Notch1 and its target gene, Hes1, play crucial roles in liver fibrosis. Based on the evidence described above, we focused on Notch1 and its target gene Hes1 in our study. Our findings showed that Notch1 and Hes1 mRNA expression decreased upon the activation of freshly isolated HSCs, in agreement with an earlier report[27]. To investigate the effects of the Notch1 receptor and Hes1 in HSC-T6 cells, we over-expressed Notch1 and Hes1 in HSC-T6 cells and found that Notch1 inhibited α-SMA, COL1α1 and COL1α2 promoter activities, while Hes1 enhanced the α-SMA and COL1α2 promoter activities. These findings suggest that the Notch1 receptor, as an upstream gene in the Notch signaling pathway, has pleiotropic effects not displayed by its downstream target, the Hes1 transcription factor. Hes1 is a bHLH transcription factor, and Hes1 homodimers auto-inhibit their own transcription by directly binding to the N-box in the Hes1 promoter. This negative feedback leads to the rapid disappearance of the extremely unstable Hes1 protein and allows a new round of expression[16]. This negative feedback may keep expression of the Hes1 protein in a reasonable range when pcDNA3.1-NICD1 is transfected into HSCs. On the other hand, Hes1 protein expression will be much higher when pcDNA3.1-Hes1 is transfected into HSCs. Because of the pleiotropic effects of Notch1 and the negative feedback of Hes1, Notch1 may keep the Hes1 protein at a reasonable level and restrain the promoter activities of α-SMA, COL1α1 and COL1α2 in HSCs, while over-expression of Hes1 may enhance the promoter activities of α-SMA and COL1α2.

We have shown that Hes1 participated in the activation of HSCs. Thus, another important question is which factors affect Hes1 expression in HSCs. Previous studies have suggested that Notch signaling may interact with TGF-β/BMP signaling and regulate the expression of Hes1 in many cell types[16]. To determine whether a similar mechanism exists in HSC-T6 cells, we analyzed the effect of CA-ALK3 and CA-ALK5. CA-ALK3 alone increased the expression of Hes1, and more importantly, CA-ALK3 strengthened the NICD1-mediated effects on Hes1 expression in HSC-T6 cells. CA-ALK5, on the other hand, could not alone affect Hes1 expression in HSC-T6 cells, but it did reduce the effects of NICD1 on the expression of Hes1. Earlier studies suggested a mechanism in which NICD1 binds phosphorylated SMAD1/5/8 (P-SMAD1/5/8) and forms a NICD1-P-SMAD1/5/8 complex, which then migrates into the nucleus, causing the activation of the Hes1 promoter in HSC-T6 cells[28,29]. CA-ALK5 can increase SMAD2/3 phosphorylation (P-SMAD2/3) and attenuate the levels of P-SMAD1/5/8 through SMAD6, ultimately leading to a significant reduction in the NICD1-P-SMAD1/5/8 complex and inhibition of Hes1 promoter activity[16]. Thus, our results demonstrate that TGF/BMP signaling interacts with Notch1 to regulate Hes1 expression in HSC-T6 cells. Clearly, the role of Notch1 and TGF-β1/BMP signaling in the regulation of the Hes1 promoter should be further investigated.

In conclusion, Notch signaling appears to interact with TGF-β/BMP signaling and co-regulates Hes1 expression in HSCs. Notch1 may keep Hes1 protein expression at a reasonable level through Hes1 auto-negative feedback, allowing Notch1 to repress the expression of α-SMA and COL1α2. This repression is consistent with the effect of capturing Hes1 using a Hes1 ODN decoy, which could, nonetheless, reduce the effects of NICD1 on Hes1 expression. Over-expression of Hes1 *via* transfection, which bypasses the negative feedback, enhances the promoter activities of α-SMA and COL1α2. This may provide an anti-fibrotic strategy against hepatic fibrosis. Further investigations of the molecular mechanisms of Hes1-mediated regulation of α-SMA and COL1α2 should provide additional support for such an approach.

ACKNOWLEDGMENTS

We are grateful to the Institute of Molecular Biology of China, Three Gorges University, for providing us with an experimental platform, and thank Li-Li Zou for technical assistance. We thank Dr. Yun-Bo Shi of the American NIH for his helpful suggestions on the manuscript.

COMMENTS

Background

It is well known that a better understanding of the molecular mechanisms underlying hepatic stellate cell (HSC) activation is an important prerequisite for developing new therapeutic modalities for liver fibrosis. The Notch signaling pathway is critical for the regulation of cell differentiation. Recently, Notch has been implicated in human liver fibrosis diseases. It has been confirmed that Notch3 may regulate the activation of HSCs, but it is unknown whether other members of the Notch family, such as Notch1, Notch2 and Notch4, play a part in HSC activation and what the underlying mechanisms might be.

Research frontiers

During hematopoiesis and immune development, Notch is critical for T/B lineage specification and for the generation of splenic marginal zone B cells. Earlier research mainly focused on the interconnections between Notch and hematopoiesis or immune system-related molecules, aiming to find a preferable method to modulate hematopoiesis or treat immune disorders. In our paper, we explored whether Notch signaling has a function in regulating HSC activation.

Innovations and breakthroughs

This study illuminates the role of Notch1 and its target gene Hes1 in HSC activation. Furthermore, we found that Notch signaling appears to interact with transforming growth factor-β (TGF-β)/bone morphogenetic protein (BMP) signaling and co-regulates Hes1 expression in HSCs. This finding indicates that Notch1 and its target gene Hes1 may contribute to liver fibrosis by regulating HSC activation.

Applications

This study demonstrated that over-expression of Notch1 or selective interruption of Hes1 decreases the expression of myofibroblastic markers in rat hepatic stellate cells, which provides a potential novel therapeutic target for liver fibrosis.

Peer review

The submitted manuscript entitled, "*Hes1*, an important gene for activation of hepatic stellate cells, is regulated by Notch1 and TGF-β/BMP signaling" presents a very interesting study. The finding highlights the crosstalk between Notch and TGF-β/BMP signaling modules in the regulation of Hes1 in hepatic stellate cells towards the understanding of anti-fibrotic mechanism. Overall, the study is very well conceived, designed and executed as well as well written.

REFERENCES

1 **Friedman SL**. Hepatic stellate cells: protean, multifunctional, and enigmatic cells of the liver. *Physiol Rev* 2008; **88**: 125-172 [PMID: 18195085 DOI: 10.1152/physrev.00013.2007]
2 **Wells RG**. The role of matrix stiffness in hepatic stellate cell activation and liver fibrosis. *J Clin Gastroenterol* 2005; **39**: S158-S161 [PMID: 15758652 DOI: 10.1097/01.mcg.0000155516.02468.0f]
3 **Bataller R**, Brenner DA. Hepatic stellate cells as a target for the treatment of liver fibrosis. *Semin Liver Dis* 2001; **21**: 437-451 [PMID: 11586471 DOI: 10.1055/s-2001-17558]
4 **Purps O**, Lahme B, Gressner AM, Meindl-Beinker NM, Dooley S. Loss of TGF-beta dependent growth control during HSC transdifferentiation. *Biochem Biophys Res Commun* 2007; **353**: 841-847 [PMID: 17204247 DOI: 10.1016/j.bbrc.2006.12.125]
5 **Choi SS**, Diehl AM. Epithelial-to-mesenchymal transitions in the liver. *Hepatology* 2009; **50**: 2007-2013 [PMID: 19824076 DOI: 10.1002/hep.23196]
6 **Sugiyama D**, Kulkeaw K, Mizuochi C. TGF-beta-1 up-regulates extra-cellular matrix production in mouse hepatoblasts. *Mech Dev* 2013; **130**: 195-206 [PMID: 23041440 DOI: 10.1016/j.mod.2012.09.003]
7 **Weiskirchen R**, Meurer SK, Gressner OA, Herrmann J, Borkham-Kamphorst E, Gressner AM. BMP-7 as antagonist of organ fibrosis. *Front Biosci* (Landmark Ed) 2009; **14**: 4992-5012 [PMID: 19482601 DOI: 10.2741/3583]
8 **Artavanis-Tsakonas S**, Rand MD, Lake RJ. Notch signaling: cell fate control and signal integration in development. *Science* 1999; **284**: 770-776 [PMID: 10221902 DOI: 10.1126/science.284.5415.770]
9 **Iso T**, Kedes L, Hamamori Y. HES and HERP families: multiple effectors of the Notch signaling pathway. *J Cell Physiol* 2003; **194**: 237-255 [PMID: 12548545 DOI: 10.1002/jcp.10208]
10 **Kageyama R**, Ohtsuka T, Tomita K. The bHLH gene Hes1 regulates differentiation of multiple cell types. *Mol Cells* 2000; **10**: 1-7 [PMID: 10774739 DOI: 10.1007/s10059-000-0001-0]
11 **Harman BC**, Jenkinson EJ, Anderson G. Entry into the thymic microenvironment triggers Notch activation in the earliest migrant T cell progenitors. *J Immunol* 2003; **170**: 1299-1303 [PMID: 12538689 DOI: 10.4049/jimmunol.170.3.1299]
12 **Maillard I**, Adler SH, Pear WS. Notch and the immune system. *Immunity* 2003; **19**: 781-791 [PMID: 14670296 DOI: 10.1016/S1074-7613(03)00325-X]
13 **Bielesz B**, Sirin Y, Si H, Niranjan T, Gruenwald A, Ahn S, Kato H, Pullman J, Gessler M, Haase VH, Susztak K. Epithelial Notch signaling regulates interstitial fibrosis development in the kidneys of mice and humans. *J Clin Invest* 2010; **120**: 4040-4054 [PMID: 20978353 DOI: 10.1172/JCI43025]
14 **Liu T**, Hu B, Choi YY, Chung M, Ullenbruch M, Yu H, Lowe JB, Phan SH. Notch1 signaling in FIZZ1 induction of myofibroblast differentiation. *Am J Pathol* 2009; **174**: 1745-1755 [PMID: 19349363 DOI: 10.2353/ajpath.2009.080618]
15 **Fu Y**, Chang A, Chang L, Niessen K, Eapen S, Setiadi A, Karsan A. Differential regulation of transforming growth factor beta signaling pathways by Notch in human endothelial cells. *J Biol Chem* 2009; **284**: 19452-19462 [PMID: 19473993 DOI: 10.1074/jbc.M109.011833]
16 **Beets K**, Huylebroeck D, Moya IM, Umans L, Zwijsen A. Robustness in angiogenesis: notch and BMP shaping waves. *Trends Genet* 2013; **29**: 140-149 [PMID: 23279848 DOI: 10.1016/j.tig.2012.11.008]
17 **Nyhan KC**, Faherty N, Murray G, Cooey LB, Godson C, Crean JK, Brazil DP. Jagged/Notch signalling is required for a subset of TGFβ1 responses in human kidney epithelial cells. *Biochim Biophys Acta* 2010; **1803**: 1386-1395 [PMID: 20833210 DOI: 10.1016/j.bbamcr.2010.09.001]
18 **Dees C**, Zerr P, Tomcik M, Beyer C, Horn A, Akhmetshina A, Palumbo K, Reich N, Zwerina J, Sticherling M, Mattson MP, Distler O, Schett G, Distler JH. Inhibition of Notch signaling prevents experimental fibrosis and induces regression of established fibrosis. *Arthritis Rheum* 2011; **63**: 1396-1404 [PMID: 21312186 DOI: 10.1002/art.30254]
19 **Eda H**, Kulig KM, Steiner TA, Shimada H, Patel K, Park E, Kim ES, Borenstein JT, Neville CM, Keller BT. A nanofiber membrane maintains the quiescent phenotype of hepatic stellate cells. *Dig Dis Sci* 2012; **57**: 1152-1162 [PMID: 22359192 DOI: 10.1007/s10620-012-2084-9]
20 **Fujii M**, Takeda K, Imamura T, Aoki H, Sampath TK, Enomoto S, Kawabata M, Kato M, Ichijo H, Miyazono K. Roles of bone morphogenetic protein type I receptors and Smad proteins in osteoblast and chondroblast differentiation. *Mol Biol Cell* 1999; **10**: 3801-3813 [PMID: 10564272 DOI: 10.1091/mbc.10.11.3801]
21 **Nakao A**, Imamura T, Souchelnytskyi S, Kawabata M, Ishisaki A, Oeda E, Tamaki K, Hanai J, Heldin CH, Miyazono K, ten Dijke P. TGF-beta receptor-mediated signalling through Smad2, Smad3 and Smad4. *EMBO J* 1997; **16**: 5353-5362 [PMID: 9311995 DOI: 10.1093/emboj/16.17.5353]
22 **Tsukada S**, Parsons CJ, Rippe RA. Mechanisms of liver fibrosis. *Clin Chim Acta* 2006; **364**: 33-60 [PMID: 16139830]
23 **Hernandez-Gea V**, Friedman SL. Pathogenesis of liver fibrosis. *Annu Rev Pathol* 2011; **6**: 425-456 [PMID: 21073339 DOI: 10.1146/annurev-pathol-011110-130246]
24 **Chen YX**, Weng ZH, Zhang SL. Notch3 regulates the activation of hepatic stellate cells. *World J Gastroenterol* 2012; **18**: 1397-1403 [PMID: 22493555 DOI: 10.3748/wjg.v18.i12.1397]
25 **Sawitza I**, Kordes C, Reister S, Häussinger D. The niche of stellate cells within rat liver. *Hepatology* 2009; **50**: 1617-1624 [PMID: 19725107 DOI: 10.1002/hep.23184]
26 **Reister S**, Kordes C, Sawitza I, Häussinger D. The epigenetic regulation of stem cell factors in hepatic stellate cells. *Stem Cells Dev* 2011; **20**: 1687-1699 [PMID: 21219128 DOI: 10.1089/scd.2010.0418]
27 **Xie G**, Karaca G, Swiderska-Syn M, Michelotti GA, Krüger L, Chen Y, Premont RT, Choi SS, Diehl AM. Cross-talk between Notch and Hedgehog regulates hepatic stellate cell fate in mice. *Hepatology* 2013; **58**: 1801-1813 [PMID: 23703657 DOI: 10.1002/hep.26511]
28 **Larrivée B**, Prahst C, Gordon E, del Toro R, Mathivet T, Duarte A, Simons M, Eichmann A. ALK1 signaling inhibits angiogenesis by cooperating with the Notch pathway. *Dev Cell* 2012; **22**: 489-500 [PMID: 22421041 DOI: 10.1016/j.devcel.2012.02.005]
29 **Moya IM**, Umans L, Maas E, Pereira PN, Beets K, Francis A, Sents W, Robertson EJ, Mummery CL, Huylebroeck D, Zwijsen A. Stalk cell phenotype depends on integration of Notch and Smad1/5 signaling cascades. *Dev Cell* 2012; **22**: 501-514 [PMID: 22364862 DOI: 10.1016/j.devcel.2012.01.007]

P- Reviewer: Higuera-de la Tijera MF, Kovacs SJ, Parvez MK
S- Editor: Qi Y **L- Editor**: Wang TQ **E- Editor**: Liu XM

World Journal of Gastroenterology

Submit a Manuscript: http://www.wjgnet.com/esps/
Help Desk: http://www.wjgnet.com/esps/helpdesk.aspx
DOI: 10.3748/wjg.v21.i3.888

World J Gastroenterol 2015 January 21; 21(3): 888-896
ISSN 1007-9327 (print) ISSN 2219-2840 (online)

ORIGINAL ARTICLE

Basic Study

Should temporary extracorporeal continuous portal diversion replace meso/porta-caval shunts in "small-for-size" syndrome in porcine hepatectomy?

Da-Dong Wang, Yong Xu, Zi-Man Zhu, Xiang-Long Tan, Yu-Liang Tu, Ming-Ming Han, Jing-Wang Tan

Da-Dong Wang, Yong Xu, Zi-Man Zhu, Xiang-Long Tan, Yu-Liang Tu, Ming-Ming Han, Jing-Wang Tan, Department of Hepatobiliary Surgery, The First Affiliated Hospital of Chinese PLA General Hospital, Beijing 100048, China

Author contributions: Tan JW designed the research; Wang DD, Xu Y and Zhu ZM performed the research; Tan XL, Tu YL and Han MM analyzed the data; and Wang DD wrote the paper.

Correspondence to: Jing-Wang Tan, MD, Department of Hepatobiliary Surgery, The First Affiliated Hospital of Chinese PLA General Hospital, 51 FuCheng Road, Haidian District, Beijing 100048, China. jingwangtan@126.com
Telephone: +86-10-66848633
Fax: +86-10-66848634

Received: April 4, 2014
Peer-review started: April 6, 2014
First decision: June 10, 2014
Revised: July 3, 2014
Accepted: September 5, 2014
Article in press: September 5, 2014
Published online: January 21, 2015

Abstract

AIM: To investigate the feasibility of temporary extracorporeal continuous porta-caval diversion (ECPD) to relieve portal hyperperfusion in "small-for-size" syndrome following massive hepatectomy in pigs.

METHODS: Fourteen pigs underwent 85%-90% liver resection and were then randomly divided into the control group (n = 7) and diversion group (n = 7). In the diversion group, portal venous blood was aspirated through the portal catheter and into a tube connected to a centrifugal pump. After filtration, the blood was returned to the pig through a double-lumen catheter inserted into the internal jugular or subclavian vein. With the conversion pump, portal venous inflow was partially diverted to the inferior vena cava through a catheter inserted *via* the gastroduodenal vein at 100-130 mL/min. Portal hemodynamics, injury, and regeneration in the liver remnant were compared between the two groups.

RESULTS: Compared to the control group, porta-caval diversion *via* ECPD significantly mitigated excessive portal venous flow and portal vein pressure (PVP); the portal vein flow (PVF), hepatic artery flow (HAF), and PVP in the two groups were not significantly different at baseline; however, the PVF (431.8 ± 36.6 *vs* 238.8 ± 29.3, $P < 0.01$; 210.3 ± 23.4 *vs* 122.3 ± 20.6, $P < 0.01$) and PVP (13.8 ± 2.6 *vs* 8.7 ± 1.4, $P < 0.01$; 15.6 ± 2.1 *vs* 10.1 ± 1.3, $P < 0.05$) in the control group were significantly higher than those in the diversion group, respectively. The HAF in the control group was significantly lower than that in the diversion group at 2 h and 48 h post hepatectomy, and ECPD significantly attenuated injury to the sinusoidal lining and hepatocytes, increased the regeneration index of the liver remnant, and relieved damage that the liver remnant suffered due to endotoxin and bacterial translocation.

CONCLUSION: ECPD, which can dynamically modulate portal inflow, can reduce injury to the liver remnant and facilitate liver regeneration, and therefore should replace permanent meso/porta-caval shunts in "small-for-size" syndrome.

Key words: Small-for-size syndrome; Extracorporeal continuous porta-caval diversion; Massive hepatectomy; Regeneration

Core tip: Meso/porta-caval shunts have usually been adopted to relieve portal hyperperfusion in "small-for-size" syndrome (SFSS) or postoperative liver failure; however, these methods cannot dynamically adjust portal inflow to affect "functional competition". In this study, extracorporeal continuous porta-caval diversion was temporarily adopted to relieve hyperperfusion, dynamically adjust the effect of portal inflow towards functional competition, and preserve optimal portal inflow. This also reduces injury to the sinusoidal endothelium, decreases endotoxin/bacterial translocation, and facilitates liver regeneration in SFSS after massive hepatectomy, and therefore could replace permanent meso/porta-caval shunts, which have no benefit or harm towards liver regeneration in late stages.

Wang DD, Xu Y, Zhu ZM, Tan XL, Tu YL, Han MM, Tan JW. Should temporary extracorporeal continuous portal diversion replace meso/porta-caval shunts in "small-for-size" syndrome in porcine hepatectomy? *World J Gastroenterol* 2015; 21(3): 888-896 Available from: URL: http://www.wjgnet.com/1007-9327/full/v21/i3/888.htm DOI: http://dx.doi.org/10.3748/wjg.v21.i3.888

INTRODUCTION

When the residual liver volume is below a certain threshold, the liver remnant cannot sustain metabolic, synthetic, and detoxifying functions[1-4], and postoperative liver failure (PLF) or "small-for-size" syndrome (SFSS) will ensue. Portal hypertension and splanchnic pooling following major hepatectomy or a small graft have been reported to contribute to the high postoperative morbidity and mortality rates associated with these procedures[5-10]. Some studies have shown that the placement of a portal-systemic shunt or splenic artery ligation improves survival following subtotal hepatectomy or a small graft, probably as a result of decompression of the portal blood flow. However, excessive diversion or hypoperfusion by the portal-systemic shunt retards regeneration of the liver remnant or small graft[11]. In this study, extracorporeal continuous porta-caval diversion (ECPD) was temporarily adopted to relieve hyperperfusion. This system is theoretically appealing, as it can dynamically adjust portal inflow to affect functional competition between the portal vein and systemic circulation, and preserve optimal portal inflow to allow hypertrophy of the liver remnant. Following the establishment of a stable, critical pig model of 85%-90% hepatectomy, the effect of ECPD in preventing sinusoidal microcirculatory injury from portal hypertension following extended hepatectomy and its advantages was analyzed.

MATERIALS AND METHODS

Animal husbandry

Fourteen male Bama miniature pigs (15-20 kg), 4 to 6 mo of age, were obtained from the Pig and Poultry Production Institute (GuangXi province, China). The pigs were raised in a closed herd and kept under strict quarantine. All animals in this study were treated humanely and in accordance with institutional and national guidelines for ethical treatment of animals. Experiments were conducted in accordance with the Chinese legislation on the protection of animals and "Principles of laboratory animal care" (NIH publication No. 85-23, revised 1985).

Surgical technique

The pigs were food-deprived for 8 h before the operation. All pigs were anesthetized by initial sedation with a deep intramuscular injection of ketamine (15-20 mg/kg) and chlorpromazine (6-8 mg/kg), 15 min after the administration of atropine (0.01 mg/kg). An upper-midline incision with right or bilateral subcostal extensions (inverse "L" or Mercedes incision) was performed. A subtotal hepatectomy with less than 60 mL of blood loss and without hepatic pedicle occlusion was performed. The extent of the hepatectomy was referred to bench dissection of 10 pigs, according to a previous study: extended hepatectomy involving approximately 85%-90% of the liver was accomplished by 75%-80% hepatectomy plus removal of the partial posterior segment[12]. A 16-gauge double-lumen catheter was inserted into the main portal vein *via* the gastroduodenal vein, and was connected to a RM6240 physiology device (Chengdu, China) to measure the portal vein pressure (PVP). Another double-lumen catheter was advanced into the suprahepatic inferior vena cava through the internal jugular vein to monitor central vein pressure (CVP). Two ultrasonic flow probes (3 mm, 10 mm) were connected to a flow meter (HT107, Transonic Systems, Ithaca, NY, United States) to measure hepatic artery flow (HAF) and portal vein flow (PVF), respectively.

Study protocols and porta-cava diversion

The 14 animals that underwent subtotal (85%-90%) hepatectomy with less than 60 mL of blood loss and without hepatic pedicle occlusion were divided into two groups: the control group (n = 7) and the diversion group (n = 7). In the diversion group, hepatectomy was followed by ECPD. The diversion flow was 100-130 mL/min, and the room temperature was 18 to 23 ℃.

Establishing the extracorporeal catheter circuit

Portal venous blood was aspirated through the portal

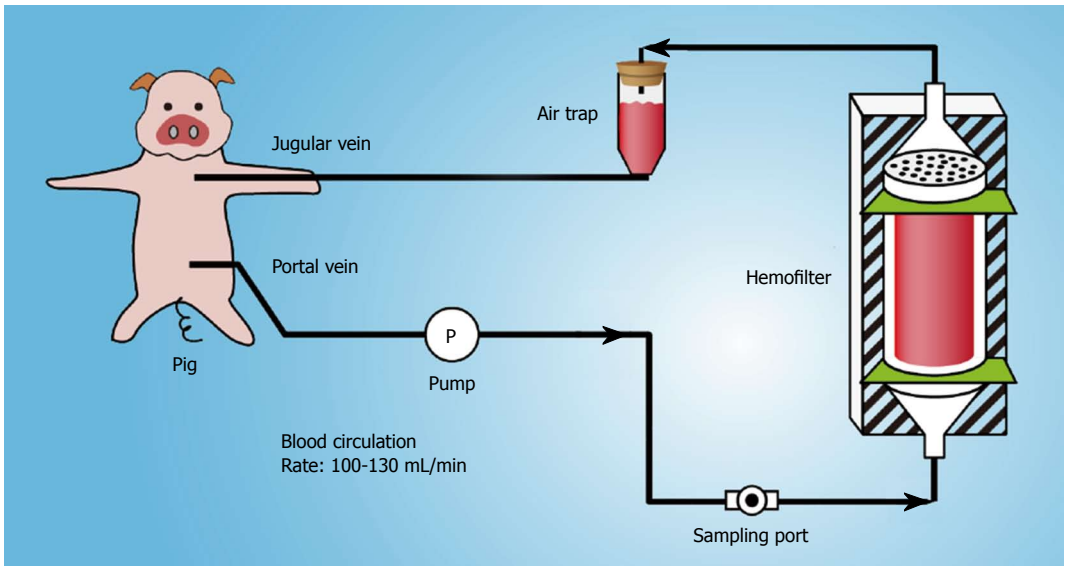

Figure 1 Schematic drawing of porta-caval diversion in the pig following hepatectomy. This system comprises a whole-blood circulation loop, conversion pump and hemofilter. In this system, blood flows directly from the pig though the portal vein and is returned to the pig *via* the jugular vein.

catheter and into a tube connected to a centrifugal pump (Plasma Separation Apparatus, Asahi Medical Co., Ltd., Japan) (Figure 1). After filtration, the blood was returned to the pig through a double-lumen catheter inserted into the internal jugular or subclavian vein. The adequacy of anticoagulation was monitored by the activated clotting time (ACT), and heparin was administered as required to maintain an ACT greater than 180 s. Standard monitoring (ECG, arterial line for blood pressure and blood gases, and Foley catheter for urine output) was performed for all pigs. With the conversion pump, the portal venous inflow was partially diverted to the inferior vena cava through a catheter inserted *via* the gastroduodenal vein at 100-130 mL/min. The portal hemodynamics, liver injury and regeneration were investigated and compared between the two groups.

Postoperative management

After the operation, one daily dose of 375 mg penicillin was given intramuscularly to all pigs, and 500 mL of normal saline and 500 mL of a 10% glucose solution were administered during recovery. Thereafter, the pigs were monitored daily until euthanasia at 49-50 h post-hepatectomy (PH). Food and water intake and serum glucose levels were evaluated at each daily postoperative assessment, and animals that had limited or no intake or low serum glucose levels (< 70-80 mg/dL) were administered 50 g of intravenous (IV) glucose (500 mL of a 10% glucose solution). At euthanasia, the liver remnant was removed, weighed, and sampled.

Hemodynamic measurement

A double-lumen catheter was placed in the internal jugular vein to monitor invasive venous pressure. The catheter was tunneled subcutaneously to exit at the back of the neck for postoperative access. A single-lumen catheter was introduced into the portal vein to monitor portal venous pressure (PVP). Ultrasonic flow probes were connected to a flow meter (HT107, Transonic Systems, Ithaca, NY, United States) to measure hepatic artery flow (HAF) and portal vein flow (PVF). PVP, HAF, and PVF were recorded at baseline, 48 h PH, and 50 h PH (stopping ECPD for 1 h), before euthanasia.

Blood and serum analysis

Serum samples were collected pre-hepatectomy and serially during the follow-up period, at 2 h, 24 h and 48 h PH. In these samples, the levels of alanine aminotransferase (ALT), total bilirubin (TB), hyaluronic acid (HA), and thymidine kinase (TK) activity were determined. HA was measured by a radiometric assay with an HA test kit (Pharmacia Diagnostics, Shanghai, China). HA is eliminated mainly in the hepatic sinusoidal endothelium; increased serum HA levels indicate sinusoidal endothelial damage[13,14]. Serum TK activity provides an index of hepatic regeneration[15,16]. TK activity was measured using the LIAISON TK assay (Jingmei Biotech Co. Ltd., Shenzhen, China).

Tissue analysis

Hepatic tissue was sampled in the two groups at 1 h PH, and each biopsy sample was divided into 2 sections. The tissue specimens for electron microscopy were fixed in 2.5% glutaraldehyde and 2% paraformaldehyde in 0.1 mol/L sodium cacodylate buffer (pH 7.3). The other set of samples was preserved in 10% neutral buffered formalin, embedded in paraffin, and stained with hematoxylin and eosin using standard histological techniques. Clusters of differentiation molecule 31 (CD_{31}) immunoglobulin helps maintain endothelial stability by interacting with other CD_{31} molecules at the extracellular border of adjacent cells. Sections of hepatic tissue were

Table 1 Characteristics of the experimental groups and hemodynamic studies

	Control group	Diversion group	*P* value
Body weight (kg)	17.4 ± 3.3	18.1 ± 3.5	0.97
Left tri-lobes (g)	351.2 ± 14.9	365.5 ± 15.8	0.81
ETL (g)	442.7 ± 18.4	457.0 ± 19.7	0.86
WRL (g)	390.7 ± 19.4	401.8 ± 20.4	0.79
ERL (g)	55.7 ± 3.8	60.8 ± 4.1	0.91
Proportion of ERL (%)	12.8 ± 2.3	13.2 ± 3.5	0.87
OT (min)	115 ± 23	121 ± 28	0.45
Blood loss (mL)	35.7 ± 13.8	45.1 ± 16.1	0.73

Data are expressed as mean ± SD. Estimated total liver weight = (weight of left tri-lobes) × 100/80. ETL: Estimated total liver weight; ERL: Estimated residual liver weight; WRL: Weight of resected liver.

immunostained with porcine anti-CD_{31} antibody (Serotec, Oxford, United Kingdom) to evaluate the integrity of the endothelial cells in the hepatic sinusoid, as previously described[17,18].

The pigs were re-opened at 48 h PH and HAF, PVF, and PVP were measured. Porta-cava conversion was stopped in the diversion group, and these parameters were measured again 1 h later. The pigs were then sacrificed, the liver excised, weighed, and processed, and hepatic tissue was sampled again from the two groups.

Increase rate of the liver remnant, PCNA index and apoptosis index

The increase rate of the liver remnant after hepatectomy was calculated using the following equation: increase rate = regenerated liver volume at sacrifice/estimated remnant liver volume at operation × 100%.

Liver samples at 48 h PH were stained for Proliferating Cell Nuclear Antigen (PCNA), a stable cell-cycle nuclear protein. The rate of DNA synthesis correlates with the rate of cell proliferation. Data are expressed as the percentage of PCNA-stained hepatocytes per total number of hepatocytes. The mean number of PCNA-stained hepatocytes per 10 high-power fields was calculated for the two groups, divided by the total cell number, and then compared.

Four-micrometer-thick sections were stained with hematoxylin and eosin and analyzed by *in situ* terminal deoxynucleotidyl transferase-mediated dUTP-biotin nick end labeling (TUNEL) using an apoptosis *in situ* detection kit (Jiamei Biotech Co. Ltd, Shenzhen, China) according to the manufacturer's instructions. For each pig, ten consecutive high-power fields were examined for counting at 400 × magnification. The apoptosis index (AI) is defined as the mean number of apoptotic cells per 10 high-power fields, and was measured for the two groups, divided by the total cell number, and then compared.

Endotoxin/bacterial translocation

LPS level: The LPS level was quantified by the limulus amebocyte lysate (LAL) assay based on the methods first introduced by Iwanaga and his colleagues[19] using the commercially available chromogenic LAL endpoint kit (Yihua BioScience Ltd.; Shanghai, China), following the manufacturer's instructions. A calculated value of 0.1 EU/mL (10 pg/mL) in the specimens was considered the threshold to be considered endotoxin positive. To control for endotoxin contamination, a sterile water sample was used as a negative control. Standards and samples were analyzed in duplicate.

Real-time polymerase chain reaction assay for bacterial DNA: DNA was isolated from the blood using the Fast DNA Spin Kit (Cat. 69506; Qiagen, United States) according to the manufacturer's instructions. Subsequently, total bacteria quantification was performed with 16S rRNA gene-targeted primers, which have demonstrated uniform success in quantifying a wide range of bacteria (49 different strains). The sequences of the universal primers were 5'-TTCCGGTTGATCCTGCCGGA-3' (forward) and 5'-GGTTACCTTGTTACGACTT-3' (reverse)[20]. Serially diluted genomic DNA from selected bacterial isolates was used as a real-time PCR control. Bacterial counts from real-time PCR are expressed as $\log_{10}$ cells per gram tissue (cells/g) mean ± SE[20,21].

Statistical analysis

All variables are expressed as mean ± SD and were compared between the two groups by the Student's *t*-test, using the PASW Statistics 18 software (SPSS Inc., Chicago, IL, United States). *P*-values < 0.05 were considered significant.

RESULTS

Operative outcomes and hemodynamic studies

The operative outcomes of the two groups were not significantly different, as shown in Table 1. The evolution of hemodynamic parameters is shown in Table 2. The PVF, HAF, and PVP in the two groups were not significantly different at baseline. However, at other time points, the PVF and PVP in the control group were significantly higher than those in the diversion group ($P < 0.01$). The HAF in the control group was significantly lower than that in the diversion group ($P < 0.05$).

Blood and serum analysis

Hepatocellular injury: The preoperative and serial postoperative measurements of serum ALT and total bilirubin (TB) are shown in Figure 2A, B, with significant differences noted. There were no significant differences between the two groups before the operation or at 2 h PH ($P > 0.05$). At other time points, the control group showed significantly elevated values compared to the diversion group ($P < 0.05$).

Endothelial cell injury

In the control group, HA levels were significantly higher than those in the diversion group (Figure 3, $P < 0.05$). There was significant endothelial denudation, sinusoidal dilation, hydropic changes in hepatocytes, and hemorrhage into the hepatic parenchyma (Figure 3A).

Table 2 Serial changes in portal vein flow, hepatic artery flow and portal vein pressure

	Control group	Diversion group	*P* value
PVF, mL/min per 100 g			
BAS	61.9 ± 9.6	64.1 ± 10.6	0.87
2 h PH	431.8 ± 36.6	238.8 ± 29.3	< 0.01
48 h PH (re-open)	210.3 ± 23.4	122.3 ± 20.6	< 0.01
Pre-EUT[1]	204.5 ± 21.4	211.4 ± 26.3	0.94
HAF, mL/min per 100 g			
BAS	19.4 ± 4.5	19.9 ± 4.1	0.96
2 h PH	6.1 ± 2.5	14.9 ± 2.5	< 0.01
48 h PH (re-open)	5.5 ± 2.1	13.2 ± 4.2	0.011
Pre-EUT[1]	5.3 ± 2.0	11.2 ± 3.4	0.014
P/A			
BAS	3.1 ± 0.2	3.4 ± 0.2	0.89
2 h PH	74.0 ± 8.1	14.8 ± 3.1	0.01
48 h PH	40.8 ± 6.6	9.5 ± 1.8	< 0.01
Pre-EUT[1]	41.3 ± 6.3	19.1 ± 2.5	< 0.01
PVP, mmHg			
BAS	6.4 ± 1.8	6.0 ± 0.8	0.94
2 h PH	13.8 ± 2.6	8.7 ± 1.4	< 0.01
48 h PH	15.6 ± 2.1	10.1 ± 1.3	0.021
Pre-EUT[1]	15.1 ± 1.9	11.4 ± 1.8	0.032

[1]ECPD was stopped for 1 h. This table depicts the changes in hemodynamic parameters measured at baseline, 1 h, and 48 h PH and before euthanasia in the two groups of animals. All flow values are reported in mL/min per 100 g hepatic tissue. NS: Not significant; BAS: Baseline; EUT: Euthanasia; HAF: Hepatic artery flow; P/A: Portal-to-arterial flow ratio; PR: Portal reperfusion; PVF: Portal vein flow; PVP: Portal vein pressure; HAF: Hepatic artery flow.

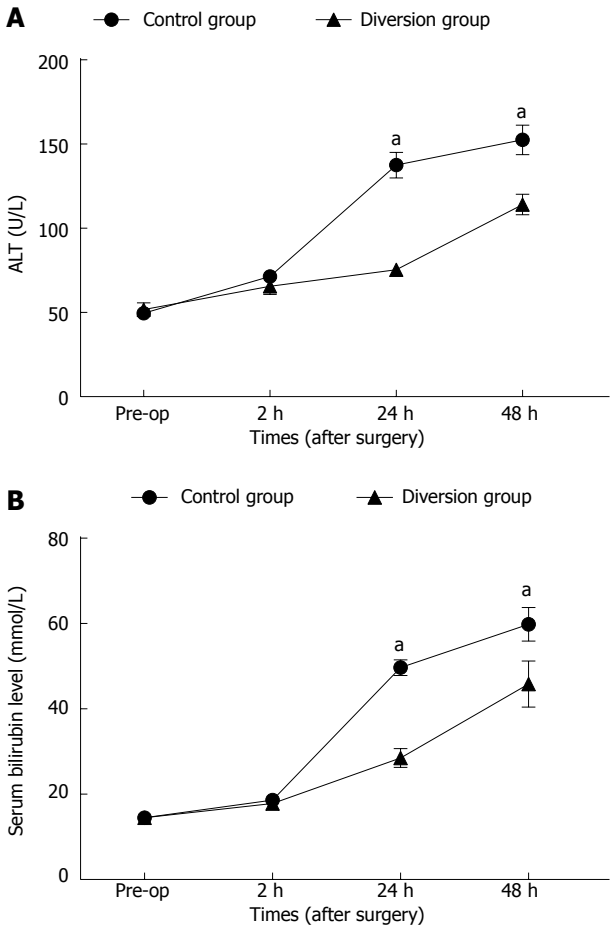

Figure 2 Change in alanine aminotransferase levels and bilirubin levels in the two groups. [a]*P* < 0.05, diversion group *vs* control group.

The sinusoidal endothelial lining was partially destroyed and detached into the sinusoidal space, with enlargement of the Disse's spaces (Figure 3C, arrowheads). CD_{31} immunostaining showed significant destruction of the endothelial lining (Figure 3E). In contrast, in the diversion group, there was no intraparenchymal hemorrhage (Figure 3B), the sinusoidal endothelial cells and hepatocytes were well-preserved, and the structure of the endothelial lining was visible (Figure 3D, arrows). Furthermore, CD_{31} immunostaining showed a mild sinusoidal microarchitecture injury in the diversion group (Figure 3F).

DISCUSSION

Portal hyper-reperfusion following subtotal hepatectomy, in which the vascular bed of the liver remnant experiences a drastic decrease, has been demonstrated in animal experiments and clinical settings[3-5]. It has been reported to contribute to the high postoperative morbidity and mortality rates[3,6-10], *via* reduction in reticuloendothelial function[21], bacterial translocation[22], hepatic ischemia, and sepsis caused by small bowel infarction[23]. In many reports[24-26], to decompress portal hypertension in clinical or experimental settings, inflow modulations have been used, including a mesocaval or portacaval shunt (MCS/PCS)[8,24,27] and splenectomy or splenic-artery ligation[26,28,29]. These methods for portal decompression improved the prognosis of small grafts or liver remnants. Interestingly, there seems to be a reverse trend from the use of right-liver grafts to the use of left-liver grafts because of these inflow modifications. However, these techniques have many shortcomings, including surgical procedure-related complications[26,28-30] and the potential risk of excessively diverting the portal flow to systemic circulation, which could retard liver regeneration[8,26,28].

In fact, it has been demonstrated in our previous study, also in the clinical setting, that it is difficult to define the size of the PCS or MCS[18]. When a small-diameter shunt was selected, thrombus of the orifice often occurred and the shunt closed. In such cases, the pigs with extended hepatectomy did not benefit from the portal decompression. In cases where a large PCS was placed, the PVP decreased and the liver remnant failed to regenerate because of poor portal flow, due to "functional competition" between the portal vein and systemic circulation. Thus, an excessive decrease in PVP was as harmful to liver regeneration as high portal-vein pressure. In order to attain an optimum PVF with dynamic regulation following an extended hepatectomy, a partial, transient diversion of portal flow (that is, ECPD) might be beneficial to adjust the portal flow to affect "functional competition". In this study, ECPD was used to optimize portal inflow by regulating the conversion flow. It has

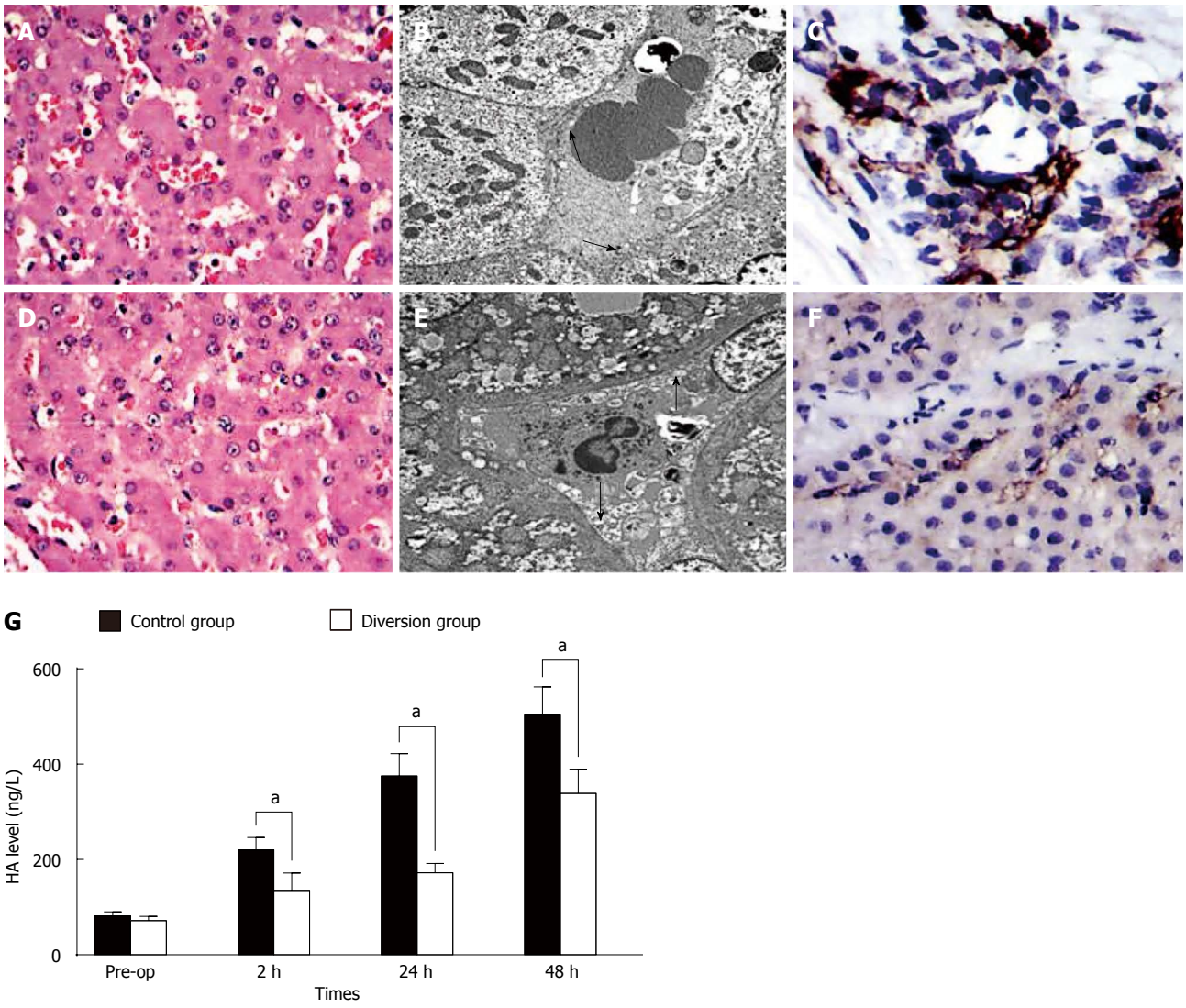

Figure 3 Sinusoidal endothelium. A, B: HE (magnification × 400); C, D: Transmission electron microscopy photographs (magnification × 6K); E, F: CD_{31} immunohistochemical staining of tissue samples taken at 1 h post hepatectomy; G: Serial changes in the hyaluronic acid level in the two groups. The arrows and the arrowheads indicate the injuried sinusoidal endothelial cells.

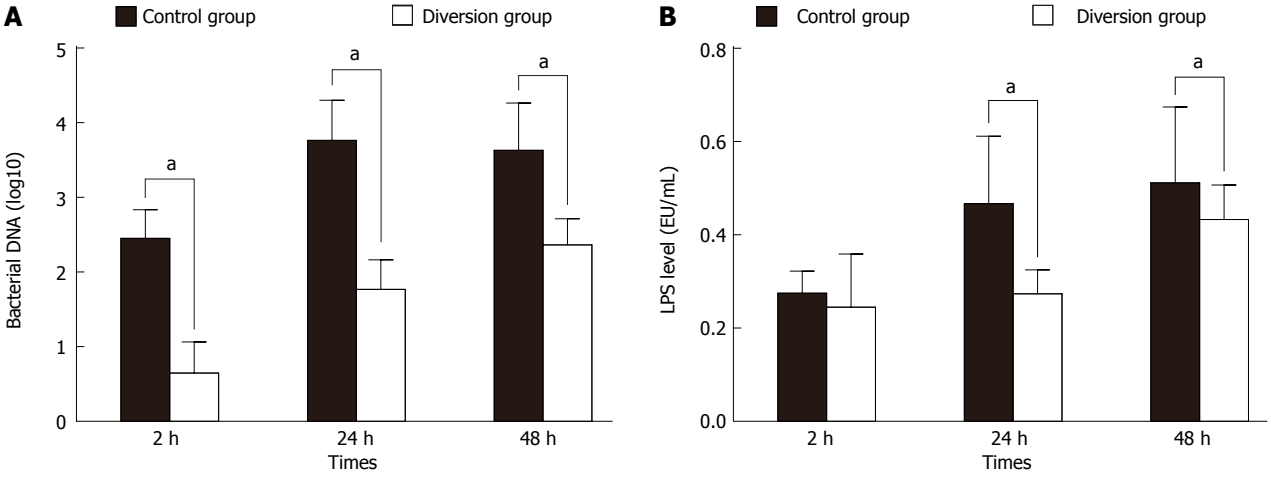

Figure 4 Serial changes in the levels of lipopolysaccharide and bacterial DNA detected in serum in the two groups (A, B). The serum lipopolysaccharide level in the control group was not significantly different at 2 h post hepatectomy (PH) ($P > 0.05$), but was significantly higher than that in the diversion group at 24 h and 48 h PH. At all time points, bacterial DNA levels in the control group were significantly elevated compared with the diversion group. $^{a}P < 0.05$, diversion group *vs* control

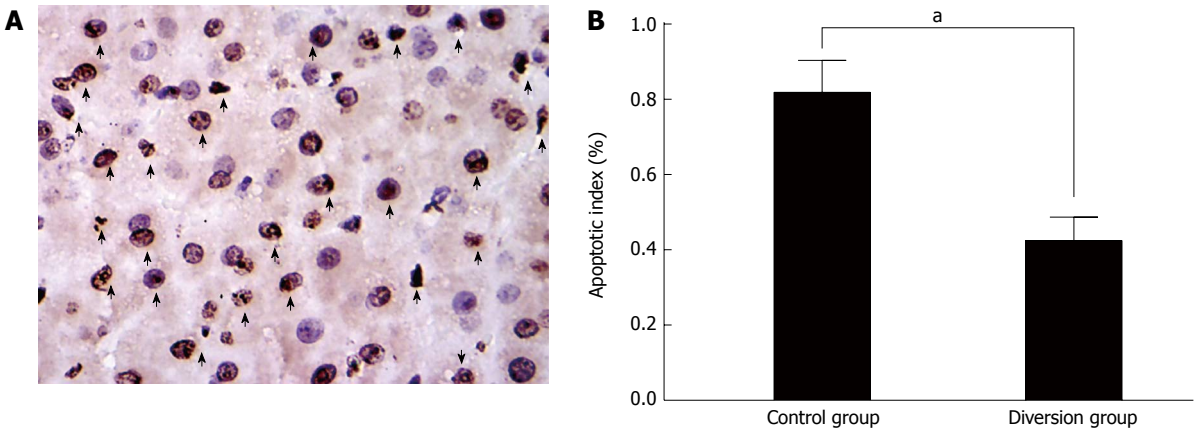

Figure 5 Portal hyperperfusion. A: Transferase-mediated dUTP-biotin nick end labeling (TUNEL) staining after hepatectomy 48 h post hepatectomy (PH). A large number of TUNEL-positive cells (arrows, identified morphologically by dark brown staining nuclei) are present in the liver remnant; 400 × magnification; B: Microphotometric evaluation of apoptotic index (AI) in TUNEL-stained tissue 48 h PH. Values are expressed as means ± SD; $n = 6$ in both groups. The differences between the groups are statistically significant. $^aP < 0.05$, diversion group *vs* control group.

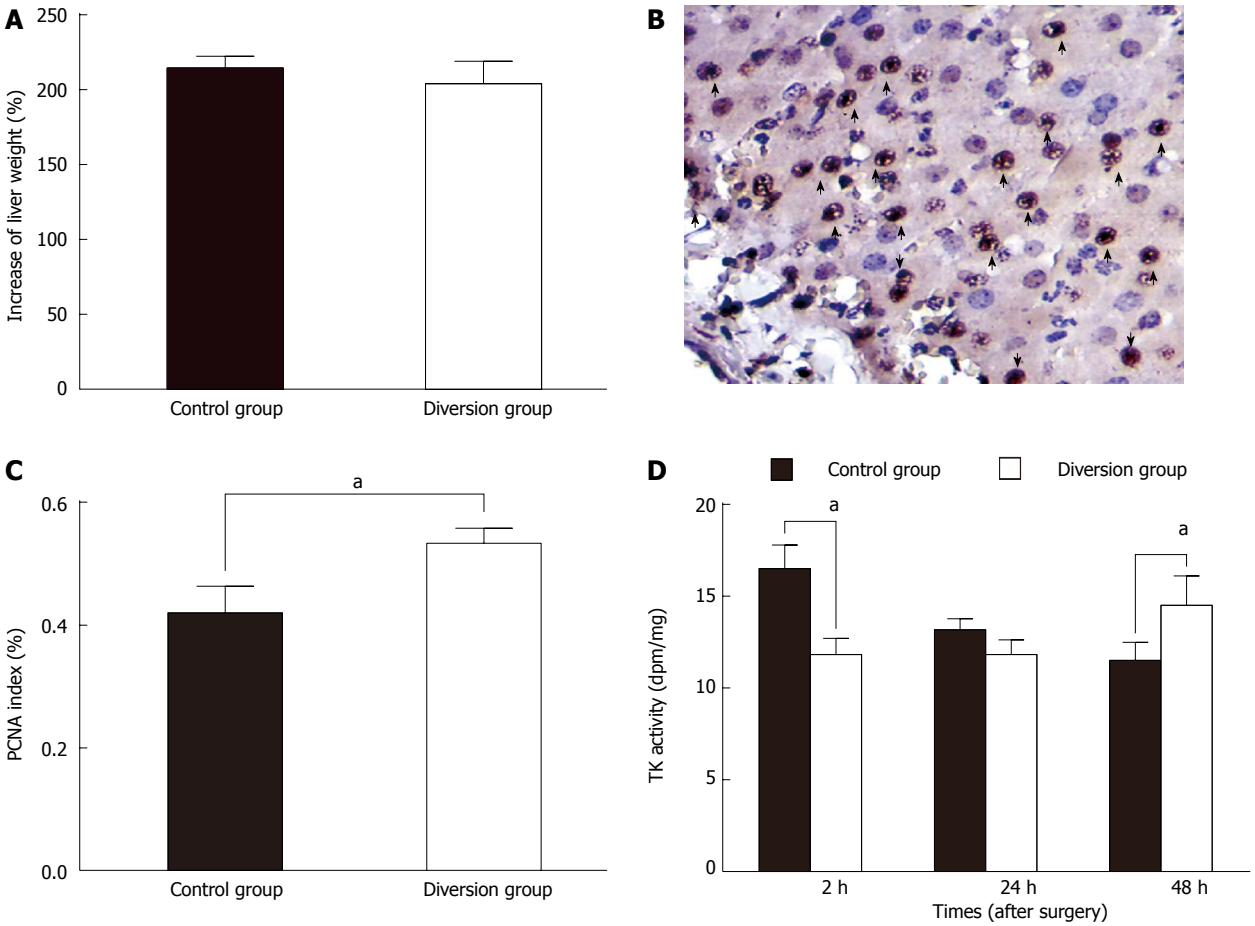

Figure 6 This indicated that the hyperperfusion could be relieved in a short time, which can be attributed to rapid regeneration of the liver remnant after massive hepatectomy. A: Increase rate of the liver remnant in both groups at 48 h PH (post hepatectomy). There was no significant difference between the control and diversion groups (P = NS); B: Proliferation cell nuclear antigen (PCNA) staining in the liver remnant (positive cells identified by dark-brown-stained nuclei, indicated by arrows; magnification × 400); C: Microphotometric evaluation of PCNA index in PCNA-stained tissue at 48 h PH. Values are expressed as means ± SD for both groups; D: The change in thymidine kinase (TK) activity in both groups. TK activity in the control group was significantly elevated compared with the diversion group at 2 h PH ($P = 0.04$), but there was no significant difference between the groups at 24 h PH (P = NS). However, TK activity in the control group was significantly reduced compared to that in the diversion group at 48 h PH. $^aP < 0.05$, diversion group *vs* control group. NS: Not significant.

been reported that approximately triple the baseline portal venous inflow following a 70% hepatectomy[7] optimally promotes liver regeneration. In this study, the portal inflow in the diversion group was easily adjusted

to 3.0-3.5 times the baseline inflow, and liver regeneration parameters were similar to the control group without portal decompression (Figure 4). However, in the diversion group, vascular shear stress in the portal vein (a determining factor in regeneration) was significantly lower than that in the control group. Moreover, the damage to hepatic parenchyma (Figure 2) and sinusoidal endothelium (Figure 3) with portal hyperperfusion, and the AI in the diversion group were significantly reduced compared with the control group (Figure 5).

However, after diverting the portal flow to the systemic circulation for 48 h, the liver volume rose to more than twice the postoperative residual volume (Figure 4A), and the PVP approached its baseline value (Table 2). When the ECPD was stopped, the PVP rose only slightly (Table 1). This indicated that the hyperperfusion could be relieved in a short time, which can be attributed to rapid regeneration of the liver remnant after massive hepatectomy (Figure 6). Therefore, with regard to portal hyperperfusion in massive hepatotectomy, ECPD sometimes only needs to be adopted for a short time.

It was shown previously that innate immunity is significantly impaired after liver surgery; RES function greatly decreases after major hepatectomy[6,7]. However, portal hypertension may also cause endotoxin absorption and an increase in bacterial translocation, causing a rise in the serum endotoxin level and severe inflammation[31,32]. In this study, the serum endotoxin level and bacterial DNA in the diversion group with ECPD were significantly depressed compared to the control group without portal decompression, indicating that portal hypertension may aggravate endotoxin absorption or bacterial translocation (Figure 4). Therefore, ECPD provides an important strategy to improve liver regeneration by reducing LPS/bacterial translocation.

Continuous hemofiltration/hemodiafiltration is a routine clinical treatment used as renal replacement in critically ill patients[33]. The placement of a catheter in the portal vein makes ECPD feasible and safe. In clinical major hepatectomy or living donor liver transplantation, the catheter may be inserted *via* the gastroepiploic vein into the portal vein, using omental wrapping of the catheter tube to prevent bleeding while removing the catheter. Alternatively, the catheter can be inserted percutaneously. According to the present study, a catheter placed into a portal vein in major hepatectomy with a high risk of PLF may permit the dynamic monitoring or relief of portal hyperperfusion. Therefore, once high portal pressure is detected, ECPD is a viable alternative method to prevent or treat portal hyperperfusion in PLF or SFSS; moreover, this could be personalized and extracorporeal blood flow can be changed depending on the parameters measured *in vivo*.

Overall, ECPD can effectively relieve hyperperfusion in SFSS or PLF, and can dynamically adjust portal flow to the functional competition between the portal vein and systemic circulation, positioning it as an alternative to SFSS in clinical settings. In the future, this experimental model could still be improved, so that it could be personalized and extracorporeal blood flow can be changed depending on the parameters measured *in vivo* in each animal, which could aid its adoption towards clinical use.

COMMENTS

Background

Portal hypertension and splanchnic pooling following major hepatectomy or a small graft have been reported to contribute to high postoperative morbidity and mortality rates associated with these procedures. The placement of a portal-systemic shunt or splenic artery ligation improves survival following subtotal hepatectomy or a small graft, probably as a result of decompression of portal blood flow. However, excessive diversion or hypoperfusion by a portal-systemic shunt retards regeneration of the liver remnant or small graft, and meso/porta-caval shunts are permanent, having no benefit or harm to liver regeneration in late stages.

Research frontiers

A portal-systemic shunt is adopted to relieve portal hyperperfusion following subtotal hepatectomy or a small graft, however, it can not avoid "functional competition" between the portal vein and systemic circulation.

Innovations and breakthroughs

Meso/porta-caval shunts cannot dynamically adjust portal inflow to affect "functional competition". In this study, extracorporeal continuous porta-caval diversion (ECPD) was temporarily adopted to relieve hyperperfusion, dynamically adjusted portal inflow to affect functional competition, and preserved optimal portal inflow, which could perhaps replace permanent meso/porta-caval shunts that have no benefit or harm towards liver regeneration in late stages.

Applications

Continuous hemofiltration/hemodiafiltration is a routine clinical treatment used as a renal replacement. The placement of a catheter in the portal vein also makes ECPD feasible and safe, and could be personalized so that extracorporeal blood flow can be dynamically changed depending on parameters measured in real time.

Peer review

This article is very interesting and useful. The methodology is explained clearly and the techniques used for recording and measuring the results are right. Temporary extracorporeal continuous portal diversion is a real solution for "small-for-size" syndrome in this experimental model.

REFERENCES

1 **Lo CM**, Liu CL, Fan ST. Portal hyperperfusion injury as the cause of primary nonfunction in a small-for-size liver graft-successful treatment with splenic artery ligation. *Liver Transpl* 2003; **9**: 626-628 [PMID: 12783407 DOI: 10.1053/jlts.2003.50081]

2 **Wang H**, Ohkohchi N, Enomoto Y, Usuda M, Miyagi S, Masuoka H, Sekiguchi S, Kawagishi N, Fujimori K, Sato A, Satomi S. Effect of portocaval shunt on residual extreme small liver after extended hepatectomy in porcine. *World J Surg* 2006; **30**: 2014-2022; discussion 2023-2024 [PMID: 16927066 DOI: 10.1007/s00268-005-0294-4]

3 **Oliver RH**, Sutton PM. The effects of partial hepatectomy on portal pressure in rats. *Br J Surg* 1966; **53**: 138-141 [PMID: 4952331]

4 **Lee SS**, Hadengue A, Girod C, Braillon A, Lebrec D. Reduction of intrahepatic vascular space in the pathogenesis of portal hypertension. In vitro and in vivo studies in the rat. *Gastroenterology* 1987; **93**: 157-161 [PMID: 3582902]

5 **Campos BD**, Botha JF. Strategies to optimize donor safety with smaller grafts for adult-to-adult living donor liver transplantation. *Curr Opin Organ Transplant* 2012; **17**: 230-234 [PMID: 22569511 DOI: 10.1097/MOT.0b013e32835365b2]

6 **Schindl MJ**, Redhead DN, Fearon KC, Garden OJ, Wigmore

SJ. The value of residual liver volume as a predictor of hepatic dysfunction and infection after major liver resection. *Gut* 2005; **54**: 289-296 [PMID: 15647196 DOI: 10.1136/gut.2004.046524]
7 **Sirinek KR**, Thomford NR. The effect of vasopressin on portal hypertension following hepatectomy. *Surg Gynecol Obstet* 1974; **139**: 573-577 [PMID: 4419573]
8 **Boillot O**, Delafosse B, Méchet I, Boucaud C, Pouyet M. Small-for-size partial liver graft in an adult recipient; a new transplant technique. *Lancet* 2002; **359**: 406-407 [PMID: 11844516 DOI: 10.1016/S0140-6736(02)07593-1]
9 **Fukuchi T**, Hirose H, Onitsuka A, Hayashi M, Senga S, Imai N, Shibata M, Yamauchi K, Futamura N, Sumi Y. Effects of portal-systemic shunt following 90% partial hepatectomy in rats. *J Surg Res* 2000; **89**: 126-131 [PMID: 10729240 DOI: 10.1006/jsre.1999.5810]
10 **Szawlowski AW**, Saint-Aubert B, Gouttebel MC, Astre C, Joyeux H. Experimental model of extended repeated partial hepatectomy in the dog. *Eur Surg Res* 1987; **19**: 375-380 [PMID: 3446496]
11 **Fondevila C**, Hessheimer AJ, Taurá P, Sánchez O, Calatayud D, de Riva N, Muñoz J, Fuster J, Rimola A, García-Valdecasas JC. Portal hyperperfusion: mechanism of injury and stimulus for regeneration in porcine small-for-size transplantation. *Liver Transpl* 2010; **16**: 364-374 [PMID: 20209596 DOI: 10.1002/lt.21989]
12 **Zhang XK**, Gauthier T, Burczynski FJ, Wang GQ, Gong YW, Minuk GY. Changes in liver membrane potentials after partial hepatectomy in rats. *Hepatology* 1996; **23**: 549-551 [PMID: 8617436 DOI: 10.1002/hep.510230321]
13 **Itasaka H**, Suehiro T, Wakiyama S, Yanaga K, Shimada M, Sugimachi K. Significance of hyaluronic acid for evaluation of hepatic endothelial cell damage after cold preservation/reperfusion. *J Surg Res* 1995; **59**: 589-595 [PMID: 7475005 DOI: 10.1006/jsre.1995.1209]
14 **Eriksson S**, Fraser JR, Laurent TC, Pertoft H, Smedsrød B. Endothelial cells are a site of uptake and degradation of hyaluronic acid in the liver. *Exp Cell Res* 1983; **144**: 223-228 [PMID: 6840207]
15 **McGowan JA**, Fausto N. Ornithine decarboxylase activity and the onset of deoxyribonucleic acid synthesis in regenerating liver. *Biochem J* 1978; **170**: 123-127 [PMID: 629771]
16 **Kahn D**, Stadler J, Terblanche J, van Hoorn-Hickman R. Thymidine kinase: an inexpensive index of liver regeneration in a large animal model. *Gastroenterology* 1980; **79**: 907-911 [PMID: 7419015]
17 **Couvelard A**, Scoazec JY, Feldmann G. Expression of cell-cell and cell-matrix adhesion proteins by sinusoidal endothelial cells in the normal and cirrhotic human liver. *Am J Pathol* 1993; **143**: 738-752 [PMID: 8362973]
18 **Castillo-Suescun F**, Oniscu GC, Hidalgo E. Hemodynamic consequences of spontaneous splenorenal shunts in deceased donor liver transplantation. *Liver Transpl* 2011; **17**: 891-895 [PMID: 21425432 DOI: 10.1002/lt.22304]
19 **Iwanaga S**, Morita T, Harada T, Nakamura S, Niwa M, Takada K, Kimura T, Sakakibara S. Chromogenic substrates for horseshoe crab clotting enzyme. Its application for the assay of bacterial endotoxins. *Haemostasis* 1978; **7**: 183-188 [PMID: 658779]
20 **Lane DJ**. 16S/23S rRNA sequencing. In: Stackebrandt E, Goodfellow M, editors. Nucleic acid techniques in bacterial systematics. New York: John Wiley and Sons, 1991: 115-175
21 **Such J**, Francés R, Muñoz C, Zapater P, Casellas JA, Cifuentes A, Rodríguez-Valera F, Pascual S, Sola-Vera J, Carnicer F, Uceda F, Palazón JM, Pérez-Mateo M. Detection and identification of bacterial DNA in patients with cirrhosis and culture-negative, nonneutrocytic ascites. *Hepatology* 2002; **36**: 135-141 [PMID: 12085357 DOI: 10.1053/jhep.2002.33715]
22 **Amann RI**, Ludwig W, Schleifer KH. Phylogenetic identification and in situ detection of individual microbial cells without cultivation. *Microbiol Rev* 1995; **59**: 143-169 [PMID: 7535888]
23 **Ito T**, Kiuchi T, Yamamoto H, Oike F, Ogura Y, Fujimoto Y, Hirohashi K, Tanaka AK. Changes in portal venous pressure in the early phase after living donor liver transplantation: pathogenesis and clinical implications. *Transplantation* 2003; **75**: 1313-1317 [PMID: 12717222 DOI: 10.1097/01.TP.0000063707.90525.10]
24 **Taniguchi M**, Shimamura T, Suzuki T, Yamashita K, Oura T, Watanabe M, Kamiyama T, Matsushita M, Furukawa H, Todo S. Transient portacaval shunt for a small-for-size graft in living donor liver transplantation. *Liver Transpl* 2007; **13**: 932-934 [PMID: 17538989 DOI: 10.1002/lt.21080]
25 **Troisi R**, Ricciardi S, Smeets P, Petrovic M, Van Maele G, Colle I, Van Vlierberghe H, de Hemptinne B. Effects of hemi-portocaval shunts for inflow modulation on the outcome of small-for-size grafts in living donor liver transplantation. *Am J Transplant* 2005; **5**: 1397-1404 [PMID: 15888047 DOI: 10.1111/j.1600-6143.2005.00850.x]
26 **Ishizaki Y**, Kawasaki S, Sugo H, Yoshimoto J, Fujiwara N, Imamura H. Left lobe adult-to-adult living donor liver transplantation: Should portal inflow modulation be added? *Liver Transpl* 2012; **18**: 305-314 [PMID: 21932379 DOI: 10.1002/lt.22440]
27 **Takada Y**, Ueda M, Ishikawa Y, Fujimoto Y, Miyauchi H, Ogura Y, Ochiai T, Tanaka K. End-to-side portocaval shunting for a small-for-size graft in living donor liver transplantation. *Liver Transpl* 2004; **10**: 807-810 [PMID: 15162477 DOI: 10.1002/lt.20164]
28 **Shimada M**, Ijichi H, Yonemura Y, Harada N, Shiotani S, Ninomiya M, Terashi T, Yoshizumi T, Soejima Y, Suehiro T, Maehara Y. The impact of splenectomy or splenic artery ligation on the outcome of a living donor adult liver transplantation using a left lobe graft. *Hepatogastroenterology* 2004; **51**: 625-629 [PMID: 15143878]
29 **Kishi Y**, Sugawara Y, Akamatsu N, Kaneko J, Tamura S, Kokudo N, Makuuchi M. Splenectomy and preemptive interferon therapy for hepatitis C patients after living-donor liver transplantation. *Clin Transplant* 2005; **19**: 769-772 [PMID: 16313323 DOI: 10.1111/j.1399-0012.2005.00419.x]
30 **Konishi N**, Ishizaki Y, Sugo H, Yoshimoto J, Miwa K, Kawasaki S. Impact of a left-lobe graft without modulation of portal flow in adult-to-adult living donor liver transplantation. *Am J Transplant* 2008; **8**: 170-174 [PMID: 18021282 DOI: 10.1111/j.1600-6143.2007.02037.x]
31 **Lin RS**, Lee FY, Lee SD, Tsai YT, Lin HC, Lu RH, Hsu WC, Huang CC, Wang SS, Lo KJ. Endotoxemia in patients with chronic liver diseases: relationship to severity of liver diseases, presence of esophageal varices, and hyperdynamic circulation. *J Hepatol* 1995; **22**: 165-172 [PMID: 7790704]
32 **Nakatani Y**, Fukui H, Kitano H, Nagamoto I, Tsujimoto T, Kuriyama S, Kikuchi E, Hoppou K, Tsujii T. Endotoxin clearance and its relation to hepatic and renal disturbances in rats with liver cirrhosis. *Liver* 2001; **21**: 64-70 [PMID: 11169075]
33 **Rimmelé T**, Kellum JA. High-volume hemofiltration in the intensive care unit: a blood purification therapy. *Anesthesiology* 2012; **116**: 1377-1387 [PMID: 22534247 DOI: 10.1097/ALN.0b013e318256f0c0]

P- Reviewer: Delgado JS, Mihaila RG, Pellicano R
S- Editor: Ma YJ **L- Editor**: Webster JR **E- Editor**: Zhang DN

World Journal of Gastroenterology

Submit a Manuscript: http://www.wjgnet.com/esps/
Help Desk: http://www.wjgnet.com/esps/helpdesk.aspx
DOI: 10.3748/wjg.v21.i3.897

World J Gastroenterol 2015 January 21; 21(3): 897-904
ISSN 1007-9327 (print) ISSN 2219-2840 (online)

ORIGINAL ARTICLE

Case Control Study

Genetic association of apolipoprotein E polymorphisms with inflammatory bowel disease

Ebtissam Saleh Al-Meghaiseeb, Mulfi Mubarak Al-Otaibi, Abdulrahman Al-Robayan, Reem Al-Amro, Ahmd Saad Al-Malki, Misbahul Arfin, Abdulrahman K Al-Asmari

Ebtissam Saleh Al-Meghaiseeb, Mulfi Mubarak Al-Otaibi, Abdulrahman Al-Robayan, Reem Al-Amro, Ahmd Saad Al-Malki, Department of Gastroenterology, Prince Sultan Military Medical City, Riyadh 11159, Saudi Arabia
Misbahul Arfin, Abdulrahman K Al-Asmari, Research Center, Prince Sultan Military Medical City, Riyadh 11159, Suadi Arabia
Author contributions: Al-Meghaiseeb ES, Al-Robayan A, Al-Otaibi MM, Al-Amro R and Al-Malki AS performed clinical examinations; Al-Meghaiseeb ES and Al-Robayan A collected demographic data; Al-Otaibi MM, Al-Amro R and Al-Malki AS searched the literature; Arfin M analyzed genotyping results and drafted the manuscript; and Al-Asmari AK designed the study, supervised and edited the manuscript.
Supported by KACST Project# 11-MED2204-21.

Correspondence to: Abdulrahman K Al-Asmari, Senior Consultant and Director of Research Center, Prince Sultan Military Medical City, P.O. Box 7897, Riyadh 11159, Saudi Arabia. abdulrahman.alasmari@gmail.com
Telephone: +966-1-4777714
Fax: +966-1-4777714
Received: June 2, 2014
Peer-review started: June 3, 2014
First decision: June 27, 2014
Revised: August 28, 2014
Accepted: September 29, 2014
Article in press: September 30, 2014
Published online: January 21, 2015

Abstract

AIM: To study the association of apolipoprotein E (APOE) polymorphisms with the susceptibility of inflammatory bowel disease (IBD) in Saudi patients.

METHODS: APOE genotyping was performed to evaluate the allele and genotype frequencies in 378 Saudi subjects including IBD patients with ulcerative colitis (n = 84) or Crohn's disease (n = 94) and matched controls (n = 200) using polymerase chain reaction and reverse-hybridization techniques.

RESULTS: The frequencies of the APOE ε2 allele and ε2/ε3 and ε2/ε4 genotypes were significantly higher in IBD patients than in controls ($P < 0.05$), suggesting that the ε2 allele and its heterozygous genotypes may increase the susceptibility to IBD. On the contrary, the frequencies of the ε3 allele and ε3/ε3 genotype were lower in IBD patients as compared to controls, suggesting a protective effect of APOE ε3 for IBD. The prevalence of the ε4 allele was also higher in the patient group compared to controls, suggesting that the ε4 allele may also increase the risk of IBD. Our results also indicated that the APOE ε4 allele was associated with an early age of IBD onset. No effect of gender or type of IBD (familial or sporadic) on the frequency distribution of APOE alleles and genotypes was noticed in this study.

CONCLUSION: APOE polymorphism is associated with risk of developing IBD and early age of onset in Saudi patients, though further studies with a large-size population are warranted.

Key words: Apolipoprotein E; Polymorphism; Inflammatory bowel disease; Saudi

Core tip: This study shows apolipoprotein E (APOE) polymorphism is associated with risk of developing inflammatory bowel disease (IBD) in Saudi patients.

Allele ε2 and its heterozygous genotypes increase the susceptibility to IBD, whereas the ε3 allele and ε3/ε3 genotype are protective for IBD. The APOE ε4 allele also increases the risk for IBD and is associated with early age at onset. The frequency distribution of APOE alleles and genotypes is not affected by gender or type of IBD (familial or sporadic).

Al-Meghaiseeb ES, Al-Otaibi MM, Al-Robayan A, Al-Amro R, Al-Malki AS, Arfin M, Al-Asmari AK. Genetic association of apolipoprotein E polymorphisms with inflammatory bowel disease. *World J Gastroenterol* 2015; 21(3): 897-904 Available from: URL: http://www.wjgnet.com/1007-9327/full/v21/i3/897.htm DOI: http://dx.doi.org/10.3748/wjg.v21.i3.897

INTRODUCTION

The inflammatory bowel diseases (IBDs), encompassing Crohn's disease (CD; OMIM 266600) and ulcerative colitis (UC; OMIM 191390), are chronic inflammatory disorders of the gastrointestinal tract. IBD has emerged as a global disease with increasing incidence and prevalence in different parts of the world[1-5]. The precise etiology of IBD is still unknown, but available evidence suggests that it is a complex multifactorial disease in which immune dysregulation caused by genetic and/or environmental factors plays an important role[6-8]. IBD appears to be caused by immunogenic responses against environmental factors and/or microbes inhabiting the distal ileum and colon of genetically susceptible hosts.

The incidence of IBD is higher in North America and Europe than in Asia and Africa, possibly due to the variation in environmental factors and genetic makeup. The hygiene hypothesis was suggested to be responsible for the rising prevalence of various autoimmune and inflammatory disorders in developed populations, which are thought to result from the lack of early exposure to bacterial infections due to good sanitary conditions[9]. The changes in dietary and intestinal microbial milieu are thought to play a key pathogenic role in the etiology of IBD, however the precise environmental factors influencing IBD prevalence have not been determined yet[10]. Intriguingly, the characteristics of Western and Asian IBD patients differ in epidemiology, phenotype and genetic susceptibility[11-14], highlighting ethnic variations.

Various epidemiologic and population-based studies have indicated that genetic factors contribute to the pathogenesis of IBD[15-17]. Apolipoprotein E (APOE) has an important role in cholesterol and lipid metabolism, and has also been shown to alter both innate and adaptive immune responses[18]. Several studies have indicated that APOE inhibits the production of T lymphocytes and regulates immune reactions by interacting with several cytokines[19-21]. Further, it has been suggested that APOE plays a key role in regulating immune response in various autoimmune diseases[22-24].

The gene encoding APOE is located on chromosome 19. It has 3 polymorphic alleles (ε2, ε3 and ε4) differing from one another by the presence of either a C or T nucleotide at codons 112 and 158. These alleles encode three different isoproteins differing significantly in structure and function, including receptor binding capacity and lipid metabolism[25]. By different combinations of these three alleles, six genotypes (ε2/ε2, ε3/ε3, ε2/ε3, ε3/ε4, ε2/ε4, and ε4/ε4) are formed[26,27]. Although the frequency of these alleles/genotypes varies significantly among different ethnic populations, APOE ε3/ε3 is the most common genotype and ε3 the most predominant allele in majority of the population[28,29]. Several studies have indicated an association between APOE alleles and genotypes with onset and severity of various autoimmune diseases[24,30-33]. Recently, association of APOE allele/genotype with UC has been reported in Chinese patients[34,35]. In this study, we examined the APOE allele/genotype frequencies in Saudi CD and UC patients and matched controls.

MATERIALS AND METHODS

Subjects

A total of 378 Saudi subjects including 178 IBD patients visiting the Gastroenterology Clinic and 200 age- and sex-matched healthy donors visiting the community health clinic of Prince Sultan Military Medical City, Riyadh were recruited in this study. Venous blood was collected from all the patients and controls. IBD patients were divided into familial (n = 20) and sporadic (n = 158) forms. They were grouped into patients with CD (n = 94, including 56 men and 38 women) with a mean age of 32 years (range: 17-65 years), and patients with UC (n = 84, including 34 men and 50 women) with mean age of 34 years (range: 22-68 years). Two hundred healthy Saudis (120 men and 80 women) were included in the study as controls. None of the controls had any history of IBD, diabetes, rheumatoid arthritis, systemic lupus erythematosus or other autoimmune diseases. The diagnoses of IBD (CD and UC) was based on the conventional endoscopic, radiologic, and histologic criteria as describe by Lennard-Jones[36]. Patient information such as age at diagnosis, disease location, disease characteristics, and extraintestinal location were used to divide the patients into groups. Patients with any other autoimmune disease or having clinical features of both UC and CD (intermediate colitis) were excluded from the study. Patients with CD were also assessed on the basis of the Montreal classification[37]. This study was approved by the ethical committee of PSMMC and written informed consent was obtained from all the subjects.

DNA extraction and genotyping

Genomic DNA was extracted from the blood of IBD patients and controls using QIAamp DNA mini kit (Qiagen, Venlo, Limburg, the Netherlands). APOE genotyping was performed using an APOE StripAssay

Table 1 Apolipoprotein E allele frequencies *n* (%)

Allele	IBD (*n* = 356)	Control (*n* = 400)	*P* value	RR	EF/PF
ε3	293 (82.30)	383 (95.75)	< 0.01	0.206	0.549
ε4	36 (10.11)	17 (4.25)	< 0.01	2.531	0.411
ε2	27 (7.59)	0 (0)	< 0.01	-	-

EF: Etiologic fraction; IBD: Inflammatory bowel disease; PF: Preventive fraction; RR: Relative risk; *n:* Number of alleles.

Table 2 Apolipoprotein E genotype frequencies *n* (%)

Genotype	IBD (*n* = 178)	Control (*n* = 200)	*P* value	RR	EF/PF
ε3/ε3	118 (66.29)	183 (91.5)	< 0.01	0.183	0.637
ε3/ε4	25 (14.05)	17 (8.5)	0.10	1.759	0.256
ε2/ε3	24 (13.48)	0 (0)	< 0.01	-	-
ε2/ε4	11 (6.18)	0 (0)	< 0.01	-	-
ε2/ε2	0 (0)	0 (0)	-	-	-
ε4/ε4	0 (0)	0 (0)	-	-	-

EF: Etiologic fraction; IBD: Inflammatory bowel disease; PF: Preventive fraction; RR: Relative risk; *n:* Number of alleles.

kit based on a PCR and reverse-hybridization technique (ViennaLab Diagnostics GmbH, Vienna, Austria). To cross-check the results, the APOE genotyping was also performed by PCR and restriction fragment length polymorphism technique as previously described[38].

Briefly, genomic DNA (200-300 ng) was amplified in 25 μL reaction tubes for 40 cycles of 94 ℃ for 30 s, 68 ℃ for 10 s, 72 ℃ for 1 min; PCR products obtained were separated by electrophoresis on 1.5% agarose gel in TAE buffer, and visualized by ethidium bromide fluorescence. Fragments with the expected size were cut from the gel, purified using a GFX PCR DNA Gel band purification kit (GE Healthcare, Little Chalfont, Buckinghamshire, UK). Purified DNA was digested with *Hha*I enzyme and separated by agarose gel electrophoresis to identify the genotype. The frequencies of various genotypes in patients and controls were determined and compared. Both the above-mentioned procedures yielded completely matching results.

Statistical analysis

Frequencies of various alleles and genotypes for APOE polymorphism were analyzed by Fisher's exact test and a $P < 0.05$ was considered as significant. The strength of the association of disease with respect to a particular allele/genotype is expressed by odd ratio interpreted as relative risk (RR) according to the method of Woolf as outlined by Schallreuter *et al*[39]. The RR was calculated only for those alleles and genotypes that were increased or decreased in IBD patients as compared to normal Saudis. RR was calculated using the following formula:

$RR = (a \times d)/(b \times c)$

Where a is number of patients expressing the allele or genotype; b is the number of patients without allele or genotype expression; c is number of controls expressing the allele or genotype; and d is the number of controls without allele or genotype expression.

The etiologic fraction (EF) indicates the hypothetical genetic component of the disease. EF values of > 0.00-0.99 are significant. It is calculated for positive associations (RR > 1) using the following formula proposed by Svejgaard *et al*[40]:

$EF = (RR-1)f/RR$, where $f = a/(a+b)$

Preventive fraction (PF) indicates the hypothetical protective effect of one allele/genotype for a disease. It is calculated for negative associations (RR < 1) using the following formula[40]:

$PF = (1-RR)f/[RR(1-f)] + f$, where $f = a/(a+b)$

Values of < 1.0 indicate the protective effect of an allele/genotype against the manifestation of disease.

RESULTS

The results of APOE genotyping in the IBD patients and the healthy controls are summarized in Tables 1, 2, 3 4 and 5. In both the IBD patient and control groups the genotype distributions were in Hardy-Weinberg equilibrium. The ε2 allele was present in 7.59% of IBD patients, while altogether absent in controls ($P < 0.01$) (Table 1). The frequency of allele ε4 was also significantly higher in patients compared with controls ($P < 0.01$), whereas the frequency of the ε3 allele was significantly lower ($P < 0.01$).

The frequency of various genotypes of APOE also showed variations in patient and control groups. The prevalences of genotypes ε2/ε3, and ε2/ε4 were 13.48, and 6.18% in patients, while totally absent in the control group ($P < 0.01$) (Table 2). The difference in the frequencies of the ε3/ε4 genotype was not statistically significant between the patient and control groups, albeit that there is a trend towards a higher frequency in IBD patients. The frequency of the ε3/ε3 genotype was significantly higher in controls than that in IBD patients ($P < 0.01$). The genotypes ε2/ε2 and ε4/ε4 were absent in both patients and controls.

The frequencies of alleles and genotypes of APOE

Table 3 Gender comparison of apolipoprotein E genotypes and alleles *n* (%)

Genotype/allele	Male (*n* = 90)	Female (*n* = 88)	*P* value
ε3/ε3	66 (73.33)	52 (59.09)	< 0.05[1]
ε3/ε4	11 (12.22)	14 (15.91)	0.52
ε2/ε3	9 (10.00)	15 (17.05)	0.19
ε2/ε4	4 (4.45)	7 (7.95)	0.36
ε3	152 (84.45)	133 (75.57)	0.04[1]
ε4	13 (7.22)	21 (11.93)	0.15
ε2	15 (8.33)	22 (12.50)	0.22

[1]Statistically significant.

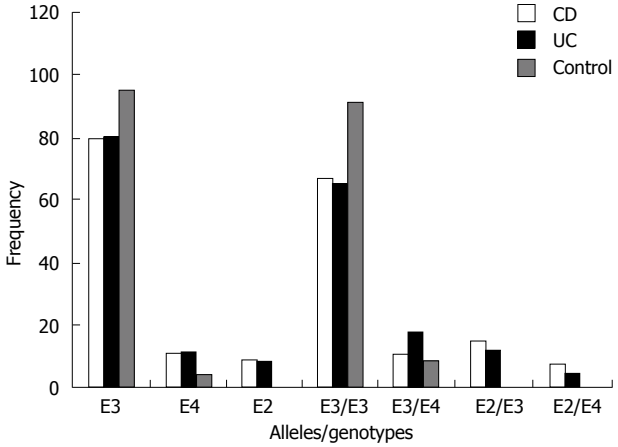

Figure 1 Comparison of apolipoprotein E genotypes and alleles in Crohn's disease and ulcerative colitis patients and controls. CD: Crohn's disease; UC: Ulcerative colitis.

polymorphism were not significantly different in male and female patients, except for the ε3 allele and homozygous ε3/ε3 genotype, which were present in significantly higher frequencies in female than male patients ($P < 0.05$) (Table 3).

The difference in the frequencies of APOE alleles and genotypes in the CD and UC patients was not significant (Table 4, Figure 1). Moreover, when compared with controls separately, an almost similar pattern was noticed for both UC and CD, except that the frequency of genotype ε3/ε4 was significantly higher in UC patients ($P = 0.03$), but not in CD patients ($P = 0.66$), as compared to controls. However, the RR values calculated for the ε3/ε4 genotype in UC and CD (RR = 2.34 and 1.28, respectively) indicated a similar positive association for both. Similarly, the stratification of IBD patients into familial and sporadic forms showed no significant difference in the frequency distribution of either alleles or genotypes of APOE (Table 5). The APOE ε4 allele was significantly associated with an early age of onset in IBD ($P \leqslant 0.05$). The groups of patients with genotype ε3/ε4 ($n = 25$), and ε2/ε4 ($n = 11$) had lower age of onset than the patients with genotype ε3/ε3 and ε2/ε3.

Table 4 Apolipoprotein E genotypes and alleles in Crohn's disease and ulcerative colitis *n* (%)

Genotype/allele	CD (*n* = 94)	UC (*n* = 84)
ε3/ε3	63 (67.02[1])	55 (65.48[1])
ε3/ε4	10 (10.64[2])	15 (17.86[1,3])
ε2/ε3	14 (14.89[1])	10 (11.90[1])
ε2/ε4	7 (7.45[1])	4 (4.76[1])
ε3	150 (79.79[1])	135 (80.36[1])
ε4	21 (11.17[1])	19 (11.31[1])
ε2	17 (9.04[1])	14 (8.33[1])

[1]$P < 0.05$ *vs* controls; [3]Relative risk = 2.34, [2]Relative risk = 1.28. CD: Crohn's disease; UC: Ulcerative colitis.

Table 5 Apolipoprotein E genotypes and alleles in familial and sporadic inflammatory bowel disease *n* (%)

Genotype/allele	Familial (*n* = 20)	Sporadic (*n* = 158)	*P* value
ε3/ε3	14 (70.00)	104 (65.82)	0.80
ε3/ε4	4 (20.00)	21 (13.30)	0.49
ε2/ε3	2 (10.00)	22 (13.92)	1.00
ε2/ε4	0 (0)	11 (6.96)	0.61
ε3	34 (85.00)	251 (79.43)	0.52
ε4	4 (10.00)	32 (10.13)	1.00
ε2	2 (5.00)	33 (10.44)	0.40

DISCUSSION

Our results showed a higher frequency of the APOE ε2 allele and predominance of ε2/ε3 and ε2/ε4 genotypes in IBD patients in comparison with matched controls, suggesting that allele ε2 carriers are at a higher risk of developing IBD. The APOE ε2 isoprotein differs from the APOE ε3 isoprotein by one amino acid, at position 158, with ε2 containing cysteine and ε3 containing arginine. This single amino acid difference causes a marked reduction in binding capacity of APOE ε2 to the low density lipoprotein family of receptors[25], which in turn results in severe metabolic disturbances, particularly type Ⅲ hyperlipidemia. Additionally, the two cysteines in APOE ε2 (positions 112 and 158) allow it to form disulfide-linked multimeric protein complexes[41]. These unique properties of APOE ε2 may contribute to its role in the etiology of IBD and other lipid-associated diseases.

Disturbances in the lipid, apolipoprotein, and lipoprotein profiles and cholesterol efflux in IBD patients have been reported[42-44]. Thus, genetic variations of apoproteins, essential in lipoprotein metabolism, may affect susceptibility to IBD. APOE is involved in transport and metabolism of cholesterol, triglyceride and other lipids. The lipid transporting and catabolic activity in APOE ε2 carriers is significantly slower compared to ε3 and ε4 carriers, due to low receptor binding affinity of ε2. Individuals with APOE ε2 are unable to efficiently clear lipids from plasma/tissues, which facilitates the

accumulation of chylomicron, very low density lipoprotein and lipids[45]. It has been suggested that APOE protein might be involved in the pathogenesis of diseases *via* the sequestration of lipids contributing to the epidermal barrier function[46].

We also observed a significantly higher frequency of the ε2/ε3 genotype in Saudi IBD patients as compared to matched controls. This genotype has been associated with significant imbalance in lipids and lipoprotein metabolism, as well as with ischemic cerebrovascular diseases[47,48]. Parameters associated with atherosclerosis, such as inflammation, carotid intima media thickness, homocysteine and insulin resistance, are increased in IBD as reported by several researchers[49-53]. In addition, several studies have suggested that IBD is a risk factor for ischemic heart diseases, including atherosclerosis[49,53,54]. Furthermore, it has been reported that IBD is an independent predictor of hypertriglyceridemia[55] and hypocholesterolemia[56].

Results of this study showed a higher frequency of the ε4 allele in patients group compared to controls, suggesting that it also may increase the risk of IBD. Similarly, a higher frequency of the ε4 allele has been reported in Chinese UC patients[34]. These authors therefore suggested that APOE ε4 confers greater risk for the development of UC in Chinese. Our results indicate that allele ε4 increases the risk for both UC and CD in Saudi patients. The ε4 allele of the APOE gene is an established risk factor for low bone mineral density[57,58], and the high frequency of APOE ε4 in UC and CD patients may be responsible for low bone mineral density in patients with UC[34,59]. To the best of our knowledge, no published report has indicated any association of APOE polymorphism with CD, and this is the first report showing a significant association with both CD and UC.

APOE is multifunctional in nature, and the presence of APOE ε4 has been associated with an enhanced inflammatory immune response[60-62]. Though the exact mechanisms by which APOE ε4 regulates the innate immune response is far from clear. Significantly higher levels of the pro-inflammatory cytokines tumor necrosis factor-α and interleukin-6 have been reported in animals expressing the ε4 allele compared to those with the ε3 allele[60]. Increased oxidative stress in the APOE ε4 cells has been suggested to contribute to higher cytokine production by enhancing the activation of nuclear factor-κB[63]. Moreover, increased expression of interleukin-1β, macrophage inflammatory protein (MIP)-1α, and tumor necrosis factor-α, as well as the transactivation of nuclear factor-κB, have been observed in APOE ε4 macrophages[64]. Recently Li *et al*[34] postulated that the epistatic interaction of MIP-1α and APOE polymorphism may contribute to individual variation in MIP-1α levels in mucosa of UC patients.

Our results also indicate that the APOE ε4 allele is associated with early age at onset of IBD. Polymorphism in the APOE gene has been defined as a modifying factor for age at onset in neurodegenerative and autoimmune diseases[30,65,66]. Our results are also in accordance with various reports showing an association of the ε4 allele with early onset of some autoimmune and neurodegenerative diseases[30,64,67,68]. The APOE ε4 allele is believed to be responsible for reducing high-density lipoprotein and increasing low-density lipoprotein in high-fat intake individuals[69], which are critical risk factors for occlusive lipid disorders. The implication of APOE ε4 in lipid metabolism and development of immunologic responses to lipid antigens may contribute to IBD in Saudis with high-fat intake as reported earlier for psoriasis[70-72]. APOE ε4 has also been linked to lower C-reactive protein, and it has been suggested that this effect is a consequence of intrinsic functional differences among the ε2, ε3, and ε4 APOE proteins in plasma[73]. Our results also show that association of APOE polymorphism was not affected by the sex of the host and the association was similar in both CD and UC.

In conclusion, this study shows a significant relation between APOE polymorphisms and IBD. The ε2 allele is associated with increased susceptibility for IBD, whereas the ε3 allele may be protective for IBD in Saudis. In addition, the ε4 allele may be a risk factor of severity or early onset of IBD. However, this association of APOE polymorphisms with the risk of IBD warrants further studies with a larger population. Similar studies on different ethnic populations will be helpful in defining the role of APOE as a putative pharmacologic target for IBD.

ACKNOWLEDGMENTS

The authors thank S. Sadaf Rizvi and Mohammad Al-Asmari for their help with laboratory work.

COMMENTS

Background

Inflammatory bowel diseases (IBD), including ulcerative colitis, and Crohn's disease, are chronic inflammatory disorders of the gastrointestinal tract. The precise etiology of IBD is still unknown, but available data suggests a definite role of immune dysregulation caused by genetic and/or environmental factors. Apolipoprotein E (APOE) plays a pivotal role in immunogenic response by interacting with several cytokines and regulating macrophage functions. Therefore, the role of APOE polymorphism was studied in Saudi patients with IBD.

Research frontiers

The gene encoding APOE is located on chromosome 19 and has three polymorphic alleles (ε2, ε3 and ε4) differing from one another by the presence of either a C or T nucleotide at codons 112 and 158. Alleles ε2, ε3 and ε4 encode different APOE isoproteins, which not only differ in structure, but also in function, including receptor binding capacity and lipid metabolism. The frequency of APOE alleles varies significantly among different ethnic populations. Several studies have indicated an association between APOE alleles and genotypes with onset and severity of various autoimmune diseases. Such association studies will help in the better prognosis and treatment of various autoimmune diseases.

Innovations and breakthroughs

There are increasing prevalences of obesity and lipid disorders in the Saudi population due to sedentary lifestyle, lack of exercise, and unique dietary habits of rich fat, sugar and red meat. Being a closed society with high rate of consanguinity, it is ideal for genetic association studies. However, the genetic studies on IBD/other autoimmune disorders in KSA and other Arab countries are scarce and inconclusive. This is the first report from a Saudi population

showing the role of APOE polymorphism in the etiology of ulcerative colitis and Crohn's disease.

Applications

The study results suggest that APOE polymorphism is associated with risk of developing IBD in Saudi patients. The ε2 allele and its heterozygous genotypes increase the susceptibility to IBD, whereas the ε3 allele and ε3/ε3 genotype are protective. The APOE ε4 allele also increases the risk for IBD and is associated with early age at onset. Similar studies on different ethnic populations will be helpful in defining the role of APOE as a putative pharmacologic target for IBD. Understanding this relationship may be potentially useful for predicting the vulnerability of individuals/populations to various autoimmune diseases.

Peer review

In this study, the authors studied the association between APOE polymorphism and IBD in a Saudi Arabian population.

REFERENCES

1 **Cosnes J**, Gower-Rousseau C, Seksik P, Cortot A. Epidemiology and natural history of inflammatory bowel diseases. *Gastroenterology* 2011; **140**: 1785-1794 [PMID: 21530745]

2 **Fadda MA**, Peedikayil MC, Kagevi I, Kahtani KA, Ben AA, Al HI, Sohaibani FA, Quaiz MA, Abdulla M, Khan MQ, Helmy A. Inflammatory bowel disease in Saudi Arabia: a hospital-based clinical study of 312 patients. *Ann Saudi Med* 2012; **32**: 276-282 [PMID: 22588439 DOI: 10.5144/0256-4947]

3 **Gunisetty S**, Tiwari S, Bardia A, Phanibhushan M, Satti V, Habeeb M, Khan A. The epidemiology and prevalence of Ulcerative colitis in the South of India. *O J Immunol* 2012; **2**: 144-148 [DOI: 10.4236/oji.2012.24018]

4 **Molodecky NA**, Soon IS, Rabi DM, Ghali WA, Ferris M, Chernoff G, Benchimol EI, Panaccione R, Ghosh S, Barkema HW, Kaplan GG. Increasing incidence and prevalence of the inflammatory bowel diseases with time, based on systematic review. *Gastroenterology* 2012; **142**: 46-54.e42; quiz e30 [PMID: 22001864]

5 **Zeng Z**, Zhu Z, Yang Y, Ruan W, Peng X, Su Y, Peng L, Chen J, Yin Q, Zhao C, Zhou H, Yuan S, Hao Y, Qian J, Ng SC, Chen M, Hu P. Incidence and clinical characteristics of inflammatory bowel disease in a developed region of Guangdong Province, China: a prospective population-based study. *J Gastroenterol Hepatol* 2013; **28**: 1148-1153 [PMID: 23432198 DOI: 10.1111/jgh.12164]

6 **Podolsky DK**. Inflammatory bowel disease. *N Engl J Med* 2002; **347**: 417-429 [PMID: 12167685 DOI: 10.1056/NEJMra020831]

7 **Strober W**, Fuss I, Mannon P. The fundamental basis of inflammatory bowel disease. *J Clin Invest* 2007; **117**: 514-521 [PMID: 17332878]

8 **Xavier RJ**, Podolsky DK. Unravelling the pathogenesis of inflammatory bowel disease. *Nature* 2007; **448**: 427-434 [PMID: 17653185 DOI: 10.1038/nature06005]

9 **Gent AE**, Hellier MD, Grace RH, Swarbrick ET, Coggon D. Inflammatory bowel disease and domestic hygiene in infancy. *Lancet* 1994; **343**: 766-767 [PMID: 7907734 DOI: 10.1016/S0140-6736(94)91841-4]

10 **Matricon J**, Barnich N, Ardid D. Immunopathogenesis of inflammatory bowel disease. *Self Nonself* 2010; **1**: 299-309 [PMID: 21487504 DOI: 10.4161/self.1.4.13560]

11 **Yang SK**, Hong WS, Min YI, Kim HY, Yoo JY, Rhee PL, Rhee JC, Chang DK, Song IS, Jung SA, Park EB, Yoo HM, Lee DK, Kim YK. Incidence and prevalence of ulcerative colitis in the Songpa-Kangdong District, Seoul, Korea, 1986-1997. *J Gastroenterol Hepatol* 2000; **15**: 1037-1042 [PMID: 11059934 DOI: 10.1046/j.1440-1746.2000.02252.x]

12 **Ling KL**, Ooi CJ, Luman W, Cheong WK, Choen FS, Ng HS. Clinical characteristics of ulcerative colitis in Singapore, a multiracial city-state. *J Clin Gastroenterol* 2002; **35**: 144-148 [PMID: 12172359]

13 **Inoue N**, Tamura K, Kinouchi Y, Fukuda Y, Takahashi S, Ogura Y, Inohara N, Núñez G, Kishi Y, Koike Y, Shimosegawa T, Shimoyama T, Hibi T. Lack of common NOD2 variants in Japanese patients with Crohn's disease. *Gastroenterology* 2002; **123**: 86-91 [PMID: 12105836]

14 **Leong RW**, Lau JY, Sung JJ. The epidemiology and phenotype of Crohn's disease in the Chinese population. *Inflamm Bowel Dis* 2004; **10**: 646-651 [PMID: 15472528 DOI: 10.1097/00054725-200409000-00022]

15 **Kim ES**, Kim WH. Inflammatory bowel disease in Korea: epidemiological, genomic, clinical, and therapeutic characteristics. *Gut Liver* 2010; **4**: 1-14 [PMID: 20479907 DOI: 10.5009/gnl.2010.4.1.1]

16 **Yun J**, Xu CT, Pan BR. Epidemiology and gene markers of ulcerative colitis in the Chinese. *World J Gastroenterol* 2009; **15**: 788-803 [PMID: 19230040]

17 **Waterman M**, Xu W, Stempak JM, Milgrom R, Bernstein CN, Griffiths AM, Greenberg GR, Steinhart AH, Silverberg MS. Distinct and overlapping genetic loci in Crohn's disease and ulcerative colitis: correlations with pathogenesis. *Inflamm Bowel Dis* 2011; **17**: 1936-1942 [PMID: 21830272 DOI: 10.1002/ibd.21579]

18 **Laskowitz DT**, Lee DM, Schmechel D, Staats HF. Altered immune responses in apolipoprotein E-deficient mice. *J Lipid Res* 2000; **41**: 613-620 [PMID: 10744782]

19 **Yin M**, Zhang L, Sun XM, Mao LF, Pan J. Lack of apoE causes alteration of cytokines expression in young mice liver. *Mol Biol Rep* 2010; **37**: 2049-2054 [PMID: 19644765 DOI: 10.1007/s11033-009-9660-x]

20 **Baitsch D**, Bock HH, Engel T, Telgmann R, Müller-Tidow C, Varga G, Bot M, Herz J, Robenek H, von Eckardstein A, Nofer JR. Apolipoprotein E induces antiinflammatory phenotype in macrophages. *Arterioscler Thromb Vasc Biol* 2011; **31**: 1160-1168 [PMID: 21350196 DOI: 10.1161/ATVBAHA.111.222745]

21 **Zhang H**, Wu LM, Wu J. Cross-talk between apolipoprotein E and cytokines. *Mediators Inflamm* 2011; **2011**: 949072 [PMID: 21772670 DOI: 10.1155/2011/949072]

22 **Zhang HL**, Wu J. Apolipoprotein E4 and psoriasis. *Arch Dermatol Res* 2010; **302**: 151 [PMID: 20033191 DOI: 10.1007/s00403-009-1015-x]

23 **Postigo J**, Genre F, Iglesias M, Fernández-Rey M, Buelta L, Carlos Rodríguez-Rey J, Merino J, Merino R. Exacerbation of type II collagen-induced arthritis in apolipoprotein E-deficient mice in association with the expansion of Th1 and Th17 cells. *Arthritis Rheum* 2011; **63**: 971-980 [PMID: 21225684]

24 **Song LJ**, Liu WW, Fan YC, Qiu F, Chen QL, Li XF, Ding F. The positive correlations of apolipoprotein E with disease activity and related cytokines in systemic lupus erythematosus. *Diagn Pathol* 2013; **8**: 175 [PMID: 24144108 DOI: 10.1186/1746-1596-8-175]

25 **Artiga MJ**, Bullido MJ, Sastre I, Recuero M, García MA, Aldudo J, Vázquez J, Valdivieso F. Allelic polymorphisms in the transcriptional regulatory region of apolipoprotein E gene. *FEBS Lett* 1998; **421**: 105-108 [PMID: 9468288]

26 **Utermann G**, Hees M, Steinmetz A. Polymorphism of apolipoprotein E and occurrence of dysbetalipoproteinaemia in man. *Nature* 1977; **269**: 604-607 [PMID: 199847]

27 **Hatters DM**, Peters-Libeu CA, Weisgraber KH. Apolipoprotein E structure: insights into function. *Trends Biochem Sci* 2006; **31**: 445-454 [PMID: 16820298 DOI: 10.1016/j.tibs.2006.06.008]

28 **Yin R**, Pan S, Wu J, Lin W, Yang D. Apolipoprotein E gene polymorphism and serum lipid levels in the Guangxi Hei Yi Zhuang and Han populations. *Exp Biol Med* (Maywood) 2008; **233**: 409-418 [PMID: 18367629 DOI: 10.3181/0709-RM-254]

29 **Al-Dabbagh NM**, Al-Dohayan N, Arfin M, Tariq M. Apolipoprotein E polymorphisms and primary glaucoma in Saudis. *Mol Vis* 2009; **15**: 912-919 [PMID: 19421411]

30 **Pertovaara M**, Lehtimäki T, Rontu R, Antonen J, Pasternack A, Hurme M. Presence of apolipoprotein E epsilon4 allele predisposes to early onset of primary Sjogren's syndrome.

Rheumatology (Oxford) 2004; **43**: 1484-1487 [PMID: 15328426 DOI: 10.1093/rheumatology/keh383]
31 **Mooyaart AL**, Valk EJ, van Es LA, Bruijn JA, de Heer E, Freedman BI, Dekkers OM, Baelde HJ. Genetic associations in diabetic nephropathy: a meta-analysis. *Diabetologia* 2011; **54**: 544-553 [PMID: 21127830 DOI: 10.1007/s00125-010-1996-1]
32 **Maehlen MT**, Provan SA, de Rooy DP, van der Helm-van Mil AH, Krabben A, Saxne T, Lindqvist E, Semb AG, Uhlig T, van der Heijde D, Mero IL, Olsen IC, Kvien TK, Lie BA. Associations between APOE genotypes and disease susceptibility, joint damage and lipid levels in patients with rheumatoid arthritis. *PLoS One* 2013; **8**: e60970 [PMID: 23613766]
33 **Al Harthi F**, Huraib GB, Zouman A, Arfin M, Tariq M, Al-Asmari A. Apolipoprotein E gene polymorphism and serum lipid profile in Saudi patients with psoriasis. *Dis Markers* 2014; **2014**: 239645 [PMID: 24782577]
34 **Li K**, Wang B, Sui H, Liu S, Yao S, Guo L, Mao D. Polymorphisms of the macrophage inflammatory protein 1 alpha and ApoE genes are associated with ulcerative colitis. *Int J Colorectal Dis* 2009; **24**: 13-17 [PMID: 18762952]
35 **Liang WD**, Yang JF, Yan J, Jin J, Li KS, Li JS, Bi YT. [Association of combined polymorphisms in MIP-1α and ApoE genes with the susceptibility of inflammatory bowel disease]. *Zhonghua Yixue Zazhi* 2011; **91**: 1250-1253 [PMID: 21756796]
36 **Lennard-Jones JE**. Classification of inflammatory bowel disease. *Scand J Gastroenterol Suppl* 1989; **170**: 2-6; discussion 16-19 [PMID: 2617184]
37 **Silverberg MS**, Satsangi J, Ahmad T, Arnott ID, Bernstein CN, Brant SR, Caprilli R, Colombel JF, Gasche C, Geboes K, Jewell DP, Karban A, Loftus EV, Peña AS, Riddell RH, Sachar DB, Schreiber S, Steinhart AH, Targan SR, Vermeire S, Warren BF. Toward an integrated clinical, molecular and serological classification of inflammatory bowel disease: report of a Working Party of the 2005 Montreal World Congress of Gastroenterology. *Can J Gastroenterol* 2005; **19** Suppl A: 5A-36A [PMID: 16151544]
38 **Al- Dabbagh NM**, Al-Saleh S, Al-Dohayan N, Al-Asmari AK, Arfin M, Tariq M. The role of Apolipoprotein E gene polymorphisms in Primary Glaucoma and Pseudoexfoliation Syndrome. Glaucoma - Basic and Clinical Aspects. *INTECH* 2013; (Pt 7): 130-156 [DOI: 10.5772/54614]
39 **Schallreuter KU**, Levenig C, Kühnl P, Löliger C, Hohl-Tehari M, Berger J. Histocompatibility antigens in vitiligo: Hamburg study on 102 patients from northern Germany. *Dermatology* 1993; **187**: 186-192 [PMID: 8219421]
40 **Svejgaard A**, Platz P, Ryder LP. HLA and disease 1982--a survey. *Immunol Rev* 1983; **70**: 193-218 [PMID: 6339368]
41 **Halford J**, Mazeika G, Slifer S, Speer M, Saunders AM, Strittmatter WJ, Morgenlander JC. APOE2 allele increased in tardive dyskinesia. *Mov Disord* 2006; **21**: 540-542 [PMID: 16261623 DOI: 10.1002/mds.20768]
42 **Agouridis AP**, Elisaf M, Milionis HJ. An overview of lipid abnormalities in patients with inflammatory bowel disease. *Ann Gastroenterol* 2011; **24**: 181-187 [PMID: 24713706]
43 **Koutroubakis IE**, Malliaraki N, Vardas E, Ganotakis E, Margioris AN, Manousos ON, Kouroumalis EA. Increased levels of lipoprotein (a) in Crohn's disease: a relation to thrombosis? *Eur J Gastroenterol Hepatol* 2001; **13**: 1415-1419 [PMID: 11742189]
44 **Ripollés Piquer B**, Nazih H, Bourreille A, Segain JP, Huvelin JM, Galmiche JP, Bard JM. Altered lipid, apolipoprotein, and lipoprotein profiles in inflammatory bowel disease: consequences on the cholesterol efflux capacity of serum using Fu5AH cell system. *Metabolism* 2006; **55**: 980-988 [PMID: 16784973 DOI: 10.1016/j.metabol.2006.03.006]
45 **Miyauchi H**. [Immunohistochemical study for the localization of apolipoprotein AI, B100, and E in normal and psoriatic skin]. *Igaku Kenkyu* 1991; **61**: 79-86 [PMID: 1823509]
46 **Furumoto H**, Nakamura K, Imamura T, Hamamoto Y, Shimizu T, Muto M, Asagami C. Association of apolipoprotein allele epsilon 2 with psoriasis vulgaris in Japanese population. *Arch Dermatol Res* 1997; **289**: 497-500 [PMID: 9341968]
47 **Couderc R**, Mahieux F, Bailleul S, Fenelon G, Mary R, Fermanian J. Prevalence of apolipoprotein E phenotypes in ischemic cerebrovascular disease. A case-control study. *Stroke* 1993; **24**: 661-664 [PMID: 8488520 DOI: 10.1161/01.STR.24.5.661]
48 **Hsia SH**, Connelly PW, Hegele RA. Restriction isotyping of apolipoprotein E R145C in type III hyperlipoproteinemia. *J Investig Med* 1995; **43**: 187-194 [PMID: 7735921]
49 **Danesh J**, Wheeler JG, Hirschfield GM, Eda S, Eiriksdottir G, Rumley A, Lowe GD, Pepys MB, Gudnason V. C-reactive protein and other circulating markers of inflammation in the prediction of coronary heart disease. *N Engl J Med* 2004; **350**: 1387-1397 [PMID: 15070788 DOI: 10.1056/NEJMoa032804]
50 **Papa A**, Santoliquido A, Danese S, Covino M, Di Campli C, Urgesi R, Grillo A, Guglielmo S, Tondi P, Guidi L, De Vitis I, Fedeli G, Gasbarrini G, Gasbarrini A. Increased carotid intima-media thickness in patients with inflammatory bowel disease. *Aliment Pharmacol Ther* 2005; **22**: 839-846 [PMID: 16225493 DOI: 10.1111/j.1365-2036.2005.02657.x]
51 **Danese S**, Sgambato A, Papa A, Scaldaferri F, Pola R, Sans M, Lovecchio M, Gasbarrini G, Cittadini A, Gasbarrini A. Homocysteine triggers mucosal microvascular activation in inflammatory bowel disease. *Am J Gastroenterol* 2005; **100**: 886-895 [PMID: 15784037]
52 **Bregenzer N**, Hartmann A, Strauch U, Schölmerich J, Andus T, Bollheimer LC. Increased insulin resistance and beta cell activity in patients with Crohn's disease. *Inflamm Bowel Dis* 2006; **12**: 53-56 [PMID: 16374259]
53 **Dagli N**, Poyrazoglu OK, Dagli AF, Sahbaz F, Karaca I, Kobat MA, Bahcecioglu IH. Is inflammatory bowel disease a risk factor for early atherosclerosis? *Angiology* 2010; **61**: 198-204 [PMID: 19398421 DOI: 10.1177/0003319709333869]
54 **Rungoe C**, Basit S, Ranthe MF, Wohlfahrt J, Langholz E, Jess T. Risk of ischaemic heart disease in patients with inflammatory bowel disease: a nationwide Danish cohort study. *Gut* 2013; **62**: 689-694 [PMID: 22961677 DOI: 10.1136/gutjnl-2012-303285]
55 **Visschers RG**, Olde Damink SW, Schreurs M, Winkens B, Soeters PB, van Gemert WG. Development of hypertriglyceridemia in patients with enterocutaneous fistulas. *Clin Nutr* 2009; **28**: 313-317 [PMID: 19327876 DOI: 10.1016/j.clnu.2009.03.001]
56 **Crook MA**, Velauthar U, Moran L, Griffiths W. Hypocholesterolaemia in a hospital population. *Ann Clin Biochem* 1999; **36** (Pt 5): 613-616 [PMID: 10505211]
57 **Shiraki M**, Shiraki Y, Aoki C, Hosoi T, Inoue S, Kaneki M, Ouchi Y. Association of bone mineral density with apolipoprotein E phenotype. *J Bone Miner Res* 1997; **12**: 1438-1445 [PMID: 9286760 DOI: 10.1359/jbmr.1997.12.9.1438]
58 **Wong SY**, Lau EM, Li M, Chung T, Sham A, Woo J. The prevalence of Apo E4 genotype and its relationship to bone mineral density in Hong Kong Chinese. *J Bone Miner Metab* 2005; **23**: 261-265 [PMID: 15838630]
59 **Ulivieri FM**, Lisciandrano D, Ranzi T, Taioli E, Cermesoni L, Piodi LP, Nava MC, Vezzoli M, Bianchi PA. Bone mineral density and body composition in patients with ulcerative colitis. *Am J Gastroenterol* 2000; **95**: 1491-1494 [PMID: 10894585]
60 **Lynch JR**, Tang W, Wang H, Vitek MP, Bennett ER, Sullivan PM, Warner DS, Laskowitz DT. APOE genotype and an ApoE-mimetic peptide modify the systemic and central nervous system inflammatory response. *J Biol Chem* 2003; **278**: 48529-48533 [PMID: 14507923 DOI: 10.1074/jbc.M306923200]
61 **Jofre-Monseny L**, Minihane AM, Rimbach G. Impact of apoE genotype on oxidative stress, inflammation and disease risk. *Mol Nutr Food Res* 2008; **52**: 131-145 [PMID: 18203129

DOI: 10.1002/mnfr.200700322]
62 **Vitek MP**, Brown CM, Colton CA. APOE genotype-specific differences in the innate immune response. *Neurobiol Aging* 2009; **30**: 1350-1360 [PMID: 18155324 DOI: 10.1016/j.neurobiolaging.2007.11.014]
63 **Ophir G**, Amariglio N, Jacob-Hirsch J, Elkon R, Rechavi G, Michaelson DM. Apolipoprotein E4 enhances brain inflammation by modulation of the NF-kappaB signaling cascade. *Neurobiol Dis* 2005; **20**: 709-718 [PMID: 15979312 DOI: 10.1016/j.nbd.2005.05.002]
64 **Jofre-Monseny L**, Loboda A, Wagner AE, Huebbe P, Boesch-Saadatmandi C, Jozkowicz A, Minihane AM, Dulak J, Rimbach G. Effects of apoE genotype on macrophage inflammation and heme oxygenase-1 expression. *Biochem Biophys Res Commun* 2007; **357**: 319-324 [PMID: 17416347 DOI: 10.1016/j.bbrc.2007.03.150]
65 **Kwon OD**, Khaleeq A, Chan W, Pavlik VN, Doody RS. Apolipoprotein E polymorphism and age at onset of Alzheimer's disease in a quadriethnic sample. *Dement Geriatr Cogn Disord* 2010; **30**: 486-491 [PMID: 21252542 DOI: 10.1159/000322368]
66 **Peng H**, Wang C, Chen Z, Sun Z, Jiao B, Li K, Huang F, Hou X, Wang J, Shen L, Xia K, Tang B, Jiang H. The APOE ε2 allele may decrease the age at onset in patients with spinocerebellar ataxia type 3 or Machado-Joseph disease from the Chinese Han population. *Neurobiol Aging* 2014; **35**: 2179.e15-2179.e18 [PMID: 24746364 DOI: 10.1016/j.neurobiolaging]
67 **Harwood DG**, Barker WW, Ownby RL, St George-Hyslop P, Mullan M, Duara R. Apolipoprotein E polymorphism and age of onset for Alzheimer's disease in a bi-ethnic sample. *Int Psychogeriatr* 2004; **16**: 317-326 [PMID: 15559755]
68 **Kampman O**, Anttila S, Illi A, Mattila KM, Rontu R, Leinonen E, Lehtimäki T. Apolipoprotein E polymorphism is associated with age of onset in schizophrenia. *J Hum Genet* 2004; **49**: 355-359 [PMID: 15221639 DOI: 10.1007/s10038-004-0157-0]
69 **Grant WB**. A multicountry ecological study of risk-modifying factors for prostate cancer: apolipoprotein E epsilon4 as a risk factor and cereals as a risk reduction factor. *Anticancer Res* 2010; **30**: 189-199 [PMID: 20150635]
70 **Kelly ME**, Clay MA, Mistry MJ, Hsieh-Li HM, Harmony JA. Apolipoprotein E inhibition of proliferation of mitogen-activated T lymphocytes: production of interleukin 2 with reduced biological activity. *Cell Immunol* 1994; **159**: 124-139 [PMID: 7994749]
71 **Koga T**, Duan H, Urabe K, Furue M. In situ localization of CD83-positive dendritic cells in psoriatic lesions. *Dermatology* 2002; **204**: 100-103 [PMID: 11937733]
72 **Oestreicher JL**, Walters IB, Kikuchi T, Gilleaudeau P, Surette J, Schwertschlag U, Dorner AJ, Krueger JG, Trepicchio WL. Molecular classification of psoriasis disease-associated genes through pharmacogenomic expression profiling. *Pharmacogenomics J* 2001; **1**: 272-287 [PMID: 11911124]
73 **Chasman DI**, Kozlowski P, Zee RY, Kwiatkowski DJ, Ridker PM. Qualitative and quantitative effects of APOE genetic variation on plasma C-reactive protein, LDL-cholesterol, and apoE protein. *Genes Immun* 2006; **7**: 211-219 [PMID: 16511556 DOI: 10.1038/sj.gene]

P- Reviewer: Il Kim T, Kochhar R, Sperti C **S- Editor**: Qi Y
L- Editor: AmEditor **E- Editor**: Wang CH

World Journal of Gastroenterology

Submit a Manuscript: http://www.wjgnet.com/esps/
Help Desk: http://www.wjgnet.com/esps/helpdesk.aspx
DOI: 10.3748/wjg.v21.i3.905

World J Gastroenterol 2015 January 21; 21(3): 905-912
ISSN 1007-9327 (print) ISSN 2219-2840 (online)

ORIGINAL ARTICLE

Case Control Study

RhoC, vascular endothelial growth factor and microvascular density in esophageal squamous cell carcinoma

Zhi-Hua Zhao, Yan Tian, Jian-Pin Yang, Jun Zhou, Kui-Sheng Chen

Zhi-Hua Zhao, Yan Tian, Jian-Pin Yang, Jun Zhou, Kui-Sheng Chen, Department of Pathology, the First Affiliated Hospital of Zhengzhou University, Zhengzhou 450052, Henan Province, China

Author contributions: Zhao ZH, Tian Y and Chen KS designed the research; Zhao ZH, Tian Y, Chen KS, Yang JP and Zhou J performed the research; Zhao ZH, Tian Y and Chen KS contributed new reagents or analytic tools; Zhao ZH and Tian Y analyzed the data; Zhao ZH and Tian Y wrote the paper.

Supported by First Affiliated Hospital of Zhengzhou University, Henan-based Research Projects with Cutting-Edge Technology, No. 132300410126 and No. 132300410458.

Correspondence to: Kui-Sheng Chen, MD, Professor, Department of Pathology, the First Affiliated Hospital of Zhengzhou University, No. 1 Jianshe East Rd, Erqi District, Zhengzhou 450052, Henan Province, China. 15036607301@163.com
Telephone: +86-371-66658175
Fax: +86-371-66658175

Received: March 27, 2014
Peer-review started: March 27, 2014
First decision: August 6, 2014
Revised: August 23, 2014
Accepted: November 8, 2014
Article in press: November 11, 2014
Published online: January 21, 2015

Abstract

AIM: To investigate the expression of Ras homolog (Rho)C, vascular endothelial growth factor (VEGF) and CD105 in esophageal squamous cell carcinoma.

METHODS: Semi-quantitative reverse transcriptase polymerase chain reaction, *in situ* hybridization and immunohistochemical streptavidin-biotin- peroxidase methods were used to detect expression of RhoC mRNA and protein, and VEGF protein in 62 cases with esophageal squamous cell carcinoma, 31 cases with adjacent atypical hyperplastic tissues, and 62 cases with normal esophageal mucosa. CD105 antibody labeling was used to measure microvascular density. Expression levels were compared according to clinicopathologic and patient parameters.

RESULTS: Expression of RhoC mRNA showed a positive correlation with the protein level in esophageal squamous cell carcinoma, as well as with VEGF protein levels. RhoC mRNA expression was mainly located within the cytoplasm of the tumor cells, appearing as blue to purple particles by *in situ* hybridization. The differences in RhoC mRNA expression in esophageal squamous cell carcinoma, adjacent atypical hyperplasia and normal esophageal mucosa were significant ($P < 0.05$). The relative expression of RhoC mRNA in cancer tissues with lymph node metastasis was significantly higher than in the tissues without lymph node metastasis ($P < 0.05$). VEGF protein expression was consistent with microvascular density ($t = 25.52$, $P < 0.05$). Positive expression of VEGF protein in esophageal squamous cell carcinoma of different histologic gradings did not differ significantly. Positive expression of VEGF protein in carcinoma tissues with deep infiltration was significantly higher than in tissues with only superficial infiltration ($P < 0.05$). The positive expression of VEGF protein in cancer tissues with lymph node metastasis was significantly higher than in the tissues without lymph node metastasis ($P < 0.05$).

CONCLUSION: RhoC protein may upregulate VEGF expression, thereby promoting tumor angiogenesis. RhoC mRNA and protein expression was correlated with metastasis.

Key words: Esophageal squamous cell carcinoma; Gene silencing; Ras homolog C; Vascular endothelial growth factor

Core tip: Recent studies have found that Ras homolog (Rho)C plays an important role in promoting angiogenesis in breast cancer. RhoC overexpression in breast cancer epithelial cells can improve expression of vascular endothelial growth factor (VEGF) and other angiogenic factors. Detection of the expression of RhoC, VEGF and microvascular density in esophageal squamous cell carcinoma and the relationship with metastasis and invasion have not been reported.

Zhao ZH, Tian Y, Yang JP, Zhou J, Chen KS. RhoC, vascular endothelial growth factor and microvascular density in esophageal squamous cell carcinoma. *World J Gastroenterol* 2015; 21(3): 905-912 Available from: URL: http://www.wjgnet.com/1007-9327/full/v21/i3/905.htm DOI: http://dx.doi.org/10.3748/wjg.v21.i3.905

INTRODUCTION

Ras homolog (Rho) family members (RhoA, RhoB and RhoC) are a class of small GTP binding proteins, which play an important role in cell signaling pathways, cell transformation, and tumor cell infiltration and metastasis[1,2]. The relationship between RhoC and malignancy has become one of the research hotspots in oncology. Recent studies have found that RhoC plays an important role in promoting angiogenesis in breast cancer[3,4]. RhoC overexpression in breast cancer epithelial cells can improve the expression of vascular endothelial growth factor (VEGF) and other angiogenic factors. Detection of the expression of RhoC, VEGF and microvascular density (MVD) in esophageal squamous cell carcinoma and the relationship with metastasis and invasion have not been reported.

In the present study, we detected expression of RhoC mRNA and protein and VEGF protein in esophageal squamous cell carcinoma, adjacent atypical hyperplasia, and normal esophageal mucosa. CD105 antibody labeling was also used to detect MVD in esophageal squamous cell carcinoma to explore the relationship with RhoC and VEGF expression, and to clarify the clinicopathologic significance of the RhoC, VEGF, and MVD in the occurrence and development of esophageal squamous cell carcinoma.

MATERIALS AND METHODS

General data

We collected surgical specimens from 62 cases of esophageal squamous cell carcinoma at the Tumor Hospital of Henan Anyang City between February and March 2006. There were 36 male and 26 female cases, aged 38-75 years (mean: 60.6 ± 9.5 years). None of the patients had a preoperative history of chemotherapy, radiotherapy or immunotherapy. Esophageal squamous cell carcinoma was divided into four types[5]: ulcer type (n = 28), medullary type (n = 29), mushroom umbrella type (n = 4), and narrow type (n = 1). Fifteen cases were Grade Ⅰ, 25 were Grade Ⅱ, and 22 were Grade Ⅲ; 20 were accompanied by lymph node metastasis, and 42 were not. Seven cases (superficial group) had tumor infiltration of the mucosa, submucosa or superficial muscles, and 55 cases (deep group) had tumor infiltration of the deep muscular or outer layer. All cases were confirmed to be esophageal squamous cell carcinoma by conventional pathology. Specimens were taken from outside the necrosis area, ⩽ 3 cm mucosa tissue adjacent to carcinoma, and remote normal mucosa.

Each section was fixed with 40 g/L formaldehyde, conventionally dehydrated, paraffin-embedded, and serially sectioned at a thickness of 4-6 μm for hematoxylin and eosin staining, *in situ* hybridization, and immunohistochemical staining.

Semi-quantitative reverse transcriptase-PCR

The total RNA of the tissue was extracted using the RNAiso Plus kit (Takara, Otsu, Shiga, Japan) and RT-PCR was performed using PrimeScript One Step RT-PCR Kit Ver. 2 (Takara). The results were analyzed with the GeneGenius Gel Imaging System (Syngene, Cambridge, United Kingdom). The ratio of the gray value of the RhoC amplified bands to the gray value of the β-actin bands was taken as the relative expression level of target gene mRNA.

In situ hybridization

In situ hybridization was carried out as described previously[6]. The probe sequence of RhoC was 5'-CGT TGG GGC AGA AGT GCT TCA-3', which was synthesized by Beijing Bioko Biotechnology Co. Ltd.

Immunohistochemistry

Immunohistochemical staining was conducted using a streptavidin-biotin-peroxidase assay kit and in strict accordance with manufacturer's instructions (Beijing Zhongshan Golden Bridge Biotechnology Development Company, China). Breast biopsy specimens with known positive expression of RhoC were taken as positive controls. Antibody was replaced by normal goat serum as a negative control and PBS as a blank control. The results were observed in a double-blind manner as described previously[7]. Yellow or brown particles in the cytoplasm or cell membrane were considered to be positive. Unstained cells were negative. Stained cells, regardless of the area and intensity, were all taken as positive.

Statistical analysis

SPSS version 13.0 software (SPSS Inc., Chicago, IL,

United States) was used to conduct χ^2 or rank sum tests. A $P < 0.05$ was considered to be statistically significant.

RESULTS

RhoC mRNA expression

RhoC mRNA expression was mainly located within the cytoplasm of the tumor cells, showing as blue to purple particles (Figure 1A). RhoC mRNA levels significantly differed among normal esophageal mucosa, adjacent atypical hyperplasia, and carcinoma sample ($P < 0.05$) (Table 1). The lower the degree of differentiation, the higher the expression of RhoC mRNA, and the difference was significant by rank sum test ($P < 0.05$) (Table 2). The difference in relative RhoC mRNA expression levels in the carcinoma tissues of the shallow and deep infiltration groups was significant ($P < 0.05$). The relative expression of RhoC mRNA in cancer tissues with lymph node metastasis was significantly higher than in the group without lymph node metastasis ($P < 0.05$). Sex, age and other factors of patients with esophageal squamous cell carcinoma were independent of the relative content of RhoC mRNA ($P > 0.05$).

RhoC protein expression

RhoC protein showed as pale to dark yellow particles, mainly located in the cytoplasm (Figure 1B). The differences in the expression of RhoC protein among the three type of tissue sample were significant ($P < 0.05$) (Table 1). The lower the degree of differentiation, the higher the expression of RhoC protein, and the difference was significant ($P < 0.05$). The positive expression of RhoC protein in cancer tissues with lymph node metastasis was significantly higher than in the tissues without lymph node metastasis ($P < 0.05$). Sex, age and other factors of patients with esophageal squamous cell carcinoma were unrelated to positive expression of RhoC protein ($P > 0.05$) (Table 2).

Expression of VEGF protein

The differences in VEGF protein expression in the three groups were significant ($P < 0.05$) (Table 1, Figure 1C). Positive expression of VEGF protein in esophageal squamous cell carcinoma of different histologic grading did not differ significantly ($P > 0.05$) (Table 2). Positive expression of VEGF protein in carcinoma tissues of the deep infiltrating groups was significantly higher than that in the superficial infiltrating group ($P < 0.05$). The positive expression of VEGF protein in cancer tissues with lymph node metastasis was significantly higher than in the tissues without lymph node metastasis ($P < 0.05$). Sex, age and other factors of patients with esophageal squamous cell carcinoma were independent of positive expression of VEGF protein ($P > 0.05$) (Table 2).

MVD_{CD105} test results

Detection of MVD by CD105 showed that positive protein expression signals of CD105 were mainly located in the vascular endothelial cell cytoplasm within the tumor stroma, or in cancer nests, with pale to dark yellow particles (Figure 1D). CD105-antibody-labeled MVD gradually increased in Grade Ⅰ, Ⅱ and Ⅲ esophageal squamous cell carcinoma, but the differences among the groups were not significant ($F = 0.298$, $P > 0.05$). MVD in the cancer tissues of the deep group was higher than that of the superficial group (34.47 ± 11.69). MVD (39.00 ± 8.84 *vs* 41.0 ± 3.26) in esophageal squamous cell carcinoma with lymph node metastasis was significantly higher than in the group without lymph node metastasis (39.00 ± 8.84 *vs* 36.33 ± 3.76), and the differences among groups were significant (Table 2, Figure 1D).

Correlational analysis for RhoC, VEGF and CD105 expression

Among the 52 cases with positive RhoC protein expression, 46 had positive mRNA expression, and in 10 cases with negative RhoC protein expression, six had negative mRNA expression. RhoC protein expression showed a positive correlation with RhoC mRNA expression in esophageal squamous cell carcinoma ($P < 0.01$) (Table 3). In the cases with positive RhoC protein expression, positive expression of VEGF protein was 50.0% (13/26), whereas in cases with negative RhoC expression, the rate was 82.6% (19/23), showing a positive correlation between the two ($P < 0.05$). In the cases with positive RhoC protein expression, MVD was 41.99 ± 9.83, whereas in cases with negative RhoC protein expression, MVD was 31.07 ± 6.38, and the difference was significant ($t = 25.52$, $P < 0.01$). MVD of 42 cases with positive VEGF protein expression was 38.88 ± 0.041, of which, 20 cases had negative VEGF protein expression with MVD of 36.45 ± 0.036. The difference was significant ($t = 25.52$, $P < 0.05$), indicating that VEGF protein expression was consistent with MVD.

DISCUSSION

RhoC is a member of the Rho family[8] and is a GTP-binding protein that hydrolyses GTP to inactivated GDP, acting as a signal converter or a molecular switch in cell signal transduction pathways to produce a variety of biological effects that act on the cytoskeleton or target proteins[9,10]. The most important function of RhoC is regulating cell motility and migration by regulating the actin cytoskeleton, and inducing aggregation of actin, integrins and associated proteins such as fibronectin[11,12]. The actin cytoskeleton plays an important role in cell shape changes, cell movement and phagocytosis, but also in various activities such as cell proliferation, growth and apoptosis[13,14]. It has been shown that RhoC overexpression is related to the development of a variety of malignancies. Clark *et al*[15] found that RhoC acts as a molecular switch in tumor metastasis in their study of the invasive and transfer phenotype of melanoma. Ikoma *et al*[16] found that RhoC overexpression leads to significantly increased mRNA expression of matrix

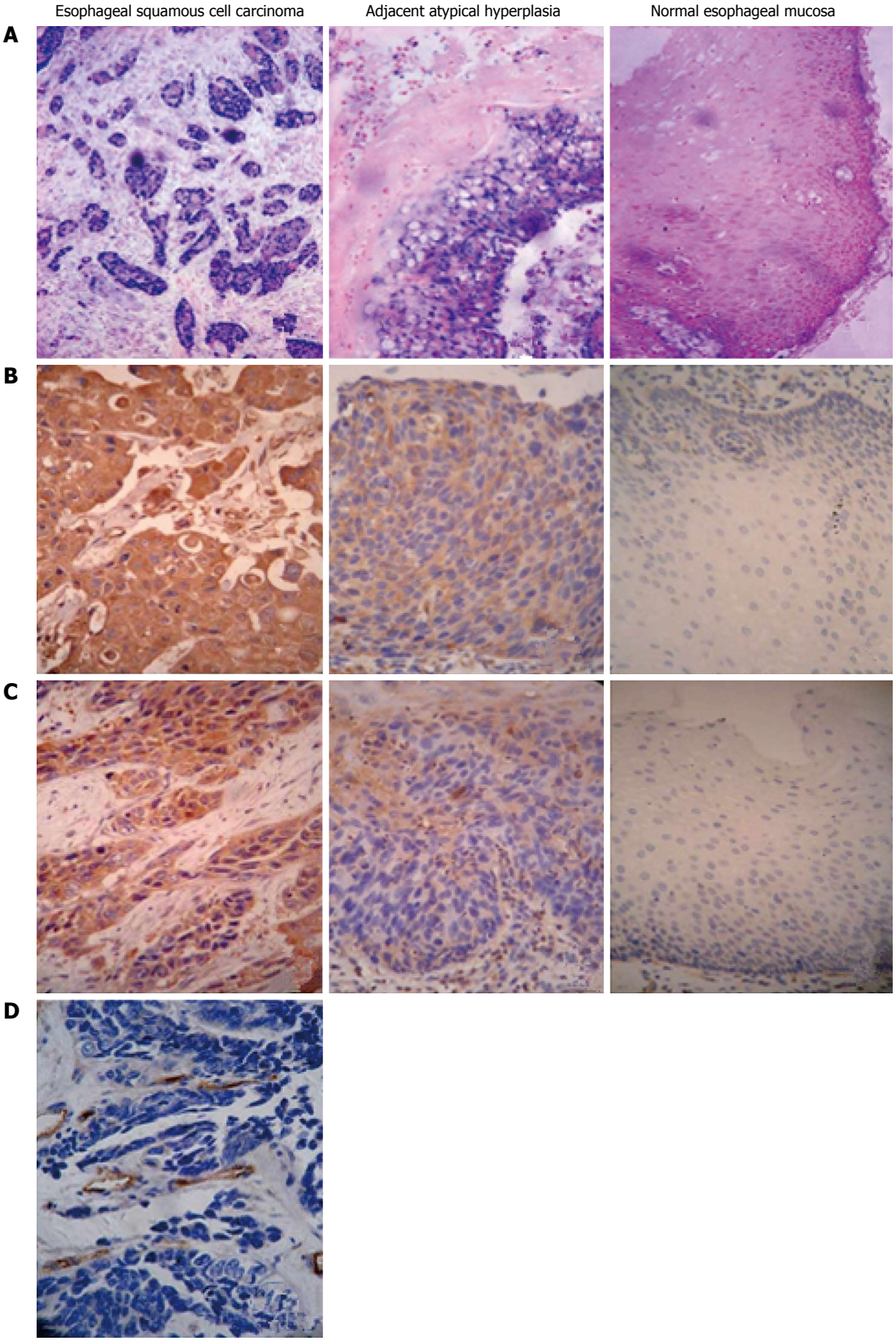

Figure 1 RhoC protein, vascular endothelial growth factor protein and CD105 immunohistochemistry. A: *In situ* hybridization with nuclear fast red for Ras homolog C (RhoC) mRNA. Immunohistochemistry with streptavidin-biotin-peroxidase for B: RhoC; C: Vascular endothelial growth factor protein; and D: CD105. 200 × magnification.

Table 1 Ras homolog C mRNA relative content, expression of Ras homolog C mRNA and protein and vascular endothelial growth factor protein in normal esophageal mucosa, adjacent atypical hyperplasia, and cancer tissues

Site	Cases (*n*)	RhoC mRNA relative content	χ^2	*P* value	RhoC mRNA expression			χ^2	*P* value	RhoC protein expression			χ^2	*P* value	VEGF protein expression			χ^2	*P* value
					-	+	Positive rate			-	+	Positive rate			-	+	Positive rate		
Normal esophageal mucosa tissues	62	0.653 ± 0.069			49	13	21%			50	12	19.4%			44	18	29%		
Adjacent atypical hyperplasia tissues	31	0.731 ± 0.065	99.629	0.000	21	10	32.3%	47.735	0.000	20	11	35.5%	54.25	0.000	14	17	54.8%	18.994	0.000
Cancer tissues	62	0.902 ± 0.119			12	50	80.6%			10	52	83.9%			20	42	67.7%		

RhoC: Ras homolog C; VEGF: Vascular endothelial growth factor.

Table 2 Ras homolog C mRNA relative content, expression of Ras homolog C mRNA and protein and vascular endothelial growth factor protein in esophageal squamous cell carcinoma and the relationship with clinicopathologic parameters

Clinicopathologic parameters	Cases (*n*)	RhoC mRNA relative content	*F* (t, χ^2)	*P* value	RhoC mRNA expression			χ^2	*P* value	RhoC protein expression			χ^2	*P* value	VEGF protein expression			χ^2	*P* value
					-	+	Positive rate			-	+	Positive rate			-	+	Positive rate		
Gender																			
Male	36	0.922 ± 0.123	0.586	0.118	7	29	80.6	0.000	0.983	6	30	83.3	0.018	0.892	11	25	69.4	0.004	0.950
Female	26	0.874 ± 0.109			5	21	80.8			4	22	84.6			9	17	65.4		
Age (yr)																			
≥ 60	33	0.911 ± 0.108	0.619	0.538	6	27	81.8	0.062	0.803	7	26	78.8	1.348	0.246	12	21	63.6	0.217	0.642
< 60	29	0.892 ± 0.132			6	23	79.3			3	26	89.7			8	21	72.4		
Histologic grading																			
Ⅰ	15	0.795 ± 0.056			7	8	53.3			7	8	53.3			8	7	46.7		
Ⅱ	25	0.898 ± 0.086	22.535	0.000	3	22	88.0	9.520	0.009	2	23	92.0	13.744	0.001	7	18	72.0	4.014	0.134
Ⅲ	22	0.979 ± 0.128			2	20	90.9			1	21	95.5			5	17	77.3		
Invasion depth																			
Shallow group	7	0.751 ± 0.036			4	3	42.9			4	3	42.9			6	1	14.3		
Deep group	55	0.924 ± 0.111	8.716	0.000	8	47	85.5	7.219	0.007	6	49	89.1	9.812	0.002	14	41	74.5	10.319	0.001
Lymphatic metastasis																			
Without	42	0.840 ± 0.074	9.042	0.000	11	31	73.8	3.898	0.048	10	32	76.2	5.678	0.017	18	24	57.1	6.693	0.010
With	20	1.032 ± 0.086			1	19	95.0			0	20	100.0			2	18	90.0		

RhoC: Ras homolog C; VEGF: Vascular endothelial growth factor.

metalloprotein (MMP)-2, MMP-9, and tissue inhibitor of matrix metalloprotein. RhoC increases the expression and activity of MMPs, which lead to enhanced tumor aggressiveness. RhoC gene overexpression also leads to increased expression of angiogenic factors (particularly VEGF) and then activation of mitogen-activated protein kinase, phospholipase C, and phosphatidylinositol 3-kinase to promote tumor invasion and metastasis. Van Golen *et al*[3] suggested that RhoC overexpression could increase the expression of VEGF and other angiogenic factors in breast epithelial cells. The extracellular C3 transferase enzyme of *Clostridium* inhibits RhoC function, which can significantly reduce the yield of angiogenic factors. Current studies evaluating RhoC gene expression in esophageal squamous cell carcinoma are limited to a few observational reports. Joint detection of RhoC, VEGF and CD105 in esophageal squamous cell carcinoma has not been reported.

The relative content of RhoC protein and mRNA suggest that RhoC overexpression may be involved in malignant transformation of esophageal epithelial cells, which may play an important role in the incidence and development of esophageal cancer. Protein and mRNA expression and the relative content of RhoC were significantly increased with the invasion depth of carcinoma, and were significantly higher in the tissues of patients with lymph node metastasis than those without metastasis. These results indicate that abnormal RhoC expression may be closely associated with invasion and lymph node metastasis in esophageal squamous cell carcinoma, which is consistent with the findings of Faried *et al*[17]. RhoC mRNA and protein expression and their relative content were significantly reduced with decreased degree of differentiation of esophageal cancer tissues. This suggests that RhoC gene plays an important role in the induction of tumor cell differentiation, and its

Table 3 Relationship among Ras homolog C protein, Ras homolog C mRNA, vascular endothelial growth factor protein and CD105 staining of measure microvascular density

RhoC protein expression	*n*	RhoC mRNA expression		*r*	*P* value	VEGF expression		*r*	*P* value	MVD_{CD105} (mean ± SD)	*r*	*P* value	VEGF protein expression	*n*	MVD_{CD105} (mean ± SD)	*t*	*P* value
		+	-			+	-										
+	52	46	6	0.451	0.000	40	12	0.448	0.000	41.99 ± 9.83	0.451	0.000	+	42	38.88 ± 0.041	5.147	0.027
-	10	4	6			2	8			31.07 ± 6.38			-	20	36.45 ± 0.036		

MVD_{CD105}: CD105 staining of measure microvascular density; RhoC: Ras homolog C; VEGF: Vascular endothelial growth factor.

overexpression may be associated with histologic grading and degree of malignancy in esophageal squamous cell carcinoma. Zhang *et al*[7] have reported that the degree of RhoC protein expression is unrelated to the degree of differentiation of esophageal cancer, and the cause of the discrepancy may be related to the different sources and numbers of specimens and antibodies.

As one of the most critical angiogenic growth factors, VEGF provides favorable conditions for the growth and metastasis of the majority of malignant tumors[18]. On the one hand, VEGF causes capillary lumen formation by acting directly on the proliferation and migration of the receptor-mediated capillary endothelial cells. On the other hand, vascular permeability is increased, which changes the tumor interstitium and plays an important role in cancer invasion and metastasis, through its autocrine or paracrine activity[19-23]. The results of the present study showed that VEGF protein expression in the lymph node metastasis group was significantly higher than in the groups without metastasis. Positive VEGF expression in the deep infiltration group was significantly higher than in the shallow infiltration group, indicating that high expression of VEGF protein can induce invasion and metastasis of esophageal squamous cell cancer. In esophageal squamous cell carcinoma with varying degrees of differentiation, the positive rate of VEGF protein expression did not differ significantly, suggesting that VEGF protein expression had nothing to do with histologic grade.

Research has shown that vascular endothelial markers such as CD34 and CD31 are expressed in tumor blood vessels, whereas the CD105 antibody is preferentially bound to the activated endothelial cells in tumor tissue. DC34 and CD31 are not expressed or only weakly expressed in the vascular endothelial cells of normal tissues, thus CD105 is a more specific marker for assessing the proliferation of vascular endothelial cells[24]. MVD in esophageal squamous cell the carcinoma tissues increased significantly with the depth of invasion. MVD in the group with lymph node metastasis was significantly higher than in the group without metastasis. CD105 expression in esophageal squamous cell carcinoma with different stages had no significant differences, which was similar to previous results[25,26]. Newborn capillaries can promote metastasis of tumor cells several ways: (1) amount of neovascularization; (2) high permeability of the new blood capillaries; and (3) degradative enzymes changing the tumor extracellular matrix[27]. Therefore, the number of blood vessels in the tumor stroma is an important factor affecting cancer prognosis and metastasis. The extent of angiogenesis in tumor tissues can be determined by assessing MVD[28]. Determination of MVD in esophageal squamous cell carcinoma could become one of the indicators to determine invasive and metastatic potential.

RhoA and RhoC can promote tumor angiogenesis by the Rho-associated kinase signaling pathway, as well as assisting distant metastasis of tumor cells through the vascular endothelium[29,30]. The results of our study showed that expression of RhoC protein was positively correlated with VEGF protein expression and MVD. The differences in MVD and expression of VEGF in patients with RhoC protein expression were significant compared with patients with negative RhoC protein expression. These findings indicate that RhoC overexpression promotes tumor angiogenesis by increasing expression of VEGF protein. We also found that MVD increased with high levels of VEGF protein expression. VEGF and CD105 staining in tumor tissues is similar, which confirms that VEGF specifically promotes tumor angiogenesis, which is consistent with previous findings in gastric cancer[31].

In summary, our results indicate that RhoC plays an important role in esophageal carcinogenesis and development. RhoC overexpression may be able to increase the expression of VEGF, thereby promoting tumor angiogenesis. VEGF protein overexpression and MVD_{CD105} were closely related to the invasion and metastasis of esophageal squamous cell carcinoma, which may be considered as an indicator for determining the lymph node metastatic potential of esophageal squamous cell carcinoma.

COMMENTS

Background

The physiological and pathological roles of Ras homolog (Rho)C, vascular endothelial growth factor (VEGF) and microvascular density (MVD) have attracted considerable attention in recent years. However, expression of RhoC, VEGF and MVD in esophageal squamous cell carcinoma and the relationship with metastasis and invasion have not been reported.

Research frontiers

This study was performed to explore the expression of RhoC, VEGF and MVD in esophageal squamous cell carcinoma and the relationship with metastasis and invasion. The study implied that the expression of RhoC, VEGF and MVD play an important role in esophageal squamous cell carcinoma.

Innovations and breakthroughs

The results of this study suggested that RhoC protein may upregulate the

expression of VEGF, thereby promote tumor angiogenesis. RhoC mRNA and protein expression was related to metastasis.

Applications

The results imply that the RhoC gene plays an important role in esophageal carcinogenesis and development. VEGF protein overexpression and MVD_{CD105} were closely related with the invasion and metastasis of esophageal squamous cell carcinoma, which may be considered as an indicator for judging the lymph node metastatic potential in esophageal squamous cell carcinoma.

Peer review

This is a well-presented article on relationship among the expression of RhoC, VEGF and MVD in esophageal squamous cell carcinoma, which has not been reported domestically or abroad. The study is innovative, the results are convincing, and the findings are presented clearly.

REFERENCES

1 **Wheeler AP**, Ridley AJ. Why three Rho proteins? RhoA, RhoB, RhoC, and cell motility. *Exp Cell Res* 2004; **301**: 43-49 [PMID: 15501444 DOI: 10.1016/j.yexcr.2004.08.012]

2 **Fukata M**, Nakagawa M, Kaibuchi K. Roles of Rho-family GTPases in cell polarisation and directional migration. *Curr Opin Cell Biol* 2003; **15**: 590-597 [PMID: 14519394 DOI: 10.1016/S0955-0674(03)00097-8]

3 **van Golen KL**, Wu ZF, Qiao XT, Bao LW, Merajver SD. RhoC GTPase, a novel transforming oncogene for human mammary epithelial cells that partially recapitulates the inflammatory breast cancer phenotype. *Cancer Res* 2000; **60**: 5832-5838 [PMID: 11059780]

4 **van Golen KL**, Wu ZF, Qiao XT, Bao L, Merajver SD. RhoC GTPase overexpression modulates induction of angiogenic factors in breast cells. *Neoplasia* 2000; **2**: 418-425 [PMID: 11191108 DOI: 10.1038/sj.neo.7900115]

5 **Du BL**. Esophageal squamous cell carcinoma. 1st ed. Beijing: China Science and Technology Press, 1994: 62-108

6 **Li SL**, Liu ZW, Zhao QM, Yu JX, Zhao ZH, Gao DL, Pang X, Chen KS, Zhang YH. RECK mRNA and protein expression and significance in ESCC. *Zhongguo Zhongliu Linchuang* 2007; **34**: 1280-1286

7 **Zhang HZ**, Liu JG, Wei YP, Wu C, Cao YK, Wang M. [Expressions of RhoC and osteopontin in esophageal squamous carcinoma and association with the patients' prognosis]. *Nanfang Yike Daxue Xuebao* 2006; **26**: 1612-1615 [PMID: 17121713]

8 **Aspenström P**. Effectors for the Rho GTPases. *Curr Opin Cell Biol* 1999; **11**: 95-102 [PMID: 10047515 DOI: 10.1016/S0955-0674(99)80011-8]

9 **Zhao L**, Wang H, Li J, Liu Y, Ding Y. Overexpression of Rho GDP-dissociation inhibitor alpha is associated with tumor progression and poor prognosis of colorectal cancer. *J Proteome Res* 2008; **7**: 3994-4003 [PMID: 18651761 DOI: 10.1021/pr800271b]

10 **Morris SW**, Valentine MB, Kirstein MN, Huebner K. Reassignment of the human ARH9 RAS-related gene to chromosome 1p13-p21. *Genomics* 1993; **15**: 677-679 [PMID: 8468062 DOI: 10.1006/geno.1993.1124]

11 **Dutt P**, Nguyen N, Toksoz D. Role of Lbc RhoGEF in Galpha12/13-induced signals to Rho GTPase. *Cell Signal* 2004; **16**: 201-209 [PMID: 14636890 DOI: 10.1016/S0898-6568(03)00132-3]

12 **Iwaki N**, Karatsu K, Miyamoto M. Role of guanine nucleotide exchange factors for Rho family GTPases in the regulation of cell morphology and actin cytoskeleton in fission yeast. *Biochem Biophys Res Commun* 2003; **312**: 414-420 [PMID: 14637153 DOI: 10.1016/j.bbrc.2003.10.140]

13 **Durkin ME**, Avner MR, Huh CG, Yuan BZ, Thorgeirsson SS, Popescu NC. DLC-1, a Rho GTPase-activating protein with tumor suppressor function, is essential for embryonic development. *FEBS Lett* 2005; **579**: 1191-1196 [PMID: 15710412 DOI: 10.1016/j.febslet.2004.12.090]

14 **Heasman SJ**, Ridley AJ. Mammalian Rho GTPases: new insights into their functions from in vivo studies. *Nat Rev Mol Cell Biol* 2008; **9**: 690-701 [PMID: 18719708 DOI: 10.1038/nrm2476]

15 **Clark EA**, Golub TR, Lander ES, Hynes RO. Genomic analysis of metastasis reveals an essential role for RhoC. *Nature* 2000; **406**: 532-535 [PMID: 10952316 DOI: 10.1038/35020106]

16 **Ikoma T**, Takahashi T, Nagano S, Li YM, Ohno Y, Ando K, Fujiwara T, Fujiwara H, Kosai K. A definitive role of RhoC in metastasis of orthotopic lung cancer in mice. *Clin Cancer Res* 2004; **10**: 1192-1200 [PMID: 14871999 DOI: 10.1158/1078-0432.CCR-03-0275]

17 **Faried A**, Faried LS, Usman N, Kato H, Kuwano H. Clinical and prognostic significance of RhoA and RhoC gene expression in esophageal squamous cell carcinoma. *Ann Surg Oncol* 2007; **14**: 3593-3601 [PMID: 17896152 DOI: 10.1245/s10434-007-9562-x]

18 **Chung J**, Yoon S, Datta K, Bachelder RE, Mercurio AM. Hypoxia-induced vascular endothelial growth factor transcription and protection from apoptosis are dependent on alpha6beta1 integrin in breast carcinoma cells. *Cancer Res* 2004; **64**: 4711-4716 [PMID: 15256436 DOI: 10.1158/0008-5472.CAN-04-0347]

19 **Weidner N**. Intratumor microvessel density as a prognostic factor in cancer. *Am J Pathol* 1995; **147**: 9-19 [PMID: 7541613]

20 **Bosari S**, Lee AK, DeLellis RA, Wiley BD, Heatley GJ, Silverman ML. Microvessel quantitation and prognosis in invasive breast carcinoma. *Hum Pathol* 1992; **23**: 755-761 [PMID: 1377162 DOI: 10.1016/0046-8177(92)90344-3]

21 **Wang FL**, Wei LX, Chen YZ. Relationship between vascular endothelial growth factor, microvessel density and metastasis and prognosis of breast cancer lymph node. *Zhonghua Binglixue Zazhi* 2000; **29**: 172-175

22 **Adams J**, Carder PJ, Downey S, Forbes MA, MacLennan K, Allgar V, Kaufman S, Hallam S, Bicknell R, Walker JJ, Cairnduff F, Selby PJ, Perren TJ, Lansdown M, Banks RE. Vascular endothelial growth factor (VEGF) in breast cancer: comparison of plasma, serum, and tissue VEGF and microvessel density and effects of tamoxifen. *Cancer Res* 2000; **60**: 2898-2905 [PMID: 10850435]

23 **Li YP**. Relationship between angiogenesis, microvessel counts and metastasis and prognosis of breast cancer. *Guowai Yixue Zhongliu Fence* 1999; **26**: 356-357

24 **Seon BK**, Matsuno F, Haruta Y, Kondo M, Barcos M. Long-lasting complete inhibition of human solid tumors in SCID mice by targeting endothelial cells of tumor vasculature with antihuman endoglin immunotoxin. *Clin Cancer Res* 1997; **3**: 1031-1044 [PMID: 9815781]

25 **Liu HN**, Cao HC, Wang ZM, Wang JJ, Zhang YX, Su YP, Huo JA. VEGF expression in esophageal tissues on prognosis. *Zhongguo Shiyong Yiyao* 1999; **2**: 450-452

26 **Liu DB**, Chen KN, Cao XZ, Wang T. [Expression of p53 and vascular endothelial growth factor in esophageal squamous cell carcinoma and their clinical significance]. *Ai Zheng* 2002; **21**: 989-993 [PMID: 12508548]

27 **Blood CH**, Zetter BR. Tumor interactions with the vasculature: angiogenesis and tumor metastasis. *Biochim Biophys Acta* 1990; **1032**: 89-118 [PMID: 1694687]

28 **Fox SH**, Whalen GF, Sanders MM, Burleson JA, Jennings K, Kurtzman S, Kreutzer D. Angiogenesis in normal tissue adjacent to colon cancer. *J Surg Oncol* 1998; **69**: 230-234 [PMID: 9881940]

29 **Croft DR**, Sahai E, Mavria G, Li S, Tsai J, Lee WM, Marshall CJ, Olson MF. Conditional ROCK activation in vivo induces tumor cell dissemination and angiogenesis. *Cancer Res* 2004; **64**: 8994-9001 [PMID: 15604264 DOI: 10.1158/0008-5472.CAN-04-2052]

30 **Pillé JY**, Denoyelle C, Varet J, Bertrand JR, Soria J, Opolon P, Lu H, Pritchard LL, Vannier JP, Malvy C, Soria C, Li H. Anti-RhoA and anti-RhoC siRNAs inhibit the proliferation and

invasiveness of MDA-MB-231 breast cancer cells in vitro and in vivo. *Mol Ther* 2005; **11**: 267-274 [PMID: 15668138 DOI: 10.1016/j.ymthe.2004.08.029]

31 **Jing YM**, Zhou SF. Expression of CD105 marker microvessel density and vascular endothelial growth factor in gastric cancer. *Hebei Yiyao* 2004; **10**: 1-5

P- Reviewer: Kim SM, Li BS **S- Editor**: Gou SX
L- Editor: AmEditor **E- Editor**: Zhang DN

World Journal of Gastroenterology

Submit a Manuscript: http://www.wjgnet.com/esps/
Help Desk: http://www.wjgnet.com/esps/helpdesk.aspx
DOI: 10.3748/wjg.v21.i3.913

World J Gastroenterol 2015 January 21; 21(3): 913-918
ISSN 1007-9327 (print) ISSN 2219-2840 (online)

ORIGINAL ARTICLE

Retrospective Study

Association of nonalcoholic fatty liver disease and liver cancer

Perla Oliveira Schulz, Fabio Gonçalves Ferreira, Maria de Fátima Araújo Nascimento, Andrea Vieira, Mauricio Alves Ribeiro, André Ibrahim David, Luiz Arnaldo Szutan

Perla Oliveira Schulz, Andrea Vieira, Gastroenterology Service, Internal Medicine Department, Santa Casa School of Medical Sciences, São Paulo 01277-900, Brazil
Maria de Fátima Araújo Nascimento, Pathology Department, Santa Casa School of Medical Sciences, São Paulo 01277-900, Brazil
André Ibrahim David, GI Transplant Service, Gastroenterology Department, University of São Paulo, São Paulo 01246-903, Brazil
Fabio Gonçalves Ferreira, Mauricio Alves Ribeiro, Luiz Arnaldo Szutan, Department of Surgery, Liver and Portal Hypertension Group, Santa Casa School of Medical Sciences, São Paulo 01277-900, Brazil
Author contributions: Schulz PO performed the research and collected and analyzed the data; Ferreira FG contributed to the design of the study; Nascimento MFA performed the histological analysis; Vieira A, Ribeiro MA, David AI and Szutan LA contributed to the design of the study and analysis of the data; Schulz PO and Ferreira FG wrote the manuscript.
Supported by CAPES-MEC-Brazil - Grant master's thesis.

Correspondence to: Fabio Gonçalves Ferreira, MD, PhD, Department of Surgery, Liver and Portal Hypertension Group, Santa Casa School of Medical Sciences, R Apinajes, 1060 ap 93, São Paulo 01277-900, Brazil. drfabioferreira@uol.com.br
Telephone: +55-11-992110057
Fax: +55-11-33378164
Received: June 3, 2014
Peer-review started: June 3, 2014
First decision: June 27, 2014
Revised: July 18, 2014
Accepted: September 18, 2014
Article in press: September 19, 2014
Published online: January 21, 2015

Abstract

AIM: To investigate the association between nonalcoholic fatty liver disease (NAFLD) and liver cancer, and NAFLD prevalence in different liver tumors.

METHODS: This is a retrospective study of the clinical, laboratory and histological data of 120 patients diagnosed with primary or secondary hepatic neoplasms and treated at a tertiary center where they underwent hepatic resection and/or liver transplantation, with subsequent evaluation of the explant or liver biopsy. The following criteria were used to exclude patients from the study: a history of alcohol abuse, hepatitis B or C infection, no tumor detected in the liver tissue examined by histological analysis, and the presence of chronic autoimmune hepatitis, hemochromatosis, Wilson's disease, or hepatoblastoma. The occurrence of NAFLD and the association with its known risk factors were studied. The risk factors considered were diabetes mellitus, impaired glucose tolerance, impaired fasting glucose, body mass index, dyslipidemia, and arterial hypertension. Presence of reticulin fibers in the hepatic neoplasms was assessed by histological analysis using slide-mounted specimens stained with either hematoxylin and eosin or Masson's trichrome and silver impregnation. Analysis of tumor-free liver parenchyma was carried out to determine the association between NAFLD and its histological grade.

RESULTS: No difference was found in the association of NAFLD with the general population (34.2% and 30.0% respectively, 95%CI: 25.8-43.4). Evaluation by cancer type showed that NAFLD was more prevalent in patients with liver metastasis of colorectal cancer than in patients with hepatocellular carcinoma and intrahepatic cholangiocarcinoma (OR = 3.99, 95%CI: 1.78-8.94, $P < 0.001$ *vs* OR = 0.60, 95%CI: 0.18-2.01, $P = 0.406$ and OR = 0.70, 95%CI: 0.18-2.80, $P = 0.613$,

respectively). There was a higher prevalence of liver fibrosis in patients with hepatocellular carcinoma (OR = 3.50, 95%CI: 1.06-11.57, *P* = 0.032). Evaluation of the relationship between the presence of NAFLD, nonalcoholic steatohepatitis, and liver fibrosis, and their risk factors, showed no significant statistical association for any of the tumors studied.

CONCLUSION: NAFLD is more common in patients with liver metastases caused by colorectal cancer.

Key words: Hepatocellular carcinoma; Colorectal liver metastases; Intrahepatic cholangiocarcinoma; Liver fibrosis; Nonalcoholic fatty liver disease; Nonalcoholic steatohepatitis

Core tip: There has not been a study clearly showing a relation between the nonalcoholic steatohepatitis cirrhosis and hepatocellular carcinoma (HCC). Some studies have suggested that the early stage of hepatic steatosis can be a favorable microenvironment for the development of liver metastases of colorectal cancer (LMCC). Others have suggested that hepatic steatosis has a protective role in the development of LMCC. Our analysis of the association of nonalcoholic fatty liver disease (NAFLD) with liver primary and secondary malignancies found a statistically higher prevalence of NAFLD in patients with LMCC, but not in non-cirrhotic HCC patients.

Schulz PO, Ferreira FG, Nascimento MFA, Vieira A, Ribeiro MA, David AI, Szutan LA. Association of nonalcoholic fatty liver disease and liver cancer. *World J Gastroenterol* 2015; 21(3): 913-918 Available from: URL: http://www.wjgnet.com/1007-9327/full/v21/i3/913.htm DOI: http://dx.doi.org/10.3748/wjg.v21.i3.913

INTRODUCTION

With the increasing prevalence of obesity and insulin resistance in the Western world, nonalcoholic fatty liver disease (NAFLD) has become a major cause of chronic liver disease[1]. Based on studies using different diagnostic methods, the current estimates of NAFLD worldwide prevalence vary from 6.3% to 33.0% (average = 20%)[2]. Molecular and pathophysiological changes caused by NAFLD may lead to liver cancer, increasing the incidence rate and modifying the epidemiology of primary and metastatic liver cancer[3-6]. It is predicted that NAFLD will emerge as the main risk factor for the development of hepatocellular carcinoma (HCC), which is the primary and most common liver cancer (70%-85% of cases), as the incidence of hepatitis B and C becomes reduced due to the expected development of better antiviral vaccines and drugs[7,8].

The actual incidence rate of the NAFLD-HCC association is unknown, but it has been reported that 30%-40% of the tumors diagnosed in patients with cryptogenic cirrhosis may be associated with obesity, insulin resistance, metabolic disorders, and NAFLD[9]. Furthermore, an increased incidence rate of intrahepatic cholangiocarcinoma (IHCC), as compared to extrahepatic cholangiocarcinoma in Western countries[6], suggests a possible interference of NAFLD[7,10-12] by the same pathophysiological mechanisms related to HCC and in the genesis of bile duct tumors[7]. NAFLD and colorectal cancer share some of the same risk factors, namely obesity, insulin resistance, and diabetes. One study demonstrated an increased risk of colorectal cancer in patients with NAFLD[13], while other studies have suggested that metabolic syndrome could be a predictor for the development of liver metastases of colorectal neoplasms[14].

To date, no study in the publicly available literature has shown an association between NAFLD and hepatic malignancy, either primary or secondary. The aim of this study was to evaluate the possible association of NAFLD with the most common primary and secondary liver cancers.

MATERIALS AND METHODS

Study design

This retrospective study encompasses clinical, laboratory and histological data of 120 patients diagnosed with either primary or secondary hepatic neoplasms. Patients were treated in the Hospital of Santa Casa Medical School of São Paulo between the dates of January 2007 and December 2011. All of the studies were conducted following approval by the local Ethics in Human Research Committee.

All of the 120 patients underwent hepatic resection and/or liver transplantation followed by subsequent evaluation of the explant or liver biopsy. Patients were excluded from the study due to: history of alcohol abuse, defined as intake of 20 g/d or more[15]; hepatitis B or C infection; absence of tumor-free liver tissue in histological material; presence of chronic autoimmune hepatitis, hemochromatosis, or Wilson's disease; hepatoblastoma cases due to very specific characteristics and histopathological features.

The medical records of the included patients were reviewed for clinical data such as age, sex, and comorbidities. Comorbidities were defined as: previous diagnosis of diabetes mellitus (DM) or impaired glucose tolerance (GI) and/or impaired fasting glucose (defined as $\geqslant$ 100 mg/dL); overweight, using the patient's height and weight to calculate the body mass index (BMI) and with the overweight threshold set as a BMI of $\geqslant$ 25 kg/m^2; history of dyslipidemia or laboratory tests demonstrating low-density lipoprotein > 160 mg/dL or triglyceride levels > 150 mg/dL; previous diagnosis of arterial hypertension, defined as systolic blood pressure $\geqslant$ 140 and/or diastolic blood pressure $\geqslant$ 90 mmHg.

Table 1 Neoplasms of 120 patients with primary and secondary hepatic neoplasm *n* (%)

Neoplasms	Incidence rate	Age, yr	Sex (male)	Steatosis	Fibrosis	NASH
NCLM	48 (40.0)	56.9	19 (39.6)	11 (22.9)	24 (50.0)	2 (4.2)
LMCC	40 (33.3)	57.5	25 (62.5)	22 (55.0)	15 (37.5)	0 (0.0)
HCC	16 (13.3)	57.9	13 (81.3)	4 (25.0)	12 (75.0)	0 (0.0)
IHCC	11 (9.2)	63.3	2 (18.2)	3 (27.3)	7 (63.6)	0 (0.0)
Others	5 (4.2)	64.4	0 (0.0)	1 (20.0)	2 (40.0)	0 (0.0)

HCC: Hepatocellular carcinoma; IHCC: Intrahepatic cholangiocarcinoma; LMCC: Liver metastasis of colorectal cancer; NASH: Nonalcoholic steatohepatitis; NCLM: Non-colorectal liver metastasis; Others: Lymphoproliferative tumors and sarcoma.

Table 2 Association of risk factors for nonalcoholic fatty liver disease with steatosis and liver fibrosis in 120 patients with primary and secondary hepatic neoplasm

NAFLD risk factor (*n*)	Liver steatosis			Liver fibrosis		
	n (%)	*P* value	OR (95%CI)	*n* (%)	*P* value	OR (95%CI)
GI and/or DM (41)	14 (34.1)	0.182	1.70 (0.78 -3.71)	31 (51.7)	0.196	0.62 (0.30-1.28)
Dyslipidemia (17)	9 (52.9)	0.078	2.50 (0.88-7.06)	8 (47.1)	0.793	0.87 (0.31-2.44)
Hypertension (55)	24 (43.6)	< 0.001[1]	3.99 (1.73-9.16)	31 (56.4)	0.200	1.60 (0.78-3.31)
Overweight (53)	26 (49.1)	0.002	3.76 (1.56-9.05)	30 (56.6)	0.165	1.74 (0.79-3.81)

[1]A statistically significant difference. DM: Diabetes mellitus; GI: Glucose intolerance; NAFLD: Nonalcoholic fatty liver disease.

Histopathology

All 120 histopathological examinations were reviewed by a pathologist with over 30 years of experience in liver pathology, who was blinded to the clinical, laboratory and/or patient demographics. The histological diagnosis of hepatic neoplasms was made using slide-mounted specimens stained with hematoxylin and eosin or Masson's trichrome and silver impregnation to assess reticulin fibers. Using the Kleiner *et al*[16] classification scoring system, we assessed the histological grade of lesions in the tumor-free liver parenchyma.

Statistical analysis

Descriptive statistics using the previously defined variables were performed to assess the results. The Statistical Package for Social Sciences version 13.0 was used for statistical calculations. Epi Info version 3.4.3 was used to evaluate confidence intervals (CIs) and odds ratios (ORs). Descriptive analyses were performed on the summary measures for quantitative variables. Qualitative variables were calculated, and absolute and relative frequencies were determined. The Student's *t*-test was used for comparisons of NAFLD with liver malignancy. The Mann-Whitney test was used for nonparametric variables. The χ^2 test and Fisher's exact test were used for statistical analysis. Significance level for all tests was defined at 5% ($P < 0.05$).

RESULTS

The demographic characteristics and histological features of the 120 included patients are listed in Table 1. Milder degrees of steatosis (grade 1; 39 cases) and liver fibrosis (grades 1 and 2, 51 cases) were predominant. When the association of steatosis with fibrosis was evaluated, no statistically significant difference ($P = 0.564$) was observed.

Neither liver fibrosis nor NAFLD showed any statistically significant relationship with their risk factors for any of the tumors studied (Table 2). Although two individuals with steatohepatitis had GI and/or DM, these findings were not statistically significant ($P = 0.507$). An analysis based on the type of liver cancer showed an association of steatosis only in liver metastasis due to colorectal cancer (Table 3) and fibrosis only in HCC.

DISCUSSION

The clinical course of NAFLD may vary according to the initial histological diagnosis and can range from a reversible benign outcome (steatosis) to the development of an inflammatory steatohepatitis (NASH) in 10%-20% of cases. Once established, 3%-5% of NASH cases progress to cirrhosis within 15-20 years, with an increase in risk of developing HCC[2,17]. In the Western population, the cumulative annual incidence rate of HCC in patients with NASH and cirrhosis was reported as 2.6%[18], while in the Asian population this rate was reported as 11.3%[19].

Recently, Hamady *et al*[20] identified hepatic steatosis as an independent risk factor for recurrence following curative resection of liver metastasis from colorectal cancer (LMCC) and was also associated with a worse prognosis. The biological characteristics of these metastases include bilateral distribution, lymph node involvement, and the presence of extrahepatic disease at diagnosis. Changes in inflammatory cytokines and extracellular matrix remodeling proteinases were associated with an increased risk of metastasis in many different organ systems[21].

Table 3 Prevalence of steatosis and hepatic fibrosis according to type of hepatic neoplasm

Histologic type (*n*)	Liver steatosis			Liver fibrosis		
	n (%)	*P* value	OR (95%CI)	*n* (%)	*P* value	OR (95%CI)
LMCC (40)	22 (55.0)	< 0.001[1]	3.99 (1.78-8.94)	15 (37.5)	0.053	0.47 (0.21-1.02)
NCLM (48)	11 (22.9)	0.034	0.42 (0.18-0.95)	24 (50.0)	1.000	1.00 (0.48-2.08)
HCC (16)	4 (25.0)	0.406	0.60 (0.18-2.01)	12 (75.0)	0.032[1]	3.50 (1.06-11.57)
IHCC (11)	3 (27.3)	0.613	0.70 (0.18-2.80)	7 (63.6)	0.343	1.85 (0.51-6.68)

[1]A statistically significant difference. HCC: Hepatocellular carcinoma; IHCC: Intrahepatic cholangiocarcinoma; LMCC: Liver metastasis of colorectal cancer; NCLM: Non-colorectal liver metastasis.

Significant changes that occur in steatosis and NASH cause an increase in certain signaling molecules, such as transforming growth factor-beta (TGF-β) and some cell matrix metalloproteinases, which may be important in tumor formation and angiogenesis stimulation[21-24]. However, other studies indicated that LMCC is less frequent in subjects with NAFLD and suggested that steatosis may be, in fact, an unfavorable factor for the development of LMCC[25-29]. Therefore, it is not clear whether NAFLD influences the development of LMCC, as demonstrated in this study, or has a protective effect (blocking LMCC development).

The incidence rate of malignant liver tumors in patients involved in the current study was similar to that reported in the literature[6,7]. No statistical differences were found in the association of hepatic steatosis neoplasms compared with the general population (34.2% in the study group *vs* 20%-30% in the general population[2]). However, when analysis was performed in our study according to the different cancer types, we found a higher prevalence of hepatic steatosis in patients with LMCC, even in cases with milder liver fibrosis, suggesting that even milder degrees of steatosis may be used as predictors for the development of hepatic neoplasms. Steatosis and liver cancer share several risk factors (including obesity, hyperinsulinemia, GI, and DM), with hepatic steatosis directly changing the liver microcirculation and inflammatory cytokines promoting the development of liver metastases[4,30]. It is also possible, however, that there is no direct relationship of steatosis with the onset of metastasis. Previous exposure to chemotherapy has been shown to result in an increase in both steatosis and steatohepatitis, in up to 92% of cases studied[4,31,32]. Furthermore, steatosis induced by neoadjuvant chemotherapy was shown to lead to greater circulation disorder with increased susceptibility to complications, such as micro-metastases[31]. Yet another possibility is that the association of NAFLD with liver colorectal metastases may occur randomly, as suggested by the high prevalence of hepatic steatosis in the general population, with no real relationship existing between these two diseases.

A discrete prevalence (with no statistically significant association) of steatosis was observed in the presence of GI and/or DM, hypertension, dyslipidemia, and overweight status. GI, DM and obesity are considered risk factors for the development of most of the hepatic neoplasms studied[12-14,33-40]. The presence of these factors, and not that of hepatic steatosis, could contribute to the development of neoplasms. However, cases of primary and secondary hepatic neoplasms associated with the presence of NAFLD even in the absence of these metabolic risk factors have been reported in other studies[41,42], suggesting that hepatic steatosis could be a predictor of these neoplasms, regardless of the presence or absence of obesity, GI and/or DM[42].

The main limitations of the present study were its retrospective design and its use of incomplete patient medical records as the source of information, which in some cases represented an absence of demographic information, anthropometric measurements, laboratory data, and other patient details. A prospective study may have provided more accurate evidence of a causal relationship between NAFLD and hepatic neoplasms. However, such a study design is logistically very difficult to perform due to the low annual incidence rate of different cancers in non-cirrhotic liver[42].

Surveillance screening of hepatic neoplasms in every obese or diabetic non-cirrhotic individual would not be cost-effective, considering that both metabolic disorders are epidemic in Brazil and several other countries around the world[37,43]. Thus, defining risk factors responsible for the development of liver cancer is crucial for increasing response rates of patients diagnosed at an early disease stage and treated with appropriate therapies for malignant tumors, which would consequently lead to a better prognosis.

In conclusion, the present study found no statistically significant association of NAFLD in patients with liver neoplasms in the general population. Only liver metastasis of colorectal cancer showed a significant association with NAFLD.

COMMENTS

Background

Some studies have suggested that early stages of hepatic steatosis can be considered a favorable microenvironment for the development of liver metastases of colorectal cancer (LMCC) as well as for the development of primary liver cancers such as hepatocellular carcinoma and intrahepatic cholangiocarcinoma. Yet, other studies have suggested a protective role of hepatic steatosis in the development of LMCC.

Research frontiers

Nonalcoholic fatty liver disease (NAFLD) includes a spectrum of diseases

starting with simple steatosis, steatohepatitis (NASH), fibrosis, and finally cirrhosis. Associations of NAFLD with cirrhotic stage and primary liver cancer have already been shown. Although primary liver cancer has been extensively studied, there has not been strong scientific evidence reported for non-cirrhotic NAFLD patients. In early stages of steatosis, the associations with liver cancer have ranged from protection to NAFLD as a causal factor in the development of LMCC.

Innovations and breakthroughs

This study found a significant association between NAFLD and liver metastasis of colorectal cancer, but not with any of the other liver neoplasms studied.

Applications

Surveillance screening of hepatic neoplasms in every obese or diabetic non-cirrhotic individual would be cost prohibitive since both metabolic disorders are epidemic. Thus, defining risk factors responsible for the development of liver cancer is crucial for increasing response rates of patients diagnosed at an early disease stage and treated with appropriate therapies for malignant tumors, which would consequently lead to a better prognosis.

Peer review

The authors evaluated the role of hepatic steatosis as a risk factor in patients who underwent liver surgery for either primary liver tumors (hepatocellular carcinoma and colorectal carcinoma) or liver metastases (colorectal or other tumors). Although the study did not include a large number of patients with steatosis/fibrosis and there were no patients with NASH, the study does provide important insights into the influence of NAFLD in the development of liver cancer.

REFERENCES

1 **Marchesini G**, Babini M. Nonalcoholic fatty liver disease and the metabolic syndrome. *Minerva Cardioangiol* 2006; **54**: 229-239 [PMID: 16778754]

2 **Vernon G**, Baranova A, Younossi ZM. Systematic review: the epidemiology and natural history of non-alcoholic fatty liver disease and non-alcoholic steatohepatitis in adults. *Aliment Pharmacol Ther* 2011; **34**: 274-285 [PMID: 21623852 DOI: 10.1111/j.1365-2036.2011.04724.x]

3 **Jemal A**, Bray F, Center MM, Ferlay J, Ward E, Forman D. Global cancer statistics. *CA Cancer J Clin* 2011; **61**: 69-90 [PMID: 21296855 DOI: 10.3322/caac.20107]

4 **van der Bilt JD**, Kranenburg O, Borren A, van Hillegersberg R, Borel Rinkes IH. Ageing and hepatic steatosis exacerbate ischemia/reperfusion-accelerated outgrowth of colorectal micrometastases. *Ann Surg Oncol* 2008; **15**: 1392-1398 [PMID: 18335279 DOI: 10.1245/s10434-007-9758-0]

5 **El-Serag HB**, Rudolph KL. Hepatocellular carcinoma: epidemiology and molecular carcinogenesis. *Gastroenterology* 2007; **132**: 2557-2576 [PMID: 17570226 DOI: 10.1053/j.gastro.2007.04.061]

6 **Khan SA**, Thomas HC, Davidson BR, Taylor-Robinson SD. Cholangiocarcinoma. *Lancet* 2005; **366**: 1303-1314 [PMID: 16214602 DOI: 10.1016/S0140-6736(05)67530-7]

7 **Michelini E**, Lonardo A, Ballestri S, Costantini M, Caporali C, Bonati ME, Bertolotti M, Iori R, Loria P. Is cholangiocarcinoma another complication of insulin resistance: a report of three cases. *Metab Syndr Relat Disord* 2007; **5**: 194-202 [PMID: 18370827 DOI: 10.1089/met.2006.0018]

8 **Baffy G**, Brunt EM, Caldwell SH. Hepatocellular carcinoma in non-alcoholic fatty liver disease: an emerging menace. *J Hepatol* 2012; **56**: 1384-1391 [PMID: 22326465 DOI: 10.1016/j.jhep.2011.10.027]

9 **Hill-Baskin AE**, Markiewski MM, Buchner DA, Shao H, DeSantis D, Hsiao G, Subramaniam S, Berger NA, Croniger C, Lambris JD, Nadeau JH. Diet-induced hepatocellular carcinoma in genetically predisposed mice. *Hum Mol Genet* 2009; **18**: 2975-2988 [PMID: 19454484 DOI: 10.1093/hmg/ddp236]

10 **Shaib Y**, El-Serag HB. The epidemiology of cholangiocarcinoma. *Semin Liver Dis* 2004; **24**: 115-125 [PMID: 15192785 DOI: 10.1055/s-2004-828889]

11 **Reddy SK**, Hyder O, Marsh JW, Sotiropoulos GC, Paul A, Alexandrescu S, Marques H, Pulitano C, Barroso E, Aldrighetti L, Geller DA, Sempoux C, Herlea V, Popescu I, Anders R, Rubbia-Brandt L, Gigot JF, Mentha G, Pawlik TM. Prevalence of nonalcoholic steatohepatitis among patients with resectable intrahepatic cholangiocarcinoma. *J Gastrointest Surg* 2013; **17**: 748-755 [PMID: 23355033 DOI: 10.1007/s11605-013-2149-x]

12 **Welzel TM**, Graubard BI, Zeuzem S, El-Serag HB, Davila JA, McGlynn KA. Metabolic syndrome increases the risk of primary liver cancer in the United States: a study in the SEER-Medicare database. *Hepatology* 2011; **54**: 463-471 [PMID: 21538440 DOI: 10.1002/hep.24397]

13 **Wong VW**, Wong GL, Tsang SW, Fan T, Chu WC, Woo J, Chan AW, Choi PC, Chim AM, Lau JY, Chan FK, Sung JJ, Chan HL. High prevalence of colorectal neoplasm in patients with non-alcoholic steatohepatitis. *Gut* 2011; **60**: 829-836 [PMID: 21339204 DOI: 10.1136/gut.2011.237974]

14 **Shen Z**, Ye Y, Bin L, Yin M, Yang X, Jiang K, Wang S. Metabolic syndrome is an important factor for the evolution of prognosis of colorectal cancer: survival, recurrence, and liver metastasis. *Am J Surg* 2010; **200**: 59-63 [PMID: 20074697 DOI: 10.1016/j.amjsurg.2009.05.005]

15 **Cotrim HP**, Parise ER, Oliveira CP, Leite N, Martinelli A, Galizzi J, Silva Rde C, Mattos A, Pereira L, Amorim W, Ivantes C, Souza F, Costa M, Maia L, Pessoa M, Oliveira F. Nonalcoholic fatty liver disease in Brazil. Clinical and histological profile. *Ann Hepatol* 2011; **10**: 33-37 [PMID: 21301007]

16 **Kleiner DE**, Brunt EM, Van Natta M, Behling C, Contos MJ, Cummings OW, Ferrell LD, Liu YC, Torbenson MS, Unalp-Arida A, Yeh M, McCullough AJ, Sanyal AJ. Design and validation of a histological scoring system for nonalcoholic fatty liver disease. *Hepatology* 2005; **41**: 1313-1321 [PMID: 15915461 DOI: 10.1002/hep.20701]

17 **de Alwis NM**, Day CP. Non-alcoholic fatty liver disease: the mist gradually clears. *J Hepatol* 2008; **48** Suppl 1: S104-S112 [PMID: 18304679 DOI: 10.1016/j.jhep.2008.01.009]

18 **Ascha MS**, Hanouneh IA, Lopez R, Tamimi TA, Feldstein AF, Zein NN. The incidence and risk factors of hepatocellular carcinoma in patients with nonalcoholic steatohepatitis. *Hepatology* 2010; **51**: 1972-1978 [PMID: 20209604 DOI: 10.1002/hep.23527]

19 **Yatsuji S**, Hashimoto E, Tobari M, Taniai M, Tokushige K, Shiratori K. Clinical features and outcomes of cirrhosis due to non-alcoholic steatohepatitis compared with cirrhosis caused by chronic hepatitis C. *J Gastroenterol Hepatol* 2009; **24**: 248-254 [PMID: 19032450 DOI: 10.1111/j.1440-1746.2008.05640.x]

20 **Hamady ZZ**, Rees M, Welsh FK, Toogood GJ, Prasad KR, John TK, Lodge JP. Fatty liver disease as a predictor of local recurrence following resection of colorectal liver metastases. *Br J Surg* 2013; **100**: 820-826 [PMID: 23354994 DOI: 10.1002/bjs.9057]

21 **Fingleton B**. Matrix metalloproteinases: roles in cancer and metastasis. *Front Biosci* 2006; **11**: 479-491 [PMID: 16146745 DOI: 10.2741/1811]

22 **Yu Q**, Stamenkovic I. Cell surface-localized matrix metalloproteinase-9 proteolytically activates TGF-beta and promotes tumor invasion and angiogenesis. *Genes Dev* 2000; **14**: 163-176 [PMID: 10652271]

23 **Kharbanda KK**, Rogers DD, Wyatt TA, Sorrell MF, Tuma DJ. Transforming growth factor-beta induces contraction of activated hepatic stellate cells. *J Hepatol* 2004; **41**: 60-66 [PMID: 15246209 DOI: 10.1016/j.jhep.2004.03.019]

24 **Gorden DL**, Fingleton B, Crawford HC, Jansen DE, Lepage M, Matrisian LM. Resident stromal cell-derived MMP-9 promotes the growth of colorectal metastases in the liver microenvironment. *Int J Cancer* 2007; **121**: 495-500 [PMID: 17417772 DOI: 10.1002/ijc.22594]

25 **Hayashi S**, Masuda H, Shigematsu M. Liver metastasis rare in

colorectal cancer patients with fatty liver. *Hepatogastroenterology* 1997; **44**: 1069-1075 [PMID: 9261601]
26 **Tamura R**, Masuda H, Ishii Y, Nemoto N. Relationship between fatty liver and liver metastasis in rats given injection of rat colon cancer cell line. *Hepatogastroenterology* 1999; **46**: 167-171 [PMID: 10228783]
27 **Karube H**, Masuda H, Hayashi S, Ishii Y, Nemoto N. Fatty liver suppressed the angiogenesis in liver metastatic lesions. *Hepatogastroenterology* 2000; **47**: 1541-1545 [PMID: 11148998]
28 **Augustin G**, Bruketa T, Korolija D, Milosevic M. Lower incidence of hepatic metastases of colorectal cancer in patients with chronic liver diseases: meta-analysis. *Hepatogastroenterology* 2013; **60**: 1164-1168 [PMID: 23803379 DOI: 10.5754/hge11561]
29 **Murono K**, Kitayama J, Tsuno NH, Nozawa H, Kawai K, Sunami E, Akahane M, Watanabe T. Hepatic steatosis is associated with lower incidence of liver metastasis from colorectal cancer. *Int J Colorectal Dis* 2013; **28**: 1065-1072 [PMID: 23392476 DOI: 10.1007/s00384-013-1656-2]
30 **VanSaun MN**, Lee IK, Washington MK, Matrisian L, Gorden DL. High fat diet induced hepatic steatosis establishes a permissive microenvironment for colorectal metastases and promotes primary dysplasia in a murine model. *Am J Pathol* 2009; **175**: 355-364 [PMID: 19541928 DOI: 10.2353/ajpath.2009.080703]
31 **Vauthey JN**, Pawlik TM, Ribero D, Wu TT, Zorzi D, Hoff PM, Xiong HQ, Eng C, Lauwers GY, Mino-Kenudson M, Risio M, Muratore A, Capussotti L, Curley SA, Abdalla EK. Chemotherapy regimen predicts steatohepatitis and an increase in 90-day mortality after surgery for hepatic colorectal metastases. *J Clin Oncol* 2006; **24**: 2065-2072 [PMID: 16648507 DOI: 10.1200/JCO.2005.05.3074]
32 **Karoui M**, Penna C, Amin-Hashem M, Mitry E, Benoist S, Franc B, Rougier P, Nordlinger B. Influence of preoperative chemotherapy on the risk of major hepatectomy for colorectal liver metastases. *Ann Surg* 2006; **243**: 1-7 [PMID: 16371728 DOI: 10.1097/01.sla.0000193603.26265.c3]
33 **El-Serag HB**, Richardson PA, Everhart JE. The role of diabetes in hepatocellular carcinoma: a case-control study among United States Veterans. *Am J Gastroenterol* 2001; **96**: 2462-2467 [PMID: 11513191 DOI: 10.1111/j.1572-0241.2001.04054.x]
34 **Nair S**, Mason A, Eason J, Loss G, Perrillo RP. Is obesity an independent risk factor for hepatocellular carcinoma in cirrhosis? *Hepatology* 2002; **36**: 150-155 [PMID: 12085359 DOI: 10.1053/jhep.2002.33713]
35 **Calle EE**, Rodriguez C, Walker-Thurmond K, Thun MJ. Overweight, obesity, and mortality from cancer in a prospectively studied cohort of U.S. adults. *N Engl J Med* 2003; **348**: 1625-1638 [PMID: 12711737 DOI: 10.1056/NEJMoa021423]
36 **Qian Y**, Fan JG. Obesity, fatty liver and liver cancer. *Hepatobiliary Pancreat Dis Int* 2005; **4**: 173-177 [PMID: 15908310]
37 **Pischon T**, Nöthlings U, Boeing H. Obesity and cancer. *Proc Nutr Soc* 2008; **67**: 128-145 [PMID: 18412987 DOI: 10.1017/S0029665108006976]
38 **Amarapurkar DN**, Patel ND, Kamani PM. Impact of diabetes mellitus on outcome of HCC. *Ann Hepatol* 2008; **7**: 148-151 [PMID: 18626433]
39 **Fair AM**, Montgomery K. Energy balance, physical activity, and cancer risk. *Methods Mol Biol* 2009; **472**: 57-88 [PMID: 19107429 DOI: 10.1007/978-1-60327-492-0_3]
40 **Schlienger JL**, Luca F, Vinzio S, Pradignac A. [Obesity and cancer]. *Rev Med Interne* 2009; **30**: 776-782 [PMID: 19524333 DOI: 10.1016/j.revmed.2009.04.007]
41 **Ertle J**, Dechêne A, Sowa JP, Penndorf V, Herzer K, Kaiser G, Schlaak JF, Gerken G, Syn WK, Canbay A. Non-alcoholic fatty liver disease progresses to hepatocellular carcinoma in the absence of apparent cirrhosis. *Int J Cancer* 2011; **128**: 2436-2443 [PMID: 21128245 DOI: 10.1002/ijc.25797]
42 **Alexander J**, Torbenson M, Wu TT, Yeh MM. Non-alcoholic fatty liver disease contributes to hepatocarcinogenesis in non-cirrhotic liver: a clinical and pathological study. *J Gastroenterol Hepatol* 2013; **28**: 848-854 [PMID: 23302015 DOI: 10.1111/jgh.12116]
43 **Flegal KM**, Carroll MD, Ogden CL, Curtin LR. Prevalence and trends in obesity among US adults, 1999-2008. *JAMA* 2010; **303**: 235-241 [PMID: 20071471 DOI: 10.1001/jama.2009.2014]

P- Reviewer: Balaban YH, Rajeshwari K, Zhu X **S- Editor**: Qi Y
L- Editor: A **E- Editor**: Wang CH

World Journal of Gastroenterology

Submit a Manuscript: http://www.wjgnet.com/esps/
Help Desk: http://www.wjgnet.com/esps/helpdesk.aspx
DOI: 10.3748/wjg.v21.i3.919

World J Gastroenterol 2015 January 21; 21(3): 919-925
ISSN 1007-9327 (print) ISSN 2219-2840 (online)

ORIGINAL ARTICLE

Retrospective Study

Clinical characteristics and management of gastric tube cancer with endoscopic submucosal dissection

Michita Mukasa, Hidetoshi Takedatsu, Ken Matsuo, Hiroaki Sumie, Hikaru Yoshida, Atsushi Hinosaka, Yasutomo Watanabe, Osamu Tsuruta, Takuji Torimura

Michita Mukasa, Hidetoshi Takedatsu, Ken Matsuo, Hiroaki Sumie, Hikaru Yoshida, Atsushi Hinosaka, Yasutomo Watanabe, Osamu Tsuruta, Takuji Torimura, Division of Gastroenterology, Department of Medicine, Kurume University School of Medicine, 67 Asahi-machi, Kurume, Fukuoka 830-0011, Japan

Author contributions: Mukasa M, Matsuo K, Sumie H, Yoshida H, Hinosaka A and Watanabe Y performed the majority of the experiments; Takedatsu H, Tsuruta O and Torimura T designed the study and wrote the manuscript.

Correspondence to: Hidetoshi Takedatsu, MD, PhD, Division of Gastroenterology, Department of Medicine, Kurume University School of Medicine, 67 Asahi-machi, Kurume, Fukuoka 830-0011, Japan. takedatsu_hidetoshi@kurume-u.ac.jp
Telephone: 81-942-353311
Fax: +81-942-342623

Received: June 5, 2014
Peer-review started: June 6, 2014
First decision: July 27, 2014
Revised: July 22, 2014
Accepted: September 18, 2014
Article in press: September 19, 2014
Published online: January 21, 2015

Abstract

AIM: To identify the characteristics of gastric tube cancer (GTC) and the complications associated with endoscopic submucosal dissection (ESD) for GTC.

METHODS: Between 2007 and 2012, 11 individuals with early gastric cancer in the reconstructed gastric tube after esophagectomy who underwent ESD in this hospital were studied. The characteristics of GTC were identified, and the complications of ESD for GTC were analyzed at three phases: preoperative, intraoperative, and postoperative.

RESULTS: A total of 11 consecutive patients with 11 GTCs were selected for this study. All cases underwent *en bloc* resections by ESD. The median procedure time was 142 min. The average GTC diameter was 26.1 mm, and the average size of the resected lesions was 45.5 mm. The histopathological diagnosis in all cases was a differentiated adenocarcinoma. In the preoperative phase, anastomotic strictures (5/11, 45%) and food residues (4/11, 36.4%) in the gastric tube were the main complications. In the intraoperative phase, bleeding was observed in 5 cases (45%). The postoperative complications observed were delayed bleeding in 2 cases (18.2%) and stenosis in one case (9.1%). The case with stenosis was successfully treated using endoscopic balloon dilatation.

CONCLUSION: Minor complications were frequently observed. However, all GTCs underwent *en bloc* resection with ESD without any serious complications. ESD is considered a useful treatment for GTC.

Key words: Gastric tube cancer; Endoscopic submucosal dissection; Complications; Endoscopy; Esophagectomy

Core tip: The pulled-up stomach conduit, when reconstructed and used as an esophageal substitute after esophagectomy, has the potential to develop gastric tube cancer (GTC). Although endoscopic submucosal dissection (ESD) for early gastric cancer is

common, there are only a few reports on ESD for GTC. In this study, we identified the characteristics of GTC and the complications associated with ESD for GTC. Minor complications, such as anastomotic stricture, food residue, and intraoperative bleeding, were frequently observed. However, all GTCs were safely resected *en bloc* with ESD without serious complications. ESD can be considered a useful treatment modality for GTC.

Mukasa M, Takedatsu H, Matsuo K, Sumie H, Yoshida H, Hinosaka A, Watanabe Y, Tsuruta O, Torimura T. Clinical characteristics and management of gastric tube cancer with endoscopic submucosal dissection. *World J Gastroenterol* 2015; 21(3): 919-925 Available from: URL: http://www.wjgnet.com/1007-9327/full/v21/i3/919.htm DOI: http://dx.doi.org/10.3748/wjg.v21.i3.919

INTRODUCTION

Esophageal cancer is associated with metachronous malignancies in other organs, and its incidence rate ranges from 11.3% to 12.0%[1-4]. Gastric cancer and head and neck cancer are the most commonly identified malignancies in this regard[1,2]. The pulled-up stomach conduit, which can be used as an esophageal substitute after esophagectomy, has the potential to develop a second primary cancer known as gastric tube cancer (GTC). GTC has been increasingly observed in recent years as advancements in treatments for esophageal cancer have contributed to prolonged patient survival[5,6].

Surgical resection has been considered the standard treatment for GTC; however, surgery is not usually preferred because of its associated high morbidity and mortality[5,7]. As a result, it is necessary to find alternatives to the surgical treatment of GTC. At present, the use of endoscopic resection, including endoscopic submucosal dissection (ESD) for early gastric cancer (EGC), is accepted as a standard of care and is commonly performed[8-10]. ESD is a technique that was developed to enable the resection of large lesions that cannot be removed using conventional endoscopic mucosal resection (EMR). The other major advantage of ESD is its ability to achieve a higher rate of *en bloc* resection, which allows it to provide more accurate histological assessment than EMR. The indications for endoscopic resection and the histopathological criteria for the curative endoscopic resection of EGC were provided by the Japanese Gastric Cancer Association gastric cancer treatment guidelines in 2010[11].

Recently, the indications and criteria for ESD were expanded to include the treatment of GTC after esophagectomy[12-15]. ESD for GTC after esophagectomy is a technically difficult procedure because of the limited working space and unusual fluid-pooling area in the reconstructed gastric tube, in addition to the presence of severe gastric fibrosis with staples under the suture line. At present, there are very few data on the clinical significance of endoscopic treatment for GTC[5], and a therapeutic strategy for GTC has not yet been established.

Table 1 Patient characteristics *n* (%)

Characteristics	
Patient	11
Gender (M/F)	10/1
Tumors	11
Mean age	70.5 (65-78)
Median period from esophagectomy to initial ESD for GTC, in months (range)	52.4 (4-144)
Gastric tube reconstruction	
Anterosternal subcutaneous route	7 (63.6)
Posterior mediastinal route	3 (27.3)
Substernal route	1 (9.1)
Size (Major axis)	26.1 mm (10-68 mm)
Macroscopic type	
0-Ⅱa	4 (36.4)
0-Ⅱc	5 (45.5)
0-Ⅱa + Ⅱc	1 (9.1)
Unclassified	1 (9.1)
Histological diagnosis	
Differentiated	11 (100)
Undifferentiated	0 (0)
Depth	
Mucosal	9 (81.8)
Submucosal	2 (18.2)
Helicobacter pylori infection	
Positive	9 (81.8)
Negative	2 (18.2)

ESD: Endoscopic submucosal dissection; GTC: Gastric tube cancer.

During the period of this study, 11 cases of early GTC after esophagectomy were diagnosed at the hospital after detailed surveillance endoscopy. All GTCs were successfully resected *en bloc* with ESD. The aim of this retrospective study was to identify the clinical characteristics of GTC and the complications associated with ESD for GTC.

MATERIALS AND METHODS

Patients

Between April 2007 and September 2012, all patients with EGC in the reconstructed gastric tube after esophagectomy who underwent ESD were retrospectively investigated at the Kurume University Hospital in Japan. The clinical characteristics of the patients with EGC are summarized in Table 1. The clinical indications of ESD for EGC were based on the Gastric Cancer Treatment Guidelines[11]. These indications were applied for GTC after esophagectomy with gastric tube reconstruction (GTR). The hospital ethics committee approved the study protocol, and all participating patients had provided prior written informed consent.

Endoscopic procedures

All ESD procedures were performed by highly skilled endoscopists using video endoscopes and a standard video

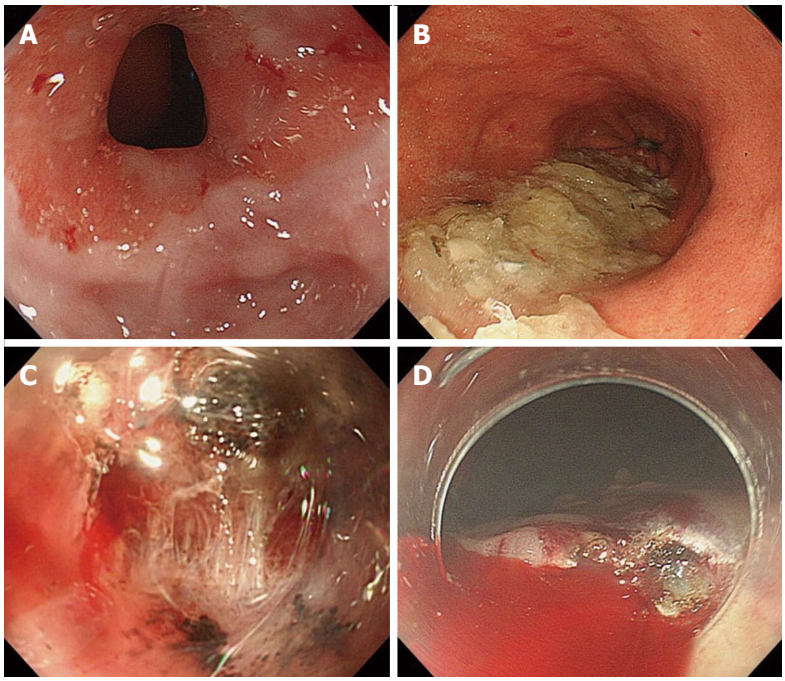

Figure 1 Complications of endoscopic submucosal dissection for gastric tube cancer. A: Anastomotic stricture in the gastric tube; B: Food residue in the gastric tube; C: Fibrosis of the submucosal layer in the gastric tube originated from the gastric body; D: Intraoperative bleeding during endoscopic submucosal dissection.

endoscope system (CV260SL/CLV260SL endoscopic system; Olympus Medical Systems, Tokyo, Japan). An insulation-tipped diathermic knife (IT knife; Olympus) was used for all ESD procedures[16]. A Dual knife (Olympus) or Flush knife (Fujifilm, Tokyo, Japan) was used to mark the dots for the initial incision, and the IT knife was used for the submucosal dissection. In addition, 0.4% sodium hyaluronate (MucoUp; Johnson & Johnson, Tokyo, Japan) diluted with normal saline solution containing epinephrine and a minute amount of indigo carmine dye (1:1) was used as the submucosal injection solution[17]. The resected GTC specimens were then extended on the boards with pins for fixation in 20% formalin. Each lesion, together with the surrounding mucosa, was cut into 2- to 5-mm-wide serial-step sections. The histopathological criteria for diagnosing GTC were based on the Japanese classifications of gastric carcinomas[11,18].

Measurements

The parameters and outcome measures studied were patient characteristics, *Helicobacter pylori* infection, endoscopic findings, tumor size, histopathological results, operative time (from marking to complete lesion removal), and complications, such as stenosis, perforation, and bleeding during the three phases: preoperative; intraoperative; and postoperative. In this study, delayed bleeding was defined as cases with hematemesis or melena requiring endoscopic intervention in the postoperative phase.

RESULTS

Patient characteristics

Eleven consecutive patients with 11 lesions were included (10 men and 1 woman), having a mean age of 70.5 years. The characteristics of these patients are shown in Tables 1 and 2. All of the patients had earlier undergone esophagectomy with gastric tube reconstruction (GTR) for esophageal cancer of the squamous cell carcinoma type. Seven cases had GTR through the anterosternal subcutaneous route; 3 had GTR through the posterior mediastinal route; and 1 had a substernal GTR. GTC occurred an average length of 52.4 mo (4-144 mo) after esophagectomy. All cases underwent *en bloc* resections with ESD. The median procedure time was 142 min (range, 32-445 min). The average GTC diameter was 26.1 mm (10-68 mm), and the average size of the resected lesion was 45.5 mm in diameter (21-74 mm). During endoscopy, the cases were macroscopically classified as follows: 4 cases were 0-Ⅱa type; 5 were 0-Ⅱc type; 1 case was 0-Ⅱa + Ⅱc type; and 1 was unclassified. The histopathological diagnosis in all cases was differentiated adenocarcinoma. Based on the depth of invasion, 9 cases were observed to be limited to the mucosa (M), and in 2 cases, the tumor had penetrated into the submucosa (SM). HP infection was observed in most of the GTC patients (9/11, 81.9%).

Complications of ESD for GTC

The complications of ESD for GTC were investigated at three phases: preoperative; intraoperative; and postoperative. In the preoperative phase, anastomotic strictures (Figure 1A) and food residue (Figure 1B) in the gastric tube were the main complications (Table 3). Anastomotic strictures were defined as an anastomotic narrowing that did not allow a standard endoscope with a diameter of 10 mm to pass without resistance.

Table 2 Detailed patient characteristics

Case	Sex	Age	Gastric tube reconstruction	Wall	Location	Macroscopic finding	Period from esophagectomy (mo)	*H. pylori* infection	Tumor size (mm)	Resected size (mm)	Depth	Resection time (min)
1	M	66	Post	Left	Body	0-Ⅱa + Ⅱc	117	Positive	28	62	SM	184
2	M	77	Ant	Left	Body	0-Ⅱa	96	Negative	16	40	M	175
3	M	67	Sub	Posterior	Body	0-Ⅱa	50	Positive	10	21	M	180
4	M	62	Ant	Right	Body	0-Ⅱa	4	Positive	31	48	M	57
5	M	78	Ant	Anterior	Antrum	0-Ⅱc	38	Positive	15	28	M	65
6	M	66	Post	Posterior	Antrum	unclassified	144	Negative	68	74	SM	445
7	M	74	Ant	Left	Body	0-Ⅱc	12	Positive	32	45	M	208
8	F	78	Ant	Anterior	Antrum	0-Ⅱa	44	Positive	20	49	M	32
9	M	78	Ant	Left	Body	0-Ⅱc	6	Positive	12	31	M	32
10	M	65	Ant	Posterior	Antrum	0-Ⅱc	45	Positive	30	52	M	44
11	M	64	Post	Left	Body	0-Ⅱc	21	Positive	25	53	M	141

Ant: Anterosternal subcutaneous route; Sub: Substernal route; Post: Posterior mediastinal route; *H. pylori*: *Helicobacter pylori*.

In this study, there were 5 cases (45%) of anastomotic stenosis in the preoperative phase, and balloon dilatation was required in all cases. Furthermore, overtube insertion was impossible in all 6 cases (including 5 preoperative cases and one postoperative) with anastomotic stenosis, although balloon dilatation for stenosis was performed. Migration of the overtube was frequently observed through the anterosternal subcutaneous route (4/7, 57.1%) compared with the other routes (2/4, 50.0%); however, this observation had no association with the insertion technique. The insertion of a scope-mounted hood was possible except in one case. In addition, food residue was observed in 4 cases (36.4%), although it is imperative to abstain from eating before treatment.

The intraoperative complications included were bleeding and perforation due to fibrosis of the submucosal layer (Figure 1C), an unusual fluid-pooling area, and limited working space (Table 4). Fibrosis of the submucosal layer at the site of the original stomach was frequently observed in the gastric tube and predominantly originated from the gastric body (5/7, 71.4%) more so than the antrum (1/4, 25%). As a result, intraoperative bleeding (Figure 1D) was more frequently observed in gastric tubes originating from the body of the stomach (body *vs* antrum, 5/7 *vs* 0/4). In addition, the resection time was longer in the gastric tube originating from the gastric body except for one case of the antrum, which developed SM infiltration (body *vs* antrum, 139.6 min *vs* 47 min). In this study, perforation was not observed as a complication (0%).

The postoperative complications were postoperative bleeding and stenosis (Table 4). Emergency hemostasis was performed for postoperative bleeding in 2 cases (18.2%) of gastric tube cancers originating from the body of the stomach. Stenosis after ESD was observed in only one case of an extensive resection of a gastric tube cancer originating from the antrum (9.1%). This case was successfully treated with endoscopic balloon dilatation.

DISCUSSION

GTC is an important issue in the long-term follow-up of patients who undergo curative esophagectomy for esophageal cancer. Because recent advances in the diagnosis and treatment of esophageal cancer have improved patient survival after esophagectomy, the occurrence of GTC has been increasing[5,6]. The frequency of GTC in patients after esophagectomy is reported to be approximately 0.5%-6.3%[12,19,20]. Several reports have shown the efficacy and safety of EMR for GTC[3,21]. Compared with surgery, endoscopic treatment, including EMR, is considered a less invasive treatment for GTC. Several investigators have reported the application of ESD for GTC, although the indications of ESD for GTC have yet to be established[12,13]. ESD has advantages over EMR in terms of the size and depth of the resected specimens and has been successfully applied for the *en bloc* resection of various cancers[22,23]. Because the *en bloc* resection rate of ESD for GTC is reported to be 88%-95%, which is much higher than that of EMR (14.3%)[12,13,15], ESD provides a more accurate histological assessment than EMR. According to the treatment guidelines for gastric cancer in Japan[11], the indications for ESD

Table 3 Complications in the preoperative phase

Case	Anastomotic stenosis	Endoscopic dilation	Mounted attachment	Attaching overtube	Food residue
1	–	–	Possible	Possible	–
2	–	–	Possible	Possible	–
3	+	+	Possible	Impossible	+
4	+	+	Possible	Possible	–
5	+	+	Impossible	Impossible	–
6	–	–	Possible	Impossible	–
7	+	+	Possible	Impossible	–
8	–	–	Possible	Possible	+
9	–	–	Possible	Impossible	+
10	+	+	Possible	Impossible	+
11	–	–	Possible	Possible	–

Table 4 Complications in the intraoperative and postoperative phase

Case	Submergence	Fibrosis of submucosa	Bleeding	Delayed bleeding	Stenosis
1	+	Moderate	Severe	+	–
2	+	Moderate	Severe	–	–
3	–	Moderate	Severe	+	–
4	–	Slight	None	–	–
5	–	Slight	None	–	–
6	–	Severe	None	–	+
7	+	Moderate	Severe	–	–
8	–	Slight	None	–	–
9	–	Slight	None	–	–
10	+	Slight	None	–	–
11	+	Severe	Severe	–	–

in EGC tend to be mucosal cancer within 2 cm in size without ulcers. Furthermore, these guidelines have extended the indications for ESD in the following cases: (1) differentiated type, mucosal (M) cancer without ulcer, and larger than 2 cm; (2) differentiated type, M cancer with ulcer, and 3 cm or smaller; and (3) undifferentiated type, M cancer without ulcer, and 2 cm or smaller. The guidelines also state that an additional lymph node resection is not necessary when lymphovascular invasion is absent and when the tumor is not deeper than submucosal 1 (SM1; Approximately 500 μm). In the present study, we performed ESD for GTC following an extended indication for EGC, and the *en bloc* resection of all GTCs was successfully achieved using ESD.

Previous studies have shown a lower prevalence of HP infection in GTC patients[3,6]. Bile reflux was frequently observed in patients after esophagectomy and most likely contributed to intestinal metaplasia and the development of GTC[13,24]. On the other hand, Nonaka *et al*[20] observed that 98% of GTC patients had an HP infection, which is considered to be a major cause of gastric cancer. This result raises the possibility that HP infection is a major cause of GTC after esophagectomy, in addition to EGC occurring in the unresected stomach[25]. As for the results of this study, 81.8% of GTC patients were HP positive. Further studies, such as the prospective assessment of mucosal status and HP infection after surgery, will be required to clarify the activity of these carcinogenetic factors in the gastric tube.

Only a few reports have investigated the minor complications of ESD, such as anastomotic stricture, food residue, bleeding, and stenosis in the GTC. The precise incidence of complications has not been clearly elucidated in previous reports because these reports have involved a small number of patients or a mixed sample with surgical resections and ESD for EGC in the remnant stomach after gastrectomy[5,12,15]. Although anastomotic stenosis was observed at a high frequency (45.5%, 5/11) and the endoscopic extension was performed before the ESD, overtube insertion was impossible in most of those cases. Food residues were observed in 36.4% (4/11) of the cases and had to be fully removed before ESD. However, these complications were not associated with an extended resection time. Bleeding was observed in 45.5% of the patients during ESD. Intraoperative bleeding was more frequently observed in the gastric tube originating from the body of the stomach (71.4%, 5/7) than in those originating from the antrum (25%, 1/4). Emergency hemostasis was performed for postoperative bleeding in the gastric tube originating from the body in 2 cases (18.2%). Our results suggest that ESD for GTC originating from the body can be considered a high risk for intra- and postoperative bleeding. Stenosis after ESD was observed in only one case (9.1%) in the largest tumor size (68 mm) found in our study. Ono *et al*[26] have reported that resecting areas larger than three-quarters of the circumference of the esophageal lumen can be considered an important risk factor for postoperative stenosis in ESD of superficial esophageal cancer. The risk factors for postoperative stenosis may be associated

with the tumor size of the GTC. A greater accumulation of cases will be required to assess the complications of ESD for GTC in detail.

Regarding major complications, Nonaka *et al*[20] showed that perforations and delayed bleeding occurred in 3.8% of patients, similar to the complication rates of ESD for EGC performed on unresected stomachs[16,27]. The influence of fibrosis and deformity due to the previous surgery would be one such explanation of the decrease in the *en bloc* resection rate. Moreover, the operative time was longer for ESD in the gastric tube than in the whole stomach. Anatomical deformities and a limited working space due to the anastomosis or stump line are possible reasons for the time-consuming nature of these procedures. Previous reports of perforation during ESD of a whole stomach specimen have found rates of 0% to 12%[28]. A high rate of perforation (18%) was reported during ESD in a gastric tube[15]. Once perforation has occurred in the gastric tube, pneumoperitoneum and pneumomediastinum are likely to occur, potentially leading to peritonitis or mediastinitis. In the current study, all patients who experienced perforations were successfully treated with immediate closure using endoclips and subsequent nasogastric suction.

In conclusion, minor complications, such as anastomotic stricture, food residue, and intraoperative bleeding, are frequently observed in ESD for GTC; however, all GTCs were safely resected *en bloc* using ESD without serious complications. ESD can be considered a useful treatment modality for GTC.

COMMENTS

Background

The pulled-up stomach conduit, which can be reconstructed and used as an esophageal substitute after esophagectomy, has the potential to develop gastric tube cancer (GTC). At present, the use of endoscopic resection including endoscopic submucosal dissection (ESD) for early gastric cancer (EGC) is accepted as a standard of care and is commonly performed. However, there are only a few reports of ESD for GTC. The aim of this study was to identify the characteristics of GTC and the complications associated with ESD for GTC.

Research frontiers

Esophageal cancer is associated with metachronous malignancies in other organs, and the reported incidence rate ranges from 11.3% to 12.0%. The pulled-up stomach conduit that is used as an esophageal substitute after esophagectomy has the potential to develop a second primary cancer known as GTC. GTC has been increasingly observed in recent years as advancements in the treatment of esophageal cancer have contributed to prolonged patient survival. This research hotspot calls for the investigation of approaches for managing and treating GTC after esophagectomy.

Innovations and breakthroughs

Recently, the indications and criteria for ESD have been expanded to include the treatment of GTC after esophagectomy. ESD for GTC after esophagectomy is a technically difficult procedure because of the limited working space and unusual fluid-pooling area in the reconstructed gastric tube, as well as the presence of severe gastric fibrosis with staples under the suture line. At present, there are very few data on the clinical significance of endoscopic treatment for GTC, and no therapeutic strategy for GTC has yet been established. In the present study, the authors showed the usefulness of ESD for GTC following the extended indication of ESD for EGC.

Applications

GTCs underwent *en bloc* resection by ESD without any serious complications, although minor complications were frequently observed. The study's results suggest that ESD can be considered a useful treatment for GTC.

Terminology

GTC is a gastric cancer in the reconstructed gastric tube after esophagectomy. ESD is an advanced technique of therapeutic endoscopy for superficial gastrointestinal neoplasms. Three steps characterize this procedure, as follows: injecting fluid into the submucosa to elevate the lesion; cutting the surrounding mucosa of the lesion; and dissecting the submucosa beneath the lesion.

Peer review

Mukasa *et al* describe the characteristics of GTC and the complications associated with ESD for GTC. Eleven consecutive patients with 11 GTC were selected for this study. All cases underwent *en bloc* resections with ESD. In the preoperative phase, anastomotic strictures and food residues in the gastric tube were the main complications. In the intraoperative phase, bleeding was the major complication, whereas in the postoperative phase, delayed bleeding and stenosis were observed. The authors concluded that ESD can be considered a useful treatment for GTC. Although surgical resection has been considered a standard treatment for GTC, more recently, the indications and criteria for ESD have been expanded to include the treatment of GTC after esophagectomy as well.

REFERENCES

1 **Kokawa A**, Yamaguchi H, Tachimori Y, Kato H, Watanabe H, Nakanishi Y. Other primary cancers occurring after treatment of superficial oesophageal cancer. *Br J Surg* 2001; **88**: 439-443 [PMID: 11260113 DOI: 10.1046/j.1365-2168.2001.01696.x]

2 **Nagasawa S**, Onda M, Sasajima K, Takubo K, Miyashita M. Multiple primary malignant neoplasms in patients with esophageal cancer. *Dis Esophagus* 2000; **13**: 226-230 [PMID: 11206637]

3 **Okamoto N**, Ozawa S, Kitagawa Y, Shimizu Y, Kitajima M. Metachronous gastric carcinoma from a gastric tube after radical surgery for esophageal carcinoma. *Ann Thorac Surg* 2004; **77**: 1189-1192 [PMID: 15063232 DOI: 10.1016/j.athoracsur.2003.09.071]

4 **Poon RT**, Law SY, Chu KM, Branicki FJ, Wong J. Multiple primary cancers in esophageal squamous cell carcinoma: incidence and implications. *Ann Thorac Surg* 1998; **65**: 1529-1534 [PMID: 9647053]

5 **Sugiura T**, Kato H, Tachimori Y, Igaki H, Yamaguchi H, Nakanishi Y. Second primary carcinoma in the gastric tube constructed as an esophageal substitute after esophagectomy. *J Am Coll Surg* 2002; **194**: 578-583 [PMID: 12022598]

6 **Kise Y**, Kijima H, Shimada H, Tanaka H, Kenmochi T, Chino O, Tajima T, Makuuchi H. Gastric tube cancer after esophagectomy for esophageal squamous cell cancer and its relevance to Helicobacter pylori. *Hepatogastroenterology* 2003; **50**: 408-411 [PMID: 12749234]

7 **Ahn HS**, Kim JW, Yoo MW, Park do J, Lee HJ, Lee KU, Yang HK. Clinicopathological features and surgical outcomes of patients with remnant gastric cancer after a distal gastrectomy. *Ann Surg Oncol* 2008; **15**: 1632-1639 [PMID: 18379851 DOI: 10.1245/s10434-008-9871-8]

8 **Gotoda T**. Endoscopic resection of early gastric cancer. *Gastric Cancer* 2007; **10**: 1-11 [PMID: 17334711 DOI: 10.1007/s10120-006-0408-1]

9 **Soetikno R**, Kaltenbach T, Yeh R, Gotoda T. Endoscopic mucosal resection for early cancers of the upper gastrointestinal tract. *J Clin Oncol* 2005; **23**: 4490-4498 [PMID: 16002839 DOI: 10.1200/JCO.2005.19.935]

10 **Rembacken BJ**, Gotoda T, Fujii T, Axon AT. Endoscopic mucosal resection. *Endoscopy* 2001; **33**: 709-718 [PMID: 11490390 DOI: 10.1055/s-2001-16224]

11 **Japanese Gastric Cancer Association**. Japanese gastric cancer treatment guidelines 2010 (ver. 3). *Gastric Cancer* 2011; **14**: 113-123 [PMID: 21573742 DOI: 10.1007/s10120-011-0042-4]

12 **Osumi W**, Fujita Y, Hiramatsu M, Kawai M, Sumiyoshi K, Umegaki E, Tokioka S, Yoda Y, Egashira Y, Abe S, Higuchi K, Tanigawa N. Endoscopic submucosal dissection allows less-invasive curative resection for gastric tube cancer after esophagectomy - a case series. *Endoscopy* 2009; **41**: 777-780

[PMID: 19746318 DOI: 10.1055/s-0029-1215024]
13 **Bamba T**, Kosugi S, Takeuchi M, Kobayashi M, Kanda T, Matsuki A, Hatakeyama K. Surveillance and treatment for second primary cancer in the gastric tube after radical esophagectomy. *Surg Endosc* 2010; **24**: 1310-1317 [PMID: 19997933 DOI: 10.1007/s00464-009-0766-y]
14 **Hoteya S**, Yamashita S, Kikuchi D, Nakamura M, Fujimoto A, Matsui A, Nishida N, Mitani T, Kuroki Y, Iizuka T, Yahagi N. Endoscopic submucosal dissection for submucosal invasive gastric cancer and curability criteria. *Dig Endosc* 2011; **23**: 30-36 [PMID: 21198914 DOI: 10.1111/j.1443-1661.2010.01040.x]
15 **Nishide N**, Ono H, Kakushima N, Takizawa K, Tanaka M, Matsubayashi H, Yamaguchi Y. Clinical outcomes of endoscopic submucosal dissection for early gastric cancer in remnant stomach or gastric tube. *Endoscopy* 2012; **44**: 577-583 [PMID: 22402983 DOI: 10.1055/s-0031-1291712]
16 **Ono H**, Hasuike N, Inui T, Takizawa K, Ikehara H, Yamaguchi Y, Otake Y, Matsubayashi H. Usefulness of a novel electrosurgical knife, the insulation-tipped diathermic knife-2, for endoscopic submucosal dissection of early gastric cancer. *Gastric Cancer* 2008; **11**: 47-52 [PMID: 18373177 DOI: 10.1007/s10120-008-0452-0]
17 **Fujishiro M**, Yahagi N, Kashimura K, Mizushima Y, Oka M, Matsuura T, Enomoto S, Kakushima N, Imagawa A, Kobayashi K, Hashimoto T, Iguchi M, Shimizu Y, Ichinose M, Omata M. Different mixtures of sodium hyaluronate and their ability to create submucosal fluid cushions for endoscopic mucosal resection. *Endoscopy* 2004; **36**: 584-589 [PMID: 15243879 DOI: 10.1055/s-2004-814524]
18 **Japanese Gastric Cancer Association**. Japanese classification of gastric carcinoma: 3rd English edition. *Gastric Cancer* 2011; **14**: 101-112 [PMID: 21573743 DOI: 10.1007/s10120-011-0041-5]
19 **Motoyama S**, Saito R, Kitamura M, Suzuki H, Nakamura M, Okuyama M, Imano H, Inoue Y, Ogawa J. Prospective endoscopic follow-up results of reconstructed gastric tube. *Hepatogastroenterology* 2003; **50**: 666-669 [PMID: 12828056]
20 **Nonaka S**, Oda I, Sato C, Abe S, Suzuki H, Yoshinaga S, Hokamura N, Igaki H, Tachimori Y, Taniguchi H, Kushima R, Saito Y. Endoscopic submucosal dissection for gastric tube cancer after esophagectomy. *Gastrointest Endosc* 2014; **79**: 260-270 [PMID: 24060521 DOI: 10.1016/j.gie.2013.07.059]
21 **Suzuki H**, Kitamura M, Saito R, Motoyama S, Ogawa J. Cancer of the gastric tube reconstructed through the posterior mediastinal route after radical surgery for esophageal cancer. *Jpn J Thorac Cardiovasc Surg* 2001; **49**: 466-469 [PMID: 11517585]
22 **Fujishiro M**, Yahagi N, Nakamura M, Kakushima N, Kodashima S, Ono S, Kobayashi K, Hashimoto T, Yamamichi N, Tateishi A, Shimizu Y, Oka M, Ogura K, Kawabe T, Ichinose M, Omata M. Successful outcomes of a novel endoscopic treatment for GI tumors: endoscopic submucosal dissection with a mixture of high-molecular-weight hyaluronic acid, glycerin, and sugar. *Gastrointest Endosc* 2006; **63**: 243-249 [PMID: 16427929 DOI: 10.1016/j.gie.2005.08.002]
23 **Onozato Y**, Ishihara H, Iizuka H, Sohara N, Kakizaki S, Okamura S, Mori M. Endoscopic submucosal dissection for early gastric cancers and large flat adenomas. *Endoscopy* 2006; **38**: 980-986 [PMID: 17058161 DOI: 10.1055/s-2006-944809]
24 **Dixon MF**, Mapstone NP, Neville PM, Moayyedi P, Axon AT. Bile reflux gastritis and intestinal metaplasia at the cardia. *Gut* 2002; **51**: 351-355 [PMID: 12171955]
25 **Asaka M**, Kimura T, Kato M, Kudo M, Miki K, Ogoshi K, Kato T, Tatsuta M, Graham DY. Possible role of Helicobacter pylori infection in early gastric cancer development. *Cancer* 1994; **73**: 2691-2694 [PMID: 8194007]
26 **Ono S**, Fujishiro M, Niimi K, Goto O, Kodashima S, Yamamichi N, Omata M. Predictors of postoperative stricture after esophageal endoscopic submucosal dissection for superficial squamous cell neoplasms. *Endoscopy* 2009; **41**: 661-665 [PMID: 19565442 DOI: 10.1055/s-0029-1214867]
27 **Isomoto H**, Shikuwa S, Yamaguchi N, Fukuda E, Ikeda K, Nishiyama H, Ohnita K, Mizuta Y, Shiozawa J, Kohno S. Endoscopic submucosal dissection for early gastric cancer: a large-scale feasibility study. *Gut* 2009; **58**: 331-336 [PMID: 19001058 DOI: 10.1136/gut.2008.165381]
28 **Kakushima N**, Fujishiro M. Endoscopic submucosal dissection for gastrointestinal neoplasms. *World J Gastroenterol* 2008; **14**: 2962-2967 [PMID: 18494043]

P- Reviewer: Herszenyi L **S- Editor**: Qi Y **L- Editor**: A
E- Editor: Wang CH

World Journal of Gastroenterology

Submit a Manuscript: http://www.wjgnet.com/esps/
Help Desk: http://www.wjgnet.com/esps/helpdesk.aspx
DOI: 10.3748/wjg.v21.i3.926

World J Gastroenterol 2015 January 21; 21(3): 926-934
ISSN 1007-9327 (print) ISSN 2219-2840 (online)

ORIGINAL ARTICLE

Retrospective Study

Deficient DNA mismatch repair is associated with favorable prognosis in Thai patients with sporadic colorectal cancer

Krittiya Korphaisarn, Ananya Pongpaibul, Chanin Limwongse, Ekkapong Roothumnong, Wipawi Klaisuban, Akarin Nimmannit, Artit Jinawath, Charuwan Akewanlop

Krittiya Korphaisarn, Charuwan Akewanlop, Division of Medical Oncology, Department of Medicine, Faculty of Medicine Siriraj Hospital, Bangkok 10700, Thailand
Ananya Pongpaibul, Wipawi Klaisuban, Department of Pathology, Faculty of Medicine Siriraj Hospital, Bangkok 10700, Thailand
Chanin Limwongse, Ekkapong Roothumnong, Division of Medical Genetics, Department of Medicine, Faculty of Medicine Siriraj Hospital, Bangkok 10700, Thailand
Akarin Nimmannit, Office for Research and Development, Faculty of Medicine Siriraj Hospital, Bangkok 10700, Thailand
Artit Jinawath, Department of Pathology, Faculty of Medicine Ramathibodi Hospital, Bangkok 10400, Thailand
Author contributions: Korphaisarn K performed the research, acquired and analyzed the data, and drafted the manuscript; Pongpaibul A, Klaisuban W, Limwongse C, Roothumnong E and Jinawath A co-supervised the field activities; Nimmannit A designed the analysis strategy, and reviewed and edited manuscript; and Akewanlop C designed the study, supervised the study, critically revised the manuscript, and approved the final version for publication.
Supported by Siriraj Research Development Fund No. 459/2554(EC2).

Correspondence to: Charuwan Akewanlop, MD, Division of Medical Oncology, Department of Medicine, Faculty of Medicine Siriraj Hospital, 13th Floor Chalerm-Prakiat Building, Bangkok-noi, Bangkok 10700, Thailand. charuwan.ake@mahidol.ac.th
Telephone: +66-2-4197000
Fax: +66-2-4181788
Received: June 7, 2014
Peer-review started: June 8, 2014
First decision: June 27, 2014
Revised: July 30, 2014
Accepted: September 18, 2014
Article in press: September 19, 2014
Published online: January 21, 2015

Abstract

AIM: To determine the prognostic significance of deficient mismatch repair (dMMR) and *BRAF* V600E in Thai sporadic colorectal cancer (CRC) patients.

METHODS: We studied a total of 211 out of 405 specimens obtained from newly diagnosed CRC patients between October 1, 2006 and December 31, 2007 at Siriraj Hospital, Mahidol University. Formalin-fixed paraffin-embedded blocks of CRC tissue samples were analyzed for dMMR by detection of MMR protein expression loss by immunohistochemistry or microsatellite instability using polymerase chain reaction (PCR)-DHPLC. *BRAF* V600E mutational analysis was performed in DNA extracted from the same archival tissues by two-round allele-specific PCR and analyzed by high sensitivity DHPLC. Associations between patient characteristics, MMR and *BRAF* status with disease-free survival (DFS) and overall survival (OS) were determined by Kaplan-Meier survival plots and log-rank test together with Cox's proportional hazard regression.

RESULTS: dMMR and *BRAF* V600E mutations were identified in 31 of 208 (14.9%) and 23 of 211 (10.9%) tumors, respectively. dMMR was more commonly found in patients with primary colon tumors rather than rectal cancer (20.4% *vs* 7.6%, P =0.01), but there was no difference in MMR status between the right-sided and left-sided colon tumors (20.8% *vs* 34.6%, P = 0.24). dMMR was associated with early-stage rather than metastatic disease (17.3% *vs* 0%, P = 0.015). No clinicopathological features such primary site or tumor differentiation were associated with the *BRAF* mutation. Six of 31 (19.3%) samples with dMMR carried the *BRAF*

mutation, while 17 of 177 (9.6%) with proficient MMR (pMMR) harbored the mutation (P = 0.11). Notably, patients with dMMR tumors had significantly superior DFS (HR = 0.30, 95%CI: 0.15-0.77; P = 0.01) and OS (HR = 0.29, 95%CI: 0.10-0.84; P = 0.02) compared with patients with pMMR tumors. By contrast, the *BRAF* V600E mutation had no prognostic impact on DFS and OS.

CONCLUSION: The prevalence of dMMR and *BRAF* V600E in Thai sporadic CRC patients was 15% and 11%, respectively. The dMMR phenotype was associated with a favorable outcome.

Key words: Sporadic colorectal cancer; Mismatch repair; *BRAF*; Overall survival

Core tip: This study is the first report of prevalence and outcome in sporadic colorectal cancer that habour deficient mismatch repair (dMMR) and *BRAF* gene mutation in Thai population. The prevalence of dMMR and *BRAF* V600E mutation was 15% and 11%, respectively. This study confirmed the favorable outcome in patients with dMMR tumors, which is consistent to the results of previous reports in Caucasian population. The method we used to detect *BRAF* mutation is allele specific polymerase chain reaction which has the highest sensitivity to detect this mutation when compared to previously reported methods.

Korphaisarn K, Pongpaibul A, Limwongse C, Roothumnong E, Klaisuban W, Nimmannit A, Jinawath A, Akewanlop C. Deficient DNA mismatch repair is associated with favorable prognosis in Thai patients with sporadic colorectal cancer. *World J Gastroenterol* 2015; 21(3): 926-934 Available from: URL: http://www.wjgnet.com/1007-9327/full/v21/i3/926.htm DOI: http://dx.doi.org/10.3748/wjg.v21.i3.926

INTRODUCTION

Colorectal tumorigenesis is a multistep process that arises from the accumulation of genetic alterations, including chromosomal abnormalities, gene mutations, and epigenetic changes[1]. With regards to genetic abnormalities, defective DNA mismatch repair (dMMR) is a type of genomic instability in tumor tissue caused by a failure to correct errors during normal DNA replication[2]. dMMR can be identified either by the presence of microsatellite instability (MSI) analyzed by polymerase chain reaction (PCR) amplification of microsatellite foci in tumor tissue, or lack of protein expression for any of the MMR genes, *MLH1*, *MSH2*, *MSH6*, and *PMS2*, detected by immunohistochemistry (IHC). Tumors with dMMR have been reported in 15%-20% of sporadic colorectal cancers (CRC), and dMMR is associated with distinct clinicopathological features such as proximal tumor site, high grade, early stage, and better prognosis[3].

The *BRAF* gene has 18 exons and encodes a serine/threonine protein kinase belonging to the RAS-RAF-MEK-ERK kinase pathway that is involved in CRC development[4,5]. The most common activating mutation is found in exon 15 at nucleotide position 1799, whereby a thymine (T) to adenine (A) transversion within codon 600 leads to substitution of valine by glutamate at the amino acid level. This leads to the oncogenic *BRAF* V600E mutation[6]. *KRAS* and *BRAF* mutations have been reported to be mutually exclusive events within tumors[6,7]. Several studies reported *BRAF* mutations in 5%-20% of patients with sporadic CRC, with a high frequency in dMMR tumors[4,8-10]. However, *BRAF* mutations are very rare in CRC patients with hereditary nonpolyposis colorectal cancer (HNPCC)[11].

Recently, the correlation between dMMR and *BRAF* mutation and CRC prognosis has been widely studied[8,12,13]. Patients with tumors harboring dMMR were associated with a more favorable survival than those with proficient MMR (pMMR)[3,14,15]. By contrast, patients with the *BRAF* mutation were associated with a worse clinical outcome, especially patients with pMMR tumors[12,13,16].

These data, however, all pertain to a Caucasian population, and there is only scarce information available for Asian populations. In this study, we systematically determined the prevalence of dMMR and *BRAF* mutations in Thai patients with sporadic CRC and established correlations with various clinicopathological features to determine their prognostic impact on clinical outcome.

MATERIALS AND METHODS

Tissue samples

Formalin-fixed paraffin-embedded tissue blocks from patients diagnosed with primary colon or rectal adenocarcinoma who underwent surgery between October 1, 2006 and December 31, 2007 were obtained for this study. We excluded patients with a known family history of CRC, those suspected to have hereditary or familial CRC, and those who did not receive treatment and follow-up at our institution. The study protocol was approved by the Siriraj Institutional Review Board, Faculty of Medicine Siriraj Hospital, Mahidol University, Thailand. This study was supported by the Siriraj Research Development Fund.

Demographic information regarding age, gender, primary tumor site, date of diagnosis, date of surgery, stage at diagnosis, date of disease recurrence, date of last follow-up, and date of death were collected. Staging was classified by AJCC/UICC TMN stage (v.3 2010). Disease-free survival (DFS) is defined as the interval between the date of diagnosis and the date of disease recurrence or death, while overall survival (OS) is the interval between the date of diagnosis and the date of death from any

cause. The primary objective of this study was to determine the prevalence of dMMR and *BRAF* V600E mutations in sporadic CRC patients; the secondary objectives were to examine correlations between MMR status and *BRAF* mutations, and the association of each marker with various clinicopathological characteristics and their prognostic impact on DFS and OS.

Determination of MMR status

MMR status was determined by analysis of MMR protein expression by IHC or MSI testing. dMMR was defined by the presence of either high-level MSI (MSI-H) or loss of MMR protein expression. pMMR was defined by the presence of either microsatellite stable (MSS)/low-level MSI (MSI-L) or the presence of normal MMR protein expression.

IHC analysis of MMR expression

IHC for four MMR proteins, MLH1, MSH2, MSH6 and PMS2, was performed on tissue microarray slides (TMAs). TMAs were assembled from paraffin-embedded tissues using a manual tissue microarrayer (UNITMA Quick-Ray 2 mm-diameter tissue cores). Hematoxylin and eosin stained slides were prepared from paraffin blocks and areas of neoplastic tissue were identified by a gastrointestinal pathologist (A.P.) who selected samples for TMA construction. Duplicated IHC for each MMR protein was performed for each patient sample. Staining for MMR proteins was performed using the following primary antibodies: mouse anti-human MLH-1 (clone G168-728; Cell Marque Corporation, Rocklin, CA), mouse anti-human MSH-2 (clone G219-1129; Cell Marque Corporation, Rocklin, CA), mouse anti-human MSH-6 (clone BC/44; Biocare, Concord, CA), and rabbit anti-human PMS2 (clone EPR3947; Cell Marque Corporation, Rocklin, CA). Loss of MMR protein was defined as the absence of nuclear staining of tumor cells in the presence of positive nuclear staining in normal epithelial cells and lymphocytes. Assessment of IHC staining was performed by the same pathologist (A.P.).

MSI testing

MSI was analyzed by PCR amplification of microsatellite foci from the five-marker Bethesda panel, which includes two mononucleotide (BAT-25 and BAT-26) and three dinucleotide (D5S346, D2S123, and D17S250) repeats. Samples with instability in two or more of these markers were defined as MSI-H, whereas those with one unstable marker were designated as MSI-L. Samples with no detectable alterations were defined as MSS.

Determination of BRAF mutation

Formalin-fixed paraffin-embedded tissues with tumorous regions were macroscopically dissected into 10 μm-thick sections using microtome blades, and then placed into separate tubes for DNA extraction using a standard phenol/chloroform extraction protocol. Probes were designed to target the most common *BRAF* mutation, a valine to glutamate transition at amino acid position 600 (V600E). *BRAF* V600E was detected using a previously-described two-round allele specific-polymerase chain reaction (AS-PCR)[17]. The primary AS-PCR reaction was performed using common-primer pairs (CF; 5'-TAATGCTTGCTCTGATAGGA-3', CR; 5' GGAAAAATAGCCTCAATTCT-3') and a *BRAF* V600E-specific primer (Mt; 5'-AAATAGGTGATTTTGGTCTGGCTACGGA-3'), which is located between common-primer pairs, and CR was used as a reverse primer. The final concentration of AS-PCR reactions comprised 100 ng genomic DNA, 0.02 U/μL of Immolase DNA polymerase (Bioline, Taunton, MA), 1 × buffer, 1.5 mmol/L $MgCl_2$, 0.2 μmol/L dNTP, 0.4 μmol/L of each common primer and 0.8 umol/L Mt primer. The reaction was amplified with a Mastercycler pro S (Eppendorf, Eppendorf AG, Hamburg, Germany) using the following protocol: activation at 95 ℃ for 10 min followed by 35 cycles at 95 ℃ for 30 s, 60 ℃ for 30s, 72 ℃ for 30 s and a final extension at 72 ℃ for 10 min. Secondary AS-PCR was amplified under the same conditions as the primary reaction, but genomic DNA template was replaced with 1 μL of the primary AS-PCR product. Secondary AS-PCR product was analyzed by high-sensitivity denaturing high performance liquid chromatography (HS-DHPLC) (Transgenomic Inc., Foster city, CA) equipped with WAVE Optimized HS Staining Solution I and a fluorescence detector in sizing mode. This assay has been shown to have a detection limit of at least 0.5% V600E-positive tumor cells.

Statistical analysis

Sample size determination was based on a *BRAF* mutation and dMMR estimated prevalence of 15% with a 95%CI of 5%: accounting for 5% of possible cases with no paraffin-embedded tumors tissue blocks, a total sample size of 210 patients was required.

Patient characteristics were described by descriptive statistics. Pearson's χ^2 test was applied to evaluate associations between *BRAF*/MMR status and clinicopathological variables. The association between patient characteristics and either *BRAF* status or MMR status with OS and DFS was explored by Kaplan-Meier estimation and log-rank test together with Cox's proportional hazard regression. Calculations were carried out using SPSS-version 18 software. *P* values of less than 0.05 were considered statistically significant.

RESULTS

A total of 405 patients were diagnosed with colon and rectal adenocarcinoma between October 1, 2006 and December 31, 2007. We investigated 211 patients for whom tissue blocks were available. The median age was 63 years (33-95 years). The ratio of males to females was 1:1. One-hundred and fifty patients (71.1%) had stage Ⅱ and Ⅲ disease while 29 patients (13.7%) were diagnosed with stage Ⅳ disease. The majority of primary

Table 1 Clinical characteristics of 211 patients with sporadic colorectal cancer *n* (%)

Variables	Value
No. of patients	211 (100)
Median age (yr, range)	63 (33-95)
Age (yr)	
≤ 50	30 (14.2)
> 50	181 (85.8)
Sex	
Female	105 (49.8)
Male	106 (50.2)
Site	
Right-sided	43 (20.8)
Left-sided	73 (34.6)
Rectum	91 (43.1)
Synchronous lesions	4 (1.9)
Stage	
Ⅰ	32 (15.2)
Ⅱ	65 (30.8)
Ⅲ	85 (40.3)
Ⅳ	29 (13.7)
Bowel wall invasion	
pT1	4 (1.9)
pT2	44 (20.8)
pT3	146 (69.2)
pT4	17 (8.1)
Lymph node metastasis	
pN0	105 (49.8)
pN1	60 (28.4)
pN2	46 (21.8)
Distant metastasis	
No	182 (86.3)
Yes	29 (13.7)
Invasion	
NO	118 (55.9)
LVI	47 (22.3)
PNI	15 (7.1)
Both LVI/PNI	31 (14.7)
Differentiation	
Well	32 (15.2)
Moderately	171 (81)
Poorly	8 (3.8)

pT: Pathological tumor stage; pN: Pathological nodal stage; ALI: Angiolymphatic invasion; PNI: Perineural invasion.

site tumors were rectal (91 patients, 43.1%), followed by left-sided colon tumors (73 patients, 34.6%). Patient and tumor characteristics are shown in Table 1.

Prevalence of dMMR and the BRAF V600E mutation

Of the 211 patients, IHC for MMR proteins and MSI detection was analyzed in 164 and 47 tumors, respectively. dMMR was identified in 10 out of 164 tumors and 21 out of 44 tumors; therefore dMMR was detected in a total of 31 out of 208 tumors (14.9%). We were unable to analyze the results in three patients because of unamplified DNA by PCR. Of the 10 patients with dMMR, interpretation of the IHC staining was as follows: MLH-1 expression was absent in four tumors, while six tumors were negative for MSH-2 expression. Interpretation parameters for IHC of MMR status is shown in Table 2.

The *BRAF* V600E mutation was identified in 23 of 211 patients (10.9%). The prevalence of the *BRAF* mutation and dMMR with specific types of mutations is shown in Table 3.

Table 2 Interpretation of immunohistochemistry for mismatch repair status

MMR mutation	IHC staining			
	MLH-1	MSH-2	MSH-6	PMS-2
MLH-1	-	+	+	-
MSH-2	+	-	-	+
MSH-6	+	+	-	+
PMS-2	+	+	+	-

MMR: Mismatch repair; IHC: Immunohistochemistry.

Table 3 Prevalence of mismatch repair and *BRAF* status *n* (%)

Variables	All cases
MMR status	*n* = 211
IHC method	164 (77.73)
pMMR	154
dMMR	10
MLH-1	4
MSH-2	6
MSH-6	0
PMS-2	0
MSI method	44 (20.85)
MSI-H	21
MSI-L/MSI-S	23
Unknown	3 (1.42)
BRAF status	
Wild type	188 (89.1)
Mutation	23 (10.9)

pMMR: Proficient mismatch repair; dMMR: Deficient mismatch repair; MSI-H: High-level MSI; MSI-L: Low-level MSI; MSS: Microsatellite stable.

Association between dMMR/BRAF mutation and clinicopathological factors

The association of dMMR and *BRAF* mutations with clinicopathological factors was evaluated by Pearson's χ^2 test. These factors included gender, age, site of the primary tumor, UICC stage, lymphovascular or/and perineural invasion, histologic grade, pT, pN, and M stage. dMMR was more commonly found in patients with primary colon tumors rather than rectal cancer (20.4% *vs* 7.6%, $P = 0.01$) but no difference in MMR status was found between right-sided and left-sided colon tumors ($P = 0.24$). dMMR was associated with early stage rather than metastatic disease (17.3% *vs* 0%, $P = 0.015$). None of the abovementioned factors were found to be significantly associated with the *BRAF* mutation (Table 4).

Association between dMMR and BRAF mutation

Two-hundred and eight tumor samples with data for both MMR and the *BRAF* mutation were available: 25/31 cases (80.6%) with dMMR were negative for *BRAF* V600E, and 6/31 (19.4%) were positive for *BRAF* mutation; whereas 160/177 cases (90.4%) with pMMR were negative for *BRAF* mutation, and 17/177 (9.6%)

Table 4 Association between mismatch repair/*BRAF* status and clinicopathological factors

Variable	MMR status (n = 208)			*BRAF* status (n = 211)		
	pMMR	dMMR	*P* value	Wild type	Mutant	*P* value
Gender						
Female	87	16	0.800	94	11	0.844
Male	90	15		94	12	
Age (yr)						
≤ 50	24	6	0.397	29	1	0.151
> 50	153	25		159	22	
Site						
Right-sided	31	11	0.037[a]	36	7	0.510
Left-sided	59	12		67	6	
Rectum	84	7		81	10	
Synchronous lesions	3	1		4	0	
Stage						
Ⅰ	25	7	0.053	30	2	0.552
Ⅱ	55	8		58	7	
Ⅲ	68	16		73	12	
Ⅳ	29	0		27	2	
Invasion						
No	99	17	0.910	106	12	0.701
LVI or PNI or both	78	14		82	11	
Differentiation						
Well-moderately	172	28	0.067	180	23	0.313
Poorly	5	3		8	0	
Bowel wall invasion						
pT1	3	1	0.511	4	0	0.410
pT2	34	9		39	5	
pT3	126	18		128	18	
pT4	14	3		17	0	
Lymph node metastasis						
pN-	88	15	0.891	96	9	0.280
pN+	89	16		92	14	
Distant metastasis						
No	148	31	0.015[a]	161	21	0.456
Yes	29	0		21	2	

[a]$P < 0.05$ *vs* control. MMR: Mismatch repair; pT: Pathological tumor stage; pN: Pathological nodal stage; ALI: Angiolymphatic invasion; PNI: Perineural invasion.

were positive for *BRAF* mutation ($P = 0.11$) (Table 5).

Survival analysis

The median follow-up time was 56.7 mo. At the last follow-up (December 5, 2012), there were 133 patients alive and 78 patients deceased. Estimated 5-year survival for the entire population was 64.5%.

Univariate analysis by Kaplan-Meier survival analysis and log rank test was performed using clinical parameters and known prognostic factors to evaluate their significance with DFS and OS. These factors included age, gender, primary tumor site, UICC stage, T stage, regional lymph node involvement, distant metastasis, histological grade, angiolymphatic (LVI) and/or perineural invasion (PNI), MMR status, and the *BRAF* V600E mutation. Factors with statistical significance for DFS were UICC stage ($P < 0.01$), pT3 ($P = 0.01$), regional lymph node involvement ($P < 0.01$), and LVI and/or PNI ($P < 0.01$). Factors that were statistically significant for OS were UICC stage, pT3, pT4, regional lymph node involvement, and LVI and/or PNI ($P < 0.01$ for all) (Table 6). Patients with dMMR tumors were found to have significantly better DFS ($P < 0.01$) and OS ($P < 0.01$) (Figure 1). There was no significant difference in either DFS or OS with respect to adjuvant chemotherapy

Table 5 Association between mismatch repair status and *BRAF* V600E

BRAF	MMR status		*P* value
	dMMR	pMMR	
Normal	25	160	0.11
V600E	6	17	

MMR: Mismatch repair; dMMR: Deficient mismatch repair; pMMR: Proficient mismatch repair.

Table 6 Univariate analysis of prognostic factors influencing disease-free survival and overall survival

Variable	n	DFS		OS	
		Median survival (mo)	*P* value	Median survival (mo)	*P* value
Gender					
Female	105	NR		NR	
Male	106	NR	0.528	NR	0.640
Age (yr)					
≤ 50	30	NR		NR	
> 50	181	NR	0.695	NR	0.424
Site					
Right-sided	43	NR		NR	
Left-sided	73	NR		NR	
Rectum	91	NR		NR	
Synchronous lesions	4	NR	0.682	NR	0.788
Stage					
Ⅰ	32	NR		NR	
Ⅱ	65	NR	< 0.0001[a]	NR	< 0.0001[a]
Ⅲ	85	66.7	< 0.0001[a]	NR	< 0.0001[a]
Ⅳ	29	10.4	< 0.0001[a]	21.6	< 0.0001[a]
Invasion					
No invasion	118	NR		NR	
LVI or PNI or both	93	52.8	0.002[a]	57.13	< 0.0001[a]
Differentiation					
Well-moderately	203	NR		NR	
Poorly	8	29.83	0.575	40.67	0.306
Bowel wall invasion					
pT1-T2	48	NR		NR	
pT3	146	62.23	0.011[a]	NR	< 0.0001[a]
pT4	17	66.73	0.122	66.733	< 0.0001[a]
Lymph node metastasis					
pN-	105	NR		NR	
pN+	106	27.57	< 0.0001[a]	54	< 0.0001[a]
Distant metastasis					
No	182	-	-	NR	< 0.0001[a]
Yes	29	-	-	21.6	
BRAF status					
Wild type	188	NR	0.794	NR	0.465
Mutation	23	NR		NR	
MMR status					
pMMR	177	NR	0.004[a]	NR	0.006[a]
dMMR	31	NR		NR	

[a]$P < 0.05$ *vs* control. DFS: Disease-free survival; OS: Overall survival; NR: Not reached; ALI: Angiolymphatic invasion; PNI: Perineural invasion; pT: Pathological tumor stage; pN: Pathological nodal stage; pMMR: Proficient mismatch repair; dMMR: Deficient MMR.

Table 7 Independent risk factors correlating with disease-free survival and overall survival of stage Ⅰ-Ⅳ colorectal cancer patients by Cox's proportional hazard regression analysis

Variable	Adjusted analysis for DFS			Adjusted analysis for OS		
	HR	95%CI	*P* value	HR	95%CI	*P* value
Stage						
Stage Ⅰ[1]						
Stage Ⅱ	1.23	0.43-3.62	0.702	1.47	0.40-5.40	0.559
Stage Ⅲ	4.03[a]	1.57-10.32	0.004[a]	4.94[a]	1.50-16.27	0.009[a]
Stage Ⅳ	-			32.64[a]	9.57-111.27	< 0.001[a]
Invasion						
No invasion[1]						
LVI/PNI/both	1.17	0.75-1.81	0.486	1.36	0.85-2.19	0.204
Differentiation						
Well-moderate[1]						
Poorly	2.57	0.87-7.43	0.083	3.78	1.27-11.21	0.017[a]
MMR status						
pMMR[1]						
dMMR	0.30	0.15-0.77	0.013[a]	0.29[a]	0.10-0.84	0.023[a]

[1]Reference. [a]$P < 0.05$ *vs* control. DFS: Disease-free survival; OS: Overall survival; HR: Hazard ratio; MMR: Mismatch repair; pMMR: Proficient MMR; dMMR: Deficient MMR.

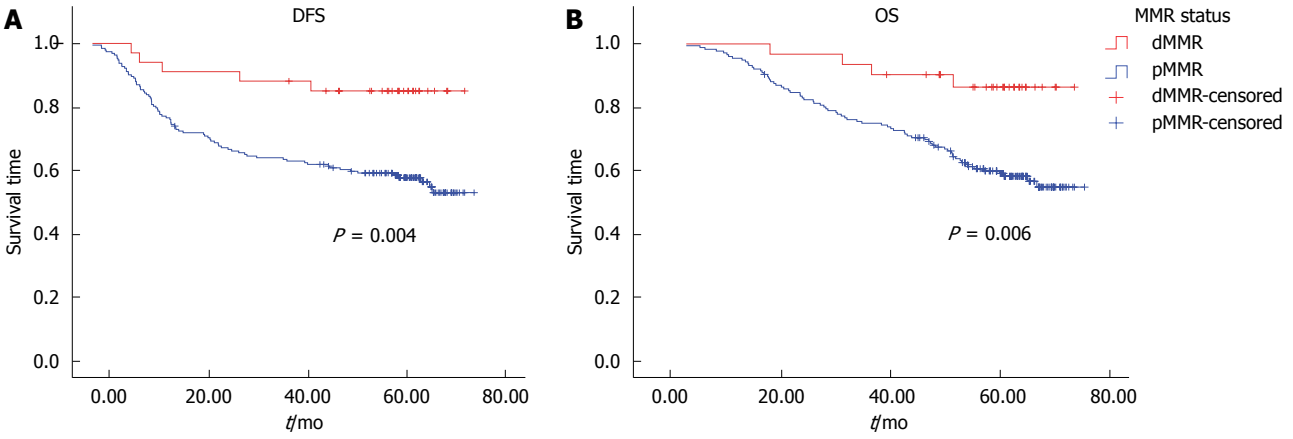

Figure 1 Kaplan-Meier survival curve of colorectal cancer patients according to mismatch repair status. A: Disease-free survival (DFS); B: Overall survival (OS); MMR: Mismatch repair; pMMR: Proficient MMR; dMMR: Deficient MMR.

in dMMR patients ($P = 0.35$, 0.21, respectively). However, there was no significant difference in either DFS or OS with respect to *BRAF* mutation (Figure 2).

Multivariate Cox proportional hazard regression analysis of factors influencing DFS and OS was performed using the factors mentioned previously. The independent risk factor for worse DFS was stage Ⅲ (HR = 4.03, 95%CI: 1.57-10.32, $P < 0.01$) and risk factors for worse OS were stage Ⅲ (HR = 4.94, 95%CI: 1.50-16.27, $P < 0.01$), stage Ⅳ (HR = 32.64, 95%CI: 9.57-112.27, $P < 0.01$) and poor differentiation (HR = 3.78, 95%CI: 1.27-11.21, $P = 0.02$). dMMR remained a significant prognostic factor for longer DFS (HR = 0.30, 95%CI: 0.15-0.77, $P = 0.01$) and OS (HR = 0.29, 95%CI: 0.10-0.84, $P = 0.02$) (Table 7).

DISCUSSION

In this study, we performed an analysis of MMR status and the *BRAF* V600E mutation in sporadic CRC using archival paraffin-embedded tissue blocks from patients diagnosed between 2006 and 2007. All patients included in the study underwent resection of their primary tumor to ensure sufficient tumor tissues would be available for the analysis. Therefore, the incidence of stage Ⅳ disease in this study (14%) was lower than previously reported from our institution in the same period (32%)[18]. Because we only selected patients who had undergone primary tumor resection, selection bias might have been introduced by not using all of the patients. The primary objective was to determine the prevalence of each biomarker. Sample size determination was based on *BRAF* mutation and dMMR estimated incidences of 15% as reported in previous studies[3,4,8-10].

IHC is an excellent method to determine MMR status. This method is inexpensive, technically simple with demonstrably good correlation with MSI-H[9,14]. Review of the literature suggested that IHC has an overall sensitivity of approximately 90% and specificity of greater than 99% in detecting MSI in sporadic CRC[19]. In our study, we used antibodies against all four MMR

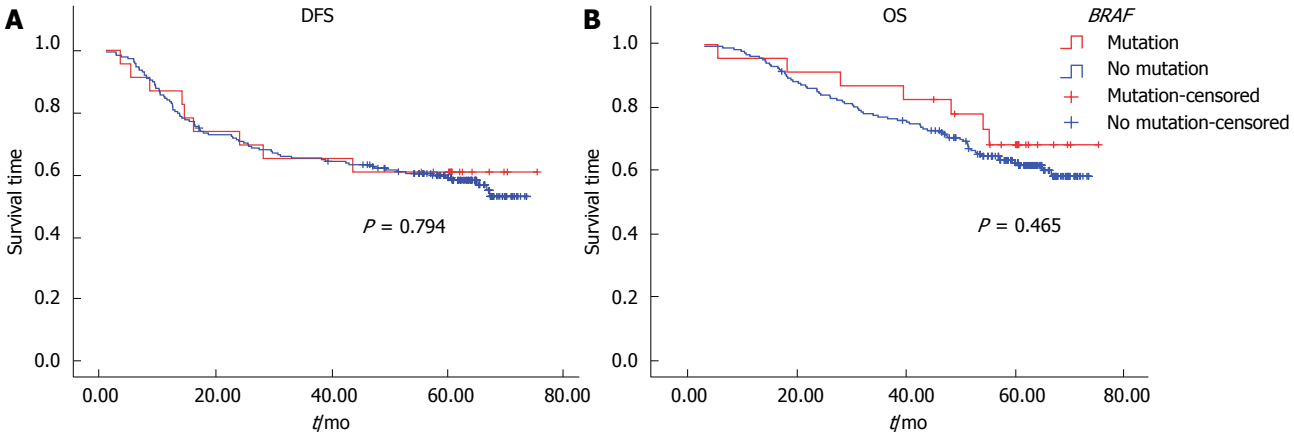

Figure 2 Kaplan-Meier survival curve of colorectal cancer patients according to the presence of the *BRAF* mutation. A: Disease-free survival (DFS); B: Overall survival (OS).

proteins to increase detection sensitivity for specific loss of protein expression other than MLH-1 and MSH-2, the two most common dMMR genes. TMA is an approach that allows high-throughput IHC to be performed on large numbers of small punched-out tissue cores from different tumors[20], thus providing time- and cost-saving benefits. TMA-IHC for MMR protein expression was validated in tumors from HNPCC patients and found to have concordant results when compared to MSI analysis and conventional IHC on whole slides[21].

Approximately 15%-20% of sporadic CRC carried dMMR. The proportion of samples with dMMR was higher in tumors located in or above the splenic flexure, stage Ⅱ rather than stage Ⅲ disease, poorly differentiated tumors, and those of mucinous subtype[9]. Several studies, including a meta-analysis, found that patients with dMMR tumors had significantly better survival compared with that of pMMR patients[9,14,22].

In this study, we performed IHC staining of 211 cases. MSI analysis was completed in 47 cases with uninformative IHC staining results. The final result indicated 14.9% (31/208) of sporadic CRC patients harbored dMMR tumors detected by both TMA-IHC and MSI analysis (10/164 and 21/47 cases, respectively), which was comparable with 11.3% (36 of 318) found in sporadic CRC patients in South Korea[23] and in that reported in the literature[3]. dMMR was more commonly found in patients with primary colon tumors rather than rectal cancer, but there was no difference in the prevalence of dMMR in right-sided and left-sided colon tumors. This might be related to the small number of patients included in the study and the fact that the majority (78%) of patients had left-sided tumors. We did not find any association between dMMR and high grade tumors ($P = 0.067$). This result should be interpreted carefully because the majority were moderately differentiated tumors, accounting for 79.1% of cases, while only 15.1 and 3.8% were well and poorly differentiated tumors, respectively. However, this study confirmed that dMMR was independently associated with favorable outcome in both DFS and OS.

Recently *BRAF* mutations have been widely studied with respect to their prognostic and predictive value in CRC. Studies have shown that the *BRAF* mutation was associated with a poor outcome in CRC patients with pMMR but not with dMMR[9,10]. The prevalence of the *BRAF* mutation in this study was 10.9%, which was comparable with Caucasian patients, but the result was higher than that reported by studies in Taiwan (1.7%), South Korea (4.5%) and Japan (6.5%)[24-26]. The main difference between our study and others is that our data were analyzed using allele-specific PCR to detect *BRAF* V600E, which is more highly sensitive in detecting this mutation than other methods. Several other approaches are suitable for evaluating this *BRAF* mutation, including direct sequencing, real-time PCR with melt curve analysis, and AS-PCR[27]. The *BRAF* mutation was strongly associated with dMMR, right-sided and poorly differentiated tumors[9]. A recent study showed that the *BRAF* V600E mutation was independently associated with worse DFS in patients with stage Ⅲ colon cancer receiving adjuvant chemotherapy[15]. In this study, there was no association between the *BRAF* mutation and any pathological features, no significant difference in the prevalence of the *BRAF* mutation in dMMR and pMMR tumors, and also no prognostic impact for either DFS or OS. This is likely a result of too few patients analyzed to determine the prognostic impact.

In conclusion, we found that the prevalence of dMMR and the *BRAF* V600E mutation in Thai sporadic CRC patients was 15 and 11%, respectively. However, only the dMMR phenotype was associated with favorable DFS and OS in our study cohort.

ACKNOWLEDGMENTS

The authors are grateful to Professor Peter Hokland for his kind help in critically reading our manuscript.

COMMENTS

Background

Colorectal tumorigenesis is a multistep process, which can arise from the

accumulation of genetic alterations. DNA mismatch repair (dMMR) and *BRAF* gene have been widely studied in this disease. The correlation between dMMR and BRAF mutation and colorectal cancer (CRC) prognosis has been reported. Patients with tumors harboring dMMR were found to be associated with a more favorable survival than those having proficient MMR (pMMR). In contrast, BRAF mutation was found to be associated with worse clinical outcome especially in patients with pMMR tumors. Unfortunately, most of these data have been studied in western country, and there is only scare information in the Asian population.

Research frontiers

In this study, the authors have systematically determined the prevalence of dMMR and *BRAF* mutation in sporadic CRC patients and established the correlations between MMR status and *BRAF* mutation, association with various clinicopathological features, and prognostic impact on the outcome of Thai patients with sporadic CRC.

Innovations and breakthroughs

The method the authors used to detect BRAF mutation is allele specific polymerase chain reaction which has the highest sensitivity to detect this mutation when compared to previously reported methods. This study is the first reported data in Thai population.

Applications

This study confirmed the favorable outcome in patients with dMMR tumors, which is consistent to the results of previous reports in Caucasian population.

Peer review

This is a good retrospective study in which this is the first reported data in Thai population. The method that used to detected *BRAF* mutation has the highest sensitivity to detect this mutation when compare to previously reported studies and the result of the study can imply that patients with dMMR tumors had a significantly better survival in both Asian and Caucasian population.

REFERENCES

1 **Worthley DL**, Whitehall VL, Spring KJ, Leggett BA. Colorectal carcinogenesis: road maps to cancer. *World J Gastroenterol* 2007; **13**: 3784-3791 [PMID: 17657831]

2 **Duval A**, Hamelin R. Mutations at coding repeat sequences in mismatch repair-deficient human cancers: toward a new concept of target genes for instability. *Cancer Res* 2002; **62**: 2447-2454 [PMID: 11980631]

3 **Popat S**, Hubner R, Houlston RS. Systematic review of microsatellite instability and colorectal cancer prognosis. *J Clin Oncol* 2005; **23**: 609-618 [PMID: 15659508 DOI: 10.1200/JCO.2005.01.086]

4 **Rajagopalan H**, Bardelli A, Lengauer C, Kinzler KW, Vogelstein B, Velculescu VE. Tumorigenesis: RAF/RAS oncogenes and mismatch-repair status. *Nature* 2002; **418**: 934 [PMID: 12198537 DOI: 10.1038/418934a]

5 **Davies H**, Bignell GR, Cox C, Stephens P, Edkins S, Clegg S, Teague J, Woffendin H, Garnett MJ, Bottomley W, Davis N, Dicks E, Ewing R, Floyd Y, Gray K, Hall S, Hawes R, Hughes J, Kosmidou V, Menzies A, Mould C, Parker A, Stevens C, Watt S, Hooper S, Wilson R, Jayatilake H, Gusterson BA, Cooper C, Shipley J, Hargrave D, Pritchard-Jones K, Maitland N, Chenevix-Trench G, Riggins GJ, Bigner DD, Palmieri G, Cossu A, Flanagan A, Nicholson A, Ho JW, Leung SY, Yuen ST, Weber BL, Seigler HF, Darrow TL, Paterson H, Marais R, Marshall CJ, Wooster R, Stratton MR, Futreal PA. Mutations of the BRAF gene in human cancer. *Nature* 2002; **417**: 949-954 [PMID: 12068308 DOI: 10.1038/nature00766]

6 **Ikenoue T**, Hikiba Y, Kanai F, Tanaka Y, Imamura J, Imamura T, Ohta M, Ijichi H, Tateishi K, Kawakami T, Aragaki J, Matsumura M, Kawabe T, Omata M. Functional analysis of mutations within the kinase activation segment of B-Raf in human colorectal tumors. *Cancer Res* 2003; **63**: 8132-8137 [PMID: 14678966]

7 **Fransén K**, Klintenäs M, Osterström A, Dimberg J, Monstein HJ, Söderkvist P. Mutation analysis of the BRAF, ARAF and RAF-1 genes in human colorectal adenocarcinomas. *Carcinogenesis* 2004; **25**: 527-533 [PMID: 14688025 DOI: 10.1093/carcin/bgh049]

8 **Maestro ML**, Vidaurreta M, Sanz-Casla MT, Rafael S, Veganzones S, Martínez A, Aguilera C, Herranz MD, Cerdán J, Arroyo M. Role of the BRAF mutations in the microsatellite instability genetic pathway in sporadic colorectal cancer. *Ann Surg Oncol* 2007; **14**: 1229-1236 [PMID: 17195912 DOI: 10.1245/s10434-006-9111-z]

9 **Hutchins G**, Southward K, Handley K, Magill L, Beaumont C, Stahlschmidt J, Richman S, Chambers P, Seymour M, Kerr D, Gray R, Quirke P. Value of mismatch repair, KRAS, and BRAF mutations in predicting recurrence and benefits from chemotherapy in colorectal cancer. *J Clin Oncol* 2011; **29**: 1261-1270 [PMID: 21383284 DOI: 10.1200/JCO.2010.30.1366]

10 **MacDonald CM**, Boursier L, D'Cruz DP, Dunn-Walters DK, Spencer J. Mathematical analysis of antigen selection in somatically mutated immunoglobulin genes associated with autoimmunity. *Lupus* 2010; **19**: 1161-1170 [PMID: 20501523 DOI: 10.1093/annonc/mdq258]

11 **Deng G**, Bell I, Crawley S, Gum J, Terdiman JP, Allen BA, Truta B, Sleisenger MH, Kim YS. BRAF mutation is frequently present in sporadic colorectal cancer with methylated hMLH1, but not in hereditary nonpolyposis colorectal cancer. *Clin Cancer Res* 2004; **10**: 191-195 [PMID: 14734469 DOI: 10.1158/1078-0432.CCR-1118-3]

12 **Ogino S**, Nosho K, Kirkner GJ, Kawasaki T, Meyerhardt JA, Loda M, Giovannucci EL, Fuchs CS. CpG island methylator phenotype, microsatellite instability, BRAF mutation and clinical outcome in colon cancer. *Gut* 2009; **58**: 90-96 [PMID: 18832519 DOI: 10.1136/gut.2008.155473]

13 **Samowitz WS**, Sweeney C, Herrick J, Albertsen H, Levin TR, Murtaugh MA, Wolff RK, Slattery ML. Poor survival associated with the BRAF V600E mutation in microsatellite-stable colon cancers. *Cancer Res* 2005; **65**: 6063-6069 [PMID: 16024606 DOI: 10.1158/0008-5472.CAN-05-0404]

14 **Lanza G**, Gafà R, Santini A, Maestri I, Guerzoni L, Cavazzini L. Immunohistochemical test for MLH1 and MSH2 expression predicts clinical outcome in stage II and III colorectal cancer patients. *J Clin Oncol* 2006; **24**: 2359-2367 [PMID: 16710035]

15 **Roth AD**, Tejpar S, Delorenzi M, Yan P, Fiocca R, Klingbiel D, Dietrich D, Biesmans B, Bodoky G, Barone C, Aranda E, Nordlinger B, Cisar L, Labianca R, Cunningham D, Van Cutsem E, Bosman F. Prognostic role of KRAS and BRAF in stage II and III resected colon cancer: results of the translational study on the PETACC-3, EORTC 40993, SAKK 60-00 trial. *J Clin Oncol* 2010; **28**: 466-474 [PMID: 20008640 DOI: 10.1200/JCO.2009.23.3452]

16 **Yokota T**, Ura T, Shibata N, Takahari D, Shitara K, Nomura M, Kondo C, Mizota A, Utsunomiya S, Muro K, Yatabe Y. BRAF mutation is a powerful prognostic factor in advanced and recurrent colorectal cancer. *Br J Cancer* 2011; **104**: 856-862 [PMID: 21285991 DOI: 10.1038/bjc.2011.19]

17 **Kannim S**, Thongnoppakhun W, Auewarakul CU. Two-round allele specific-polymerase chain reaction: a simple and highly sensitive method for JAK2V617F mutation detection. *Clin Chim Acta* 2009; **401**: 148-151 [PMID: 19135044 DOI: 10.1016/j.cca.2008.12.010]

18 **Techawathanawanna S**, Nimmannit A, Akewanlop C. Clinical characteristics and disease outcome of UICC stages I-III colorectal cancer patients at Siriraj Hospital. *J Med Assoc Thai* 2012; **95** Suppl 2: S189-S198 [PMID: 22574549]

19 **Shia J**, Ellis NA, Klimstra DS. The utility of immunohistochemical detection of DNA mismatch repair gene proteins. *Virchows Arch* 2004; **445**: 431-441 [PMID: 15455227]

20 **Bubendorf L**, Nocito A, Moch H, Sauter G. Tissue microarray (TMA) technology: miniaturized pathology archives for high-throughput in situ studies. *J Pathol* 2001; **195**: 72-79 [PMID: 11568893]

21 **Hendriks Y**, Franken P, Dierssen JW, De Leeuw W, Wijnen J, Dreef E, Tops C, Breuning M, Bröcker-Vriends A, Vasen

H, Fodde R, Morreau H. Conventional and tissue microarray immunohistochemical expression analysis of mismatch repair in hereditary colorectal tumors. *Am J Pathol* 2003; **162**: 469-477 [PMID: 12547705]

22 **Des Guetz G**, Schischmanoff O, Nicolas P, Perret GY, Morere JF, Uzzan B. Does microsatellite instability predict the efficacy of adjuvant chemotherapy in colorectal cancer? A systematic review with meta-analysis. *Eur J Cancer* 2009; **45**: 1890-1896 [PMID: 19427194 DOI: 10.1016/j.ejca.2009.04.018]

23 **Park JW**, Chang HJ, Park S, Kim BC, Kim DY, Baek JY, Kim SY, Oh JH, Choi HS, Park SC, Jeong SY. Absence of hMLH1 or hMSH2 expression as a stage-dependent prognostic factor in sporadic colorectal cancers. *Ann Surg Oncol* 2010; **17**: 2839-2846 [PMID: 20549564 DOI: 10.1245/s10434-010-1135-8]

24 **Shen H**, Yuan Y, Hu HG, Zhong X, Ye XX, Li MD, Fang WJ, Zheng S. Clinical significance of K-ras and BRAF mutations in Chinese colorectal cancer patients. *World J Gastroenterol* 2011; **17**: 809-816 [PMID: 21390154 DOI: 10.3748/wjg.v17.i6.809]

25 **Lee S**, Cho NY, Choi M, Yoo EJ, Kim JH, Kang GH. Clinicopathological features of CpG island methylator phenotype-positive colorectal cancer and its adverse prognosis in relation to KRAS/BRAF mutation. *Pathol Int* 2008; **58**: 104-113 [PMID: 18199160 DOI: 10.1111/j.1440-1827.2007.02197.x]

26 **Yokota T**, Shibata N, Ura T, Takahari D, Shitara K, Muro K, Yatabe Y. Cycleave polymerase chain reaction method is practically applicable for V-Ki-ras2 Kirsten rat sarcoma viral oncogene homolog (KRAS)/V-raf murine sarcoma viral oncogene homolog B1 (BRAF) genotyping in colorectal cancer. *Transl Res* 2010; **156**: 98-105 [PMID: 20627194 DOI: 10.1016/j.trsl.2010.05.007]

27 **Sharma SG**, Gulley ML. BRAF mutation testing in colorectal cancer. *Arch Pathol Lab Med* 2010; **134**: 1225-1228 [PMID: 20670148 DOI: 10.1043/2009-0232-RS.1]

P- Reviewer: Wang YD **S- Editor**: Qi Y **L- Editor**: A
E- Editor: Wang CH

World Journal of Gastroenterology

Submit a Manuscript: http://www.wjgnet.com/esps/
Help Desk: http://www.wjgnet.com/esps/helpdesk.aspx
DOI: 10.3748/wjg.v21.i3.935

World J Gastroenterol 2015 January 21; 21(3): 935-943
ISSN 1007-9327 (print) ISSN 2219-2840 (online)

ORIGINAL ARTICLE

Retrospective Study

Prognosis after resection for hepatitis B virus-associated intrahepatic cholangiocarcinoma

Zhen-Feng Wu, Xiao-Yu Wu, Nan Zhu, Zhe Xu, Wei-Su Li, Hai-Bin Zhang, Ning Yang, Xue-Quan Yao, Fu-Kun Liu, Guang-Shun Yang

Zhen-Feng Wu, Xiao-Yu Wu, Zhe Xu, Wei-Su Li, Xue-Quan Yao, Fu-Kun Liu, Department of Surgical Oncology, Jiangsu Province Hospital of Traditional Chinese Medicine, the Affiliated Hospital of Nanjing University of Chinese Medicine, Nanjing 210029, Jiangsu Province, China

Nan Zhu, Hai-Bin Zhang, Ning Yang, Guang-Shun Yang, Fifth Department of Hepatic Surgery, Eastern Hepatobiliary Surgery Hospital, Second Military Medical University, Shanghai 200438, China

Author contributions: Yao XQ, Wu ZF, Wu XY and Zhu N conceived and designed the study; Wu ZF and Li WS acquired the data; Xu Z, Yang N and Liu FK controlled the quality of data and algorithms; Zhang HB, Wu ZF and Yang GS analysed and interpreted the data; Wu ZF and Liu FK performed statistical analysis; Wu ZF, Wu XY and Zhu N contributed equally to this work.

Supported by National Natural Science Foundation of China, No. 81402523.

Correspondence to: Xue-Quan Yao, MD, Department of Surgical Oncology, Jiangsu Province Hospital of Traditional Chinese Medicine, the Affiliated Hospital of Nanjing University of Chinese Medicine, No. 155 Hanzhong Road, Nanjing 210029, Jiangsu Province, China. xuequan000@126.com
Telephone: +86-25-86617141
Fax: +86-25-86617141

Received: May 14, 2014
Peer-review started: May 14, 2014
First decision: June 18, 2014
Revised: July 12, 2014
Accepted: September 18, 2014
Article in press: September 19, 2014
Published online: January 21, 2015

Abstract

AIM: To investigate the prognostic factors after resection for hepatitis B virus (HBV)-associated intrahepatic cholangiocarcinoma (ICC) and to assess the impact of different extents of lymphadenectomy on patient survival.

METHODS: A total of 85 patients with HBV-associated ICC who underwent curative resection from January 2005 to December 2006 were analyzed. The patients were classified into groups according to the extent of lymphadenectomy (no lymph node dissection, sampling lymph node dissection and regional lymph node dissection). Clinicopathological characteristics and survival were reviewed retrospectively.

RESULTS: The cumulative 1-, 3-, and 5-year survival rates were found to be 60%, 18%, and 13%, respectively. Multivariate analysis revealed that liver cirrhosis (HR = 1.875, 95%CI: 1.197-3.278, P = 0.008) and multiple tumors (HR = 2.653, 95%CI: 1.562-4.508, P < 0.001) were independent prognostic factors for survival. Recurrence occurred in 70 patients. The 1-, 3-, and 5-year disease-free survival rates were 36%, 3% and 0%, respectively. Liver cirrhosis (HR = 1.919, P = 0.012), advanced TNM stage (stage Ⅲ/Ⅳ) (HR = 2.027, P < 0.001), and vascular invasion (HR = 3.779, P = 0.02) were independent prognostic factors for disease-free survival. Patients with regional lymph node dissection demonstrated a similar survival rate to patients with sampling lymph node dissection. Lymphadenectomy did not significantly improve the survival rate of patients with negative lymph node status.

CONCLUSION: The extent of lymphadenectomy does not seem to have influence on the survival of patients with HBV-associated ICC, and routine lymph node

dissection is not recommended, particularly for those without lymph node metastasis.

Key words: Intrahepatic cholangiocarcinoma; Hepatitis B virus; Lymph node metastases; Postoperative survival; Lymph node dissection

Core tip: Some recently published studies show a relation between chronic hepatitis B infection and the development of intrahepatic cholangiocarcinoma. Hepatitis B-associated patients with cholangiocarcinoma appear to have different clinicopathological characteristics compared with seronegative patients. In this context, the authors analyzed the data of patients with hepatitis B virus-associated intrahepatic cholangiocarcinoma who underwent curative resection retrospectively. They found in multivariate analysis that liver cirrhosis and multiple tumors were independent prognostic factors for overall survival. Independent prognostic factors for disease-free survival were liver cirrhosis, vascular invasion and advanced TNM stage. The patients were divided into three groups depending on the extent of lymph node dissection (no lymph node dissection, sampling lymph node dissection and regional lymph node dissection). The outcomes were not statistically different between the three groups.

Wu ZF, Wu XY, Zhu N, Xu Z, Li WS, Zhang HB, Yang N, Yao XQ, Liu FK, Yang GS. Prognosis after resection for hepatitis B virus-associated intrahepatic cholangiocarcinoma. *World J Gastroenterol* 2015; 21(3): 935-943 Available from: URL: http://www.wjgnet.com/1007-9327/full/v21/i3/935.htm DOI: http://dx.doi.org/10.3748/wjg.v21.i3.935

INTRODUCTION

Intrahepatic cholangiocarcinoma (ICC), which arises from the more peripheral branches of the intrahepatic bile duct, is the second most common primary liver cancer after hepatocellular carcinoma (HCC), accounting for 5%-10% of primary liver malignancies[1,2]. It demonstrates a relatively high prevalence in parts of East Asia[3].

Recently, an increasing number of studies have shown that viral hepatitis B and C are statistically related to ICC[4-8]. The mechanism for the development of ICC in patients with HBV infection is still uncertain. Hepatitis B and C virus infections are the most common risk factors for HCC. Hepatitis-associated HCC contains elements of cholangiocarcinoma[9,10], suggesting that the two malignancies share a common origin from bipotential stem cells and pathogenic mechanisms[9,11]. Clinically, some studies have also found that both viral hepatitis-associated ICC and HCC have similar age profiles and different age distributions between patients with chronic hepatitis B and those with chronic hepatitis C[7,8,12]. In addition, in our previous study, we have found that HBV-associated ICC have specific clinicopathological characteristics[13]. Compared with seronegative ICC patients, HBV-associated ICC patients tend to be male and younger, with higher α-fetoprotein levels and a lower frequency of lymphatic metastasis, which has been proved by other studies[7,12]. It is suggested that HBV-associated ICC and HCC share common disease processes for carcinogenesis, and should be distinguished from those without HBV infection, because they have different clinicopathological characteristics and surgical outcomes[14].

The prognosis of ICC is generally poor as compared with that of HCC[15,16], because it is frequently associated with lymph node involvement, intrahepatic metastasis, and peritoneal dissemination[17,18]. In consideration of similar pathogenesis and clinicopathological characteristics, studies should be conducted to ascertain whether HBV-associated ICC can be successfully treated by the methods used to treat HCC. Curative resection is still known to be the only effective therapeutic measure. However, there is no established consensus on the prognostic significance of lymph node dissection (LND), or even the extent of LND[19]. Prognostic factors after resection for HBV-associated ICC have not been confirmed due to its rarity and low resectability. Therefore, this study was conducted to investigate the outcomes of HBV-associated ICC patients after hepatic resection, and to analyze the prognostic factors affecting the survival and recurrence of the patients. The study also investigated the impact of the extent of LND on survival.

MATERIALS AND METHODS

Patients

Primary curative resection was performed in 127 out of 146 patients diagnosed with ICC at Eastern Hepatobiliary Surgery Hospital, Second Military Medical University (Shanghai, China) from January 2005 to December 2006. Only 114 patients were available for data analysis, and the rest of the patients could not be followed after operation.

With respect to a case of hepatitis B surface antigen being positive [HBsAg (+)], it is impossible to determine whether it is a chronic infection, acute infection, or false positive result. Generally speaking, the case of anti-hepatitis B core (HBc) being positive [anti-HBc (+)] only indicates that there may be past infection or that it may be present after the disappearance of HBsAg and the appearance of anti-HBs antibody, thus indicating recent infection. It can also be considered a sentinel marker for detection of occult HBV infection (HBsAg carrier)[20]. Therefore, the present study defined chronic HBV infection as either HBsAg (+) or anti-HBc (+)[21].

Data analysis was conducted on 85 patients (74.6%) with chronic HBV infection. The diagnosis of ICC was confirmed by pathological examination. Patients with hilar cholangiocarcinoma, gallbladder cancer, or

combined type carcinoma consisting of HCC and ICC were excluded from this study. Curative resection was defined as negative surgical margins on microscopic examination, absence of macroscopic intrahepatic metastasis in the residual liver at the time of surgery, and absence of abdominal dissemination. The study protocol was approved by the clinical research ethics committee of the hospital. Written consent was obtained from all patients according to the policies of the committee.

Preoperative investigations

Preoperative evaluation was conducted before the decision for surgery was made. We evaluated resectability of ICC by ultrasonography, computed tomography (CT), and magnetic resonance image (MRI) examinations. Liver function was evaluated *via* Child-Pugh classification. Before the operation, patients at or over the age of 60 were routinely evaluated for formal cardiopulmonary and general conditions. Resection criteria were constant during the study period, including the number of resectable tumors, presence or absence of tumor thrombus and gross metastatic focus, and adequate liver function reserve, as reported in our previous study[22,23].

Surgical procedures and parameter definitions

Liver resection was carried out using finger fracture and clamp crushing with intermittent Pringle's maneuver under room temperature. Lymphadenectomy was not conducted uniformly for every patient. 35 out of 85 patients did not undergo lymphadenectomy, neither did they present lymph node metastasis in the preoperative evaluation and intraoperative assessment. We classified the extent of lymphadenectomy into lymph node sampling and regional LND. Lymph node sampling was performed in 22 patients, and the lymph nodes along the hepatoduodenal ligament were removed. Regional LND was performed in 28 patients who underwent complete excision of soft tissue and lymph nodes at the hepatic hilum, common hepatic artery stations, hepatoduodenal ligament, and posterior to the upper portion of the pancreatic head. The extent of LND was similar for right- and left-sided tumors, with the exception of dissection of lymph nodes along the lesser curvature of the stomach for tumors located in the left lobe of the liver. The patients were divided into three groups according to the extent of LND: (1) LND (-) group: with no lymphadenectomy; (2) lymph node sampling group: with lymph node sampling; and (3) regional LND group: with regional lymphadenectomy.

ICC was classified on the basis of gross appearance, as raised by the Liver Cancer Study Group of Japan (LCSGJ), including types of mass-forming (MF), periductal infiltrating (PI), and intraductal growth (IG). Tumor-node-metastasis (TNM) staging of tumors complied with the guidelines of the 7th edition of the American Joint Committee on Cancer/International Union against Cancer (AJCC/UICC). In this study, multiple tumors referred to more than one tumorous node (including micrometastases that could be discovered only on pathological examination); tumor size referred to the maximum tumor diameter; major liver resection was defined as resection of three or more hepatic segments; minor liver resection was defined as resection of one or two hepatic segments.

Follow-up

The clinical data from all patients were recorded prospectively. Follow-up after resection consisted of routine blood tests, physical examination, and abdominal ultrasonography every 3 mo postoperatively for the first 2 years and twice a year thereafter at our hospital. Suspected recurrences were confirmed by CT or MRI. If unavailable to undergo this procedure, the patient was followed by telephone or letter every year, as reported in our previous study[22,23].

Statistical analysis

Overall survival (OS) and disease-free survival (DFS) rates and curves were analyzed by the Kaplan-Meier method, and differences were compared by the log-rank test. Comparisons between groups were made using the Chi-square test or Fisher's exact test. After univariate analysis, only significant variables with $P < 0.05$ were adopted in the multivariate analysis. Multivariate analysis was conducted by means of the Cox proportional hazards model to identify prognostic factors. All statistical analyses were carried out with software package SPSS 18.0 (SPSS Inc., Chicago, IL). A P value < 0.05 was considered statistically significant.

RESULTS

Clinicopathological characteristics of the patients

The follow-up duration was calculated from the day of operation to either the day of death or the date of December 31, 2012. There were a total of 66 males and 19 females with a median age of 54 years (range: 28-79 years). Out of the 85 patients, 40 underwent major liver resection while 45 underwent minor resection. Additional procedures were carried out in 10 patients (Table 1). Eight patients had surgical complications, including biliary leakage in 3 cases, subphrenic infection in 2 cases, liver abscess in 1 case, bowel obstruction in 1 case, and bleeding in 1 case.

Survival and recurrence

The cumulative 1-, 3-, and 5-year survival rates were 60%, 18%, and 13%, respectively (Figure 1). The median survival time was 25 mo. Univariate analysis revealed that the following prognostic factors were predictive of worse survival: liver cirrhosis ($P = 0.002$), tumor number ($P < 0.001$), tumor size ($P = 0.006$), lymph node metastasis ($P = 0.005$), vascular invasion ($P = 0.013$), and TNM classification ($P < 0.001$; Table 2). Age, gender, and other tumor-related factors were not significantly related with survival. Through multivariate analysis by means of Cox's proportional hazards model, liver cirrhosis (HR = 1.875, 95%CI: 1.197-3.278, $P = 0.008$) and multiple tumors (HR

Table 1 Operative procedures for intrahepatic cholangiocarcinoma

Operative modality	Number
Hepatic resection (n = 85)	
Major resection (n = 40)	
Partial hepatectomy	24
Right trisectionectomy	1
Left trisectionectomy	4
Right hemihepatectomy	1
Left hemihepatectomy	8
Central bisectionectomy	2
Minor resection (n = 45)	
Partial hepatectomy	33
Right anterior sectionectomy	2
Right posterior sectionectomy	3
Left lateral sectionectomy	4
Bisegmentectomy	3
Combined resection (n = 10)	
Spleen	2
Gallbladder	8

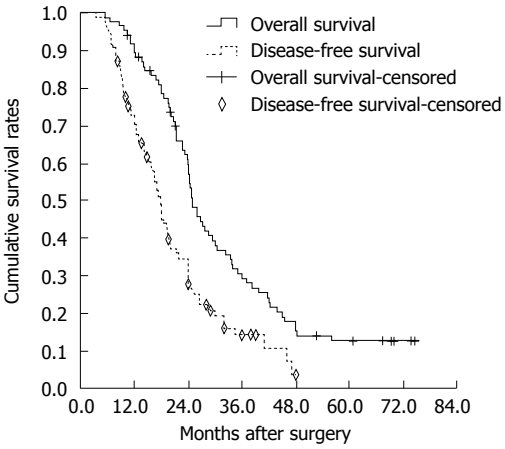

Figure 1 Overall survival and disease-free survival curves of the 85 hepatitis B virus-associated intrahepatic cholangiocarcinoma patients after curative resection. The median overall survival was 25 mo. The median disease-free survival was 17.9 mo.

= 2.653, 95%CI: 1.562-4.508, $P < 0.001$) were identified as independent prognostic factors (Table 2).

Seventy patients had recurrence (82.4%). The 1-, 3-, and 5-year DFS rates were 36%, 3% and 0%, respectively. (Figure 1). The sites of recurrence are shown in Table 3. The most common recurrence pattern was intrahepatic. Two patients (2.9%) with recurrence underwent further liver resection, while 48 patients (68.6%) underwent post-recurrence TACE. Other measures taken against recurrence included radiotherapy (n = 11), systemic chemotherapy (n = 2), and supportive therapy or Chinese herbal therapy (n = 7) in patients with liver dysfunction. Univariate analysis revealed that liver cirrhosis (P = 0.003), tumor number ($P < 0.001$), lymph node metastasis ($P < 0.001$), vascular invasion ($P < 0.001$), and TNM classification ($P < 0.001$) were significant risk factors for recurrence (Table 4). Multivariate analysis revealed that liver cirrhosis (HR = 1.919, P = 0.012), advanced TNM stage (stage Ⅲ or Ⅳ) (HR = 2.027, $P < 0.001$), and vascular invasion (HR = 3.779, P = 0.02) were

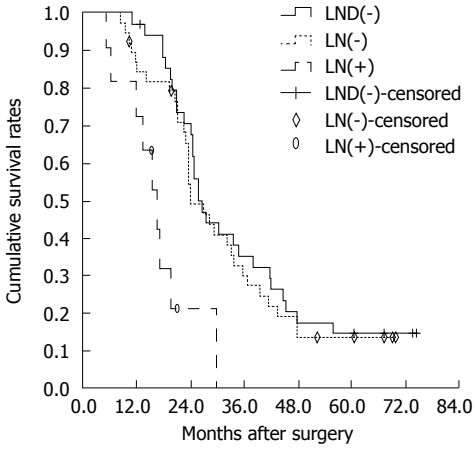

Figure 2 Overall survival curves of patients in lymph node dissection (-), lymph node (-) and lymph node (+) groups. There was no statistically significant difference in OS between the lymph node dissection (LND) (-) and LN (-) groups (P = 0.729). There were significant differences between LN (-) and LN (+) groups (P = 0.033). A statistically significant difference between LND (-) and LN (+) groups was observed (P = 0.004). LND: Lymph node dissection; LN: Lymph node.

independent prognostic factors affecting DFS (Table 4).

Influence of LND on survival

The pathological characteristics associated with the extent of lymphadenectomy are as shown in Table 5. The LND (-) group did not demonstrate lymph node metastases as revealed by preoperative imaging (CT and MRI) and intraoperative assessment. No survival difference was recorded between the LND (-) group and the group of patients without lymph node metastasis [LN (-) group] (P =0.729). Among patients who underwent lymph node sampling or dissection, the LN (-) group showed better survival than the group of patients with lymph node metastasis [LN (+) group] (P = 0.033) (Figure 2). No survival difference was recorded between the lymph node sampling and regional LND groups (P = 0.089) (Figure 3). Among the patients with negative lymph node status, a survival difference was not present between the lymph node sampling group and regional LND group (P = 0.182). Therefore, lymphadenectomy did not significantly improve the survival rate in node negative patients (Figure 4).

DISCUSSION

We analyzed a group of 85 patients who underwent potentially curative surgery for HBV-associated ICC. The cumulative 1-, 3-, and 5-year survival rates were 60%, 18%, and 13%, respectively. Several clinicopathological factors that were suspected to significantly influence survival and recurrence were examined. In some studies, vascular invasion, lymph node metastasis, microscopic presence of tumor cells on the resection margin, multiple tumors, and tumor size were found to be significant prognostic factors for survival[24-30]. In this study, univariate analysis showed that liver cirrhosis, tumor number, tumor size, lymph node metastasis, vascular invasion, and TNM classification were

Table 2 Univariate and multivariate analyses of prognostic factors for overall survival of hepatitis B virus-associated intrahepatic cholangiocarcinoma patients included in this study

Variable	*n*	Univariate analysis			Multivariateanalyses		
		1-yr	5-yr	*P* value	HR	95%CI	*P* value
Gender				0.205	NA	NA	NA
Female	19	66%	23%				
Male	66	58%	10%				
Age				0.769	NA	NA	NA
≤ 60	59	64%	13%				
> 60	26	50%	12%				
Capsule formation				0.522	NA	NA	NA
Yes	32	55%	10%				
No	53	63%	14%				
Cirrhosis				0.002	1.981	1.197-3.278	0.008
Yes	48	56%	0%				
No	37	65%	27%				
Child-Pugh class				0.257	NA	NA	NA
A	76	61%	14%				
B	9	18%	0%				
AFP (ng/mL)				0.342	NA	NA	NA
≤ 20	48	51%	11%				
> 20	37	72%	15%				
CA19-9 (U/mL)				0.342	NA	NA	NA
≤ 37	55	66%	14%				
> 37	30	50%	10%				
Gross type				0.402	NA	NA	NA
MF	63	61%	13%				
PI + IG	22	56%	11%				
Differentiation				0.119	NA	NA	NA
Well or Moderate	63	64%	16%				
Poor	22	50%	0%				
Tumor number				< 0.001	2.653	1.562-4.508	< 0.001
Single	60	69%	17%				
Multiple	25	38%	0%				
Tumor size				0.006	NA	NA	NA
< 5 cm	43	70%	21%				
≥ 5 cm	42	49%	5%				
LN metastasis				0.005	NA	NA	NA
Yes	11	31%	0%				
No	74	64%	14%				
Vascular invasion				0.013	NA	NA	NA
Yes	11	24%	0%				
No	74	64%	14%				
TNM classification				< 0.001	NA	NA	NA
Stage Ⅰ or Ⅱ	61	66%	17%				
Stage Ⅲ or Ⅳ	24	43%	0%				
Width of resection margin				0.274	NA	NA	NA
< 1 cm	37	69%	17%				
≥ 1 cm	48	53%	9%				
Surgical procedure				0.962	NA	NA	NA
Major hepatectomy	40	61%	13%				
Minor hepatectomy	45	59%	12%				

AFP: Alpha-fetoprotein; CA19-9: Carbohydrate antigen 19-9; MF: Mass-forming; PI: Periductal infiltrating; IG: Intraductal growth; TNM: Tumor-node-metastasis; NA: Not available; HR: Hazard ratio; LN: Lymph node.

Table 3 Sites of initial recurrences in hepatitis B virus-associated intrahepatic cholangiocarcinoma patients after curative resection

Site of initial recurrence	No. of patients
Liver, lymph nodes	6
Liver, lung	1
Liver	46
Lymph nodes	8
Peritoneum	5
Wound site	1
Bone	1
Lung	2

significant prognostic factors for survival. Multivariate analysis showed that liver cirrhosis and multiple tumors were independent prognostic factors for survival.

The recurrence rate was reported to be 61%-65%[24,25,28,29]. The most common recurrence site was the remnant liver, as reported in other studies [24,25,28]. In this study, liver cirrhosis, vascular invasion, and advanced TNM stage (stage Ⅲ or Ⅳ) were independent prognostic factors for DFS.

The presence of liver cirrhosis was obviously more common in HBV-associated ICC. In this study, there were

Table 4 Univariate and multivariate analyses of prognostic factors for disease-free survival in hepatitis B virus-associated intrahepatic cholangiocarcinoma patients included in this study

Variable	*n*	Univariate analysis			Multivariateanalyses		
		1-yr	5-yr	*P* value	HR	95%CI	*P* value
Gender				0.312	NA	NA	NA
Female	19	50%	0%				
Male	66	32%	4%				
Age				0.853	NA	NA	NA
≤ 60	59	33%	1%				
> 60	26	42%	5%				
Capsule formation				0.970	NA	NA	NA
Yes	32	40%	7%				
No	53	33%	0%				
Cirrhosis				0.003	1.919	1.153-3.192	0.012
Yes	48	22%	0%				
No	37	52%	5%				
Child-Pugh class				0.237	NA	NA	NA
A	76	50%	20%				
B	9	27%	0%				
AFP (ng/mL)				0.648	NA	NA	NA
≤ 20	48	32%	3%				
> 20	37	40%	2%				
CA19-9 (U/mL)				0.189	NA	NA	NA
≤ 37	55	39%	3%				
> 37	30	29%	2%				
Gross type				0.917	NA	NA	NA
MF	63	37%	3%				
PI + IG	22	30%	0%				
Differentiation				0.076	NA	NA	NA
Well or Moderate	63	42%	3%				
Poor	22	18%	0%				
Tumor number				< 0.001	NA	NA	NA
Single	60	48%	3%				
Multiple	25	5%	0%				
Tumor size				0.091	NA	NA	NA
< 5 cm	43	44%	1%				
≥ 5 cm	42	27%	5%				
LN metastasis				< 0.001	NA	NA	NA
Yes	11	0%	0%				
No	74	40%	3%				
Vascular invasion					3.779	1.601-8.923	0.020
Yes	11						
No	74						
TNM classification				< 0.001	NA	NA	NA
Stage Ⅰ or Ⅱ	61	0%	0%				
Stage Ⅲ or Ⅳ	24	51%	20%				
Width of resection margin				< 0.001	NA	NA	NA
< 1 cm	37	49%	4%				
≥ 1 cm	48	0%	0%				
Surgical procedure				0.391	NA	NA	NA
Major hepatectomy	40	41%	2%				
Minor hepatectomy	45	31%	3%				

AFP: Alpha-fetoprotein; CA19-9: Carbohydrate antigen 19-9; MF: Mass-forming; PI: Periductal infiltrating; IG: Intraductal growth; TNM: Tumor-node-metastasis; NA: Not available; HR: Hazard ratio; LN: Lymph node.

48 patients (56.5%) with liver cirrhosis. Cirrhosis was an independent prognostic factor for HCC. However, there is little documentation showing that this is associated with ICC. We have demonstrated that cirrhosis not only is an independent prognostic factor for DFS, but also is significantly related to poor survival of the patients with HBV-associated ICC after surgery. It may be due to the fact that HBV-associated ICC shares common disease processes for carcinogenesis with HCC.

Lymph node metastasis was found to be an important prognostic factor in previous studies[27,30]. It was associated with OS and DFS on univariate analysis, but not on multivariate analysis in this study, probably because the sample size was relatively small.

It remains unclear whether the clearance of the route of lymph node metastasis is beneficial to survival[24]. There are no clear guidelines on LND. It is reported that extended lymphadenectomy in ICC patients did not seem to show any advantage without control of liver metastases, because most recurrences occurred

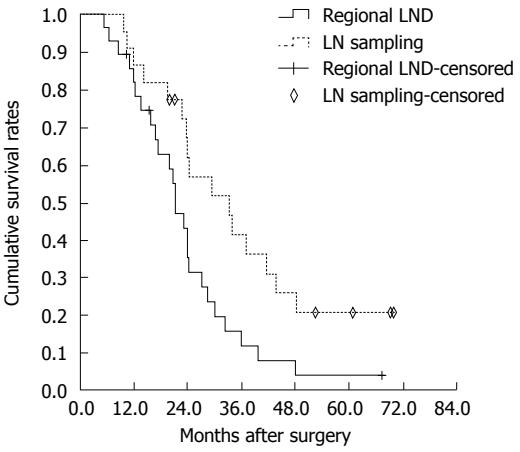

Figure 3 Overall survival curves of hepatitis B virus-associated intrahepatic cholangiocarcinoma patients undergoing sampling lymph node sampling and regional lymph node dissection. There were no significant differences between the two groups (P = 0.089). LND: Lymph node dissection; LN: Lymph node.

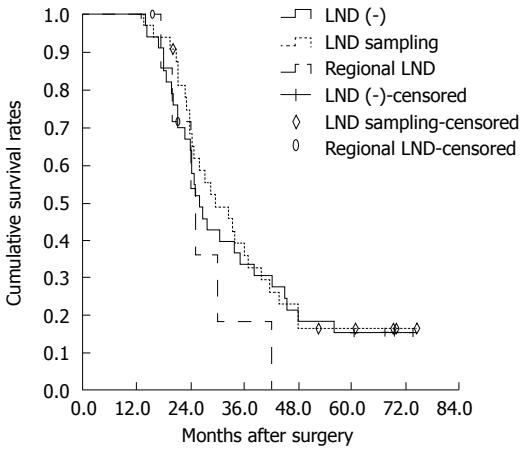

Figure 4 Overall survival curves of hepatitis B virus-associated intrahepatic cholangiocarcinoma patients without lymph node involvement. There was no survival difference between lymph node sampling and regional LND groups (P = 0.182). There was no statistically significant difference in overall survival between LND (-) and lymph node sampling groups (P = 0.709). There were also no significant differences between LND (-) and regional LND groups (P = 0.309). LND: Lymph node dissection.

Table 5 Comparison of the pathological factors according to the extent of lymph node dissection

Variable	LND (-)	LN sampling	Regional LND	*P* value
Cirrhosis				0.439
Yes	17	13	18	
No	18	9	10	
Gross type				0.617
MF	24	17	22	
PI + IG	11	5	6	
Differentiation				0.478
Well or Moderate	25	15	23	
Poor	10	7	5	
Capsule formation				0.931
Yes	14	8	10	
No	21	14	18	
Tumor number				0.512
Single	27	14	18	
Multiple	8	8	10	
Tumor size				0.145
< 5 cm	21	12	10	
⩾ 5 cm	14	10	18	
Pathologica LN metastasis				0.085
Yes	NA	2	9	
No	NA	20	19	
Vascular invasion				0.181
Yes	2	3	6	
No	33	19	22	

MF: Mass-forming; PI: Periductal infiltrating; IG: Intraductal growth; LN: Lymph node; LND: Lymph node dissection; NA: Not available.

in patients with known liver metastases[17,24]. However, other reports indicated that extensive hepatectomy with extended LND produced a better outcome[31,32]. Defining the role of lymphadenectomy is important, because lymphadenectomy is a factor controllable by a surgeon out of numerous prognostic factors. The present study has demonstrated that regional LND group has a survival rate similar to that of the lymph node sampling group. The extent of lymphadenectomy (lymph node sampling *vs* regional LND) does not affect the survival. The patients without LND have similar survival to patients with LND or negative lymph node status. It is revealed that lymphadenectomy does not significantly improve the survival of patients with negative lymph node status.

Nevertheless, this study was limited by its retrospective design. More than five surgeons were involved in treating ICC in this study. It was difficult to determine the exact reasons and extent of LND performed for each patient.

In conclusion, liver cirrhosis and multiple tumors are independent prognostic factors for survival in patients with HBV-associated ICC. The extent of LND does not seem to have influence on the survival of patients with HBV-associated ICC. LND cannot significantly improve the survival of patients with negative lymph node status. We recommend intraoperative lymph node exploration, as opposed to routine regional LND. Regional LND should be performed when lymph node involvement is clinically recognized or it is positive as demonstrated by a frozen section examination.

COMMENTS

Background

Some recently published studies show a relation between chronic hepatitis B infection and the development of intrahepatic cholangiocarcinoma. Patients with hepatitis B-associated cholangiocarcinoma appear to have different clinicopathological characteristics compared with seronegative patients.

Research frontiers

Hepatitis B virus (HBV)-associated intrahepatic cholangiocarcinoma (ICC) have different clinicopathological characteristics and surgical outcomes, and should be distinguished from those without HBV infection. Because of the rarity and low resectability of HBV-associated ICC, prognostic factors after resection for HBV-associated ICC have not been clearly established. The influences of the extent of lymph node dissection (LND) on survival were also not been clearly established.

Innovations and breakthroughs

This study was conducted to investigate the outcomes of HBV-associated ICC patients after hepatic resection, and analyzed the prognostic factors affecting the survival and recurrence. The impact of the extent of LND on survival was

also investigated.

Applications

Liver cirrhosis and multiple tumors are independent prognostic factors for survival in patients with HBV-associated ICC. The extent of lymph node dissection does not seem to have influence on the survival of patients with HBV-associated ICC. Lymphadenectomy cannot significantly improve the survival of lymph node negative patients.

Peer review

The reported data are interesting. Some recently published studies show a relation between chronic hepatitis B infection and the development of intrahepatic cholangiocarcinoma. Patients with hepatitis B-associated cholangiocarcinoma appear to have different clinicopathological characteristics compared with seronegative patients.

REFERENCES

1 **Casavilla FA**, Marsh JW, Iwatsuki S, Todo S, Lee RG, Madariaga JR, Pinna A, Dvorchik I, Fung JJ, Starzl TE. Hepatic resection and transplantation for peripheral cholangiocarcinoma. *J Am Coll Surg* 1997; **185**: 429-436 [PMID: 9358085 DOI: 10.1016/S1072-7515(01)00953-X]

2 **Ikai I**, Arii S, Okazaki M, Okita K, Omata M, Kojiro M, Takayasu K, Nakanuma Y, Makuuchi M, Matsuyama Y, Monden M, Kudo M. Report of the 17th Nationwide Follow-up Survey of Primary Liver Cancer in Japan. *Hepatol Res* 2007; **37**: 676-691 [PMID: 17617112 DOI: 10.1111/j.1872-034X.2007.00119.x]

3 **Aishima S**, Kuroda Y, Nishihara Y, Iguchi T, Taguchi K, Taketomi A, Maehara Y, Tsuneyoshi M. Proposal of progression model for intrahepatic cholangiocarcinoma: clinicopathologic differences between hilar type and peripheral type. *Am J Surg Pathol* 2007; **31**: 1059-1067 [PMID: 17592273 DOI: 10.1097/PAS.0b013e31802b34b6]

4 **Kobayashi M**, Ikeda K, Saitoh S, Suzuki F, Tsubota A, Suzuki Y, Arase Y, Murashima N, Chayama K, Kumada H. Incidence of primary cholangiocellular carcinoma of the liver in japanese patients with hepatitis C virus-related cirrhosis. *Cancer* 2000; **88**: 2471-2477 [PMID: 10861422]

5 **Lee TY**, Lee SS, Jung SW, Jeon SH, Yun SC, Oh HC, Kwon S, Lee SK, Seo DW, Kim MH, Suh DJ. Hepatitis B virus infection and intrahepatic cholangiocarcinoma in Korea: a case-control study. *Am J Gastroenterol* 2008; **103**: 1716-1720 [PMID: 18557716 DOI: 10.1111/j.1572-0241.2008.01796.x]

6 **Hai S**, Kubo S, Yamamoto S, Uenishi T, Tanaka H, Shuto T, Takemura S, Yamazaki O, Hirohashi K. Clinicopathologic characteristics of hepatitis C virus-associated intrahepatic cholangiocarcinoma. *Dig Surg* 2005; **22**: 432-439 [PMID: 16479112 DOI: 10.1159/000091446]

7 **Lee CH**, Chang CJ, Lin YJ, Yeh CN, Chen MF, Hsieh SY. Viral hepatitis-associated intrahepatic cholangiocarcinoma shares common disease processes with hepatocellular carcinoma. *Br J Cancer* 2009; **100**: 1765-1770 [PMID: 19436294 DOI: 10.1038/sj.bjc.6605063]

8 **Zhou H**, Wang H, Zhou D, Wang H, Wang Q, Zou S, Tu Q, Wu M, Hu H. Hepatitis B virus-associated intrahepatic cholangiocarcinoma and hepatocellular carcinoma may hold common disease process for carcinogenesis. *Eur J Cancer* 2010; **46**: 1056-1061 [PMID: 20202823 DOI: 10.1016/j.ejca.2010.02.005]

9 **Bhagat V**, Javle M, Yu J, Agrawal A, Gibbs JF, Kuvshinoff B, Nava E, Iyer R. Combined hepatocholangiocarcinoma: case-series and review of literature. *Int J Gastrointest Cancer* 2006; **37**: 27-34 [PMID: 17290078]

10 **Koh KC**, Lee H, Choi MS, Lee JH, Paik SW, Yoo BC, Rhee JC, Cho JW, Park CK, Kim HJ. Clinicopathologic features and prognosis of combined hepatocellular cholangiocarcinoma. *Am J Surg* 2005; **189**: 120-125 [PMID: 15701504 DOI: 10.1016/j.amjsurg.2004.03.018]

11 **Zhang F**, Chen XP, Zhang W, Dong HH, Xiang S, Zhang WG, Zhang BX. Combined hepatocellular cholangiocarcinoma originating from hepatic progenitor cells: immunohistochemical and double-fluorescence immunostaining evidence. *Histopathology* 2008; **52**: 224-232 [PMID: 18184271 DOI: 10.1111/j.1365-2559.2007.02929.x]

12 **Peng NF**, Li LQ, Qin X, Guo Y, Peng T, Xiao KY, Chen XG, Yang YF, Su ZX, Chen B, Su M, Qi LN. Evaluation of risk factors and clinicopathologic features for intrahepatic cholangiocarcinoma in Southern China: a possible role of hepatitis B virus. *Ann Surg Oncol* 2011; **18**: 1258-1266 [PMID: 21207172 DOI: 10.1245/s10434-010-1458-5]

13 **Wu ZF**, Yang N, Li DY, Zhang HB, Yang GS. Characteristics of intrahepatic cholangiocarcinoma in patients with hepatitis B virus infection: clinicopathologic study of resected tumours. *J Viral Hepat* 2013; **20**: 306-310 [PMID: 23565611 DOI: 10.1111/jvh.12005]

14 **Zhou HB**, Wang H, Li YQ, Li SX, Wang H, Zhou DX, Tu QQ, Wang Q, Zou SS, Wu MC, Hu HP. Hepatitis B virus infection: a favorable prognostic factor for intrahepatic cholangiocarcinoma after resection. *World J Gastroenterol* 2011; **17**: 1292-1303 [PMID: 21455328 DOI: 10.3748/wjg.v17.i10.1292]

15 **Zhou XD**, Tang ZY, Fan J, Zhou J, Wu ZQ, Qin LX, Ma ZC, Sun HC, Qiu SJ, Yu Y, Ren N, Ye QH, Wang L, Ye SL. Intrahepatic cholangiocarcinoma: report of 272 patients compared with 5,829 patients with hepatocellular carcinoma. *J Cancer Res Clin Oncol* 2009; **135**: 1073-1080 [PMID: 19294418 DOI: 10.1007/s00432-009-0547-y]

16 **Tang D**, Nagano H, Nakamura M, Wada H, Marubashi S, Miyamoto A, Takeda Y, Umeshita K, Dono K, Monden M. Clinical and pathological features of Allen's type C classification of resected combined hepatocellular and cholangiocarcinoma: a comparative study with hepatocellular carcinoma and cholangiocellular carcinoma. *J Gastrointest Surg* 2006; **10**: 987-998 [PMID: 16843869 DOI: 10.1016/j.gassur.2006.01.018]

17 **Shimada M**, Yamashita Y, Aishima S, Shirabe K, Takenaka K, Sugimachi K. Value of lymph node dissection during resection of intrahepatic cholangiocarcinoma. *Br J Surg* 2001; **88**: 1463-1466 [PMID: 11683741 DOI: 10.1046/j.0007-1323.2001.01879.x]

18 **Yamamoto M**, Takasaki K, Yoshikawa T. Lymph node metastasis in intrahepatic cholangiocarcinoma. *Jpn J Clin Oncol* 1999; **29**: 147-150 [PMID: 10225697 DOI: 10.1093/jjco/29.3.147]

19 **Uenishi T**, Hirohashi K, Kubo S, Yamamoto T, Hamba H, Tanaka H, Kinoshita H. Histologic factors affecting prognosis following hepatectomy for intrahepatic cholangiocarcinoma. *World J Surg* 2001; **25**: 865-869 [PMID: 11572025 DOI: 10.1007/s00268-001-0042-3]

20 **Vitale F**, Tramuto F, Orlando A, Vizzini G, Meli V, Cerame G, Mazzucco W, Virdone R, Palazzo U, Villafrate MR, Tagger A, Romano N. Can the serological status of anti-HBc alone be considered a sentinel marker for detection of occult HBV infection? *J Med Virol* 2008; **80**: 577-582 [PMID: 18297707 DOI: 10.1002/jmv.21121]

21 **Shiota G**, Oyama K, Udagawa A, Tanaka K, Nomi T, Kitamura A, Tsutsumi A, Noguchi N, Takano Y, Yashima K, Kishimoto Y, Suou T, Kawasaki H. Occult hepatitis B virus infection in HBs antigen-negative hepatocellular carcinoma in a Japanese population: involvement of HBx and p53. *J Med Virol* 2000; **62**: 151-158 [PMID: 11002243]

22 **Yang T**, Zhang J, Lu JH, Yang LQ, Yang GS, Wu MC, Yu WF. A new staging system for resectable hepatocellular carcinoma: comparison with six existing staging systems in a large Chinese cohort. *J Cancer Res Clin Oncol* 2011; **137**: 739-750 [PMID: 20607551 DOI: 10.1007/s00432-010-0935-3]

23 **Wu ZF**, Zhang HB, Yang N, Zhao WC, Fu Y, Yang GS. Postoperative adjuvant transcatheter arterial chemoembolisation improves survival of intrahepatic cholangiocarcinoma patients

with poor prognostic factors: results of a large monocentric series. *Eur J Surg Oncol* 2012; **38**: 602-610 [PMID: 22417704 DOI: 10.1016/j.ejso.2012.02.185]

24 **Choi SB**, Kim KS, Choi JY, Park SW, Choi JS, Lee WJ, Chung JB. The prognosis and survival outcome of intrahepatic cholangiocarcinoma following surgical resection: association of lymph node metastasis and lymph node dissection with survival. *Ann Surg Oncol* 2009; **16**: 3048-3056 [PMID: 19626372 DOI: 10.1245/s10434-009-0631-1]

25 **Ohtsuka M**, Ito H, Kimura F, Shimizu H, Togawa A, Yoshidome H, Miyazaki M. Results of surgical treatment for intrahepatic cholangiocarcinoma and clinicopathological factors influencing survival. *Br J Surg* 2002; **89**: 1525-1531 [PMID: 12445060 DOI: 10.1046/j.1365-2168.2002.02268.x]

26 **Nakagawa T**, Kamiyama T, Kurauchi N, Matsushita M, Nakanishi K, Kamachi H, Kudo T, Todo S. Number of lymph node metastases is a significant prognostic factor in intrahepatic cholangiocarcinoma. *World J Surg* 2005; **29**: 728-733 [PMID: 15880276 DOI: 10.1007/s00268-005-7761-9]

27 **Shimada K**, Sano T, Sakamoto Y, Esaki M, Kosuge T, Ojima H. Clinical impact of the surgical margin status in hepatectomy for solitary mass-forming type intrahepatic cholangiocarcinoma without lymph node metastases. *J Surg Oncol* 2007; **96**: 160-165 [PMID: 17443744 DOI: 10.1002/jso.20792]

28 **Nakagohri T**, Asano T, Kinoshita H, Kenmochi T, Urashima T, Miura F, Ochiai T. Aggressive surgical resection for hilar-invasive and peripheral intrahepatic cholangiocarcinoma. *World J Surg* 2003; **27**: 289-293 [PMID: 12607053 DOI: 10.1007/s00268-002-6696-7]

29 **Weber SM**, Jarnagin WR, Klimstra D, DeMatteo RP, Fong Y, Blumgart LH. Intrahepatic cholangiocarcinoma: resectability, recurrence pattern, and outcomes. *J Am Coll Surg* 2001; **193**: 384-391 [PMID: 11584966 DOI: 10.1016/S1072-7515(01)01016-X]

30 **Tajima Y**, Kuroki T, Fukuda K, Tsuneoka N, Furui J, Kanematsu T. An intraductal papillary component is associated with prolonged survival after hepatic resection for intrahepatic cholangiocarcinoma. *Br J Surg* 2004; **91**: 99-104 [PMID: 14716802 DOI: 10.1002/bjs.4366]

31 **Asakura H**, Ohtsuka M, Ito H, Kimura F, Ambiru S, Shimizu H, Togawa A, Yoshidome H, Kato A, Miyazaki M. Long-term survival after extended surgical resection of intrahepatic cholangiocarcinoma with extensive lymph node metastasis. *Hepatogastroenterology* 2005; **52**: 722-724 [PMID: 15966191]

32 **Uenishi T**, Yamazaki O, Horii K, Yamamoto T, Kubo S. A long-term survivor of intrahepatic cholangiocarcinoma with paraaortic lymph node metastasis. *J Gastroenterol* 2006; **41**: 391-392 [PMID: 16741622 DOI: 10.1007/s00535-006-1757-6]

P- Reviewer: Bo J, Chiang TA, Shaikh S **S- Editor**: Qi Y
L- Editor: Wang TQ **E- Editor**: Wang CH

World Journal of Gastroenterology

Submit a Manuscript: http://www.wjgnet.com/esps/
Help Desk: http://www.wjgnet.com/esps/helpdesk.aspx
DOI: 10.3748/wjg.v21.i3.944

World J Gastroenterol 2015 January 21; 21(3): 944-952
ISSN 1007-9327 (print) ISSN 2219-2840 (online)

ORIGINAL ARTICLE

Clinical Trials Study

Centralized isolation of *Helicobacter pylori* from multiple centers and transport condition influences

Ya-Nan Gong, You-Ming Li, Ning-Min Yang, Hong-Zhang Li, Feng Guo, Lang Lin, Qun-Ying Wang, Jia-Kun Zhang, Zi-Zhong Ji, Ji-Bo Mao, Jun-Liang Mao, Zheng-Chao Shi, Wu-Heng Tang, Xin-Jian Zhu, Wei Shao, Xiao-Feng Zhang, Xing-Hua Wang, Yue-Feng Tong, Mi-Zu Jiang, Guang-Lan Chen, Zhi-Yong Wang, Hui-Min Tu, Guo-Fa Jiang, Jian-Sheng Wu, Xu-Peng Chen, Qiu-Long Ding, Hong Ouyang, Feng-Zhe Jin, Yan-Li Xu, Jian-Zhong Zhang

Ya-Nan Gong, Jian-Zhong Zhang, State Key Laboratory for Infectious Disease Prevention and Control, National Institute for Communicable Disease Control and Prevention, Chinese Center for Disease Control and Prevention, Beijing 102206, China
Ya-Nan Gong, Jian-Zhong Zhang, Collaborative Innovation Center for Diagnosis and Treatment of Infectious Diseases, Hangzhou 310003, Zhejiang Province, China
You-Ming Li, The First Affiliated Hospital, College of Medicine, Zhejiang University, Hangzhou 310003, Zhejiang Province, China
Ning-Min Yang, Zhiyuan Medical Inspection Institute Co., Ltd., Hangzhou 310021, Zhejiang Province, China
Hong-Zhang Li, Sanmen People's Hospital, Taizhou 317100, Zhejiang Province, China
Feng Guo, The First People's Hospital of Xiaoshan District, Hangzhou 311200, Zhejiang Province, China
Lang Lin, The First People's Hospital of Cangnan, Wenzhou 325800, Zhejiang Province, China
Qun-Ying Wang, Jinhua Municipal Central Hospital, Jinhua 321001, Zhejiang Province, China
Jia-Kun Zhang, The First People's Hospital of Pingyang, Wenzhou 325400, Zhejiang Province, China
Zi-Zhong Ji, The First Hospital of Jiaxing, Jiaxing 314001, Zhejiang Province, China
Ji-Bo Mao, Zhoushan Hospital, Zhoushan 316021, Zhejiang Province, China
Jun-Liang Mao, The First People's Hospital of Wenling, Wenling 317500, Zhejiang Province, China
Zheng-Chao Shi, Rui'an People's Hospital, Rui'an 325200, Zhejiang Province, China
Wu-Heng Tang, Maternal and Child Health Hospital of Zhoushan City, Zhoushan 316000, Zhejiang Province, China
Xin-Jian Zhu, Shangyu People's Hospital, Shaoxing 312300, Zhejiang Province, China
Wei Shao, People's Hospital of Putuo District, Zhoushan 316399, Zhejiang Province, China
Xiao-Feng Zhang, Hangzhou First People's Hospital, Hangzhou 310006, Zhejiang Province, China
Xing-Hua Wang, Qingtian People's Hospital, Lishui 323900, Zhejiang Province, China
Yue-Feng Tong, The First People's Hospital of Yongkang, Yongkang 321300, Zhejiang Province, China
Mi-Zu Jiang, The Children's Hospital Zhejiang University School of Medicine, Hangzhou 310003, Zhejiang Province, China
Guang-Lan Chen, Lishui People's Hospital, Lishui 323000, Zhejiang Province, China
Zhi-Yong Wang, The Affiliated Hospital of Hangzhou Normal University, Hangzhou 310015, Zhejiang Province, China
Hui-Min Tu, Wuxi No. 4 Hospital Affiliated to Suzhou University, Wuxi 214062, Zhejiang Province, China
Guo-Fa Jiang, Jinhua Wenrong Hospital, Jinhua 321001, Zhejiang Province, China
Jian-Sheng Wu, The First Affiliated Hospital of Wenzhou Medical College, Wenzhou 325000, Zhejiang Province, China
Xu-Peng Chen, Yueqing People's Hospital, Wenzhou 325600, Zhejiang Province, China
Qiu-Long Ding, Tiantai People's Hospital, Taizhou 317200, Zhejiang Province, China
Hong Ouyang, Lin'an people's Hospital, Lin'an 311300, Zhejiang Province, China
Feng-Zhe Jin, Rui'an City TCM Hospital, Rui'an 325200, Zhejiang Province, China
Yan-Li Xu, Medical College of Hebei University of Engineering, Handan 056038, Hebei Province, China

Author contributions: Gong YN and Xu YL analyzed data and drafted this paper; Li YM and Yang NM were involved in designing the protocol and providing results of this study; Zhang JZ had the idea for this study and final responsibility for the decision to submit for publication; Li HZ, Guo F, Lin L, Wang QY, Zhang JK, Ji ZZ, Mao JB, Mao JL, Shi ZC, Tang WH, Zhu XJ, Shao W, Zhang XF, Wang XH, Tong YF, Jiang MZ, Chen GL, Wang ZY, Tu HM, Jiang GF, Wu JS, Chen XP, Ding QL, Ouyang H and Jin FZ were responsible for sample collection, the order of authorship was based on specific contribution; all authors were involved in data interpretation and critical revisions of the

report, and approved the final version.
Supported by Grants from the Science and Technology Program of Zhejiang Province China, No. 2001C23140, National Technology RD Program in the 12th Five-Year Plan of China, No. 2012BAI06B02, the Major Technology Project as part of "Prevention and Control of Major Infectious Diseases including AIDS and Viral Hepatitis", No. 2013ZX10004216-002, the National Key Scientific Instrument and Equipment Development Project, No. 2012YQ180117, the Medical and Health Science and Technology Plan Project of Zhejiang Province, No. 2012KYB248, and the Science and Technology Project of Zhejiang province, No. 2011C23140.

Correspondence to: Jian-Zhong Zhang, MD, PhD, State Key Laboratory for Infectious Disease Prevention and Control, National Institute for Communicable Disease Control and Prevention, Chinese Center for Disease Control and Prevention, 155 Changbai Road, Changping District, Beijing 102206, China. zhangjianzhong@icdc.cn
Telephone: +86-10-58900707
Fax: +86-10-58900700
Received: June 16, 2014
Peer-review started: June 16, 2014
First decision: July 21, 2014
Revised: August 11, 2014
Accepted: September 18, 2014
Article in press: September 19, 2014
Published online: January 21, 2015

Abstract

AIM: To evaluate the efficacy of centralized culture and possible influencing factors.

METHODS: From January 2010 to July 2012, 66452 patients with suspected *Helicobacter pylori* (*H. pylori*) infection from 26 hospitals in Zhejiang and Jiangsu Provinces in China underwent gastrointestinal endoscopy. Gastric mucosal biopsies were taken from the antrum for culture. These biopsies were transported under natural environmental temperature to the central laboratory in Hangzhou city and divided into three groups based on their transport time: 5, 24 and 48 h. The culture results were reported after 72 h and the positive culture rates were analyzed by a χ^2 test. An additional 5736 biopsies from *H. pylori*-positive patients (5646 rapid urease test-positive and 90 ^{14}C-urease breath test-positive) were also cultured for quality control in the central laboratory setting.

RESULTS: The positive culture rate was 31.66% (21036/66452) for the patient samples and 71.72% (4114/5736) for the *H. pylori*-positive quality control specimens. In the 5 h transport group, the positive culture rate was 30.99% (3865/12471), and 32.84% (14960/45553) in the 24 h transport group. In contrast, the positive culture rate declined significantly in the 48 h transport group (26.25%; $P < 0.001$). During transportation, the average natural temperature increased from 4.67 to 29.14 ℃, while the positive culture rate declined from 36.67% (1462/3987) to 24.12% (1799/7459). When the temperature exceeded 24 ℃, the positive culture rate decreased significantly, especially in the 48 h transport group (23.17%).

CONCLUSION: Transportation of specimens within 24 h and below 24 ℃ is reasonable and acceptable for centralized culture of multicenter *H. pylori* samples.

Key words: Centralized isolation; *Helicobacter pylori*; Influencing factor; Multiple centers; Personalized treatment

Core tip: This is the first large-scale study on the centralized culture of *Helicobacter pylori* in a large number of clinical samples from multiple centers. The efficacy of centralized culture and possible influencing factors were evaluated. The results confirm the feasibility of establishing a culture center for individualized medical use. The findings of this study can be promisingly applied in clinical and public health practice.

Gong YN, Li YM, Yang NM, Li HZ, Guo F, Lin L, Wang QY, Zhang JK, Ji ZZ, Mao JB, Mao JL, Shi ZC, Tang WH, Zhu XJ, Shao W, Zhang XF, Wang XH, Tong YF, Jiang MZ, Chen GL, Wang ZY, Tu HM, Jiang GF, Wu JS, Chen XP, Ding QL, Ouyang H, Jin FZ, Xu YL, Zhang JZ. Centralized isolation of *Helicobacter pylori* from multiple centers and transport condition influences. *World J Gastroenterol* 2015; 21(3): 944-952 Available from: URL: http://www.wjgnet.com/1007-9327/full/v21/i3/944.htm DOI: http://dx.doi.org/10.3748/wjg.v21.i3.944

INTRODUCTION

Helicobacter pylori (*H. pylori*), one of the most common human pathogens, can lead to gastric ulcers, gastritis, gastric cancer, and mucosa-associated lymphoid tumors[1]. According to the Maastricht Ⅳ and Chinese Consensus Report, two antibiotics combined with one proton-pump inhibitor are recommended as standard first-line treatment to eradicate *H. pylori*[2,3]. However, in recent years, the success rates have declined below 80% in most European and Asian countries[4-6]. There are many reasons accounting for eradication failure, such as poor patient compliance, low gastric pH, and resistant bacteria. In fact, the main reason for the decline is the increasing *H. pylori* resistance to the antibiotics used[7,8]. In China, the resistance to clarithromycin, a key antibiotic in the triple

therapy, has reached above 20% and should not be used in anti-*H.pylori* therapy without a susceptibility test[2,9-11].

Accumulated evidence suggests that culture-susceptibility tests may improve the eradication rate of *H. pylori*[12-17]. However, *H. pylori* is a rather fastidious bacterium at culture, especially when a low bacterial load is present[18]. The ideal situation for culture-susceptibility test is not available in many clinical settings, since most endoscopic units do not have direct access to a microbiology laboratory. Therefore, gastric biopsy specimens should be transported to a central laboratory for *H. pylori* culture. During transportation, time and temperature could influence the survivability of *H. pylori* and these issues are still in debate[19-23]. Some investigators emphasized the need for rapid transport at a low temperature[21]. Others demonstrated that *H. pylori* could survive at room temperature for 24 h without loss of the ability to recover[22]. The transport of samples at natural temperature is required for a routine clinical application system. In order to assess the factors, transportation[24] and isolation tests of thousands of *H. pylori* strains were performed in our lab, but the complexity of large-scale clinical application could not be accurately represented. The feasibility of centralized isolation of *H. pylori* in a large number of clinical samples from multiple centers and influencing factors need to be tested for actual practice.

A central laboratory for *H. pylori* isolation was set up in Zhiyuan Medical Inspection Institute Co., Ltd., in Hangzhou city, which has provided a personalized treatment strategy for *H. pylori* eradication in recent years. In order to evaluate the efficacy of centralized culture and possible influencing factors, we conducted research in the central laboratory to analyze positive culture rates of a large number of clinical samples collected from 26 hospitals in nine cities.

MATERIALS AND METHODS

Sample collection

The sampling was conducted in Zhejiang Province and Jiangsu Province, China. Between January 2010 and July 2012, consecutive participants with suspected *H. pylori* infection underwent gastrointestinal endoscopy. The gastric mucosal biopsies were taken from the greater curvature of gastric antrum using sterile disposable biopsy forceps. Additionally, in order to assess the positive rate of *H. pylori* culture, specimens from *H. pylori*-positive patients (5646 rapid urease test-positive and 90 ^{14}C-urease breath test-positive) were also collected as a control. The *H. pylori*-positive samples were all collected from Wenzhou city, including The First Affiliated Hospital of Wenzhou Medical College and The First People's Hospital of Pingyang.

This study was approved by the Ethics Committee of National Institute for Communicable Disease Control and Prevention, Chinese Center for Disease Control and Prevention and the Ethics Committee of Zhiyuan Medical Inspection Institute Co., Ltd., and written informed consent was obtained from all patients.

Transport and culture procedure

The gastric mucosal sample from each patient was stored in sterile tube that contained 1 mL brain-heart infusion with 20% glycerol and kept under 4 ℃ before transportation. All the fresh biopsy specimens were transported at external temperature to Zhiyuan Medical Inspection Institute Co., Ltd., for centralized isolation. The 66452 specimens were divided into three independent groups based on transport time: 5, 24 and 48 h. The first group (5 h; n = 12471) was collected from Hangzhou city between 9 am and 12 pm and cultured at 2 pm on the same day. The second group (24 h; n = 45553) was collected from other cities hundreds of kilometers away from Hangzhou between 9 am and 12 pm and sent to Hangzhou for culture at 9 am the next day. The third group (48 h; n = 8428) were collected from Jinhua city and transported to Hangzhou for culture 48 h later because of the limitations of local hospital conditions. The *H. pylori*-positive control samples were transported the same as the 24 h group.

The samples were ground/broken and cultivated on Columbia agar plates (Oxoid of Thermo Fisher Scientific Inc., Waltham, MA, United States) supplemented with 5% defibrinated sheep blood, 3 μg/mL synergist, 2.5 μg/mL vancomycin, 2 μg/mL amphotericin B, and 2 μg/mL bacillosporin B under microaerophilic conditions (5% O_2, 10% CO_2, 85% N_2) for 72 h. Translucent colonies (0.5-2.0 mm) from the original agar plates were selected for gram staining and urease, oxidase and catalase tests. Colonies with curved gram-negative rods resembling *Helicobacter spp* and positive in three enzyme tests were identified as *H. pylori*.

Meteorological data

The information concerning daily measured maximum, minimum and average temperatures in each city related with this study in Zhejiang Province from January 1, 2010 to December 31, 2012 was supplied by the Meteorological Bureau of Zhejiang Province. The average daily temperature was the average value of temperatures at four time points each day (2 am, 8 am, 2 pm and 8 pm). In our investigation, we used the regional level meteorological data from six cities (Hangzhou, Jiaxing, Jinhua, Taizhou, Wenzhou, and Zhoushan) to calculate the monthly maximum, minimum and average temperatures and draw the temperature change curves.

Statistical analysis

The results of isolation and identification of *H. pylori* for all specimens were reported 72 h after culture and all calculations were performed using SPSS 18.0 software (SPSS Inc., Chicago, IL, United States). The positive culture rates were assessed with a χ^2 test. A $P \leqslant 0.05$ was considered as statistically significant.

RESULTS

Sample collection

The random 66452 samples were collected from 24 hospitals in nine cities: Hangzhou (n = 6), Jiaxing (n = 1), Jinhua (n = 3), Shaoxing (n = 1), Taizhou (n = 3), Wenzhou (n = 4), Zhoushan (n = 3), Lishui (n = 2) and Wuxi (n = 1). The 5736 *H. pylori*-positive specimens were collected from another two hospitals in Wenzhou city. Eight of the 26 sampling hospitals are Class 2A hospitals, which are primarily county-level hospitals providing medical service to the communities. The other hospitals belong to Class 3A, which are regional hospitals and possess the highest medical level in Chinese hospital grading. The distribution and numbers of samples in each year and city are shown in Figure 1A.

Culture results

Of the 66452 specimens, 31.66% (21036/66452) were *H. pylori*-positive. The positive culture rates of specimens in 2010, 2011 and 2012 were 28.64% (4897/17098), 30.28% (6513/21509) and 34.57% (9626/27845), respectively. The differences showed statistical significance ($P < 0.001$). The positive culture rate for Class 2A hospitals was 31.96% (8103/25350) and that of Class 3A hospitals was 31.47% (12933/41102).

The positive culture rates of samples from nine cities varied from 26.59% (2354/8852) in Jinhua city to 42.51% (332/781) in Lishui city (Figure 1B). The positive culture rate of Hangzhou city, which was the culture center, was 30.99% (3866/12473).

Even in the same city, the positive culture rates of different sampling hospitals were different. The culture positive rates from four hospitals in Hangzhou city were 29.97% (3316/11064), 38.95% (298/705), 25.73% (79/307) and 47.66% (61/128) (Figure 2).

Culture results of different transport groups

The positive culture rates from the 5, 24, and 48 h transport groups were 30.99% (3865/12471), 32.84% (14960/45553) and 26.25% (2211/8428), respectively. The positive culture rate of the 48 h transport group was significantly lower than the other two groups ($P < 0.001$). The positive culture rate from the 48 h group was significantly lower than the 24 h group in samples from the same city, (26.25% *vs* 33.73%, $P < 0.001$).

Culture results from natural transport temperatures

The average natural temperature in Zhejiang province varied within one year from 4.67 to 29.14 ℃. The average temperatures in January, May, June and July were 4.66, 20.85, 24.24 and 28.85 ℃, respectively. The change curves of average temperatures were similar in six cities, and the monthly average temperature, average maximum and minimum temperatures of the six cities during this study are shown in Figure 3A.

As the temperature increased, the total positive culture rate declined from 36.67% (1462/3987) in December to 24.12% (1799/7459) in July. Although the average temperature elevated significantly from January to May, the positive culture rates were similar. When the average temperature exceeded 24 ℃ in June and July, the positive culture rates declined significantly ($P < 0.001$), with the lowest positive culture rate in July (24.12%; 1799/7459). This phenomenon was particularly evident in Wenzhou city whose positive culture rates changed from 38.44% (316/822) in January to 25.38% (389/1533) in July. The positive culture rates in the other months changed slightly even when the temperatures changed significantly (Figure 3B). Positive culture rates of six cities in Zhejiang Province in January, May, June and July are shown in Figure 4.

Culture results of H. pylori-positive specimens

Of the *H. pylori*-positive specimens, the isolation of *H. pylori* was successful in 71.72% (4114/5736) of cases, demonstrating the positive predictive value of *H. pylori* isolation in the central cultural platform.

DISCUSSION

Isolation of all samples was conducted in the same laboratory to eliminate the intrinsic variability from multiple laboratories. The advantage of our study is that it contains largest sample size to date, involving a wide range of demographic characteristics, geographic areas and hospitals from various medical levels (nearly all the gastrointestinal endoscopic tests were done in Class 2A and 3A hospitals in China). Compared with a previous study[25], the limitations of small sample size and collection of data from different laboratories were certainly avoided in this study, and more reliable information for the centralized culture of *H. pylori* was provided.

Previous studies reported *H. pylori*-positive isolation rates ranging from 75% to 94%[25,26]. Considering the differences between the *H. pylori* cultures used for clinical study and those for individual medical service, as well as the amount of samples and the time-efficient characteristics (a limited time of about seven days for clinical report was usually set in the latter), the positive culture rate of 71.72% found in this study is acceptable.

In China, the total infectious rate of *H. pylori* was relatively high, reaching 40%-60% in adults. In this study, the positive culture rate of the suspected *H. pylori* infection group was 31.66%. Combined with the culture rate of positive control samples, a 44% infectious rate was calculated, in agreement with the reported data, indicating the positive culture rate of random samples was reasonable. In addition, the cost of culture and sensitivity tests for six antibiotics is approximately $18, whereas the urease breath test costs $29 in Zhejiang province. The random samples were collected without any *H. pylori* detection, leading to a lower cost (51.25% reduced) and economic burden in this population compared with the detection strategy.

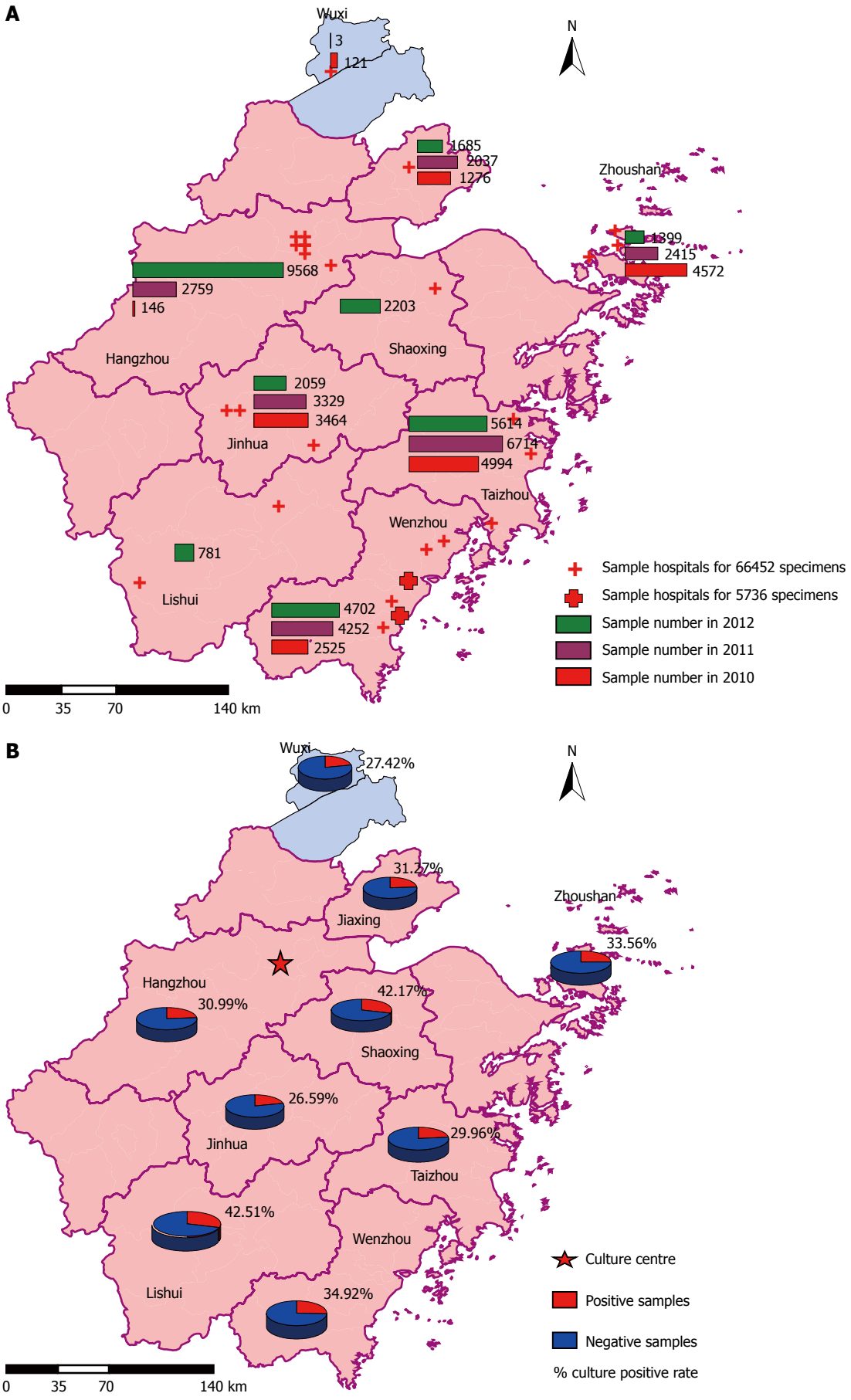

Figure 1 Distributions of samples and *Helicobacter pylori* positive culture rates. A: Distribution of the 26 hospitals and sample numbers from 2010 to 2012 in each city; B: Positive rates in nine cities in Zhejiang and Jiangsu Provinces. The map was drawn by ARCGIS 9.3. software.

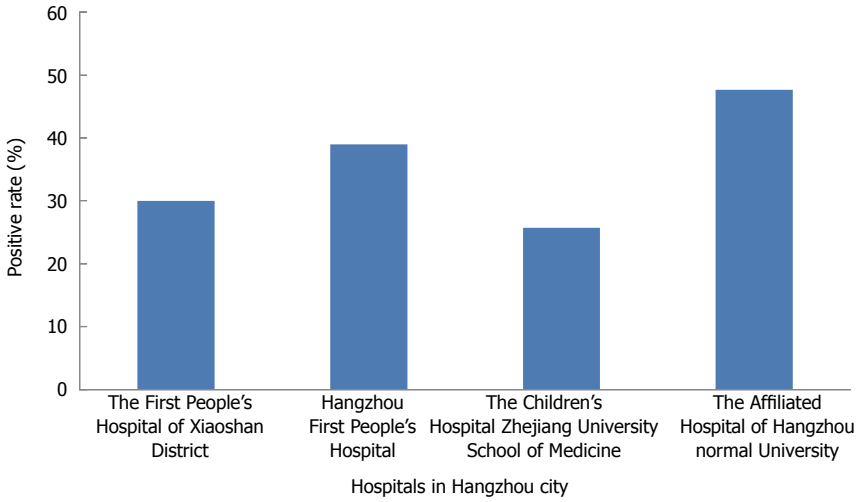

Figure 2 Positive culture rates in four different hospitals in Hangzhou.

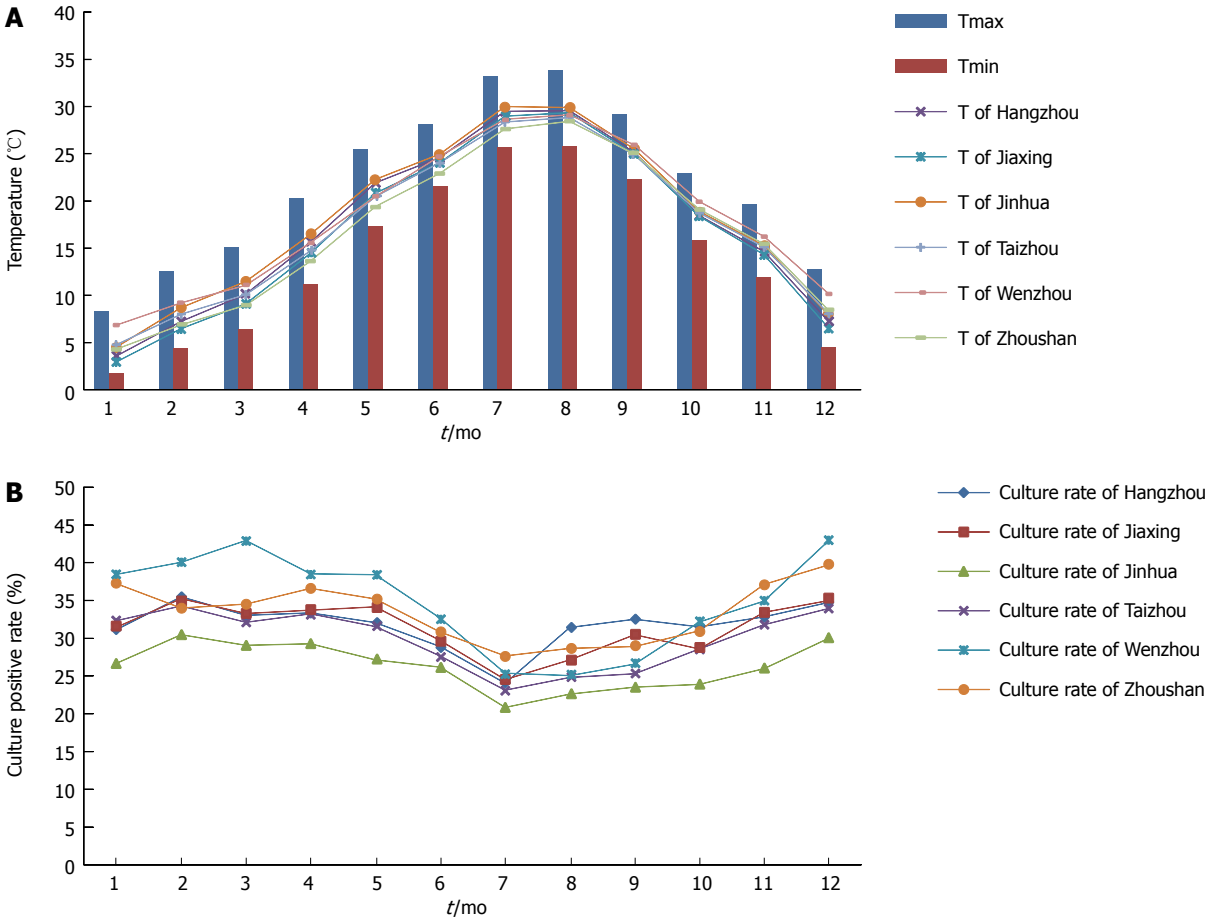

Figure 3 Temperatures and positive culture rate in six cities within three years. A: The maximum (T_{max}), minimum (T_{min}) and average (T) temperatures; B: Positive culture rates.

Factors influencing the isolation rates during transportation have been discussed by previous studies[18,23,27,28]. Use of dry ice and need for storage at a constant temperature of 4 ℃ were recommended, but they cannot be put into actual practice in the *H. pylori* isolation for individualized medical need in a large number of cases because dry ice is too costly and constant 4 ℃ preservation condition is hard to maintain. Despite the appearance as a necessary condition for the optimal diagnosis of *Helicobacter* infections *via* bacteriologic methods in a small-sample study[29], transport on ice was not recommended, as repeated freezing and thawing is more harmful for the successful isolation of *H. pylori*. Thus, in our study, transportation of biopsy specimens under ambient temperature was performed. Our results indicate that the samples were maintained without influencing the culture rates within 24 h, especially

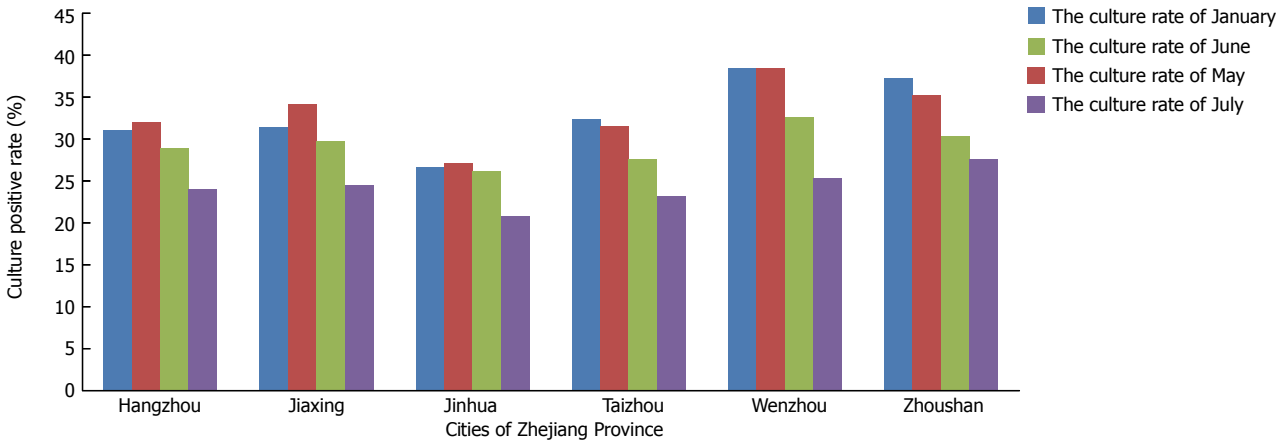

Figure 4 Positive culture rates of six cities in Zhejiang Province in January, May, June and July.

when the mean temperature was lower than 24 ℃. A prolonged or delayed transport time and higher natural temperature (daily average temperature above 24 ℃) could significantly influence the positive culture rates, probably due to contamination and overgrowth of other bacteria. Based on these factors, the proper position of the culture center should be taken into account, and measures to lower ambient temperature should be taken in summer.

Besides the two strong influencing factors, other factors such as sampling and operation levels should also be considered, since variability in the positive culture rates was observed among the four hospitals in Hangzhou city that shared the same sample population and transport conditions. In one study[30], low isolation rates were obtained from failed eradication therapy patients. The patients from Class 2A and 3A hospitals might have different backgrounds of antibiotics use. In this study, a novel design was to compare the culture rates between Class 2A and Class 3A hospitals. The results show no obvious differences, indicating the medical levels of hospitals can be ignored. In addition, the positive culture rates significantly increased over three years, probably due to the improved sampling skills and experience of the laboratory personnel. This indicates that the positive culture rate may increase, even within an *H. pylori*-isolation platform for individualized medical need in a large number of cases.

There were also some limitations in this study. First, we only compared the positive culture rates of four hospitals in Hangzhou city. The other two hospitals were excluded, as the number of samples was small and the sampling was not consecutive. Second, we only selected six cities to assess the temperature effects on positive culture rates, because the samples collected in Lishui, Wuxi and Shaoxing were missed for some months, and the meteorological data was incomplete. Even with these exclusions, the selected data accounted for the majority and was sufficient to compare these differences. Third, although the *H. pylori*-positive group was available to assess the culture results, there was no direct comparison or control group in this study for all samples, such as a non-culture based test, and the positive culture rates in this study were considered acceptable.

In general, this was the first large-scale study on centralized culture of *H. pylori*, confirming the feasibility of establishing a culture center for individualized medical use. We believe the findings of this study can be promisingly applied in clinical and public health practice. The resistance to clarithromycin often poses a challenge in clinical design. For example, as the eradication rate of two couplet therapeutics decreased ten years ago, triple therapy was recommended, thus doctors had to choose quadruple or sequential therapy in failed cases. However, this cycle is likely to continue, and the eradication rate of quadruple or sequential therapies will be reduced to unacceptable levels. Establishment of a personalized treatment strategy may potentially resolve the public health problem and reduce economic burden on the patients and the community, especially in those populations with high resistance.

COMMENTS

Background

The centralized culture of *Helicobacter pylori* (*H. pylori*) in a large number of clinical samples from multiple centers was established. The efficacy of centralized culture and possible influencing factors was evaluated.

Research frontiers

Antibiotic resistance is a worldwide problem that prevents *H. pylori* eradication. Personalized treatment strategy based on culture and antimicrobial susceptibility tests is one of the most promising ways to solve the problem.

Innovations and breakthroughs

Previous studies have discussed factors influencing *H. pylori* isolation rates during transportation. This is the first large-scale study on centralized culture of *H. pylori*, confirming the feasibility of establishing a culture center for individualized medical use.

Applications

The findings of this study can be promisingly applied in clinical and public health practice. Establishment of a personalized treatment strategy may potentially resolve the public health problem and reduce economic burden on the patients and the community, especially in those populations with high resistance.

Terminology

Clarithromycin is one of the core antibiotics of a triple regimen for *H. pylori* eradication. If the clarithromycin resistance rate of *H. pylori* increases to 15%-20%

in a population, this antibiotic should not be used without a susceptibility test.

Peer review

In this study, the authors evaluated the efficacy of centralized culture and discussed the possible influencing factors. It reveals that centralized culture of multicenter samples is feasible. The results of this study can be promisingly applied in individualized medical use and clinical *H. pylori* eradication.

REFERENCES

1 **Parsonnet J**. Helicobacter pylori: the size of the problem. *Gut* 1998; **43** Suppl 1: S6-S9 [PMID: 9764031 DOI: 10.1136/gut.43.2008.S6]

2 **Malfertheiner P**, Megraud F, O'Morain CA, Atherton J, Axon AT, Bazzoli F, Gensini GF, Gisbert JP, Graham DY, Rokkas T, El-Omar EM, Kuipers EJ. Management of Helicobacter pylori infection--the Maastricht IV/ Florence Consensus Report. *Gut* 2012; **61**: 646-664 [PMID: 22491499 DOI: 10.1136/gutjnl-2012-302084]

3 **Hu FL**, Hu PJ, Liu WZ, De Wang J, Lv NH, Xiao SD, Zhang WD, Cheng H, Xie Y. Third Chinese National Consensus Report on the management of Helicobacter pylori infection. *J Dig Dis* 2008; **9**: 178-184 [PMID: 18956598 DOI: 10.1111/j.1751-2980.2008.00342.x]

4 **Altintas E**, Sezgin O, Ulu O, Aydin O, Camdeviren H. Maastricht II treatment scheme and efficacy of different proton pump inhibitors in eradicating Helicobacter pylori. *World J Gastroenterol* 2004; **10**: 1656-1658 [PMID: 15162544]

5 **Gumurdulu Y**, Serin E, Ozer B, Kayaselcuk F, Ozsahin K, Cosar AM, Gursoy M, Gur G, Yilmaz U, Boyacioglu S. Low eradication rate of Helicobacter pylori with triple 7-14 days and quadriple therapy in Turkey. *World J Gastroenterol* 2004; **10**: 668-671 [PMID: 14991935]

6 **Suzuki H**, Nishizawa T, Hibi T. Helicobacter pylori eradication therapy. *Future Microbiol* 2010; **5**: 639-648 [PMID: 20353303 DOI: 10.2217/fmb.10.25]

7 **Mégraud F**, Lamouliatte H. Review article: the treatment of refractory Helicobacter pylori infection. *Aliment Pharmacol Ther* 2003; **17**: 1333-1343 [PMID: 12786627 DOI: 10.1046/j.1365-2036.2003.01592.x]

8 **Mégraud F**. H pylori antibiotic resistance: prevalence, importance, and advances in testing. *Gut* 2004; **53**: 1374-1384 [PMID: 15306603 DOI: 10.1136/gut.2003.022111]

9 **Gao W**, Cheng H, Hu F, Li J, Wang L, Yang G, Xu L, Zheng X. The evolution of Helicobacter pylori antibiotics resistance over 10 years in Beijing, China. *Helicobacter* 2010; **15**: 460-466 [PMID: 21083752 DOI: 10.1111/j.1523-5378.2010.00788.x]

10 **Su P**, Li Y, Li H, Zhang J, Lin L, Wang Q, Guo F, Ji Z, Mao J, Tang W, Shi Z, Shao W, Mao J, Zhu X, Zhang X, Tong Y, Tu H, Jiang M, Wang Z, Jin F, Yang N, Zhang J. Antibiotic resistance of Helicobacter pylori isolated in the Southeast Coastal Region of China. *Helicobacter* 2013; **18**: 274-279 [PMID: 23418857 DOI: 10.1111/hel.12046]

11 **Malfertheiner P**, Megraud F, O'Morain C, Bazzoli F, El-Omar E, Graham D, Hunt R, Rokkas T, Vakil N, Kuipers EJ. Current concepts in the management of Helicobacter pylori infection: the Maastricht III Consensus Report. *Gut* 2007; **56**: 772-781 [PMID: 17170018 DOI: 10.1136/gut.2006.101634]

12 **Dore MP**, Leandro G, Realdi G, Sepulveda AR, Graham DY. Effect of pretreatment antibiotic resistance to metronidazole and clarithromycin on outcome of Helicobacter pylori therapy: a meta-analytical approach. *Dig Dis Sci* 2000; **45**: 68-76 [PMID: 10695616]

13 **Realdi G**, Dore MP, Piana A, Atzei A, Carta M, Cugia L, Manca A, Are BM, Massarelli G, Mura I, Maida A, Graham DY. Pretreatment antibiotic resistance in Helicobacter pylori infection: results of three randomized controlled studies. *Helicobacter* 1999; **4**: 106-112 [PMID: 10382124 DOI: 10.1046/j.1523-5378.1999.99002.x]

14 **Glupczynski Y**, Mégraud F, Lopez-Brea M, Andersen LP. European multicentre survey of in vitro antimicrobial resistance in Helicobacter pylori. *Eur J Clin Microbiol Infect Dis* 2001; **20**: 820-823 [PMID: 11783701 DOI: 10.1007/s100960100611]

15 **Wang G**, Zhao Q, Li S. Study of drug sensitivity test in Helicobacter pylori eradication therapy. *J Clin Intern Med* 2008; **25**: 474-477

16 **Romano M**, Iovene MR, Montella F, Vitale LM, De S : imone T, Del Vecchio Blanco C. Pretreatment antimicrobial-susceptibility testing in the eradication of H. pylori infection. *Am J Gastroenterol* 2000; **95**: 3317-3318 [PMID: 11095372 DOI: 10.1111/j.1572-0241.2000.03317.x]

17 **Romano M**, Marmo R, Cuomo A, De Simone T, Mucherino C, Iovene MR, Montella F, Tufano MA, Del Vecchio Blanco C, Nardone G. Pretreatment antimicrobial susceptibility testing is cost saving in the eradication of Helicobacter pylori. *Clin Gastroenterol Hepatol* 2003; **1**: 273-278 [PMID: 15017668 DOI: 10.1016/S1542-3565(03)00131-9]

18 **Soltesz V**, Zeeberg B, Wadström T. Optimal survival of Helicobacter pylori under various transport conditions. *J Clin Microbiol* 1992; **30**: 1453-1456 [PMID: 1624562]

19 **Yuen B**, Zbinden R, Fried M, Bauerfeind P, Bernardi M. Cultural recovery and determination of antimicrobial susceptibility in Helicobacter pylori by using commercial transport and isolation media. *Infection* 2005; **33**: 77-81 [PMID: 15827875 DOI: 10.1007/s15010-005-4071-y]

20 **Xia HX**, Keane CT, O'Morain CA. Determination of the optimal transport system for Helicobacter pylori cultures. *J Med Microbiol* 1993; **39**: 334-337 [PMID: 8246249 DOI: 10.1099/00222615-39-5-334]

21 **Roosendaal R**, Kuipers EJ, Peña AS, de Graaff J. Recovery of Helicobacter pylori from gastric biopsy specimens is not dependent on the transport medium used. *J Clin Microbiol* 1995; **33**: 2798-2800 [PMID: 8567932]

22 **Heep M**, Scheibl K, Degrell A, Lehn N. Transport and storage of fresh and frozen gastric biopsy specimens for optimal recovery of Helicobacter pylori. *J Clin Microbiol* 1999; **37**: 3764-3766 [PMID: 10523597]

23 **Siu LK**, Leung WK, Cheng AF, Sung JY, Ling TK, Ling JM, Ng EK, Lau JY, Chung SC. Evaluation of a selective transport medium for gastric biopsy specimens to be cultured for Helicobacter pylori. *J Clin Microbiol* 1998; **36**: 3048-3050 [PMID: 9738066]

24 **Xia HX**, Keane CT, Chen J, Zhang J, Walsh EJ, Moran AP, Hua JS, Megraud F, O'Morain CA. Transportation of Helicobacter pylori cultures by optimal systems. *J Clin Microbiol* 1994; **32**: 3075-3077 [PMID: 7883907]

25 **Grove DI**, McLeay RA, Byron KE, Koutsouridis G. Isolation of Helicobacter pylori after transport from a regional laboratory of gastric biopsy specimens in saline, Portagerm pylori or cultured on chocolate agar. *Pathology* 2001; **33**: 362-364 [PMID: 11523941]

26 **Debongnie JC**, Delmee M, Mainguet P, Beyaert C, Haot J, Legros G. Cytology: a simple, rapid, sensitive method in the diagnosis of Helicobacter pylori. *Am J Gastroenterol* 1992; **87**: 20-23 [PMID: 1728119]

27 **van der Hulst RW**, Verheul SB, Weel JF, Gerrits Y, ten Kate FJ, Dankert J, Tytgat GN. Effect of specimen collection techniques, transport media, and incubation of cultures on the detection rate of Helicobacter pylori. *Eur J Clin Microbiol Infect Dis* 1996; **15**: 211-215 [PMID: 8740855 DOI: 10.1007/BF01591356]

28 **Veenendaal RA**, Lichtendahl-Bernards AT, Peña AS, Endtz HP, van Boven CP, Lamers CB. Effect of transport medium and transportation time on culture of Helicobacter pylori from gastric biopsy specimens. *J Clin Pathol* 1993; **46**: 561-563 [PMID: 8331182 DOI: 10.1136/jcp.46.6.561]

29 **Meunier O**, Walter P, Chamouard P, Piemont Y, Monteil H. [Isolation of Helicobacter pylori: necessity of control

of transport conditions]. *Pathol Biol* (Paris) 1997; **45**: 82-85 [PMID: 9097852]

30 **Savarino V**, Zentilin P, Pivari M, Bisso G, Raffaella Mele M, Bilardi C, Borro P, Dulbecco P, Tessieri L, Mansi C, Borgonovo G, De Salvo L, Vigneri S. The impact of antibiotic resistance on the efficacy of three 7-day regimens against Helicobacter pylori. *Aliment Pharmacol Ther* 2000; **14**: 893-900 [PMID: 10886045 DOI: 10.1046/j.1365-2036.2000.00780.x]

P- Reviewer: Buzas GM, Yula E **S- Editor**: Qi Y
L- Editor: AmEditor **E- Editor**: Zhang DN

World Journal of Gastroenterology

Submit a Manuscript: http://www.wjgnet.com/esps/
Help Desk: http://www.wjgnet.com/esps/helpdesk.aspx
DOI: 10.3748/wjg.v21.i3.953

World J Gastroenterol 2015 January 21; 21(3): 953-960
ISSN 1007-9327 (print) ISSN 2219-2840 (online)

ORIGINAL ARTICLE

Observational Study

Transient elastography improves detection of liver cirrhosis compared to routine screening tests

Thomas Göbel, Janine Schadewaldt-Tümmers, Lucas Greiner, Christopher Poremba, Dieter Häussinger, Andreas Erhardt

Thomas Göbel, Janine Schadewaldt-Tümmers, Dieter Häussinger, Andreas Erhardt, Klinik für Gastroenterologie, Hepatologie und Infektiologie, Universitätsklinikum Düsseldorf, 40225 Düsseldorf, Germany
Thomas Göbel, Lucas Greiner, Andreas Erhardt, Klinik für Gastroenterologie, Hepatologie und Diabetologie, Petrus-Krankenhaus Wuppertal, 42283 Wuppertal, Germany
Christopher Poremba, Pathologie München-Nord, Ernst-Platz-Straße 2, 80992 München, Germany
Author contributions: Göbel T, Schadewaldt-Tümmers J and Erhardt A wrote the manuscript; Erhardt A and Schadewaldt-Tümmers J analysed the data; Erhardt A and Schadewaldt-Tümmers J investigated the patients; Poremba C investigated liver biopsy samples; Greiner L and Häussinger D reviewed the paper; Erhardt A, Schadewaldt-Tümmers J and Häussinger D designed the study.

Correspondence to: Andreas Erhardt, Professor, Klinik für Gastroenterologie, Hepatologie und Diabetologie, Petrus-Krankenhaus Wuppertal, Carnaper Str. 48, 42283 Wuppertal, Germany. andreas.erhardt@cellitinnen.de
Telephone: +49-202-2992861
Fax: +49-202-2992865
Received: June 7, 2014
Peer-review started: June 8, 2014
First decision: June 27, 2014
Revised: July 27, 2014
Accepted: September 18, 2014
Article in press: September 19, 2014
Published online: January 21, 2015

Abstract

AIM: To investigate the diagnostic significance of transient elastography (TE) in a daily routine clinical setting in comparison to clinical signs, laboratory parameters and ultrasound.

METHODS: TE, ultrasound, laboratory parameters and cutaneous liver signs were assessed in 291 consecutive patients with chronic liver disease of various aetiologies who underwent liver biopsy in daily routine.

RESULTS: Sensitivity of TE for the detection of liver cirrhosis was 90.4%, compared to 80.1% for ultrasound, 58.0% for platelet count and 45.1% for cutaneous liver signs ($P < 0.0001$ for comparisons with histology). AUROC for TE was 0.760 (95%CI: 0.694-0.825). Combination of TE with ultrasound increased sensitivity to 96.1% and AUROC to 0.825 (95%CI: 0.768-0.882). TE correlated with laboratory parameters of cirrhosis progression like albumin ($r = -0.43$), prothrombin time ($r = -0.44$), and bilirubin ($r = 0.34$; $P < 0.001$ for each). Particularly, in patients with Child Pugh score A or normal platelet count TE improved sensitivity for the detection of liver cirrhosis compared to ultrasound by 14.1% ($P < 0.04$) and 16.3% ($P < 0.02$), respectively.

CONCLUSION: Transient elastography is superior to routine diagnostic tests allowing detection of liver cirrhosis in additional 10%-16% of patients with chronic liver disease that would have been missed by clinical examinations.

Key words: Transient elastography; Fibroscan; Liver cirrhosis; Liver disease; Chronic hepatitis

Core tip: Diagnosis of liver cirrhosis is often missed in routine clinical practice. Novel non-invasive tools like transient elastography (TE) are available but their

diagnostic performance for the detection of cirrhosis has only been poorly evaluated in a routine clinical setting, where screening and diagnosis is mainly based on clinical signs, simple laboratory parameters and conventional ultrasound. The present investigation shows that TE is found to be superior to routine diagnostic tests allowing detection of liver cirrhosis in an additional 10%-15% of patients. The highest diagnostic benefit is seen in patients with early cirrhosis or normal platelet count.

Göbel T, Schadewaldt-Tümmers J, Greiner L, Poremba C, Häussinger D, Erhardt A. Transient elastography improves detection of liver cirrhosis compared to routine screening tests. *World J Gastroenterol* 2015; 21(3): 953-960 Available from: URL: http://www.wjgnet.com/1007-9327/full/v21/i3/953.htm DOI: http://dx.doi.org/10.3748/wjg.v21.i3.953

INTRODUCTION

Patients with liver cirrhosis have a significantly reduced life expectancy compared to non-cirrhotic patients due to complications such as ascites, bleeding of oesophageal varices, hepatic encephalopathy, hepatorenal or hepatopulmonary syndrome and hepatocellular carcinoma (HCC)[1]. Particularly the increasing incidence of HCC secondary to hepatic cirrhosis contributes significantly to the high mortality seen in these patients[2]. Hence, most guidelines recommend regular screening for HCC in patients with liver cirrhosis at least every six months[3,4]. However, diagnosis of liver cirrhosis is frequently missed in a routine clinical setting[5]. The limitations of available diagnostic tools for the detection of hepatic cirrhosis (clinical signs, laboratory parameters, imaging techniques and liver biopsy) are currently driving interest towards non-invasive tests.

Transient elastography (TE) is a non-invasive instrument that determines liver stiffness by generating a low frequency elastic wave of 50 Hz and a high frequency ultrasound wave of 1500 m/s, which allows measurement of the transmission of the elastic wave into liver tissue. Liver stiffness correlates with the degree of fibrosis, a higher degree of fibrosis implying greater stiffness. TE is a valid tool for the differentiation of cirrhotic from non-cirrhotic liver with sensitivities of 77%-100%, specificities of 78%-98% and mean AUROCs of 0.94 (95%CI: 0.93-0.95), but has limitations in discriminating lower fibrosis stages[6].

Although cutaneous liver signs are part of the routine physical examination, their diagnostic value for determination of the severity of liver disease has been poorly evaluated[7]. Among them, spider naevi (84%) and palmar erythema (70.4%) have the highest sensitivities for the diagnosis of liver cirrhosis.

There are numerous laboratory markers which can be used individually or in combination to determine the extent of fibrosis. However, most of these markers and scores have no causal relationship with fibrogenesis[8]. Among the individual measures, the platelet count is the most convenient rough guide for the evaluation of the fibrosis stage and correlates moderately with the histologically determined stage of fibrosis (r = -0.46 to -0.50)[9]. Another frequently used measure of serum fibrosis is the APRI ("aspartate aminotransferase to platelet ratio") index, which is calculated from the AST level and the platelet count. The APRI score has so far only been evaluated in patients with viral hepatitis. A threshold level for significant fibrosis has been defined (Ishak score F3 to F6) at a score of > 1.5, liver cirrhosis at a score of > 2, whereas a score of < 0.5 is said to rule out significant fibrosis[10].

Conventional ultrasound allows accurate diagnosis of liver cirrhosis in 82%-88 % of cases[11]. However, its value depends on the experience of the operator and the quality of the ultrasound instrument. Furthermore, diagnosis of hepatic cirrhosis by ultrasound relies to a significant extent on indirect parameters of liver cirrhosis such as evidence of portal hypertension.

Despite the increasing propagation of transient elastography no studies have investigated the diagnostic performance of transient elastography compared to clinical signs and only one in comparison to ultrasound including only a limited number of cirrhotic patients[12]. Therefore, the present investigation evaluated the benefit of transient elastography for the assessment of liver cirrhosis in a large cohort of patients with chronic liver disease compared to diagnostic tools available in the daily routine like cutaneous liver signs, laboratory parameters and ultrasound.

MATERIALS AND METHODS

Between 2005 and 2008 a total of 291 patients with chronic liver disease of different aetiologies who underwent liver biopsy in a tertiary care centre were additionally investigated by transient elastography, ultrasound, biochemical parameters and cutaneous liver signs within 12 mo after liver biopsy. Ultrasound examination, blood sampling, physical examination and transient elastography were performed on the same day. Ultrasound examination was done unaware of the results of transient elastography and of liver biopsy.

Inclusion was restricted to patients with chronic liver disease (duration of liver disease > 6 mo) and absence of acute flares defined as acute ALT elevation higher than 5 times the upper limit of the patient's individual baseline level. In four out of 291 patients liver stiffness could not be assessed by transient elastography due to morbid obesity. Histologically confirmed liver cirrhosis was present in 182 patients.

Liver histology and quantification of liver fibrosis

Liver biopsy was performed percutaneously by the Menghini technique using a 1.6-mm-diameter needle. Liver fibrosis was evaluated semiquantitatively according to the scoring system of Desmet *et al*[13] or Bondini *et al*[14]. All liver specimens were stained with HE, Elastica-van-

Table 1 Baseline clinical and biochemical characteristics of all patients

	All (n = 291)	HCV (n = 92)	ASH/NASH (n = 109)	HBV (n = 35)	Cryptogenic (n = 13)	HDV (n = 10)	Other causes (n = 32)
Age, yr	54 ± 15	59 ± 13[b]	53 ± 15	51 ± 13[b]	59 ± 15	43 ± 9[a]	50 ± 17[a]
Gender,%							
Female	39.9	41.3	36.7	28.6	38.5	30	59.4[a]
Male	60.1	58.7	63.3	71.4	61.5	70	40.6
Cirrhosis, %	62.5	76.1	56	68.6	100[b]	70	25.0[d]
BMI, kg/m²	25.5 ± 4.2	24.6 ± 3.9[a]	25.8 ± 4.8	27.2 ± 3.3	25.3 ± 3.0	23.2 ± 4.9	25.2 ± 3.6
Bilirubin, mg/dL	2.7± 4.8	1.5 ± 2.5[b]	4.3 ± 7.0	1.5 ± 1.5[b]	1.8 ± 1.3	2.0 ± 1.6	4.1 ± 5.8
Albumin, g/dL	3.6 ± 0.7	3.8 ± 0.6[b]	3.4 ± 0.7[a]	3.8 ± 0.7	3.4 ± 0.7	3.4 ± 0.6	3.7 ± 0.4
Immunoglobulins, g/dL	1.7 ± 0.7	1.8 ± 0.7	1.5 ± 0.7	1.7 ± 0.8	1.5 ± 0.4	2.6 ± 0.7[b]	1.7 ± 0.5
AST, U/L	116 ± 175	100 ± 54	113 ± 187	76 ± 51	70 ± 55	155 ± 94	243 ± 400
ALT, U/L	106 ± 176	102 ± 71	73 ± 100[b]	72 ± 52	43 ± 20	131 ± 62	300 ± 462[a]
AFP, μg/L[1]	6.2	9.7	5.8	3.4	5.9	7.2	2.9
Platelets, [a]1000/μL	170 ± 83	152 ± 82	181 ± 79	165 ± 78	168 ± 77	127 ± 74	208 ± 96
Prothrombin time, %	83 ± 18	88 ± 16[b]	78 ± 21[b]	85 ± 13	81 ± 23	73 ± 14	86 ± 15

[1]Median value. [a]$P \leq 0.05$; [b]$P \leq 0.01$ *vs* all other patients. HCV: Hepatitis C virus; HBV: Hepatitis B virus; HDV: Hepatitis D virus; ASH: Alcoholic steatohepatitis; NASH: Non-alcoholic steatohepatitis.

Gieson (EvG), Gomori, PAS-Diastase and iron stain and analysed by experienced pathologists blinded to the results of transient elastography and ultrasound.

Liver stiffness measurement

Liver stiffness was assessed by transient elastography (Fibroscan®) as described previously[15]. At least 10 measurements were performed. Only procedures with a success rate of 60% were considered reliable. The median value was taken as representative. Liver cirrhosis was assumed in case of a median value ≥ 13 kPa which has been identified in previous studies and a large meta-analysis[15,16].

Conventional ultrasound examination

Liver cirrhosis was suspected if two of the following criteria were present: (1) nodular appearance of the liver surface; (2) inhomogeneous liver texture; (3) rarefaction or tortuosity of hepatic veins; (4) dilatation of portal vein beyond 12 mm; (5) splenomegaly; (6) presence of ascites; (7) collateral circulation and (8) hypertrophy of the quadrate lobe[17].

Cutaneous liver signs

Liver cirrhosis was assumed in patients presenting with at least one of the following cutaneous liver signs: spider angiomata, venectasias of the abdominal wall, glossy tongue, Terry's nails, palmar erythema and gynaecomastia.

Platelet count and APRI index

A platelet count < 150000/μL and an APRI index > 2 were used as a cutoff for the diagnosis of liver cirrhosis. APRI-index was determined only in patients with viral hepatitis. The APRI index was calculated as follows: AST (× upper limit of normal) × 100/ platelet count (10^9/L).

Statistical analysis

A χ^2 was used for comparison of categorical variables. McNemar's test was used on nominal data. Student t test and Mann-Whitney test were used for comparison of continuous variables. The significance level was set at $P < 0.05$, all P values were two tailed. Statistical analysis was performed with the SPSS software 18.0 (SPSS, Munich, Germany).

RESULTS

Among all 291 investigated patients with chronic liver disease 31.6 % had hepatitis C, 37.5 % ASH/NASH, 12% hepatitis B, 3.4% hepatitis D, 11 % had other more rare causes of chronic liver disease (primary biliary cirrhosis, primary sclerosing cholangitis, autoimmune hepatitis, hereditary haemochromatosis, Wilson's disease) and 4.5% liver disease of unknown cause ("cryptogenic"). Chronic alcohol consumption was defined as daily intake above 20 g in females and 40g in males. 182 of all 291 patients had histologically proven liver cirrhosis. According to the Child Pugh score 58.8% of these patients were classified as A, 20.9% as B and 8.2% of patients as C. A total of 12.1% of patients with liver cirrhosis could not be classified according to Child Pugh score due to missing data. The majority of biochemical and clinical parameters did not differ between the different aetiologies of chronic liver disease (Table 1). Notably, patients with hepatitis D infection displayed higher ALT, AST, immunoglobulin levels, and lower prothrombin time despite a younger age compared to most of the other patient groups (Table 1).

Sensitivity of transient elastography for the detection of liver cirrhosis was 90.4 % (Table 2). TE could not be performed in 4 patients due to morbid obesity, these patients were nevertheless included in the calculation of sensitivity. The positive predictive value was 75.2%. Specificity was 51.2% and the negative predictive value was 76.7%. Sensitivity for the detection of liver cirrhosis by transient elastography was about 10% higher compared to ultrasound and exceeded that of platelet

Table 2 Sensitivity, specificity, positive and negative predictive value of the different non-invasive examinations for detection of liver cirrhosis

	All					Viral hepatitis[1]				
	Sensitivity	Specificity	PPV	NPV	*P* value[3]	Sensitivity	Specificity	PPV	NPV	*P* value[3]
Liver stiffness ≥ 13 kPa	90.4	51.4	75.2	76.7		91.3	44.4	82.5	64.0	
Ultrasound[2]	80.1	82.4	88.7	70.6	0.02	96.6	61.2	81.4	90.9	0.04
Platelets < 150.000/μL	58.0	80.2	83.3	52.8	0.03	63.1	72.2	86.7	40.6	0.05
Cutaneous liver signs[2]	45.1	72.1	70.4	47.2	0.0001	42.7	64.7	77.4	28.6	0.01
APRI-Score ≥ 2	NA	NA	NA	NA	NA	56.1	63.3	87.7	24.1	

[1]*n* = 139; only patients with chronic hepatitis B, C and D were included; [2]According to the definitions in the patients and methods section; available for 257 patients; [3]For comparison of sensitivities with liver stiffness as reference. NA: Not applicable; PPV: Positive predictive value; NPV: Negative predictive value.

Table 3 Sensitivities for detection of liver cirrhosis by different combinations of non-invasive examinations

	All patients (*n* = 182)				
	Sensitivity	Specificity	PPV	NPV	*P* value[1]
Liver stiffness ≥ 13 kPa and/or ultrasound cirrhosis	96.1%	50.5%	76.5%	88.5%	
Liver stiffness ≥ 13 kPa and/or platelets < 150.000/μL	93.9%	49.1%	75.4%	82.8%	< 0.0001
Ultrasound and/or platelets < 150.000/μL	88.2%	68.0%	82.6%	76.9%	< 0.0001
Ultrasound and/or cutaneous liver signs	87.6%	62.0%	79.7%	74.7%	< 0.0001
Platelets < 150000/μL and/or cutaneous liver signs	79.4%	63.7%	78.5%	65%	< 0.004

[1]Sensitivity compared to the combination of liver stiffness and/or ultrasound. NS: Not significant; PPV: Positive predictive value; NPV: Negative predictive value.

count, APRI index and cutaneous liver signs by more than 30% (Table 2). In the subgroup of patients with viral hepatitis, sensitivity and specificity of ultrasound was slightly superior to that of transient elastography (Table 2). The highest liver stiffness values were found in patients with cryptogenic cirrhosis, although these patients had the lowest ALT levels (data not shown). The combination of liver stiffness with ultrasound or platelet count allowed detection of liver cirrhosis at a slightly higher rate (96.1% and 93.9% respectively) than transient elastography alone (90.4%). Combinations of screening tests including transient elastography were superior to combinations of ultrasound with cutaneous liver signs or platelet counts (Table 3). Area under the receiver operating characteristic curve (AUROC) for detection of liver cirrhosis by transient elastography was 0.760 (95%CI: 0.694-0.825) compared to an AUROC of 0.796 (95%CI: 0.740-0.863) for detection of liver cirrhosis by conventional ultrasound. The combination of transient elastography with ultrasound resulted in an AUROC of 0.825 (95%CI: 0.768-0.882).

Transient elastography correlated with the severity of liver cirrhosis, like presence of ascites, cutaneous liver signs and particularly with biochemical parameters included in the Child-Pugh score (Table 4). The correlation coefficient of transient elastography with bilirubin was $r = 0.34$ ($P < 0.0001$), with albumin $r = -0.43$ ($P < 0.0001$), with prothrombin time $r = -0.44$ ($P < 0.001$) and immunoglobulins $r = 0.34$ ($P < 0.001$). No correlation was seen between transient elastography and AFP, platelets, ALT or BMI.

In the subgroup of patients with normal platelet count ($n = 161$) of the present population transient elastography showed the highest sensitivities for the detection of cirrhosis compared to other screening methods like ultrasound, platelet count, cutaneous liver signs (Table 5). Among patients with Child-Pugh A liver cirrhosis TE was superior with respect to sensitivity compared to other tests by more than 15% (Table 5). In advanced liver cirrhosis (*i.e.*, Child-Pugh B and C patients) gain in sensitivity of transient elastography compared to ultrasound was only small (98.1% *vs* 96.2%). Performance of platelet count (sensitivity 74.1 %) and cutaneous liver signs (sensitivity 64.3%) improved with more advanced cirrhosis but were still worse than corresponding results of conventional ultrasound or transient elastography.

DISCUSSION

Diagnosis of liver cirrhosis and especially early stages of liver cirrhosis with its important clinical implications is often difficult and detection might be missed in daily clinical practice. Autopsy studies in Western populations revealed that one third of patients with liver cirrhosis are not identified during their lifetime[5,18]. This dissatisfying misclassification of liver cirrhosis and the fact that an invasive liver biopsy is supposed to be the "gold standard" has led to the development of several non-invasive technologies.

Transient elastography has been extensively evaluated with more or less complex fibrosis scores and other diagnostic tools[19] but a comparison with routinely available markers in a large series of patients with histologically confirmed liver cirrhosis is still lacking. Therefore, the present study was explicitly designed to reflect a routine clinical setting and investigated the

Table 4 Comparison of transient elastography with clinical and biochemical parameters

	⩾ 13 kPa (*n* = 161)	⩾ 27.5 kPa[1] (*n* = 94)	⩾ 54 kPa[1] (*n* = 48)	⩾ 27.5kPa *vs* < 27.5 kPa *P* value	⩾ 54 kPa *vs* < 54 kPa *P* value	⩾ 54 kPa *vs* 27.5-54 kPa *P* value
Age, yr	60 ± 14	56 ± 13	55 ± 13	NS	NS	NS
BMI, kg/m²	26.2 ± 3.7	25.5 ± 4.0	24.8 ± 3.7	NS	0.05	NS
Bilirubin, mg/dL	1.1 ± 1.0	3.2 ± 5.6	4.4 ± 6.9	0.0001	0.007	0.04
Albumin, g/dL	3.9 ± 0.4	3.4 ± 0.7	3.2 ± 0.7	0.0001	0.0001	0.02
Immunoglobulins, g/dL	1.6 ± 0.7	2.0 ± 0.7	2.1 ± 0.8	0.02	0.007	0.03
AST, U/L	79 ± 49	102 ± 71	115 ± 83	0.02	0.015	0.07
ALT, U/L	79 ± 56	71 ± 51	69 ± 54	NS	NS	NS
AFP, μg/L[2]	7.6	7.7	7.8	NS	NS	NS
Platelets, 1000/μL	145 ± 68	144 ± 82	151 ± 77	NS	NS	NS
Prothrombin time, %	88 ± 13	76 ± 19	70 ± 18	0.0001	0.0001	0.02
APRI-Score[3]	2.4 ± 1.8	3.6 ± 3.1	4.3 ± 3.6	0.03	NS	NS
Platelets < 150.000/μL, %	59.7	60.6	56.3	NS	NS	NS
Ultrasound cirrhosis, %	73.1	88.9	93.6	0.02	0.01	NS
Splenomegaly, %	57.8	71.4	72.3	0.09	NS	NS
Ascites, %	16.4	35.5	52.1	0.01	0.0001	0.01
Cutaneous liver signs, %	43.3	55.3	63.2	NS	0.09	NS

[1]Cut-off values in accordance to Foucher *et al*[30]; [2]AFP is given as median value; [3]APRI-Score was only applied to patients with chronic viral hepatitis. NS: Not significant.

Table 5 Usefulness of transient elastography in cirrhotic patients with Child-Pugh A or normal platelet count

	Child-Pugh A[1]					Normal platelet count[2]				
	Sensitivity	Specificity	PPV	NPV	*P* value[3]	Sensitivity	Specificity	PPV	NPV	*P* value[3]
Liver stiffness ⩾ 13 kPa	91.5%	48.8%	59.5	87.5		85.3%	62.4%	66.7	82.8	
Ultrasound	75.2%	75.2%	72.5	77.8	0.02	71.2%	86.4%	82.5	76.9	0.04
Platelets < 150.000/μL	55.1%	78.6%	68.6	67.3	NS	NA	NA	NA	NA	
Cutaneous liver signs	42.0%	74.8%	59.2	59.7	0.01	46.2%	81.3%	66.7	65.0	0.001

[1]*n* = 107; [2]*n* = 161; Normal platelet count was 150.000-400.000/μL; [3]Values are given for the comparison of sensitivities with transient elastography. NA: Not applicable; NS: Not significant; PPV: Positive predictive value; NPV: Negative predictive value.

additional benefit of transient elastography for the identification of liver cirrhosis compared to clinical signs, simple laboratory parameters and ultrasound. Although measurement of transient elastography requires hardware equipment, it has the potential of a bedside test. High reproducibility of transient elastography for the determination of liver cirrhosis was shown in non-obese persons[20]. In contrast, reproducibility of transient elastography for differentiating fibrosis stages below F3 was poor. Hence, the present study focused on the identification of cirrhosis.

There are many other non-invasive surrogate markers and scores for determination of liver fibrosis and cirrhosis[8]. Recently, magnetic resonance elastography has been evaluated in patients with chronic liver disease[21]. However, these parameters or tests are either not routinely available, expensive or not properly evaluated and were therefore not integrated in the present investigation. Histopathological examination of liver is still considered the gold standard for evaluation of liver fibrosis[22] and was taken as reference in the present study. Liver biopsy has significant diagnostic limitations due the risk of serious complications, sampling and intra- or interobserver errors[23,24]. Error rates of 20%-45% for disease staging have been reported[25]. These limitations of liver biopsy can influence the diagnostic performance of transient elastography.

The major finding of the present study was a significant increase by 10 % of the sensitivity for the detection of liver cirrhosis by the use of transient elastography compared to best routine screening tests available (Table 2). Furthermore, combinations of different tests might improve diagnostic accuracy[26]. In the present investigation the combination of transient elastography with ultrasound allows detection of early stages of liver cirrhosis with the highest sensitivity followed by the combination of transient elastography with a platelet count below 150000/μL (Table 4).

It has to be kept in mind that these findings apply to the selected group of patients in which liver cirrhosis was determined according to the histological evaluation. The present investigation may therefore be biased as patients with advanced and clinically apparent liver cirrhosis might not have been considered for liver biopsy at all. However, if liver cirrhosis can easily be clinically assessed, liver biopsy or non-invasive tests are no longer needed. As expected, patients that were staged Child-Pugh A had greater diagnostic benefit from transient elastography than the overall cohort of patients and especially patients with advanced Child Pugh B or C cirrhosis (Table 5). The

superiority of TE compared to other conventional tests also applied to patients with normal platelet count (Table 5). Unravelling fibrosis in these "unsuspicious" patients with early cirrhosis has important clinical and therapeutic consequences.

Sensitivity of cutaneous liver signs to detect liver cirrhosis varied between 31% and 84% in a recent report[7]. Low sensitivities were found for cutaneous signs like glossy tongue, gynaecomastia and white nails, while presence of spider naevi and palmar erythema showed higher sensitivities. Cutaneous liver signs were not sub-differentiated in the present study as this would have resulted in too small populations. Sensitivities for abdominal ultrasound so far reported were comparable to the present study[11,27]. However, ultrasound largely depends on the quality of the technical equipment used and the operator's skills. Platelet count is often used as a rough estimation for the presence of liver cirrhosis. The present investigation suggests that platelet count and cutaneous liver signs are not useful for the identification of early liver cirrhosis as sensitivities were below 60%. However, there are also several drawbacks of transient elastography. First, in 1%-9% of the cases transient elastography is technically not feasible due to obesity, ascites, scars, narrowing of the intercostal spaces or other reasons[6]. Technical failures of transient elastography were seen in 2% of the present study (n = 4 patients with morbid obesity). These diagnostic failures were still included in the calculations. In addition, acute disease deteriorations with high ALT values and cholestasis can lead to a systematic overestimation of liver stiffness[28,29]. Therefore only patients with chronic liver disease without flares were included in the present study. Misclassification of transient elastography can also occur in the case of macronodular cirrhosis, high body mass index and liver tumors[30].

A major advantage of transient elastography compared to other non-invasive tests is that it not only indicates the presence or absence but also severity of liver cirrhosis. Different cutoffs have been established that predict or exclude the presence of oesophageal varices, hepatocellular carcinoma, and the Child Pugh score[30,31]. In the present study liver stiffness was positively correlated to parameters of liver function like albumin, prothrombin time and bilirubin (Table 4). In addition, transient elastography correlated to immunoglobulins as further markers of liver cirrhosis stage. Thus, transient elastography like the Child Pugh score should be a valuable tool to estimate progression of liver cirrhosis.

This study also has its limitations: this investigation was performed at a tertiary centre, therefore a high proportion of more advanced stages in patients with chronic liver disease can be expected. This is apparent from the fact that the rate of histologically proven liver cirrhosis in all liver biopsies performed is quite high (n = 182/291; 62.5%). Furthermore, the procedures of the independently prospective performed transient elastography, ultrasound and clinical investigations were compared to liver biopsies which were done in advance with a maximum time range of one year. Usually, the development of chronic liver disease is a continuous, but mostly slow process over many years or decades and therefore rapid changes of liver stiffness or sonographic appearance is generally not expected. Acute flares of chronic disease were excluded as it is already known that measurement of liver stiffness is influenced by acute hepatitis[28]. Investigators of transient elastography and ultrasound were furthermore unaware of the results of liver biopsy to exclude further bias.

Summarising, transient elastography allowed the identification of an additional 10% of cirrhotic patients among patients with chronic liver disease compared to routinely available non-invasive tests and examinations like ultrasound, platelet count, or cutaneous liver signs. Patients with early cirrhosis had the greatest diagnostic benefit from transient elastography. Combination of transient elastography with conventional ultrasound or platelet count further improved diagnostic accuracy.

COMMENTS

Background

The detection of liver cirrhosis is crucial for patients as this condition may lead to complications like hepatocellular carcinoma, variceal bleeding or hepatic decompensation. Autopsy studies reveal that one third of patients with liver cirrhosis are missed during their lifetime. Liver biopsy is thought to be the "gold standard" but non-invasive tools like transient elastography are increasingly available.

Research frontiers

Transient elastography is a valid tool for the differentiation of cirrhotic from non-cirrhotic liver but no studies have investigated the diagnostic performance of transient elastography compared to clinical signs and conventional ultrasound. Therefore, the present investigation evaluated the benefit of transient elastography for the assessment of liver cirrhosis in a large cohort of patients with chronic liver disease compared to diagnostic tools available in the daily routine like cutaneous liver signs, laboratory parameters and conventional ultrasound.

Innovations and breakthroughs

The major finding of the present study was a significant increase by 10% of the sensitivity for the detection of liver cirrhosis by the use of transient elastography compared to routine screening tests. Patients with early cirrhosis had the greatest diagnostic benefit from transient elastography. Furthermore, liver stiffness positively correlated with parameters of liver function like albumin, prothrombin time and bilirubin.

Terminology

Liver cirrhosis: end-stage of chronic liver disease which is characterised by progressive scarring of liver tissue ("fibrosis") while healthy cells are vanishing. This leads to a functional loss of the organ, development of portal hypertension and also represents a precancerosis for liver malignancies; transient elastography: non-invasive method that determines liver stiffness by generating an elastic wave. Liver stiffness correlates with the degree of fibrosis, a higher degree of fibrosis implying greater stiffness.

Peer review

Transient elastography has been compared with routinely available markers (clinical signs, simple laboratory parameters and ultrasound) in a large series of patients with histologically confirmed liver cirrhosis. A major advantage of transient elastography compared to other non-invasive tests is that it not only indicates the presence or absence but also severity of liver cirrhosis. In the present study liver stiffness was positively correlated to parameters of liver function like albumin, prothrombin time and bilirubin.

REFERENCES

1 **Niederau C**, Lange S, Heintges T, Erhardt A, Buschkamp

M, Hürter D, Nawrocki M, Kruska L, Hensel F, Petry W, Häussinger D. Prognosis of chronic hepatitis C: results of a large, prospective cohort study. *Hepatology* 1998; **28**: 1687-1695 [PMID: 9828236 DOI: 10.1002/hep.510280632]

2 **El-Serag HB**. Hepatocellular carcinoma: recent trends in the United States. *Gastroenterology* 2004; **127**: S27-S34 [PMID: 15508094 DOI: 10.1053/j.gastro.2004.09.013]

3 **European Association for the Study of the Liver**, European Organisation For Research And Treatment Of Cancer. EASL-EORTC clinical practice guidelines: management of hepatocellular carcinoma. *J Hepatol* 2012; **56**: 908-943 [PMID: 22424438 DOI: 10.1016/j.jhep.2011.12.001]

4 **Greten TF**, Malek NP, Schmidt S, Arends J, Bartenstein P, Bechstein W, Bernatik T, Bitzer M, Chavan A, Dollinger M, Domagk D, Drognitz O, Düx M, Farkas S, Folprecht G, Galle P, Geißler M, Gerken G, Habermehl D, Helmberger T, Herfarth K, Hoffmann RT, Holtmann M, Huppert P, Jakobs T, Keller M, Klempnauer J, Kolligs F, Körber J, Lang H, Lehner F, Lordick F, Lubienski A, Manns MP, Mahnken A, Möhler M, Mönch C, Neuhaus P, Niederau C, Ocker M, Otto G, Pereira P, Pott G, Riemer J, Ringe K, Ritterbusch U, Rummeny E, Schirmacher P, Schlitt HJ, Schlottmann K, Schmitz V, Schuler A, Schulze-Bergkamen H, von Schweinitz D, Seehofer D, Sitter H, Straßburg CP, Stroszczynski C, Strobel D, Tannapfel A, Trojan J, van Thiel I, Vogel A, Wacker F, Wedemeyer H, Wege H, Weinmann A, Wittekind C, Wörmann B, Zech CJ. [Diagnosis of and therapy for hepatocellular carcinoma]. *Z Gastroenterol* 2013; **51**: 1269-1326 [PMID: 24243572 DOI: 10.1055/s-0033-1355841]

5 **Graudal N**, Leth P, Mårbjerg L, Galløe AM. Characteristics of cirrhosis undiagnosed during life: a comparative analysis of 73 undiagnosed cases and 149 diagnosed cases of cirrhosis, detected in 4929 consecutive autopsies. *J Intern Med* 1991; **230**: 165-171 [PMID: 1650808 DOI: 10.1111/j.1365-2796.1991.tb00425.x]

6 **Friedrich-Rust M**, Ong MF, Martens S, Sarrazin C, Bojunga J, Zeuzem S, Herrmann E. Performance of transient elastography for the staging of liver fibrosis: a meta-analysis. *Gastroenterology* 2008; **134**: 960-974 [PMID: 18395077 DOI: 10.1053/j.gastro.2008.01.034]

7 **Niederau C**, Lange S, Frühauf M, Thiel A. Cutaneous signs of liver disease: value for prognosis of severe fibrosis and cirrhosis. *Liver Int* 2008; **28**: 659-666 [PMID: 18312288 DOI: 10.1111/j.1478-3231.2008.01694.x]

8 **Gressner OA**, Weiskirchen R, Gressner AM. Biomarkers of hepatic fibrosis, fibrogenesis and genetic pre-disposition pending between fiction and reality. *J Cell Mol Med* 2007; **11**: 1031-1051 [PMID: 17979881 DOI: 10.1111/j.1582-4934.2007.00092.x]

9 **Lackner C**, Struber G, Liegl B, Leibl S, Ofner P, Bankuti C, Bauer B, Stauber RE. Comparison and validation of simple noninvasive tests for prediction of fibrosis in chronic hepatitis C. *Hepatology* 2005; **41**: 1376-1382 [PMID: 15915455 DOI: 10.1002/hep.20717]

10 **Wai CT**, Greenson JK, Fontana RJ, Kalbfleisch JD, Marrero JA, Conjeevaram HS, Lok AS. A simple noninvasive index can predict both significant fibrosis and cirrhosis in patients with chronic hepatitis C. *Hepatology* 2003; **38**: 518-526 [PMID: 12883497 DOI: 10.1053/jhep.2003.50346]

11 **Aubé C**, Oberti F, Korali N, Namour MA, Loisel D, Tanguy JY, Valsesia E, Pilette C, Rousselet MC, Bedossa P, Rifflet H, Maïga MY, Penneau-Fontbonne D, Caron C, Calès P. Ultrasonographic diagnosis of hepatic fibrosis or cirrhosis. *J Hepatol* 1999; **30**: 472-478 [PMID: 10190731 DOI: 10.1016/S0168-8278(99)80107-X]

12 **Wang JH**, Changchien CS, Hung CH, Eng HL, Tung WC, Kee KM, Chen CH, Hu TH, Lee CM, Lu SN. FibroScan and ultrasonography in the prediction of hepatic fibrosis in patients with chronic viral hepatitis. *J Gastroenterol* 2009; **44**: 439-446 [PMID: 19308312 DOI: 10.1007/s00535-009-0017-y]

13 **Desmet VJ**, Gerber M, Hoofnagle JH, Manns M, Scheuer PJ. Classification of chronic hepatitis: diagnosis, grading and staging. *Hepatology* 1994; **19**: 1513-1520 [PMID: 8188183 DOI: 10.1002/hep.1840190629]

14 **Bondini S**, Kleiner DE, Goodman ZD, Gramlich T, Younossi ZM. Pathologic assessment of non-alcoholic fatty liver disease. *Clin Liver Dis* 2007; **11**: 17-23, vii [PMID: 17544969 DOI: 10.1016/j.cld.2007.02.002]

15 **Erhardt A**, Lörke J, Vogt C, Poremba C, Willers R, Sagir A, Häussinger D. [Transient elastography for diagnosing liver cirrhosis]. *Dtsch Med Wochenschr* 2006; **131**: 2765-2769 [PMID: 17136655 DOI: 10.1055/s-2006-957180]

16 **Friedrich-Rust M**, Zeuzem S. [Transient elastography (FibroScan) for the non-invasive assessment of liver fibrosis: current status and perspectives]. *Z Gastroenterol* 2007; **45**: 387-394 [PMID: 17503318 DOI: 10.1055/s-2007-963008]

17 **Di Lelio A**, Cestari C, Lomazzi A, Beretta L. Cirrhosis: diagnosis with sonographic study of the liver surface. *Radiology* 1989; **172**: 389-392 [PMID: 2526349 DOI: 10.1148/radiology.172.2.2526349]

18 **Fujimoto K**, Sawabe M, Sasaki M, Kino K, Arai T. Undiagnosed cirrhosis occurs frequently in the elderly and requires periodic follow ups and medical treatments. *Geriatr Gerontol Int* 2008; **8**: 198-203 [PMID: 18822004 DOI: 10.1111/j.1447-0594.2008.00470.x]

19 **Castera L**, Forns X, Alberti A. Non-invasive evaluation of liver fibrosis using transient elastography. *J Hepatol* 2008; **48**: 835-847 [PMID: 18334275 DOI: 10.1016/j.jhep.2008.02.008]

20 **Fraquelli M**, Rigamonti C, Casazza G, Conte D, Donato MF, Ronchi G, Colombo M. Reproducibility of transient elastography in the evaluation of liver fibrosis in patients with chronic liver disease. *Gut* 2007; **56**: 968-973 [PMID: 17255218 DOI: 10.1136/gut.2006.111302]

21 **Huwart L**, Sempoux C, Vicaut E, Salameh N, Annet L, Danse E, Peeters F, ter Beek LC, Rahier J, Sinkus R, Horsmans Y, Van Beers BE. Magnetic resonance elastography for the noninvasive staging of liver fibrosis. *Gastroenterology* 2008; **135**: 32-40 [PMID: 18471441 DOI: 10.1053/j.gastro.2008.03.076]

22 **Bravo AA**, Sheth SG, Chopra S. Liver biopsy. *N Engl J Med* 2001; **344**: 495-500 [PMID: 11172192 DOI: 10.1056/NEJM200102153440706]

23 **Bedossa P**, Dargère D, Paradis V. Sampling variability of liver fibrosis in chronic hepatitis C. *Hepatology* 2003; **38**: 1449-1457 [PMID: 14647056 DOI: 10.1016/j.hep.2003.09.022]

24 **Regev A**, Berho M, Jeffers LJ, Milikowski C, Molina EG, Pyrsopoulos NT, Feng ZZ, Reddy KR, Schiff ER. Sampling error and intraobserver variation in liver biopsy in patients with chronic HCV infection. *Am J Gastroenterol* 2002; **97**: 2614-2618 [PMID: 12385448 DOI: 10.1111/j.1572-0241.2002.06038.x]

25 **Afdhal NH**. Diagnosing fibrosis in hepatitis C: is the pendulum swinging from biopsy to blood tests? *Hepatology* 2003; **37**: 972-974 [PMID: 12717376 DOI: 10.1053/jhep.2003.50223]

26 **Sebastiani G**, Vario A, Guido M, Noventa F, Plebani M, Pistis R, Ferrari A, Alberti A. Stepwise combination algorithms of non-invasive markers to diagnose significant fibrosis in chronic hepatitis C. *J Hepatol* 2006; **44**: 686-693 [PMID: 16490278 DOI: 10.1016/j.jhep.2006.01.007]

27 **Goyal N**, Jain N, Rachapalli V, Cochlin DL, Robinson M. Non-invasive evaluation of liver cirrhosis using ultrasound. *Clin Radiol* 2009; **64**: 1056-1066 [PMID: 19822238 DOI: 10.1016/j.crad.2009.05.010]

28 **Sagir A**, Erhardt A, Schmitt M, Häussinger D. Transient elastography is unreliable for detection of cirrhosis in patients with acute liver damage. *Hepatology* 2008; **47**: 592-595 [PMID: 18098325 DOI: 10.1002/hep.22056]

29 **Millonig G**, Reimann FM, Friedrich S, Fonouni H, Mehrabi A, Büchler MW, Seitz HK, Mueller S. Extrahepatic cholestasis increases liver stiffness (FibroScan) irrespective of fibrosis. *Hepatology* 2008; **48**: 1718-1723 [PMID: 18836992 DOI: 10.1002/hep.22577]

30 **Foucher J**, Chanteloup E, Vergniol J, Castéra L, Le Bail B, Adhoute X, Bertet J, Couzigou P, de Lédinghen V. Diagnosis of cirrhosis by transient elastography (FibroScan): a prospective study. *Gut* 2006; **55**: 403-408 [PMID: 16020491 DOI: 10.1136/gut.2005.069153]

31 **Sporea I**, Rațiu I, Bota S, Şirli R, Jurchiş A. Are different cut-off values of liver stiffness assessed by transient elastography according to the etiology of liver cirrhosis for predicting significant esophageal varices? *Med Ultrason* 2013; **15**: 111-115 [PMID: 23702500]

P- Reviewer: Peltec A, Sirin G **S- Editor**: Qi Y **L- Editor**: A
E- Editor: Wang CH

World Journal of Gastroenterology

Submit a Manuscript: http://www.wjgnet.com/esps/
Help Desk: http://www.wjgnet.com/esps/helpdesk.aspx
DOI: 10.3748/wjg.v21.i3.961

World J Gastroenterol 2015 January 21; 21(3): 961-968
ISSN 1007-9327 (print) ISSN 2219-2840 (online)

ORIGINAL ARTICLE

Observational Study

Pure laparoscopic hepatectomy as repeat surgery and repeat hepatectomy

Masashi Isetani, Zenichi Morise, Norihiko Kawabe, Hirokazu Tomishige, Hidetoshi Nagata, Jin Kawase, Satoshi Arakawa

Masashi Isetani, Zenichi Morise, Norihiko Kawabe, Hirokazu Tomishige, Hidetoshi Nagata, Jin Kawase, Satoshi Arakawa, Department of Surgery, Fujita Health University School of Medicine, Banbuntane Houtokukai Hospital, Aichi, Nagoya 454-8509, Japan
Author contributions: Isetani M and Morise Z wrote the manuscript; Kawabe N, Tomishige H, Nagata H, Kawase J, and Arakawa S collected the data and assisted in writing the manuscript.

Correspondence to: Zenichi Morise, MD, PhD, FACS, Department of Surgery, Fujita Health University School of Medicine, Banbuntane Houtokukai Hospital, 3-6-10 Otobashi Nakagawa-ku, Aichi, Nagoya 454-8509, Japan. zmorise@fujita-hu.ac.jp
Telephone: +81-52-3235680
Fax: +81-52-3234502
Received: April 16, 2014
Peer-review started: April 17, 2014
First decision: July 21, 2014
Revised: August 10, 2014
Accepted: September 18, 2014
Article in press: September 19, 2014
Published online: January 21, 2015

Abstract

AIM: To assess clinical outcomes of laparoscopic hepatectomy (LH) in patients with a history of upper abdominal surgery and repeat hepatectomy.

METHODS: This study compared the perioperative courses of patients receiving LH at our institution that had or had not previously undergone upper abdominal surgery. Of the 80 patients who underwent LH, 22 had prior abdominal surgeries, including hepatectomy (n = 12), pancreatectomy (n = 3), cholecystectomy and common bile duct excision (n = 1), splenectomy (n = 1), total gastrectomy (n = 1), colectomy with the involvement of transverse colon (n = 3), and extended hysterectomy with extensive lymph-node dissection up to the upper abdomen (n = 1). Clinical indicators including operating time, blood loss, hospital stay, and morbidity were compared among the groups.

RESULTS: Eighteen of the 22 patients who had undergone previous surgery had severe adhesions in the area around the liver. However, there were no conversions to laparotomy in this group. In the 58 patients without a history of upper abdominal surgery, the median operative time was 301 min and blood loss was 150 mL. In patients with upper abdominal surgical history or repeat hepatectomy, the operative times were 351 and 301 min, and blood loss was 100 and 50 mL, respectively. The median postoperative stay was 17, 13 and 12 d for patients with no history of upper abdominal surgery, patients with a history, and patients with repeat hepatectomy, respectively. There were five cases with complications in the group with no surgical history, compared to only one case in the group with a prior history. There were no statistically significant differences in the perioperative results between the groups with and without upper abdominal surgical history, or with repeat hepatectomy.

CONCLUSION: LH is feasible and safe in patients with a history of upper abdominal surgery or repeat hepatectomy.

Key words: Chronic liver disease; Laparoscopic hepatectomy; Liver tumor; Repeat hepatectomy; Surgical history

Core tip: The clinical outcomes of laparoscopic hepatectomy (LH) in patients with a history of upper abdominal surgery and repeat hepatectomy were evaluated. Of 80 patients who underwent pure LH, 22 had prior upper abdominal surgeries, and 12 underwent repeat hepatectomy. There were no conversions to laparotomy. There were no significant differences in operative time, blood loss, morbidity, or postoperative hospital stay between patients with and without prior abdominal surgery. LH with upper abdominal surgical history and repeat hepatectomy is feasible and safe for select patients.

Isetani M, Morise Z, Kawabe N, Tomishige H, Nagata H, Kawase J, Arakawa S. Pure laparoscopic hepatectomy as repeat surgery and repeat hepatectomy. *World J Gastroenterol* 2015; 21(3): 961-968 Available from: URL: http://www.wjgnet.com/1007-9327/full/v21/i3/961.htm DOI: http://dx.doi.org/10.3748/wjg.v21.i3.961

INTRODUCTION

The liver is the organ where most tumors metastasize, including colorectal, lung, breast, and ovarian cancers. Hepatic recurrence after previous resection of hepatocellular carcinoma (HCC) can also occur[1-3]. Therefore, conventional open surgery for hepatic resection is frequently performed in patients with a history of abdominal surgery[1-5]. Recently, laparoscopic procedures have been widely applied in various fields of surgery, and the number of favorable reports on laparoscopic hepatectomy (LH) is increasing[6-11]. However, there are still technical difficulties with LH related to liver mobilization, control of hemorrhaging, avoiding or repairing bile duct injuries, and vascular control. Moreover, surgeons need to contend with restricted manipulation, the lack of manual sensation, and disorientation from the lack of an overview[12,13]. Therefore, LH is typically only indicated for small and easily accessible lesions[7,14]. Indications for pure LH include HCC when there is an adequate hepatic reserve, metastatic liver tumors when there is no evidence of uncontrollable extrahepatic metastasis, and benign tumors when the diagnosis is uncertain or there are obvious symptoms.

An additional complication for LH is the presence of postoperative adhesions around the liver in patients who have had previous upper abdominal surgery. These adhesions and other postoperative changes can increase the risk of intraoperative bleeding and injury to vascular or biliary structures. Despite the increasing frequency of hepatectomy for patients with a history of abdominal surgical procedures, only a few reports of LH procedures for these patients are available[15-17]. Therefore, the purpose of this study was to assess the outcomes of LH for the patients with prior upper abdominal surgery and repeat hepatectomies.

MATERIALS AND METHODS

Patients and categorization

A total of 80 patients who underwent pure LH procedures at our hospital were included in this study. Patients undergoing hybrid procedures (LH combined with manipulation through a mini-laparotomy for reconstruction and other complicated procedures) for resection of hilar carcinoma, gallbladder carcinoma, or liver tumors with hepatic vein root involvement were excluded from this study. Lesions in all segments of the liver (segments 1-8) were included.

Patients were divided into groups based on the presence or absence of prior surgical history: no history (NH; $n = 58$) or upper abdominal surgical history (UASH; $n = 22$). Within the UASH group, a subgroup of patients was identified who had repeat hepatectomy (RH; $n = 12$). For these groups of patients, clinical indicators of perioperative course were retrospectively examined from medical records, including operative time, intraoperative blood loss, conversion to laparotomy, morbidity, and postoperative hospital stay. For patients in the UASH group, adhesions from previous surgery were evaluated by reviewing recorded video and graded according to Beck *et al*[18] mild adhesions were considered grade 1 (thin, filmy, and divided by blunt dissection) or grade 2 (thin, vascular, and easily divided by sharp dissection); severe adhesions were considered grade 3 (extensive, thick, and vascular, requiring division by sharp dissection) or grade 4 (dense, and the bowel is at risk of injury with division).

LH procedure

Patients were put in a supine to lateral position depending on the location of the tumor (left lateral position for tumors in the right dorsal liver). The first trocar was inserted at the umbilicus with an open method when the patient had no previous operative scar, otherwise the trocar was placed where adhesions were expected to be absent or minimal, while avoiding the previous incision site. After pneumoperitoneum (8 mmHg, occasionally increased up to 12 mmHg) was established through a 12-mm-port, a flexible laparoscope was introduced and then 3 to 4 additional trocars were inserted. When encountering adhesions that prevented adequate visualization, access to the operative field, and insertion of additional trocars, adhesiolysis was carefully performed with an electrocautery pen and ultrasonic shears. Intraoperative ultrasonography was routinely performed to assess the tumor conditions and determine the transection line. For the cases requiring anatomical

Table 1 Upper abdominal surgical histories

Surgical history		Procedure type	Adhesion
Hepatectomy (n = 12)	S4a56a resection, lymph node dissection	Laparoscopic	Severe
	Central bisectorectomy	Open	Severe
	S3 segmentectomy	Laparoscopic	Mild
	(3rd resection) S3 segmentectomy, Pt S5-6	Laparoscopic	Severe
	Pt S5 (severe cholecystitis)	Laparoscopic	Severe
	Extended posterior sectorectomy	Open	Severe
	(3rd resection) Lateral sectorectomy, S4b-8a resection	Open	Severe
	Pt S4 and S3	Open	Severe
	Anterior sectorectomy (distal gastrectomy)	Open	Severe
	Pt S6	Open	Severe
	Pt S6	Open	Severe
	S5 segmentectomy	Open	Severe
Pancreatectomy (n = 3)	Pancreatoduodenectomy	Open	Severe
	Distal pancreatectomy	Open	Severe
	Distal pancreatectomy	Open	Severe
Colectomy (involving transverse colon) (n = 3)		Open	Severe
		Laparoscopic	Mild
		Open	Severe
Common bile duct excision (n = 1)		Open	Severe
Splenectomy (n = 1)		Laparoscopic	Mild
Total gastrectomy (n = 1)		Laparoscopic	Mild
Extended hysterectomy[1] (n = 1)		Open	Severe

[1]Extended hysterectomy with extensive lymph node dissection up to the upper abdomen. The degree of adhesions was classified according to Beck *et al*[18] (mild = grade 1-2, severe = grade 3-4). Pt: Partial resection; S: Segment.

resection of one or more sectors, extrahepatic Glissonian pedicle encirclement/control and Pringle maneuvers were applied. The superficial hepatic parenchyma was transected using ultrasonic shears and the deeper portion of the parenchyma was transected using irrigation monopolar/bipolar cautery and a bipolar sealing device (BiClamp forceps, ERBE VIO System 200D, ERBE Elektromedizin GmbH, Tuebingen, Germany). A laparoscopic cavitron ultrasonic surgical aspirator was used for the portion of the parenchyma near the major vessels. After completing resection of the liver, the specimen was inserted into a protective plastic bag and extracted through the incision created by extending the port site. In the cases with an uncertain tumor location or uncontrollable bleeding, the operation was converted to a hand-assisted laparoscopic surgery or conventional open surgery.

Terminology

An upper abdominal surgery was defined as a distinct scar above the umbilicus[19] from which the operative procedure involved the subphrenic and subcostal area around the liver. If a laparoscopic procedure involved this area, it was defined as upper abdominal surgery regardless of port placements, including hepatectomy, biliary and pancreatic surgery, splenectomy, radical gastrectomy, colectomy with the involvement of transverse colon, and extended hysterectomy with extensive lymph node dissection up to upper abdomen. However, the patients with laparoscopic cholecystectomy were excluded due to mild adhesions that are usually observed. Colorectal cancer surgery was only included when the transverse colon was involved in the procedure.

Anatomical resection of the liver was defined as the procedure in which the Glissonian pedicle was divided at the root bifurcation and all the parenchyma related to the pedicle was resected. The nomenclature from the Brisbane 2000 Guidelines for liver anatomy and resection was used to describe the extent of the hepatic resection: major resection = hemihepatectomy and central bisectionectomy, as well as right posterior, anterior, and left median sectorectomies, which have cutting surfaces that are larger than that of a hemihepatectomy[11,20].

Statistical analysis

Groups were compared using Student's t, Fisher's exact and χ^2 tests with SPSS, version 11 statistical software (SPSS Inc., Chicago, IL, United States), with $P < 0.05$ indicating significance.

RESULTS

Characteristics of patients who underwent LH

The types of previous upper abdominal surgical procedures and extent of adhesions for each patient in the UASH group are given in Table 1. A subgroup of these patients underwent repeat hepatectomies, the details of which are presented in Table 2. Analysis of the three groups revealed that there were no differences with respect to age, sex, disease, tumor characteristics, or type of hepatectomy (Table 3).

Perioperative outcome

Although 81.8% (18/22) of UASH and 91.7% (11/12)

Table 2 Characteristics of the patients with repeat hepatectomies

Sex	Age	Cause for Hx	Method for diagnosis	Hx procedures	No. of tumors	Size of tumors (mm)	Child-Pugh class	Surgery interval (mo)	Adhesion grade	Operating time (min)	Bleeding (mL)	Hospital stay (d)
M	63	IPT	CT with contrast	Pt S4a5	1	20	A	12	3	540	100	30
F	71	HCC	CT with contrast	Pt S1 (3rd Hx)	1	8	A	22	4	216	0	9
M	74	Met	CT with contrast	Pt S5, S7	4	28	A	70	4	570	840	21
F	81	HCC	CT with contrast	Pt S2-3	1	18	A	87	4	104	5	12
F	69	HCC	CT with contrast	Pt S5-6	2	30	A	28	2	168	30	9
M	65	HCC	CT with contrast	Pt S1l	1	23	A	16	4	165	50	10
F	80	HCC	CT with contrast	S3 resection	1	18	B	46	4	224	50	13
M	60	HCC	CT with contrast	Pt S4	1	35	A	16	3	286	50	14
M	77	Met	CT with contrast	Pt S4 - 8	1	20	A	15	4	245	21	9
M	72	GBCa	Pathology from 1st Hx for IPT	S4a56a resection	1	60	A	0.5	4	488	143	24
M	57	HCC	CT with contrast	Pt S7, S2	2	21	A	32	4	388	50	10
M	67	HCC	CT with contrast	PtS8	1	11	A	97	3	432	365	14

Adhesion grades according to Beck *et al*[18]. CT: Computed tomography; GBCa: Gall bladder carcinoma; HCC: Hepatocellular carcinoma; Hx: Hepatectomy; IPT: Inflammatory pseudo-tumor; Met: Metastasis; Pt: Partial resection; S: Segment.

Table 3 Demographic factors and background diseases of the patients

Factor	NH (*n* = 58)	UASH (*n* = 22)	RH (*n* = 12)
Age, yr	70 (48-82)	68 (57-81)	70 (57-81)
Sex, male/female	34/24	12/10	8/4
Chronic liver disease, yes/no	37/21	11/11	7/5
Cause for hepatectomy			
Hepatocellular carcinoma	38	12	8
Metastasis	11	8	2
Others	9	2	2
Tumor			
n	1 (1-4)	1 (1-6)	1 (1-4)
Size (mm)	24 (7-107)	23 (8-60)	21 (8-60)
Type of LH procedure			
Major/minor	11/47	1/21	0/12
Anatomical/non-anatomical	23/35	6/16	2/10

Twelve patients in the RH group are also included in the UASH group. Values are expressed as median (range). Major resection: hemihepatectomy, central bisectionectomy, right posterior sectorectomy, right anterior sectorectomy and left median sectorectomy. Anatomical resection: the procedures in which the Glissonian pedicle was divided at the root in bifurcation and all the parenchyma related to the pedicle was resected. LH: Laparoscopic hepatectomy; NH: No history of upper abdominal surgery; RH: Repeat hepatectomy; UASH: Upper abdominal surgery history.

of RH patients had severe adhesions, there were no conversions to a laparotomy. However, there were two cases of conversion among the NH patients due to massive hemorrhage or difficulty of tumor identification. The median operative times did not differ among the groups (Table 4). Although the blood loss was reduced in the RH group, the difference was not statistically different. Seven patients in the NH group had complications, leading to a median hospital stay of 17 d, whereas only one UASH patient had leakage of pancreatic juice from the area around the pancreatico-jejunostomy, which recovered conservatively. However,

Table 4 Perioperative courses of the patients with laparoscopic liver resection

	NH (*n* = 58)	UASH (*n* = 22)	RH (*n* = 12)
Operative time (min)	301 (112-710)	351 (104-848)	301 (104-570)
Blood loss (mL)	150 (NC-3270)	100 (NC-3569)	50 (NC-840)
Conversion to laparotomy (*n*)	2	0	0
Morbidity (*n*)	7	1	0
Postoperative hospital stay (d)	17 (5-254[1])	14 (8-52)	12 (9-30)

Twelve patients in the RH group are also included in the group of UASH. Values are expressed as median (range). [1]Although this patient developed no complication directly related to operative manipulation during and immediately after surgery, her postoperative stay was extended due to uncontrollable massive ascites. NC: Small and non-countable; NH: No history of upper abdominal surgery; RH: Repeat hepatectomy; UASH: Upper abdominal surgery history.

Table 5 Perioperative courses of the patients with laparoscopic liver resection (excluding those with major hepatectomy)

	NH (*n* = 47)	UASH (*n* = 21)	RH (*n* = 12)
Operative time (min)	287 (112-696)	334 (104-682)	301 (104-570)
Blood loss (mL)	100 (NC-3270)	100 (NC-850)	50 (NC-840)
Conversion to laparotomy (*n*)	2	0	0
Morbidity (*n*)	5	1	0
Postoperative hospital stay (d)	17 (5-254[1])	13 (8-52)	12 (9-30)

Twelve patients in the RH group are also included in the group of UASH. Values are expressed as median (range). [1]Although this patient developed no complication related directly to operative manipulation during and immediately after surgery, her postoperative stay was extended due to uncontrollable massive ascites. NC: Small and non-countable; NH: No history of upper abdominal surgery; RH: Repeat hepatectomy; UASH: Upper abdominal surgery history.

Table 6 Summary of previous reports of laparoscopic repeat hepatectomy

Ref.	*n*	Age (yr)	Disease	First Hx (open/lap)	Procedure	Bleeding (mL)	Operating time (min)	Con. (*n*)	POHS (d)	Morbidity	Mortality
Nguyen *et al*[16]	2		Met								
Belli[1] *et al*[15]	12	69 (58-75)	HCC	4:8	LLS (*n* = 5), Pt (*n* = 4), Seg (*n* = 3)	297 ± 134 272.2 ± 120	114.4 ± 11.0 63.9 ± 13.3	1	7.4 ± 2.5 6.2 ± 3.0	26.6%	0%
Hu *et al*[28]	6	49 (46-61)	HCC	3:3 (Lap RFA, *n* = 2)	LLS (*n* = 2), Pt (*n* = 4)	283.3 ± 256.3	140.8 ± 35.7	0	5.67 ± 1.63	16.7%	0%
Shafaee *et al*[27]	76	61 (29-82)	Met (*n* = 63), HCC (*n* = 3), others (*n* = 10)	28:44	LLS (*n* = 4), Pt seg (*n* = 53), above-seg (*n* = 19)	300 (0-5000)	180 (80-570)	8	6 (2-42)	26%	0%
Ahn *et al*[17]	4	57 (54-60)	HCC (*n* = 3), Met (*n* =1)	0:4	LLS (*n* = 1), Pt (*n* = 3)	481.7 ± 449.5	312.3 ± 158.4	1	10.6 ± 7.4	23.4%	0%
Cannon *et al*[29]	17										
Tsuchiya *et al*[30]	3	73 (52-79)	HCC	0:3		281.3 (mean)	264.6 (mean)	0	8.6 (mean)		0%
Kanazawa *et al*[31]	20	70 (46-83)	HCC	15:5	Pt	78 (1-1500)	239 (69-658)	2 (HALS)	9 (5-22)	5%	0%
Montalti *et al*[32]	9		Met								
Present article	12	70 (57-81)	HCC (*n* = 8), Met (*n* = 2), others (*n* = 2)	8:4	Pt (*n* = 10), Subseg (*n* = 2)	50 (NC-840)	301 (104-570)	0	12 (9-30)	0%	0%

Data are expressed as median (range) or mean ± SD, unless stated otherwise. [1]In the paper from Belli, operating time, bleeding and POHS are described separately for patients whose previous hepatectomy was open (upper) or laparoscopic (lower). Con: Conversion to laparotomy; HALS: Hand-assisted laparoscopic surgery; HCC: Hepatocellular carcinoma; Hx: Hepatectomy; LAP: Laparoscopic; LLS: Left lateral sectorectomy; Met: Metastasis, NC: Small and non-countable; POHS: Postoperative hospital stay; Pt: Partial resection; RFA: Radiofrequency ablation; Seg: Segmentectomy; Subseg: Subsegmentectomy.

the morbidity and hospital durations did not differ among the groups, and there were no postoperative deaths.

Because the number of major hepatectomies in the UASH and RH groups was small, and these procedures often entail longer operative times, larger blood loss, and longer postoperative hospital stays, the results were re-analyzed after excluding these patients. No differences were observed in any of the parameters tested (Table 5).

DISCUSSION

Postoperative adhesions are known to increase the operative time of subsequent surgeries, due to the need for adhesiolysis and the risk of bowel injury[18]. Furthermore, there is an increased risk of intraoperative complications and conversion from laparoscopic procedures to laparotomy in patients with postoperative adhesions[21]. Indeed, a history of abdominal surgery was once considered a contraindication for laparoscopic surgery, though technical and instrumental improvements have allowed for laparoscopic procedures such as cholecystectomy, appendectomy, colectomy, and gastrectomy to be safely applied in these patients[18,22-25]. However, LH remains a technically demanding procedure. Resection of the liver parenchyma can be performed after completing adequate adhesiolysis and mobilization of the involved liver area. Fibrotic adhesions can hinder the visualization and dissection of the hepatoduodenal ligament and hilar area, which are often crucial steps in LH procedures. The liver capsule bleeds easily during adhesiolysis and mobilization, thus increasing blood loss and creating a suboptimal operative field[26].

The results of perioperative indicators are similar to previous reports[15-17,27-32], which are summarized in Table 6. However, patients in the present study had longer postoperative hospital stays, which was likely due to the higher age and poorer liver function of our patients, in addition to cultural and healthcare management differences. Importantly, the perioperative results were not significantly different between the groups with and without an upper abdominal surgical history, despite the high incidence of severe postoperative adhesions. The prevalence of severe adhesions in patients in the UASH group is consistent with the report by Ahn *et al*[17]. In their study, patients without a surgical history frequently had chronic liver disease, which can make transection of the liver parenchyma more difficult. Therefore, these challenges offset the complications caused by adhesions in the group with a surgical history, resulting in a lack of perioperative differences between the groups. In comparison, a larger proportion of our patients had chronic liver disease compared to their study, both in the NH group (60% *vs* 45%) and the UASH group (50% *vs* 9%). On the other hand, our study had a smaller proportion of patients who had undergone

major hepatectomy (15% *vs* 39%), with more anatomical resections (36%, mostly minor) due to chronic liver disease.

We previously reported that pure LH is useful for patients with severe liver dysfunction, as it minimizes the disturbance in liver-cirrhotic collateral blood/lymphatic flow caused by laparotomy and liver mobilization, as well as the mesenchymal injury caused by compression of the liver[33,34]. Pure LH, therefore, limits complications, such as massive ascites, which can lead to severe postoperative liver failure. In the present series, we found that the smaller working space required by LH allowed for minimal adhesion dissections and a direct tumor approach. We believe that this is one of the reasons why our patients with a surgical history, and with repeat hepatectomy, had similar perioperative results to the patients without a history. Although perioperative results are different with major hepatectomies (longer operative time and postoperative hospital stay, larger blood loss), inclusion of these few cases did not significantly alter the results between the groups. The majority of cases in previous reports and in the present series underwent partial hepatectomy as a repeat procedure, therefore alterations of hepatic parenchyma and intrahepatic anatomy from the first hepatectomy should be relatively small. Since alterations of hilar and intrahepatic vascular structures should greatly impact the second hepatectomy, further examination of major or anatomical repeat hepatectomies is needed. However, the results of the present study suggest that an advantage of pure laparoscopy for smaller repeat resections of impaired liver is the fact that the hepatectomy is facilitated by the minimal adhesiolysis required with a laparoscopic view and manipulation.

The perioperative morbidity and mortality with conventional open repeat hepatectomy are comparable to those with the first hepatectomy[2,35]. However, repeat LH has recently been safely applied to patients with recurrent HCC, and is recommended as a good alternative treatment option[15,27]. In our series, 12 repeat LH procedures, two of which were third hepatectomies, were performed for recurrent liver tumors without morbidity. Another treatment option involves a hybrid procedure with adhesiolysis through a previous mini-laparotomy, which may be effective for patients with massive adhesions and without any free space in the abdomen. We experienced one such case in our series in a patient with a history of severe acute pancreatitis caused by main pancreatic duct tumor embolus. He underwent adhesiolysis through a previous mini-laparotomy followed by the pure LH. In this operation, the magnified laparoscopic view facilitated the hepatectomy with minimal adhesiolysis and in the small working space.

In conclusion, this study demonstrates that pure LH in patients with a history of upper abdominal surgery is feasible and safe in select patients. Moreover, repeat hepatectomy can be facilitated with a laparoscopic approach, especially in patients with impaired liver function.

COMMENTS

Background

The liver is the most common site for tumor metastases from colorectal, lung, breast, and ovarian cancers, in addition to recurrence of hepatocellular carcinoma. Thus, hepatic resection is frequently performed in patients with a history of abdominal surgery. Recently, laparoscopic procedures have been widely applied in various surgical fields. However, despite the favorable results reported from laparoscopic hepatectomy (LH), technical difficulties still remain with this procedure. In addition, this procedure is complicated by adhesions at the area around the liver that occur in patients who have previously undergone upper abdominal surgery.

Research frontiers

Although the importance and application of hepatectomy for patients with a history of abdominal surgical procedures have increased, reports of the use of LH in such cases are limited. In this study, the outcomes of LH for the patients with prior upper abdominal surgery and of repeat hepatectomy in our series were evaluated and compared to those from patients without prior surgical histories.

Innovations and breakthroughs

This study demonstrates that pure LH as a repeat surgery and repeat hepatectomy is feasible and safe in select patients. Furthermore, this procedure facilitates repeat hepatectomy in patients with impaired liver function.

Applications

Pure LH as a repeat surgery and repeat hepatectomy is safely applicable to patients with liver metastasis from intra-abdominal organ malignancies, metachronous repeat hepatic tumors, or impaired liver function.

Terminology

Upper abdominal surgery was defined as an operative procedure involving the subphrenic and subcostal area around the liver, including hepatectomy, biliary and pancreatic surgery, splenectomy, radical gastrectomy, colectomy with the involvement of transverse colon, and extended hysterectomy with extensive lymph node dissection up to upper abdomen. Anatomical resection of the liver was defined as the procedure in which the Glissonian pedicle was divided at the root bifurcation and all the parenchyma related to the pedicle was resected. A major resection referred to hemihepatectomy, central bisectionectomy, and right posterior, anterior, and left median sectorectomies.

Peer review

The article is useful for surgeons, gastroenterologists, and oncologists and confirms the safety of laparoscopic hepatectomies in patients with previous abdominal surgeries. The number of analyzed patients was sufficient to allow a statistical analysis and to draw conclusions. The surgical technique, the results, and the statistical analysis are well presented.

REFERENCES

1 **Petrowsky H**, Gonen M, Jarnagin W, Lorenz M, DeMatteo R, Heinrich S, Encke A, Blumgart L, Fong Y. Second liver resections are safe and effective treatment for recurrent hepatic metastases from colorectal cancer: a bi-institutional analysis. *Ann Surg* 2002; **235**: 863-871 [PMID: 12035044 DOI: 10.1097/00000658-200206000-00015]

2 **Wanebo HJ**, Chu QD, Avradopoulos KA, Vezeridis MP. Current perspectives on repeat hepatic resection for colorectal carcinoma: a review. *Surgery* 1996; **119**: 361-371 [PMID: 8643998 DOI: 10.1016/S0039-6060(96)80133-4]

3 **Itamoto T**, Nakahara H, Amano H, Kohashi T, Ohdan H, Tashiro H, Asahara T. Repeat hepatectomy for recurrent hepatocellular carcinoma. *Surgery* 2007; **141**: 589-597 [PMID: 17462458 DOI: 10.1016/j.surg.2006.12.014]

4 **Heslin MJ**, Medina-Franco H, Parker M, Vickers SM, Aldrete J, Urist MM. Colorectal hepatic metastases: resection, local ablation, and hepatic artery infusion pump are associated

with prolonged survival. *Arch Surg* 2001; **136**: 318-323 [PMID: 11231853 DOI: 10.1001/archsurg.136.3.318]
5 **Weitz J**, Blumgart LH, Fong Y, Jarnagin WR, D'Angelica M, Harrison LE, DeMatteo RP. Partial hepatectomy for metastases from noncolorectal, nonneuroendocrine carcinoma. *Ann Surg* 2005; **241**: 269-276 [PMID: 15650637 DOI: 10.1097/01.sla.0000150244.72285.ad]
6 **Nguyen KT**, Gamblin TC, Geller DA. World review of laparoscopic liver resection-2,804 patients. *Ann Surg* 2009; **250**: 831-841 [PMID: 19801936 DOI: 10.1097/SLA.0b013e3181b0c4df]
7 **Cherqui D**, Husson E, Hammoud R, Malassagne B, Stéphan F, Bensaid S, Rotman N, Fagniez PL. Laparoscopic liver resections: a feasibility study in 30 patients. *Ann Surg* 2000; **232**: 753-762 [PMID: 11088070 DOI: 10.1097/00000658-200012000-00004]
8 **Kaneko H**, Takagi S, Otsuka Y, Tsuchiya M, Tamura A, Katagiri T, Maeda T, Shiba T. Laparoscopic liver resection of hepatocellular carcinoma. *Am J Surg* 2005; **189**: 190-194 [PMID: 15720988 DOI: 10.1016/j.amjsurg.2004.09.010]
9 **Sasaki A**, Nitta H, Otsuka K, Takahara T, Nishizuka S, Wakabayashi G. Ten-year experience of totally laparoscopic liver resection in a single institution. *Br J Surg* 2009; **96**: 274-279 [PMID: 19224518 DOI: 10.1002/bjs.6472]
10 **Buell JF**, Thomas MT, Rudich S, Marvin M, Nagubandi R, Ravindra KV, Brock G, McMasters KM. Experience with more than 500 minimally invasive hepatic procedures. *Ann Surg* 2008; **248**: 475-486 [PMID: 18791368]
11 **Cho JY**, Han HS, Yoon YS, Shin SH. Feasibility of laparoscopic liver resection for tumors located in the posterosuperior segments of the liver, with a special reference to overcoming current limitations on tumor location. *Surgery* 2008; **144**: 32-38 [PMID: 18571582 DOI: 10.1016/j.surg.2008.03.020]
12 **Buell JF**, Thomas MJ, Doty TC, Gersin KS, Merchen TD, Gupta M, Rudich SM, Woodle ES. An initial experience and evolution of laparoscopic hepatic resectional surgery. *Surgery* 2004; **136**: 804-811 [PMID: 15467665 DOI: 10.1016/j.surg.2004.07.002]
13 **Vibert E**, Perniceni T, Levard H, Denet C, Shahri NK, Gayet B. Laparoscopic liver resection. *Br J Surg* 2006; **93**: 67-72 [PMID: 16273531 DOI: 10.1002/bjs.5150]
14 **Otsuka Y**, Tsuchiya M, Maeda T, Katagiri T, Isii J, Tamura A, Yamazaki K, Kubota Y, Suzuki T, Suzuki T, Kagami S, Kaneko H. Laparoscopic hepatectomy for liver tumors: proposals for standardization. *J Hepatobiliary Pancreat Surg* 2009; **16**: 720-725 [PMID: 19652902 DOI: 10.1007/s00534-009-0139-x]
15 **Belli G**, Cioffi L, Fantini C, D'Agostino A, Russo G, Limongelli P, Belli A. Laparoscopic redo surgery for recurrent hepatocellular carcinoma in cirrhotic patients: feasibility, safety, and results. *Surg Endosc* 2009; **23**: 1807-1811 [PMID: 19277781 DOI: 10.1007/s00464-009-0344-3]
16 **Nguyen KT**, Laurent A, Dagher I, Geller DA, Steel J, Thomas MT, Marvin M, Ravindra KV, Mejia A, Lainas P, Franco D, Cherqui D, Buell JF, Gamblin TC. Minimally invasive liver resection for metastatic colorectal cancer: a multi-institutional, international report of safety, feasibility, and early outcomes. *Ann Surg* 2009; **250**: 842-848 [PMID: 19806058 DOI: 10.1097/SLA.0b013e3181bc789c]
17 **Ahn KS**, Han HS, Yoon YS, Cho JY, Kim JH. Laparoscopic liver resection in patients with a history of upper abdominal surgery. *World J Surg* 2011; **35**: 1333-1339 [PMID: 21452069 DOI: 10.1007/s00268-011-1073-z]
18 **Beck DE**, Ferguson MA, Opelka FG, Fleshman JW, Gervaz P, Wexner SD. Effect of previous surgery on abdominal opening time. *Dis Colon Rectum* 2000; **43**: 1749-1753 [PMID: 11156462 DOI: 10.1007/BF02236862]
19 **Karayiannakis AJ**, Polychronidis A, Perente S, Botaitis S, Simopoulos C. Laparoscopic cholecystectomy in patients with previous upper or lower abdominal surgery. *Surg Endosc* 2004; **18**: 97-101 [PMID: 14569455 DOI: 10.1007/s00464-003-9001-4]
20 **Yoon YS**, Han HS, Choi YS, Jang JY, Suh KS, Kim SW, Lee KU, Park YH. Total laparoscopic right posterior sectionectomy for hepatocellular carcinoma. *J Laparoendosc Adv Surg Tech A* 2006; **16**: 274-277 [PMID: 16796440 DOI: 10.1089/lap.2006.16.274]
21 **Wiebke EA**, Pruitt AL, Howard TJ, Jacobson LE, Broadie TA, Goulet RJ, Canal DF. Conversion of laparoscopic to open cholecystectomy. An analysis of risk factors. *Surg Endosc* 1996; **10**: 742-745 [PMID: 8662431 DOI: 10.1007/BF00193048]
22 **Wu JM**, Lin HF, Chen KH, Tseng LM, Tsai MS, Huang SH. Impact of previous abdominal surgery on laparoscopic appendectomy for acute appendicitis. *Surg Endosc* 2007; **21**: 570-573 [PMID: 17103279 DOI: 10.1007/s00464-006-9027-5]
23 **Law WL**, Lee YM, Chu KW. Previous abdominal operations do not affect the outcomes of laparoscopic colorectal surgery. *Surg Endosc* 2005; **19**: 326-330 [PMID: 15624064 DOI: 10.1007/s00464-004-8114-8]
24 **Curet MJ**. Special problems in laparoscopic surgery. Previous abdominal surgery, obesity, and pregnancy. *Surg Clin North Am* 2000; **80**: 1093-1110 [PMID: 10987026 DOI: 10.1016/S0039-6109(05)70215-2]
25 **Nunobe S**, Hiki N, Fukunaga T, Tokunaga M, Ohyama S, Seto Y, Yamaguchi T. Previous laparotomy is not a contraindication to laparoscopy-assisted gastrectomy for early gastric cancer. *World J Surg* 2008; **32**: 1466-1472 [PMID: 18340481 DOI: 10.1007/s00268-008-9542-8]
26 **Szomstein S**, Lo Menzo E, Simpfendorfer C, Zundel N, Rosenthal RJ. Laparoscopic lysis of adhesions. *World J Surg* 2006; **30**: 535-540 [PMID: 16555020 DOI: 10.1007/s00268-005-7778-0]
27 **Shafaee Z**, Kazaryan AM, Marvin MR, Cannon R, Buell JF, Edwin B, Gayet B. Is laparoscopic repeat hepatectomy feasible? A tri-institutional analysis. *J Am Coll Surg* 2011; **212**: 171-179 [PMID: 21276531 DOI: 10.1016/j.jamcollsurg.2010.10.012]
28 **Hu M**, Zhao G, Xu D, Liu R. Laparoscopic repeat resection of recurrent hepatocellular carcinoma. *World J Surg* 2011; **35**: 648-655 [PMID: 21184074 DOI: 10.1007/s00268-010-0919-0]
29 **Cannon RM**, Brock GN, Marvin MR, Buell JF. Laparoscopic liver resection: an examination of our first 300 patients. *J Am Coll Surg* 2011; **213**: 501-507 [PMID: 21624840 DOI: 10.1016/j.jamcollsurg.2011.04.032]
30 **Tsuchiya M**, Otsuka Y, Maeda T, Ishii J, Tamura A, Kaneko H. Efficacy of laparoscopic surgery for recurrent hepatocellular carcinoma. *Hepatogastroenterology* 2012; **59**: 1333-1337 [PMID: 22591625 DOI: 10.5754/hge12302]
31 **Kanazawa A**, Tsukamoto T, Shimizu S, Kodai S, Yamamoto S, Yamazoe S, Ohira G, Nakajima T. Laparoscopic liver resection for treating recurrent hepatocellular carcinoma. *J Hepatobiliary Pancreat Sci* 2013; **20**: 512-517 [PMID: 23404252 DOI: 10.1007/s00534-012-0592-9]
32 **Montalti R**, Berardi G, Laurent S, Sebastiani S, Ferdinande L, Libbrecht LJ, Smeets P, Brescia A, Rogiers X, de Hemptinne B, Geboes K, Troisi RI. Laparoscopic liver resection compared to open approach in patients with colorectal liver metastases improves further resectability: Oncological outcomes of a case-control matched-pairs analysis. *Eur J Surg Oncol* 2014; **40**: 536-544 [PMID: 24555996 DOI: 10.1016/j.ejso.2014.01.005]
33 **Morise Z**, Sugioka A, Kawabe N, Umemoto S, Nagata H, Ohshima H, Kawase J, Arakawa S, Yoshida R. Pure laparoscopic hepatectomy for hepatocellular carcinoma patients with severe liver cirrhosis. *Asian J Endosc Surg* 2011; **4**: 143-146 [PMID: 22776279 DOI: 10.1111/j.1758-5910.2011.00081.x]
34 **Morise Z**. Pure laparoscopic hepatectomy for HCC patients. In: Lau WY. Hepatocellular Carcinoma - Clinical Research. Zagreb. Croatia: InTech, 2012: 183-196

35 **Vaillant JC**, Balladur P, Nordlinger B, Karaitianos I, Hannoun L, Huguet C, Parc R. Repeat liver resection for recurrent colorectal metastases. *Br J Surg* 1993; **80**: 340-344 [PMID: 8472146 DOI: 10.1002/bjs.1800800324]

P- Reviewer: Dhiman RK, Ferreira Galvao FH, Furka A, Mihaila RG
S- Editor: Qi Y **L- Editor**: A **E- Editor**: Zhang DN

World Journal of Gastroenterology

Submit a Manuscript: http://www.wjgnet.com/esps/
Help Desk: http://www.wjgnet.com/esps/helpdesk.aspx
DOI: 10.3748/wjg.v21.i3.969

World J Gastroenterol 2015 January 21; 21(3): 969-976
ISSN 1007-9327 (print) ISSN 2219-2840 (online)

ORIGINAL ARTICLE

Observational Study

Accuracy of routine multidetector computed tomography to identify arterial variants in patients scheduled for pancreaticoduodenectomy

Feng Yang, Yang Di, Ji Li, Xiao-Yi Wang, Lie Yao, Si-Jie Hao, Yong-Jian Jiang, Chen Jin, De-Liang Fu

Feng Yang, Yang Di, Ji Li, Xiao-Yi Wang, Lie Yao, Si-Jie Hao, Yong-Jian Jiang, Chen Jin, De-Liang Fu, Department of Pancreatic Surgery, Pancreatic Disease Institute, Huashan Hospital, Shanghai Medical College, Fudan University, Shanghai 200040, China

Author contributions: Yang F and Fu DL designed the study; Yang F, Di Y, Li J, Wang XY, Yao L, Hao SJ and Jiang YJ collected data for this research; Yang F, Jin C and Fu DL analyzed the data; Yang F wrote the manuscript; and Jin C and Fu DL edited the manuscript.

Supported by New Outstanding Youth Program of Shanghai Municipal Health Bureau, No. XYQ2013090; Shanghai Young Physician Training Program and the Zhuo-Xue Project of Fudan University; and The key Project of Oncological Subject of the Ministry of Health of China 2012.

Correspondence to: De-Liang Fu, Professor, Department of Pancreatic Surgery, Pancreatic Disease Institute, Huashan Hospital, Shanghai Medical College, Fudan University, 12 Central Urumqi Road, Shanghai 200040, China. surgeonfu@163.com
Telephone: +86-21-52887164
Fax: +86-21-52888277

Received: June 4, 2014
Peer-review started: June 5, 2014
First decision: July 9, 2014
Revised: July 30, 2014
Accepted: September 18, 2014
Article in press: September 19, 2014
Published online: January 21, 2015

Abstract

AIM: To assess the efficacy of cross-sectional multidetector computed tomography (MDCT) imaging without arterial reconstruction to identify aberrant right hepatic artery (RHA) and celiac artery stenosis (CAS) in patients scheduled for pancreaticoduodenectomy.

METHODS: Patients with peri-ampullary and pancreatic head tumors who underwent routine preoperative MDCT and subsequent computed tomography (CT) angiography (CTA), conventional angiography or pancreaticoduodenectomy between September 2007 and August 2013 were identified. Retrospective analysis of imaging data was undertaken using CTA, conventional angiographic and surgical findings as the reference standards. The accuracy, sensitivity, specificity, positive predictive value (PPV) and negative predictive value (NPV) of MDCT in evaluation of aberrant RHA and CAS were calculated.

RESULTS: A group of 458 patients met the inclusion criteria of this study to detect aberrant RHA, and 181 cases were included to identify CAS. Fifty-four (11.8%) patients were confirmed to have aberrant RHA, while 12 (6.6%) patients with CAS were demonstrated. MDCT yielded an accuracy of 98.5%, sensitivity of 96.3% and specificity of 98.8% in the detection of aberrant RHA. The sensitivity, specificity, PPV and NPV of MDCT for detecting CAS were 58.3%, 98.2%, 70% and 97.1%, respectively.

CONCLUSION: Routine MDCT is recommended such that surgeons and radiologists be alerted to the importance of arterial variants on preoperative CT scans in patients scheduled for pancreaticoduodenectomy.

Key words: Pancreaticoduodenectomy; Aberrant hepatic artery; Celiac artery stenosis; Multidetector computed tomography; Angiography

Core tip: Few studies have investigated the ability of routine multidetector computed tomography (CT) scans without arterial reconstruction, which are commonplace in medical practice, to assess peri-pancreatic arterial variants such as aberrant right hepatic artery and celiac artery stenosis prior to pancreaticoduodenectomy. This study demonstrated that a routine multidetector CT scan is useful to evaluate aberrant right hepatic artery in the preoperative planning of pancreatic surgery, although it is limited by lower sensitivity for evaluating celiac artery stenosis. It is recommended that surgeons and radiologists be alerted to the importance of arterial variants on preoperative CT scans in patients scheduled for pancreaticoduodenectomy.

Yang F, Di Y, Li J, Wang XY, Yao L, Hao SJ, Jiang YJ, Jin C, Fu DL. Accuracy of routine multidetector computed tomography to identify arterial variants in patients scheduled for pancreaticoduodenectomy. *World J Gastroenterol* 2015; 21(3): 969-976 Available from: URL: http://www.wjgnet.com/1007-9327/full/v21/i3/969.htm DOI: http://dx.doi.org/10.3748/wjg.v21.i3.969

INTRODUCTION

The complex nature of the peri-pancreatic vasculature and its variations add to the difficulty of surgical resection. Previous reports[1-5] demonstrated that hepatic artery anomalies and celiac artery stenosis (CAS) were not rare in patients with peri-ampullary and pancreatic head neoplasms. One relatively common aberration in hepatic artery anatomy is the replaced or accessory right hepatic artery (R/A RHA), but it failed to be identified in nearly half of patients preoperatively[6]. R/A RHA usually runs laterally to the portal vein (PV) behind the pancreatic head and enters the right side of the hepatoduodenal ligament posterolateral to the common bile duct (CBD). The presence of R/A RHA may modify the surgical approach when special conditions, such as CAS or occlusion[7-9], are encountered. Usually the presence of CAS is of no clinical significance, as blood supply to the pancreas, liver, stomach and spleen is maintained through a well-developed system of pancreaticoduodenal collateral pathways from the superior mesenteric artery (SMA). However, it can lead to liver ischemia after occlusion of the gastroduodenal artery (GDA), which may cause severe complications after a Whipple procedure[10]. Thus, surgeons should be vigilant for these anomalous arteries to avoid potentially disastrous complications.

Preoperative angiography helps to identify abnormalities in the peri-pancreatic vasculature, enabling better preparation for management during surgery. It also provides a reliable method to diagnose CAS in the presence of direct visualization of stenosis on lateral views, retrograde blood flow through markedly developed pancreaticoduodenal arcades and prominent collateral vessels in the peri-pancreatic region. CT angiography (CTA) is an effective alternate imaging tool to conventional angiography that has high spatial resolution, making noninvasive evaluation of the vascular architecture surrounding the pancreas from any angle possible. It also allows the display of both the pancreas (including the mass) and the vascular map in a single view. Studies have demonstrated that there is no significant difference in sensitivity between CTA and conventional angiography with the use of multiplanar and volume set analysis[9]. Nevertheless, the necessity for conventional angiography remains controversial because of its invasive nature. Conventional angiography cannot visualize the pancreas directly. In addition, whether or not it can thoroughly depict the vascular variations depends on the site of vascular access.

Routine multidetector CT (MDCT) is the standard examination method for the initial detection and characterization of pancreatic tumors, and for evaluation of resectability. However, there are few studies focusing on the assessment of peri-pancreatic arterial variants by means of preoperative MDCT without arterial reconstruction. The question is how accurately can MDCT show aberrant RHA or CAS in clinical practice? The purpose of this study was to assess the efficacy of routine MDCT to identify aberrant RHA and CAS in patients scheduled for pancreaticoduodenectomy using CTA, conventional angiographic and surgical findings as the reference standard.

MATERIALS AND METHODS

Patients

All patients with peri-ampullary and pancreatic head tumors who underwent routine preoperative MDCT and subsequent CTA, conventional angiography, or pancreaticoduodenectomy between September 2007 and August 2013 were identified from a review of patients treated at the Huashan Hospital. The patients who did not have a CTA examination or conventional angiography, and those who did not receive pancreaticoduodenectomy, were excluded. The remaining patients comprised the final study population. Medical records, surgical notes and imaging reports of these patients were reviewed. Two pancreatic surgeons familiar with the peri-pancreatic vascular anatomy but blinded to all other information including surgical records and the findings of CTA and conventional angiography reviewed the radiological films of the arterial phase of MDCT retrospectively. The Huashan Hospital institutional review board approved this study, and patient informed consent was obtained for all procedures.

Imaging techniques

MDCT was used to evaluate the tumor and its relationship with peri-pancreatic vascular structures. CT investigations were performed on 16-slice or 64-slice MDCT equipment (GE Medical Systems) after intravenous injection of 2

mL/kg of 300 mg I/mL Omnipaque (GE Healthcare Shanghai Co., Ltd.) at a flow rate of four mL/s. The major scanning parameters were set at a voltage of 120 kV, tube current of 280 mA, rotation time of 0.5-0.8 s and a section thickness of 3.75 mm. Arterial phase images of the routine MDCT were reviewed to evaluate aberrant RHA and CAS in all patients. Neither multiplanar reformation (MPR) nor maximum intensity projection (MIP) was used to review the MDCT images. These arterial variants were graded as "visualized" or "non-visualized".

Abdominal CTA was performed using 64-slice CT. Approximately 100 mL of iodine contrast agent (300 mg I/mL Omnipaque) was administered into the antecubital vein at a flow rate of three mL/s with a power injector. The collimation was set to 64 mm × 0.6 mm. The delay time, which depended on a bolus test using smartprep software (GE Healthcare), was roughly 15-18 s. The reconstructed slice thickness was one mm (field of view, 26 cm × 26 cm; matrix, 512 × 512; pixel size, 0.5 mm × 0.5 mm). Axial images were reconstructed with both three mm slice thickness and a reconstruction interval. An experienced technician in the 3D laboratory performed the three-dimensional arteriography on a dedicated 3D workstation (Siemens syngo MultiModality Workplace). MIP and volume rendering (VR) were used for the 3D post processing to analyze the arteries on the workstation.

The indication of conventional angiography was patients with locally advanced pancreatic head cancer who received adjuvant interventional chemotherapy (regional intra-arterial infusion chemotherapy). During the procedure, we also assessed the resectability of the tumors. Conventional angiography was performed as previous described[1,11]. In brief, a catheter (5-Fr Rosch hepatic catheter; Wilson-Cook Medical Inc., Winston-Salem, N.C., United States) was introduced through the right femoral artery by the Seldinger technique. The celiac or selective hepatic angiography and superior mesenteric angiography were carried out with selective injections of contrast medium in the celiac trunk and in the SMA. Serial anterior-posterior images were obtained at a rate of one of every two seconds for the first eight seconds and a slower rate thereafter.

Surgery

Patients who had lesions that were definitely resectable according to preoperative evaluation received surgical therapy. Two experienced pancreatic surgeons, who perform more than 60 Whipple procedures every year, performed the surgery. During the procedure, they paid particular attention to whether the patients had aberrant RHA. They were informed of the CTA and conventional angiography results regarding hepatic arterial anatomy before surgery if the patients had preoperative angiography examination. The MDCT results were compared with intra-operative findings, which were used as a standard of reference.

Image interpretation and data analysis

We assessed the studies for the presence of R/A RHA, replaced common hepatic artery (RCHA) and CAS. The presence or absence of aberrant hepatic arteries was evaluated using CTA, conventional angiography and surgery as the standards of reference. For CAS, we used CTA and conventional angiography as the reference standards. The sensitivity, specificity and accuracy of the diagnosis of these arterial variants on MDCT were calculated using the following definitions. True positives included patients with arterial variants identified by both reference standards and MDCT. True negatives included patients without arterial variants identified by both reference standards and MDCT. False positives included patients without arterial variants identified by reference standards, but positive indication by MDCT. False negatives included patients with arterial variants identified with reference standards, but received a negative indication by MDCT.

RESULTS

During the study period, 932 patients with pancreatic head and peri-ampullary tumors were evaluated with preoperative routine contrast-enhanced MDCT. Among them, 376 patients underwent pancreaticoduodenectomy, 122 received CTA and 102 received conventional angiography. Four hundred and seventy-four patients were excluded from the study that evaluated the accuracy of routine MDCT identification of aberrant RHA. Seven hundred and fifty-one patients were excluded from the study assessing the accuracy of routine MDCT in identifying CAS. Hence, 458 patients who underwent CTA, conventional angiography or surgery and 181 patients who received CTA or conventional angiography met the inclusion criteria of this study (Figure 1). The demographic and clinical characteristics of the patients are shown in Table 1.

The diagnostic accuracy results for routine MDCT in identifying arterial variants compared with the gold standards are summarized in Table 2. Among the 458 patients, 54 were confirmed to have aberrant RHA, with an incidence of 11.8%. MDCT demonstrated a sensitivity of 96.3%, a specificity of 98.8% and an overall diagnostic accuracy of 98.5%. A replaced right hepatic artery (RRHA) was found in 6.3% (29/458) of patients (Figure 2). MDCT demonstrated a sensitivity of 89.7%, a specificity of 99.1% and a diagnostic accuracy of 98.5%. Three patients with false-negative MDCT were all misdiagnosed with accessory right hepatic arteries (ARHA), and the four false positive results were as follows: two cases with ARHA were misdiagnosed as RRHA and two cases without aberrant RHA were misdiagnosed as RRHA. ARHA was found in 3.3% (15/458) of patients (Figure 3). MDCT identified 11/15 patients with ARHA and gave a false positive result in six of 443 patients without ARHA. Therefore, the sensitivity, specificity, positive

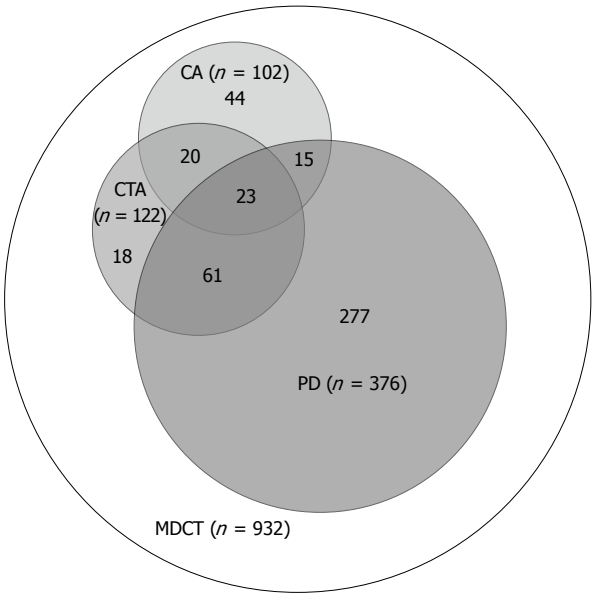

Figure 1 Patients included (grey) in the analysis and those excluded (white). PD: Pancreaticoduodenectomy; CTA: Computed tomography angiography; CA: Conventional angiography; MDCT: Multidetector computed tomography.

Table 1 Patient baseline characteristics *n* (%)

Characteristics	Patients assessed for aberrant RHA (*n* = 458)	Patients assessed for CAS (*n* = 181)
Age, (yr)	57.2 ± 12.9	57.3 ± 13.6
Male	242 (52.8)	102 (56.4)
Unresectable disease	82 (17.9)	82 (45.3)
Diagnosis		
Pancreatic adenocarcinoma	291 (63.5)	150 (82.9)
Pancreatic cystic neoplasm	34 (7.4)	6 (3.3)
Pancreatic neuroendocrine tumor	14 (3.1)	4 (2.2)
Ampullary adenocarcinoma	31 (6.8)	9 (5.0)
Duodenal adenocarcinoma	19 (4.1)	1 (0.6)
Others	69 (15.1)	11 (6.1)
Surgery		
Whipple	318 (69.4)	87 (48.1)
PPPD	58 (12.7)	12 (6.6)
Palliative bypass	13 (2.8)	4 (2.2)

CAS: Celiac artery stenosis; RHA: Right hepatic artery.

predictive value (PPV) and negative predictive value (NPV) of MDCT for detecting ARHA were 73.3%, 98.6%, 64.7% and 99.1%, respectively. RCHA was found in 2.2% (10/458) of patients (Figure 4). MDCT showed an accuracy of 100%, sensitivity of 100% and specificity of 100%.

Among the 181 patients scheduled for evaluation of CAS (Figure 5), twelve (6.6%) demonstrated positive results by CTA and conventional angiography. Three patients had false positive results and five had false negative results by routine MDCT. Thus, the sensitivity, specificity, PPV and NPV of MDCT for detecting CAS were 58.3%, 98.2%, 70% and 97.1%, respectively.

DISCUSSION

Visceral ischemia after pancreaticoduodenectomy caused by intraoperative hepatic artery injury or pre-existing CAS is a rare, but potentially serious, complication[5,10]. The prevention and adequate management of these ischemic complications are challenging. Many studies have highlighted the importance of identifying peri-pancreatic arterial variants before pancreaticoduodenectomy[12-16]. Variant hepatic and celiac arterial anatomy have been reported in 49% of the patients with pancreatic or hepatobiliary neoplasms[17]. Intra-operative palpation for the presence of the aberrant hepatic artery can be unreliable when the patient has prior surgery or is obese, when there is local inflammation, enlarged lymph nodes or an existing biliary stent. Despite advances in imaging technology, cross sectional CT scans are commonly used in the initial detection of peri-ampullary tumors, and are often performed to determine tumor resectability and stage[18].

Few studies have investigated routine MDCT without arterial reconstruction, which is commonplace in medical practice, in the assessment of peri-pancreatic arterial variants prior to surgery. Although conventional angiography is obsolete in primary staging, it is occasionally used to evaluate peri-pancreatic vessels before surgery. In our institution, we used this invasive technique mainly for multiphase regional intra-arterial infusion chemotherapy for pancreatic cancer[1,11]. Compared with routine arteriography, MDCT is noninvasive and directly visualizes the pancreas and the tumor. The introduction of modern MDCT scanners has greatly advanced the role of CTA in clinical practice and makes visualization of small visceral vessels possible[19]. In this study, we found that MDCT without arterial reconstruction could detect right hepatic arterial variants before pancreatic surgery very accurately. The result is consistent with other reports, which demonstrated that axial spiral CT scan (8-mm section thickness, 4-mm overlapping reconstructions) had a sensitivity, specificity and accuracy of 96%, 87% and 88%, respectively, for detecting aberrant hepatic arteries[20].

Turrini and colleagues[6] analyzed preoperative CT scans and showed that the detection rate of R/A RHA was 29% by radiologists and 51% by surgeons. Their results revealed that surgeons were more likely to identify aberrant RHA than radiologists on a CT scan. The reason for such a low detection rate may relate to technical aspects, such as the small caliber of R/A RHA identified on thick-cut CT images and not enough attention being paid to the arterial variants. Pre-operative radiological information about peri-pancreatic arterial variations was not always included. Although CT image reconstruction could provide preoperative vascular information, it was only done in a small number of patients. The excessive workload of radiologists, lack of interest in some cases, and lack of consolidated multidisciplinary teams may explain why on many occasions, image reconstruction was not available. In the present study, we found that aberrant RHA was usually well demonstrated with routine

Table 2 Diagnostic accuracy of routine multidetector computed tomography in preoperative identification of arterial variants

Arterial variants	Sensitivity	Specificity	Accuracy	PPV	NPV
Aberrant RHA	96.3 (86.2-99.4)	98.8 (97-99.5)	98.5	91.2 (80-96.7)	99.5 (98-99.9)
RRHA	89.7 (71.5-97.3)	99.1 (97.5-99.7)	98.5	86.7 (68.4-95.6)	99.3 (97.8-99.8)
ARHA	73.3 (44.8-91.1)	98.6 (96.9-99.4)	97.8	64.7 (38.6-84.7)	99.1 (97.5-99.7)
RCHA	100 (65.5-100)	100 (98.9-100)	100	100 (65.5-100)	100 (98.9-100)
CAS	58.3 (28.6-83.5)	98.2 (94.5-99.5)	95.6	70 (35.4-91.9)	97.1 (92.9-98.9)

RCHA: Replaced common hepatic artery; ARHA: Accessory right hepatic artery; RHA: Right hepatic artery; CAS: Celiac artery stenosis; RRHA: Replaced right hepatic artery; PPV: Positive predictive value; NPV: Negative predictive value.

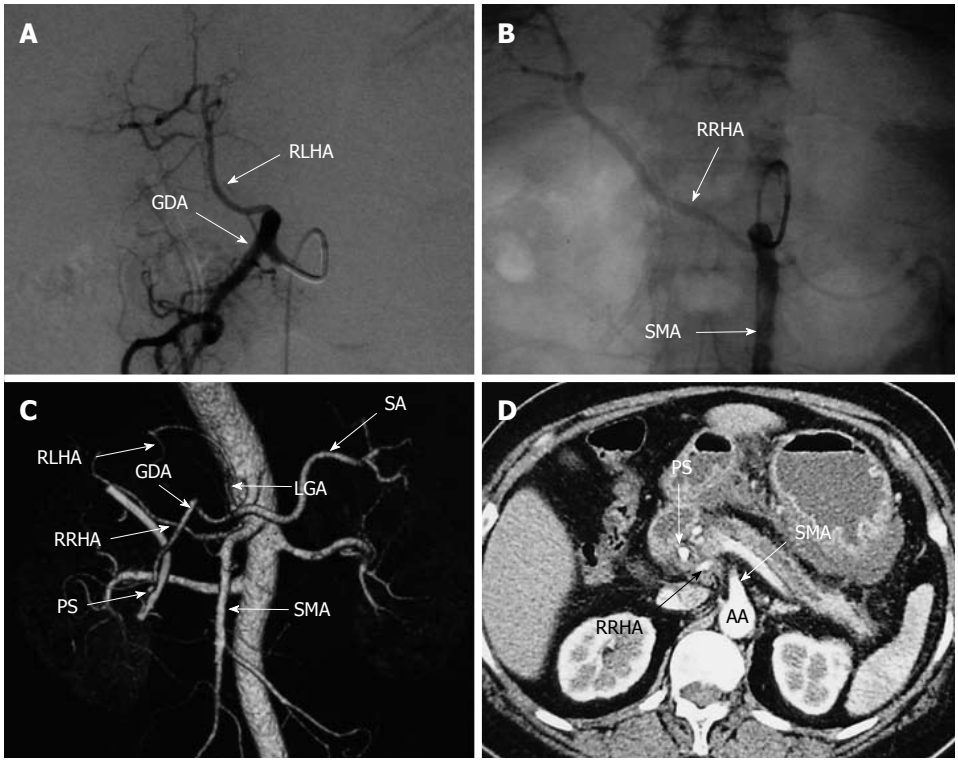

Figure 2 Sixty-year-old woman with replaced right hepatic artery and replaced left hepatic artery. A: Visceral angiogram with celiac injection demonstrating an RLHA; B: Visceral angiogram with SMA injection revealed an RRHA originating from the proximal SMA; C: Volume-rendered reformatted image depicting Michels type Ⅳ; D: MDCT showing an RRHA originating from the SMA traveling behind the portal vein. RRHA: Replaced right hepatic artery; RLHA: Replaced left hepatic artery; SMA: Superior mesenteric artery; SA: Splenic artery; GDA: Gastroduodenal artery; LGA: Left gastric artery; PS: Plastic stent; AA: Abdominal aorta.

MDCT by careful examination of the portacaval space, as well as the SMA and celiac axis. RRHA was shown originating from the SMA, passing behind the superior mesenteric vein (SMV), traveling through or behind the pancreatic head and entering the hepatoduodenal ligament. ARHA was observed as a vessel following a similar path as RRHA, and was found to be an additional vessel to the native RHA. RCHA, which originated from the SMA, was revealed to run behind or cross anteriorly to the PV/SMV, either within or along the ventral side of the pancreas, with no CHA found arising from the celiac axis. In compliance with these rules, we made errors in only a few patients when analyzing the CT images *via* picture archiving and communication systems (PACS). A dilated inferior pancreaticoduodenal artery arising from SMA may also be seen within the portacaval space; however, this is usually found in patients with CAS or arteriovenous malformation. The main difficulty in identifying an aberrant hepatic artery is the close proximity from which the celiac trunk and SMA originate on the aorta.

Previously reported incidences of CAS ranged from 2% to 49.7%[4]. In our study, CTA and conventional angiography detected CAS in twelve (6.6%) of 181 patients, with incidence similar to previous studies[5,21]. Park *et al*[21] showed that the incidence of celiac axis stenosis in an asymptomatic Korean population was 7.3%. Gaujoux and colleagues[5] detected CAS in 11% of patients who underwent pancreaticoduodenectomy. The lower incidence of CAS in the present study may partly reflect the lower incidence of atherosclerosis in the Chinese population compared with Westerners. Few studies have reported the value of MDCT to detect and characterize CAS. In a prospective study, the sensitivity of MDCT with arterial reconstruction to detect significant CAS was 96% with only one false

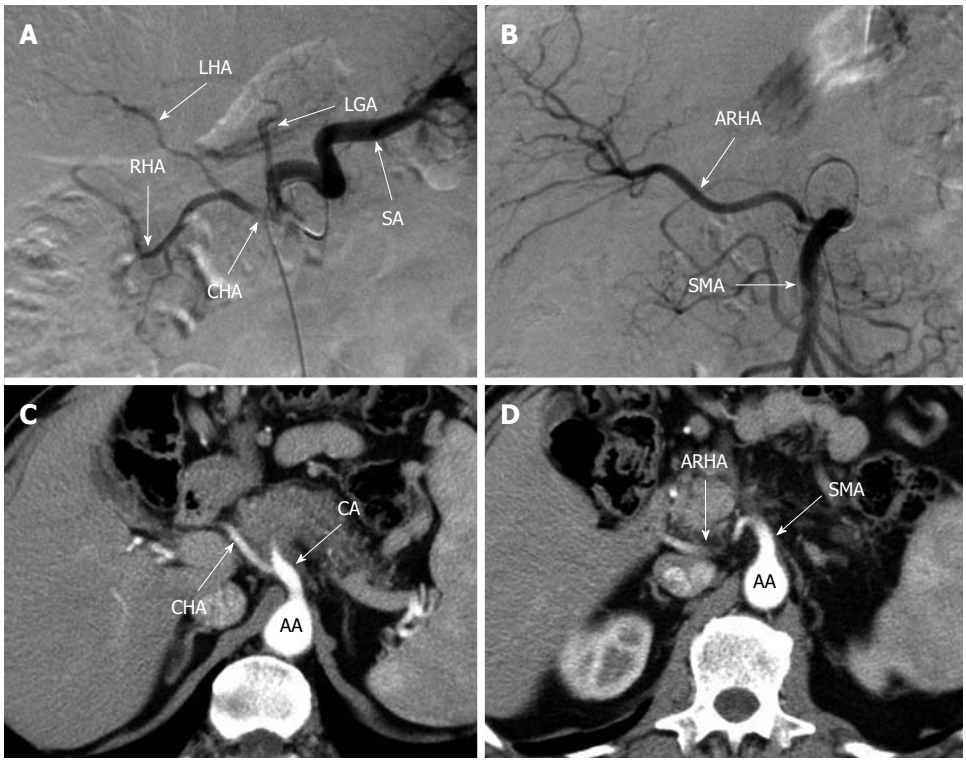

Figure 3 Sixty-five-year-old man with an accessory right hepatic artery. Conventional angiography with celiac injection (A) demonstrating a classic hepatic arterial anatomy, and one with SMA injection (B) showing an ARHA originating from the proximal SMA. MDCT showing the CHA arising from the CA (C), and an ARHA originating from the SMA, traveling behind the pancreatic head (D). ARHA: Accessory right hepatic artery; CHA: Common hepatic artery; SA: Splenic artery; LGA: Left gastric artery; RHA: Right hepatic artery; LHA: Left hepatic artery; SMA: Superior mesenteric artery; AA: Abdominal aorta; CA: Celiac axis.

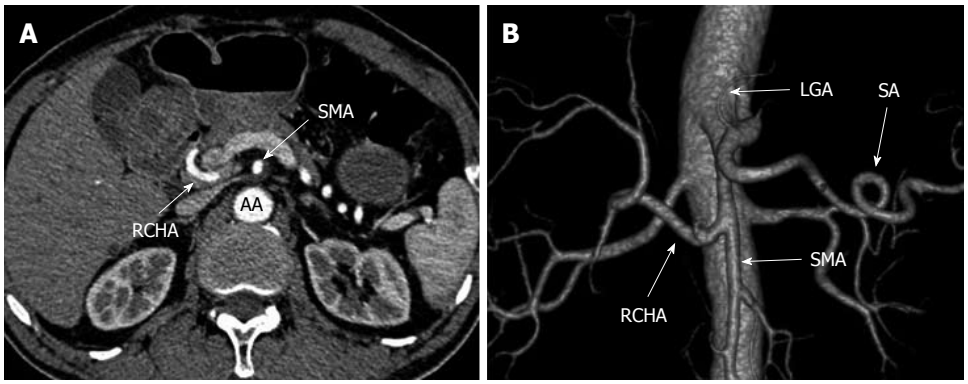

Figue 4 Sixty-eight-year-old man with a replaced common hepatic artery. A: MDCT demonstrating an RCHA originating from the SMA, running behind the superior mesenteric vein, with no common hepatic artery found arising from the celiac axis; B: Volumetric three-dimensional CT angiography demonstrating Michels type Ⅸ. RCHA: Replaced common hepatic artery; MDCT: Multidetector computed tomography; CT: Computed tomography; SMA: Superior mesenteric artery; SA: Splenic artery; LGA: Left gastric artery; AA: Abdominal aorta.

negative[5]. Typically, a fishhook appearance is seen in sagittal reformatted images in patients with significant CAS. However, this appearance cannot be visualized on a transverse section CT scan, which demonstrates CAS as a stenosis at the origin of the celiac trunk, or a large arcade from the pancreaticoduodenal arcade. Our study used routine MDCT without arterial reconstruction, and revealed a sensitivity of 58.3%, which was significantly lower than that of the above study. The high specificity in our study indicated that routine MDCT without arterial reconstruction had a high rate of missed diagnoses, with few misdiagnoses of CAS. The reason for the low sensitivity may be that only high degree stenosis (hemodynamically significant) was demonstrated, while mild stenosis was hard to see at the origin of the celiac artery. Considering its limitation for evaluating CAS, we suggest that angiography should be performed for patients scheduled for pancreaticduodenectomy who have extensive pancreatic arterial collateralization on preoperative CT imaging[22].

In the present study, we only investigated the main arteries surrounding the pancreatic head, as these vessels were clinically relevant for pancreatic surgery. Variations in the pancreaticoduodenal arcade, gastric arteries,

Figure 5 Sixty-five-year-old man with celiac axis stenosis. Computed tomography scan of the abdomen (A) and celiac artery angiogram (B) revealing stenosis of the celiac axis (arrow). (C) Superior mesenteric arteriogram demonstrating retrograde filling of the hepatic artery through a dilatation of the pancreaticoduodenal arcade.

gastroepiploic arteries and portosplenic confluence are quite rare and less important for pancreatic surgery[17]. The current study included a large number of patients, and all patients underwent arteriography or surgery (reference standard). Nonetheless, one of the limitations of this study is that it was performed in a single center, albeit one highly experienced in pancreatic CT scans. Thus, the results need to be confirmed in multicenter prospective studies. Another limitation is that we did not assess the differences in the identification rate of arterial variants among various generations of CT scanners. Usui *et al*[23] reported no significant differences in the detection of arteries surrounding the stomach between 8-channel and 16-channel MDCT. We believe this also not likely to generate differences in our results.

Our study demonstrated that routine MDCT without arterial reconstruction is very useful to evaluate aberrant RHA in the preoperative planning of pancreatic surgery, although its usefulness is limited for evaluating CAS. In the case of pancreaticoduodenectomy, preoperative detection of CAS is still advisable, despite its low sensitivity. It is recommended that surgeons and radiologists be alerted to the importance of arterial variants on preoperative CT scans in patients who are scheduled for pancreaticoduodenectomy.

ACKNOWLEDGMENTS

We thank the Radiological Department of Huashan Hospital for their superb technical assistance.

COMMENTS

Background

Peri-pancreatic arterial variations, such as hepatic artery anomalies and celiac artery stenosis (CAS), add to the difficulty of pancreaticoduodenectomy, and may occasionally lead to potentially disastrous complications.

Research frontiers

Routine multidetector computed tomography (MDCT) is the standard examination for the initial detection and characterization of pancreatic tumors. The current important issue regarding the accuracy of preoperative MDCT without arterial reconstruction to identify arterial variants in patients scheduled for pancreaticoduodenectomy remains to be elucidated.

Innovations and breakthroughs

Although computed tomography (CT) angiography and conventional angiography are effective imaging tools to evaluate the vascular architecture surrounding the pancreas, they are often not available because of the excessive workload of radiologists, lack of interest in some cases, lack of consolidated multidisciplinary teams, or their invasive natures. Few studies have investigated the ability of routine MDCT without arterial reconstruction, which is more commonplace in usual medical practice, in the assessment of peri-pancreatic arterial variants before surgery. The present study demonstrated that routine MDCT was highly accuracy, sensitive and specific to detect aberrant right hepatic arteries, although it was limited by a lower sensitivity to detect CAS.

Applications

The study results suggested that routine MDCT without arterial reconstruction is useful to evaluate aberrant right hepatic arteries in the preoperative planning of pancreaticoduodenectomy. Surgeons and radiologists should be alerted to the importance of arterial variants on preoperative CT scans in patients scheduled for the Whipple procedure.

Terminology

Aberrant hepatic arteries are defined as accessory, occurring in addition to the normal arterial supply; or replaced, representing the primary arterial supply to the lobe. CAS, also known as celiac artery compression syndrome, is a relatively common finding. In the presence of CAS, arterial blood supply to the pancreas, liver, stomach, and spleen is sustained *via* a well-developed system of pancreaticoduodenal collateral pathways in most patients.

Peer review

The results in this well-written manuscript adequately support its objective. In some ways, the present study also supports the necessity of multidisciplinary teams for pancreatic surgery.

REFERENCES

1 **Yang F**, Long J, Fu DL, Jin C, Yu XJ, Xu J, Ni QX. Aberrant hepatic artery in patients undergoing pancreaticoduodenectomy. *Pancreatology* 2008; **8**: 50-54 [PMID: 18230918 DOI: 10.1159/000114867]

2 **Biehl TR**, Traverso LW, Hauptmann E, Ryan JA. Preoperative visceral angiography alters intraoperative strategy during the Whipple procedure. *Am J Surg* 1993; **165**: 607-612 [PMID: 8098185 DOI: 10.1016/S0002-9610(05)80444-1]

3 **Rong GH**, Sindelar WF. Aberrant peripancreatic arterial anatomy. Considerations in performing pancreatectomy for malignant neoplasms. *Am Surg* 1987; **53**: 726-729 [PMID: 3425998]

4 **Sakorafas GH**, Sarr MG, Peros G. Celiac artery stenosis: an underappreciated and unpleasant surprise in patients undergoing pancreaticoduodenectomy. *J Am Coll Surg* 2008; **206**: 349-356 [PMID: 18222391 DOI: 10.1016/j.jamcollsurg.2007.09.002]

5 **Gaujoux S**, Sauvanet A, Vullierme MP, Cortes A, Dokmak S, Sibert A, Vilgrain V, Belghiti J. Ischemic complications after pancreaticoduodenectomy: incidence, prevention, and management. *Ann Surg* 2009; **249**: 111-117 [PMID: 19106685 DOI: 10.1097/SLA.0b013e3181930249]

6 **Turrini O**, Wiebke EA, Delpero JR, Viret F, Lillemoe KD, Schmidt CM. Preservation of replaced or accessory right hepatic artery during pancreaticoduodenectomy for adenocarcinoma: impact on margin status and survival. *J Gastrointest Surg* 2010; **14**: 1813-1819 [PMID: 20697832 DOI: 10.1007/s11605-010-1272-1]

7 **Bong JJ**, Karanjia ND, Menezes N, Worthington TR, Lightwood RG. Total gastric necrosis due to aberrant arterial anatomy and retrograde blood flow in the gastroduodenal artery: a complication following pancreaticoduodenectomy. *HPB* (Oxford) 2007; **9**: 466-469 [PMID: 18345296 DOI: 10.1080/13651820701713741]

8 **Murakami Y**, Uemura K, Yokoyama Y, Sasaki M, Morifuji M, Hayashidani Y, Sudo T, Sueda T. Celiac axis occlusion with replaced common hepatic artery and pancreatoduodenectomy. *J Gastrointest Surg* 2004; **8**: 520-522 [PMID: 15120379 DOI: 10.1016/j.gassur.2004.01.003]

9 **Smith SL**, Rae D, Sinclair M, Satyadas T. Does moderate celiac axis stenosis identified on preoperative multidetector computed tomographic angiography predict an increased risk of complications after pancreaticoduodenectomy for malignant pancreatic tumors? *Pancreas* 2007; **34**: 80-84 [PMID: 17198187 DOI: 10.1097/01.mpa.0000240607.49183.7e]

10 **Hackert T**, Stampfl U, Schulz H, Strobel O, Büchler MW, Werner J. Clinical significance of liver ischaemia after pancreatic resection. *Br J Surg* 2011; **98**: 1760-1765 [PMID: 22021030 DOI: 10.1002/bjs.7675]

11 **Jin C**, Yao L, Long J, Fu DL, Yu XJ, Xu J, Yang F, Ni QX. Effect of multiple-phase regional intra-arterial infusion chemotherapy on patients with resectable pancreatic head adenocarcinoma. *Chin Med J* (Engl) 2009; **122**: 284-290 [PMID: 19236805]

12 **Shukla PJ**, Barreto SG, Kulkarni A, Nagarajan G, Fingerhut A. Vascular anomalies encountered during pancreatoduodenectomy: do they influence outcomes? *Ann Surg Oncol* 2010; **17**: 186-193 [PMID: 19838756 DOI: 10.1245/s10434-009-0757-1]

13 **Sulpice L**, Rayar M, Paquet C, Bergeat D, Merdrignac A, Cunin D, Meunier B, Boudjema K. Does an aberrant right hepatic artery really influence the short- and long-term results of a pancreaticoduodenectomy for malignant disease? A matched case-controlled study. *J Surg Res* 2013; **185**: 620-625 [PMID: 24011920 DOI: 10.1016/j.jss.2013.07.015]

14 **Venara A**, Pittet O, Lu TL, Demartines N, Halkic N. Aberrant right hepatic artery with a prepancreatic course visualized prior to pancreaticoduodenectomy. *J Gastrointest Surg* 2013; **17**: 1024-1026 [PMID: 23288717 DOI: 10.1007/s11605-012-2127-8]

15 **Jah A**, Jamieson N, Huguet E, Praseedom R. The implications of the presence of an aberrant right hepatic artery in patients undergoing a pancreaticoduodenectomy. *Surg Today* 2009; **39**: 669-674 [PMID: 19639433 DOI: 10.1007/s00595-009-3947-3]

16 **Stauffer JA**, Bridges MD, Turan N, Nguyen JH, Martin JK. Aberrant right hepatic arterial anatomy and pancreaticoduodenectomy: recognition, prevalence and management. *HPB* (Oxford) 2009; **11**: 161-165 [PMID: 19590642 DOI: 10.1111/j.1477-2574.2009.00037.x]

17 **Winston CB**, Lee NA, Jarnagin WR, Teitcher J, DeMatteo RP, Fong Y, Blumgart LH. CT angiography for delineation of celiac and superior mesenteric artery variants in patients undergoing hepatobiliary and pancreatic surgery. *AJR Am J Roentgenol* 2007; **189**: W13-W19 [PMID: 17579128]

18 **Fishman EK**, Horton KM. Imaging pancreatic cancer: the role of multidetector CT with three-dimensional CT angiography. *Pancreatology* 2001; **1**: 610-624 [PMID: 12120244 DOI: 10.1159/000055871]

19 **Willmann JK**, Weishaupt D, Böhm T, Pfammatter T, Seifert B, Marincek B, Bauerfeind P. Detection of submucosal gastric fundal varices with multi-detector row CT angiography. *Gut* 2003; **52**: 886-892 [PMID: 12740347 DOI: 10.1136/gut.52.6.886]

20 **Chambers TP**, Fishman EK, Bluemke DA, Urban B, Venbrux AC. Identification of the aberrant hepatic artery with axial spiral CT. *J Vasc Interv Radiol* 1995; **6**: 959-964 [PMID: 8850677 DOI: 10.1016/S1051-0443(95)71222-2]

21 **Park CM**, Chung JW, Kim HB, Shin SJ, Park JH. Celiac axis stenosis: incidence and etiologies in asymptomatic individuals. *Korean J Radiol* 2001; **2**: 8-13 [PMID: 11752963 DOI: 10.3348/kjr.2001.2.1.8]

22 **Yang F**, Jin C, Fu D. Celiac axis compression syndrome and pancreatic head cancer. *Pancreatology* 2014; **14**: 310-311 [PMID: 25207337 DOI: 10.1016/j.pan.2014.05.795]

23 **Usui S**, Hiranuma S, Ichikawa T, Maeda M, Kudo SE, Iwai T. Preoperative imaging of surrounding arteries by three-dimensional CT: is it useful for laparoscopic gastrectomy? *Surg Laparosc Endosc Percutan Tech* 2005; **15**: 61-65 [PMID: 15821615]

P- Reviewer: Symeonidis NG, Tsuchiya A **S- Editor**: Qi Y
L- Editor: Stewart G **E- Editor**: Wang CH

World Journal of Gastroenterology

Submit a Manuscript: http://www.wjgnet.com/esps/
Help Desk: http://www.wjgnet.com/esps/helpdesk.aspx
DOI: 10.3748/wjg.v21.i3.977

World J Gastroenterol 2015 January 21; 21(3): 977-981
ISSN 1007-9327 (print) ISSN 2219-2840 (online)

ORIGINAL ARTICLE

Prospective Study

Paclitaxel-eluting balloon dilation of biliary anastomotic stricture after liver transplantation

Anna Hüsing, Holger Reinecke, Vito R Cicinnati, Susanne Beckebaum, Christian Wilms, Hartmut H Schmidt, Iyad Kabar

Anna Hüsing, Vito R Cicinnati, Susanne Beckebaum, Christian Wilms, Hartmut H Schmidt, Iyad Kabar, Department of Transplant Medicine, University Hospital Münster, 48149 Münster, Germany
Holger Reinecke, Division of Angiology, Department of Cardiology and Angiology, University Hospital Münster, 48149 Münster, Germany
Author contributions: Hüsing A, Reinecke H, Schmidt HH and Kabar I designed the study; Kabar I, Wilms C and Hüsing A performed the study; Hüsing A, Cicinnati VR, Wilms C, Beckebaum S and Kabar I collected the patient data; Hüsing A, Beckebaum S, Cicinnati VR, Reinecke H and Kabar I analyzed the data; Kabar I, Hüsing A, Cicinnati VR and Schmidt HH wrote the paper.

Correspondence to: Iyad Kabar, MD, Department of Transplant Medicine, University Hospital Münster, Albert-Schweitzer-Campus 1, Gebäude A14, 48149 Münster, Germany. iyad.kabar@ukmuenster.de
Telephone: +49-251-8344957
Fax: +49-251-8357771
Received: July 8, 2014
Peer-review started: July 9, 2014
First decision: August 15, 2014
Revised: September 2, 2014
Accepted: October 14, 2014
Article in press: October 15, 2014
Published online: January 21, 2015

Abstract

AIM: To investigate the safety and effectiveness of endoscopic therapy with a paclitaxel-eluting balloon (PEB) for biliary anastomotic stricture (AS) after liver transplantation (LT).

METHODS: This prospective pilot study enrolled 13 consecutive eligible patients treated for symptomatic AS after LT at the University Hospital of Münster between January 2011 and March 2014. The patients were treated by endoscopic therapy with a PEB and followed up every 8 wk by endoscopic retrograde cholangiopancreatography (ERCP). In cases of re-stenosis, further balloon dilation with a PEB was performed. Follow-up was continued until 24 mo after the last intervention.

RESULTS: Initial technical feasibility, defined as successful balloon dilation with a PEB during the initial ERCP procedure, was achieved in 100% of cases. Long-term clinical success (LTCS), defined as no need for further endoscopic intervention for at least 24 mo, was achieved in 12 of the 13 patients (92.3%). The mean number of endoscopic interventions required to achieve LTCS was only 1.7 ± 1.1. Treatment failure, defined as the need for definitive alternative treatment, occurred in only one patient, who developed recurrent stenosis with increasing bile duct dilatation that required stent placement.

CONCLUSION: Endoscopic therapy with a PEB is very effective for the treatment of AS after LT, and seems to significantly shorten the overall duration of endoscopic treatment by reducing the number of interventions needed to achieve LTCS.

Key words: Liver transplantation; Anastomotic stricture; Endoscopic therapy; Endoscopic retrograde cholangiopancreatography; Balloon dilation; Paclitaxel-eluting balloon

Core tip: Biliary anastomotic stricture is common after liver transplantation and can significantly impair both organ and patient survival. Endoscopic treatment of an anastomotic stricture usually requires many interventions before long-term resolution is achieved. This study investigated the safety and efficacy of an innovative approach using endoscopic therapy with a paclitaxel-eluting balloon for the treatment of biliary anastomotic stricture after liver transplantation. Our data are very promising and show excellent long-term results. Furthermore, use of a paclitaxel-eluting balloon seems to reduce the number of endoscopic interventions needed to achieve sustained resolution of the stricture.

Hüsing A, Reinecke H, Cicinnati VR, Beckebaum S, Wilms C, Schmidt HH, Kabar I. Paclitaxel-eluting balloon dilation of biliary anastomotic stricture after liver transplantation. *World J Gastroenterol* 2015; 21(3): 977-981 Available from: URL: http://www.wjgnet.com/1007-9327/full/v21/i3/977.htm DOI: http://dx.doi.org/10.3748/wjg.v21.i3.977

INTRODUCTION

Biliary complications are common after liver transplantation (LT) because the vascular supply to the biliary tract is easily injured, and such complications are a major cause of morbidity and graft failure. Biliary complications are reported to occur in 10%-25% of LT recipients, and may include stricture, leakage, and formation of biliary stones, casts, and sludge[1-3]. Biliary stricture is one of the most commonly reported complications after LT and can be divided into two types: anastomotic stricture (AS) and non-anastomotic stricture. This categorization helps to predict the response to treatment, with AS responding more favorably to endoscopic intervention than non-anastomotic stricture[3,4].

AS is the most frequent biliary complication after LT, accounting for 8%-20% of all complications. Endoscopic retrograde cholangiopancreatography (ERCP) is considered to be the gold standard for diagnosis and treatment of biliary complications after LT. Current standard endoscopic interventions for AS include balloon dilation and stent placement. Most patients require repeated endoscopic procedures for 12 to 24 mo, during which they undergo an average of 5-6 endoscopic interventions. The reported success rate of balloon dilation alone is about 40%, and the reported overall long-term success rate after endoscopic interventions is 75%-80%. However, AS recurrence after successful endoscopic treatment has been reported in up to 30% of cases[5-7].

In recent years, fully covered self-expandable metal stents have been used to treat biliary strictures after LT when standard endoscopic treatment failed. Treatment with such stents has a success rate of nearly 80%, but also has a high complication rate of up to 47%, mainly due to stent migration, stent occlusion, and *de novo* stricture formation[1,8,9].

New treatment modalities are needed to reduce procedure-related morbidity and the overall duration of endoscopic treatment, as well as to improve long-term results. The short-term outcome data of this study published in 2012 were very promising[10]. The aim of this pilot study was to evaluate the long-term safety and effectiveness of endoscopic therapy with a paclitaxel-eluting balloon (PEB) for AS after LT.

MATERIALS AND METHODS

This prospective study was conducted between January 2011 and March 2014 in the Department of Transplant Medicine, University Hospital of Münster. Thirteen consecutive eligible patients were enrolled between January 2011 and September 2011, and follow-up was performed until March 2014.

All patients gave written informed consent, and the study was conducted in accordance with the guidelines of the Declaration of Helsinki (2004 revision). The study protocol was finalized after consultation with the local institutional review board.

All patients with newly diagnosed AS after LT who had undergone end-to-end choledochocholedochostomy were eligible for inclusion in the study. Patients who had undergone choledochojejunostomy were excluded.

AS was defined as a narrowing of the bile duct, predominantly at the anastomotic site, with markedly reduced passage of contrast material observed on fluoroscopy during ERCP. ERCP was performed if there were clinical, biochemical, or histological signs of cholestasis, or dilated bile ducts on imaging examinations (ultrasonography, computed tomography, or magnetic resonance tomography). Four of the 13 patients (30.8%) had dilated bile ducts on non-invasive imaging examinations.

Endoscopic procedure

ERCP was performed using a therapeutic duodenoscope (TJF-180V, Olympus Corp., Tokyo, Japan) under conscious sedation (midazolam and propofol, with or without opiates) and antibiotic prophylaxis (ciprofloxacin 750 mg orally 2 h before and 6 h after the procedure). The bile duct was accessed using a sphincterotome (TriTome, TRI 20, Cook Medical, Winston-Salem, NC, United States) and a wire (0.035 inches, THSF-35-480, Cook Medical) to guide cannulation. Cholangiography was performed to assess the biliary anastomosis. The guidewire was then advanced through the stricture.

If AS was diagnosed, endoscopic treatment was performed, comprising sphincterotomy followed by dilation with a PEB (DIOR paclitaxel coated coronary balloon dilatation catheter, paclitaxel 3 μg/mm^2; Eurocor, Bonn, Germany). The PEB was coated with a 1:1 mixture of paclitaxel and shellac that prevented release

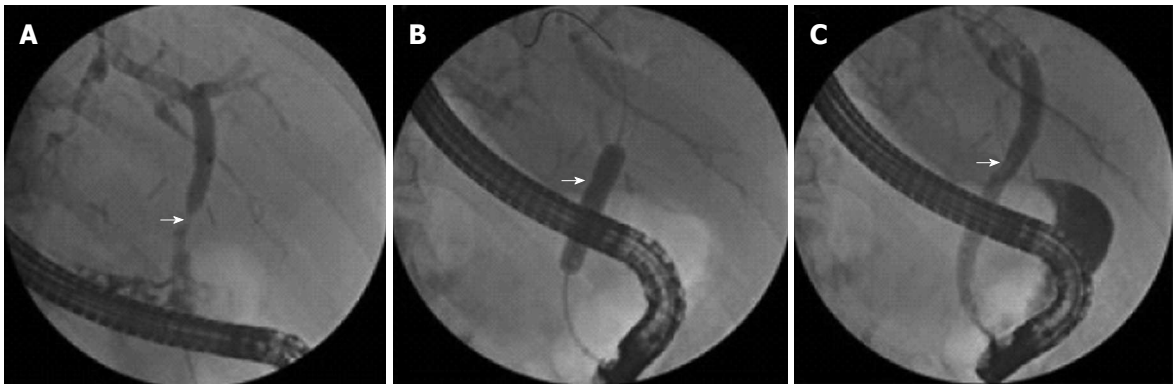

Figure 1 Endoscopic therapy for a biliary anastomotic stricture. A: Anastomotic stricture after liver transplantation (arrow); B: The inflated balloon has a waist at the narrowest part of the stricture (arrow); C: Resolution of the stricture after balloon dilation.

Table 1 Laboratory parameters

	Before intervention	7 d after intervention	24 mo after last intervention
Bilirubin (reference value < 1.2 mg/dL)	6.8 ± 4.1	2.2 ± 1.3	1.4 ± 0.6
GPT (reference value 10-35 U/L)	149.1 ± 120.1	51.5 ± 21.3	35.1 ± 3.9
GGT (reference value < 39 U/L)	614.5 ± 330.0	107.1 ± 62.8	37.7 ± 10.1

GPT: Glutamic-pyruvic transaminase; GGT: Gamma-glutamyl transferase.

of paclitaxel in the working channel of the endoscope. Contact of the hydrophilic shellac mixture with a body fluid such as bile opens the structure to allow pressure-induced release of paclitaxel on the inflated balloon. The PEB was inflated at the anastomotic site to a pressure of up to 12 bar, and left in place for 30 s (Figure 1). After the initial balloon dilation, ERCP was performed every 8 wk to re-evaluate the stricture. If cholangiography showed a patent anastomosis, no further endoscopic treatment was performed. If the stricture persisted, further dilation with a PEB was performed. Follow-up was continued until 24 mo after the last intervention.

Definitions and statistical analysis

The main outcome parameter of this prospective study was long-term clinical success (LTCS), defined as a period of at least 24 mo without the need for further endoscopic intervention, confirmed by the absence of stricture recurrence on follow-up ERCP examinations, laboratory test results indicating cholestasis, or clinical signs of jaundice or cholangitis. The secondary outcome parameters were initial technical feasibility, sustained clinical success (SCS), and treatment failure.

Initial technical feasibility was defined as successful advancement of a guidewire through the AS followed by balloon dilation during the initial ERCP procedure. SCS was defined as a period of at least 6 mo with no need for further endoscopic intervention, confirmed by the absence of stricture recurrence on follow-up ERCP examinations. Treatment failure was defined as the need for definitive alternative treatment at any time during the follow-up period, such as stent placement, percutaneous transhepatic drainage, or surgical intervention.

Descriptive statistical analyses were performed. Data are presented as the mean ± SD. All statistical analyses were performed using SPSS version 20 for Windows.

RESULTS

A total of 13 patients (2 women, 11 men, mean age 50.4 ± 13.8 years) who were referred for endoscopic treatment of newly diagnosed AS after LT were included in the study. The mean time from LT to the initial ERCP procedure was 9.4 ± 3.2 mo. The indications for LT were alcoholic cirrhosis (n = 5), hepatitis B virus infection (n = 2), hepatitis C virus infection (n = 2), hepatocellular carcinoma (n = 3), and primary biliary cirrhosis (n = 1).

The initial technical feasibility rate was 100%, and no intra-procedural complications were recorded. Liver enzyme levels and cholestasis parameters decreased after the initial procedure in all patients (Table 1). Two patients developed acute cholangitis within 3 d after the last intervention, which resolved after antibiotic therapy with imipenem. There were no cases of post-ERCP pancreatitis. The mean follow-up period was 30.3 ± 3.3 mo. SCS was achieved in 12 of 13 patients (92.3%): after one dilation in nine patients (69%), after two dilations in one patient, and after three dilations in two patients. Despite initial technical feasibility, the remaining patient developed AS recurrence with increasing bile duct

dilatation proximal to the stenosis after three dilations with a PEB, and eventually underwent conventional stent placement. This case was considered to be a treatment failure. AS recurrence after SCS was observed in 2/12 patients (16.6%). The time interval between the initial balloon dilation and AS recurrence was 8.89 ± 0.63 mo. In each of these two patients, one additional dilation was needed to achieve LTCS. LTCS was eventually achieved in all 12 patients (92.3%) who achieved SCS, after a mean of 1.7 ± 1.1 balloon dilations.

After successful endoscopic treatment of the stenosis, the bilirubin and liver enzyme levels decreased over time in all patients (Table 1).

DISCUSSION

Biliary tract complications are common after LT, and present a therapeutic challenge for endoscopists. Endoscopic intervention is currently the gold standard treatment for AS after LT[1-3], but the optimal treatment strategy for this complication is still unclear. Repeated endoscopic interventions over a prolonged treatment period of up to 24 mo are usually needed to achieve SCS[4-7]. Moreover, there are few data available regarding the rate of AS recurrence after SCS[4]. When endoscopic therapy is unsuccessful, surgical treatment is indicated[2,11].

The limitations of the currently available treatment options clearly demonstrate the need for development of new interventions. Considering the fibroproliferative aspect of AS, a therapeutic approach that combines balloon dilation with application of an antiproliferative agent directly to the site of the stenosis seems logical. The mitotic inhibitor paclitaxel has antiproliferative effects as well as antifibrotic effects *via* inhibition of transforming growth factor-beta/Smad activity[12,13]. Use of PEBs has previously been shown to be clinically safe and effective for the treatment of coronary and femoropopliteal arterial stenoses[14,15].

This is the first study to investigate endoscopic treatment with a PEB for AS after LT. SCS was achieved in 92.3% of cases, and was achieved after only one balloon dilation in 69% of cases. AS recurrence after SCS occurred in 16.6% of patients, which is much less frequent than the previously reported recurrence rate of about 30%[5-7]. All cases of AS recurrence were successfully treated by repeat balloon dilation. LTCS was achieved in 92.3% of cases, after 1.7 ± 1.1 balloon dilations. This is a notable achievement in comparison with previous reports that five or six interventions were generally required to achieve sustained resolution of AS[1-3,5].

Successful endoscopic treatment was associated with significantly decreased levels of bilirubin and liver enzymes (Table 1).

In this pilot study, endoscopic therapy with a PEB achieved a high rate of LTCS and a low rate of AS recurrence after SCS, indicating very promising outcomes for our treatment approach for AS after LT. Use of a PEB seems to reduce the number of interventional procedures required to achieve LTCS, thereby shortening the overall duration of endoscopic treatment. A reduced number of endoscopic interventions may also result in a decreased overall complication rate. Larger randomized clinical trials are needed to confirm our findings.

COMMENTS

Background

Biliary anastomotic stricture (AS) is an important cause of morbidity and graft failure after liver transplantation (LT). The reported success rate of endoscopic therapy for AS after LT is variable, and the optimal treatment for this complication is still unclear.

Research frontiers

Patients with AS after LT usually undergo repeated endoscopic interventions, with balloon dilation with or without stent implantation, over a long time period. However, the reported success rate of balloon dilation alone is relatively low, and stent placement has a high complication rate.

Innovations and breakthroughs

Paclitaxel is an antifibrotic and antiproliferative agent. As AS after LT results from inflammatory fibrosis, this study investigated the effectiveness of endoscopic therapy with a paclitaxel-eluting balloon (PEB) for the treatment of such strictures. This is the first study to investigate the use of a PEB for the treatment of AS after LT.

Applications

The results of this study show that endoscopic therapy with a PEB may significantly reduce the number of interventions required to achieve complete resolution of AS after LT, thereby shortening the overall duration of endoscopic therapy.

Terminology

After LT, AS may develop at the site of bile duct anastomosis. AS is caused by fibrosis during healing, and most cases develop within the first year after LT. Paclitaxel is a mitotic inhibitor that is used as a chemotherapeutic agent for the treatment of malignant tumors. Because of its antiproliferative effects, paclitaxel is also used to treat and prevent coronary restenosis.

Peer review

In this paper, the authors reported the results of an extended follow up of their series of patients, included in a previous publication from the same group. Although new information is limited, the paper is interesting and well written.

REFERENCES

1 **Ryu CH**, Lee SK. Biliary strictures after liver transplantation. *Gut Liver* 2011; **5**: 133-142 [PMID: 21814591 DOI: 10.5009/gnl.5.133]

2 **Pascher A**, Neuhaus P. Bile duct complications after liver transplantation. *Transpl Int* 2005; **18**: 627-642 [PMID: 15910286 DOI: 10.1111/tri.18.627]

3 **Williams ED**, Draganov PV. Endoscopic management of biliary strictures after liver transplantation. *World J Gastroenterol* 2009; **15**: 3725-3733 [PMID: 19673012 DOI: 10.3748/wjg.15.3725]

4 **Kao D**, Zepeda-Gomez S, Tandon P, Bain VG. Managing the post-liver transplantation anastomotic biliary stricture: multiple plastic versus metal stents: a systematic review. *Gastrointest Endosc* 2013; **77**: 679-691 [PMID: 23473000 DOI: 10.1016/j.gie.77.679]

5 **Zoepf T**, Maldonado-Lopez EJ, Hilgard P, Malago M, Broelsch CE, Treichel U, Gerken G. Balloon dilatation vs. balloon dilatation plus bile duct endoprostheses for treatment of anastomotic biliary strictures after liver transplantation. *Liver Transpl* 2006; **12**: 88-94 [PMID: 16382450 DOI: 10.1002/lt.12.88]

6 **Kulaksiz H**, Weiss KH, Gotthardt D, Adler G, Stremmel W, Schaible A, Dogan A, Stiehl A, Sauer P. Is stenting necessary after balloon dilation of post-transplantation biliary strictures? Results of a prospective comparative study. *Endoscopy* 2008; **40**: 746-751 [PMID: 18702031 DOI: 10.1055/s.40.746]

7 **Costamagna G**, Pandolfi M, Mutignani M, Spada C, Perri V.

Long-term results of endoscopic management of postoperative bile duct strictures with increasing numbers of stents. *Gastrointest Endosc* 2001; **54**: 162-168 [PMID: 11474384 DOI: 10.1016/j.gie.54.162]

8 **Sauer P**, Chahoud F, Gotthardt D, Stremmel W, Weiss KH, Büchler M, Schemmer P, Weitz J, Schaible A. Temporary placement of fully covered self-expandable metal stents in biliary complications after liver transplantation. *Endoscopy* 2012; **44**: 536-538 [PMID: 22370701 DOI: 10.1055/s.44.536]

9 **Traina M**, Tarantino I, Barresi L, Volpes R, Gruttadauria S, Petridis I, Gridelli B. Efficacy and safety of fully covered self-expandable metallic stents in biliary complications after liver transplantation: a preliminary study. *Liver Transpl* 2009; **15**: 1493-1498 [PMID: 19877248 DOI: 10.1002/lt.15.1493]

10 **Kabar I**, Cicinnati VR, Beckebaum S, Cordesmeyer S, Avsar Y, Reinecke H, Schmidt HH. Use of paclitaxel-eluting balloons for endotherapy of anastomotic strictures following liver transplantation. *Endoscopy* 2012; **44**: 1158-1160 [PMID: 23188664 DOI: 10.1055/s.44.1158]

11 **Buxbaum JL**, Biggins SW, Bagatelos KC, Ostroff JW. Predictors of endoscopic treatment outcomes in the management of biliary problems after liver transplantation at a high-volume academic center. *Gastrointest Endosc* 2011; **73**: 37-44 [PMID: 21074761 DOI: 10.1016/j.gie.73.37]

12 **Zhou J**, Zhong DW, Wang QW, Miao XY, Xu XD. Paclitaxel ameliorates fibrosis in hepatic stellate cells via inhibition of TGF-beta/Smad activity. *World J Gastroenterol* 2010; **16**: 3330-3334 [PMID: 20614491 DOI: 10.3748/wjg.16.3330]

13 **Zhang D**, Sun L, Xian W, Liu F, Ling G, Xiao L, Liu Y, Peng Y, Haruna Y, Kanwar YS. Low-dose paclitaxel ameliorates renal fibrosis in rat UUO model by inhibition of TGF-beta/Smad activity. *Lab Invest* 2010; **90**: 436-447 [PMID: 20142807 DOI: 10.1038/labinvest.90.436]

14 **Scheller B**, Hehrlein C, Bocksch W, Rutsch W, Haghi D, Dietz U, Böhm M, Speck U. Treatment of coronary in-stent restenosis with a paclitaxel-coated balloon catheter. *N Engl J Med* 2006; **355**: 2113-2124 [PMID: 17101615 DOI: 10.1056/NEJMoa.355.2113]

15 **Werk M**, Albrecht T, Meyer DR, Ahmed MN, Behne A, Dietz U, Eschenbach G, Hartmann H, Lange C, Schnorr B, Stiepani H, Zoccai GB, Hänninen EL. Paclitaxel-coated balloons reduce restenosis after femoro-popliteal angioplasty: evidence from the randomized PACIFIER trial. *Circ Cardiovasc Interv* 2012; **5**: 831-840 [PMID: 23192918]

P- Reviewer: Camellini L, Guo XZ
S- Editor: Ma YJ **L- Editor**: A **E- Editor**: Liu XM

World Journal of Gastroenterology

Submit a Manuscript: http://www.wjgnet.com/esps/
Help Desk: http://www.wjgnet.com/esps/helpdesk.aspx
DOI: 10.3748/wjg.v21.i3.982

World J Gastroenterol 2015 January 21; 21(3): 982-987
ISSN 1007-9327 (print) ISSN 2219-2840 (online)

ORIGINAL ARTICLE

Prospective Study

New aspects in the pathomechanism and diagnosis of the laryngopharyngeal reflux-clinical impact of laryngeal proton pumps and pharyngeal pH metry in extraesophageal gastroesophageal reflux disease

Valentin Becker, Romina Drabner, Simone Graf, Christoph Schlag, Simon Nennstiel, Anna Maria Buchberger, Roland M Schmid, Dieter Saur, Monther Bajbouj

Valentin Becker, Romina Drabner, Simone Graf, Christoph Schlag, Simon Nennstiel, Roland M Schmid, Dieter Saur, Monther Bajbouj, II. Medizinische Klinik, Klinikum rechts der Isar, Technische Universität München, 81675 München, Germany

Anna Maria Buchberger, Hals-Nasen Ohren Klinik, Klinikum rechts der Isar, Technische Universität München, 81675 München, Germany

Author contributions: Becker V, Bajbouj M and Schmid RM are responsible for the study design; Becker V, Bajbouj M, Schlag C and Nennstiel S performed patient recruitment; Drabner R and Saur D was immunohistochemistry and histopathology; Graf S and Buchberger AM performed ENT diagnostics.

Correspondence to: Dr. Valentin Becker, II. Medizinische Klinik, Klinikum rechts der Isar, Technische Universität München, 22 Ismaninger str., 81675 München, Germany. valentin.becker@lrz.tum.de
Telephone: +49-89-41405847
Fax: +49-89-41404816

Received: July 15, 2014
Peer-review started: July 16, 2014
First decision: August 15, 2014
Revised: August 22, 2014
Accepted: October 14, 2014
Article in press: October 15, 2014
Published online: January 21, 2015

Abstract

AIM: To determine the laryngeal H+K+-ATPase and pharyngeal pH in patients with laryngopharyngeal reflux (LPR)-symptoms as well as to assess the symptom scores during PPI therapy.

METHODS: Endoscopy was performed to exclude neoplasia and to collect biopsies from the posterior cricoid area (immunohistochemistry and PCR analysis). Immunohistochemical staining was performed with monoclonal mouse antibodies against human H+K+-ATPase. Quantitative real-time RT-PCR for each of the H+K+-ATPase subunits was performed. The pH values were assessed in the aerosolized environment of the oropharynx (DxpH Catheter) and compared to a subsequently applied combined pH/MII measurement.

RESULTS: Twenty patients with LPR symptoms were included. In only one patient, the laryngeal H+K+-ATPase was verified by immunohistochemical staining. In another patient, real-time RT-PCR for each H+K+-ATPase subunit was positive. Fourteen out of twenty patients had pathological results in DxpH, and 6/20 patients had pathological results in pH/MII. Four patients had pathological results in both functional tests. Nine out of twenty patients responded to PPIs.

CONCLUSION: The laryngeal H+K+-ATPase can only be sporadically detected in patients with LPR symptoms and is unlikely to cause the LPR symptoms. Alternative hypotheses for the pathomechanism are needed. The role of pharyngeal pH-metry remains unclear

and its use can only be recommended for patients in a research study setting.

Key words: Laryngopharyngeal reflux; Proton pump inhibitor; Gastroesophageal reflux disease; Pathomechanism

Core tip: The pathophysiology and objective diagnosis of laryngopharyngeal reflux (LPR) is still unclear. The response to standard therapy (proton pump inhibitors) is poor. Laryngeal proton pumps (H+K+-ATPase) are often considered to be potential causes of LPR. The clinical significance of laryngeal proton pumps (H+K+-ATPase) is unclear. We present the first prospective series evaluating the laryngeal H+K+-ATPase, pharyngeal pH and symptom scores in patients with LPR symptoms. Laryngeal H+K+-ATPases can only be sporadically detected, and they are unlikely to cause LPR symptoms. The role of pharyngeal pH-metry remains unclear and its use can only be recommended for patients in the research study setting.

Becker V, Drabner R, Graf S, Schlag C, Nennstiel S, Buchberger AM, Schmid RM, Saur D, Bajbouj M. New aspects in the pathomechanism and diagnosis of the laryngopharyngeal reflux-clinical impact of laryngeal proton pumps and pharyngeal pH metry in extraesophageal gastroesophageal reflux disease. *World J Gastroenterol* 2015; 21(3): 982-987 Available from: URL: http://www.wjgnet.com/1007-9327/full/v21/i3/982.htm DOI: http://dx.doi.org/10.3748/wjg.v21.i3.982

INTRODUCTION

The incidence of laryngopharyngeal reflux (LPR) has dramatically grown in recent years[1]. LPR includes numerous clinically relevant symptoms, such as chronic cough, chronic globus sensations, hoarseness, asthma, sinusitis, subglottic stenosis, laryngospasm, and halitosis[2,3]. These symptoms remain a diagnostic and therapeutic challenge for the involved physicians.

The pathomechanism of LPR is still unclear. The most commonly discussed theory is that LPR symptoms are a result of direct alteration of the laryngeal mucosa by gastric fluids due to gastroesophageal reflux disease (GERD). Multichannel impedance monitoring in combination with pH-metry (pH/MII) and 2-channel pH-metry are safe and reliable tools to objectify gastroesophageal reflux events as source of LPR symptoms[4,5]. Based on the actual hypothesis of the LPR pathomechanism, standard therapy consists of high dose proton pump inhibitor therapy for up to 6 mo[6]. However, in randomized trials, there is insufficient evidence to conclude that treatment with PPIs is superior to placebo[7]. Nevertheless, there are data suggesting that LPR-patients might benefit from antireflux surgery[8]. However, the correlation between GERD, LPR symptoms and the response to PPI is comparatively poor, and an interventional antireflux therapy (*e.g.*, Fundoplication) might harbor significant risks. In a recently published study, we were able to demonstrate that a pathological acidic environment in the oropharynx in LPR-patients was not correlated to objectified gastroesophageal reflux episodes[9]. These results were reconfirmed in another study with the same design[10]. Based on these data, the generally accepted pathomechanism of the direct alteration of the laryngeal epithelium by gastric contents, resulting in LPR-symptoms, needs to be reconsidered and alternative mechanisms should be discussed.

There are data supporting that LPR symptoms can also be associated with acid production[11] by laryngeal H+/K+-ATPase proton-pumps. H+K+-ATPase proton pumps were identified by immunohistochemistry in pathologic specimens of the larynx. Hence, local laryngeal acid production might be responsible for LPR symptoms because the laryngeal area is very sensitive to acid[10]. To objectively evaluate the laryngeal acid levels, selective pH values in the aerosolized environment can continuously be assessed with a pH measurement system. In this study, the pH-antimon probe is positioned in the oropharynx above the upper sphincter of the esophagus (DxpH, Restech, San Diego, United States). The special shape of the catheter keeps liquids out of the pH-sensor. Only the aerosol pH values are detected, and reference values are available.

The aim of this study was to correlate the laryngeal H+K+-ATPase expression, results of the pharyngeal pH metry, pH/MII and symptom response to PPI therapy, evaluating the laryngeal acid production as a potential alternative cause of LPR symptoms

MATERIALS AND METHODS

Between June 2011 and December 2012, a total of 20 consecutive patients (male = 11; 40-78 years old) with oropharyngeal symptoms suspicious of atypical GERD were included. The study was approved by the Ethics Committee of the Technical University of Munich (Study Number 5024/11). All authors had access to the study data and reviewed and approved the final manuscript. Before study inclusion, PPIs had to be stopped for at least 14 d. Informed consent to participate in the study and evaluate the data was obtained from all patients. To exclude neoplasia or erosive reflux diseases, an upper endoscopic examination was performed under conscious sedation with propofol in accordance with German medical practice regulations[12]. Standard biopsies (Radial Jaw® 4 Biopsy Forceps, Boston Scientific) were collected from the post cricoid area during the same session under the direct supervision of an experienced otolaryngologist (SG) (two biopsies for PCR analysis and two biopsies for immunohistochemistry) (Figure 1).

Dx-pH measurement and pH/MII monitoring

The Dx-pH measurement was performed standardized

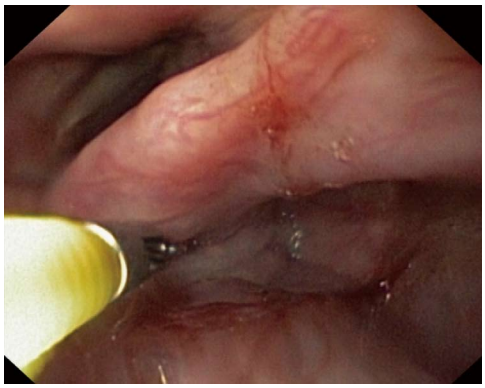

Figure 1 Endoscopic biopsies from the posterio cricoid area.

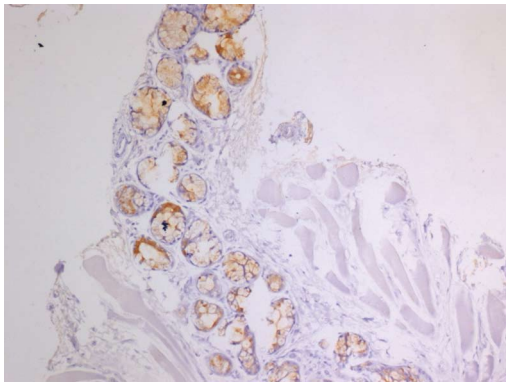

Figure 2 Immunohistochemical analysis of the H+K+-ATPase expression (brown color) in formalin fixed, paraffin embedded human laryngeal tissue.

as established previously[13-15]. Meals and body position were documented. Duration of measurement was minimum 22 h. Criteria for pathological results were Ryan Score > 9.4 in an upright position (pH < 5.5) or > 6.8 in a supine position (pH < 5.0)[13].

Combined pH/ MII monitoring (Tecnomatix ZAN S 61 C 01 E, Sandhill Scientific, Highlands Ranch, United States) was also performed as established previously[16,17]. Duration of measurement was minimum 22 h. Criteria for pathological results were pH level < 4 for more than 4% of the examination period and/or more than 73 mixed and/or fluid reflux events in impedance monitoring[17]. Both measurements (DxpH and pH/MII) were performed during the same time period.

Quantitative reverse-transcriptase PCR

RNA was isolated from tissue biopsies using the RNeasy Mini kit (Qiagen, Hilden, Germany) according to the manufacturer's advice. To remove genomic DNA, DNAse (RNase Free DNase Set Qiagen, Hilden, Germany) was used. Isolated RNA was transcribed reverse into complementary DNA (cDNA) with random hexamere primers as described previously[18]. Quantitative mRNA analysis was performed using real-time PCR with SYBR ®Green dye (APPLIED BIOSYSTEMS®, LIFE TECHNOLOGIES™, Darmstadt, Germany) and standard curves were generated as previously described[19,20]. As a housekeeping gene, Cyclophilin was used for normalization. The following primers were used for amplification of the α and β subunits of the human H+K+-ATPase: alpha subunit forward primer: CTTTGCCATCCAGGCTAGTGA and reverse primer: GGTGACGACAACCACAGCAAT; beta subunit forward primer: CCAGGTGGGTGTGGATCAG and reverse primer: GAGGCACAGGGCGAAGAG (www.eurofinsdna.com).

Hematoxylin and eosin stain and Immunohistochemistry

For histopathological analysis (Figure 2), tissue was fixed in 4% buffered formalin. After embedment in paraffin, tissue was sectioned (2.5 μm thick) and stained with hematoxylin and eosin as previously described[21]. For immunodetection, formalin-fixed paraffin-embedded tissue sections were deparaffinized in Histo-Clear (Roti®-Histol, Carl Roth GmbH, Karlsruhe, Germany) and ethanol. To recover antigens, sections were incubated in antigen unmasking solution (pH = 9, Vector Laboratories, Burlingame, CA) and placed in a microwave for 15 minutes at 360 watts. The following primary antibodies were used for immunostaining: Anti-Proton pump/H+K+-ATPase α subunit (1:285; D031-3, Clone 1H9) and H+K+-ATPase β subunit (1:285; D032-3, Clone 1B6; both from MBL® international corporation, Woburn, MA). Following primary antibodies, samples were treated with secondary antibodies conjugated to biotin (Vector Laboratories). Peroxidase conjugated streptavidin and 3,3'-diaminobenzidine tetrahydrochloride (DAB, Sigma-Aldrich, Munich, Germany) were used as a chromogen for detection as previously described[22]. Sections were counterstained with hematoxylin. As positive controls, biopsies from human corpus mucosa were used.

RESULTS

No complications or technical problems were documented during all procedures. Upper endoscopic examination did not reveal any relevant pathology, such as neoplasia or severe erosive esophagitis.

Twenty patients with LPR symptoms were included (Table 1). Fourteen out of twenty patients had pathological results in DxpH; 6/20 patients had pathological results in pH/MII. Four patients had pathological results in both functional tests. In one patient, laryngeal H+K+-ATPase expression was verified by immunohistochemical staining. In this patient, DxpH and pH/MII showed pathological results, and the PPI response was reported. In another patient, real-time RT-PCR for each of the H+K+-ATPase subunits was positive. Pathological results were assessed with DxpH; there were regular results in the pH/MII measurements and the PPI response was noted as positive (Figure 3).

Symptom relief (at least reduction of three points on a ten point scale) with PPI was reported in 9 of 20 patients. In patients with pathological DxpH, 9 of 14 patients reported significant symptom relief. Seventy percent of

Table 1 Patient data and results

No	Gender	Age	pHDx	Rayn	Rayn	Impedance	deMeester	Epithelium /Glands	Immuno-histo	PCR	Therapy response	Symptom-score
			+ path	> 9.4 upright position	> 6.8 supine position	+ path	Score < 22.0	+ pos	+ pos	+ pos	+ pos	before/after therapy
1	M	74	+	23.92	2.17	+	29.9	-	-	-	+	7/4
2	F	49	+	17.84	2.17	-	7.2	-	-	-	-	6/6
3	M	78	+	20.88	11.31	+	38.2	-	-	-	-	7/6
4	M	57	-	4.04	2.17	-	7.1	-	-	-	-	6/5
5	M	46	+	19.35	2.17	-	3.7	-	-	-	+	6/3
6	F	59	+	115.85	7.99	+	25.4	+	+	-	+	8/5
7	M	53	-	2.12	2.17	-	1.5	-	-	-	-	8/8
8	F	40	-	2.12	2.17	-	11.0	-	-	-	-	5/3
9	M	52	+	53.3	2.17	+	24.1	-	-	-	+	5/1
10	M	46	+	52.39	2.17	-	0.9	-	-	-	-	6/5
11	F	62	+	2.12	7.57	-	3.2	-	-	+	+	8/5
12	F	77	+	37.01	2.17	-	14.2	-	-	-	-	7/7
13	F	63	-	2.12	2.17	-	7.2	-	-	-	-	8/8
14	M	51	+	124.43	9.26	-	7.1	-	-	-	-	4/4
15	F	64	+	201.59	2.17	-	9.4	-	-	-	+	6/3
16	F	75	+	38.98	9.33	-	1.3	-	-	-	+	7/4
17	M	55	-	2.12	2.17	+	37.0	-	-	-	-	6/6
18	M	53	+	23.23	2.17	-	0.9	-	-	-	+	8/4
19	F	75	+	41.12	2.17	-	12.8	-	-	-	+	8/5
20	M	65	-	4.15	2.17	+	28.8	-	-	-	-	7/6

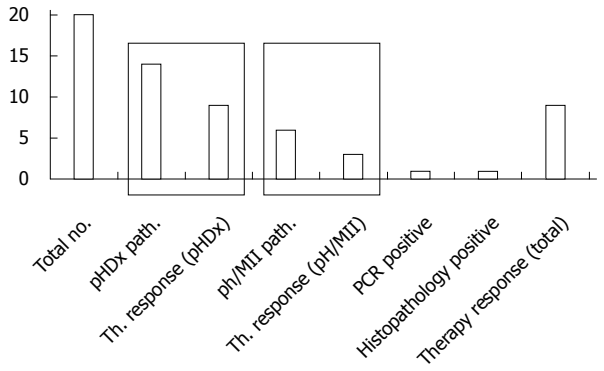

Figure 3 Pathological results of the respective diagnostic procedures and therapy response (number of patients).

the patients had pathological results in DxpH, and only 30% of the patients were pathological in pH/MII.

DISCUSSION

The primary aim of the study was to correlate the laryngeal H+K+-ATPase expression, results of the pharyngeal pH-metry, pH/MII and symptom response to PPI therapy and evaluate laryngeal acid production as a potential alternative pathomechanism for LPR symptoms.

Since the identification of laryngeal H+K+-ATPase proton pumps in pathologic specimens by immunohistochemistry, the clinical significance of laryngeal H+K+-ATPase proton pumps has been controversial[11]. We verified a pathologic, acidic environment in the oropharynx in most of the examined LPR-patients without any correlation with the objectified gastroesophageal reflux episodes[9]. This finding supports the theory of laryngeal acid production. However, the pharyngeal acid levels were only documented with the Dx-pH system. As reported in previous trials, Dx-pH more often detects pathological acid pH levels than the standard pH/MII. On the other hand, the pharyngeal system regularly misses proximal pH exposure that is documented in regular pH/MII[9,10]. Hence, the clinical significance of this Dx-pH system is not clear. In the current study, Dx-pH revealed pathological values in 70% of the patients, whereas 30% of the patients had pathological values in pH/MII.

As mentioned previously, the Dx-pH system potentially detects a high number of false-positive patients; as a result, the pH/MII is the gold standard. However, the evidence of involvement of laryngeal H+K+-ATPase proton pumps is much higher in patients with LPR symptoms, which might explain the pathological acid environment of the oropharynx in patients without gastroesophageal reflux. The lack of detection of H+K+-ATPase could be explained in different ways. First, H+K+-ATPases are only located in the seromucinous glands of the human larynx and not in the squamous epithelium. Due to endoscopic sampling error with random biopsies during standard endoscopy, submucosal glands with H+K+-ATPase proton pumps can easily be missed, which was previously described in Barrett's esophagus[23]. In our study, the submucosal glands were only detected in one patient. In this patient, the immunohistochemistry was positive. Second, the idea of an "activated" or "inducible" state of the proton pumps needs to be discussed[24]. Inflammation, infection or gastroesophageal reflux might

"activate" H+K+-ATPase proton pumps, resulting in increased proton secretion[24,25]. Determining whether both laryngeal H+K+-ATPase proton pumps and gastric H+K+-ATPase proton pumps respond to PPI therapy might be of clinical significance. As confirmed by the Altman group, the α and β-subunits of the H+K+-ATPase proton pumps have identical components as those found in the stomach[11]. Therefore, PPI therapy should be an effective therapy for LPR patients. However, the concentration of the laryngeal H+K+-ATPase proton pumps is much lower than the concentration in the stomach[26]. Compared to the distal esophagus, relatively low acid levels might result in relevant symptoms because the larynx area is extremely sensitive to pH alterations[10]. This might explain the need for high dose, long-term PPI therapy in LPR patients to terminate proton secretion and resolve symptoms.

However, the detection of only one patient with histopathological evidence of H+K+-ATPase and one patient with positive PCR challenges the theory that laryngeal H+K+-ATPase proton pumps cause LPR symptoms. We conclude that laryngeal H+K+-ATPase proton pumps lack clinical relevance in patients with LPR symptoms. Alternative pathomechanisms must be discussed, including that LPR patients can have a pathologically acidic environment in the oropharynx without being correlated to the number of gastroesophageal reflux episodes. Still, it is important to note that this is a feasibility study with limitations, including the small number of patients and single-center setting. Both patients with detectable laryngeal H+K+ATPase proton pumps responded to PPI therapy, and nine of fourteen (64%) Dx-pH positive patients responded to therapy, which is a remarkable number of patients with LPR symptoms.

As previously mentioned, the results and clinical significance of pharyngeal pH testing are controversial[27]. Recently, a study group of a retrospective chart review reported that patients with atypical reflux symptoms have better symptom relief after surgical antireflux procedures in the group with pathological pharyngeal pH levels than the study group with pathological result esophageal pH levels. The median follow up was 18 mo[28]. However, the study has several limitations. Symptom relief was only judged as a symptomatic parameter, and no objective data with the Dx-pH system were analyzed. Objective data would have been very interesting for the pathomechanism of LPR. Furthermore, only patients with previously performed esophageal and pharyngeal pH testing were included (retrospectively), which leads to a relevant patient selection. Hence, the impact of the study results is unclear. To objectively evaluate gastroesophageal reflux episodes leading to LPR symptoms, pH/MII is the most accurate diagnostic instrument[4]. However, simultaneous measurements of combined pH/MII and Dx-pH were not correlated[10]. Furthermore, the pharyngeal probe missed almost 90% of all proximal reflux episodes detected by MII, but the data are reproducible[9]. Therefore, it is unclear what the pharyngeal pH probe is actually measuring. Based on these data, the results of pharyngeal pH metry should not be used to establish the diagnosis of laryngopharyngeal reflux or to guide therapy, including surgical anti-reflux procedures.

In conclusion, laryngeal H+K+-ATPases can only be sporadically detected in patients with LPR symptoms, and they are unlikely to cause LPR symptoms. Alternative pathomechanisms must be discussed. The role of pharyngeal pH-metry remains unclear, and its use can only be recommended for patients in the research study setting.

COMMENTS

Background

The pathophysiology and objective diagnosis of laryngopharyngeal reflux (LPR) is still unclear. Correlation between gastroesophageal reflux disease (GERD), LPR-symptoms and the response to proton pump inhibitors (PPI) is poor. Recently, laryngeal proton pumps (H+K+-ATPases) were identified and linked as potential causative agents for LPR. However, their clinical significance is unclear. Pharyngeal pH-metry was introduced for use in clinical procedures even though its role in the diagnosis of atypical GERD has questionable impact.

Research frontiers

The study aim was to evaluate laryngeal H+K+-ATPases and pharyngeal pH in patients with LPR-symptoms as well as to assess the symptom scores and PPI therapy response.

Innovations and breakthroughs

Previous studies have identified laryngeal H+K+-ATPase proton pumps in pathologic specimens by immunohistochemistry. Furthermore, the acidic environment in the oropharynx can be verified without gastroesophageal reflux episodes. Therefore, acid production in the laryngeal epithelium is increasingly discussed. This is the first study to correlate pharyngeal pH metry results with laryngeal H+K+-ATPase proton pumps, subjective evaluation and therapy response.

Applications

For patients with LPR symptoms, a positive correlation and therapeutic effect of PPI therapy might offer a new diagnostic and therapeutic approach.

Terminology

LPR has dramatically grown in recent years and includes numerous clinically relevant symptoms such as chronic cough, globus sensations in the throat, asthma, chronic sinusitis, subglottic stenosis, laryngospasm, halitosis, hoarseness and dysphonia.

Peer review

This paper is a well written study about new aspects of LPR. The study is well designed and the diverse results are well discussed.

REFERENCES

1 **Hicks DM**, Ours TM, Abelson TI, Vaezi MF, Richter JE. The prevalence of hypopharynx findings associated with gastroesophageal reflux in normal volunteers. *J Voice* 2002; **16**: 564-579 [PMID: 12512644 DOI: 10.1016/S0892-1997(02)00132-7]

2 **Ford CN**. Evaluation and management of laryngopharyngeal reflux. *JAMA* 2005; **294**: 1534-1540 [PMID: 16189367 DOI: 10.1001/jama.294.12.1534]

3 **Rohof WO**, Hirsch DP, Boeckxstaens GE. Pathophysiology and management of gastroesophageal reflux disease. *Minerva Gastroenterol Dietol* 2009; **55**: 289-300 [PMID: 19829285]

4 **Bredenoord AJ**. Impedance-pH monitoring: new standard for measuring gastro-oesophageal reflux. *Neurogastroenterol Motil* 2008; **20**: 434-439 [PMID: 18416700 DOI: 10.1111/j.1365-2982.2008.01131.x]

5 **Bajbouj M**, Becker V, Neuber M, Schmid RM, Meining A. Combined pH-metry/impedance monitoring increases the diagnostic yield in patients with atypical gastroesophageal

reflux symptoms. *Digestion* 2007; **76**: 223-228 [PMID: 18174685 DOI: 10.1159/000112728]
6 **Dore MP**, Pedroni A, Pes GM, Maragkoudakis E, Tadeu V, Pirina P, Realdi G, Delitala G, Malaty HM. Effect of antisecretory therapy on atypical symptoms in gastroesophageal reflux disease. *Dig Dis Sci* 2007; **52**: 463-468 [PMID: 17211695 DOI: 10.1007/s10620-006-9573-7]
7 **Chang AB**, Lasserson TJ, Gaffney J, Connor FL, Garske LA. Gastro-oesophageal reflux treatment for prolonged non-specific cough in children and adults. *Cochrane Database Syst Rev* 2011; (**1**): CD004823 [DOI: 10.1002/14651858.CD004823.pub4]
8 **Koch OO**, Antoniou SA, Kaindlstorfer A, Asche KU, Granderath FA, Pointner R. Effectiveness of laparoscopic total and partial fundoplication on extraesophageal manifestations of gastroesophageal reflux disease: a randomized study. *Surg Laparosc Endosc Percutan Tech* 2012; **22**: 387-391 [DOI: 10.1097/SLE.0b013e31825efb5b]
9 **Becker V**, Graf S, Schlag C, Schuster T, Feussner H, Schmid RM, Bajbouj M. First agreement analysis and day-to-day comparison of pharyngeal pH monitoring with pH/impedance monitoring in patients with suspected laryngopharyngeal reflux. *J Gastrointest Surg* 2012; **16**: 1096-1101 [PMID: 22450948 DOI: 10.1007/s11605-012-1866-x]
10 **Ummarino D**, Vandermeulen L, Roosens B, Urbain D, Hauser B, Vandenplas Y. Gastroesophageal reflux evaluation in patients affected by chronic cough: Restech versus multichannel intraluminal impedance/pH metry. *Laryngoscope* 2013; **123**: 980-984 [PMID: 23023943 DOI: 10.1002/lary.23738]
11 **Altman KW**, Haines GK 3rd, Hammer ND, Radosevich JA. The H /K -ATPase (proton) pump is expressed in human laryngeal submucosal glands. *Laryngoscope* 2003; **113**: 1927 [DOI: 10.1097/00005537-200311000-00013]
12 **Riphaus A**, Wehrmann T, Weber B, Arnold J, Beilenhoff U, Bitter H, von Delius S, Domagk D, Ehlers AF, Faiss S, Hartmann D, Heinrichs W, Hermans ML, Hofmann C, In der Smitten S, Jung M, Kähler G, Kraus M, Martin J, Meining A, Radke J, Rösch T, Seifert H, Sieg A, Wigginghaus B, Kopp I. [S3-guidelines--sedation in gastrointestinal endoscopy]. *Z Gastroenterol* 2008; **46**: 1298-1330 [PMID: 19012203 DOI: 10.1055/s-2008-1027850]
13 **Ayazi S**, Hagen JA, Zehetner J, Oezcelik A, Abate E, Kohn GP, Sohn HJ, Lipham JC, Demeester SR, Demeester TR. Proximal esophageal pH monitoring: improved definition of normal values and determination of a composite pH score. *J Am Coll Surg* 2010; **210**: 345-350 [PMID: 20193899 DOI: 10.1016/j.jamcollsurg.2009.12.006]
14 **Ayazi S**, Lipham JC, Hagen JA, Tang AL, Zehetner J, Leers JM, Oezcelik A, Abate E, Banki F, DeMeester SR, DeMeester TR. A new technique for measurement of pharyngeal pH: normal values and discriminating pH threshold. *J Gastrointest Surg* 2009; **13**: 1422-1429 [PMID: 19421822 DOI: 10.1007/s11605-009-0915-6]
15 **Sifrim D**, Holloway R, Silny J, Xin Z, Tack J, Lerut A, Janssens J. Acid, nonacid, and gas reflux in patients with gastroesophageal reflux disease during ambulatory 24-hour pH-impedance recordings. *Gastroenterology* 2001; **120**: 1588-1598 [PMID: 11375941 DOI: 10.1053/gast.2001.24841]
16 **Becker V**, Bajbouj M, Waller K, Schmid RM, Meining A. Clinical trial: persistent gastro-oesophageal reflux symptoms despite standard therapy with proton pump inhibitors - a follow-up study of intraluminal-impedance guided therapy. *Aliment Pharmacol Ther* 2007; **26**: 1355-1360 [PMID: 17900268 DOI: 10.1111/j.1365-2036.2007.03529.x]
17 **Shay S**, Tutuian R, Sifrim D, Vela M, Wise J, Balaji N, Zhang X, Adhami T, Murray J, Peters J, Castell D. Twenty-four hour ambulatory simultaneous impedance and pH monitoring: a multicenter report of normal values from 60 healthy volunteers. *Am J Gastroenterol* 2004; **99**: 1037-1043 [PMID: 15180722 DOI: 10.1111/j.1572-0241.2004.04172.x]
18 **Saur D**, Paehge H, Schusdziarra V, Allescher HD. Distinct expression of splice variants of neuronal nitric oxide synthase in the human gastrointestinal tract. *Gastroenterology* 2000; **118**: 849-858 [PMID: 10784584 DOI: 10.1016/S0016-5085(00)70171-5]
19 **Saur D**, Seidler B, Schneider G, Algül H, Beck R, Senekowitsch-Schmidtke R, Schwaiger M, Schmid RM. CXCR4 expression increases liver and lung metastasis in a mouse model of pancreatic cancer. *Gastroenterology* 2005; **129**: 1237-1250 [PMID: 16230077 DOI: 10.1053/j.gastro.2005.06.056]
20 **von Burstin J**, Eser S, Paul MC, Seidler B, Brandl M, Messer M, von Werder A, Schmidt A, Mages J, Pagel P. E-cadherin regulates metastasis of pancreatic cancer in vivo and is suppressed by a SNAIL/HDAC1/HDAC2 repressor complex. *Gastroenterology* 2009: 137, 361-371, 371 e361-e365
21 **Seidler B**, Schmidt A, Mayr U, Nakhai H, Schmid RM, Schneider G, Saur D. A Cre-loxP-based mouse model for conditional somatic gene expression and knockdown in vivo by using avian retroviral vectors. *Proc Natl Acad Sci USA* 2008; **105**: 10137-10142 [PMID: 18621715 DOI: 10.1073/pnas.0800487105]
22 **Eser S**, Messer M, Eser P, von Werder A, Seidler B, Bajbouj M, Vogelmann R, Meining A, von Burstin J, Algül H, Pagel P, Schnieke AE, Esposito I, Schmid RM, Schneider G, Saur D. In vivo diagnosis of murine pancreatic intraepithelial neoplasia and early-stage pancreatic cancer by molecular imaging. *Proc Natl Acad Sci USA* 2011; **108**: 9945-9950 [PMID: 21628592 DOI: 10.1073/pnas.1100890108]
23 **Gatenby PA**, Ramus JR, Caygill CP, Shepherd NA, Watson A. Relevance of the detection of intestinal metaplasia in non-dysplastic columnar-lined oesophagus. *Scand J Gastroenterol* 2008; **43**: 524-530 [PMID: 18415743 DOI: 10.1080/00365520701879831]
24 **Roussa E**, Thévenod F, Sabolic I, Herak-Kramberger CM, Nastainczyk W, Bock R, Schulz I. Immunolocalization of vacuolar-type H+-ATPase in rat submandibular gland and adaptive changes induced by acid-base disturbances. *J Histochem Cytochem* 1998; **46**: 91-100 [PMID: 9405498 DOI: 10.1177/002215549804600112]
25 **Layden TJ**, Agnone LM, Schmidt LN, Hakim B, Goldstein JL. Rabbit esophageal cells possess an Na+,H+ antiport. *Gastroenterology* 1990; **99**: 909-917 [PMID: 2168329]
26 **Herrmann M**, Selige J, Raffael S, Sachs G, Brambilla A, Klein T. Systematic expression profiling of the gastric H+/K+ ATPase in human tissue. *Scand J Gastroenterol* 2007; **42**: 1275-1288 [PMID: 17852870 DOI: 10.1080/00365520701405579]
27 **Merati AL**, Lim HJ, Ulualp SO, Toohill RJ. Meta-analysis of upper probe measurements in normal subjects and patients with laryngopharyngeal reflux. *Ann Otol Rhinol Laryngol* 2005; **114**: 177-182 [PMID: 15825565]
28 **Worrell SG**, DeMeester SR, Greene CL, Oh DS, Hagen JA. Pharyngeal pH monitoring better predicts a successful outcome for extraesophageal reflux symptoms after antireflux surgery. *Surg Endosc* 2013; **27**: 4113-4118 [DOI: 10.1007/s00464-013-3076-3]

P- Reviewer: Dormann AJ, Pehl C
S- Editor: Qi Y **L- Editor**: A **E- Editor**: Liu XM

World Journal of Gastroenterology

Submit a Manuscript: http://www.wjgnet.com/esps/
Help Desk: http://www.wjgnet.com/esps/helpdesk.aspx
DOI: 10.3748/wjg.v21.i3.988

World J Gastroenterol 2015 January 21; 21(3): 988-996
ISSN 1007-9327 (print) ISSN 2219-2840 (online)

ORIGINAL ARTICLE

Prospective Study

Albumin and magnetic resonance imaging-liver volume to identify hepatitis B-related cirrhosis and esophageal varices

Hang Li, Tian-Wu Chen, Zhen-Lin Li, Xiao-Ming Zhang, Cheng-Jun Li, Xiao-Li Chen, Guang-Wen Chen, Jia-Ni Hu, Yong-Quan Ye

Hang Li, Tian-Wu Chen, Xiao-Ming Zhang, Cheng-Jun Li, Xiao-Li Chen, Sichuan Key Laboratory of Medical Imaging, and Department of Radiology, Affiliated Hospital of North Sichuan Medical College, Nanchong 637000, Sichuan Province, China
Hang Li, Guang-Wen Chen, Department of Radiology, Sichuan Provincial People's Hospital, Chengdu 610070, Sichuan Province, China
Zhen-Lin Li, Department of Radiology, West China Hospital of Sichuan University, Chengdu 610041, Sichuan Province, China
Jia-Ni Hu, Yong-Quan Ye, Department of Radiology, Wayne State University, Detroit, MI 48201, United States
Author contributions: Li H, Li ZL, Zhang XM and Li CJ contributed equally to this work; Li H, Chen TW, Chen XL, Li ZL, Zhang XM and Li CJ designed the research; Li H, Chen XL, Chen GW, Hu JN and Ye YQ performed the research; Li H, Chen TW, Li ZL, Chen XL, Chen GW, Hu JN and Ye YQ contributed new reagents/analytic tools; Li H, Chen XL and Chen TW analyzed the data; Li H, Chen TW and Chen XL wrote the paper.
Supported by National Natural Science Foundation of China, No. 81050033; Key Projects in the Sichuan Province Science and Technology Pillar Program, No. 2011SZ0237; the Science Foundation for Distinguished Young Scholars of Sichuan Province in China, No. 2010JQ0039; Key Science and Technology Project of Chinese Ministry of Public Health, No. 2014114; and Natural Science Key Project of North Sichuan Medical College, No. CBY12-A-ZD03.

Correspondence to: Tian-Wu Chen, MD, Sichuan Key Laboratory of Medical Imaging, and Department of Radiology, Affiliated Hospital of North Sichuan Medical College, 63 Wenhua Road, Shunqing District, Nanchong 637000, Sichuan Province, China. chentw@aliyun.com
Telephone: +86-817-2262236
Fax: +86-817-2262236
Received: July 18, 2014
Peer-review started: July 20, 2014
First decision: August 27, 2014
Revised: September 11, 2014
Accepted: October 20, 2014
Article in press: October 21, 2014
Published online: January 21, 2015

Abstract

AIM: To investigate whether liver lobe volume and albumin (ALB) could predict the presence and severity of liver cirrhosis, and esophageal varices.

METHODS: Seventy-one cirrhotic patients with hepatitis B and 21 healthy individuals were enrolled in this study. All the participants underwent abdominal enhanced magnetic resonance imaging to measure each liver lobe volume, and biochemical workup for testing ALB and Child-Pugh class. All cirrhotic patients underwent upper gastrointestinal endoscopy to show the presence of cirrhotic esophageal varices. Right liver lobe volume (RV), left medial liver lobe volume (LMV), left lateral liver lobe volume (LLV), and caudate lobe volume (CV) were measured using enhanced magnetic resonance imaging. The ratios of RV to ALB (RV/ALB), LMV to ALB (LMV/ALB), LLV to ALB (LLV/ALB) and CV to ALB (CV/ALB) were calculated. Statistical analyses were performed to determine whether and how the combination of liver lobe volume measured using magnetic resonance imaging and albumin could predict the presence and severity of liver cirrhosis, and the presence of esophageal varices.

RESULTS: RV, LMV, LLV and CV decreased (r = -0.51-0.373; all $P < 0.05$), while RV/ALB increased (r = 0.424; $P < 0.05$), with the progress of Child-Pugh class

of liver cirrhosis. RV, LMV, CV, LLV/ALB and CV/ALB could identify presence of liver cirrhosis; LLV and LMV could distinguish Child-Pugh class A from B; RV, LMV, LLV, CV, RV/ALB and LLV/ALB could distinguish class A from C; RV and LLV/ALB could differentiate B from C; and RV, RV/ALB and CV/ALB could identify presence of esophageal varices (all $P < 0.05$). Among these parameters, CV/ALB could best identify the presence of liver cirrhosis, with an area under receiver operating characteristic curve (AUC) of 0.860, a sensitivity of 82.0% and a specificity of 83.0%. LLV could best distinguish class A from B, with an AUC of 0.761, a sensitivity of 74.4% and a specificity of 73.1%. RV could best distinguish class A from C, with an AUC of 0.900, a sensitivity of 90.3% and a specificity of 84.5%. LLV/ALB could best distinguish class B from C, with an AUC of 0.900, a sensitivity of 93.8% and a specificity of 81.5%. RV/ALB could best identify esophageal varices, with an AUC of 0.890, a sensitivity of 80.0% and a specificity of 83.5%.

CONCLUSION: The combination of liver lobe volume and ALB has potential to identify presence and severity of cirrhosis, and presence of esophageal varices.

Key words: Magnetic resonance imaging; Liver cirrhosis; Liver lobe volume; Esophageal varices; Child-Pugh class

Core tip: We determined whether and how the combination of albumin and liver lobe volume (measured using magnetic resonance imaging) could predict the presence and severity of liver cirrhosis, and the presence of esophageal varices. The ratio of caudate lobe volume to albumin could identify the occurrence of cirrhosis, and that of left lateral liver lobe volume, right liver lobe volume, and the ratio of left lateral liver lobe volume to albumin could differentiate Child-Pugh class A from B, A from C, and B from C, respectively. The right liver lobe volume to albumin ratio could identify the presence of esophageal varices.

Li H, Chen TW, Li ZL, Zhang XM, Li CJ, Chen XL, Chen GW, Hu JN, Ye YQ. Albumin and magnetic resonance imaging-liver volume to identify hepatitis B-related cirrhosis and esophageal varices. *World J Gastroenterol* 2015; 21(3): 988-996 Available from: URL: http://www.wjgnet.com/1007-9327/full/v21/i3/988.htm DOI: http://dx.doi.org/10.3748/wjg.v21.i3.988

INTRODUCTION

Liver cirrhosis is a common condition that causes progressive liver dysfunction. In the early stages of cirrhosis, the liver is still compensating and application of adequate therapy can help prolong sufficient liver function. When the liver function decompensates, the patient is in end-stage liver disease and has a high risk of developing complications, such as gastrointestinal bleeding[1]. Therefore, it is important to follow up the progress of this disease and determine the stage of cirrhosis[2]. The modified Child-Pugh classification system has been confirmed as an independent prognostic factor for survival of cirrhotic patients, and can be utilized to adequately assess liver transplantation candidates[3,4].

The morphology of the liver changes with the progress of Child-Pugh classification. Previous studies reported that changes in liver lobe volume were positively correlated with prognosis and Child-Pugh classifications[4]. One interesting study focused on the correlation between the ratio of right liver lobe diameter to albumin and Child-Pugh classifications, and clarifying the significant correlation in classifying cirrhosis[5]. In addition, esophageal varices are one of the major complications of liver cirrhosis, with a risk of bleeding from varices of approximately 25%-35%[6]. Prophylactic endoscopic variceal ligation can decrease the incidence of first variceal bleeding and mortality in cirrhotic patients who have large varices[6]. Nevertheless, repeated endoscopic examinations are not accepted for patients and are expensive. As a safe, effective and repeatable noninvasive modality, magnetic resonance imaging (MRI) has increasingly been used to assess liver diseases[7,8]. Previous studies reported that liver volume indexes measured on MRI could be used as a method for grading the severity of cirrhosis[9,10]. To the best of our knowledge, there was no study focusing on the combination of liver lobe volume measured on MRI with albumin to assess the presence of cirrhosis and define its Child-Pugh classifications[11]. There were also no reports on the combination of liver lobe volume with albumin to determine the presence of esophageal varices in cirrhotic patients. Therefore, we aimed to determine how liver lobe volume and the ratio of the liver lobe volume to albumin could determine the presence and Child-Pugh class of liver cirrhosis, and the presence of esophageal varices.

MATERIALS AND METHODS

Patients

The institutional human research review committee of our hospital approved this study. Written informed consent was obtained from each patient before the prospective study.

The study included 96 consecutive patients with confirmed liver cirrhosis between February 2012 and December 2013. The inclusion criteria were: (1) the diagnosis of cirrhosis in patients with hepatitis B was based on physical findings, laboratory investigations, image findings or histopathological findings, whenever available, according to the American Association for the Study of Liver Diseases practice guidelines on chronic hepatitis B (2007)[12]; (2) the patients underwent abdominal triple-phase enhanced MRI scans, biochemical workup

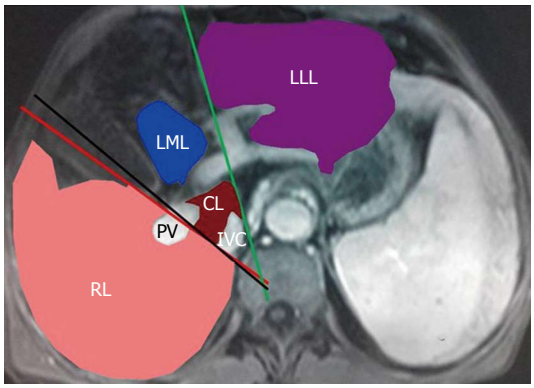

Figure 1 Outline of each liver lobe. Right liver lobe is differentiated from the left liver lobe by the middle liver fissure (black line), and the discrimination between the left lateral liver lobe and the left medial liver lobe is provided by the liver interlobar fissure (green line) on the level of the fossa for gallbladder. The connecting line (red) between the inferior vena cava (IVC) and the right branch of the portal vein (PV) is used to distinguish the right lobe (RL) from the caudate lobe (CL). The profiles of the RL, left lateral liver lobe (LLL), left medial liver lobe (LML) and CL are drawn on the axial portal venous phase enhanced magnetic resonance imaging, and marked in pink, blue, purple and red, respectively.

and upper gastrointestinal endoscopy; and (3) image data showed patients without portal vein-emboli or hepatic carcinoma. This biochemical workup was used to achieve the Child-Pugh score calculation using five parameters including, albumin (ALB), ascites, bilirubin, prothrombin activity and encephalopathy[3]. The endoscopy was to demonstrate the presence of esophageal varices. The exclusion criteria were: (1) patients had a history of treatments for portal hypertension (n = 10); (2) patients had primary hematological disorders, such as lymphoma and leukemia (n = 2); and (3) patients had active alcohol abuse (less than six months of alcohol abstinence) (n = 13). Consequently, 71 patients (36 men and 35 women; age range, 31-76 years; median age, 59 years) were enrolled into this study. In this cohort, 33 patients (46.5%) had ascites, 15 patients (21.1%) had esophageal varices, 10 patients (14.1%) had both ascites and esophageal varices, and 13 patients (18.3%) had neither ascites nor esophageal varices. According to the Child-Pugh classification system, 27, 28 and 16 patients were categorized into Child-Pugh class A, B and C, respectively.

Additionally, 21 random consecutive healthy volunteers with no history of chronic liver disease (12 men and 9 women; median age 58 years; range: 38-70 years) who underwent upper abdominal triphasic enhancement MRI and biochemical workup at our institution served as the reference group.

MRI technique

Each participant underwent MRI scans supinely with a 3.0-T scanner (Signa Excite; GE Medical Systems, Milwaukee, WI, United States) in an 8-channel phased array body coil after the establishment of respiratory signals from the diaphragm to the inferior border of the spleen to cover the entire liver. The routine MRI sequences included spoiled gradient recalled T1- and fast recovery fast spin echo T2-weighted imaging. Subsequently, each patient received an injection of standard dose (0.2 mmol/kg of body weight) of gadodiamide (Magnevist; Bayer Healthcare, Germany) at a standard flow rate (3 mL/s) through a 21-gauge peripheral venous access followed by a 20-mL saline solution flush. After the previous injection, each participant underwent axial three-dimensional liver acquisition with volume acceleration (3D-LAVA), with a repetition time of 3.9 ms, an echo time of 1.8 ms, a field of view of 34 cm × 34 cm, a slice thickness of 5.0 mm, a slice gap of zero and a matrix of 256 mm × 224 mm.

Image data analysis

The analysis of the original MRI data was performed on a workstation (GE Advantage Workstation Version 4.4-09; Sun Microsystems, Palo Alto, CA, United States). The portal venous phase images were used for the above-mentioned analysis because the boundary of each liver lobe could be traced more clearly on the portal venous phase than on arterial or delayed phase[13]. As depicted in the Goldsmith and Woodburne system[14], the liver comprises four lobes including left lateral and medial lobes, right lobe and caudate lobe (Figure 1). Each liver lobe volume was measured retrospectively and independently by two experienced abdominal radiologists (Tian-wu Chen and Hang Li), without the knowledge of clinical data. On each axial 3D-LAVA image, liver lobe contour was manually drawn, excluding the inferior vena cava and gallbladder, and the cross-sectional area of each liver lobe was automatically calculated by the software[15]. This previous data analysis on each contiguous transverse level was repeated until the entire liver lobe was covered. Right liver lobe volume (RV), left medial liver lobe volume (LMV), left lateral liver lobe volume (LLV), and caudate lobe volume (CV) were acquired by the sum of the corresponding liver lobe areas × section thickness[15]. Based on each liver lobe volume and albumin, the ratios of RV to albumin (RV/ALB), of LMV to albumin (LMV/ALB), of LLV to albumin (LLV/ALB), and of CV to albumin (CV/ALB) were calculated.

Statistical analysis

The MRI data of the 71 cirrhotic patients were randomly chosen to test the interobserver variability of the measurements. In the 71 cirrhotic patients, the interobserver agreement in liver lobe volume measurements between the two independent observers was assessed using coefficient of variation coefficient of variation (mean ± SD, × 100)[16]. When coefficient of variation was less than 10%, interobserver variability was considered to be small, and the averaged value of the two observers' measurements was regarded as the final liver lobe volume parameter[17]. If coefficient of variation exceeded 10%, the previous observers made two further measurements and an average of the four measurements was used as the final liver lobe

Table 1 Interobserver variability of each liver lobe volume parameter between two observers' measurements in cirrhotic patients with hepatitis B

Liver lobe volume parameters	Mean coefficient of variation (range)	≤ 10% (*n*)	> 10% (*n*)
RV	7.5% (2%-14%)	59	12
LMV	8.6% (3%-15%)	61	10
LLV	8.2% (3%-13%)	63	8
CV	6.0% (2%-11%)	69	2
RV/ALB	5.5% (1%-11%)	70	1
LMV/ALB	6.4% (1%-10%)	71	0
LLV/ALB	6.2% (2%-10%)	71	0
CV/ALB	4.0% (2%-9%)	71	0

RV: Right liver lobe volume; LMV: Left medial liver lobe volume; LLV: Left lateral liver lobe volume; CV: Caudate lobe volume; ALB: Albumin.

volume parameter.

The relationship between each liver lobe volume parameter and Child-Pugh class was tested by Spearman's rank correlation analyses. The Mann-Whitney *U* test was used to compare liver lobe volume parameters among Child-Pugh classifications, with Bonferroni correction for multigroup comparisons. The two independent samples test was performed to compare each liver lobe volume parameter between patients with and without esophageal varices. If there were significant positive findings in any liver lobe volume parameter classified by Child-Pugh classifications, receiver-operating characteristic (ROC) analysis was performed to determine if the cutoff values of liver lobe volume parameter could help identify the presence and the Child-Pugh class of cirrhosis. When statistically positive findings were found in the comparison of any liver lobe volume parameter between patients with and without esophageal varices, ROC analysis was performed to determine if the cutoff values of the liver lobe volume parameters could help predict the presence of esophageal varices. *P* values < 0.05 were accepted as significant.

RESULTS

Interobserver variability of each liver lobe volume parameter measurement in cirrhotic patients

The mean coefficient of variation in each liver lobe volume parameter measurement and the numbers of patients with coefficient of variation less than 10% and exceeding 10% are shown in Table 1. For two observers' measurements of each liver lobe volume parameter in the 71 cirrhotic patients, the interobserver variability was low when the coefficient of variation was less than 10%, and the averaged value of each liver lobe volume parameter obtained by the two observers was used for subsequent analyses. For the two observers' measurements of RV in 12 patients, LMV in 10 patients, LLV in eight patients, CV in two patients and RV/ALB in one patient, the coefficient of variation exceeded 10%; therefore, two additional measurements were obtained and an average of the four measurements was used as the final liver lobe volume parameter.

Analysis of liver lobe volume parameters and possible clinical data associated with the presence of cirrhosis and Child-Pugh classification

The possible clinical data, including the gender, age, body weight, body mass index, and liver lobe volume parameters of all the participants are shown in Table 2. Cirrhotic patients were more likely to have lower RV ($P < 0.001$) and LMV ($P = 0.001$), and larger CV ($P = 0.001$), LLV/ALB ($P < 0.001$) and CV/ALB ($P < 0.001$) than the healthy volunteers. RV, LMV, CV, LLV/ALB and CV/ALB could identify the presence of liver cirrhosis. However, no significant differences were found in gender ($P = 0.756$), age ($P = 0.135$), body weight ($P = 0.08$), body mass index ($P = 0.056$), LLV ($P = 0.06$), RV/ALB ($P = 0.631$) and LMV/ALB ($P = 0.564$) between cirrhotic patients and healthy volunteers.

RV ($r = -0.519$, $P < 0.001$), LMV ($r = -0.415$, $P = 0.007$), LLV ($r = -0.437$, $P = 0.002$) and CV ($r = -0.373$, $P = 0.01$) decreased, while RV/ALB ($r = 0.424$; $P = 0.005$) increased, with progressive Child-Pugh class of cirrhosis. Spearman's rank correlation analyses could not be performed to assess the correlations of LMV/ALB, LLV/ALB or CV/ALB with Child-Pugh class of cirrhosis because no upward or downward trend was found in these parameters, as shown in Table 2. LLV ($P = 0.002$) and LMV ($P = 0.004$) could distinguish class A from B; RV ($P < 0.001$), LMV ($P = 0.019$), LLV ($P = 0.001$), CV ($P = 0.001$), RV/ALB ($P = 0.001$) and LLV/ALB ($P = 0.015$) could distinguish class A from C; and RV ($P = 0.001$) and LLV/ALB ($P < 0.001$) could differentiate class B from C.

Comparisons of liver lobe volume parameters between cirrhotic patients with and without esophageal varices

We only predicted the esophageal varices rather than gastric varices because esophageal varices are one of the major complications of liver cirrhosis, with the risk of bleeding from varices of approximately 25%-35%[5]. Comparison of each liver lobe volume parameter between cirrhotic patients with and without esophageal varices is illustrated in Table 3. As shown by the two independent samples test, RV in patients without esophageal varices was larger than in those with esophageal varices ($P < 0.001$). RV/ALB ($P < 0.001$); CV/ALB ($P = 0.04$) in patients with esophageal varices were larger than in those without esophageal varices.

ROC analysis of liver lobe volume parameters for differentiating the presence of cirrhosis and Child-Pugh classification, and predicting the presence of esophageal varices

In this study, ROC analyses of liver lobe volume parameters were performed to discriminate between patients with and without liver cirrhosis, and distinguish Child-Pugh class A from B, A from C, and B from C. The ROC analyses were also carried out to differentiate

Table 2 Main clinical data of the healthy volunteers and patients with cirrhosis in different Child-Pugh classes

	No cirrhosis	Child-Pugh class of cirrhosis		
	(*n* = 21)	Class A (*n* = 27)	Class B (*n* = 28)	Class C (*n* = 16)
Gender (M/F)	12/9	12/15	13/15	11/5
Age	56.23 ± 13.02	59.43 ± 12.93	54.57 ± 12.59	53.56 ± 16.13
Body weight (kg)	65.42 ± 5.34	60.53 ± 3.20	57.61 ± 2.05	55.33 ± 1.53
BMI (kg/m^2)	23.15 ± 0.54	22.42 ± 0.45	21.25 ± 0.31	19.41 ± 0.24
RV (mm^3)	806.45 ± 198.89[1]	649.60 ± 123.46	586.98 ± 137.28[3]	470.58 ± 46.03[4]
LMV (mm^3)	234.29 ± 70.341	193.23 ± 47.05[2]	161.27 ± 43.04	147.47 ± 83.75[4]
LLV (mm^3)	215.51 ± 133.63	279.60 ± 95.33[2]	218.69 ± 35.47	208.49 ± 36.17[4]
CV (mm^3)	20.28 ± 9.35[1]	34.36 ± 10.46	29.15 ± 12.23	22.41 ± 10.94[4]
ALB (g/L)	45.27 ± 3.46	37.82 ± 4.07	33.24 ± 2.56	26.76 ± 3.23
RV/ALB	17.59 ± 4.31	16.98 ± 3.03	18.61 ± 4.12	20.45 ± 3.55[4]
LMV/ALB	5.52 ± 1.73	5.16 ± 1.39	5.15 ± 1.45	6.43 ± 3.81
LLV/ALB	5.14 ± 3.41[1]	7.29 ± 2.95	7.08 ± 1.26[3]	9.19 ± 1.40[4]
CV/ALB	0.48 ± 0.24[1]	0.87 ± 0.28	0.95 ± 0.43	0.96 ± 0.45

[1]Different from Cirrhosis group, $P < 0.05$; [2]Different from Class B, $P < 0.05$; [3]Different from Class C, $P < 0.05$; [4]Different from Class A, $P < 0.05$. BMI: Body mass index; RV: Right liver lobe volume; LMV: Left medial liver lobe volume; LLV: Left lateral liver lobe volume; CV: Caudate lobe volume; ALB: Albumin.

Table 3 Comparison of liver lobe volume parameters between patients with and without esophageal varices

Parameters	Esophageal varices	
	No (*n* = 46)	Yes (*n* = 25)
RV (mm^3)	687.85 ± 175.73[1]	534.87 ± 85.86
LMV (mm^3)	190.01 ± 63.70	167.18 ± 66.70
LLV (mm^3)	544.26 ± 98.74	216.05 ± 39.04
CV (mm^3)	27.52 ± 12.83	27.61 ± 8.54
RV/ALB	16.98 ± 3.36[1]	21.26 ± 3.01
LMV/ALB	5.26 ± 1.68	5.96 ± 2.96
LLV/ALB	6.91 ± 2.77	7.78 ± 1.92
CV/ALB	0.78 ± 0.41[1]	0.97 ± 0.31

[1]Different from the patients with esophageal varices, $P < 0.05$. RV: Right liver lobe volume; LMV: Left medial liver lobe volume; LLV: Left lateral liver lobe volume; CV: Caudate lobe volume; ALB: Albumin.

between patients with and without esophageal varices. The AUC, cutoff values, satisfactory sensitivity and specificity for the previous differentiations are shown in Table 4. Among these parameters, CV/ALB (AUC = 0.86), LLV (AUC = 0.761), RV (AUC = 0.9) and LLV/ALB (AUC = 0.9) were the best noninvasive factors to distinguish cirrhotic patients from healthy participants (Figure 2A), Child-Pugh class A from B (Figure 2B), A from C (Figure 2C), and B from C (Figure 2D), respectively. RV/ALB (AUC = 0.890) was the best predictor for identifying the presence of esophageal varices in cirrhotic patients (Figure 2E). The best liver lobe volume parameters for differentiating the presence of cirrhosis and Child-Pugh classification, and predicting the presence of esophageal varices, are shown in Table 5.

Table 4 Volume parameters of each liver lobe in determining the presence and Child-Pugh class of liver cirrhosis, and predicting the presence of esophageal varices

Parameters	Cut-off	Differentiations	AUC	Sensitivity	Specificity
RV (mm^3)	692.3	No cirrhosis *vs* cirrhosis	0.816	70.6%	75%
	508.9	Class A *vs* C	0.900	90.3%	84.5%
	522.2	Class B *vs* C	0.803	70.0%	88%
	579.45	No varices *vs* varices	0.780	71.4%	70.0%
LMV (mm^3)	201.3	No cirrhosis *vs* cirrhosis	0.754	70.6%	77.0%
	181.1	Class A *vs* B	0.728	68.0%	71.0%
	155.4	Class A *vs* C	0.751	82.1%	75.0%
LLV (mm^3)	233.2	Class A *vs* B	0.761	74.4%	73.1%
	224.9	Class A *vs* C	0.792	82.1%	75.0%
CV (mm^3)	23.8	No cirrhosis *vs* cirrhosis	0.756	69.0%	65.0%
	25.1	Class A *vs* C	0.806	85.7%	69.0%
RV/ALB	19.9	Class A *vs* C	0.801	68.8%	79.6%
	20.46	No varices *vs* varices	0.890	80.0%	83.5%
LLV/ALB	0.9	No cirrhosis *vs* cirrhosis	0.763	70.6%	71.0%
	8.3	Class A *vs* C	0.752	68.8%	65.5%
	7.5	Class B *vs* C	0.900	93.8%	81.5%
CV/ALB	0.6	No cirrhosis *vs* cirrhosis	0.860	82.0%	83.0%
	0.825	No varices *vs* varices	0.673	64.0%	67.0%

RV: Right liver lobe volume; LMV: Left medial liver lobe volume; LLV: Left lateral liver lobe volume; CV: Caudate lobe volume; ALB: Albumin.

DISCUSSION

Most of published studies have investigated the value of various imaging methods for diagnosing liver cirrhosis and evaluating related complications[3,10,18]. MRI could provide satisfactory quality of three-dimensional reconstruction images and clear anatomy of each liver lobe[19]. The most significant intra- and extra-hepatic changes related to this condition are atrophy of the right liver lobe, hypertrophy of the caudate lobe and the lateral segment of the left lobe, the presence of ascites, decreased albumin, and varicose veins[10,20]; therefore, we investigated the utility of the liver lobe volume obtained on MRI and the ratio of the liver lobe volume to albumin to determine the presence and Child-Pugh class of liver cirrhosis, and to identify the presence of

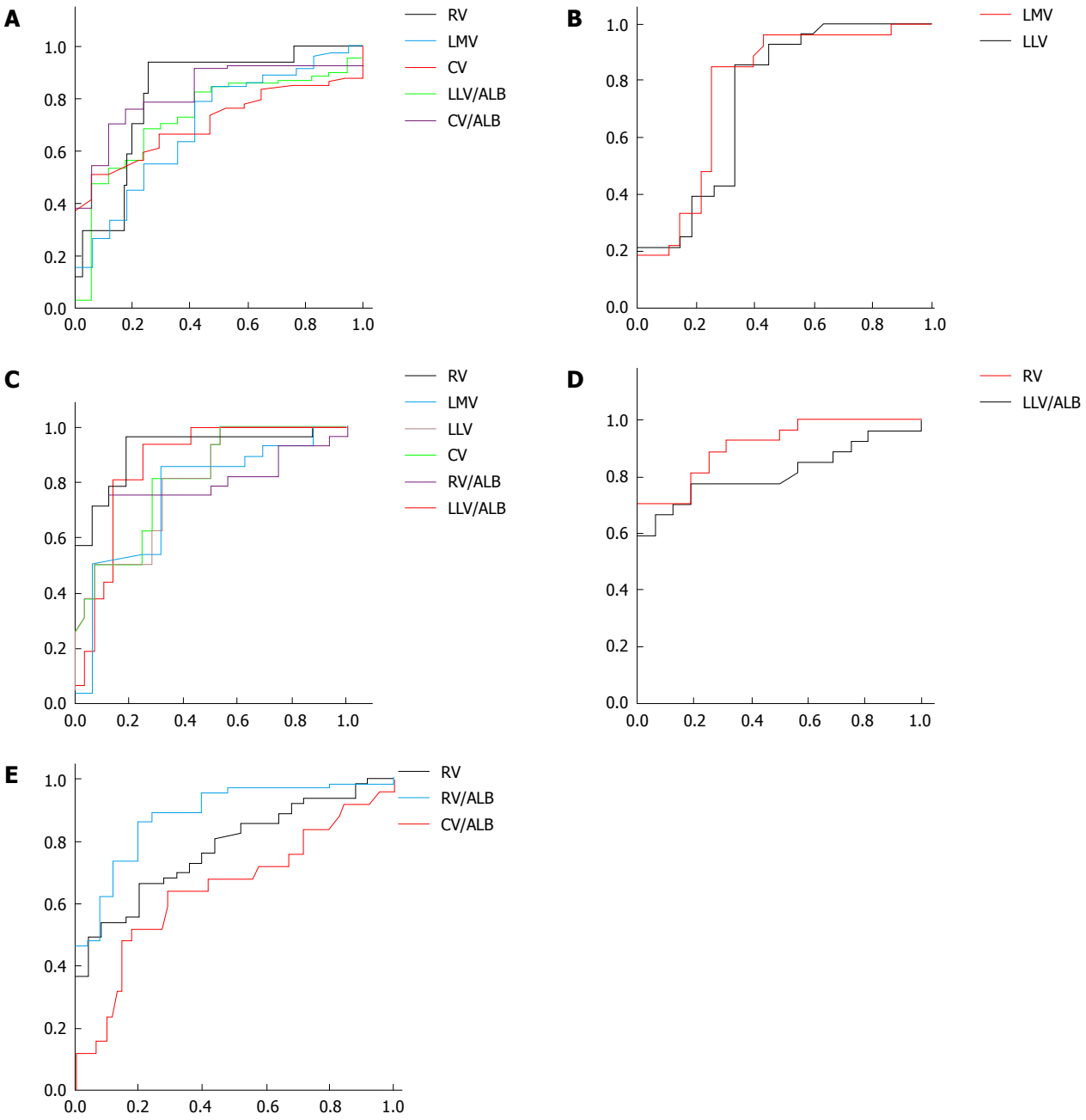

Figure 2 Receiver operating characteristic curves of liver lobe volume parameters to identify the presence, and Child-Pugh class, of liver cirrhosis in patients with hepatitis B, and the presence of esophageal varices. The figures show that the ratio of caudate lobe volume to albumin (CV/ALB), left lateral liver lobe volume (LLV), right liver lobe volume (RV), the ratio of LLV to albumin (LLV/ALB) and the ratio of RV to albumin (RV/ALB) could be recommended as an indicator for distinguishing cirrhotic patients from healthy participants (A), Child-Pugh class A from B (B), class A from C (C), class B from C (D), and cirrhotic patients with esophageal varices from those without esophageal varices (E), respectively.

esophageal varices.

As shown in this study, RV, LMV, LLV, and CV decreased, while RV/ALB increased, with progressive Child-Pugh class of cirrhosis. Regarding the variation of liver lobe volume, patients with compensated cirrhosis typically exhibit hypertrophy of the caudate lobe and the lateral segment of the left lobe, and atrophy of the right lobe and medial segment of the left lobe when the healthy liver progresses to the stage of compensated cirrhosis[10,21]. The pathological mechanism may be that the right portal vein branch enters directly into the parenchyma of the right liver lobe[22]. In cases of cirrhosis, hepatic fibrosis and cirrhosis nodules cause compression and irregular stenoses of the intrahepatic branches of this portal vein, and reduce flow through the right portal branch, resulting in the obvious atrophy of right liver lobe. Conversely, the portal branch runs through the falciform ligament, which is still outside the liver parenchyma, before entering the left liver lobe, resulting in a relatively greater blood supply to the lateral segment. Hypertrophy of the caudate lobe can be explained similarly in that most portal branches (78%)

Table 5 Volume parameters of liver lobes for best identifying the presence and Child-Pugh class of liver cirrhosis, and predicting the presence of esophageal varices

Parameter	Cut-off	Differentiations	Sensitivity	Specificity
CV/ALB	0.6	No cirrhosis *vs* cirrhosis	82.0%	83.00%
RV (mm^3)	508.9	Class A *vs* C	90.3%	84.5%
LLV/ALB	7.5	Class B *vs* C	93.8%	81.5%
LLV (mm^3)	233.2	Class A *vs* B	74.4%	73.1%
RV/ALB (mm^3)	20.46	No varices *vs* varices	80.0%	83.5%

RV: Right liver lobe volume; LMV: Left medial liver lobe volume; LLV: Left lateral liver lobe volume; CV: Caudate lobe volume; ALB: Albumin.

distributed in the caudate lobe arise from the bifurcation of the portal vein and have a shorter intrahepatic course than the vessels in the right lobe[2]. The cause of atrophy of the medial liver lobe may be that the left portal branch inflow to this lobe decreases, as does the right portal branch flow because of the diminishing compensatory hepatic function of the lateral liver lobe and the caudate lobe.

As cirrhosis progresses to decompensated cirrhosis, hypertrophy of the lateral liver lobe and the caudate lobe reaches a maximum, and then the two hypertrophied liver lobes begin to atrophy, with further progressive Child-Pugh class. As regards RV/ALB, our results agreed with those of Alempijevic, who found that the ratio of right liver lobe diameter on ultrasonography to serum albumin was significantly correlated with Child-Pugh class[6]. Based on the more and more obvious decrease of the albumin with the progressive Child-Pugh class of cirrhosis, we presumed that albumin reduced more obviously than RV, leading to the increase of RV/ALB.

As shown by the Mann-Whitney tests, RV, LMV, CV, LLV/ALB and CV/ALB could identify the presence of liver cirrhosis. Clinically, the Child-Pugh Class A patients usually show a good median survival term without orthotopic liver transplantation. The Child-Pugh Class C patients are considered conventional candidates for the procedure. Child-Pugh Class B patients can be considered a heterogeneous group, as their clinical condition may remain stable for more than a year or may rapidly deteriorate[23]. Therefore, it was important to differentiate the Child-Pugh classification. Our study indicated that LLV and LMV could distinguish class A from B; RV, LMV, LLV, CV, RV/ALB and LLV/ALB could distinguish class A from C; and RV and LLV/ALB could differentiate class B from C. Additionally, we also performed ROC analysis to determine how to use RV, LMV, LLV, CV, RV/ALB, LLV/ALB and CV/ALB to identify the occurrence and Child-Pugh class of liver cirrhosis for the first time. Among these parameters, CV/ALB could be the best factor to identify the presence of liver cirrhosis, with an AUC of more than 0.8. LLV, RV and LLV/ALB could best distinguish class A from B, with an AUC of more than 0.75; class A from C, with an AUC of 0.9; and class B from C with an AUC of 0.9, respectively. A previous study reported that liver volume could reflect the liver functional reserve, similar to the Child-Pugh class[24,25]. Our findings further indicate that LLV, RV and LLV/ALB could best reflect the decrease of liver functional reserve from class A from B, A from C, and class B from C.

In addition, cirrhosis can result in esophageal varices, which may induce fulminant massive hemorrhage of the upper gastrointestinal tract. Two recent studies reported that the ratio of right liver lobe diameter on ultrasonography to albumin could be a noninvasive parameter providing accurate information pertinent to determination of presence of esophageal varices[6,26]. As demonstrated in this study, RV, LMV and LLV were larger, and CV, RV/ALB, LMV/ALB, LLV/ALB and CV/ALB were lower in cirrhotic patients with esophageal varices than without esophageal varices. For the first time, we performed the ROC analysis of the previous parameters to predict the presence of esophageal varices, and found that RV/ALB could be the best parameter to predict the presence of esophageal varices, with an AUC of 0.89.

There is a limitation to our study. The sample size was relatively small. In particularly, the healthy control group was small while the cirrhotic group included both compensated and decompensated patients. Moreover, a large number of patients presented with clinical decompensation (ascites) but had no sign of esophageal varices on upper endoscopy, and the possible reason to explain this limitation may be attribute to the small sample size of the compensated patients. Despite this limitation, our study indicated that liver lobe volume parameters could help differentiate the presence of cirrhosis and its Child-Pugh class, and could identify the presence of esophageal varices. We will perform further studies with larger samples to confirm the results.

In conclusion, we confirmed that RV, LMV, LLV and CV decreased, while RV/ALB increased with Child-Pugh class of cirrhosis. CV/ALB could be used to identify the occurrence of cirrhosis, and LLV, RV and LLV/ALB could be recommended for differentiating Child-Pugh class A from B, A from C, and B from C, respectively. RV/ALB could help identify the presence of esophageal varices in cirrhotic patients. The findings could be helpful for the selection of appropriate liver lobe volume parameters to identify the presence and Child-Pugh class of cirrhosis, and the presence of esophageal varices for choosing appropriate treatment.

COMMENTS

Background

It is important to follow up the progress of liver cirrhosis and determine the stage of this disease. The modified Child-Pugh classification system has been confirmed as an independent prognostic factor for survival of cirrhotic patients. Previous studies reported that the changes in liver lobe volume were positively correlated with prognosis of Child-Pugh classes. There was an interesting study focusing on the correlation of the ratio of right liver lobe diameter to albumin with Child-Pugh class. In addition, esophageal varices are one of the major complications of liver cirrhosis, with the risk of bleeding from varices. However, how liver lobe volume and the ratio of liver lobe volume to albumin

could determine the Child-Pugh class of liver cirrhosis and the presence of esophageal varices remained unclear.

Research frontiers

Liver lobe volume measured on magnetic resonance imaging (MRI) or the ratio of right liver lobe diameter to albumin correlates with the Child-Pugh class of liver cirrhosis. However, whether liver lobe volume and the ratio of each liver lobe volume to albumin could predict the Child-Pugh class of liver cirrhosis and the presence of esophageal varices has not been determined.

Innovations and breakthroughs

The authors investigated the association of liver lobe volume measured on magnetic resonance imaging and the ratio of each liver lobe volume to albumin with Child-Pugh class of liver cirrhosis and with the presence of esophageal varices. They utilized receiver-operating characteristic curve analysis to identify the Child-Pugh class of cirrhosis and the presence of esophageal varices.

Applications

The authors found that liver lobe volume measured on magnetic resonance imaging and the ratio of each liver lobe volume to albumin could predict the presence, and Child-Pugh class, of liver cirrhosis, and the presence of esophageal varices. The ratio of caudate lobe volume to albumin could be used to identify the occurrence of cirrhosis. The left lateral liver lobe volume, right liver lobe volume, and the ratio of left lateral liver lobe volume to albumin could be recommended for differentiating Child-Pugh class A from B, A from C, and B from C, respectively. The ratio of right liver lobe volume to albumin could be recommended as an indicator for identifying the presence of esophageal varices in cirrhotic patients.

Terminology

The modified Child-Pugh classification system of liver cirrhosis is considered the cornerstone in prognostic evaluation of cirrhotic patients, and contains five variables, including serum levels of bilirubin and albumin, prothrombin time, ascites, and encephalopathy, and allows categorization of patients into Child-Pugh Class A, B and C.

Peer review

The authors study the potential of combination of liver lobe volumes (measured by MRI) and albumin levels in the identification of liver cirrhosis severity and esophageal varices in patients affected by hepatitis B virus. In addition, the authors observed an interesting correlation between radiological and biochemical parameters for the prediction of "presence of cirrhosis", "Child-Pugh stage of the disease" and "presence of esophageal varices".

REFERENCES

1 **Tsochatzis EA**, Bosch J, Burroughs AK. Liver cirrhosis. *Lancet* 2014; **383**: 1749-1761 [PMID: 24480518 DOI: 10.1016/S0140-6736(14)60121-5]

2 **Ito K**, Mitchell DG, Hann HW, Outwater EK, Kim Y, Fujita T, Okazaki H, Honjo K, Matsunaga N. Progressive viral-induced cirrhosis: serial MR imaging findings and clinical correlation. *Radiology* 1998; **207**: 729-735 [PMID: 9609897 DOI: 10.1148/radiology.207.3.9609897]

3 **Durand F**, Valla D. Assessment of the prognosis of cirrhosis: Child-Pugh versus MELD. *J Hepatol* 2005; **42** Suppl: S100-S107 [PMID: 15777564 DOI: 10.1016/j.jhep.2004.11.015]

4 **Zhou XP**, Lu T, Wei YG, Chen XZ. Liver volume variation in patients with virus-induced cirrhosis: findings on MDCT. *AJR Am J Roentgenol* 2007; **189**: W153-W159 [PMID: 17715084 DOI: 10.2214/AJR.07.2181]

5 **Alempijevic T**, Bulat V, Djuranovic S, Kovacevic N, Jesic R, Tomic D, Krstic S, Krstic M. Right liver lobe/albumin ratio: contribution to non-invasive assessment of portal hypertension. *World J Gastroenterol* 2007; **13**: 5331-5335 [PMID: 17879402]

6 **Psilopoulos D**, Galanis P, Goulas S, Papanikolaou IS, Elefsiniotis I, Liatsos C, Sparos L, Mavrogiannis C. Endoscopic variceal ligation vs. propranolol for prevention of first variceal bleeding: a randomized controlled trial. *Eur J Gastroenterol Hepatol* 2005; **17**: 1111-1117 [PMID: 16148558]

7 **Talwalkar JA**, Yin M, Fidler JL, Sanderson SO, Kamath PS, Ehman RL. Magnetic resonance imaging of hepatic fibrosis: emerging clinical applications. *Hepatology* 2008; **47**: 332-342 [PMID: 18161879 DOI: 10.1002/hep.21972]

8 **Taouli B**, Ehman RL, Reeder SB. Advanced MRI methods for assessment of chronic liver disease. *AJR Am J Roentgenol* 2009; **193**: 14-27 [PMID: 19542391 DOI: 10.2214/AJR.09.2601]

9 **Ito K**, Mitchell DG, Hann HW, Kim Y, Fujita T, Okazaki H, Honjo K, Matsunaga N. Viral-induced cirrhosis: grading of severity using MR imaging. *AJR Am J Roentgenol* 1999; **173**: 591-596 [PMID: 10470885 DOI: 10.2214/ajr.173.3.10470885]

10 **Ito K**, Mitchell DG, Hann HW, Outwater EK, Kim Y. Compensated cirrhosis due to viral hepatitis: using MR imaging to predict clinical progression. *AJR Am J Roentgenol* 1997; **169**: 801-805 [PMID: 9275900 DOI: 10.2214/ajr.169.3.9275900]

11 **North Italian Endoscopic Club for the Study and Treatment of Esophageal Varices**. Prediction of the first variceal hemorrhage in patients with cirrhosis of the liver and esophageal varices. A prospective multicenter study. *N Engl J Med* 1988; **319**: 983-989 [PMID: 3262200 DOI: 10.1056/NEJM198810133191505]

12 **Lok AS**, McMahon BJ. Chronic hepatitis B. *Hepatology* 2007; **45**: 507-539 [PMID: 17256718 DOI: 10.1002/hep.21513]

13 **Li H**, Chen TW, Zhang XM, Li ZL, Zhang JL, Wang D, Li T, Wu JL, Guo X, Chen XL, Li L, Xie XY, Zhang ZS. Liver lobe volumes and the ratios of liver lobe volumes to spleen volume on magnetic resonance imaging for staging liver fibrosis in a minipig model. *PLoS One* 2013; **8**: e79681 [PMID: 24223184 DOI: 10.1371/journal.pone.0079681]

14 **Goldsmith NA**, Woodburne RT. The surgical anatomy pertaining to liver resection. *Surg Gynecol Obstet* 1957; **105**: 310-318 [PMID: 13467662]

15 **Mazonakis M**, Damilakis J, Maris T, Prassopoulos P, Gourtsoyiannis N. Comparison of two volumetric techniques for estimating liver volume using magnetic resonance imaging. *J Magn Reson Imaging* 2002; **15**: 557-563 [PMID: 11997897 DOI: 10.1002/jmri.10109]

16 **Hara AK**, Burkart DJ, Johnson CD, Felmlee JP, Ehman RL, Ilstrup DM, Harmsen WS. Variability of consecutive in vivo MR flow measurements in the main portal vein. *AJR Am J Roentgenol* 1996; **166**: 1311-1315 [PMID: 8633438 DOI: 10.2214/ajr.166.6.8633438]

17 **Johnson CR**, Khandelwal SR, Schmidt-Ullrich RK, Ravalese J, Wazer DE. The influence of quantitative tumor volume measurements on local control in advanced head and neck cancer using concomitant boost accelerated superfractionated irradiation. *Int J Radiat Oncol Biol Phys* 1995; **32**: 635-641 [PMID: 7790249 DOI: 10.1016/0360-3016(95)00031-S]

18 **Alempijevic T**, Kovacevic N. Right liver lobe diameter: albumin ratio: a new non-invasive parameter for prediction of oesophageal varices in patients with liver cirrhosis (preliminary report). *Gut* 2007; **56**: 1166-1167; authro reply 1167 [PMID: 17625152]

19 **Chen XL**, Chen TW, Li ZL, Zhang XM, Chen N, Zeng NL, Li H, Tang HJ, Pu Y, Li CP. Spleen size measured on enhanced MRI for quantitatively staging liver fibrosis in minipigs. *J Magn Reson Imaging* 2013; **38**: 540-547 [PMID: 23349034 DOI: 10.1002/jmri.24007]

20 **Cho KC**, Patel YD, Wachsberg RH, Seeff J. Varices in portal hypertension: evaluation with CT. *Radiographics* 1995; **15**: 609-622 [PMID: 7624566 DOI: 10.1148/radiographics.15.3.7624566]

21 **Saygili OB**, Tarhan NC, Yildirim T, Serin E, Ozer B, Agildere AM. Value of computed tomography and magnetic resonance imaging for assessing severity of liver cirrhosis secondary to viral hepatitis. *Eur J Radiol* 2005; **54**: 400-407 [PMID: 15899343 DOI: 10.1016/j.ejrad.2004.08.001]

22 **Zhou L**, Chen TW, Zhang XM, Yang Z, Tang HJ, Deng D, Zeng NL, Wang LY, Chen XL, Li H, Li CP, Li L, Xie XY, Hu J. Liver dynamic contrast-enhanced MRI for staging liver fibrosis in a piglet model. *J Magn Reson Imaging* 2014; **39**: 872-878 [PMID: 24123400 DOI: 10.1002/jmri.24248]

23 **Abdalla EK**, Denys A, Chevalier P, Nemr RA, Vauthey JN.

Total and segmental liver volume variations: implications for liver surgery. *Surgery* 2004; **135**: 404-410 [PMID: 15041964 DOI: 10.1016/j.surg.2003.08.024]

24 **Keeffe EB**. Summary of guidelines on organ allocation and patient listing for liver transplantation. *Liver Transpl Surg* 1998; **4**: S108-S114 [PMID: 9742503]

25 **Schiano TD**, Bodian C, Schwartz ME, Glajchen N, Min AD. Accuracy and significance of computed tomographic scan assessment of hepatic volume in patients undergoing liver transplantation. *Transplantation* 2000; **69**: 545-550 [PMID: 10708109 DOI: 10.1097/00007890-200002270-00014]

26 **Esmat S**, Omarn D, Rashid L. Can we consider the right hepatic lobe size/albumin ratio a noninvasive predictor of oesophageal varices in hepatitis C virus-related liver cirrhotic Egyptian patients? *Eur J Intern Med* 2012; **23**: 267-272 [PMID: 22385886 DOI: 10.1016/j.ejim.2011.11.010]

P- Reviewer: Higuera-de la Tijera MF, Kovacs SJ, Lisotti A, Maroni L, Raggi CMF
S- Editor: Qi Y **L- Editor**: Stewart G **E- Editor**: Liu XM

World Journal of Gastroenterology

Submit a Manuscript: http://www.wjgnet.com/esps/
Help Desk: http://www.wjgnet.com/esps/helpdesk.aspx
DOI: 10.3748/wjg.v21.i3.997

World J Gastroenterol 2015 January 21; 21(3): 997-1000
ISSN 1007-9327 (print) ISSN 2219-2840 (online)

CASE REPORT

Preoperative trans-jugular porto-systemic shunt for oncological gastric surgery in a cirrhotic patient

Andrea Liverani, Luigi Solinas, Tatiana Di Cesare, Luca Velari, Tiziano Neri, Francesco Cilurso, Francesco Favi, Giancarlo Bizzarri

Andrea Liverani, Luigi Solinas, Tatiana Di Cesare, Tiziano Neri, Francesco Cilurso, Francesco Favi, Department of General Surgery, Regina Apostolorum Hospital, 00100 Rome, Italy
Luca Velari, Giancarlo Bizzarri, Department of Radiology, Regina Apostolorum Hospital, 00100 Rome, Italy
Author contributions: Liverani A designed the research and had final approval of the version to be published; Solinas L and Di Cesare T performed the research; Velari L and Bizzarri G contributed new reagents or analytic tools; Neri T and Cilurso F made substantial contributions to the conception and design; Favi F analyzed the data; Liverani A, Solinas L and Di Cesare T wrote the paper.

Correspondence to: Tatiana Di Cesare, MD, Department of General Surgery, Regina Apostolorum Hospital, Via San Francesco 50, 00040 Albano Laziale (RM), 00100 Rome, Italy. tatiana.dicesare@hotmail.it
Telephone: +39-6-932989
Fax: +39-6-9321138
Received: March 6, 2014
Peer-review started: March 7, 2014
First decision: April 28, 2014
Revised: May 13, 2014
Accepted: October 15, 2014
Article in press: October 15, 2014
Published online: January 21, 2015

Abstract

Abdominal surgery in cirrhotic patients with portal hypertension is associated with high incidence of disease and mortality. In these patients, oncological gastric procedures with lymph-nodes dissection show much higher complication rates than in normotensive portal vein patients. Thus, normalization of portal vein pressure may be a favorable determinant factor to reduce complications. We report a case of a patient with hepatitis C virus-related hepatic cirrhosis, esophageal varices, portal hypertension and gastric cancer. We demonstrated the efficacy of a preoperative trans-jugular porto-systemic shunt to perform oncological radical resection more safely. We retained preoperative the trans-jugular porto-systemic shunt in the patients with elevated portal pressure and gastric cancer to perform a gastrectomy more safely and to decrease morbidity and mortality of these cases.

Key words: Gastric cancer; Cirrhotic patients; Esophageal varices; Portal hypertension; Trans-jugular porto-systemic shunt; Gastric surgery

Core tip: We suggest a preoperative trans-jugular porto-systemic shunt in patients with portal hypertension and gastric cancer to perform a safer gastrectomy. This procedure decreases intraoperational blood loss and postoperative morbidity. Moreover, the normalization of portal vein pressure permits the performance of an oncological nodes dissection. Finally, this technique may reduce perioperative mortality.

Liverani A, Solinas L, Di Cesare T, Velari L, Neri T, Cilurso F, Favi F, Bizzarri G. Preoperative trans-jugular porto-systemic shunt for oncological gastric surgery in a cirrhotic patient. *World J Gastroenterol* 2015; 21(3): 997-1000 Available from: URL: http://www.wjgnet.com/1007-9327/full/v21/i3/997.htm DOI: http://dx.doi.org/10.3748/wjg.v21.i3.997

INTRODUCTION

Abdominal surgery in cirrhotic patients with portal hypertension is associated with high incidence of disease and mortality. In these patients, oncological gastric procedures with lymph-nodes dissection show a much higher rate of complications than in normotensive portal vein patients. Thus, normalization of portal vein pressure may be a favorable determinant factor to reduce complications.

CASE REPORT

An 80-year-old female patient presented an endoscopic report of gastric neoplasia. Two months previously, she was subjected to an endoscopic oesophageal varices ligation because of variceal rupture (Figure 1). The Child-Pugh classification was B and portal pressure was up to 28 mmHg.

Preoperative oncological staging showed the absence of local or distant metastasis, and the patient was a candidate for radical resection. To reduce portal pressure and the risks of esophagogastric variceal rupture relapse, a preoperative transjugular intrahepatic portosystemic shunt (TIPSS) was proposed and successfully created. The right gastric vein was coiled. Normal portal pressure was reached, with values ranging from 12 to 15 mmHg.

Radiological procedure: the patient was placed a supine position in the angiographic suite. A rotation of the head to the left was required.

We used a spontaneous breathing general anesthesia for the radiological procedure, using a laryngeal mask, with a mixture of O_2, N_2O and isoflurane (1%-2%).

Puncture of the right internal jugular vein was performed with real-time sonography guidance using an 18-gauge needle.

A 0.035 degree angle Hydrophilic Coated Guidewires (Terumo Glidewire®, Tokyo, Japan) was inserted into the jugular vein, down to the inferior vena cava (IVC).

A 12-F introducer sheath was positioned in the right atrium and then into the IVC to measure the pressure. The hepatic vein was then catheterized directly using the curved metallic cannula of the TIPSS set (AngioDynamics®; Queensberry, NY, United States) and the guidewire (Terumo Glidewire®). The blood flow through the vein was sufficient to visualize the structure of the hepatic vein. Percutaneous puncture of portal vein was performed by placing a small introducer to permit portography (Figure 2).

The right hepatic vein was catheterized and the portal vein puncture was performed through the wall of the hepatic vein 1-3 cm from its origin. The catheter was turned anteriorly and advanced into the liver parenchyma for 4-5 cm. It was then slowly moved back and at the same time it was aspirated with a syringe. The correct puncture was checked *via* portography and a guidewire was introduced into the mesenteric vein.

Pressure was measured to evaluate the portosystemic differential pressure. A venogram was used to define the measure of the intrahepatic tract using a marked pigtail catheter.

Figure 1 Oesophageal and gastric varices.

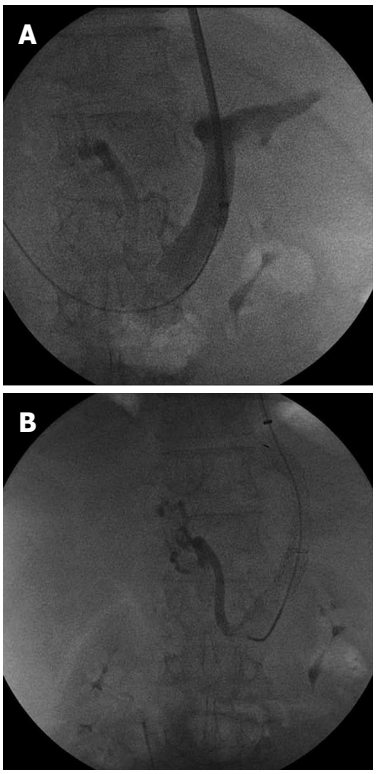

Figure 2 Portography. A: Transjugular intrahepatic porto-systemic shunt 1; B: Transjugular intrahepatic porto-systemic shunt 2.

Afterwards, an Amplatz Super Stiff™ Guidewire (Boston Scientific; Natick, MA, United States) was inserted into the splenic or mesenteric vein, and the intrahepatic tract was dilated using an 8 mm low-profile balloon (Wanda™, Boston Scientific; Natick, MA, United States).

The GORE® VIATORR® stent graft comprises a self-expanding nitinol endoprosthesis with a high radial strength and is covered with an ultrathin expanded polytetrafluoroethylene tube.

The 12-F introducer sheath was positioned into the portal system for 3 cm and moved back to have release of the uncovered tract within the portal vein. Once the

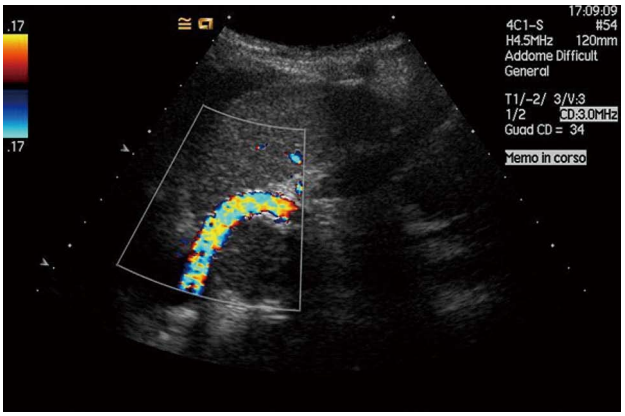

Figure 3 Ecocolor Doppler transjugular intrahepatic porto-systemic shunt.

Figure 4 Computed tomography. A: Computed tomography after a transjugular intrahepatic porto-systemic shunt; B: Coil embolization of right gastric vein.

endoprosthesis was positioned, the whole device was carefully removed until a resistance was felt, thus showing that the proximal tract of the device was positioned at the junction of the portal vein with the intrahepatic tract. The introducer was advanced largely upstream of the beginning of the endoprosthesis and, while positioning the system in place, the coated portion of the VIATORR® (60-20-10 mm, Figure 3) was released.

The endoprosthesis was then expanded, with the low-profile balloon catheter used previously. After complete deployment of the Viatorr, blood flow through the shunt was measured to check its function, and the mean atrial and portal pressures were evaluated to ascertain the hemodynamic significance of the procedure (PSG < 12 mmHg).

In conclusion, the right gastric vein, which fueled the massive variceal was embolized with coils. One month later, the patient was readmitted to the Surgical Department and a D-2 distal gastrectomy with a B2 gastrojejunal anastomosis was performed.

No intraoperative complications were observed and no transfusions were requested during the procedure. No postoperative bleeding or hepatic dysfunctions occurred, and the postoperative course was uneventful, except for delayed gastric stump empting with hospital discharge in 14 d.

DISCUSSION

A cirrhotic patient with portal hypertension as a candidate for an extrahepatic abdominal major procedure is a surgical challenge, especially if variceal bleeding is present. In these cases, morbidity and mortality is higher, ranging from 10% to 60%[1]. Gastric surgery in patients with portal hypertension is associated with mortality in excess of 10% and a morbidity rate of 25%[2].

The two major factors that contribute to higher operative mortality are propensity for bleeding and ascites, which increase the risk of infection. Less frequently hepatic insufficiency, hepato-renal syndrome or sepsis are determinants for postoperative complications, and often determine a fatal multiorgan failure[3].

Thus, it would seem important to achieve the best and most relevant preoperative control all correctable factors, such as ascites control, correction of coagulopathies, malnutrition and protein catabolism, amelioration of Child's class or, finally, reduction of portal pressure.

In fact, a preoperative procedure to reduce or normalize portal pressure seems to decrease surgical risks, with lower incidence of complications and death[4-6].

At present, TIPSS is the preferred noninvasive procedure for treating portal hypertension and variceal bleeding[7-9]; however, its use preoperatively before extrahepatic abdominal surgery is rarely described (Figure 4).

In our patient, recent recurrent variceal bleeding had been referred and an oncological gastric procedure was mandatory.

We retained the preoperative TIPSS in the patients with elevated portal pressure and gastric cancer to perform a gastrectomy more safely, and to decrease the morbidity and mortality of these cases.

COMMENTS

Case characteristics

The patient had esophageal varices bleeding twice that were treated by endoscopy. In the last month the patient suffered dysphagia, epigastric pain and weight loss.

Clinical diagnosis

Gastroscopy showed an endoluminal hemorrhagic pyloric lesion of the stomach.

Differential diagnosis

Histopathological examination after endoscopic biopsy showed gastric carcinoma.

Laboratory diagnosis

Anemia, low dosage of albumin and coagulopathy.

Imaging diagnosis

A total body computed tomography scan showed the gastric lesion, esophageal varices, hepatic cirrhosis and ascites.

Treatment

Trans-jugular porto-systemic shunt (TIPSS) and gastric resection was performed in two steps.

Experiences and lessons

This case showed that preoperative TIPSS before gastric surgery reduced

perioperative morbidity and mortality.

Peer review

TIPSS is a useful and safe radiological procedure to treat portal vein hypertension. Cirrhotic patients undergoing oncological gastric surgery can be submitted to TIPSS 40-60 d before surgery. This procedure decreases intraoperative bleeding, morbidity and mortality.

REFERENCES

1 **Guglielmi A**, Girlanda R, Lombardo F, de Manzoni G, Frameglia M, Pelosi G, Baldin M. TIPS allowing for an endoscopic mucosal resection of early gastric cancer in a cirrhotic patient with severe hypertensive gastropathy: report of a case. *Surg Today* 1999; **29**: 902-905 [PMID: 10489133 DOI: 10.1007/BF02482783]

2 **Catalano G**, Urbani L, De Simone P, Morelli L, Coletti L, Cioni R, Matocci G, Mosca F, Filipponi F. Expanding indications for TIPSS: portal decompression before elective oncologic gastric surgery in cirrhotic patients. *J Clin Gastroenterol* 2005; **39**: 921-923 [PMID: 16208123 DOI: 10.1097/01.mcg.0000180798.41704.43]

3 **Minicozzi A**, Veraldi GF, Borzellino G. Minimally invasive treatment of portal hypertension, abdominal aortic aneurysm, and colon cancer: a case report. *Surg Laparosc Endosc Percutan Tech* 2010; **20**: 281-283 [PMID: 20729703 DOI: 10.1097/SLE.0b013e3181e1348d]

4 **Norton SA**, Vickers J, Callaway MP, Alderson D. The role of preoperative TIPSS to facilitate curative gastric surgery. *Cardiovasc Intervent Radiol* 2003; **26**: 398-399 [PMID: 14667124 DOI: 10.1007/s00270-003-0018-9]

5 **Gil A**, Martínez-Regueira F, Hernández-Lizoain JL, Pardo F, Olea JM, Bastarrika G, Cienfuegos JA, Bilbao JI. The role of transjugular intrahepatic portosystemic shunt prior to abdominal tumoral surgery in cirrhotic patients with portal hypertension. *Eur J Surg Oncol* 2004; **30**: 46-52 [PMID: 14736522 DOI: 10.1016/j.ejso.2003.10.014]

6 **Rumstadt B**, Schilling D. The preoperative placement of transjugular intrahepatic portosystemic shunt for treatment of a patient with portal hypertension and gastric cancer. *Hepatogastroenterology* 2008; **55**: 303-304 [PMID: 18507130]

7 **von Renteln D**, Riecken B, Muehleisen H, Caca K. Transjugular intrahepatic portosystemic shunt and endoscopic submucosal dissection for treatment of early gastric cancer in a cirrhotic patient. *Endoscopy* 2008; **40** Suppl 2: E32-E33 [PMID: 18283618 DOI: 10.1055/s-2007-966800]

8 **Han SG**, Han KJ, Cho HG, Gham CW, Choi CH, Hwang SY, Song SY. A case of successful treatment of stomal variceal bleeding with transjugular intrahepatic portosystemic shunt and coil embolization. *J Korean Med Sci* 2007; **22**: 583-587 [PMID: 17596678 DOI: 10.3346/jkms.2007.22.3.583]

9 **Palikhe M**, Xue H, Jha RK, Li YC, Yuan J, Wang J, Zhang M. Changes in portal hemodynamics after TIPS in liver cirrhosis and portal hypertension. *Scand J Gastroenterol* 2013; **48**: 570-576 [PMID: 23452021]

P- Reviewer: Anand BS **S- Editor**: Gou SX
L- Editor: Stewart G **E- Editor**: Zhang DN

World Journal of Gastroenterology

Submit a Manuscript: http://www.wjgnet.com/esps/
Help Desk: http://www.wjgnet.com/esps/helpdesk.aspx
DOI: 10.3748/wjg.v21.i3.1001

World J Gastroenterol 2015 January 21; 21(3): 1001-1008
ISSN 1007-9327 (print) ISSN 2219-2840 (online)

CASE REPORT

Novel *LIPA* mutations in Mexican siblings with lysosomal acid lipase deficiency

Yuritzi Santillán-Hernández, Enory Almanza-Miranda, Winnie W Xin, Kendrick Goss, Aurea Vera-Loaiza, María T Gorráez-de la Mora, Raul E Piña-Aguilar

Yuritzi Santillán-Hernández, Aurea Vera-Loaiza, Medical Genetics Department, Centro Médico Nacional "20 de Noviembre", ISSSTE, México City 03100, México
Enory Almanza-Miranda, Pediatric Gastroenterology Department, Centro Médico Nacional "20 de Noviembre", ISSSTE, México City 03229, México
Winnie W Xin, Kendrick Goss, Neurogenetics DNA Diagnostic Laboratory, Massachusetts General Hospital, Boston, MA 02114, United States
María T Gorráez-de la Mora, Pathology Department, Centro Médico Nacional "20 de Noviembre", ISSSTE, México City 03229, México
Raul E Piña-Aguilar, Medical Genomics Division, Centro Médico Nacional "20 de Noviembre", ISSSTE, México City 03100, México
Author contributions: Santillán-Hernández Y, Almanza-Miranda E, Vera-Loaiza A and Piña-Aguilar RE designed the report; Goss K and Xin WW performed the genetic analyses; Piña-Aguilar RE, Almanza-Miranda E, Vera-Loaiza A and Santillán-Hernández Y collected the patient's clinical data; Gorráez-de la Mora MT performed the pathology studies and analyzed histological data; Piña-Aguilar RE, Almanza-Miranda E, Vera-Loaiza A, Goss K and Xin WW analyzed the data and wrote the paper.

Correspondence to: Raul E Piña-Aguilar, MD, Medical Genomics Division, Centro Médico Nacional "20 de Noviembre", ISSSTE, San Lorenzo #502D, Col. del Valle, Del. Benito Juarez, México City 03100, México. rpina.a@hotmail.com
Telephone: +52-55-52005003-14645
Received: June 18, 2014
Peer-review started: June 18, 2014
First decision: July 21, 2014
Revised: August 12, 2014
Accepted: September 29, 2014
Article in press: September 30, 2014

Published online: January 21, 2015

Abstract

Lysosomal acid lipase (LAL) deficiency is an under-recognized lysosomal disease caused by deficient enzymatic activity of LAL. In this report we describe two affected female Mexican siblings with early hepatic complications. At two months of age, the first sibling presented with alternating episodes of diarrhea and constipation, and later with hepatomegaly, elevated transaminases, high levels of total and low-density lipoprotein cholesterol, and low levels of high-density lipoprotein. Portal hypertension and grade 2 esophageal varices were detected at four years of age. The second sibling presented with hepatomegaly, elevated transaminases and mildly elevated low-density lipoprotein and low high-density lipoprotein at six months of age. LAL activity was deficient in both patients. Sequencing of *LIPA* revealed two previously unreported heterozygous mutations in exon 4: c.253C>A and c.294C>G. These cases highlight the clinical continuum between the so-called Wolman disease and cholesteryl ester storage disease, and underscore that LAL deficiency represents a single disease with a degree of clinical heterogeneity.

Key words: Cholesteryl ester storage disease; Liver fibrosis; Dyslipidemia; Liver steatosis; Wolman disease

Core tip: Lysosomal acid lipase deficiency is a rare genetic disorder related to the metabolism of cholesterol and triglycerides inside the lysosome. In this report, we present the findings from two siblings with no lysosomal acid lipase activity caused by two previously unidentified mutations in exon 4 of *LIPA*.

The patients had early hepatic presentation, including severe cirrhosis and esophageal varices in the elder sibling, underscoring the significant morbidity that can occur at all ages of lysosomal acid lipase deficiency and highlighting possible compensatory mechanisms in liver function in children.

Santillán-Hernández Y, Almanza-Miranda E, Xin WW, Goss K, Vera-Loaiza A, Gorráez-de la Mora MT, Piña-Aguilar RE. Novel *LIPA* mutations in Mexican siblings with lysosomal acid lipase deficiency. *World J Gastroenterol* 2015; 21(3): 1001-1008 Available from: URL: http://www.wjgnet.com/1007-9327/full/v21/i3/1001.htm DOI: http://dx.doi.org/10.3748/wjg.v21.i3.1001

INTRODUCTION

Lysosomal acid lipase deficiency (LALD; OMIM #278000) is an autosomal recessive disease caused by mutations in *LIPA* at chromosomal locus 10q23.31, which encodes a hydrolase involved in the degradation of lysosomal cholesterol esters and triglycerides. Clinically, LALD has been historically reported as one of two principal phenotypic presentations: early onset, often called Wolman disease (WD), and late onset, termed cholesteryl ester storage disease (CESD)[1].

The early presentation of LALD has an estimated prevalence of 1/350000 in infants, with symptoms such as diarrhea, massive hepatosplenomegaly, malabsorption, cachexia and adrenal calcifications, which typically develop within the first three months of life. Liver cirrhosis results in fatal liver failure before one year of age[1]. The exact prevalence of LALD in children and adults is not yet established, and ranges from 1 in 150000 to 300000 in Caucasians[1] and 1 in 40000 in German newborns[2]. The clinical signs and symptoms are heterogeneous, including hepatic steatosis leading to hepatomegaly and hepatic fibrosis and cirrhosis, splenomegaly, type Ⅱ hyperlipoproteinemia, and accelerated atherosclerosis. Although some patients remain asymptomatic until adulthood, infants and children can have significant morbidity and early mortality as a result of liver cirrhosis and liver failure[3].

A review analyzing 135 CESD patients published in the literature found that the mean age at presentation was 5 years (range: 1-44 years), with hepatomegaly as the most common manifestation[3]. In that review, Bernstein *et al*[3] noted that the age at presentation was between 0 and 2 years in the most severely affected cases, corresponding to 27% of patients and highlighting the significance of liver morbidity (cirrhosis, fibrosis, and failure). Another recent review showed that all 71 pediatric LALD cases had hepatomegaly, with 63% presenting symptoms before five years of age[4]. The early signs of portal hypertension and its correlation to hepatic fibrosis and the progression of disease are unknown. Although liver manifestations of the disease usually predominate, dyslipidemia and associated cardiac complications have also been reported[1,3]. The principal causes of death reported in CESD patients were liver failure and bleeding of esophageal varices[3]. However, bleeding of esophageal varices was reported in only 8% of patients[3], and this complication is primarily described in Mexican patients[5].

In this report, we describe the cases of two Mexican siblings with LALD that was attributed to previously undescribed mutations in exon 4 of *LIPA*. These siblings presented symptoms within the first year of life and developed portal hypertension before four years of age. Both cases demonstrated early clinical signs and symptoms and relatively rapid clinical progression of the disease compared to previously reported cases.

CASE REPORT

Sibling 1

This report describes the case of a 9-year-old girl with healthy, non-consanguineous parents from Mexico, who was apparently normal at birth and met normal development milestones. She became symptomatic at two months of age, presenting with alternating episodes of diarrhea and constipation, and reduced weight and height. Hepatomegaly was detected by abdominal radiography at six months of age during the evaluation for diarrhea. An initial laboratory workup indicated leukocytosis (16000/mL) and eosinophilia (2700/mL), and a bone marrow analysis showed an increase of myeloid series, with augmented cellularity and the presence of megakaryocytes, without immature cells. The patient then underwent additional testing to rule out a hematologic malignancy. Further workup included karyotype in peripheral blood, reported as 46, XX[20].

Laboratory assessments at two years of age showed: hemoglobin, 14.1 g/dL; leukocytes, 13200/mL; eosinophilia, 3200/mL (24.6% of white blood cell differential count); platelets, 330000; abnormal liver enzymes and dyslipidemia (Table 1) with evidence of chronic Epstein-Barr virus infection. Serology for hepatitis A, B and C was negative. Hepatosplenomegaly was confirmed by abdominal ultrasound.

A computed tomography scan at four years of age revealed an enlarged liver, with a longitudinal diameter of 18 cm and spleen length of 13.4 cm, without adrenal calcifications. The patient was transferred to the pediatric gastroenterology department in our hospital for further investigation for metabolic disease. She presented gastrointestinal bleeding and endoscopy revealed grade 2 (Sohendra) esophageal varices.

When the patient was five years of age, a hepatic biopsy showed multinodular microvesicular steatosis in 10% of hepatocytes, with irregular small nodules separated by gross bands of porto-portal fibrosis with no zonal preference, ballooning degeneration and pseudoacinar regeneration, and no stasis of bilirubin or deposition of copper or iron (Figure 1A, B). The portal triads were expanded by fibrous tissue, with sparse duct

Table 1 Hepatic function test, lipid profile and coagulation values in patients

Parameter (unit)	Sibling 1		Sibling 2		Reference value
	2 yr	9 yr	6 mo	4 yr	
AST (U/L)	229	192	61	221	8-50
ALT (U/L)	344	193	56	181	7-45
Alkaline phosphatase (U/L)	365	545	328	402	4 yr: 169-372 9 yr: 212-468
Lactate dehydrogenase (U/L)	258	281	288	236	4-6 yr: 145-345 7-9 yr: 143-290
Total bilirubin (mg/dL)	0.8	0.42	0.2	0.42	0.1-0.9
Indirect bilirubin (mg/dL)	0.7	0.2	0.1	0.28	
Total cholesterol (mg/dL)	343.0	211.0	165.0	221.0	< 170
Triglycerides (mg/dL)	316.0	118.0	154.0	181.0	< 90
LDL-cholesterol (mg/dL)	277.1	157.4	123.0	154.8	< 100 (optimal)
HDL-cholesterol (mg/dL)	22.3	30.0	30.0	30.0	⩾ 60
Trombin time (min)	21.87	23.1	21.1	20.8	15-22
Prothrombin time (min)	13.9	14.8	12.0	12.4	11-15
pTT (min)	30.2	35.1	27.8	32.0	25-33
INR (%)	1.15 (92.8%)	1.3 (58.4%)	1 (100.8%)	1.1 (72.8%)	0.8-1.1 (89%-129%)

proliferation. Cells with foamy cytoplasm were observed in the portal space and in the fibrous tissue, which demonstrated diastase resistance and Periodic acid-Schiff positivity. Kupffer sinusoidal cells were immunopositive for CD68 (Figure 1C) and immunonegative for Hepar-1 and pan-cytokeratin, with fine granules containing autofluorescent ceroid-like material (Figure 1D).

Doppler ultrasound at six years of age showed a homogenous parenchyma, with normal echogenicity and without intrahepatic lesions or increased flux in portal circulation.

A duodenal biopsy performed when the patient was seven years of age showed preserved architecture of duodenal mucosa, but with groups of histiocytes with fluorescent ceroid material occupying about 40% of the *lamina propria* of villi (Figure 1E) that were associated with lymphocytes. A liver biopsy also demonstrated the same changes, with minimal steatosis that was decreased from the biopsy performed at five years. The histology indicated micronodular cirrhosis, widened portal spaces and fibrotic tissue with histiocytes, with an absence of a central vein and nodules of hepatic regeneration.

The pathologic findings of the biopsies were interpreted as a possible diagnosis of Niemann-Pick disease. Thus, sphingomyelinase activity was measured by mass spectrometry, and quantified as 2.3 μmol/L per hour (reference value ⩾ 2 μmol/L per hour). A skin biopsy was taken to determine cholesterol esterification and filipin staining in cultured fibroblasts to eliminate Niemann-Pick type C disease (performed at Mayo Clinic, United States), revealing low-density lipoprotein esterification that was 2% of normal control cells, similar to patients with Niemann-Pick type C disease, but with normal filipin staining.

The patient was not given any lipid-lowering drugs; recent laboratory test results are shown in Table 1. Associated with the progression of her liver disease and the associated portal hypertension and splenomegaly, the patient's platelet count decreased to 96000 (reference range: 150000-500000). Endoscopy performed at nine years of age revealed continued presence of grade 2 esophageal varices (Figure 1F) and one medium gastric varix; the esophageal varices were ligated. The last Doppler ultrasound showed a longitudinal liver diameter of 14.7 cm, increased liver echogenicity, micronodular pattern, spleen longitudinal length of 14.6 cm, and increase in portal flux and collateral circulation with porto-systemic shunts (splenorenal shunt and umbilical vein recanalization) (Figure 2). The patient is currently being treated with propranolol (2 mg/kg per day) for gastrointestinal bleeding prophylaxis and vitamin K (10 mg/d) for prolonged bleeding times.

Sibling 2

Given the suspicion of a probable lysosomal storage disease in sibling 1, we began the study of her now 4-year-old sister at six months of age. The initial physical examination revealed reduced height and hepatomegaly, which was confirmed by an abdominal ultrasound showing the liver with a longitudinal diameter of 8.4 cm and increased echogenicity, and a spleen length of 7.1 cm. Laboratory tests revealed alterations in liver function and lipid profile (Table 1); however, a bone marrow aspirate indicated no evidence of storage disease. Sphingomyelinase activity was 2.8 μmol/L per hour. A recent endoscopy showed no varices, but Doppler ultrasound demonstrated increased hepatic flux, without porto-systemic shunts (Figure 2).

LAL enzymatic and molecular analyses

Following exclusion of Niemann-Pick diseases, a diagnosis of LALD was considered for both siblings. LAL activity was determined using a fluorescence-based whole blood assay with 4-methylumbelliferone[6], which revealed < 0.02 pmol/punch*h (normal range: 24.00-134.00 pmol/punch*h) in dried blood and 0.000 nmol/punch*h in whole blood (normal range: 0.027-0.152 nmol/punch*h). LAL activity from dried

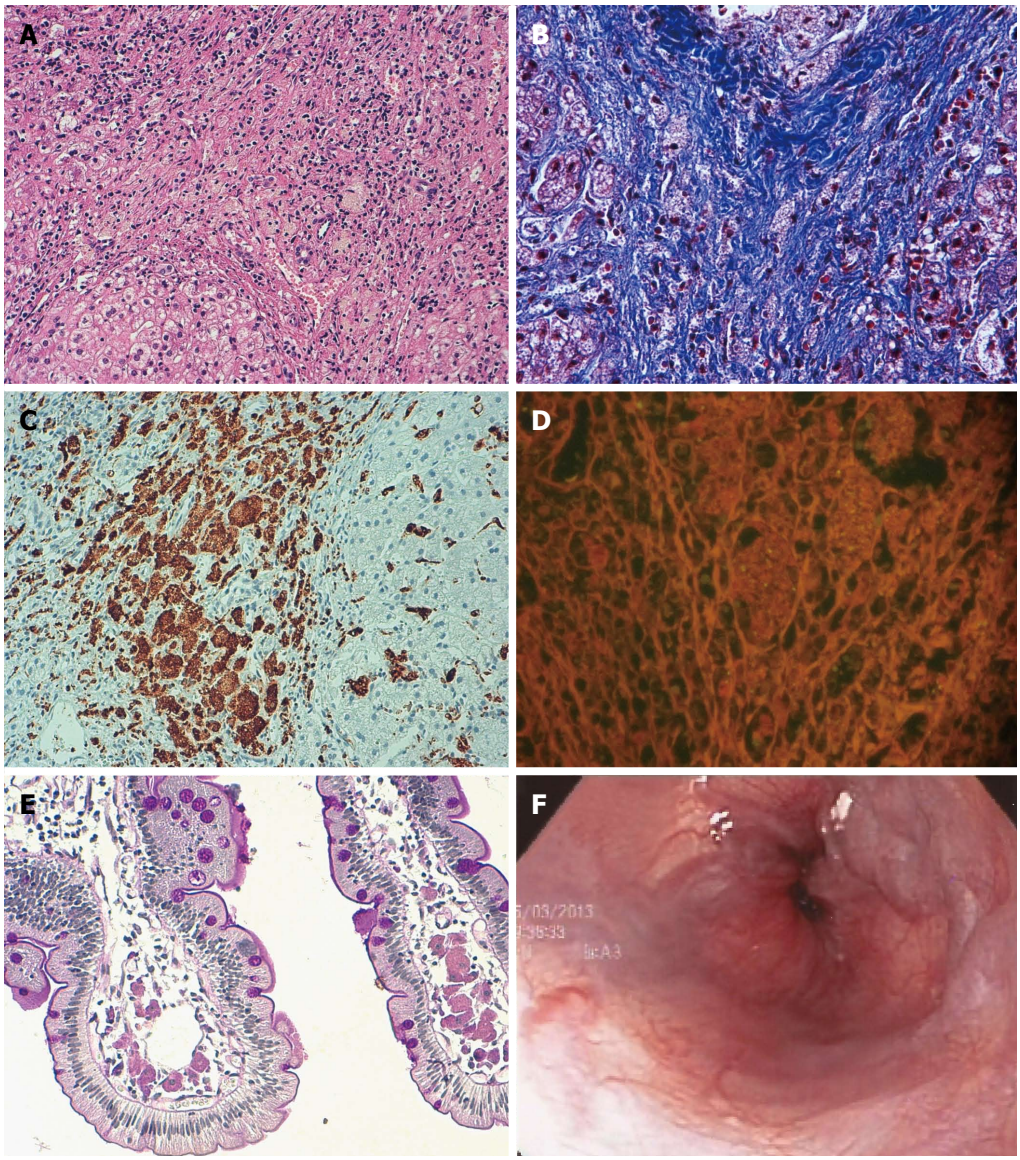

Figure 1 Liver histopathology and endoscopy images from sibling 1. A: Presence of ballooning and pseudoacinar regeneration, with foamy cells (HE, magnification × 400); B: Presence of portal triads expanded by fibrosis tissue and foamy cells (Masson's tricromic, magnification × 400); C: Positive CD68 immunoreactivity in cells (CD68 immunostaining); D: Autofluorescence of foamy cells in portal spaces (Masson's tricromic, magnification × 400); E: Duodenal biopsy shows histiocytes with ceroid material in the lamina propria of the villi; F: Endoscopy showing esophageal varices.

blood samples was 40.06 pmol/punch*h in the father, and 19.53 pmol/punch*h (low normal) in the mother.

LIPA sequencing

Genomic DNA was extracted from dried blood spots, and exons 1-10 of *LIPA* were amplified by polymerase chain reaction and labeled with Big Dye Terminator (Applied Biosystems of Thermo Fisher Scientific Inc., Waltham, MA, United States) and resolved by capillary electrophoresis on a 3730XL Genetic Analyzer (Applied Biosystems). Sequencing revealed a previously reported single nucleotide polymorphism within intron 5 (rs2297472; c.539-5C>T), along with two previously unreported missense mutations in exon 4: c.253C>A (p.Gln85Lys) and c.294C>G (p.Asn98Lys) (Figure 3). Subsequent sequencing of exon 4 in the parents showed that the father was a carrier of the c.294C>G mutation, and the mother carried the c.253C>A mutation. This confirmed the *trans*-state of mutations in the siblings.

Bioinformatics analyses using the Polyphen-2 and Sorting Intolerant From Tolerant (SIFT) predictive tools indicated that the exon 4 mutations are likely to be pathogenic, which was also indirectly demonstrated by the undetectable level of LAL activity in whole blood and the very low incorporation of low-density lipoprotein cholesterol in fibroblasts. These mutations were not found in other patients with LALD studied at the Massachusetts General Hospital, in the 1092 control individuals of diverse ethnic background studied in the 1000 Genomes Project (http://www.1000genomes.org), or in the 6500 samples from NHLBI GO Exome Sequencing Project (http://evs.gs.washington.edu/EVS),

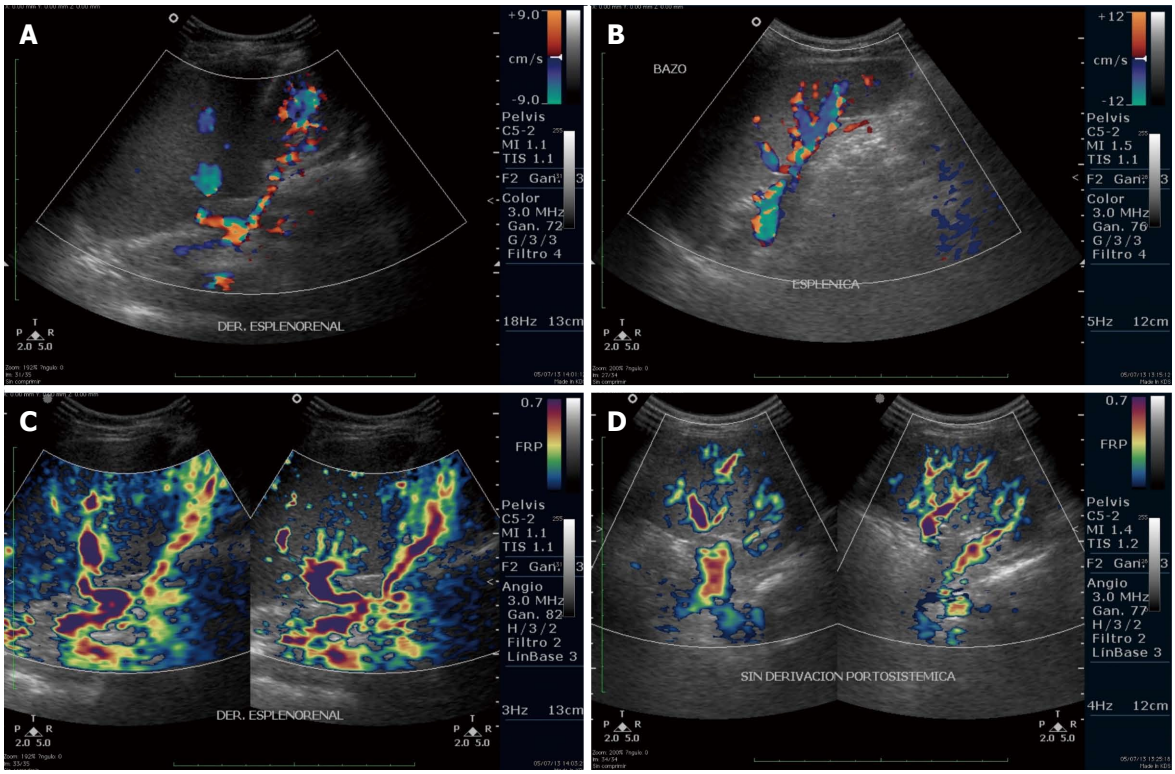

Figure 2 Comparison of Doppler ultrasound images from sibling 1 (A,C) and sibling 2 (B,D). A: Splenic vein with a spontaneous splenorenal shunt; B: Splenic vein with collateral vessels at the hilum, without porto-systemic shunts; C: Dilated and tortuous vessels, collateral circulation and a spontaneous splenorenal shunt; D: Absence of a splenorenal shunt.

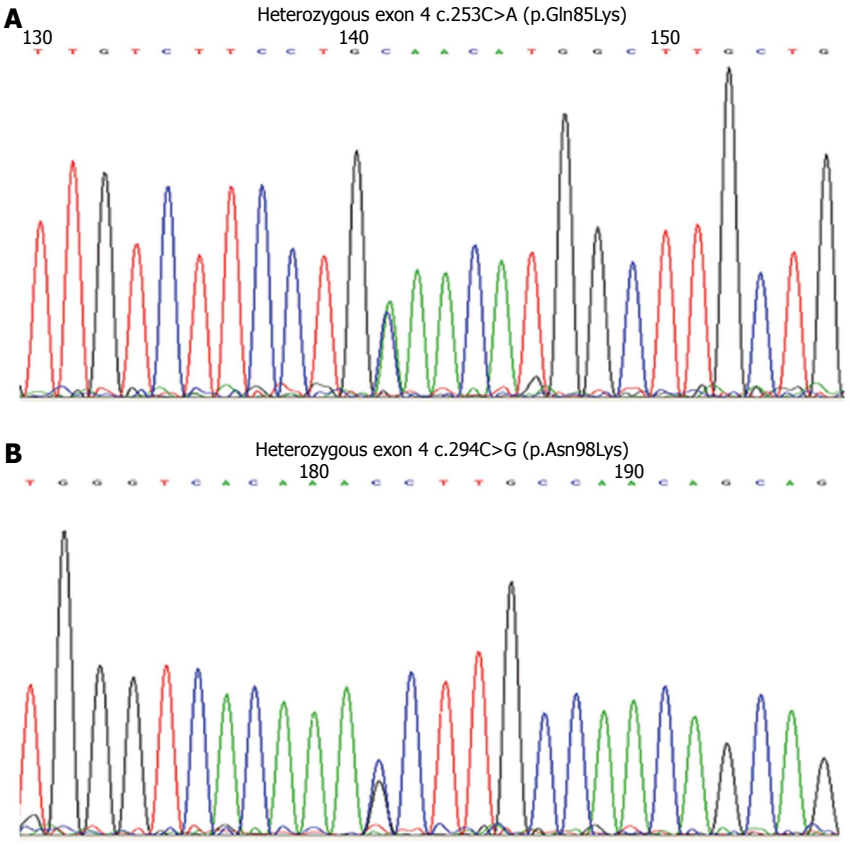

Figure 3 Electropherograms showing the mutations in exon 4 of the *LIPA* gene. A: Mutation in exon 4: c.253C>A (p.Gln85Lys); B: Mutation in exon 4: c.294C>G (p.Asn98Lys).

suggesting that they are very rare.

DISCUSSION

There are several previous reports of severe LALD in patients of Mexican origin. A Mexican family was studied at Baylor College of Medicine in Texas with three affected members who developed esophageal varices, hepatic failure and pulmonary complications early in life[7-10]. Another Mexican female studied at the same institute represented the first case of hepatic transplantation in CESD after developing several complications[11]. In Mexico, two infants were diagnosed with Wolman disease by the characteristic adrenal calcification at autopsy[12,13], and another case was diagnosed by the presence of crystal structures upon electron microscopy[14]. Considering the severity of hepatic failure, it was thought that Mexican patients had more severe alleles or genes that modulated CESD[5]. Only two reports included a molecular diagnosis: a male infant affected by LALD (Mexican father and American mother) had Trp95X/fs219 mutations[15]; and a female infant with a sibling that died at three months had compound heterozygosity for one new mutation: p.Gln98His/p.Gly342Arg[16].

The mutations found at amino acids 85 and 98 in exon 4 reported here are novel and were associated with undetectable whole blood enzyme activity, though a different mutation has been reported at amino acid 85 (p.Gln85Arg)[3,17]. Although structural features of the LAL protein are not well defined, exon 4 may be functionally important as the majority of mutations are within this exon[3,17] and its deletion causes LALD[3]. The absence of detectable activity is an interesting finding because these siblings had early non-fatal complications, suggesting that LALD is a continuous phenotype with some cases presenting overlapping features of Wolman disease and CESD, and indicating that enzymatic activity cannot predict the phenotype[3]. Studies of the natural history of LALD and correlating genotype and phenotype are urgently needed.

An exon 8 splice junction mutation (E8SJM) is present in the majority of LALD cases[1]. A review of the 55 published cases of LALD with molecular analysis of *LIPA* demonstrated that 89% of patients had the E8SJM mutation in at least one allele[3]. Ethnicity influences the prevalence of LALD, as a recent screen showed an increased frequency of E8SJM carriers in Caucasian and Hispanic populations (1:300) compared to African American, Asian and Ashkenazi groups[18]. The cases reported here demonstrate that despite a high prevalence of the E8SJM allele, LALD can originate from alternate mutations. In the Human Mutation Database, there are only 48 *LIPA* mutations reported to date in infant (19 mutations) and child/adult (27 mutations) cases[17]. Thus, further studies of carrier frequency of mutations in the full *LIPA* gene are required.

Clinicians, particularly pediatric gastroenterologists/hepatologists, should be aware of LALD in view of the frequent reported pediatric presentations[3] and the potential for misdiagnosis. Children can have all the complications related to the progression of cirrhosis, such as portal hypertension, ascites, esophageal/gastric varices, coagulopathy and bleeding; but these complications may not follow the adult pattern. Therefore, the detection of fibrosis, which progresses to cirrhosis, is a priority for the assessment of hepatic dysfunction, the need for hepatic transplantation and prognosis. Hepatic biopsy is still the most reliable assessment of progressive liver disease, so it is necessary to develop and validate noninvasive techniques that correlate with histopathology in order to identify fibrosis and to evaluate response to treatment, such as the recently developed dry blood spot assay for diagnostic confirmation of LALD[6]. It is also necessary to explore the use of Doppler ultrasound for identifying subtle changes in portal flow, and the presence of compensatory changes like recanalization of umbilical vein and splenic renal shunts. Magnetic resonance spectroscopy can be used to quantify intrahepatic fat in LALD[19], but cannot evaluate the presence of fibrosis.

The progression to fibrosis in sibling 1 corresponded with an increase in alanine aminotransferase levels, altering the ratio with aspartate aminotransferase. The patient also presented with a porto-systemic shunt (Figure 2) that likely maintained stable portal hypertension and decreased the risk of variceal bleeding, despite the extensive fibrosis. It is not clear if these changes are the natural course of hepatic compromise in pediatric LALD patients. Other cases of LALD in Mexican patients demonstrate a rapid progression to hepatic failure[7-10].

Treatment for LALD has been limited to the use of lipid-lowering drugs or hepatic transplantation, which was performed in nine patients with mixed-results but with no long-term follow-up[3]. Sebelipase alfa (Synageva BioPharma Corp., Lexington, MA, United States), a recombinant human LAL, is under development for use as an enzymatic replacement therapy. The initial trial in adults showed a decrease in serum lipids and liver volume and normalization of liver transaminases[20,21], and a phase 3 global trial is currently underway[22]. Timely diagnosis, as well as incorporation of LAL activity in newborn screening, will be needed to optimize the time to begin enzymatic replacement therapy. Further research is needed for evaluating additional therapies for CESD patients, such as bone marrow and hepatic transplantation.

CONCLUSION

LALD is an underdiagnosed pediatric disease requiring an increased awareness and early diagnosis, particularly in Caucasian and Hispanic individuals. This report presents the cases of two siblings carrying two previously unreported mutations in exon 4 of *LIPA* that likely resulted in a deficiency of LAL activity with early

symptomatology and complications.

ACKNOWLEDGMENTS

We would like to thank Radhika Tripuraneni, MD, MPH, for critical reading of the manuscript, Angelica Toriz-Ortiz, MD, for ultrasound imaging, and the medical staff of the Endoscopy and Pathology Department of CMN "20 de Noviembre", along with all the personnel involved in the care of the patients.

This work was presented in abstract form at 2013's National Week of Gastroenterology (Semana Nacional de Gastroenterologia de la AMG) in Veracruz, Mexico and at IX Congress of SLEIMPN in Medellín, Colombia.

COMMENTS

Case characteristics

Two siblings were affected by lysosomal acid lipase deficiency with early manifestations and hepatic complications, with the elder presenting with bleeding episodes, esophageal varices and portal hypertension.

Clinical diagnosis

The two cases presented similar characteristics: sibling 1 presented with gastrointestinal manifestations (alternating diarrhea and constipation episodes), hepatomegaly, reduced height and weight; sibling 2 presented with reduced height and hepatomegaly on physical examination.

Differential diagnosis

Other lysosomal storage diseases with hepatomegaly and Niemann-Pick cells, such as acid sphingomyelinase-deficiency (Niemann-Pick B), Niemann-Pick C, and Tangier disease.

Laboratory diagnosis

High levels of total cholesterol, low-density lipoprotein, aspartate and alanine aminotransferases, and low levels of high-density lipoprotein, normal bilirubin and undetectable lysosomal acid lipase activity in blood.

Imaging diagnosis

For both cases, abdominal ultrasound showed hepatomegaly and Doppler ultrasound showed abnormal portal flux velocities. Endoscopy in sibling 1 revealed esophageal varices.

Pathological diagnosis

In sibling 1, liver biopsy at five years of age showed microvesicular steatosis, foamy cells, fibrosis and cirrhosis.

Treatment

Both siblings were treated with a beta-blocker. Endoscopic variceal ligation was performed in sibling 1.

Related reports

Only one case of a Mexican infant with lysosomal acid lipase deficiency included *LIPA* mutation analysis. Other reports demonstrate that patients with the late presentation of this condition show severe hepatic disease with rapid progression.

Term explanation

Trans-state of mutations refers to mutations present in different alleles inherited from each parent.

Experiences and lessons

Limitations with enzymatic and molecular diagnosis along with a poor awareness of rare diseases can lead to a wrong diagnosis, as demonstrated in the patients reported here. New biochemical genetics techniques are available to achieve a correct diagnosis.

Peer review

The authors highlight the presentation of lysosomal acid lipase deficiency with hepatic complications and the importance of newly identified gene mutations. They also noted that enzyme levels were very low in the mother, a carrier of the mutation, suggesting that function is also impacted in a heterozygous state.

REFERENCES

1 **Grabowski GA**, Du H. Lysosomal Acid Lipase Deficiencies: The Wolman Disease/Cholesteryl Ester Storage Disease Spectrum. The Online Metabolic and Molecular Bases of Inherited Diseases. New York: McGraw-Hill, 2012
2 **Muntoni S,** Wiebusch H, Jansen-Rust M, Rust S, Seedorf U, Schulte H, Berger K, Funke H, Assmann G. Prevalence of cholesteryl ester storage disease. *Arterioscler Thromb Vasc Biol* 2007; **27**: 1866-1868 [PMID: 1763452]
3 **Bernstein DL**, Hülkova H, Bialer MG, Desnick RJ. Cholesteryl ester storage disease: review of the findings in 135 reported patients with an underdiagnosed disease. *J Hepatol* 2013; **58**: 1230-1243 [PMID: 23485521 DOI: 10.1016/j.jhep.2013.02.014]
4 **Zhang B**, Porto AF. Cholesteryl ester storage disease: protean presentations of lysosomal acid lipase deficiency. *J Pediatr Gastroenterol Nutr* 2013; **56**: 682-685 [PMID: 23403440 DOI: 10.1097/MPG.0b013e31828b36ac]
5 **Assmnann G**, Seedorf U. Acid Lipase Deficiency: Wolman Disease and Cholesteryl Ester Storage Disease. The Online Metabolic and Molecular Bases of Inherited Diseases. New York: McGraw-Hill, 2009
6 **Hamilton J**, Jones I, Srivastava R, Galloway P. A new method for the measurement of lysosomal acid lipase in dried blood spots using the inhibitor Lalistat 2. *Clin Chim Acta* 2012; **413**: 1207-1210 [PMID: 22483793 DOI: 10.1016/j.cca.2012.03.019]
7 **Beaudet AL**, Lipson MH, Ferry GD, Nichols BL. Acid lipase in cultured fibroblasts: cholesterol ester storage disease. *J Lab Clin Med* 1974; **84**: 54-61 [PMID: 4833843]
8 **Beaudet AL**, Ferry GD, Nichols BL, Rosenberg HS. Cholesterol ester storage disease: clinical, biochemical, and pathological studies. *J Pediatr* 1977; **90**: 910-914 [PMID: 859064]
9 **Michels VV**, Driscoll DJ, Ferry GD, Duff DF, Beaudet AL. Pulmonary vascular obstruction associated with cholesteryl ester storage disease. *J Pediatr* 1979; **94**: 621-623 [PMID: 430306]
10 **Cagle PT**, Ferry GD, Beaudet AL, Hawkins EP. Pulmonary hypertension in an 18-year-old girl with cholesteryl ester storage disease (CESD) *Am J Med Genet* 1986; **24**: 711-722 [PMID: 3740103]
11 **Ferry GD**, Whisennand HH, Finegold MJ, Alpert E, Glombicki A. Liver transplantation for cholesteryl ester storage disease. *J Pediatr Gastroenterol Nutr* 1991; **12**: 376-378 [PMID: 2072231]
12 **Peña-Alonso YR**, Ramón-García G. Enfermedad de Wolman en una niña mexicana. *Bol Med Hos Infant Mex* 1994; **51**: 660-664
13 **Ramón-García G**, Díaz-Ponce H, Díaz-Pérez C, Delgado-González E. [A 3-month-old girl with fever, abdominal distension, vomiting, and jaundice]. *Gac Med Mex* 2000; **136**: 361-367 [PMID: 10992637]
14 **Fernández-Aragón M**, Cervantes-Bustamante R, De León-Bojorge B, Zárate-Mondragón F, Mata-Rivera N, Barrios EM, Campos MG, Ramírez-Mayans JA. [Cholesterol ester storage disease]. *Rev Gastroenterol Mex* 2004; **69**: 171-175 [PMID: 15759790]
15 **Anderson RA**, Bryson GM, Parks JS. Lysosomal acid lipase mutations that determine phenotype in Wolman and cholesterol ester storage disease. *Mol Genet Metab* 1999; **68**: 333-345 [PMID: 10562460 DOI: 10.1006/mgme.1999.2904]
16 **Gómez-Nájera M**, Barajas-Medina H, Gallegos-Rivas MC, Mendez-Sashida P, Goss K, Sims KB, Radhikatripuraneni, Valles-Ayoub Y. New Diagnostic Method for Lysosomal Acid Lipase Deficiency and the Need to Recognize its Manifestation in Infants (Wolman Disease). *J Pediatr Gastroenterol Nutr* 2013; Epub ahead of print [PMID: 24048164]
17 **Stenson PD**, Mort M, Ball EV, Howells K, Phillips AD,

Thomas NS, Cooper DN. The Human Gene Mutation Database: 2008 update. *Genome Med* 2009; **1**: 13 [PMID: 19348700 DOI: 10.1186/gm13]

18 **Scott SA**, Liu B, Nazarenko I, Martis S, Kozlitina J, Yang Y, Ramirez C, Kasai Y, Hyatt T, Peter I, Desnick RJ. Frequency of the cholesteryl ester storage disease common LIPA E8SJM mutation (c.894G>A) in various racial and ethnic groups. *Hepatology* 2013; **58**: 958-965 [PMID: 23424026 DOI: 10.1002/hep.26327]

19 **Thelwall PE**, Smith FE, Leavitt MC, Canty D, Hu W, Hollingsworth KG, Thoma C, Trenell MI, Taylor R, Rutkowski JV, Blamire AM, Quinn AG. Hepatic cholesteryl ester accumulation in lysosomal acid lipase deficiency: non-invasive identification and treatment monitoring by magnetic resonance. *J Hepatol* 2013; **59**: 543-549 [PMID: 23624251 DOI: 10.1016/j.jhep.2013.04.016]

20 **Balwani M**, Breen C, Enns GM, Deegan PB, Honzík T, Jones S, Kane JP, Malinova V, Sharma R, Stock EO, Valayannopoulos V, Wraith JE, Burg J, Eckert S, Schneider E, Quinn AG. Clinical effect and safety profile of recombinant human lysosomal acid lipase in patients with cholesteryl ester storage disease. *Hepatology* 2013; **58**: 950-957 [PMID: 23348766 DOI: 10.1002/hep.26289]

21 **Valayannopoulos V**, Malinova V, Honzík T, Balwani M, Breen C, Deegan PB, Enns GM, Jones SA, Kane JP, Stock EO, Tripuraneni R, Eckert S, Schneider E, Hamilton G, Middleton MS, Sirlin C, Kessler B, Bourdon C, Boyadjiev SA, Sharma R, Twelves C, Whitley CB, Quinn AG. Sebelipase alfa over 52 weeks reduces serum transaminases, liver volume and improves serum lipids in patients with lysosomal acid lipase deficiency. *J Hepatol* 2014; **61**: 1135-1142 [PMID: 24993530 DOI: 10.1016/j.jhep.2014.06.022]

22 **Synageva BioPharma Corp**. A Multicenter Study of SBC-102 (Sebelipase Alfa) in Patients With Lysosomal Acid Lipase Deficiency/ARISE (Acid Lipase Replacement Investigating Safety and Efficacy. Active clinical trial, information. 14 April 2014. Available from: URL: http://www.clinicaltrials.gov/ct2/show/NCT01757184

P- Reviewer: Hoare M, Kovacs SJ, Liaskou E, Mohn A
S- Editor: Qi Y **L- Editor**: Wang TQ **E- Editor**: Ma S

World Journal of Gastroenterology

Submit a Manuscript: http://www.wjgnet.com/esps/
Help Desk: http://www.wjgnet.com/esps/helpdesk.aspx
DOI: 10.3748/wjg.v21.i3.1009

World J Gastroenterol 2015 January 21; 21(3): 1009-1013
ISSN 1007-9327 (print) ISSN 2219-2840 (online)

CASE REPORT

Simeprevir with peginterferon and ribavirin induced interstitial pneumonitis: First case report

Katsuyoshi Tamaki, Akihiko Okubo

Katsuyoshi Tamaki, Department of Hepatology, Tourai-kai Okubo Hospital, Tokushima 770-0923, Japan
Akihiko Okubo, Department of Respirology, Tourai-kai Okubo Hospital, Tokushima 770-0923, Japan
Author contributions: Tamaki K and Okubo A equally contributed to this paper.

Correspondence to: Katsuyoshi Tamaki, MD, PhD, Department of Hepatology, Tourai-kai Okubo Hospital, 2-30 Omichi, Tokushima 770-0923, Japan. cer.tamaki@gmail.com
Telephone: +81-88-6229156
Fax: +81-88-6229157
Received: May 9, 2014
Peer-review started: May 10, 2014
First decision: June 10, 2014
Revised: June 23, 2014
Accepted: July 22, 2014
Article in press: July 22, 2014
Published online: January 21, 2015

Abstract

The effectiveness of hepatitis C treatment has improved with the development of interferon (IFN), and it has drastically improved with the development of peg-interferon-α (PEG-IFN) in combination with ribavirin (RBV) and, more recently, with the addition of a protease inhibitor. Simeprevir, which is a second-generation protease inhibitor, has shown clinically favorable safety and tolerability profiles. Simeprevir received its first global approval in Japan in September 2013 for the treatment of genotype 1 chronic hepatitis C in combination with PEG-IFN and RBV. One serious adverse event associated with IFN therapy is interstitial pneumonitis, which can be fatal. We experienced a patient with interstitial pneumonitis that was induced by simeprevir with PEG-IFN and RBV therapy for chronic hepatitis C in the early stages of therapy (8 wk after initiating therapy). This is the first case report of interstitial pneumonitis with simeprevir with PEG-IFN and RBV in the world. In addition, it is very interesting that the onset of interstitial pneumonitis was earlier than that in conventional PEG-IFN and RBV therapy. This finding suggests that simeprevir augments the adverse event. We present this case report in light of relevant literature on interstitial pneumonitis with conventional PEG-IFN and RBV therapy.

Key words: Simeprevir; Chronic hepatitis C; Interstitial pneumonitis; Peg-interferon-α; Adverse events

Core tip: Simeprevir is recently being used as a protease inhibitor for hepatitis C. Several reports have indicated that simeprevir has clinically favorable safety and tolerability profiles. However, this is the first report of interstitial pneumonitis that was induced by simeprevir with peg-interferon and ribavirin therapy for chronic hepatitis C. Therefore, it is necessary to carefully observe the presence of respiratory symptoms in patients receiving this treatment.

Tamaki K, Okubo A. Simeprevir with peginterferon and ribavirin induced interstitial pneumonitis: First case report. *World J Gastroenterol* 2015; 21(3): 1009-1013 Available from: URL: http://www.wjgnet.com/1007-9327/full/v21/i3/1009.htm DOI: http://dx.doi.org/10.3748/wjg.v21.i3.1009

INTRODUCTION

Approximately 150 million people worldwide are

infected with the hepatitis C virus (HCV). HCV can lead to chronic hepatitis, liver cirrhosis, and hepatocellular carcinoma; the treatment of patients with HCV typically includes interferon (IFN) therapy.

The treatment of HCV has evolved over the past 20 years. Before 2011, the standard treatment was a combination of IFN alpha-polyethylene glycol [peg-IFN-α (PEG-IFN)], given as a weekly injection, and oral ribavirin (RBV). In patients infected with HCV genotype 1, the most common genotype worldwide, the standard treatment is a combination of PEG-IFN and RBV for 48 wk. This treatment results in only 40%-50% sustained virological response (SVR)[1-3].

The effectiveness of treatment has improved with the development of IFN, and it has drastically improved with the development of PEG-IFN in combination with RBV and, more recently, with the addition of a protease inhibitor.

The first direct-acting antivirals (DAAs), the NS3-4A serine protease inhibitors boceprevir and telaprevir, improved the rate of SVR; however, their toxicity in combination with PEG-IFN and RBV limited their overall efficacy[4]. In Japan, telaprevir or simeprevir is recently being used as a protease inhibitor for hepatitis C. Compared with PEG-IFN and RBV therapy, telaprevir-based triple therapy (with PEG-IFN and RBV) has a high frequency and severe dermatological and hematological adverse events (anemia)[5,6].

Several reports have indicated that simeprevir has clinically favorable safety and tolerability profiles. The report from the OPERA-1 study described adverse events in treatment-naïve patients graded as 1 or 2 in severity. The most common adverse events reported for recipients of simeprevir were fatigue, nausea, asthenia, diarrhea, bone pain, and dry skin[7]. One serious adverse event associated with IFN therapy includes interstitial pneumonitis, which can be fatal. Therefore, it is necessary to carefully observe the presence of respiratory symptoms (*i.e.*, cough, dyspnea) in patients receiving this treatment.

Here, we present a case of interstitial pneumonitis that was induced by simeprevir with PEG-IFN and RBV therapy for chronic hepatitis C and began in the early stages of therapy (8 wk after the initiation of therapy). This is first case report of interstitial pneumonitis with simeprevir with PEG-IFN and RBV in the world.

In addition, the onset of interstitial pneumonitis was earlier than that of interstitial pneumonitis in conventional PEG-IFN and RBV therapy. This suggests simeprevir augments this adverse event. We report our case with relevant literature on interstitial pneumonitis with conventional PEG-IFN and RBV therapy.

CASE REPORT

A 70-year-old female was diagnosed with chronic hepatitis C in 1994, and she underwent treatment at the outpatient clinic of our hospital (Table 1). She had no history of autoimmune or pulmonary disease. In 2011, she was treatment naïve when she began a 72-wk PEG-IFNα-2A + RBV therapy. HCV RNA became undetectable at week 16, and it remained undetectable throughout the remaining treatment. However, a relapse occurred 2 mo later during a follow-up examination.

Table 1 Patient's laboratory findings prior to receiving treatment

Parameters	Value
WBC	5600/μL
RBC	481 × 10^4/μL
Hb	14.1 g/dL
Plt	15.2 × 10^4/μL
PT-INR	1.17
AST	63 IU/L
ALT	48 IU/L
TP	7.6 g/dL
Alb	3.7 g/dL
TBIL	1.3 mg/dL
ALP	554 IU/L
γ-GTP	27 IU/L
CRP	< 0.10 mg/dL
LDH	285 U/L
UA	4.6 mg/dL
BUN	5.8 mg/dL
Cr	0.7 mg/dL
Na	141 mEq/L
K	4.2 mEq/L
HBsAg	(-)
HCVAb	(+)
HCV-RNA	5.6 LogIU/mL
Genotype	1B

WBC: White blood cells; RBC: Red blood cells; Plt: Platelets; PT: Prothrombin time; AST: Aspartate aminotransferase; ALT: Alanine aminotransferase; TP: Total protein; Alb: Albumin; TBIL: Total bilirubin; ALP: Alkaline phosphatase; γ-GTP: Gamma glutamyl transpeptidase; CRP: C-reactive protein; LDH: Lactate dehydrogenase; UA: Uric acid; BUN: Blood urea nitrogen; Cr: Creatinine; Na: Natrium; K: Potasium; HBsAg: Hepatitis B surface antigen; HCV: Hepatitis C virus antibody; HCV-RNA: Hepatitis C virus ribonucleic acid.

From January 2014, she was treated with triple therapy that included simeprevir, PEG-IFNα-2A, and RBV. The HCV RNA level immediately decreased at week 1 to 2.2 $\log_{10}$ IU/mL, and HCV RNA was undetectable at week 4. There were no adverse events or abnormalities other than mild anemia and neutropenia identified with hemogram and biochemistry at week 7. However, she visited our hospital for dyspnea on effort and a mild dry cough that appeared at approximately week 8. Her basal oxygen saturation was 98% (room air); however, her physical examination revealed a bibasailar mild, fine crackle, and high-resolution computed tomography (CT) revealed bilateral ground-glass opacities (Figure 1A). In addition, her KL-6 was elevated to 3021 U/mL.

Based on these findings, we diagnosed her with interstitial pneumonitis caused by simeprevir with PEG-IFNα-2A and RBV therapy. Interstitial pneumonitis was grade 2 on the World Health Organization grading scale (Table 2). Following her diagnosis, we immediately discontinued the treatment and administered 20 mg of

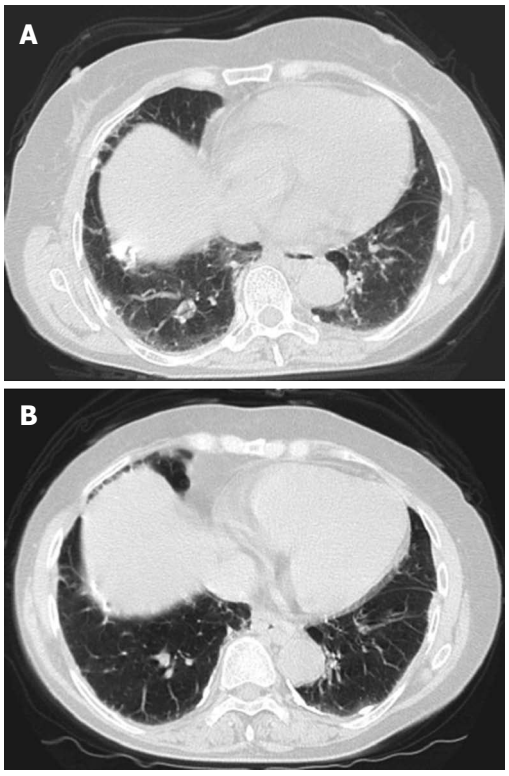

Figure 1 Computed tomography. A: Computed tomography (CT) revealed bilateral ground-glass opacities; B: After 3 wk, the ground-glass opacities improved on chest CT.

oral prednisolone daily.

After beginning prednisolone therapy, her respiratory symptoms gradually improved, and the ground-glass opacities improved on chest CT (Figure 1B). Prednisolone was then gradually tapered down by 5 mg every 3 d, and her respiratory symptoms disappeared. She had maintained persistent undetectable HCV RNA and achieved normal ALT levels at a follow-up visit 2 mo after the end of the treatment.

DISCUSSION

Simeprevir received its first global approval in Japan in September 2013 for the treatment of genotype 1 chronic hepatitis C in combination with PEG-IFN and RBV. Simeprevir is administered as a pill once daily. It is a small-molecule macrocyclic drug that targets and selectively inhibits HCV NS3/4A serine protease, thereby blocking the enzyme that enables HCV to replicate in host cells[8].

Compared with a placebo, treatment with simeprevir, PEG-IFN, and RBV resulted in significantly higher SVR rates in the overall patient population[9]. In a Japanese study, SVR at 12 wk after the end of treatment was achieved in 88.6% of simeprevir-treated patients and 61.7% of placebo-treated patien[10]. In Phase I and phase II studies conducted in Japan, the rate of adverse events was reported to be 97.7% (426/436). The most common adverse events and their incidence were as follows: rash

Table 2 Post medical history and complication (interstitial pneumonitis)

	Positive	Negative
Incidence	11	113
Incidence rate	0.026%	0.27%
Dead	1	12
Dead/incidence	9.1%	10.6%

Japanese Welfare Ministry report include an interstitial pneumonitis incidence number. Total estimated number of patients was 42600 and total an interstitial pneumonitis incidence number was 124 (0.29%).

(46.6%), pruritus (24.1%), hyperbilirubinemia (22.2%), constipation (6.7%), and photosensitivity reaction (1.8%). However, no interstitial pneumonitis was reported in these studies. Nearly all patients receiving simeprevir with PEG-IFN and RBV experience adverse events that can be serious. Fatigue and flu-like symptoms are common, and psychiatric symptoms, weight loss, seizures, peripheral neuropathy, and bone marrow suppression can also occur. RBV causes hemolysis and skin complications and is teratogenic[11]. The adverse events associated with PEG-IFNα-2A that were described previously in a Japanese Welfare Ministry report include an interstitial pneumonia incidence rate of 0.3%. The shortest onset time was 11 wk, and the longest reported onset time was 38 wk (mean 16 wk). This is the first case of interstitial pneumonia with triple therapy (simeprevir with PEG-IFNα-2A and RBV). This case was observed in week 8; this was earlier than the cases of interstitial pneumonitis with PEG-IFNα-2A observed previously. Moreover, the immunological and pharmacokinetic properties of PEG-IFNα-2a, with the longest half-life, may act to trigger the pathophysiologic mechanisms of interstitial pneumonitis. The mechanism of this adverse event remains unclear; however, it is considered idiosyncratic and is probably related to the IFN immunomodulatory activity that includes the induction of enzymes, suppression of cell proliferation, enhancement of macrophage phagocytic activity, inhibition of suppressor T cells, and liberation of proinflammatory cytokines[12-14]. Although co-administration of RBV does not affect the pharmacokinetics of PEG-IFN, these drugs altogether have enhanced toxicity. In addition, clinically relevant drug-drug interactions between PEG-IFN alfa-2a (40 KD) and agents metabolized *via* the hepatic P450 system are unlikely to occur[15].

Simeprevir inhibits OATP1B1/3 and P-glycoprotein transporters. Co-administration of simeprevir with drugs that are substrates of OATP1B1/3 and P-glycoprotein transport may result in increased plasma concentrations of these drugs[16]. Therefore, it is possible that a combination of drugs will result in greater pulmonary toxicity. However, further studies are required to confirm this possibility. The fact that reports of pneumonitis associated with RBV monotherapy and simeprevir monotherapy have not been published till date enhances the probability of interstitial pneumonitis induced by

PEG-IFN in the present case.

In spite of the additional efficacy and safety of PEG-IFN, which is largely used in combination with simeprevir to treat chronic hepatitis C, we report a case of interstitial pneumonitis related to PEG-IFNα-2a, notifying physicians about this pulmonary nonspecific adverse event with potential severity, given the insufficiency of publications regarding this risk during the treatment of chronic hepatitis C.

In most cases, symptoms of pneumonitis are reversible after cessation of treatment with IFN and RBV. There is no consensus with regard to the treatment of interstitial pneumonitis induced with IFN and RBV. Upon review of the literature, three options are possible. The first option is to stop the combination treatment of HCV and wait until the disease resolves, which was done in a limited number of cases. The second option is to administer steroids, although the dosage and route of administration regimes vary widely. The third option, *i.e.*, adding azathioprine to steroids in therapy-resistant relapsing cases, may be beneficial for resolving interstitial pneumonitis[17]. A shorter overall treatment duration is acceptable in patients with chronic HCV infection because it reduces the exposure to PEG-IFN and RBV, thereby resulting in a reduced incidence of adverse events[18-20].

In conclusion, interstitial pneumonitis with triple therapy, including simeprevir, PEG-IFNα-2A, and RBV, is rare but can be fatal. Larger and longer studies are required to assess the efficacy and safety of simeprevir for HCV infection.

COMMENTS

Case characteristics

A 70-year-old female with interstitial pneumonitis that was induced by simeprevir with peg-interferon-α (PEG-IFN) and ribavirin (RBV) therapy for chronic hepatitis C.

Clinical diagnosis

The patient had dyspnea on effort and a mild dry cough.

Differential diagnosis

Anemia is associated with the use of RBV, respiratory infections, bactrerial pneumonia.

Laboratory diagnosis

Laboratory tests showed elevated KL-6 (3021 U/mL) suggesting interstitial pneumonitis.

Imaging diagnosis

The patient's chest computed tomography revealed bilateral ground-glass opacities.

Treatment

The authors immediately discontinued triple therapy (simeprevir with PEG-IFN and RBV) and administered 20 mg of oral prednisolone daily.

Term explanation

Drug-induced lung injury may involve the airways, lung parenchyma, mediastinum, pleura, pulmonary vasculature, and the most common form of drug-induced lung toxicity is drug-induced interstitial pneumonitis.

Experiences and lessons

This is the first report of interstitial pneumonitis that was induced by simeprevir with PEG-IFN and RBV therapy for chronic hepatitis C.

Peer review

The case is well documented showing enough data to sustain the diagnosis of interstitial pneumonitis developed by the patient after 8 wk of treatment.

REFERENCES

1 **Fried MW**, Shiffman ML, Reddy KR, Smith C, Marinos G, Gonçales FL, Häussinger D, Diago M, Carosi G, Dhumeaux D, Craxi A, Lin A, Hoffman J, Yu J. Peginterferon alfa-2a plus ribavirin for chronic hepatitis C virus infection. *N Engl J Med* 2002; **347**: 975-982 [PMID: 12324553]

2 **Hadziyannis SJ**, Sette H, Morgan TR, Balan V, Diago M, Marcellin P, Ramadori G, Bodenheimer H, Bernstein D, Rizzetto M, Zeuzem S, Pockros PJ, Lin A, Ackrill AM. Peginterferon-alpha2a and ribavirin combination therapy in chronic hepatitis C: a randomized study of treatment duration and ribavirin dose. *Ann Intern Med* 2004; **140**: 346-355 [PMID: 14996676]

3 **Manns MP**, McHutchison JG, Gordon SC, Rustgi VK, Shiffman M, Reindollar R, Goodman ZD, Koury K, Ling M, Albrecht JK. Peginterferon alfa-2b plus ribavirin compared with interferon alfa-2b plus ribavirin for initial treatment of chronic hepatitis C: a randomised trial. *Lancet* 2001; **358**: 958-965 [PMID: 11583749]

4 **deLemos AS**, Chung RT. Hepatitis C treatment: an incipient therapeutic revolution. *Trends Mol Med* 2014; **20**: 315-321 [PMID: 24636306 DOI: 10.1016/j.molmed.2014.02.002]

5 **Torii H**, Sueki H, Kumada H, Sakurai Y, Aoki K, Yamada I, Ohtsuki M. Dermatological side-effects of telaprevir-based triple therapy for chronic hepatitis C in phase III trials in Japan. *J Dermatol* 2013; **40**: 587-595 [PMID: 23734933 DOI: 10.1111/1346-8138.12199]

6 **Matthews SJ**, Lancaster JW. Telaprevir: a hepatitis C NS3/4A protease inhibitor. *Clin Ther* 2012; **34**: 1857-1882 [PMID: 22951253 DOI: 10.1016/j.clinthera.2012.07.011]

7 **Lenz O**, de Bruijne J, Vijgen L, Verbinnen T, Weegink C, Van Marck H, Vandenbroucke I, Peeters M, Simmen K, Fanning G, Verloes R, Picchio G, Reesink H. Efficacy of re-treatment with TMC435 as combination therapy in hepatitis C virus-infected patients following TMC435 monotherapy. *Gastroenterology* 2012; **143**: 1176-1178.e1-e6 [PMID: 22885330 DOI: 10.1053/j.gastro.2012.07.117]

8 **Vaidya A**, Perry CM. Simeprevir: first global approval. *Drugs* 2013; **73**: 2093-2106 [PMID: 24293133 DOI: 10.1007/s40265-013-0153-9]

9 **Zeuzem S**, Berg T, Gane E, Ferenci P, Foster GR, Fried MW, Hezode C, Hirschfield GM, Jacobson I, Nikitin I, Pockros PJ, Poordad F, Scott J, Lenz O, Peeters M, Sekar V, De Smedt G, Sinha R, Beumont-Mauviel M. Simeprevir increases rate of sustained virologic response among treatment-experienced patients with HCV genotype-1 infection: a phase IIb trial. *Gastroenterology* 2014; **146**: 430-441.e6 [PMID: 24184810 DOI: 10.1053/j.gastro.2013.10.058]

10 **Hayashi N**, Izumi N, Kumada H, Okanoue T, Tsubouchi H, Yatsuhashi H, Kato M, Ki R, Komada Y, Seto C, Goto S. Simeprevir with peginterferon/ribavirin for treatment-naïve hepatitis C genotype 1 patients in Japan: CONCERTO-1, a phase III trial. *J Hepatol* 2014; **61**: 219-227 [PMID: 24727123 DOI: 10.1016/j.jhep.2014.04.004]

11 **Izumi N**, Hayashi N, Kumada H, Okanoue T, Tsubouchi H, Yatsuhashi H, Kato M, Ki R, Komada Y, Seto C, Goto S. Once-daily simeprevir with peginterferon and ribavirin for treatment-experienced HCV genotype 1-infected patients in Japan: the CONCERTO-2 and CONCERTO-3 studies. *J Gastroenterol* 2014; **49**: 941-953 [PMID: 24626851 DOI: 10.1007/s00535-014-0949-8]

12 **Tilg H**. New insights into the mechanisms of interferon alfa: an immunoregulatory and anti-inflammatory cytokine. *Gastroenterology* 1997; **112**: 1017-1021 [PMID: 9041265]

13 **Borden EC**, Parkinson D. A perspective on the clinical effectiveness and tolerance of interferon-alpha. *Semin Oncol* 1998; **25**: 3-8 [PMID: 9482534]

14 **Dalgard O**, Bjøro K, Hellum K, Myrvang B, Bjøro T, Haug E, Bell H. Thyroid dysfunction during treatment of chronic hepatitis C with interferon alpha: no association with either interferon dosage or efficacy of therapy. *J Intern Med* 2002; **251**: 400-406 [PMID: 11982739]
15 **Brennan BJ**, Xu ZX, Grippo JF. Effect of peginterferon alfa-2a (40KD) on cytochrome P450 isoenzyme activity. *Br J Clin Pharmacol* 2013; **75**: 497-506 [PMID: 22765278 DOI: 10.1111/j.1365-2125.2012.04373.x]
16 **Goldenberg MM**. Pharmaceutical approval update. *P T* 2014; **39**: 112-118 [PMID: 24669177]
17 **Slavenburg S**, Heijdra YF, Drenth JP. Pneumonitis as a consequence of (peg)interferon-ribavirin combination therapy for hepatitis C: a review of the literature. *Dig Dis Sci* 2010; **55**: 579-585 [PMID: 19399621 DOI: 10.1007/s10620-009-0797-1]
18 **Kwo PY**. Response-guided therapy for HCV. *Gastroenterol Hepatol* (N Y) 2011; **7**: 43-45 [PMID: 21346852]
19 **McEwan P**, Yuan Y, Litauen G, Kim R. Cost benefit analysis of response guided therapy: dynamic disease Markov modeling for patients with chronic hepatitis (HCV) by fibrosis stages. *J Hepatol* 2011; **54** (S461); Abs1167
20 **Reddy KR**, Lin F, Zoulim F. Response-guided and -unguided treatment of chronic hepatitis C. *Liver Int* 2012; **32** Suppl 1: 64-73 [PMID: 22212575 DOI: 10.1111/j.1478-3231.2011.02713.x]

P- Reviewer: Hegade VS, Larrubia JR **S- Editor**: Ma YJ
L- Editor: A **E- Editor**: Zhang DN

World Journal of Gastroenterology

Submit a Manuscript: http://www.wjgnet.com/esps/
Help Desk: http://www.wjgnet.com/esps/helpdesk.aspx
DOI: 10.3748/wjg.v21.i3.1014

World J Gastroenterol 2015 January 21; 21(3): 1014-1019
ISSN 1007-9327 (print) ISSN 2219-2840 (online)

CASE REPORT

Pancreatic mass as an initial manifestation of polyarteritis nodosa: A case report and review of the literature

Yoshihiro Yokoi, Ippei Nakamura, Takeshi Kaneko, Tomoki Sawayanagi, Youichi Watahiki, Makoto Kuroda

Yoshihiro Yokoi, Takeshi Kaneko, Tomoki Sawayanagi, Youichi Watahiki, Department of Surgery, Shinshiro Municipal Hospital, Aichi 441-1387, Japan
Ippei Nakamura, Department of Internal Medicine, Shinshiro Municipal Hospital, Aichi 441-1387, Japan
Makoto Kuroda, Department of Pathology, Fujita Health University, Aichi 470-1192, Japan
Author contributions: Yokoi Y, Nakamura I, Kaneko T, Sawayanagi T and Watahiki Y participated in the diagnosis, management and follow-up of this clinical case; Kuroda M provided a critical and valuable discussion on the histopathological study.

Correspondence to: Yoshihiro Yokoi, MD, Department of Surgery, Shinshiro Municipal Hospital, 32-1 Kitahata, Shinshiro, Aichi 441-1387, Japan. y.yokoi@hospital.shinshiro.aichi.jp
Telephone: +81-536-222171
Fax: +81-536-222850
Received: June 3, 2014
Peer-review started: June 4, 2014
First decision: July 9, 2014
Revised: July 29, 2014
Accepted: September 18, 2014
Article in press: September 19, 2014
Published online: January 21, 2015

Abstract

Classic polyarteritis nodosa (PAN) that targets medium-sized muscular arteries and microscopic polyangiitis (MPA), characterized by inflammation of small-caliber vessels and the presence of circulating myeloperoxidase anti-neutrophil cytoplasmic antibodies (MPO-ANCA), are distinct clinicopathological entities of systemic vasculitis. A 66-year-old woman presented with fever, cholestasis and positive MPO-ANCA. Radiological examination showed a pancreatic mass compressing the bile duct. Therefore, we performed pancreatoduodenectomy. Histopathological examination revealed that necrotizing vasculitis predominantly affecting the medium-sized vessels, spared arterioles or capillaries in the pancreas, a finding consistent with PAN. Unexpectedly, renal biopsy revealed small-caliber vasculitis and glomerulonephritis, supporting MPA. The initial manifestation of a pancreatic mass associated with vasculitis has only been reported in 7 articles. Its diagnosis is challenging because no reliable clinico-radiological findings have been observed. Clinicians should be aware of such cases and early diagnosis followed by immunosuppression is mandatory. Our findings may reflect a polyangiitis overlap syndrome coexisting between pancreatic PAN and renal MPA.

Key words: Classic polyarteritis nodosa; Microscopic polyangiitis; Myeloperoxidase anti-neutrophil cytoplasmic antibodies; Pancreatic mass; Polyangiitis overlap syndrome

Core tip: A 66-year-old woman presented with a pancreatic mass accompanied by fever, cholestasis and positive myeloperoxidase anti-neutrophil cytoplasmic antibodies. The resected pancreas showed extensive fibrosis associated with necrotizing vasculitis, targeting medium-sized vessels but sparing small-caliber vessels, a finding compatible with polyarteritis nodosa. Unexpectedly, renal biopsy revealed small-caliber vasculitis and glomerulonephritis, supporting microscopic polyangiitis. The initial manifestation of a pancreatic mass associated with vasculitis has only been reported in 7 articles. Although rare, vasculitis should be included in a differential diagnosis for pancreatic masses. Additionally, our findings may reflect a polyangiitis overlap syndrome coexisting between pancreatic polyarteritis nodosa and renal microscopic polyangiitis.

Yokoi Y, Nakamura I, Kaneko T, Sawayanagi T, Watahiki Y, Kuroda M. Pancreatic mass as an initial manifestation of polyarteritis nodosa: A case report and review of the literature. *World J Gastroenterol* 2015; 21(3): 1014-1019 Available from: URL: http://www.wjgnet.com/1007-9327/full/v21/i3/1014.htm DOI: http://dx.doi.org/10.3748/wjg.v21.i3.1014

INTRODUCTION

Systemic vasculitis is characterized by a variety of clinical manifestations and courses, depending upon the organ involved. Among the classifications for systemic vasculitis, the Chapel Hill consensus conference (CHCC) nomenclature is widely accepted[1,2]. Vasculitis affecting small-caliber blood vessels (arterioles, venules or capillaries) often accompanies anti-neutrophil cytoplasmic antibodies which are postulated to play a major pathological role in developing necrotizing vasculitis[3]. Such ANCA-associated vasculitis includes the following 3 clinicopathological variants: microscopic polyangiitis (MPA), granulomatosis with polyangiitis (GPA) and eosinophilic granulomatosis with polyangiitis[2]. Among them, MPA is characterized by non-granulomatous inflammation, few or no immune deposits (pauci-immune), glomerulonephritis and the presence of myeloperoxidase (MPO)-ANCA[2].

Another category of vasculitis, classic polyarteritis nodosa (PAN), targets small and medium-sized muscular arteries, spares small-caliber vessels and causes diffuse vascular inflammation, ischemia or rupture of affected organs[4]. Although PAN frequently complicates the skin, joints, kidneys and gastrointestinal system, initial and symptomatic involvement of the pancreatobiliary system has only been reported in rare cases[5-8].

Herein, we report a patient presenting with fever, cholestasis and a pancreatic mass compressing the bile duct as a clinical feature of PAN.

CASE REPORT

A 66-year-old woman presented with a 2 wk history of intermittent high-grade fever (approximately 39 ℃). She did not report arthralgia, myalgia or abdominal symptoms. Approximately 1 mo before admission, she underwent tympanotomy for left otitis media. Her medical history was noncontributory. She denied alcohol and drug use. Laboratory examination showed elevated biliary enzyme levels, including an alkaline phosphatase level of 717 U/L (115-359 U/L), gamma glutamyl transpeptidase levels of 238 U/L (10-47 U/L) and C-reactive protein (CRP) levels of 8.30 mg/dL (< 0.30 mg/dL). Serum levels of amylase, aspartate aminotransferase, alanine aminotransferase, blood urea nitrogen, creatinine, carcinoembryonic antigen, carbohydrate antigen 19-9 and procalcitonin were normal. The levels of glycated hemoglobin were slightly elevated. Leukocytosis and eosinophilia were not present. Immunological data showed slight elevations of IgG [1902 mg/dL (820-1740 mg/dL)] and IgA [628 mg/dL (90-400 mg/dL)], but IgM and IgG4 levels were normal. Autoimmune investigations showed elevated MPO-ANCA levels [473 IU/mL (< 3.5 IU/mL)] in addition to a slight elevation of anti-nuclear antibodies (1:64) and rheumatoid factor. Proteinase 3-ANCA, serum hepatitis B surface antigen and hepatitis C virus antibodies were not detected. No bacteria grew on blood culture. Urinalysis revealed proteinuria (2+) and hematuria (2+) with hyaline casts.

A hypoechoic 2.0 cm mass was observed in the pancreatic head on an abdominal ultrasonogram (Figure 1A). The corresponding lesion was an ill-defined hypodense mass with poor enhancement, observed by using a CT scan, and it compressed the distal common bile duct (CBD) and pancreatic duct (PD) (Figure 1B-E). The walls of the gallbladder and bile duct were thickened (Figure 1D, E). A chest CT scan showed slight changes, including bronchial dilation and peripheral inflammation with a centrilobular distribution. Angiographic reconstruction using a CT scan showed normal visceral arteries of the superior mesenteric artery (SMA) and celiac systems. Vascular stenosis or aneurysms were not detectable. Endoscopic retrograde cholangiopancreatography (ERCP) demonstrated a double duct sign with compression of the distal CBD and tortuous dilation of the PD (Figure 1F). Bile cytology and culture were negative according to the results obtained after using the sample *via* naso-biliary drainage.

We could not exclude the possibility of pancreatic cancer as a cause of the patient's fever and therefore we performed a pylorus-preserving pancreatoduodenectomy. The pancreatic mass was soft on palpation and did not invade the adjacent tissues. Intraoperative ultrasonography revealed an ill-defined pancreatic mass with low echogenicity. The postoperative course was uneventful and the patient's fever completely resolved with a reduction of CRP levels.

In the resected pancreas, the focal stenosis in the CBD was approximately 2 cm distal to the ampulla of Vater. There was marked fibrosis adjacent to the intrapancreatic CBD and PD (Figure 2A). The affected small to medium-sized arteries in the fibrosis were characterized by necrotizing arteritis with subintimal fibrinoid necrosis, disruption of the elastic laminae, perivascular fibrosis and inflammatory cell infiltration (Figure 2A, B). Vessel occlusion or thrombus was also observed (Figure 2A). Small-caliber vessels such as the arterioles, capillaries or venules were spared. Granulomatous inflammation and significant eosinophil infiltration were not found. The fibrotic lesion extended longitudinally towards the hepatic hilus along the bile duct. Necrotizing vasculitis was also observed in the walls of the proximal bile duct and gallbladder but their mucosal layers were well preserved (Figure 2C). The duodenum also showed arterial changes. These vascular changes were compatible with classical PAN.

To confirm systemic vasculitis, a renal needle biopsy was performed. Global sclerosis affected 20% of the

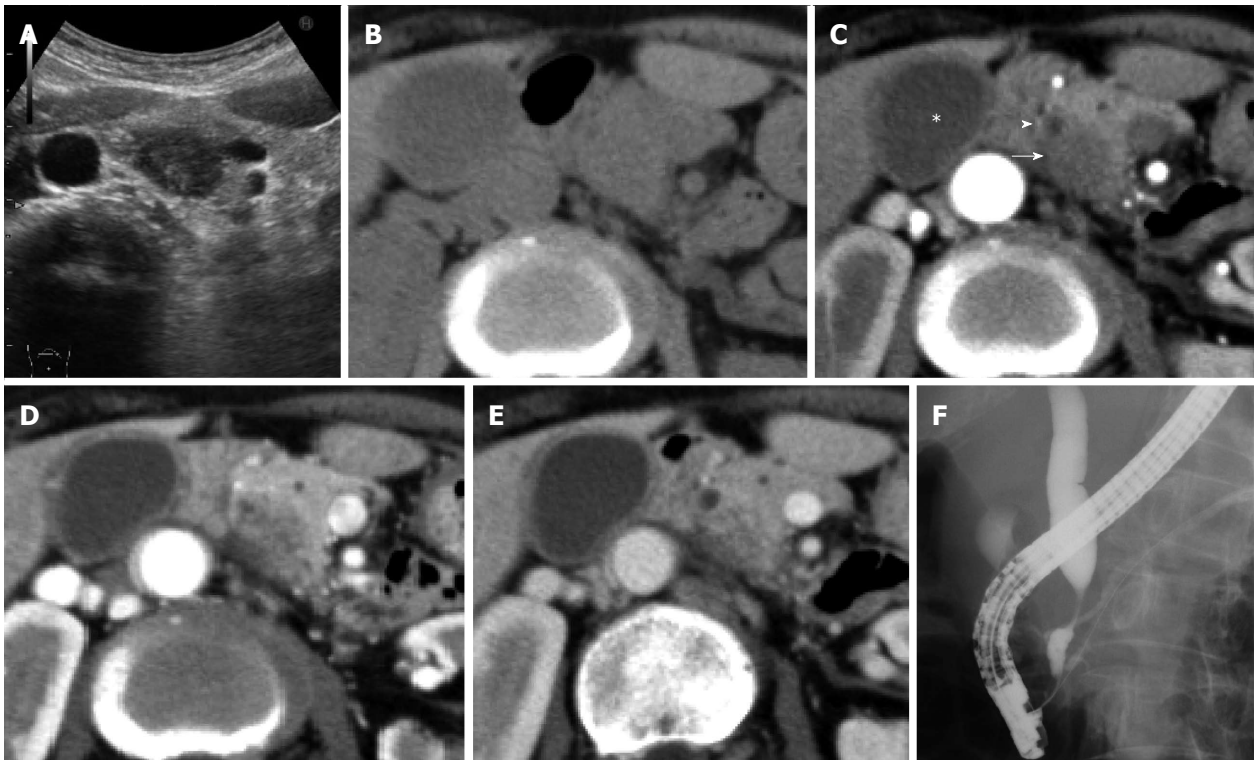

Figure 1 Preoperative images. A: An ultrasonogram showing a slightly ill-defined hypoechoic mass at the pancreatic head; B-E Abdominal CT scans: The pancreatic mass is slightly hypodense on simple CT; C: Enhanced CT shows a non-enhancing mass (arrow) located adjacent to the bile duct (arrowhead) at the arterial phase. Note that the walls of the gallbladder (asterisk) and bile duct are thickened; D and E; The mass has sporadic enhancement at the later phase; F: A Cholangiogram showing a tapered distal biliary stricture consistent with extrinsic compression by the pancreatic mass. CT: Computed tomography.

glomeruli, whereas a cellular crescent was observed in 10% (Figure 2D). Interstitial fibrosis was observed in the tubulointerstitial area. Both active and healed stages of vasculitis were observed in the small arteries and capillaries (Figure 2E). Immune complexes were not detectable. These pathological findings were compatible with the renal changes of MPA according to the CHCC nomenclature[1,2].

Therapy with prednisone and cyclophosphamide was undertaken to induce remission of the systemic vasculitis. The patient has remained asymptomatic 6 mo after the operation.

DISCUSSION

In the present patient, a pancreatic mass accompanied by fever and cholestasis was observed; surgical removal successfully improved the patient's clinical symptoms and data. Pathological study demonstrated extensive vascular injury in the pancreas, bile duct, gallbladder and duodenum. The affected vessels were small and medium-sized arteries and arterioles and capillaries were spared, a finding consistent with classic PAN[1,2,4]. Initial clinical manifestation of vasculitis in the pancreatobiliary system is uncommon, with only a few reports documenting pancreatitis or cholecystitis[7]. Other forms of pancreatic vasculitis, including mass formation, are extremely rare. The articles reporting a pancreatic mass associated with vasculitis were collected through a literature search with the words "vasculitis", "pancreas", "tumor" or "mass" in their title. Among them, 7 articles providing radiological and histopathological descriptions were reviewed (Table 1). Including our case, there were 3 PAN[5,6], 3 GPA[8-10] and 2 localized PAN[11,12]. The former 2 were major vasculitis presenting with a tumor-like lesion in the urogenital system and breast or kidney, respectively[6]. The median age was 62 years (range: 44-66 years), with a male predominance (5:3 ratio). Three patients were Japanese, 2 were white and 1 was Jewish. The symptoms were varied and nonspecific, including abdominal pain (5 patients), fever (3 patients), otitis media (2 patients) and jaundice (1 patient). All lesions were 2-3 cm in diameter and were localized in the head (6 patients), neck (1 patient) and both body and tail of the pancreas (1 patient). The gallbladder was also affected in 2 PAN patients. Among 4 cases analyzed, ANCA was positive in 3 (GPA, 2; PAN, 1). Use of glucocorticoids and a cytotoxic agent was effective in all cases if treated, otherwise rapid deterioration of necrotizing vasculitis was fatal, as shown in case 5. These findings indicate that early introduction of immunosuppressive treatment based on accurate diagnosis is crucial for a better outcome.

One of the obstacles in treatment strategy for a vasculitis-induced pancreatic mass is the difficulty in diagnosing it. Our review showed that 7 of 8 patients were diagnosed only after surgery or autopsy (Table 1). Besides neoplasm, the pancreatic mass can encompass a variety of diseases, such as an inflammatory pseudotumor

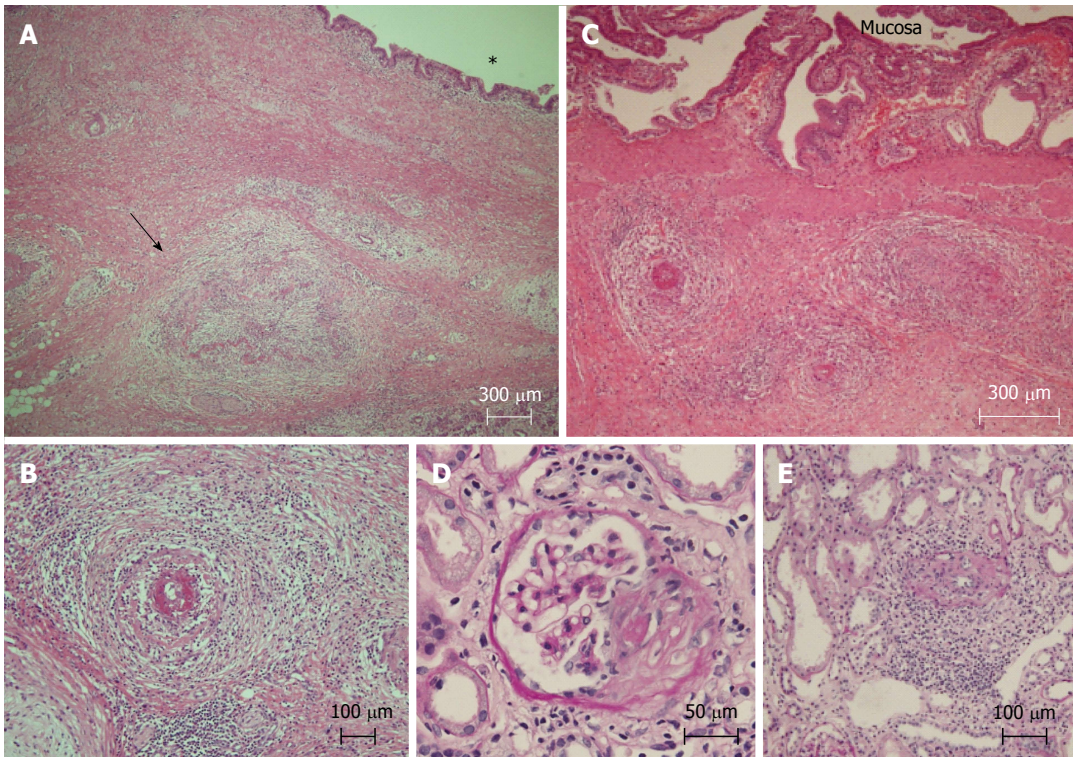

Figure 2 Histological findings of the pancreas, gallbladder and kidney. A: Pancreatic fibrotic changes adjacent to the bile duct (asterisk) are evident. An obliterated medium-sized artery (arrow) is accompanied by cellular infiltration and destruction of the wall. The bile duct mucosa is intact (hematoxylin-eosin stain; original magnification, × 40); B: The affected small-sized artery in the pancreatic fibrosis is characterized by necrotizing arteritis with subintimal fibrinoid necrosis and inflammatory cell infiltration (hematoxylin-eosin stain; original magnification, × 100); C: The arteries of the gallbladder are also involved: the mucosa is preserved (hematoxylin-eosin stain; original magnification, × 40); D and E: Renal biopsy showed segmental sclerosis and collapse with a fibrocellular crescent (D: Periodic acid-Shiff's stain, original magnification, × 200) and vasculitis of a small-sized artery (E: Periodic acid-Shiff's stain, original magnification, × 100).

Table 1 Reported cases of pancreatic tumor associated with vasculitis

Ref.	Age/sex/ race *etc.*	Final diagnosis	Symptoms	Sites involved	Prior diagnosis	Tumor size imaging findings	Diagnostic criteria	Outcome	
								Pancreas	Patient
Ito *et al*[11]	44/M/ Japanese	Localized PAN	Epigastralgia	Head	No	ND ERCP: CBD stenosis	ND	Underwent PD	Discharged
O'Neil *et al*[8]	62/M/ White	GPA	Jaundice Otitis media Nasal ulceration	Head Gallbladder	No	3 cm CT: mass US: hypoechoic ERCP: CBD stenosis	ANCA (+) Needle biopsy: non diagnostic Renal biopsy: confirmed	Improved on CYC + CS	Improved on CYC + CS
Damani *et al*[5]	46/F/ ND	PAN	Right upper abdominal pain	Neck	No	2 cm US: hypoechoic CT: low attenuation, nonenhancing mass	Needle biopsy: non diagnostic Postoperative histopathology	Cholecystectomy Distal Px	Died (20 d) Various complication
Kariv *et al*[6]	65/ M/ Jewish	PAN	Epigastralgia Weight loss Low grade fever	Head	No	3 cm CT: mass	Needle biopsy: chronic pancreatitis	Underwent PD	Remission on CS
Matsubayashi *et al*[9]	65/M/ Japanese	GPA	Left abdominal pain Constipation Low grade fever Tympanitis	Body and Tail	S/O GPA	ND CT: Enlargement of pancreas with sporadic low density lesions	^{12}PR3-ANCA (+) Autopsy	No	Died Hemorrhagic pneumonia Diffuse necrotizing pancreatitis
Tinazzi *et al*[10]	48/F/ ND	GPA	Mid-epigastric pain	Head	No	2 cm: US: Hypoechoic MRCP: Obstruction of pancreatic duct	Postoperative histopathology	Underwent PD	Improved on CYC + CS
Gonzalez-Gay *et al*[12]	75/M/ White	Localized PAN	Epigastralgia	Head	No	ND	Postoperative histopathology	Underwent PD	Discharged

Our case	66 /F/ Japanese	PAN Renal MPA	Otitis media Fever	Head Gallbladder Bile duct Duodenum	No	2 cm US: Hypoechoic CT: Hypodense Non-enhancing	MPO-ANCA(+) Postoperative histopathology	Underwent PD	Improved on CYC + CS Discharged

PAN: Polyarteritis nodosa; ERCP: Endoscopic retrograde cholangiopancreatography; CBD: Common bile duct; PD: Pancreatoduodenectomy; GPA: Granulomatosis with polyangiitis; US: Ultrasonography; ANCA: Anti-neutrophil cytoplasmic antibody; CYC: Cyclophosphamide; CS: Corticosteroids; Px: Pancreatectomy; S/O: Suspect of; PR3: Proteinase 3; MRCP: Magnetic resonance cholangiopancreatography; MPA: Microscopic polyangiitis; MPO: Myeloperoxidase.

(IPT). IPT includes autoimmune pancreatitis, groove pancreatitis and lipomatosis[13]. As shown in Table 1, regardless of different types of vasculitis, vasculitis-associated masses were hypoechoic and hypodense with poor encasement on a CT scan, making it difficult for differentiation from pancreatic cancer or IPT. For a focal pancreatic lesion, fine-needle biopsy is widely used with abdominal or endoscopic ultrasonography and it is useful in autoimmune pancreatitis[14]. However, fine-needle biopsy has potential sampling error problems; indeed, ultrasound or CT-guided needle biopsy failed to be diagnostic for pancreatic GPA (case 2) and PAN (cases 3 and 4). Negative findings do not exclude the possibility of malignancy and there is a risk of needle tract seeding or dissemination of tumor cells[15]. Thus, the diagnostic procedure is challenging. Some clinicians do away with the preoperative evaluation in patients with operable focal lesions of a clinically and radiologically suspicious malignancy. The common use of ANCA tests in the future would enhance preoperative diagnosis and avoid unnecessary radical operations.

Another interesting finding in this case was the coexistence of different entities of vasculitis, such as PAN in the pancreatobiliary system and MPA in the kidneys. The renal histopathological findings of small-caliber vessel (arteries and capillaries) vasculitis and positive MPO-ANCA supported the MPA diagnosis[2,3]. PAN and MPA had often been diagnosed together until the proposal of the CHCC nomenclature and distinguishing between these 2 entities is not clinically always straightforward[16]. Our case may represent the so-called polyangiitis overlap syndrome which is characterized by systemic vasculitis with features that overlap more than 1 type of vasculitis[17]. Alternatively, it is possibly a coincidence or part of the MAP or PAN spectrum. Renal MAP has been reported to complicate vasculitic disorders that can be attributed to PAN, such as a rupture of branch of the celiac[18] or SMA system[19] and coronary angiitis[20].

In conclusion, we encountered a patient with a pancreatic mass associated with PAN. A literature review revealed that pancreatic masses have been reported in 7 patients with primary vasculitis. Because of its rarity and lack of reliable discrimination from pancreatic cancer, clinicians should be aware of such cases and that early diagnosis followed by immunosuppressive treatment is mandatory.

COMMENTS

Case characteristics

A 66-year-old woman presented with a pancreatic mass accompanied by fever.

Differential diagnosis

An inflammatory pseudotumor and pancreatic neoplasms, including cancer.

Laboratory diagnosis

Laboratory examination showed elevated levels of biliary enzymes (alkaline phosphatase and gamma glutamyl transpeptidase), C-reactive protein and myeloperoxidase-anti nuclear cytoplasmic antibodies.

Imaging diagnosis

An abdominal computed tomography revealed an ill-defined 2.0 cm pancreatic mass with poor enhancement compressing the distal common bile duct (CBD) and pancreatic duct, as well as the thickened walls of the CBD and gallbladder.

Pathological diagnosis

The resected pancreas revealed extensive fibrosis associated with necrotizing vasculitis targeting medium-sized vessels and sparing small-caliber vessels.

Treatment

The patient underwent surgical resection followed by immunosuppression after pathological diagnosis of polyarteritis nodosa.

Related reports

A pancreatic mass as an initial manifestation of vasculitis is extremely rare, with only 7 cases reported in the literature.

Experiences and lessons

The case emphasizes that vasculitis should be included in the differential diagnosis of a pancreatic mass accompanied by fever.

Peer review

Although immunosuppression is the optimal treatment for a vasculitis-associated pancreatic tumor, the diagnosis is challenging because of its rarity and lack of discrimination from pancreatic cancer.

REFERENCES

1 **Jennette JC**, Falk RJ, Andrassy K, Bacon PA, Churg J, Gross WL, Hagen EC, Hoffman GS, Hunder GG, Kallenberg CG. Nomenclature of systemic vasculitides. Proposal of an international consensus conference. *Arthritis Rheum* 1994; **37**: 187-192 [PMID: 8129773 DOI: 10.1002/art.1780370206]

2 **Jennette JC**, Falk RJ, Bacon PA, Basu N, Cid MC, Ferrario F, Flores-Suarez LF, Gross WL, Guillevin L, Hagen EC, Hoffman GS, Jayne DR, Kallenberg CG, Lamprecht P, Langford CA, Luqmani RA, Mahr AD, Matteson EL, Merkel PA, Ozen S, Pusey CD, Rasmussen N, Rees AJ, Scott DG, Specks U, Stone JH, Takahashi K, Watts RA. 2012 revised International Chapel Hill Consensus Conference Nomenclature of Vasculitides. *Arthritis Rheum* 2013; **65**: 1-11 [PMID: 23045170 DOI: 10.1002/art.37715]

3 **Kallenberg CG**. Pathogenesis of ANCA-associated vasculitides. *Ann Rheum Dis* 2011; **70** Suppl 1: i59-i63 [PMID: 21339221 DOI: 10.1136/ard.2010.138024]

4 **Fauci AS**, Haynes B, Katz P. The spectrum of vasculitis: clinical, pathologic, immunologic and therapeutic considerations. *Ann Intern Med* 1978; **89**: 660-676 [PMID: 31121 DOI: 10.7326/0003-4819-89-5-660]

5 **Damani NN**, Asch MR, Redston M. The diagnostic challenge of vasculitis in a patient presenting with acute cholecystitis and a focal pancreatic mass: case report. *Can Assoc Radiol J* 1997; **48**: 179-182 [PMID: 9193416]

6 **Kariv R**, Sidi Y, Gur H. Systemic vasculitis presenting as a tumorlike lesion. Four case reports and an analysis of 79 reported cases. *Medicine* (Baltimore) 2000; **79**: 349-359 [PMID:

11144033 DOI: 10.1097/00005792-200011000-00001]
7 **Pagnoux C**, Mahr A, Cohen P, Guillevin L. Presentation and outcome of gastrointestinal involvement in systemic necrotizing vasculitides: analysis of 62 patients with polyarteritis nodosa, microscopic polyangiitis, Wegener granulomatosis, Churg-Strauss syndrome, or rheumatoid arthritis-associated vasculitis. *Medicine* (Baltimore) 2005; **84**: 115-128 [PMID: 15758841 DOI: 10.1097/01.md.0000158825.87055.0b]
8 **O'Neil KM**, Jones DM, Lawson JM. Wegener's granulomatosis masquerading as pancreatic carcinoma. *Dig Dis Sci* 1992; **37**: 702-704 [PMID: 1563310 DOI: 10.1007/BF01296425]
9 **Matsubayashi H**, Seki T, Niki S, Mizumura Y, Taguchi Y, Moriyasu F, Go K. Wegener's granulomatosis with onset of acute pancreatitis and rapid progress. A case report. *Pancreatology* 2001; **1**: 263-266 [PMID: 12120205 DOI: 10.1159/000055821]
10 **Tinazzi I**, Caramaschi P, Parisi A, Faccioli N, Capelli P, Biasi D. Pancreatic granulomatous necrotizing vasculitis: a case report and review of the literature. *Rheumatol Int* 2007; **27**: 989-991 [PMID: 17265156 DOI: 10.1007/s00296-007-0314-9]
11 **Ito M**, Sano K, Inaba H, Hotchi M. Localized necrotizing arteritis. A report of two cases involving the gallbladder and pancreas. *Arch Pathol Lab Med* 1991; **115**: 780-783 [PMID: 1677801]
12 **Gonzalez-Gay MA**, Vazquez-Rodriguez TR, Miranda-Filloy JA, Pazos-Ferro A, Garcia-Rodeja E. Localized vasculitis of the gastrointestinal tract: a case report and literature review. *Clin Exp Rheumatol* 2008; **26**: S101-S104 [PMID: 18799064]
13 **Adsay NV**, Basturk O, Klimstra DS, Klöppel G. Pancreatic pseudotumors: non-neoplastic solid lesions of the pancreas that clinically mimic pancreas cancer. *Semin Diagn Pathol* 2004; **21**: 260-267 [PMID: 16273945 DOI: 10.1053/j.semdp.2005.07.003]
14 **Kanno A**, Ishida K, Hamada S, Fujishima F, Unno J, Kume K, Kikuta K, Hirota M, Masamune A, Satoh K, Notohara K, Shimosegawa T. Diagnosis of autoimmune pancreatitis by EUS-FNA by using a 22-gauge needle based on the International Consensus Diagnostic Criteria. *Gastrointest Endosc* 2012; **76**: 594-602 [PMID: 22898417 DOI: 10.1016/j.gie.2012.05.014]
15 **Hirooka Y**, Goto H, Itoh A, Hashimoto S, Niwa K, Ishikawa H, Okada N, Itoh T, Kawashima H. Case of intraductal papillary mucinous tumor in which endosonography-guided fine-needle aspiration biopsy caused dissemination. *J Gastroenterol Hepatol* 2003; **18**: 1323-1324 [PMID: 14535994 DOI: 10.1046/j.1440-1746.2003.03040.x]
16 **Basu N**, Watts R, Bajema I, Baslund B, Bley T, Boers M, Brogan P, Calabrese L, Cid MC, Cohen-Tervaert JW, Flores-Suarez LF, Fujimoto S, de Groot K, Guillevin L, Hatemi G, Hauser T, Jayne D, Jennette C, Kallenberg CG, Kobayashi S, Little MA, Mahr A, McLaren J, Merkel PA, Ozen S, Puechal X, Rasmussen N, Salama A, Salvarani C, Savage C, Scott DG, Segelmark M, Specks U, Sunderköetter C, Suzuki K, Tesar V, Wiik A, Yazici H, Luqmani R. EULAR points to consider in the development of classification and diagnostic criteria in systemic vasculitis. *Ann Rheum Dis* 2010; **69**: 1744-1750 [PMID: 20448283 DOI: 10.1136/ard.2009.119032]
17 **Leavitt RY**, Fauci AS. Polyangiitis overlap syndrome. Classification and prospective clinical experience. *Am J Med* 1986; **81**: 79-85 [PMID: 2873744 DOI: 10.1016/0002-9343(86)90186-5]
18 **Ito Y**, Tanaka A, Sugiura Y, Sezaki R. An autopsy case of intraabdominal hemorrhage in microscopic polyangiitis. *Intern Med* 2011; **50**: 1501-1502 [PMID: 21757839 DOI: 10.2169/internalmedicine.50.5549]
19 **Ueda S**, Matsumoto M, Ahn T, Adachi S, Oku K, Takagi M, Fukui H, Yoshikawa M. Microscopic polyangiitis complicated with massive intestinal bleeding. *J Gastroenterol* 2001; **36**: 264-270 [PMID: 11324731 DOI: 10.1007/s005350170114]
20 **Shah AS**, Din JN, Payne JR, Dhaun N, Denvir MA, Mills NL. Coronary angiitis and cardiac arrest in antineutrophil cytoplasmic-antibody associated systemic vasculitis. *Circulation* 2011; **123**: e230-e231 [PMID: 21321177 DOI: 10.1161/CIRCULATIONAHA.110.981936]

P- Reviewer: Ranieri G **S- Editor**: Qi Y **L- Editor**: Roemmele A
E- Editor: Wang CH

World Journal of Gastroenterology

Submit a Manuscript: http://www.wjgnet.com/esps/
Help Desk: http://www.wjgnet.com/esps/helpdesk.aspx
DOI: 10.3748/wjg.v21.i3.1020

World J Gastroenterol 2015 January 21; 21(3): 1020-1023
ISSN 1007-9327 (print) ISSN 2219-2840 (online)

CASE REPORT

Rare case of pancreatic cancer with leptomeningeal carcinomatosis

In Kyung Yoo, Hong Sik Lee, Chang Duk Kim, Hoon Jai Chun, Yoon Tae Jeen, Bora Keum, Eun Sun Kim, Hyuk Soon Choi, Jae Min Lee, Seung Han Kim, Seung Joo Nam, Jong Jin Hyun

In Kyung Yoo, Hong Sik Lee, Chang Duk Kim, Hoon Jai Chun, Yoon Tae Jeen, Bora Keum, Eun Sun Kim, Hyuk Soon Choi, Jae Min Lee, Seung Han Kim, Seung Joo Nam, Division of Gastroenterology and Hepatology, Department of Internal Medicine, Institute of Digestive Disease and Nutrition, Korea University College of Medicine, Seoul 136-705, South Korea
Jong Jin Hyun, Division of Gastroenterology and Hepatology, Department of Internal Medicine, Korea University Ansan Hospital 123, Gyeonggi-do 425-707, South Korea
Author contributions: Kim CD and Chun HJ designed the report; Jeen YT, Keum B and Kim ES collected the patient's clinical data; Choi HS, Lee JM, Kim SH and Nam SJ performed the research; Yoo IK wrote the paper; and Lee HS approved the final version of the paper to be published; all authors finally revised this paper.

Correspondence to: Hong Sik Lee, MD, PhD, Division of Gastroenterology and Hepatology, Department of Internal Medicine, Institute of Digestive Disease and Nutrition, Korea University College of Medicine, Inchon-ro 73, Seongbuk-gu, Seoul 136-705, South Korea. hslee60@korea.ac.kr
Telephone: +82-10-86502455
Fax: +82-2-9531943
Received: May 28, 2014
Peer-review started: May 29, 2014
First decision: June 27, 2014
Revised: July 6, 2014
Accepted: September 5, 2014
Article in press: September 5, 2014
Published online: January 21, 2015

Abstract

Leptomeningeal carcinomatosis occurs very rarely in patients with pancreatic cancer. Leptomeningeal carcinomatosis is characterized by multifocal seeding of the leptomeninges by malignant cells that originate from a solid tumor. To the best of our knowledge, brain metastasis from pancreatic cancer is extremely rare. Leptomeningeal carcinomatosis is estimated to occur in 3% to 8% of cases of solid tumors. The clinical manifestation usually involves neurological symptoms, including dizziness, headache, vomiting, nausea, and hemiparesis, symptoms similar to those of meningitis or brain tumors. Diagnostic methods for leptomeningeal carcinomatosis include brain magnetic resonance imaging and cerebrospinal fluid examination. Here, we describe a case of leptomeningeal carcinomatosis in which the primary tumor was later determined to be pancreatic cancer. Brain magnetic resonance imaging findings showed mild enhancement of the leptomeninges, and cerebrospinal fluid cytology was negative at first. However, after repeated spinal taps, atypical cells were observed on cerebrospinal fluid analysis and levels of tumor markers such as carbohydrate antigen 19-9 in cerebrospinal fluid were elevated. Abdominal computed tomography, performed to determine the presence of extracerebral tumors, revealed pancreatic cancer. Pancreatic cancer was confirmed histopathologically on examination of an endoscopic ultrasound-guided fine needle aspiration specimen.

Key words: Pancreatic cancer; Radiation therapy; Tumor marker; Leptomeningeal carcinomatosis; Prognosis

Core tip: Leptomeningeal carcinomatosis with pancreatic cancer is a relatively rare finding. To date, only a few cases of brain metastasis originating from pancreatic cancer have been reported. Here, we report on a patient presenting with neurologic symptoms who was found to have pancreatic cancer with leptomeningeal metastasis, and we review the relevant literature.

Yoo IK, Lee HS, Kim CD, Chun HJ, Jeen YT, Keum B, Kim ES, Choi HS, Lee JM, Kim SH, Nam SJ, Hyun JJ. Rare case of pancreatic cancer with leptomeningeal carcinomatosis. *World J Gastroenterol* 2015; 21(3): 1020-1023 Available from: URL: http://www.wjgnet.com/1007-9327/full/v21/i3/1020.htm DOI: http://dx.doi.org/10.3748/wjg.v21.i3.1020

INTRODUCTION

Pancreatic cancer is the fourth frequent cause of cancer-related deaths in the United States[1]. At the time of diagnosis, most patients have locally advanced or metastasized disease and therefore do not qualify for surgical treatment, resulting in a very poor prognosis with a 5-year survival rate of less than 5%[2]. However, central nervous system (CNS) involvement is rare in pancreatic cancer. Metastatic leptomeningeal carcinomatosis (LC) is estimated to occur in 3% to 8% of cases of solid tumors[3]. Particularly, in patients with pancreatic cancer, the development of metastasis to the CNS is rare (occurring in approximately 0.3% of cases). According to the literature, leptomeningeal metastasis from pancreatic cancer has been reported in only 12 cases.

In this report, we discuss a rare case of pancreatic cancer leading to LC.

CASE REPORT

An 80-year-old man was admitted to the neurology department of our hospital in February 2014 because of episodes of headache and seizure. The headaches began 5 wk before hospital admission and increased in intensity and frequency. Seizure episodes were observed 5 d before admission to the hospital. The duration of each seizure was approximately 10 s, and these were accompanied by upward deviation of the eyeballs. The seizures were generalized tonic-clonic seizures, and the patient was responsive after 3 to 4 min. He had a 40-year history of smoking one pack of cigarettes per a day and no specific family history of other diseases.

The patient had no other complaints except for recent weight loss of 5 kg over 4 mo. On physical examination, he exhibited no focal neurological signs such as abnormal reflexes, sensory deficit, nystagmus, or neck stiffness. His vital signs were as follows: blood pressure, 110/70 mmHg; pulse rate, 72 beats/min; and respiratory rate, 20 breaths/min. Breathing sounds were clear, and heart sounds were regular and without murmur. Findings of the laboratory workup on admission were normal. Magnetic resonance imaging (MRI) of the brain (Figure 1) revealed mild leptomeningeal enhancement in the cerebellar folia and bilateral temporoparietal meninges and solid enhancement in the pineal gland. Laboratory analysis showed relatively normal cerebrospinal fluid (CSF), 4 white blood cells per μL, slightly elevated protein level of 65.3 mg/dL (normal range: 10-45 mg/dL), a slightly decreased glucose level of 31 mg/dL (normal range: 50-75 mg/dL), an adenosine deaminase level of 3.8 IU/L, and negative results on tuberculosis (Tb) polymerase chain reaction and acid-fast bacilli staining. CSF cytology showed no atypical cells. The opening pressure was 12.5 cmH_2O (normal range: 8-15 cmH_2O). Although the CSF analysis results indicated no specific abnormality, Tb treatment was started as a preventative measure for Tb meningitis, which was prevalent in South Korea. On the basis of these results, the possibility of a pineal gland tumor with leptomeningeal metastasis or an extracerebral tumor with LC was also explored. However, the brain tumor with pineal gland involvement which seeding to meninges is very rare and definitive diagnosis was not made before autopsy. Accordingly, computed tomography (CT) and serum tumor marker measurement were performed to determine the presence of extracerebral tumors. Contrast CT of the chest and abdomen/pelvis showed an infiltrating mass in the body of the pancreas encasing the celiac trunk, with lymph node enlargement in the left paraaortic area, indicative of liver metastases (Figure 2). The serum carbohydrate antigen (CA) 19-9 level was elevated at 8310 IU/mL (normal range, 0-37 IU/mL). Endoscopic ultrasonography showed an ill-defined lesion in the body of the pancreas; the presence of adenocarcinoma cells was confirmed by histopathological examination of a fine-needle aspiration specimen.

A repeat examination of CSF was performed, including tumor marker measurement. Elevated levels of CA 19-9 (10000 IU/mL; normal range, 0-32 IU/mL) and carcinoembryonic antigen (CEA) (23.2 ng/mL; normal range, 0-5 mg/mL) were detected. At the third spinal tap for CSF, atypical cells were present, which were not detected previously. The pineal gland tumor which metastasis to meninges is mostly germ cell tumor even its prevalence is rare, and usually show elevation of α-Fetoprotein or β-chorionic gonadotropin in CSF. Given the markedly elevated CA 19-9 level in serum and CSF and the clinical and radiologic findings (brain MRI and abdominal CT), a diagnosis of metastatic pancreatic cancer, rather than leptomeningeal seeding from the pineal gland tumor or meningitis, was made.

The patient's Eastern Cooperative Oncology Group performance status was 3, and he was capable of limited self-care, being confined to a bed or chair for more than 50% of the time for which he was awake. He wished to continue treatment for as long as tolerable. Whole brain radiation with a palliative intent was initiated. Intrathecal chemotherapy was deferred because of the patient's poor performance status. After four rounds of radiation therapy, the patient was transferred to another, affiliated hospital near house for his wish. Therefore, the patient could not be followed-up thereafter.

DISCUSSION

Pancreatic cancer is a common malignancy and often presents at an advanced stage. Despite advances in early

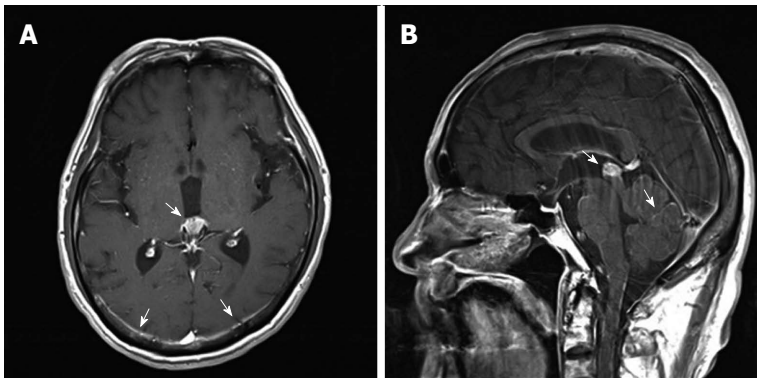

Figure 1 Brain magnetic resonance imaging findings. A: Pineal gland and parietal leptomeningeal enhancement on a T1 axial image (arrows); B: Pineal gland and cerebellar folia enhancement on a T1 sagittal image (arrows).

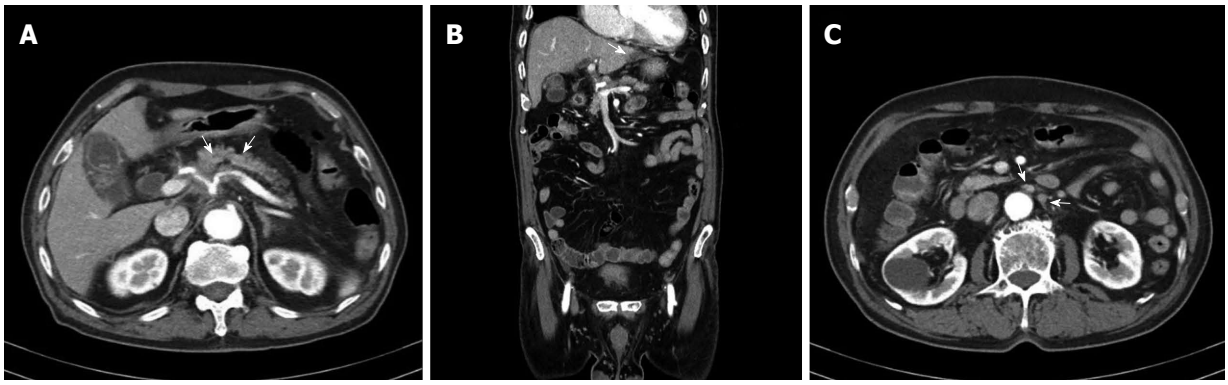

Figure 2 Computed tomography scans of the abdomen and pelvis. A: An infiltrating pancreatic neoplasm involving the body encasing the celiac axis (arrows); B: Low-density lesion at the left lateral segment of the liver (arrow); C: Lymph node enlargement in the left paraaortic area (arrows).

diagnosis and therapy, the survival rate has not changed during recent years. This is because early diagnosis is difficult owing to nonspecific symptoms or the absence of symptoms and because the etiology of pancreatic cancer is unknown.

LC, wherein tumor cells metastasize to the leptomeninges and CSF, is a particularly virulent syndrome with extremely high morbidity and mortality[4-7].

Patients with LC can present with symptoms similar to those of infectious meningitis, such as headache, neck stiffness, nausea, and vomiting[8].

The diagnosis of LC is difficult in most patients because this requires the detection of malignant cells on CSF cytology. As seen in this case, malignant cells are rarely found initially. They are detected in the initial CSF sample in only 50% of patients with LC. Repeat CSF analysis has been found to improve the yield to 90%[9]. At the time of lumbar puncture, an elevated opening pressure of the CSF, an elevated protein level, and a decreased glucose level could aid in the diagnosis[10]. Measurement of levels of specific tumor markers in the CSF, in particular, CEA, CA 125, CA 19-9, and CYFRA 21-1, may also help in early diagnosis of LC[11]. According to the literature, CYFRA 21-1 and neuron-specific enolase levels are usually elevated in CSF in cases of lung cancer and the CEA level is elevated in cases of solid adenocarcinomas, mainly gastrointestinal tumors. These studies suggest that tumor marker levels be considered diagnostic for LC when levels in CSF are greater than those in serum. Because tumor markers are produced directly by tumors or by non-tumor cells in response to the presence of a tumor, elevated tumor marker levels can be detected earlier than radiological radiographic abnormalities[12]. Levels of CSF tumor markers such as CA 19-9 in particular have predictive value for breast cancer and LC[13,14]. However, diagnostic data relating to CSF tumor marker levels are not available for pancreatic cancer with LC, because of the rare occurrence of CNS metastasis from pancreatic cancer. In our case of pancreatic cancer with LC, we found markedly elevated levels of CA 19-9 (10000 IU/mL), and we would like to emphasize that this finding is unique. Further study of CA 19-9 levels in CSF would be meaningful on accumulation of more cases of pancreatic cancer with LC.

Brain MRI with gadolinium-enhanced, T1-weighted images can support the diagnosis in patients with negative cytology findings[15]. On MRI, LC shows thin, diffuse leptomeningeal contrast enhancement and multiple nodular deposits in the subarachnoid space, cerebellar folia, or cortical surface, and can show mass lesions, as in the case presented here.

The treatment goal for LC is to improve or stabilize

the patient's neurologic status and to prolong survival. According to the National Comprehensive Cancer Network, treatment decisions should be based on the patients' risk group stratification. Patients in the poor risk group (Karnofsky Performance Status score less than 60, multiple serious major neurologic deficits, bulky CNS disease, and encephalopathy) are usually offered supportive care and palliative radiation therapy is considered. Patients in the good risk group (Karnofsky Performance Status score more than 60, no major neurologic deficits, minimal systemic disease) receive radiation therapy and chemotherapy.

To our knowledge, this is the first case of LC from pancreatic cancer in South Korea and the detection of an elevated CA 19-9 level in the CSF in such a patient. When neurological symptoms and signs are present, clinicians should consider the possibility of LC from a solid tumor and perform investigations to exclude neurological involvement.

COMMENTS

Case characteristics

An 80-year-old male presenting with neurologic symptoms who was found to have pancreatic cancer with leptomeningeal metastasis.

Clinical diagnosis

Seizure episodes were observed 5 d before admission.

Differential diagnosis

An extracerebral tumor with leptomeningeal metastasis, Tb meningitis, pineal gland tumor with leptomeningeal metastasis.

Laboratory diagnosis

WBC 10.0 k/uL; HGB 13 g/dL; CA 19-9 (serum) 8310 IU /mL; CA 19-9 (CSF) 10000 IU /mL; CEA (CSF) 23.2 ng/mL; metabolic panel and liver function test were within normal limits.

Imaging diagnosis

Brain magnetic resonance imaging revealed mild leptomeningeal enhancement and abdominal computed tomography showed an infiltrating mass in the body of the pancreas encasing the celiac trunk.

Pathological diagnosis

Histopathological examination of transesophageal ultrasound-guided fine needle aspiration revealed adenocarcinoma on pancreas and at the third spinal tap for cerebrospinal fluid (CSF), atypical cells were present.

Treatment

The patient was treated with whole brain radiation.

Related reports

According to the literature, leptomeningeal metastasis from pancreatic cancer has been reported in only 12 cases.

Term explanation

Leptomeningeal carcinomatosis is characterized by multifocal seeding of the leptomeninges by malignant cells that originate from a solid tumor.

Experiences and lessons

When neurological symptoms and signs are present in patient, clinicians should consider the possibility of leptomeningeal carcinomatosis from a solid tumor and perform investigations to exclude neurological involvement.

Peer review

This article applies repeated CSF taping and checking elevated level of CA 19-9 could help to diagnosis the rare case of pancreatic cancer with leptomeningeal carcinomatosis.

REFERENCES

1 **Siegel R**, Naishadham D, Jemal A. Cancer statistics, 2013. *CA Cancer J Clin* 2013; **63**: 11-30 [PMID: 23335087 DOI: 10.3322/caac.21166]

2 **Hidalgo M**. Pancreatic cancer. *N Engl J Med* 2010; **362**: 1605-1617 [PMID: 20427809 DOI: 10.1056/NEJMra0901557]

3 **Lee JL**, Kang YK, Kim TW, Chang HM, Lee GW, Ryu MH, Kim E, Oh SJ, Lee JH, Kim SB, Kim SW, Suh C, Lee KH, Lee JS, Kim WK, Kim SH. Leptomeningeal carcinomatosis in gastric cancer. *J Neurooncol* 2004; **66**: 167-174 [PMID: 15015782 DOI: 10.1023/B:NEON.0000013462.43156.f4]

4 **Chamberlain MC**. Neurotoxicity of intra-CSF liposomal cytarabine (DepoCyt) administered for the treatment of leptomeningeal metastases: a retrospective case series. *J Neurooncol* 2012; **109**: 143-148 [PMID: 22539243 DOI: 10.1007/s11060-012-0880-x]

5 **Chamberlain MC**, Sandy AD, Press GA. Leptomeningeal metastasis: a comparison of gadolinium-enhanced MR and contrast-enhanced CT of the brain. *Neurology* 1990; **40**: 435-438 [PMID: 2314584 DOI: 10.1212/WNL.40.3_Part_1.435]

6 **Groves MD**, Glantz MJ, Chamberlain MC, Baumgartner KE, Conrad CA, Hsu S, Wefel JS, Gilbert MR, Ictech S, Hunter KU, Forman AD, Puduvalli VK, Colman H, Hess KR, Yung WK. A multicenter phase II trial of intrathecal topotecan in patients with meningeal malignancies. *Neuro Oncol* 2008; **10**: 208-215 [PMID: 18316473 DOI: 10.1215/15228517-2007-059]

7 **Niwińska A**, Rudnicka H, Murawska M. Breast cancer leptomeningeal metastasis: propensity of breast cancer subtypes for leptomeninges and the analysis of factors influencing survival. *Med Oncol* 2013; **30**: 408 [PMID: 23322521 DOI: 10.1007/s12032-012-0408-4]

8 **Pavlidis N**. The diagnostic and therapeutic management of leptomeningeal carcinomatosis. *Ann Oncol* 2004; **15** Suppl 4: iv285-iv291 [PMID: 15477323]

9 **Kesari S**, Batchelor TT. Leptomeningeal metastases. *Neurol Clin* 2003; **21**: 25-66 [PMID: 12690644 DOI: 10.1016/S0733-8619(02)00032-4]

10 **Leal T**, Chang JE, Mehta M, Robins HI. Leptomeningeal Metastasis: Challenges in Diagnosis and Treatment. *Curr Cancer Ther Rev* 2011; **7**: 319-327 [PMID: 23251128 DOI: 10.2174/157339411797642597]

11 **Wang P**, Piao Y, Zhang X, Li W, Hao X. The concentration of CYFRA 21-1, NSE and CEA in cerebro-spinal fluid can be useful indicators for diagnosis of meningeal carcinomatosis of lung cancer. *Cancer Biomark* 2013; **13**: 123-130 [PMID: 23838141 DOI: 10.3233/CBM-130338]

12 **Shi Q**, Pu CQ, Wu WP, Huang XS, Yu SY, Tian CL, Huang DH, Zhang JT. [Value of tumor markers in the cerebrospinal fluid in the diagnosis of meningeal carcinomatosis]. *Nanfang Yi ke Daxue Xuebao* 2010; **30**: 1192-1194 [PMID: 20501426]

13 **Kosmas C**, Tsavaris NB, Tsakonas G, Soukouli G, Gassiamis A, Mylonakis N, Karabelis A. Cerebrospinal fluid tumor marker levels in predicting response to treatment and survival of carcinomatous meningitis in patients with advanced breast cancer. *Med Sci Monit* 2005; **11**: CR398-CR401 [PMID: 16049383]

14 **Tajima Y**, Horiguchi K, Nakano S, Hirono S, Higuchi Y, Oide T, Iwadate Y, Saeki N. [Leptomeningeal carcinomatosis following 27 years remission from breast cancer with epidermoid: a case report]. *No Shinkei Geka* 2012; **40**: 343-349 [PMID: 22466234]

15 **Wasserstrom WR**, Glass JP, Posner JB. Diagnosis and treatment of leptomeningeal metastases from solid tumors: experience with 90 patients. *Cancer* 1982; **49**: 759-772 [PMID: 6895713]

P- Reviewer: Fölsch UR, Kapan S **S- Editor**: Ma YJ
L- Editor: A **E- Editor**: Wang CH

World Journal of Gastroenterology

Submit a Manuscript: http://www.wjgnet.com/esps/
Help Desk: http://www.wjgnet.com/esps/helpdesk.aspx
DOI: 10.3748/wjg.v21.i3.1024

World J Gastroenterol 2015 January 21; 21(3): 1024-1027
ISSN 1007-9327 (print) ISSN 2219-2840 (online)

CASE REPORT

Protein C deficiency related obscure gastrointestinal bleeding treated by enteroscopy and anticoagulant therapy

Wei-Fan Hsu, Yuk-Ming Tsang, Chung-Jen Teng, Chen-Shuan Chung

Wei-Fan Hsu, Chung-Jen Teng, Chen-Shuan Chung, Department of Internal Medicine, Far Eastern Memorial Hospital, New Taipei City 22060, Taiwan
Yuk-Ming Tsang, Department of Radiology, Far Eastern Memorial Hospital, New Taipei City 22060, Taiwan
Chen-Shuan Chung, College of Medicine, Fu Jen Catholic University, New Taipei City 24205, Taiwan
Chen-Shuan Chung, Taiwan Association for the Study of Small Intestinal Diseases, New Taipei City 22060, Taiwan
Author contributions: Hsu WF and Chung CS designed the research; Chung CS performed the enteroscopy; Tsang YM reviewed the computed tomography and angiography findings; Teng CJ reviewed the disease of protein C deficiency; Hsu WF wrote the paper; and Chung CS approved the final version.

Correspondence to: Chen-Shuan Chung, MD, MSc, Department of Internal Medicine, Far Eastern Memorial Hospital, 21, Section 2, Nan-Ya South Road, Banciao District, New Taipei City 22060, Taiwan. chungchenshuan_3@yahoo.com.tw
Telephone: +886-2-89667000-1704
Fax: +886-2-77380091
Received: May 3, 2014
Peer-review started: May 4, 2014
First decision: June 27, 2014
Revised: July 6, 2014
Accepted: July 30, 2014
Article in press: July 30, 2014
Published online: January 21, 2015

Abstract

Obscure gastrointestinal bleeding is an uncommonly encountered and difficult-to-treat clinical problem in gastroenterology, but advancements in endoscopic and radiologic imaging modalities allow for greater accuracy in diagnosing obscure gastrointestinal bleeding. Ectopic varices account for less than 5% of all variceal bleeding cases, and jejunal variceal bleeding due to extrahepatic portal hypertension is rare. We present a 47-year-old man suffering from obscure gastrointestinal bleeding. Computed tomography of the abdomen revealed multiple vascular tufts around the proximal jejunum but no evidence of cirrhosis, and a visible hypodense filling defect suggestive of thrombus was visible in the superior mesenteric vein. Enteroscopy revealed several serpiginous varices in the proximal jejunum. Serologic data disclosed protein C deficiency (33.6%). The patient was successfully treated by therapeutic balloon-assisted enteroscopy and long-term anticoagulant therapy, which is normally contraindicated in patients with gastrointestinal bleeding. Diagnostic modalities for obscure gastrointestinal bleeding, such as capsule endoscopy, computed tomography enterography, magnetic resonance enterography, and enteroscopy, were also reviewed in this article.

Key words: Angiography; Computed tomography; Enteroscopy; Obscure gastrointestinal bleeding; Protein C deficiency; Superior mesenteric venous thrombosis

Core tip: This article presents a rare case of obscure gastrointestinal bleeding-jejunal variceal bleeding and superior mesenteric venous thrombosis. The variceal bleeding and superior mesenteric venous thrombosis were secondary to protein C deficiency. It is worth mentioning that the bleeding was controlled under anticoagulant therapy after therapeutic enteroscopy.

Hsu WF, Tsang YM, Teng CJ, Chung CS. Protein C deficiency related obscure gastrointestinal bleeding treated by enteroscopy and anticoagulant therapy. *World J Gastroenterol* 2015; 21(3): 1024-1027 Available from: URL: http://www.wjgnet.

com/1007-9327/full/v21/i3/1024.htm DOI: http://dx.doi.org/10.3748/wjg.v21.i3.1024

INTRODUCTION

Recent advancements in endoscopic and radiologic imaging modalities allow for greater accuracy in diagnosing obscure gastrointestinal bleeding (OGIB), an uncommonly encountered and difficult-to-treat clinical problem in gastroenterology[1]. Ectopic varices, which comprise large portosystemic venous collaterals located anywhere other than the gastroesophageal region[2], account for less than 5% of all variceal bleeding cases[3] and usually are due to previous abdominal surgery, intrahepatic portal hypertension, and rarely extrahepatic causes[4]. We present a case of thrombosis in the superior mesenteric vein (SMV) complicated by jejunal variceal bleeding secondary to protein C deficiency. OGIB was successfully treated by balloon-assisted enteroscopy and anticoagulant therapy.

CASE REPORT

A 47-year-old man presented with a 10-d history of tarry stool passage. The patient had no other underlying disease. Results of physical examinations were unremarkable with the exception of pale conjunctiva. Laboratory studies revealed a hemoglobin level of 6.9 g/dL (normal range: 13-17 g/dL), a platelet count of 200 × 10^3/μL (normal range, 140-400 × 10^3/μL), an international normalized ratio (INR) of prothrombin time of 1.01, an activated partial thromboplastin time of 26.8 s (normal range: 23.3-39.3 s), and normal aminotransferase levels. Esophagogastroduodenoscopic and colonoscopic examinations revealed no evidence of stigmata of recent hemorrhage. The preliminary diagnosis was OGIB. Computed tomography (CT) of the abdomen revealed multiple vascular tufts around the proximal jejunum but no evidence of cirrhosis (Figure 1A). A hypodense filling defect suggestive of thrombus was visible in the SMV (Figure 1B). Celiac angiography revealed engorged collateral veins in the left upper quadrant of the abdomen without contrast agent in the main trunk of the SMV (Figure 2). Antegrade single-balloon enteroscopy (SIF-Q260; Olympus Medical systems, Tokyo, Japan) revealed several serpiginous varicose veins (Figure 3) with poor distensibility of the proximal jejunum. A mixture of 0.5 mL N-butyl-2-cyanoacrylate and 0.5 mL lipioidol was endoscopically injected into said veins. Serologic data disclosed protein C deficiency (33.6%). Anti-smooth muscle antibody, antinuclear antibody, anti-cardiolipin antibody, homocysteine, antithrombin Ⅲ, and tumor markers were all within normal limits. The patient was therefore placed on oral warfarin therapy (INR 2.0), and he lived uneventfully 17 mo after the enteroscopy.

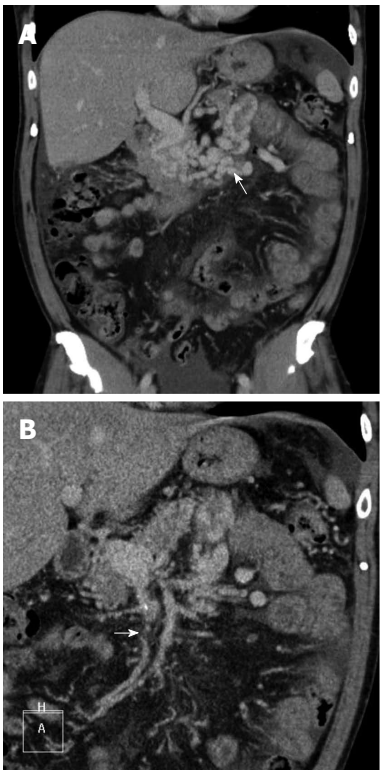

Figure 1 Computed tomographic scan reveals vascular tufts around the proximal jejunum (A, arrow), and thrombi are visible as hypodense lesions in the contrasted superior mesenteric vein (B, arrow).

DISCUSSION

Variceal bleeding due to portal hypertension developing in locations other than the esophagus and stomach accounts for less than 5% of all variceal bleeding cases[3]. Jejunal variceal bleeding due to extrahepatic portal hypertension is rare. Small intestinal varices normally present as melena or hematochezia[5]. Bleeding from chronic mesenteric thrombosis is a rare cause of OGIB and without prompt diagnosis it can result in death[6].

Diagnosis of small bowel disorders is challenging because of the small intestine's length (about 6 to 7 m), mobility, and tortuosity. With the development of diagnostic modalities, such as capsule endoscopy[7], CT enterography (CTE)[8], and magnetic resonance enterography (MRE)[9], correct and timely diagnosis of small intestinal lesions can be achieved without unnecessary surgical intervention in some cases. Capsule endoscopy not only has the advantage of non-invasiveness but also has a high sensitivity and high negative predictive value in predicting rebleeding in patients with OGIB[7]. However, the diagnostic specificity of capsule endoscopy is a concern, because 13% of asymptomatic persons may have minor lesions that are not detected by capsule endoscopic evaluation. In addition, capsule endoscopy cannot be performed with therapeutic intents or in patients with certain contraindications, such as gastrointestinal obstruction, pregnancy, or swallowing

Figure 2 Celiac angiography reveals engorged collateral veins in the left upper quadrant of the abdomen without contrast agent in the main trunk of the superior mesenteric vein.

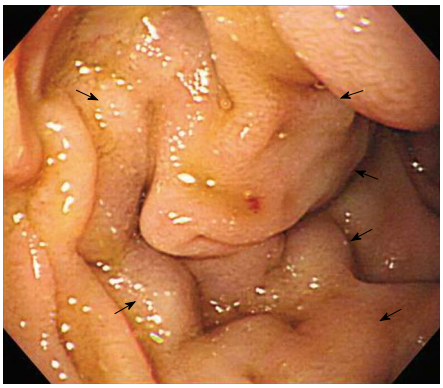

Figure 3 Antegrade single-balloon enteroscopy shows several serpinginous varicose veins (arrows).

difficulty[10]. CTE and MRE are useful methods for detecting small inflammatory and hypervascular lesions in the small intestine[8,9]. Limitations of enterography include exposure to radiation, the need for large volumes of oral contrast agents, adverse reactions to contrast agents (*e.g.*, contrast allergy), and the risk of developing contrast-induced nephropathy[11]. Deep small-bowel enteroscopy can be used to simultaneously detect and treat lesions as well as take biopsy specimens for pathologic analysis[12]; however, the technique requires years of experience to perform and is associated with rare complications, including pancreatitis and perforation[13,14]. Diagnosis and treatment of OGIB could be dramatically improved by adequately combining two or more of the modalities. In our institute we routinely perform second-look upper and lower endoscopy for patients with OGIB, as recommended by a number of clinical guidelines[1,15]. If the second-look endoscopy reveals negative findings, antegrade or retrograde single-balloon enteroscopy guided by capsule endoscopy or CT images is performed.

Small intestinal ectopic varices normally present as tortuous collateral vessels in the mesenteric side of the small intestine on abdominal images[16,17]. Angiographic findings characteristic of OGIB include prolonged contrast agent retention in the collateral vascular tufts[18,19], while endoscopic findings include a spherical bulge, localized prominence, and nodular or serpinginous varices[20,21]. These image findings were identified in our patient. As shown in this and in previous reports, jejunal variceal bleeding can be treated by injecting N-butyl-2-cyanoacrylate under enteroscopy[22]. Radiographic embolization *via* feeding venous occlusions has been suggested in acute settings[23]. Surgery is only recommended for patients without liver cirrhosis or for patients with compensated liver cirrhosis and extrahepatic portal vein thrombosis[24].

Protein C is a vitamin K-dependent anticoagulant protein that inactivates coagulation factors Va and Ⅷa, and its deficiency (< 55%) results in a thrombophilic state[25]. Long-term oral anticoagulants at an INR of 2 to 3 have been shown to be effective in preventing thrombosis in patients with protein C deficiency[25].

In conclusion, OGIB is an uncommonly encountered and difficult-to-treat clinical problem in gastroenterology; however, recent advancements in imaging modalities have greatly enhanced diagnosis and treatment. Ectopic variceal bleeding should be considered in patients with OGIB, and small intestinal variceal bleeding secondary to thrombophilia can be managed by balloon-assisted enteroscopy and anticoagulant therapy.

COMMENTS

Case characteristics

A 47-year-old man presented with a 10-d history of tarry stool passage.

Clinical diagnosis

Esophagogastroduodenoscopic and colonoscopic examinations revealed no evidence of stigmata of recent hemorrhage, and the preliminary diagnosis was obscure gastrointestinal bleeding.

Differential diagnosis

Common differential diagnoses of obscure gastrointestinal bleeding include angiodysplasia, small bowel Crohn's disease, small bowel tumors, intestinal infections (such as tuberculosis and parasites), nonspecific intestinal ulcers, and variceal bleeding.

Laboratory diagnosis

HGB 6.9 gm/dL; platelet count of 200 × $10^3/\mu L$; PT INR 1.01; aPTT 26.8 s; Serologic data disclosed a protein C level of 33.6%.

Imaging diagnosis

Abdominal computed tomography revealed multiple vascular tufts around the proximal jejunum with a hypodense filling defect in the superior mesenteric vein, and antegrade single-balloon enteroscopy revealed several serpiginous varicose veins in the proximal jejunum.

Pathological diagnosis

No pathological diagnosis in this article.

Treatment

A mixture of 0.5 mL N-butyl-2-cyanoacrylate and 0.5 mL lipioidol was endoscopically injected into varices, and the patient was placed on long-term oral warfarin therapy (PT INR 2.0).

Related reports

Ectopic varices account for less than 5% of all variceal bleeding cases, and jejunal variceal bleeding due to superior mesenteric venous thrombosis and protein C deficiency is rare.

Term explanation

Protein C is a vitamin K-dependent anticoagulant protein that inactivates coagulation factors Va and Ⅷa, and its deficiency (< 55%) results in a thrombophilic state.

Experiences and lessons

This case report reminds us that the cause of jejunal varices should be carefully evaluated, and small intestinal variceal bleeding secondary to thrombophilia

can be managed by balloon-assisted enteroscopy and anticoagulant therapy.

Peer review

Although single-balloon enteroscopy with N-butyl-2-cyanoacrylate and lipioidol injection for varicose veins had been reported before, it was a rare circumstance that the jejunal varices came from superior mesenteric venous thrombosis and protein C deficiency.

REFERENCES

1 **Dye CE**, Gaffney RR, Dykes TM, Moyer MT. Endoscopic and radiographic evaluation of the small bowel in 2012. *Am J Med* 2012; **125**: 1228.e1-1228.e12 [PMID: 23062406 DOI: 10.1016/j.amjmed.2012.06.017]

2 **Lebrec D**. Ectopic varices in patients with portal hypertension. *Arch Surg* 1980; **115**: 890 [PMID: 7387382]

3 **Kinkhabwala M**, Mousavi A, Iyer S, Adamsons R. Bleeding ileal varicosity demonstrated by transhepatic portography. *AJR Am J Roentgenol* 1977; **129**: 514-516 [PMID: 409211 DOI: 10.2214/ajr.129.3.514]

4 **Lebrec D**, Benhamou JP. Ectopic varices in portal hypertension. *Clin Gastroenterol* 1985; **14**: 105-121 [PMID: 3872747]

5 **Khan AA**, Sarwar S, Alam A, Butt AK, Shafqat F, Tarique S, Ahmed I, Alvi A, Niazi A. Ectopic intestinal varices as a rare cause of lower gastrointestinal haemorrhage. *J Coll Physicians Surg Pak* 2003; **13**: 526-527 [PMID: 12971876]

6 **Soper NJ**, Rikkers LF, Miller FJ. Gastrointestinal hemorrhage associated with chronic mesenteric venous occlusion. *Gastroenterology* 1985; **88**: 1964-1967 [PMID: 3873375]

7 **Lai LH**, Wong GL, Chow DK, Lau JY, Sung JJ, Leung WK. Long-term follow-up of patients with obscure gastrointestinal bleeding after negative capsule endoscopy. *Am J Gastroenterol* 2006; **101**: 1224-1228 [PMID: 16771942 DOI: 10.1111/j.1572-0241.2006.00565.x]

8 **Fletcher JG**, Huprich J, Loftus EV, Bruining DH, Fidler JL. Computerized tomography enterography and its role in small-bowel imaging. *Clin Gastroenterol Hepatol* 2008; **6**: 283-289 [PMID: 18328436 DOI: 10.1016/j.cgh.2007.12.049]

9 **Masselli G**, Vecchioli A, Gualdi GF. Crohn disease of the small bowel: MR enteroclysis versus conventional enteroclysis. *Abdom Imaging* 2006; **31**: 400-409 [PMID: 16447084 DOI: 10.1007/s00261-005-0395-4]

10 **Goldstein JL**, Eisen GM, Lewis B, Gralnek IM, Zlotnick S, Fort JG. Video capsule endoscopy to prospectively assess small bowel injury with celecoxib, naproxen plus omeprazole, and placebo. *Clin Gastroenterol Hepatol* 2005; **3**: 133-141 [PMID: 15704047]

11 **Graça BM**, Freire PA, Brito JB, Ilharco JM, Carvalheiro VM, Caseiro-Alves F. Gastroenterologic and radiologic approach to obscure gastrointestinal bleeding: how, why, and when? *Radiographics* 2010; **30**: 235-252 [PMID: 20083596 DOI: 10.1148/rg.301095091]

12 **Pasha SF**, Hara AK, Leighton JA. Diagnostic evaluation and management of obscure gastrointestinal bleeding: a changing paradigm. *Gastroenterol Hepatol* (N Y) 2009; **5**: 839-850 [PMID: 20567529]

13 **Mehdizadeh S**, Ross A, Gerson L, Leighton J, Chen A, Schembre D, Chen G, Semrad C, Kamal A, Harrison EM, Binmoeller K, Waxman I, Kozarek R, Lo SK. What is the learning curve associated with double-balloon enteroscopy? Technical details and early experience in 6 U.S. tertiary care centers. *Gastrointest Endosc* 2006; **64**: 740-750 [PMID: 17055868 DOI: 10.1016/j.gie.2006.05.022]

14 **May A**, Nachbar L, Pohl J, Ell C. Endoscopic interventions in the small bowel using double balloon enteroscopy: feasibility and limitations. *Am J Gastroenterol* 2007; **102**: 527-535 [PMID: 17222315 DOI: 10.1111/j.1572-0241.2007.01063.x]

15 **Raju GS**, Gerson L, Das A, Lewis B. American Gastroenterological Association (AGA) Institute technical review on obscure gastrointestinal bleeding. *Gastroenterology* 2007; **133**: 1697-1717 [PMID: 17983812 DOI: 10.1053/j.gastro.2007.06.007]

16 **Lee JY**, Song SY, Kim J, Koh BH, Kim Y, Jeong WK, Kim MY. Percutaneous transsplenic embolization of jejunal varices in a patient with liver cirrhosis: a case report. *Abdom Imaging* 2013; **38**: 52-55 [PMID: 22527157 DOI: 10.1007/s00261-012-9894-2]

17 **Seeger M**, Günther R, Hinrichsen H, Both M, Helwig U, Arlt A, Stelck B, Bräsen JH, Sipos B, Schafmayer C, Braun F, Bröring DC, Schreiber S, Hampe J. Chronic portal vein thrombosis: transcapsular hepatic collateral vessels and communicating ectopic varices. *Radiology* 2010; **257**: 568-578 [PMID: 20829527 DOI: 10.1148/radiol.10100157]

18 **Menu Y**, Gayet B, Nahum H. Bleeding duodenal varices: diagnosis and treatment by percutaneous portography and transcatheter embolization. *Gastrointest Radiol* 1987; **12**: 111-113 [PMID: 3493935]

19 **Weishaupt D**, Pfammatter T, Hilfiker PR, Wolfensberger U, Marincek B. Detecting bleeding duodenal varices with multislice helical CT. *AJR Am J Roentgenol* 2002; **178**: 399-401 [PMID: 11804902 DOI: 10.2214/ajr.178.2.1780399]

20 **Soga K**, Tomikashi K, Miyawaki K, Okuda K, Sugiyama Y, Sekikawa S, Wakabayashi N, Konishi H, Mitsufuji S, Kataoka K, Yoshikawa T. Endoscopic injection sclerotherapy with ethanolamine oleate with iopamidol for esophagojejunal varices in idiopathic portal hypertension. *Dig Dis Sci* 2009; **54**: 1592-1596 [PMID: 18810636 DOI: 10.1007/s10620-008-0505-6]

21 **Almadi MA**, Almessabi A, Wong P, Ghali PM, Barkun A. Ectopic varices. *Gastrointest Endosc* 2011; **74**: 380-388 [PMID: 21612777 DOI: 10.1016/j.gie.2011.03.1177]

22 **Gubler C**, Glenck M, Pfammatter T, Bauerfeind P. Successful treatment of anastomotic jejunal varices with N-butyl-2-cyanoacrylate (Histoacryl): single-center experience. *Endoscopy* 2012; **44**: 776-779 [PMID: 22833023 DOI: 10.1055/s-0032-1309834]

23 **Smith-Laing G**, Scott J, Long RG, Dick R, Sherlock S. Role of percutaneous transhepatic obliteration of varices in the management of hemorrhage from gastroesophageal varices. *Gastroenterology* 1981; **80**: 1031-1036 [PMID: 7009311]

24 **Norton ID**, Andrews JC, Kamath PS. Management of ectopic varices. *Hepatology* 1998; **28**: 1154-1158 [PMID: 9755256 DOI: 10.1002/hep.510280434]

25 **Dahlbäck B**. Advances in understanding pathogenic mechanisms of thrombophilic disorders. *Blood* 2008; **112**: 19-27 [PMID: 18574041 DOI: 10.1182/blood-2008-01-077909]

P- Reviewer: Dina I, Lin HC, Wang SJ **S- Editor**: Qi Y
L- Editor: Wang TQ **E- Editor**: Zhang DN

World Journal of Gastroenterology

Submit a Manuscript: http://www.wjgnet.com/esps/
Help Desk: http://www.wjgnet.com/esps/helpdesk.aspx
DOI: 10.3748/wjg.v21.i3.1028

World J Gastroenterol 2015 January 21; 21(3): 1028-1031
ISSN 1007-9327 (print) ISSN 2219-2840 (online)

CASE REPORT

Focal nodular hyperplasia coexistent with hepatoblastoma in a 36-d-old infant

Ying Gong, Lian Chen, Zhong-Wei Qiao, Yang-Yang Ma

Ying Gong, Zhong-Wei Qiao, Department of Radiology, Children's Hospital of Fudan University, Shanghai 201102, China
Lian Chen, Yang-Yang Ma, Department of Pathology, Children's Hospital of Fudan University, Shanghai 201102, China
Author contributions: Gong Y and Qiao ZW analyzed the CT imaging and wrote the paper; Chen L and Ma YY contributed to the interpretation of histopathologic data.
Supported by National Key Clinical Specialty Construction Programs of China (2014-2016); and Medical Guide Project of Shanghai Municipal Science and Technology Commission, No. 134119a4100 (to Qiao ZW).

Correspondence to: Zhong-Wei Qiao, MD, PhD, Department of Radiology, Children's Hospital of Fudan University, 399 WanYuan Road, Shanghai 201102, China. zqiao@fudan.edu.cn
Telephone: +86-21-64931802
Fax: +86-21-64931901
Received: April 26, 2014
Peer-review started: April 30, 2014
First decision: June 10, 2014
Revised: July 3, 2014
Accepted: September 5, 2014
Article in press: September 5, 2014
Published online: January 21, 2015

Abstract

Focal nodular hyperplasia (FNH) is a benign hepatic tumor characterized by hepatocyte hyperplasia and a central stellate scar. The association of FNH with other hepatic lesions, such as adenomas, hemangiomas and hepatocellular carcinoma, has been previously reported, but FNH associated with another hepatic tumor is rare in infants. Here we report a case of FNH coexistent with hepatoblastoma in a 36-d-old girl. Computed tomography (CT) imaging showed an ill-delineated, inhomogeneous enhanced mass with a central star-like scar in the right lobe of the liver. The tumor showed early mild enhancement at the arterial phase (from 40HU without contrast to 52HU at the arterial phase), intense enhancement at the portal phase (87.7HU) and 98.1HU in the 3-min delay scan. A central scar in the tumor presented as low density on non-contrast CT and slightly enhanced at delayed contrast-enhanced scanning. This infant underwent surgical resection of the tumor. Histopathology demonstrated typical FNH coexistent with a focal hepatoblastoma, which showed epithelioid tumor cells separated by proliferated fibrous tissue.

Key words: Focal nodular hyperplasia; Hepatoblastoma; Infant; Computed tomography

Core tip: Focal nodular hyperplasia (FNH) is infrequent in infants, and hepatoblastoma is the most common primary malignant liver tumor in infants. The case reported here was a 36-d-old girl suffering from FNH coexistent with hepatoblastoma. Computed tomography imaging showed an ill-delineated, inhomogeneous enhanced mass with a central star-like scar in the right lobe of the liver. The patient underwent surgical resection of the tumor, and histopathology demonstrated typical FNH coexistent with a focal hepatoblastoma.

Gong Y, Chen L, Qiao ZW, Ma YY. Focal nodular hyperplasia coexistent with hepatoblastoma in a 36-d-old infant. *World J Gastroenterol* 2015; 21(3): 1028-1031 Available from: URL: http://www.wjgnet.com/1007-9327/full/v21/i3/1028.htm DOI: http://dx.doi.org/10.3748/wjg.v21.i3.1028

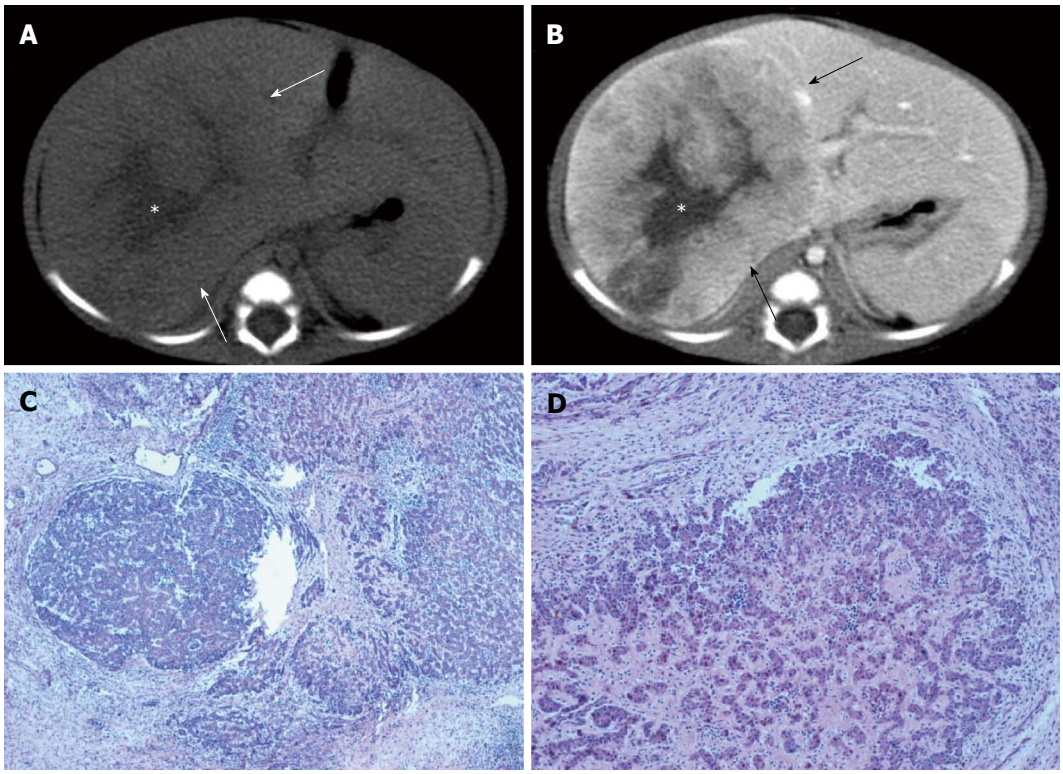

Figure 1 Computed tomography findings. A: Non-contrast computed tomography (CT) of the liver showed a slightly hypo-dense mass in the right lobe of the liver (arrow) with a hypo-dense central star-like scar (asterisk); B: Contrast-enhanced CT of the liver in the portal venous phase showed inhomogeneous and intense enhancement of the mass (arrow), with the central star-like scar (asterisk); C: Histopathology showed typical focal nodular hyperplasia, with hepatocytic nodules separated by bands of fibrous tissue (HE stain, original magnification × 50); D: Foci of hepatoblastoma showed epithelioid tumor cells separated by proliferated fibrous tissue (HE stain, original magnification × 100).

INTRODUCTION

Focal nodular hyperplasia (FNH) is a benign liver tumor, often asymptomatic and discovered incidentally[1,2]. Although FNH can be found at any age, it is rare in children, and comprises only 2% of all pediatric liver tumors[3]. There have been various reports on the association between FNH and other hepatic lesions, such as hepatocellular adenomas[4], hemangiomas[5], hepatocellular carcinoma[6] and metastases[7]. We herein report a case of FNH associated with hepatoblastoma in a 36-d-old female infant. To the best of our knowledge, only one case of FNH complicated by hepatoblastoma has been reported in a 4-year-old boy after treatment of stage IV neuroblastoma[8].

CASE REPORT

A 36-d-old girl presented to the hospital with a history of jaundice. Physical examination revealed a palpable solid mass fixed on the right quarter of the abdomen approximately 7 cm × 8 cm × 8 cm in diameter. The baby was full-term and delivered normally without asphyxia. Her mother had a history of progesterone administration before and in the early stages of pregnancy.

Sonography revealed a huge uneven hypo-echoic mass in the right lobe of the liver. Computed tomography (CT) imaging showed an ill-delineated, inhomogeneous enhanced mass with a central star-like scar in right lobe of the liver (Figure 1A, B). The tumor showed early mild enhancement at the arterial phase (from 40HU without contrast to 52HU at the arterial phase), intense enhancement at the portal phase (87.7HU) and 98.1HU in the 3-min delay scan, with slight enhancement of the central scar.

Laboratory evaluations included serum total bilirubin (TBIL) 93.1 μmol/L (normal 5.1-17.1 μmol/L), direct bilirubin (DBIL) 42.6 μmol/L (normal 0-6 μmol/L) and an alpha-fetoprotein (AFP) level of 74390 ng/mL (normal 0-77 ng/mL). Serum markers for both hepatitis B and hepatitis C virus were negative.

The infant underwent surgical resection of the tumor. The histopathology demonstrated FNH coexistent with hepatoblastoma (Figure 1C and D).

DISCUSSION

Up to 75% of pediatric liver tumors are malignant[9], and FNH constitutes 5% of benign liver tumors in children[10]. Although FNH is found at any age, even in newborn[11,12], it is rare in children, and two age peaks have been described, around 6 years and 18 years[10].

The pathogenesis of FNH is not well understood[2,13-15]. The most widely accepted theory is that FNH is the result of congenital or acquired vascular abnormalities[14,15]. Numerous studies have reported an increased incidence of

FNH in long-term survivors of childhood malignancies or following hematopoietic stem cell transplantation[8,14-17]. It was thought that FNH was a complication of chemotherapy or radiation therapy in these patients[15].

The features of FNH on MRI and CT include homogeneity, arterial phase enhancement suggestive of hypervascularity, a lack of lesion capsule, and the presence of a central scar[15,18]. Ultrasound, CT, and especially MRI have proven effective at distinguishing FNH from other benign and malignant lesions in adults. In children, due to its infrequency and more variable imaging features, the accuracy of radiologic diagnosis of FNH is challenging. Atypical or variable radiologic features such as absence or non-enhancement of the central scar may be more common in children than adults[9]. Atypical features make it difficult to differentiate FNH from other benign or malignant lesions, including hepatic adenoma, hemangioma or infantile hemangioendothelioma, hepatoblastoma, and hepatocellular carcinoma.

Although there is no evidence in the literature of malignant degeneration of FNH, there are several reports of FNH occurring simultaneously with malignant neoplasms[6-9]. Gutweiler *et al*[8] described a case of hepatoblastoma concomitant with FNH after treatment of neuroblastoma in a 4-year-old boy. Similarly, Lautz *et al*[9] described a patient with hepatocellular carcinoma and concomitant FNH with a history of neuroblastoma. At present, most children with FNH should continue to undergo surgical resection due to symptoms, increasing size, or inability to confidently rule out malignancies[9].

COMMENTS

Case characteristics

A 36-d-old girl presented to the hospital with a history of jaundice.

Clinical diagnosis

Physical examination revealed a palpable solid mass fixed on the right quarter of the abdomen.

Differential diagnosis

Hepatoblastoma, hemangioma or infantile hemangioendothelioma.

Laboratory diagnosis

Serum level of total bilirubin was 93.1 umol/L, direct bilirubin was 42.6 μmol/L, and alpha-fetoprotein level was 74390 ng/mL.

Imaging diagnosis

Sonography and computed tomography (CT) imaging revealed a mass in the right lobe of the liver. The tumor showed early mild enhancement at the arterial phase, intense enhancement at the portal phase and slight enhancement of the central scar in the 3-min delay scan.

Pathological diagnosis

Histopathology demonstrated typical focal nodular hyperplasia (FNH) coexistent with a focal hepatoblastoma.

Treatment

The infant underwent surgical resection of the tumor.

Related reports

There are several reports of FNH occurring in children after treatment of malignant neoplasms. However, no cases of FNH and hepatoblastoma have been reported in infants.

Experiences and lessons

Hepatoblastoma is more common in infants than FNH. The tumor in this infant showed a typical central scar on CT imaging, and histopathology confirmed FNH coexistent with a focal hepatoblastoma.

Peer review

FNH coexistent with a focal hepatoblastoma is rare in infants. The dynamic CT images in this infant are helpful to diagnose FNH in the liver, but it is challenging to confirm a coexistent focal hepatoblastoma.

REFERENCES

1 **Finch MD**, Crosbie JL, Currie E, Garden OJ. An 8-year experience of hepatic resection: indications and outcome. *Br J Surg* 1998; **85**: 315-319 [PMID: 9529482 DOI: 10.1046/j.1365-2168.1998.00585.x]

2 **Nguyen BN**, Fléjou JF, Terris B, Belghiti J, Degott C. Focal nodular hyperplasia of the liver: a comprehensive pathologic study of 305 lesions and recognition of new histologic forms. *Am J Surg Pathol* 1999; **23**: 1441-1454 [PMID: 10584697 DOI: 10.1097/00000478-199912000-00001]

3 **Reymond D**, Plaschkes J, Lüthy AR, Leibundgut K, Hirt A, Wagner HP. Focal nodular hyperplasia of the liver in children: review of follow-up and outcome. *J Pediatr Surg* 1995; **30**: 1590-1593 [PMID: 8583330 DOI: 10.1016/0022-3468(95)90162-0]

4 **Nagorney DM**. Benign hepatic tumors: focal nodular hyperplasia and hepatocellular adenoma. *World J Surg* 1995; **19**: 13-18 [PMID: 7740799 DOI: 10.1007/bf00316973]

5 **Toshikuni N**, Kawaguchi K, Miki H, Kihara Y, Sawayama T, Yamasaki S, Takano S, Minato T. Focal nodular hyperplasia coexistent with hemangioma and multiple cysts of the liver. *J Gastroenterol* 2001; **36**: 206-211 [PMID: 11291886 DOI: 10.1007/s005350170131]

6 **Zhang SH**, Cong WM, Wu MC. Focal nodular hyperplasia with concomitant hepatocellular carcinoma: a case report and clonal analysis. *J Clin Pathol* 2004; **57**: 556-559 [PMID: 15113871 DOI: 10.1136/jcp.2003.012823]

7 **Nisar PJ**, Zaitoun AM, Damera A, Hodi Z, Tierney GM, Beckingham IJ. Metastatic rectal adenocarcinoma to the liver associated with focal nodular hyperplasia. *J Clin Pathol* 2002; **55**: 967-969 [PMID: 12461070 DOI: 10.1136/jcp.55.12.967]

8 **Gutweiler JR**, Yu DC, Kim HB, Kozakewich HP, Marcus KJ, Shamberger RC, Weldon CB. Hepatoblastoma presenting with focal nodular hyperplasia after treatment of neuroblastoma. *J Pediatr Surg* 2008; **43**: 2297-2300 [PMID: 19040959 DOI: 10.1016/j.jpedsurg.2008.08.069]

9 **Lautz T**, Tantemsapya N, Dzakovic A, Superina R. Focal nodular hyperplasia in children: clinical features and current management practice. *J Pediatr Surg* 2010; **45**: 1797-1803 [PMID: 20850623 DOI: 10.1016/j.jpedsurg.2009.12.027]

10 **Jha P**, Chawla SC, Tavri S, Patel C, Gooding C, Daldrup-Link H. Pediatric liver tumors--a pictorial review. *Eur Radiol* 2009; **19**: 209-219 [PMID: 18682957 DOI: 10.1007/s00330-008-1106-7]

11 **De Luca G**, Zamparelli M, Fadda C, Martone A. Focal nodular hyperplasia of the liver in infancy: a case report. *J Pediatr Surg* 2006; **41**: 456-457 [PMID: 16481271 DOI: 10.1016/j.jpedsurg.2005.11.026]

12 **Kang J**, Choi HJ, Yu E, Hwang I, Kim YM, Cha HJ. A case report of fetal telangiectatic focal nodular hyperplasia. *Pediatr Dev Pathol* 2007; **10**: 416-417 [PMID: 17929986 DOI: 10.2350/06-07-0139]

13 **Ndimbie OK**, Goodman ZD, Chase RL, Ma CK, Lee MW. Hemangiomas with localized nodular proliferation of the liver. A suggestion on the pathogenesis of focal nodular hyperplasia. *Am J Surg Pathol* 1990; **14**: 142-150 [PMID: 2301700 DOI: 10.1097/00000478-199002000-00006]

14 **Kumagai H**, Masuda T, Oikawa H, Endo K, Endo M, Takano T. Focal nodular hyperplasia of the liver: direct evidence of circulatory disturbances. *J Gastroenterol Hepatol* 2000; **15**: 1344-1347 [PMID: 11129233 DOI: 10.1046/j.1440-1746.2000.2354.x]

15 **Towbin AJ**, Luo GG, Yin H, Mo JQ. Focal nodular hyperplasia in children, adolescents, and young adults. *Pediatr Radiol* 2011;

41: 341-349 [PMID: 20949264 DOI: 10.1007/s00247-010-1839-8]
16 **Bouyn CI**, Leclere J, Raimondo G, Le Pointe HD, Couanet D, Valteau-Couanet D, Hartmann O. Hepatic focal nodular hyperplasia in children previously treated for a solid tumor. Incidence, risk factors, and outcome. *Cancer* 2003; **97**: 3107-3113 [PMID: 12784348 DOI: 10.1002/cncr.11452]
17 **Joyner BL**, Levin TL, Goyal RK, Newman B. Focal nodular hyperplasia of the liver: a sequela of tumor therapy. *Pediatr Radiol* 2005; **35**: 1234-1239 [PMID: 16052333 DOI: 10.1007/s00247-005-1558-8]
18 **Cheon JE**, Kim WS, Kim IO, Jang JJ, Seo JK, Yeon KM. Radiological features of focal nodular hyperplasia of the liver in children. *Pediatr Radiol* 1998; **28**: 878-883 [PMID: 9799323 DOI: 10.1007/s002470050487]

P- Reviewer: Chen Y, Otte JB, Tang KF **S- Editor**: Ma YJ
L- Editor: A **E- Editor**: Zhang DN

World Journal of Gastroenterology

Submit a Manuscript: http://www.wjgnet.com/esps/
Help Desk: http://www.wjgnet.com/esps/helpdesk.aspx
DOI: 10.3748/wjg.v21.i3.1032

World J Gastroenterol 2015 January 21; 21(3): 1032-1035
ISSN 1007-9327 (print) ISSN 2219-2840 (online)

CASE REPORT

Gastrotracheal fistula: Treatment with a covered self-expanding Y-shaped metallic stent

Fei Wang, Hong Yu, Ming-Hui Zhu, Quan-Peng Li, Xian-Xiu Ge, Jun-Jie Nie, Lin Miao

Fei Wang, Hong Yu, Quan-Peng Li, Xian-Xiu Ge, Jun-Jie Nie, Lin Miao, Institute of Digestive Endoscopy and Medical Center for Digestive Diseases, Second Affiliated Hospital of Nanjing Medical University, Nanjing 210011, Jiangsu Province, China
Ming-Hui Zhu, Department of Gastroenterology, People's Hospital of Jingjiang, Taizhou 214500, Jiangsu Province, China
Author contributions: Wang F and Yu H contributed equally to this work; all the authors contributed to this article.

Correspondence to: Lin Miao, MD, Institute of Digestive Endoscopy and Medical Center for Digestive Diseases, Second Affiliated Hospital of Nanjing Medical University, 121 Jiangjiayuan, Nanjing 210011, Jiangsu Province, China. miaofrest@163.com
Telephone: +86-25-58509932
Fax: +86-25-58509931
Received: April 25, 2014
Peer-review started: April 27, 2014
First decision: May 29, 2014
Revised: June 27, 2014
Accepted: July 24, 2014
Article in press: July 25, 2014
Published online: January 21, 2015

Abstract

A 67-year-old man had a sev-ere cough and pulmonary infection for 1 wk before seeking evaluation at our hospital. He had undergone esophagectomy with gastric pull-up and radiotherapy for esophageal cancer 3 years previously. After admission to our hospital, gastroscopy and bronchoscopy revealed a fistulous communication between the posterior tracheal wall near the carina and the upper residual stomach. We measured the diameter of the trachea and bronchus and determined the site and size of the fistula using multislice computed tomography and gastroscopy. A covered self-expanding Y-shaped metallic stent was implanted into the trachea and bronchus. Subsequently, the fistula was closed completely. The patient tolerated the stent well and had good palliation of his symptoms.

Key words: Gastrotracheal fistula; Y-shaped metallic stent; Esophageal cancer; Gastroesophageal surgery

Core tip: Gastrotracheal fistula (GTF), the fistula between the tracheobronchial tree and stomach after gastric pull-up surgery, is an extremely rare complication of esophagectomy and the condition is life-threatening. For these patients, the goal of therapy is palliative rather than curative. During the past decade, metallic airway stents have been used in patients with GTFs. However, fistulas close to the carina often require the placement of Y-shaped stents for successful palliation. We report a patient post-esophagectomy with a GTF near the carina that was successfully treated with a covered self-expanding Y-shaped metallic stent.

Wang F, Yu H, Zhu MH, Li QP, Ge XX, Nie JJ, Miao L. Gastrotracheal fistula: Treatment with a covered self-expanding Y-shaped metallic stent. *World J Gastroenterol* 2015; 21(3): 1032-1035 Available from: URL: http://www.wjgnet.com/1007-9327/full/v21/i3/1032.htm DOI: http://dx.doi.org/10.3748/wjg.v21.i3.1032

INTRODUCTION

A gastrotracheal fistula (GTF), the fistula between the tracheobronchial tree and stomach after gastric

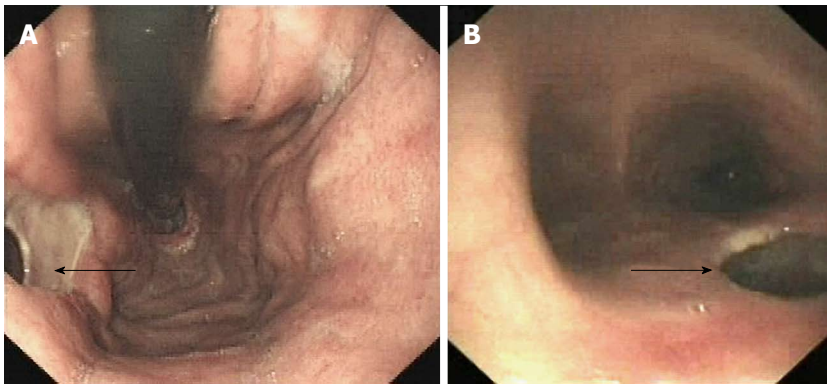

Figure 1 Gastroscopy revealed a fistula (arrow, A) in the upper body of the stomach, bronchoscopy confirmed the presence of a fistula (arrow, B) in the lower trachea near the carina.

pull-up surgery, is an extremely rare complication of esophagectomy and the condition is life-threatening[1]. If a malignant GTF is untreated, the patient will suffer continued tracheobronchial soilage, develop pulmonary sepsis rapidly and die. The average survival of patients with this complication is 1-6 wk with supportive care alone[2]. For these patients, the goal of therapy is palliative rather than curative. During the past decade, metallic airway stents, such as covered self-expandable metal stents (SEMS), have been used in patients with GTFs. Various studies[3,4] involving the use of covered SEMSs or partially covered SEMSs for malignant fistulas have proved that 87%-91% of patients acquire successful fistula closure. Inserting a covered metallic airway stent into the trachea or bronchus has proven to be an effective method to seal off the fistula[5]. However, fistulas close to the carina often require the placement of Y-shaped stents for successful palliation[6]. We report a patient post-esophagectomy with a GTF near the carina that was successfully treated with a covered self-expanding Y-shaped metallic stent.

CASE REPORT

A 67-year-old man had a severe cough and pulmonary infection for 1 wk before admission to our hospital. He had undergone esophagectomy with a gastric pull-up and radiotherapy for esophageal cancer 3 years previously. After admission to our hospital, gastroscopy revealed a fistula in the upper body of the stomach (Figure 1A) and bronchoscopy confirmed the presence of a fistula in the lower trachea near the carina (Figure 1B). We measured the diameter of the trachea and bronchus and determined the site and size of the fistula using multislice computed tomography (CT) and gastroscopy. A covered self-expanding Y-shaped metallic stent (body, 30 mm × 70 mm; right limb, 14 mm × 30 mm; left limb, 18 mm × 40 mm, Changzhou New District Garson Medical Stent Apparatus Co., Ltd, Changzhou, Jiangsu province, China) was implanted into the trachea and bronchus. Stent insertion was performed fluoroscopically, controlled by flexible bronchoscopy under general anesthesia and jet ventilation. Correct placement was ensured by inserting 2 guide wires in both main bronchi. The 2 bronchial arms of the Y-stent were introduced over the 2 guide wires. Utmost care was taken that these wires did not cross inside the trachea but ran parallel when introducing the stent over these wires. After both bronchial arms opened completely, the tracheal part was released. Subsequently, the fistula was closed completely. After stent placement, gastroscopy (Figure 2A) and bronchoscopy (Figure 2B) confirmed that the Y-stent tightly sealed the fistula. Fluoroscopy also revealed correct placement of the stent (Figure 3). The patient tolerated the stent well and the cough and pulmonary infection improved after the stent placement. However, he died of disease progression with a patent stent 1 mo later.

DISCUSSION

GTF is an extremely rare complication and can most often be observed after gastroesophageal surgery[1]. GTF may develop because of dissection injury or post-operative mediastinitis in the early post-operative period. GTF occurring in the late post-operative period is most often due to tumor recurrence, radiation necrosis and tracheobronchial erosion along the gastric staple-line[7]. CT scanning can demonstrate the defect between the trachea and the residual stomach. Bronchoscopy and gastroscopy are helpful for the identification and localization of the fistula.

The treatment options for GTF include surgery, external drainage and endoscopic treatment. Surgical repair of the fistula, which includes tracheal resection, lower lobectomy or creation of a muscle flap, may impose an excessive burden on a debilitated patient[2]. Therefore, the use of covered metallic stents is a good choice in the palliative treatment of these patients. Recently, Han *et al*[8] reported that metallic stent placement for tracheobronchial diseases was technically successful in 96% of patients, with 85% of patients presenting with symptom improvement 1-7 d after stent placement. Furthermore, for the patient with a thermic effect of feeding (TEF), maintaining sufficient ventilation is

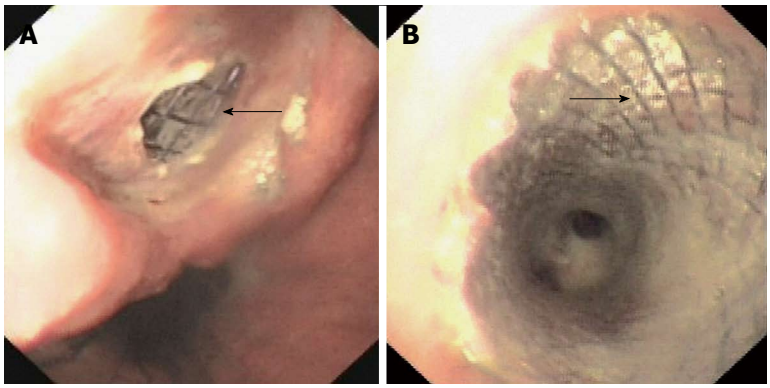

Figure 2 Gastroscopy confirmed that the Y-stent tightly sealed the fistula (arrow, A), bronchoscopy confirmed that the Y-stent tightly sealed the fistula (arrow, B).

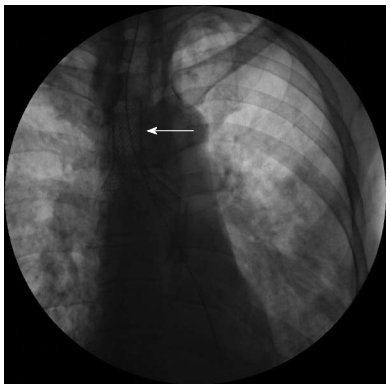

Figure 3 Fluoroscopy image. Fluoroscopy revealed the correct placement of the stent (arrow).

difficult. Passing the fistula with the bronchoscope and ventilating the patient through the bronchoscope lying distally to the fistula is usually possible without problems in a high TEF. However, in a fistula at the level of the tracheal bifurcation or near the carina, it is not feasible. Thus, jet ventilation is necessary. In our case, stent insertion was performed under general anesthesia with jet ventilation.

However, choosing a stent that will fully cover the fistula and allow sufficient tolerance compression is very important for successful stenting. For the patient described herein, the replaced stomach showed a large lumen compared with the lumen of the original esophagus. Therefore, esophageal stenting was not feasible. After consultation with specialists, we chose the covered self-expanding Y-shaped metallic stent.

The self-expanding Y-shaped metallic stents not only cover the fistula, but also have lower rates of migration because they imitate the bifurcation and attach to the main carina[9]. When the metallic stent is in place, it can expand to fill the space between the stent and the mucosa. The flexibility and radial force enable stents to fit the contours of the trachea or bronchus and make stents well-suited to prevent luminal contents from leaking[4].

However, metallic stents are not as effective against neoplasms and proliferating granulation tissue. One of the Y stent-related complications is the retention of secretions because the cilia cannot function when a covered metal stent is in place. Prevention of these stent-related complications remains one of the major challenges for developing new stent designs.

GTF is a rare but serious complication which is most often encountered after gastroesophageal surgery. The implantation of a covered self-expanding Y-shaped metallic stent proved to be an effective treatment for a GTF.

COMMENTS

Case characteristics

A 67-year-old man had a severe cough and pulmonary infection for 1 wk before seeking evaluation at our hospital.

Clinical diagnosis

He had undergone esophagectomy with gastric pull-up and radiotherapy for esophageal cancer 3 years previously. After admission to the hospital, gastroscopy and bronchoscopy revealed a fistulous communication between the posterior tracheal wall near the carina and the upper residual stomach.

Imaging diagnosis

The authors measured the diameter of the trachea and bronchus and determined the site and size of the fistula using multislice computed tomography and gastroscopy.

Treatment

A covered self-expanding Y-shaped metallic stent was implanted into the trachea and bronchus. Subsequently, the fistula was closed completely.

Experiences and lessons

The patient tolerated the stent well and had good palliation of his symptoms.

Peer review

In this article, the authors describe the case of a 67-year-old man with a gastrotracheal fistula after an esophagectomy with gastric pull-up, which was conservatively treated by the bronchoscopic placement of a covered self-expanding Y stent.

REFERENCES

1 **Marty-Ané CH**, Prudhome M, Fabre JM, Domergue J, Balmes M, Mary H. Tracheoesophagogastric anastomosis fistula: a rare complication of esophagectomy. *Ann Thorac Surg* 1995; **60**: 690-693 [PMID: 7677505 DOI: 10.1016/0003-4975(95)00284-R]

2 **Reed MF**, Mathisen DJ. Tracheoesophageal fistula. *Chest Surg Clin N Am* 2003; **13**: 271-289 [PMID: 12755313 DOI:

10.1016/S1052-3359(03)00030-9]
3 **May A**, Ell C. Palliative treatment of malignant esophagorespiratory fistulas with Gianturco-Z stents. A prospective clinical trial and review of the literature on covered metal stents. *Am J Gastroenterol* 1998; **93**: 532-535 [PMID: 9576443 DOI: 10.1016/S0002-9270(98)00037-9]
4 **Ross WA**, Alkassab F, Lynch PM, Ayers GD, Ajani J, Lee JH, Bismar M. Evolving role of self-expanding metal stents in the treatment of malignant dysphagia and fistulas. *Gastrointest Endosc* 2007; **65**: 70-76 [PMID: 17185082 DOI: 10.1016/j.gie.2006.04.040]
5 **Li YD**, Li MH, Han XW, Wu G, Li WB. Gastrotracheal and gastrobronchial fistulas: management with covered expandable metallic stents. *J Vasc Interv Radiol* 2006; **17**: 1649-1656 [PMID: 17057007 DOI: 10.1097/01.RVI.0000236609.33842.50]
6 **Hürtgen M**, Herber SC. Treatment of malignant tracheoesophageal fistula. *Thorac Surg Clin* 2014; **24**: 117-127 [PMID: 24295667 DOI: 10.1016/j.thorsurg.2013.09.006]
7 **Bennie MJ**, Sabharwal T, Dussek J, Adam A. Bronchogastric fistula successfully treated with the insertion of a covered bronchial stent. *Eur Radiol* 2003; **13**: 2222-2225 [PMID: 12928968 DOI: 10.1007/s00330-002-1698-2]
8 **Han XW**, Wu G, Li YD, Zhang QX, Guan S, Ma N, Ma J. Overcoming the delivery limitation: results of an approach to implanting an integrated self-expanding Y-shaped metallic stent in the carina. *J Vasc Interv Radiol* 2008; **19**: 742-747 [PMID: 18440464 DOI: 10.1016/j.jvir.2008.01.022]
9 **Gompelmann D**, Eberhardt R, Schuhmann M, Heussel CP, Herth FJ. Self-expanding Y stents in the treatment of central airway stenosis: a retrospective analysis. *Ther Adv Respir Dis* 2013; **7**: 255-263 [PMID: 23823488 DOI: 10.1177/1753465813489766]

P- Reviewer: Konishi T, Melloni G, Petronella P
S- Editor: Gou SX **L- Editor**: Roemmele A **E- Editor**: Liu XM

World Journal of Gastroenterology

Submit a Manuscript: http://www.wjgnet.com/esps/
Help Desk: http://www.wjgnet.com/esps/helpdesk.aspx
DOI: 10.3748/wjg.v21.i3.1036

World J Gastroenterol 2015 January 21; 21(3): 1036-1039
ISSN 1007-9327 (print) ISSN 2219-2840 (online)

CASE REPORT

Primary pancreatic paraganglioma: A report of two cases and literature review

Lei Meng, Jin Wang, Song-Hua Fang

Lei Meng, Song-Hua Fang, Department of Radiology, Sir Run Run Shaw Hospital, Sir Run Run Shaw Institute of Clinical Medicine of Zhejiang University, Hangzhou 310016, Zhejiang Province, China
Jin Wang, Department of Pathology, Sir Run Run Shaw Hospital, Sir Run Run Shaw Institute of Clinical Medicine of Zhejiang University, Hangzhou 310016, Zhejiang Province, China
Author contributions: Fang SH designed research; Meng L performed research and wrote the paper; and Wang J performed pathological and immunohistochemical examinations.

Correspondence to: Song-Hua Fang, Chief Physician, Department of Radiology, Sir Run Run Shaw Hospital, Sir Run Run Shaw Institute of Clinical Medicine of Zhejiang University, 3 East Qingchun Road, Hangzhou 310016, Zhejiang Province, China. fangsonghua@163.com
Telephone: +86-571-86006762
Fax: +86-571-86044822
Received: April 26, 2014
Peer-review started: April 27, 2014
First decision: May 29, 2014
Revised: June 23, 2014
Accepted: July 24, 2014
Article in press: July 25, 2014
Published online: January 21, 2015

Abstract

Paraganglioma is a rare tumor of paraganglia, derived from neural crest cells in sympathetic or parasympathetic ganglions. Primary paraganglioma originating from the pancreas is rare. We report two patients with paraganglioma in the head of the pancreas, in whom computed tomography showed a sharply marginated, hypervascular tumor with cystic areas. Significant intratumoral vessels and early contrast filling of the draining veins from the mass were not found. Although the pancreatic paraganglioma was located at the pancreatic head, the bile ducts often revealed no dilation, and sometimes the main pancreatic duct was mildly dilated. These findings are helpful in differentiating pancreatic paraganglioma from other pancreatic neoplasms. It is often difficult to distinguish between nonfunctional pancreatic paragangliomas and pancreatic endocrine tumors. In many reports,pancreatic paragangliomas show the retroperitoneal extension of a paraganglioma into the pancreas rather than a true pancreatic neoplasm. In surgical treatment, we could select simple excision of the tumor rather than radical surgery.

Key words: Paraganglioma; Pancreas; X-ray tomography; Computed tomography

Core tip: Primary paraganglioma that arises in the pancreas is rare. We herein present two pathologically proven cases of pancreatic paraganglioma, retrospectively analyze their clinical and imaging features, and review the literature.

Meng L, Wang J, Fang SH. Primary pancreatic paraganglioma: A report of two cases and literature review. *World J Gastroenterol* 2015; 21(3): 1036-1039 Available from: URL: http://www.wjgnet.com/1007-9327/full/v21/i3/1036.htm DOI: http://dx.doi.org/10.3748/wjg.v21.i3.1036

INTRODUCTION

Paraganglioma is a rare tumor of paraganglia, derived from neural crest cells in sympathetic or parasympathetic ganglions[1,2]. Intra-adrenal paraganglioma is found

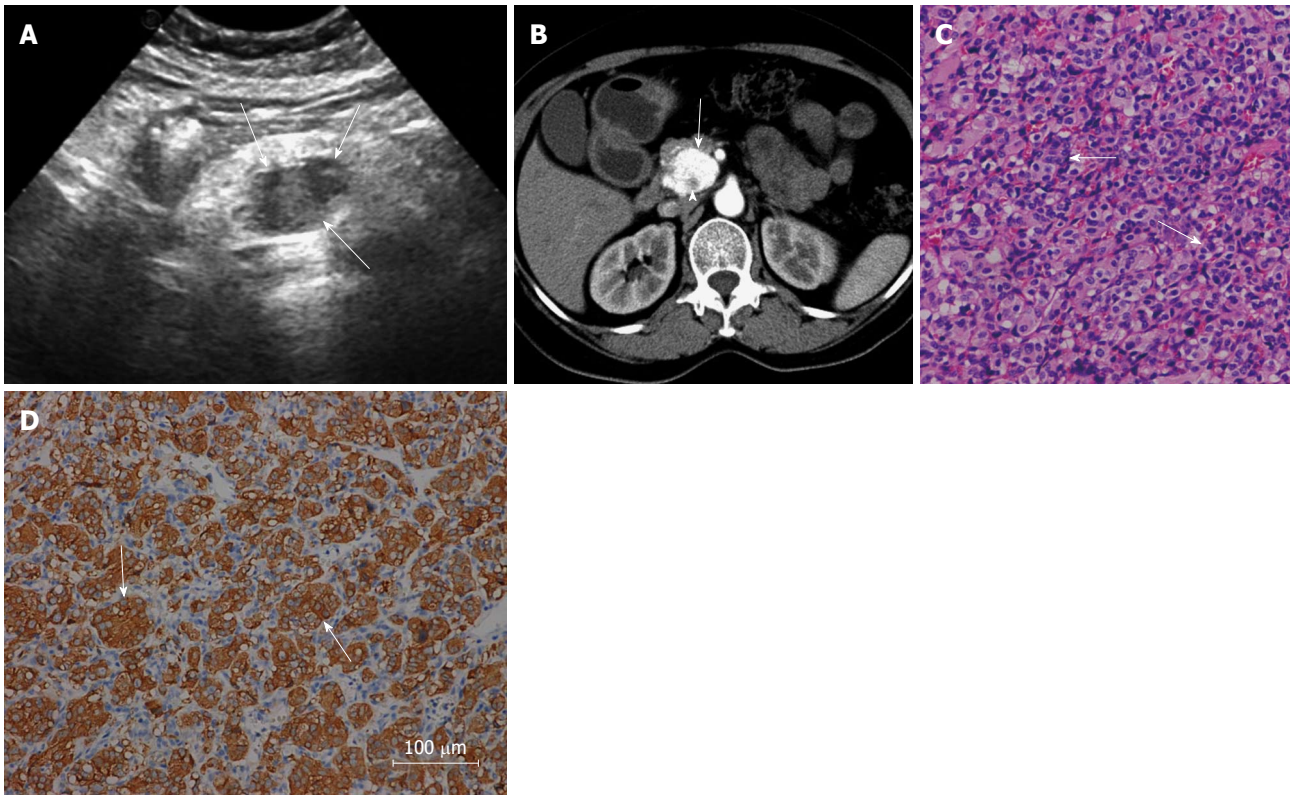

Figure 1 Fifty-four-year-old woman felt left upper abdominal pain for 20 d. A: Ultrasonography revealed an ill-defined hypoechoic mass in the pancreatic head (arrows); B: On contrast-enhanced computed tomography, the mass (arrow) in the pancreatic head was found with heterogeneous marked enhancement in the arterial phase, while non-enhancing patchy areas were seen in the tumor (arrowhead); C: Microscopically, the chief cells had round or ovoid nuclei (arrows), arranged in nest-like structures with dilated capillary intervals (hematoxylin-eosin; original magnification, 200 ×); D: Immunohistochemical study revealed positive staining for synaptophysin (200 ×).

mainly in the adrenal medulla, and extra-adrenal paraganglioma is located in the head, neck, mediastinum and retroperitoneum. Primary paraganglioma that arises in the pancreas is rare[3].

CASE REPORT

Case 1

A 54-year-old woman felt left upper abdominal pain for 20 d. She denied obvious symptoms of gastric bleeding and vomiting. Blood tests and blood pressure were normal. On medical examination, no mass of upper abdomen was palpated. Her abdomen was soft without tenderness and jaundice.

She underwent upper abdominal ultrasound, which showed an ill-defined hypoechoic mass in the pancreatic head (Figure 1A). The mass measured 2.6 cm × 2.3 cm, and the blood flow signal was plentiful. Unenhanced computed tomography (CT) revealed a poor-defined isodense mass in the head of the pancreas. On contrast-enhanced CT, the mass in the pancreatic head was found with heterogeneous striking enhancement during the arterial phase (Figure 1B), while non-enhancing patchy areas were seen in the tumor (Figure 1B). During the venous phase, the same mass was well-defined with homogeneous marked enhancement. No invasion of the adjacent organs was seen around the pancreas. Intraoperatively, a well-defined mass, 3 cm × 2.5 cm, was found with a rich supply of blood and soft texture in the pancreatic head.

Gross pathological examination revealed an encapsulated mass from the pancreas, 3 cm × 2.5 cm, with gray-red soft tissue and moderate texture. Microscopically, the tumor showed round or polygonal cells with rich cytoplasm on the hematoxylin-eosin-stained tissue sections. The tumor cells had round or ovoid nuclei (Figure 1C), arranged in nest-like structure with dilated capillary intervals. Immunohistochemical study revealed positive staining for S-100, cytokeratin (CK), non-specific enolase (NSE), CgA and Syn (Figure 1D), but negative reactions to CD34, CD117, DOG, SMA, Des and HMB47. The tumors were finally diagnosed as primary pancreatic paraganglioma.

Case 2

A 41-year-old woman was found to have an upper abdominal mass incidentally on ultrasound examination 6 d earlier. She denied obvious symptoms of gastric bleeding and abdominal discomfort. Blood tests and liver and renal functions were normal. On medical examination, no mass of upper abdomen was palpated. Her abdomen was soft without tenderness and jaundice. She had no acute pain, and her signs of life were normal.

On ultrasound examination, she was found to have a

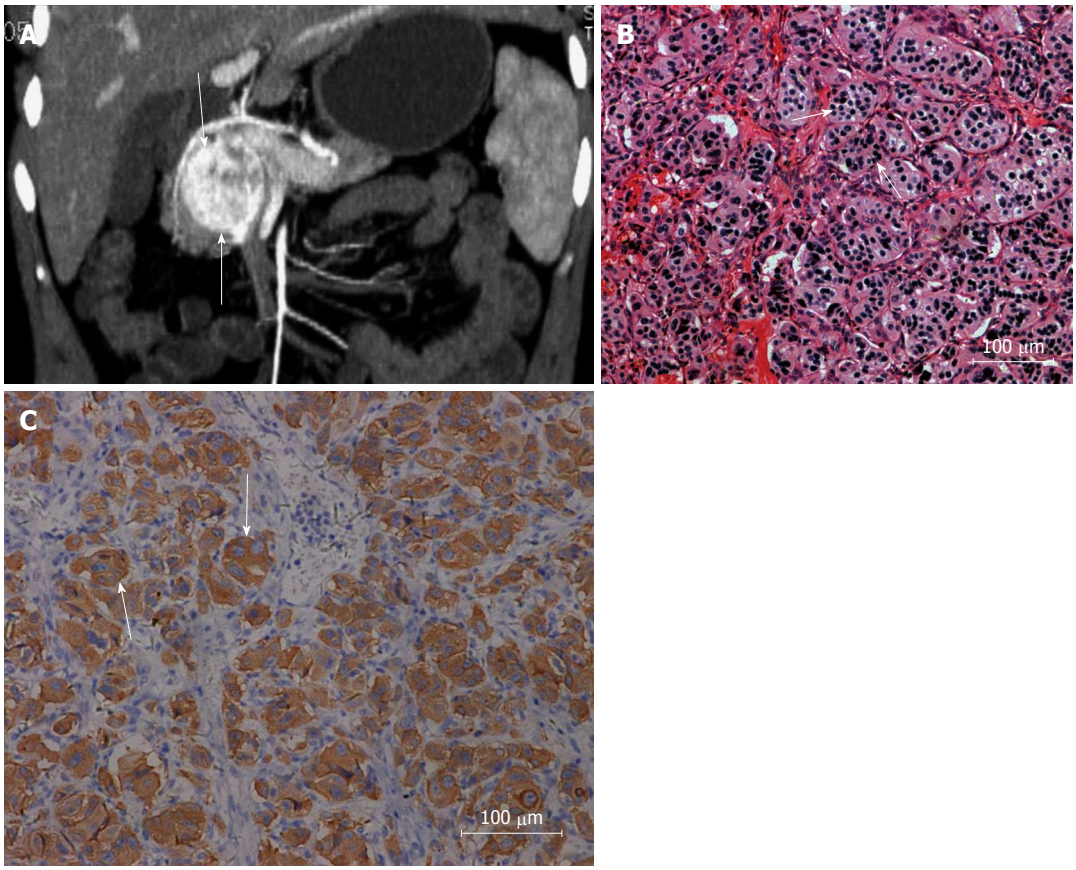

Figure 2 Forty-one-year-old woman was found to have an upper abdominal mass on ultrasound examination 6 d earlier. A: On coronal reconstruction imaging, a well-demarcated mass (arrows) was found with marked enhancement in the arterial phase after contrast enhancement; B: Under microscopic examination, a few cells had large nuclei with hyperchromatism and pink cytoplasm, arranged in organ-like or nest-like structures (arrows) (hematoxylin-eosin; original magnification, 200 ×); C: Immunohistochemistry showed positive staining for synaptophysin (200 ×).

well-demarcated hypoechoic mass in the pancreatic head with homogeneous echo of other pancreatic tissues. The mass measured 6.2 cm × 4.4 cm × 4.5 cm, and some blood flow signal was seen. The diameter of the main pancreatic duct was 0.73 cm and the diameter of the common bile duct was 0.46 cm.

Unenhanced CT revealed a poor-defined mass in the pancreatic head with low and heterogeneous density. On contrast-enhanced CT, a well-demarcated mass in the head of the pancreas, 4.2 cm × 4 cm, was found with marked enhancement (Figure 2A), while some patchy areas were not enhanced. The main pancreatic duct was mildly dilated.

Intraoperatively, a mass measuring 6 cm × 5 cm with well-demarcated margins was found in the pancreatic head without infiltration of the adjacent organs and blood vessels. The main pancreatic duct was dilated with a diameter of 0.4 cm. No significant lymph nodes were seen around the pancreas.

Gross pathological examination revealed a well-defined mass from the pancreas, 4 cm × 4 cm, with gray-yellow soft tissue and hard texture. Under microscopic examination, the tumor cell nuclei were round or ovoid. Nuclear staining was deeper in some areas. A few cells had large nuclei with hyperchromatism and pink cytoplasm, arranged in organ-like or nest-like structures (Figure 2B). The stroma was rich in capillaries.

Immunohistochemistry showed S-100, CK, NSE, CgA and Syn positivity (Figure 2C). Insulin,somatostatin and glucagon were negative. At last, the tumors were diagnosed as primary paraganglioma arising from the pancreas.

DISCUSSION

The paraganglion system is composed of numerous neuroepithelial cells (chief cells). There are many neuronal secretion granules with catecholamines in the cytoplasm. Microscopically, the chief cells are surrounded by the sustentacular cells, arranged in nest-like structures (cell balls). Intra-adrenal paraganglioma is mainly present in the adrenal medulla as pheochromocytoma. Extra-adrenal paraganglioma is divided into two major categories. One type is chemodectoma, which is located in the parasympathetic nervous system in the head, neck or mediastinum, and is non-chromaffin. The other type is ectopic pheochromocytoma, which is located in the sympathetic nervous system in the retroperitoneum or along the aorta, and contains chromaffin.

Primary paraganglioma that arises in the pancreas

is rare. It is characterized on imaging features as sharply marginated, hypervascular tumor with cystic areas;the latter reveals necrotic or cystic change. Our two pathologically proven cases were in accordance with the above imaging features. Kim *et al*[3] reported a well-defined, extremely hypervascular pancreatic paraganglioma with significant intratumoral vessels and early contrast filling of the draining veins from the mass. In our two cases, these imaging characteristics were not found.

Although the pancreatic paraganglioma is located at the pancreatic head, the bile ducts often reveal no dilation, and sometimes the main pancreatic duct is mildly dilated. The CT findings are different from those of pancreatic carcinoma, which is usually characterized as a mild to moderate enhanced tumor with prominent dilation of the biliary and pancreatic ducts, as well as retroperitoneal invasion[4]. Clinically, functional pancreatic endocrine tumor is usually < 3 cm, with striking and homogenous enhancement in the arterial phase. The diameter of nonfunctional pancreatic endocrine tumor is usually > 5 cm. The tumor always has necrosis, cystic change or calcification, so it shows heterogeneous or ring-liked enhancement[5]. It is often difficult to distinguish between nonfunctional pancreatic paragangliomas and pancreatic endocrine tumors. In many reports, pancreatic paragangliomas show the retroperitoneal extension of a paraganglioma into the pancreas rather than a true pancreatic neoplasm[6]. In relation to surgical treatment, the prognosis is equally good for simple excision of the tumor and radical surgery such as pancreaticoduodenectomy. In our patients, combinatorial image analysis helped us to diagnose pancreatic paraganglioma and we could select the non-excessive surgical treatment without post-surgical functional disorder of the pancreas[7].

In conclusion, we report two patients with paraganglioma in the head of the pancreas, in whom CT showed a well-defined tumor with cystic areas and rich blood supply. These findings are helpful in differentiating pancreatic paraganglioma from other pancreatic neoplasms. For surgical treatment, we could select simple excision of the tumor rather than radical surgery.

COMMENTS

Case characteristics

Case 1 felt left upper abdominal pain for 20 d. Case 2 denied obvious symptoms of gastric bleeding and abdominal discomfort.

Clinical diagnosis

The mass was found in the pancreatic head.

Differential diagnosis

Computed tomography (CT) findings are helpful to differentiate between pancreatic paraganglioma and other pancreatic neoplasms, such as pancreatic carcinoma and pancreatic endocrine tumor.

Laboratory diagnosis

Blood tests and liver and renal functions were normal.

Imaging diagnosis

CT findings are a well-defined, hypervascular tumor with cystic areas.

Pathological diagnosis

The tumors were finally diagnosed as primary pancreatic paraganglioma by microscopic examination and immunohistochemical study.

Treatment

Simple excision of the tumor was performed.

Related reports

Primary paraganglioma that arises in the pancreas is rare. Lightfoot *et al* found pancreatic paragangliomas in many reports show the retroperitoneal extension of a paraganglioma into the pancreas rather than a true pancreatic neoplasm.

Term explanation

Paraganglioma is a rare tumor of the paraganglia, derived from neural crest cells in sympathetic or parasympathetic ganglions. These tumors can be widely distributed from the adrenal medulla to the head, neck, mediastinum and retroperitoneum.

Experiences and lessons

It is often difficult to distinguish between pancreatic paragangliomas and pancreatic endocrine tumors.

Peer review

The authors reported two patients with paraganglioma in the head of the pancreas, a rare pancreatic tumor. The imaging features of pancreatic paraganglioma are well described. These findings are helpful to differentiate between pancreatic paraganglioma and other pancreatic neoplasms.

REFERENCES

1 **Borgohain M**, Gogoi G, Das D, Biswas M. Pancreatic paraganglioma: An extremely rare entity and crucial role of immunohistochemistry for diagnosis. *Indian J Endocrinol Metab* 2013; **17**: 917-919 [PMID: 24083178 DOI: 10.4103/2230-8210.117217]

2 **Jamilloux Y**, Favier J, Pertuit M, Delage-Corre M, Lopez S, Teissier MP, Mathonnet M, Galinat S, Barlier A, Archambeaud F. A MEN1 syndrome with a paraganglioma. *Eur J Hum Genet* 2014; **22**: 283-285 [PMID: 23778871 DOI: 10.1038/ejhg.2013.128]

3 **Kim SY**, Byun JH, Choi G, Yu E, Choi EK, Park SH, Lee MG. A case of primary paraganglioma that arose in the pancreas: the Color Doppler ultrasonography and dynamic CT features. *Korean J Radiol* 2008; **9** Suppl: S18-S21 [PMID: 18607119 DOI: 10.3348/kjr.2008.9.s.s18]

4 **He J**, Zhao F, Li H, Zhou K, Zhu B. Pancreatic paraganglioma: A case report of CT manifestations and literature review. *Quant Imaging Med Surg* 2011; **1**: 41-43 [PMID: 23256053 DOI: 10.3978/j.issn.2223-4292.2011.08.02]

5 **Procacci C**, Carbognin G, Accordini S, Biasiutti C, Bicego E, Romano L, Guarise A, Minniti S, Pagnotta N, Falconi M. Nonfunctioning endocrine tumors of the pancreas: possibilities of spiral CT characterization. *Eur Radiol* 2001; **11**: 1175-1183 [PMID: 11471608 DOI: 10.1007/s003300000714]

6 **Lightfoot N**, Santos P, Nikfarjam M. Paraganglioma mimicking a pancreatic neoplasm. *JOP* 2011; **12**: 259-261 [PMID: 21546704]

7 **Ohkawara T**, Naruse H, Takeda H, Asaka M. Primary paraganglioma of the head of pancreas: contribution of combinatorial image analyses to the diagnosis of disease. *Intern Med* 2005; **44**: 1195-1196 [PMID: 16357461 DOI: 10.2169/internalmedicine.44.1195]

P- Reviewer: Hackert T, Yang LB **S- Editor**: Gou SX
L- Editor: A **E- Editor**: Liu XM

World Journal of Gastroenterology

Submit a Manuscript: http://www.wjgnet.com/esps/
Help Desk: http://www.wjgnet.com/esps/helpdesk.aspx
DOI: 10.3748/wjg.v21.i3.1040

World J Gastroenterol 2015 January 21; 21(3): 1040-1043
ISSN 1007-9327 (print) ISSN 2219-2840 (online)

CASE REPORT

Successful endoscopic hemoclipping of massive lower gastrointestinal bleeding from paratyphoid A fever

Hui Wang, Xiao-Lin Dong, Xiao-Ming Yu, Kyu Sung Chung, Jian-Peng Gao

Hui Wang, Xiao-Lin Dong, Xiao-Ming Yu, Kyu Sung Chung, Jian-Peng Gao, Department of Gastroenterology, The Affiliated YanAn Hospital of Kunming Medical University, Kunming 650051, Yunnan Province, China

Author contributions: Wang H and Yu XM performed the endoscopy; Dong XL received the patient and assisted in collecting the patient's data; Wang H wrote the manuscript; Gao JP and Chung KS edited the manuscript; all authors read and approved the final manuscript.

Correspondence to: Jian-Peng Gao, MD, Department of Gastroenterology, The Affiliated YanAn Hospital of Kunming Medical University, 245 East Renmin Road, Kunming 650051, Yunnan Province, China. gaojianpengkm@163.com
Telephone: +86-871-63211282
Fax: +86-871-63211282

Received: June 7, 2014
Peer-review started: June 8, 2014
First decision: June 27, 2014
Revised: August 14, 2014
Accepted: September 18, 2014
Article in press: September 19, 2014
Published online: January 21, 2015

Abstract

Paratyphoid fever can be complicated by massive lower gastrointestinal bleeding with ileocolonic ulcerations, which are commonly localized using colonoscopy. The most common manifestations include multiple, variable-sized, round or oval-shaped, punched-out ulcers. Occasionally, massive lower gastrointestinal bleeding can occur from erosion of blood vessels. We present a rare case of severe lower gastrointestinal bleeding due to paratyphoid A fever that was successfully controlled with hemoclippings. A 30-year-old man experienced high fever and hematochezia whose blood culture showed *Salmonella paratyphi* A. A complete colonoscopy was successfully performed up to the level of the terminal ileum, which showed multiple, shallow, ulcerated lesions over the entire terminal ileum. A bleeding vessel was seen in one of the ulcers, with overlaying blood clots. Endoscopic hemostasis was successfully performed with four pieces of endoclip and without immediate complication. This report highlights the use of colonoscopy and endoscopic therapy with endoclips for lower gastrointestinal bleeding, which should be considered before surgery.

Key words: Endoscopic hemoclipping hemostasis; Lower gastrointestinal bleeding; Paratyphoid A fever

Core tip: We present a case of severe lower gastrointestinal bleeding due to paratyphoid A fever that was well-controlled by hemoclippings. Although this type of complication is rare with paratyphoid A fever, clinicians should be cognizant of the possibility for intestinal bleeding from the ulcers in the ileum and proximal colon, which can appear as multiple, variable-sized, round or oval-shaped, punched-out ulcers. Colonoscopy and endoscopic therapy with endoclips should be considered before surgery.

Wang H, Dong XL, Yu XM, Chung KS, Gao JP. Successful endoscopic hemoclipping of massive lower gastrointestinal bleeding from paratyphoid A fever. *World J Gastroenterol* 2015; 21(3): 1040-1043 Available from: URL: http://www.wjgnet.com/1007-9327/full/v21/i3/1040.htm DOI: http://dx.doi.org/10.3748/wjg.v21.i3.1040

INTRODUCTION

Paratyphoid fever can be complicated by ileocolonic ulcerations and massive lower gastrointestinal bleeding (LGIB). The infectious organisms causing the condition localize to the Peyer's patches of the terminal ileum. Hyperplasia and necrosis in these areas can result in multiple, variable-sized, round or oval-shaped, punched-out ulcers. Conservative therapy is commonly used for treating paratyphoid fever and gastrointestinal infections that are complicated by a minor episode of LGIB. However, a life-threatening hemorrhage can occur in 3%-10% of patients[1], which is associated with a high mortality unless specifically treated[2]. Although antimicrobial therapy is usually the mainstay treatment[3], surgical involvement is sometimes necessary[4]. Occasionally, a massive LGIB can occur from erosion of blood vessels. Colonoscopy has recently been advocated for localizing the site of bleeding among patients with typhoid fever, and favorable results have been found with endoscopic hemostasis without immediate complications[5,6]. However, diagnostic methodologies and treatment strategies for LGIB in patients with typhoid fever have not yet been established[4,7]. Here we present a rare case of severe LGIB due to paratyphoid A fever that was successfully controlled by endoscopic therapy with endoclips.

CASE REPORT

A 30-year-old man was admitted to our hospital with a six-day history of fever, poor appetite, and abdominal discomfort. He had no history of recent travel. The vital signs were normal except for a body temperature of 39.8 ℃. The physical examination was unremarkable except for tenderness in the right lower quadrant. Abnormal laboratory values were as follows: alanine aminotransferase, 57 U/L; aspartate aminotransferase, 82 U/L; and white cell count, 3.64 × 10^9/L. Stool tests showed the presence of occult blood. A blood culture identified *Salmonella paratyphi* A that was sensitive to levofloxacin, and intravenous treatment was thus administered.

On the second day of hospitalization, the patient experienced hematochezia and dizziness. Hemoglobin levels dropped from 12.2 to 7.3 g/dL, and the patient was transfused with two units of packed red blood cells to maintain hemodynamic stability.

A complete colonoscopy was successfully performed up to the level of the terminal ileum. Multiple, shallow, ulcerated lesions were observed over the entire terminal ileum, and there was a bleeding vessel visible with overlaying blood clots in one of the ulcers (Figure 1). Four pieces of endoclip were successfully placed without complication (Figure 2), and the patient immediately became hemodynamically stable.

A ten-day course of levofloxacin (400 mg/d) was continued. The patient became afebrile and did not have subsequent bleeding. A colonoscopy was repeated after 12 d showing isolated ulcerations and normal intervening mucosa in the terminal ileum and cecum (Figure 3). The patient made a rapid recovery and was discharged after a total of 12 d in good health with a hemoglobin level of 9.7 g/dL. A colonoscopy was again performed 30 d after discharge, which showed complete resolution of the inflammation.

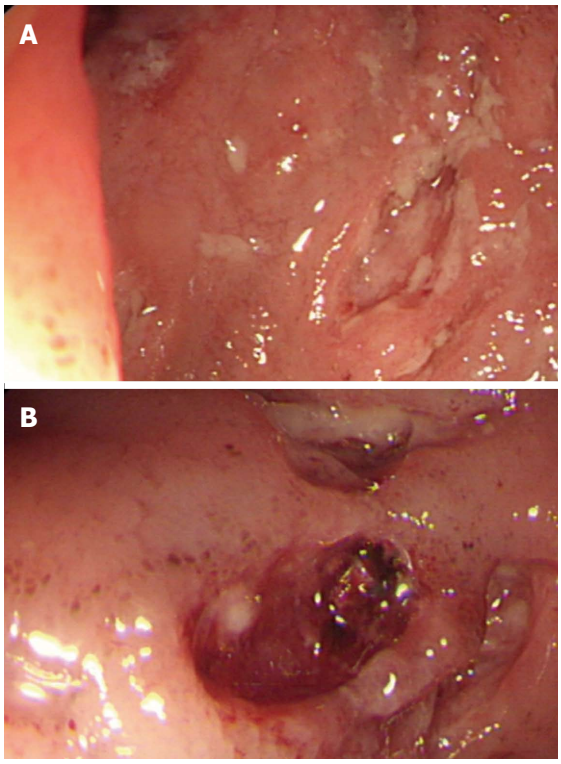

Figure 1 Endoscopy of the terminal ileum. Endoscopy revealed the presence. A: Multiple ulcerative lesions; B: An exposed bleeding vessel.

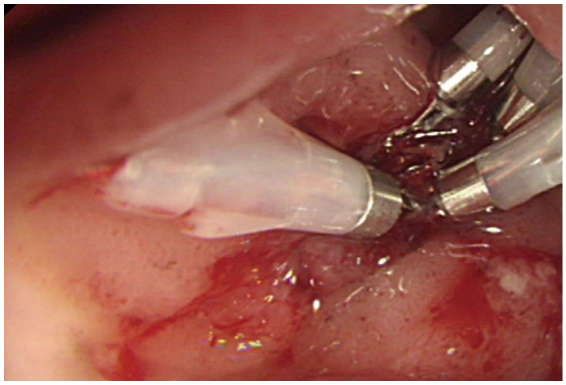

Figure 2 Hemoclippings were successfully placed at the exposed vessel.

DISCUSSION

There are few articles concerning the management of typhoid or paratyphoid fever in patients with LGIB. Surgical intervention based on a selective angiography is the first choice of management[2]. When treating the patient in the present case, bleeding was stopped with hemoclippings,

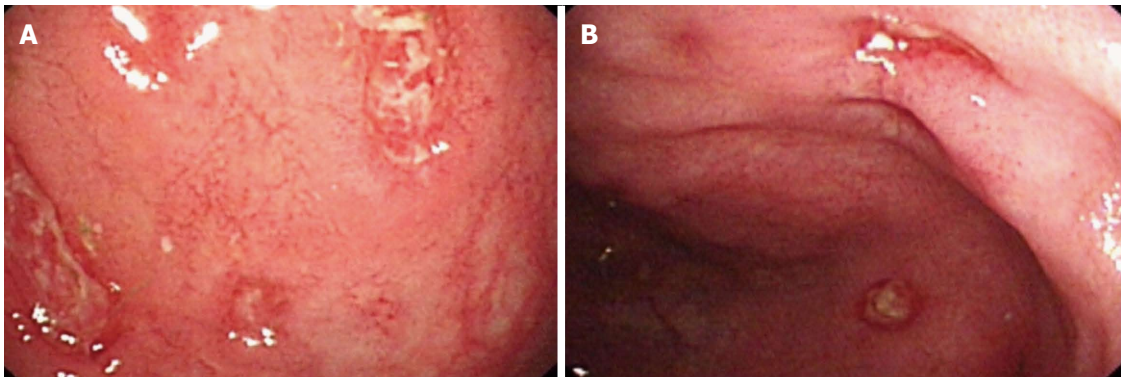

Figure 3 Repeat colonoscopy of the terminal ileum and cecum. Endoscopy revealed the presence. A: Isolated ulcerations and normal intervening mucosa in the terminal ileum; B: Isolated ulcerations and normal intervening mucosa in the cecum.

as it was not known during the colonoscopy that this was a case of paratyphoid A fever. Endoclips are effective for active vascular bleeding, non-bleeding visible vessels and adherent clots[8]. Yoshida *et al*[9] reported the control of massive colonic bleeding with hemoclippings in patients with ulcerative colitis. Hemoclippings have an advantage over epinephrine injections for preventing recurrent bleeding[10], without adding the risk of thermal injury over electrocoagulation[11].

To our knowledge, this is the first case of endoscopic hemoclipping hemostasis against massive LGIB in a patient with paratyphoid A fever. We advocate the use of hemoclipping with colonoscopy and endoscopic therapy in cases of LGIB with paratyphoid fever before radiologic or surgical intervention, particularly in patients that are hemodynamically compromised. In summary, clinicians should consider paratyphoid A fever among the other causes in patients with intestinal bleeding from ulcers in the ileum and proximal colon.

COMMENTS

Case characteristics

A 30-year-old man with massive lower gastrointestinal bleeding from paratyphoid A fever was successfully treated with endoscopic hemoclipping.

Clinical diagnosis

The patient was diagnosed with massive lower gastrointestinal bleeding from paratyphoid A fever.

Differential diagnosis

Differential diagnoses were inflammatory bowel disease and intestinal tuberculosis.

Laboratory diagnosis

The patient was diagnosed with paratyphoid A fever by blood culture and the following blood test results were obtained: alanine aminotransferase, 57 U/L; aspartate aminotransferase, 82 U/L; white cell count 3.64 × 10^9/L; hemoglobin level dropped from 12.2 to 7.3 g/dL.

Imaging diagnosis

A complete colonoscopy up to the level the terminal ileum revealed multiple shallow ulcer lesions and a bleeding vessel with overlaying blood clots in one of the ulcers in the terminal ileum.

Treatment

The patient was treated with levofloxacin and endoscopic therapy in the form of endoclips.

Related reports

Massive lower gastrointestinal bleeding from paratyphoid A fever is rare, with few cases of successful treatment using endoscopic hemoclipping reported in the literature.

Experiences and lessons

Clinicians must be alert to typhoid fever in patients with intestinal bleeding from ulcers in the ileum and proximal colon and colonoscopy and endoscopic therapy in the form of endoclips should be considered before surgery.

Peer review

The authors report an interesting case involving massive lower gastrointestinal bleeding from paratyphoid A fever that was successfully treated with endoscopic hemoclipping. The treatment option described in the article may be helpful for readers who have patients suffering the same condition.

REFERENCES

1 **Gläser A**. [Pathology and clinical aspects of bone neoplasms]. *Zentralbl Chir* 1976; **101**: 321-329 [PMID: 952122 DOI: 10.1001/archinte.158.6.633]
2 **Rubin CM**, Fairhurst JJ. Life-threatening haemorrhage from typhoid fever. *Br J Radiol* 1988; **61**: 415-416 [PMID: 3260117 DOI: 10.1259/0007-1285-61-725-415]
3 **Mandal BK**. Modern treatment of typhoid fever. *J Infect* 1991; **22**: 1-4 [PMID: 2002221 DOI: 10.1016/0163-4453(91)90758-K]
4 **Zuckerman MJ**, Meza AD, Ho H, Menzies IS, Dudrey EF. Lower gastrointestinal bleed in a patient with typhoid fever. *Am J Gastroenterol* 2000; **95**: 843-845 [PMID: 10710109 DOI: 10.1111/j.1572-0241.2000.01874.x]
5 **Kang JY**. Endoscopic diagnosis of ileal ulceration in typhoid fever. *Gastrointest Endosc* 1988; **34**: 442-443 [PMID: 3263299 DOI: 10.1016/S0016-5107(88)71422-4]
6 **Lee JH**, Kim JJ, Jung JH, Lee SY, Bae MH, Kim YH, Son HJ, Rhee PL, Rhee JC. Colonoscopic manifestations of typhoid fever with lower gastrointestinal bleeding. *Dig Liver Dis* 2004; **36**: 141-146 [PMID: 15002823 DOI: 10.1016/j.dld.2003.10.013]
7 **Sharma V**, Prashar BS, Kanga AK, Thakur S. Typhoid fever--an update. *Indian J Med Sci* 1998; **52**: 163-165 [PMID: 9770883]
8 **Saltzman JR**, Strate LL, Di Sena V, Huang C, Merrifield B, Ookubo R, Carr-Locke DL. Prospective trial of endoscopic clips versus combination therapy in upper GI bleeding (PROTECCT--UGI bleeding). *Am J Gastroenterol* 2005; **100**: 1503-1508 [PMID: 15984972 DOI: 10.1111/j.1572-0241.2005.41561.x]
9 **Yoshida Y**, Kawaguchi A, Mataki N, Matsuzaki K, Hokari R, Iwai A, Nagao S, Itoh K, Miura S. Endoscopic treatment of massive lower GI hemorrhage in two patients with ulcerative colitis. *Gastrointest Endosc* 2001; **54**: 779-781 [PMID:

11726862 DOI: 10.1067/mge.2001.119601]
10 **Odom KD**. Recovering the ESWL patient. *J Post Anesth Nurs* 1988; **3**: 14-16 [PMID: 3351772 DOI: 10.3748/wjg.v18.i18.2219]
11 **Chuttani R**, Barkun A, Carpenter S, Chotiprasidhi P, Ginsberg GG, Hussain N, Liu J, Silverman W, Taitelbaum G, Petersen B. Endoscopic clip application devices. *Gastrointest Endosc* 2006; **63**: 746-750 [PMID: 16650531 DOI: 10.1016/j.gie.2006.02.042]

P- Reviewer: Ciacci C **S- Editor**: Qi Y **L- Editor**: A
E- Editor: Wang CH

World Journal of Gastroenterology

Submit a Manuscript: http://www.wjgnet.com/esps/
Help Desk: http://www.wjgnet.com/esps/helpdesk.aspx
DOI: 10.3748/wjg.v21.i3.1044

World J Gastroenterol 2015 January 21; 21(3): 1044-1048
ISSN 1007-9327 (print) ISSN 2219-2840 (online)

CASE REPORT

Ulcerative colitis with inflammatory polyposis in a teenage boy: A case report

Jin-Shan Feng, Ying Ye, Can-Can Guo, Bo-Tao Luo, Xue-Bao Zheng

Jin-Shan Feng, Can-Can Guo, Xue-Bao Zheng, Research Institute of Traditional Chinese Medicine, Guangdong Medical College, Zhanjiang 524023, Guangdong Province, China
Ying Ye, Department of Gastroenterology, Guangdong Medical College affiliated Lianjiang Hospital, Lianjiang 524400, Guangdong Province, China
Bo-Tao Luo, Department of Pathology, School of Basic Medicine Sciences, Guangdong Medical College, Zhanjiang 524023, Guangdong Province, China
Author contributions: Feng JS and Ye Y contributed equally to this work; Feng JS, Ye Y, Luo BT and Zheng XB performed research; Guo CC collected data; Feng JS and Ye Y wrote the paper.

Correspondence to: Xue-Bao Zheng, MD, Research Institute of Traditional Chinese Medicine, Guangdong Medical College, 2 Wenmingdong Road, Zhanjiang 524023, Guangdong Province, China. xuebaozheng@sina.com
Telephone: +86-759-2388010
Fax: +86-759-2388009
Received: June 2, 2014
Peer-review started: June 3, 2014
First decision: June 27, 2014
Revised: July 29, 2014
Accepted: September 18, 2014
Article in press: September 19, 2014
Published online: January 21, 2015

Abstract

Ulcerative colitis in addition to inflammatory polyposis is common. The benign sequel of ulcerative colitis can sometimes mimic colorectal carcinoma. This report describes a rare case of inflammatory polyposis with hundreds of inflammatory polyps in ulcerative colitis which was not easy to distinguish from other polyposis syndromes. A 16-year-old Chinese male suffering from ulcerative colitis for 6 mo underwent colonoscopy, and hundreds of polyps were observed in the sigmoid, causing colonic stenosis. The polyps were restricted to the sigmoid. Although rectal inflammation was detected, no polyps were found in the rectum. A diagnosis of inflammatory polyposis and ulcerative colitis was made. The patient underwent total colectomy and ileal pouch anal anastomosis. The patient recovered well and was discharged on postoperative day 8. Endoscopic surveillance after surgery is crucial as ulcerative colitis with polyposis is a risk factor for colorectal cancer. Recognition of polyposis requires clinical, endoscopic and histopathologic correlation, and helps with chemoprophylaxis of colorectal cancer, as the drugs used postoperatively for colorectal cancer, ulcerative colitis and polyposis are different.

Key words: Ulcerative colitis; Inflammatory polyposis; Teenager; Colorectal cancer

Core tip: This case report describes ulcerative colitis with inflammatory polyps in a teenage boy. The macropathology of inflammatory polyps excised from the colon was similar to that of familial adenomatous polyps and hyperplastic polyps. In this article, we discuss the difficulties in distinguishing inflammatory polyposis from similar polyps and emphasize the importance of the chemoprophylaxis of colorectal cancer developed from ulcerative colitis and polyps.

Feng JS, Ye Y, Guo CC, Luo BT, Zheng XB. Ulcerative colitis with inflammatory polyposis in a teenage boy: A case report. *World J Gastroenterol* 2015; 21(3): 1044-1048 Available from: URL: http://www.wjgnet.com/1007-9327/full/v21/i3/1044.htm DOI: http://dx.doi.org/10.3748/wjg.v21.i3.1044

INTRODUCTION

Ulcerative colitis (UC) is one of two major types of inflammatory bowel disease (IBD); the other is Crohn's disease (CD). The age of onset follows a bimodal pattern, with a major peak at 15-25 years and a smaller peak at 55-65 years, although the disease can occur at any age[1]. Inflammatory polyps are usually found in the setting of severe inflammatory diseases such as IBD, and carcinoma can occur in inflammatory polyps, especially unusual inflammatory polyps in complex formations. Here we present the case of a 16-year-old male with inflammatory polyposis (IP) in addition to UC, and describe its appearance on colonoscopy and gross specimen following surgery. To the best of our knowledge, such a severe condition at such a young age is rare, and it is necessary to distinguish the polyposis in this case from other polyposis syndromes.

CASE REPORT

A 16-year-old Chinese male suffering from recurrent abdominal pain and diarrhea with mucosanguineous feces for six months was referred to our department on September 18, 2012. The patient had occasional fever with dark red stool and stench on one or two occasions. He showed no obvious weight loss, had no relevant family history, and did not smoke or drink alcohol. Six months previously he had been diagnosed with UC based on colonoscopy (Figure 1A) and histology of biopsy (Figure 1B, C). At that time, physical examination showed no obvious abdominal abnormality. Laboratory examinations showed C reactive protein (CRP) of 19.0 mg/L, hemoglobin (HGB) of 63 g/L, and platelets (PLT) of 503×10^9/L. The patient received mesalazine for six months, but the symptoms recurred.

Six months later on September 21, 2012, a second colonoscopy was performed, revealing a large number of polyps in the sigmoid lumen, mucosal swelling, friability, erosions, loss of vascular pattern, and substantial superficial punctate hemorrhage. The large number of polyps had also resulted in stenosis in the sigmoid lumen (Figure 2A). The lens was unable to pass through the stenosis into the enteric cavity. The rectal mucosa showed inflammation and ulcer formation, but no polyps.

The patient underwent a total colectomy and ileal pouch anal anastomosis (IPAA) on October 7, 2012. Macroscopic examination of the resected colon revealed a large number of diffuse inflammatory polyp-like protrusions (more than a few hundreds) at both ends of the excision. Polyp diameter ranged from 0.3 to 0.8 cm. Histological analysis showed inflammatory polyposis (Figure 2B-D), and no granulomatous, adenomatous or malignant changes were noted. After surgery, the patient's condition improved and he was discharged on postoperative day 8. Examination was performed six months later, and an increase in stool frequency was observed. The boy's quality of life was normal, and acute and chronic complications such as bleeding, pelvic abscess, pouchitis, pouch failure, intestinal obstruction, and chronic pelvic infection were not found.

DISCUSSION

Inflammatory polyps are often found in inflammatory diseases of the colonic mucosa, such as UC in remission, and they may produce symptoms of pain[2] and obstruction[3], especially giant polyps[4]. In this case, the patient developed UC at an early age which was quickly complicated by severe inflammatory polyposis, which is unusual in UC. As seen in the endoscope image, numerous polyps were mainly located in the sigmoid which led to stenosis, and there was no histological evidence of neoplasm or CD which may have resulted in stenosis of the lumen (Figure 2B-D). According to endoscopic and surgical findings, it is necessary to distinguish inflammatory polyposis from other polyposis syndromes.

Another type of polyposis is familial adenomatous polyposis (FAP) which is characterized by the presence of hundreds to thousands of adenomatous polyps throughout the colon. The World Health Organization (WHO) diagnostic criteria for FAP are as follows: (1) 100 or more colorectal adenomas or (2) a germline mutation of the APC gene; or (3) a family history of FAP and at least one of the following: epidermoid cysts, osteomas, and desmoid tumor. There appears to be no significant ethnic or racial differences in the incidence of FAP. In this case, the gross findings in the excised specimen were similar to FAP, which confused the diagnosis. The potential relationship between FAP and UC is not clear. A 50-year-old man with no known history or symptoms of IBD presenting with filiform polyposis involving the entire colon, clinically mimicking FAP, and showing histologic features similar to neuromuscular and vascular hamartoma of the small bowel was reported[5]. Leal and colleagues found that patients with UC had significantly higher protein levels of Bax, APAF-1, and Caspase-9 than patients with FAP[6]. The average age of onset of polyposis in FAP is 16 years, which was the age of our patient. However, the histologic appearance of the resected specimen did not match the criteria for FAP (Figure 2B-D).

Hyperplastic polyposis (HP) is another type of polyposis. HP is usually diagnosed in individuals in their 40's to 60's, although it has been reported in patients as young as 11 years[7]. The syndrome and its inherent risk of malignant disease should be considered when polyps are numerous (more than 20, *i.e.*, polyposis), large (> 1 cm), and proximally located (especially if more than five are proximal to the sigmoid colon), and especially when there are serrated adenomas[8,9]. A family history of HP is uncommon, but colorectal cancer (CRC) in a first-degree relative of a patient with HP is common and reflects inherited increased risk, perhaps associated with the putative heterozygous state[10].

There are similar characteristics in UC, FAP and HP, respectively. Firstly, individuals with these diseases are

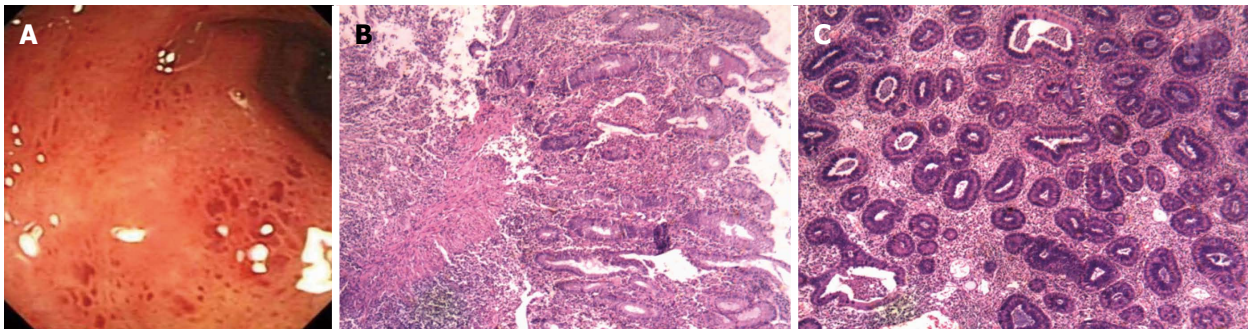

Figure 1 Colonoscopy and histologic findings in the early onset of colon inflammation. A: Inflammation in the colon, no polyps were found in the colon; B: Mucosal epithelial necrosis, destruction, distortion and branching of lamina propria glands. The distance between the glands in some regions was increased and goblet cells decreased significantly; a large number of lymphocytes and plasma cells infiltrated the lamina propria, there were neutrophils in crypts, and lymphocytes increased significantly in the base of the mucosa; a large number of lymphocytes and plasma cells infiltrated the submucosa; C: Lamina propria glands were distorted and branched accompanied by crypt abscesses and parts of the glands showed atrophy. The distance between the glands in some regions was increased, in which goblet cells were decreased. Inflammation in the lamina propria was uniform, with infiltration of numerous lymphocytes and plasma cells, and stromal vessels were significantly dilated and congested (HE staining).

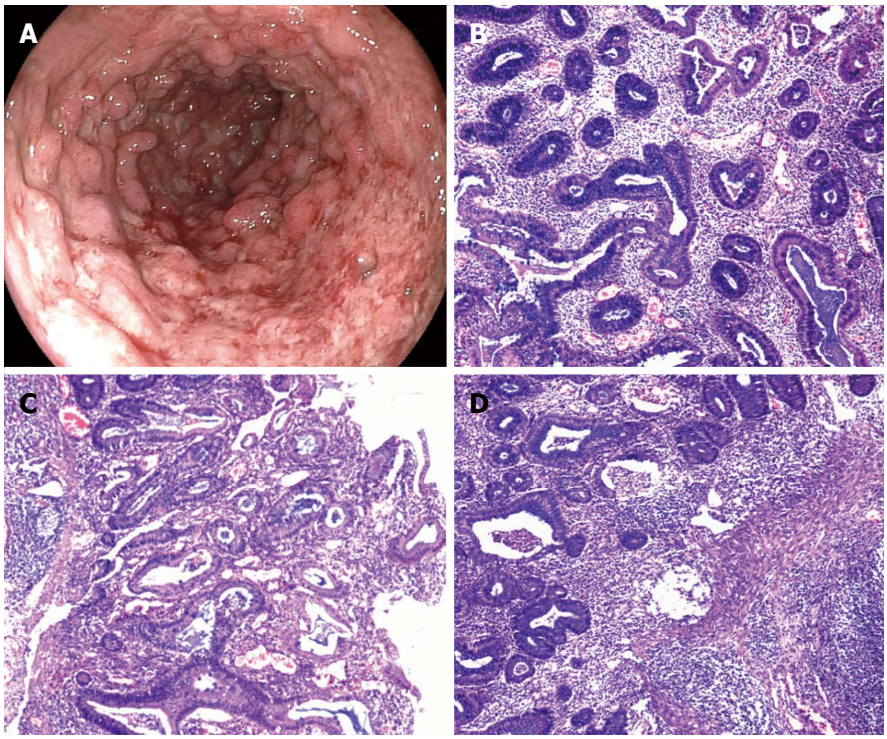

Figure 2 Colonoscopy and histologic finding 6 mo later. A: Diffuse congestion and edema in the mucosa accompanied by focal hemorrhage and exudation, showing the different shapes, sizes, erosive lesions and superficial ulcers, and most of the regional mucosal hyperplasia was granular with pseudopolyp formation; B-D: Formation of necrosis and shallow ulcers in part of the mucosal epithelial and glands in the lamina propria were distorted and branching. Several glands showed atrophy and goblet cells were decreased. Neutrophils infiltrated the lamina propria. The stromal blood vessels were significantly dilated and congested (HE staining).

clearly at increased risk of CRC. FAP is an autosomal-dominant CRC syndrome that can be caused by a germline mutation in the adenomatous polyposis coli (APC) gene on chromosome 5q21[11]. For patients who inherit the FAP mutation, there is a virtually 100% risk of colon cancer[12,13]. Colon cancer will develop in some patients as early as pre-teenage years[14]. The proportion of FAP patients with CRC who are under 20 years old is 2%-15%[15]. In addition, FAP is associated with an increased risk for the development of other malignancies, such as desmoid tumors, lymphoma, adrenal cancer, gastric cancer and ileal adenomas. A high incidence of duodenal polyps has also been described in FAP patients (79.3%)[16].

Recent studies have proposed that, large right-sided sessile "serrated" hyperplastic polyps are prone to oncogenetic and epigenetic changes leading to genetic instability and neoplasia[17,18]. HP will progress to adenocarcinoma through a "serrated neoplastic pathway" and a B type Raf kinase (BRAF) proto-oncogene mutation[19]. About 30% of CRCs develop through this pathway[20]. However, BRAF mutations were not present

in any of the polyps of patients with hyperplastic/serrated polyposis in addition to IBD[21]. These findings suggest the possibility of another pathway related to carcinogenesis in IBD. The genetic abnormalities in HP also include oncogenes and tumor suppressor genes, especially abnormalities in KRAS and TGFBR2, and loss of chromosome 1p.

UC is also associated with an increased risk of CRC, depending on age at diagnosis, especially in those less than 15 years of age, and is also dependent on the extent of disease at diagnosis[22]. The risk of CRC in patients with UC is approximately 7%-14% by 25 years of age, and the overall incidence rate of CRC is 1.67 per 1000 patient-year[23]. A recent study showed that the risk of developing CRC in patients with UC has steadily decreased over the last six decades, but the extent and duration of the disease has increased this risk[24]. The available data indicate a similar proportion of CRC in FAP and UC patients[15,22]. Whether patients with FAP in addition to UC have a higher risk of CRC is unknown and requires further investigation.

Secondly, abdominal pain and bloody diarrhea with or without mucus are common symptoms of UC and FAP. For patients with UC in addition to other polyposis, it is possible that the early symptoms of UC masked the symptoms of polyposis, however, in some cases, UC is an initial symptom of polyposis, and vice versa. It was reported that late-onset UC can present as filiform polyposis, although there were no associated diverticula, inflammatory lesions or adenomas on endoscopy and the histology of intervening mucosa was strongly suggestive of UC in remission[25]. Thus, there may be a relationship between FAP and UC which needs to be clarified. Another report suggested a link between IBD and FAP as the offspring of an FAP patient suffered from IBD[26]. In this case, however, none of his family members suffered from IBD or other polyposis syndromes, and his polyps were diagnosed after inflammation was observed.

There are some differences among the three types of lesions mentioned above. UC, HP and FAP are all closely related to CRC, however, the chemoprophylaxis for CRC is important, but is contraindicated in UC and neoplastic polyposis. For CRC and some neoplastic polyposis, non-steroidal anti-inflammatory drugs (NSAIDs) are beneficial, but are harmful in UC. NSAIDs play a role in postponing surgery in patients with mild colonic polyposis, in patients with rectal polyposis after prior colectomy, and as an adjunct to endoscopic surveillance; the use of any NSAID regardless of type is associated with a reduced risk of adenomatous polyps[27]. However, the risk is increased in CD and UC[28] and NSAIDs have been reported to induce irreversible exacerbation of IBD[29,30]. As a chemopreventive agent in CRC, the effectiveness of aspirin in FAP is unclear[31]. Researchers have found that the use of aspirin and COX-2 inhibitors was not associated with HP risk[27]. In UC patients, the use of 5-aminosalicylic acid (5-ASA) can reduce the risk of CRC[32], however, 5-ASA appears to have no effect on reducing the number or shrinking the size of polyps in the APC^{Min} mouse model of FAP[33].

In conclusion, a teenage boy with UC in addition to polyposis with a possible higher risk of CRC is described. Thus, the recognition of polyps requires the correlation of clinical, endoscopic and histopathologic examinations. It is important to make an accurate diagnosis as the chemoprophylaxis for CRC is contraindicated in patients with neoplastic polyps or pseudopolyps. Endoscopic surveillance is neccessary for patients who have undergone colectomy.

COMMENTS

Case characteristics

Hundreds of polyps were found at the onset of ulcerative colitis in a teenage boy.

Clinical diagnosis

Ulcerative colitis complicated by inflammatory polyps: Large numbers of polyps resulted in stenosis in the sigmoid lumen.

Differential diagnosis

Endoscopic and surgical examinations were required to distinguish inflammatory polyposis from familial adenomatous polyposis and hyperplastic polyposis.

Laboratory diagnosis

Laboratory diagnosis was ulcerative colitis with inflammatory polyps.

Imaging diagnosis

Colonoscopy images showed hundreds of polyps in the sigmoid causing colonic stenosis.

Pathological diagnosis

Pathological diagnosis indicated inflammatory changes in the colon.

Treatment

The patient underwent a total colectomy and ileal pouch anal anastomosis.

Term explanation

There are no uncommon terms in this case report.

Experiences and lessons

Some inflammatory polyposis syndromes are similar to familial adenomatous polyposis and hyperplastic polyposis. These disorders should be carefully distinguished and accurately diagnosed to ensure an appropriate therapeutic regimen.

Peer review

Inflammatory polyposis is not novel in ulcerative colitis but the review of the literature is sound and complete for this case report.

REFERENCES

1 **Jang ES**, Lee DH, Kim J, Yang HJ, Lee SH, Park YS, Hwang JH, Kim JW, Jeong SH, Kim N, Jung HC, Song IS. Age as a clinical predictor of relapse after induction therapy in ulcerative colitis. *Hepatogastroenterology* 2009; **56**: 1304-1309 [PMID: 19950781]

2 **Meenakshisundaram**. Isolated diffuse hyperplastic gastric polyposis: a rare case. *J Clin Diagn Res* 2012; **6**: 1428-1429 [PMID: 23205366 DOI: 10.7860/JCDR/2012/4413.2378]

3 **Adelson JW**, deChadarévian JP, Azouz EM, Guttman FM. Giant inflammatory polyposis causing partial obstruction and pain in "healed" ulcerative colitis in an adolescent. *J Pediatr Gastroenterol Nutr* 1988; **7**: 135-140 [PMID: 3335975 DOI: 10.1097/00005176-198801000-00025]

4 **Maggs JR**, Browning LC, Warren BF, Travis SP. Obstructing giant post-inflammatory polyposis in ulcerative colitis: Case report and review of the literature. *J Crohns Colitis* 2008; **2**: 170-180 [PMID: 21172208 DOI: 10.1016/j.crohns.2007.10.007]

5 **Oakley GJ**, Schraut WH, Peel R, Krasinskas A. Diffuse filiform polyposis with unique histology mimicking familial adenomatous polyposis in a patient without inflammatory bowel disease. *Arch Pathol Lab Med* 2007; **131**: 1821-1824

[PMID: 18081442 DOI: 10.1043/1543-2165(2007)131]
6 **Leal RF**, Ayrizono Mde L, Milanski M, Fagundes JJ, Moraes JC, Meirelles LR, Velloso LA, Coy CS. Detection of epithelial apoptosis in pelvic ileal pouches for ulcerative colitis and familial adenomatous polyposis. *J Transl Med* 2010; **8**: 11 [PMID: 20113505 DOI: 10.1186/1479-5876-8-11]
7 **Keljo DJ**, Weinberg AG, Winick N, Tomlinson G. Rectal cancer in an 11-year-old girl with hyperplastic polyposis. *J Pediatr Gastroenterol Nutr* 1999; **28**: 327-332 [PMID: 10067739 DOI: 10.1097/00005176-199903000-00023]
8 **Macrae FA**, Young GP. Neoplastic and nonneoplastic polyps of the colon and rectum [M]//YAMADA T. Textbook of gastroenterology. Oxford, UK, Blackwell Publishing Ltd, 2009: 1611-1639 [DOI: 10.1002/9781444303254.ch63]
9 **Lin YC**, Chiu HM, Lee YC, Shun CT, Wang HP, Wu MS. Hyperplastic polyps identified during screening endoscopy: reevaluated by histological examinations and genetic alterations. *J Formos Med Assoc* 2014; **113**: 417-421 [PMID: 24961182 DOI: 10.1016/j.jfma.2012.07.030]
10 **Smith RJ**, Bryant RG. Metal substitutions incarbonic anhydrase: a halide ion probe study. *Biochem Biophys Res Commun* 1975; **66**: 1281-1286 [PMID: 3]
11 **Burt R**, Neklason DW. Genetic testing for inherited colon cancer. *Gastroenterology* 2005; **128**: 1696-1716 [PMID: 15887160 DOI: 10.1053/j.gastro.2005.03.036]
12 **Burt RW**, Samowitz WS. The adenomatous polyp and the hereditary polyposis syndromes. *Gastroenterol Clin North Am* 1988; **17**: 657-678 [PMID: 2852640]
13 **Petersen GM**, Slack J, Nakamura Y. Screening guidelines and premorbid diagnosis of familial adenomatous polyposis using linkage. *Gastroenterology* 1991; **100**: 1658-1664 [PMID: 1673441]
14 **Church JM**, McGannon E, Burke C, Clark B. Teenagers with familial adenomatous polyposis: what is their risk for colorectal cancer? *Dis Colon Rectum* 2002; **45**: 887-889 [PMID: 12130875]
15 **Vasen HF**, Möslein G, Alonso A, Aretz S, Bernstein I, Bertario L, Blanco I, Bülow S, Burn J, Capella G, Colas C, Engel C, Frayling I, Friedl W, Hes FJ, Hodgson S, Järvinen H, Mecklin JP, Møller P, Myrhøi T, Nagengast FM, Parc Y, Phillips R, Clark SK, de Leon MP, Renkonen-Sinisalo L, Sampson JR, Stormorken A, Tejpar S, Thomas HJ, Wijnen J. Guidelines for the clinical management of familial adenomatous polyposis (FAP). *Gut* 2008; **57**: 704-713 [PMID: 18194984 DOI: 10.1136/gut.2007.136127]
16 **Cordero-Fernández C**, Garzón-Benavides M, Pizarro-Moreno A, García-Lozano R, Márquez-Galán JL, López Ruiz T, Sobrino S, Bozada JM, Laguna OB. Gastroduodenal involvement in patients with familial adenomatous polyposis. Prospective study of the nature and evolution of polyps: evaluation of the treatment and surveillance methods applied. *Eur J Gastroenterol Hepatol* 2009; **21**: 1161-1167 [PMID: 19357520 DOI: 10.1097/MEG.0b013e3283297cf2]
17 **Chow E**, Lipton L, Lynch E, D'Souza R, Aragona C, Hodgkin L, Brown G, Winship I, Barker M, Buchanan D, Cowie S, Nasioulas S, du Sart D, Young J, Leggett B, Jass J, Macrae F. Hyperplastic polyposis syndrome: phenotypic presentations and the role of MBD4 and MYH. *Gastroenterology* 2006; **131**: 30-39 [PMID: 16831587 DOI: 10.1053/j.gastro.2006.03.046]
18 **Jass JR**. Hyperplastic polyps of the colorectum-innocent or guilty? *Dis Colon Rectum* 2001; **44**: 163-166 [PMID: 11227930 DOI: 10.1007/BF02234287]
19 **Ahn HS**, Hong SJ, Kim HK, Yoo HY, Kim HJ, Ko BM, Lee MS. Hyperplastic Polyposis Syndrome Identified with a BRAF Mutation. *Gut Liver* 2012; **6**: 280-283 [PMID: 22570761 DOI: 10.5009/gnl.2012.6.2.280]
20 **Dörk T**, Dworniczak B, Aulehla-Scholz C, Wieczorek D, Böhm I, Mayerova A, Seydewitz HH, Nieschlag E, Meschede D, Horst J, Pander HJ, Sperling H, Ratjen F, Passarge E, Schmidtke J, Stuhrmann M. Distinct spectrum of CFTR gene mutations in congenital absence of vas deferens. *Hum Genet* 1997; **100**: 365-377 [PMID: 9272157]
21 **Srivastava A**, Redston M, Farraye FA, Yantiss RK, Odze RD. Hyperplastic/serrated polyposis in inflammatory bowel disease: a case series of a previously undescribed entity. *Am J Surg Pathol* 2008; **32**: 296-303 [PMID: 18223333 DOI: 10.1097/PAS.0b013e318150d51b]
22 **Ekbom A**, Helmick C, Zack M, Adami HO. Ulcerative colitis and colorectal cancer. A population-based study. *N Engl J Med* 1990; **323**: 1228-1233 [PMID: 2215606 DOI: 10.1056/NEJM199011013231802]
23 **Castano-Milla C**, Chaparro M, Gisbert JP. Has the Risk of Developing Colorectal Cancer in Patients With Ulcerative Colitis Been Overstated? a Meta-Analysis. *Gastroenterology* 2012; **142**: S251-S251 [DOI: 10.1016/S0016-5085(12)60944-5]
24 **Castaño-Milla C**, Chaparro M, Gisbert JP. Systematic review with meta-analysis: the declining risk of colorectal cancer in ulcerative colitis. *Aliment Pharmacol Ther* 2014; **39**: 645-659 [PMID: 24612141 DOI: 10.1111/apt.12651]
25 **Papathanasopoulos AA**, Katsanos KH, Tsianos EV. Late-onset ulcerative colitis presenting as filiform polyposis. *J Crohns Colitis* 2010; **4**: 488-489 [PMID: 21122551 DOI: 10.1016/j.crohns.2010.07.009]
26 **Brignola C**, Belloli C, De Simone G, Varesco L, Walger P, Areni A, Calabrese C, Di Febo G, Barbara L. Familial adenomatous polyposis and inflammatory bowel disease associated in two kindreds. *Dig Dis Sci* 1995; **40**: 402-405 [PMID: 7851206 DOI: 10.1007/BF02065428]
27 **Murff HJ**, Shrubsole MJ, Chen Z, Smalley WE, Chen H, Shyr Y, Ness RM, Zheng W. Nonsteroidal anti-inflammatory drug use and risk of adenomatous and hyperplastic polyps. *Cancer Prev Res* (Phila) 2011; **4**: 1799-1807 [PMID: 21764857 DOI: 10.1158/1940-6207.capr-11-0107]
28 **Ananthakrishnan AN**, Higuchi LM, Huang ES, Khalili H, Richter JM, Fuchs CS, Chan AT. Aspirin, nonsteroidal anti-inflammatory drug use, and risk for Crohn disease and ulcerative colitis: a cohort study. *Ann Intern Med* 2012; **156**: 350-359 [PMID: 22393130 DOI: 10.1059/0003-4819-156-5-201203060-00007]
29 **Hovde O**, Farup PG. NSAID-induced irreversible exacerbation of ulcerative colitis. *J Clin Gastroenterol* 1992; **15**: 160-161 [PMID: 1401830]
30 **Bonner GF**. Exacerbation of inflammatory bowel disease associated with use of celecoxib. *Am J Gastroenterol* 2001; **96**: 1306-1308 [PMID: 11316199 DOI: 10.1016/s0002-9270(01)02293-6]
31 **Kim B**, Giardiello FM. Chemoprevention in familial adenomatous polyposis. *Best Pract Res Clin Gastroenterol* 2011; **25**: 607-622 [PMID: 22122775 DOI: 10.1016/j.bpg.2011.08.002]
32 **Velayos FS**, Terdiman JP, Walsh JM. Effect of 5-aminosalicylate use on colorectal cancer and dysplasia risk: a systematic review and metaanalysis of observational studies. *Am J Gastroenterol* 2005; **100**: 1345-1353 [PMID: 15929768 DOI: 10.1111/j.1572-0241.2005.41442.x]
33 **Ritland SR**, Leighton JA, Hirsch RE, Morrow JD, Weaver AL, Gendler SJ. Evaluation of 5-aminosalicylic acid (5-ASA) for cancer chemoprevention: lack of efficacy against nascent adenomatous polyps in the Apc(Min) mouse. *Clin Cancer Res* 1999; **5**: 855-863 [PMID: 10213222]

P- Reviewer: Mao AP, Mulberg AE **S- Editor**: Qi Y
L- Editor: A **E- Editor**: Wang CH

Published by **Baishideng Publishing Group Inc**
8226 Regency Drive, Pleasanton, CA 94588, USA
Telephone: +1-925-223-8242
Fax: +1-925-223-8243
E-mail: bpgoffice@wjgnet.com
Help Desk: http://www.wjgnet.com/esps/helpdesk.aspx
http://www.wjgnet.com

ISSN 1007-9327